EIGHTH EDITION

Spectrometric Identification of Organic Compounds

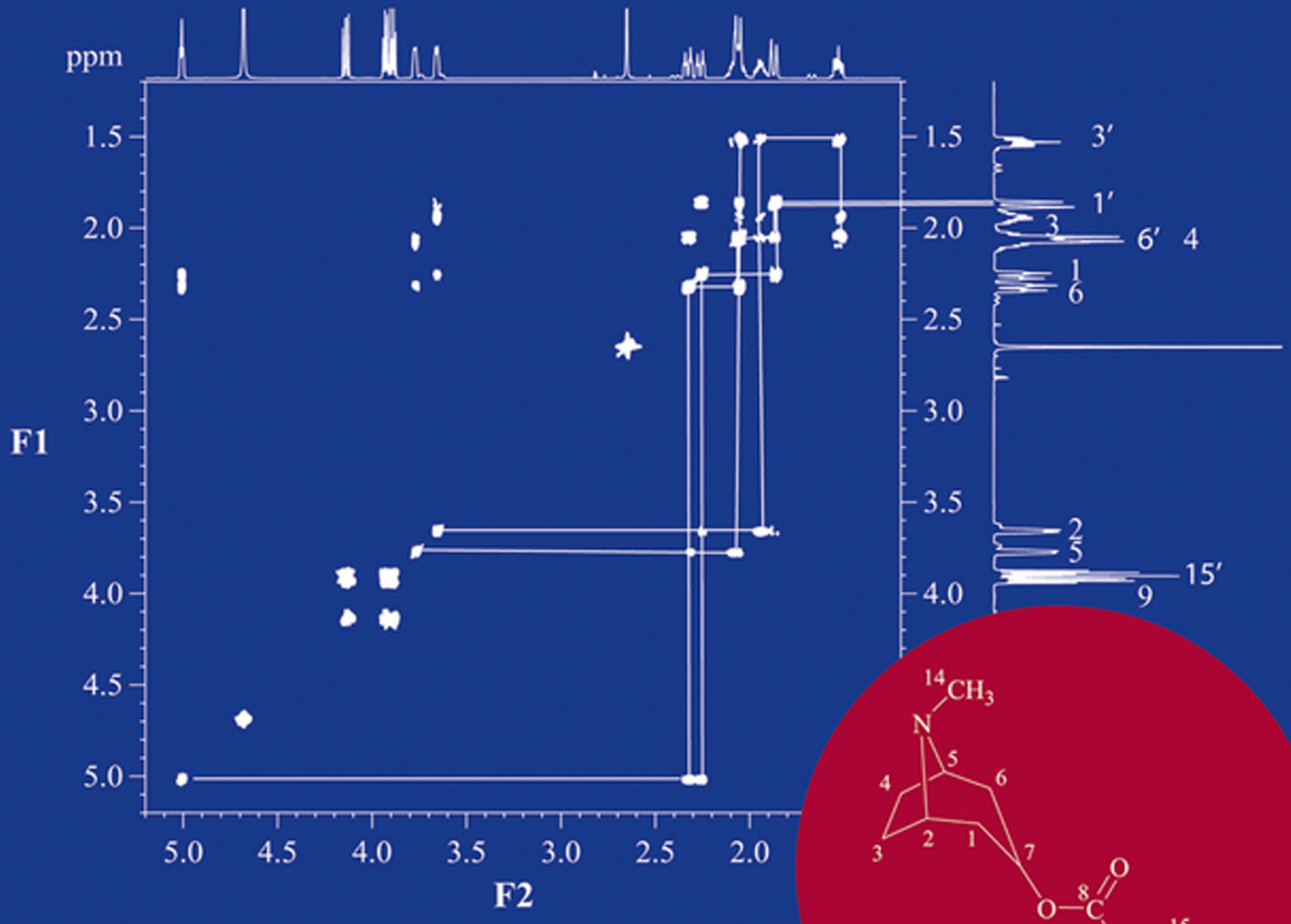

Robert M. Silverstein
Francis X. Webster
David J. Kiemle
David L. Bryce

WILEY

EIGHTH EDITION

SPECTROMETRIC IDENTIFICATION OF ORGANIC COMPOUNDS

ROBERT M. SILVERSTEIN

FRANCIS X. WEBSTER

DAVID J. KIEMLE

State University of New York College of Environmental Science & Forestry

DAVID L. BRYCE

University of Ottawa

WILEY

Vice President and Publisher:	Petra Recter
Sponsoring Editor:	Joan Kalkut
Senior Project Editor:	Jennifer Yee
Sponsoring Editor:	Mary O'Sullivan
Project Editor:	Ellen Keohane
Designer:	Maddy Lesure
Cover Designer:	Kenji Ngieng
Associate Production Manager:	Joyce Poh
Senior Production Editor:	Jolene Ling
Production Management Services:	Laserwords
Cover Illustration Credit:	© David J. Kiemle

This book was set in Stix Regular 10pt by Laserwords.

This book is printed on acid free paper. ∞

Library of Congress Cataloging-in-Publication Data

Silverstein, Robert M. (Robert Milton), 1916-2007.
Spectrometric identification of organic compounds / Robert M. Silverstein, Francis X. Webster, David J. Kiemle, State University of New York, College of Environmental Science & Forestry; David L. Bryce, University of Ottawa. – Eighth edition.
pages cm
Includes index.
ISBN 978-0-470-61637-6 (pbk.)
1. Spectrum analysis–Textbooks. 2. Organic compounds–Spectra–Textbooks. I. Webster, Francis X. II. Kiemle, David J. III. Bryce, David L. (David Lawson), 1975- IV. Title.
QD272.S6S55 2015
543'.5–dc23

2014018634

Printed in the United States of America

10 9 8 7 6 5 4 3 2 1

PREFACE TO EIGHTH EDITION

This problem-solving textbook, known as "Silverstein" to many of its generations of readers, has been a popular and very useful resource for students and instructors over the past 50 years. The book presents a unified approach to the structural determination of organic compounds based largely on mass spectrometry (MS), infrared (IR) spectroscopy, and multinuclear and multidimensional nuclear magnetic resonance (NMR) spectroscopy. We are very pleased to present the newly revised eighth edition. The strengths for which *Spectrometric Identification of Organic Compounds* is known are preserved and updated. Such strengths include the pragmatic approach to problem solving and the wealth of useful NMR and mass spectrometric data available in tabular form. Some of the more important revisions to this edition of the book are briefly detailed below.

Throughout the text, wording has been updated for consistency and to be more reflective of modern usage. We have replaced the older terminologies "spectrometry" and "spectrometric" in reference to IR and NMR with the more widely used "spectroscopy" and "spectroscopic" throughout the text, even though we are aware there are valid arguments for keeping the former. The original familiar title of the book has been maintained. New information on polymers and phosphorus functional groups has been added to Chapter 2 on IR spectroscopy. Chapter 3 on proton NMR spectroscopy has been overhauled, some sections having been thoroughly revised. The latest techniques in cutting-edge NMR signal enhancement methods are highlighted. We have attempted to maintain an appropriate balance between theory and practice. The concepts of chemical and magnetic equivalence, central to understanding many NMR spectra, are explained with more clarity. Chapters 4 and 5 on ^{13}C NMR and two-dimensional NMR feature clearer explanations and revised sections, which more accurately convey how some of the experiments actually work. The important roles of gradients and of more advanced data acquisition methods in modern NMR research are also briefly highlighted in Chapter 5. Chapter 6, on multinuclear magnetic resonance, includes details on additional isotopes of interest to the chemist and several additional tables of chemical shifts and coupling constants. Hopefully, this chapter will encourage the reader to pursue studies of isotopes beyond ^{1}H and ^{13}C when present in their molecules of interest. Chapters 7 and 8, which feature solved problems and assigned problems, have been revised but the core content consisting of the problems themselves has been maintained from the previous edition. Reviewers have consistently noted the values of the problems to students in these two chapters.

We would like to thank the Wiley staff, including Jennifer Yee, Ellen Keohane, and Mary O'Sullivan, for their hard work and dedication to this project. We are also grateful to the following reviewers for their invaluable suggestions that greatly improved the manuscript:

Scott Burt, Brigham Young University, Provo, Utah

Charles Garner, Baylor University, Waco, Texas

Kevin Gwaltney, Kennesaw State University, Kennesaw, Georgia

Vera Kolb, University of Wisconsin-Parkside

James Nowick, University of California, Irvine

Michael Wentzel, Augsburg College, Minneapolis, Minnesota

David L. Bryce, Ottawa, Ontario
Francis X. Webster, Syracuse, New York
David J. Kiemle, Syracuse, New York

PREFACE TO FIRST EDITION

During the past several years, we have been engaged in isolating small amounts of organic compounds from complex mixtures and identifying these compounds spectrometrically.

At the suggestion of Dr. A. J. Castro of San Jose State College, we developed a one unit course entitled "Spectrometric Identification of Organic Compounds," and presented it to a class of graduate students and industrial chemists during the 1962 spring semester. This book has evolved largely from the material gathered for the course and bears the same title as the course.*

We should first like to acknowledge the financial support we received from two sources: The Perkin-Elmer Corporation and Stanford Research Institute.

A large debt of gratitude is owed to our colleagues at Stanford Research Institute. We have taken advantage of the generosity of too many of them to list them individually, but we should like to thank Dr. S. A. Fuqua, in particular, for many helpful discussions of NMR spectrometry. We wish to acknowledge also the cooperation at the management level, Dr. C. M. Himel, chairman of the Organic Research Department, and Dr. D. M. Coulson, chairman of the Analytical Research Department.

Varian Associates contributed the time and talents of its NMR Applications Laboratory. We are indebted to Mr. N. S. Bhacca, Mr. L. F. Johnson, and Dr. J. N. Shoolery for the NMR spectra and for their generous help with points of interpretation.

The invitation to teach at San Jose State College was extended to Dr. Bert M. Morris, head of the Department of Chemistry, who kindly arranged the administrative details.

The bulk of the manuscript was read by Dr. R. H. Eastman of the Stanford University whose comments were most helpful and are deeply appreciated.

Finally, we want to thank our wives. As a test of a wife's patience, there are few things to compare with an author in the throes of composition. Our wives not only endured, they also encouraged, assisted, and inspired.

R. M. Silverstein
G. C. Bassler

Menlo Park, California
April 1963

*A brief description of the methodology had been published: R. M. Silverstein and G. C. Bassler, *J. Chem. Educ.* **39**, 546 (1962).

CONTENTS

CHAPTER 1

MASS SPECTROMETRY

1.1 INTRODUCTION

The concept of mass spectrometry is relatively simple: a compound is ionized (ionization method), the ions are separated on the basis of their mass/charge ratio (ion separation method), and the number of ions representing each mass/charge unit is recorded as a spectrum. There are many ionization methods and many methods for separating the resulting ions (see Section 1.2). For instance, in the commonly used electron impact (EI) mode, the mass spectrometer bombards molecules in the vapor phase with a high-energy electron beam and records the result as a spectrum of positive ions, which have been separated on the basis of mass/charge (m/z).*

To illustrate, the EI mass spectrum of benzamide is given in Figure 1.1 showing a plot of abundance (% of the base peak, the most intense peak in the spectrum) versus m/z. The positive ion peak at m/z 121 represents the intact molecule (M) less one electron, which was removed by the impacting electron beam; it is designated as the molecular ion, $M^{\cdot+}$. The energetic molecular ion produces a series of fragment ions, some of which are rationalized in Figure 1.1.

It is routine to couple a mass spectrometer to some form of chromatographic instrument, such as a gas chromatograph (GC-MS) or a liquid chromatograph (LC-MS). The mass spectrometer finds widespread use in the analysis of compounds whose mass spectrum is known and in the analysis of completely unknown compounds. In the case of known compounds, a computer search is conducted comparing the mass spectrum of the compound in question with a library of mass spectra. Electron impact mass spectrometry is particularly useful in this regard since EI mass spectrometry leads to considerable fragmentation. Congruence of mass spectra is convincing evidence for identification and is often even admissible in court. In the case of an unknown compound, the molecular ion, the fragmentation pattern, and evidence from other forms of spectrometry (e.g., IR and NMR) can lead to the identification of a new compound. Our focus and goal in this chapter is to develop skill in the latter use,

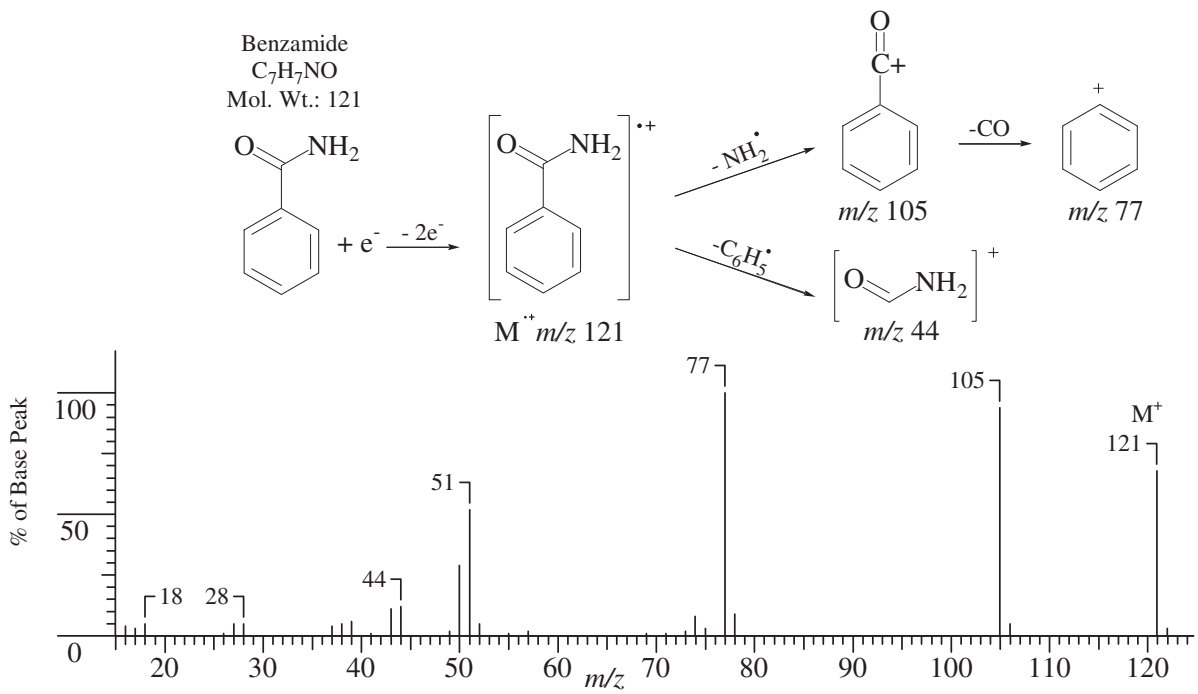

FIGURE 1.1 The EI mass spectrum of benzamide, above which is a fragmentation pathway to explain some of the important ions.

*The unit of mass is the Dalton (Da), defined as $\frac{1}{12}$ of the mass of an atom of the isotope ^{12}C, which is arbitrarily 12.0000 … mass units.

especially using the EI method. For other applications or for more detail, mass spectrometry texts and spectral compilations are listed online at www.wiley.com/college/silverstein.

1.2 INSTRUMENTATION

As with all modern analytical instrumentation, there has been recent, rapid growth and change in instrumentation for mass spectrometry. Instead of discussing individual instruments, the discussion will be broken down into (1) ionization methods and (2) ion separation methods. In general, the method of ionization is independent of the method of ion separation and vice versa, although there are exceptions. Some of the ionization methods depend on a specific chromatographic front end (e.g., LC-MS), while still others are precluded from using chromatography for introduction of the sample (e.g., FAB and MALDI). Before delving further into instrumentation, let us make a distinction between two types of mass spectrometers based on resolution.

The minimum requirement for the organic chemist is the ability to record the molecular weight of the compound under examination to the nearest whole number. Thus, the spectrum should show a peak at, say, m/z 400, which is distinguishable from a peak at m/z 399 or at m/z 401. In order to select possible molecular formulas by measuring isotope peak intensities (see Section 1.5.2.1), adjacent peaks must be cleanly separated. Arbitrarily, the valley between two such peaks should not be more than 10% of the height of the larger peak. This degree of resolution is qualitatively termed "unit" resolution and can be obtained up to a mass of approximately 3000 Da on readily available "unit resolution" instruments.

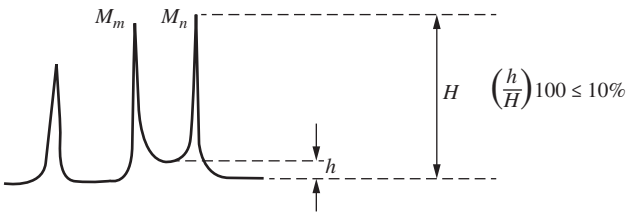

To determine the resolution* of an instrument, consider two adjacent peaks of approximately equal intensity. These peaks should be chosen so that the height of the valley between the peaks is less than 10% of the intensity of the peaks. The resolution (R) is $R = M_n/(M_n - M_m)$, where M_n is the higher mass number of the two adjacent peaks, and M_m is the lower mass number.

There are two important categories of mass spectrometers: low (unit) resolution and high resolution. Low-resolution instruments can be defined arbitrarily as the instruments that separate unit masses up to m/z 3000 [$R = 3000/(3000 - 2999) = 3000$]. A high-resolution instrument (e.g., $R = 20{,}000$) can distinguish between $C_{16}H_{26}O_2$ and $C_{15}H_{24}NO_2$ [$R = 250.1933/(250.1933 - 250.1807) = 19857$]. This important class of mass spectrometers, which can have R as large as 100,000, can measure the mass of an ion with sufficient accuracy to determine its atomic composition (molecular formula). As a practical matter, the term high-resolution mass spectrometry will be used to designate *accurate mass measurement*. The number of decimal places needed for an unambiguous determination of elemental composition is related to the mass of the ion. For instance, an accuracy of 0.0025 Da should be sufficient for ions with a mass of less than 500 Da.

All mass spectrometers share common features (see Figure 1.2). Introduction of the sample into the mass spectrometer is an important consideration, but it often depends on the type of ionization method (see below). All mass spectrometers have methods for ionizing the sample and for separating the ions on the basis of m/z. These methods are discussed in detail below. Once separated, the ions must be detected and quantified. A typical ion collector consists of collimating slits that direct only one set of ions at a time into the collector, where they are detected and amplified by an electron multiplier. Ion detectors are designed to balance sensitivity, accuracy, and response time. Generally speaking, fast response times and high accuracy are mutually exclusive. The method of ion detection is dependent to some extent on the method of ion separation.

*This definition is the most common way to calculate resolution, but not the only way.

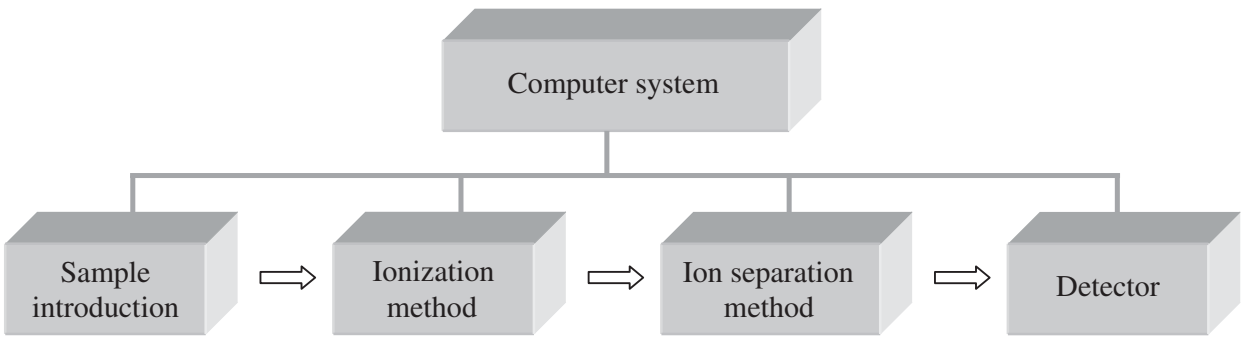

FIGURE 1.2 Block diagram of features of a typical mass spectrometer.

Nearly all mass spectrometers today are interfaced with a computer. Typically, the computer controls the operation of the instrument, which includes any chromatography, collects and stores the data, and provides either graphical output (essentially a bar graph) or tabular lists of the data.

1.3 IONIZATION METHODS

The large number of ionization methods, some of which are highly specialized, precludes complete coverage. The most common ones in the three general areas of gas-phase, desorption, and evaporative ionization are described below.

1.3.1 Gas-Phase Ionization Methods

Gas-phase methods for generating ions for mass spectrometry are the oldest and most popular methods for organic chemists. These methods are applicable to compounds that have a minimum vapor pressure of ca. 10^{-6} Torr at a temperature at which the compound is stable; this criterion applies to a large number of nonionic organic molecules with MW<1000 Da.

1.3.1.1 Electron Impact Ionization. Electron impact (EI) has historically been the most widely used method for generating ions for mass spectrometry. It is also the main focus in this chapter for interpreting mass spectra for structure determination. Vapor-phase sample molecules are bombarded with high-energy electrons (generally 70 eV), the purpose of which is to eject an electron from a sample molecule to produce a radical cation, known as the molecular ion. Because the ionization potential of typical organic compounds is generally less than 15 eV, the bombarding electrons impart 50 eV (or more) of excess energy to the newly created molecular ion, which is dissipated, in part, by the breaking of covalent bonds, which have strengths between 3 and 10 eV.

Bond breaking is usually extensive and critically, highly reproducible, and characteristic of the compound. Furthermore, this fragmentation process is also partly predictable and is the source of the powerful structure elucidation potential of mass spectrometry. Often, the excess energy imparted to the molecular ion is too great, which leads to a mass spectrum with no discernible molecular ion. Reduction of the ionization voltage is a commonly used strategy to obtain a molecular ion; the strategy is often successful because there is greatly reduced fragmentation. The disadvantage of this strategy is that the spectrum changes and cannot be compared to standard literature spectra.

To many organic chemists, mass spectrometry is synonymous with EI mass spectrometry. This view is understandable for two reasons. First, historically, EI was universally available before other ionization methods were developed. Much of the early work was EI mass spectrometry. Second, the major libraries and databases of mass spectral data, which are relied upon so heavily and cited so often, are of EI mass spectra. Some of the readily accessible databases contain EI mass spectra of over 390000 compounds and they are easily searched by efficient computer algorithms. The uniqueness of the EI mass spectrum for a given organic compound, even for diastereomers, is an almost certainty. This uniqueness, coupled with the great sensitivity of the method, is what makes GC-MS such a powerful and popular analytical tool. We will discuss EI mass spectra beginning in Section 1.5.

1.3.1.2 Chemical Ionization. Electron impact ionization often leads to such extensive fragmentation that no molecular ion is observed. One way to avoid this problem is to use an indirect ionization method; chemical ionization (CI) is popular and readily available on many commercial instruments. In CI, sample molecules (in the vapor phase) are not subjected to bombardment by high-energy electrons. Instead, a reagent gas (usually methane, isobutane, ammonia, but others are also used) is introduced into the ionization source and ionized. Sample molecules collide with ionized reagent gas molecules ($CH_5^+, C_4H_9^+$, etc.) in the relatively high-pressure CI source and undergo secondary ionization (i.e., chemical ionization) by proton transfer producing an $[M+1]^+$ ion, by electrophilic addition producing $[M+15]^+, [M+29]^+, [M+41]^+$, or $[M+18]^+$ (with NH_4^+ ions), or by charge exchange (rare) producing a $[M]^+$ ion. Chemical ionization spectra sometimes have prominent $[M-1]^+$ ion peaks because of hydride abstraction. The ions thus produced are even electron species. The excess energy transfered to the sample molecules during the ionization phase is small, generally less than 5 eV, so that much less fragmentation takes place. There are several important consequences, the most valuable of which are an abundance of quasimolecular ions and greater sensitivity because the total ion current is concentrated into a few ions. There is however, less information on structure. The quasimolecular ions are usually quite stable and they are readily detected. Oftentimes, there are only one or two fragment ions produced and sometimes there are none.

For example, the EI mass spectrum of 3, 4-dimethoxyacetophenone (Figure 1.3) shows, in addition to the molecular ion at m/z 180, numerous fragment peaks in the range of m/z 15 to 167; these include the base peak at m/z 165 and prominent peaks at m/z 137 and m/z 77. The CI mass spectrum (methane, CH_4, as reagent gas) shows the quasimolecular ion ($[M+1]^+$, m/z 181) as the base peak (100%), and no fragment ion peaks. The only other peaks, each of just a few percent intensity, are the molecular ion peak, m/z 180, m/z 209 ($[M+29]^+$ or $M+C_2H_5^+$), and m/z 221 ($[M+41]^+$ or $M+C_3H_5^+$). These last two peaks are a result of electrophilic addition of carbocations and are very useful in identifying the molecular ion. The excess methane carrier gas is ionized by electron impact to the primary ions CH_4^+ and CH_3^+. These react with the excess methane to give secondary ions.

$$CH_3^+ + CH_4 \longrightarrow C_2H_5^+ \text{ and } H_2$$

$$CH_4 + C_2H_5^+ \longrightarrow C_3H_5^+ \text{ and } 2H_2$$

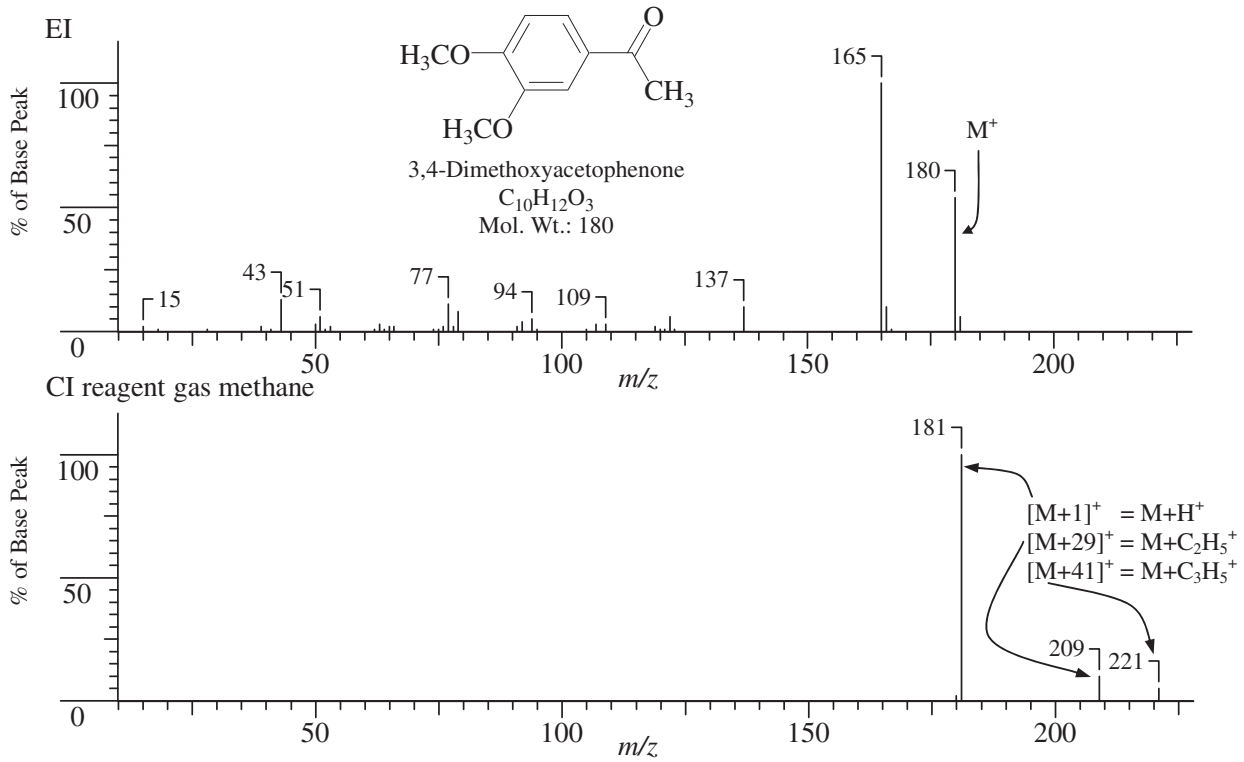

FIGURE 1.3 The EI and CI mass spectra of 3,4-dimethoxyacetophenone.

The energy content of the various secondary ions (from, respectively, methane, isobutane, and ammonia) decrease in the order: $C_3H_5^+ > t\text{-}C_4H_9^+ > NH_4^+$. Thus, by choice of reagent gas, we can control the tendency of the CI produced $[M + 1]^+$ ion to fragment. For example, when methane is the reagent gas, dioctyl phthalate shows its $[M + 1]^+$ peak (m/z 391) as the base peak; more importantly, the fragment peaks (e.g., m/z 113 and 149) are 30% to 60% of the intensity of the base beak. When isobutane is used, the $[M + 1]^+$ peak is still large, while the fragment peaks are only roughly 5% as intense as the $[M + 1]^+$ peak.

Chemical ionization mass spectrometry is neither useful for peak matching (either manually or by computer) nor is it particularly useful for structure elucidation; its main use is for the detection of molecular ions and hence molecular weights.

1.3.2 Desorption Ionization Methods

Desorption ionization methods are those techniques in which sample molecules are emitted directly from a condensed phase into the vapor phase as ions. The primary use of these methods is for large, nonvolatile, or ionic compounds. There can be significant disadvantages. Desorption methods generally do not use available sample efficiently. Often times, the information content is limited. For unknown compounds, the methods are used primarily to provide molecular weight, and in some cases to obtain an exact mass. However, even for this purpose, it should be used with caution because the molecular ion or the quasimolecular ion may not be evident. The resulting spectra are often complicated by abundant matrix ions.

1.3.2.1 Field Desorption Ionization. In the field desorption (FD) method, the sample is applied to a metal emitter on the surface of which is found carbon microneedles. The microneedles activate the surface, which is maintained at the accelerating voltage and functions as the anode. Very high voltage gradients at the tips of the needles remove an electron from the sample, and the resulting cation is repelled away from the emitter. The ions generated have little excess energy so there is minimal fragmentation, that is, the molecular ion is usually the only significant ion seen. For example, with cholest-5-ene-3,16,22,26-tetrol, the EI and CI mass spectra do not show a molecular ion peak. However, the FD mass spectrum (Figure 1.4) shows predominately the molecular ion with virtually no fragmentation.

1.3.2.2 Fast Atom Bombardment Ionization. Fast atom bombardment (FAB) uses high-energy xenon or argon atoms (6 keV to 10 keV) to bombard samples dissolved in a liquid of low vapor pressure (e.g., glycerol). The matrix protects the sample from excessive radiation damage. A related method, liquid secondary ionization mass spectrometry, LSIMS, is similar except that it uses somewhat more energetic cesium ions (10 keV to 30 keV).

In both methods, positive ions (by cation attachment ($[M + 1]^+$ or $[M + 23, Na]^+$) and negative ions (by

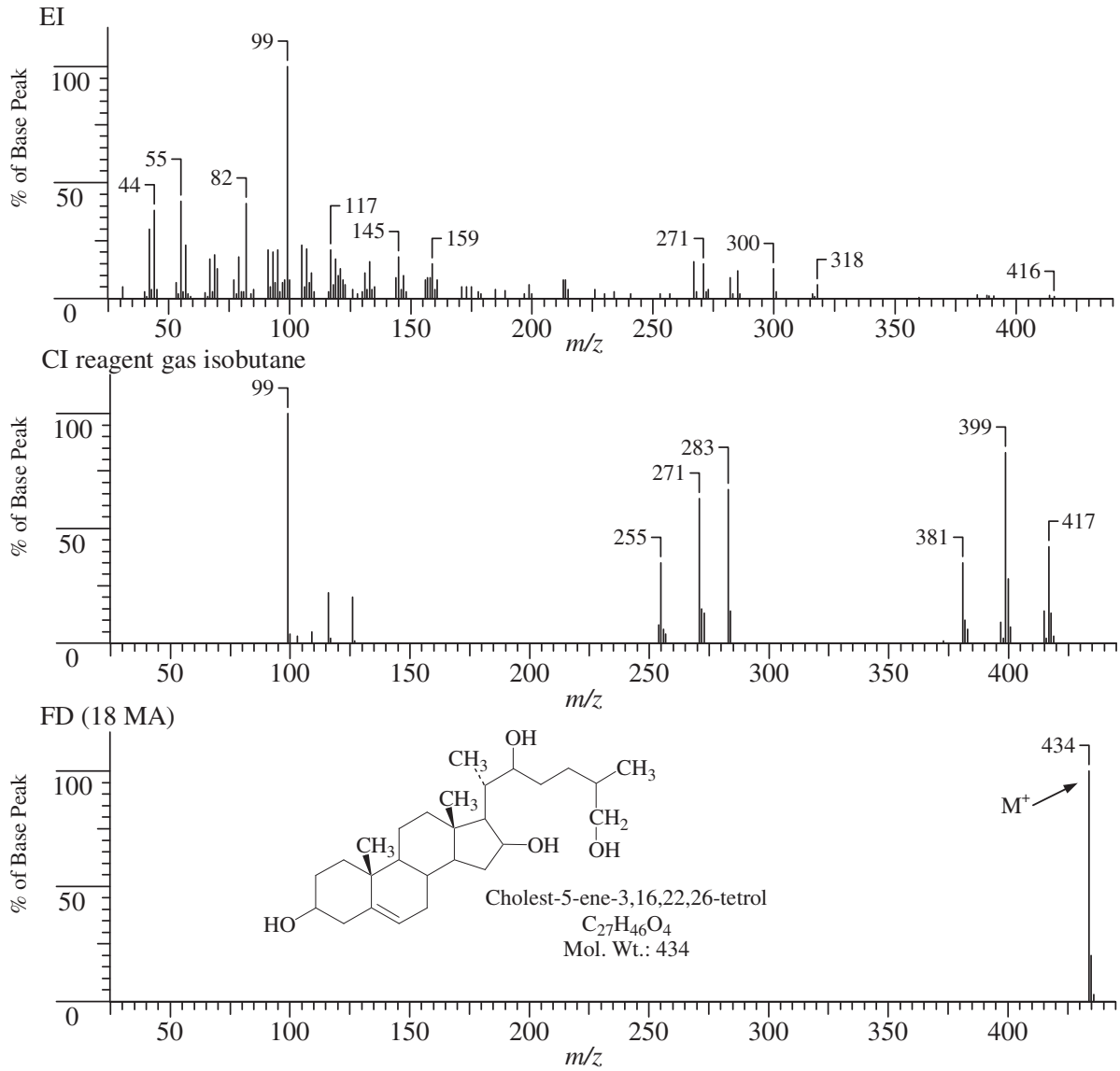

FIGURE 1.4 The electron impact (EI), chemical ionization (CI), and field desorption (FD) mass spectra of cholest-5-ene-3, 16, 22, 26-tetrol.

deprotonation $[M - 1]^-$) are formed; both types of ions are usually singly charged and, depending on the instrument, FAB can be used in high-resolution mode. FAB is used primarily with large nonvolatile molecules, particularly to determine molecular weight. For most classes of compounds, the rest of the spectrum is less useful, partially because the lower mass ranges may be composed of ions produced by the matrix itself. However, for certain classes of compounds that are composed of "building blocks," such as polysaccharides and peptides, some structural information may be obtained because fragmentation usually occurs at the glycosidic and peptide bonds, respectively, thereby affording a method of sequencing these classes of compounds.

The upper mass limit for FAB (and LSIMS) ionization is between 10 kDa and 20 kDa, and FAB is really most useful up to about 6 kDa. FAB is seen most often with double focusing magnetic sector instruments where it has a resolution of about 0.3 m/z over the entire mass range; FAB can, however, be used with most types of mass analyzers. The biggest drawback to using FAB is that the spectrum always shows a high level of matrix generated ions, which limit sensitivity and which may obscure important fragment ions.

1.3.2.3 Plasma Desorption Ionization. Plasma desorption ionization is a highly specialized technique used almost exclusively with a time-of-flight (TOF) mass analyzer (Section 1.4.4). The fission products from californium-252 (^{252}Cf), with energies in the range of 80 MeV to 100 MeV, are used to bombard and ionize the sample. Each time a ^{252}Cf splits, two particles are produced moving in opposite directions. One of the particles hits a triggering detector and signals a start time. The other particle strikes the sample matrix ejecting some sample ions into a time-of-flight mass spectrometer (TOF-MS). The sample ions

are most often released as singly, doubly, or triply protonated moieties. These ions are of fairly low energy so that structurally useful fragmentation is rarely observed and, for polysaccharides and polypeptides, sequencing information is not available. The mass accuracy of the method is limited by the TOF mass spectrometer. The technique is useful on compounds with molecular weights up to at least 45 kDa.

1.3.2.4 Laser Desorption Ionization. A pulsed laser beam can be used to ionize samples for mass spectrometry. Because this method of ionization is pulsed, it must be used with either a TOF or a Fourier transform mass spectrometer (Section 1.4.5). Two types of lasers have found widespread use: a CO_2 laser, which emits radiation in the far infrared region, and a frequency-quadrupled neodymium/yttrium-aluminum-garnet (Nd/YAG) laser, which emits radiation in the UV region at 266 nm. Without matrix assistance, the method is limited to low molecular weight molecules (<2 kDa).

The power of the method is greatly enhanced by using matrix assistance (matrix-assisted laser desorption ionization, or MALDI). Two matrix materials, 2,5-dihydroxybenzoic acid and sinapinic acid, which have absorption bands coinciding with the laser employed, have found widespread use and sample molecular weights of up to two to three hundred thousand Da have been successfully analyzed. A few picomoles of sample are mixed with the matrix compound followed by pulsed irradiation, which causes sample ions (usually singly charged monomers but occasionally multiply charged ions and dimers have been observed) to be ejected from the matrix into the mass spectrometer.

The ions have little excess energy and show little propensity to fragment. For this reason, the method is fairly useful for mixtures. MALDI is used most often with a TOF-MS or a Fourier transform mass spectrometer (FT-MS); both mass analyzers are capable of accurate mass measurement. As with other matrix-assisted methods, MALDI suffers from background interference from the matrix material, which is further exacerbated by matrix adduction. Thus, the assignment of a molecular ion of an unknown compound can be uncertain.

1.3.3 Evaporative Ionization Methods

There are two important methods in which ions or, less often, neutral compounds in solution (often containing formic acid) have their solvent molecules stripped by evaporation, with simultaneous ionization leaving behind the ions for mass analysis. Coupled with liquid chromatography instrumentation, these methods have become immensely popular.

1.3.3.1 Thermospray Mass Spectrometry. In the thermospray method, a solution of the sample is introduced into the mass spectrometer by means of a heated capillary tube. The tube nebulizes and partially vaporizes the solvent, forming a stream of fine droplets which enter the ion source. When the solvent completely evaporates, the sample ions can be mass analyzed. This method can handle high flow rates and buffers; it was an early solution to interfacing mass spectrometers with aqueous liquid chromatography. The method has largely been supplanted by electrospray.

1.3.3.2 Electrospray Mass Spectrometry. The electrospray (ES) ion source (Figure 1.5) is operated at or near atmospheric pressure and, thus is also called atmospheric pressure ionization or API. The sample in solution (usually a polar, volatile solvent) enters the ion source through a stainless steel capillary, which is surrounded by a co-axial flow of nitrogen, called the nebulizing gas. The tip of the capillary is maintained at a high potential with respect to a counter-electrode. The potential difference produces a field gradient of up to 5 kV/cm. As the solution exits the capillary, an aerosol of charged droplets forms. The flow of nebulizing gas directs the effluent toward the mass spectrometer.

Droplets in the aerosol shrink as the solvent evaporates, thereby concentrating the charged sample ions. When

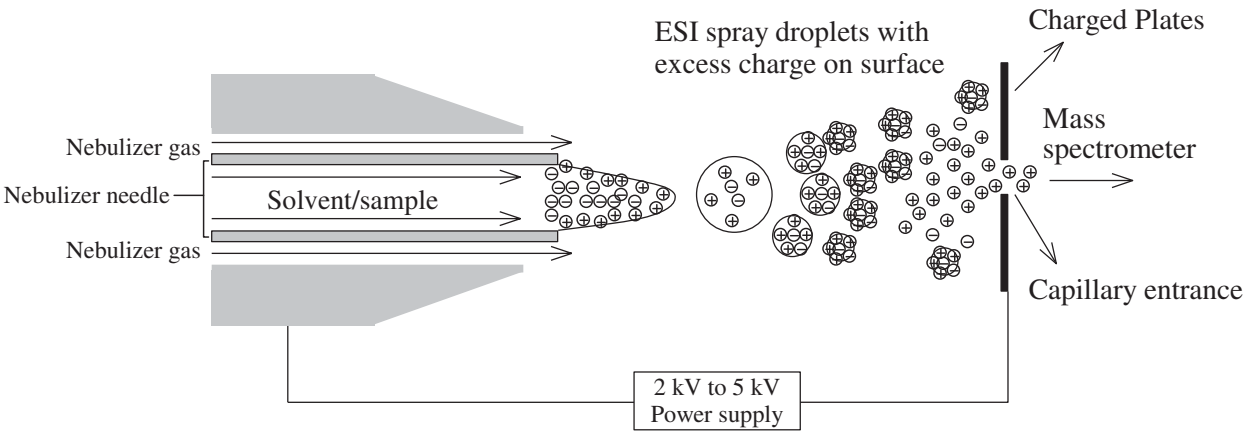

FIGURE 1.5 A diagram showing the evaporation of solvent leading to individual ions in an electrospray instrument.

the electrostatic repulsion among the charged sample ions reaches a critical point, the droplet undergoes a so-called Coulombic explosion, which releases the sample ions into the vapor phase. The vapor phase ions are focused with a number of sampling orifices into the mass analyzer.

Electrospray MS has undergone an explosion of activity since about 1990, mainly for compounds that have multiple charge-bearing sites. With proteins, for example, ions with multiple charges are formed. Since the mass spectrometer measures mass to charge ratio (m/z) rather than mass directly, these multiply charged ions are recorded at apparent mass values of $\frac{1}{2}, \frac{1}{3}, \ldots \frac{1}{n}$ of their actual masses, where n is the number of charges (z). Large proteins can have 40 or more charges so that molecules of up to 100 kDa can be detected in the range of conventional quadrupole, ion trap, or magnetic sector mass spectrometers. The appearance of the spectrum is a series of peaks increasing in mass, which correspond to pseudomolecular ions possessing sequentially one less proton and therefore one less charge.

Determination of the actual mass of the ion requires that the charge of the ion be known. If two peaks, which differ by a single charge, can be identified, the calculation is reduced to simple algebra. Recall that each ion of the sample molecule (M_s) has the general form $(M_s + zH)^{z+}$ where H is the mass of a proton (1.0079 Da). For two ions differing by one charge, $m_1 = [M_s + (z+1)H]/(z+1)$ and $m_2 = [(M_s + zH)/z]$. Solving the two simultaneous equations for the charge z, yields $z = (m_1 - H)/(m_2 - m_1)$. A simple computer program automates this calculation for every peak in the spectrum and calculates the mass directly.

Many manufacturers have introduced inexpensive mass spectrometers dedicated to electrospray for two reasons. First, the method has been very successful while remaining a fairly simple method to employ. Second, the analysis of proteins and smaller peptides has grown in importance, and they are probably analyzed best by the electrospray method.

Figure 1.6 compares the EI mass spectrum (lower portion of the figure) of lactose to its ES mass spectrum (upper portion of figure). Lactose is considered in more detail in Chapter 5. The EI mass spectrum is completely useless because lactose has low vapor pressure, it is thermally labile, and the spectrum shows no characteristic peaks. The ES mass spectrum shows a weak molecular ion peak at m/z 342 and a characteristic $[M + 23]^+$ peak, the molecular ion peak plus sodium. Because sodium ions are ubiquitous in aqueous solution, these sodium adducts are very common.

The ES mass spectrum of a tetra peptide comprised of valine, glycine, serine, and glutamic acid (VGSE) is given in Figure 1.7. VGSE is also an example compound in Chapter 5. The base beak is the $[M + 1]^+$ ion at m/z 391 and the sodium adduct, $[M + 23]^+$, is nearly 90% of the base peak. In addition, there is some useful fragmentation information characteristic of each of the amino acids. For small peptides, it is not uncommon to find some helpful fragmentation, but for proteins it is less likely.

Methods of ionization are summarized in Table 1.1.

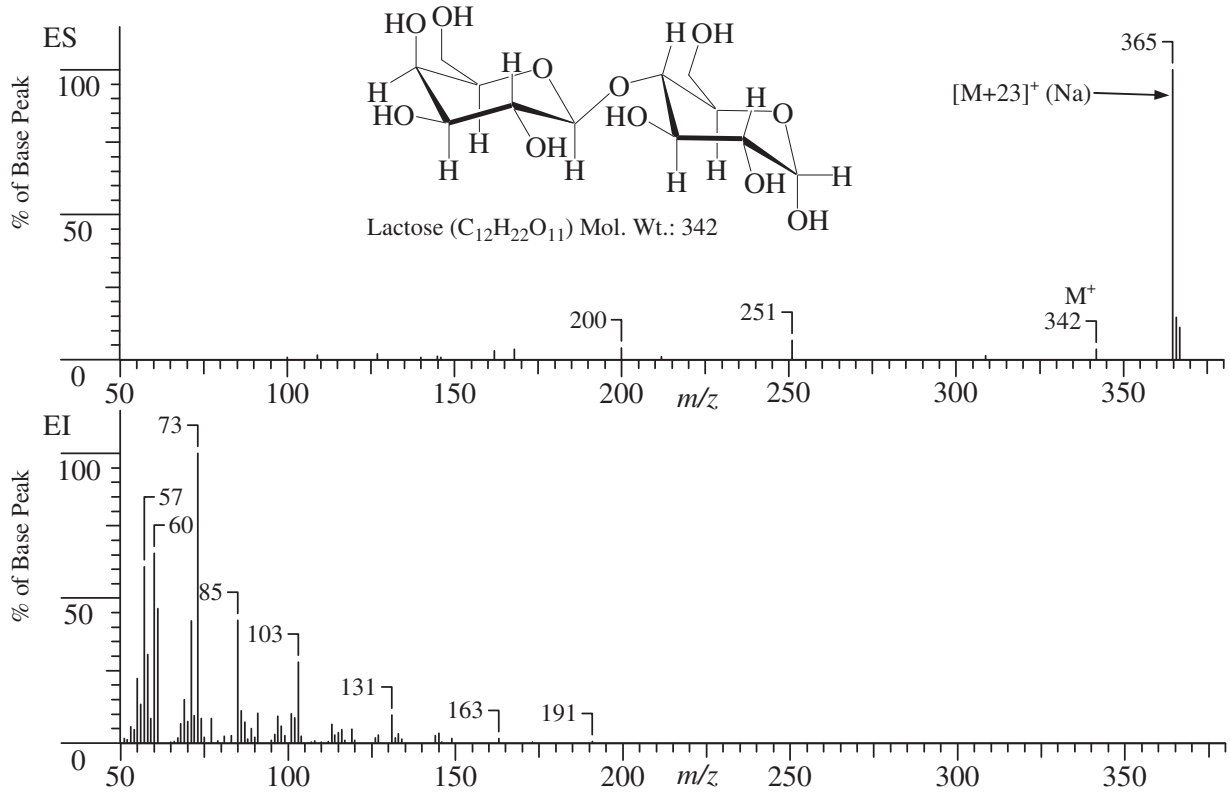

FIGURE 1.6 The EI and ES mass spectra of lactose.

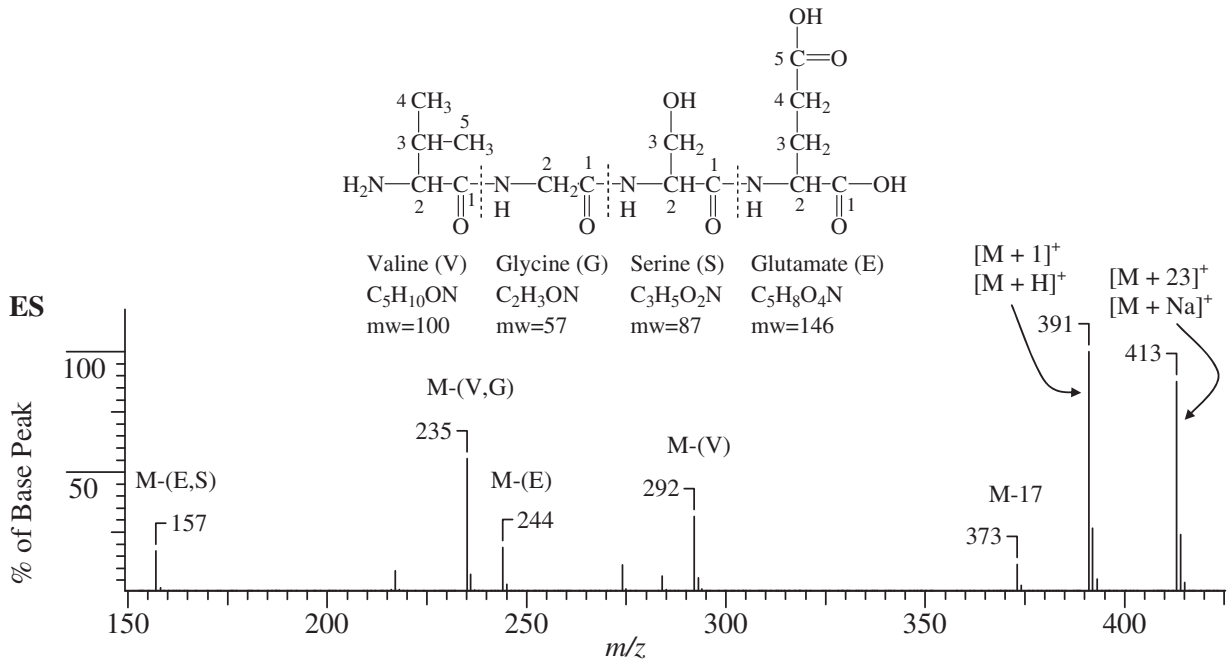

FIGURE 1.7 The electrospray (ES) mass spectrum for the tetra peptide whose structure is given in the figure. See text for explanation.

TABLE 1.1 Summary of Ionization Methods

Ionization Method	Ions Formed	Sensitivity	Advantage	Disadvantage
Electron impact	M^+	ng – pg	Data base searchable Structural information	M^+ occasionally absent
Chemical ionization	M + 1, M + 18, etc.	ng – pg	M^+ usually present	Little structural information
Field desorption	M^+	μg – ng	Nonvolatile compounds	Specialized equipment
Fast atom bombardment	M + 1, M + cation M + matrix	μg – ng	Nonvolatile compounds Sequencing information	Matrix interference Difficult to interpret
Plasma desorption	M+	μg – ng	Nonvolatile compounds	Matrix interference
Laser desorption	M + 1, M + matrix	μg – ng	Nonvolatile compounds Burst of ions	Matrix interference
Thermospray	M^+	μg – ng	Nonvolatile compounds	Outdated
Electrospray	M^+, M^{++}, M^{+++}, etc.	ng – pg	Nonvolatile compounds interfaces w/LC Forms multiply charged ions	Limited classes of compounds Little structural information

1.4 MASS ANALYZERS

The mass analyzer, which separates the mixture of ions that is generated during the ionization step by m/z in order to obtain a spectrum, is the heart of each mass spectrometer, and there are several different types with different characteristics. Each of the major types of mass analyzers is described below. This section concludes with a brief discussion of tandem MS and related processes.

1.4.1 Magnetic Sector Mass Spectrometers

Mass spectrometers were originally developed in the early twentieth century; the 1922 Nobel Prize in chemistry was awarded partly for the development of the mass spectrograph. All of the early instruments were of the magnetic sector type. The magnetic sector mass spectrometer uses a magnetic field to deflect moving ions around a curved path (see Figure 1.8). Even though magnetic sector mass spectrometers were the first commercially available instruments, they remain important today. Separation of ions occurs based on the mass/charge ratio, with lighter ions deflected to a greater extent than the heavier ions. Resolution depends on each ion entering the magnetic field (from the source) with the same kinetic energy, accomplished by accelerating the ions (which have a charge z) with a voltage V. Each ion acquires kinetic energy $E = zV = mv^2/2$. When an accelerated ion enters the magnetic field (B), it experiences a deflecting force (Bzv), which bends the path of the ion orthogonal to its original

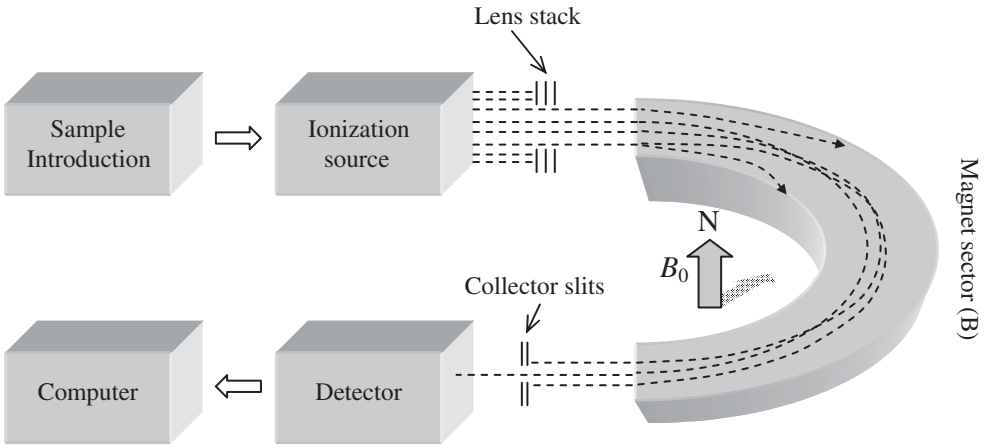

FIGURE 1.8 Schematic diagram of a single focusing, 180° sector mass analyzer. The magnetic field is perpendicular to the page. The radius of curvature varies from one instrument to another.

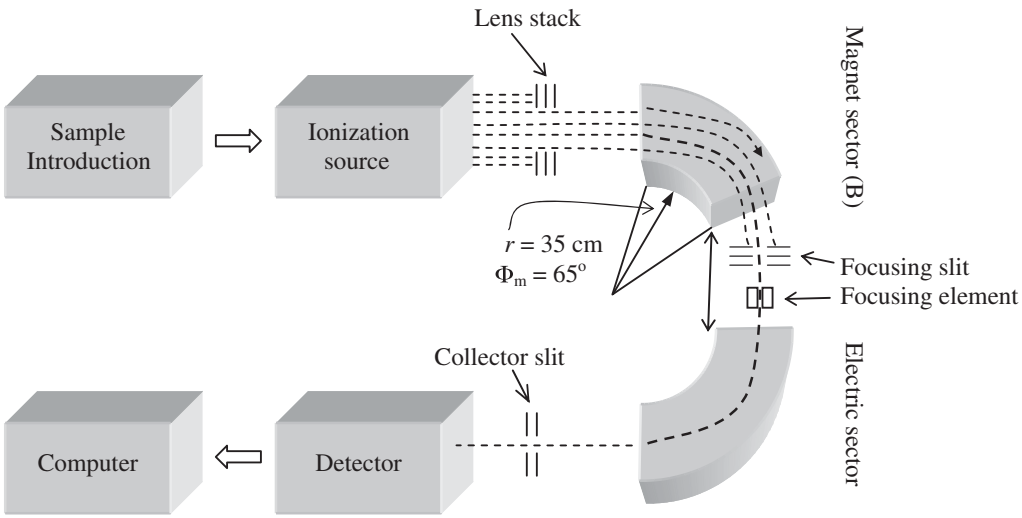

FIGURE 1.9 Schematic of double-focusing mass spectrometer.

direction. The ion is now traveling in a circular path of radius r, given by $Bzv = mv^2/r$. The two equations can be combined to give the familiar magnetic sector equation: $m/z = B^2r^2/2V$. Because the radius of the instrument is fixed, the magnetic field is scanned to bring the ions of different m/z sequentially into focus. As these equations show, a magnetic sector instrument separates ions on the basis of momentum, which is the product of mass and velocity, rather than mass alone; therefore, ions of the same mass but different energies will come into focus at different points.

An electrostatic analyzer (ESA) can greatly reduce the energy distribution of an ion beam by forcing ions of the same charge (z) and kinetic energy (regardless of mass) to follow the same path. A slit at the exit of the ESA further focuses the ion beam before it enters the detector. The combination of an ESA and a magnetic sector is known as double focusing because the two fields counteract the dispersive effects each has on direction and velocity.

The resolution of a double-focusing magnetic sector instrument (Figure 1.9) can be as high as 100000 through the use of extremely small slit widths. This very high resolution allows the measurement of "exact masses," which unequivocally provide molecular formulas and is enormously useful. By comparison, slits allowing an energy distribution for about 5000 resolution give at least 0.5 m/z accuracy across the entire mass range, that is, the "unit resolution" that is used in a standard mass spectrometer. The upper mass limit for commercial magnetic sector instruments is about m/z 15000. Raising this upper limit is theoretically possible but impractical.

1.4.2 Quadrupole Mass Spectrometers

The quadrupole mass analyzer (sometimes abbreviated QMF for quadrupole mass filter), also known as the transmission quadrupole, is much smaller and cheaper than a magnetic

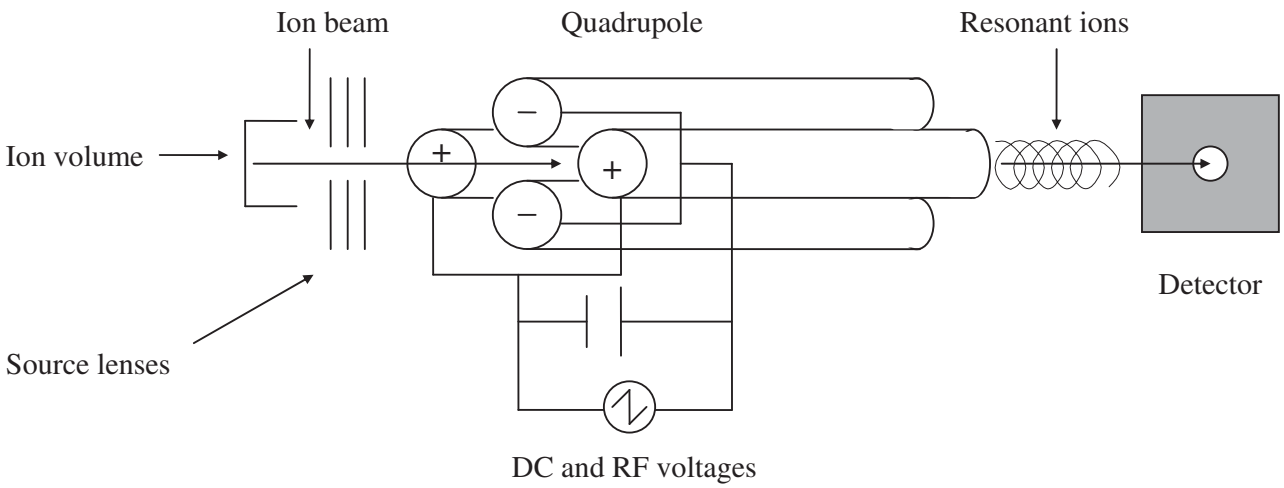

FIGURE 1.10 Schematic representation of a quadrupole "mass filter" or ion separator.

sector instrument. A quadrupole setup (seen schematically in Figure 1.10) consists of four cylindrical (or of hyperbolic cross-section) rods (100 mm to 200 mm long) mounted parallel to each other, at the corners of a square. A complete mathematical analysis of the quadrupole mass analyzer is complex, but we can discuss how it works in a simplified form. This nonmagnetic mass analyzer uses a constant DC voltage, which is modified by a radiofrequency voltage, applied to the rods. Ions are introduced to the "tunnel" formed by the four rods of the quadrupole in the center of the square at one end to the rods and travel down the axis.

For any given combination of DC voltage and modified voltage applied at the appropriate frequency (always at a constant ratio), only ions with a certain m/z value possess a stable trajectory and therefore are able to pass all the way to the end of the quadrupole to the detector. All ions with different m/z values travel unstable or erratic paths and collide with one of the rods or pass outside the quadrupole. An easy way to look at the quadrupole mass analyzer is as a tunable mass filter. In other words, as the ions enter at one end, only one m/z ion will pass through. In practice, the filtering can be carried out at a very fast rate so that the entire mass range can be scanned in considerably less than 1 second.

The development of the QMF forever changed mass spectrometry. Lower cost and ease-of-use led to "benchtop" instruments, which in turn led to everyday use by chemists and technicians. Also, the very fast scan times enabled the coupling of the quadrupole mass spectrometer with the gas chromatograph.

With respect to resolution and mass range, the quadrupole is generally inferior to the magnetic sector. For instance, the current upper mass range is generally less than 5000 m/z. On the other hand, sensitivity is generally high because there is no need for resolving slits, which would remove a portion of the ions. An important advantage of quadrupoles is that they operate most efficiently on ions of low velocity, which means that their ion sources can operate close to ground potential (i.e., low voltage). Since the entering ions generally have energies of less than 100 eV, the quadrupole mass spectrometer is ideal for interfacing to LC systems and for atmospheric pressure ionization (API) techniques such as electrospray (see Section 1.3.3.2). These techniques work best on ions of low energy so that fewer high-energy collisions will occur before they enter the quadrupole.

1.4.3 Ion Trap Mass Spectrometer

The ion trap, also known as the quadrupole ion trap, is sometimes considered as a variant of the quadrupole, since it resulted as a direct outgrowth of quadrupole research. However, the ion trap is much more versatile and clearly has greater potential for development. At one time the ion trap had a bad reputation because the earliest versions gave inferior results compared to quadrupoles. These problems have been overcome and the EI spectra obtained with an ion trap are now fully searchable with commercial databases. Furthermore, the ion trap is more sensitive than the quadrupole arrangement, and the ion trap is routinely configured to carry out tandem experiments with no extra hardware needed.

In one sense, an ion trap is aptly named because, unlike the quadrupole, which merely acts as a mass filter, the ion trap literally "traps" ions for relatively long periods of time, with important consequences. The simplest use of the trapped ions is to sequentially eject them to a detector, producing a conventional mass spectrum. Before other uses of trapped ions are briefly described, a closer look at the ion trap itself will be helpful.

The ion trap generally consists of three electrodes (hence, it is often called a 3D quadrupole ion trap or 3D QIT): one ring electrode with a hyperbolic inner surface, and two hyperbolic endcap electrodes at either end (a cross section of an ion trap is found in Figure 1.11). The ring electrode is operated with a sinusoidal radiofrequency field while the endcap electrodes are operated in one of three modes. The endcap may be operated at ground potential, or with either a DC or an AC voltage.

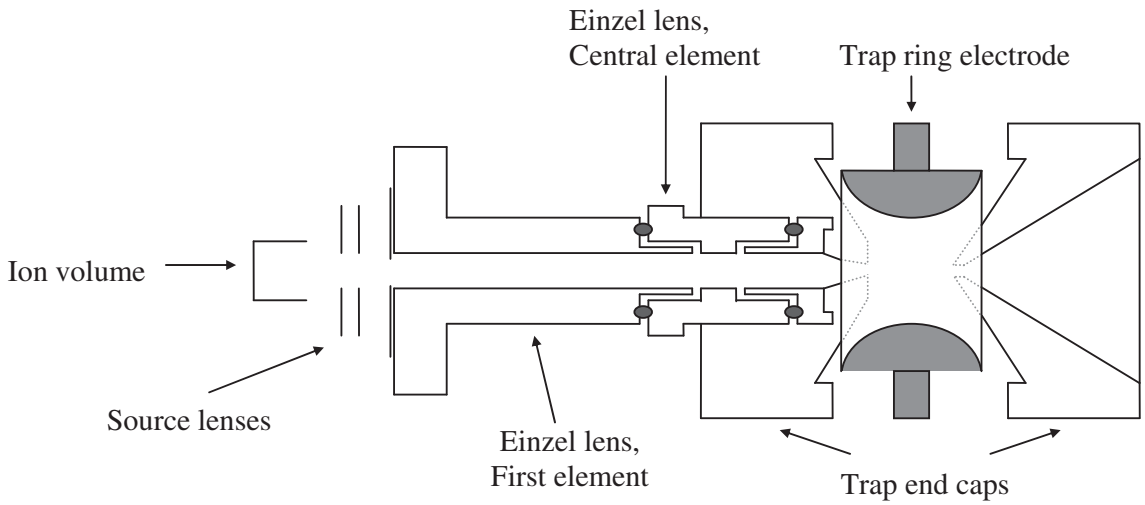

FIGURE 1.11 Cross-sectional view of an ion trap.

The mathematics that describes the motion of ions within the ion trap are given by the Mathieu equation. Details and discussions of three-dimensional ion stability diagrams can be found in either March and Hughes (1989) or Nourse and Cooks (1990). The beauty of the ion trap is that by controlling the three parameters of RF voltage, AC voltage, and DC voltage, a wide variety of experiments can be run quite easily (for details see March and Hughes, 1989).

There are three basic modes in which the ion trap can be operated. First, when the ion trap is operated with a fixed RF voltage and no DC bias between the endcap and ring electrodes, all ions above a certain cutoff m/z ratio will be trapped. As the RF voltage is raised, the cutoff m/z is increased in a controlled manner and the ions are sequentially ejected and detected. The result is the standard mass spectrum and this procedure is called the "mass-selective instability" mode of operation. The maximum RF potential that can be applied between the electrodes limits the upper mass range in this mode. Ions of mass contained beyond the upper limit are removed after the RF potential is brought back to zero.

The second mode of operation uses a DC potential across the endcaps; the general result is that there is now both a low- and high-end cutoff (m/z) of ions. The possibilities of experiments in this mode of operation are tremendous, and most operations with the ion trap use this mode. As few as one ion mass can be selected. Selective ion monitoring is an important use of this mode of operation. There is no practical limit on the number of ionic masses that can be selected.

The third mode of operation is similar to the second, with the addition of an auxiliary oscillatory field between the endcap electrodes, which results in adding kinetic energy selectively to a particular ion. With a small amplitude auxiliary field, selected ions gain kinetic energy slowly, during which time they usually undergo a fragmenting collision; the result can be a nearly 100% MS-MS efficiency. If the inherent sensitivity of the ion trap is considered along with the nearly 100% tandem efficiency, the use of the ion trap for the tandem MS experiment greatly outshines the so-called triple quad (see below).

Another way to use this kinetic energy addition mode is to selectively reject unwanted ions from the ion trap. These could be ions derived from solvent or from the matrix in FAB or LSIMS experiments. A constant frequency field at high voltage during the ionization period will selectively reject a single ion. Multiple ions can also be selected in this mode.

1.4.4 Time-of-Flight Mass Spectrometer

The concept of time-of-flight (TOF) mass spectrometers is simple. Ions are accelerated through a potential (V) and are then allowed to "drift" down a tube to a detector. If the assumption is made that all of the ions arriving at the beginning of the drift tube have the same energy given by $zeV = mv^2/2$, then ions of different mass will have different velocities: $v = (2zeV/m)^{\frac{1}{2}}$. If a spectrometer possesses a drift tube of length L, the time of flight for an ion is given by: $t = (L^2 m/2zeV)^{\frac{1}{2}}$, from which the mass for a given ion can be easily calculated.

The critical aspect of this otherwise simple instrument is the need to produce the ions at an accurately known start time and position. These constraints generally limit TOF spectrometers to use pulsed ionization techniques, which include plasma and laser desorption (e.g., MALDI, matrix assisted laser desorption ionization).

The resolution of TOF instruments is usually less than 20000 because some variation in ion energy is unavoidable. Also, since the difference in arrival times at the detector can be less than 10^{-7} seconds, fast electronics are necessary for adequate resolution. On the positive side, the mass range of these instruments is unlimited, and, like quadrupoles, they have excellent sensitivity due to lack of resolving slits. Thus, the technique is most useful for large biomolecules.

1.4.5 Fourier Transform Mass Spectrometer

In a Fourier transform mass spectrometer (formerly called an ion cyclotron resonance mass spectrometer), ions are held in a cell with an electric trapping potential within a strong magnetic field. Within the cell, each ion orbits in a direction perpendicular to the magnetic field, with a frequency proportional to the ion's m/z value. A radiofrequency pulse applied to the cell brings all of the cycloidal frequencies into resonance simultaneously to yield an interferogram, conceptually similar to the free induction decay (FID) signal in NMR or the interferogram generated in FTIR experiments. The interferogram, which is a time domain spectrum, is Fourier transformed into a frequency domain spectrum, which then yields the conventional m/z spectrum. Pulsed Fourier transform methods applied to nuclear magnetic resonance spectroscopy are discussed in Chapters 3, 4, and 5.

Because the instrument is operated at fixed magnetic field strength, extremely high field superconducting magnets can be used. Also, because mass range is directly proportional to magnetic field strength, very high mass detection is possible. Finally, since all of the ions from a single ionization event can be trapped and analyzed, the method is very sensitive and works well with pulsed ionization methods. The most compelling aspect of the method is its high resolution, making FT mass spectrometers an attractive alternative to other mass analyzers. The FT mass spectrometer can be coupled to chromatographic instrumentation and various ionization methods, which means that it can be easily used with small molecules. Further information on FT mass spectrometers can be found in the book by Gross (1990).

1.4.6 Tandem Mass Spectrometry

Tandem mass spectrometry or MS-MS ("MS squared") is useful in studies with both known and unknown compounds; with certain ion traps, MS to the nth ($MS^{(n)}$) is possible where $n = 2$ to 9. In practice, n rarely exceeds 2 or 3. With MS-MS, a "parent" ion from the initial fragmentation (the initial fragmentation gives rise to the conventional mass spectrum) is selected and allowed or induced to fragment further thus giving rise to "daughter" ions. In complex mixtures, these daughter ions provide unequivocal evidence for the presence of a known compound. For unknown or new compounds, these daughter ions provide potential for further structural information.

One popular use of MS-MS involves ionizing a crude sample, selectively "fishing out" an ion characteristic for the compound under study and obtaining the diagnostic spectrum of the daughter ions produced from that ion. In this way, a compound can be unequivocally detected in a crude sample, with no prior chromatographic (or other separation steps) being required. Thus, MS-MS can be a very powerful screening tool. This type of analysis alleviates the need for complex separations of mixtures for many routine analyses. For instance, the analysis of urine samples from humans (or from other animals such as race horses) for the presence of drugs or drug metabolites can be carried out routinely on whole urine (i.e., no purification or separation) by MS-MS. For unknown compounds, these daughter ions can provide structural information as well.

One way to carry out MS-MS is to link two or more mass analyzers in series to produce an instrument capable of selecting a single ion, and examining how that ion (either a parent or daughter ion) fragments. For instance, three quadrupoles can be linked (a so-called triple quad) to produce a tandem mass spectrometer. In this arrangement, the first quadrupole selects a specific ion for further analysis, the second quadrupole functions as a collision cell (collision induced dissociation, CID) and is operated with radiofrequency only, and the third quadrupole separates the product ions to produce a spectrum of daughter ions. The field of tandem mass spectrometry is already rather mature with good books available (Benninghoven et al., 1987; Wilson et al., 1989).

In order for an instrument to carry out MS-MS, it must be able to do the three operations outlined above. As we have seen, however, ion-trap systems capable of MS-MS and $MS^{(n)}$ do not use a tandem arrangement of mass analyzers at all, but rather use a single ion trap for all three operations simultaneously. As has already been stated, these ion-trap tandem mass spectrometer experiments are very sensitive and are now user friendly. The ion trap brings the capability for carrying out MS-MS experiments to the benchtop at relatively low cost.

A summary of mass analyzers and ionization methods is displayed in Table 1.2.

1.5 INTERPRETATION OF EI MASS SPECTRA

Our discussion of interpreting mass spectra is limited to EI mass spectrometry. Fragmentation in EI mass spectra is rich with structural information; mastery of EI mass spectra is especially useful for the organic chemist.

EI mass spectra are routinely obtained at an electron beam energy of 70 eV. The desired and simplest event that occurs is the removal of a single electron from the molecule in the gas phase by an electron of the electron beam to form the molecular ion, which is a radical cation. For example, methanol forms a molecular ion in which the single dot represents the remaining odd electron as seen in Scheme 1.1. When the charge can be localized on one particular atom, the charge is shown on that atom:

$$CH_3OH + e^- \rightarrow CH_3OH^{+\cdot}(m/z\ 32) + 2e^-$$

(Sch 1.1)

Many of these molecular ions rapidly disintegrate in 10^{-10} seconds to 10^{-3} seconds to give, in the simplest

TABLE 1.2 Summary of Mass Analyzers

Mass Analyzer	Mass Range	Resolution	Sensitivity	Advantage	Disadvantage
Magnetic sector	1 – 15000 m/z	0.0001	Low	High resolution	Low sensitivity Very expensive High technical expertise
Quadrupole	1 – 5000 m/z	Unit	High	Easy to use Inexpensive High sensitivity	Low resolution Low mass range
Ion trap	1 – 5000 m/z	Unit	High	Easy to use Inexpensive High sensitivity Tandem MS (MS^n)	Low resolution Low mass range
Time of flight	Unlimited	0.0001	High	High mass range Simple design	Very high resolution
Fourier transform	Up to 70 kDa	0.0001	High	Very high resolution and mass range	Very expensive High technical expertise

case, a positively charged fragment ion and a radical. Many fragment ions are thus formed, and each of these can cleave to yield smaller fragments; examples of possible cleavages for methanol are given in Scheme 1.2.

$$CH_3OH^{\cdot+} \longrightarrow CH_2OH^+(m/z\ 31) + H^{\cdot}$$
$$CH_3OH^{\cdot+} \longrightarrow CH_3{}^+(m/z\ 15) + {}^{\cdot}OH$$
$$CH_2OH^+ \longrightarrow CHO^+(m/z\ 29) + H_2$$

(Sch 1.2)

If some of the molecular ions remain intact long enough to reach the detector, we see a molecular ion peak. It is important to recognize the molecular ion peak because this gives the molecular weight of the compound. With unit resolution, this weight is the molecular weight to the nearest whole number.

A mass spectrum is a presentation of the masses of the positively charged fragments (including the molecular ion) versus their relative abundances. The most intense peak in the spectrum, called the base peak, is assigned a value of 100%, and the intensities (height × sensitivity factor) of the other peaks, including the molecular ion peak, are reported as percentages of the base peak. Of course, the molecular ion peak may sometimes be the base peak. In Figure 1.1, the molecular ion peak is m/z 121, and the base peak is m/z 77.

A tabular or graphic presentation of a spectrum may be used. A graph has the advantage of presenting patterns that, with experience, can be quickly recognized. However, a graph must be drawn so that there is no difficulty in distinguishing mass units. Mistaking a peak at, say, m/z 79 for m/z 80 can result in total confusion. The molecular ion peak is usually the peak of highest mass number except for the isotope peaks.

1.5.1 Recognition of the Molecular Ion Peak

Quite often, under electron impact (EI), recognition of the molecular ion peak $(M)^+$ poses a problem. The peak may be very weak or it may not appear at all; how can we be sure that it is the molecular ion peak and not a fragment peak or an impurity? Often the best solution, if there is doubt, is to obtain a chemical ionization spectrum (see Section 1.3.1.2). The usual result is an intense peak at $[M + 1]^+$ and little fragmentation.

Many peaks can be ruled out as possible molecular ions simply on grounds of reasonable structure requirements. The nitrogen rule is often helpful. It states that a molecule of even-numbered molecular weight must contain either no nitrogen atoms or an even number of nitrogen atoms; an odd-numbered molecular weight requires an odd number of nitrogen atoms.* This rule holds for all compounds containing carbon, hydrogen, oxygen, nitrogen, sulfur, and the halogens, as well as many of the less usual atoms such as phosphorus, boron, silicon, arsenic, and the alkaline earths.

A useful corollary of the nitrogen rule states that fragmentation at a single bond gives an odd-numbered ion fragment from an even-numbered molecular ion, and an even-numbered ion fragment from an odd-numbered molecular ion. For this corollary to hold, the ion fragment must contain all of the nitrogen (if any) of the molecular ion.

Consideration of the breakdown pattern coupled with other information will also assist in identifying molecular ions. It should be kept in mind that Appendix A contains fragment formulas as well as molecular formulas. Some of the formulas may be discarded as trivial in attempts to solve a particular problem.

The intensity of the molecular ion peak depends on the stability of the molecular ion. The most stable molecular ions are those of purely aromatic systems. If substituents that have favorable modes of cleavage are present, the molecular ion peak will be less intense, and the fragment peaks relatively more intense. In general, the following group of compounds will, in order of decreasing ability, give prominent molecular ion peaks: aromatic compounds > conjugated alkenes >

*For the nitrogen rule to hold, only unit atomic masses (i.e., integers) are used in calculating the formula masses.

cyclic compounds > organic sulfides > short, normal alkanes > mercaptans. Recognizable molecular ions are usually produced for these compounds in order of decreasing ability: ketones > amines > esters > ethers > carboxylic acids ~ aldehydes ~ amides ~ halides. The molecular ion is frequently not detectable in aliphatic alcohols, nitrites, nitrates, nitro compounds, nitriles, and in highly branched compounds.

The presence of an M − 15 peak (loss of CH_3), or an M − 18 peak (loss of H_2O), or an M − 31 peak (loss of OCH_3 from methyl esters), and so on, is taken as confirmation of a molecular ion peak. An M − 1 peak is common, and occasionally an M − 2 peak (loss of H_2 by either fragmentation or thermolysis), or even a rare M − 3 peak (from alcohols) is reasonable. Peaks in the range of M − 3 to M − 14, however, indicate that contaminants may be present or that the presumed molecular ion peak is actually a fragment ion peak. Losses of fragments of masses of 19 to 25 are also unlikely (except for loss of F = 19 or HF = 20 from fluorinated compounds). Loss of 16 (O), 17 (OH), or 18 (H_2O) are likely only if an oxygen atom is in the molecule.

1.5.2 Determination of a Molecular Formula

1.5.2.1 Unit-Mass Molecular Ion and Isotope Peaks. So far, we have discussed the mass spectrum in terms of unit resolutions: The unit mass of the molecular ion of C_7H_7NO (Figure 1.1) is m/z 121—that is, the sum of the unit masses of the most abundant isotopes: $(7 \times 12$ [for $^{12}C]) + (7 \times 1$ [for $^{1}H]) + (1 \times 14$ [for $^{14}N] + (1 \times 16$ [for$^{16}O]) = 121$.

In addition, molecular species exist that contain the less abundant isotopes, and these give rise to the "isotope peaks" at M + 1, M + 2, etc. In Figure 1.1, the M + 1 peak is approximately 8% of the intensity of the molecular ion peak, which for this purpose, is assigned an intensity of 100%. Contributing to the M + 1 peak are the isotopes, ^{13}C, ^{2}H, ^{15}N, and ^{17}O. Table 1.3 gives the abundances of these isotopes relative to those of the most abundant isotopes. The only contributor to the M + 2 peak of C_7H_7NO is ^{18}O, whose relative abundance is very low (or a combination of two of the isotopes that contribute to the M + 1, for example, one ^{13}C and one ^{2}H); thus the M + 2 peak is undetected. If only C, H, N, O, F, P, and I are present, the approximate expected percentage (M + 1) and percentage (M + 2) intensities can be calculated by use of the following equations for a compound of formula $C_nH_mN_xO_y$ (note: F, P, and I are monoisotopic and do not contribute and can be ignored for the calculation):

$$\%\,(M+1) \approx (1.1 \cdot n) + (0.36 \cdot x) \text{ and } \%\,(M+2) \approx (1.1 \cdot n)^2/200 + (0.2 \cdot y)$$

If these isotope peaks are intense enough to be measured accurately, the above calculations may be useful in determining the molecular formula.*

If sulfur or silicon is present, the M + 2 peak will be more intense. In the case of a single sulfur atom, ^{34}S contributes approximately 4.40% to the M + 2 peak; for a single silicon in the molecule, ^{30}Si contributes about 3.35% to the M + 2 peak (see Section 1.6.15). A single chlorine atom results in a contribution of 32.50% to the M + 2 peak, while a single bromine atom contributes 98.00% to the M + 2 isotope peak. The effect of several bromine and chlorine atoms is described in Section 1.6.16. Note the appearance of additional isotope peaks in the case of multiple bromine and chlorine atoms. Obviously the mass spectrum should be routinely scanned for the relative intensities of the M + 2, M + 4, and higher isotope peaks, and the relative intensities should be carefully measured. Since F, P, and I are monoisotopic, they can be difficult to spot.

For most of the Problems in this text, the unit-resolution molecular ion, used in conjunction with IR and NMR, will suffice for determining the molecular formula by browsing

*There are limitations beyond the difficulty of measuring small peaks: The $^{13}C/^{12}C$ ratio differs with the source of the compound—synthetic compared with a natural source. A natural product from different organisms or regions may show differences. Furthermore, isotope peaks may be more intense than the calculated value because of ion – molecule interactions that vary with the sample concentration or with the class of compound involved.

TABLE 1.3 Relative Isotopic Abundances of Common Elements

Element	Isotope	Relative Abundance	Isotope	Relative Abundance	Isotope	Relative Abundance
Carbon	^{12}C	100	^{13}C	1.11		
Hydrogen	^{1}H	100	^{2}H	0.016		
Nitrogen	^{14}N	100	^{15}N	0.38		
Oxygen	^{16}O	100	^{17}O	0.04	^{18}O	0.2
Fluorine	^{19}F	100				
Silicon	^{28}Si	100	^{29}Si	5.1	^{30}Si	3.35
Phosphorus	^{31}P	100				
Sulfur	^{32}S	100	^{33}S	0.78	^{34}S	4.4
Chlorine	^{35}Cl	100			^{37}Cl	32.5
Bromine	^{79}Br	100			^{81}Br	98
Iodine	^{127}I	100				

Appendix A. For several more difficult Problems, the high-resolution formula masses—for use with Appendix A (see Section 1.5.2.2)—have been supplied.

Table 1.3 lists the principal stable isotopes of the common elements and their relative abundance calculated on the basis of 100 molecules containing the most common isotope. Note that this presentation differs from many isotopic abundance tables, in which the sum of all the isotopes of an element adds up to 100%.

1.5.2.2 High-Resolution Molecular Ion. A unique molecular formula (or fragment formula) can often be derived from a sufficiently accurate mass measurement alone (high-resolution mass spectrometry). This is possible because the nuclide masses are not integers (see Table 1.4). For example, we can distinguish at a unit mass of 28 among CO, N_2, CH_2N, and C_2H_4. The exact mass of CO is: 12.0000 (for ^{12}C) + 15.9949 (for ^{16}O) = 27.9949; the exact mass of N_2 is: 2×14.0031 (for ^{14}N) = 28.0062. Similar calculations give an exact mass of 28.0187 for CH_2N and 28.0312 for C_2H_4.

Thus, the mass observed for the molecular ion of CO, for example, is the sum of the exact formula masses of the most abundant isotope of carbon and of oxygen. This differs from a molecular weight of CO based on atomic weights that are the average of weights of all natural isotopes of an element (e.g., C = 12.01, O = 15.999).

Table 1.4 gives the masses to four or five decimal places for the common naturally occurring isotopes; it also gives the familiar atomic weights (average weights for the elements).

TABLE 1.4 Exact Masses of Isotopes

Element	Atomic Weight	Nuclide	Mass
Hydrogen	1.00794	^{1}H	1.00783
		D(^{2}H)	2.01410
Carbon	12.01115	^{12}C	12.00000 (std)
		^{13}C	13.00336
Nitrogen	14.0067	^{14}N	14.0031
		^{15}N	15.0001
Oxygen	15.9994	^{16}O	15.9949
		^{17}O	16.9991
		^{18}O	17.9992
Fluorine	18.9984	^{19}F	18.9984
Silicon	28.0855	^{28}Si	27.9769
		^{29}Si	28.9765
		^{30}Si	29.9738
Phosphorus	30.9738	^{31}P	30.9738
Sulfur	32.0660	^{32}S	31.9721
		^{33}S	32.9715
		^{34}S	33.9679
Chlorine	35.4527	^{35}Cl	34.9689
		^{37}Cl	36.9659
Bromine	79.9094	^{79}Br	78.9183
		^{81}Br	80.9163
Iodine	126.9045	^{127}I	126.9045

Appendix A lists molecular and fragment formulas in order of the unit masses. Under each unit mass, the formulas are listed in order of the standard *Chemical Abstract* system. The calculated formula mass (FM) to four decimal places is given for each formula. Appendix A is designed for browsing, on the assumption that the student has a unit molecular mass from a unit-resolution mass spectrometer and clues from other spectra. Note that the table includes only C, H, N, and O.

1.5.3 Use of the Molecular Formula. Index of Hydrogen Deficiency

If organic chemists had to choose a single item of information above all others that are usually available from spectra or from chemical manipulations, they would certainly choose the molecular formula.

In addition to the kinds and numbers of atoms, the molecular formula gives the index of hydrogen deficiency. The index of hydrogen deficiency is the number of *pairs* of hydrogen atoms that must be removed from the corresponding "saturated" formula to produce the molecular formula of the compound of interest. The index of hydrogen deficiency is also called the number of "sites (or degrees) of unsaturation"; this description is incomplete since hydrogen deficiency can result from cyclic structures as well as from multiple bonds. The index is thus the sum of the number of rings, the number of double bonds, and twice the number of triple bonds.

The index of hydrogen deficiency can be calculated for compounds containing carbon, hydrogen, nitrogen, halogen, oxygen, and sulfur having the generalized molecular formula, $C_nH_mX_xN_yO_z$, from the equation

$$\text{Index} = (n) - (m/2) - (x/2) + (y/2) + 1$$

Thus, the compound C_7H_7NO has an index of $7 - 3.5 + 0.5 + 1 = 5$. Note that divalent atoms (oxygen and sulfur) are not counted in the formula.

For the generalized molecular formula $\alpha_I\beta_{II}\gamma_{III}\delta_{IV}$, the index is given by (IV) − (I/2) + (III/2) + 1, where α is H, D, or halogen (i.e., any monovalent atom), β is O, S, or any other bivalent atom, γ is N, P, or any other trivalent atom, and δ is C, Si, or any other tetravalent atom. The numerals I – IV designate the numbers of the mono-, di-, tri-, and tetravalent atoms, respectively.

For simple molecular formulas, we can arrive at the index by comparison of the formula of interest with the molecular formula of the corresponding saturated compound. Compare C_6H_6 and C_6H_{14}; the index is 4 for the former and 0 for the latter.

The index for C_7H_7NO is 5, and a possible structure is benzamide (see Figure 1.1). Of course, other isomers (i.e., compounds with the same molecular formula) are possible, such as

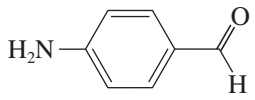

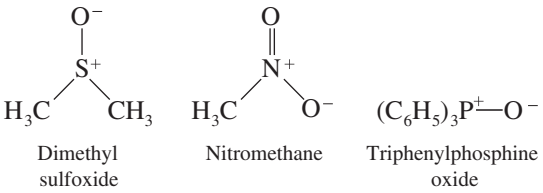

FIGURE 1.12 "Polar" Lewis structures of dimethyl sulfoxide, nitromethane, and triphenylphosphine oxide that correctly account for the index of hydrogen deficiency.

Note that the benzene ring itself accounts for four sites of unsaturation: three for the double bonds and one for the ring.

"Polar" structures must be used for compounds containing an atom in a higher valence state, such as sulfur or phosphorus. Thus, if we treat sulfur in dimethyl sulfoxide (DMSO) formally as a divalent atom, the calculated index, 0, is compatible with the structure in Figure 1.12. We must use only formulas with filled valence shells; that is, the Lewis octet rule must be obeyed.

Similarly, if we treat the nitrogen in nitromethane as a trivalent atom, the index is 1, which is compatible with Figure 1.12. If we treat phosphorus in triphenylphosphine oxide as trivalent, the index is 12, which fits the Lewis structure in Figure 1.12. As an example, let us consider the molecular formula $C_{13}H_9N_2O_4BrS$. The index of hydrogen deficiency would be $13 - \frac{10}{2} + \frac{2}{2} + 1 = 10$ and a consistent structure would be

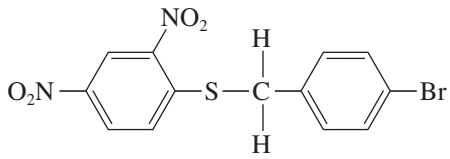

(Index of hydrogen deficiency = 4 per benzene ring and 1 per NO_2 group.)

The formula above for the index can be applied to fragment ions as well as to the molecular ion. When it is applied to even-electron (all electrons paired) ions, the result is always an odd multiple of 0.5. As an example, consider $C_7H_5O^+$ with an index of 5.5. A reasonable structure is

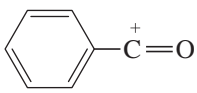

since 5.5 pairs of hydrogen atoms would be necessary to obtain the corresponding saturated formula $C_7H_{16}O$ ($C_nH_{2n+2}O$). Odd-electron fragment ions will always give integer values of the index.

Such simple considerations give the chemist very ready information about structure. As another example, a compound containing a single oxygen atom might quickly be determined to be an ether or a carbonyl compound simply by the degree of hydrogen deficiency. Much of the potential structural information is readily confirmed with information from IR and NMR spectra (See Chapters 2, 3, and 4).

1.5.4 Fragmentation

As a first impression, fragmenting a molecule with a huge excess of energy would seem a brute-force approach to molecular structure. The rationalizations used to correlate spectral patterns with structure, however, can only be described as elegant, though sometimes arbitrary. The insight of such pioneers as McLafferty, Beynon, Stenhagen, Ryhage, and Meyerson led to a number of rational mechanisms for fragmentation. These were masterfully summarized and elaborated by Biemann (1962), Budzikiewicz et al. (1967), and others.

Generally, the tendency is to represent the molecular ion with a localized charge. The approach of Budzikiewicz et al. (1967) is to localize the positive charge on either a π bond (except in conjugated systems), or on a heteroatom. Whether or not this concept is totally rigorous, it is, at the least, a pedagogic *tour de force*. We shall use such locally charged molecular ions in this book.

Structures **A**, **B**, and **C** in Figure 1.13, for example, represent the molecular ion of cyclohexadiene. Compound **A** is a delocalized structure with one less electron than the original uncharged diene; both the electron and the positive charge are delocalized over the π system. Since the electron removed to form the molecular ion is a π electron, other structures, such as **B** or **C** (resonance structures) can be used. Structures such as **B** and **C** localize the electron and the positive charge and thus are useful for describing fragmentation processes.

Fragmentation is initiated by electron impact. Only a small part of the driving force for fragmentation is energy transferred as the result of the impact. The major driving force is the cation-radical character that is imposed upon the structure.

Fragmentation of the odd-electron molecular ion (radical-cation, $M^{\cdot+}$) may occur by homolytic or heterolytic cleavage of a single bond. In homolytic cleavage (Scheme 1.3, ***I***) each electron moves independently as shown by a (single-barbed) fishhook: the fragments are an even-electron cation and a free radical (odd electron). To prevent clutter, only one of each pair of fishhooks need to be shown (Scheme 1.3, ***II***). In heterolytic cleavage, a pair of electrons move together

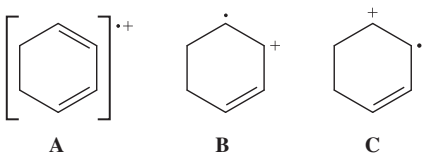

FIGURE 1.13 Different representations of the radical cation of cyclohexadiene.

toward the charged site as shown by the conventional curved arrow; the fragments are again an even-electron cation and a radical, but here the final charge site is on the alkyl product (Scheme 1.3, ***III***).

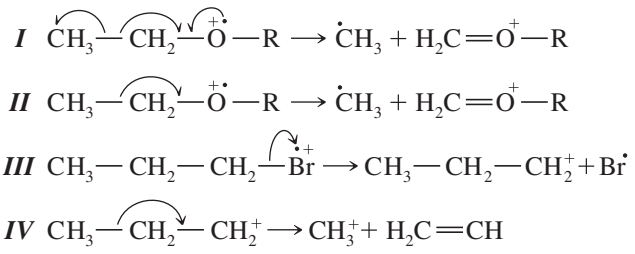

(Sch 1.3)

In the absence of rings (whose fragmentation requires cleavage of two or more bonds), most of the prominent fragments in a mass spectrum are even-electron cations formed as above by a single cleavage. Further fragmentation of an even-electron cation usually results in another even-electron cation and an even-electron neutral molecule or fragment (Scheme 1.3, ***IV***).

Simultaneous or consecutive cleavage of several bonds may occur when energy benefits accrue from formation of a highly stabilized cation and/or a stable radical, or a neutral molecule, often through a well-defined low-energy pathway. These are treated in Section 1.5.5 (rearrangements) and in Section 1.6 under individual chemical classes.

The probability of cleavage of a particular bond is related to the bond strength, to the possibility of low energy transitions, and to the stability of the fragments, both charged and uncharged, formed in the fragmentation process. Our knowledge of pyrolytic cleavages can be used, to some extent, to predict likely modes of cleavage of the molecular ion. Because of the extremely low pressure in the mass spectrometer, there are very few fragment collisions; we are dealing largely with unimolecular decompositions. This assumption, backed by a large collection of reference spectra, is the basis for the vast amount of information available from the fragmentation pattern of a molecule. Whereas conventional organic chemistry deals with reactions initiated by chemical reagents, by thermal energy, or by light, mass spectrometry is concerned with the consequences suffered by an organic molecule at a vapor pressure of about 10^{-6} mm Hg struck by an ionizing electron beam.

A number of general guidelines for predicting prominent peaks in EI spectra can be written and rationalized by using standard concepts of physical organic chemistry:

1. The relative intensity of the molecular ion peak is greatest for the straight-chain compound and decreases as the degree of branching increases (see rule 3).

2. The relative intensity of the molecular ion peak usually decreases with increasing molecular weight in a homologous series. Fatty esters appear to be an exception.

3. Cleavage is favored at alkyl-substituted carbon atoms: the more substituted, the more likely is cleavage. This is a consequence of the increased stability of a tertiary carbocation over a secondary, which in turn is more stable than a primary. Generally, the largest substituent at a branch is eliminated most readily as a radical, presumably because a long-chain radical can achieve some stability by delocalization of the lone electron.

Cation stability order:

$$CH_3^+ < R_2CH_2^+ < R_3CH^+ < R_3C^+$$

4. Double bonds, cyclic structures, and especially aromatic (or heteroaromatic) rings stabilize the molecular ion and thus increase the probability of its appearance.

5. Double bonds favor allylic cleavage and give the resonance-stabilized allylic carbocation. This rule does not hold for simple alkenes because of the ready migration of the double bond, but it does hold for cycloalkenes.

6. Saturated rings tend to lose alkyl side chains at the α bond. This is merely a special case of branching (rule 3). The positive charge tends to stay with the ring fragment. See Scheme 1.4. Unsaturated rings can undergo a retro-Diels-Alder reaction (see Scheme 1.5).

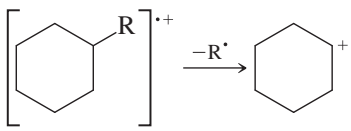

(Sch 1.4)

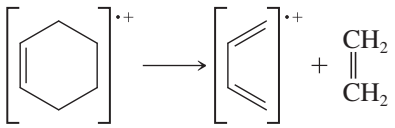

(Sch 1.5)

7. In alkyl-substituted aromatic compounds, cleavage is very probable at the bond β to the ring, giving the resonance-stabilized benzyl ion or, more likely, the tropylium ion (see Scheme 1.6).

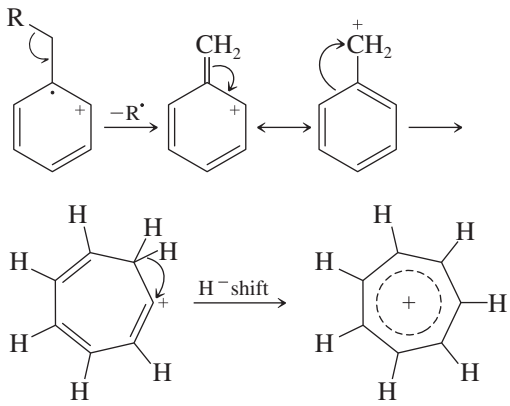

(Sch 1.6)

8. The C—C bonds next to a heteroatom are frequently cleaved, leaving the charge on the fragment containing the heteroatom whose nonbonding electrons provide resonance stabilization.
9. Cleavage is often associated with elimination of small, stable, neutral molecules, such as carbon monoxide, alkenes, water, ammonia, hydrogen sulfide, hydrogen cyanide, mercaptans, ketenes, or alcohols, often with rearrangement (Section 1.5.5).

It should be kept in mind that the fragmentation guidelines above apply to EI mass spectrometry. Since other ionizing techniques (CI, etc.) often produce molecular ions with much lower energy or quasimolecular ions with very different fragmentation patterns, different rules govern the fragmentation of these molecular ions.

1.5.5 Rearrangements

Rearrangement ions are fragments whose origin cannot be described by simple cleavage of bonds in the molecular ion but are a result of intramolecular atomic rearrangement during fragmentation. Rearrangements involving migration of hydrogen atoms in molecules that contain a heteroatom are especially common. One important example is the so-called McLafferty rearrangement; it is illustrated in Scheme 1.7 for the general case.

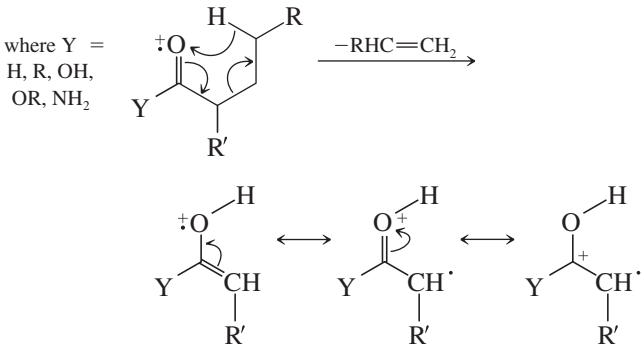

(Sch 1.7)

To undergo a McLafferty rearrangement, a molecule must possess an appropriately located heteroatom (e.g., O), a π system (usually a double bond), and an abstractable hydrogen atom γ to the C═O system.

Such rearrangements often account for prominent characteristic peaks and are consequently very useful for our purpose. They can frequently be rationalized on the basis of low-energy transitions and increased stability of the products. Rearrangements resulting in elimination of a stable neutral molecule are common (e.g., the alkene product in the McLafferty rearrangement) and will be encountered in the discussion of mass spectra of chemical classes.

Rearrangement peaks, with loss of a neutral molecule, can be recognized by considering the unit mass number (m/z) for fragment ions and for their corresponding molecular ions. A simple (no rearrangement) cleavage of an even-numbered molecular ion gives an odd-numbered fragment ion and simple cleavage of an odd-numbered molecular ion gives an even-numbered fragment. Observation of a fragment ion mass different by 1 unit from that expected for a fragment resulting from simple cleavage (e.g., an even-numbered fragment mass from an even-numbered molecular ion mass) indicates rearrangement of a hydrogen atom has accompanied fragmentation. Rearrangement peaks may be recognized by considering the corollary to the "nitrogen rule" (Section 1.5.1). Thus, an even-numbered peak derived from an even-numbered molecular ion is a result of two cleavages, which may involve a rearrangement.

Seemingly random rearrangements of hydrocarbons were noted by the early mass spectrometrists in the petroleum industry. For example, the rearrangement of the *neo*-pentyl radical-cation to the ethyl cation, shown in Scheme 1.8, defies a straightforward explanation.

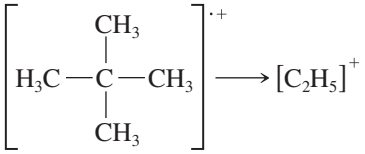

(Sch 1.8)

1.6 MASS SPECTRA OF SOME CHEMICAL CLASSES

Mass spectra of a number of chemical classes are briefly described in this section in terms of the most useful generalizations for identification. For more details, the references cited should be consulted (in particular, the thorough treatment by Budzikiewicz et al., 1967). Databases are available both from publishers and as part of instrument capabilities. The references are selective rather than comprehensive. A table of frequently encountered fragment ions is given in Appendix B. A table of fragments (uncharged) that are commonly eliminated and some structural inferences are presented in Appendix C. More exhaustive listings of common fragment ions have been compiled (see References).

1.6.1 Hydrocarbons

1.6.1.1 Saturated Hydrocarbons. Most of the early work in mass spectrometry was done on hydrocarbons of interest to the petroleum industry. Guidelines 1 – 3, (Section 1.5.4) apply quite generally; rearrangement peaks, though common, are not usually intense (random rearrangements), and numerous reference spectra are available.

The molecular ion peak of a straight-chain, saturated hydrocarbon is always present, though of low intensity for

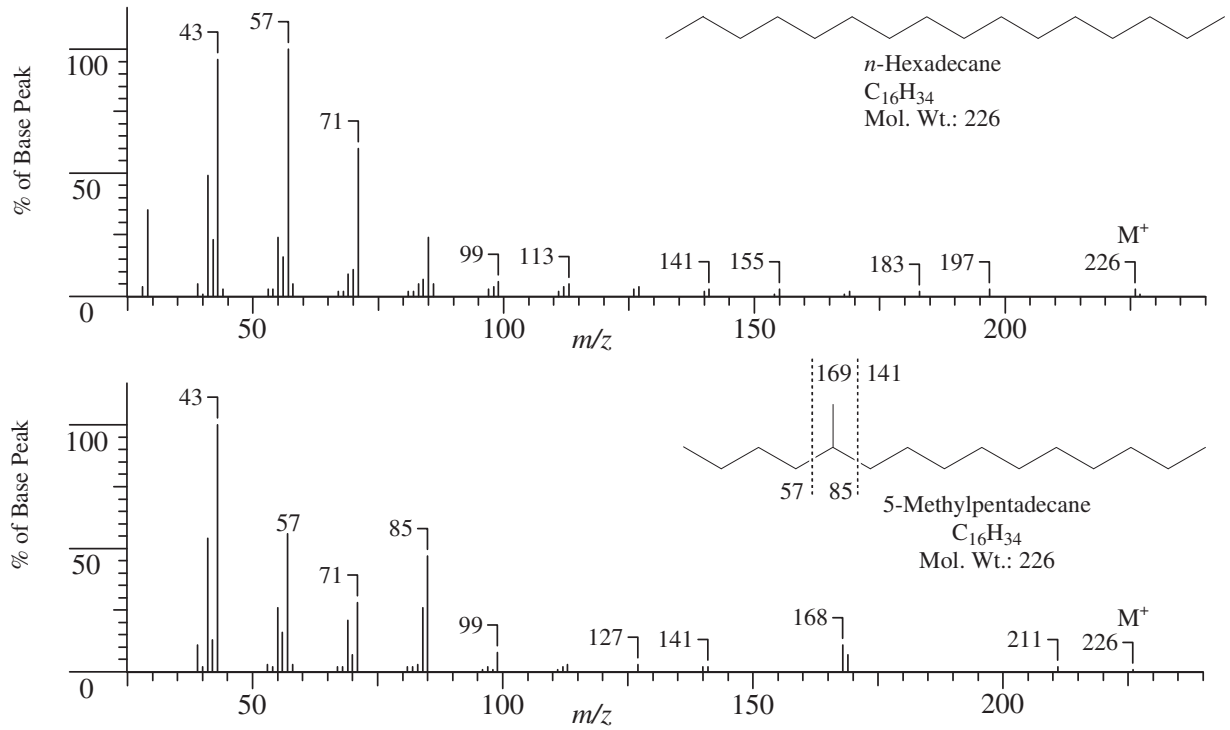

FIGURE 1.14 EI mass spectra of isomeric C_{16} hydrocarbons.

long-chain compounds. The fragmentation pattern is characterized by clusters of peaks, and the corresponding peaks of each cluster are 14 mass units (—CH_2—) apart. The largest peak in each cluster represents a C_nH_{2n+1} fragment and thus occurs at $m/z = 14n + 1$; this peak is accompanied by C_nH_{2n} and C_nH_{2n-1} fragments. The most abundant fragments are at C_3 and C_4, and the fragment abundances logarithmically decrease down to $[M - C_2H_5]^+$; the $[M - CH_3]^+$ peak is characteristically very weak or missing. Compounds containing more than eight carbon atoms show fairly similar spectra; identification then depends on the molecular ion peak.

Spectra of branched saturated hydrocarbons are grossly similar to those of straight-chain compounds, but the smooth curve of decreasing intensities is broken by preferred fragmentation at each branch. The smooth curve for the *n*-alkane in Figure 1.14 (top) is in contrast to the discontinuity at C_{12} for the branched alkane (Figure 1.14, bottom). This discontinuity indicates that the longest branch of 5-methylpentadecane has 10 carbon atoms.

In the bottom spectrum of Figure 1.14, the peaks at m/z 169 and 85 represent cleavage on either side of the branch with charge retention on the substituted carbon atom. Subtraction of the molecular weight from the sum of these fragments accounts for the fragment —CH—CH_3. Again, we appreciate the absence of a C_{11} unit, which cannot form by a single cleavage. Finally, the presence of a distinct M − 15 peak also indicates a methyl branch. The fragment resulting from cleavage at a branch tends to lose a single hydrogen atom so that the resulting C_nH_{2n} peak is prominent and sometimes more intense than the corresponding C_nH_{2n+1} peak.

A saturated ring in a hydrocarbon increases the relative intensity of the molecular ion peak and favors cleavage at the bond connecting the ring to the rest of the molecule (guideline 6, Section 1.5.4). Fragmentation of the ring is usually characterized by the loss of two carbon atoms as C_2H_4 (28) and C_2H_5 (29). This tendency to lose even-numbered fragments gives a spectrum that contains a greater proportion of even-numbered mass ions than the spectrum of an acyclic hydrocarbon. As in branched hydrocarbons, C—C cleavage is accompanied by the loss of a hydrogen atom. The characteristic peaks are therefore in the C_nH_{2n-1} and C_nH_{2n-2} series.

The mass spectrum of cyclohexane (Figure 1.15) shows a much more intense molecular ion than those of acyclic compounds, since fragmentation requires the cleavage of two carbon-carbon bonds. This spectrum has its base peak at m/z 56 (because of a loss of C_2H_4) and a large peak at m/z 41, which is a fragment in the C_nH_{2n-1} series with $n = 3$.

1.6.1.2 Alkenes (Olefins). The molecular ion peak of alkenes, especially polyalkenes, is usually distinct. Location of the double bond in acyclic alkenes is sometimes difficult because of its facile migration in the fragments. In cyclic (especially polycyclic) alkenes, location of the double bond is frequently evident as a result of a strong tendency for allylic cleavage without much double-bond migration (guideline 5, Section 1.5.4). Conjugation with a carbonyl group also fixes the position of the double bond. As with

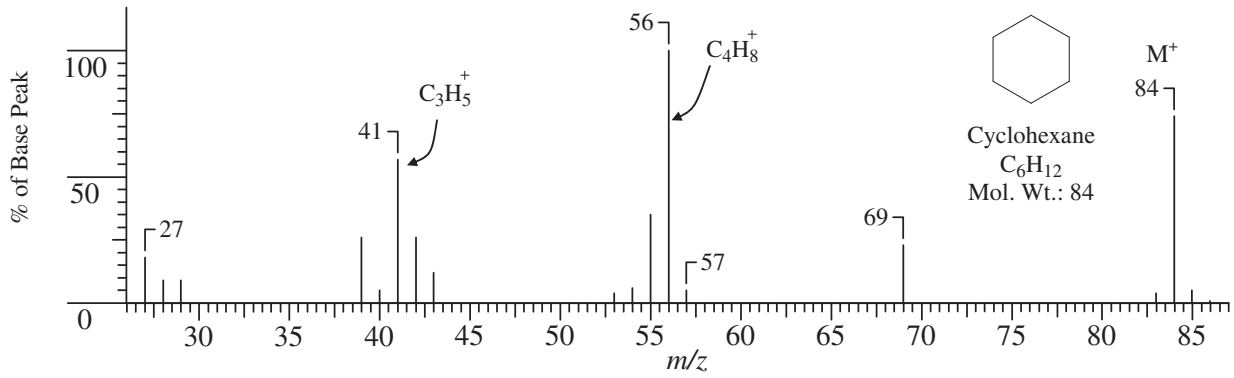

FIGURE 1.15 EI mass spectrum of cyclohexane.

saturated hydrocarbons, acyclic alkenes are characterized by clusters of peaks at intervals of 14 units. In these clusters the C_nH_{2n-1} and C_nH_{2n} peaks are more intense than the C_nH_{2n+1} peaks.

The mass spectrum of β-myrcene, a monoterpene, is shown in Figure 1.16. The peaks at m/z 41, 55, and 69 correspond to the formula C_nH_{2n-1} with $n = 3$, 4, and 5, respectively. Formation of the m/z 41 peak must involve isomerization. The peaks at m/z 67 and 69 are the fragments from cleavage of a bi-allylic bond, which is shown in Scheme 1.9.

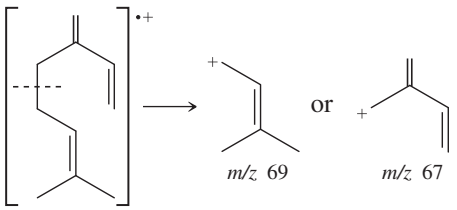

(Sch 1.9)

The peak at m/z 93 is rationalized in Scheme 1.10 as a structure of formula $C_7H_9^+$ formed by double bond isomerization (resulting in increased conjugation), followed by allylic cleavage. The ion at m/z 93 has at least two important resonance forms that contribute to its stability. As an exercise, the student is encouraged to draw them.

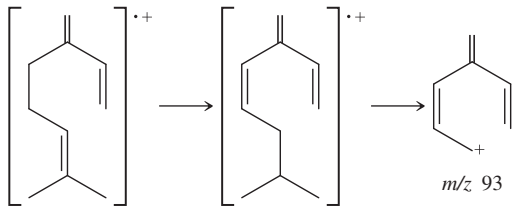

(Sch 1.10)

Cyclic alkenes usually show a distinct molecular ion peak. A unique mode of cleavage is the *retro*-Diels-Alder reaction. This reaction is illustrated with limonene in Scheme 1.11 (see Figure 1.17). A retro-Diels-Alder reaction in this example gives two isoprene molecules. Since the reaction is an example of a rearrangement, one of the isoprene moieties is a neutral molecule.

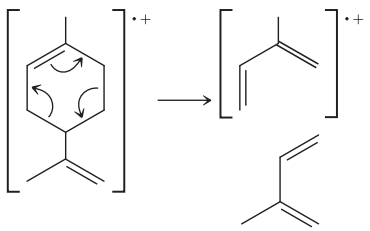

(Sch 1.11)

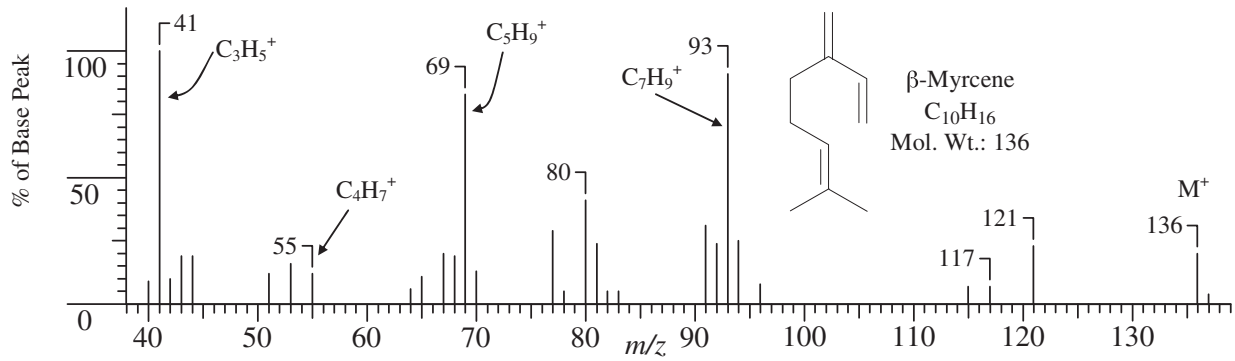

FIGURE 1.16 EI mass spectrum of β-myrcene.

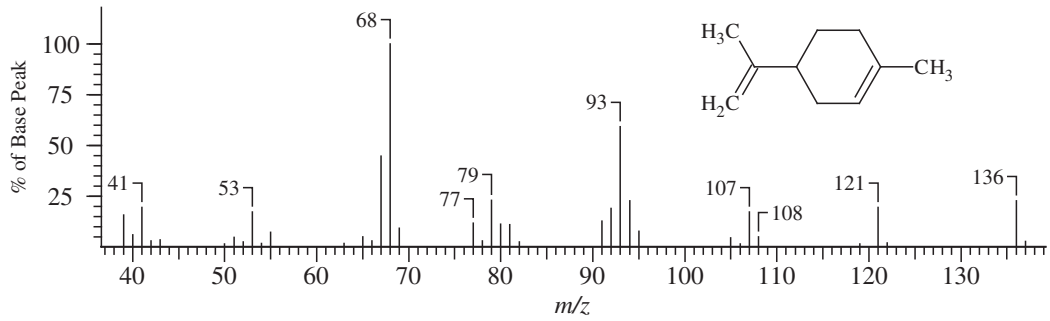

FIGURE 1.17 EI mass spectrum of limonene.

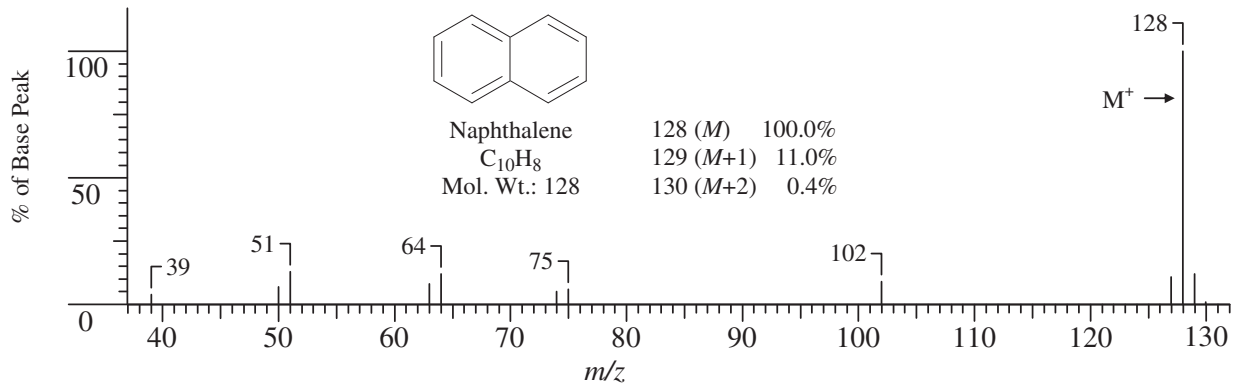

FIGURE 1.18 EI mass spectrum of naphthalene.

1.6.1.3 Aromatic and Aralkyl Hydrocarbons. An aromatic ring in a molecule stabilizes the molecular ion peak (guideline 4, Section 1.5.4), which is usually sufficiently large that accurate intensity measurements can be made on the M + 1 and M + 2 peaks.

Shown in Figure 1.18 is the mass spectrum of naphthalene. The molecular ion peak is also the base peak, and the largest fragment peak, m/z 51, is only 12.5% as intense as the molecular ion peak.

An alkyl-substituted benzene ring frequently gives a prominent peak (often the base peak) at m/z 91 ($C_6H_5CH_2^+$). Branching at the α-carbon leads to masses higher than 91, by increments of 14, the largest substituent being eliminated most readily (guideline 3, Section 1.5.4). The mere presence of a peak at mass 91, however, does not preclude branching at the α-carbon because this highly stabilized fragment may result from rearrangements. A distinct and sometimes prominent M − 1 peak results from similar benzylic cleavage of a C—H bond.

It has been proposed that, in most cases, the ion of mass 91 is a tropylium rather than a benzylic cation. This explains the ready loss of a methyl group, which seems to violate guideline 7, from xylenes (Scheme 1.12, see Figure 1.19). By comparison, toluene does not easily lose a methyl group. The incipient molecular radical ion of xylene rearranges to the methylcycloheptatriene radical ion, which then cleaves to the tropylium ion ($C_7H_7^+$). The frequently observed peak at m/z 65 results from the elimination of a neutral acetylene molecule from the tropylium ion.

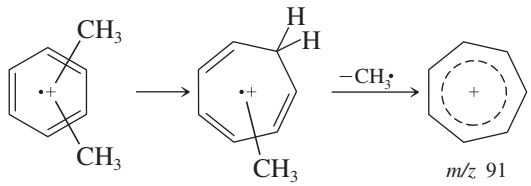

(Sch 1.12)

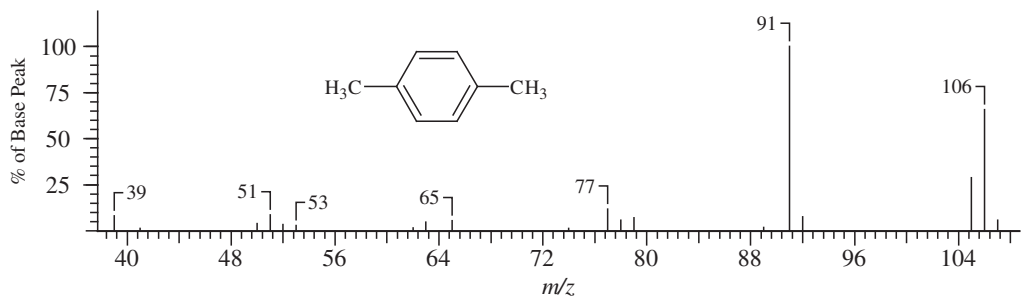

FIGURE 1.19 EI mass spectrum of *p*-xylene.

Hydrogen migration with elimination of a neutral alkene molecule accounts for the peak at m/z 92 observed when the alkyl group is longer than C_2. Scheme 1.13 illustrates with a general example. Note again that this is an example of a rearrangement.

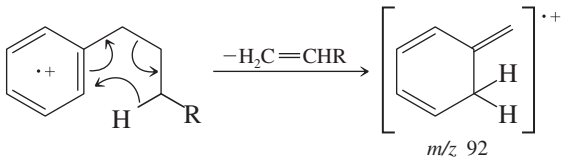

(Sch 1.13)

A characteristic cluster of ions resulting from an α cleavage and hydrogen migration in monoalkylbenzenes appears at m/z 77 ($C_6H_5^+$), 78 ($C_6H_6^+$), and 79 ($C_6H_7^+$).

Alkylated polyphenyls and alkylated polycyclic aromatic hydrocarbons exhibit the same β cleavage as alkylbenzene compounds.

1.6.2 Hydroxy Compounds

1.6.2.1 Alcohols. The molecular ion peak of a primary or secondary alcohol is usually quite small and for a tertiary alcohol is often undetectable. The molecular ion of 1-pentanol is extremely weak compared with its near homologs. Expedients such as CI, or derivatization, may be used to obtain the molecular weight.

Cleavage of the C—C bond next to the oxygen atom is of general occurrence (guideline 8, Section 1.5.4). Thus, primary alcohols show a prominent peak resulting from $^+CH_2$—OH (m/z 31). Secondary and tertiary alcohols cleave analogously to give a prominent peak resulting from $^+$CHR—OH (m/z 45, 59, 73, etc.) and $^+$CRR′—OH (m/z 59, 73, 87, etc.), respectively. The largest substituent is expelled most readily (guideline 3). It is not unusual that the C—H bond next to the oxygen atom is cleaved; this less (or least) favored pathway gives rise to an M − 1 peak.

Primary alcohols, in addition to the principal C—C cleavage next to the oxygen atom, show a homologous series of peaks of progressively decreasing intensity resulting from cleavage at C—C bonds successively removed from the oxygen atom. In long-chain (>C_6) alcohols, the fragmentation becomes dominated by the hydrocarbon pattern; in fact, the spectrum resembles that of the corresponding alkene. The spectrum in the vicinity of a very weak or missing molecular ion peak of a primary alcohol is sometimes complicated by weak M − 2 and M − 3 peaks.

A distinct and sometimes prominent peak can usually be found at M − 18 from loss of water. This peak is most noticeable in spectra of primary alcohols. This elimination by electron impact has been rationalized and a mechanism in which a δ-hydrogen is lost is shown in Scheme 1.14, ***I***. A similar mechanism can be drawn in which a γ-hydrogen is lost. The M − 18 peak is frequently exaggerated by thermal decomposition of higher alcohols on hot inlet surfaces. Elimination of water, together with elimination of an alkene from primary alcohols (see Scheme 1.14, ***II***), accounts for the presence of a peak at M − (alkene + H_2O), that is, a peak at M − 46, M − 74, M − 102, …

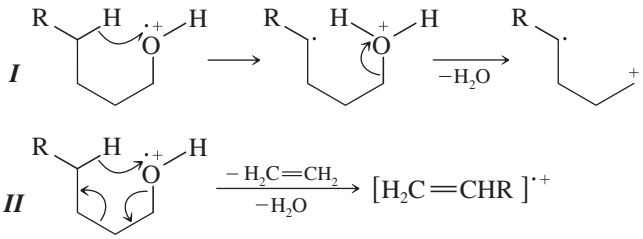

(Sch 1.14)

Alcohols containing branched methyl groups (e.g., terpene alcohols) frequently show a fairly strong peak at M − 33 resulting from loss of CH_3 and H_2O.

Cyclic alcohols undergo fragmentation by complicated pathways; for example, cyclohexanol (Figure 1.20) (M = m/z 100) forms $C_6H_{11}O^+$ by simple loss of the α-hydrogen, loses H_2O to form $C_6H_{10}^+$ (which appears to have more than one possible bridged bicyclic structure), and forms $C_3H_5O^+$ (m/z 57) by a complex ring cleavage pathway.

A peak at m/z 31 (see above) is quite diagnostic for a primary alcohol provided it is more intense than peaks at m/z 45, 59, 73 …. However, the first-formed ion of a secondary alcohol can decompose further to give a moderately intense m/z 31 peak.

Figure 1.21 gives the characteristic spectra of isomeric primary, secondary, and tertiary C_5 alcohols.

Benzyl alcohols and their substituted homologs and analogs constitute a distinct class. Generally, the parent peak is strong. A moderate benzylic peak (M − OH) may be present as expected from cleavage β to the ring.

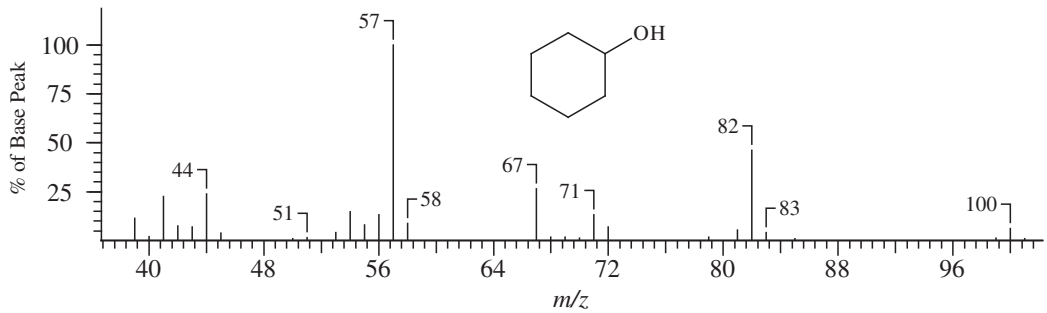

FIGURE 1.20 EI mass spectrum of cyclohexanol.

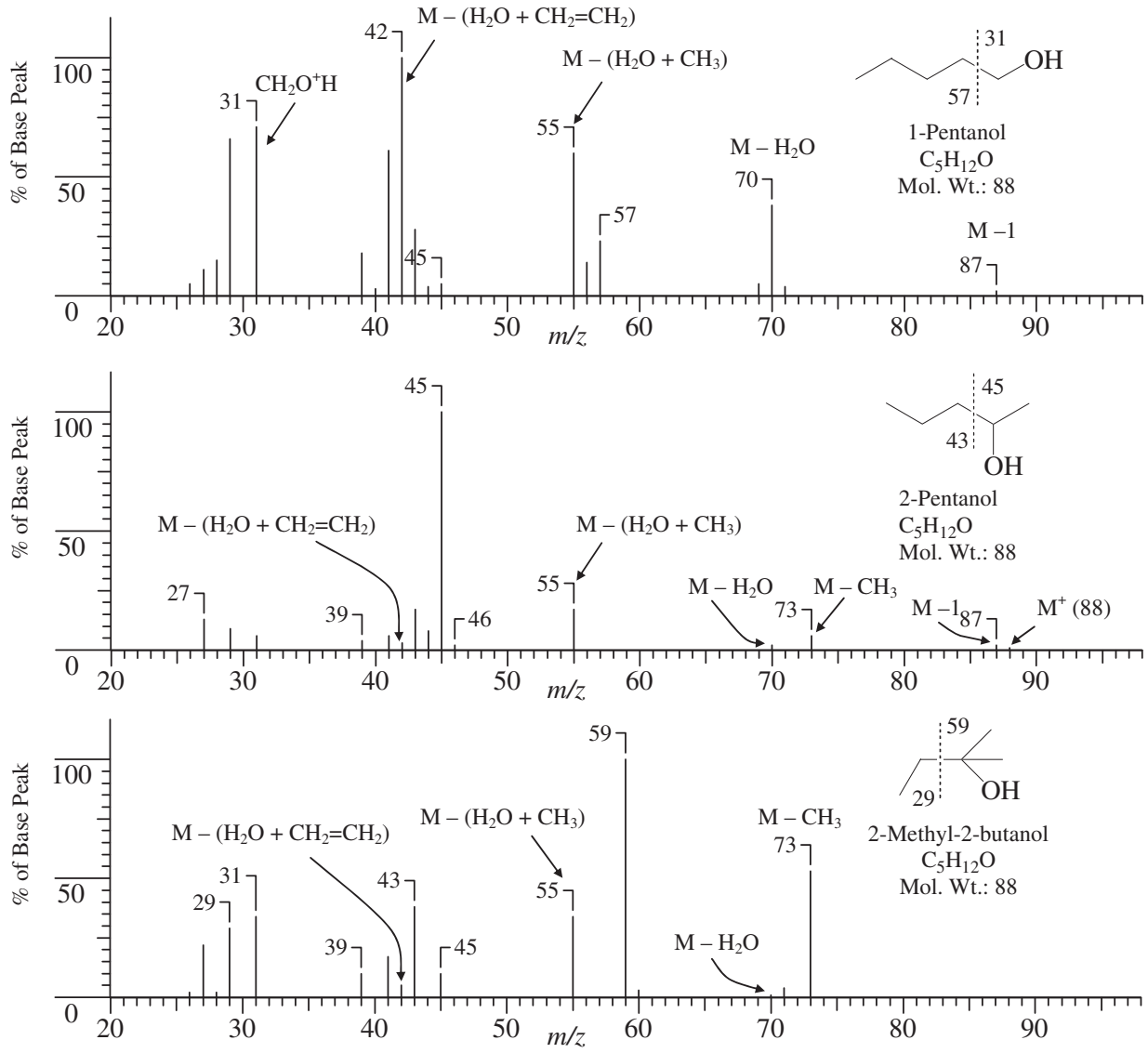

FIGURE 1.21 EI mass spectra of isomeric pentanols.

A complicated sequence leads to prominent M − 1, M − 2, and M − 3 peaks. Benzyl alcohol itself (Figure 1.22) fragments to give sequentially the M − 1 ion, the $C_6H_7^+$ ion by loss of CO, and the $C_6H_5^+$ ion by loss of H_2 (see Scheme 1.15).

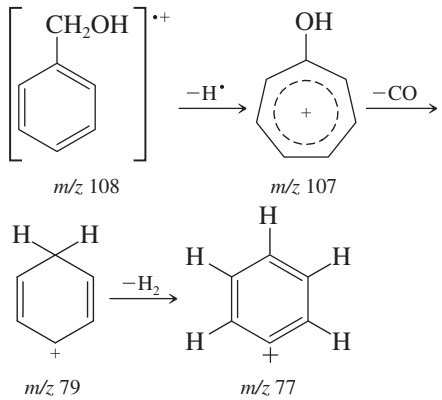

(Sch 1.15)

Loss of H_2O to give a distinct M − 18 peak is a common feature, especially pronounced and mechanistically straightforward in some *ortho*-substituted benzyl alcohols (see Figure 1.23). The loss of water shown in Scheme 1.16 works equally well with an oxygen atom at the *ortho*-position (a phenol). The aromatic cluster at *m/z* 77, 78, and 79 resulting from complex degradation is prominent here also.

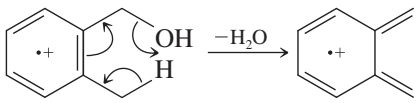

(Sch 1.16)

1.6.2.2 Phenols. A conspicuous molecular ion peak facilitates identification of phenols. In phenol itself, the molecular ion peak is the base peak, and the M − 1 peak is small. In cresols, the M − 1 peak is larger than that of the molecular ion as a result of a facile benzylic C—H cleavage.

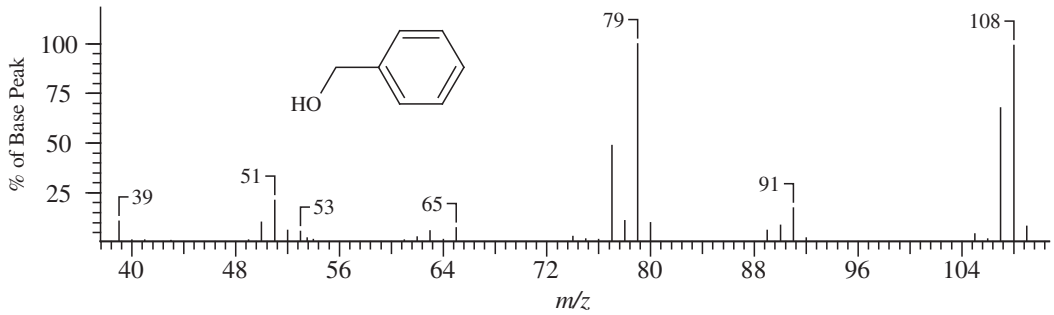

FIGURE 1.22 EI mass spectrum of benzyl alcohol.

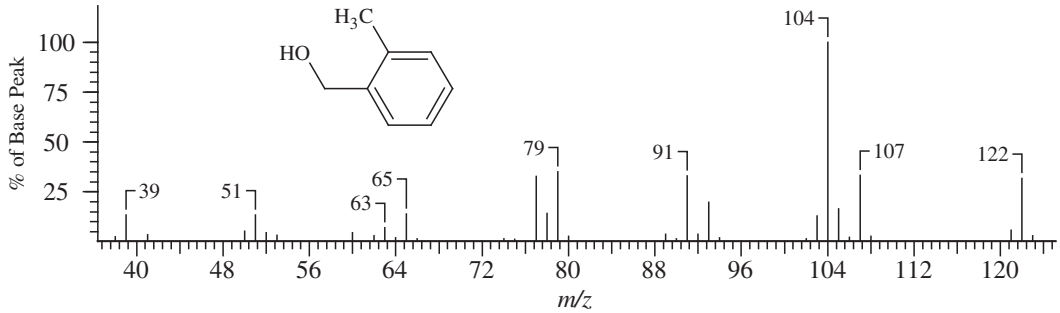

FIGURE 1.23 EI mass spectrum of *o*-methylbenzyl alcohol.

A rearrangement peak at m/z 77 and peaks resulting from the loss of CO (M − 28) and CHO (M − 29) are usually found in the mass spectra of phenols.

The mass spectrum of *o*-ethylphenol, a typical phenol, is shown in Figure 1.24. This spectrum shows that a methyl group is lost much more readily than an α-hydrogen.

1.6.3 Ethers

1.6.3.1 Aliphatic Ethers (and Acetals). The molecular ion peak (two mass units larger than that of an analogous hydrocarbon) is small, but larger sample size usually will make the molecular ion peak or the M + 1 peak obvious ($H^{\cdot}$ transfer during ion-molecule collision).

The presence of an oxygen atom can be deduced from strong peaks at m/z 31, 45, 59, 73, … These peaks represent the RO^+ and $ROCH_2{}^+$ fragments. A typical aliphatic ether is shown in Figure 1.25. Fragmentation occurs in two principal ways:

1. Cleavage of the C—C bond next to the oxygen atom (α, β bond, guideline 8, Section 1.5.4). One or the other of these oxygen-containing ions may account for the base peak. In the case shown in Figure 1.25, the first cleavage (i.e., at the branch position leading to loss of the larger fragment) is preferred. However, the first-formed fragment decomposes further by loss of ethylene to give the base peak; this decomposition is important when the α-carbon is substituted (see McLafferty rearrangement, Section 1.5.5)

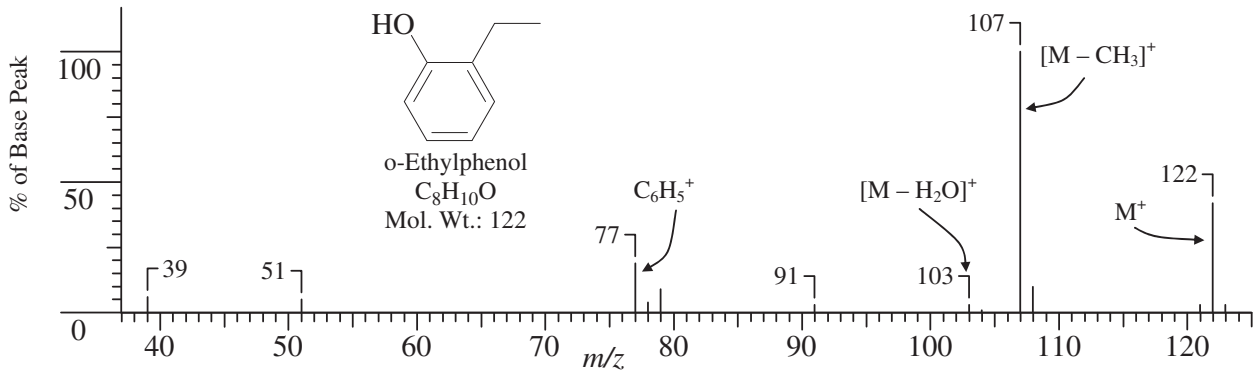

FIGURE 1.24 EI mass spectrum of *o*-ethylphenol.

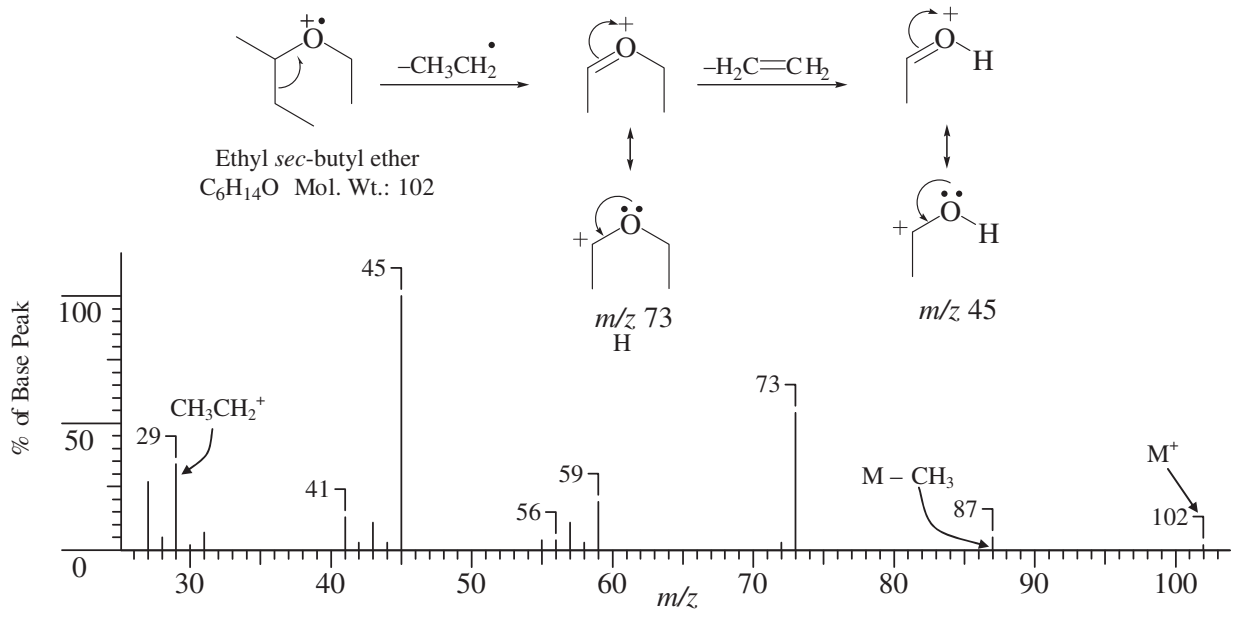

FIGURE 1.25 EI mass spectrum of ethyl *sec*-butyl ether.

2. C—O bond cleavage with the charge remaining on the alkyl fragment. The spectrum of long-chain ethers becomes dominated by the hydrocarbon pattern.

Acetals are a special class of ethers. Their mass spectra are characterized by an extremely weak molecular ion peak, by the prominent peaks at M – R and M – OR (and/or M – OR′), and a weak peak at M – H. Each of these cleavages is mediated by an oxygen atom and thus facile. As usual, elimination of the largest group is preferred. As with aliphatic ethers, the first-formed oxygen-containing fragments can decompose further with hydrogen migration and alkene elimination. Ketals behave similarly.

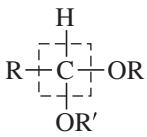

1.6.3.2 Aromatic Ethers. The molecular ion peak of aromatic ethers is prominent. Primary cleavage occurs at the bond β to the ring, and the first-formed ion can decompose further. Thus, anisole (Figure 1.26, MW 108) gives ions of m/z 93 and 65. The characteristic aromatic peaks at m/z 78 and 77 may arise from anisole.

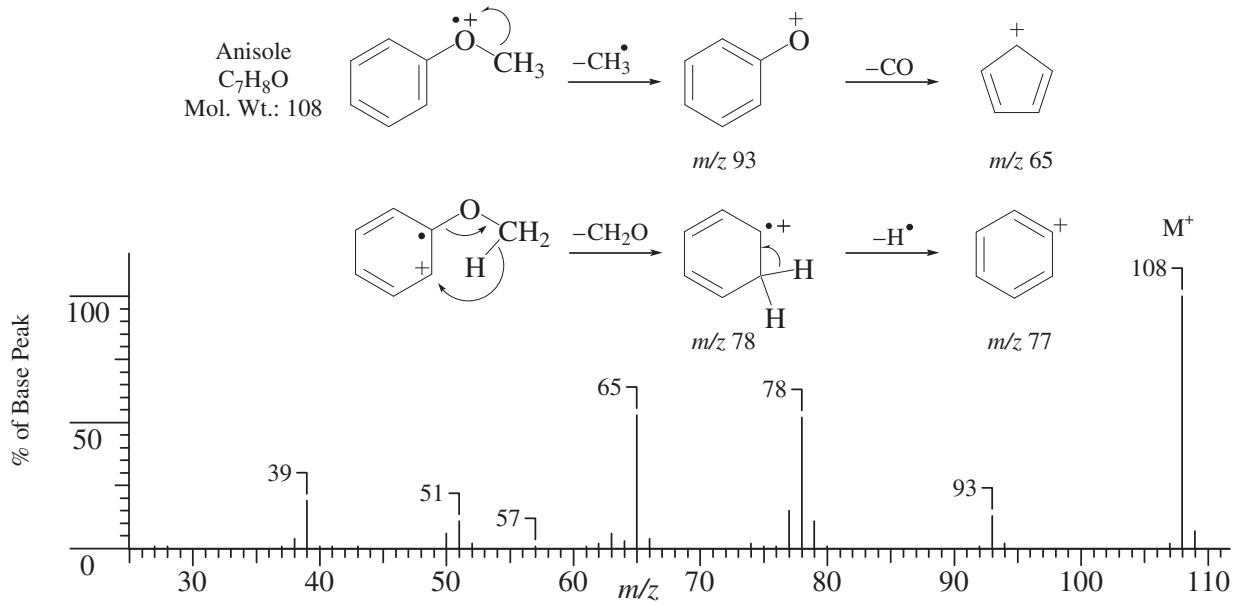

FIGURE 1.26 EI mass spectrum of anisole.

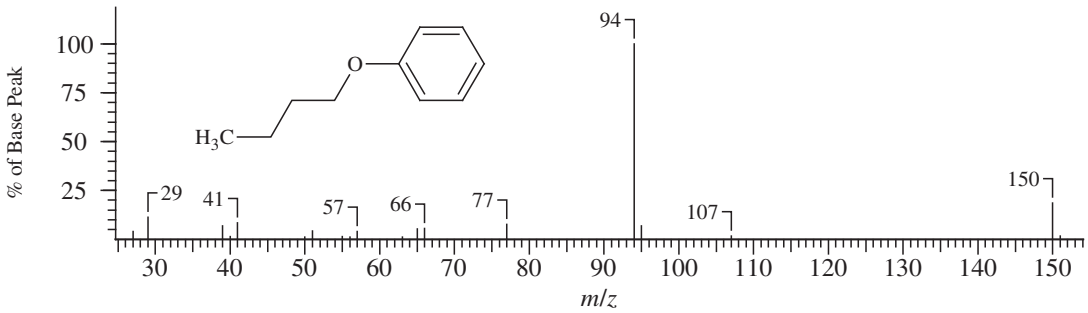

FIGURE 1.27 EI mass spectrum of butyl phenyl ether.

When the alkyl portion of an aromatic alkyl ether is C_2 or larger, cleavage β to the ring is accompanied by hydrogen migration (Scheme 1.17) as noted above for alkylbenzenes. Clearly, cleavage is mediated by the ring rather than by the oxygen atom; C—C cleavage next to the oxygen atom is insignificant. An example of this type is illustrated in the spectrum of butyl phenyl ether, Figure 1.27.

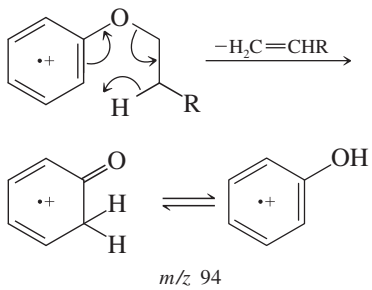

(Sch 1.17)

Diphenyl ethers show peaks at M − H, M − CO, and M − CHO by complex rearrangements.

1.6.4 Ketones

1.6.4.1 Aliphatic Ketones. The molecular ion peak of ketones is usually quite pronounced. Major fragmentation peaks of aliphatic ketones result from cleavage at one of the C—C bonds adjacent to the oxygen atom, the charge remaining with the resonance-stabilized acylium ion (Scheme 1.18). Thus, as with alcohols and ethers, cleavage is mediated by the oxygen atom. This cleavage gives rise to a peak at m/z 43 or 57 or 71…. The base peak very often results from loss of the larger alkyl group.

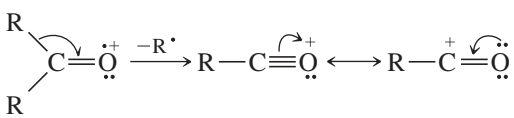

(Sch 1.18)

When one of the alkyl chains attached to the C═O group is C_3 or longer, cleavage of the C—C bond once removed (α,β-bond) from the C═O group occurs with hydrogen migration to give a major peak (McLafferty rearrangement, Scheme 1.19). Simple cleavage of the α,β-bond, which does not occur to any extent, would give an ion of low stability because it would have two adjacent positive centers.

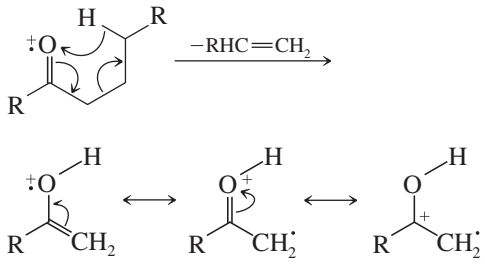

(Sch 1.19)

Note that in long-chain ketones the hydrocarbon peaks are indistinguishable (without the aid of high-resolution techniques) from the acyl peaks, since the mass of the C═O unit (28) is the same as two methylene units. The multiple cleavage modes in ketones sometimes make difficult the determination of the carbon chain configuration. Reduction of the carbonyl group to a methylene group yields the corresponding hydrocarbon whose fragmentation pattern leads to the carbon skeleton.

1.6.4.2 Cyclic Ketones. The molecular ion peak in cyclic ketones is prominent. As with acyclic ketones, the primary cleavage of cyclic ketones is adjacent to the C═O group, but the ion thus formed must undergo further cleavage in order to produce a fragment. The base peak in the spectrum of cyclopentanone and of cyclohexanone (Figure 1.28) is m/z 55. The mechanisms are similar in both cases: hydrogen shift to convert a primary radical to a conjugated secondary radical followed by formation of the resonance-stabilized ion, m/z 55. The other distinctive peaks at m/z 83 and 42 in the spectrum of cyclohexanone have been rationalized as depicted in Figure 1.28.

1.6.4.3 Aromatic Ketones. The molecular ion peak of an aromatic ketone is prominent. Cleavage of aryl alkyl ketones occurs at the bond β to the ring, leaving a characteristic $ArC{\equiv}O^+$ fragment (m/z 105 when Ar = phenyl), which usually accounts for the base peak. Loss of CO from this fragment gives the "aryl" ion (m/z 77 in the case of acetophenone). Cleavage of the bond adjacent to the ring to form a $RC{\equiv}O^+$ fragment (R = alkyl) is less important though somewhat enhanced by electron-withdrawing groups

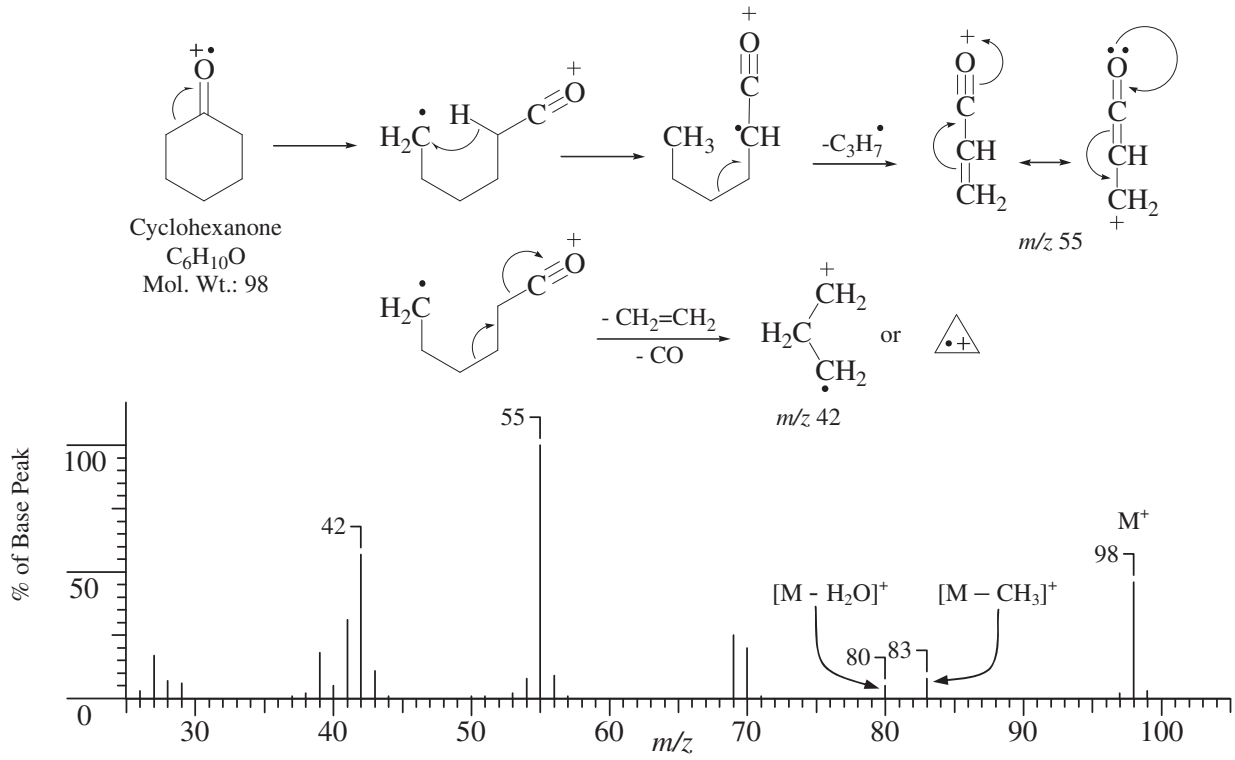

FIGURE 1.28 EI mass spectrum of cyclohexanone.

(and diminished by electron-donating groups) in the *para*-position of the Ar group.

When the alkyl chain is C_3 or longer, cleavage of the C—C bond once removed from the C═O group occurs with hydrogen migration. This is the same cleavage noted for aliphatic ketones that proceeds through a cyclic transition state and results in elimination of an alkene and formation of a stable ion.

The mass spectrum of an unsymmetrical diaryl ketone, *p*-chlorobenzophenone, is displayed in Figure 1.29. The molecular ion peak (m/z 216) is prominent and the intensity of the M + 2 peak (33.99%, relative to the molecular ion peak) demonstrates that chlorine is in the structure (see the discussion of Table 1.5 and Figure 1.35 in Section 1.6.16).

Since the intensity of the m/z 141 peak is about $\frac{1}{3}$ the intensity of the m/z 139 peak, these peaks, which are

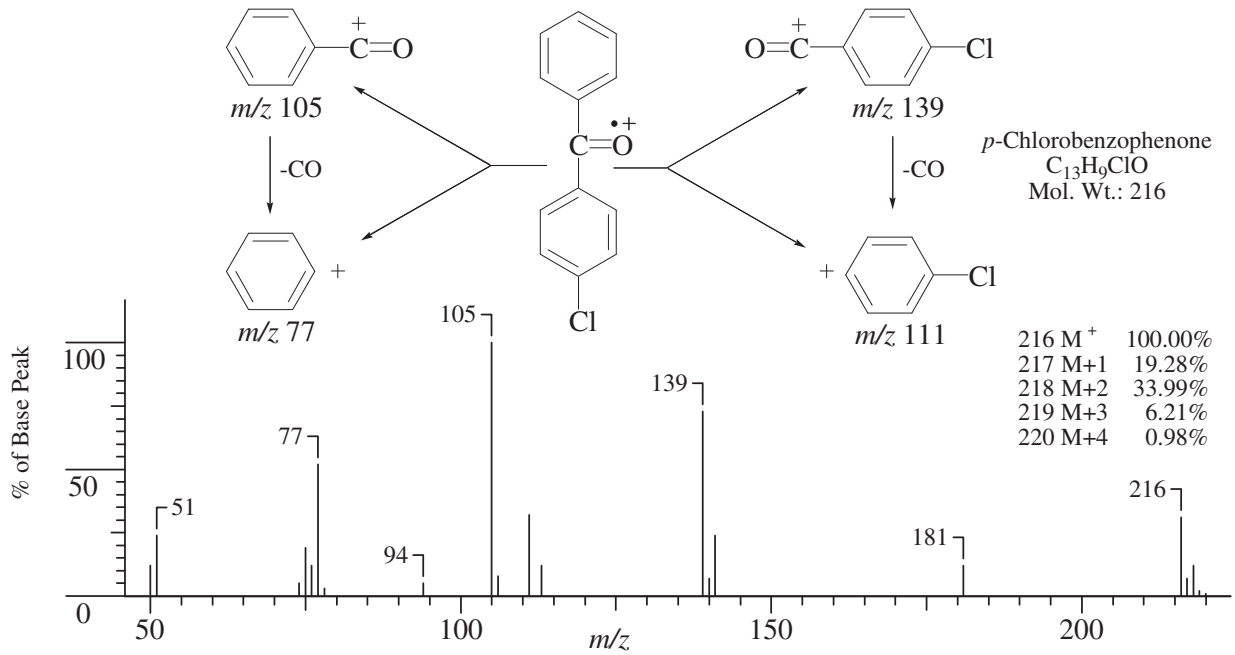

FIGURE 1.29 EI mass spectrum of *p*-chlorobenzophenone.

due to fragments which contain chlorine, correspond to the same fragment. The same can be said about the fragments producing the m/z 111 and 113 peaks.

The fragmentation leading to the major peaks is sketched in Figure 1.29. The Cl—ArC≡O^+ peak is larger than the Cl—Ar^+ peak, and the ArC≡O^+ peak is larger than the Ar^+ peak (β cleavage favored). If the [fragment + 2] peaks for the Cl-substituted moieties are taken into account however, there is little difference in abundance between Cl—$ArCO^+$ and $ArCO^+$, or between Cl—Ar^+ and Ar^+; the inductive (electron withdrawing) and resonance (electron releasing) effects of the *para*-substituted Cl are roughly balanced out as they are in electrophilic aromatic substitution reactions.

1.6.5 Aldehydes

1.6.5.1 Aliphatic Aldehydes. The molecular ion peak of aliphatic aldehydes is usually discernible. Cleavage of the C—H and C—C bonds next to the oxygen atom results in an M − 1 peak and in an M − R peak (m/z 29, CHO^+). The M − 1 peak is a good diagnostic peak even for long-chain aldehydes, but the m/z 29 peak present in C_4 and higher aldehydes results from the hydrocarbon $C_2H_5{}^+$ ion.

In the C_4 and higher aldehydes, McLafferty cleavage of the α,β C—C bond occurs to give a major peak at m/z 44, 58, or 72, …, depending on the α substituents. This is the resonance-stabilized ion (Scheme 1.20) formed through the cyclic transition state as shown in Scheme 1.7, where Y═H.

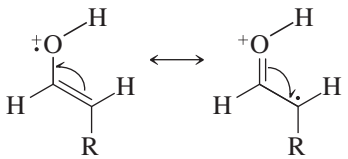

(Sch 1.20)

In straight-chain aldehydes, other unique, diagnostic peaks are at M − 18 (loss of water), M − 28 (loss of ethylene), M − 43 (loss of CH_2═CH—O·), and M − 44 (loss of CH_2═CH—OH). The rearrangements leading to these peaks have been rationalized (see Budzikiewicz et al., 1967). As the chain lengthens, the hydrocarbon pattern (m/z 29, 43, 57, 71, …) becomes dominant. These features are evident in the spectrum of nonanal (Figure 1.30).

1.6.5.2 Aromatic Aldehydes. Aromatic aldehydes are characterized by a large molecular ion peak and by an M − 1 peak (Ar—C═O^+) that is always large and may be larger than the molecular ion peak. The M − 1 ion, C_6H_5—CO^+ when Ar = phenyl, eliminates CO to give the phenyl ion (m/z 77), which in turn eliminates acetylene to give the $C_4H_3{}^+$ ion (m/z 51).

1.6.6 Carboxylic Acids

1.6.6.1 Aliphatic Acids. The molecular ion peak of a straight-chain monocarboxylic acid is weak but usually discernible. The most characteristic (sometimes the base) peak is m/z 60 resulting from the McLafferty rearrangement (Scheme 1.21). Branching at the α-carbon enhances this cleavage.

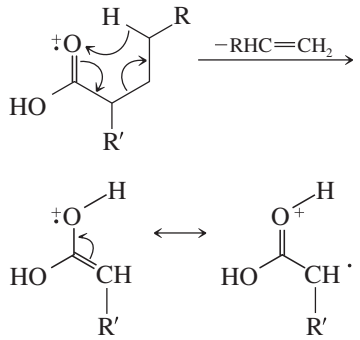

(Sch 1.21)

In short-chain acids, peaks at M − OH and M − CO_2H are prominent: these represent cleavage of bonds next to C═O. In long-chain acids, the spectrum consists of two series of peaks resulting from cleavage at each C—C bond with retention of charge either on the oxygen-containing fragment (m/z 45, 59, 73, 87, …) or on the alkyl fragment (m/z 29, 43, 57, 71, 85, …). As previously discussed, the hydrocarbon pattern also shows peaks at m/z 27, 28; 41, 42;

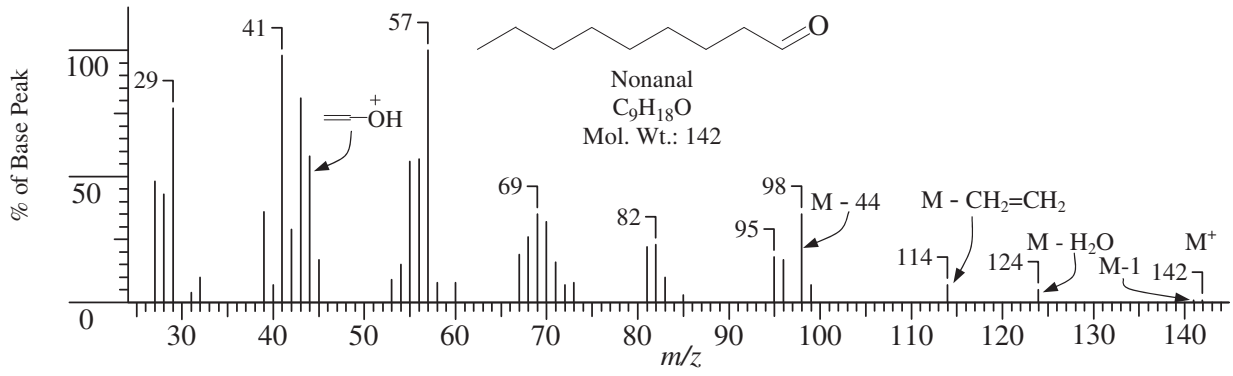

FIGURE 1.30 EI mass spectrum of nonanal.

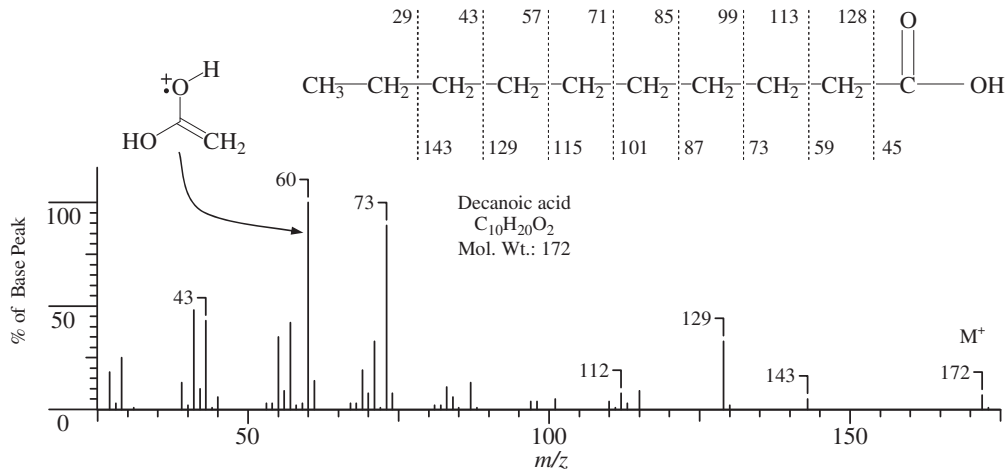

FIGURE 1.31 EI mass spectrum of decanoic acid.

55, 56; 69, 70; …. In summary, besides the McLafferty rearrangement peak, the spectrum of a long-chain acid resembles the series of hydrocarbon clusters at intervals of 14 mass units. In each cluster, however, is a prominent peak at $C_nH_{2n-1}O_2$. Decanoic acid, (Figure 1.31), nicely illustrates many of the points discussed above.

Dibasic acids usually have low volatility and hence are converted to esters to increase vapor pressure. Trimethylsilyl esters are often successful.

1.6.6.2 Aromatic Acids. The molecular ion peak of aromatic acids is large. The other prominent peaks are formed by loss of OH (M − 17) and of CO_2H (M − 45). Loss of H_2O (M − 18) is prominent if a hydrogen-bearing *ortho* group is available as outlined in Scheme 1.22. This is one example of the general "*ortho* effect" noted when the substituents can be in a six-membered transition state to facilitate loss of a neutral molecule of H_2O, ROH, or NH_3.

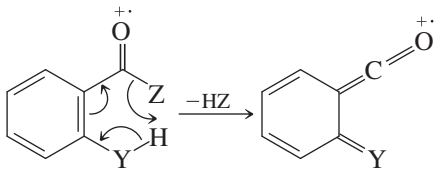

(Sch 1.22)

1.6.7 Carboxylic Esters

1.6.7.1 Aliphatic Esters. The molecular ion peak of a methyl ester of a straight-chain aliphatic acid is usually distinct. Even waxes usually show a discernible molecular ion peak. The molecular ion peak is weak in the range m/z 130 to ~200, but becomes somewhat more intense beyond this range. The most characteristic peak results from the familiar McLafferty rearrangement (Scheme 1.23 gives the rearrangement for an ester) and cleavage one bond removed from the C═O group. Thus, a methyl ester of an aliphatic acid unbranched at the α-carbon gives a strong peak at m/z 74, which in fact, is the base peak in straight-chain methyl esters from C_6 to C_{26}. The alcohol moiety and/or the α substituent can often be deduced by the location of the peak resulting from this cleavage.

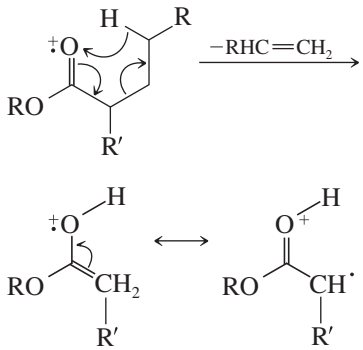

(Sch 1.23)

For the general ester, four ions can result from bond cleavage next to C═O.

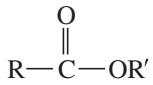

The ion R^+ is prominent for the short-chain esters but diminishes rapidly with increasing chain length and is barely perceptible in methyl hexanoate. The ion $R{-}C{\equiv}O^+$ gives an easily recognizable peak for esters. In methyl esters, it occurs at M − 31. It is the base peak in methyl acetate and is still 4% of the base peak in the C_{26} methyl ester. The ions $[OR']^+$ and $[C(=O)OR']^+$ are usually of little importance. The latter is discernible when $R'{=}CH_3$ (see m/z 59 peak of Figure 1.32).

First, consider esters in which the acid portion is the predominant portion of the molecule. The fragmentation pattern for methyl esters of straight-chain acids can be described in the same terms used for the pattern of the free acid. Cleavage at each C—C bond gives an alkyl ion (m/z 29, 43, 57, …) and an oxygen-containing ion, $C_nH_{2n-1}O_2^+$ (m/z 59, 73, 87, …). Thus, there are hydrocarbon clusters at intervals of 14 mass units; in each cluster is a

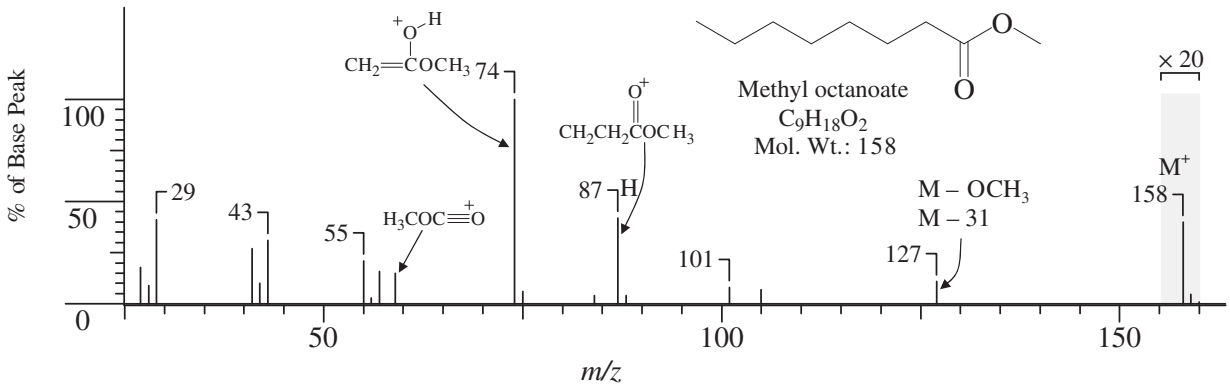

FIGURE 1.32 EI mass spectrum of methyl octanoate.

prominent peak at $C_nH_{2n-1}O_2^+$. The peak (m/z 87) formally represented by the ion $[CH_2CH_2COOCH_3]^+$ is always more intense than its homologs, but the reason is not immediately obvious. However, it seems clear that the $C_nH_{2n-1}O_2^+$ ions do not at all arise from simple cleavage.

The spectrum of methyl octanoate is presented as Figure 1.32. This spectrum illustrates one difficulty in using the M + 1 peak to arrive at a molecular formula (previously mentioned, Section 1.5.2.1). The measured value for the M + 1 peak is 12%. The calculated value is 10.0%. The measured value is high because of an ion-molecule reaction induced by the relatively large sample that was used to see the weak molecular ion peak.

Now let us consider esters in which the alcohol portion is the predominant portion of the molecule. Esters of fatty alcohols (except methyl esters) eliminate a molecule of acid in the same manner that alcohols eliminate water. A scheme similar to that described earlier for alcohols, involving a single hydrogen transfer to the alcohol oxygen of the ester, can be written. An alternative mechanism involves a hydride transfer to the carbonyl oxygen (McLafferty rearrangement).

The loss of acetic acid by the mechanism described above is so facile in steroidal acetates that they frequently show no detectable molecular ion peak. Steroidal systems also seem unusual in that they often display significant molecular ions as alcohols, even when the corresponding acetates do not.

Esters of long-chain alcohols show a diagnostic peak at m/z 61, 75, or 89 … from elimination of the alkyl moiety as an alkene and transfer of *two* hydrogen atoms to the fragment containing the oxygen atoms, which in essence is the protonated carboxylic acid.

Esters of dibasic acids $ROOC(CH_2)_nCOOR$, in general, give recognizable molecular ion peaks. Intense peaks are found at $[ROOC(CH_2)_nC{=}O]^+$ and at $[ROOC(CH_2)_n]^+$.

1.6.7.2 Benzyl and Phenyl Esters. Benzyl acetate (also furfuryl acetate and other similar acetates) and phenyl acetate eliminate the neutral molecule ketene (Scheme 1.24); frequently this gives rise to the base peak.

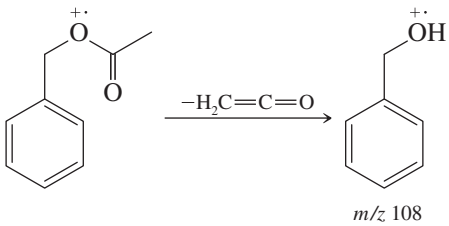

(Sch 1.24)

Of course, the m/z 43 peak $(CH_3C{=}O)^+$ and m/z 91 $(C_7H_7)^+$ peaks are prominent for benzyl acetate.

1.6.7.3 Esters of Aromatic Acids. The molecular ion peak of methyl esters of aromatic acids is prominent ($ArCOOR, R{=}CH_3$). As the size of the alcohol moiety increases, the intensity of the molecular ion peak decreases rapidly to practically zero at C_5. The base peak results from elimination of $\cdot OR$, and elimination of $\cdot COOR$ accounts for another prominent peak. In methyl esters, these peaks are at M − 31 and M − 59, respectively.

As the alkyl moiety increases in length, three modes of cleavage become important: (1) McLafferty rearrangement, (2) rearrangement of two hydrogen atoms with elimination of an allylic radical, and (3) retention of the positive charge by the alkyl group.

The familiar McLafferty rearrangement pathway gives rise to a peak for the aromatic acid, $(ArCOOH)^+$. The second, similar pathway gives the protonated aromatic acid, $(ArCOOH_2)^+$. The third mode of cleavage gives the alkyl cation, R^+.

Appropriately, *ortho*-substituted benzoates eliminate ROH through the general *"ortho"* effect described above under aromatic acids. Thus, the base peak in the spectrum of methyl salicylate is m/z 120; this ion eliminates carbon monoxide to give a strong peak at m/z 92.

A strong characteristic peak at mass 149 is found in the spectra of all esters of phthalic acid, starting with the diethyl

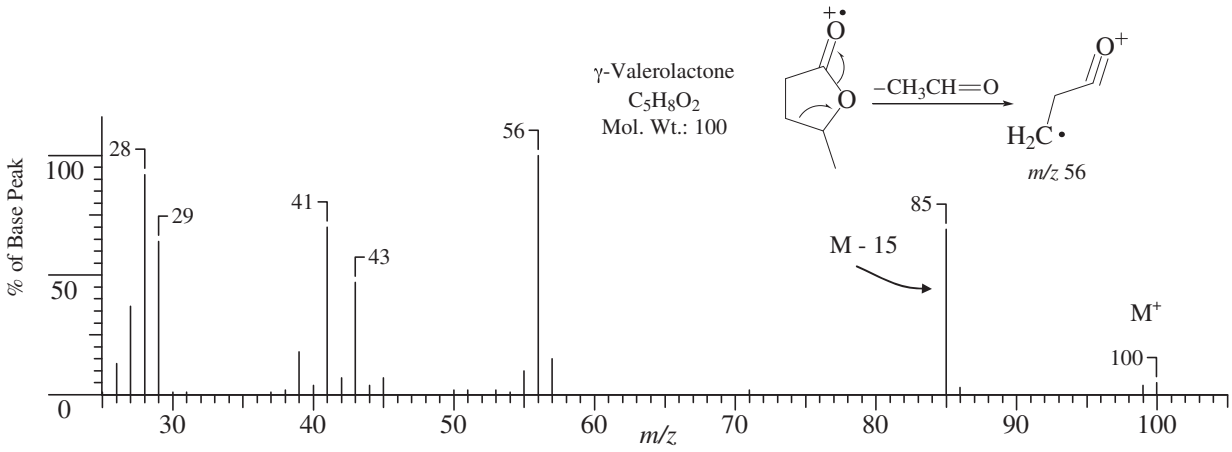

FIGURE 1.33 EI mass spectrum of γ-valerolactone.

ester. This peak is not significant in the dimethyl or methyl ethyl ester of phthalic acid, nor in esters of isophthalic or terephthalic acids, all of which give the expected peaks at $M-R, M-2R, M-CO_2R$, and $M-2CO_2R$. Since long-chain phthalate esters are widely used as plasticizers, a strong peak at m/z 149 may indicate contamination. The m/z 149 fragment (essentially a protonated phthalic anhydride) is probably formed by two ester cleavages involving the shift of two hydrogen atoms and then another hydrogen atom, followed by elimination of H_2O.

1.6.8 Lactones

The molecular ion peak of five-membered ring lactones is distinct but is weaker when an alkyl substituent is present at C_4. Facile cleavage of the side chain at C_4 (guidelines 3 and 8, Section 1.5.4) gives a strong peak at M − alkyl.

The base peak (m/z 56) of γ-valerolactone (Figure 1.33) and the same strong peak of butyrolactone are rationalized, which shows the elimination of acetaldehyde.

Labeling experiments indicate that some of the m/z 56 peak in γ-valerolactone arises from the $C_4H_8{}^+$ ion. The other intense peaks in γ-valerolactone are at m/z 27 ($C_2H_3{}^+$), 28 ($C_2H_4{}^+$), 29 ($C_2H_5{}^+$), 41 ($C_3H_5{}^+$), and 43 ($C_3H_7{}^+$), and 85 ($C_4H_5O_2{}^+$, loss of the methyl group). In butyrolactone, there are strong peaks at m/z 27, 28, 29, 41, and 42 ($C_3H_6{}^+$).

1.6.9 Amines

1.6.9.1 Aliphatic Amines. The molecular ion peak of an aliphatic monoamine is an odd number, but it is usually quite weak and, in long-chain or highly branched amines, undetectable. The base peak frequently results from C—C cleavage next to the nitrogen atom (α, β guideline 8, Section 1.5.4); for primary amines unbranched at the α-carbon, this is m/z 30 ($CH_2NH_2{}^+$) shown in Scheme 1.25. This cleavage accounts for the base peak in all primary amines and secondary and tertiary amines that are not branched at the α-carbon. Loss of the largest branch ($\cdot R''$ in Scheme 1.25) from the α-C atom is preferred.

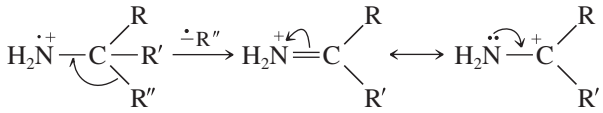

(Sch 1.25)

When branching at the α-carbon is absent, an M − 1 peak is usually visible. This is the same type of cleavage noted above for alcohols. The effect is more pronounced in amines because of the better resonance stabilization of the ion fragment by the less electronegative N atom compared with the O atom.

Primary straight-chain amines show a homologous series of peaks of progressively decreasing intensity (the cleavage at the ϵ-bond is slightly more important than at the neighboring bonds) at m/z 30, 44, 58,…resulting from cleavage at C—C bonds successively removed from the nitrogen atom with retention of the charge on the *N*-containing fragment. These peaks are accompanied by the hydrocarbon pattern of C_nH_{2n+1}, C_nH_{2n}, and C_nH_{2n-1} ions. Thus, we note characteristic clusters at intervals of 14 mass units, each cluster containing a peak resulting from a $C_nH_{2n+2}N$ ion. Because of the very facile cleavage to form the base peak, the fragmentation pattern in the high mass region becomes extremely weak.

Cyclic fragments apparently occur during the fragmentation of longer chain amines. The fragment shown in Scheme 1.26 gives a six-membered ring; five-membered rings are also commonly formed.

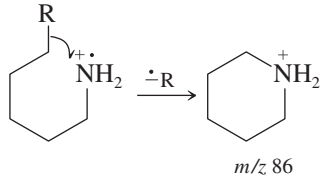

(Sch 1.26)

A peak at m/z 30 is good though not conclusive evidence for a straight-chain primary amine. Further decomposition of the first-formed ion from a secondary or tertiary amine leads to a peak at m/z 30, 44, 58, 72, …. This is a process similar to that described for aliphatic alcohols and ethers above and, similarly, is enhanced by branching at one of the α-carbon atoms.

Cleavage of amino acid esters occurs at both C—C bonds (dashed lines below) next to the nitrogen atom; loss of the carbalkoxy group (—COOR′) is preferred. The aliphatic amine fragment ($^{+}NH_2{=}CHCH_2CH_2R$) decomposes further to give a peak at m/z 30.

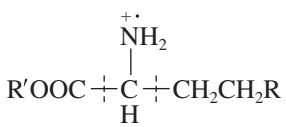

1.6.9.2 Cyclic Amines. In contrast to acyclic amines, the molecular ion peaks of cyclic amines are usually intense unless there is substitution at the α position; for example, the molecular ion peak of pyrrolidine is strong. Primary cleavage at the bonds next to the N atom leads either to loss of an α-hydrogen atom to give a strong M − 1 peak or to opening of the ring; the latter event is followed by elimination of ethylene to give $\cdot CH_2{-}{}^{+}NH{=}CH_2$ (m/z 43, base peak), hence by loss of a hydrogen atom to give $CH_2{=}N^{+}{=}CH_2$ (m/z 42). *N*-methyl pyrrolidine also gives a $C_2H_4N^{+}$ (m/z 42) peak, apparently by more than one pathway.

Piperidine likewise shows a strong molecular ion and M − 1 (base) peak. Ring opening followed by several available sequences leads to characteristic peaks at m/z 70, 57, 56, 44, 43, 42, 30, 29, and 28. Substituents are cleaved from the ring (guideline 6, Section 1.5.4).

1.6.9.3 Aromatic Amines (Anilines). The molecular ion peak (odd number) of an aromatic monoamine is intense. Loss of one of the amino H atoms of aniline gives a moderately intense M − 1 peak; loss of a neutral molecule of HCN followed by loss of a hydrogen atom gives prominent peaks at m/z 66 and 65, respectively.

It was noted above that cleavage of alkyl aryl ethers occurs with rearrangement involving cleavage of the ArO—R bond: that is, cleavage was controlled by the ring rather than by the oxygen atom. In the case of alkyl aryl amines, cleavage of the C—C bond next to the nitrogen atom is dominant (Scheme 1.27): that is, the heteroatom controls cleavage.

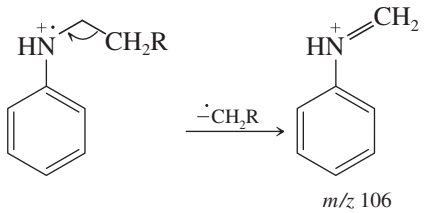

(Sch 1.27)

1.6.10 Amides

1.6.10.1 Aliphatic Amides. The molecular ion peak of straight-chain monoamides is usually discernible. The dominant modes of cleavage depend on the length of the acyl moiety and on the lengths and number of the alkyl groups attached to the nitrogen atom.

The base peak (m/z 59, $H_2NC(=OH^{+})CH_2^{\cdot}$) in all straight-chain primary amides higher than propionamide results from the familiar McLafferty rearrangement. Branching at the α-carbon (CH_3, etc.) gives a homologous peak at m/z 73 or 87, ….

Primary amides give a strong peak at m/z 44 from cleavage of the R—$CONH_2$ bond: ($O{=}C{=}{}^{+}NH_2$); this is the base peak in C_1—C_3 primary amides and in isobutyramide. A moderate peak at m/z 86 results from γ,δ C—C cleavage, possibly accompanied by cyclization (Scheme 1.28).

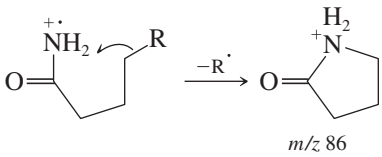

(Sch 1.28)

Secondary and tertiary amides with an available hydrogen on the γ-carbon of the acyl moiety and methyl groups on the N atom show the dominant peak resulting from the McLafferty rearrangement. When the *N*-alkyl groups are C_2 or longer and the acyl moiety is shorter than C_3, another mode of cleavage predominates. This is cleavage of the *N*-alkyl group β to the nitrogen atom, and cleavage of the carbonyl C—N bond with migration of an α-hydrogen atom of the acyl moiety (expelling a neutral ketene molecule) and leaving $^{+}NH_2{=}CH_2$ (m/z 30).

1.6.10.2 Aromatic Amides. Benzamide (Figure 1.1) is a typical example. Loss of NH_2 from the molecular ion yields a resonance-stabilized benzoyl cation that in turn undergoes cleavage to a phenyl cation. A separate fragmentation pathway gives rise to a modest m/z 44 peak.

1.6.11 Aliphatic Nitriles

The molecular ion peaks of aliphatic nitriles (except for acetonitrile and propionitrile) are weak or absent, but the M + 1 peak can usually be located by its behavior on increasing the sample size (Section 1.5.2.1). A weak but diagnostically useful M − 1 peak is formed by loss of an α-hydrogen to form the stable ion: $RCH{=}C{=}N^{+}$.

The base peak of straight-chain nitriles between C4 and C9 is m/z 41. This peak corresponds to the ion resulting from hydrogen rearrangement in a six-membered transition state, similar to a McLafferty rearrangement giving a peak at m/z 41 $CH_2{=}C{=}N^{+}{-}H$. However, this peak lacks diagnostic value because of the presence of $C_3H_5^{+}$ (m/z 41) for all molecules containing a hydrocarbon chain.

A peak at m/z 97 is characteristic and intense (sometimes the base peak) in straight-chain nitriles C_8 and higher.

The mechanism depicted in Scheme 1.29 has been proposed to account for this ion.

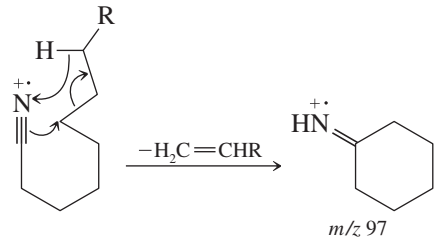

(Sch 1.29)

Simple cleavage at each C—C bond (except the one next to the N atom) gives a characteristic series of homologous peaks of even mass number down the entire length of the chain (m/z 40, 54, 68, 82, …) resulting from the $(CH_2)_nC{\equiv}N^+$ ions. Accompanying these peaks are the usual peaks of the hydrocarbon pattern.

1.6.12 Nitro Compounds

1.6.12.1 Aliphatic Nitro Compounds. The molecular ion peak (odd number) of an aliphatic mononitro compound is weak or absent (except in the lower homologs). The main peaks are attributable to the hydrocarbon fragments up to $M - NO_2$. Presence of a nitro group is indicated by an appreciable peak at m/z 30 (NO^+) and a smaller peak at mass 46 ($NO_2{}^+$).

1.6.12.2 Aromatic Nitro Compounds. The molecular ion peak of aromatic nitro compounds (odd number for one N atom) is strong. Prominent peaks result from elimination of an NO_2 radical (M − 46, the base peak in nitrobenzene), and of a neutral NO molecule with rearrangement to form the phenoxy cation (M − 30); both are good diagnostic peaks. Loss of acetylene from the M − 46 ion accounts for a strong peak at M − 72; loss of CO from the M − 30 ion gives a peak at M − 58. A diagnostic peak at m/z 30 results from the NO^+ ion.

The isomeric *o*-, *m*-, and *p*-nitroanilines each give a strong molecular ion (even number). They all give prominent peaks resulting from two sequences. The first pathway entails a loss of an NO_2 group (M − 46) to give an m/z 92; this ion loses HCN to give an m/z 65. The second sequence records a loss of NO (M − 30) to give m/z 108, which loses CO to give m/z 80.

Aside from differences in intensities, the three isomers give very similar spectra. The *meta* and *para* compounds give a small peak at m/z 122 from loss of an O atom, whereas the *ortho* compound eliminates OH as depicted in Scheme 1.30 to give a small peak at m/z 121.

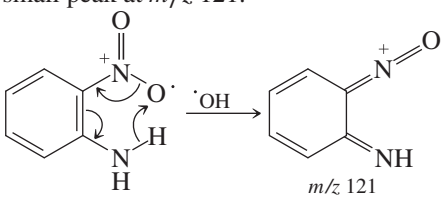

(Sch 1.30)

1.6.13 Aliphatic Nitrites

The molecular ion peak (odd number) of aliphatic nitrites (one N present) is weak or absent. The peak at m/z 30 (NO^+) is always large and is often the base peak. There is a large peak at m/z 60 ($CH_2{=}{=}{}^+ONO$) in all nitrites unbranched at the α-carbon; this represents cleavage of the C—C bond next to the ONO group. An α branch can be identified by a peak at m/z 74, 88, or 102 …. Absence of a large peak at m/z 46 permits differentiation from nitro compounds. Hydrocarbon peaks are prominent, and their distribution and intensities describe the arrangement of the carbon chain.

1.6.14 Aliphatic Nitrates

The molecular ion peak (odd number) of aliphatic nitrates (one nitrogen present) is weak or absent. A prominent (frequently the base) peak is formed by cleavage of the C—C bond next to the ONO_2 group with loss of the heaviest alkyl group attached to the α-carbon. The $NO_2{}^+$ peak at m/z 46 is also prominent. As in the case of aliphatic nitrites, the hydrocarbon fragment ions are distinct.

1.6.15 Sulfur Compounds

The contribution (4.4%, see Table 1.3 and Figure 1.34) of the ^{34}S isotope to the M + 2 peak, and often to a (fragment + 2) peak, affords ready recognition of sulfur-containing compounds. A homologous series of sulfur containing fragments is four mass units higher than the hydrocarbon fragment series. The number of sulfur atoms can be determined from the size of the contribution of the ^{34}S isotope to the M + 2 peak. The mass of the sulfur atom(s) present is subtracted from the molecular weight. In diisopentyl disulfide, for example, the molecular weight is 206, and the molecule contains two sulfur atoms. The formula for the rest of the molecule is therefore found under mass 142, that is, $206 - (2 \times 32)$.

1.6.15.1 Aliphatic Mercaptans (Thiols). The molecular ion peak of aliphatic mercaptans, except for higher tertiary mercaptans, is usually strong enough so that the M + 2 peak can be accurately measured. In general, the cleavage modes resemble those of alcohols. Cleavage of the C—C bond (α,β-bond) next to the SH group gives the characteristic ion $CH_2{=}{=}SH^+$ (m/z 47). Sulfur is poorer than nitrogen, but better than oxygen, at stabilizing such a fragment. Cleavage at the β,γ bond gives a peak at m/z 61 of about one-half the intensity of the m/z 47 peak. Cleavage at the γ,δ-bond gives a small peak at m/z 75, and cleavage at the δ,ϵ-bond gives a peak at m/z 89 that is more intense than the peak at m/z 73; presumably the m/z 89 ion is stabilized by cyclization:

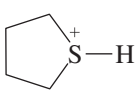

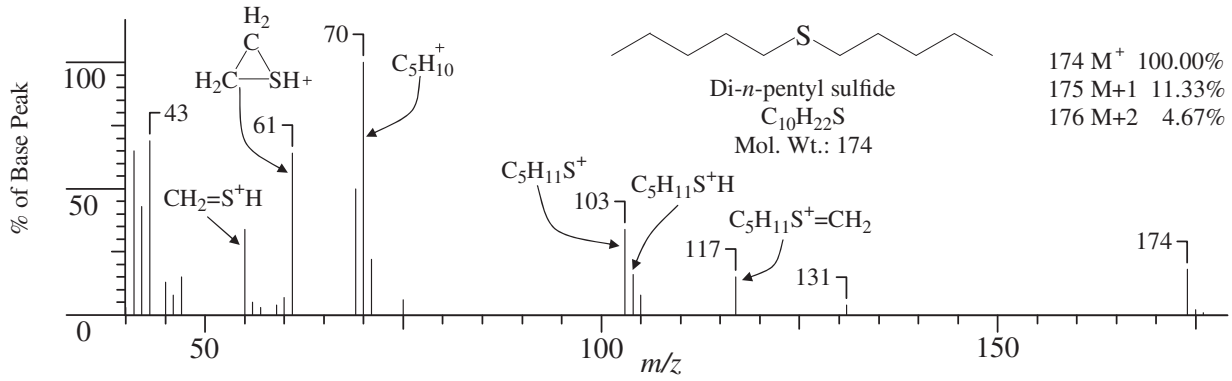

FIGURE 1.34 EI mass spectrum of di-*n*-pentyl sulfide.

Again analogous to alcohols, primary mercaptans fragment to give H_2S and a strong M − 34 peak, the resulting ion then eliminating ethylene: thus the homologous series $M - H_2S - (CH_2{=}CH_2)_n$ arises.

Secondary and tertiary mercaptans cleave at the α-carbon atom with loss of the largest group to give a prominent peak $M - CH_3, M - C_2H_5, M - C_3H_7, \ldots$. However, a peak at m/z 47 may also appear as a rearrangement peak of secondary and tertiary mercaptans. A peak at M − 33 (loss of HS) is usually present for secondary mercaptans.

In long-chain mercaptans, the hydrocarbon pattern is superimposed on the mercaptan pattern. As for alcohols, the alkenyl peaks (i.e., m/z 41, 55, 69, …) are as intense or even more so than the alkyl peaks (m/z 43, 57, 71, …).

1.6.15.2 Aliphatic Sulfides. The molecular ion peak of aliphatic sulfides is usually intense enough so that the M + 2 peak can be accurately measured. The cleavage modes generally resemble those of ethers. Cleavage of one or the other of the α, β C—C bonds occurs, with loss of the largest group being favored. These first-formed ions decompose further with hydrogen transfer and elimination of an alkene. The steps for aliphatic ethers also occur for sulfides (Scheme 1.31); the end result is the ion $RCH{=}SH^+$ (see Figure 1.34 for an example.)

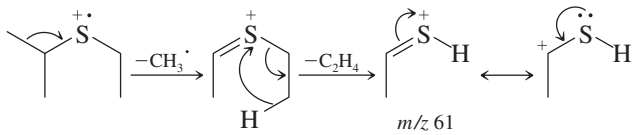

(Sch 1.31)

For a sulfide unbranched at either δ-carbon atom, this ion is $CH_2{=}SH^+$ (m/z 47), and its intensity may lead to confusion with the same ion derived from a mercaptan. However, the absence of $M - H_2S$ or M − SH peaks in sulfide spectra makes the distinction.

A moderate to strong peak at m/z 61 is present (see alkyl sulfide cleavage, Figure 1.34) in the spectrum of all except tertiary sulfides. When an α-methyl substituent is present, m/z 61 is the ion $CH_3CH{=}SH^+$, resulting from the double cleavage. Methyl primary sulfides cleave at the α, β-bond to give the m/z 61 ion, $CH_3{-}S^+{=}CH_2$.

However, a strong m/z 61 peak in the spectrum of a straight-chain sulfide calls for a different explanation. Scheme 1.32 offers a plausible explanation.

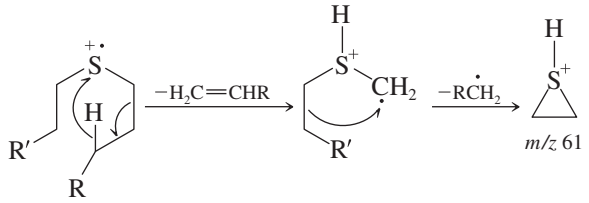

(Sch 1.32)

Sulfides give a characteristic ion by cleavage of the C—S bond with retention of charge on sulfur. The resulting RS^+ ion gives a peak at m/z $32 + CH_3, 32 + C_2H_5, 32 + C_3H_7, \ldots$. The ion of m/z 103 seems especially favored possibly because of formation of a rearranged cyclic ion (Scheme 1.33). These features are illustrated by the spectrum of di-*n*-pentyl sulfide (Figure 1.34).

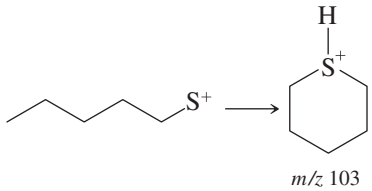

(Sch 1.33)

As with long-chain ethers, the hydrocarbon pattern may dominate the spectrum of long-chain sulfides; the C_nH_{2n} peaks seem especially prominent. In branched chain sulfides, cleavage at the branch may reduce the relative intensity of the characteristic sulfide peaks.

1.6.15.3 Aliphatic Disulfides. The molecular ion peak for at least up to C_{10} disulfides is strong. A major peak found in these spectra results from cleavage of one of the C—S bonds with retention of the charge on the alkyl fragment. Another major peak results from the same cleavage along

with a shift of a hydrogen atom to form the RSSH fragment, which retains the charge. Other peaks apparently result from cleavage between the sulfur atoms without rearrangement, and with migration of one or two hydrogen atoms to give, respectively, RS^+, $RS^+ - 1$, and $RS^+ - 2$.

1.6.16 Halogen Compounds

A compound that contains one chlorine atom will have an M + 2 peak approximately one-third the intensity of the molecular ion peak because of the presence of a molecular ion containing the ^{37}Cl isotope (see Table 1.4). A compound that contains one bromine atom will have an M + 2 peak almost equal in intensity to the molecular ion because of the presence of a molecular ion containing the ^{81}Br isotope. A compound that contains two chlorines, or two bromines, or one chlorine and one bromine will show a distinct M + 4 peak, in addition to the M + 2 peak, because of the presence of a molecular ion containing two atoms of the heavy isotope. In general, the number of chlorine and/or bromine atoms in a molecule can be ascertained by the number of alternate peaks beyond the molecular ion peak. Thus, three chlorine atoms in a molecule will give peaks at M + 2, M + 4, and M + 6; in polychloro compounds, the peak of highest mass may be so weak as to escape notice.

The relative abundances of the peaks (molecular ion, M + 2, M + 4, and so on) have been calculated by Beynon et al. (1968) for compounds containing chlorine and bromine (atoms other than chlorine and bromine were ignored). A portion of these results is presented here, somewhat modified, as Table 1.5. We can now tell what combination of chlorine and bromine atoms is present. It should be noted that Table 1.5 presents the isotope contributions in terms of percent of the molecular ion peak. Figure 1.35 provides the corresponding bar graphs.

As required by Table 1.5, the M + 2 peak in the spectrum of *p*-chlorobenzophenone (Figure 1.29) is about one-third the intensity of the molecular ion peak (m/z 218). As mentioned earlier, the chlorine containing fragments (m/z 141 and 113) show [fragment + 2] peaks of the proper intensity.

TABLE 1.5 Intensities of Isotope Peaks (Relative to the Molecular Ion) for Combinations of Chlorine and Bromine

Halogen Present	% M + 2	% M + 4	% M + 6	% M + 8	% M + 10	% M + 12
Cl	32.6					
Cl_2	65.3	10.6				
Cl_3	97.8	31.9	3.5			
Cl_4	131.0	63.9	14.0	1.2		
Cl_5	163.0	106.0	34.7	5.7	0.4	
Cl_6	196.0	161.0	69.4	17.0	2.2	0.1
Br	97.9					
Br_2	195.0	95.5				
Br_3	293.0	286.0	93.4			
BrCl	130.0	31.9				
$BrCl_2$	163.0	74.4	10.4			
Br_2Cl	228.0	159.0	31.2			

Unfortunately, the application of isotope contributions, though generally useful for aromatic halogen compounds, is limited by the weak molecular ion peak of many aliphatic halogen compounds of more than about six carbon atoms for a straight chain, or fewer for a branched chain. However, the halogen-containing fragments are recognizable by the ratio of the (fragment + 2) peaks to fragment peaks in monochlorides or monobromides. In polychloro or polybromo compounds, these (fragment + isotope) peaks form a distinctive series of multiplets (Figure 1.36). Coincidence of a fragment ion with one of the isotope fragments, with another disruption of the characteristic ratios, must always be kept in mind.

1.6.16.1 Aliphatic Chlorides. The molecular ion peak is detectable only in the lower monochlorides. Fragmentation of the molecular ion is mediated by the chlorine atom but to a much lesser degree than is the case in oxygen-, nitrogen-, or sulfur-containing compounds. Thus, cleavage of a straight-chain monochloride at the C—C bond adjacent to the chlorine atom accounts for a small peak at m/z 49, $CH_2{=}Cl^+$ (and, of course, the isotope peak at m/z 51).

Cleavage of the C—Cl bond leads to a small Cl^+ peak and to a R^+ peak, which is prominent in the lower chlorides but quite small when the chain is longer than about C_5.

Straight-chain chlorides longer than C_6 give $C_3H_6Cl^+$, $C_4H_8Cl^+$, and $C_5H_{10}Cl^+$ ions. Of these, the $C_4H_8Cl^+$ ion forms the most intense (sometimes the base) peak; a five-membered cyclic structure (Scheme 1.34) may explain its stability.

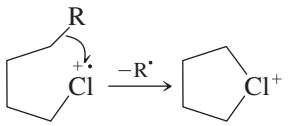

(Sch 1.34)

Loss of HCl occurs, possibly by 1,3 elimination, to give a peak (weak or moderate) at M − 36.

In general, the spectrum of an aliphatic monochloride is dominated by the hydrocarbon pattern to a greater extent than that of a corresponding alcohol, amine, or mercaptan.

1.6.16.2 Aliphatic Bromides. The remarks under aliphatic chlorides apply quite generally to the corresponding bromides.

1.6.16.3 Aliphatic Iodides. Aliphatic iodides give the strongest molecular ion peak of the aliphatic halides. Since iodine is monoisotopic, there is no distinctive isotope peak. The presence of an iodine atom can sometimes be deduced from isotope peaks that are suspiciously low in relation to the molecular ion peaks, and from several distinctive peaks; in polyiodo compounds, the large interval between major peaks is characteristic.

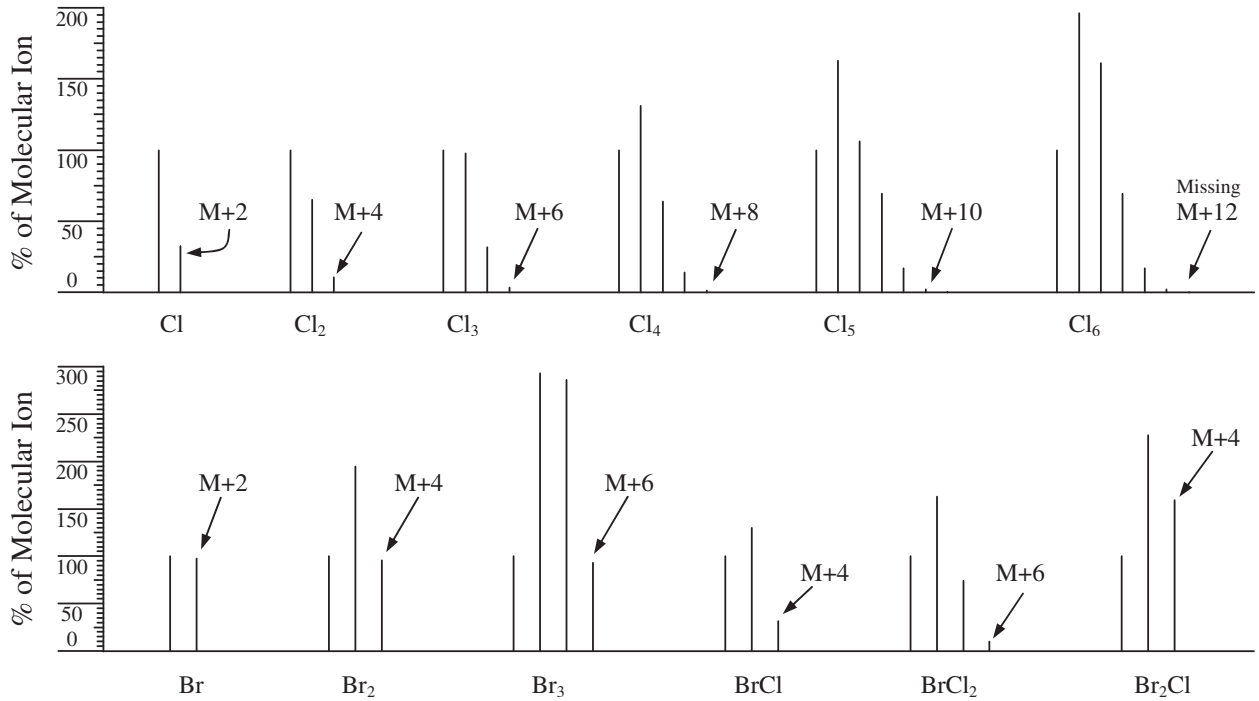

FIGURE 1.35 Predicted patterns of M, M + 2, M + 4, … for compounds with various combinations of chlorine and bromine.

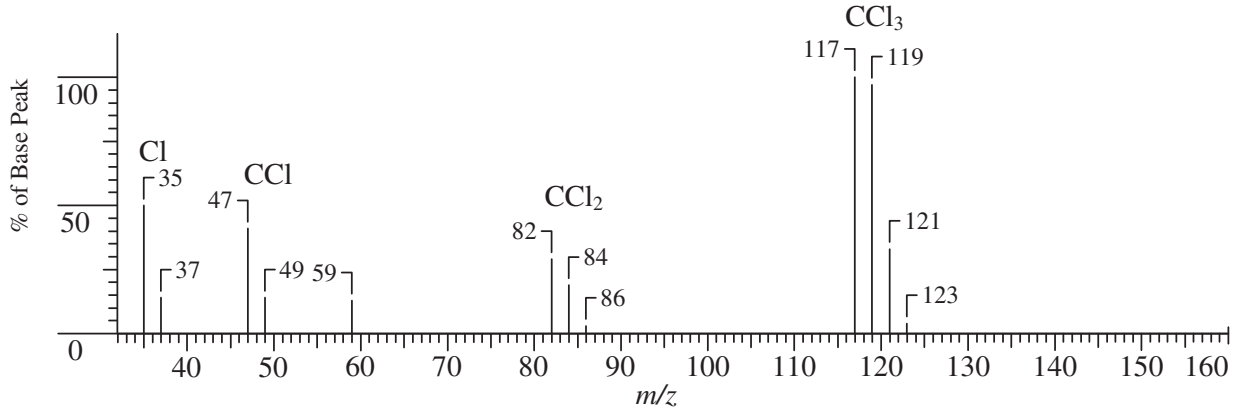

FIGURE 1.36 EI mass spectrum of carbon tetrachloride (CCl_4).

Iodides cleave much as do chlorides and bromides, but the $C_4H_8I^+$ ion is not as evident as the corresponding chloride and bromide ions.

1.6.16.4 Aliphatic Fluorides. Aliphatic fluorides give the weakest molecular ion peak of the aliphatic halides. Fluorine is monoisotopic, and its detection in polyfluoro compounds depends on suspiciously small isotopic peaks relative to the molecular ion, on the intervals between peaks, and on characteristic peaks. Of these, the most characteristic is m/z 69 resulting from the ion CF_3^+, which is the base peak in all perfluorocarbons. Prominent peaks are noted at m/z 119, 169, 219…; these are increments of CF_2. The stable ions $C_3F_5^+$ and $C_4F_7^+$ give large peaks at m/z 131 and 181. The M − F peak is frequently visible in perfluorinated compounds. In monofluorides, cleavage of the α,β C—C bond is less important than in the other monohalides, but cleavage of a C—H bond on the α-carbon atom is more important. This reversal is a consequence of the high electronegativity of the F atom and is rationalized by placing the positive charge on the α-carbon atom. The secondary carbonium ion thus depicted in Scheme 1.35 by a loss of a hydrogen atom is more stable than the primary carbonium ion resulting from loss of an alkyl radical.

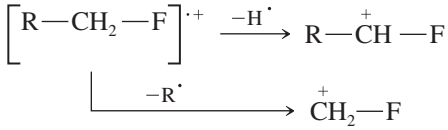

(Sch 1.35)

1.6.16.5 Benzyl Halides. The molecular ion peak of benzyl halides is usually detectable. The benzyl (or tropylium) ion from loss of the halide (guideline 8, Section 1.5.4) is favored even over β-bond cleavage of an alkyl substituent. A substituted phenyl ion (α-bond cleavage) is prominent when the ring is polysubstituted.

1.6.16.6 Aromatic Halides. The molecular ion peak of an aryl halide is readily apparent. The M – X peak is large for all compounds in which X is attached directly to the ring.

1.6.17 Heteroaromatic Compounds

The molecular ion peak of heteroaromatics and alkylated heteroaromatics is intense. Cleavage of the bond β to the ring, as in alkylbenzenes, is the general rule; in pyridine, the position of substitution determines the ease of cleavage of the β-bond (see below).

Localizing the charge of the molecular ion on the heteroatom, rather than in the ring π structure, provides a satisfactory rationale for the observed mode of cleavage. The present treatment follows that used by Djerassi (Budzikiewicz et al., 1967).

The five-membered ring heteroaromatics (furan, thiophene, and pyrrole) show very similar ring cleavage patterns. The first step in each case is cleavage of the carbon-heteroatom bond, followed by loss of either a neutral acetylene molecule or by loss of radical fragments. Thus, furan exhibits two principal peaks: $C_3H_3^+$(m/z 39) and $HC{\equiv}O^+$ (m/z 29). For thiophene, there are three peaks, $C_3H_3^+$(m/z 39), $HC{\equiv}S^+$ (m/z 45), and $C_2H_2S^+$ (m/z 58). For pyrrole, there are three peaks: $C_3H_3^+$(m/z 39), $HC{=}NH^+$ (m/z 28) and $C_2H_2\ NH^+$ (m/z 41). Pyrrole also eliminates a neutral molecule of HCN to give an intense peak at m/z 40. The base peak of 2,5-dimethylfuran is m/z 43 ($CH_3C{\equiv}O^+$).

Cleavage of the β C—C bond in alkylpyridines (Scheme 1.36) depends on the position of the ring substitution, being more pronounced when the alkyl group is in the 3 position. An alkyl group of more than three carbon atoms in the 2 position can undergo migration of a hydrogen atom to the ring nitrogen.

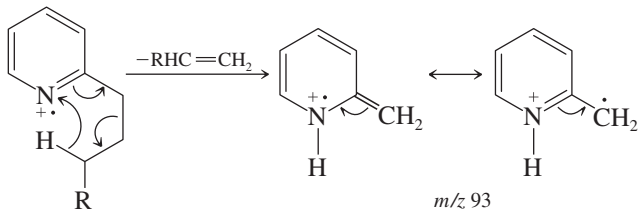

(Sch 1.36)

A similar cleavage is found in pyrazines since all ring substituents are necessarily ortho to one of the nitrogen atoms.

REFERENCES

For a list of Chapter References, please visit: www.wiley.com/college/silverstein.

STUDENT EXERCISES

1.1 Using Table 1.4, calculate the exact mass for the compounds below (**a** – **o**).

1.2 Determine the index of hydrogen deficiency for the compounds below.

1.3 Write the structure for the molecular ion for each compound (**a** – **o**) showing, when possible, the location of the radical cation.

1.4 Predict three major fragmentation/rearrangement pathways for the compounds below. For each pathway, cite the guideline from Section 1.5.4 that supports your prediction.

1.5 For each fragmentation/rearrangement pathway from exercise 1.4, show a detailed mechanism using either single barbed or double barbed arrows as appropriate.

1.6 Match each of the exact masses to the mass spectra shown on the following pages (labelled **A – W**). Note that two compounds have the same exact mass, and you will need to consider the CI mass spectrum when given. The masses are: (a) 56.0264, (b) 73.0896, (c) 74.0363, (d) 89.0479, (e) 94.0535, (f) 96.0572, (g) 98.0736, (h) 100.0893, (i) 102.0678, (j) 113.0845, (k) 114.1043, (l) 116.0841, (m) 116.1206, (n) 122.0733, (o) 122.0733, (p) 126.1041, (q) 138.0687, (r) 150.0041, (s) 152.0476, (t) 156.9934, (u) 161.9637, (v) 169.9735, (w) 208.0094.

1.7 For each of the mass spectra (**A**–**W**), determine if there are any of the following heteroatoms in the compound: S, Cl, Br.

1.8 For each exact mass corresponding to mass spectra **A**–**W**, determine the molecular formula. Remember to look at the heteroatoms that were determined in exercise 1.7.

1.9 Determine the index of hydrogen deficiency for each of the formulas in exercise 1.6.

1.10 List the base peak and molecular ion peak for each of the EI mass spectra (**A** – **W**).

1.11 Choose three ions (besides the molecular ion) from each EI mass spectrum (**A** – **W**, except for H), determine the molecular formula for each fragment ion, and give the molecular formula for the portion that is lost from the molecular ion. Indicate which ions result from a rearrangement.

Exercise 1.1

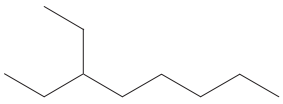

a

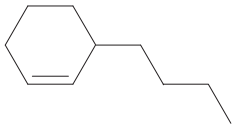

b

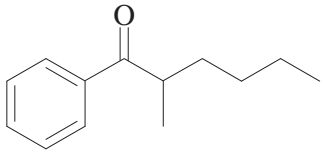

c

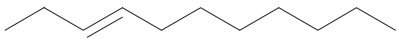

d

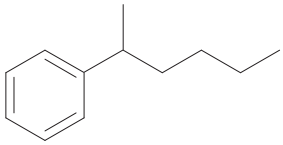

e

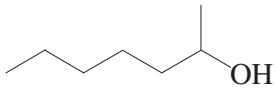

f

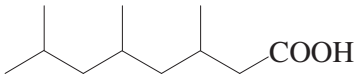

g

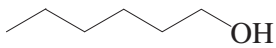

h

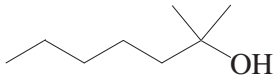

i

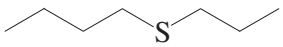

j

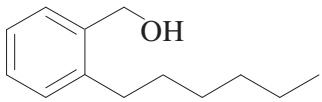

k

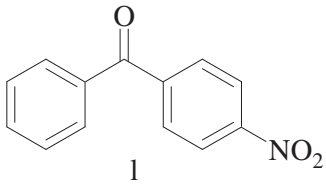

l

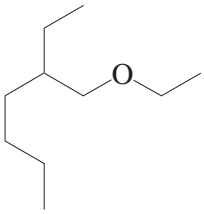

m

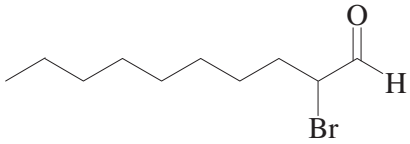

n

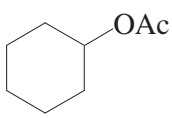

o

A

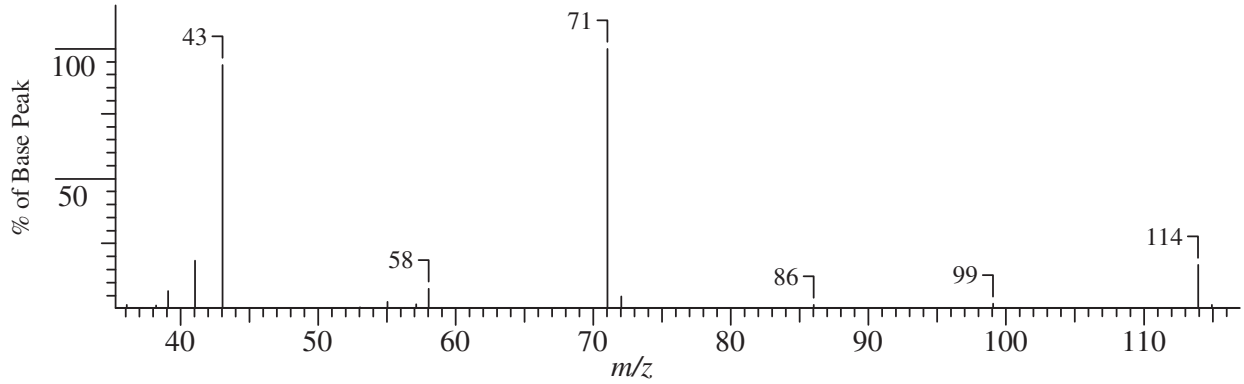

B

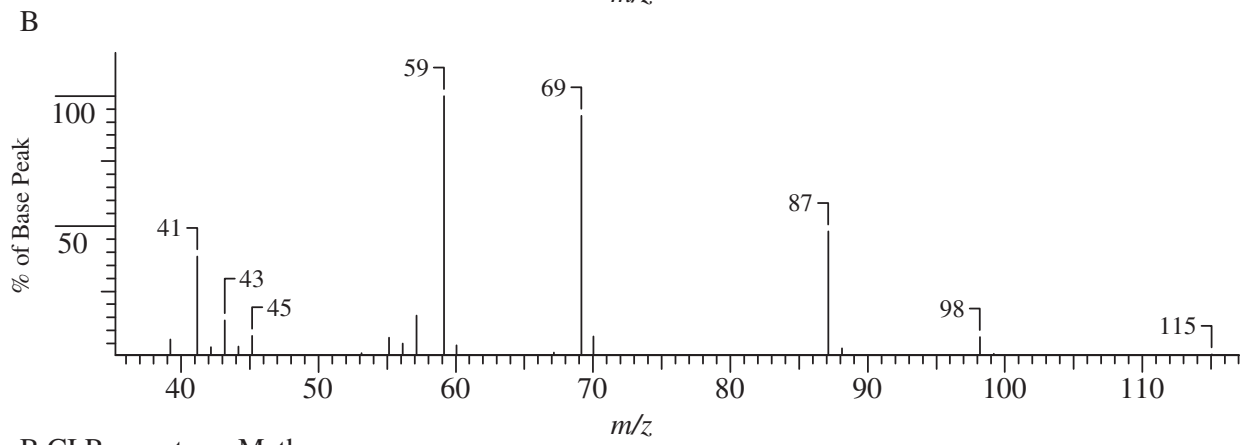

B CI Reagent gas Methane

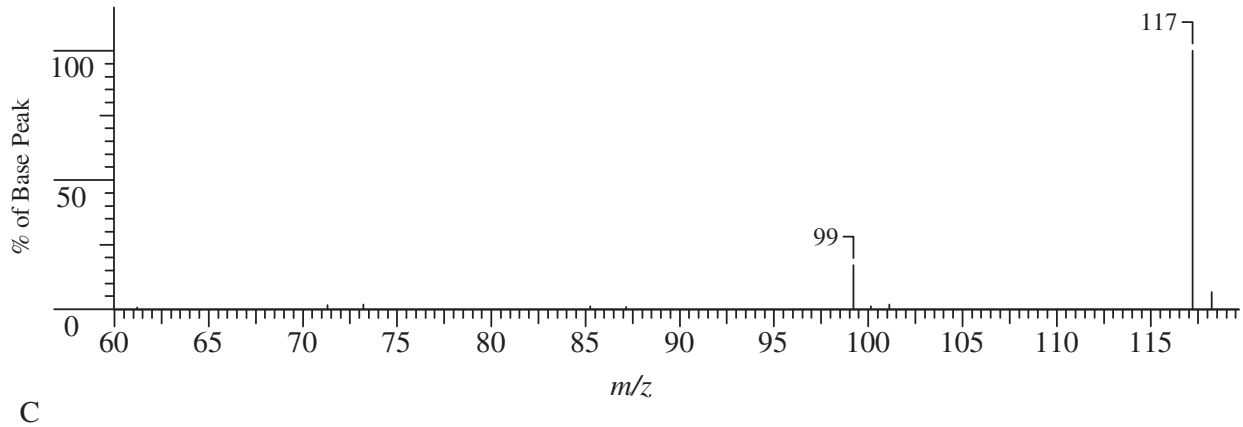

C

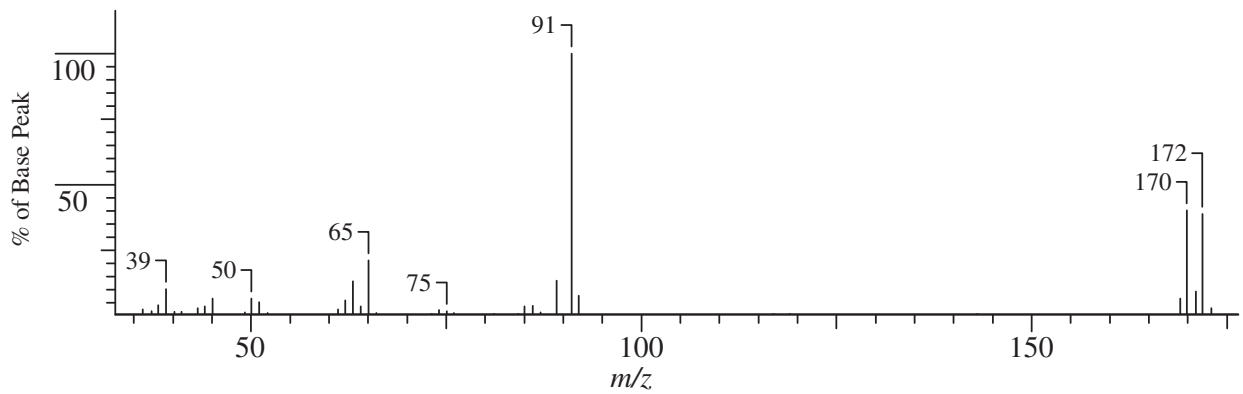

D

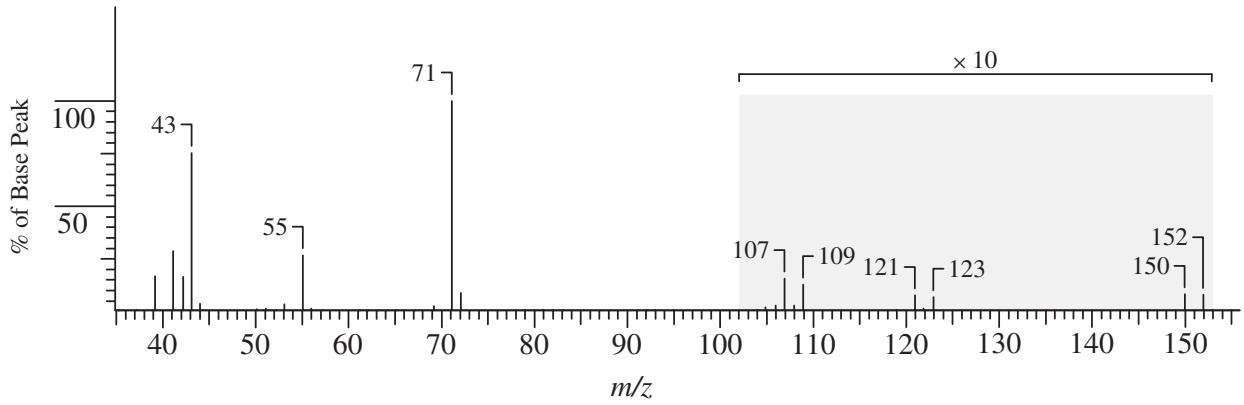
% of Base Peak
100
50
43
55
71
× 10
107
109
121
123
150
152
40 50 60 70 80 90 100 110 120 130 140 150
m/z

E

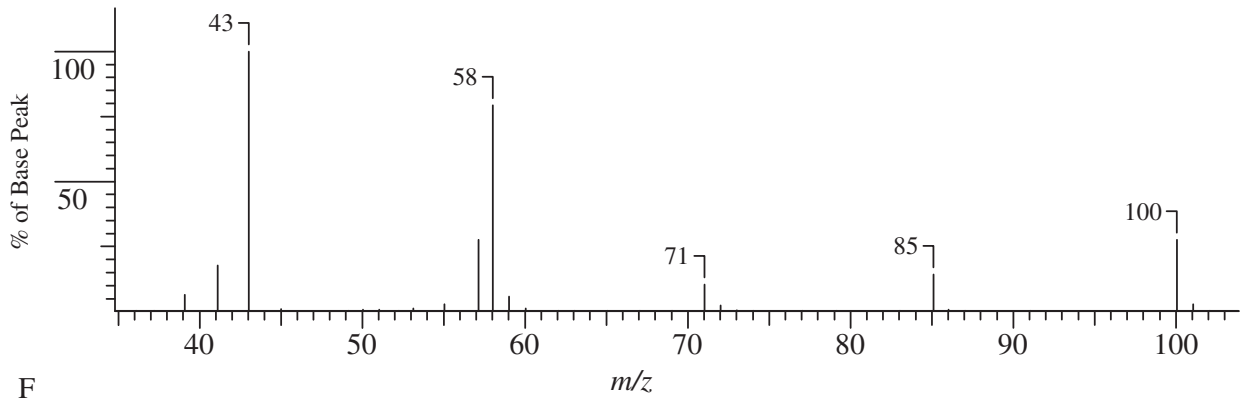
% of Base Peak
100
50
43
58
71
85
100
40 50 60 70 80 90 100
m/z

F

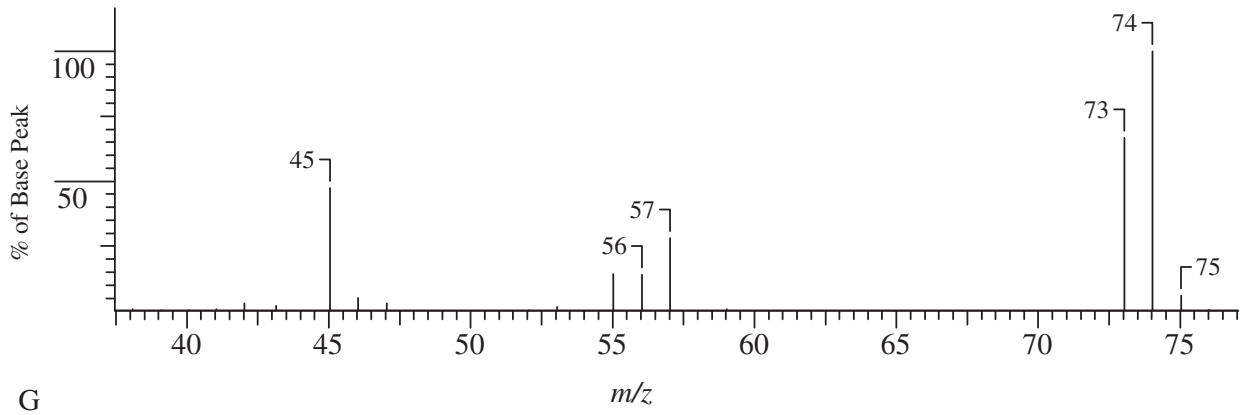
% of Base Peak
100
50
45
56
57
73
74
75
40 45 50 55 60 65 70 75
m/z

G

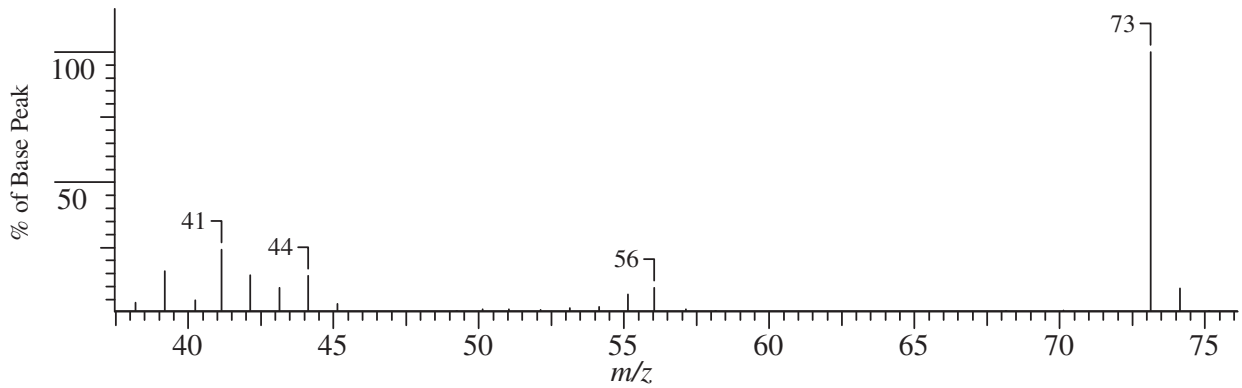
% of Base Peak
100
50
41
44
56
73
40 45 50 55 60 65 70 75
m/z

H

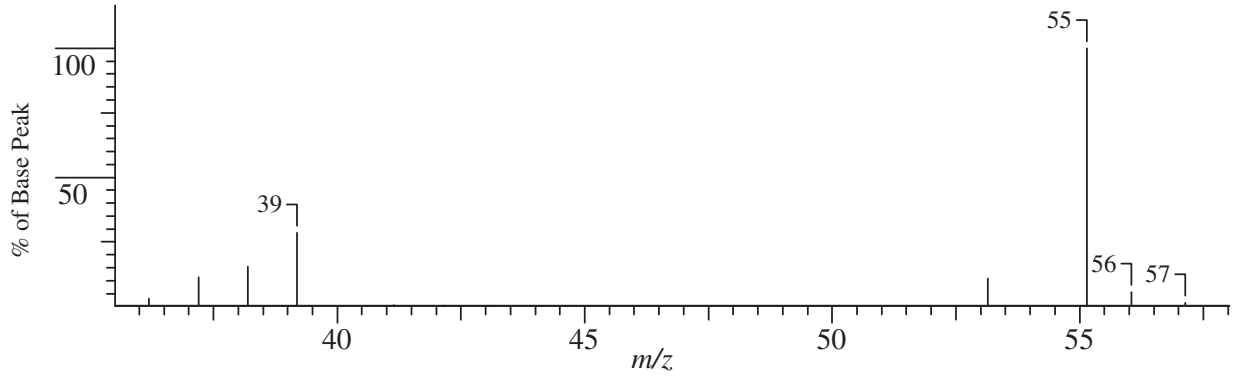

H CI Reagent gas Methane

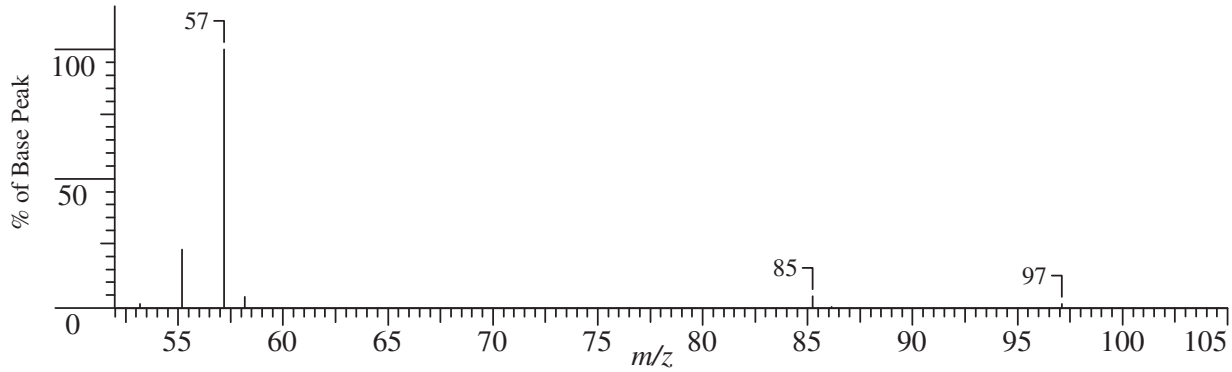

I

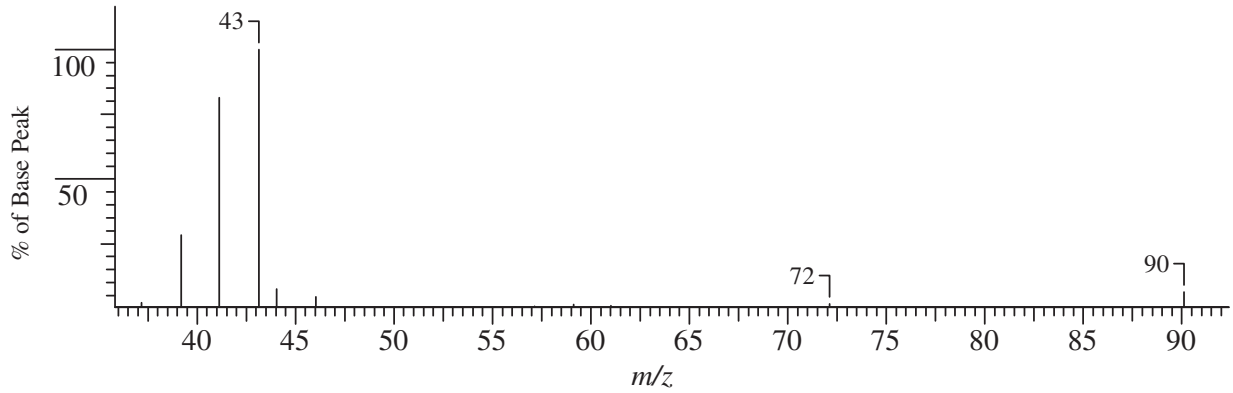

I CI Reagent gas Methane

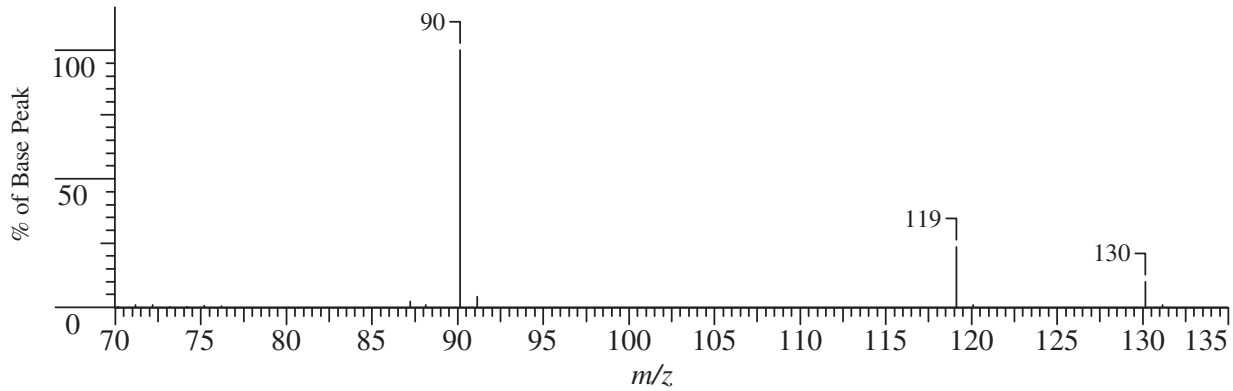

J

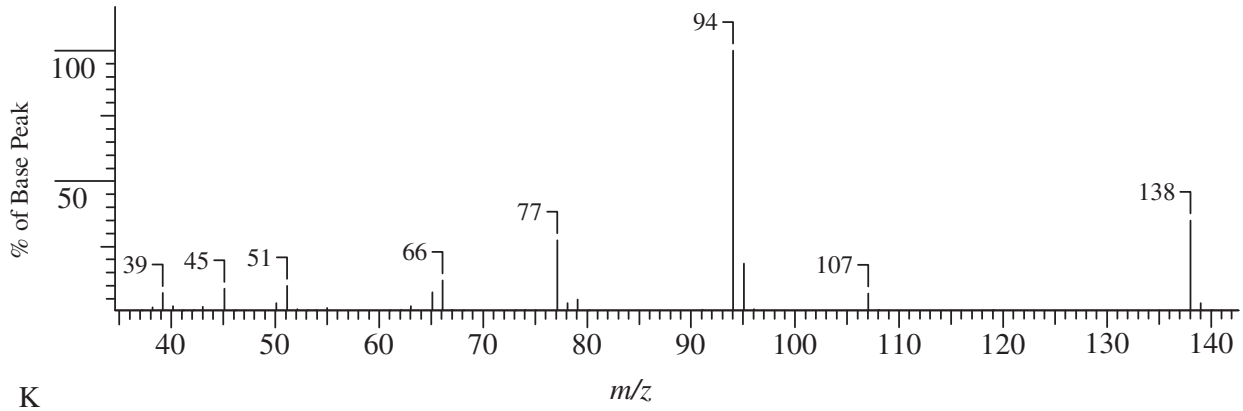
% of Base Peak
100
50
94
138
77
39
45
51
66
107
40
50
60
70
80
90
100
110
120
130
140
m/z

K

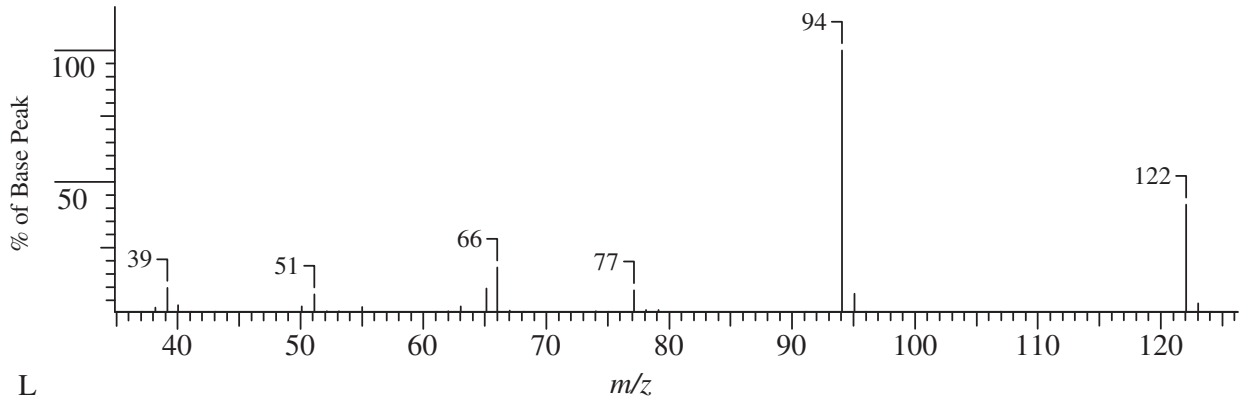
% of Base Peak
100
50
94
122
66
39
51
77
40
50
60
70
80
90
100
110
120
m/z

L

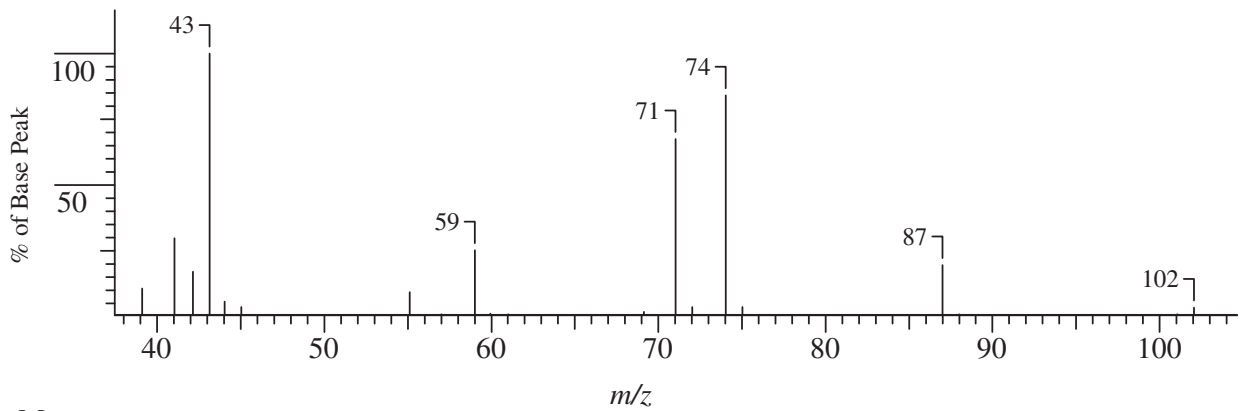
% of Base Peak
100
50
43
74
71
59
87
102
40
50
60
70
80
90
100
m/z

M

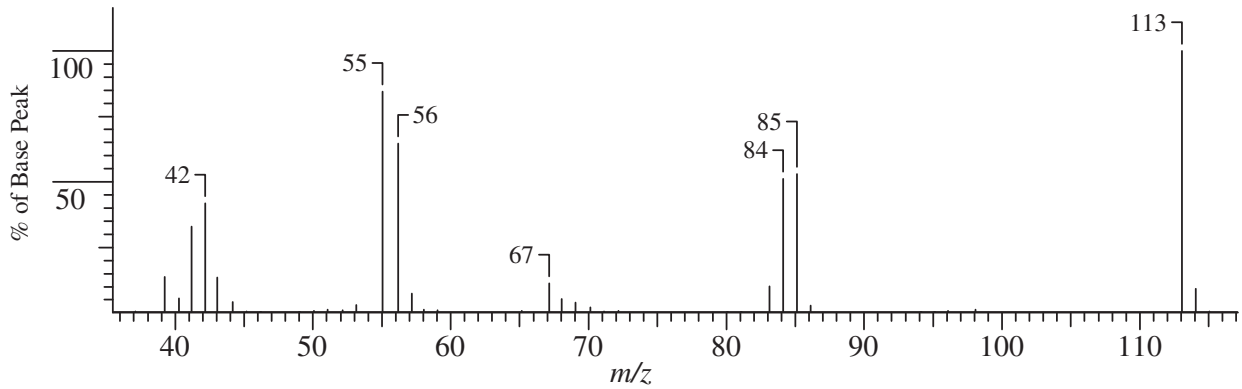
% of Base Peak
100
50
113
55
56
85
84
42
67
40
50
60
70
80
90
100
110
m/z

N

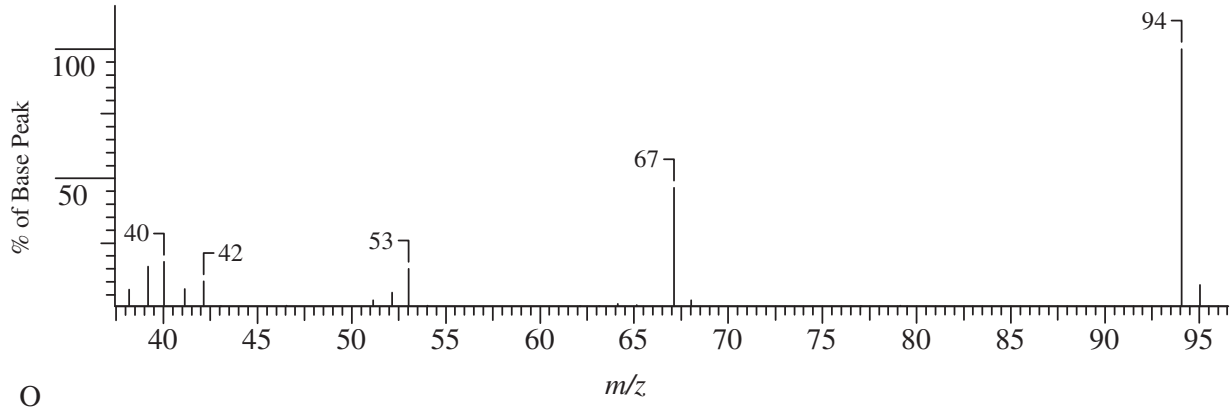
% of Base Peak
100
50
94
67
40
42
53
40 45 50 55 60 65 70 75 80 85 90 95
m/z

O

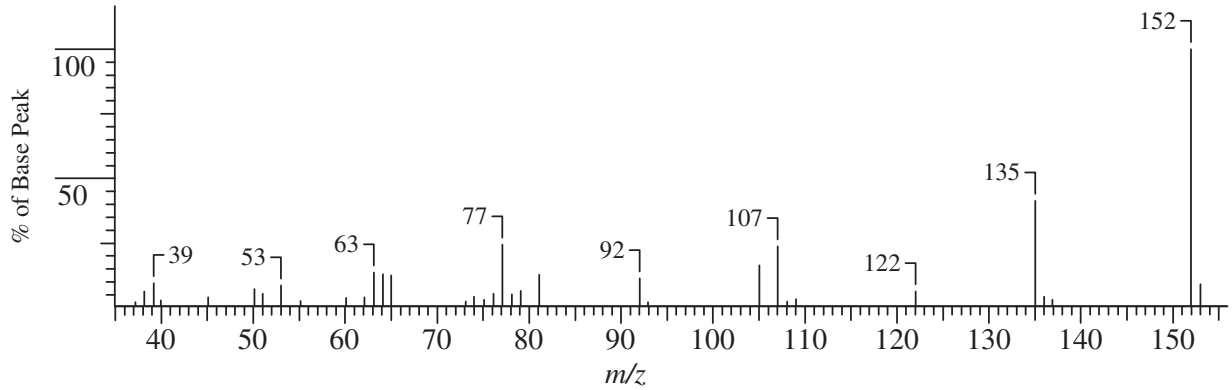
% of Base Peak
100
50
152
135
77
107
63
92
39
53
122
40 50 60 70 80 90 100 110 120 130 140 150
m/z

P

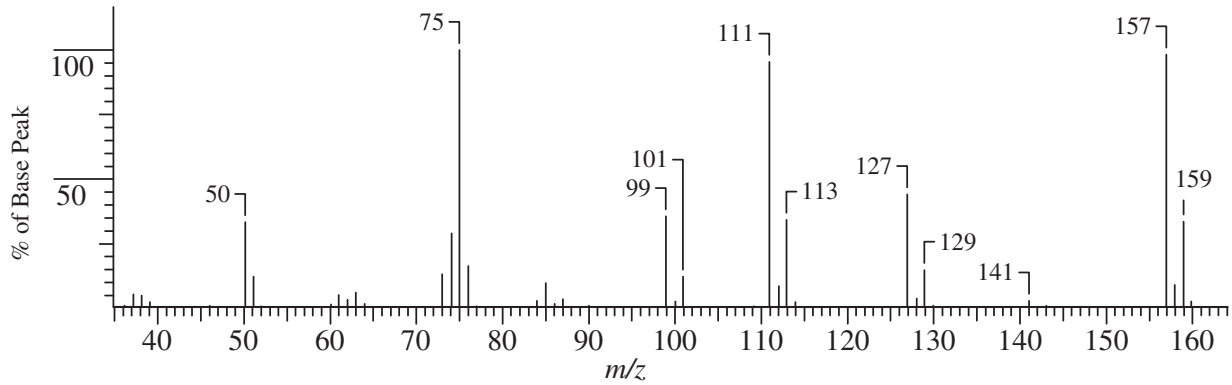
% of Base Peak
100
50
75
111
157
101
99
127
159
50
113
129
141
40 50 60 70 80 90 100 110 120 130 140 150 160
m/z

Q

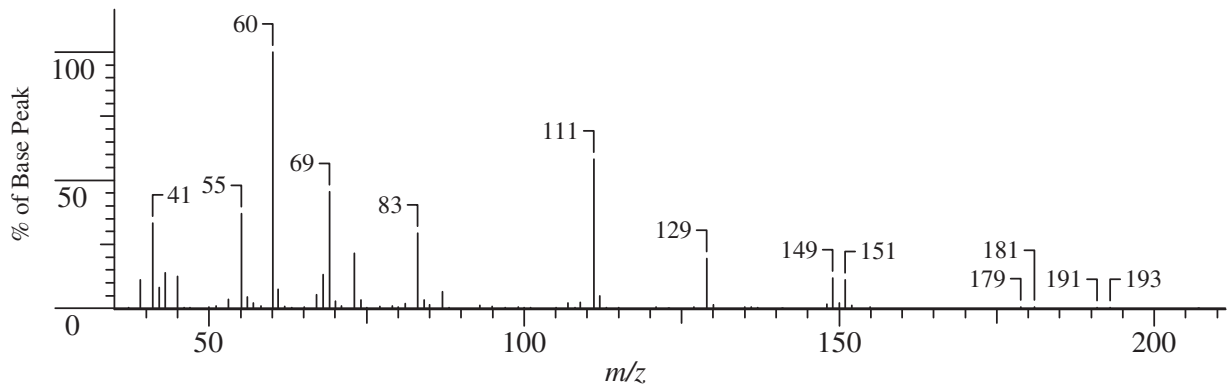
% of Base Peak
100
50
0
60
111
69
41
55
83
129
149
151
181
179
191
193
50 100 150 200
m/z

Q CI Reagent gas Methane

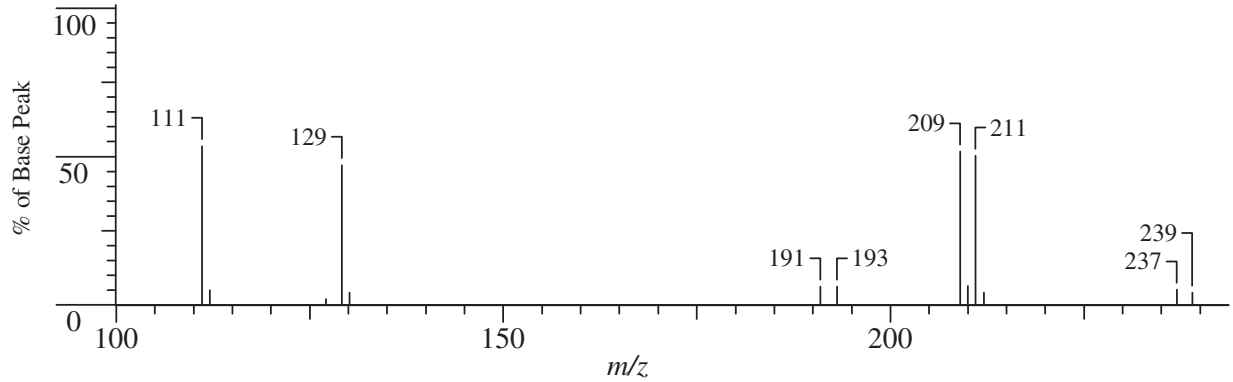

R

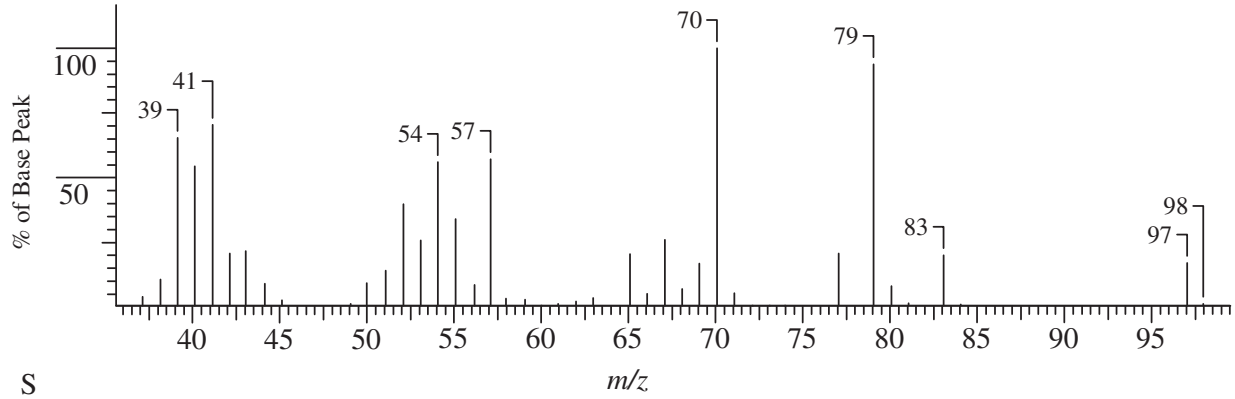

S

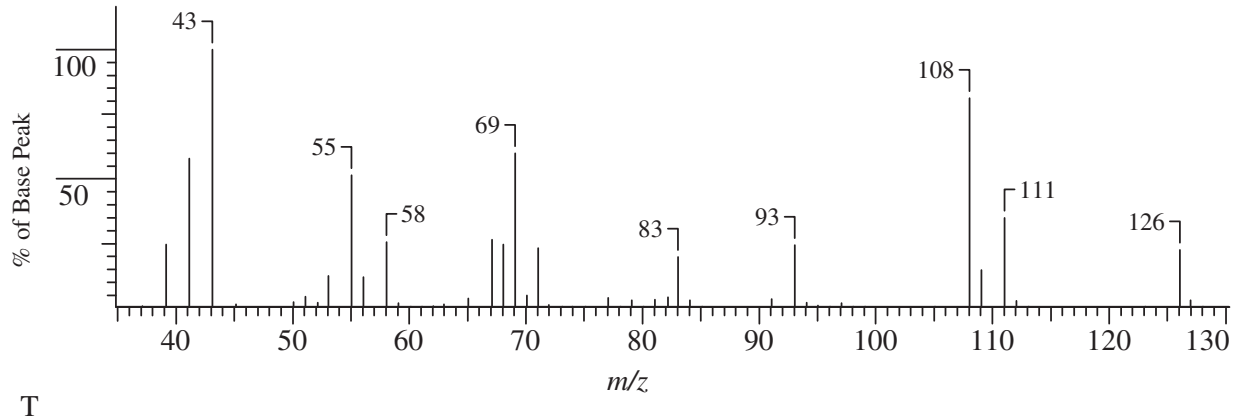

T

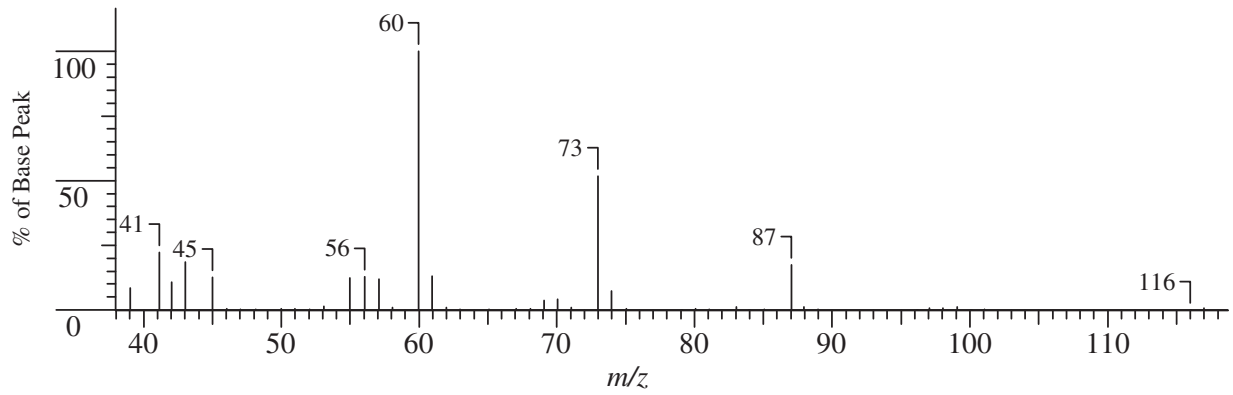

T CI Reagent gas Methane

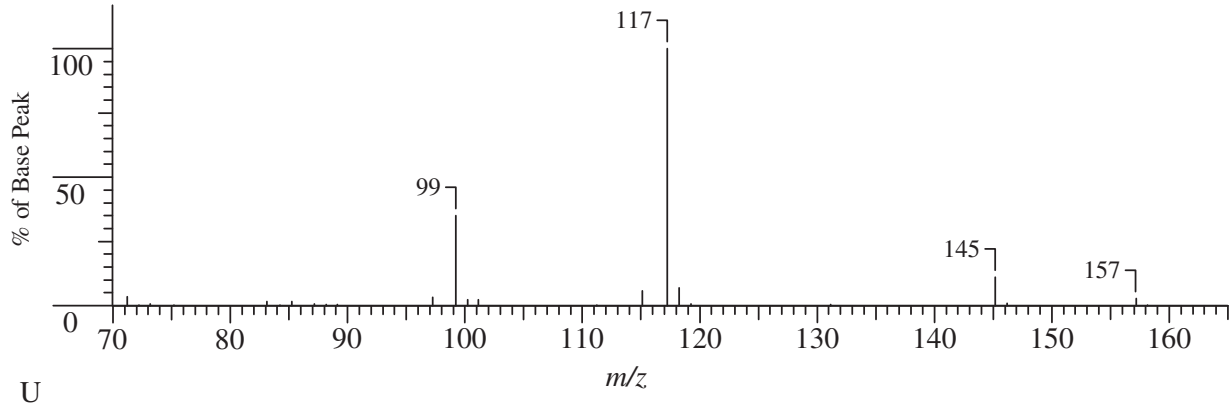

U

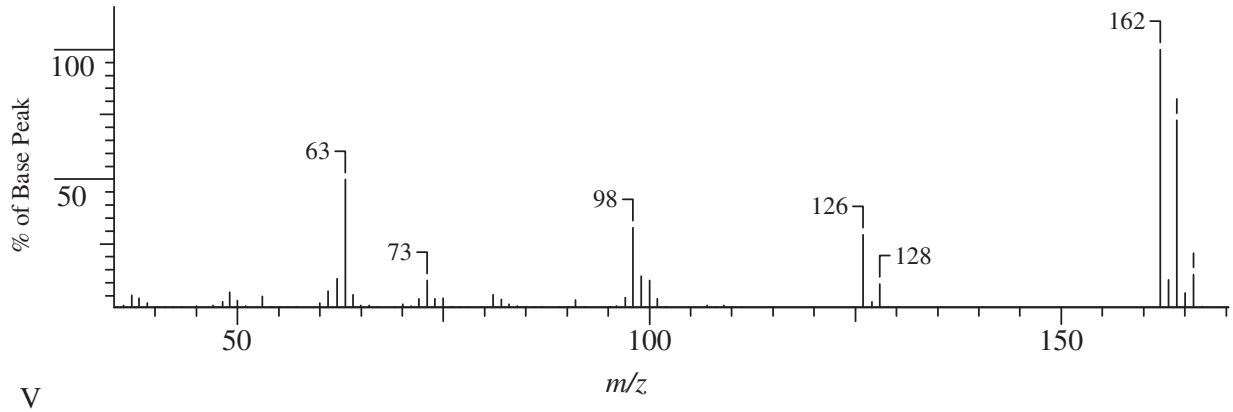

V

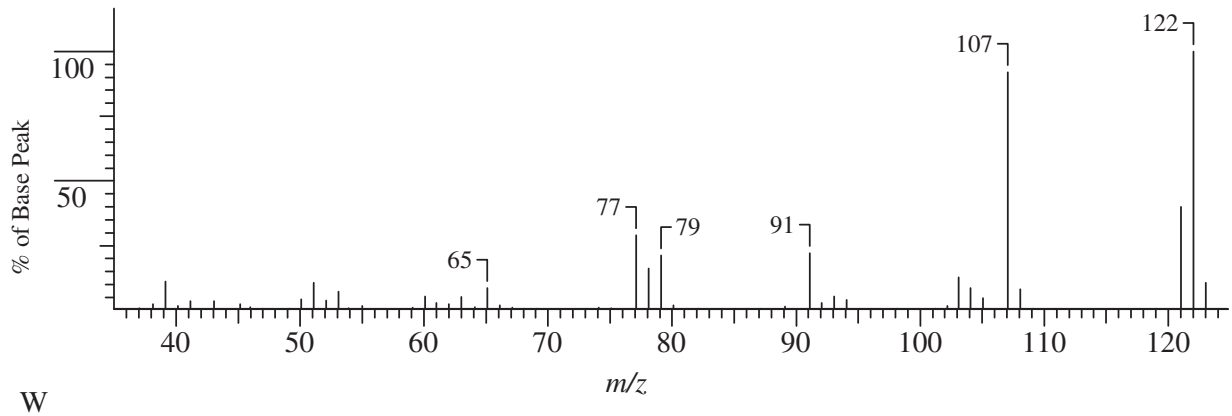

W

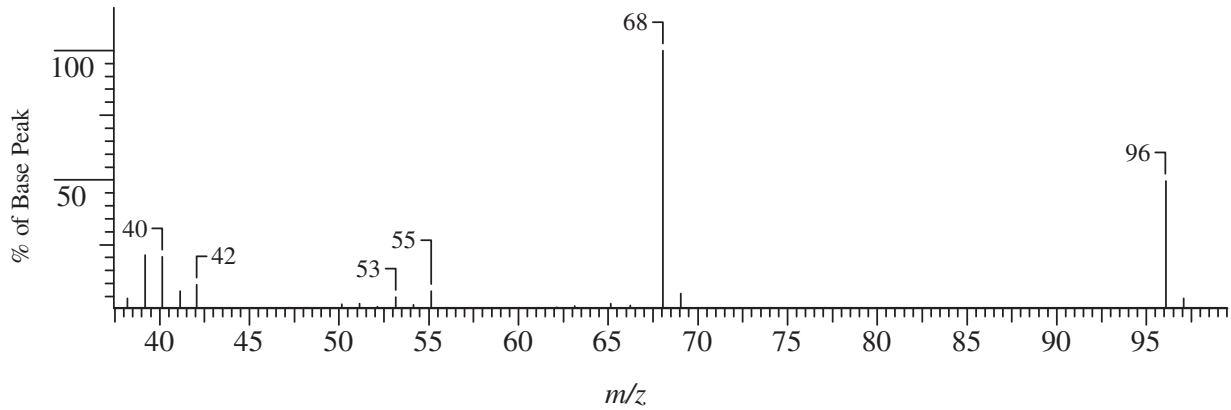

APPENDIX A FORMULA MASSES (FM) FOR VARIOUS COMBINATIONS OF CARBON, HYDROGEN, NITROGEN, AND OXYGEN[a]

	FM		FM		FM		FM
12		H_4N_2	32.0375	C_2H_6O	46.0419	CH_3N_2O	59.0246
C	12.0000	CH_4O	32.0262	**47**		CH_5N_3	59.0484
13		**33**		HNO_2	47.0007	$C_2H_3O_2$	59.0133
CH	13.0078	HO_2	32.9976	CH_3O_2	47.0133	C_2H_5NO	59.0371
14		H_3NO	33.0215	CH_5NO	47.0371	$C_2H_7N_2$	59.0610
N	14.0031	**34**		**48**		C_3H_7O	59.0497
CH_2	14.0157	H_2O_2	34.0054	O_3	47.9847	C_3H_9N	59.0736
15		**38**		H_2NO_2	48.0085	**60**	
HN	15.0109	C_3H_2	38.0157	H_4N_2O	48.0324	CH_2NO_2	60.0085
CH_3	15.0235	**39**		CH_4O_2	48.0211	CH_4N_2O	60.0324
16		C_2HN	39.0109	**49**		CH_6N_3	60.0563
O	15.9949	C_3H_3	39.0235	H_3NO_2	49.0164	$C_2H_4O_2$	60.0211
H_2N	16.0187	**40**		**52**		C_2H_6NO	60.0450
CH_4	16.0313	C_2H_2N	40.0187	C_4H_4	52.0313	$C_2H_8N_2$	60.0688
17		C_3H_4	40.0313	**53**		C_3H_8O	60.0575
HO	17.0027	**41**		C_3H_3N	53.0266	C_5	60.0000
H_3N	17.0266	CHN_2	41.0140	C_4H_5	53.0391	**61**	
18		C_2H_3N	41.0266	**54**		CH_3NO_2	61.0164
H_2O	18.0106	C_3H_5	41.0391	$C_2H_2N_2$	54.0218	CH_5N_2O	61.0402
24		**42**		C_3H_2O	54.0106	CH_7N_3	61.0641
C_2	24.0000	N_3	42.0093	C_3H_4N	54.0344	$C_2H_5O_2$	61.0289
26		CNO	41.9980	C_4H_6	54.0470	C_2H_7NO	61.0528
CN	26.0031	CH_2N_2	42.0218	**55**		**62**	
C_2H_2	26.0157	C_2H_2O	42.0106	$C_2H_3N_2$	55.0297	CH_2O_3	62.0003
27		C_2H_4N	42.0344	C_3H_3O	55.0184	CH_4NO_2	62.0242
CHN	27.0109	C_3H_6	42.0470	C_3H_5N	55.0422	CH_6N_2O	62.0480
C_2H_3	27.0235	**43**		C_4H_7	55.0548	$C_2H_6O_2$	62.0368
28		HN_3	43.0170	**56**		**63**	
N_2	28.0062	CHNO	43.0058	C_2O_2	55.9898	HNO_3	62.9956
CO	27.9949	CH_3N_2	43.0297	C_2H_2NO	56.0136	CH_5NO_2	63.0320
CH_2N	28.0187	C_2H_3O	43.0184	$C_2H_4N_2$	56.0375	**64**	
C_2H_4	28.0313	C_2H_5N	43.0422	C_3H_4O	56.0262	C_5H_4	64.0313
29		C_3H_7	43.0548	C_3H_6N	56.0501	**65**	
HN_2	29.0140	**44**		C_4H_8	56.0626	C_4H_3N	65.0266
CHO	29.0027	N_2O	44.0011	**57**		C_5H_5	65.0391
CH_3N	29.0266	CO_2	43.9898	C_2H_3NO	57.0215	**66**	
C_2H_5	29.0391	CH_2NO	44.0136	$C_2H_5N_2$	57.0453	C_4H_4N	66.0344
30		CH_4N_2	44.0375	C_3H_5O	57.0340	C_5H_6	66.0470
NO	29.9980	C_2H_4O	44.0262	C_3H_7N	57.0579	**67**	
H_2N_2	30.0218	C_2H_6N	44.0501	C_4H_9	57.0705	$C_3H_3N_2$	67.0297
CH_2O	30.0106	C_3H_8	44.0626	**58**		C_4H_3O	67.0184
CH_4N	30.0344	**45**		CH_2N_2O	58.0167	C_4H_5N	67.0422
C_2H_6	30.0470	CH_3NO	45.0215	CH_4N_3	58.0406	C_5H_7	67.0548
31		CH_5N_2	45.0453	$C_2H_2O_2$	58.0054	**68**	
HNO	31.0058	C_2H_5O	45.0340	C_2H_4NO	58.0293	$C_3H_4N_2$	68.0375
H_3N_2	31.0297	C_2H_7N	45.0579	$C_2H_6N_2$	58.0532	C_4H_4O	68.0262
CH_3O	31.0184	**46**		C_3H_6O	58.0419	C_4H_6N	68.0501
CH_5N	31.0422	NO_2	45.9929	C_3H_8N	58.0657	C_5H_8	68.0626
32		CH_2O_2	46.0054	C_4H_{10}	58.0783	**69**	
O_2	31.9898	CH_4NO	46.0293	**59**		C_3H_3NO	69.0215
H_2NO	32.0136	CH_6N_2	46.0532	$CHNO_2$	59.0007	$C_3H_5N_2$	69.0453

[a]With permission from J.H. Beynon, *Mass Spectrometry and its Application to Organic Chemistry*, Amsterdam, 1960. The columns headed FM contain the *formula masses* based on the exact mass of the most abundant isotope of each element; these masses are based on the most abundant isotope of carbon having a mass of 12.0000. Note that the table includes only C, H, N, and O.

APPENDIX A (*Continued*)

FM		FM		FM		FM	
C_4H_5O	69.0340	$C_2H_6NO_2$	76.0399	$C_4H_9N_2$	85.0767	$C_3H_8NO_2$	90.0555
C_4H_7N	69.0579	$C_2H_8N_2O$	76.0637	C_5H_9O	85.0653	$C_3H_{10}N_2O$	90.0794
C_5H_9	69.0705	$C_3H_8O_2$	76.0524	$C_5H_{11}N$	85.0892	$C_4H_{10}O_2$	90.0681
70		C_5H_2N	76.0187	C_6H_{13}	85.1018	C_7H_6	90.0470
$C_2H_4N_3$	70.0406	C_6H_4	76.0313	**86**		**91**	
$C_3H_2O_2$	70.0054	**77**		$C_2H_2N_2O_2$	86.0116	$C_2H_3O_4$	91.0031
C_3H_4NO	70.0293	CH_3NO_3	77.0113	$C_2H_4N_3O$	86.0355	$C_2H_5NO_3$	91.0269
$C_3H_6N_2$	70.0532	$C_2H_5O_3$	77.0238	$C_2H_6N_4$	86.0594	$C_2H_7N_2O_2$	91.0508
C_4H_6O	70.0419	$C_2H_7NO_2$	77.0477	$C_3H_4NO_2$	86.0242	$C_2H_9N_3O$	91.0746
C_4H_8N	70.0657	C_6H_5	77.0391	$C_3H_6N_2O$	86.0480	$C_3H_7O_3$	91.0395
C_5H_{10}	70.0783	**78**		$C_3H_8N_3$	86.0719	$C_3H_9NO_2$	91.0634
71		$C_2H_6O_3$	78.0317	$C_4H_6O_2$	86.0368	C_6H_5N	91.0422
$C_2H_3N_2O$	71.0246	C_5H_4N	78.0344	C_4H_8NO	86.0606	C_7H_7	91.0548
$C_2H_5N_3$	71.0484	C_6H_6	78.0470	$C_4H_{10}N_2$	86.0845	**92**	
$C_3H_3O_2$	71.0133	**79**		$C_5H_{10}O$	86.0732	$C_2H_4O_4$	92.0109
C_3H_5NO	71.0371	C_5H_5N	79.0422	$C_5H_{12}N$	86.0970	$C_2H_6NO_3$	92.0348
$C_3H_7N_2$	71.0610	C_6H_7	79.0548	C_6H_{14}	86.1096	$C_2H_8N_2O_2$	92.0586
C_4H_7O	71.0497	**80**		**87**		$C_3H_8O_3$	92.0473
C_4H_9N	71.0736	$C_3H_2N_3$	80.0249	$C_2H_7N_4$	87.0672	C_6H_4O	92.0262
C_5H_{11}	71.0861	$C_4H_4N_2$	80.0375	$C_3H_3O_3$	87.0082	C_6H_6N	92.0501
72		C_5H_4O	80.0262	$C_3H_5NO_2$	87.0320	C_7H_8	92.0626
$C_2H_2NO_2$	72.0085	C_5H_6N	80.0501	$C_3H_7N_2O$	87.0559	**93**	
$C_2H_4N_2O$	72.0324	C_6H_8	80.0626	$C_3H_9N_3$	87.0798	$C_2H_5O_4$	93.0187
$C_2H_6N_3$	72.0563	**81**		$C_4H_7O_2$	87.0446	$C_2H_7NO_3$	92.0426
$C_3H_4O_2$	72.0211	$C_3H_3N_3$	81.0328	C_4H_9NO	87.0684	$C_5H_5N_2$	93.0453
C_3H_6NO	72.0449	$C_4H_5N_2$	81.0453	$C_4H_{11}N_2$	87.0923	C_6H_5O	93.0340
$C_3H_8N_2$	72.0688	C_5H_5O	81.0340	$C_5H_{11}O$	87.0810	C_6H_7N	93.0579
C_4H_8O	72.0575	C_5H_7N	81.0579	$C_5H_{13}N$	87.1049	C_7H_9	93.0705
$C_4H_{10}N$	72.0814	C_6H_9	81.0705	**88**		**94**	
C_5H_{12}	72.0939	**82**		$C_2H_4N_2O_2$	88.0273	$C_2H_6O_4$	94.0266
73		$C_3H_4N_3$	82.0406	$C_2H_6N_3O$	88.0511	$C_4H_4N_3$	94.0406
$C_2H_3NO_2$	73.0164	C_4H_4NO	82.0293	$C_2H_8N_4$	88.0750	C_5H_4NO	94.0293
$C_2H_5N_2O$	73.0402	$C_4H_6N_2$	82.0532	$C_3H_4O_3$	88.0160	$C_5H_6N_2$	94.0532
$C_2H_7N_3$	73.0641	C_5H_6O	82.0419	$C_3H_6NO_2$	88.0399	C_6H_6O	94.0419
$C_3H_5O_2$	73.0289	C_5H_8N	82.0657	$C_3H_8N_2O$	88.0637	C_6H_8N	94.0657
C_3H_7NO	73.0528	C_6H_{10}	82.0783	$C_3H_{10}N_3$	88.0876	C_7H_{10}	94.0783
$C_3H_9N_2$	73.0767	**83**		$C_4H_8O_2$	88.0524	**95**	
C_4H_9O	73.0653	$C_3H_5N_3$	83.0484	$C_4H_{10}NO$	88.0763	$C_4H_5N_3$	95.0484
$C_4H_{11}N$	73.0892	$C_4H_3O_2$	83.0133	$C_4H_{12}N_2$	88.1001	C_5H_5NO	95.0371
74		C_4H_5NO	83.0371	$C_5H_{12}O$	88.0888	$C_5H_7N_2$	95.0610
$C_2H_2O_3$	74.0003	$C_4H_7N_2$	83.0610	**89**		C_6H_7O	95.0497
$C_2H_4NO_2$	74.0242	C_5H_7O	83.0497	$C_2H_5N_2O_2$	89.0351	C_6H_9N	95.0736
$C_2H_6N_2O$	74.0480	C_5H_9N	83.0736	$C_2H_7N_3O$	89.0590	C_7H_{11}	95.0861
$C_2H_8N_3$	74.0719	C_6H_{11}	83.0861	$C_2H_9N_4$	89.0829	**96**	
$C_3H_6O_2$	74.0368	**84**		$C_3H_5O_3$	89.0238	$C_4H_6N_3$	96.0563
C_3H_8NO	74.0606	$C_3H_6N_3$	84.0563	$C_3H_7NO_2$	89.0477	$C_5H_4O_2$	96.0211
$C_3H_{10}N_2$	74.0845	$C_4H_4O_2$	84.0211	$C_3H_9N_2O$	89.0715	C_5H_6NO	96.0449
$C_4H_{10}O$	74.0732	C_4H_6NO	84.0449	$C_3H_{11}N_3$	89.0954	$C_5H_8N_2$	96.0688
75		$C_4H_8N_2$	84.0688	$C_4H_9O_2$	89.0603	C_6H_8O	96.0575
$C_2H_3O_3$	75.0082	C_5H_8O	84.0575	$C_4H_{11}NO$	89.0841	$C_6H_{10}N$	96.0814
$C_2H_5NO_2$	75.0320	$C_5H_{10}N$	84.0814	C_7H_5	89.0391	C_7H_{12}	96.0939
$C_2H_7N_2O$	75.0559	C_6H_{12}	84.0939	**90**		**97**	
$C_2H_9N_3$	75.0798	**85**		$C_2H_4NO_3$	90.0191	$C_3H_5N_4$	97.0515
$C_3H_7O_2$	75.0446	$C_3H_5N_2O$	85.0402	$C_2H_6N_2O_2$	90.0429	$C_4H_5N_2O$	97.0402
C_3H_9NO	75.0684	$C_3H_7N_3$	85.0641	$C_2H_8N_3O$	90.0668	$C_5H_5O_2$	97.0289
76		$C_4H_5O_2$	85.0289	$C_2H_{10}N_4$	90.0907	C_5H_7NO	97.0528
$C_2H_4O_3$	76.0160	C_4H_7NO	85.0528	$C_3H_6O_3$	90.0317	$C_5H_9N_2$	97.0767

APPENDIX A (*Continued*)

FM		FM		FM		FM	
C_6H_9O	97.0653	**102**		$C_4H_{11}NO_2$	105.0790	$C_4H_6N_4$	110.0594
$C_6H_{11}N$	97.0892	$C_2H_6N_4O$	102.0542	$C_6H_5N_2$	105.0453	$C_5H_6N_2O$	110.0480
C_7H_{13}	97.1018	$C_3H_4NO_3$	102.0191	C_7H_5O	105.0340	$C_5H_8N_3$	110.0719
98		$C_3H_6N_2O_2$	102.0429	C_7H_7N	105.0579	$C_6H_6O_2$	110.0368
$C_3H_4N_3O$	98.0355	$C_3H_8N_3O$	102.0668	C_8H_9	105.0705	C_6H_8NO	110.0606
$C_3H_6N_4$	98.0594	$C_3H_{10}N_4$	102.0907	**106**		$C_6H_{10}N_2$	110.0845
$C_4H_4NO_2$	98.0242	$C_4H_6O_3$	102.0317	$C_2H_4NO_4$	106.0140	$C_7H_{10}O$	110.0732
$C_4H_6N_2O$	98.0480	$C_4H_8NO_2$	102.0555	$C_2H_6N_2O_3$	106.0379	$C_7H_{12}N$	110.0970
$C_4H_8N_3$	98.0719	$C_4H_{10}N_2O$	102.0794	$C_2H_8N_3O_2$	106.0617	C_8H_{14}	110.1096
$C_5H_6O_2$	98.0368	$C_4H_{12}N_3$	102.1032	$C_2H_{10}N_4O$	106.0856	**111**	
C_5H_8NO	98.0606	$C_5H_{10}O_2$	102.0681	$C_3H_6O_4$	106.0266	$C_4H_5N_3O$	111.0433
$C_5H_{10}N_2$	98.0845	$C_5H_{12}NO$	102.0919	$C_3H_8NO_3$	106.0504	$C_4H_7N_4$	111.0672
$C_6H_{10}O$	98.0732	$C_5H_{14}N_2$	102.1158	$C_3H_{10}N_2O_2$	106.0743	$C_5H_5NO_2$	111.0320
$C_6H_{12}N$	98.0970	$C_6H_{14}O$	102.1045	$C_4H_{10}O_3$	106.0630	$C_5H_7N_2O$	111.0559
C_7H_{14}	98.1096	C_8H_6	102.0470	C_6H_4NO	106.0293	$C_5H_9N_3$	111.0789
99		**103**		$C_6H_6N_2$	106.0532	$C_6H_7O_2$	111.0446
$C_3H_5N_3O$	99.0433	$C_2H_5N_3O_2$	103.0382	C_7H_6O	106.0419	C_6H_9NO	111.0684
$C_3H_7N_4$	99.0672	$C_2H_7N_4O$	103.0621	C_7H_8N	106.0657	$C_6H_{11}N_2$	111.0923
$C_4H_3O_3$	99.0082	$C_3H_3O_4$	103.0031	C_8H_{10}	106.0783	$C_7H_{11}O$	111.0810
$C_4H_5NO_2$	99.0320	$C_3H_5NO_3$	103.0269	**107**		$C_7H_{13}N$	111.1049
$C_4H_7N_2O$	99.0559	$C_3H_7N_2O_2$	103.0508	$C_2H_5NO_4$	107.0218	C_8H_{15}	111.1174
$C_4H_9N_3$	99.0798	$C_3H_9N_3O$	103.0746	$C_2H_7N_2O_3$	107.0457	**112**	
$C_5H_7O_2$	99.0446	$C_3H_{11}N_4$	103.0985	$C_2H_9N_3O_2$	107.0695	$C_3H_4N_4O$	112.0386
C_5H_9NO	99.0685	$C_4H_7O_3$	103.0395	$C_3H_7O_4$	107.0344	$C_4H_4N_2O_2$	112.0273
$C_5H_{11}N_2$	99.0923	$C_4H_9NO_2$	103.0634	$C_3H_9NO_3$	107.0583	$C_4H_6N_3O$	112.0511
$C_6H_{11}O$	99.0810	$C_4H_{11}N_2O$	103.0872	$C_5H_5N_3$	107.0484	$C_4H_8N_4$	112.0750
$C_6H_{13}N$	99.1049	$C_4H_{13}N_3$	103.1111	C_6H_5NO	107.0371	$C_5H_4O_3$	112.0160
C_7H_{15}	99.1174	$C_5H_{11}O_2$	103.0759	$C_6H_7N_2$	107.0610	$C_5H_6NO_2$	112.0399
100		$C_5H_{13}NO$	103.0998	C_7H_7O	107.0497	$C_5H_8N_2O$	112.0637
$C_2H_4N_4O$	100.0386	C_7H_5N	103.0422	C_7H_9N	107.0736	$C_5H_{10}N_3$	112.0876
$C_3H_4N_2O_2$	100.0273	C_8H_7	103.0548	C_8H_{11}	107.0861	$C_6H_8O_2$	112.0524
$C_3H_6N_3O$	100.0511	**104**		**108**		$C_6H_{10}NO$	112.0763
$C_3H_8N_4$	100.0750	$C_2H_4N_2O_3$	104.0222	$C_2H_6NO_4$	108.0297	$C_6H_{12}N_2$	112.1001
$C_4H_4O_3$	100.0160	$C_2H_6N_3O_2$	104.0460	$C_2H_8N_2O_3$	108.0535	$C_7H_{12}O$	112.0888
$C_4H_6NO_2$	100.0399	$C_2H_8N_4O$	104.0699	$C_3H_8O_4$	108.0422	$C_7H_{14}N$	112.1127
$C_4H_8N_2O$	100.0637	$C_3H_4O_4$	104.0109	$C_4H_4N_4$	108.0437	C_8H_{16}	112.1253
$C_4H_{10}N_3$	100.0876	$C_3H_6NO_3$	104.0348	$C_5H_4N_2O$	108.0324	**113**	
$C_5H_8O_2$	100.0524	$C_3H_8N_2O_2$	104.0586	$C_5H_6N_3$	108.0563	$C_3H_5N_4O$	113.0464
$C_5H_{10}NO$	100.0763	$C_3H_{10}N_3O$	104.0825	$C_6H_4O_2$	108.0211	$C_4H_5N_2O_2$	113.0351
$C_5H_{12}N_2$	100.1001	$C_3H_{12}N_4$	104.1063	C_6H_6NO	108.0449	$C_4H_7N_3O$	113.0590
$C_6H_{12}O$	100.0888	$C_4H_8O_3$	104.0473	$C_6H_8N_2$	108.0688	$C_4H_9N_4$	113.0829
$C_6H_{14}N$	100.1127	$C_4H_{10}NO_2$	104.0712	C_7H_8O	108.0575	$C_5H_5O_3$	113.0238
C_7H_{16}	100.1253	$C_4H_{12}N_2O$	104.0950	$C_7H_{10}N$	108.0814	$C_5H_7NO_2$	113.0477
101		$C_5H_{12}O_2$	104.0837	C_8H_{12}	108.0939	$C_5H_9N_2O$	113.0715
$C_3H_3NO_3$	101.0113	$C_6H_4N_2$	104.0375	**109**		$C_5H_{11}N_3$	113.0954
$C_3H_5N_2O_2$	101.0351	C_7H_4O	104.0262	$C_2H_7NO_4$	109.0375	$C_6H_9O_2$	113.0603
$C_3H_7N_3O$	101.0590	C_7H_6N	104.0501	$C_4H_5N_4$	109.0515	$C_6H_{11}NO$	113.0841
$C_3H_9N_4$	101.0829	C_8H_8	104.0626	$C_5H_5N_2O$	109.0402	$C_6H_{13}N_2$	113.1080
$C_4H_5O_3$	101.0238	**105**		$C_5H_7N_3$	109.0641	$C_7H_{13}O$	113.0967
$C_4H_7NO_2$	101.0477	$C_2H_5N_2O_3$	105.0300	$C_6H_5O_2$	109.0289	$C_7H_{15}N$	113.1205
$C_4H_9N_2O$	101.0715	$C_2H_7N_3O_2$	105.0539	C_6H_7NO	109.0528	C_8H_{17}	113.1331
$C_4H_{11}N_3$	101.0954	$C_2H_9N_4O$	105.0777	$C_6H_9N_2$	109.0767	**114**	
$C_5H_9O_2$	101.0603	$C_3H_5O_4$	105.0187	C_7H_9O	109.0653	$C_3H_6N_4O$	114.0542
$C_5H_{11}NO$	101.0841	$C_3H_7NO_3$	105.0426	$C_7H_{11}N$	109.0892	$C_4H_4NO_3$	114.0191
$C_5H_{13}N_2$	101.1080	$C_3H_9N_2O_2$	105.0664	C_8H_{13}	109.1018	$C_4H_6N_2O_2$	114.0429
$C_6H_{13}O$	101.0967	$C_3H_{11}N_3O$	105.0903	**110**		$C_4H_8N_3O$	114.0668
$C_6H_{15}N$	101.1205	$C_4H_9O_3$	105.0552	$C_4H_4N_3O$	110.0355	$C_4H_{10}N_4$	114.0907

APPENDIX A (*Continued*)

FM		FM		FM		FM	
$C_5H_6O_3$	114.0317	$C_4H_9N_2O_2$	117.0664	$C_4H_8O_4$	120.0422	C_7H_9NO	123.0684
$C_5H_8NO_2$	114.0555	$C_4H_{11}N_3O$	117.0903	$C_4H_{10}NO_3$	120.0661	$C_7H_{11}N_2$	123.0923
$C_5H_{10}N_2O$	114.0794	$C_4H_{13}N_4$	117.1142	$C_4H_{12}N_2O_2$	120.0899	$C_8H_{11}O$	123.0810
$C_5H_{12}N_3$	114.1032	$C_5H_9O_3$	117.0552	$C_5H_4N_4$	120.0437	$C_8H_{13}N$	123.1049
$C_6H_{10}O_2$	114.0681	$C_5H_{11}NO_2$	117.0790	$C_5H_{12}O_3$	120.0786	C_9H_{15}	123.1174
$C_6H_{12}NO$	114.0919	$C_5H_{13}N_2O$	117.1029	$C_6H_4N_2O$	120.0324	**124**	
$C_6H_{14}N_2$	114.1158	$C_5H_{15}N_3$	117.1267	$C_6H_6N_3$	120.0563	$C_2H_8N_2O_4$	124.0484
$C_7H_{14}O$	114.1045	$C_6H_{13}O_2$	117.0916	C_7H_6NO	120.0449	$C_4H_4N_4O$	124.0386
$C_7H_{16}N$	114.1284	$C_6H_{15}NO$	117.1154	$C_7H_8N_2$	120.0688	$C_5H_4N_2O_2$	124.0273
C_8H_{18}	114.1409	C_8H_7N	117.0579	C_8H_8O	120.0575	$C_5H_6N_3O$	124.0511
C_9H_6	114.0470	C_9H_9	117.0705	$C_8H_{10}N$	120.0814	$C_5H_8N_4$	124.0750
115		**118**		C_9H_{12}	120.0939	$C_6H_4O_3$	124.0160
$C_3H_5N_3O_2$	115.0382	$C_2H_4N_3O_3$	118.0253	**121**		$C_6H_6NO_2$	124.0399
$C_3H_7N_4O$	115.0621	$C_2H_6N_4O_2$	118.0491	$C_2H_5N_2O_4$	121.0249	$C_6H_8N_2O$	124.0637
$C_4H_5NO_3$	115.0269	$C_3H_4NO_4$	118.0140	$C_2H_7N_3O_3$	121.0488	$C_6H_{10}N_3$	124.0876
$C_4H_7N_2O_2$	115.0508	$C_3H_6N_2O_3$	118.0379	$C_2H_9N_4O_2$	121.0726	$C_7H_8O_2$	124.0524
$C_4H_9N_3O$	115.0746	$C_3H_8N_3O_2$	118.0617	$C_3H_7NO_4$	121.0375	$C_7H_{10}NO$	124.0763
$C_4H_{11}N_4$	115.0985	$C_3H_{10}N_4O$	118.0856	$C_3H_9N_2O_3$	121.0614	$C_7H_{12}N_2$	124.1001
$C_5H_7O_3$	115.0395	$C_4H_6O_4$	118.0266	$C_3H_{11}N_3O_2$	121.0852	C_8N_2	124.0062
$C_5H_9NO_2$	115.0634	$C_4H_8NO_3$	118.0504	$C_4H_9O_4$	121.0501	$C_8H_{12}O$	124.0888
$C_5H_{11}N_2O$	115.0872	$C_4H_{10}N_2O_2$	118.0743	$C_4H_{11}NO_3$	121.0739	$C_8H_{14}N$	124.1127
$C_5H_{13}N_3$	115.1111	$C_4H_{12}N_3O$	118.0981	$C_5H_5N_4$	121.0515	C_9H_{16}	124.1253
$C_6H_{11}O_2$	115.0759	$C_4H_{14}N_4$	118.1220	$C_6H_5N_2O$	121.0402	**125**	
$C_6H_{13}NO$	115.0998	$C_5H_{10}O_3$	118.0630	$C_6H_7N_3$	121.0641	$C_4H_3N_3O_2$	125.0226
$C_6H_{15}N_2$	115.1236	$C_5H_{12}NO_2$	118.0868	$C_7H_5O_2$	121.0289	$C_4H_5N_4O$	125.0464
$C_7H_{15}O$	115.1123	$C_5H_{14}N_2O$	118.1107	C_7H_7NO	121.0528	$C_5H_5N_2O_2$	125.0351
$C_7H_{17}N$	115.1362	$C_6H_{14}O_2$	118.0994	$C_7H_9N_2$	121.0767	$C_5H_7N_3O$	125.0590
C_9H_7	115.0548	$C_7H_6N_2$	118.0532	C_8H_9O	121.0653	$C_5H_9N_4$	125.0829
116		C_8H_6O	118.0419	$C_8H_{11}N$	121.0892	$C_6H_5O_3$	125.0238
$C_2H_4N_4O_2$	116.0335	C_8H_8N	118.0657	C_9H_{13}	121.1018	$C_6H_7NO_2$	125.0477
$C_3H_4N_2O_3$	116.0222	C_9H_{10}	118.0783	**122**		$C_6H_9N_2O$	125.0715
$C_3H_6N_3O_2$	116.0460	**119**		$C_2H_6N_2O_4$	122.0328	$C_6H_{11}N_3$	125.0954
$C_3H_8N_4O$	116.0699	$C_2H_5N_3O_3$	119.0331	$C_2H_8N_3O_3$	122.0566	$C_7H_9O_2$	125.0603
$C_4H_4O_4$	116.0109	$C_2H_7N_4O_2$	119.0570	$C_2H_{10}N_4O_2$	122.0805	$C_7H_{11}NO$	125.0841
$C_4H_6NO_3$	116.0348	$C_3H_5NO_4$	119.0218	$C_3H_8NO_4$	122.0453	$C_7H_{13}N_2$	125.1080
$C_4H_8N_2O_2$	116.0586	$C_3H_7N_2O_3$	119.0457	$C_3H_{10}N_2O_3$	122.0692	$C_8H_{13}O$	125.0967
$C_4H_{10}N_3O$	116.0825	$C_3H_9N_3O_2$	119.0695	$C_4H_{10}O_4$	122.0579	$C_8H_{15}N$	125.1205
$C_4H_{12}N_4$	116.1063	$C_3H_{11}N_4O$	119.0934	$C_5H_6N_4$	122.0594	C_9H_{17}	125.1331
$C_5H_8O_3$	116.0473	$C_4H_7O_4$	119.0344	$C_6H_4NO_2$	122.0242	**126**	
$C_5H_{10}NO_2$	116.0712	$C_4H_9NO_3$	119.0583	$C_6H_6N_2O$	122.0480	$C_3H_2N_4O_2$	126.0178
$C_5H_{12}N_2O$	116.0950	$C_4H_{11}N_2O_2$	119.0821	$C_6H_8N_3$	122.0719	$C_4H_4N_3O_2$	126.0304
$C_5H_{14}N_3$	116.1189	$C_4H_{13}N_3O$	119.1060	$C_7H_6O_2$	122.0368	$C_4H_6N_4O$	126.0542
$C_6H_{12}O_2$	116.0837	$C_5H_{11}O_3$	119.0708	C_7H_8NO	122.0606	$C_5H_4NO_3$	126.0191
$C_6H_{14}NO$	116.1076	$C_5H_{13}NO_2$	119.0947	$C_7H_{10}N_2$	122.0845	$C_5H_6N_2O_2$	126.0429
$C_6H_{16}N_2$	116.1315	$C_6H_5N_3$	119.0484	$C_8H_{10}O$	122.0732	$C_5H_8N_3O$	126.0668
$C_7H_4N_2$	116.0375	C_7H_5NO	119.0371	$C_8H_{12}N$	122.0970	$C_5H_{10}N_4$	126.0907
$C_7H_{16}O$	116.1202	$C_7H_7N_2$	119.0610	C_9H_{14}	122.1096	$C_6H_6O_3$	126.0317
C_8H_6N	116.0501	C_8H_7O	119.0497	**123**		$C_6H_8NO_2$	126.0555
C_9H_8	116.0626	C_8H_9N	119.0736	$C_2H_7N_2O_4$	123.0406	$C_6H_{10}N_2O$	126.0794
117		C_9H_{11}	119.0861	$C_2H_9N_3O_3$	123.0644	$C_6H_{12}N_3$	126.1032
$C_2H_5N_4O_2$	117.0413	**120**		$C_3H_9NO_4$	123.0532	$C_7H_{10}O_2$	126.0681
$C_3H_3NO_4$	117.0062	$C_2H_6N_3O_3$	120.0410	$C_5H_5N_3O$	123.0433	$C_7H_{12}NO$	126.0919
$C_3H_5N_2O_3$	117.0300	$C_2H_8N_4O_2$	120.0648	$C_5H_7N_4$	123.0672	$C_7H_{14}N_2$	126.1158
$C_3H_7N_3O_2$	117.0539	$C_3H_6NO_4$	120.0297	$C_6H_5NO_2$	123.0320	$C_8H_{14}O$	126.1045
$C_3H_9N_4O$	117.0777	$C_3H_8N_2O_3$	120.0535	$C_6H_7N_2O$	123.0559	$C_8H_{16}N$	126.1284
$C_4H_5O_4$	117.0187	$C_3H_{10}N_3O_2$	120.0774	$C_6H_9N_3$	123.0798	C_9H_{18}	126.1409
$C_4H_7NO_3$	117.0426	$C_3H_{12}N_4O$	120.1012	$C_7H_7O_2$	123.0446	**127**	

APPENDIX A (*Continued*)

FM		FM		FM		FM	
$C_3H_3N_4O_2$	127.0257	$C_8H_{19}N$	129.1519	$C_4H_{10}N_3O_2$	132.0774	C_8H_8NO	134.0606
$C_4H_5N_3O_2$	127.0382	C_9H_7N	129.0579	$C_4H_{12}N_4O$	132.1012	$C_8H_{10}N_2$	134.0845
$C_4H_7N_4O$	127.0621	$C_{10}H_9$	129.0705	$C_5H_8O_4$	132.0422	$C_9H_{10}O$	134.0732
$C_5H_5NO_3$	127.0269	**130**		$C_5H_{10}NO_3$	132.0661	$C_9H_{12}N$	134.0970
$C_5H_7N_2O_2$	127.0508	$C_3H_4N_3O_3$	130.0253	$C_5H_{12}N_2O_2$	132.0899	$C_{10}H_{14}$	134.1096
$C_5H_9N_3O$	127.0746	$C_3H_6N_4O_2$	130.0491	$C_5H_{14}N_3O$	132.1138	**135**	
$C_5H_{11}N_4$	127.0985	$C_4H_4NO_4$	130.0140	$C_5H_{16}N_4$	132.1377	$C_3H_7N_2O_4$	135.0406
$C_6H_7O_3$	127.0395	$C_4H_6N_2O_3$	130.0379	$C_6H_4N_4$	132.0437	$C_3H_9N_3O_3$	135.0644
$C_6H_9NO_2$	127.0634	$C_4H_8N_3O_2$	130.0617	$C_6H_{12}O_3$	132.0786	$C_3H_{11}N_4O_2$	135.0883
$C_6H_{11}N_2O$	127.0872	$C_4H_{10}N_4O$	130.0856	$C_6H_{14}NO_2$	132.1025	$C_4H_9NO_4$	135.0532
$C_6H_{13}N_3$	127.1111	$C_5H_6O_4$	130.0266	$C_6H_{16}N_2O$	132.1264	$C_4H_{11}N_2O_3$	135.0770
$C_7H_{11}O_2$	127.0759	$C_5H_8NO_3$	130.0504	$C_7H_9N_3$	132.0563	$C_4H_{13}N_3O_2$	135.1009
$C_7H_{13}NO$	127.0998	$C_5H_{10}N_2O_2$	130.0743	$C_7H_{16}O_2$	132.1151	$C_5H_3N_4O$	135.0308
$C_7H_{15}N_2$	127.1236	$C_5H_{12}N_3O$	130.0981	C_8H_6NO	132.0449	$C_5H_{11}O_4$	135.0657
$C_8H_{15}O$	127.1123	$C_5H_{14}N_4$	130.1220	$C_8H_8N_2$	132.0688	$C_5H_{13}NO_3$	135.0896
$C_8H_{17}N$	127.1362	$C_6H_{10}O_3$	130.0630	C_9H_8O	132.0575	$C_6H_5N_3O$	135.0433
C_9H_{19}	127.1488	$C_6H_{12}NO_2$	130.0868	$C_9H_{10}N$	132.0814	$C_6H_7N_4$	135.0672
128		$C_6H_{14}N_2O$	130.1107	$C_{10}H_{12}$	132.0939	$C_7H_5NO_2$	135.0320
$C_3H_4N_4O_2$	128.0335	$C_6H_{16}N_3$	130.1346	**133**		$C_7H_7N_2O$	135.0559
$C_4H_4N_2O_3$	128.0222	$C_7H_4N_3$	130.0406	$C_3H_5N_2O_4$	133.0249	$C_7H_9N_3$	135.0798
$C_4H_6N_3O_2$	128.0460	$C_7H_{14}O_2$	130.0994	$C_3H_7N_3O_3$	133.0488	$C_8H_7O_2$	135.0446
$C_4H_8N_4O$	128.0699	$C_7H_{16}NO$	130.1233	$C_3H_9N_4O_2$	133.0726	C_8H_9NO	135.0684
$C_5H_4O_4$	128.0109	$C_7H_{18}N_2$	130.1471	$C_4H_7NO_4$	133.0375	$C_8H_{11}N_2$	135.0923
$C_5H_6NO_3$	128.0348	$C_8H_6N_2$	130.0532	$C_4H_9N_2O_3$	133.0614	$C_9H_{11}O$	135.0810
$C_5H_8N_2O_2$	128.0586	$C_8H_{18}O$	130.1358	$C_4H_{11}N_3O_2$	133.0852	$C_9H_{13}N$	135.1049
$C_5H_{10}N_3O$	128.0825	C_9H_8N	130.0657	$C_4H_{13}N_4O$	133.1091	$C_{10}H_{15}$	135.1174
$C_5H_{12}N_4$	128.1063	$C_{10}H_{10}$	130.0783	$C_5H_9O_4$	133.0501	**136**	
$C_6H_8O_3$	128.0473	**131**		$C_5H_{11}NO_3$	133.0739	$C_3H_8N_2O_4$	136.0484
$C_6H_{10}NO_2$	128.0712	$C_3H_3N_2O_4$	131.0093	$C_5H_{13}N_2O_2$	133.0978	$C_3H_{10}N_3O_3$	136.0723
$C_6H_{12}N_2O$	128.0950	$C_3H_5N_3O_3$	131.0331	$C_5H_{15}N_3O$	133.1216	$C_3H_{12}N_4O_2$	136.0961
$C_6H_{14}N_3$	128.1189	$C_3H_7N_4O_2$	131.0570	$C_6H_5N_4$	133.0515	$C_4H_{10}NO_4$	136.0610
$C_7H_{12}O_2$	128.0837	$C_4H_5NO_4$	131.0218	$C_6H_{13}O_3$	133.0865	$C_4H_{12}N_2O_3$	136.0848
$C_7H_{14}NO$	128.1076	$C_4H_7N_2O_3$	131.0457	$C_6H_{15}NO_2$	133.1103	$C_5H_2N_3O_2$	136.0147
$C_7H_{16}N_2$	128.1315	$C_4H_9N_3O_2$	131.0695	$C_7H_5N_2O$	133.0402	$C_5H_4N_4O$	136.0386
$C_8H_{16}O$	128.1202	$C_4H_{11}N_4O$	131.0934	$C_7H_7N_3$	133.0641	$C_5H_{12}O_4$	136.0735
$C_8H_{18}N$	128.1440	$C_5H_7O_4$	131.0344	C_8H_7NO	133.0528	$C_6H_4N_2O_2$	136.0273
C_9H_{20}	128.1566	$C_5H_9NO_3$	131.0583	$C_8H_9N_2$	133.0767	$C_6H_6N_3O$	136.0511
$C_{10}H_8$	128.0626	$C_5H_{11}N_2O_2$	131.0821	C_9H_9O	133.0653	$C_6H_8N_4$	136.0750
129		$C_5H_{13}N_3O$	131.1060	$C_9H_{11}N$	133.0892	$C_7H_4O_3$	136.0160
$C_3H_3N_3O_3$	129.0175	$C_5H_{15}N_4$	131.1298	$C_{10}H_{13}$	133.1018	$C_7H_6NO_2$	136.0399
$C_3H_5N_4O_2$	129.0413	$C_6H_{11}O_3$	131.0708	**134**		$C_7H_8N_2O$	136.0637
$C_4H_5N_2O_3$	129.0300	$C_6H_{13}NO_2$	131.0947	$C_3H_6N_2O_4$	134.0328	$C_7H_{10}N_3$	136.0876
$C_4H_7N_3O_2$	129.0539	$C_6H_{15}N_2O$	131.1185	$C_3H_8N_3O_3$	134.0566	$C_8H_8O_2$	136.0524
$C_4H_9N_4O$	129.0777	$C_6H_{17}N_3$	131.1424	$C_3H_{10}N_4O_2$	134.0805	$C_8H_{10}NO$	136.0763
$C_5H_5O_4$	129.0187	$C_7H_5N_3$	131.0484	$C_4H_8NO_4$	134.0453	$C_8H_{12}N_2$	136.1001
$C_5H_7NO_3$	129.0426	$C_7H_{15}O_2$	131.1072	$C_4H_{10}N_2O_3$	134.0692	$C_9H_{12}O$	136.0888
$C_5H_9N_2O_2$	129.0664	$C_7H_{17}NO$	131.1311	$C_4H_{12}N_3O_2$	134.0930	$C_9H_{14}N$	136.1127
$C_5H_{11}N_3O$	129.0903	$C_8H_7N_2$	131.0610	$C_4H_{14}N_4O$	134.1169	$C_{10}H_{16}$	136.1253
$C_5H_{13}N_4$	129.1142	C_9H_7O	131.0497	$C_5H_{10}O_4$	134.0579	**137**	
$C_6H_9O_3$	129.0552	C_9H_9N	131.0736	$C_5H_{12}NO_3$	134.0817	$C_3H_9N_2O_4$	137.0563
$C_6H_{11}NO_2$	129.0790	$C_{10}H_{11}$	131.0861	$C_5H_{14}N_2O_2$	134.1056	$C_3H_{11}N_3O_3$	137.0801
$C_6H_{13}N_2O$	129.1029	**132**		$C_6H_4N_3O$	134.0355	$C_4H_{11}NO_4$	137.0688
$C_6H_{15}N_3$	129.1267	$C_3H_4N_2O_4$	132.0171	$C_6H_6N_4$	134.0594	$C_5H_3N_3O_2$	137.0226
$C_7H_{13}O_2$	129.0916	$C_3H_6N_3O_3$	132.0410	$C_6H_{14}O_3$	134.0943	$C_5H_5N_4O$	137.0464
$C_7H_{15}NO$	129.1154	$C_3H_8N_4O_2$	132.0648	$C_7H_6N_2O$	134.0480	$C_6H_5N_2O_2$	137.0351
$C_7H_{17}N_2$	129.1393	$C_4H_6NO_4$	132.0297	$C_7H_8N_3$	134.0719	$C_6H_7N_3O$	137.0590
$C_8H_{17}O$	129.1280	$C_4H_8N_2O_3$	132.0535	$C_8H_6O_2$	134.0368	$C_6H_9N_4$	137.0829

APPENDIX A (*Continued*)

FM		FM		FM		FM	
$C_7H_5O_3$	137.0238	$C_6H_8N_2O_2$	140.0586	$C_8H_{16}NO$	142.1233	$C_9H_8N_2$	144.0688
$C_7H_7NO_2$	137.0477	$C_6H_{10}N_3O$	140.0825	$C_8H_{18}N_2$	142.1471	$C_9H_{20}O$	144.1515
$C_7H_9N_2O$	137.0715	$C_6H_{12}N_4$	140.1063	$C_9H_6N_2$	142.0532	$C_{10}H_8O$	144.0575
$C_7H_{11}N_3$	137.0954	$C_7H_8O_3$	140.0473	$C_9H_{18}O$	142.1358	$C_{10}H_{10}N$	144.0814
$C_8H_9O_2$	137.0603	$C_7H_{10}NO_2$	140.0712	$C_9H_{20}N$	142.1597	$C_{11}H_{12}$	144.0939
$C_8H_{11}NO$	137.0841	$C_7H_{12}N_2O$	140.0950	$C_{10}H_8N$	142.0657	**145**	
$C_8H_{13}N_2$	137.1080	$C_7H_{14}N_3$	140.1189	$C_{10}H_{22}$	142.1722	$C_4H_5N_2O_4$	145.0249
$C_9H_{13}O$	137.0967	$C_8H_{12}O_2$	140.0837	$C_{11}H_{10}$	142.0783	$C_4H_7N_3O_3$	145.0488
$C_9H_{15}N$	137.1205	$C_8H_{14}NO$	140.1076	**143**		$C_4H_9N_4O_2$	145.0726
$C_{10}H_{17}$	137.1331	$C_8H_{16}N_2$	140.1315	$C_4H_3N_2O_4$	143.0093	$C_5H_7NO_4$	145.0375
138		$C_9H_{16}O$	140.1202	$C_4H_5N_3O_3$	143.0331	$C_5H_9N_2O_3$	145.0614
$C_3H_{10}N_2O_4$	138.0641	$C_9H_{18}N$	140.1440	$C_4H_7N_4O_2$	143.0570	$C_5H_{11}N_3O_2$	145.0852
$C_5H_4N_3O_2$	138.0304	$C_{10}H_6N$	140.0501	$C_5H_5NO_4$	143.0218	$C_5H_{13}N_4O$	145.1091
$C_5H_6N_4O$	138.0542	$C_{10}H_{20}$	140.1566	$C_5H_7N_2O_3$	143.0457	$C_6H_5N_4$	145.0501
$C_6H_4NO_3$	138.0191	$C_{11}H_8$	140.0626	$C_5H_9N_3O_2$	143.0695	$C_6H_{11}NO_3$	145.0739
$C_6H_6N_2O_2$	138.0429	**141**		$C_5H_{11}N_4O$	143.0934	$C_6H_{13}N_2O_2$	145.0978
$C_6H_8N_3O$	138.0668	$C_4H_3N_3O_3$	141.0175	$C_6H_7O_4$	143.0344	$C_6H_{15}N_3O$	145.1216
$C_6H_{10}N_4$	138.0907	$C_4H_5N_4O_2$	141.0413	$C_6H_9NO_3$	143.0583	$C_6H_{17}N_4$	145.1455
$C_7H_6O_3$	138.0317	$C_5H_3NO_4$	141.0062	$C_6H_{11}N_2O_2$	143.0821	$C_7H_5N_4$	145.0515
$C_7H_8NO_2$	138.0555	$C_5H_5N_2O_3$	141.0300	$C_6H_{13}N_3O$	143.1060	$C_7H_{13}O_3$	145.0865
$C_7H_{10}N_2O$	138.0794	$C_5H_7N_3O_2$	141.0539	$C_6H_{15}N_4$	143.1298	$C_7H_{15}NO_2$	145.1103
$C_7H_{12}N_3$	138.1032	$C_5H_9N_4O$	141.0777	$C_7H_{11}O_3$	143.0708	$C_7H_{17}N_2O$	145.1342
$C_8H_{10}O_2$	138.0681	$C_6H_5O_4$	141.0187	$C_7H_{13}NO_2$	143.0947	$C_7H_{19}N_3$	145.1580
$C_8H_{12}NO$	138.0919	$C_6H_7NO_3$	141.0426	$C_7H_{15}N_2O$	143.1185	$C_8H_5N_2O$	145.0402
$C_8H_{14}N_2$	138.1158	$C_6H_9N_2O_2$	141.0664	$C_7H_{17}N_3$	143.1424	$C_8H_7N_3$	145.0641
$C_9H_{14}O$	138.1045	$C_6H_{11}N_3O$	141.0903	$C_8H_{15}O_2$	143.1072	$C_8H_{17}O_2$	145.1229
$C_9H_{16}N$	138.1284	$C_6H_{13}N_4$	141.1142	$C_8H_{17}NO$	143.1311	$C_8H_{19}NO$	145.1467
$C_{10}H_{18}$	138.1409	$C_7H_9O_3$	141.0552	$C_8H_{19}N_2$	143.1549	C_9H_7NO	145.0528
139		$C_7H_{11}NO_2$	141.0790	$C_9H_7N_2$	143.0610	$C_9H_9N_2$	145.0767
$C_4H_3N_4O_2$	139.0257	$C_7H_{13}N_2O$	141.1029	$C_9H_{19}O$	143.1436	$C_{10}H_9O$	145.0653
$C_5H_3N_2O_3$	139.0144	$C_7H_{15}N_3$	141.1267	$C_9H_{21}N$	143.1675	$C_{10}H_{11}N$	145.0892
$C_5H_5N_3O_2$	139.0382	$C_8H_{13}O_2$	141.0916	$C_{10}H_7O$	143.0497	$C_{11}H_{13}$	145.1018
$C_5H_7N_4O$	139.0621	$C_8H_{15}NO$	141.1154	$C_{10}H_9N$	143.0736	**146**	
$C_6H_5NO_3$	139.0269	$C_8H_{17}N_2$	141.1393	$C_{11}H_{11}$	143.0861	$C_4H_6N_2O_4$	146.0328
$C_6H_7N_2O_2$	139.0508	$C_9H_{17}O$	141.1280	**144**		$C_4H_8N_3O_3$	146.0566
$C_6H_9N_3O$	139.0747	$C_9H_{19}N$	141.1519	$C_4H_4N_2O_4$	144.0171	$C_4H_{10}N_4O_2$	146.0805
$C_6H_{11}N_4$	139.0985	$C_{10}H_7N$	141.0579	$C_4H_6N_3O_3$	144.0410	$C_5H_8NO_4$	146.0453
$C_7H_7O_3$	139.0395	$C_{10}H_{21}$	141.1644	$C_4H_8N_4O_2$	144.0648	$C_5H_{10}N_2O_3$	146.0692
$C_7H_9NO_2$	139.0634	$C_{11}H_9$	141.0705	$C_5H_6NO_4$	144.0297	$C_5H_{12}N_3O_2$	146.0930
$C_7H_{11}N_2O$	139.0872	**142**		$C_5H_8N_2O_3$	144.0535	$C_5H_{14}N_4O$	146.1169
$C_7H_{13}N_3$	139.1111	$C_4H_4N_3O_3$	142.0253	$C_5H_{10}N_3O_2$	144.0774	$C_6H_{10}O_4$	146.0579
$C_8H_{11}O_2$	139.0759	$C_4H_6N_4O_2$	142.0491	$C_5H_{12}N_4O$	144.1012	$C_6H_{12}NO_3$	146.0817
$C_8H_{13}NO$	139.0998	$C_5H_4NO_4$	142.0140	$C_6H_8O_4$	144.0422	$C_6H_{14}N_2O_2$	146.1056
$C_8H_{15}N_2$	139.1236	$C_5H_6N_2O_3$	142.0379	$C_6H_{10}NO_3$	144.0661	$C_6H_{16}N_3O$	146.1295
$C_9H_3N_2$	139.0297	$C_5H_8N_3O_2$	142.0617	$C_6H_{12}N_2O_2$	144.0899	$C_7H_6N_4$	146.0594
$C_9H_{15}O$	139.1123	$C_5H_{10}N_4O$	142.0856	$C_6H_{14}N_3O$	144.1138	$C_7H_{14}O_3$	146.0943
$C_9H_{17}N$	139.1362	$C_6H_6O_4$	142.0266	$C_6H_{16}N_4$	144.1377	$C_7H_{16}NO_2$	146.1182
$C_{10}H_{19}$	139.1488	$C_6H_8NO_3$	142.0504	$C_7H_{12}O_3$	144.0786	$C_7H_{18}N_2O$	146.1420
$C_{11}H_7$	139.0548	$C_6H_{10}N_2O_2$	142.0743	$C_7H_{14}NO_2$	144.1025	$C_8H_2O_3$	146.0003
140		$C_6H_{12}N_3O$	142.0981	$C_7H_{16}N_2O$	144.1264	$C_8H_6N_2O$	146.0480
$C_4H_4N_4O_2$	140.0335	$C_6H_{14}N_4$	142.1220	$C_7H_{18}N_3$	144.1502	$C_8H_8N_3$	146.0719
$C_5H_4N_2O_3$	140.0222	$C_7H_{10}O_3$	142.0630	$C_8H_6N_3$	144.0563	$C_8H_{18}O_2$	146.1307
$C_5H_6N_3O_2$	140.0460	$C_7H_{12}NO_2$	142.0868	$C_8H_{16}O_2$	144.1151	$C_9H_6O_2$	146.0368
$C_5H_8N_4O$	140.0699	$C_7H_{14}N_2O$	142.1107	$C_8H_{18}NO$	144.1389	C_9H_8NO	146.0606
$C_6H_4O_4$	140.0109	$C_7H_{16}N_3$	142.1346	$C_8H_{20}N_2$	144.1628	$C_9H_{10}N_2$	146.0845
$C_6H_6NO_3$	140.0348	$C_8H_{14}O_2$	142.0994	C_9H_6NO	144.0449	$C_{10}H_{10}O$	146.0732

APPENDIX A (*Continued*)

FM		FM		FM		FM	
$C_{10}H_{12}N$	146.0970	$C_5H_{15}N_3O_2$	149.1165	$C_9H_{13}NO$	151.0998	$C_6H_{10}N_4O$	154.0856
$C_{11}H_{14}$	146.1096	$C_6H_5N_4O$	149.0464	$C_9H_{15}N_2$	151.1236	$C_7H_6O_4$	154.0266
147		$C_6H_{13}O_4$	149.0814	$C_{10}H_{15}O$	151.1123	$C_7H_8NO_3$	154.0504
$C_4H_7N_2O_4$	147.0406	$C_6H_{15}NO_3$	149.1052	$C_{10}H_{17}N$	151.1362	$C_7H_{10}N_2O_2$	154.0743
$C_4H_9N_3O_3$	147.0644	$C_7H_5N_2O_2$	149.0351	$C_{11}H_{19}$	151.1488	$C_7H_{12}N_3O$	154.0981
$C_4H_{11}N_4O_2$	147.0883	$C_7H_7N_3O$	149.0590	**152**		$C_7H_{14}N_4$	154.1220
$C_5H_9NO_4$	147.0532	$C_7H_9N_4$	149.0829	$C_4H_{12}N_2O_4$	152.0797	$C_8H_{10}O_3$	154.0630
$C_5H_{11}N_2O_3$	147.0770	$C_8H_5O_3$	149.0238	$C_5H_4N_4O_2$	152.0335	$C_8H_{12}NO_2$	154.0868
$C_5H_{13}N_3O_2$	147.1009	$C_8H_7NO_2$	149.0477	$C_6H_4N_2O_3$	152.0222	$C_8H_{14}N_2O$	154.1107
$C_5H_{15}N_4O$	147.1247	$C_8H_9N_2O$	149.0715	$C_6H_6N_3O_2$	152.0460	$C_8H_{16}N_3$	154.1346
$C_6H_{11}O_4$	147.0657	$C_8H_{11}N_3$	149.0954	$C_6H_8N_4O$	152.0699	$C_9H_{14}O_2$	154.0994
$C_6H_{13}NO_3$	147.0896	$C_9H_9O_2$	149.0603	$C_7H_6NO_3$	152.0348	$C_9H_{16}NO$	154.1233
$C_6H_{15}N_2O_2$	147.1134	$C_9H_{11}NO$	149.0841	$C_7H_8N_2O_2$	152.0586	$C_9H_{18}N_2$	154.1471
$C_6H_{17}N_3O$	147.1373	$C_9H_{13}N_2$	149.1080	$C_7H_{10}N_3O$	152.0825	$C_{10}H_{18}O$	154.1358
$C_7H_5N_3O$	147.0433	$C_{10}H_{13}O$	149.0967	$C_7H_{12}N_4$	152.1063	$C_{10}H_{20}N$	154.1597
$C_7H_7N_4$	147.0672	$C_{10}H_{15}N$	149.1205	$C_8H_8O_3$	152.0473	$C_{11}H_8N$	154.0657
$C_7H_{15}O_3$	147.1021	$C_{11}H_{17}$	149.1331	$C_8H_{10}NO_2$	152.0712	$C_{11}H_{22}$	154.1722
$C_7H_{17}NO_2$	147.1260	**150**		$C_8H_{12}N_2O$	152.0950	$C_{12}H_{10}$	154.0783
$C_8H_5NO_2$	147.0320	$C_4H_{10}N_2O_4$	150.0641	$C_8H_{14}N_3$	152.1189	**155**	
$C_8H_7N_2O$	147.0559	$C_4H_{12}N_3O_3$	150.0879	$C_9H_{12}O_2$	152.0837	$C_5H_3N_2O_4$	155.0093
$C_8H_9N_3$	147.0798	$C_4H_{14}N_4O_2$	150.1118	$C_9H_{14}NO$	152.1076	$C_5H_5N_3O_3$	155.0331
$C_9H_7O_2$	147.0446	$C_5H_{12}NO_4$	150.0766	$C_9H_{16}N_2$	152.1315	$C_5H_7N_4O_2$	155.0570
C_9H_9NO	147.0684	$C_5H_{14}N_2O_3$	150.1005	$C_{10}H_{16}O$	152.1202	$C_6H_5NO_4$	155.0218
$C_9H_{11}N_2$	147.0923	$C_6H_4N_3O_2$	150.0304	$C_{10}H_{18}N$	152.1440	$C_6H_7N_2O_3$	155.0457
$C_{10}H_{11}O$	147.0810	$C_6H_6N_4O$	150.0542	$C_{11}H_6N$	152.0501	$C_6H_9N_3O_2$	155.0695
$C_{10}H_{13}N$	147.1049	$C_6H_{14}O_4$	150.0892	$C_{11}H_{20}$	152.1566	$C_6H_{11}N_4O$	155.0934
$C_{11}H_{15}$	147.1174	$C_7H_6N_2O_2$	150.0429	$C_{12}H_8$	152.0626	$C_7H_7O_4$	155.0344
148		$C_7H_8N_3O$	150.0668	**153**		$C_7H_9NO_3$	155.0583
$C_4H_8N_2O_4$	148.0484	$C_7H_{10}N_4$	150.0907	$C_5H_3N_3O_3$	153.0175	$C_7H_{11}N_2O_2$	155.0821
$C_4H_{10}N_3O_3$	148.0723	$C_8H_6O_3$	150.0317	$C_5H_5N_4O_2$	153.0413	$C_7H_{13}N_3O$	155.1060
$C_4H_{12}N_4O_2$	148.0961	$C_8H_8NO_2$	150.0555	$C_6H_5N_2O_3$	153.0300	$C_8H_{11}O_3$	155.0708
$C_5H_{10}NO_4$	148.0610	$C_8H_{10}N_2O$	150.0794	$C_6H_7N_3O_2$	153.0539	$C_8H_{13}NO_2$	155.0947
$C_5H_{12}N_2O_3$	148.0849	$C_8H_{12}N_3$	150.1032	$C_6H_9N_4O$	153.0777	$C_8H_{15}N_2O$	155.1185
$C_5H_{16}N_4O$	148.1325	$C_9H_{10}O_2$	150.0681	$C_7H_5O_4$	153.0187	$C_8H_{17}N_3$	155.1424
$C_6H_4N_4O$	148.0386	$C_9H_{12}NO$	150.0919	$C_7H_7NO_3$	153.0426	$C_9H_{15}O_2$	155.1072
$C_6H_{12}O_4$	148.0735	$C_9H_{14}N_2$	150.1158	$C_7H_9N_2O_2$	153.0664	$C_9H_{17}NO$	155.1311
$C_6H_{14}NO_3$	148.0974	$C_{10}H_{14}O$	150.1045	$C_7H_{11}N_3O$	153.0903	$C_9H_{19}N_2$	155.1549
$C_6H_{16}N_2O_2$	148.1213	$C_{10}H_{16}N$	150.1284	$C_7H_{13}N_4$	153.1142	$C_{10}H_7N_2$	155.0610
$C_7H_6N_3O$	148.0511	$C_{11}H_{18}$	150.1409	$C_8H_9O_3$	153.0552	$C_{10}H_{19}O$	155.1436
$C_7H_8N_4$	148.0750	**151**		$C_8H_{11}NO_2$	153.0790	$C_{10}H_{21}N$	155.1675
$C_7H_{16}O_3$	148.1100	$C_4H_{11}N_2O_4$	151.0719	$C_8H_{13}N_2O$	153.1029	$C_{11}H_7O$	155.0497
$C_8H_6NO_2$	148.0399	$C_4H_{13}N_3O_3$	151.0958	$C_8H_{15}N_3$	153.1267	$C_{11}H_9N$	155.0736
$C_8H_8N_2O$	148.0637	$C_5H_3N_4O_2$	151.0257	$C_9H_{13}O_2$	153.0916	$C_{11}H_{23}$	155.1801
$C_8H_{10}N_3$	148.0876	$C_5H_{13}NO_4$	151.0845	$C_9H_{15}NO$	153.1154	$C_{12}H_{11}$	155.0861
$C_9H_8O_2$	148.0524	$C_6H_3N_2O_3$	151.0144	$C_9H_{17}N_2$	153.1393	**156**	
$C_9H_{10}NO$	148.0763	$C_6H_5N_3O_2$	151.0382	$C_{10}H_{17}O$	153.1280	$C_5H_4N_2O_4$	156.0171
$C_9H_{12}N_2$	148.1001	$C_6H_7N_4O$	151.0621	$C_{10}H_{19}N$	153.1519	$C_5H_6N_3O_3$	156.0410
$C_{10}H_{12}O$	148.0888	$C_7H_5NO_3$	151.0269	$C_{11}H_7N$	153.0579	$C_5H_8N_4O_2$	156.0648
$C_{10}H_{14}N$	148.1127	$C_7H_7N_2O_2$	151.0508	$C_{11}H_{21}$	153.1644	$C_6H_6NO_4$	156.0297
$C_{11}H_{16}$	148.1253	$C_7H_9N_3O$	151.0746	$C_{12}H_9$	153.0705	$C_6H_8N_2O_3$	156.0535
149		$C_7H_{11}N_4$	151.0985	**154**		$C_6H_{10}N_3O_2$	156.0774
$C_4H_9N_2O_4$	149.0563	$C_8H_7O_3$	151.0395	$C_5H_4N_3O_3$	154.0253	$C_6H_{12}N_4O$	156.1012
$C_4H_{11}N_3O_3$	149.0801	$C_8H_9NO_2$	151.0634	$C_5H_6N_4O_2$	154.0491	$C_7H_8O_4$	156.0422
$C_4H_{13}N_4O_2$	149.1040	$C_8H_{11}N_2O$	151.0872	$C_6H_4NO_4$	154.0140	$C_7H_{10}NO_3$	156.0661
$C_5H_{11}NO_4$	149.0688	$C_8H_{13}N_3$	151.1111	$C_6H_6N_2O_3$	154.0379	$C_7H_{12}N_2O_2$	156.0899
$C_5H_{13}N_2O_3$	149.0927	$C_9H_{11}O_2$	151.0759	$C_6H_8N_3O_2$	154.0617	$C_7H_{14}N_3O$	156.1138

APPENDIX A (*Continued*)

	FM		FM		FM		FM
$C_7H_{16}N_4$	156.1377	$C_7H_{14}N_2O_2$	158.1056	$C_7H_{14}NO_3$	160.0974	$C_8H_{10}N_4$	162.0907
$C_8H_{12}O_3$	156.0786	$C_7H_{16}N_3O$	158.1295	$C_7H_{16}N_2O_2$	160.1213	$C_8H_{18}O_3$	162.1256
$C_8H_{14}NO_2$	156.1025	$C_7H_{18}N_4$	158.1533	$C_7H_{18}N_3O$	160.1451	$C_9H_6O_3$	162.0317
$C_8H_{16}N_2O$	156.1264	$C_8H_6N_4$	158.0594	$C_7H_{20}N_4$	160.1690	$C_9H_8NO_2$	162.0555
$C_8H_{18}N_3$	156.1502	$C_8H_{14}O_3$	158.0943	$C_8H_6N_3O$	160.0511	$C_9H_{10}N_2O$	162.0794
$C_9H_6N_3$	156.0563	$C_8H_{16}NO_2$	158.1182	$C_8H_8N_4$	160.0750	$C_9H_{12}N_3$	162.1032
$C_9H_{16}O_2$	156.1151	$C_8H_{18}N_2O$	158.1420	$C_8H_{16}O_3$	160.1100	$C_{10}H_{10}O_2$	162.0681
$C_9H_{18}NO$	156.1389	$C_8H_{20}N_3$	158.1659	$C_8H_{18}NO_2$	160.1338	$C_{10}H_{12}NO$	162.0919
$C_9H_{20}N_2$	156.1628	$C_9H_6N_2O$	158.0480	$C_8H_{20}N_2O$	160.1577	$C_{10}H_{14}N_2$	162.1158
$C_{10}H_6NO$	156.0449	$C_9H_8N_3$	158.0719	$C_9H_6NO_2$	160.0399	$C_{11}H_{14}O$	162.1045
$C_{10}H_8N_2$	156.0688	$C_9H_{18}O_2$	158.1307	$C_9H_8N_2O$	160.0637	$C_{11}H_{16}N$	162.1284
$C_{10}H_{20}O$	156.1515	$C_9H_{20}NO$	158.1546	$C_9H_{10}N_3$	160.0876	$C_{12}H_{18}$	162.1409
$C_{10}H_{22}N$	156.1753	$C_{10}H_6O_2$	158.0368	$C_9H_{20}O_2$	160.1464	**163**	
$C_{11}H_8O$	156.0575	$C_{10}H_8NO$	158.0606	$C_{10}H_8O_2$	160.0524	$C_5H_{11}N_2O_4$	163.0719
$C_{11}H_{10}N$	156.0814	$C_{10}H_{10}N_2$	158.0845	$C_{10}H_{10}NO$	160.0763	$C_5H_{13}N_3O_3$	163.0958
$C_{11}H_{24}$	156.1879	$C_{10}H_{22}O$	158.1672	$C_{10}H_{12}N_2$	160.1001	$C_5H_{15}N_4O_2$	163.1196
$C_{12}H_{12}$	156.0939	$C_{11}H_{10}O$	158.0732	$C_{11}H_{12}O$	160.0888	$C_6H_{13}NO_4$	163.0845
157		$C_{11}H_{12}N$	158.0970	$C_{11}H_{14}N$	160.1127	$C_6H_{15}N_2O_3$	163.1083
$C_5H_5N_2O_4$	157.0249	$C_{12}H_{14}$	158.1096	$C_{12}H_{16}$	160.1253	$C_6H_{17}N_3O_2$	163.1322
$C_5H_7N_3O_3$	157.0488	**159**		**161**		$C_7H_5N_3O_2$	163.0382
$C_5H_9N_4O_2$	157.0726	$C_5H_7N_2O_4$	159.0406	$C_5H_9N_2O_4$	161.0563	$C_7H_7N_4O$	163.0621
$C_6H_7NO_4$	157.0375	$C_5H_9N_3O_3$	159.0644	$C_5H_{11}N_3O_3$	161.0801	$C_7H_{15}O_4$	163.0970
$C_6H_9N_2O_3$	157.0614	$C_5H_{11}N_4O_2$	159.0883	$C_5H_{13}N_4O_2$	161.1040	$C_7H_{17}NO_3$	163.1209
$C_6H_{11}N_3O_2$	157.0852	$C_6H_9NO_4$	159.0532	$C_6H_{11}NO_4$	161.0688	$C_8H_5NO_3$	163.0269
$C_6H_{13}N_4O$	157.1091	$C_6H_{11}N_2O_3$	159.0770	$C_6H_{13}N_2O_3$	161.0927	$C_8H_7N_2O_2$	163.0508
$C_7H_9O_4$	157.0501	$C_6H_{13}N_3O_2$	159.1009	$C_6H_{15}N_3O_2$	161.1165	$C_8H_9N_3O$	163.0746
$C_7H_{11}NO_3$	157.0739	$C_6H_{15}N_4O$	159.1247	$C_6H_{17}N_4O$	161.1404	$C_8H_{11}N_4$	163.0985
$C_7H_{13}N_2O_2$	157.0978	$C_7H_{11}O_4$	159.0657	$C_7H_5N_4O$	161.0464	$C_9H_7O_3$	163.0395
$C_7H_{15}N_3O$	157.1216	$C_7H_{13}NO_3$	159.0896	$C_8H_5N_2O_2$	161.0351	$C_9H_9NO_2$	163.0634
$C_7H_{17}N_4$	157.1455	$C_7H_{15}N_2O_2$	159.1134	$C_8H_7N_3O$	161.0590	$C_9H_{11}N_2O$	163.0872
$C_8H_5N_4$	157.0515	$C_7H_{17}N_3O$	159.1373	$C_8H_9N_4$	161.0829	$C_9H_{13}N_3$	163.1111
$C_8H_{13}O_3$	157.0865	$C_8H_5N_3O$	159.0433	$C_8H_{17}O_3$	161.1178	$C_{10}H_{11}O_2$	163.0759
$C_8H_{15}NO_2$	157.1103	$C_8H_7N_4$	159.0672	$C_8H_{19}NO_2$	161.1416	$C_{10}H_{13}NO$	163.0998
$C_8H_{17}N_2O$	157.1342	$C_8H_{15}O_3$	159.1021	$C_9H_5O_3$	161.0238	$C_{10}H_{15}N_2$	163.1236
$C_8H_{19}N_3$	157.1580	$C_8H_{17}NO_2$	159.1260	$C_9H_7NO_2$	161.0477	$C_{11}H_{15}O$	163.1123
$C_9H_5N_2O$	157.0402	$C_8H_{19}N_2O$	159.1498	$C_9H_9N_2O$	161.0715	$C_{11}H_{17}N$	163.1362
$C_9H_7N_3$	157.0641	$C_8H_{21}N_3$	159.1737	$C_9H_{11}N_3$	161.0954	$C_{12}H_{19}$	163.1488
$C_9H_{17}O_2$	157.1229	$C_9H_5NO_2$	159.0320	$C_{10}H_9O_2$	161.0603	**164**	
$C_9H_{19}NO$	157.1467	$C_9H_7N_2O$	159.0559	$C_{10}H_{11}NO$	161.0841	$C_5H_{12}N_2O_4$	164.0797
$C_9H_{21}N_2$	157.1706	$C_9H_9N_3$	159.0798	$C_{10}H_{13}N_2$	161.1080	$C_5H_{14}N_3O_3$	164.1036
$C_{10}H_7NO$	157.0528	$C_9H_{19}O_2$	159.1385	$C_{11}H_{13}O$	161.0967	$C_5H_{16}N_4O_2$	164.1275
$C_{10}H_9N_2$	157.0767	$C_9H_{21}NO$	159.1624	$C_{11}H_{15}N$	161.1205	$C_6H_4N_4O_2$	164.0335
$C_{10}H_{21}O$	157.1593	$C_{10}H_7O_2$	159.0446	$C_{12}H_{17}$	161.1331	$C_6H_{14}NO_4$	164.0923
$C_{10}H_{23}N$	157.1832	$C_{10}H_9NO$	159.0684	**162**		$C_6H_{16}N_2O_3$	164.1162
$C_{11}H_9O$	157.0653	$C_{10}H_{11}N_2$	159.0923	$C_5H_{10}N_2O_4$	162.0641	$C_7H_6N_3O_2$	164.0460
$C_{11}H_{11}N$	157.0892	$C_{11}H_{11}O$	159.0810	$C_5H_{12}N_3O_3$	162.0879	$C_7H_8N_4O$	164.0699
$C_{12}H_{13}$	157.1018	$C_{11}H_{13}N$	159.1049	$C_5H_{14}N_4O_2$	162.1118	$C_7H_{16}O_4$	164.1049
158		$C_{12}H_{15}$	159.1174	$C_6H_{12}NO_4$	162.0766	$C_8H_6NO_3$	164.0348
$C_5H_6N_2O_4$	158.0328	**160**		$C_6H_{14}N_2O_3$	162.1005	$C_8H_8N_2O_2$	164.0586
$C_5H_8N_3O_3$	158.0566	$C_5H_8N_2O_4$	160.0484	$C_6H_{16}N_3O_2$	162.1244	$C_8H_{10}N_3O$	164.0825
$C_5H_{10}N_4O_2$	158.0805	$C_5H_{10}N_3O_3$	160.0723	$C_6H_{18}N_4O$	162.1482	$C_8H_{12}N_4$	164.1063
$C_6H_8NO_4$	158.0453	$C_5H_{12}N_4O_2$	160.0961	$C_7H_6N_4O$	162.0542	$C_9H_8O_3$	164.0473
$C_6H_{10}N_2O_3$	158.0692	$C_6H_{10}NO_4$	160.0610	$C_7H_{14}O_4$	162.0892	$C_9H_{10}NO_2$	164.0712
$C_6H_{12}N_3O_2$	158.0930	$C_6H_{12}N_2O_3$	160.0848	$C_7H_{16}NO_3$	162.1131	$C_9H_{12}N_2O$	164.0950
$C_6H_{14}N_4O$	158.1169	$C_6H_{14}N_3O_2$	160.1087	$C_7H_{18}N_2O_2$	162.1369	$C_9H_{14}N_3$	164.1189
$C_7H_{10}O_4$	158.0579	$C_6H_{16}N_4O$	160.1325	$C_8H_6N_2O_2$	162.0429	$C_{10}H_{12}O_2$	164.0837
$C_7H_{12}NO_3$	158.0817	$C_7H_{12}O_4$	160.0735	$C_8H_8N_3O$	162.0668	$C_{10}H_{14}NO$	164.1076

APPENDIX A (*Continued*)

FM		FM		FM		FM	
$C_{10}H_{16}N_2$	164.1315	$C_7H_7N_2O_3$	167.0457	$C_8H_{11}NO_3$	169.0739	$C_7H_{13}N_3O_2$	171.1009
$C_{11}H_{16}O$	164.1202	$C_7H_9N_3O_2$	167.0695	$C_8H_{13}N_2O_2$	169.0978	$C_7H_{15}N_4O$	171.1247
$C_{11}H_{18}N$	164.1440	$C_7H_{11}N_4O$	167.0934	$C_8H_{15}N_3O$	169.1216	$C_8H_{11}O_4$	171.0657
$C_{12}H_{20}$	164.1566	$C_8H_7O_4$	167.0344	$C_8H_{17}N_4$	169.1455	$C_8H_{13}NO_3$	171.0896
165		$C_8H_9NO_3$	167.0583	$C_9H_{13}O_3$	169.0865	$C_8H_{15}N_2O_2$	171.1134
$C_5H_{13}N_2O_4$	165.0876	$C_8H_{11}N_2O_2$	167.0821	$C_9H_{15}NO_2$	169.1103	$C_8H_{17}N_3O$	171.1373
$C_5H_{15}N_3O_3$	165.1114	$C_8H_{13}N_3O$	167.1060	$C_9H_{17}N_2O$	169.1342	$C_8H_{19}N_4$	171.1611
$C_6H_5N_4O_2$	165.0413	$C_8H_{15}N_4$	167.1298	$C_9H_{19}N_3$	169.1580	$C_9H_5N_3O$	171.0433
$C_6H_{15}NO_4$	165.1001	$C_9H_{11}O_3$	167.0708	$C_{10}H_7N_3$	169.0641	$C_9H_7N_4$	171.0672
$C_7H_5N_2O_3$	165.0300	$C_9H_{13}NO_2$	167.0947	$C_{10}H_{17}O_2$	169.1229	$C_9H_{15}O_3$	171.1021
$C_7H_7N_3O_2$	165.0539	$C_9H_{15}N_2O$	167.1185	$C_{10}H_{19}NO$	169.1467	$C_9H_{17}NO_2$	171.1260
$C_7H_9N_4O$	165.0777	$C_9H_{17}N_3$	167.1424	$C_{10}H_{21}N_2$	169.1706	$C_9H_{19}N_2O$	171.1498
$C_8H_5O_4$	165.0187	$C_{10}H_{15}O_2$	167.1072	$C_{11}H_7NO$	169.0528	$C_9H_{21}N_3$	171.1737
$C_8H_7NO_3$	165.0426	$C_{10}H_{17}NO$	167.1311	$C_{11}H_9N_2$	169.0767	$C_{10}H_7N_2O$	171.0559
$C_8H_9N_2O_2$	165.0664	$C_{10}H_{19}N_2$	167.1549	$C_{11}H_{21}O$	169.1593	$C_{10}H_9N_3$	171.0798
$C_8H_{11}N_3O$	165.0903	$C_{11}H_7N_2$	167.0610	$C_{11}H_{23}N$	169.1832	$C_{10}H_{19}O_2$	171.1385
$C_8H_{13}N_4$	165.1142	$C_{11}H_{19}O$	167.1436	$C_{12}H_9O$	169.0653	$C_{10}H_{21}NO$	171.1624
$C_9H_9O_3$	165.0552	$C_{11}H_{21}N$	167.1675	$C_{12}H_{11}N$	169.0892	$C_{10}H_{23}N_2$	171.1863
$C_9H_{11}NO_2$	165.0790	$C_{12}H_9N$	167.0736	$C_{12}H_{25}$	169.1957	$C_{11}H_7O_2$	171.0446
$C_9H_{13}N_2O$	165.1029	$C_{12}H_{23}$	167.1801	$C_{13}H_{13}$	169.1018	$C_{11}H_9NO$	171.0684
$C_9H_{15}N_3$	165.1267	$C_{13}H_{11}$	167.0861	**170**		$C_{11}H_{11}N_2$	171.0923
$C_{10}H_{13}O_2$	165.0916	**168**		$C_6H_6N_2O_4$	170.0328	$C_{11}H_{23}O$	171.1750
$C_{10}H_{15}NO$	165.1154	$C_6H_4N_2O_4$	168.0171	$C_6H_8N_3O_3$	170.0566	$C_{11}H_{25}N$	171.1988
$C_{10}H_{17}N_2$	165.1393	$C_6H_6N_3O_3$	168.0410	$C_6H_{10}N_4O_2$	170.0805	$C_{12}H_{11}O$	171.0810
$C_{11}H_{17}O$	165.1280	$C_6H_8N_4O_2$	168.0648	$C_7H_8NO_4$	170.0453	$C_{12}H_{13}N$	171.1049
$C_{11}H_{19}N$	165.1519	$C_7H_6NO_4$	168.0297	$C_7H_{10}N_2O_3$	170.0692	$C_{13}H_{15}$	171.1174
$C_{12}H_7N$	165.0579	$C_7H_8N_2O_3$	168.0535	$C_7H_{12}N_3O_2$	170.0930	**172**	
$C_{12}H_{21}$	165.1644	$C_7H_{10}N_3O_2$	168.0774	$C_7H_{14}N_4O$	170.1169	$C_6H_8N_2O_4$	172.0484
$C_{13}H_9$	165.0705	$C_7H_{12}N_4O$	168.1012	$C_8H_{10}O_4$	170.0579	$C_6H_{10}N_3O_3$	172.0723
166		$C_8H_8O_4$	168.0422	$C_8H_{12}NO_3$	170.0817	$C_6H_{12}N_4O_2$	172.0961
$C_5H_{14}N_2O_4$	166.0954	$C_8H_{10}NO_3$	168.0661	$C_8H_{14}N_2O_2$	170.1056	$C_7H_{10}NO_4$	172.0610
$C_6H_4N_3O_3$	166.0253	$C_8H_{12}N_2O_2$	168.0899	$C_8H_{16}N_3O$	170.1295	$C_7H_{12}H_{12}N_2O_3$	172.0848
$C_6H_6N_4O_2$	166.0491	$C_8H_{14}N_3O$	168.1138	$C_8H_{18}N_4$	170.1533	$C_7H_{14}N_3O_2$	172.1087
$C_7H_6N_2O_3$	166.0379	$C_8H_{16}N_4$	168.1377	$C_9H_6N_4$	170.0594	$C_7H_{16}N_4O$	172.1325
$C_7H_8N_3O_2$	166.0617	$C_9H_{12}O_3$	168.0786	$C_9H_{14}O_3$	170.0943	$C_8H_{12}O_4$	172.0735
$C_7H_{10}N_4O$	166.0856	$C_9H_{14}NO_2$	168.1025	$C_9H_{16}NO_2$	170.1182	$C_8H_{14}NO_3$	172.0974
$C_8H_6O_4$	166.0266	$C_9H_{16}N_2O$	168.1264	$C_9H_{18}N_2O$	170.1420	$C_8H_{16}N_2O_2$	172.1213
$C_8H_8NO_3$	166.0504	$C_9H_{18}N_3$	168.1502	$C_9H_{20}N_3$	170.1659	$C_8H_{18}N_3O$	172.1451
$C_8H_{10}N_2O_2$	166.0743	$C_{10}H_{16}O_2$	168.1151	$C_{10}H_6N_2O$	170.0480	$C_8H_{20}N_4$	172.1690
$C_8H_{12}N_3O$	166.0981	$C_{10}H_{18}NO$	168.1389	$C_{10}H_8N_3$	170.0719	$C_9H_6N_3O$	172.0511
$C_8H_{14}N_4$	166.1220	$C_{10}H_{20}N_2$	168.1628	$C_{10}H_{18}O_2$	170.1307	$C_9H_8N_4$	172.0750
$C_9H_{10}O_3$	166.0630	$C_{11}H_8N_2$	168.0688	$C_{10}H_{20}NO$	170.1546	$C_9H_{16}O_3$	172.1100
$C_9H_{12}NO_2$	166.0868	$C_{11}H_{20}O$	168.1515	$C_{10}H_{22}N_2$	170.1784	$C_9H_{18}NO_2$	172.1338
$C_9H_{14}N_2O$	166.1107	$C_{11}H_{22}N$	168.1753	$C_{11}H_8NO$	170.0606	$C_9H_{20}N_2O$	172.1577
$C_9H_{16}N_3$	166.1346	$C_{12}H_8O$	168.0575	$C_{11}H_{10}N_2$	170.0845	$C_9H_{22}N_3$	172.1815
$C_{10}H_{14}O_2$	166.0994	$C_{12}H_{10}N$	168.0814	$C_{11}H_{22}O$	170.1671	$C_{10}H_6NO_2$	172.0399
$C_{10}H_{16}NO$	166.1233	$C_{12}H_{24}$	168.1879	$C_{11}H_{24}N$	170.1910	$C_{10}H_8N_2O$	172.0637
$C_{10}H_{18}N_2$	166.1471	$C_{13}H_{12}$	168.0939	$C_{12}H_{10}O$	170.0732	$C_{10}H_{10}N_3$	172.0876
$C_{11}H_{18}O$	166.1358	**169**		$C_{12}H_{12}N$	170.0970	$C_{10}H_{20}O_2$	172.1464
$C_{11}H_{20}N$	166.1597	$C_6H_5N_2O_4$	169.0249	$C_{12}H_{26}$	170.2036	$C_{10}H_{22}NO$	172.1702
$C_{12}H_8N$	166.0657	$C_6H_7N_3O_3$	169.0488	$C_{13}H_{14}$	170.1096	$C_{10}H_{24}N_2$	172.1941
$C_{12}H_{22}$	166.1722	$C_6H_9N_4O_2$	169.0726	**171**		$C_{11}H_8O_2$	172.0524
$C_{13}H_{10}$	166.0783	$C_7H_7NO_4$	169.0375	$C_6H_7N_2O_4$	171.0406	$C_{11}H_{10}NO$	172.0763
167		$C_7H_9N_2O_3$	169.0614	$C_6H_9N_3O_3$	171.0644	$C_{11}H_{12}N_2$	172.1001
$C_6H_5N_3O_3$	167.0331	$C_7H_{11}N_3O_2$	169.0852	$C_6H_{11}N_4O_2$	171.0883	$C_{11}H_{24}O$	172.1828
$C_6H_7N_4O_2$	167.0570	$C_7H_{13}N_4O$	169.1091	$C_7H_9NO_4$	171.0532	$C_{12}H_{12}O$	172.0888
$C_7H_5NO_4$	167.0218	$C_8H_9O_4$	169.0501	$C_7H_{11}N_2O_3$	171.0770	$C_{12}H_{14}N$	172.1127

APPENDIX A (*Continued*)

FM		FM		FM		FM	
$C_{13}H_{16}$	172.1253	$C_{11}H_{12}NO$	174.0919	$C_{11}H_{12}O_2$	176.0837	$C_{12}H_{20}N$	178.1597
173		$C_{11}H_{14}N_2$	174.1158	$C_{11}H_{14}NO$	176.1076	$C_{13}H_8N$	178.0657
$C_6H_9N_2O_4$	173.0563	$C_{12}H_{14}O$	174.1045	$C_{11}H_{16}N_2$	176.1315	$C_{13}H_{22}$	178.1722
$C_6H_{11}N_3O_3$	173.0801	$C_{12}H_{16}N$	174.1284	$C_{12}H_{16}O$	176.1202	$C_{14}H_{10}$	178.0783
$C_6H_{13}N_4O_2$	173.1040	$C_{13}H_{18}$	174.1409	$C_{12}H_{18}N$	176.1440	**179**	
$C_7H_{11}NO_4$	173.0688	**175**		$C_{13}H_{20}$	176.1566	$C_6H_{15}N_2O_4$	179.1032
$C_7H_{13}N_2O_3$	173.0927	$C_6H_{11}N_2O_4$	175.0719	**177**		$C_6H_{17}N_3O_3$	179.1271
$C_7H_{15}N_3O_2$	173.1165	$C_6H_{13}N_3O_3$	175.0958	$C_6H_{13}N_2O_4$	177.0876	$C_7H_5N_3O_3$	179.0331
$C_7H_{17}N_4O$	173.1404	$C_6H_{15}N_4O_2$	175.1196	$C_6H_{15}N_3O_3$	177.1114	$C_7H_7N_4O_2$	179.0570
$C_8H_{13}O_4$	173.0814	$C_7H_{13}NO_4$	175.0845	$C_6H_{17}N_4O_2$	177.1353	$C_7H_{17}NO_4$	179.1158
$C_8H_{15}NO_3$	173.1052	$C_7H_{15}N_2O_3$	175.1083	$C_7H_5N_4O_2$	177.0413	$C_8H_5NO_4$	179.0218
$C_8H_{17}N_2O_2$	173.1291	$C_7H_{17}N_3O_2$	175.1322	$C_7H_{15}NO_4$	177.1001	$C_8H_7N_2O_3$	179.0457
$C_8H_{19}N_3O$	173.1529	$C_7H_{19}N_4O$	175.1560	$C_7H_{17}N_2O_3$	177.1240	$C_8H_9N_3O_2$	179.0695
$C_8H_{21}N_4$	173.1768	$C_8H_7N_4O$	175.0621	$C_7H_{19}N_3O_2$	177.1478	$C_8H_{11}N_4O$	179.0934
$C_9H_7N_3O$	173.0590	$C_8H_{15}O_4$	175.0970	$C_8H_5N_2O_3$	177.0300	$C_9H_7O_4$	179.0344
$C_9H_9N_4$	173.0829	$C_8H_{17}NO_3$	175.1209	$C_8H_7N_3O_2$	177.0539	$C_9H_9NO_3$	179.0583
$C_9H_{17}O_3$	173.1178	$C_8H_{19}N_2O_2$	175.1447	$C_8H_9N_4O$	177.0777	$C_9H_{11}N_2O_2$	179.0821
$C_9H_{19}NO_2$	173.1416	$C_8H_{21}N_3O$	175.1686	$C_8H_{17}O_4$	177.1127	$C_9H_{13}N_3O$	179.1060
$C_9H_{21}N_2O$	173.1655	$C_9H_5NO_3$	175.0269	$C_8H_{19}NO_3$	177.1365	$C_9H_{15}N_4$	179.1298
$C_{10}H_5O_3$	173.0238	$C_9H_7N_2O_2$	175.0508	$C_9H_7NO_3$	177.0426	$C_{10}H_{11}O_3$	179.0708
$C_{10}H_7NO_2$	173.0477	$C_9H_9N_3O$	175.0746	$C_9H_9N_2O_2$	177.0664	$C_{10}H_{13}NO_2$	179.0947
$C_{10}H_9N_2O$	173.0715	$C_9H_{11}N_4$	175.0985	$C_9H_{11}N_3O$	177.0903	$C_{10}H_{15}N_2O$	179.1185
$C_{10}H_{11}N_3$	173.0954	$C_9H_{19}O_3$	175.1334	$C_9H_{13}N_4$	177.1142	$C_{10}H_{17}N_3$	179.1424
$C_{10}H_{21}O_2$	173.1542	$C_9H_{21}NO_2$	175.1573	$C_{10}H_9O_3$	177.0552	$C_{11}H_{15}O_2$	179.1072
$C_{10}H_{23}NO$	173.1781	$C_{10}H_7O_3$	175.0395	$C_{10}H_{11}NO_2$	177.0790	$C_{11}H_{17}NO$	179.1311
$C_{11}H_9O_2$	173.0603	$C_{10}H_9NO_2$	175.0634	$C_{10}H_{13}N_2O$	177.1029	$C_{11}H_{19}N_2$	179.1549
$C_{11}H_{11}NO$	173.0841	$C_{10}H_{11}N_2O$	175.0872	$C_{10}H_{15}N_3$	177.1267	$C_{12}H_{19}O$	179.1436
$C_{11}H_{13}N_2$	173.1080	$C_{10}H_{13}N_3$	175.1111	$C_{11}H_{13}O_2$	177.0916	$C_{12}H_{21}N$	179.1675
$C_{12}H_{13}O$	173.0967	$C_{11}H_{11}O_2$	175.0759	$C_{11}H_{15}NO$	177.1154	$C_{13}H_9N$	179.0736
$C_{12}H_{15}N$	173.1205	$C_{11}H_{13}NO$	175.0998	$C_{11}H_{17}N_2$	177.1393	$C_{13}H_{23}$	179.1801
$C_{13}H_{17}$	173.1331	$C_{11}H_{15}N_2$	175.1236	$C_{12}H_{17}O$	177.1280	$C_{14}H_{11}$	179.0861
174		$C_{12}H_{15}O$	175.1123	$C_{12}H_{19}N$	177.1519	**180**	
$C_6H_{10}N_2O_4$	174.0641	$C_{12}H_{17}N$	175.1362	$C_{13}H_{21}$	177.1644	$C_6H_{16}N_2O_4$	180.1111
$C_6H_{12}N_3O_3$	174.0879	$C_{13}H_3O$	175.0184	**178**		$C_7H_6N_3O_3$	180.0410
$C_6H_{14}N_4O_2$	174.1118	$C_{13}H_{19}$	175.1488	$C_6H_{14}N_2O_4$	178.0954	$C_7H_8N_4O_2$	180.0648
$C_7H_{12}NO_4$	174.0766	**176**		$C_6H_{16}N_3O_3$	178.1193	$C_8H_6NO_4$	180.0297
$C_7H_{14}N_2O_3$	174.1005	$C_6H_{12}N_2O_4$	176.0797	$C_6H_{18}N_4O_2$	178.1431	$C_8H_8N_2O_3$	180.0535
$C_7H_{16}N_3O_2$	174.1244	$C_6H_{14}N_3O_3$	176.1036	$C_7H_6N_4O_2$	178.0491	$C_8H_{10}N_3O_2$	180.0774
$C_7H_{18}N_4O$	174.1482	$C_6H_{16}N_4O_2$	176.1275	$C_7H_{16}NO_4$	178.1080	$C_8H_{12}N_4O$	180.1012
$C_7H_{16}N_4O$	174.1244	$C_7H_{14}NO_4$	176.0923	$C_7H_{18}N_2O_3$	178.1318	$C_9H_8O_4$	180.0422
$C_8H_6N_4O$	174.0542	$C_7H_{16}N_2O_3$	176.1162	$C_8H_6N_2O_3$	178.0379	$C_9H_{10}NO_3$	180.0661
$C_8H_{14}O_4$	174.0892	$C_7H_{18}N_3O_2$	176.1400	$C_8H_8N_3O_2$	178.0617	$C_9H_{12}N_2O_2$	180.0899
$C_8H_{16}NO_3$	174.1131	$C_7H_{20}N_4O$	176.1639	$C_8H_{10}N_4O$	178.0856	$C_9H_{14}N_3O$	180.1138
$C_8H_{18}N_2O_2$	174.1369	$C_8H_6N_3O_2$	176.0460	$C_8H_{18}O_4$	178.1205	$C_9H_{16}N_4$	180.1377
$C_8H_{20}N_3O$	174.1608	$C_8H_8N_4O$	176.0699	$C_9H_6O_4$	178.0266	$C_{10}H_{12}O_3$	180.0786
$C_8H_{22}N_4$	174.1846	$C_8H_{16}O_4$	176.1049	$C_9H_8NO_3$	178.0504	$C_{10}H_{14}NO_2$	180.1025
$C_9H_6N_2O_2$	174.0429	$C_8H_{18}NO_3$	176.1287	$C_9H_{10}N_2O_2$	178.0743	$C_{10}H_{16}N_2O$	180.1264
$C_9H_{10}N_4$	174.0907	$C_8H_{20}N_2O_2$	176.1526	$C_9H_{12}N_3O$	178.0981	$C_{10}H_{18}N_3$	180.1502
$C_9H_{18}O_3$	174.1256	$C_9H_6NO_3$	176.0348	$C_9H_{14}N_4$	178.1220	$C_{11}H_{16}O_2$	180.1151
$C_9H_{20}NO_2$	174.1495	$C_9H_8N_2O_2$	176.0586	$C_{10}H_{10}O_3$	178.0630	$C_{11}H_{18}NO$	180.1389
$C_9H_{22}N_2O$	174.1733	$C_9H_{10}N_3O$	176.0825	$C_{10}H_{12}NO_2$	178.0868	$C_{11}H_{20}N_2$	180.1628
$C_{10}H_6O_3$	174.0317	$C_9H_{12}N_4$	176.1063	$C_{10}H_{14}N_2O$	178.1107	$C_{12}H_8N_2$	180.0688
$C_{10}H_8NO_2$	174.0555	$C_9H_{20}O_3$	176.1413	$C_{10}H_{16}N_3$	178.1346	$C_{12}H_{20}O$	180.1515
$C_{10}H_{10}N_2O$	174.0794	$C_{10}H_8O_3$	176.0473	$C_{11}H_{14}O_2$	178.0994	$C_{12}H_{22}N$	180.1753
$C_{10}H_{12}N_3$	174.1032	$C_{10}H_{10}NO_2$	176.0712	$C_{11}H_{16}NO$	178.1233	$C_{13}H_8O$	180.0575
$C_{10}H_{22}O_2$	174.1620	$C_{10}H_{12}N_2O$	176.0950	$C_{11}H_{18}N_2$	178.1471	$C_{13}H_{10}N$	180.0814
$C_{11}H_{10}O_2$	174.0681	$C_{10}H_{14}N_3$	176.1189	$C_{12}H_{18}O$	178.1358	$C_{13}H_{24}$	180.1879

APPENDIX A (*Continued*)

FM		FM		FM		FM	
$C_{14}H_{12}$	180.0939	$C_{13}H_{12}N$	182.0970	$C_{11}H_{22}NO$	184.1702	$C_{10}H_8N_3O$	186.0668
181		$C_{13}H_{26}$	182.2036	$C_{11}H_{24}N_2$	184.1941	$C_{10}H_{10}N_4$	186.0907
$C_7H_5N_2O_4$	181.0249	$C_{14}H_{14}$	182.1096	$C_{12}H_8O_2$	184.0524	$C_{10}H_{18}O_3$	186.1256
$C_7H_7N_3O_3$	181.0488	**183**		$C_{12}H_{10}NO$	184.0763	$C_{10}H_{20}NO_2$	186.1495
$C_7H_9N_4O_2$	181.0726	$C_7H_7N_2O_4$	183.0406	$C_{12}H_{12}N_2$	184.1001	$C_{10}H_{22}N_2O$	186.1733
$C_8H_7NO_4$	181.0375	$C_7H_9N_3O_3$	183.0644	$C_{12}H_{24}O$	184.1828	$C_{10}H_{24}N_3$	186.1972
$C_8H_9N_2O_3$	181.0614	$C_7H_{11}N_4O_2$	183.0883	$C_{12}H_{26}N$	184.2067	$C_{11}H_8NO_2$	186.0555
$C_8H_{11}N_3O_2$	181.0852	$C_8H_9NO_4$	183.0532	$C_{13}H_{12}O$	184.0888	$C_{11}H_{10}N_2O$	186.0794
$C_8H_{13}N_4O$	181.1091	$C_8H_{11}N_2O_3$	183.0770	$C_{13}H_{14}N$	184.1127	$C_{11}H_{12}N_3$	186.1032
$C_9H_9O_4$	181.0501	$C_8H_{13}N_3O_2$	183.1009	$C_{13}H_{28}$	184.2192	$C_{11}H_{22}O_2$	186.1620
$C_9H_{11}NO_3$	181.0739	$C_8H_{15}N_4O$	183.1247	$C_{14}H_{16}$	184.1253	$C_{11}H_{24}NO$	186.1859
$C_9H_{13}N_2O_2$	181.0978	$C_9H_{11}O_4$	183.0657	**185**		$C_{11}H_{26}N_2$	186.2098
$C_9H_{15}N_3O$	181.1216	$C_9H_{13}NO_3$	183.0896	$C_7H_9N_2O_4$	185.0563	$C_{12}H_{10}O_2$	186.0681
$C_9H_{17}N_4$	181.1455	$C_9H_{15}N_2O_2$	183.1134	$C_7H_{11}N_3O_3$	185.0801	$C_{12}H_{12}NO$	186.0919
$C_{10}H_{13}O_3$	181.0865	$C_9H_{17}N_3O$	183.1373	$C_7H_{13}N_4O_2$	185.1040	$C_{12}H_{14}N_2$	186.1158
$C_{10}H_{15}NO_2$	181.1103	$C_9H_{19}N_4$	183.1611	$C_8H_{11}NO_4$	185.0688	$C_{12}H_{26}O$	186.1985
$C_{10}H_{17}N_2O$	181.1342	$C_{10}H_7N_4$	183.0672	$C_8H_{13}N_2O_3$	185.0927	$C_{13}H_{14}O$	186.1045
$C_{10}H_{19}N_3$	181.1580	$C_{10}H_{15}O_3$	183.1021	$C_8H_{15}N_3O_2$	185.1165	$C_{13}H_{16}N$	186.1284
$C_{11}H_7N_3$	181.0641	$C_{10}H_{17}NO_2$	183.1260	$C_8H_{17}N_4O$	185.1404	$C_{14}H_{18}$	186.1409
$C_{11}H_{17}O_2$	181.1229	$C_{10}H_{19}N_2O$	183.1498	$C_9H_{13}O_4$	185.0814	**187**	
$C_{11}H_{19}NO$	181.1467	$C_{10}H_{21}N_3$	183.1737	$C_9H_{15}NO_3$	185.1052	$C_7H_{11}N_2O_4$	187.0719
$C_{11}H_{21}N_2$	181.1706	$C_{11}H_7N_2O$	183.0559	$C_9H_{17}N_2O_2$	185.1291	$C_7H_{13}N_3O_3$	187.0958
$C_{12}H_7NO$	181.0528	$C_{11}H_9N_3$	183.0798	$C_9H_{19}N_3O$	185.1529	$C_7H_{15}N_4O_2$	187.1196
$C_{12}H_9N_2$	181.0767	$C_{11}H_{19}O_2$	183.1385	$C_9H_{21}N_4$	185.1768	$C_8H_{13}NO_4$	187.0845
$C_{12}H_{21}O$	181.1593	$C_{11}H_{21}NO$	183.1624	$C_{10}H_7N_3O$	185.0590	$C_8H_{15}N_2O_3$	187.1083
$C_{12}H_{23}N$	181.1832	$C_{11}H_{23}N_2$	183.1863	$C_{10}H_9N_4$	185.0829	$C_8H_{17}N_3O_2$	187.1322
$C_{13}H_9O$	181.0653	$C_{12}H_7O_2$	183.0446	$C_{10}H_{17}O_3$	185.1178	$C_8H_{19}N_4O$	187.1560
$C_{13}H_{11}N$	181.0892	$C_{12}H_9NO$	183.0684	$C_{10}H_{19}NO_2$	185.1416	$C_9H_7N_4O$	187.0621
$C_{13}H_{25}$	181.1957	$C_{12}H_{11}N_2$	183.0923	$C_{10}H_{21}N_2O$	185.1655	$C_9H_{15}O_4$	187.0970
$C_{14}H_{13}$	181.1018	$C_{12}H_{23}O$	183.1750	$C_{10}H_{23}N_3$	185.1894	$C_9H_{17}NO_3$	187.1209
182		$C_{12}H_{25}N$	183.1988	$C_{11}H_9N_2O$	185.0715	$C_9H_{19}N_2O_2$	187.1447
$C_7H_6N_2O_4$	182.0328	$C_{13}H_{11}O$	183.0810	$C_{11}H_{11}N_3$	185.0954	$C_9H_{21}N_3O$	187.1686
$C_7H_8N_3O_3$	182.0566	$C_{13}H_{13}N$	183.1049	$C_{11}H_{21}O_2$	185.1542	$C_9H_{23}N_4$	187.1925
$C_7H_{10}N_4O_2$	182.0805	$C_{13}H_{27}$	183.2114	$C_{11}H_{23}NO$	185.1781	$C_{10}H_7N_2O_2$	187.0508
$C_8H_8NO_4$	182.0453	$C_{14}H_{15}$	183.1174	$C_{11}H_{25}N_2$	185.2019	$C_{10}H_9N_3O$	187.0746
$C_8H_{10}N_2O_3$	182.0692	**184**		$C_{12}H_9O_2$	185.0603	$C_{10}H_{11}N_4$	187.0985
$C_8H_{12}N_3O_2$	182.0930	$C_7H_8N_2O_4$	184.0484	$C_{12}H_{11}NO$	185.0841	$C_{10}H_{19}O_3$	187.1334
$C_8H_{14}N_4O$	182.1169	$C_7H_{10}N_3O_3$	184.0723	$C_{12}H_{13}N_2$	185.1080	$C_{10}H_{21}NO_2$	187.1573
$C_9H_{10}O_4$	182.0579	$C_7H_{12}N_4O_2$	184.0961	$C_{12}H_{25}O$	185.1906	$C_{10}H_{23}N_2O$	187.1811
$C_9H_{12}NO_3$	182.0817	$C_8H_{10}NO_4$	184.0610	$C_{12}H_{27}N$	185.2145	$C_{10}H_{25}N_3$	187.2050
$C_9H_{14}N_2O_2$	182.1056	$C_8H_{12}N_2O_3$	184.0848	$C_{13}H_{13}O$	185.0967	$C_{11}H_7O_3$	187.0395
$C_9H_{16}N_3O$	182.1295	$C_8H_{14}N_3O_2$	184.1087	$C_{13}H_{15}N$	185.1205	$C_{11}H_9NO_2$	187.0634
$C_9H_{18}N_4$	182.1533	$C_8H_{16}N_4O$	184.1325	$C_{14}H_{17}$	185.1331	$C_{11}H_{11}N_2O$	187.0872
$C_{10}H_6N_4$	182.0594	$C_9H_{12}O_4$	184.0735	**186**		$C_{11}H_{13}N_3$	187.1111
$C_{10}H_{14}O_3$	182.0943	$C_9H_{14}NO_3$	184.0974	$C_7H_{10}N_2O_4$	186.0641	$C_{11}H_{23}O_2$	187.1699
$C_{10}H_{16}NO_2$	182.1182	$C_9H_{16}N_2O_2$	184.1213	$C_7H_{12}N_3O_3$	186.0879	$C_{11}H_{25}NO$	187.1937
$C_{10}H_{18}N_2O$	182.1420	$C_9H_{18}N_3O$	184.1451	$C_7H_{14}N_4O_2$	186.1118	$C_{12}H_{11}O_2$	187.0759
$C_{10}H_{20}N_3$	182.1659	$C_9H_{20}N_4$	184.1690	$C_8H_{12}NO_4$	186.0766	$C_{12}H_{13}NO$	187.0998
$C_{11}H_8N_3$	182.0719	$C_{10}H_6N_3O$	184.0511	$C_8H_{14}N_2O_3$	186.1005	$C_{12}H_{15}N_2$	187.1236
$C_{11}H_{18}O_2$	182.1307	$C_{10}H_8N_4$	184.0750	$C_8H_{16}N_3O_2$	186.1244	$C_{13}H_{15}O$	187.1123
$C_{11}H_{20}NO$	182.1546	$C_{10}H_{16}O_3$	184.1100	$C_8H_{18}N_4O$	186.1482	$C_{13}H_{17}N$	187.1362
$C_{11}H_{22}N_2$	182.1784	$C_{10}H_{18}NO_2$	184.1338	$C_9H_6N_4O$	186.0542	$C_{14}H_{19}$	187.1488
$C_{12}H_8NO$	182.0606	$C_{10}H_{20}N_2O$	184.1577	$C_9H_{14}O_4$	186.0892	**188**	
$C_{12}H_{10}N_2$	182.0845	$C_{10}H_{22}N_3$	184.1815	$C_9H_{16}NO_3$	186.1131	$C_7H_{12}N_2O_4$	188.0797
$C_{12}H_{22}O$	182.1671	$C_{11}H_8N_2O$	184.0637	$C_9H_{18}N_2O_2$	186.1369	$C_7H_{14}N_3O_3$	188.1036
$C_{12}H_{24}N$	182.1910	$C_{11}H_{10}N_3$	184.0876	$C_9H_{20}N_3O$	186.1608	$C_7H_{16}N_4O_2$	188.1275
$C_{13}H_{10}O$	182.0732	$C_{11}H_{20}O_2$	184.1464	$C_{10}H_6N_2O_2$	186.0429	$C_8H_{14}NO_4$	188.0923

APPENDIX A (*Continued*)

FM		FM		FM		FM	
$C_8H_{16}N_2O_3$	188.1162	**190**		$C_{14}H_9N$	191.0736	$C_{13}H_{21}O$	193.1593
$C_8H_{18}N_3O_2$	188.1400	$C_7H_{14}N_2O_4$	190.0954	$C_{14}H_{23}N$	191.1801	$C_{13}H_{23}N$	193.1832
$C_8H_{20}N_4O$	188.1639	$C_7H_{16}N_3O_3$	190.1193	$C_{15}H_{11}$	191.0861	$C_{14}H_9O$	193.0653
$C_9H_6N_3O_2$	188.0460	$C_7H_{18}N_4O_2$	190.1431	**192**		$C_{14}H_{11}N$	193.0892
$C_9H_8N_4O$	188.0699	$C_8H_6N_4O_2$	190.0491	$C_7H_{16}N_2O_4$	192.1111	$C_{14}H_{25}$	193.1957
$C_9H_{16}O_4$	188.1049	$C_8H_{16}NO_4$	190.1080	$C_7H_{18}N_3O_3$	192.1349	$C_{15}H_{13}$	193.1018
$C_9H_{18}NO_3$	188.1287	$C_8H_{18}N_2O_3$	190.1318	$C_7H_{20}N_4O_2$	192.1588	**194**	
$C_9H_{20}N_2O_2$	188.1526	$C_8H_{20}N_3O_2$	190.1557	$C_8H_6N_3O_3$	192.0410	$C_7H_{18}N_2O_4$	194.1267
$C_9H_{22}N_3O$	188.1764	$C_8H_{22}N_4O$	190.1795	$C_8H_8N_4O_2$	192.0648	$C_8H_6N_2O_4$	194.0328
$C_9H_{24}N_4$	188.2003	$C_9H_8N_3O_2$	190.0617	$C_8H_{18}NO_4$	192.1236	$C_8H_8N_3O_3$	194.0566
$C_{10}H_8N_2O_2$	188.0586	$C_9H_{10}N_4O$	190.0856	$C_8H_{20}N_2O_3$	192.1475	$C_8H_{10}N_4O_2$	194.0805
$C_{10}H_{10}N_3O$	188.0825	$C_9H_{18}O_4$	190.1205	$C_9H_6NO_4$	192.0297	$C_9H_8NO_4$	194.0453
$C_{10}H_{12}N_4$	188.1063	$C_9H_{20}NO_3$	190.1444	$C_9H_8N_2O_3$	192.0535	$C_9H_{10}N_2O_3$	194.0692
$C_{10}H_{20}O_3$	188.1413	$C_9H_{22}N_2O_2$	190.1682	$C_9H_{10}N_3O_2$	192.0774	$C_9H_{12}N_3O_2$	194.0930
$C_{10}H_{22}NO_2$	188.1651	$C_{10}H_8NO_3$	190.0504	$C_9H_{12}N_4O$	192.1012	$C_9H_{14}N_4O$	194.1169
$C_{10}H_{24}N_2O$	188.1890	$C_{10}H_{10}N_2O_2$	190.0743	$C_9H_{20}O_4$	192.1362	$C_{10}H_{10}O_4$	194.0579
$C_{11}H_8O_3$	188.0473	$C_{10}H_{12}N_3O$	190.0981	$C_{10}H_8O_4$	192.0422	$C_{10}H_{12}NO_3$	194.0817
$C_{11}H_{10}NO_2$	188.0712	$C_{10}H_{14}N_4$	190.1220	$C_{10}H_{10}NO_3$	192.0661	$C_{10}H_{14}N_2O_2$	194.1056
$C_{11}H_{12}N_2O$	188.0950	$C_{10}H_{22}O_3$	190.1569	$C_{10}H_{12}N_2O_2$	192.0899	$C_{10}H_{16}N_3O$	194.1295
$C_{11}H_{14}N_3$	188.1189	$C_{11}H_{10}O_3$	190.0630	$C_{10}H_{14}N_3O$	192.1138	$C_{10}H_{18}N_4$	194.1533
$C_{11}H_{24}O_2$	188.1777	$C_{11}H_{12}NO_2$	190.0868	$C_{10}H_{16}N_4$	192.1377	$C_{11}H_{14}O_3$	194.0943
$C_{12}H_{12}O_2$	188.0837	$C_{11}H_{14}N_2O$	190.1107	$C_{11}H_{12}O_3$	192.0786	$C_{11}H_{16}NO_2$	194.1182
$C_{12}H_{14}NO$	188.1076	$C_{11}H_{16}N_3$	190.1346	$C_{11}H_{14}NO_2$	192.1025	$C_{11}H_{18}N_2O$	194.1420
$C_{12}H_{16}N_2$	188.1315	$C_{12}H_{14}O_2$	190.0994	$C_{11}H_{16}N_2O$	192.1264	$C_{11}H_{20}N_3$	194.1659
$C_{13}H_{16}O$	188.1202	$C_{12}H_{16}NO$	190.1233	$C_{11}H_{18}N_3$	192.1502	$C_{12}H_8N_3$	194.0719
$C_{13}H_{18}N$	188.1440	$C_{12}H_{18}N_2$	190.1471	$C_{12}H_{16}O_2$	192.1151	$C_{12}H_{18}O_2$	194.1307
$C_{14}H_{20}$	188.1566	$C_{13}H_{18}O$	190.1358	$C_{12}H_{18}NO$	192.1389	$C_{12}H_{20}NO$	194.1546
189		$C_{13}H_{20}N$	190.1597	$C_{12}H_{20}N_2$	192.1628	$C_{12}H_{22}N_2$	194.1784
$C_7H_{13}N_2O_4$	189.0876	$C_{14}H_{22}$	190.1722	$C_{13}H_8N_2$	192.0688	$C_{13}H_8NO$	194.0606
$C_7H_{15}N_3O_3$	189.1114	$C_{15}H_{10}$	190.0783	$C_{13}H_{20}O$	192.1515	$C_{13}H_{10}N_2$	194.0845
$C_7H_{17}N_4O_2$	189.1353	**191**		$C_{13}H_{22}N$	192.1753	$C_{13}H_{22}O$	194.1671
$C_8H_{15}NO_4$	189.1001	$C_7H_{15}N_2O_4$	191.1032	$C_{14}H_{10}N$	192.0814	$C_{13}H_{24}N$	194.1910
$C_8H_{17}N_2O_3$	189.1240	$C_7H_{17}N_3O_3$	191.1271	$C_{14}H_{24}$	192.1879	$C_{14}H_{10}O$	194.0732
$C_8H_{19}N_3O_2$	189.1478	$C_7H_{19}N_4O_2$	191.1509	$C_{15}H_{12}$	192.0939	$C_{14}H_{12}N$	194.0970
$C_8H_{21}N_4O$	189.1717	$C_8H_7N_4O_2$	191.0570	**193**		$C_{14}H_{26}$	194.2036
$C_9H_7N_3O_2$	189.0539	$C_8H_{17}NO_4$	191.1158	$C_7H_{17}N_2O_4$	193.1189	$C_{15}H_{14}$	194.1096
$C_9H_9N_4O$	189.0777	$C_8H_{19}N_2O_3$	191.1396	$C_7H_{19}N_3O_3$	193.1427	**195**	
$C_9H_{17}O_4$	189.1127	$C_8H_{21}N_3O_2$	191.1635	$C_8H_7N_3O_3$	193.0488	$C_8H_7N_2O_4$	195.0406
$C_9H_{19}NO_3$	189.1365	$C_9H_7N_2O_3$	191.0457	$C_8H_9N_4O_2$	193.0726	$C_8H_9N_3O_3$	195.0644
$C_9H_{21}N_2O_2$	189.1604	$C_9H_9N_3O_2$	191.0695	$C_8H_{19}NO_4$	193.1315	$C_8H_{11}N_4O_2$	195.0883
$C_9H_{23}N_3O$	189.1842	$C_9H_{11}N_4O$	191.0934	$C_9H_7NO_4$	193.0375	$C_9H_9NO_4$	195.0532
$C_{10}H_7NO_3$	189.0426	$C_9H_{19}O_4$	191.1284	$C_9H_9N_2O_3$	193.0614	$C_9H_{11}N_2O_3$	195.0770
$C_{10}H_9N_2O_2$	189.0664	$C_9H_{21}NO_3$	191.1522	$C_9H_{11}N_3O_2$	193.0852	$C_9H_{13}N_3O_2$	195.1009
$C_{10}H_{11}N_3O$	189.0903	$C_{10}H_7O_4$	191.0344	$C_9H_{13}N_4O$	193.1091	$C_9H_{15}N_4O$	195.1247
$C_{10}H_{13}N_4$	189.1142	$C_{10}H_9NO_3$	191.0583	$C_{10}H_9O_4$	193.0501	$C_{10}H_{11}O_4$	195.0657
$C_{10}H_{21}O_3$	189.1491	$C_{10}H_{11}N_2O_2$	191.0821	$C_{10}H_{11}NO_3$	193.0739	$C_{10}H_{13}NO_3$	195.0896
$C_{10}H_{23}NO_2$	189.1730	$C_{10}H_{13}N_3O$	191.1060	$C_{10}H_{13}N_2O_2$	193.0978	$C_{10}H_{15}N_2O_2$	195.1134
$C_{11}H_9O_3$	189.0552	$C_{10}H_{15}N_4$	191.1298	$C_{10}H_{15}N_3O$	193.1216	$C_{10}H_{17}N_3O$	195.1373
$C_{11}H_{11}NO_2$	189.0790	$C_{11}H_{11}O_3$	191.0708	$C_{10}H_{17}N_4$	193.1455	$C_{10}H_{19}N_4$	195.1611
$C_{11}H_{13}N_2O$	189.1029	$C_{11}H_{13}NO_2$	191.0947	$C_{11}H_{13}O_3$	193.0865	$C_{11}H_7N_4$	195.0672
$C_{11}H_{15}N_3$	189.1267	$C_{11}H_{15}N_2O$	191.1185	$C_{11}H_{15}NO_2$	193.1103	$C_{11}H_{15}O_3$	195.1021
$C_{12}H_{13}O_2$	189.0916	$C_{11}H_{17}N_3$	191.1424	$C_{11}H_{17}N_2O$	193.1342	$C_{11}H_{17}NO_2$	195.1260
$C_{12}H_{15}NO$	189.1154	$C_{12}H_{15}O_2$	191.1072	$C_{11}H_{19}N_3$	193.1580	$C_{11}H_{19}N_2O$	195.1498
$C_{12}H_{17}N_2$	189.1393	$C_{12}H_{17}NO$	191.1311	$C_{12}H_{17}O_2$	193.1229	$C_{11}H_{21}N_3$	195.1737
$C_{13}H_{17}O$	189.1280	$C_{12}H_{19}N_2$	191.1549	$C_{12}H_{19}NO$	193.1467	$C_{12}H_7N_2O$	195.0559
$C_{13}H_{19}N$	189.1519	$C_{13}H_{19}O$	191.1436	$C_{12}H_{21}N_2$	193.1706	$C_{12}H_9N_3$	195.0798
$C_{14}H_{21}$	189.1644	$C_{13}H_{21}N$	191.1675	$C_{13}H_9N_2$	193.0767	$C_{12}H_{19}O_2$	195.1385

APPENDIX A (*Continued*)

FM		FM		FM		FM	
$C_{12}H_{21}NO$	195.1624	$C_{11}H_{17}O_3$	197.1178	$C_9H_{15}N_2O_3$	199.1083	$C_{12}H_{28}N_2$	200.2254
$C_{12}H_{23}N_2$	195.1863	$C_{11}H_{19}NO_2$	197.1416	$C_9H_{17}N_3O_2$	199.1322	$C_{13}H_{12}O_2$	200.0837
$C_{13}H_9NO$	195.0684	$C_{11}H_{21}N_2O$	197.1655	$C_9H_{19}N_4O$	199.1560	$C_{13}H_{14}NO$	200.1076
$C_{13}H_{11}N_2$	195.0923	$C_{11}H_{23}N_3$	197.1894	$C_{10}H_7N_4O$	199.0621	$C_{13}H_{16}N_2$	200.1315
$C_{13}H_{23}O$	195.1750	$C_{12}H_9N_2O$	197.0715	$C_{10}H_{15}O_4$	199.0970	$C_{13}H_{28}O$	200.2141
$C_{13}H_{25}N$	195.1988	$C_{12}H_{11}N_3$	197.0954	$C_{10}H_{17}NO_3$	199.1209	$C_{14}H_{16}O$	200.1202
$C_{14}H_{11}O$	195.0810	$C_{12}H_{21}O_2$	197.1542	$C_{10}H_{19}N_2O_2$	199.1447	$C_{14}H_{18}N$	200.1440
$C_{14}H_{13}N$	195.1049	$C_{12}H_{23}NO$	197.1781	$C_{10}H_{21}N_3O$	199.1686	$C_{15}H_{20}$	200.1566
$C_{14}H_{27}$	195.2114	$C_{12}H_{25}N_2$	197.2019	$C_{10}H_{23}N_4$	199.1925	**201**	
$C_{15}H_{15}$	195.1174	$C_{13}H_9O_2$	197.0603	$C_{11}H_7N_2O_2$	199.0508	$C_8H_{13}N_2O_4$	201.0876
196		$C_{13}H_{11}NO$	197.0841	$C_{11}H_9N_3O$	199.0746	$C_8H_{15}N_3O_3$	201.1114
$C_8H_8N_2O_4$	196.0484	$C_{13}H_{13}N_2$	197.1080	$C_{11}H_{11}N_4$	199.0985	$C_8H_{17}N_4O_2$	201.1353
$C_8H_{10}N_3O_3$	196.0723	$C_{13}H_{25}O$	197.1906	$C_{11}H_{19}O_3$	199.1334	$C_9H_{15}NO_4$	201.1001
$C_8H_{12}N_4O_2$	196.0961	$C_{13}H_{27}N$	197.2145	$C_{11}H_{21}NO_2$	199.1573	$C_9H_{17}N_2O_3$	201.1240
$C_9H_{10}NO_4$	196.0610	$C_{14}H_{13}O$	197.0967	$C_{11}H_{23}N_2O$	199.1811	$C_9H_{19}N_3O_2$	201.1478
$C_9H_{12}N_2O_3$	196.0848	$C_{14}H_{15}N$	197.1205	$C_{11}H_{25}N_3$	199.2050	$C_9H_{21}N_4O$	201.1717
$C_9H_{14}N_3O_2$	196.1087	$C_{14}H_{29}$	197.2270	$C_{12}H_9NO_2$	199.0634	$C_{10}H_7N_3O_2$	201.0539
$C_9H_{16}N_4O$	196.1325	$C_{15}H_{17}$	197.1331	$C_{12}H_{11}N_2O$	199.0872	$C_{10}H_9N_4O$	201.0777
$C_{10}H_{12}O_4$	196.0735	**198**		$C_{12}H_{13}N_3$	199.1111	$C_{10}H_{17}O_4$	201.1127
$C_{10}H_{14}NO_3$	196.0974	$C_8H_{10}N_2O_4$	198.0641	$C_{12}H_{23}O_2$	199.1699	$C_{10}H_{19}NO_3$	201.1365
$C_{10}H_{16}N_2O_2$	196.1213	$C_8H_{12}N_3O_3$	198.0879	$C_{12}H_{25}NO$	199.1937	$C_{10}H_{21}N_2O_2$	201.1604
$C_{10}H_{18}N_3O$	196.1451	$C_8H_{14}N_4O_2$	198.1118	$C_{12}H_{27}N_2$	199.2176	$C_{10}H_{23}N_3O$	201.1842
$C_{10}H_{20}N_4$	196.1690	$C_9H_{12}NO_4$	198.0766	$C_{13}H_{11}O_2$	199.0759	$C_{10}H_{25}N_4$	201.2081
$C_{11}H_8N_4$	196.0750	$C_9H_{14}N_2O_3$	198.1005	$C_{13}H_{13}NO$	199.0998	$C_{11}H_7NO_3$	201.0426
$C_{11}H_{16}O_3$	196.1100	$C_9H_{16}N_3O_2$	198.1244	$C_{13}H_{15}N_2$	199.1236	$C_{11}H_9N_2O_2$	201.0664
$C_{11}H_{18}NO_2$	196.1338	$C_9H_{18}N_4O$	198.1482	$C_{13}H_{27}O$	199.2063	$C_{11}H_{11}N_3O$	201.0903
$C_{11}H_{20}N_2O$	196.1577	$C_{10}H_{14}O_4$	198.0892	$C_{13}H_{29}N$	199.2301	$C_{11}H_{13}N_4$	201.1142
$C_{11}H_{22}N_3$	196.1815	$C_{10}H_{16}NO_3$	198.1131	$C_{14}H_{15}O$	199.1123	$C_{11}H_{21}O_3$	201.1491
$C_{12}H_8N_2O$	196.0637	$C_{10}H_{18}N_2O_2$	198.1369	$C_{14}H_{17}N$	199.1362	$C_{11}H_{23}NO_2$	201.1730
$C_{12}H_{10}N_3$	196.0876	$C_{10}H_{20}N_3O$	198.1608	$C_{15}H_{19}$	199.1488	$C_{11}H_{25}N_2O$	201.1968
$C_{12}H_{20}O_2$	196.1464	$C_{10}H_{22}N_4$	198.1846	**200**		$C_{11}H_{27}N_3$	201.2207
$C_{12}H_{22}NO$	196.1702	$C_{11}H_8N_3O$	198.0668	$C_8H_{12}N_2O_4$	200.0797	$C_{12}H_9O_3$	201.0552
$C_{12}H_{24}N_2$	196.1941	$C_{11}H_{10}N_4$	198.0907	$C_8H_{14}N_3O_3$	200.1036	$C_{12}H_{11}NO_2$	201.0790
$C_{13}H_8O_2$	196.0524	$C_{11}H_{18}O_3$	198.1256	$C_8H_{16}N_4O_2$	200.1275	$C_{12}H_{13}N_2O$	201.1029
$C_{13}H_{10}NO$	196.0763	$C_{11}H_{20}NO_2$	198.1495	$C_9H_{14}NO_4$	200.0923	$C_{12}H_{15}N_3$	201.1267
$C_{13}H_{12}N_2$	196.1001	$C_{11}H_{22}N_2O$	198.1733	$C_9H_{16}N_2O_3$	200.1162	$C_{12}H_{25}O_2$	201.1855
$C_{13}H_{24}O$	196.1828	$C_{11}H_{24}N_3$	198.1972	$C_9H_{18}N_3O_2$	200.1400	$C_{12}H_{27}NO$	201.2094
$C_{13}H_{26}N$	196.2067	$C_{12}H_8NO_2$	198.0555	$C_9H_{20}N_4O$	200.1639	$C_{13}H_{13}O_2$	201.0916
$C_{14}H_{12}O$	196.0888	$C_{12}H_{10}N_2O$	198.0794	$C_{10}H_8N_4O$	200.0699	$C_{13}H_{15}NO$	201.1154
$C_{14}H_{14}N$	196.1127	$C_{12}H_{12}N_3$	198.1032	$C_{10}H_{16}O_4$	200.1049	$C_{13}H_{17}N_2$	201.1393
$C_{14}H_{28}$	196.2192	$C_{12}H_{22}O_2$	198.1620	$C_{10}H_{18}NO_3$	200.1287	$C_{14}H_{17}O$	201.1280
$C_{15}H_{16}$	196.1253	$C_{12}H_{24}NO$	198.1859	$C_{10}H_{20}N_2O_2$	200.1526	$C_{14}H_{19}N$	201.1519
197		$C_{12}H_{26}N_2$	198.2098	$C_{10}H_{22}N_3O$	200.1764	$C_{15}H_{21}$	201.1644
$C_8H_9N_2O_4$	197.0563	$C_{13}H_{10}O_2$	198.0681	$C_{10}H_{24}N_4$	200.2003	**202**	
$C_8H_{11}N_3O_3$	197.0801	$C_{13}H_{12}NO$	198.0919	$C_{11}H_8N_2O_2$	200.0586	$C_8H_{14}N_2O_4$	202.0954
$C_8H_{13}N_4O_2$	197.1040	$C_{13}H_{14}N_2$	198.1158	$C_{11}H_{10}N_3O$	200.0825	$C_8H_{16}N_3O_3$	202.1193
$C_9H_{11}NO_4$	197.0688	$C_{13}H_{26}O$	198.1985	$C_{11}H_{12}N_4$	200.1063	$C_8H_{18}N_4O_2$	202.1431
$C_9H_{13}N_2O_3$	197.0927	$C_{13}H_{28}N$	198.2223	$C_{11}H_{20}O_3$	200.1413	$C_9H_6N_4O_2$	202.0491
$C_9H_{15}N_3O_2$	197.1165	$C_{14}H_{14}O$	198.1045	$C_{11}H_{22}NO_2$	200.1651	$C_9H_{16}NO_4$	202.1080
$C_9H_{17}N_4O$	197.1404	$C_{14}H_{16}N$	198.1284	$C_{11}H_{24}N_2O$	200.1890	$C_9H_{18}N_2O_3$	202.1318
$C_{10}H_{13}O_4$	197.0814	$C_{14}H_{30}$	198.2349	$C_{11}N_{26}N_3$	200.2129	$C_9H_{20}N_3O_2$	202.1557
$C_{10}H_{15}NO_3$	197.1052	$C_{15}H_{18}$	198.1409	$C_{12}H_8O_3$	200.0473	$C_9H_{22}N_4O$	202.1795
$C_{10}H_{17}N_2O_2$	197.1291	**199**		$C_{12}H_{10}NO_2$	200.0712	$C_{10}H_8N_3O_2$	202.0617
$C_{10}H_{19}N_3O$	197.1529	$C_8H_{11}N_2O_4$	199.0719	$C_{12}H_{12}N_2O$	200.0950	$C_{10}H_{10}N_4O$	202.0856
$C_{10}H_{21}N_4$	197.1768	$C_8H_{13}N_3O_3$	199.0958	$C_{12}H_{14}N_3$	200.1189	$C_{10}H_{18}O_4$	202.1205
$C_{11}H_7N_3O$	197.0590	$C_8H_{15}N_4O_2$	199.1196	$C_{12}H_{24}O_2$	200.1777	$C_{10}H_{20}NO_3$	202.1444
$C_{11}H_9N_4$	197.0829	$C_9H_{13}NO_4$	199.0845	$C_{12}H_{26}NO$	200.2015	$C_{10}H_{22}N_2O_2$	202.1682

APPENDIX A (*Continued*)

FM		FM		FM		FM	
$C_{10}H_{24}N_3O$	202.1921	$C_8H_{20}N_4O_2$	204.1588	$C_{13}H_{21}N_2$	205.1706	$C_{11}H_{19}N_4$	207.1611
$C_{10}H_{26}N_4$	202.2160	$C_9H_6N_3O_3$	204.0410	$C_{14}H_9N_2$	205.0767	$C_{12}H_{15}O_3$	207.1021
$C_{11}H_8NO_3$	202.0504	$C_9H_8N_4O_2$	204.0648	$C_{14}H_{21}O$	205.1593	$C_{12}H_{17}NO_2$	207.1260
$C_{11}H_{10}N_2O_2$	202.0743	$C_9H_{18}NO_4$	204.1236	$C_{14}H_{23}N$	205.1832	$C_{12}H_{19}N_2O$	207.1498
$C_{11}H_{12}N_3O$	202.0981	$C_9H_{20}N_2O_3$	204.1475	$C_{15}H_9O$	205.0653	$C_{12}H_{21}N_3$	207.1737
$C_{11}H_{14}N_4$	202.1220	$C_9H_{22}N_3O_2$	204.1713	$C_{15}H_{11}N$	205.0892	$C_{13}H_9N_3$	207.0798
$C_{11}H_{22}O_3$	202.1569	$C_9H_{24}N_4O$	204.1952	$C_{15}H_{25}$	205.1957	$C_{13}H_{19}O_2$	207.1385
$C_{11}H_{24}NO_2$	202.1808	$C_{10}H_8N_2O_3$	204.0535	$C_{16}H_{13}$	205.1018	$C_{13}H_{21}NO$	207.1624
$C_{11}H_{26}N_2O$	202.2046	$C_{10}H_{10}N_3O_2$	204.0774	**206**		$C_{13}H_{23}N_2$	207.1863
$C_{12}H_{10}O_3$	202.0630	$C_{10}H_{12}N_4O$	204.1012	$C_8H_{18}N_2O_4$	206.1267	$C_{14}H_9NO$	207.0684
$C_{12}H_{12}NO_2$	202.0868	$C_{10}H_{20}O_4$	204.1362	$C_8H_{20}N_3O_3$	206.1506	$C_{14}H_{11}N_2$	207.0923
$C_{12}H_{14}N_2O$	202.1107	$C_{10}H_{22}NO_3$	204.1600	$C_8H_{22}N_4O_2$	206.1744	$C_{14}H_{23}O$	207.1750
$C_{12}H_{16}N_3$	202.1346	$C_{10}H_{24}N_2O_2$	204.1839	$C_9H_6N_2O_4$	206.0328	$C_{14}H_{25}N$	207.1988
$C_{12}H_{26}O_2$	202.1934	$C_{11}H_8O_4$	204.0422	$C_9H_8N_3O_3$	206.0566	$C_{15}H_{11}O$	207.0810
$C_{13}H_{14}O_2$	202.0994	$C_{11}H_{10}NO_3$	204.0661	$C_9H_{10}N_4O_2$	206.0805	$C_{15}H_{13}N$	207.1049
$C_{13}H_{16}NO$	202.1233	$C_{11}H_{12}N_2O_2$	204.0899	$C_9H_{20}NO_4$	206.1393	$C_{15}H_{27}$	207.2114
$C_{13}H_{18}N_2$	202.1471	$C_{11}H_{14}N_3O$	204.1138	$C_9H_{22}N_2O_3$	206.1631	$C_{16}H_{15}$	207.1174
$C_{14}H_{18}O$	202.1358	$C_{11}H_{16}N_4$	204.1377	$C_{10}H_8NO_4$	206.0453	**208**	
$C_{14}H_{20}N$	202.1597	$C_{11}H_{24}O_3$	204.1726	$C_{10}H_{10}N_2O_3$	206.0692	$C_8H_{20}N_2O_4$	208.1424
$C_{15}H_{22}$	202.1722	$C_{12}H_{12}O_3$	204.0786	$C_{10}H_{12}N_3O_2$	206.0930	$C_9H_8N_2O_4$	208.0484
203		$C_{12}H_{14}NO_2$	204.1025	$C_{10}H_{14}N_4O$	206.1169	$C_9H_{10}N_3O_3$	208.0723
$C_8H_{15}N_2O_4$	203.1032	$C_{12}H_{16}N_2O$	204.1264	$C_{10}H_{22}O_4$	206.1518	$C_9H_{12}N_4O_2$	208.0961
$C_8H_{17}N_3O_3$	203.1271	$C_{12}H_{18}N_3$	204.1502	$C_{11}H_{10}O_4$	206.0579	$C_{10}H_{10}NO_4$	208.0610
$C_8H_{19}N_4O_2$	203.1509	$C_{13}H_{16}O_2$	204.1151	$C_{11}H_{12}NO_3$	206.0817	$C_{10}H_{12}N_2O_3$	208.0848
$C_9H_7N_4O_2$	203.0570	$C_{13}H_{18}NO$	204.1389	$C_{11}H_{14}N_2O_2$	206.1056	$C_{10}H_{14}N_3O_2$	208.1087
$C_9H_{17}NO_4$	203.1158	$C_{13}H_{20}N_2$	204.1628	$C_{11}H_{16}N_3O$	206.1295	$C_{10}H_{16}N_4O$	208.1325
$C_9H_{19}N_2O_3$	203.1396	$C_{14}H_{20}O$	204.1515	$C_{11}H_{18}N_4$	206.1533	$C_{11}H_{12}O_4$	208.0735
$C_9H_{21}N_3O_2$	203.1635	$C_{14}H_{22}N$	204.1753	$C_{12}H_{14}O_3$	206.0943	$C_{11}H_{14}NO_3$	208.0974
$C_9H_{23}N_4O$	203.1873	$C_{15}H_{10}N$	204.0814	$C_{12}H_{16}NO_2$	206.1182	$C_{11}H_{16}N_2O_2$	208.1213
$C_{10}H_7N_2O_3$	203.0457	$C_{15}H_{24}$	204.1879	$C_{12}H_{18}N_2O$	206.1420	$C_{11}H_{18}N_3O$	208.1451
$C_{10}H_9N_3O_2$	203.0695	$C_{16}H_{12}$	204.0939	$C_{12}H_{20}N_3$	206.1659	$C_{11}H_{20}N_4$	208.1690
$C_{10}H_{11}N_4O$	203.0934	**205**		$C_{13}H_8N_3$	206.0719	$C_{12}H_8N_4$	208.0750
$C_{10}H_{19}O_4$	203.1284	$C_8H_{17}N_2O_4$	205.1189	$C_{13}H_{18}O_2$	206.1307	$C_{12}H_{16}O_3$	208.1100
$C_{10}H_{21}NO_3$	203.1522	$C_8H_{19}N_3O_3$	205.1427	$C_{13}H_{20}NO$	206.1546	$C_{12}H_{18}NO_2$	208.1338
$C_{10}H_{23}N_2O_2$	203.1761	$C_8H_{21}N_4O_2$	205.1666	$C_{13}H_{22}N_2$	206.1784	$C_{12}H_{20}N_2O$	208.1577
$C_{10}H_{25}N_3O$	203.1999	$C_9H_7N_3O_3$	205.0488	$C_{14}H_{10}N_2$	206.0845	$C_{12}H_{22}N_3$	208.1815
$C_{11}H_7O_4$	203.0344	$C_9H_9N_4O_2$	205.0726	$C_{14}H_{22}O$	206.1671	$C_{13}H_8N_2O$	208.0637
$C_{11}H_9NO_3$	203.0583	$C_9H_{19}NO_4$	205.1315	$C_{14}H_{24}N$	206.1910	$C_{13}H_{10}N_3$	208.0876
$C_{11}H_{11}N_2O_2$	203.0821	$C_9H_{21}N_2O_3$	205.1553	$C_{15}H_{10}O$	206.0732	$C_{13}H_{20}O_2$	208.1464
$C_{11}H_{13}N_3O$	203.1060	$C_9H_{23}N_3O_2$	205.1791	$C_{15}H_{12}N$	206.0970	$C_{13}H_{22}NO$	208.1702
$C_{11}H_{15}N_4$	203.1298	$C_{10}H_7NO_4$	205.0375	$C_{15}H_{26}$	206.2036	$C_{13}H_{24}N_2$	208.1941
$C_{11}H_{23}O_3$	203.1648	$C_{10}H_9N_2O_3$	205.0614	$C_{16}H_{14}$	206.1096	$C_{14}H_{10}NO$	208.0763
$C_{11}H_{25}NO_2$	203.1886	$C_{10}H_{11}N_3O_2$	205.0852	**207**		$C_{14}H_{12}N_2$	208.1001
$C_{12}H_{11}O_3$	203.0708	$C_{10}H_{13}N_4O$	205.1091	$C_8H_{19}N_2O_4$	207.1345	$C_{14}H_{24}O$	208.1828
$C_{12}H_{13}NO_2$	203.0947	$C_{10}H_{21}O_4$	205.1440	$C_8H_{21}N_3O_3$	207.1584	$C_{14}H_{26}N$	208.2067
$C_{12}H_{15}N_2O$	203.1185	$C_{10}H_{23}NO_3$	205.1679	$C_9H_7N_2O_4$	207.0406	$C_{15}H_{12}O$	208.0888
$C_{12}H_{17}N_3$	203.1424	$C_{11}H_9O_4$	205.0501	$C_9H_9N_3O_3$	207.0644	$C_{15}H_{14}N$	208.1127
$C_{13}H_{15}O_2$	203.1072	$C_{11}H_{11}NO_3$	205.0739	$C_9H_{11}N_4O_2$	207.0883	$C_{15}H_{28}$	208.2192
$C_{13}H_{17}NO$	203.1311	$C_{11}H_{13}N_2O_2$	205.0978	$C_9H_{21}NO_4$	207.1471	$C_{16}H_{16}$	208.1253
$C_{13}H_{19}N_2$	203.1549	$C_{11}H_{15}N_3O$	205.1216	$C_{10}H_9NO_4$	207.0532	**209**	
$C_{14}H_{19}O$	203.1436	$C_{11}H_{17}N_4$	205.1455	$C_{10}H_{11}N_2O_3$	207.0770	$C_9H_9N_2O_4$	209.0563
$C_{14}H_{21}N$	203.1675	$C_{12}H_{13}O_3$	205.0865	$C_{10}H_{13}N_3O_2$	207.1009	$C_9H_{11}N_3O_3$	209.0801
$C_{15}H_9N$	203.0736	$C_{12}H_{15}N$	205.1103	$C_{10}H_{15}N_4O$	207.1247	$C_9H_{13}N_4O_2$	209.1040
$C_{15}H_{23}$	203.1801	$C_{12}H_{17}N_2O$	205.1342	$C_{11}H_{11}O_4$	207.0657	$C_{10}H_{11}NO_4$	209.0688
204		$C_{12}H_{19}N_3$	205.1580	$C_{11}H_{13}NO_3$	207.0896	$C_{10}H_{13}N_2O_3$	209.0927
$C_8H_{16}N_2O_4$	204.1111	$C_{13}H_{17}O_2$	205.1229	$C_{11}H_{15}N_2O_2$	207.1134	$C_{10}H_{15}N_3O_2$	209.1165
$C_8H_{18}N_3O_3$	204.1349	$C_{13}H_{19}NO$	205.1467	$C_{11}H_{17}N_3O$	207.1373	$C_{10}H_{17}N_4O$	209.1404

APPENDIX A (*Continued*)

FM		FM		FM		FM	
$C_{11}H_{13}O_4$	209.0814	$C_{16}H_{18}$	210.1409	$C_{13}H_8O_3$	212.0473	$C_{10}H_{18}N_2O_3$	214.1318
$C_{11}H_{15}NO_3$	209.1052	**211**		$C_{13}H_{10}NO_2$	212.0712	$C_{10}H_{20}N_3O_2$	214.1557
$C_{11}H_{17}N_2O_2$	209.1291	$C_9H_{11}N_2O_4$	211.0719	$C_{13}H_{12}N_2O$	212.0950	$C_{10}H_{22}N_4O$	214.1795
$C_{11}H_{19}N_3O$	209.1529	$C_9H_{13}N_3O_3$	211.0958	$C_{13}H_{14}N_3$	212.1189	$C_{11}H_8N_3O_2$	214.0617
$C_{11}H_{21}N_4$	209.1768	$C_9H_{15}N_4O_2$	211.1196	$C_{13}H_{24}O_2$	212.1777	$C_{11}H_{10}N_4O$	214.0856
$C_{12}H_9N_4$	209.0829	$C_{10}H_{13}NO_4$	211.0845	$C_{13}H_{26}NO$	212.2015	$C_{11}H_{18}O_4$	214.1205
$C_{12}H_{17}O_3$	209.1178	$C_{10}H_{15}N_2O_3$	211.1083	$C_{13}H_{28}N_2$	212.2254	$C_{11}H_{20}NO_3$	214.1444
$C_{12}H_{19}NO_2$	209.1416	$C_{10}H_{17}N_3O_2$	211.1322	$C_{14}H_{12}O_2$	212.0837	$C_{11}H_{22}N_2O_2$	214.1682
$C_{12}H_{21}N_2O$	209.1655	$C_{10}H_{19}N_4O$	211.1560	$C_{14}H_{14}NO$	212.1076	$C_{11}H_{24}N_3O$	214.1921
$C_{12}H_{23}N_3$	209.1894	$C_{11}H_7N_4O$	211.0621	$C_{14}H_{16}N_2$	212.1315	$C_{11}H_{26}N_4$	214.2160
$C_{13}H_9N_2O$	209.0715	$C_{11}H_{15}O_4$	211.0970	$C_{14}H_{28}O$	212.2141	$C_{12}H_8NO_3$	214.0504
$C_{13}H_{11}N_3$	209.0954	$C_{11}H_{17}NO_3$	211.1209	$C_{14}H_{30}N$	212.2380	$C_{12}H_{10}N_2O_2$	214.0743
$C_{13}H_{21}O_2$	209.1542	$C_{11}H_{19}N_2O_2$	211.1447	$C_{15}H_{16}O$	212.1202	$C_{12}H_{12}N_3O$	214.0981
$C_{13}H_{23}NO$	209.1781	$C_{11}H_{21}N_3O$	211.1686	$C_{15}H_{18}N$	212.1440	$C_{12}H_{14}N_4$	214.1220
$C_{13}H_{25}N_2$	209.2019	$C_{11}H_{23}N_4$	211.1925	$C_{15}H_{32}$	212.2505	$C_{12}H_{22}O_3$	214.1569
$C_{14}H_9O_2$	209.0603	$C_{12}H_9N_3O$	211.0746	$C_{16}H_{20}$	212.1566	$C_{12}H_{24}NO_2$	214.1808
$C_{14}H_{11}NO$	209.0841	$C_{12}H_{11}N_4$	211.0985	**213**		$C_{12}H_{26}N_2O$	214.2046
$C_{14}H_{13}N_2$	209.1080	$C_{12}H_{19}O_3$	211.1334	$C_9H_{13}N_2O_4$	213.0876	$C_{12}H_{28}N_3$	214.2285
$C_{14}H_{25}O$	209.1906	$C_{12}H_{21}NO_2$	211.1573	$C_9H_{15}N_3O_3$	213.1114	$C_{13}H_{10}O_3$	214.0630
$C_{14}H_{27}N$	209.2145	$C_{12}H_{23}N_2O$	211.1811	$C_9H_{17}N_4O_2$	213.1353	$C_{13}H_{12}NO_2$	214.0869
$C_{15}H_{13}O$	209.0967	$C_{12}H_{25}N_3$	211.2050	$C_{10}H_{15}NO_4$	213.1001	$C_{13}H_{14}N_2O$	214.1107
$C_{15}H_{15}N$	209.1205	$C_{13}H_9NO_2$	211.0634	$C_{10}H_{17}N_2O_3$	213.1240	$C_{13}H_{16}N_3$	214.1346
$C_{15}H_{29}$	209.2270	$C_{13}H_{11}N_2O$	211.0872	$C_{10}H_{19}N_3O_2$	213.1478	$C_{13}H_{26}O_2$	214.1934
$C_{16}H_{17}$	209.1331	$C_{13}H_{13}N_3$	211.1111	$C_{10}H_{21}N_4O$	213.1717	$C_{13}H_{28}NO$	214.2172
210		$C_{13}H_{23}O_2$	211.1699	$C_{11}H_7N_3O_2$	213.0539	$C_{13}H_{30}N_2$	214.2411
$C_9H_{10}N_2O_4$	210.0641	$C_{13}H_{25}NO$	211.1937	$C_{11}H_9N_4O$	213.0777	$C_{14}H_{14}O_2$	214.0994
$C_9H_{12}N_3O_3$	210.0879	$C_{13}H_{27}N_2$	211.2176	$C_{11}H_{17}O_4$	213.1127	$C_{14}H_{16}NO$	214.1233
$C_9H_{14}N_4O_2$	210.1118	$C_{14}H_{11}O_2$	211.0759	$C_{11}H_{19}NO_3$	213.1365	$C_{14}H_{18}N_2$	214.1471
$C_{10}H_{12}NO_4$	210.0766	$C_{14}H_{13}NO$	211.0998	$C_{11}H_{21}N_2O_2$	213.1604	$C_{15}H_{18}O$	214.1358
$C_{10}H_{14}N_2O_3$	210.1005	$C_{14}H_{15}N_2$	211.1236	$C_{11}H_{23}N_3O$	213.1842	$C_{15}H_{20}N$	214.1597
$C_{10}H_{16}N_3O_2$	210.1244	$C_{14}H_{27}O$	211.2063	$C_{11}H_{25}N_4$	213.2081	$C_{16}H_{22}$	214.1722
$C_{10}H_{18}N_4O$	210.1482	$C_{14}H_{29}N$	211.2301	$C_{12}H_9N_2O_2$	213.0664	**215**	
$C_{11}H_{14}O_4$	210.0892	$C_{15}H_{15}O$	211.1123	$C_{12}H_{11}N_3O$	213.0903	$C_9H_{15}N_2O_4$	215.1032
$C_{11}H_{16}NO_3$	210.1131	$C_{15}H_{17}N$	211.1362	$C_{12}H_{13}N_4$	213.1142	$C_9H_{17}N_3O_3$	215.1271
$C_{11}H_{18}N_2O_2$	210.1369	$C_{15}H_{31}$	211.2427	$C_{12}H_{21}O_3$	213.1491	$C_9H_{19}N_4O_2$	215.1509
$C_{11}H_{20}N_3O$	210.1608	$C_{16}H_{19}$	211.1488	$C_{12}H_{23}NO_2$	213.1730	$C_{10}H_7N_4O_2$	215.0570
$C_{11}H_{22}N_4$	210.1846	**212**		$C_{12}H_{25}N_2O$	213.1968	$C_{10}H_{17}NO_4$	215.1158
$C_{12}H_8N_3O$	210.0668	$C_9H_{12}N_2O_4$	212.0797	$C_{12}H_{27}N_3$	213.2207	$C_{10}H_{19}N_2O_3$	215.1396
$C_{12}H_{10}N_4$	210.0907	$C_9H_{14}N_3O_3$	212.1036	$C_{13}H_9O_3$	213.0552	$C_{10}H_{21}N_3O_2$	215.1635
$C_{12}H_{18}O_3$	210.1256	$C_9H_{16}N_4O_2$	212.1275	$C_{13}H_{11}NO_2$	213.0790	$C_{10}H_{23}N_4O$	215.1873
$C_{12}H_{20}NO_2$	210.1495	$C_{10}H_{14}NO_4$	212.0923	$C_{13}H_{13}N_2O$	213.1029	$C_{11}H_7N_2O_3$	215.0457
$C_{12}H_{22}N_2O$	210.1733	$C_{10}H_{16}N_2O_3$	212.1162	$C_{13}H_{15}N_3$	213.1267	$C_{11}H_9N_3O_2$	215.0695
$C_{12}H_{24}N_3$	210.1972	$C_{10}H_{18}N_3O_2$	212.1400	$C_{13}H_{25}O_2$	213.1855	$C_{11}H_{11}N_4O$	215.0934
$C_{13}H_8NO_2$	210.0555	$C_{10}H_{20}N_4O$	212.1639	$C_{13}H_{27}NO$	213.2094	$C_{11}H_{19}O_4$	215.1284
$C_{13}H_{10}N_2O$	210.0794	$C_{11}H_8N_4O$	212.0699	$C_{13}H_{29}N_2$	213.2332	$C_{11}H_{21}NO_3$	215.1522
$C_{13}H_{12}N_3$	210.1032	$C_{11}H_{16}O_4$	212.1049	$C_{14}H_{13}O_2$	213.0916	$C_{11}H_{23}N_2O_2$	215.1761
$C_{13}H_{22}O_2$	210.1620	$C_{11}H_{18}NO_3$	212.1287	$C_{14}H_{15}NO$	213.1154	$C_{11}H_{25}N_3O$	215.1999
$C_{13}H_{24}NO$	210.1859	$C_{11}H_{20}N_2O_2$	212.1526	$C_{14}H_{17}N_2$	213.1393	$C_{11}H_{27}N_4$	215.2238
$C_{13}H_{26}N_2$	210.2098	$C_{11}H_{22}N_3O$	212.1764	$C_{14}H_{29}O$	213.2219	$C_{12}H_9NO_3$	215.0583
$C_{14}H_{10}O_2$	210.0681	$C_{11}H_{24}N_4$	212.2003	$C_{15}H_{17}O$	213.1280	$C_{12}H_{11}N_2O_2$	215.0821
$C_{14}H_{12}NO$	210.0919	$C_{12}H_8N_2O_2$	212.0586	$C_{15}H_{19}N$	213.1519	$C_{12}H_{13}N_3O$	215.1060
$C_{14}H_{14}N_2$	210.1158	$C_{12}H_{10}N_3O$	212.0825	$C_{16}H_{21}$	213.1644	$C_{12}H_{15}N_4$	215.1298
$C_{14}H_{26}O$	210.1985	$C_{12}H_{12}N_4$	212.1063	**214**		$C_{12}H_{23}O_3$	215.1648
$C_{14}H_{28}N$	210.2223	$C_{12}H_{20}O_3$	212.1413	$C_9H_{14}N_2O_4$	214.0954	$C_{12}H_{25}NO_2$	215.1886
$C_{15}H_{14}O$	210.1045	$C_{12}H_{22}NO_2$	212.1651	$C_9H_{16}N_3O_3$	214.1193	$C_{12}H_{27}N_2O$	215.2125
$C_{15}H_{16}N$	210.1284	$C_{12}H_{24}N_2O$	212.1890	$C_9H_{18}N_4O_2$	214.1431	$C_{12}H_{29}N_3$	215.2363
$C_{15}H_{30}$	210.2349	$C_{12}H_{26}N_3$	212.2129	$C_{10}H_{16}NO_4$	214.1080	$C_{13}H_{11}O_3$	215.0708

APPENDIX A (*Continued*)

FM		FM		FM		FM	
$C_{13}H_{13}NO_2$	215.0947	$C_{11}H_7NO_4$	217.0375	$C_{14}H_{22}N_2$	218.1784	$C_{11}H_{16}N_4O$	220.1325
$C_{13}H_{15}N_2O$	215.1185	$C_{11}H_9N_2O_3$	217.0614	$C_{15}H_{10}N_2$	218.0845	$C_{12}H_{12}O_4$	220.0735
$C_{13}H_{17}N_3$	215.1424	$C_{11}H_{11}N_3O_2$	217.0852	$C_{15}H_{22}O$	218.1671	$C_{12}H_{14}NO_3$	220.0974
$C_{14}H_{15}O_2$	215.1072	$C_{11}H_{13}N_4O$	217.1091	$C_{15}H_{24}N$	218.1910	$C_{12}H_{16}N_2O_2$	220.1213
$C_{14}H_{17}NO$	215.1311	$C_{11}H_{21}O_4$	217.1440	$C_{16}H_{10}O$	218.0732	$C_{12}H_{18}N_3O$	220.1451
$C_{14}H_{19}N_2$	215.1549	$C_{11}H_{23}NO_3$	217.1679	$C_{16}H_{12}N$	218.0970	$C_{12}H_{20}N_4$	220.1690
$C_{15}H_{19}O$	215.1436	$C_{11}H_{25}N_2O_2$	217.1917	$C_{16}H_{26}$	218.2036	$C_{13}H_8N_4$	220.0750
$C_{15}H_{21}N$	215.1675	$C_{11}H_{27}N_3O$	217.2156	$C_{17}H_{14}$	218.1096	$C_{13}H_{16}O_3$	220.1100
$C_{16}H_{23}$	215.1801	$C_{12}H_9O_4$	217.0501	**219**		$C_{13}H_{18}NO_2$	220.1338
216		$C_{12}H_{11}NO_3$	217.0739	$C_9H_{19}N_2O_4$	219.1345	$C_{13}H_{20}N_2O$	220.1577
$C_9H_{16}N_2O_4$	216.1111	$C_{12}H_{13}N_2O_2$	217.0978	$C_9H_{21}N_3O_3$	219.1584	$C_{13}H_{22}N_3$	220.1815
$C_9H_{18}N_3O_3$	216.1349	$C_{12}H_{15}N_3O$	217.1216	$C_9H_{23}N_4O_2$	219.1822	$C_{14}H_{10}N_3$	220.0876
$C_9H_{20}N_4O_2$	216.1588	$C_{12}H_{17}N_4$	217.1455	$C_{10}H_7N_2O_4$	219.0406	$C_{14}H_{20}O_2$	220.1464
$C_{10}H_8N_4O_2$	216.0648	$C_{12}H_{25}O_3$	217.1804	$C_{10}H_9N_3O_3$	219.0644	$C_{14}H_{22}NO$	220.1702
$C_{10}H_{18}NO_4$	216.1236	$C_{12}H_{27}NO_2$	217.2043	$C_{10}H_{11}N_4O_2$	219.0883	$C_{14}H_{24}N_2$	220.1941
$C_{10}H_{20}N_2O_3$	216.1475	$C_{13}H_{13}O_3$	217.0865	$C_{10}H_{21}NO_4$	219.1471	$C_{15}H_{10}NO$	220.0763
$C_{10}H_{22}N_3O_2$	216.1713	$C_{13}H_{15}NO_2$	217.1103	$C_{10}H_{23}N_2O_3$	219.1710	$C_{15}H_{12}N_2$	220.1001
$C_{10}H_{24}N_4O$	216.1952	$C_{13}H_{17}N_2O$	217.1342	$C_{10}H_{25}N_3O_2$	219.1948	$C_{15}H_{24}O$	220.1828
$C_{11}H_8N_2O_3$	216.0535	$C_{13}H_{19}N_3$	217.1580	$C_{11}H_9NO_4$	219.0532	$C_{15}H_{26}N$	220.2067
$C_{11}H_{10}N_3O_2$	216.0774	$C_{14}H_{17}O_2$	217.1229	$C_{11}H_{11}N_2O_3$	219.0770	$C_{16}H_{12}O$	220.0888
$C_{11}H_{12}N_4O$	216.1012	$C_{14}H_{19}NO$	217.1467	$C_{11}H_{13}N_3O_2$	219.1009	$C_{16}H_{14}N$	220.1127
$C_{11}H_{20}O_4$	216.1362	$C_{14}H_{21}N_2$	217.1706	$C_{11}H_{15}N_4O$	219.1247	$C_{16}H_{28}$	220.2192
$C_{11}H_{22}NO_3$	216.1600	$C_{15}H_9N_2$	217.0767	$C_{11}H_{23}O_4$	219.1597	$C_{17}H_{16}$	220.1253
$C_{11}H_{24}N_2O_2$	216.1839	$C_{15}H_{21}O$	217.1593	$C_{11}H_{25}NO_3$	219.1835	**221**	
$C_{11}H_{26}N_3O$	216.2077	$C_{15}H_{23}N$	217.1832	$C_{12}H_{11}O_4$	219.0657	$C_9H_{21}N_2O_4$	221.1502
$C_{11}H_{28}N_4$	216.2316	$C_{16}H_{11}N$	217.0892	$C_{12}H_{13}NO_3$	219.0896	$C_9H_{23}N_3O_3$	221.1741
$C_{12}H_8O_4$	216.0422	$C_{16}H_{25}$	217.1957	$C_{12}H_{15}N_2O_2$	219.1134	$C_{10}H_9N_2O_4$	221.0563
$C_{12}H_{10}NO_3$	216.0661	$C_{17}H_{13}$	217.1018	$C_{12}H_{17}N_3O$	219.1373	$C_{10}H_{11}N_3O_3$	221.0801
$C_{12}H_{12}N_2O_2$	216.0899	**218**		$C_{12}H_{19}N_4$	219.1611	$C_{10}H_{13}N_4O_2$	221.1040
$C_{12}H_{14}N_3O$	216.1138	$C_9H_{18}N_2O_4$	218.1267	$C_{13}H_{15}O_3$	219.1021	$C_{10}H_{23}NO_4$	221.1628
$C_{12}H_{16}N_4$	216.1377	$C_9H_{20}N_3O_3$	218.1506	$C_{13}H_{17}NO_2$	219.1260	$C_{11}H_{11}NO_4$	221.0688
$C_{12}H_{24}O_3$	216.1726	$C_9H_{22}N_4O_2$	218.1744	$C_{13}H_{19}N_2O$	219.1498	$C_{11}H_{13}N_2O_3$	221.0927
$C_{12}H_{26}NO_2$	216.1965	$C_{10}H_8N_3O_3$	218.0566	$C_{13}H_{21}N_3$	219.1737	$C_{11}H_{15}N_3O_2$	221.1165
$C_{12}H_{28}N_2O$	216.2203	$C_{10}H_{10}N_4O_2$	218.0805	$C_{14}H_9N_3$	219.0798	$C_{11}H_{17}N_4O$	221.1404
$C_{13}H_{12}O_3$	216.0786	$C_{10}H_{20}NO_4$	218.1393	$C_{14}H_{19}O_2$	219.1385	$C_{12}H_{13}O_4$	221.0814
$C_{13}H_{14}NO_2$	216.1025	$C_{10}H_{22}N_2O_3$	218.1631	$C_{14}H_{21}NO$	219.1624	$C_{12}H_{15}NO_3$	221.1052
$C_{13}H_{16}N_2O$	216.1264	$C_{10}H_{24}N_3O_2$	218.1870	$C_{14}H_{23}N_2$	219.1863	$C_{12}H_{17}N_2O_2$	221.1291
$C_{13}H_{18}N_3$	216.1502	$C_{10}H_{26}N_4O$	218.2108	$C_{15}H_9NO$	219.0684	$C_{12}H_{19}N_3O$	221.1529
$C_{13}H_{28}O_2$	216.2090	$C_{11}H_8NO_4$	218.0453	$C_{15}H_{11}N_2$	219.0923	$C_{12}H_{21}N_4$	221.1768
$C_{14}H_{16}O_2$	216.1151	$C_{11}H_{10}N_2O_3$	218.0692	$C_{15}H_{23}O$	219.1750	$C_{13}H_9N_4$	221.0829
$C_{14}H_{18}NO$	216.1389	$C_{11}H_{12}N_3O_2$	218.0930	$C_{15}H_{25}N$	219.1988	$C_{13}H_{17}O_3$	221.1178
$C_{14}H_{20}N_2$	216.1628	$C_{11}H_{14}N_4O$	218.1169	$C_{16}H_{11}O$	219.0810	$C_{13}H_{19}NO_2$	221.1416
$C_{15}H_{20}O$	216.1515	$C_{11}H_{22}O_4$	218.1518	$C_{16}H_{13}N$	219.1049	$C_{13}H_{21}N_2O$	221.1655
$C_{15}H_{22}N$	216.1753	$C_{11}H_{24}NO_3$	218.1757	$C_{16}H_{27}$	219.2114	$C_{13}H_{23}N_3$	221.1894
$C_{16}H_{10}N$	216.0814	$C_{11}H_{26}N_2O_2$	218.1996	$C_{17}H_{15}$	219.1174	$C_{14}H_9N_2O$	221.0715
$C_{16}H_{24}$	216.1879	$C_{12}H_{10}O_4$	218.0579	**220**		$C_{14}H_{11}N_3$	221.0954
$C_{17}H_{12}$	216.0939	$C_{12}H_{12}NO_3$	218.0817	$C_9H_{20}N_2O_4$	220.1424	$C_{14}H_{21}O_2$	221.1542
217		$C_{12}H_{14}N_2O_2$	218.1056	$C_9H_{22}N_3O_3$	220.1662	$C_{14}H_{23}NO$	221.1781
$C_9H_{17}N_2O_4$	217.1189	$C_{12}H_{16}N_3O$	218.1295	$C_9H_{24}N_4O_2$	220.1901	$C_{14}H_{25}N_2$	221.2019
$C_9H_{19}N_3O_3$	217.1427	$C_{12}H_{18}N_4$	218.1533	$C_{10}H_8N_2O_4$	220.0484	$C_{15}H_9O_2$	221.0603
$C_9H_{21}N_4O_2$	217.1666	$C_{12}H_{26}O_3$	218.1883	$C_{10}H_{10}N_3O_3$	220.0723	$C_{15}H_{11}NO$	221.0841
$C_{10}H_7N_3O_3$	217.0488	$C_{13}H_{14}O_3$	218.0943	$C_{10}H_{12}N_4O_2$	220.0961	$C_{15}H_{13}N_2$	221.1080
$C_{10}H_9N_4O_2$	217.0726	$C_{13}H_{16}NO_2$	218.1182	$C_{10}H_{22}NO_4$	220.1549	$C_{15}H_{25}O$	221.1906
$C_{10}H_{19}NO_4$	217.1315	$C_{13}H_{18}N_2O$	218.1420	$C_{10}H_{24}N_2O_3$	220.1788	$C_{15}H_{27}N$	221.2145
$C_{10}H_{21}N_2O_3$	217.1553	$C_{13}H_{20}N_3$	218.1659	$C_{11}H_{10}NO_4$	220.0610	$C_{16}H_{13}O$	221.0967
$C_{10}H_{23}N_3O_2$	217.1791	$C_{14}H_{18}O_2$	218.1307	$C_{11}H_{12}N_2O_3$	220.0848	$C_{16}H_{15}N$	221.1205
$C_{10}H_{25}N_4O$	217.2030	$C_{14}H_{20}NO$	218.1546	$C_{11}H_{14}N_3O_2$	220.1087	$C_{16}H_{29}$	221.2270

APPENDIX A (*Continued*)

FM		FM		FM		FM	
$C_{17}H_{17}$	221.1331	$C_{14}H_9NO_2$	223.0634	$C_{11}H_{21}N_4O$	225.1717	$C_{14}H_{28}NO$	226.2172
222		$C_{14}H_{11}N_2O$	223.0872	$C_{12}H_9N_4O$	225.0777	$C_{14}H_{30}N_2$	226.2411
$C_9H_{22}N_2O_4$	222.1580	$C_{14}H_{13}N_3$	223.1111	$C_{12}H_{17}O_4$	225.1127	$C_{15}H_{14}O_2$	226.0994
$C_{10}H_{10}N_2O_4$	222.0641	$C_{14}H_{23}O_2$	223.1699	$C_{12}H_{19}NO_3$	225.1365	$C_{15}H_{16}NO$	226.1233
$C_{10}H_{12}N_3O_3$	222.0879	$C_{14}H_{25}NO$	223.1937	$C_{12}H_{21}N_2O_2$	225.1604	$C_{15}H_{18}N_2$	226.1471
$C_{10}H_{14}N_4O_2$	222.1118	$C_{14}H_{27}N_2$	223.2176	$C_{12}H_{23}N_3O$	225.1842	$C_{15}H_{30}O$	226.2298
$C_{11}H_{12}NO_4$	222.0766	$C_{15}H_{11}O_2$	223.0759	$C_{12}H_{25}N_4$	225.2081	$C_{15}H_{32}N$	226.2536
$C_{11}H_{14}N_2O_3$	222.1005	$C_{15}H_{13}NO$	223.0998	$C_{13}H_9N_2O_2$	225.0664	$C_{16}H_{18}O$	226.1358
$C_{11}H_{16}N_3O_2$	222.1244	$C_{15}H_{27}O$	223.2063	$C_{13}H_{11}N_3O$	225.0903	$C_{16}H_{20}N$	226.1597
$C_{11}H_{18}N_4O$	222.1482	$C_{15}H_{29}N$	223.2301	$C_{13}H_{13}N_4$	225.1142	$C_{16}H_{34}$	226.2662
$C_{11}N_3O_3$	221.9940	$C_{16}H_{15}O$	223.1123	$C_{13}H_{21}O_3$	225.1491	$C_{17}H_{22}$	226.1722
$C_{12}H_{14}O_4$	222.0892	$C_{16}H_{17}N$	223.1362	$C_{13}H_{23}NO_2$	225.1730	**227**	
$C_{12}H_{16}NO_3$	222.1131	$C_{16}H_{31}$	223.2427	$C_{13}H_{25}N_2O$	225.1968	$C_{10}H_{15}N_2O_4$	227.1032
$C_{12}H_{18}N_2O_2$	222.1369	$C_{17}H_{19}$	223.1488	$C_{13}H_{27}N_3$	225.2207	$C_{10}H_{17}N_3O_3$	227.1271
$C_{12}H_{20}N_3O$	222.1608	**224**		$C_{14}H_9O_3$	225.0552	$C_{10}H_{19}N_4O_2$	227.1509
$C_{12}H_{22}N_4$	222.1846	$C_{10}H_{12}N_2O_4$	224.0797	$C_{14}H_{11}NO_2$	225.0790	$C_{11}H_{17}NO_4$	227.1158
$C_{13}H_8N_3O$	222.0668	$C_{10}H_{14}N_3O_3$	224.1036	$C_{14}H_{13}N_2O$	225.1029	$C_{11}H_{21}N_3O_2$	227.1635
$C_{13}H_{10}N_4$	222.0907	$C_{10}H_{16}N_4O_2$	224.1275	$C_{14}H_{15}N_3$	225.1267	$C_{11}H_{23}N_4O$	227.1873
$C_{13}H_{18}O_3$	222.1256	$C_{11}H_{14}NO_4$	224.0923	$C_{14}H_{25}O_2$	225.1855	$C_{12}H_7N_2O_3$	227.0457
$C_{13}H_{20}NO_2$	222.1495	$C_{11}H_{16}N_2O_3$	224.1162	$C_{14}H_{27}NO$	225.2094	$C_{12}H_9N_3O_2$	227.0695
$C_{13}H_{22}N_2O$	222.1733	$C_{11}H_{18}N_3O_2$	224.1400	$C_{14}H_{29}N_2$	225.2332	$C_{12}H_{11}N_4O$	227.0934
$C_{13}H_{24}N_3$	222.1972	$C_{11}H_{20}N_4O$	224.1639	$C_{15}H_{13}O_2$	225.0916	$C_{12}H_{19}O_4$	227.1284
$C_{14}H_{10}N_2O$	222.0794	$C_{12}H_8N_4O$	224.0699	$C_{15}H_{15}NO$	225.1154	$C_{12}H_{21}NO_3$	227.1522
$C_{14}H_{12}N_3$	222.1032	$C_{12}H_{16}O_4$	224.1049	$C_{15}H_{17}N_2$	225.1393	$C_{12}H_{23}N_2O_2$	227.1761
$C_{14}H_{22}O_2$	222.1620	$C_{12}H_{18}NO_3$	224.1287	$C_{15}H_{29}O$	225.2219	$C_{12}H_{25}N_3O$	227.1999
$C_{14}H_{24}NO$	222.1859	$C_{12}H_{20}N_2O_2$	224.1526	$C_{15}H_{31}N$	225.2458	$C_{12}H_{27}N_4$	227.2238
$C_{14}H_{26}N_2$	222.2098	$C_{12}H_{22}N_3O$	224.1764	$C_{16}H_{17}O$	225.1280	$C_{13}H_9NO_3$	227.0583
$C_{15}H_{10}O_2$	222.0681	$C_{12}H_{24}N_4$	224.2003	$C_{16}H_{19}N$	225.1519	$C_{13}H_{11}N_2O_2$	227.0821
$C_{15}H_{12}NO$	222.0919	$C_{13}H_8N_2O_2$	224.0586	$C_{16}H_{33}$	225.2584	$C_{13}H_{13}N_3O$	227.1060
$C_{15}H_{14}N_2$	222.1158	$C_{13}H_{10}N_3O$	224.0825	$C_{17}H_{21}$	225.1644	$C_{13}H_{15}N_4$	227.1298
$C_{15}H_{26}O$	222.1985	$C_{13}H_{12}N_4$	224.1063	**226**		$C_{13}H_{25}NO_2$	227.1886
$C_{15}H_{28}N$	222.2223	$C_{13}H_{20}O_3$	224.1413	$C_{10}H_{14}N_2O_4$	226.0954	$C_{13}H_{27}N_2O$	227.2125
$C_{16}H_{14}O$	222.1045	$C_{13}H_{22}NO_2$	224.1651	$C_{10}H_{16}N_3O_3$	226.1193	$C_{13}H_{29}N_3$	227.2363
$C_{16}H_{16}N$	222.1284	$C_{13}H_{24}N_2O$	224.1890	$C_{10}H_{18}N_4O_2$	226.1431	$C_{14}H_{11}O_3$	227.0708
$C_{16}H_{30}$	222.2349	$C_{13}H_{26}N_3$	224.2129	$C_{11}H_{16}NO_4$	226.1080	$C_{14}H_{13}NO_2$	227.0947
$C_{16}NO$	221.9980	$C_{14}H_{10}NO_2$	224.0712	$C_{11}H_{18}N_2O_3$	226.1318	$C_{14}H_{15}N_2O$	227.1185
$C_{17}H_{18}$	222.1409	$C_{14}H_{12}N_2O$	224.0950	$C_{11}H_{20}N_3O_2$	226.1557	$C_{14}H_{17}N_3$	227.1424
223		$C_{14}H_{14}N_3$	224.1189	$C_{11}H_{22}N_4O$	226.1795	$C_{14}H_{27}O_2$	227.2012
$C_{10}H_{11}N_2O_4$	223.0719	$C_{14}H_{24}O_2$	224.1777	$C_{12}H_8N_3O_2$	226.0617	$C_{14}H_{29}NO$	227.2250
$C_{10}H_{13}N_3O_3$	223.0958	$C_{14}H_{26}NO$	224.2015	$C_{12}H_{10}N_4O$	226.0856	$C_{15}H_{15}O_2$	227.1072
$C_{10}H_{15}N_4O_2$	223.1196	$C_{14}H_{28}N_2$	224.2254	$C_{12}H_{18}O_4$	226.1205	$C_{15}H_{17}NO$	227.1311
$C_{11}H_{13}NO_4$	223.0845	$C_{15}H_{12}O_2$	224.0837	$C_{12}H_{20}NO_3$	226.1444	$C_{15}H_{19}N_2$	227.1549
$C_{11}H_{15}N_2O_3$	223.1083	$C_{15}H_{14}NO$	224.1076	$C_{12}H_{22}N_2O_2$	226.1682	$C_{15}H_{31}O$	227.2376
$C_{11}H_{17}N_3O_2$	223.1322	$C_{15}H_{16}N_2$	224.1315	$C_{12}H_{24}N_3O$	226.1929	$C_{15}H_{33}N$	227.2615
$C_{11}H_{19}N_4O$	223.1560	$C_{15}H_{28}O$	224.2141	$C_{12}H_{26}N_4$	226.2160	$C_{16}H_{19}O$	227.1436
$C_{12}H_7N_4O$	223.0621	$C_{15}H_{30}N$	224.2380	$C_{13}H_{10}N_2O_2$	226.0743	$C_{16}H_{21}N$	227.1675
$C_{12}H_{15}O_4$	223.0970	$C_{16}H_{16}O$	224.1202	$C_{13}H_{12}N_3O$	226.0981	$C_{17}H_{23}$	227.1801
$C_{12}H_{17}NO_3$	223.1209	$C_{16}H_{18}N$	224.1440	$C_{13}H_{14}N_4$	226.1220	**228**	
$C_{12}H_{19}N_2O_2$	223.1447	$C_{16}H_{32}$	224.2505	$C_{13}H_{22}O_3$	226.1569	$C_{10}H_{16}N_2O_2$	228.1111
$C_{12}H_{21}N_3O$	223.1686	$C_{17}H_{20}$	224.1566	$C_{13}H_{24}NO_2$	226.1808	$C_{10}H_{18}N_3O_3$	228.1349
$C_{12}H_{23}N_4$	223.1925	**225**		$C_{13}H_{26}N_2O$	226.2046	$C_{10}H_{20}N_4O_2$	228.1588
$C_{13}H_9N_3O$	223.0746	$C_{10}H_{13}N_2O_4$	225.0876	$C_{13}H_{28}N_3$	226.2285	$C_{11}H_8N_4O_2$	228.0648
$C_{13}H_{11}N_4$	223.0985	$C_{10}H_{15}N_3O_3$	225.1114	$C_{14}H_{10}O_3$	226.0630	$C_{11}H_{18}NO_4$	228.1236
$C_{13}H_{19}O_3$	223.1334	$C_{10}H_{17}N_4O_2$	225.1353	$C_{14}H_{12}NO_2$	226.0868	$C_{11}H_{20}N_2O_3$	228.1475
$C_{13}H_{21}NO_2$	223.1573	$C_{11}H_{15}NO_4$	225.1001	$C_{14}H_{14}N_2O$	226.1107	$C_{11}H_{22}N_3O_2$	228.1713
$C_{13}H_{23}N_2O$	223.1811	$C_{11}H_{17}N_2O_3$	225.1240	$C_{14}H_{16}N_3$	226.1346	$C_{11}H_{24}N_4O$	228.1952
$C_{13}H_{25}N_3$	223.2050	$C_{11}H_{19}N_3O_2$	225.1478	$C_{14}H_{26}O_2$	226.1934	$C_{12}H_8N_2O_3$	228.0535

APPENDIX A (*Continued*)

FM		FM		FM		FM	
$C_{12}H_{12}N_4O$	228.1012	$C_{14}H_{15}NO_2$	229.1103	$C_{10}H_{23}N_4O_2$	231.1822	$C_{13}H_{20}N_4$	232.1690
$C_{12}H_{20}O_4$	228.1362	$C_{14}H_{17}N_2O$	229.1342	$C_{11}H_7N_2O_4$	231.0406	$C_{13}H_{28}O_3$	232.2039
$C_{12}H_{22}NO_3$	228.1600	$C_{14}H_{19}N_3$	229.1580	$C_{11}H_9N_3O_3$	231.0644	$C_{14}H_{16}O_3$	232.1100
$C_{12}H_{24}N_2O_2$	228.1839	$C_{14}H_{29}O_2$	229.2168	$C_{11}H_{11}N_4O_2$	231.0883	$C_{14}H_{18}NO_2$	232.1338
$C_{12}H_{26}N_3O$	228.2077	$C_{14}H_{31}NO$	229.2407	$C_{11}H_{21}NO_4$	231.1471	$C_{14}H_{20}N_2O$	232.1577
$C_{12}H_{28}N_4$	228.2316	$C_{15}H_{17}O_2$	229.1229	$C_{11}H_{23}N_2O_3$	231.1710	$C_{14}H_{22}N_3$	232.1815
$C_{13}H_8O_4$	228.0422	$C_{15}H_{19}NO$	229.1467	$C_{11}H_{25}N_3O_2$	231.1948	$C_{15}H_{10}N_3$	232.0876
$C_{13}H_{10}NO_3$	228.0661	$C_{15}H_{21}N_2$	229.1706	$C_{11}H_{27}N_4O$	231.2187	$C_{15}H_{20}O_2$	232.1464
$C_{13}H_{12}N_2O_2$	228.0899	$C_{16}H_{21}O$	229.1593	$C_{12}H_9NO_4$	231.0532	$C_{15}H_{22}NO$	232.1702
$C_{13}H_{14}N_3O$	228.1138	$C_{16}H_{23}N$	229.1832	$C_{12}H_{11}N_2O_3$	231.0770	$C_{15}H_{24}N_2$	232.1941
$C_{13}H_{24}O_3$	228.1726	$C_{17}H_9O$	229.0653	$C_{12}H_{13}N_3O_2$	231.1009	$C_{16}H_{10}NO$	232.0768
$C_{13}H_{26}NO_2$	228.1965	$C_{17}H_{11}N$	229.0892	$C_{12}H_{15}N_4O$	231.1247	$C_{16}H_{12}N_2$	232.1001
$C_{13}H_{28}N_2O$	228.2203	$C_{18}H_{13}$	229.1018	$C_{12}H_{23}O_4$	231.1597	$C_{16}H_{24}O$	232.1828
$C_{13}H_{30}N_3$	228.2442	**230**		$C_{12}H_{25}NO_3$	231.1835	$C_{16}H_{26}N$	232.2067
$C_{14}H_{12}O_3$	228.0786	$C_{10}H_{18}N_2O_4$	230.1267	$C_{12}H_{27}N_2O_2$	231.2074	$C_{17}H_{12}O$	232.0888
$C_{14}H_{14}NO_2$	228.1025	$C_{10}H_{20}N_3O_3$	230.1506	$C_{12}H_{29}N_3O$	231.2312	$C_{17}H_{14}N$	232.1127
$C_{14}H_{16}N_2O$	228.1264	$C_{10}H_{22}N_4O_2$	230.1744	$C_{13}H_{11}O_4$	231.0657	$C_{17}H_{28}$	232.2192
$C_{14}H_{18}N_3$	228.1502	$C_{11}H_8N_3O_3$	230.0566	$C_{13}H_{13}NO_3$	231.0896	$C_{18}H_{16}$	232.1253
$C_{14}H_{28}O_2$	228.2090	$C_{11}H_{10}N_4O_2$	230.0805	$C_{13}H_{15}N_2O_2$	231.1134	**233**	
$C_{14}H_{30}NO$	228.2329	$C_{11}H_{20}NO_4$	230.1393	$C_{13}H_{17}N_3O$	231.1373	$C_{10}H_{23}N_3O_3$	233.1741
$C_{14}H_{32}N_2$	228.2567	$C_{11}H_{22}N_2O_3$	230.1631	$C_{13}H_{19}N_4$	231.1611	$C_{10}H_{25}N_4O_2$	233.1979
$C_{15}H_{16}O_2$	228.1151	$C_{11}H_{24}N_3O_2$	230.1870	$C_{14}H_{15}O_3$	231.1021	$C_{11}H_9N_2O_4$	233.0563
$C_{15}H_{18}NO$	228.1389	$C_{11}H_{26}N_4O$	230.2108	$C_{14}H_{17}NO_2$	231.1260	$C_{11}H_{11}N_3O_3$	233.0801
$C_{15}H_{20}N_2$	228.1628	$C_{12}H_8NO_4$	230.0453	$C_{14}H_{19}N_2O$	231.1498	$C_{11}H_{23}NO_4$	233.1628
$C_{15}H_{32}O$	228.2454	$C_{12}H_{10}N_2O_3$	230.0692	$C_{14}H_{21}N_3$	231.1737	$C_{11}H_{25}N_2O_3$	233.1866
$C_{16}H_{20}O$	228.1515	$C_{12}H_{12}N_3O_2$	230.0930	$C_{15}H_9N_3$	231.0798	$C_{11}H_{27}N_3O_2$	233.2105
$C_{16}H_{22}N$	228.1753	$C_{12}H_{14}N_4O$	230.1169	$C_{15}H_{19}O_2$	231.1385	$C_{12}H_{11}NO_4$	233.0688
$C_{17}H_{10}N$	228.0814	$C_{12}H_{22}O_4$	230.1518	$C_{15}H_{21}NO$	231.1624	$C_{12}H_{13}N_2O_3$	233.0927
$C_{17}H_{24}$	228.1879	$C_{12}H_{24}NO_3$	230.1757	$C_{15}H_{23}N_2$	231.1863	$C_{12}H_{15}N_3O_2$	233.1165
$C_{18}H_{12}$	228.0939	$C_{12}H_{26}N_2O_2$	230.1996	$C_{16}H_9NO$	231.0684	$C_{12}H_{17}N_4O$	233.1404
229		$C_{12}H_{28}N_3O$	230.2234	$C_{16}H_{11}N_2$	231.0923	$C_{12}H_{25}O_4$	233.1753
$C_{10}H_{17}N_2O_4$	229.1189	$C_{12}H_{30}N_4$	230.2473	$C_{16}H_{23}O$	231.1750	$C_{12}H_{27}NO_3$	233.1992
$C_{10}H_{19}N_3O_3$	229.1427	$C_{13}H_{10}O_4$	230.0579	$C_{17}H_{11}O$	231.0810	$C_{13}H_{13}O_4$	233.0814
$C_{10}H_{21}N_4O_2$	229.1666	$C_{13}H_{12}NO_3$	230.0817	$C_{17}H_{13}N$	231.1049	$C_{13}H_{15}NO_3$	233.1052
$C_{11}H_7N_3O_3$	229.0488	$C_{13}H_{14}N_2O_2$	230.1056	$C_{17}H_{27}$	231.2114	$C_{13}H_{17}N_2O_2$	233.1291
$C_{11}H_9N_4O_2$	229.0726	$C_{13}H_{16}N_3O$	230.1295	$C_{18}H_{15}$	231.1174	$C_{13}H_{19}N_3O$	233.1529
$C_{11}H_{19}NO_4$	229.1315	$C_{13}H_{18}N_4$	230.1533	**232**		$C_{13}H_{21}N_4$	233.1768
$C_{11}H_{21}N_2O_3$	229.1553	$C_{13}H_{26}O_3$	230.1883	$C_{10}H_{20}N_2O_4$	232.1424	$C_{14}H_9N_4$	233.0829
$C_{11}H_{23}N_3O_2$	229.1791	$C_{13}H_{28}NO_2$	230.2121	$C_{10}H_{22}N_3O_3$	232.1662	$C_{14}H_{17}O_3$	233.1178
$C_{11}H_{25}N_4O$	229.2030	$C_{13}H_{30}N_2O$	230.2360	$C_{10}H_{24}N_4O_2$	232.1901	$C_{14}H_{19}NO_2$	233.1416
$C_{12}H_9N_2O_3$	229.0614	$C_{14}H_{14}O_3$	230.0943	$C_{11}H_8N_2O_4$	232.0484	$C_{14}H_{21}N_2O$	233.1655
$C_{12}H_{11}N_3O_2$	229.0852	$C_{14}H_{16}NO_2$	230.1182	$C_{11}H_{10}N_3O_3$	232.0723	$C_{15}H_9N_2O$	233.0715
$C_{12}H_{13}N_4O$	229.1091	$C_{14}H_{18}N_2O$	230.1420	$C_{11}H_{12}N_4O_2$	232.0961	$C_{15}H_{11}N_3$	233.0954
$C_{12}H_{21}O_4$	229.1440	$C_{14}H_{20}N_3$	230.1659	$C_{11}H_{22}NO_4$	232.1549	$C_{15}H_{21}O_2$	233.1542
$C_{12}H_{23}NO_3$	229.1679	$C_{14}H_{30}O_2$	230.2247	$C_{11}H_{24}N_2O_3$	232.1788	$C_{15}H_{23}NO$	233.1781
$C_{12}H_{25}N_2O_2$	229.1917	$C_{15}H_{18}O_2$	230.1307	$C_{11}H_{26}N_3O_2$	232.2026	$C_{15}H_{25}N_2$	233.2019
$C_{12}H_{27}N_3O$	229.2156	$C_{15}H_{20}NO$	230.1546	$C_{11}H_{28}N_4O$	232.2265	$C_{16}H_9O_2$	233.0603
$C_{12}H_{29}N_4$	229.2394	$C_{15}H_{22}N_2$	230.1784	$C_{12}H_{10}NO_4$	232.0610	$C_{16}H_{11}NO$	233.0841
$C_{13}H_9O_4$	229.0501	$C_{16}H_{10}N_2$	230.0845	$C_{12}H_{12}N_2O_3$	232.0848	$C_{16}H_{13}N_2$	233.1080
$C_{13}H_{11}NO_3$	229.0739	$C_{16}H_{22}O$	230.1671	$C_{12}H_{14}N_3O_2$	232.1087	$C_{16}H_{25}O$	233.1906
$C_{13}H_{13}N_2O_2$	229.0978	$C_{16}H_{24}N$	230.1910	$C_{12}H_{16}N_4O$	232.1325	$C_{16}H_{27}N$	233.2145
$C_{13}H_{15}N_3O$	229.1216	$C_{17}H_{10}O$	230.0732	$C_{12}H_{24}O_4$	232.1675	$C_{17}H_{13}O$	233.0967
$C_{13}H_{17}N_4$	229.1455	$C_{17}H_{12}N$	230.0970	$C_{12}H_{26}NO_3$	232.1914	$C_{17}H_{15}N$	233.1205
$C_{13}H_{25}O_3$	229.1804	$C_{17}H_{26}$	230.2036	$C_{12}H_{28}N_2O_2$	232.2152	$C_{17}H_{29}$	233.2270
$C_{13}H_{27}NO_2$	229.2043	$C_{18}H_{14}$	230.1096	$C_{13}H_{12}O_4$	232.0735	$C_{18}H_{17}$	233.1331
$C_{13}H_{29}N_2O$	229.2281	**231**		$C_{13}H_{14}NO_3$	232.0974	**234**	
$C_{13}H_{31}N_3$	229.2520	$C_{10}H_{19}N_2O_4$	231.1345	$C_{13}H_{16}N_2O_2$	232.1213	$C_{10}H_{22}N_2O_4$	234.1580
$C_{14}H_{13}O_3$	229.0865	$C_{10}H_{21}N_3O_3$	231.1584	$C_{13}H_{18}N_3O$	232.1451	$C_{10}H_{24}N_3O_3$	234.1819

APPENDIX A (*Continued*)

FM		FM		FM		FM	
$C_{10}H_{26}N_4O_2$	234.2057	$C_{15}H_{13}N_3$	235.1111	$C_{12}H_{21}N_4O$	237.1717	$C_{15}H_{30}N_2$	238.2411
$C_{11}H_{10}N_2O_4$	234.0641	$C_{15}H_{23}O_2$	235.1699	$C_{13}H_9N_4O$	237.0777	$C_{16}H_{14}O_2$	238.0994
$C_{11}H_{12}N_3O_3$	234.0879	$C_{15}H_{25}NO$	235.1937	$C_{13}H_{17}O_4$	237.1127	$C_{16}H_{16}NO$	238.1233
$C_{11}H_{14}N_4O_2$	234.1118	$C_{15}H_{27}N_2$	235.2176	$C_{13}H_{19}NO_3$	237.1365	$C_{16}H_{18}N_2$	238.1471
$C_{11}H_{24}NO_4$	234.1706	$C_{16}H_{11}O_2$	235.0759	$C_{13}H_{21}N_2O_2$	237.1604	$C_{16}H_{30}O$	238.2298
$C_{11}H_{26}N_2O_3$	234.1945	$C_{16}H_{13}NO$	235.0998	$C_{13}H_{23}N_3O$	237.1842	$C_{16}H_{32}N$	238.2536
$C_{12}H_{12}NO_4$	234.0766	$C_{16}H_{15}N_2$	235.1236	$C_{13}H_{25}N$	237.2081	$C_{17}H_{18}O$	238.1358
$C_{12}H_{14}N_2O_3$	234.1005	$C_{16}H_{27}O$	235.2063	$C_{14}H_9N_2O_2$	237.0664	$C_{17}H_{20}N$	238.1597
$C_{12}H_{16}N_3O_2$	234.1244	$C_{16}H_{29}N$	235.2301	$C_{14}H_{11}N_3O$	237.0903	$C_{17}H_{34}$	238.2662
$C_{12}H_{18}N_4O$	234.1482	$C_{17}H_{15}O$	235.1123	$C_{14}H_{13}N_4$	237.1142	$C_{18}H_{22}$	238.1722
$C_{12}H_{26}O_4$	234.1832	$C_{17}H_{17}N$	235.1362	$C_{14}H_{21}O_3$	237.1491	**239**	
$C_{13}H_{14}O_4$	234.0892	$C_{17}H_{31}$	235.2427	$C_{14}H_{23}NO_2$	237.1730	$C_{11}H_{15}N_2O_4$	239.1032
$C_{13}H_{16}NO_3$	234.1131	$C_{18}H_{19}$	235.1488	$C_{14}H_{25}N_2O$	237.1968	$C_{11}H_{17}N_3O_3$	239.1271
$C_{13}H_{18}N_2O_2$	234.1369	**236**		$C_{14}H_{27}N_3$	237.2207	$C_{11}H_{19}N_4O_2$	239.1509
$C_{13}H_{20}N_3O$	234.1608	$C_{10}H_{24}N_2O_4$	236.1737	$C_{15}H_9O_3$	237.0552	$C_{12}H_{17}NO_4$	239.1158
$C_{13}H_{22}N_4$	234.1846	$C_{11}H_{12}N_2O_4$	236.0797	$C_{15}H_{11}NO_2$	237.0790	$C_{12}H_{19}N_2O_3$	239.1396
$C_{14}H_{10}N_4$	234.0907	$C_{11}H_{14}N_3O_3$	236.1036	$C_{15}H_{13}N_2O$	237.1029	$C_{12}H_{21}N_3O_2$	239.1635
$C_{14}H_{18}O_3$	234.1256	$C_{11}H_{16}N_4O_2$	236.1275	$C_{15}H_{15}N_3$	237.1267	$C_{12}H_{23}N_4O$	239.1873
$C_{14}H_{20}NO_2$	234.1495	$C_{12}H_2N_3O_3$	236.0096	$C_{15}H_{25}O_2$	237.1855	$C_{13}H_9N_3O_2$	239.0695
$C_{14}H_{22}N_2O$	234.1733	$C_{12}H_4N_4O_2$	236.0335	$C_{15}H_{27}NO$	237.2094	$C_{13}H_{11}N_4O$	239.0934
$C_{14}H_{24}N_3$	234.1972	$C_{12}H_{14}NO_4$	236.0923	$C_{15}H_{29}N_2$	237.2332	$C_{13}H_{19}O_4$	239.1284
$C_{15}H_{10}N_2O$	234.0794	$C_{12}H_{16}N_2O_3$	236.1162	$C_{16}H_{13}O_2$	237.0916	$C_{13}H_{21}NO_3$	239.1522
$C_{15}H_{12}N_3$	234.1032	$C_{12}H_{18}N_3O_2$	236.1400	$C_{16}H_{15}NO$	237.1154	$C_{13}H_{23}N_2O_2$	239.1761
$C_{15}H_{22}O_2$	234.1620	$C_{12}H_{20}N_4O$	236.1639	$C_{16}H_{17}N_2$	237.1393	$C_{13}H_{25}N_3O$	239.1999
$C_{15}H_{24}NO$	234.1859	$C_{13}H_8N_4O$	236.0699	$C_{16}H_{29}O$	237.2219	$C_{13}H_{27}N_4$	239.2238
$C_{15}H_{26}N_2$	234.2098	$C_{13}H_{16}O_4$	236.1049	$C_{16}H_{31}N$	237.2458	$C_{14}H_9NO_3$	239.0583
$C_{16}H_{10}O_2$	234.0681	$C_{13}H_{18}NO_3$	236.1287	$C_{17}H_{17}O$	237.1280	$C_{14}H_{11}N_2O_2$	239.0821
$C_{16}H_{12}NO$	234.0919	$C_{13}H_{20}N_2O_2$	236.1526	$C_{17}H_{19}N$	237.1519	$C_{14}H_{13}N_3O$	239.1060
$C_{16}H_{14}N_2$	234.1158	$C_{13}H_{22}N_3O$	236.1764	$C_{17}H_{33}$	237.2584	$C_{14}H_{15}N_4$	239.1298
$C_{16}H_{26}O$	234.1985	$C_{13}H_{24}N_4$	236.2003	$C_{18}H_{21}$	237.1644	$C_{14}H_{23}O_3$	239.1648
$C_{16}H_{28}N$	234.2223	$C_{14}H_{10}N_3O$	236.0825	**238**		$C_{14}H_{25}NO_2$	239.1886
$C_{17}H_{16}N$	234.1284	$C_{14}H_{12}N_4$	236.1063	$C_{11}H_{14}N_2O_4$	238.0954	$C_{14}H_{27}N_2O$	239.2125
$C_{17}H_{30}$	234.2349	$C_{14}H_{20}O_3$	236.1413	$C_{11}H_{16}N_3O_3$	238.1193	$C_{14}H_{29}N_3$	239.2363
$C_{18}H_{18}$	234.1409	$C_{14}H_{22}NO_2$	236.1651	$C_{11}H_{18}N_4O_2$	238.1431	$C_{15}H_{11}O_3$	239.0708
235		$C_{14}H_{24}N_2O$	236.1890	$C_{12}H_{16}NO_4$	238.1080	$C_{15}H_{13}NO_2$	239.0947
$C_{10}H_{23}N_2O_4$	235.1659	$C_{14}H_{26}N_3$	236.2129	$C_{12}H_{18}N_2O_3$	238.1318	$C_{15}H_{15}N_2O$	239.1185
$C_{10}H_{25}N_3O_3$	235.1897	$C_{15}H_{10}NO_2$	236.0712	$C_{12}H_{20}N_3O_2$	238.1557	$C_{15}H_{17}N_3$	239.1424
$C_{11}H_{11}N_2O_4$	235.0719	$C_{15}H_{12}N_2O$	236.0950	$C_{12}H_{22}N_4O$	238.1795	$C_{15}H_{27}O_2$	239.2012
$C_{11}H_{13}N_3O_3$	235.0958	$C_{15}H_{14}N_3$	236.1189	$C_{13}H_8N_3O_2$	238.0617	$C_{15}H_{29}NO$	239.2250
$C_{11}H_{15}N_4O_2$	235.1196	$C_{15}H_{24}O_2$	236.1777	$C_{13}H_{10}N_4O$	238.0856	$C_{15}H_{31}N_2$	239.2489
$C_{11}H_{25}NO_4$	235.1784	$C_{15}H_{26}NO$	236.2015	$C_{13}H_{18}O_4$	238.1205	$C_{16}H_{15}O_2$	239.1072
$C_{12}H_{13}NO_4$	235.0845	$C_{15}H_{28}N_2$	236.2254	$C_{13}H_{20}NO_3$	238.1444	$C_{16}H_{17}NO$	239.1311
$C_{12}H_{15}N_2O_3$	235.1083	$C_{16}H_{12}O_2$	236.0837	$C_{13}H_{22}N_2O_2$	238.1682	$C_{16}H_{19}N_2$	239.1549
$C_{12}H_{17}N_3O_2$	235.1322	$C_{16}H_{14}NO$	236.1076	$C_{13}H_{24}N_3O$	238.1921	$C_{16}H_{31}O$	239.2376
$C_{12}H_{19}N_4O$	235.1560	$C_{16}H_{16}N_2$	236.1315	$C_{13}H_{26}N_4$	238.2160	$C_{16}H_{33}N$	239.2615
$C_{13}H_{15}O_4$	235.0970	$C_{16}H_{28}O$	236.2141	$C_{14}H_{10}N_2O_2$	238.0743	$C_{17}H_{19}O$	239.1436
$C_{13}H_{17}NO_3$	235.1209	$C_{16}H_{30}N$	236.2380	$C_{14}H_{12}N_3O$	238.0981	$C_{17}H_{21}N$	239.1675
$C_{13}H_{19}N_2O_2$	235.1447	$C_{17}H_{16}O$	236.1202	$C_{14}H_{14}N_4$	238.1220	$C_{17}H_{35}$	239.2740
$C_{13}H_{21}N_3O$	235.1686	$C_{17}H_{18}N$	236.1440	$C_{14}H_{22}O_3$	238.1569	$C_{18}H_{23}$	239.1801
$C_{13}H_{23}N_4$	235.1925	$C_{17}H_{32}$	236.2505	$C_{14}H_{24}NO_2$	238.1808	**240**	
$C_{14}H_9N_3O$	235.0746	$C_{18}H_{20}$	236.1566	$C_{14}H_{26}N_2O$	238.2046	$C_{11}H_{16}N_2O_4$	240.1111
$C_{14}H_{11}N_4$	235.0985	**237**		$C_{14}H_{28}N_3$	238.2285	$C_{11}H_{18}N_3O_3$	240.1349
$C_{14}H_{19}O_3$	235.1334	$C_{11}H_{13}N_2O_4$	237.0876	$C_{15}H_{10}O_3$	238.0630	$C_{11}H_{20}N_4O_2$	240.1588
$C_{14}H_{21}NO_2$	235.1573	$C_{11}H_{15}N_3O_3$	237.1114	$C_{15}H_{12}NO_2$	238.0868	$C_{12}H_8N_4O_2$	240.0648
$C_{14}H_{23}N_2O$	235.1811	$C_{11}H_{17}N_4O_2$	237.1353	$C_{15}H_{14}N_2O$	238.1107	$C_{12}H_{18}NO_4$	240.1236
$C_{14}H_{25}N_3$	235.2050	$C_{12}H_{15}NO_4$	237.1001	$C_{15}H_{16}N_3$	238.1346	$C_{12}H_{20}N_2O_3$	240.1475
$C_{15}H_9NO_2$	235.0634	$C_{12}H_{17}N_2O_3$	237.1240	$C_{15}H_{26}O_2$	238.1934	$C_{12}H_{22}N_3O_2$	240.1713
$C_{15}H_{11}N_2O$	235.0872	$C_{12}H_{19}N_3O_2$	237.1478	$C_{15}H_{28}NO$	238.2172	$C_{12}H_{24}N_4O$	240.1952

APPENDIX A (*Continued*)

FM		FM		FM		FM	
$C_{13}H_8N_2O_3$	240.0535	$C_{15}H_{17}N_2O$	241.1342	$C_{17}H_{24}N$	242.1910	$C_{12}H_{24}N_2O_3$	244.1788
$C_{13}H_{10}N_3O_2$	240.0774	$C_{15}H_{19}N_3$	241.1580	$C_{18}H_{10}O$	242.0732	$C_{12}H_{26}N_3O_2$	244.2026
$C_{13}H_{12}N_4O$	240.1012	$C_{15}H_{29}O_2$	241.2168	$C_{18}H_{12}N$	242.0970	$C_{12}H_{28}N_4O$	244.2265
$C_{13}H_{20}O_4$	240.1362	$C_{15}H_{31}NO$	241.2407	$C_{18}H_{26}$	242.2036	$C_{13}H_{10}NO_4$	244.0610
$C_{13}H_{22}NO_3$	240.1600	$C_{15}H_{33}N_2$	241.2646	$C_{19}H_{14}$	242.1096	$C_{13}H_{12}N_2O_3$	244.0848
$C_{13}H_{24}N_2O_2$	240.1839	$C_{16}H_{17}O_2$	241.1229	**243**		$C_{13}H_{14}N_3O_2$	244.1087
$C_{13}H_{28}N_4$	240.2316	$C_{16}H_{19}NO$	241.1467	$C_{11}H_{19}N_2O_4$	243.1345	$C_{13}H_{16}N_4O$	244.1325
$C_{14}H_8O_4$	240.0422	$C_{16}H_{21}N_2$	241.1706	$C_{11}H_{21}N_3O_3$	243.1584	$C_{13}H_{24}O_4$	244.1675
$C_{14}H_{10}NO_3$	240.0661	$C_{16}H_{33}O$	241.2533	$C_{11}H_{23}N_4O_2$	243.1822	$C_{13}H_{26}NO_3$	244.1914
$C_{14}H_{12}N_2O_2$	240.0899	$C_{16}H_{35}N$	241.2771	$C_{12}H_7N_2O_4$	243.0406	$C_{13}H_{28}N_2O_2$	244.2152
$C_{14}H_{14}N_3O$	240.1138	$C_{17}H_{21}O$	241.1593	$C_{12}H_9N_3O_3$	243.0644	$C_{13}H_{30}N_3O$	244.2391
$C_{14}H_{16}N_4$	240.1377	$C_{17}H_{23}N$	241.1832	$C_{12}H_{11}N_4O_2$	243.0883	$C_{13}H_{32}N_4$	244.2629
$C_{14}H_{24}O_3$	240.1726	$C_{18}H_{25}$	241.1957	$C_{12}H_{21}NO_4$	243.1471	$C_{14}H_{12}O_4$	244.0735
$C_{14}H_{26}NO_2$	240.1965	**242**		$C_{12}H_{23}N_2O_3$	243.1710	$C_{14}H_{14}NO_3$	244.0974
$C_{14}H_{28}N_2O$	240.2203	$C_{11}H_{18}N_2O_4$	242.1267	$C_{12}H_{25}N_3O_2$	243.1948	$C_{14}H_{16}N_2O_2$	244.1213
$C_{14}H_{30}N_3$	240.2442	$C_{11}H_{20}N_3O_3$	242.1506	$C_{12}H_{27}N_4O$	243.2187	$C_{14}H_{18}N_3O$	244.1451
$C_{15}H_{12}O_3$	240.0786	$C_{11}H_{22}N_4O_2$	242.1744	$C_{13}H_9NO_4$	243.0532	$C_{14}H_{20}N_4$	244.1690
$C_{15}H_{14}NO_2$	240.1025	$C_{12}H_8N_3O_3$	242.0566	$C_{13}H_{11}N_2O_3$	243.0770	$C_{14}H_{28}O_3$	244.2039
$C_{15}H_{16}N_2O$	240.1264	$C_{12}H_{10}N_4O_2$	242.0805	$C_{13}H_{13}N_3O_2$	243.1009	$C_{14}H_{30}NO_2$	244.2278
$C_{15}H_{18}N_3$	240.1502	$C_{12}H_{20}NO_4$	242.1393	$C_{13}H_{15}N_4O$	243.1247	$C_{14}H_{32}N_2O$	244.2516
$C_{15}H_{28}O_2$	240.2090	$C_{12}H_{22}N_2O_3$	242.1631	$C_{13}H_{23}O_4$	243.1597	$C_{15}H_{16}O_3$	244.1100
$C_{15}H_{30}NO$	240.2329	$C_{12}H_{24}N_3O_2$	242.1870	$C_{13}H_{25}NO_3$	243.1835	$C_{15}H_{18}NO_2$	244.1338
$C_{15}H_{32}N_2$	240.2567	$C_{12}H_{26}N_4O$	242.2108	$C_{13}H_{27}N_2O_2$	243.2074	$C_{15}H_{20}N_2O$	244.1577
$C_{16}H_{16}O_2$	240.1151	$C_{13}H_8NO_4$	242.0453	$C_{13}H_{29}N_3O$	243.2312	$C_{15}H_{22}N_3$	244.1815
$C_{16}H_{20}N_2$	240.1628	$C_{13}H_{10}N_2O_3$	242.0692	$C_{13}H_{31}N_4$	243.2551	$C_{15}H_{32}O_2$	244.2403
$C_{16}H_{18}NO$	240.1389	$C_{13}H_{12}N_3O_2$	242.0930	$C_{14}H_{11}O_4$	243.0657	$C_{16}H_{10}N_3$	244.0876
$C_{16}H_{32}O$	240.2454	$C_{13}H_{14}N_4O$	242.1169	$C_{14}H_{13}NO_3$	243.0896	$C_{16}H_{20}O_2$	244.1464
$C_{16}H_{34}N$	240.2693	$C_{13}H_{22}O_4$	242.1518	$C_{14}H_{15}N_2O_2$	243.1134	$C_{16}H_{22}NO$	244.1702
$C_{17}H_{20}O$	240.1515	$C_{13}H_{24}NO_3$	242.1757	$C_{14}H_{17}N_3O$	243.1373	$C_{16}H_{24}N_2$	244.1941
$C_{17}H_{22}N$	240.1753	$C_{13}H_{26}N_2O_2$	242.1996	$C_{14}H_{19}N_4$	243.1611	$C_{17}H_{10}NO$	244.0763
$C_{17}H_{36}$	240.2819	$C_{13}H_{28}N_3O$	242.2234	$C_{14}H_{27}O_3$	243.1961	$C_{17}H_{12}N_2$	244.1001
$C_{18}H_{24}$	240.1879	$C_{13}H_{30}N_4$	242.2473	$C_{14}H_{29}NO_2$	243.2199	$C_{17}H_{24}O$	244.1828
241		$C_{14}H_{10}O_4$	242.0579	$C_{14}H_{31}N_2O$	243.2438	$C_{17}H_{26}N$	244.2067
$C_{11}H_{17}N_2O_4$	241.1189	$C_{14}H_{12}NO_3$	242.0817	$C_{14}H_{33}N_3$	243.2677	$C_{18}H_{12}O$	244.0888
$C_{11}H_{19}N_3O_3$	241.1427	$C_{14}H_{14}N_2O_2$	242.1056	$C_{15}H_{15}O_3$	243.1021	$C_{18}H_{14}N$	244.1127
$C_{11}H_{21}N_4O_2$	241.1666	$C_{14}H_{16}N_3O$	242.1295	$C_{15}H_{17}NO_2$	243.1260	$C_{18}H_{28}$	244.2192
$C_{12}H_{19}NO_4$	241.1315	$C_{14}H_{18}N_4$	242.1533	$C_{15}H_{19}N_2O$	243.1498	$C_{19}H_{16}$	244.1253
$C_{12}H_{21}N_2O_3$	241.1553	$C_{14}H_{26}O_3$	242.1883	$C_{15}H_{21}N_3$	243.1737	**245**	
$C_{12}H_{23}N_3O_2$	241.1791	$C_{14}H_{28}NO_2$	242.2121	$C_{15}H_{31}O_2$	243.2325	$C_{11}H_{21}N_2O_4$	245.1502
$C_{12}H_{25}N_4O$	241.2030	$C_{14}H_{30}N_2O$	242.2360	$C_{15}H_{33}NO$	243.2564	$C_{11}H_{23}N_3O_3$	245.1741
$C_{13}H_{11}N_3O_2$	241.0852	$C_{14}H_{32}N_3$	242.2598	$C_{16}H_{19}O_2$	243.1385	$C_{11}H_{25}N_4O_2$	245.1979
$C_{13}H_{13}N_4O$	241.1091	$C_{15}H_{14}O_3$	242.0943	$C_{16}H_{21}NO$	243.1624	$C_{12}H_9N_2O_4$	245.0563
$C_{13}H_{21}O_4$	241.1440	$C_{15}H_{16}NO_2$	242.1182	$C_{16}H_{23}N_2$	243.1863	$C_{12}H_{11}N_3O_3$	245.0801
$C_{13}H_{25}N_2O_2$	241.1679	$C_{15}H_{18}N_2O$	242.1420	$C_{17}H_{23}O$	243.1750	$C_{12}H_{13}N_4O_2$	245.1040
$C_{13}H_{25}N_2O_2$	241.1917	$C_{15}H_{20}N_3$	242.1659	$C_{17}H_{25}N$	243.1988	$C_{12}H_{23}NO_4$	245.1628
$C_{13}H_{27}N_3O$	241.2156	$C_{15}H_{30}O_2$	242.2247	$C_{18}H_{11}O$	243.0810	$C_{12}H_{25}N_2O_3$	245.1866
$C_{13}H_{29}N_4$	241.2394	$C_{15}H_{32}NO$	242.2485	$C_{18}H_{13}N$	243.1049	$C_{12}H_{27}N_3O_2$	245.2105
$C_{14}H_{11}NO_3$	241.0739	$C_{15}H_{34}N_2$	242.2724	$C_{18}H_{27}$	243.2114	$C_{12}H_{29}N_4O$	245.2343
$C_{14}H_{13}N_2O_2$	241.0978	$C_{16}H_{18}O_2$	242.1307	$C_{19}H_{15}$	243.1174	$C_{13}H_{11}NO_4$	245.0688
$C_{14}H_{15}N_3O$	241.1216	$C_{16}H_{20}NO$	242.1546	**244**		$C_{13}H_{13}N_2O_3$	245.0927
$C_{14}H_{17}N_4$	241.1445	$C_{16}H_{22}N_2$	242.1784	$C_{11}H_{20}N_2O_4$	244.1424	$C_{13}H_{15}N_3O_2$	245.1165
$C_{14}H_{25}O_3$	241.1804	$C_{16}H_{34}O$	242.2611	$C_{11}H_{22}N_3O_3$	244.1662	$C_{13}H_{17}N_4O$	245.1404
$C_{14}H_{27}NO_2$	241.2043	$C_{16}H_{18}O_2$	242.1307	$C_{11}H_{24}N_4O_2$	244.1901	$C_{13}H_{25}O_4$	245.1753
$C_{14}H_{29}N_2O$	241.2281	$C_{16}H_{20}NO$	242.1546	$C_{12}H_8N_2O_4$	244.0484	$C_{13}H_{27}NO_3$	245.1992
$C_{14}H_{31}N_3$	241.2520	$C_{16}H_{22}N_2$	242.1784	$C_{12}H_{10}N_3O_3$	244.0723	$C_{13}H_{29}N_2O_2$	245.2230
$C_{15}H_{13}O_3$	241.0865	$C_{16}H_{34}O$	242.2611	$C_{12}H_{12}N_4O_2$	244.0961	$C_{13}H_{31}N_3O$	245.2469
$C_{15}H_{15}NO_2$	241.1103	$C_{17}H_{22}O$	242.1871	$C_{12}H_{22}NO_4$	244.1549	$C_{14}H_{13}O_4$	245.0814

APPENDIX A (*Continued*)

FM		FM		FM		FM	
$C_{14}H_{15}NO_3$	245.1052	$C_{16}H_{26}N_2$	246.2098	$C_{12}H_{14}N_3O_3$	248.1036	$C_{15}H_{25}N_2O$	249.1968
$C_{14}H_{17}N_2O_2$	245.1291	$C_{17}H_{10}O_2$	246.0681	$C_{12}H_{16}N_4O_2$	248.1275	$C_{15}H_{27}N_3$	249.2207
$C_{14}H_{19}N_3O$	245.1529	$C_{17}H_{12}NO$	246.0919	$C_{12}H_{26}NO_4$	248.1863	$C_{16}H_{11}NO_2$	249.0790
$C_{14}H_{21}N_4$	245.1768	$C_{17}H_{14}N_2$	246.1158	$C_{12}H_{28}N_2O_3$	248.2101	$C_{16}H_{13}N_2O$	249.1029
$C_{14}H_{29}O_3$	245.2117	$C_{17}H_{26}O$	246.1985	$C_{13}H_{14}NO_4$	248.0923	$C_{16}H_{15}N_3$	249.1267
$C_{14}H_{31}NO_2$	245.2356	$C_{17}H_{28}N$	246.2223	$C_{13}H_{16}N_2O_3$	248.1162	$C_{16}H_{25}O_2$	249.1855
$C_{15}H_{17}O_3$	245.1178	$C_{18}H_{14}O$	246.1045	$C_{13}H_{18}N_3O_2$	248.1400	$C_{16}H_{27}NO$	249.2094
$C_{15}H_{19}NO_2$	245.1416	$C_{18}H_{16}N$	246.1284	$C_{13}H_{20}N_4O$	248.1639	$C_{16}H_{29}N_2$	249.2332
$C_{15}H_{21}N_2O$	245.1655	$C_{18}H_{30}$	246.2349	$C_{13}H_{28}O_4$	248.1988	$C_{17}H_{13}O_2$	249.0916
$C_{15}H_{23}N_3$	245.1894	$C_{19}H_{18}$	246.1409	$C_{14}H_{16}O_4$	248.1049	$C_{17}H_{15}NO$	249.1154
$C_{16}H_9N_2O$	245.0715	**247**		$C_{14}H_{20}N_2O_2$	248.1526	$C_{17}H_{17}N_2$	249.1393
$C_{16}H_{11}N_3$	245.0954	$C_{11}H_{23}N_2O_4$	247.1659	$C_{14}H_{22}N_3O$	248.1764	$C_{17}H_{29}O$	249.2219
$C_{16}H_{21}O_2$	245.1542	$C_{11}H_{25}N_3O_3$	247.1897	$C_{14}H_{24}N_4$	248.2003	$C_{17}H_{31}N$	249.2458
$C_{16}H_{23}NO$	245.1781	$C_{11}H_{27}N_4O_2$	247.2136	$C_{15}H_{10}N_3O$	248.0825	$C_{18}H_{17}O$	249.1280
$C_{16}H_{25}N_2$	245.2019	$C_{12}H_{11}N_2O_4$	247.0719	$C_{15}H_{12}N_4$	248.1063	$C_{18}H_{19}N$	249.1519
$C_{17}H_{11}NO$	245.0841	$C_{12}H_{13}N_3O_3$	247.0958	$C_{15}H_{20}O_3$	248.1413	$C_{18}H_{33}$	249.2584
$C_{17}H_{13}N_2$	245.1080	$C_{12}H_{15}N_4O_2$	247.1196	$C_{15}H_{22}NO_2$	248.1651	$C_{19}H_{21}$	249.1644
$C_{17}H_{25}O$	245.1906	$C_{12}H_{25}NO_4$	247.1784	$C_{15}H_{24}N_2O$	248.1890	**250**	
$C_{17}H_{27}N$	245.2145	$C_{12}H_{27}N_2O_3$	247.2023	$C_{15}H_{26}N_3$	248.2129	$C_{11}H_{26}N_2O_4$	250.1894
$C_{18}H_{13}O$	245.0967	$C_{12}H_{29}N_3O_2$	247.2261	$C_{16}H_{10}NO_2$	248.0712	$C_{12}H_{14}N_2O_4$	250.0954
$C_{18}H_{15}N$	245.1205	$C_{13}H_{13}NO_4$	247.0845	$C_{16}H_{12}N_2O$	248.0950	$C_{12}H_{16}N_3O_3$	250.1193
$C_{18}H_{29}$	245.2270	$C_{13}H_{15}N_2O_3$	247.1083	$C_{16}H_{14}N_3$	248.1189	$C_{12}H_{18}N_4O_2$	250.1431
$C_{19}H_{17}$	245.1331	$C_{13}H_{17}N_3O_2$	247.1322	$C_{16}H_{24}O_2$	248.1777	$C_{13}H_{16}NO_4$	250.1080
246		$C_{13}H_{19}N_4O$	247.1560	$C_{16}H_{26}NO$	248.2015	$C_{13}H_{18}N_2O_3$	250.1318
$C_{11}H_{22}N_2O_4$	246.1580	$C_{13}H_{27}O_4$	247.1910	$C_{16}H_{28}N_2$	248.2254	$C_{13}H_{20}N_3O_2$	250.1557
$C_{11}H_{24}N_3O_3$	246.1819	$C_{13}H_{29}NO_3$	247.2148	$C_{17}H_{12}O_2$	248.0837	$C_{13}H_{22}N_4O$	250.1795
$C_{11}H_{26}N_4O_2$	246.2057	$C_{14}H_{15}O_4$	247.0970	$C_{17}H_{14}NO$	248.1076	$C_{14}H_{10}N_4O$	250.0856
$C_{12}H_{10}N_2O_4$	246.0641	$C_{14}H_{17}NO_3$	247.1209	$C_{17}H_{16}N_2$	248.1315	$C_{14}H_{20}NO_3$	250.1444
$C_{12}H_{12}N_3O_3$	246.0879	$C_{14}H_{19}N_2O_2$	247.1448	$C_{17}H_{28}O$	248.2141	$C_{14}H_{22}N_2O_2$	250.1682
$C_{12}H_{14}N_4O_2$	246.1118	$C_{14}H_{21}N_3O$	247.1686	$C_{17}H_{30}N$	248.2380	$C_{14}H_{24}N_3O$	250.1921
$C_{12}H_{24}NO_4$	246.1706	$C_{14}H_{23}N_4$	247.1925	$C_{18}H_{16}O$	248.1202	$C_{14}H_{26}N_4$	250.2160
$C_{12}H_{26}N_2O_3$	246.1945	$C_{15}H_9N_3O$	247.0746	$C_{18}H_{18}N$	248.1440	$C_{15}H_{10}N_2O_2$	250.0743
$C_{12}H_{28}N_3O_2$	246.2183	$C_{15}H_{11}N_4$	247.0985	$C_{18}H_{32}$	248.2505	$C_{15}H_{12}N_3O$	250.0981
$C_{12}H_{30}N_4O$	246.2422	$C_{15}H_{19}O_3$	247.1334	$C_{19}H_{20}$	248.1566	$C_{15}H_{14}N_4$	250.1220
$C_{13}H_{12}NO_4$	246.0766	$C_{15}H_{21}NO_2$	247.1573	**249**		$C_{15}H_{22}O_3$	250.1569
$C_{13}H_{14}N_2O_3$	246.1005	$C_{15}H_{23}N_2O$	247.1811	$C_{11}H_{25}N_2O_4$	249.1815	$C_{15}H_{24}NO_2$	250.1808
$C_{13}H_{16}N_3O_2$	246.1244	$C_{15}H_{25}N_3$	247.2050	$C_{11}H_{27}N_3O_3$	249.2054	$C_{15}H_{26}N_2O$	250.2046
$C_{13}H_{18}N_4O$	246.1482	$C_{16}H_{11}N_2O$	247.0872	$C_{12}H_{13}N_2O_4$	249.0876	$C_{15}H_{28}N_3$	250.2285
$C_{13}H_{26}O_4$	246.1832	$C_{16}H_{13}N_3$	247.1111	$C_{12}H_{15}N_3O_3$	249.1114	$C_{16}H_{10}O_3$	250.0630
$C_{13}H_{28}NO_3$	246.2070	$C_{16}H_{23}O_2$	247.1699	$C_{12}H_{17}N_4O_2$	249.1353	$C_{16}H_{12}NO_2$	250.0868
$C_{13}H_{30}N_2O_2$	246.2309	$C_{16}H_{25}NO$	247.1937	$C_{12}H_{27}NO_4$	249.1941	$C_{16}H_{14}N_2O$	250.1107
$C_{14}H_{14}O_4$	246.0892	$C_{16}H_{27}N_2$	247.2176	$C_{13}H_{15}NO_4$	249.1001	$C_{16}H_{16}N_3$	250.1346
$C_{14}H_{16}NO_3$	246.1131	$C_{17}H_{11}O_2$	247.0759	$C_{13}H_{17}N_2O_3$	249.1240	$C_{16}H_{26}O_2$	250.1934
$C_{14}H_{18}N_2O_2$	246.1369	$C_{17}H_{13}NO$	247.0998	$C_{13}H_{19}N_3O_2$	249.1478	$C_{16}H_{28}NO$	250.2172
$C_{14}H_{20}N_3O$	246.1608	$C_{17}H_{15}N_2$	247.1236	$C_{13}H_{21}N_4O$	249.1717	$C_{16}H_{30}N_2$	250.2411
$C_{14}H_{22}N_4$	246.1846	$C_{17}H_{27}O$	247.2063	$C_{14}H_9N_4O$	249.0777	$C_{17}H_{14}O_2$	250.0994
$C_{14}H_{30}O_3$	246.2196	$C_{17}H_{29}N$	247.2301	$C_{14}H_{17}O_4$	249.1127	$C_{17}H_{16}NO$	250.1233
$C_{15}H_{10}N_4$	246.0907	$C_{18}H_{15}O$	247.1123	$C_{14}H_{19}NO_3$	249.1365	$C_{17}H_{18}N_2$	250.1471
$C_{15}H_{18}O_3$	246.1256	$C_{18}H_{17}N$	247.1362	$C_{14}H_{21}N_2O_2$	249.1604	$C_{17}H_{30}O$	250.2298
$C_{15}H_{20}NO_2$	246.1495	$C_{18}H_{31}$	247.2427	$C_{14}H_{23}N_3O$	249.1842	$C_{17}H_{32}N$	250.2536
$C_{15}H_{22}N_2O$	246.1733	$C_{19}H_{19}$	247.1488	$C_{14}H_{25}N_4$	249.2081	$C_{18}H_{18}O$	250.1358
$C_{15}H_{24}N_3$	246.1972	**248**		$C_{15}H_9N_2O_2$	249.0664	$C_{18}H_{20}N$	250.1597
$C_{16}H_{10}N_2O$	246.0794	$C_{11}H_{24}N_2O_4$	248.1737	$C_{15}H_{11}N_3O$	249.0903	$C_{18}H_{34}$	250.2662
$C_{16}H_{12}N_3$	246.1032	$C_{11}H_{26}N_3O_3$	248.1976	$C_{15}H_{13}N_4$	249.1142	$C_{19}H_{22}$	250.1722
$C_{16}H_{22}O_2$	246.1620	$C_{11}H_{28}N_4O_2$	248.2214	$C_{15}H_{21}O_3$	249.1491		
$C_{16}H_{24}NO$	246.1859	$C_{12}H_{12}N_2O_4$	248.0797	$C_{15}H_{23}NO_2$	249.1730		

APPENDIX B COMMON FRAGMENT IONS

All fragments listed bear +1 charges. To be used in conjunction with Appendix C. Not all members of homologous and isomeric series are given. The list is meant to be suggestive rather than exhaustive. Appendix II of Hamming and Foster (1972), Table A-7 of McLafferty and Turecek's (1993) interpretative book, and the high-resolution ion data of McLafferty and Venkataraghavan (1982) are recommended as supplements.

***m/z* Ions**[a]

14 CH_2
15 CH_3
16 O
17 OH
18 H_2O, NH_4
19 F, H_3O
26 $C{\equiv}N$, C_2H_2
27 C_2H_3
28 C_2H_4, CO, N_2 (air), $CH{=}NH$
29 C_2H_5, CHO
30 CH_2NH_2, NO
31 CH_2OH, OCH_3
32 O_2 (air)
33 SH, CH_2F
34 H_2S
35 ^{35}Cl[b]
36 $H^{35}Cl$[b]
39 C_3H_3
40 $CH_2C{=}N$, Ar (air)
41 C_3H_5, $CH_2C{=}N$ + H, C_2H_2NH
42 C_3H_6, C_2H_2O
43 C_3H_7, $CH_3C{=}O$, C_2H_5N
44 $CH_2C(=O)H$ + H, CH_3CHNH_2, CO_2 (air), $NH_2C{=}O$, $(CH_3)_2N$
45 $CH_3CH(OH)$, CH_2CH_2OH, CH_2OCH_3, $C(=O)OH$
46 NO_2
47 CH_2SH, CH_3S
48 CH_3S + H
49 $CH_2{}^{35}Cl$[b]
51 CHF_2, C_4H_3
53 C_4H_5
54 $CH_2CH_2C{\equiv}N$
55 C_4H_7, $CH_2{=}CHC{=}O$
56 C_4H_8
57 C_4H_9, $C_2H_5C{=}O$
58 $CH_3C(=O)CH_2$ + H, $C_2H_5CHNH_2$, $(CH_3)_2NCH_2$, $C_2H_5NHCH_2$, C_2H_5S
59 $(CH_3)_2COH$, $CH_2OC_2H_5$, CO_2CH_3, $NH_2C(=O)CH_2$ + H, CH_3OCHCH_3, CH_3CHCH_2OH, C_2H_5CHOH
60 CH_2CO_2H + H, CH_2ONO
61 CH_3CO_2 + 2H, CH_2CH_2SH, CH_2SCH_3
65 C_5H_5

66 H_2S_2,  $\equiv C_5H_6$

67 C_5H_7
68 $CH_2CH_2CH_2C{\equiv}N$
69 C_5H_9, CF_3, $CH_3CH{=}CHC{=}O$, $CH_2{=}C(CH_3)C{=}O$
70 C_5H_{10}
71 C_5H_{11}, $C_3H_7C{=}O$
72 $C_2H_5C(=O)CH_2$ + H, $C_3H_7CHNH_2$, $(CH_3)_2N{=}C{=}O$, $C_2H_5NHCHCH_3$ and isomers
73 Homologs of 59, $(CH_3)_3Si$
74 $CH_2CO_2CH_3$ + H
75 $CO_2C_2H_5$ + 2H, $C_2H_5CO_2$ + 2H, $CH_2SC_2H_5$, $(CH_3)_2CSH$, $(CH_3O)_2CH$, $(CH_3)_2SiOH$
76 C_6H_4 (C_6H_4XY)
77 C_6H_5 (C_6H_5X)
78 C_6H_5 + H
79 C_6H_5 + 2H, ^{79}Br[b]
80 CH_3SS + H, $H^{79}Br$[b],

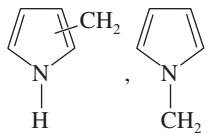

81 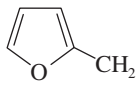 , C_6H_9

82 $(CH_2)_4C{\equiv}N$, C_6H_{10}, $C^{35}Cl_2$[b]

83 C_6H_{11}, $CH^{35}Cl_2$[b], 

85  ,  , C_6H_{13}, $C_4H_9C{=}O$, $Cl^{35}ClF_2$[b]

86 $C_3H_7C(=O)CH_2$ + H, $C_4H_9CHNH_2$ and isomers
87 $C_3H_7CO_2$, Homologs of 73, $CH_2CH_2CO_2CH_3$
88 $CH_2CO_2C_2H_5$ + H

89 $CO_2C_3H_7$ + 2H, 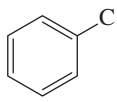

90 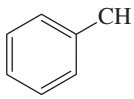 , CH_3CHONO_2

91 $(C_6H_5)CH_2$, $(C_6H_5)CH$ + H, $(C_6H_5)C$ + 2H, $(CH_2)_4{}^{35}Cl$[b], $(C_6H_5)N$

92 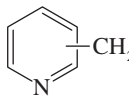 CH_2, $(C_6H_5)CH_2$ + H

APPENDIX B (*Continued*)

***m/z* Ions**[a]

93 $CH_2{}^{79}Br$[b], C_7H_9, $(C_6H_5)O$, 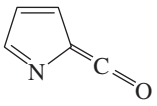

94 $(C_6H_5)O$ + H, 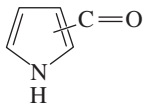

95 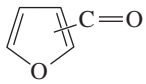

96 $(CH_2)_5C{\equiv}N$

97 C_7H_{13}, 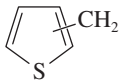

98 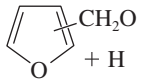

99 C_7H_{15}, $C_6H_{11}O$, 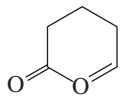

100 $C_4H_9C(=O)CH_2$ + H, $C_5H_{11}CHNH_2$

101 $CO_2C_4H_9$

102 $CH_2CO_2C_2H_7$ + H

103 $CO_2C_4H_9$ + 2H, $C_5H_{11}S$, $CH(OCH_2CH_3)_2$

104 $C_2H_5CHONO_2$

105 $C_6H_5C{=}O$, $C_6H_5CH_2CH_2$, $C_6H_5CHCH_3$

106 $C_6H_5NHCH_2$

107 $C_6H_5CH_2O$, $HO(C_6H_4)CH_2$, $C_2H_4{}^{79}Br$[b]

108 $C_6H_5CH_2O$ + H, 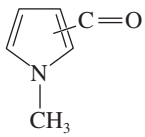

109 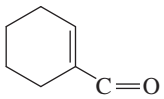

111 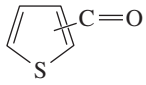

119 CF_3CF_2, $(C_6H_5)C(CH_3)_2$, $CH_3CH(C_6H_4)CH_3$, $CO(C_6H_4)CH_3$

120 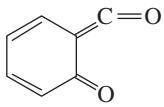

121 C_9H_{13}, 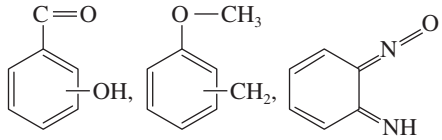

122 $C_6H_5CO_2$ + H

123 $F(C_6H_4)C{=}O$, $C_6H_5CO_2$ + 2H

125 C_6H_5SO

127 I

128 HI

130 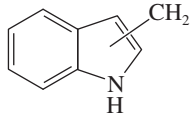

131 C_3F_5, $C_6H_5CH{=}CHC{=}O$

135 $(CH_2)_4{}^{79}Br$[b]

138 $CO_2(C_6H_4)OH$ + H

139 $^{35}Cl(C_6H_4)C{=}O$[b]

141 CH_2I

147 $(CH_3)_2Si{=}O{-}Si(CH_3)_3$

149 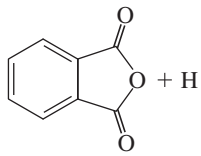

154 $(C_6H_5)_2$

[a] Ions indicated as a fragment + *n*H (*n* + 1,2,3, . . .) are ions that arise via rearrangement involving hydrogen transfer.

[b] Only the more abundant isotope is indicated.

APPENDIX C COMMON FRAGMENTS LOST

This list is suggestive rather than comprehensive. It should be used in conjunction with Appendix B. Table 5-19 of Hamming and Foster (1972) and Table A-5 of McLafferty and Turecek (1993) are recommended as supplements. All of these fragments are lost as neutral species.

Molecular Ion Minus	Fragment Lost (Inference Structure)
1	H·
2	2H·
15	CH_3·
16	O ($ArNO_2$, amine oxides, sulfoxides); ·NH_2 (carboxamides, sulfonamides)
17	HO·
18	H_2O (alcohols, aldehydes, ketones)
19	F·
20	HF
26	CH≡CH, ·CH≡N
27	CH_2=CH·, HC≡N (aromatic nitrites, nitrogen heterocycles)
28	CH_2=CH_2, CO, (quinones) (HCN + H)
29	CH_3CH_2·, (ethyl ketones, $ArCH_2CH_2CH_3$), ·CHO
30	NH_2CH_2·, CH_2O ($ArOCH_3$), NO ($ArNO_2$), C_2H_6
31	·OCH_3(methyl esters), ·CH_2OH, CH_3NH_2
32	CH_3OH, S
33	HS· (thiols), (·CH_3 and H_2O)
34	H_2S (thiols)
35	Cl·
36	HCl, $2H_2O$
37	H_2Cl (or HCl + H)
38	C_3H_2, C_2N, F_2
39	C_3H_3, HC_2N
40	CH_3C≡CH
41	CH_2=$CHCH_2$·
42	CH_2=$CHCH_3$, CH_2=C=O,  , NCO, $NCNH_2$
43	C_3H_7·(propyl ketones, $ArCH_2$—C_3H_7), CH_3C(=O)·(methyl ketones, CH_3C(=O)G, where G = various functional groups), CH_2=CH—O·, (CH_3· and CH_2=CH_2), HCNO
44	CH_2=CHOH, CO_2 (esters, anhydrides), N_2O, $CONH_2$, $NHCH_2CH_3$
45	CH_3CHOH, CH_3CH_2O·(ethyl esters), CO_2H, $CH_3CH_2NH_2$
46	(H_2O and CH_2=CH_2), CH_3CH_2OH, ·NO_2 ($ArNO_2$)
47	CH_3S·
48	CH_3SH, SO (sulfoxides), O_3
49	·CH_2Cl
51	·CHF_2
52	C_4H_4, C_2N_2
53	C_4H_5
54	CH_2=CH—CH=CH_2
55	CH_2=$CHCHCH_3$

APPENDIX C (*Continued*)

Molecular Ion Minus	Fragment Lost (Inference Structure)
56	$CH_2{=}CHCH_2CH_3$, $CH_3CH{=}CHCH_3$, 2CO
57	$C_4H_9\cdot$ (butyl ketones), C_2H_5CO (ethyl ketones, EtC=OG, G = various structural units)
58	$\cdot NCS$, (NO + CO), CH_3COCH_3, C_4H_{10}
59	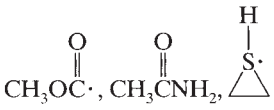
60	C_3H_7OH, $CH_2{=}C(OH)_2$ (acetate esters)[a]
61	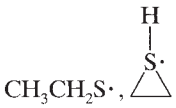
62	(H_2S and $CH_2{=}CH_2$)
63	$\cdot CH_2CH_2Cl$
64	C_5H_4, S_2, SO_2
68	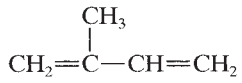
69	$CF_3\cdot$, $C_5H_9\cdot$
71	$C_5H_{11}\cdot$
73	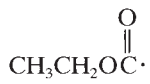
74	C_4H_9OH
75	C_6H_3
76	C_6H_4, CS_2
77	C_6H_5, CS_2H
78	C_6H_6, CS_2H_2, C_5H_4N
79	$Br\cdot$, C_5H_5N
80	HBr
85	$\cdot CClF_2$
100	$CF_2{=}CF_2$
119	$CF_3{-}CF_2\cdot$
122	C_6H_5COOH
127	$I\cdot$
128	HI

[a] McLafferty rearrangement.

CHAPTER 2

INFRARED SPECTROSCOPY

2.1 INTRODUCTION

Infrared (IR) radiation refers broadly to that part of the electromagnetic spectrum between the visible and microwave regions. Of greatest practical use to the organic chemist is the limited portion between 4000 cm^{-1} and 400 cm^{-1}. There has been some interest in the near-IR (14290 cm^{-1} to 4000 cm^{-1}) and the far-IR (700 cm^{-1} to 200 cm^{-1}) regions.

From the brief theoretical discussion that follows, it is clear that even a very simple molecule can give an extremely complex spectrum. The organic chemist takes advantage of this complexity when matching the spectrum of an unknown compound against that of an authentic sample. A peak-by-peak correlation is excellent evidence for identity. Any two compounds, except enantiomers, are unlikely to give exactly the same IR spectrum.

Although the IR spectrum is characteristic of the entire molecule, it is true that certain groups of atoms give rise to bands at or near the same frequency regardless of the structure of the rest of the molecule. It is the persistence of these characteristic bands that permits the chemist to obtain useful structural information by simple inspection and reference to generalized charts of characteristic group frequencies. We shall rely heavily on these characteristic group frequencies.

Since we are not solely dependent on IR spectra for identification, a detailed analysis of the spectrum will not be required. Following our general plan, we shall present only sufficient theory to accomplish our purpose: utilization of IR spectra in conjunction with other spectral data in order to determine or confirm molecular structure.

The importance of IR spectroscopy as a tool of the practicing organic chemist is readily apparent from the number of books devoted wholly or in part to discussions of applications of this method (see the references at www.wiley.com/college/silverstein). There are many compilations of spectra as well as indexes to spectral collections and to the literature. Among the more commonly used compilations are those published by Sadtler (1994) and by Aldrich (1989). There are also numerous specialized texts dealing with specific classes of materials such as polymers and plastics. Examples include Haslam et al. (1979), Hummel (1980), Koenig (1992), and Everall (2007).

2.2 THEORY

Radiation of wavenumbers less than about 100 cm^{-1} is absorbed and converted by an organic molecule into energy of molecular rotation. This absorption is quantized; thus, a molecular rotational spectrum consists of discrete lines.

Infrared radiation in the range from about 10000 cm^{-1} to 100 cm^{-1} is absorbed and converted by an organic molecule into energy of molecular vibration. This absorption is also quantized, but vibrational spectra appear as bands rather than as lines because a single vibrational energy change is accompanied by a number of rotational energy changes. It is with these vibrational–rotational bands, particularly those occurring between 4000 cm^{-1} and 400 cm^{-1}, that we shall be concerned. The frequency or wavelength of absorption depends on the relative masses of the atoms, the force constants of the bonds, and the geometrical arrangement of the atoms (i.e., the molecular structure).

Band positions in IR spectra are presented here as wavenumbers ($\tilde{\nu}$) whose unit is the reciprocal centimeter (cm^{-1}); this unit is proportional to the energy of vibration and modern instruments are linear in reciprocal centimeters. Wavelength (λ) was used in the older literature in units of micrometers ($\mu m = 10^{-6}$ m; earlier called microns). Wavenumbers are reciprocally related to wavelength:

$$\tilde{\nu} = 1/\lambda$$

The IR spectra in this text are generally shown with units as a linear function of cm^{-1} unless otherwise indicated. Note that spectra that are plotted as a function of wavelength are quite different in appearance from those plotted in wavenumbers, but the information content is the same (see Figure 2.5). Wavenumbers (in cm^{-1}) are directly proportional to frequency (in Hertz), and the two are related by the speed of light ($\tilde{\nu} = \nu/c$); therefore, higher frequency vibrations correspond to higher wavenumbers.

Band intensities can be expressed either as transmittance (T) or absorbance (A). Transmittance is the ratio of the radiant power transmitted by a sample to the radiant power incident on the sample. Absorbance is the logarithm, to the base 10, of the reciprocal of the transmittance; $A = \log_{10}(1/T)$. Organic chemists usually report intensity in qualitative terms (s = strong, m = medium, and w = weak).

Two of the most important types of molecular vibrations are stretching and bending. A stretching vibration is a rhythmical movement along the bond axis such that the interatomic distance is increasing or decreasing. A bending vibration may consist of a change in angle between bonds with a common atom or the movement of a group of atoms with respect to the remainder of the molecule without movement of the atoms in the group with respect to one another. For example, twisting, rocking, and torsional vibrations involve

a change in bond angles with reference to a set of coordinates arbitrarily set up within the molecule.

Only those vibrations that result in a change in the net dipole moment of the molecule are observed in the IR spectrum. The alternating electric field, produced by the changing charge distribution accompanying a vibration, couples the molecular vibration with the oscillating electric field of the electromagnetic radiation.

A molecule has as many degrees of freedom as the total degrees of freedom of its individual atoms. Each atom has three degrees of freedom corresponding to the Cartesian coordinates (x, y, z) necessary to describe its position relative to other atoms in the molecule. A molecule of n atoms therefore has $3n$ degrees of freedom. For nonlinear molecules, three degrees of freedom describe rotation and three describe translation; the remaining $3n - 6$ degrees of freedom are vibrational degrees of freedom that correspond to fundamental vibrations. Linear molecules have $3n - 5$ vibrational degrees of freedom, since only two independent degrees of freedom are required to describe rotation.

Fundamental vibrations involve no change in the center of gravity of the molecule. The three fundamental vibrations of the nonlinear triatomic water molecule are depicted in the top portion of Figure 2.1. Note the very close energetic spacing of the interacting or coupled asymmetric and symmetric stretching compared with the far-removed scissoring mode.

The CO_2 molecule is linear and contains three atoms; therefore, it has four fundamental vibrations $[(3 \times 3) - 5]$ as shown in the middle section of Figure 2.1. The symmetrical stretching vibration in (1) is inactive in the IR since it produces no net change in the dipole moment of the molecule. The bending vibrations in (3) and (4) of Figure 2.1 are equivalent and are the resolved components of bending motion oriented at any angle to the internuclear axis; they have the same frequency and are said to be doubly degenerate.

The various stretching and bending modes for an AX_2 group appearing as a portion of a molecule, for example, the CH_2 group in a hydrocarbon molecule, are shown in Figure 2.1. The $3n - 6$ rule does not apply since the CH_2 group represents only a portion of a molecule.

The theoretical number of fundamental vibrations (absorption frequencies) will seldom be observed because overtones (multiples of a given frequency) and combination tones (sum of two other vibrations) increase the number of bands, whereas other phenomena reduce the number of bands. The following will reduce the number of observed bands:

1. Fundamental wavenumbers that fall outside of the 4000 cm^{-1} to 400 cm^{-1} region.
2. Fundamental bands that are too weak to be observed.
3. Fundamental vibrational wavenumbers that are so close that the bands coalesce.
4. The occurrence of a degenerate band from several absorptions of the same frequency in highly symmetrical molecules.
5. The failure of certain fundamental vibrations to appear in the IR because of the lack of change in molecular dipole.

Assignments for stretching frequencies can be approximated by the application of Hooke's law. In the application of the law, two atoms and their connecting bond are treated as a simple harmonic oscillator composed of two masses joined by a spring. The following equation, derived from Hooke's law, states the relationship between wavenumber of oscillation, atomic masses, and the force constant of the bond:

$$\tilde{\nu} = \frac{1}{2\pi c}\sqrt{\frac{f}{(M_x M_y)/(M_x + M_y)}}$$

where

$\tilde{\nu}$ = the vibrational wavenumber (cm^{-1})
c = speed of light (cm/s)
f = force constant of bond (dyne/cm)
M_x and M_y = mass (g) of atom x and atom y, respectively.

The value of f is approximately 5×10^5 dyne/cm for single bonds and approximately two and three times this value for double and triple bonds, respectively (see Table 2.1). The force constant, f, can be thought of as a measure of bond "stiffness." This force constant can be correlated with properties such as bond order and bond strength. Because the wavenumber is directly related to the square root of the force constant, we know that the frequency of bond vibrations should decrease as bonds decrease in strength.

Application of the formula to C—H stretching using 2.10×10^{-23} g and 1.67×10^{-24} g as mass values for C and H, respectively, places the frequency of the C—H bond vibration at 3032 cm^{-1}. Actually, C—H stretching vibrations, associated with methyl and methylene groups, are generally observed in the region between 2960 cm^{-1} and 2850 cm^{-1}. The calculation is not highly accurate because effects arising from the environment of the C—H group within a molecule have been ignored. The observed frequency of IR absorption is commonly used to calculate the force constants of bonds.

The shift in absorption frequency following deuteration is often employed in the assignment of C—H stretching frequencies. The above equation can be used to estimate the change in stretching frequency as a result of deuteration. The term $M_x M_y/(M_x + M_y)$ will be equal to $M_C M_H/(M_C + M_H)$ for the C—H compound. Since $M_C \gg M_H$, this term is approximately equal to $M_C M_H/M_C$ or to M_H. Thus, for the C—D compound, the term is equal to M_D; the frequency by Hooke's law application is inversely proportional to the square root of the mass of the isotope of hydrogen. The ratio of the C—H to C—D stretching frequencies should, therefore, equal $\sqrt{2}$. If the ratio of the frequencies, following deuteration, is much less than $\sqrt{2}$,

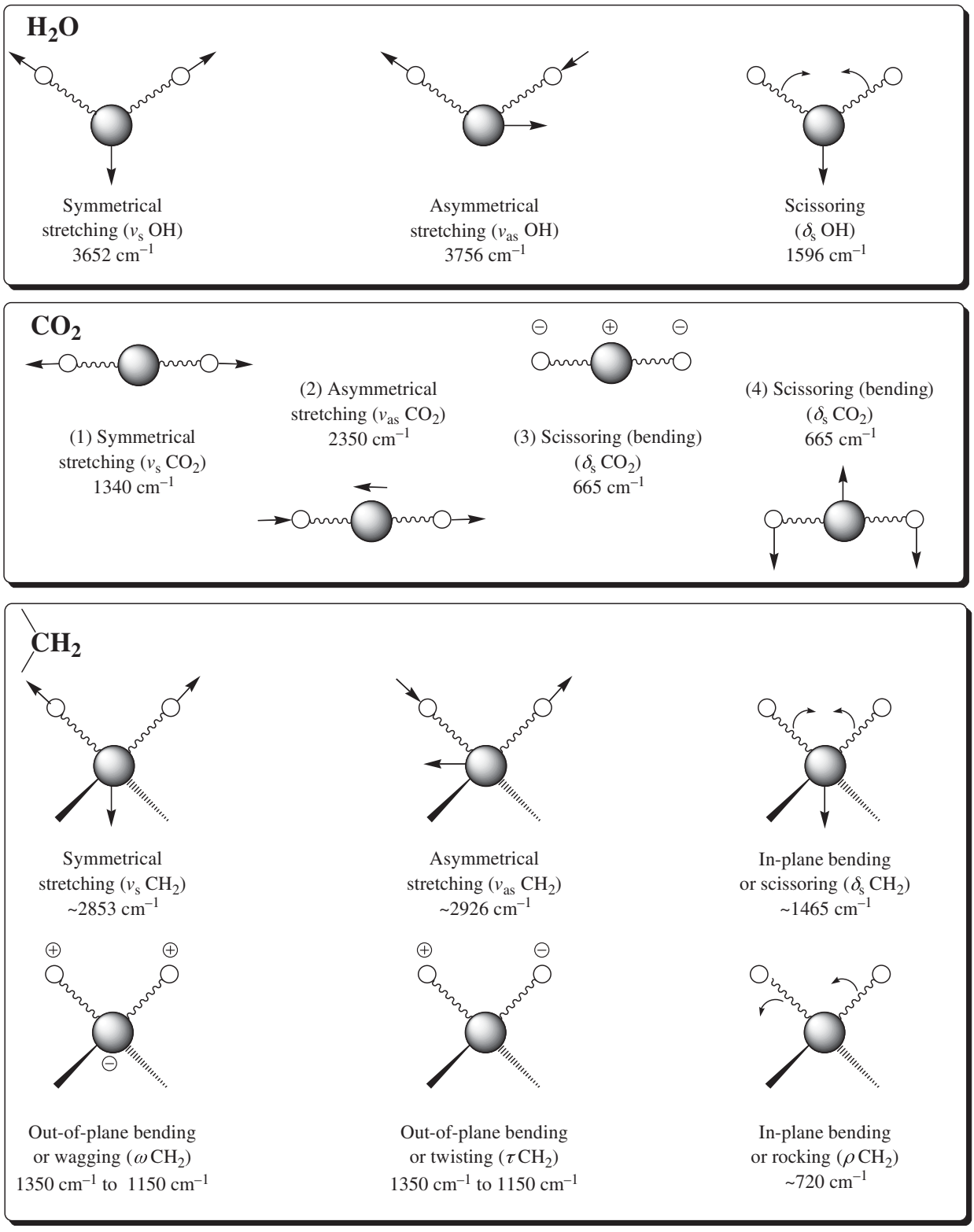

FIGURE 2.1 (Top) Vibrational modes for H_2O. (Middle) Vibrational modes for linear CO_2. (Bottom) Vibrational modes for a CH_2 group (+ and − indicate movement perpendicular to the plane of the page).

TABLE 2.1 IR Absorption Regions Using Hooke's Law

Bond Type	Force Constant f in (dyne/cm)	Absorption Region (cm^{-1})	
		Calculated	Observed
C—O	5.0×10^5	1113	1300 – 800
C—C	4.5×10^5	1128	1300 – 800
C—N	4.9×10^5	1135	1250 – 1000
C═C	9.7×10^5	1657	1900 – 1500
C═O	12.1×10^5	1731	1850 – 1600
C≡C	15.6×10^5	2101	2150 – 2100
C—D	5.0×10^5	2225	2250 – 2080
C—H	5.0×10^5	3032	3000 – 2850
O—H	7.01×10^5	3553	3800 – 2700

we can assume that the vibration is not simply a C—H stretching vibration but instead a mixed vibration involving interaction (coupling) with another vibration.

Crude approximations based on Hooke's law can be made by calculating the stretching frequencies for certain bond types as indicated in Table 2.1.

To approximate the vibrational frequencies of bond stretching by Hooke's law, the relative contributions of bond strengths and atomic masses must be considered. For example, a superficial comparison of the C—H group with the F—H group, on the basis of atomic masses, might lead to the conclusion that the stretching frequency of the F—H bond should occur at a lower frequency than that for the C—H bond. However, the increase in the force constant from left to right across the first two rows of the periodic table has a greater effect than the mass increase. Thus, the F—H group absorbs at a higher wavenumber (4138 cm^{-1}) than the C—H group (3040 cm^{-1}).

In general, functional groups that have a strong dipole give rise to strong absorptions in the IR.

2.2.1 Coupled Interactions

When two bond oscillators share a common atom, they seldom behave as individual oscillators unless the individual oscillation frequencies are widely different. This is because there is mechanical coupling interaction between the oscillators. For example, the carbon dioxide molecule (see Figure 2.1), which consists of two C═O bonds with a common carbon atom, has two fundamental stretching vibrations: an asymmetrical and a symmetrical stretching mode. The symmetrical stretching mode consists of an in-phase stretching or contracting of the C═O bonds, and absorption occurs at a wavelength longer than that observed for the carbonyl group in an aliphatic ketone. The symmetrical stretching mode produces no change in the dipole moment (μ) of the molecule and is therefore inactive in the IR, but it is easily observed in the Raman spectrum* near 1340 cm^{-1}. In the asymmetrical stretching mode, the two C═O bonds stretch out of phase; one C═O bond stretches as the other contracts. The asymmetrical stretching mode, since it produces a change in the dipole moment, is IR active; the absorption (2350 cm^{-1}) is at a higher frequency (shorter wavelength) than observed for a carbonyl group in aliphatic ketones.

$$\underset{\text{Symmetrical}\ \mu = 0}{\longleftarrow O{=}C{=}O \longrightarrow} \qquad \underset{\text{Asymmetrical}\ \mu \neq 0}{\longleftarrow O{=}\vec{C}{=}O \longleftarrow}$$

This difference in carbonyl absorption frequencies displayed by the carbon dioxide molecule results from strong mechanical coupling or interaction. In contrast, two ketonic carbonyl groups separated by one or more carbon atoms show normal carbonyl absorption near 1715 cm^{-1} because appreciable coupling is prevented by the intervening carbon atom(s).

Coupling accounts for the two N—H stretching bands in the 3497 cm^{-1} to 3077 cm^{-1} region in the spectra of primary amines and primary amides, for the two C═O stretching bands in the 1818 cm^{-1} to 1720 cm^{-1} region in carboxylic anhydride and imide spectra, and for the two C—H stretching bands in the 3000 cm^{-1} to 2760 cm^{-1} region for both methylene and methyl groups.

Useful characteristic group frequency bands often involve coupled vibrations. The spectra of alcohols have a strong band in the region between 1260 cm^{-1} and 1000 cm^{-1}, which is usually designated as the C—O stretching band. In the spectrum of methanol, this band is at 1034 cm^{-1}; in the spectrum of ethanol it occurs at 1053 cm^{-1}. Branching and unsaturation produce absorptions characteristic of these structures (see Section 2.6.9). It is evident that we are dealing not with an isolated C—O stretching vibration but rather a coupled asymmetric vibration involving C—C—O stretching.

Vibrations resulting from bond angle changes frequently couple in a manner similar to stretching vibrations. Thus, the ring C—H out-of-plane bending frequencies of aromatic molecules depend on the number of adjacent hydrogen atoms on the ring; coupling between the hydrogen atoms is affected by the bending of the C—C bond in the ring to which the hydrogen atoms are attached.

Interaction arising from coupling of stretching and bending vibrations is illustrated by the absorption of secondary acyclic amides. Secondary acyclic amides, which exist predominantly in the *trans* conformation, show strong absorption in the 1563 cm^{-1} to 1515 cm^{-1} region; this absorption involves coupling of the N—H bending and C—N stretching vibrations.

The requirements for effective coupling interaction may be summarized as follows:

1. The vibrations must be of the same symmetry species if interaction is to occur.
2. Strong coupling between stretching vibrations requires a common atom between the groups.
3. Interaction is greatest when the coupled groups absorb, individually, near the same frequency.

*Band intensity in Raman spectra depends on bond polarizability rather than molecular dipole changes.

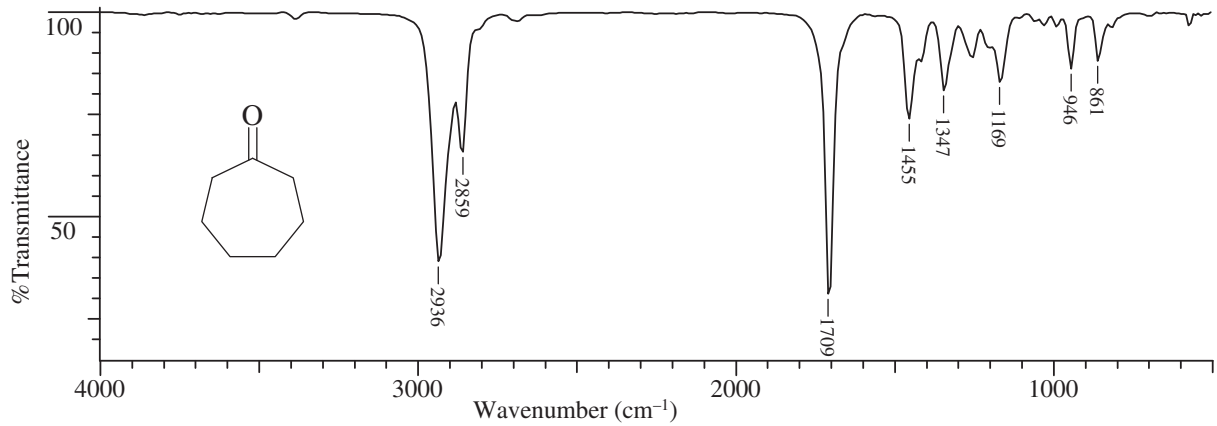

FIGURE 2.2 IR spectrum of cycloheptanone, neat.

4. Coupling between bending and stretching vibrations can occur if the stretching bond forms one side of the changing angle.
5. A common bond is required for coupling of bending vibrations.
6. Coupling is negligible when groups are separated by one or more carbon atoms and the vibrations are mutually perpendicular.

As we have seen in our discussion of interaction, coupling of two fundamental vibrational modes will produce two new modes of vibration, with frequencies higher and lower than that observed when interaction is absent. Interaction can also occur between fundamental vibrations and overtones or combination-tone vibrations. Such interaction is known as Fermi resonance. One example of Fermi resonance is afforded by the absorption pattern of carbon dioxide. In our discussion of interaction, we indicated that the symmetrical stretching band of CO_2 appears in the Raman spectrum near 1340 cm^{-1}. Actually two bands are observed: one at 1286 cm^{-1} and one at 1388 cm^{-1}. The splitting results from coupling between the fundamental C═O stretching vibration, near 1340 cm^{-1}, and the first overtone of the bending vibration. The fundamental bending vibration occurs near 666 cm^{-1}, and the first overtone near 1334 cm^{-1}.

Fermi resonance is a common phenomenon in IR and Raman spectra. It requires that the vibrational levels be of the same symmetry species and that the interacting groups be located in the molecule so that mechanical coupling is appreciable.

An example of Fermi resonance in an organic structure is the doublet appearance of the C═O stretch of certain cyclic ketones under sufficient resolution conditions. Figure 2.2 shows the appearance of the spectrum of cycloheptanone under the usual conditions of resolution; the carbonyl peak at 1709 cm^{-1} is a singlet. With adequate resolution however, the IR spectra of cyclopentanone's carbonyl region, which are given in Figure 2.3 for four different conditions, show a doublet for the carbonyl group. These doublets are due to Fermi resonance of the carbonyl group with an overtone or combination band of an α-methylene group.

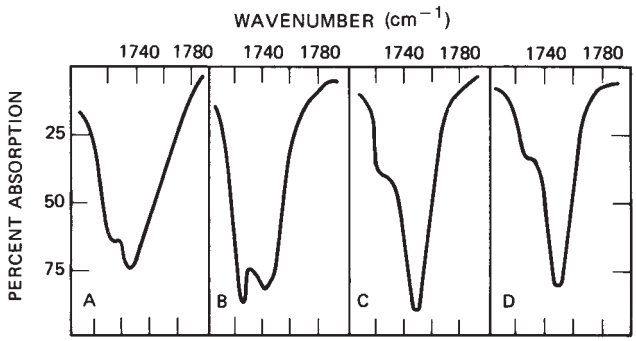

FIGURE 2.3 Infrared spectrum of cyclopentanone in various media. A. Carbon tetrachloride solution (0.15 *M*). B. Carbon disulfide solution (0.023 *M*). C. Chloroform solution (0.025 *M*). D. Liquid state (thin film). (Computed spectral slit width 2 cm^{-1}.)

2.2.2 Hydrogen Bonding

Hydrogen bonding can occur in any system containing a proton donor group (X—H) and a proton acceptor (Ÿ) if the *s* orbital of the proton can effectively overlap with the *p* or π orbital of the acceptor group. Atoms X and Y are electronegative, with Ÿ possessing lone pair electrons. The common proton donor groups in organic molecules are carboxyl, hydroxyl, amine, or amide groups. Common proton acceptor atoms are oxygen, nitrogen, and the halogens. Unsaturated groups, such as the C═C linkage, can also act as proton acceptors.

The strength of the hydrogen bond is at a maximum when the proton donor group and the axis of the lone pair orbital are collinear. The strength of the bond decreases as the distance between X and Y increases.

Hydrogen bonding alters the force constant of both groups; thus, the frequencies of both stretching and bending vibrations are altered. The X—H stretching bands move to lower frequencies (longer wavelengths) usually with increased intensity and band widening. The stretching frequency of the acceptor group, for example, C═O, is also reduced but to a lesser degree than the proton donor group. The H—X bending vibration usually shifts to a shorter

wavelength when bonding occurs; this shift is less pronounced than that of the stretching frequency.

Intermolecular hydrogen bonding involves association of two or more molecules of the same or different compounds. Intermolecular bonding may result in dimer molecules (as observed for carboxylic acids) or in polymeric molecular chains, which exist in neat samples or concentrated solutions of monohydroxy alcohols. Intramolecular hydrogen bonds are formed when the proton donor and acceptor are present in a single molecule under spatial conditions that allow the required overlap of orbitals; for example, the formation of a five- or six-membered ring. The extent of both intermolecular and intramolecular bonding is temperature dependent. The effect of concentration on intermolecular and intramolecular hydrogen bonding is markedly different. The bands that result from intermolecular bonding generally disappear at low concentrations (less than about 0.01 *M* in nonpolar solvents). Intramolecular hydrogen bonding is an internal effect and persists at very low concentrations.

The change in frequency between free OH absorption and bonded OH absorption is a measure of the strength of the hydrogen bond. Ring strain, molecular geometry, and the relative acidity and basicity of the proton donor and acceptor groups affect the strength of bonding. Intramolecular bonding involving the same bonding groups is stronger when a six-membered ring is formed than when a smaller ring results from bonding. Hydrogen bonding is strongest when the bonded structure is stabilized by resonance.

The effects of hydrogen bonding on the stretching frequencies of hydroxyl and carbonyl groups are summarized in Table 2.2. Figure 2.18 (spectrum of cyclohexylcarbinol in the O—H stretch region) clearly illustrates this effect.

An important aspect of hydrogen bonding involves interaction between functional groups of solvent and solute. If the solute is polar, then it is important to note the solvent used and the solute concentration.

2.3 INSTRUMENTATION

2.3.1 Dispersion IR

For many years, an infrared spectrum was obtained by passing an infrared beam though the sample and scanning the spectrum with a dispersion device (the familiar diffraction grating). The spectrum was scanned by rotating the diffraction grating; the absorption areas (peaks) were detected and plotted as frequencies versus intensities. Because FT-IR methods have largely replaced dispersion methods, there is no need to discuss this further.

2.3.2 Fourier Transform Infrared Spectrometer (Interferometer)

Fourier transform infrared (FT-IR) spectroscopy has been extensively developed over the past 25 years. FT-IR provides a number of advantages over the old dispersive method, including better sensitivity, resolution, and speed; therefore, FT-IR has become the only method of IR spectroscopy commonly performed today. In FT-IR, radiation containing all IR wavenumbers (e.g., 4000 cm^{-1}) to 400 cm^{-1}) is split into two beams (Figure 2.4). One beam is of fixed length, and the other is of variable length (movable mirror).

The varying distances between two path lengths result in a sequence of constructive and destructive interferences and hence variations in intensities: an interferogram. Fourier transformation converts this interferogram from the time domain into one spectral point on the more familiar form of the frequency domain. Smooth and continuous variation of the length of the piston adjusts the position of mirror B and varies the length of beam B; Fourier transformation at successive points throughout this variation gives rise to the complete IR spectrum. Passage of this radiation through a sample subjects the compound to a broadband of energies.

TABLE 2.2 Impact of Hydrogen Bonding on IR Stretching Wavenumbers

	Intermolecular Bonding			Intramolecular Bonding		
X—H · · · Y	Wavenumber Reduction			Wavenumber Reduction		
Strength	νOH	νC=O	Compound Class	νOH	νC=O	Compound Class
Weak	300[a]	15[b]	Alcohols, phenols, and intermolecular hydroxyl to carbonyl bonding	<100[a]	10	1,2-Diols, α- and most β-hydroxy ketones; *o*-chloro and *o*-alkoxy phenols
Medium				100 to 300[a]	50	1,3-Diols; some β-hydroxy ketones; β-hydroxy amino compounds; nitro compounds
Strong	500[a]	50[b]	RCO_2H dimers	>300[a]	100	*o*-Hydroxy aryl ketones; *o*-hydroxyaryl acids; β-diketones; tropolones

[a]Shift relative to "free" stretching wavenumbers.
[b]Carbonyl stretching only where applicable.

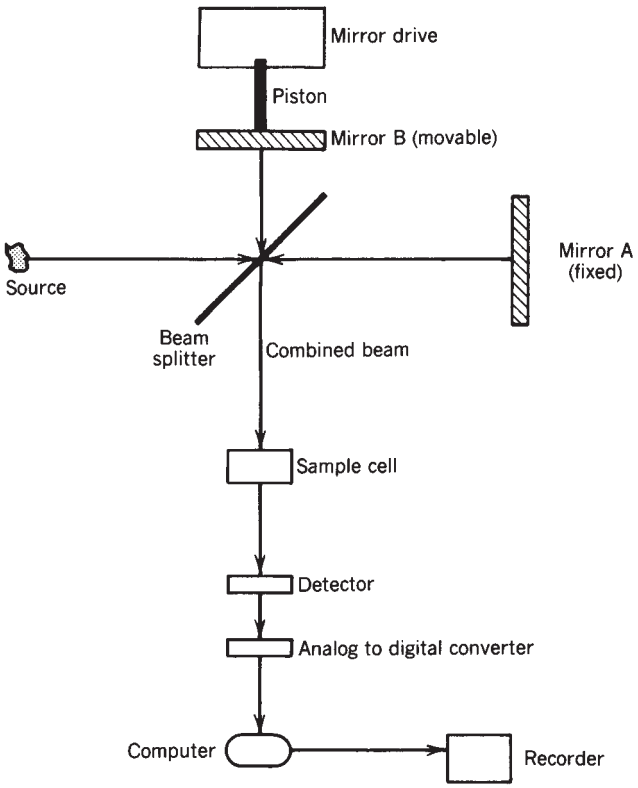

FIGURE 2.4 Schematic of an FT-IR spectrometer.

In principle, the analysis of one broadbanded pass of radiation through the sample will give rise to a complete IR spectrum.

There are a number of advantages to FT-IR methods. Since a monochromator is not used, the entire radiation range is passed through the sample simultaneously and much time is saved (Felgett's advantage). FT-IR instruments can have very high resolution (≤ 0.001 cm^{-1}). Moreover, since the data undergo analog-to-digital conversion, IR results are easily manipulated: results of several scans are combined to average out random absorption artifacts, and excellent spectra from very small samples can be obtained. Another advantage of FT-IR is that accurate analysis can be done on mixtures by computerized spectral subtraction. This technique depends on having a standard spectrum of the one component whose peaks are then subtracted from those of the mixture.

FT-IR can be interfaced with chromatographic instrumentation. The techniques of gas chromatographic FT-IR (GC-FT-IR) and liquid chromatographic FT-IR (LC-FT-IR) are particularly useful in identifying compounds in mixtures. GC-FT-IR instruments are capable of providing a vapor-phase spectrum on nanogram amounts of a compound eluted from a capillary GC column. Vapor-phase spectra resemble those run at high dilution in a nonpolar solvent; concentration-dependent peaks are shifted to higher frequency compared with those obtained from concentrated solutions, thin films, or the solid state [see Aldrich (1989)]. The combination of FT-IR spectroscopy with visible microscopy also has been used in a wide range of applications including the identification of trace contaminants, characterization of production defects down to micron area dimensions, and the study of chain order and chain packing. FT-IR microscopy allows the study of cells at the molecular level to obtain information that is rich in structural and functional information (Sasic, 2010).

2.4 SAMPLE HANDLING

Infrared spectra may be obtained for gases, liquids, or solids. The spectra of gases or low-boiling liquids may be obtained by expansion of the sample into an evacuated cell. Gas cells are available in lengths of a few centimeters to 40 m. The sampling area of a standard IR spectrometer will not accommodate cells much longer than 10 cm; long paths are achieved by multiple reflection optics.

Liquids may be examined neat or in solution. Neat liquids are examined between salt plates, usually without a spacer. Pressing a liquid sample between flat plates produces a film 0.01 mm or less in thickness, the plates being held together by capillary action. Samples of 1 mg to 10 mg are required. Thick samples of neat liquids usually absorb too strongly to produce a satisfactory spectrum. Volatile liquids are examined in sealed cells with very thin spacers. Silver chloride plates may be used for samples that dissolve sodium chloride plates.

Solutions are handled in cells of 0.1 mm to 1 mm in thickness. Volumes of 0.1 mL to 1 mL of 0.05% to 10% solutions are required for readily available cells. A compensating cell, containing pure solvent, is placed in the reference beam. The spectrum thus obtained is that of the solute except in those regions in which the solvent absorbs strongly. For example, thick samples of carbon tetrachloride absorb strongly near 800 cm^{-1}; compensation for this band is ineffective since strong absorption prevents any radiation from reaching the detector.

The solvent selected must be dry and transparent in the region of interest. When the entire spectrum is of interest, several solvents must be used. A common pair of solvents is carbon tetrachloride (CCl_4) and carbon disulfide (CS_2). Carbon tetrachloride is relatively free of absorption at frequencies above 1333 cm^{-1}, whereas CS_2 shows little absorption below 1333 cm^{-1}. Solvent and solute combinations that react must be avoided. For example, CS_2 cannot be used as a solvent for primary or secondary amines. Amino alcohols react slowly with CS_2 and CCl_4. The absorption patterns of selected solvents and mulling oils are presented in Appendix A.

Solids can be examined as a mull, a pressed disk, a deposited glassy film, or as powders using a method called diffuse reflectance. Mulls are prepared by thoroughly grinding 2 mg to 5 mg of a solid in a smooth agate mortar. Grinding is continued after the addition of one or two drops of the mulling oil. The suspended particles must be < 2 μm to avoid excessive scattering of radiation. The mull is examined as a thin film between flat salt plates. Nujol® (a high-boiling petroleum oil) is commonly used as a mulling agent. When

hydrocarbon bands interfere with the spectrum, Fluorolube® (a completely halogenated polymer containing F and Cl) or hexachlorobutadiene may be used. The use of both Nujol® and Fluorolube® mulls makes possible a scan, essentially free of interfering bands, over the 4000 cm^{-1} to 250 cm^{-1} region.

The pellet (pressed-disk) technique depends on the fact that dry, powdered potassium bromide (or other alkali metal halides) can be compacted under pressure to form transparent disks. The sample (0.5 mg to 1.0 mg) is intimately mixed with approximately 100 mg of dry, powdered KBr. Mixing can be effected by thorough grinding in a smooth agate mortar or, more efficiently, with a small vibrating ball mill, or by lyophilization. The mixture is pressed with special dies under a pressure of 70000 kPa to 100000 kPa into a transparent disk. The quality of the spectrum depends on the intimacy of mixing and the reduction of the suspended particles to ≤ 2 μm. Microdisks, 0.5 mm to 1.5 mm in diameter, can be used with a beam condenser. The microdisk technique permits examination of samples as small as 1 μg. Bands near 3448 cm^{-1} and 1639 cm^{-1}, resulting from moisture, frequently appear in spectra obtained by the pressed-disk technique.

The use of KBr disks or pellets has often been avoided in the past because of the demanding task of making good pellets. Such KBr techniques can be made less daunting by using the Mini-Press, which affords a simple procedure. The KBr-sample mixture is placed in the nut portion of the assembly with one bolt in place. The second bolt is introduced, and pressure is applied by tightening the bolts. Removal of the bolts leaves a pellet in the nut that now serves as a cell.

Deposited films are useful only when the material can be deposited from solution or cooled from a melt as microcrystals or as a glassy film. Crystalline films generally lead to excessive light scattering. Specific crystal orientation may lead to spectra differing from those observed for randomly oriented particles which exist in a mull or halide disk. The deposited film technique is particularly useful for obtaining spectra of resins and plastics. Care must be taken to free the sample of solvent by vacuum treatment or gentle heating.

In general, a dilute solution in a nonpolar solvent furnishes the best (i.e., least distorted) spectrum. Nonpolar compounds give essentially the same spectra in the condensed phase (i.e., neat liquid, a mull, a KBr disk, or a thin film) as they give in nonpolar solvents. Polar compounds, however, often show hydrogen bonding effects in the condensed phase. Unfortunately, polar compounds are frequently insoluble in nonpolar solvents, and the spectrum must be obtained either in a condensed phase or in a polar solvent; the latter introduces the possibility of solute–solvent hydrogen bonding.

In recent years, the development of IR measurements has been focused on reflectance methods. Two common reflectance methods are attenuated total reflectance (ATR) and diffuse reflectance infrared Fourier transform spectroscopy (DRIFTS). Both methods probe primarily the surface of the sample (down to a few micrometers). These spectroscopic methods of analysis were initially developed for specimens that cannot be analyzed by conventional transmission techniques. With minimal sample preparation, IR spectra can be effectively obtained for highly absorbing samples (such as aqueous solutions and biological specimens) and opaque materials such as polymers, coatings, powders, and liquids.

ATR FT-IR is based on the principle of internal reflection spectroscopy. Thus, when a beam of light passes through an optically clear, dense material (e.g., a crystal having a high refractive index), it is internally reflected from the interface of an adjoining medium of lower optical density and lower refractive index. Qualitatively, ATR works as follows: the reflected radiation waves (called standing waves) lose a minute fraction of their intensity via absorption to the functional groups of the material at the interface where the vanishing wave (evanescent wave) is formed, and hence an absorption spectrum is produced. Particular attention is required to establish good optical contact of the sample and the crystal. This can be done in various ways, for example, by casting from solution, or by pressing the sample on the surface of the crystal. However, it is important to note that pressure can have an effect on the quality and intensity of the recorded spectra, and therefore should be uniform for the entire measurement.

The DRIFTS method is based on the concept of diffusion reflectance spectroscopy. It enables one to study the surface chemistry of materials that can reflect light, such as heterogeneous catalysts, composites, powders, organic crystals, and pharmaceutical substances. In the DRIFTS accessory, the IR light reflects off the surface (a powdered sample is preferable) at all angles, and a parabolic mirror collector refocuses the diffusely reflected light to an IR detector.

FT-IR-ATR and DRIFTS spectra are similar to conventional IR spectra. The absorption band positions are identical; however, the relative intensities of corresponding bands are often different.

2.5 INTERPRETATION OF SPECTRA

There are no rigid rules for interpreting an IR spectrum. Certain requirements, however, must be met before an attempt is made to interpret a spectrum:

1. The spectrum must be adequately resolved and of adequate intensity.
2. The spectrum should be that of a reasonably pure compound.
3. The spectrometer should be calibrated so that the bands are observed at their proper frequencies or wavelengths. Proper calibration can be made with reliable standards, such as polystyrene film.
4. The method of sample handling must be specified. If a solvent is employed, the solvent, concentration, and the cell thickness should be indicated.

A precise treatment of the vibrations of a complex molecule is not feasible; thus, the IR spectrum must be interpreted from empirical comparison of spectra and extrapolation of studies of simpler molecules. Many questions arising in the interpretation of an IR spectrum can be answered by data obtained from the mass (Chapter 1) and NMR spectra (Chapters 3 to 6).

Infrared absorption of organic molecules is summarized in the chart of characteristic group absorptions in Appendix B. Many of the group absorptions vary over a wide range because the bands arise from complex interacting vibrations within the molecule. Absorption bands may, however, represent predominantly a single vibrational mode. Certain absorption bands, for example, those arising from the C—H, O—H, and C═O stretching modes, remain within fairly narrow regions of the spectrum. Important details of structure may be revealed by the exact position of an absorption band within these narrow regions. Shifts in absorption position and changes in band contours, accompanying changes in molecular environment, may also suggest important structural details.

The two important areas for a preliminary examination of a spectrum are the regions 4000 cm^{-1} to 1300 cm^{-1} and 900 cm^{-1} to 650 cm^{-1}. The high-frequency portion of the spectrum is called the functional group region. The characteristic stretching frequencies for important functional groups such as OH, NH, and C═O occur in this portion of the spectrum. The absence of absorption in the assigned ranges for the various functional groups can usually be used as evidence for the absence of such groups in the molecule. Care must be exercised, however, in such interpretations since certain structural characteristics may cause a band to become extremely broad so that it may go unnoticed. For example, intramolecular hydrogen bonding in the enolic form of acetylacetone results in a broad OH band, which may be overlooked. The absence of absorption in the 1850 cm^{-1} to 1540 cm^{-1} region excludes a structure containing a carbonyl group.

Weak bands in the high-frequency region, resulting from the fundamental absorption of functional groups, such as S—H and C═C, are extremely valuable in the determination of structure. Such weak bands would be of little value in the more complicated regions of the spectrum. Overtones and combination tones of lower frequency bands frequently appear in the high-frequency region of the spectrum. Overtone and combination-tone bands are characteristically weak except when Fermi resonance occurs. Strong skeletal bands for aromatics and heteroaromatics fall in the 1600 cm^{-1} to 1300 cm^{-1} region of the spectrum.

The lack of strong absorption bands in the 900 cm^{-1} to 650 cm^{-1} region generally indicates a nonaromatic structure. Aromatic and heteroaromatic compounds display strong out-of-plane C—H bending and ring bending absorption bands in this region that can frequently be correlated with the substitution pattern. Broad, moderately intense absorption in the low-frequency region suggests the presence of carboxylic acid dimers, amines, or amides, all of which show out-of-plane bending in this region. If the region is extended to 1000 cm^{-1}, absorption band characteristics of alkene structures are included.

The intermediate portion of the spectrum, 1300 cm^{-1} to 900 cm^{-1}, is usually referred to as the fingerprint region. The absorption pattern in this region is frequently complex, with the bands originating in interacting vibrational modes. This portion of the spectrum is extremely valuable when examined in reference to the other regions. For example, if alcoholic or phenolic O—H stretching absorption appears in the high-frequency region of the spectrum, the position of the C—C—O absorption band in the 1260 cm^{-1} to 1000 cm^{-1} region frequently makes it possible to assign the O—H absorption to alcohols and phenols with highly specific structures. Absorption in this intermediate region is probably unique for every molecular species.

Any conclusions reached after examination of a particular band should be confirmed where possible by examination of other portions of the spectrum. For example, the assignment of a carbonyl band to an aldehyde should be confirmed by the appearance of a band or a pair of bands in the 2900 cm^{-1} to 2695 cm^{-1} region of the spectrum, arising from C—H stretching vibrations of the aldehyde group. Similarly, the assignment of a carbonyl band to an ester should be confirmed by observation of a strong band in the C—O stretching region, 1300 cm^{-1} to 1100 cm^{-1}.

Similar compounds may give virtually identical spectra under normal conditions, but fingerprint differences can be detected with an expanded vertical scale or with a very large sample (major bands off scale). For example, pentane and hexane are essentially indistinguishable under normal conditions and can be differentiated only with very high sensitivity experiments.

Finally, in a fingerprint comparison of spectra, or any other situation in which the shapes of peaks are important, we should be aware of the substantial differences in the appearance of the spectrum in changing from a presentation that is linear in wavenumber to one that is linear in wavelength (Figure 2.5).

Admittedly, the full chart of characteristic absorption groups (Appendix B) is intimidating. The following statements and a simplified chart may help (Figure 2.6).

The first bit of advice is negative: do not attempt a frontal, systematic assault on an infrared spectrum. Rather, look for evidence of the presence or absence of a few common functional groups with very characteristic absorptions. Start with OH, C═O, and NH groups in Figure 2.6 since a "yes/no" answer is usually available. A "yes" answer for any of these groups sharpens the focus considerably. Certainly, the answer will contribute to development of a molecular formula from the mass spectrum (Chapter 1) and to an entry point for the NMR spectra (Chapters 3 to 6). These other spectra, in turn, will suggest further leads in the IR spectrum.

Figure 2.6 lists the common groups that provide distinctive, characteristic absorptions. Section 2.6 furnishes more detailed information, including a number of caveats.

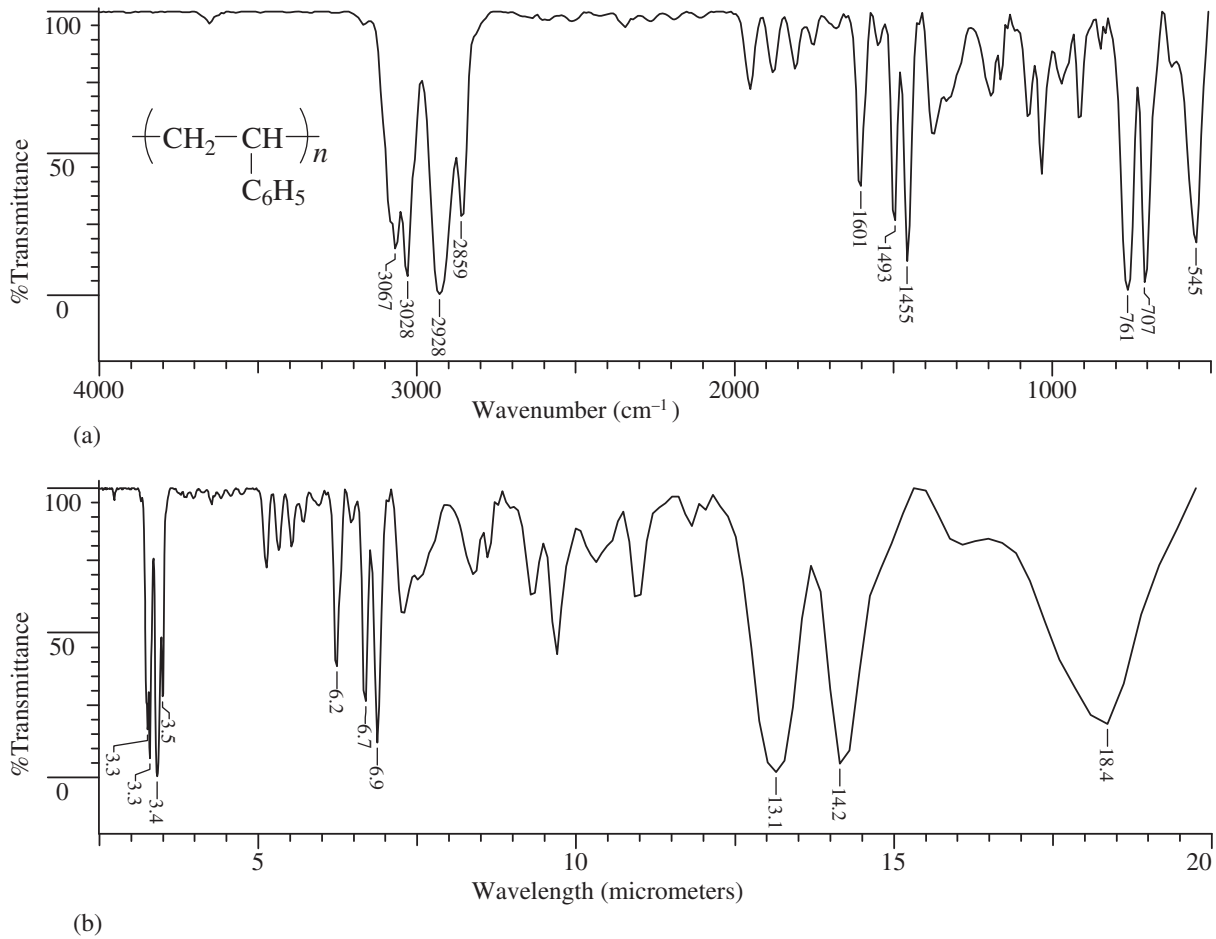

FIGURE 2.5 Polystyrene, same sample for both (a) and (b). Spectrum (a) linear in wavenumber (cm^{-1}); spectrum (b) linear in wavelength (μm).

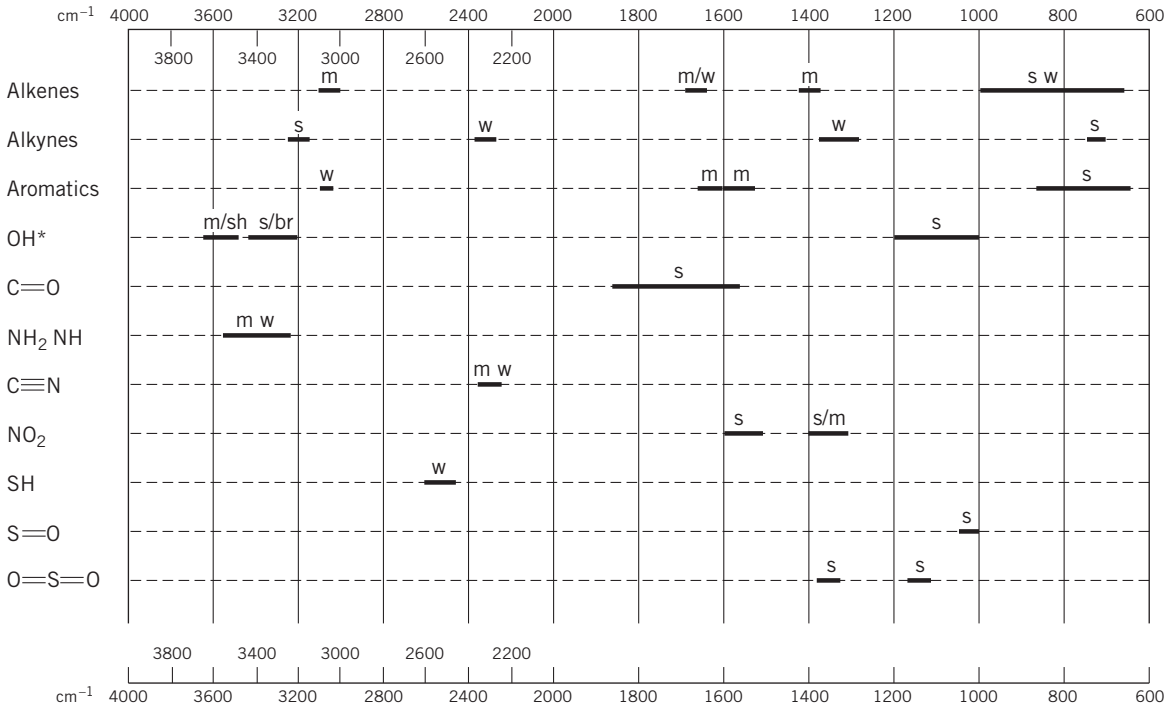

*Free OH, medium and sharp; bonded OH, strong and broad

FIGURE 2.6 Simplified chart of several common functional groups with very characteristic absorptions. s = strong, m = medium, w = weak, sh = sharp, and br = broad.

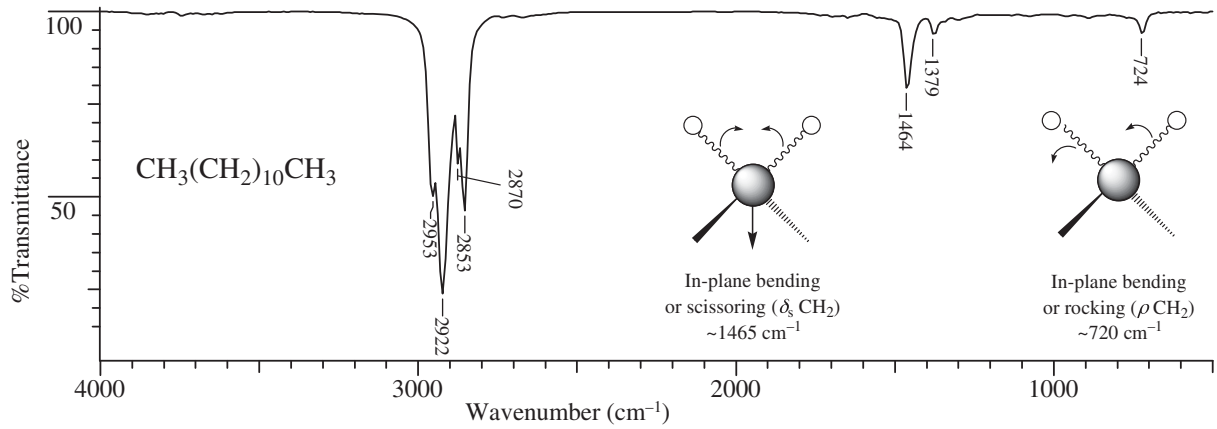

FIGURE 2.7 Dodecane. C—H stretch: 2953 cm^{-1} $\nu_{as}CH_3$, 2870 cm^{-1} $\nu_{vs}CH_3$, 2922 cm^{-1} $\nu_{as}CH_2$, 2853 cm^{-1} ν_sCH_2. C—H bend: 1464 cm^{-1} δ_sCH_2, 1450 cm^{-1} $\delta_{as}CH_3$, 1379 cm^{-1} δ_sCH_3. CH_2 rock: 724 cm^{-1} ρCH_2.

2.6 CHARACTERISTIC GROUP ABSORPTIONS OF ORGANIC MOLECULES

A table of characteristic group absorptions is presented in Appendix B. The ranges presented for group absorptions have been assigned following the examination of many compounds in which the groups occur. Although the ranges are quite well defined, the precise frequency or wavelength at which a specific group absorbs is dependent on its environment within the molecule and on its physical state.

This section is concerned with a comprehensive look at these characteristic group absorptions and their relationship to molecular structure. As a major type or class of molecule or functional group is introduced in the following sections, an example of an IR spectrum with the important peak assignments will be given for most.

2.6.1 Normal Alkanes (Paraffins)

The spectra of normal alkanes (paraffins) can be interpreted in terms of four vibrations, namely, the stretching and bending of C—H and C—C bonds. Detailed analysis of the spectra of the lower members of the alkane series has made detailed assignments of the spectral positions of specific vibrational modes possible.

Not all of the possible absorption frequencies of alkanes are of equal value in the assignment of structure. The C—C bending vibrations occur at very low frequencies (below 500 cm^{-1}) and therefore do not appear in our spectra. The bands assigned to C—C stretching vibrations are weak and appear in the broad region of 1200 cm^{-1} to 800 cm^{-1}; they are generally of little value for identification.

The most characteristic vibrations are those arising from C—H stretching and bending. Of these vibrations, those arising from methylene twisting and wagging are usually of limited diagnostic value because of their weakness and instability. This instability is a result of strong coupling to the remainder of the molecule.

The vibrational modes of alkanes are common to many organic molecules. Although the positions of C—H stretching and bending frequencies of methyl and methylene groups remain nearly constant in hydrocarbons, the attachment of CH_3 or CH_2 groups to atoms other than carbon, or to a carbonyl group or aromatic ring, may result in appreciable shifts of the C—H stretching and bending frequencies.

The spectrum of dodecane (Figure 2.7) is that of a typical straight-chain hydrocarbon.

2.6.1.1 C—H Stretching Vibrations. Absorption arising from C—H stretching in the alkanes occurs in the general region of 3000 cm^{-1} to 2840 cm^{-1}. The positions of the C—H stretching vibrations are among the most stable in the spectrum.

Methyl Groups An examination of a large number of saturated hydrocarbons containing methyl groups showed, in all cases, two distinct bands occurring at approximately 2962 cm^{-1} and 2872 cm^{-1}. The first of these results from the asymmetrical (as) stretching mode in which two C—H bonds of the methyl group are extending while the third one is contracting ($\nu_{as}CH_3$). The second arises from symmetrical (s) stretching (ν_sCH_3) in which all three of the C—H bonds extend and contract in phase. The presence of several methyl groups in a molecule results in strong absorption at these positions.

Methylene Groups The asymmetrical stretching ($\nu_{as}CH_2$) and symmetrical stretching (ν_sCH_2) occur, respectively, near 2926 cm^{-1} and 2853 cm^{-1}. The positions of these bands do not vary more than ± 10 cm^{-1} in the aliphatic and unstrained cyclic hydrocarbons. The frequency of methylene stretching is increased when the methylene group is part of a strained ring.

2.6.1.2 C—H Bending Vibrations.

Methyl Groups Two bending vibrations can occur within a methyl group. The first of these, the symmetrical

bending vibration, involves the in-phase bending of the C—H bonds (**I**). The second, the asymmetrical bending vibration, involves out-of-phase bending of the C—H bonds (**II**).

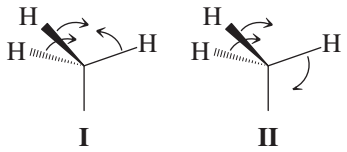

In **I**, the C—H bonds are moving like the closing petals of a flower; in **II**, one petal opens as two petals close.

The symmetrical bending vibration ($\delta_s CH_3$) occurs near 1375 cm^{-1}, and the asymmetrical bending vibration ($\delta_{as} CH_3$) near 1450 cm^{-1}.

The asymmetrical vibration generally overlaps the scissoring vibration of the methylene groups (see below). Two distinct bands are observed, however, in compounds such as diethyl ketone, in which the methylene scissoring band has been shifted to a lower frequency, 1439 to 1399 cm^{-1}, and increased in intensity because of its proximity to the carbonyl group.

The absorption band near 1375 cm^{-1}, arising from the symmetrical bending of the methyl C—H bonds, is very stable in position when the methyl group is attached to another carbon atom. The intensity of this band is greater for each methyl group in the compound than that for the asymmetrical methyl bending vibration or the methylene scissoring vibration.

Methylene Groups The bending vibrations of the C—H bonds in the methylene group have been shown schematically in Figure 2.1. The four bending vibrations are referred to as *scissoring*, *rocking*, *wagging*, and *twisting*.

The scissoring band ($\delta_s CH_2$) in the spectra of hydrocarbons occurs at a nearly constant position near 1465 cm^{-1} (see Figure 2.7).

The band resulting from the methylene rocking vibration (ρCH_2), in which all of the methylene groups rock in phase, appears near 720 cm^{-1} for straight-chain alkanes of seven or more carbon atoms. This band may appear as a doublet in the spectra of solid samples. In the lower members of the *n*-alkane series, the band appears at somewhat higher frequencies.

For hydrocarbons, because of methylene twisting and wagging vibrations, absorption is observed in the 1350 cm^{-1} to 1150 cm^{-1} region. These bands are generally appreciably weaker than those resulting from methylene scissoring. A series of bands in this region, arising from the methylene group, is characteristic of the spectra of solid samples of long-chain acids, amides, and esters.

2.6.2 Branched-Chain Alkanes

In general, the changes brought about in the spectrum of a hydrocarbon by branching result from changes in skeletal stretching vibrations and methyl bending vibrations; these occur below 1500 cm^{-1}. The spectrum of 2,2,4-trimethylpentane in Figure 2.8 is that of a typical branched alkane.

2.6.2.1 C—H Stretching Vibrations: Tertiary C—H Groups. Absorption resulting from this vibrational mode is very weak and is usually lost in other aliphatic C—H absorptions. Absorption in hydrocarbons occurs near 2890 cm^{-1}.

2.6.2.2 C—H Bending Vibrations: gem-Dimethyl Groups. Configurations in which two methyl groups are attached to the same carbon atom exhibit distinctive absorption in the C—H bending region. The isopropyl group shows a strong doublet, with peaks of almost equal intensity at 1385 cm^{-1} to 1380 cm^{-1} and 1370 cm^{-1} to 1365 cm^{-1}. The *tertiary* butyl group gives rise to two C—H bending bands, one in the 1395 cm^{-1} to 1385 cm^{-1} region and one near 1370 cm^{-1}. In the *t*-butyl doublet, the long wavelength band is more intense. When the *gem*-dimethyl group occurs at an internal position, a doublet is observed in essentially the same region where absorption occurs for the isopropyl and *t*-butyl groups. Doublets are observed for *gem*-dimethyl groups because of interaction between the in-phase and out-of-phase CH_3 bending of the two methyl groups attached to a common carbon atom.

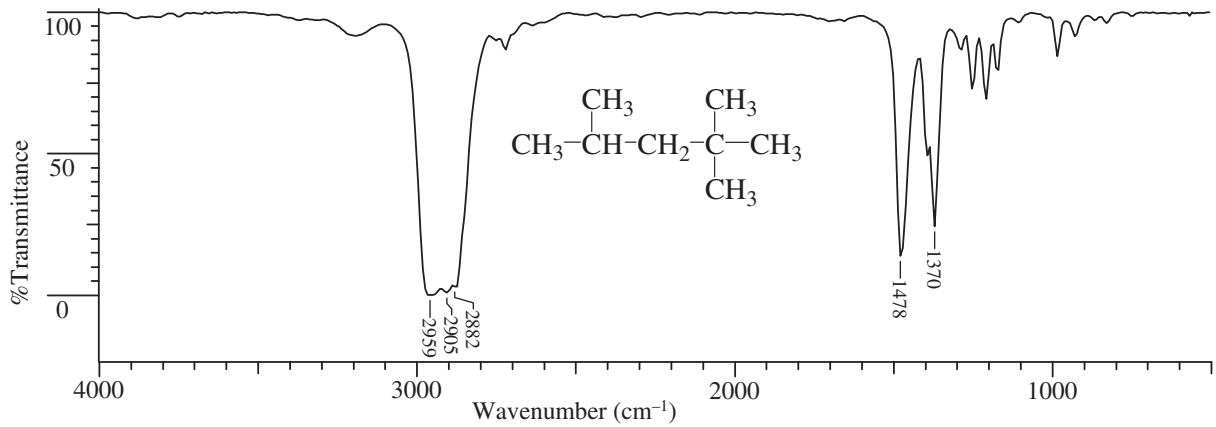

FIGURE 2.8 2,2,4-Trimethylpentane. C—H stretch (see Figure 2.7). C—H bend (see Figure 2.7). There are overlapping doublets for the *t*-butyl and the isopropyl groups at 1400 – 1340 cm^{-1}. Compare the absence of a methylene rocking band(s) 1000 cm^{-1} to 800 cm^{-1} to Figure 2.7.

Weak bands result from methyl rocking vibrations in isopropyl and *t*-butyl groups. These vibrations are sensitive to mass and interaction with skeletal stretching modes and are generally less reliable than the C—H bending vibrations. The following assignments have been made: isopropyl group, 922 cm^{-1} to 919 cm^{-1}, and *t*-butyl group, 932 cm^{-1} to 926 cm^{-1}.

2.6.3 Cyclic Alkanes

2.6.3.1 C—H Stretching Vibrations. The methylene stretching vibrations of unstrained cyclic poly(methylene) structures are much the same as those observed for acyclic alkanes. Increasing ring strain moves the C—H stretching bands progressively to higher frequencies. The ring CH_2 and CH groups in a monoalkylcyclopropane ring absorb in the region of 3100 cm^{-1} to 2990 cm^{-1}.

2.6.3.2 C—H Bending Vibrations. Cyclization decreases the frequency of the CH_2 scissoring vibration. Cyclohexane absorbs at 1452 cm^{-1}, whereas *n*-hexane absorbs at 1468 cm^{-1}. Cyclopentane absorbs at 1455 cm^{-1} and cyclopropane absorbs at 1442 cm^{-1}. This shift frequently makes it possible to observe distinct bands for methylene and methyl absorption in this region.

2.6.4 Alkenes

Alkene (olefinic) structures introduce several new modes of vibration into a hydrocarbon molecule: a C=C stretching vibration, C—H stretching vibrations in which the carbon atom is present in the alkene linkage, and in-plane and out-of-plane bending of the alkene C—H bond. The spectrum in Figure 2.9 is that of a typical terminal alkene.

2.6.4.1 C=C Stretching Vibrations Unconjugated Linear Alkenes. The C=C stretching mode of unconjugated alkenes usually shows moderate to weak absorption at 1667 cm^{-1} to 1640 cm^{-1}. Monosubstituted alkenes, that is, vinyl groups, absorb near 1640 cm^{-1}, with moderate intensity. Disubstituted *trans*-alkenes, tri- and tetraalkyl-substituted alkenes absorb at or near 1670 cm^{-1}; disubstituted *cis*-alkenes and vinylidene alkenes absorb near 1650 cm^{-1}.

The absorption of symmetrical disubstituted *trans*-alkenes or tetrasubstituted alkenes may be extremely weak or absent. The *cis*-alkenes, which lack the symmetry of the *trans* structure, absorb more strongly than *trans*-alkenes. Internal double bonds generally absorb more weakly than terminal double bonds because of pseudosymmetry.

Abnormally high absorption frequencies are observed for —CH=CF_2 and —CF=CF_2 groups. The former absorbs near 1754 cm^{-1}, and the latter near 1786 cm^{-1}. In contrast, the absorption frequency is reduced by the attachment of chlorine, bromine, or iodine.

Cycloalkenes Absorption due to the internal double bond in the unstrained cyclohexene system is essentially the same as that of a *cis*-isomer in an acyclic system. The C=C stretch vibration is coupled with the C—C stretching of the adjacent bonds. As the angle α

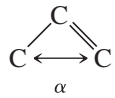

becomes smaller, the interaction becomes less until it is at a minimum of 90° in cyclobutene (1566 cm^{-1}). In the cyclopropene structure, interaction again becomes appreciable, and the absorption wavenumber increases (1641 cm^{-1}).

The substitution of alkyl groups for a hydrogen atom in strained ring systems serves to increase the frequency of C=C absorption. Cyclobutene absorbs at 1566 cm^{-1} and 1-methylcyclobutene absorbs at 1641 cm^{-1}.

The absorption frequency of external exocyclic bonds increases with decreasing ring size. Methylenecyclohexane absorbs at 1650 cm^{-1} and methylenecyclopropane absorbs at 1781 cm^{-1}.

Conjugated Systems The alkene bond stretching vibrations in conjugated dienes without a center of symmetry interact to produce two C=C stretching bands. The spectrum of an unsymmetrical conjugated diene, such as 1,3-pentadiene, shows absorption near 1650 cm^{-1} and

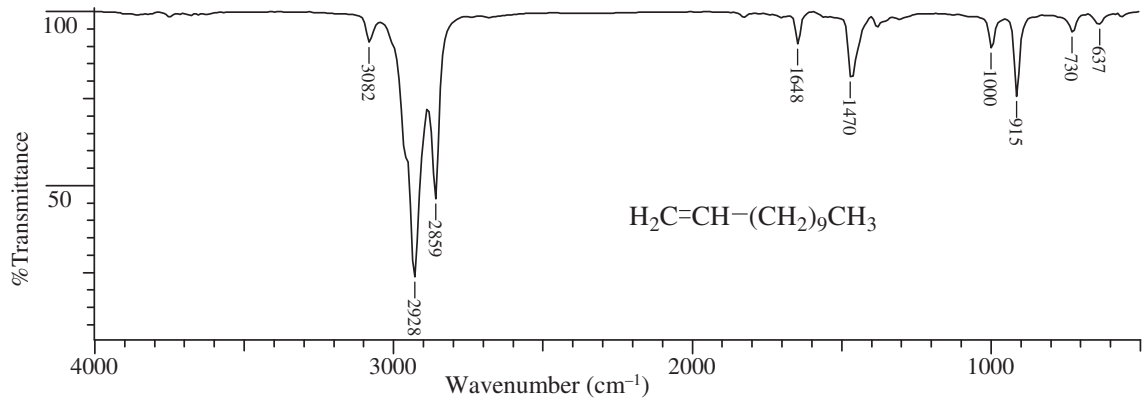

FIGURE 2.9 1-Dodecene. C—H stretch (see Figure 2.7). Note alkene C—H stretch at 3082 cm^{-1}. C=C stretch, 1648 cm^{-1}, see Appendix Table C.1. Out-of-plane C—H bend: 1000 cm^{-1}, (alkene) 915 cm^{-1}. Methylene rock: 730 cm^{-1}.

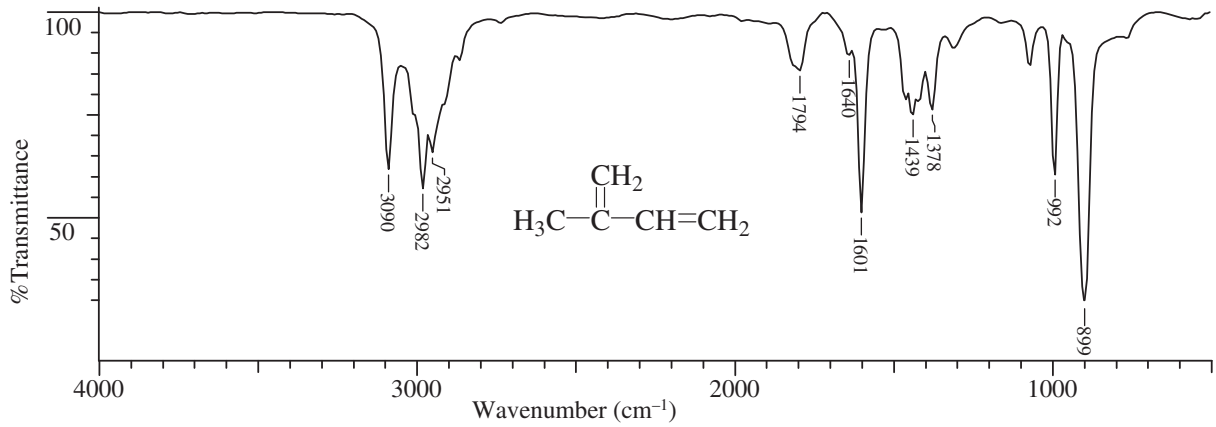

FIGURE 2.10 Isoprene. C—H stretch: =C—H 3090 cm^{-1}. Coupled C=C—C=C stretch: symmetric 1640 cm^{-1} (weak), asymmetric 1601 cm^{-1} (strong). C—H bend (saturated, alkene in-plane). C—H out-of-plane bend: 992 cm^{-1}, 899 cm^{-1} (see vinyl, Appendix Table C.1).

1600 cm^{-1}. The symmetrical molecule 1,3-butadiene shows only one band near 1600 cm^{-1}, resulting from asymmetric stretching; the symmetrical stretching band is inactive in the IR. The IR spectrum of isoprene (Figure 2.10) illustrates many of these features.

Conjugation of an alkene double bond with an aromatic ring produces enhanced alkene absorption near 1625 cm^{-1}.

The absorption frequency of the alkene bond in conjugation with a carbonyl group is lowered by about 30 cm^{-1}; the intensity of absorption is increased. In *s-cis* structures, the alkene absorption may be as intense as that of the carbonyl group. *s-Trans* structures absorb more weakly than *s-cis* structures.

Cumulated Alkenes A cumulated double-bond system, as occurs in the allenes $\left(\text{>C=C=CH}_2\right)$ absorbs near 2000 cm^{-1} to 1900 cm^{-1}. The absorption results from asymmetric C=C=C stretching. The absorption may be considered an extreme case of exocyclic C=C absorption.

2.6.4.2 Alkene C—H Stretching Vibrations. In general, any C—H stretching bands above 3000 cm^{-1} result from aromatic, heteroaromatic, alkyne, or alkene C—H stretching. Also found in the same region are the C—H stretching bands for small rings, such as cyclopropane, and the C—H bands for halogenated alkyl groups. The frequency and intensity of alkene C—H stretching absorptions are influenced by the pattern of substitution. With proper resolution, multiple bands are observed for structures in which stretching interaction may occur. For example, the vinyl group produces three closely spaced C—H stretching bands. Two of these result from symmetrical and asymmetrical stretching of the terminal C—H groups, and the third from the stretching of the remaining single C—H.

2.6.4.3 Alkene C—H Bending Vibrations. Alkene C—H bonds can undergo bending either in the same plane as the C=C bond or perpendicular to it; the bending vibrations can be either in phase or out of phase with respect to each other.

Assignments have been made for a few of the more prominent and reliable in-plane bending vibrations. The vinyl group absorbs near 1416 cm^{-1} because of a scissoring vibration of the terminal methylene. The C—H rocking vibration of a *cis*-disubstituted alkene occurs in the same general region.

The most characteristic vibrational modes of alkenes are the out-of-plane C—H bending vibrations between 1000 cm^{-1} and 650 cm^{-1}. These bands are usually the strongest in the spectra of alkenes. The most reliable bands are those of the vinyl group, the vinylidene group, and the *trans*-disubstituted alkene. Alkene absorptions are summarized in the Appendix (Tables C.1 and C.2).

In allene structures, strong absorption is observed near 850 cm^{-1}, arising from $=CH_2$ wagging. The first overtone of this band may also be seen.

2.6.5 Alkynes

The two stretching vibrations in alkynes (acetylenes) involve C≡C and C—H stretching. Absorption due to C—H bending is characteristic of acetylene and monosubstituted alkynes. The spectrum shown in Figure 2.11 is that of a typical terminal alkyne.

2.6.5.1 C≡C Stretching Vibrations. The weak C≡C stretching band of alkyne molecules occurs in the region of 2260 cm^{-1} to 2100 cm^{-1}. Because of symmetry, no C≡C band is observed in the IR for symmetrically substituted alkynes. In the IR spectra of monosubstituted alkynes, the band appears at 2140 cm^{-1} to 2100 cm^{-1}. Disubstituted alkynes, in which the substituents are different, absorb near 2260 cm^{-1} to 2190 cm^{-1}. When the substituents are similar in mass, or produce similar inductive and resonance effects, the band may be so weak as to be unobserved in the IR spectrum. For reasons of symmetry, a terminal C≡C bond produces a stronger band than an internal C≡C bond (pseudosymmetry). The intensity of the C≡C bond stretching band is increased by conjugation with a carbonyl group.

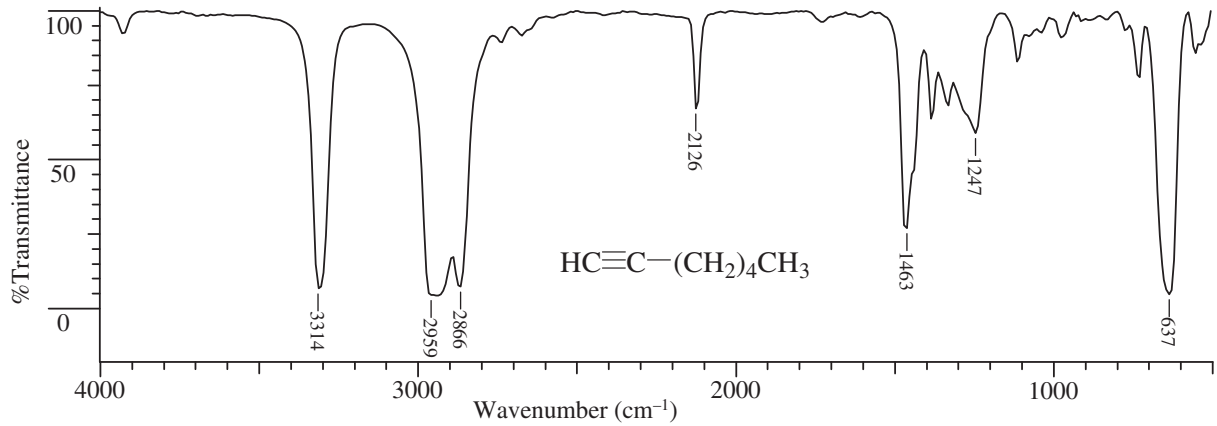

FIGURE 2.11 1-Heptyne. ≡C—H stretch, 3314 cm^{-1}. Alkyl C—H stretch 1450 – 1360 cm^{-1}, 2960 – 2860 cm^{-1}. C≡C stretch, 2126 cm^{-1}. C—H bend: 1463 cm^{-1} $\delta_s CH_2$, 1450 cm^{-1} $\delta_{as} CH_3$. ≡C—H bend overtone, 1247 cm^{-1}; ≡C—H bend fundamental, 637 cm^{-1}.

2.6.5.2 C—H Stretching Vibrations. The C—H stretching band of monosubstituted alkynes occurs in the general region of 3333 cm^{-1} to 3267 cm^{-1}. This is a strong band and is narrower than the hydrogen-bonded OH and NH bands occurring in the same region.

2.6.5.3 C—H Bending Vibrations. The C—H bending vibration of alkynes or monosubstituted alkynes leads to strong, broad absorption in the 700 cm^{-1} to 610 cm^{-1} region. The first overtone of the C—H bending vibration appears as a weak, broadband in the 1370 cm^{-1} to 1220 cm^{-1} region.

2.6.6 Mononuclear Aromatic Hydrocarbons

The most prominent and most informative bands in the spectra of aromatic compounds occur in the low-frequency range from 900 cm^{-1} to 675 cm^{-1}. These strong absorption bands result from the out-of-plane ("oop") bending of the ring C—H bonds. In-plane bending bands appear in the 1300 cm^{-1} to 1000 cm^{-1} region. Skeletal vibrations, involving carbon–carbon stretching within the ring, absorb in the 1600 cm^{-1} to 1585 cm^{-1} and 1500 cm^{-1} to 1400 cm^{-1} regions. The skeletal bands frequently appear as doublets, depending on the nature of the ring substituents.

Aromatic C—H stretching bands occur between 3100 cm^{-1} and 3000 cm^{-1}.

Weak combination and overtone bands appear in the 2000 cm^{-1} to 1650 cm^{-1} region. The pattern of the overtone bands is not a reliable guide to the substitution pattern of the ring. Because they are weak, the overtone and combination bands are most readily observed in spectra obtained from thick samples. The spectrum shown in Figure 2.12 is that of a typical aromatic (benzenoid) compound.

2.6.6.1 Out-of-Plane C—H Bending Vibrations. The in-phase, out-of-plane bending of a ring hydrogen atom is strongly coupled to adjacent hydrogen atoms. The position of absorption of the out-of-plane bending bands is therefore characteristic of the number of adjacent hydrogen atoms on the ring. The bands are frequently intense and appear at 900 cm^{-1} to 675 cm^{-1}.

Assignments for C—H out-of-plane bending bands in the spectra of substituted benzenes appear in the chart of characteristic group absorptions (Appendix B). These assignments are usually reliable for alkyl-substituted

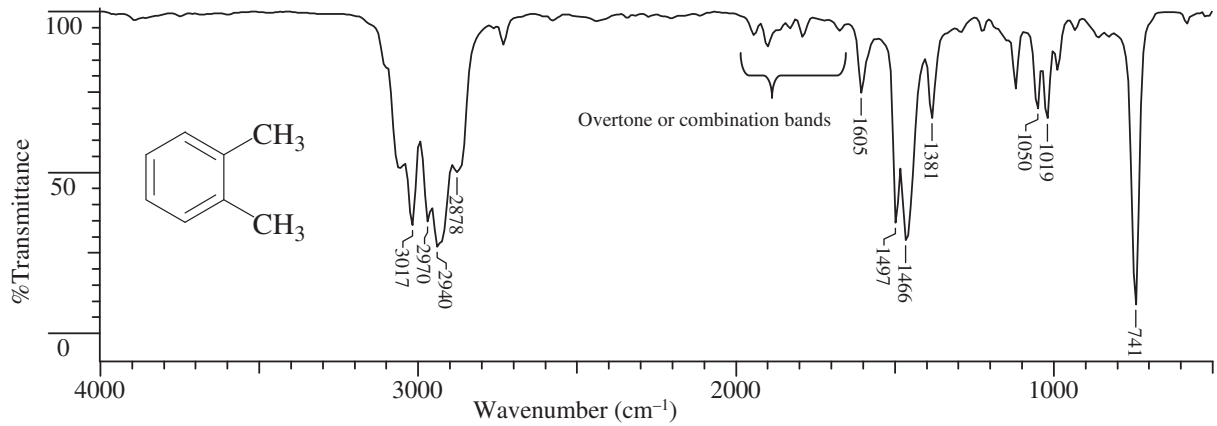

FIGURE 2.12 *o*-Xylene. Aromatic C—H stretch, 3017 cm^{-1}. Methyl bands, C—H stretch 3970, 2940, 2875 cm^{-1}. Overtone or combination bands, 2000 cm^{-1} to 1667 cm^{-1}. C—C ring stretch, 1605, 1497, 1466 cm^{-1}. In-plane C—H bend, 1050, 1019 cm^{-1}. Out-of-plane —C—H bend, 741 cm^{-1}.

TABLE 2.3 C—H Out-of-Plane Bending Vibrations of a β-Substituted Naphthalene

Substitution Pattern	Absorption Range (cm^{-1})
Isolated hydrogen	862 to 835
Two adjacent hydrogen atoms	835 to 805
Four adjacent hydrogen atoms	760 to 735

benzenes, but caution must be observed in the interpretation of spectra when polar groups are attached directly to the ring, for example, in nitrobenzenes, aromatic acids, and esters or amides of aromatic acids.

The absorption band that frequently appears in the spectra of substituted benzenes near 600 cm^{-1} to 420 cm^{-1} is attributed to out-of-plane ring bending.

2.6.7 Polynuclear Aromatic Hydrocarbons

Polynuclear aromatic compounds, like the mononuclear aromatics, show characteristic absorption in three regions of the spectrum.

The aromatic C—H stretching and the skeletal vibrations absorb in the same regions as observed for the mononuclear aromatics. The most characteristic absorption of polynuclear aromatics results from C—H out-of-plane bending in the 900 cm^{-1} to 675 cm^{-1} region. These bands can be correlated with the number of adjacent hydrogen atoms on the rings. Most β-substituted naphthalenes, for example, show three absorption bands resulting from out-of-plane C—H bending; these correspond to an isolated hydrogen atom and two adjacent hydrogen atoms on one ring and four adjacent hydrogen atoms on the other ring.

In the spectra of α-substituted naphthalenes, the bands for the isolated hydrogen and the two adjacent hydrogen atoms of β-naphthalenes are replaced by a band for three adjacent hydrogen atoms. This band is near 810 cm^{-1} to 785 cm^{-1}. Additional bands may appear because of ring bending vibrations (see Table 2.3). The positions of absorption bands for more highly substituted naphthalenes and other polynuclear aromatics are summarized by Colthup et al. (1990).

2.6.8 Polymers

In this section, we limit the discussion to a particular class of synthetic macromolecules that consist of a set of regularly repeated chemical units (i.e., a monomer). A macromolecule with only one type of chemical repeat unit in the polymer chain is called a homopolymer. A copolymer consists of a very limited number of different types of monomers joined end to end to form a chain molecule. Polymers may be linear, branched, or crosslinked and they may exist in crystalline, semicrystalline, or amorphous states. A molecule consisting of N atoms has 3N-6 normal modes of vibration (Section 2.2); a polymer molecule may contain tens of thousands of atoms, and thus, can have tens to hundreds of thousands of normal modes. This situation could conceivably lead to extremely complicated IR spectra. However, homopolymers consist of a large number of chemically identical repeat units, each of which contains a limited number of atoms. This leads to a considerable reduction in the complexity of the IR spectrum. Therefore, the IR spectrum of a polymer usually contains a number of peaks usually on the order of $\leq 3n$, where n is the number of atoms in an individual repeat unit, rather than $3N$, where N is the number of atoms in the whole molecule. The bands in the spectrum of a polymer may then be assigned largely on the basis of characteristic stretching and deformation vibrations of the specific groups in the repeat units that comprise the polymer chain.

Identification of an unknown polymer thus involves detection of characteristic absorption bands due to a particular chemical group in the repeat unit. By using a functional group frequency correlation table for small molecules (Appendix B), it is then a relatively simple task, for example, to ascertain whether the spectrum is that of an aliphatic or aromatic hydrocarbon polymer, a polyester, a polyamide, and so forth.

FT-IR spectra of the simplest polymer, polyethylene $(—CH_2—CH_2—)_n$, are shown in Figures 2.13 and 2.14. The spectrum of high-density polyethylene (HDPE)

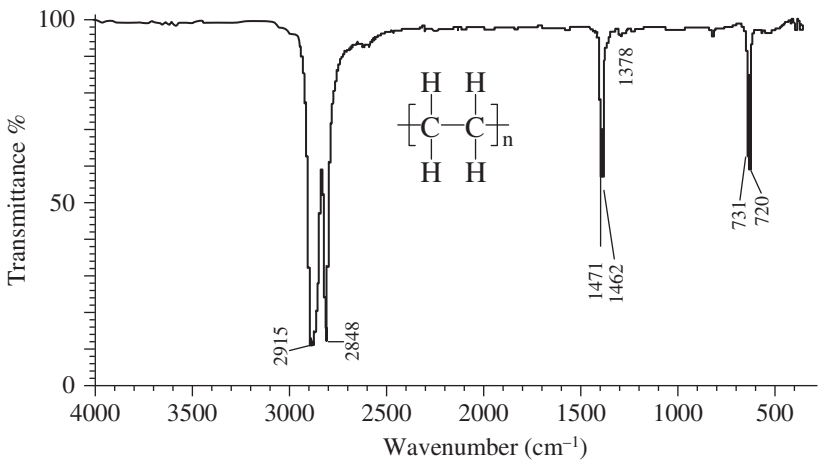

FIGURE 2.13 IR spectrum of high-density polyethylene.

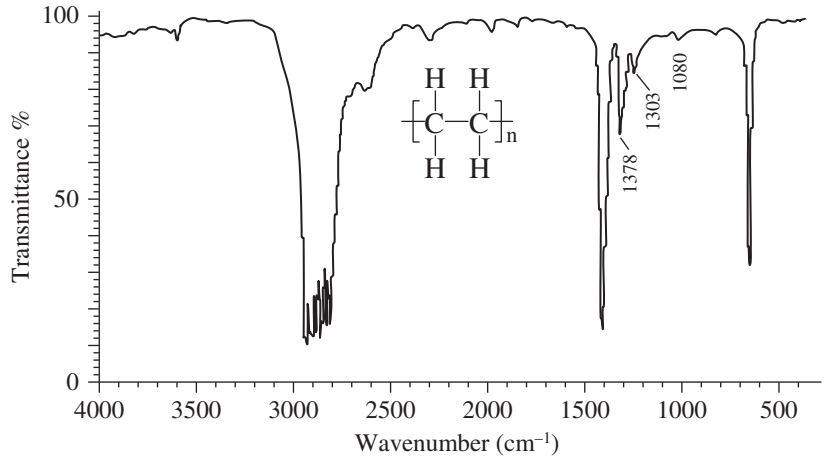

FIGURE 2.14 IR spectrum of low-density polyethylene.

(Figure 2.13) shows a strong CH_2 symmetric stretch at 2848 cm^{-1}, a CH_2 asymmetric stretch at 2915 cm^{-1}, a doublet at 1461 cm^{-1} and 1471 cm^{-1} due to a CH_2 bend, an out-of-phase CH_2 rock of the two chains in the unit cell at 720 cm^{-1}, and an in-phase CH_2 rock of the two chains in the unit cell at 730 cm^{-1}. HDPE is a linear, highly crystalline polymer with a low CH_3 group content, found almost entirely as chain end-groups of the polymer. Thus, the $\nu_{as}CH_3$ at 2950 cm^{-1}, ν_sCH_3 at 2870 cm^{-1}, and δ_sCH_3 at 1378 cm^{-1} are absent or have very low intensity. In contrast, LDPE (low-density polyethylene produced at high pressure and temperature, 82 MPa to 276 MPa and 405°C to 605°C, respectively) contains some chain branches, and consequently, an elevated content of —CH_3 groups. Hence, the CH_3 symmetrical bending at 1378 cm^{-1} of LDPE has a relatively high intensity compared to HDPE (Figure 2.14).

By measuring the relative intensity of the CH_3 vibration band, the degree of short chain branching in polyethylene can be determined. A band near 1303 cm^{-1} (CH_2 wag) and a bend at 1080 cm^{-1} (skeletal C—C stretch) are associated with the amorphous character of the polymer; thus, these bands can be used to verify the degree of crystallinity of polyethylene sample.

Figure 2.15 shows the spectrum of polypropylene where a methyl group substitutes for one of the hydrogen atoms in the units of polyethylene. The spectrum not only shows all the characteristics of a saturated aliphatic hydrocarbon but also has a number of sharp bands in the C—C stretching and C—H deformation regions, suggesting a well-defined carbon–carbon backbone. Polypropylene, like vinyl or the vinylidene class of polymer, can form stereochemical configurational isomers.

Polypropylene has three types as illustrated in Figure 2.16. The isotactic type, where all the R groups lie on the same side of the extended chain; the syndiotactic type, where the R groups have alternating positions along the chain; and the atactic type, where the placement of R group along the polymer units is random. These different tacticities have a considerable effect on the ordering and packing of the polymer in the solid state, which consequentially affects the IR spectrum of the material. The configuration of atactic-PP exhibits no overall regularity of successive repeat units. Isotactic-PP coils up into a 3_1 helix, and also packs regularly to form crystalline arrangements. In general, increasing crystallinity and order leads to a sharpening and increase in the intensity of some bands in the IR spectra. Accordingly,

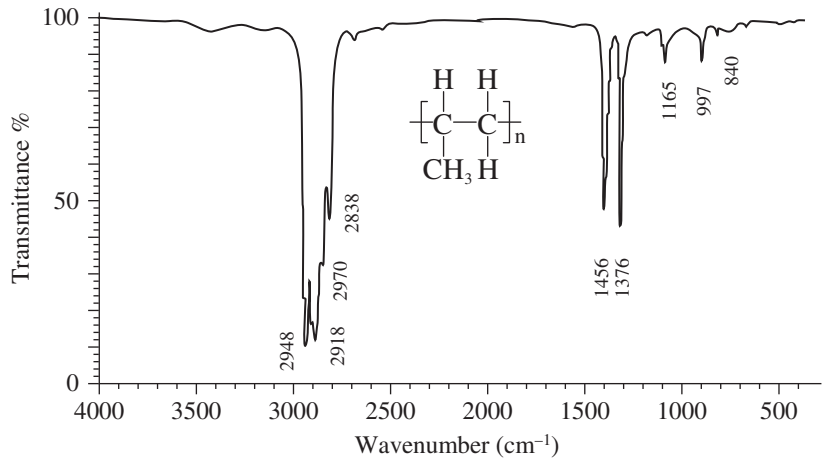

FIGURE 2.15 IR spectrum of isotactic polypropylene.

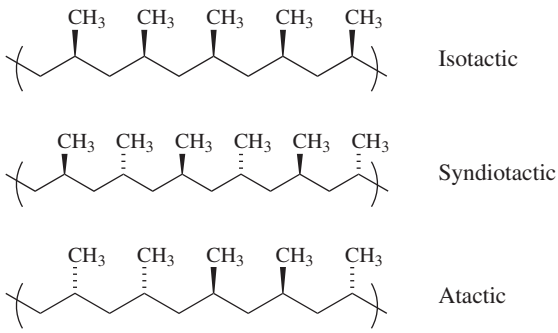

FIGURE 2.16 Stereochemical configurations of polypropylene.

the IR spectra of atactic polymers are similar to those of the amorphous polymer. However, isotactic PP has more pronounced intensity at 1170 cm^{-1}, 998 cm^{-1}, and 841 cm^{-1} compared to atactic forms.

Figure 2.17 shows the IR spectrum of polybutadiene where a $—CH{=}CH_2$ group substitutes for one of the hydrogen atoms of the units of polyethylene. Characteristic bands of the out-of-plane deformation modes of the hydrogen atoms that are attached to the carbon atoms adjacent to the double bonds appear at different positions in the IR spectra. For 1,4-*cis*-polybutadiene, this band is observed at 740 cm^{-1}, but for 1,4 *trans*-polybutadiene it is at 966 cm^{-1}.

2.6.9 Alcohols and Phenols

The characteristic bands observed in the spectra of alcohols and phenols result from O—H stretching and C—O stretching. These vibrations are sensitive to hydrogen bonding. The C—O stretching and O—H bending modes are not independent vibrational modes because they couple with the vibrations of adjacent groups.

2.6.9.1 O—H Stretching Vibrations. The non-hydrogen-bonded or "free" hydroxyl group of alcohols and phenols absorbs strongly in the 3700 cm^{-1} to 3584 cm^{-1} region. These sharp, free hydroxyl bands are observed in the vapor phase, in very dilute solution in nonpolar solvents, or for hindered OH groups. Intermolecular hydrogen bonding increases as the concentration of the solution increases, and additional bands start to appear at lower wavenumbers, 3550 cm^{-1} to 3200 cm^{-1}, at the expense of the free hydroxyl band. This effect is illustrated in Figure 2.18, in which the absorption bands in the O—H stretching region are shown for two different concentrations of cyclohexylcarbinol in carbon tetrachloride. For comparisons of this type, the path length of the cell must be altered with changing concentration, so that the same number of absorbing molecules will be present in the IR beam at each concentration. The band at 3623 cm^{-1} results from the monomer, whereas the broad absorption near 3333 cm^{-1} arises from "polymeric" structures.

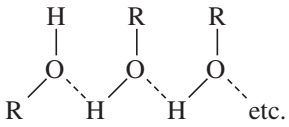

Strong intramolecular hydrogen bonding occurs in *o*-hydroxyacetophenone. The resulting absorption at 3077 cm^{-1} is broad, shallow, and independent of concentration (Figure 2.19).

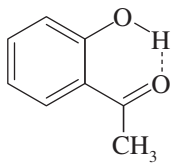

In contrast, *p*-hydroxyacetophenone

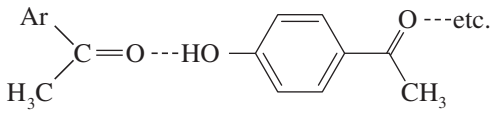

shows a sharp free hydroxy peak at 3600 cm^{-1} in dilute CCl_4 solution as well as a broad, strong intermolecular peak at 3100 cm^{-1} in the spectrum of a neat sample. In structures such as 2,6-di-*t*-butylphenol, in which steric hindrance prevents hydrogen bonding, no bonded hydroxyl band is observed, not even in spectra of neat samples.

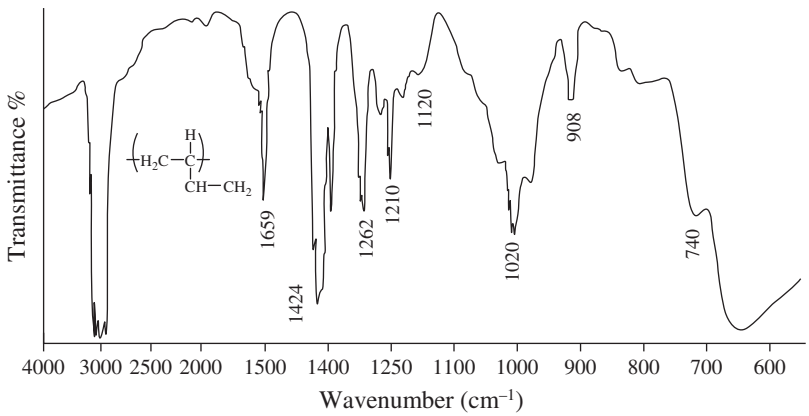

FIGURE 2.17 IR spectrum of 1,4-*cis*-polybutadiene.

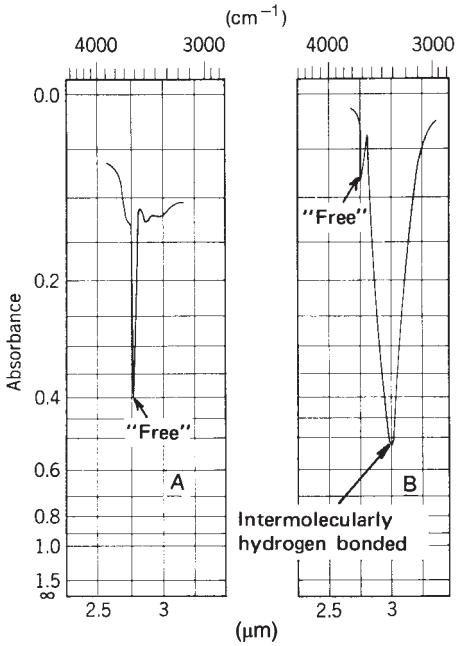

FIGURE 2.18 Infrared spectrum of the OH stretching region of cyclohexylcarbinol in CCl_4. Peak A at 0.03 *M* (0.406 mm cell); Peak B at 1.00 *M* (0.014 mm cell).

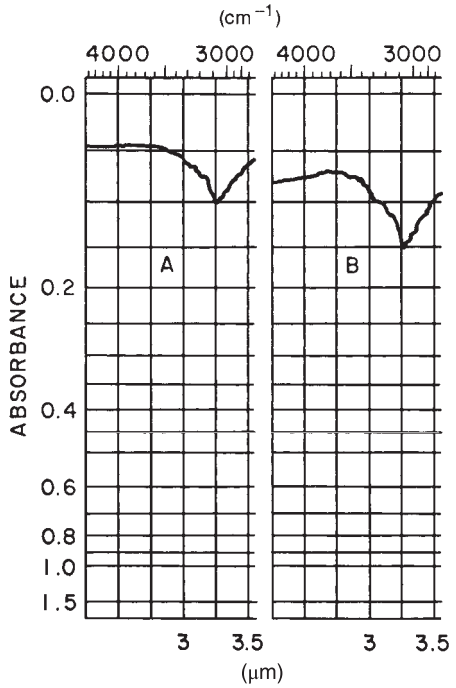

FIGURE 2.19 A portion of the IR spectra of *o*-hydroxyacetophenone. Peak A at 0.03 *M*, cell thickness: 0.41 mm. Peak B at 1.0 *M*, cell thickness: 0.015 mm.

2.6.9.2 C—O Stretching Vibrations. The C—O stretching vibrations in alcohols (Figures 2.20 and 2.22) and phenols (Figure 2.21) produce a strong band in the 1260 cm^{-1} –1000 cm^{-1} region of the spectrum.

The C—O stretching mode is coupled with the adjacent C—C stretching vibration; thus, in primary alcohols, the vibration might better be described as an asymmetric C—C—O stretching vibration. The vibrational mode is further complicated by branching and α,β-unsaturation. These effects are summarized in Table 2.4 for a series of secondary alcohols (neat samples).

The absorption ranges of the various types of alcohols are provided in Table 2.5. These values are for neat samples of the alcohols.

Mulls, pellets, or melts of phenols absorb at 1390 cm^{-1} to 1330 cm^{-1} and 1260 cm^{-1} to 1180 cm^{-1}. These bands apparently result from an interaction between O—H bending and C—O stretching. The long-wavelength band is the stronger one and both bands appear at longer wavelengths in spectra observed in solution. The spectrum of phenol in Figure 2.21 was determined on a melt to show a high degree of association.

2.6.9.3 O—H Bending Vibrations. The O—H in-plane bending vibration occurs in the general region of 1420 cm^{-1} to 1330 cm^{-1}. In primary and secondary alcohols, the O—H in-plane bending couples with the C—H wagging vibrations to produce two bands: the first near 1420 cm^{-1} and the second near 1330 cm^{-1}. These bands are of little diagnostic value. Tertiary alcohols, in which no coupling can occur, show a single band in this region, the position depending on the degree of hydrogen bonding (Figure 2.22).

The spectra of alcohols and phenols determined in the liquid state show a broad absorption band in the 769 cm^{-1} to 650 cm^{-1} region because of out-of-plane bending of the bonded O—H group.

2.6.10 Ethers, Epoxides, and Peroxides

2.6.10.1 C—O Stretching Vibrations. The characteristic response of ethers in the IR is associated with the stretching vibration of the C—O—C system. Since the vibrational characteristics of this system would not be expected to differ greatly from the C—C—C system, it is not surprising to find the response to C—O—C stretching in the same general region. However, since vibrations involving oxygen atoms result in greater dipole moment changes than those involving carbon atoms, more intense IR bands are observed for ethers. The C—O—C stretching bands of ethers, as is the case with the C—O stretching bands of alcohols, involve coupling with other vibrations within the molecule. The spectrum of anisole in Figure 2.23 is that of a typical aryl alkyl ether.

In the spectra of aliphatic ethers, the most characteristic absorption is a strong band in the 1150 cm^{-1} to 1085 cm^{-1} region because of asymmetrical C—O—C stretching; this band usually occurs near 1125 cm^{-1}. The symmetrical stretching band is usually weak and is more readily observed in the Raman spectrum.

The C—O—C group in a six-membered ring absorbs at the same frequency as in an acyclic ether. As the ring becomes smaller, the asymmetrical C—O—C stretching vibration moves progressively to lower wavenumbers (longer wavelengths), whereas the symmetrical C—O—C stretching vibration (ring breathing frequency) moves to higher wavenumbers.

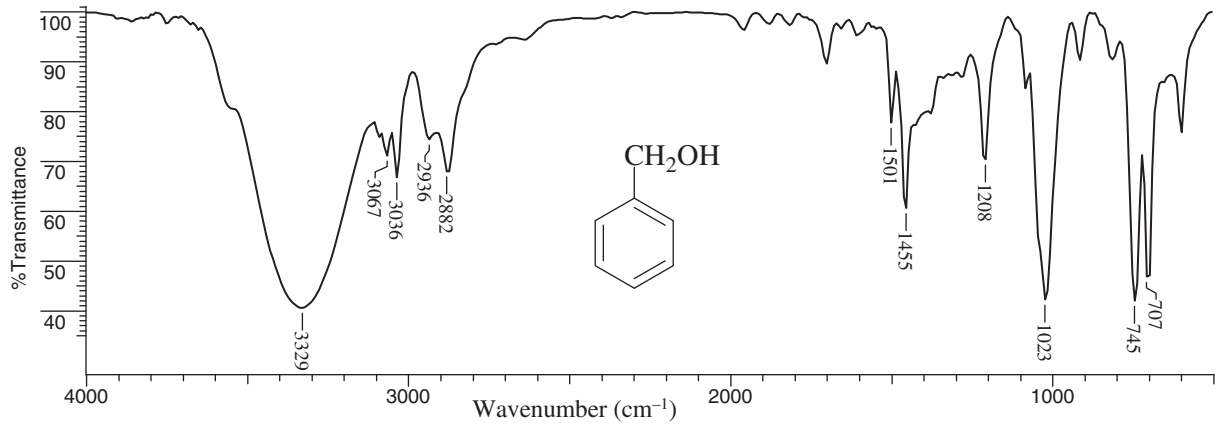

FIGURE 2.20 Benzyl alcohol. O—H stretch: intermolecular hydrogen bonded, 3329 cm^{-1}. C—H stretch: aromatic 3100 cm^{-1} to 3000 cm^{-1}. C—H stretch: methylene, 2940 cm^{-1} to 2860 cm^{-1}. Overtone or combination bands, 2000 cm^{-1} to 1667 cm^{-1}. C=C ring stretch, 1501 cm^{-1}, 1455 cm^{-1}, overlapped by CH_2 scissoring, about 1471 cm^{-1}. O—H bend, possibly augmented by C—H in-plane bend, 1209 cm^{-1}. C—O stretch, primary alcohol (see Table 2.5) 1023 cm^{-1}. Out-of-plane aromatic C—H bend, 745 cm^{-1}. Ring C—C bend, 707 cm^{-1}.

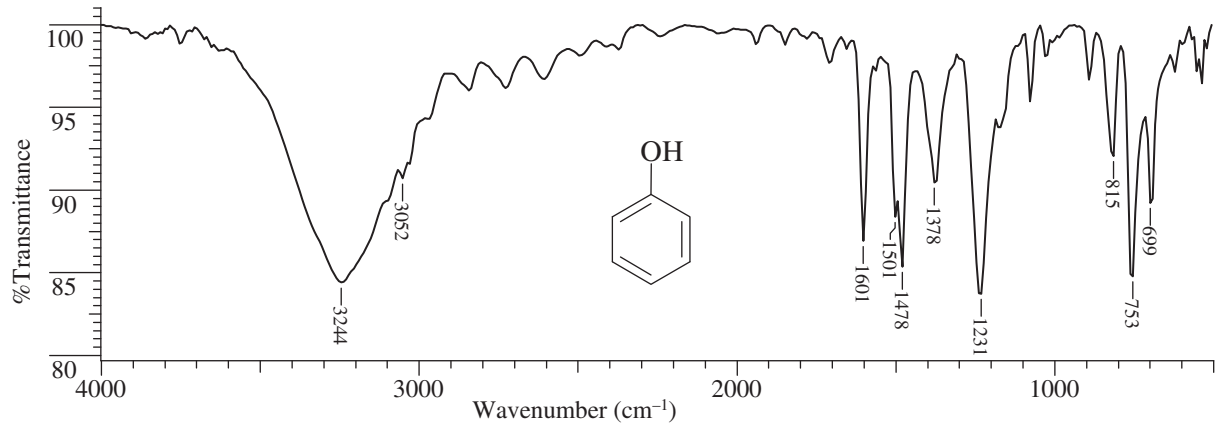

FIGURE 2.21 Phenol (melt). Broad intermolecular hydrogen bonded, O—H stretch, 3244 cm^{-1}. Aromatic C—H stretch, 3052 cm^{-1}. Overtone or combination bands, 2000 cm^{-1} to 1667 cm^{-1}. C—C ring stretch, 1601, 1501, 1478 cm^{-1}. In-plane O—H bend, 1378 cm^{-1}. C—O stretch, 1231 cm^{-1}. Out-of-plane C—H bend, 815, 753 cm^{-1}. Out-of-plane ring C—C bend, 699 cm^{-1}. (Broad) hydrogen-bonded, out-of-plane O—H bend, about 650 cm^{-1}.

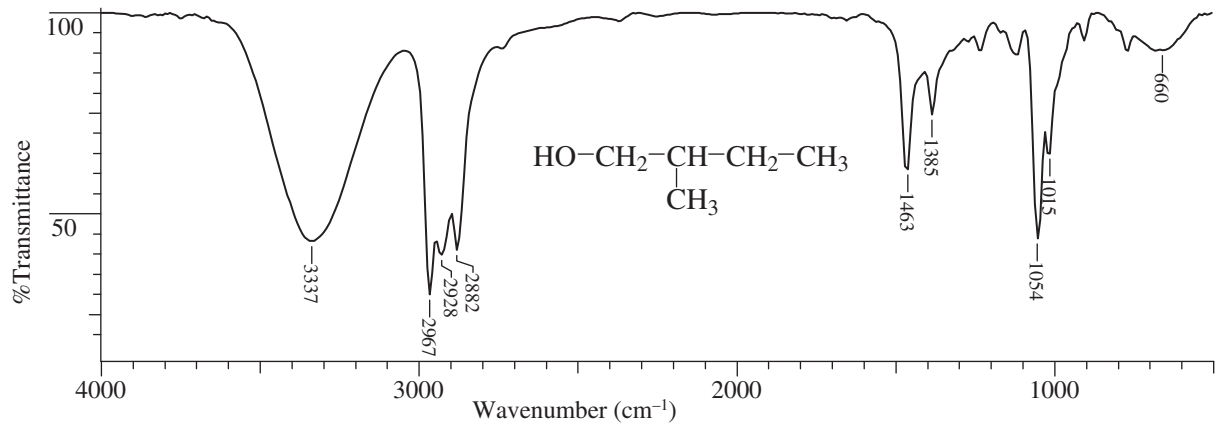

FIGURE 2.22 2-Methyl-1-butanol. O—H stretch, intermolecular hydrogen bonding 3337 cm^{-1}. C—H stretch (3000 – 2800 cm^{-1}). C—H bend (see Figure 2.8). C—O stretch 1054 cm^{-1}.

TABLE 2.4 C—C—O Stretching Vibrations of Secondary Alcohols

Secondary Alcohol	Absorption (cm^{-1})
2-Butanol	1105
3-Methyl-2-butanol	1091
1-Phenylethanol	1073
3-Buten-2-ol	1058
Diphenylmethanol	1014

TABLE 2.5 Alcoholic C—O Stretch Absorptions

Alcohol Type	Absorption Range (cm^{-1})
(1) Saturated tertiary	
(2) Secondary, highly symmetrical	1205 – 1124
(1) Saturated secondary	
(2) α-Unsaturated or cyclic tertiary	1124 – 1087
(1) Secondary, α-unsaturated	
(2) Secondary, alicyclic five- or six-membered ring	1085 – 1050
(3) Saturated primary	
(1) Tertiary, highly α-unsaturated	
(2) Secondary, di-α-unsaturated	
(3) Secondary, α-unsaturated and α-branched	
(4) Secondary, alicyclic seven- or eight-membered ring	<1050
(5) Primary, α-unsaturated and/or α-branched	

Branching on the carbon atoms adjacent to the oxygen usually leads to splitting of the C—O—C band. Isopropyl ether shows a triplet structure in the 1170 cm^{-1} to 1114 cm^{-1} region with the principal band occurring at 1114 cm^{-1}.

Spectra of aryl alkyl ethers display an asymmetrical C—O—C stretching band at 1275 cm^{-1} to 1200 cm^{-1} with symmetrical stretching near 1075 cm^{-1} to 1020 cm^{-1}. Strong absorption caused by asymmetrical C—O—C stretching in vinyl ethers occurs in the 1225 cm^{-1} to 1200 cm^{-1} region with a strong symmetrical band at 1075 cm^{-1} to 1020 cm^{-1}. Resonance structures can account for the shift in the asymmetric absorption band of arylalkyl and vinyl ethers.

The C═C stretching band of vinyl ethers occurs in the 1660 cm^{-1} to 1610 cm^{-1} region. This alkene band is characterized by its higher intensity compared with the C═C stretching band in alkenes. This band frequently appears as a doublet resulting from absorption of rotational isomers.

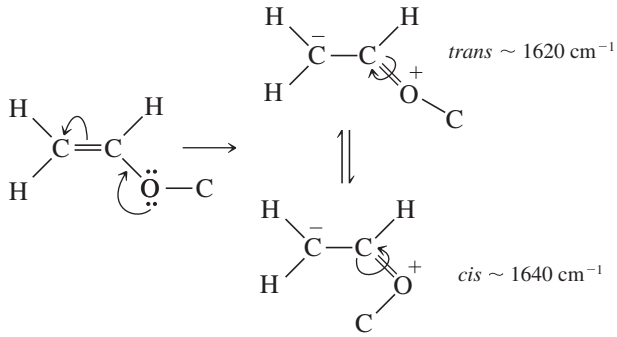

Coplanarity in the *trans*-isomer allows maximum resonance, thus more effectively reducing the double-bond character of the alkene linkage. Steric hindrance reduces resonance in the *cis*-isomer.

The two bands arising from ═C—H wagging in terminal alkenes occur near 1000 cm^{-1} and 909 cm^{-1}. In the spectra of vinyl ethers, these bands are shifted to longer wavelengths because of resonance.

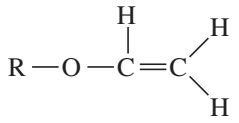

terminal CH_2 wag, 813 cm^{-1}
trans CH wag, 960 cm^{-1}

Alkyl and aryl peroxides display C—C—O absorption in the 1198 cm^{-1} to 1176 cm^{-1} region. Acyl and aroyl peroxides display two carbonyl absorption bands in the 1818 cm^{-1} to 1754 cm^{-1} region. Two bands are observed because

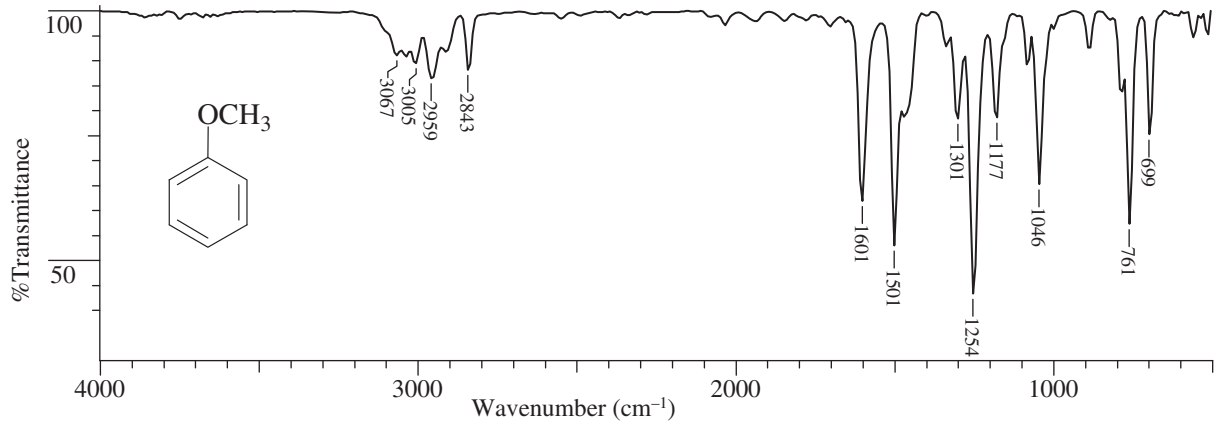

FIGURE 2.23 Anisole. Aromatic C—H stretch, 3067, 3030, 3005 cm^{-1}. Methyl C—H stretch, 2950, 2843 cm^{-1}. Overtone-combination region, 2000 cm^{-1} to 1650 cm^{-1}. C—C ring stretch, 1601, 1501 cm^{-1}. Asymmetric C—O—C stretch, 1254 cm^{-1}. Symmetric C—O—C stretch, 1046 cm^{-1}. Out-of-plane C—H bend, 784, 761 cm^{-1}. Out-of-plane ring C═O bend, 699 cm^{-1}.

of mechanical interaction between the stretching modes of the two carbonyl groups.

The symmetrical stretching, or ring breathing frequency, of the epoxy ring, with all ring bonds stretching and contracting in phase, occurs near 1250 cm^{-1}. Another band appears in the 950 cm^{-1} to 810 cm^{-1} region and is attributed to asymmetrical ring stretching in which the C—C bond is stretching during contraction of the C—O bond. A third band, referred to as the "12 micron band," appears in the 840 cm^{-1} to 750 cm^{-1} region. The C—H stretching vibrations of epoxy rings occur in the 3050 cm^{-1} to 2990 cm^{-1} region of the spectrum.

2.6.11 Ketones

2.6.11.1 C═O Stretching Vibrations. Ketones, aldehydes, carboxylic acids, carboxylic esters, lactones, acid halides, anhydrides, amides, and lactams show a strong C═O stretching absorption band in the region of 1870 cm^{-1} to 1540 cm^{-1}. Its relatively constant position, high intensity, and relative freedom from interfering bands make this one of the easiest bands to recognize in IR spectra.

Within its given range, the position of the C═O stretching band is determined by the following factors: (i) the physical state, (ii) electronic and mass effects of neighboring substituents, (iii) conjugation, (iv) hydrogen bonding (intermolecular and intramolecular), and (v) ring strain. Consideration of these factors leads to a considerable amount of information about the environment of the C═O group.

In a discussion of these effects, it is customary to refer to the absorption wavenumber of a neat sample of a saturated aliphatic ketone, 1715 cm^{-1}, as "normal." For example, acetone and cyclohexanone absorb at 1715 cm^{-1}. Changes in the environment of the carbonyl can either lower or raise the absorption wavenumber from this "normal" value. A typical ketone spectrum is displayed in Figure 2.24.

The absorption wavenumber observed for a neat sample is increased when absorption is observed in nonpolar solvents. Polar solvents reduce the wavenumber of absorption. The overall range of solvent effects does not exceed 25 cm^{-1}.

Replacement of an alkyl group of a saturated aliphatic ketone by a heteroatom (G) shifts the carbonyl absorption. The direction of the shift depends on whether the inductive effect (a) or resonance effect (b) predominates.

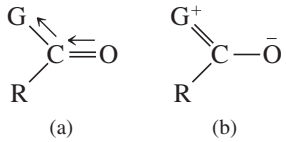

The inductive effect reduces the length of the C═O bond and thus increases its force constant and the frequency of absorption. The resonance effect increases the C═O bond length and reduces the frequency of absorption.

The absorptions of several carbonyl compound classes are summarized in Table 2.6.

Conjugation with a C═C bond results in delocalization of the π electrons of both unsaturated groups. Delocalization of the π electrons of the C═O group reduces the double-bond character of the C—O bond, causing absorption at lower wavenumbers (longer wavelengths). Conjugation with an alkene or phenyl group causes absorption in the

TABLE 2.6 The Carbonyl Absorption of Various RC(═O)G Compounds

G Effect Predominantly Inductive	
G	**νC═O (cm^{-1})**
Cl	1815 to 1785
F	~1869
Br	1812
OH (monomer)	1760
OR	1750 to 1735
G Effect Predominantly Resonance	
G	**νC═O (cm^{-1})**
NH_2	1695 – 1650
SR	1720 – 1690

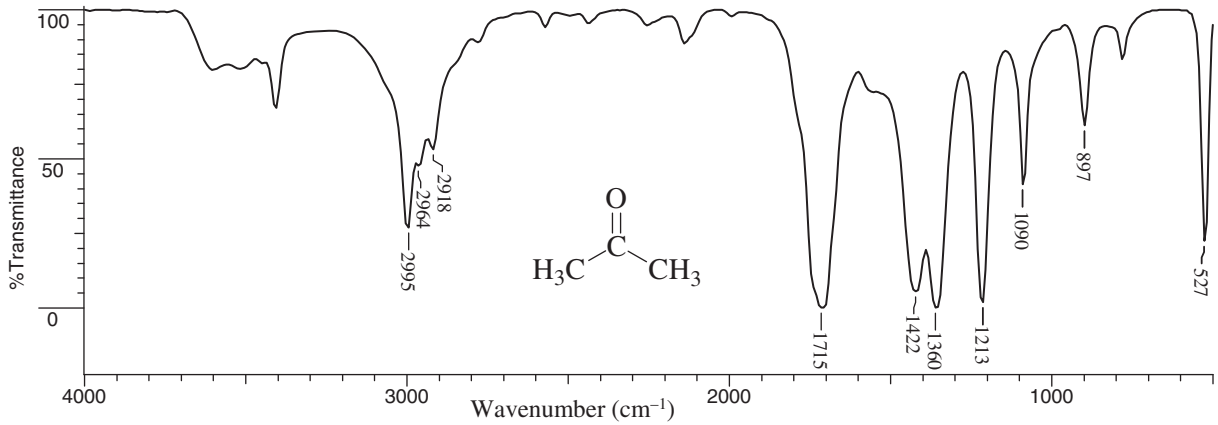

FIGURE 2.24 Acetone. ν_{as}, Methyl, 2995 cm^{-1}. ν_{as}, Methylene, 2964 cm^{-1}. ν_s, Methyl, 2918 cm^{-1}. Normal C═O stretch, 1715 cm^{-1}. δ_{as}, CH_3 1422 cm^{-1}. δ_s, CH_3 1360 cm^{-1}. C—CO—C stretch and bend, 1213 cm^{-1}.

1685 cm^{-1} to 1666 cm^{-1} region. Additional conjugation may cause a slight further reduction in wavenumber. This conjugation effect is illustrated in Figure 2.25.

Steric effects that reduce the coplanarity of the conjugated system reduce the effect of conjugation. In the absence of steric hindrance, a conjugated system will tend toward a planar conformation. Thus, α,β-unsaturated ketones may exist in *s-cis* and *s-trans* conformations. When both forms are present, absorption for each of the forms is observed. The absorption of benzalacetone in CS_2 serves as an example; both the *s-cis* and *s-trans* forms are present at room temperature.

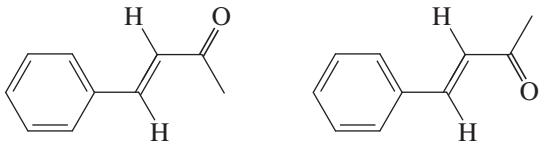

s-trans 1674 cm^{-1} *s-cis* 1699 cm^{-1}

The absorption of the alkene bond in conjugation with the carbonyl group occurs at a lower wavenumber than that of an isolated C═C bond; the intensity of the conjugated double bond absorption, when in an *s-cis* system, is greater than that of an isolated double bond.

Intermolecular hydrogen bonding between a ketone and a hydroxylic solvent such as methanol causes a slight decrease in the wavenumber of the carbonyl group. For example, a neat sample of ethyl methyl ketone absorbs at 1715 cm^{-1}, whereas a 10% solution of the ketone in methanol absorbs at 1706 cm^{-1}.

β-Diketones usually exist as mixtures of tautomeric keto and enol forms. The enolic form does not show the normal absorption of conjugated ketones. Instead, a broadband appears in the 1640 cm^{-1} to 1580 cm^{-1} region, many times more intense than a normal carbonyl absorption. The intense and displaced absorption results from intramolecular hydrogen bonding, with the bonded structure being stabilized by resonance.

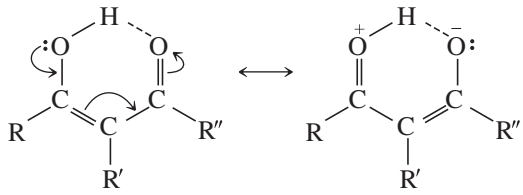

Acetylacetone as a liquid at 40°C exists about 64% in the enolic form that absorbs at 1613 cm^{-1}. The keto form and a small amount of unbonded enolic form may be responsible for two bands centered near 1725 cm^{-1}. Interaction between the two carbonyl groups in the keto form was suggested as a cause for this doublet. The enolic O—H stretching absorption is seen as a broad shallow band at 3000 cm^{-1} to 2700 cm^{-1}.

α-Diketones, in which carbonyl groups exist in formal conjugation, show a single absorption band near the frequency observed for the corresponding monoketone. Biacetyl absorbs at 1718 cm^{-1} and benzil absorbs at 1681 cm^{-1}. Conjugation is ineffective for α-diketones and the C═O groups of these diketones do not couple as do, for example, the corresponding groups in acid anhydrides (see Section 2.6.17).

Quinones, which have both carbonyl groups in the same ring, absorb in the 1690 cm^{-1} to 1655 cm^{-1} region. With extended conjugation, in which the carbonyl groups appear in different rings, the absorption shifts to the 1655 cm^{-1} to 1635 cm^{-1} region.

Acyclic α-chloroketones absorb at two frequencies because of rotational isomerism. When the chlorine atom is near the oxygen, its negative field repels the nonbonding electrons of the oxygen atom, thus increasing the force constant of the C═O bond. This conformation absorbs at a higher wavenumber (1745 cm^{-1}) than that in which the carbonyl oxygen and chlorine atom are widely separated (1725 cm^{-1}). In rigid molecules such as the monoketo steroids, α-halogenation results in equatorial or axial substitution. In the equatorial orientation, the halogen atom is near the carbonyl group and the "field effect" causes an increase

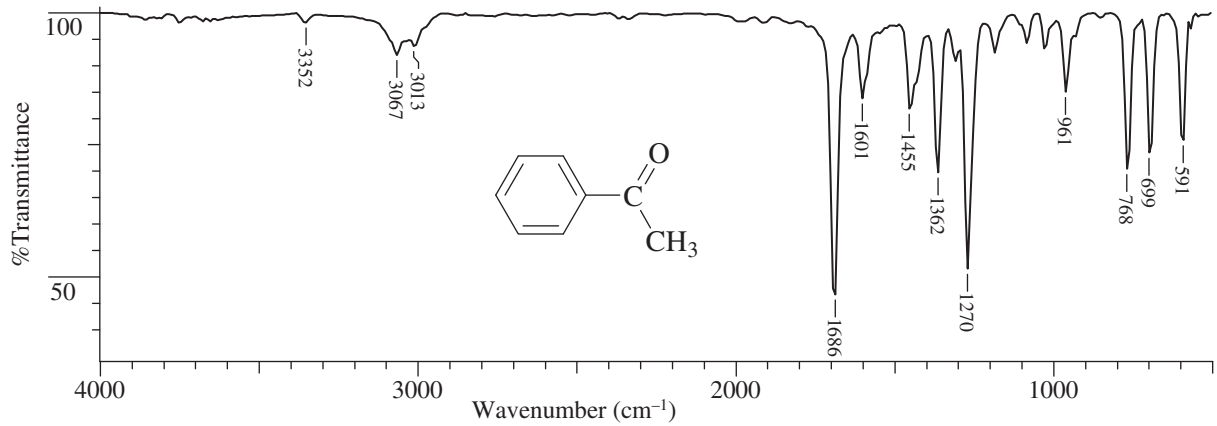

FIGURE 2.25 Acetophenone. Overtone of C═O stretch 3352 cm^{-1}; frequency about twice that of C═O stretch. C═O stretch, 1686 cm^{-1}, lower frequency than observed in Figure 2.24 because of the conjugation with the phenyl group.

in the C═O stretching frequency. In the isomer in which the halogen atom is axial to the ring, and distant from the C═O, no shift is observed.

In cyclic ketones, the C—C—C bond angle of the C—(C═O)—C group influences the absorption frequency of the carbonyl group. The C═O stretching undoubtedly is affected by adjacent C—C stretching. In acyclic ketones and in ketones with a six-membered ring, the angle is near 120°. In strained rings in which the angle is <120°, interaction with C—C bond stretching increases the energy required to produce C═O stretching and thus increases the stretching frequency. Cycloheptanone absorbs at 1709 cm^{-1}, cyclohexanone absorbs at 1715 cm^{-1}, cyclopentanone absorbs at 1751 cm^{-1}, and cyclobutanone absorbs at 1775 cm^{-1}.

2.6.11.2 C—C(═O)—C Stretching and Bending Vibrations. Ketones show moderate absorption in the 1300 cm^{-1} to 1100 cm^{-1} region as a result of C—C—C stretching and C—C(═O)—C bending in the C—C—C group. The absorption may consist of multiple bands. Aliphatic ketones absorb in the 1230 cm^{-1} to 1100 cm^{-1} region; aromatic ketones absorb at the higher frequency end of the general absorption region.

2.6.12 Aldehydes

The spectrum of octanal, illustrating typical aldehydic absorption characteristics, is shown in Figure 2.26.

2.6.12.1 C═O Stretching Vibrations. The carbonyl groups of aldehydes absorb at slightly higher frequencies than those of the corresponding methyl ketones. Aliphatic aldehydes absorb near 1740 cm^{-1} to 1720 cm^{-1}. Aldehydic carbonyl absorption responds to structural changes in the same manner as ketones. Electronegative substitution on the α-carbon increases the frequency of carbonyl absorption. Acetaldehyde absorbs at 1730 cm^{-1} and trichloroacetaldehyde absorbs at 1768 cm^{-1}. Conjugate unsaturation, as in α,β-unsaturated aldehydes and benzaldehydes, reduces the frequency of carbonyl absorption. α,β-Unsaturated aldehydes and benzaldehydes absorb in the region of 1710 cm^{-1} to 1685 cm^{-1}. Internal hydrogen bonding, such as occurs in salicylaldehyde, shifts the absorption to lower wavenumbers (1666 cm^{-1} for salicylaldehyde). Glyoxal, like the α-diketones, shows only one carbonyl absorption peak with no shift from the normal absorption position of monoaldehydic absorption.

2.6.12.2 C—H Stretching Vibrations. The majority of aldehydes show aldehydic C—H stretching absorption in the 2830 cm^{-1} to 2695 cm^{-1} region. Two moderately intense bands are frequently observed in this region. The appearance of two bands is attributed to Fermi resonance between the fundamental aldehydic C—H stretch and the first overtone of the aldehydic C—H bending vibration that usually appears near 1390 cm^{-1}. Only one C—H stretching band is observed for aldehydes, whose C—H bending band has been shifted appreciably from 1390 cm^{-1}.

Some aromatic aldehydes with strongly electronegative groups in the *ortho* position may absorb as high as 2900 cm^{-1}.

The absorption of medium intensity near 2720 cm^{-1}, accompanied by a carbonyl absorption band, is good evidence for the presence of an aldehyde group.

2.6.13 Carboxylic Acids

2.6.13.1 O—H Stretching Vibrations. In the liquid or solid state, and in CCl_4 solution at concentrations much over 0.01 M, carboxylic acids exist as dimers due to strong hydrogen bonding.

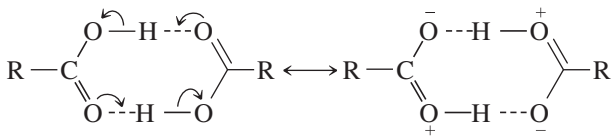

The exceptional strength of the hydrogen bonding is explained on the basis of the large contribution of the ionic resonance structure. Because of the strong bonding, a free hydroxyl stretching vibration (near 3520 cm^{-1}) is observed

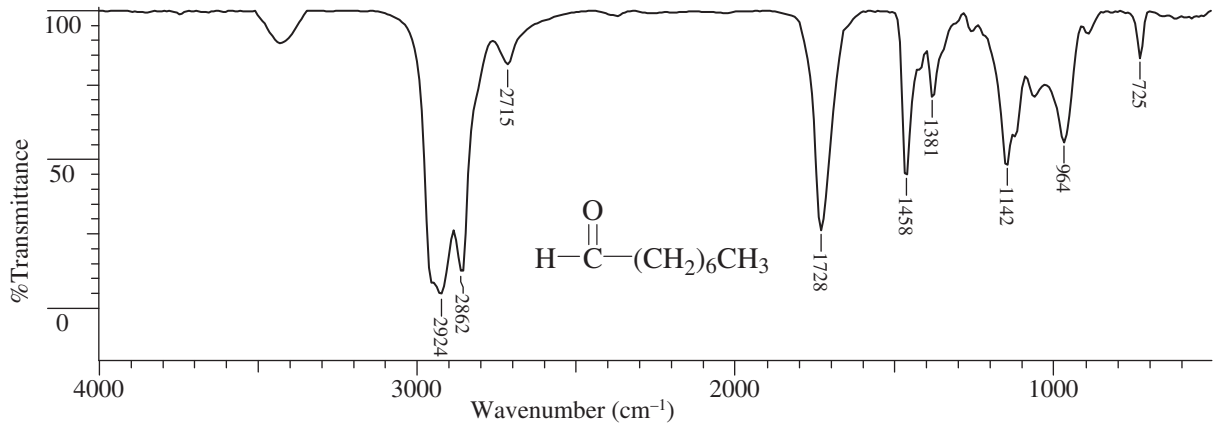

FIGURE 2.26 Octanal. Aliphatic, 2980 cm^{-1} to 2860 cm^{-1} (see Figure 2.8). Aldehydic, C—H stretch, 2715 cm^{-1}. Normal aldehydic C═O stretch, 1728 cm^{-1}. Aldehydic C—H bend, 1381 cm^{-1}.

only in very dilute solution in nonpolar solvents or in the vapor phase.

Carboxylic acid dimers display very broad, intense O—H stretching absorptions in the region of 3300 cm^{-1} to 2500 cm^{-1}. The band is usually centered near 3000 cm^{-1}. The weaker C—H stretching bands are generally seen superimposed upon the broad O—H band. Fine structure observed on the long-wavelength side of the broad O—H band represents overtones and combination tones of fundamental bands occurring at longer wavelengths. The spectrum of a typical aliphatic carboxylic acid is displayed in Figure 2.27.

Other structures with strong hydrogen bonding, such as β-diketones, also absorb in the 3300 cm^{-1} to 2500 cm^{-1} region, but the absorption is usually less intense. Also, the C═O stretching vibrations of structures such as β-diketones are shifted to lower frequencies than those observed for carboxylic acids.

Carboxylic acids can bond intermolecularly with ethers, such as dioxane and tetrahydrofuran, or with other solvents that can act as proton acceptors. Spectra determined in such solvents show bonded O—H absorption near 3100 cm^{-1}.

2.6.13.2 C═O Stretching Vibrations. The C═O stretching bands of acids are considerably more intense than ketonic C═O stretching bands. The monomers of saturated aliphatic acids absorb near 1760 cm^{-1}.

The carboxylic dimer has a center of symmetry; only the asymmetrical C═O stretching mode absorbs in the IR. Hydrogen bonding and resonance weaken the C═O bond, resulting in absorption at a lower frequency than the monomer. The C═O group in dimerized saturated aliphatic acids absorbs in the region of 1720 cm^{-1} to 1706 cm^{-1}.

Internal hydrogen bonding reduces the frequency of the carbonyl stretching absorption to a greater degree than does intermolecular hydrogen bonding. For example, salicylic acid absorbs at 1665 cm^{-1}, whereas *p*-hydroxybenzoic acid absorbs at 1680 cm^{-1}.

Unsaturation in conjugation with the carboxylic carbonyl group decreases the frequency (increases the wavelength) of absorption of both the monomer and dimer forms only slightly. In general, α,β-unsaturated and aryl conjugated acids show absorption for the dimer in the 1710 cm^{-1} to 1680 cm^{-1} region. Extension of conjugation beyond the α,β-position results in very little additional shifting of the C═O absorption.

Substitution in the α-position with electronegative groups, such as the halogens, brings about a slight increase in the C═O absorption wavenumber (10 cm^{-1} to 20 cm^{-1}). The spectra of acids with halogens in the α-position, determined in the liquid state or in solution, show dual carbonyl bands resulting from rotational isomerism (field effect). The higher frequency band corresponds to the conformation in which the halogen is in proximity to the carbonyl group.

2.6.13.3 C—O Stretching and O—H Bending Vibrations. Two bands arising from C—O stretching and O—H bending appear in the spectra of carboxylic acids near 1320 cm^{-1} to 1210 cm^{-1} and 1440 cm^{-1} to 1395 cm^{-1}, respectively. Both of these bands involve some interaction between C—O stretching and in-plane C—O—H bending. The more intense band, near 1315 cm^{-1} to 1280 cm^{-1} for dimers, is generally referred to as the C—O stretching band and usually appears as a doublet in the spectra of long-chain fatty acids. The C—O—H bending band at 1440 cm^{-1} to 1395 cm^{-1} is of moderate intensity and occurs in the same region as the CH_2 scissoring vibration of the CH_2 group adjacent to the carbonyl.

One of the characteristic bands in the spectra of dimeric carboxylic acids results from the out-of-plane bending of the bonded O—H. The band appears near 920 cm^{-1} and is characteristically broad with medium intensity.

2.6.14 Carboxylate Anion

The carboxylate anion has two strongly coupled C---O bonds with bond strengths intermediate between C═O and C—O.

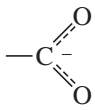

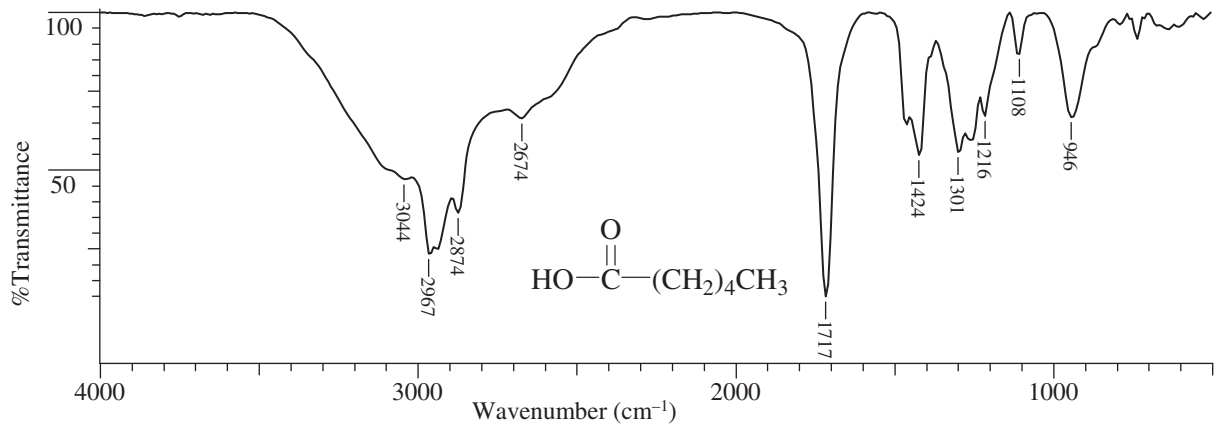

FIGURE 2.27 Hexanoic acid. Broad O—H stretch, 3300 cm^{-1} to 2500 cm^{-1}. C—H stretch (see Figure 2.8), 2967, 2874, 2855 cm^{-1}. Superimposed upon O—H stretch. Normal, dimeric carboxylic C═O stretch, 1717 cm^{-1}. C—O—H in-plane bend, 1424 cm^{-1}. C—O stretch, dimer, 1301 cm^{-1}. O—H out-of-plane bend, 946 cm^{-1}.

The carboxylate ion gives rise to two bands: a strong asymmetrical stretching band near 1650 cm^{-1} to 1550 cm^{-1} and a weaker, symmetrical stretching band near 1400 cm^{-1}.

The conversion of a carboxylic acid to a salt can serve as confirmation of the acid structure. This is conveniently done by the addition of a tertiary aliphatic amine, such as triethylamine, to a solution of the carboxylic acid in chloroform (no reaction occurs in CCl_4). The carboxylate ion thus formed shows the two characteristic carbonyl absorption bands in addition to an ammonium band in the 2700 cm^{-1} to 2200 cm^{-1} region. The O—H stretching band, of course, disappears. The spectrum of ammonium benzoate (Figure 2.28) demonstrates most of these features.

2.6.15 Esters and Lactones

Esters and lactones have two characteristically strong absorption bands arising from C═O and C—O stretching. The intense C═O stretching vibration occurs at higher frequencies (shorter wavelength) than that of normal ketones. The force constant of the carbonyl bond is increased by the electron-attracting nature of the adjacent oxygen atom (inductive effect). Overlapping occurs between esters in which the carbonyl frequency is lowered, and ketones in which the normal ketone frequency is raised. A distinguishing feature of esters and lactones, however, is the strong C—O stretching band in the region where a weaker band occurs for ketones. There is overlapping in the C═O frequencies of esters or lactones and acids, but the OH stretching and bending vibrations and the possibility of salt formation distinguish the acids.

The frequency of the ester carbonyl responds to environmental changes in the vicinity of the carbonyl group in much the same manner as ketones. The spectrum of phenyl acetate illustrates most of the important absorption characteristics for esters (Figure 2.29).

2.6.15.1 C═O Stretching Vibrations. The C═O absorption band of saturated aliphatic esters (except formates) is in the 1750 cm^{-1} to 1735 cm^{-1} region. The C═O absorption

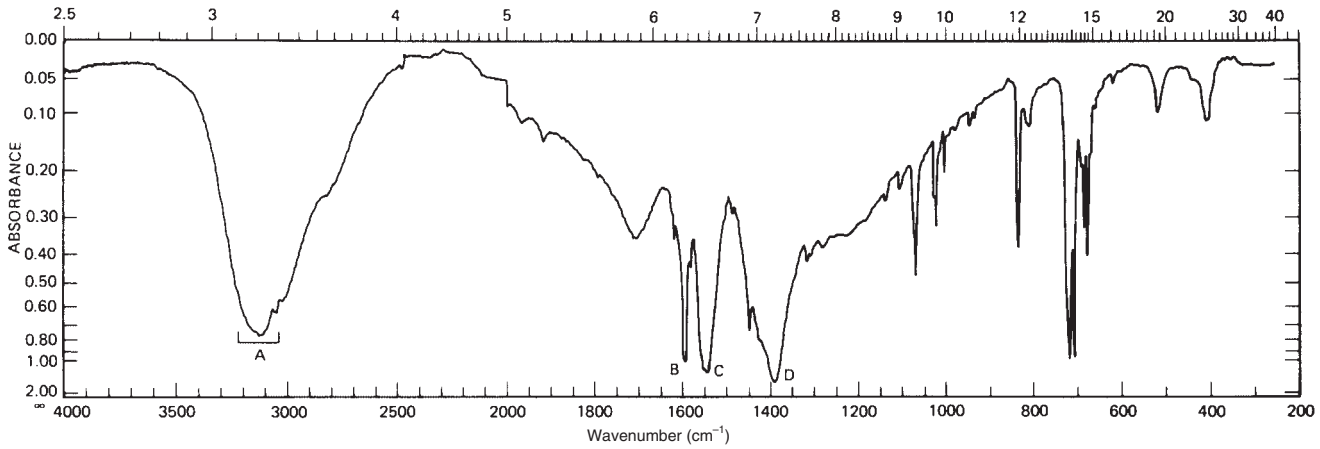

FIGURE 2.28 Benzoic acid, ammonium salt. A. N—H and C—H stretch, 3600 cm^{-1} to 2500 cm^{-1}. B. Ring C—O stretch, 1600 cm^{-1}. C. Asymmetric carboxylate anion $C(-O)_2^-$ stretch, 1550 cm^{-1}. D. Symmetric carboxylate $C(-O)_2^-$ stretch, 1385 cm^{-1}.

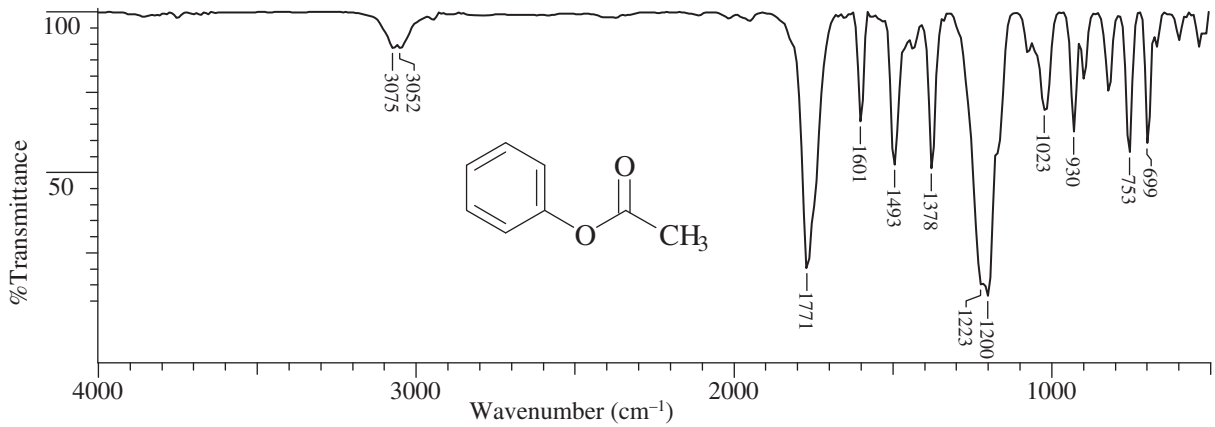

FIGURE 2.29 Phenyl acetate. Aromatic C—H stretch, 3075, 3052 cm^{-1}. C═O stretch, 1771 cm^{-1}: this is higher frequency than that from a normal ester C═O stretch (1740 cm^{-1}: see Table 2.6) because of phenyl conjugation with alcohol oxygen; conjugation of an aryl group or other unsaturation with the carbonyl group causes this C═O stretch to be at lower than normal frequency (e.g., benzoates absorb at about 1724 cm^{-1}). Ring C—C stretch, 1601 cm^{-1}. $\delta_{as}CH_3$, 1493 cm^{-1}, δ_sCH_3, 1378 cm^{-1}. Acetate C(═O)—O stretch, 1223 cm^{-1} O—C—C asymmetrical stretch, 1200 cm^{-1}.

bands of formates and of α,β-unsaturated and benzoate esters are in the region of 1730 cm^{-1} to 1715 cm^{-1}. Further conjugation has little or no additional effect on the frequency of the carbonyl absorption.

In the spectra of vinyl or phenyl esters, with unsaturation adjacent to the C—O— group, a marked rise in the carbonyl frequency is observed along with a lowering of the C—O frequency. Vinyl acetate has a carbonyl band at 1776 cm^{-1}; phenyl acetate absorbs at 1771 cm^{-1}.

α-Halogen substitution results in a rise in the C═O stretching frequency. Ethyl trichloroacetate absorbs at 1770 cm^{-1}.

In oxalates and α-keto esters, as in α-diketones, there appears to be little or no interaction between the two carbonyl groups so that normal absorption occurs in the region of 1755 cm^{-1} to 1740 cm^{-1}. In the spectra of β-keto esters, however, where enolization can occur, a band is observed near 1650 cm^{-1} that results from hydrogen bonding between the ester C═O and the enolic hydroxyl group.

The carbonyl absorption of saturated δ-lactones (six-membered ring) occurs in the same region as straight-chain, unconjugated esters. Unsaturation α to the C═O group

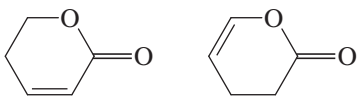

1720 cm^{-1} 1760 cm^{-1}

reduces the C═O absorption frequency. Unsaturation α to the —O— group increases it.

α-Pyrones frequently display two carbonyl absorption bands in the 1775 cm^{-1} to 1715 cm^{-1} region, probably because of Fermi resonance.

Saturated γ-lactones (five-membered ring) absorb at shorter wavelengths than esters or δ-lactones: 1795 cm^{-1} to 1760 cm^{-1}; δ-valerolactone absorbs at 1770 cm^{-1}. Unsaturation in the γ-lactone molecule affects the carbonyl absorption in the same manner as unsaturation in δ-lactones.

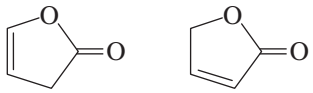

1800 cm^{-1} 1750 cm^{-1}

In unsaturated lactones, when the double bond is adjacent to the —O—, a strong C═C absorption is observed in the 1685 cm^{-1} to 1660 cm^{-1} region.

2.6.15.2 C—O Stretching Vibrations. The C—O stretching vibrations of esters actually consist of two asymmetrical coupled vibrations: C—C(═O)—O and O—C—C, the former being more important. These bands occur in the region of 1300 cm^{-1} to 1000 cm^{-1}. The corresponding symmetric vibrations are of little importance. The C—O stretch correlations are less reliable than the C═O stretch correlations.

The C—C(═O)—O band of saturated esters, except for acetates, is shown strongly in the 1210 cm^{-1} to 1163 cm^{-1} region. It is often broader and stronger than the C═O stretch absorption. Acetates of saturated alcohols display this band at 1240 cm^{-1}. Vinyl and phenyl acetates absorb at a somewhat lower wavenumber, 1190 cm^{-1} to 1140 cm^{-1}; for example, see Figure 2.29. The C—C(═O)—O stretch of esters of α,β-unsaturated acids results in multiple bands in the 1300 cm^{-1} to 1160 cm^{-1} region. Esters of aromatic acids absorb strongly in the 1310 cm^{-1} to 1250 cm^{-1} region. The analogous type of stretch in lactones is observed in the 1250 cm^{-1} to 1111 cm^{-1} region.

The O—C—C band of esters (alcohol carbon–oxygen stretch) of primary alcohols occurs at about 1164 cm^{-1} to 1031 cm^{-1} and that of esters of secondary alcohols occurs at about 1100 cm^{-1}. Aromatic esters of primary alcohols show this absorption near 1111 cm^{-1}.

Methyl esters of long-chain fatty acids present a three-band pattern with bands near 1250, 1205, and 1175 cm^{-1}. The band near 1175 cm^{-1} is the strongest.

2.6.16 Acid Halides

2.6.16.1 C═O Stretching Vibrations. Acid halides show strong absorption in the C═O stretching region. Unconjugated acid chlorides absorb in the 1815 cm^{-1} to 1785 cm^{-1} region. Acetyl fluoride in the gas phase absorbs near 1869 cm^{-1}. Conjugated acid halides absorb at a slightly lower frequency because resonance reduces the force constant of the C═O bond; aromatic acid chlorides absorb strongly at 1800 cm^{-1} to 1770 cm^{-1}. A weak band near 1750 cm^{-1} to 1735 cm^{-1} appearing in the spectra of aroyl chlorides probably results from Fermi resonance between the C═O band and the overtone of a lower wavenumber band near 875 cm^{-1}. The spectrum of a typical aromatic acid chloride is given in Figure 2.30.

2.6.17 Carboxylic Acid Anhydrides

2.6.17.1 C═O Stretching Vibrations. Anhydrides display two stretching bands in the carbonyl region. The two bands result from asymmetrical and symmetrical C═O stretching modes. Saturated acyclic anhydrides absorb near 1818 cm^{-1} and 1750 cm^{-1}. Conjugated acyclic anhydrides show absorption near 1775 cm^{-1} and 1720 cm^{-1}; the decrease in the frequency of absorption may be explained by resonance structures. The higher frequency band is the more intense.

Cyclic anhydrides with five-membered rings show absorption at higher frequencies than acyclic anhydrides because of ring strain; succinic anhydride absorbs at 1865 cm^{-1} and 1782 cm^{-1}. The lower frequency C═O band is the stronger of the two carbonyl bands in five-membered ring cyclic anhydrides.

2.6.17.2 C—O Stretching Vibrations. Other strong bands appear in the spectra of anhydrides as a result of

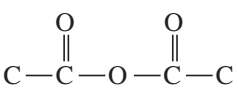

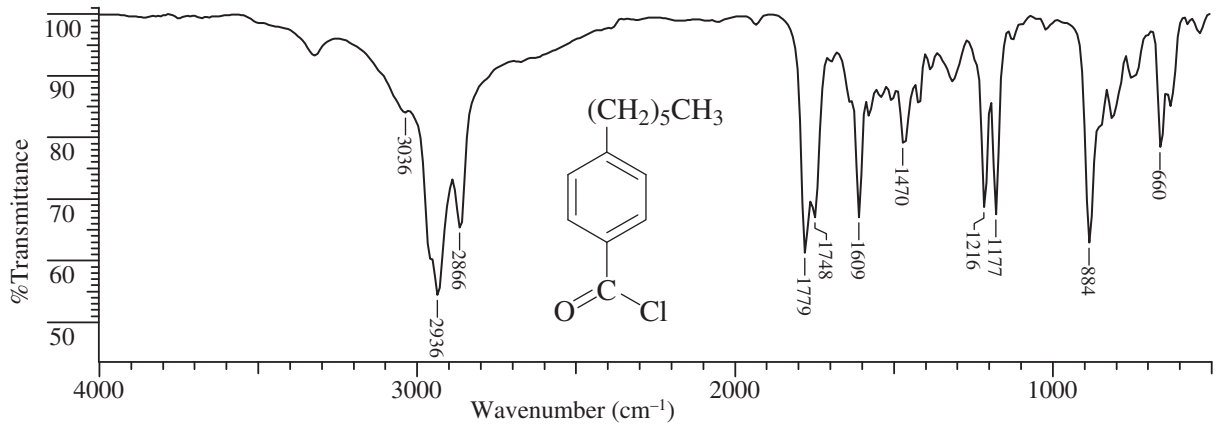

FIGURE 2.30 IR spectrum of 4-hexylbenzoyl chloride. Aromatic C—H stretch, 3036 cm^{-1}. C—H stretch, 2936 cm^{-1} and 2866 cm^{-1}. C═O stretch, 1779 cm^{-1}. Acid chloride C═O stretch wavenumbers show a small dependence on conjugation. Aroyl chlorides can be identified by a Fermi resonance band such as that seen at 1748 cm^{-1} (due to the C═O stretch and the overtone of the 884 cm^{-1} band).

stretching vibrations. Unconjugated straight-chain anhydrides absorb near 1047 cm^{-1}. Cyclic anhydrides display bands near 952 cm^{-1} to 909 cm^{-1} and 1299 cm^{-1} to 1176 cm^{-1}. The C—O stretching band for acetic anhydride is at 1125 cm^{-1}.

The spectrum of benzoic anhydride in Figure 2.31 is that of a typical aromatic anhydride.

2.6.18 Amides and Lactams

All amides show a carbonyl absorption band known as the amide I band. Its position depends on the degree of hydrogen bonding and, thus, on the physical state of the compound.

Primary amides show two N—H stretching bands resulting from symmetrical and asymmetrical N—H stretching. Secondary amides and lactams show only one N—H stretching band. As in the case of O—H stretching, the frequency of the N—H stretching is reduced by hydrogen bonding, though to a lesser degree. Overlapping occurs in the observed position of N—H and O—H stretching frequencies so that an unequivocal differentiation in structure is sometimes impossible.

Primary amides and secondary amides, and a few lactams, display a band or bands in the region of 1650 cm^{-1} to 1515 cm^{-1} caused primarily by NH_2 or NH bending. This is called the amide II band. This absorption involves coupling between N—H bending and other fundamental vibrations and requires a *trans* geometry.

Out-of-plane N—H wagging is responsible for a broadband of medium intensity in the 800 cm^{-1} to 666 cm^{-1} region.

The spectrum of acrylamide in Figure 2.32 is that of a typical primary amide of an unsaturated acid.

2.6.18.1 N—H Stretching Vibrations. In dilute solution in nonpolar solvents, primary amides show two moderately intense N—H stretching frequencies corresponding to the asymmetrical and symmetrical N—H stretching vibrations. These bands occur near 3520 cm^{-1} and 3400 cm^{-1}, respectively. In the spectra of solid samples, these bands are observed near 3350 cm^{-1} and 3180 cm^{-1} because of hydrogen bonding.

In IR spectra of secondary amides, which exist mainly in the *trans* conformation, the free N—H stretching vibration observed in dilute solutions occurs near 3500 cm^{-1} to 3400

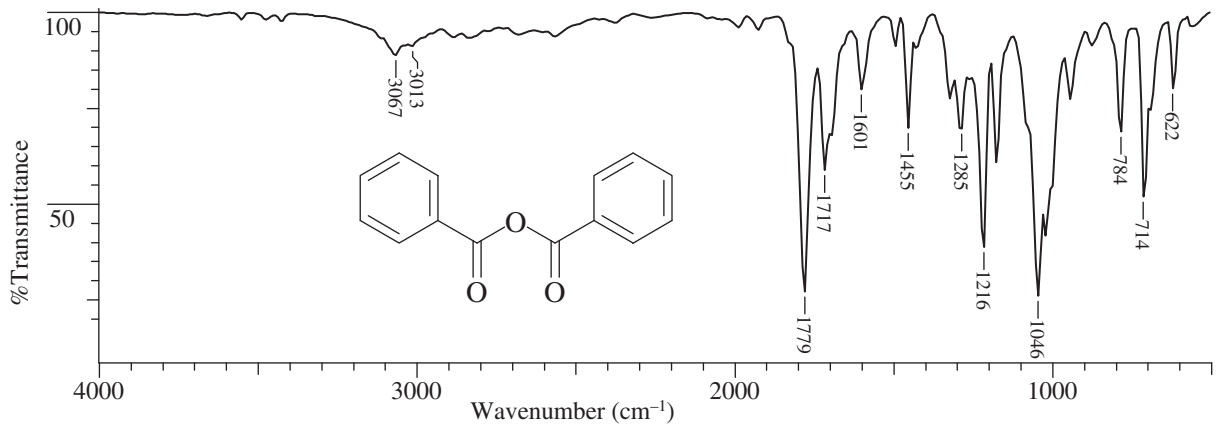

FIGURE 2.31 Benzoic anhydride. Aromatic C—H stretch, 3067, 3013 cm^{-1}. Asymmetric and symmetric C═O coupled stretching, respectively: 1779, 1717 cm^{-1}. See Table 2.6. C—CO—O—CO—C stretch, 1046 cm^{-1}.

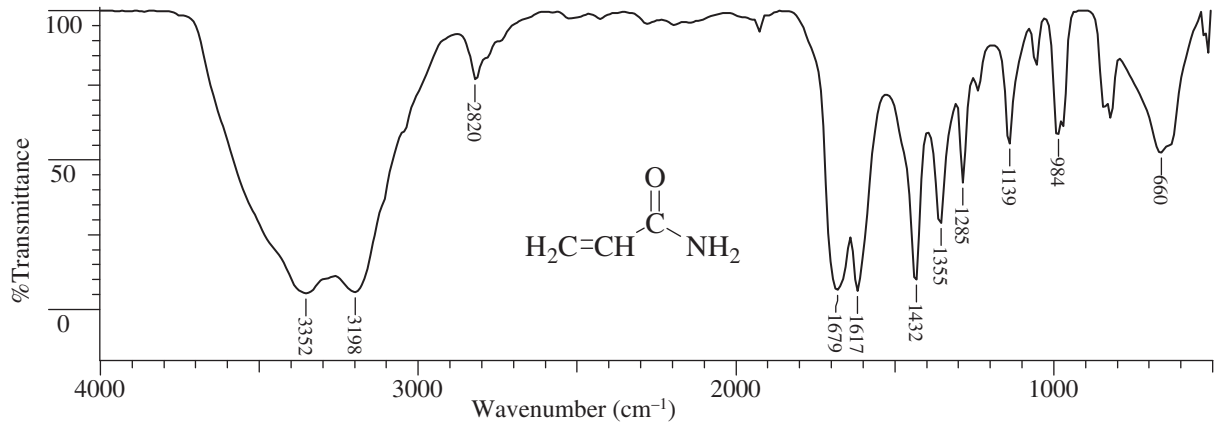

FIGURE 2.32 Acrylamide. N—H stretch, coupled, primary amide, hydrogen bonded; asymmetric, 3352 cm^{-1}; symmetric, 3198 cm^{-1}. Overlap C═O stretch, amide I band, 1679 cm^{-1}; see Table 2.6. N—H bend, amide II band, 1617 cm^{-1}. C—N stretch, 1432 cm^{-1}. Broad N—H out-of-plane bend 700 – 600 cm^{-1}.

cm^{-1}. In more concentrated solutions and in solid samples, the free N—H band is replaced by multiple bands in the 3330 cm^{-1} to 3060 cm^{-1} region. Multiple bands are observed since the amide group can bond to produce dimers with an *s-cis* conformation and polymers with an *s-trans* conformation.

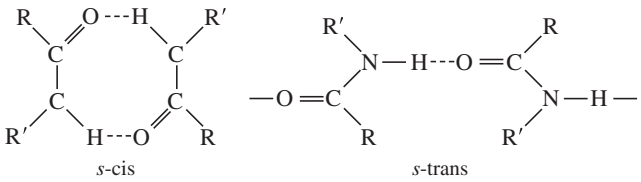

2.6.18.2 C═O Stretching Vibrations (Amide I Band). The C═O absorption of amides occurs at lower frequencies than "normal" carbonyl absorption due to the resonance effect (see Section 2.6.10.1). The position of absorption depends on the same environmental factors as the carbonyl absorption of other compounds.

Primary amides (except acetamide, whose C═O bond absorbs at 1694 cm^{-1}) have a strong amide I band in the region of 1650 cm^{-1} when examined in the solid phase. When the amide is examined in dilute solution, the absorption is observed at a higher wavenumber, near 1690 cm^{-1}. In more concentrated solutions, the C═O wavenumber is observed at some intermediate value, depending on the degree of hydrogen bonding.

Simple, open-chain, secondary amides absorb near 1640 cm^{-1} when examined in the solid state. In dilute solution, the wavenumber of the amide I band may be raised to 1680 cm^{-1} and even to 1700 cm^{-1} in the case of the anilides. In the anilide structure there is competition between the ring and the C═O for the nonbonded electron pair of the nitrogen atom.

The carbonyl frequency of tertiary amides is independent of the physical state since hydrogen bonding with another tertiary amide group is impossible. The C═O absorption occurs in the range of 1680 cm^{-1} to 1630 cm^{-1}. The absorption range of tertiary amides in solution is influenced by hydrogen bonding with the solvent: *N*,*N*-diethylacetamide absorbs at 1647 cm^{-1} in dioxane and at 1615 cm^{-1} in methanol.

Electron-attracting groups attached to the nitrogen increase the frequency of absorption since they effectively compete with the carbonyl oxygen for the electrons of the nitrogen, thus increasing the force constant of the C═O bond.

2.6.18.3 N—H Bending Vibrations (Amide II Band). All primary amides show a sharp absorption band in dilute solution (amide II band) resulting from N—H bending at a somewhat lower frequency than the C═O band. This band has an intensity of one-half to one-third of the C═O absorption band. In mulls and pellets, the band occurs near 1655 cm^{-1} to 1620 cm^{-1} and is usually under the envelope of the amide I band. In dilute solutions, the band appears at lower wavenumbers, 1620 cm^{-1} to 1590 cm^{-1}, and normally is separated from the amide I band. Multiple bands may appear in the spectra of concentrated solutions, arising from the free and associated states. The nature of the R group in R—C(═O) —NH_2 has little effect on the amide II band.

Secondary acyclic amides in the solid-state display an amide II band in the region of 1570 cm^{-1} to 1515 cm^{-1}. In dilute solution, the band occurs in the 1550 cm^{-1} to 1510 cm^{-1} region. This band results from interaction between the N—H bending and the C—N stretching of the C—N—H group. A second, weaker band near 1250 cm^{-1} also results from interaction between N—H bending and C—N stretching.

2.6.18.4 Other Vibration Bands. The C—N stretching band of primary amides occurs near 1400 cm^{-1}. A broad, medium band in the 800 cm^{-1} to 666 cm^{-1} region in the spectra of primary and secondary amides results from out-of-plane N—H wagging.

In lactams of medium ring size, the amide group is forced into the *s-cis* conformation. Solid lactams absorb strongly near 3200 cm^{-1} because of the N—H stretching vibration. This band does not shift appreciably with dilution

since the *s-cis* form remains associated at relatively low concentrations.

2.6.18.5 C═O Stretching Vibrations of Lactams. The C═O absorption of lactams with six-membered rings or larger is near 1650 cm^{-1}. Five-membered ring (γ) lactams absorb in the 1750 cm^{-1} to 1700 cm^{-1} region. Unfused four-membered ring (β) lactams absorb at 1760 cm^{-1} to 1730 cm^{-1}. Fusion of the lactam ring to another ring generally increases the frequency by 20 cm^{-1} to 50 cm^{-1}.

Most lactams do not show a band near 1550 cm^{-1} that is a characteristic of *s-trans* noncyclic secondary amides. The N—H out-of-plane wagging in lactams causes broad absorption in the 800 cm^{-1} to 700 cm^{-1} region.

2.6.19 Amines

The spectrum of a typical primary aliphatic diamine appears in Figure 2.33.

2.6.19.1 N—H Stretching Vibrations. Primary amines, examined in dilute solution, display two weak absorption bands: one near 3500 cm^{-1} and the other near 3400 cm^{-1}. These bands represent, respectively, the "free" asymmetrical and symmetrical N—H stretching modes. Secondary amines show a single weak band in the 3350 cm^{-1} to 3310 cm^{-1} region. These bands are shifted to longer wavelengths by hydrogen bonding. The associated N—H bands are weaker and frequently sharper than the corresponding O—H bands. Aliphatic primary amines (neat) absorb at 3400 cm^{-1} to 3300 cm^{-1} and 3330 cm^{-1} to 3250 cm^{-1}. Aromatic primary amines absorb at slightly higher wavenumbers. In the spectra of liquid primary and secondary amines, a shoulder usually appears on the low-frequency side of the N—H stretching band, arising from the overtone of the NH bending band intensified by Fermi resonance. Tertiary amines do not absorb in this region.

2.6.19.2 N—H Bending Vibrations. The N—H bending (scissoring) vibration of primary amines is observed in the 1650 cm^{-1} to 1580 cm^{-1} region of the spectrum. The band is medium to strong in intensity and is moved to slightly higher frequencies when the compound is associated. The N—H bending band is seldom detectable in the spectra of aliphatic secondary amines, whereas secondary aromatic amines absorb near 1515 cm^{-1}.

Liquid samples of primary and secondary amines display medium-to-strong broad absorption in the 909 cm^{-1} to 666 cm^{-1} region of the spectrum arising from NH wagging. The position of this band depends on the degree of hydrogen bonding.

2.6.19.3 C—N Stretching Vibrations. Medium-to-weak absorption bands for the unconjugated C—N linkage in primary, secondary, and tertiary aliphatic amines appear in the region of 1250 cm^{-1} to 1020 cm^{-1}. The vibrations responsible for these bands involve C—N stretching coupled with the stretching of adjacent bonds in the molecule. The position of absorption in this region depends on the class of the amine and the pattern of substitution on the α-carbon.

Aromatic amines display strong C—N stretching absorption in the 1342 cm^{-1} to 1266 cm^{-1} region. The absorption appears at higher frequencies than the corresponding absorption of aliphatic amines because the force constant of the C—N bond is increased by resonance with the ring.

Characteristic strong C—N stretching bands in the spectra of aromatic amines have been assigned as shown in Table 2.7.

2.6.20 Amine Salts

2.6.20.1 N—H Stretching Vibrations. The ammonium ion gives a strong, broad absorption in the 3300 cm^{-1} to 3030 cm^{-1} region because of N—H stretching vibrations (see Figure 2.28). There is also a combination band in the 2000 cm^{-1} to 1709 cm^{-1} region.

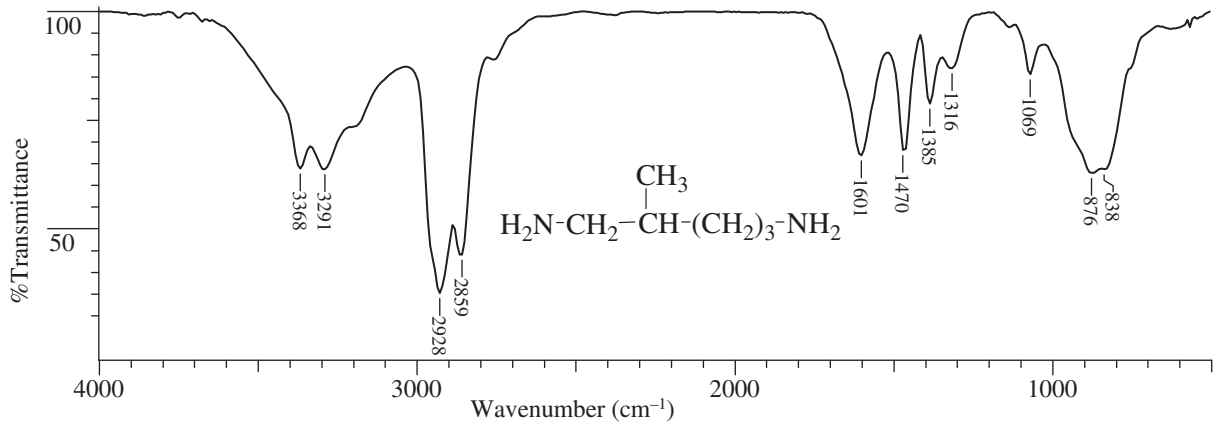

FIGURE 2.33 2-Methyl-1,5-pentanediamine. N—H stretch, hydrogen-bonded, primary amine coupled doublet: asymmetric, 3368 cm^{-1}. Symmetric, 3291 cm^{-1}. (Shoulder at about 3200 cm^{-1}, Fermi resonance band with overtone of band at 1601 cm^{-1}. Aliphatic C—H stretch, 2928, 2859 cm^{-1}. N—H bend (scissoring) 1601 cm^{-1}. $\delta_s CH_2$ (scissoring), 1470 cm^{-1}. C—N stretch, 1069 cm^{-1}. N—H wag (neat sample), ~900 cm^{-1} to 700 cm^{-1}.

TABLE 2.7 C—N Stretch of Aromatic Amines

Aromatic Amine	Absorption Region (cm^{-1})
Primary	1340 to 1250
Secondary	1350 to 1280
Tertiary	1360 to 1310

Salts of primary amines show strong, broad absorption between 3000 cm^{-1} and 2800 cm^{-1} arising from asymmetrical and symmetrical stretching in the NH_3^+ group. In addition, multiple combination bands of medium intensity occur in the 2800 cm^{-1} to 2000 cm^{-1} region, the most prominent being the band near 2000 cm^{-1}. Salts of secondary amines absorb strongly in the 3000 cm^{-1} to 2700 cm^{-1} region with multiple bands extending to 2273 cm^{-1}. A medium intensity band near 2000 cm^{-1} may be observed. Tertiary amine salts absorb at longer wavelengths than do the salts of primary and secondary amines (2700 cm^{-1} to 2250 cm^{-1}). Quaternary ammonium salts have no N—H stretching vibrations.

2.6.20.2 N——H Bending Vibrations. The ammonium ion displays a strong, broad NH_4^+ bending band near 1429 cm^{-1}. The NH_3^+ group of the salt of a primary amine absorbs near 1600 cm^{-1} to 1575 cm^{-1} and 1550 cm^{-1} to 1504 cm^{-1}. These bands originate in asymmetrical and symmetrical NH_3^+ bending, analogous to the corresponding bands of the CH_3 group. Salts of secondary amines absorb near 1620 cm^{-1} to 1560 cm^{-1}. The N—H bending band of the salts of tertiary amines is weak and of no practical value.

2.6.21 Amino Acids and Salts of Amino Acids

Amino acids are encountered in three forms:

1. The free amino acid (zwitterion).*

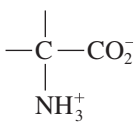

2. The hydrochloride (or other salt).

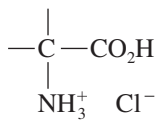

3. The sodium (or other cation) salt.

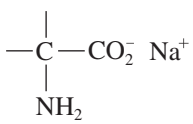

*Aromatic amino acids are not zwitterions. Thus *p*-aminobenzoic acid is

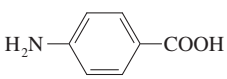

Free primary amino acids are characterized by the following absorptions (most of the work was done with α-amino acids, but the relative positions of the amino and carboxyl groups seem to have little effect):

1. A broad, strong NH_3^+ stretching band in the 3100 cm^{-1} to 2600 cm^{-1} region. Multiple combination and overtone bands extend the absorption to about 2000 cm^{-1}. This overtone region usually contains a prominent band near 2222 cm^{-1} to 2000 cm^{-1} assigned to a combination of the asymmetrical NH_3^+ bending vibration and the torsional oscillation of the NH_3^+ group. The torsional oscillation occurs near 500 cm^{-1}. The 2000 cm^{-1} band is absent if the nitrogen atom of the amino acid is substituted.
2. A weak asymmetrical NH_3^+ bending band near 1660 cm^{-1} to 1610 cm^{-1} and a fairly strong symmetrical bending band near 1550 cm^{-1} to 1485 cm^{-1}.
3. The carboxylate ion group 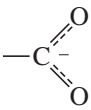 absorbs strongly near 1600 cm^{-1} to 1590 cm^{-1} and more weakly near 1400 cm^{-1}. These bands result, respectively, from asymmetrical and symmetrical $C(—O)_2$ stretching.

The spectrum of the amino acid leucine, including assignments corresponding to the preceding three categories, is shown in Figure 2.34.

Hydrochlorides of amino acids present the following patterns:

1. Broad, strong absorption in the 3333 cm^{-1} to 2380 cm^{-1} region resulting from superimposed O—H and NH_3^+ stretching bands. Absorption in this region is characterized by fine structure on the low-wavenumber side of the band.
2. A weak, asymmetrical NH_3^+ bending band near 1610 cm^{-1} to 1590 cm^{-1} and a relatively strong, symmetrical NH_3^+ bending band at 1550 cm^{-1} to 1481 cm^{-1}.
3. A strong band at 1220 cm^{-1} to 1190 cm^{-1} arising from C—C(=O)—O stretching.
4. Strong carbonyl absorption at 1755 cm^{-1} to 1730 cm^{-1} for α-amino acid hydrochlorides, and at 1730 cm^{-1} to 1700 cm^{-1} for other amino acid hydrochlorides.

Sodium salts of amino acids show the normal N—H stretching vibrations at 3400 cm^{-1} to 3200 cm^{-1} common to other amines. The characteristic carboxylate ion bands appear near 1600 cm^{-1} to 1590 cm^{-1} and near 1400 cm^{-1}.

2.6.22 Nitriles

The spectra of nitriles (R—C≡N) are characterized by weak-to-medium absorption in the triple-bond stretching region of the spectrum. Aliphatic nitriles absorb at 2260 cm^{-1} to 2240 cm^{-1}. Electron-attracting atoms, such as oxygen or chlorine, attached to the carbon atom α to the C≡N group reduce the intensity of absorption. Conjugation, such as occurs in aromatic nitriles, reduces the wavenumber

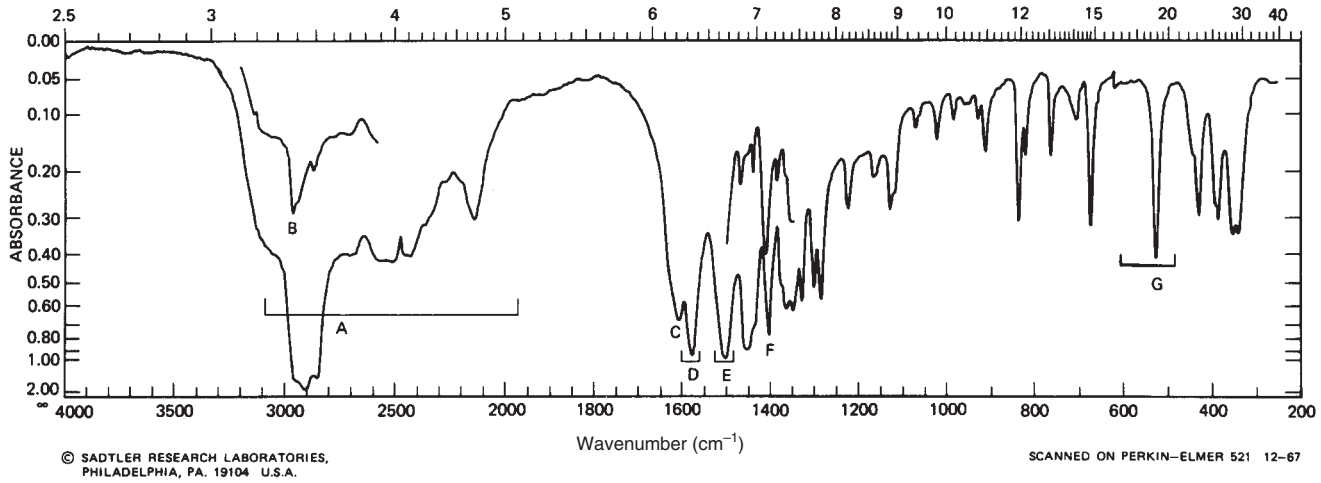

FIGURE 2.34 (±)-Leucine. A. Broad ($-NH_3^+$) N—H stretch, 3100 – 2000 cm^{-1}, extended by combination band at 2140 cm^{-1}, and other combination-overtone bands. B. Aliphatic C—H stretch (superimposed on N—H stretch), 2967 cm^{-1}. C. Asymmetric ($-NH_3^+$) N—H bend, 1610 cm^{-1}. D. Asymmetric carboxylate $(C{=}O)_2$ stretch, 1580 cm^{-1}. E. Symmetric ($-NH_3^+$) N—H bend, 1505 cm^{-1}. F. Symmetric carboxylate $(C{=}O)_2$ stretch, 1405 cm^{-1}. G. Torsional ($-NH_3^+$) N—H oscillation, 525 cm^{-1}.

of absorption to 2240 cm^{-1} to 2222 cm^{-1} and enhances the intensity. The spectrum of a typical nitrile is shown in Figure 2.35.

2.6.23 Isonitriles (R—N≡C), Cyanates (R—O—C≡N), Isocyanates (R—N=C=O), Thiocyanates (R—S—C≡N), and Isothiocyanates (R—N=C=S)

These groups show the triple bond or cumulative bond stretch in the 2280 cm^{-1} to 2000 cm^{-1} region.

2.6.24 Compounds Containing a —N=N Group

The N=N stretching vibration of a symmetrical *trans*-azo compound is forbidden in the IR but absorbs around 1576 cm^{-1} in the Raman spectrum. Unsymmetrical *para*-substituted azobenzenes in which the substituent is an electron-donating group absorb near 1429 cm^{-1}. The bands are weak because of the nonpolar nature of the bond.

2.6.25 Covalent Compounds Containing Nitrogen—Oxygen Bonds

Nitro compounds, nitrates, and nitramines contain an NO_2 group. Each of these classes shows absorption caused by asymmetrical and symmetrical stretching of the NO_2 group. Asymmetrical absorption results in a strong band in the 1661 cm^{-1} to 1499 cm^{-1} region; symmetrical absorption occurs in the region between 1389 cm^{-1} and 1259 cm^{-1}. The exact position of the bands is dependent on substitution and unsaturation in the vicinity of the NO_2 group.

2.6.25.1 N—O Stretching Vibrations.

Nitro Compounds In nitroalkanes, the bands occur near 1550 cm^{-1} and 1372 cm^{-1}. Conjugation lowers the wavenumbers of both bands, resulting in absorption near 1550 cm^{-1} to 1500 cm^{-1} and 1360 cm^{-1} to 1290 cm^{-1}.

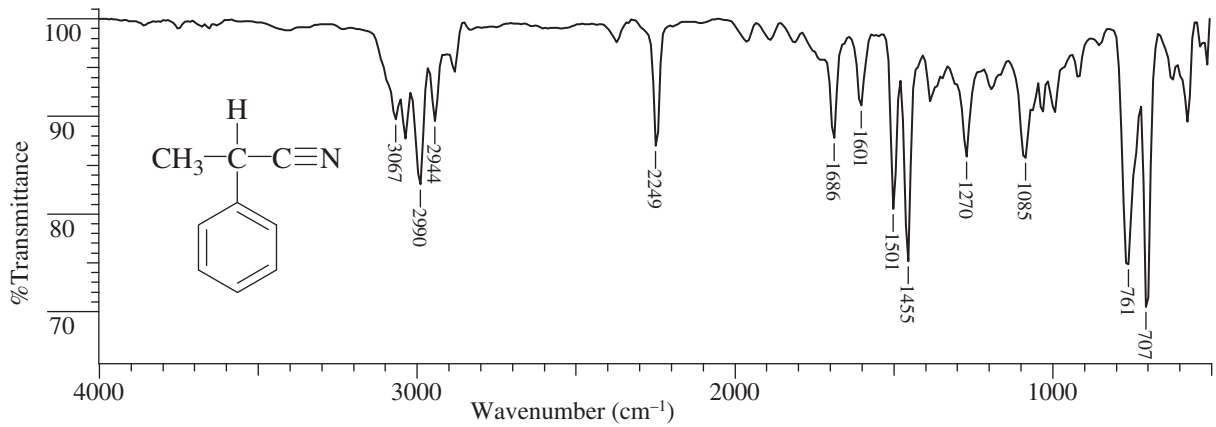

FIGURE 2.35 α-Methylbenzyl cyanide. Aromatic C—H stretch, 3067, 3030 cm^{-1}. Aliphatic C—H stretch, 2990, 2944 cm^{-1}. C≡N stretch, 2249 cm^{-1}. Out-of-plane C—H bend (aromatic ring), 761 cm^{-1}.

Attachment of electronegative groups to the α-carbon of a nitro compound causes an increase in the frequency of the asymmetrical NO_2 band and a reduction in the frequency of the symmetrical band; chloropicrin, Cl_3CNO_2, absorbs at 1610 cm^{-1} and 1307 cm^{-1}.

Aromatic nitro groups absorb near the same frequencies as observed for conjugated aliphatic nitro compounds. Interaction between the NO_2 out-of-plane bending and ring C—H out-of-plane bending frequencies destroys the reliability of the substitution pattern observed for nitroaromatics in the long-wavelength region of the spectrum. Nitroaromatic compounds show a C—N stretching vibration near 870 cm^{-1}. The spectrum of nitrobenzene, with assignments corresponding to the preceding discussion, is shown in Figure 2.36.

Because of strong resonance in aromatic systems containing NO_2 groups and electron-donating groups such as the amino group, *ortho* or *para* to one another, the symmetrical NO_2 vibration is shifted to lower frequencies and increases in intensity. *p*-Nitroaniline absorbs at 1475 cm^{-1} and 1310 cm^{-1}.

The positions of asymmetric and symmetric NO_2 stretching bands of nitramines $\backslash N - NO_2$ and the NO stretch of nitrosoamines are given in Appendix B.

Nitrates Organic nitrates show absorption for N—O stretching vibrations of the NO_2 group and for the O—N linkage. Asymmetrical stretching in the NO_2 group results in strong absorption in the 1660 cm^{-1} to 1625 cm^{-1} region; the symmetrical vibration absorbs strongly near 1300 cm^{-1} to 1255 cm^{-1}. Stretching of the π bonds of the N—O linkage produces absorption near 870 cm^{-1} to 833 cm^{-1}. Absorption observed at longer wavelengths, near 763 cm^{-1} to 690 cm^{-1}, likely results from NO_2 bending vibrations.

Nitrites Nitrites display two strong N═O stretching bands. The band near 1680 cm^{-1} to 1650 cm^{-1} is attributed to the *trans* isomer; the *cis* isomer absorbs in the 1625 cm^{-1} to 1610 cm^{-1} region. The N—O stretching band appears in the region between 850 cm^{-1} and 750 cm^{-1}. The nitrite absorption bands are among the strongest observed in IR spectra.

Nitroso Compounds Primary and secondary aliphatic *C*-nitroso compounds are usually unstable and rearrange to oximes or dimerize. Tertiary and aromatic nitroso compounds are reasonably stable, existing as monomers in the gaseous phase or in dilute solution and as dimers in neat samples. Monomeric, tertiary, aliphatic nitroso compounds show N═O absorption in the 1585 cm^{-1} to 1539 cm^{-1} region; aromatic monomers absorb between 1511 cm^{-1} and 1495 cm^{-1}.

The N→O stretching absorptions of dimeric nitroso compounds are categorized in Appendix B as to *cis* versus *trans* and aliphatic versus aromatic. Nitrosoamine absorptions are given in Appendix B.

2.6.26 Organic Sulfur Compounds

2.6.26.1 S—H Stretching Vibrations: Mercaptans.

Aliphatic mercaptans and thiophenols, as liquids or in solution, show S—H stretching absorption in the range of 2600 cm^{-1} to 2550 cm^{-1}. The S—H stretching band is characteristically weak and may go undetected in the spectra of dilute solutions or thin films. However, since few other groups show absorption in this region, it is useful in detecting S—H groups. The spectrum of 1,6-hexanedithiol in Figure 2.37 is that of a mercaptan with a detectable S—H stretch band. The band may be obscured by strong carboxyl absorption in the same region. Hydrogen bonding is much weaker for S—H groups than for O—H and N—H groups.

The S—H group of thiol acids absorbs in the same region as mercaptans and thiophenols.

2.6.26.2 C—S and C═S Stretching Vibrations.

Sulfides The stretching vibrations assigned to the C—S linkage occur in the region of 700 cm^{-1} to 600 cm^{-1}.

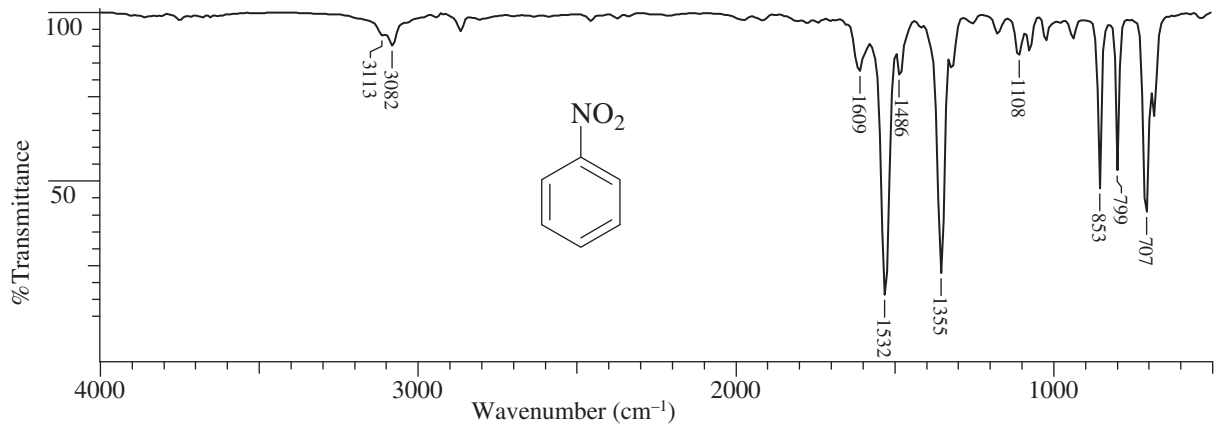

FIGURE 2.36 Nitrobenzene. Aromatic C—H stretch, 3113, 3082 cm^{-1}. Asymmetric $(ArNO_2)(N{=}O)_2$ stretch, 1532 cm^{-1}. Symmetric $(ArNO_2)(N{=}O)_2$ stretch 1355 cm^{-1}. C—N stretch for $ArNO_2$, 853 cm^{-1}. Low-frequency bands are of little use in determining the nature of ring substitution since these absorption patterns result from interaction of NO_2 and C—H out-of-plane bending frequencies. The inability of the "oop" region to reveal structural information is typical of aromatic compounds with highly polar substituents.

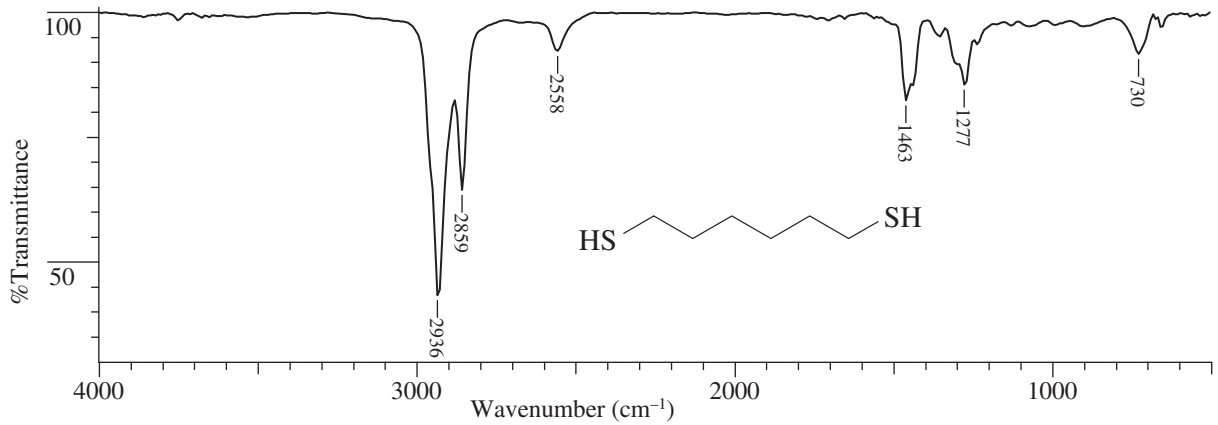

FIGURE 2.37 IR spectrum of 1,6-hexanedithiol. Aliphatic C—H stretch, 2936 cm^{-1}, 259 cm^{-1}. Moderately weak S—H stretch, 2558 cm^{-1}. C—S stretch, 730 cm^{-1}.

The weakness of absorption and variability of position make this band of little value in structural determination.

Disulfides The S—S stretching vibration is very weak and falls between 500 and 400 cm^{-1}.

Thiocarbonyl Compounds Aliphatic thials or thiones exist as trimeric, cyclic sulfides. Aralkyl thiones may exist either as monomers or trimers, whereas diaryl thiones, such as thiobenzophenone, exist only as monomers. The C═S group is less polar than the C═O group and has a considerably weaker bond. As a consequence, the band is not intense, and it falls at lower frequencies, where it is much more susceptible to coupling effects. Identification is therefore difficult and uncertain.

Compounds that contain a thiocarbonyl group show absorption in the 1250 cm^{-1} to 1020 cm^{-1} region. Thiobenzophenone and its derivatives absorb moderately in the 1224 cm^{-1} to 1207 cm^{-1} region. Since the absorption occurs in the same general region as C—O and C—N stretching, considerable interaction can occur between these vibrations within a single molecule.

Spectra of compounds in which the C═S group is attached to a nitrogen atom show an absorption band in the general C═S stretching region. In addition, several other bands in the broad region of 1563 cm^{-1} to 700 cm^{-1} can be attributed to vibrations involving interaction between C═S stretching and C—N stretching.

Thioketo compounds that can undergo enolization exist as thioketo–thioenol tautomeric systems; such systems show S—H stretching absorption. The thioenol tautomer of ethyl thiobenzoylacetate

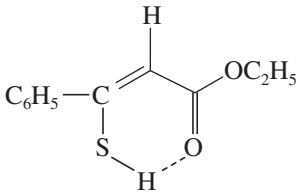

absorbs broadly at 2415 cm^{-1} because of hydrogen-bonded S—H stretching absorption.

2.6.27 Compounds Containing Sulfur—Oxygen Bonds

2.6.27.1 S═O Stretching Vibrations.

Sulfoxides Alkyl and aryl sulfoxides as liquids or in solution show strong absorption in the 1070 cm^{-1} to 1030 cm^{-1} region. This absorption occurs at 1050 cm^{-1} for dimethyl sulfoxide (DMSO). Conjugation brings about a small change in the observed frequency, in contrast to the marked reduction in frequency of the analogous C═O bond absorption accompanying conjugation. Diallyl sulfoxide absorbs at 1047 cm^{-1}. Phenyl methyl sulfoxide and cyclohexyl methyl sulfoxide absorb at 1055 cm^{-1} in dilute solution in carbon tetrachloride. The sulfoxide group is susceptible to hydrogen bonding, with the absorption shifting to slightly lower frequencies from dilute solution to the liquid phase. The frequency of S═O absorption is increased by electronegative substitution.

Sulfones Spectra of sulfones show strong absorption bands at 1350 cm^{-1} to 1300 cm^{-1} and 1160 cm^{-1} to 1120 cm^{-1}. These bands arise from asymmetric and symmetric SO_2 stretching, respectively. Hydrogen bonding results in absorption near 1300 cm^{-1} and 1125 cm^{-1}. Splitting of the high-frequency band often occurs in CCl_4 solution or in the solid state.

Sulfonyl Chlorides Sulfonyl chlorides absorb strongly in the regions of 1410 cm^{-1} to 1380 cm^{-1} and 1204 cm^{-1} to 1177 cm^{-1}. This increase in frequency, compared with the sulfones, results from the electronegativity of the chlorine atom.

Sulfonamides Solutions of sulfonamides absorb strongly at 1370 cm^{-1} to 1335 cm^{-1} and 1170 cm^{-1} to 1155 cm^{-1}. In the solid phase, these wavenumbers are lowered by

TABLE 2.8 Stretching Wavenumber of Sulfonates, Sulfates, Sulfonic acids, and Sulfonate salts

Class	Stretching Wavenumber (cm^{-1})
Sulfonates (covalent)	1372 to 1335, 1195 to 1168
Sulfates (organic)	1415 to 1380, 1200 to 1185
Sulfonic acids	1350 to 1342, 1165 to 1150
Sulfonate salts	1175, 1055

10 cm^{-1} to 20 cm^{-1}, the high-wavenumber band is broadened, and several submaxima usually appear.

Primary sulfonamides show strong N—H stretching bands at 3390 cm^{-1} to 3330 cm^{-1} and 3300 cm^{-1} to 3247 cm^{-1} in the solid state; secondary sulfonamides absorb near 3265 cm^{-1}.

Sulfonates, Sulfates, and Sulfonic Acids The asymmetric (higher frequency and shorter wavelength) and symmetric S═O stretching frequency ranges for these compounds are provided in Table 2.8.

The spectrum of a typical alkyl arenesulfonate is given in Figure 2.38. In virtually all sulfonates, the asymmetric stretch occurs as a doublet. Alkyl and aryl sulfonates show negligible differences; electron-donating groups in the *para* position of arenesulfonates cause higher frequency absorption.

Sulfonic acids are listed in narrow ranges above; these apply only to anhydrous forms. Such acids hydrate readily to give bands that are probably a result of the formation of hydronium sulfonate salts, in the 1230 cm^{-1} to 1120 cm^{-1} range.

2.6.28 Organic Halogen Compounds

The strong absorption of halogenated hydrocarbons arises from the stretching vibrations of the carbon–halogen bond (Table 2.9).

Aliphatic C—Cl absorption is observed in the broad region between 850 cm^{-1} and 550 cm^{-1}. When several chlorine atoms are attached to one carbon atom, the band is usually more intense and at the high-frequency end of the assigned limits. Carbon tetrachloride shows an intense band at 797 cm^{-1}. The first overtones of the intense fundamental bands are frequently observed. Brominated compounds absorb in the 690 cm^{-1} to 515 cm^{-1} region and iodo compounds in the 600 cm^{-1} to 500 cm^{-1} region. A strong CH_2 wagging band is observed for the CH_2X (X = Cl, Br, and I) group in the 1300 cm^{-1} to 1150 cm^{-1} region.

Fluorine-containing compounds absorb strongly over a wide range from 1400 cm^{-1} to 1000 cm^{-1} because of C—F stretching modes. A monofluoroalkane shows a strong band in the 1100 cm^{-1} to 1000 cm^{-1} region. As the number of fluorine atoms in an aliphatic molecule increases, the band pattern becomes more complex, with multiple strong bands

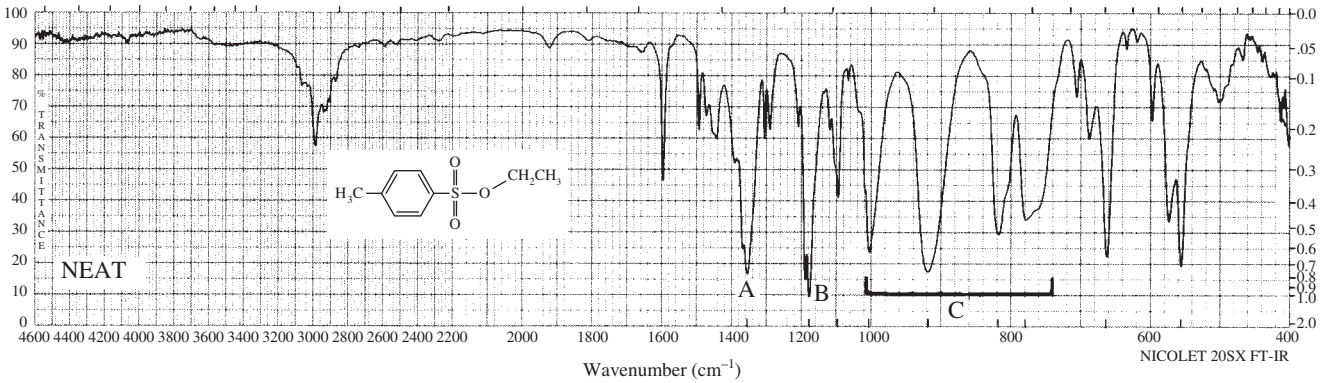

FIGURE 2.38 Ethyl *p*-toluenesulfonate. A. Asymmetric $S(=O)_2$ stretch, 1355 cm^{-1}. B. Symmetric $S(=O)_2$ stretch, 1177 cm^{-1}. C. Various strong S—O—C stretches, 1000 cm^{-1} to 769 cm^{-1}.

TABLE 2.9 Aliphatic Organohalogen Compound IR Wavenumbers

Functional Group	Wavenumber (cm^{-1})	Assignment
C—F	1100 to 1000	Monofluoroalkane C—F stretch
	1350 to 1120	CF_3 and CF_2
C—Cl	850 to 550	Aliphatic chloro compounds, C—Cl stretch
C—Br	690 to 515	Aliphatic bromo compounds, C—Br stretch
C—I	600 to 500	Aliphatic iodo compounds, C—I stretch
CH_2X (X = Cl, Br, and I)	1300 to 1500	CH_2 wagging

appearing over the broad region of C—F absorption. The CF_3 and CF_2 groups absorb strongly in the 1350 cm^{-1} to 1120 cm^{-1} region.

Chlorobenzenes absorb in the 1096 cm^{-1} to 1089 cm^{-1} region. The position within this region depends on the substitution pattern. Aryl fluorides absorb in the 1250 cm^{-1} to 1100 cm^{-1} region of the spectrum. A monofluorinated benzene ring displays a strong, narrow absorption band near 1230 cm^{-1}.

Since halogen atoms have high electronegativity, halogen substitution has a noticeable impact on the spectrum of neighboring group frequencies, including adjacent hydrogen atoms. Significant shifting of C—H frequencies can occur. The direction of the shift is dependent on the location of the C—H group, and whether the halogen adds (higher frequency) or subtracts (lower frequency) electron density from the C—H bond.

2.6.29 Silicon Compounds

2.6.29.1 Si—H Vibrations. Vibrations for the Si—H bond include the Si—H stretch (~2200 cm^{-1}) and the Si—H bend (800 cm^{-1} to 950 cm^{-1}). The Si—H stretching frequencies are increased by the attachment of an electronegative group to the silicon.

2.6.29.2 SiO—H and Si—O Vibrations. The OH stretching vibrations of the SiOH group absorb in the same region as the alcohols, 3700 cm^{-1} to 3200 cm^{-1}, and strong Si—O bands are at 830 cm^{-1} to 1110 cm^{-1}. As in alcohols, the absorption characteristics depend on the degree of hydrogen bonding.

2.6.29.3 Silicon–Halogen Stretching Vibrations. Absorption caused by Si—F stretching is in the 800 cm^{-1} to 1000 cm^{-1} region.

Bands resulting from Si—Cl stretching occur at wavenumbers below 666 cm^{-1}.

2.6.30 Phosphorus Compounds

2.6.30.1 P—H, P—C, P—O, and P=O Stretching Vibrations. The P—H bond, which occurs in many organophosphorus compounds, has stretching vibrations in the region of 2350 cm^{-1} to 2440 cm^{-1} and bending vibrations at 1120 cm^{-1} to 950 cm^{-1}. The latter may be overshadowed by other intense bands not related to the P—H bond. Replacement of hydrogen by deuterium produces a significant isotope shift of ~650 cm^{-1}, resulting in P—D stretching bands at ~1750 cm^{-1}.

The stretching vibrations of P—C bonds in aliphatic phosphine oxides appear in the range of 650 cm^{-1} to 750 cm^{-1}, although the size and structure of alkyl groups and the identity of other substituents on the phosphorus atom are expected to have some effect. When an aromatic ring is bonded directly to phosphorus, it shows the characteristic aromatic frequencies corresponding to the respective structures and positions of the substituents the same as the aromatic ring in hydrocarbons (Section 2.6.6). There are two additional bands near 1000 cm^{-1} and 1440 cm^{-1} for compounds containing an aromatic ring directly attached to phosphorus. The band at 1000 cm^{-1} is usually stronger than that at 1440 cm^{-1}.

In the phosphoryl group (P=O), unlike for C=O, the oxygen atom bonds with the phosphorus in a highly polar bond that is frequently designated as a $(\overset{+}{P}-\overset{-}{O})$ group. The latter suggests that the IR spectra of the P=O group may be largely interpreted in the context of a σ bond. The phosphoryl stretching absorption occurs over a rather wide range, extending from 1150 cm^{-1} to 1310 cm^{-1} (Figure 2.39). The frequency of this band is extremely sensitive to other substituents on the phosphorus atom, and there is a correlation between the phosphoryl frequency and the electronegativity

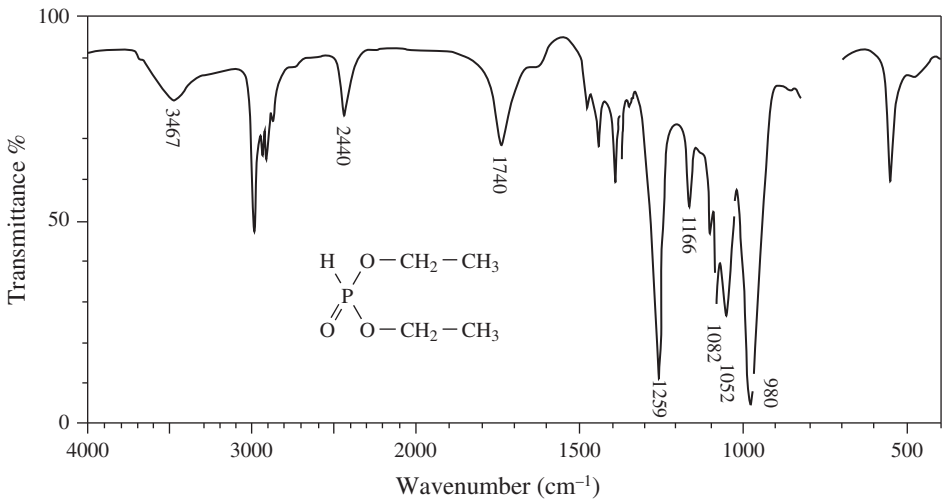

FIGURE 2.39 IR spectrum of diethyl phosphite. Broad P—O—H band, 3467 cm^{-1}. P—H band, 2440 cm^{-1}. P=O stretch, 1259 cm^{-1}. P—O—C band, 1166(w), 1062(m), 1052(m), 980(s) cm^{-1}.

TABLE 2.10 Effect of Electronegativity of Substituents on IR Wavenumber of the Phosphoryl Group

Compound	No. Electronegative Substituents	Wavenumber in IR (cm^{-1})
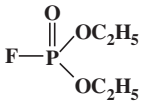 Dimethylfluorophosphate	3	1305
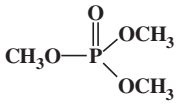 Trimethylphosphate	3	1275
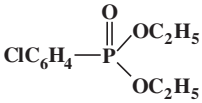 Diethyl *p*-chlorophenylphosphonic acid	2	1265
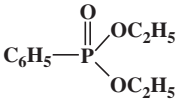 Diethylphenylphosphonate	2	1257
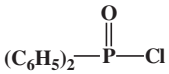 Diphenylchlorophosphine oxide	1	1236
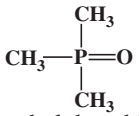 Trimethylphosphine oxide	0	1190

of the other substituents on the phosphorus atom. Table 2.10 lists the effects of some substituents on the phosphoryl IR frequency.

The phosphoryl group can interact through its oxygen atom with hydroxyl groups to form hydrogen bonds, or form complexes with heavy metal compounds, which can significantly shift the stretching bands of the P═O group to lower frequency. The metal ions bonding to a phosphoryl group can reduce the P═O absorption by more than 100 cm^{-1}. Accordingly, in complexes formed between tributylphosphate and thorium, cerium(IV), or uranyl nitrates, the P═O stretching band shifts from 1280 cm^{-1} to ~1180 cm^{-1}.

Organic esters have a characteristic band at about 1110 cm^{-1}, which has been ascribed to the C—O—C linkage. Substitution of phosphorus for carbon in an aliphatic ester group will normally shift the absorption band toward lower frequencies. The absorption of the P—O—C group of the aliphatic phosphates appears as a strong-to-moderate broadband near 1050 cm^{-1}; an exception is P—O—CH_3, in which the absorption appears as a single, well-defined, strong band, with an additional weak sharp band at 1190 cm^{-1}. Also associated with the P—O—C group is a medium-intensity band between 835 cm^{-1} and 715 cm^{-1} which becomes quite weak for an aliphatic group larger than methyl or ethyl. For an aromatic phosphate, this absorption shifts to a higher wavenumber of 1260 cm^{-1} to 1160 cm^{-1}.

2.6.31 Heteroaromatic Compounds

The spectra of heteroaromatic compounds result primarily from the same vibrational modes as observed for aromatic compounds.

2.6.31.1 C—H Stretching Vibrations. Heteroaromatics, such as pyridines, pyrazines, pyrroles, furans, and thiophenes, show C—H stretching bands in the 3077 cm^{-1} to 3003 cm^{-1} region.

2.6.31.2 N—H Stretching Frequencies. Heteroaromatics containing an N—H group show an N—H stretching

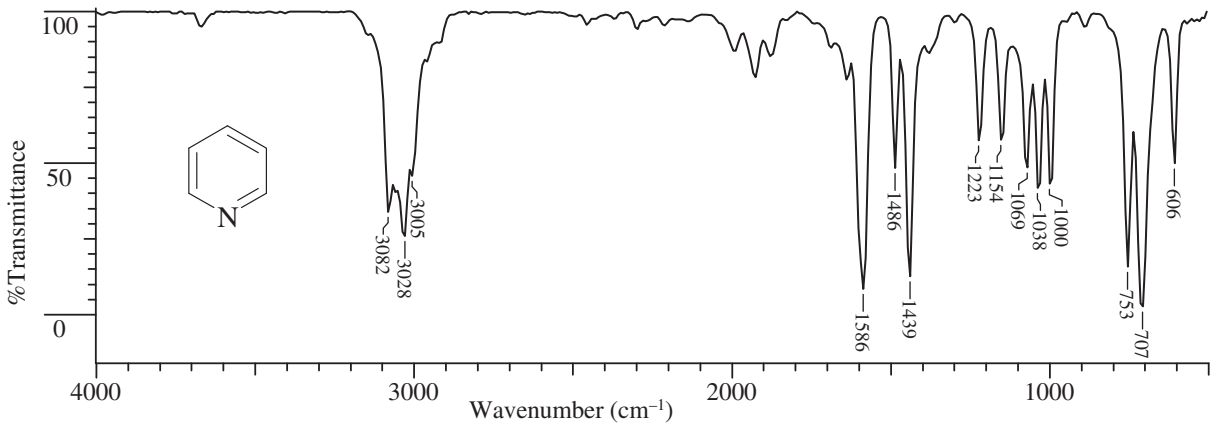

FIGURE 2.40 Pyridine. Aromatic C—H stretch, 3090 – 3000 cm^{-1}. C—C, C—N ring stretching (skeletal bands), 1600 cm^{-1} to 1430 cm^{-1}. C—H out-of-plane bending, 753, 707 cm^{-1}. See Appendix E, Table E.1 for patterns in region C for substituted pyridines.

absorption in the region of 3500 cm^{-1} to 3220 cm^{-1}. The position of the absorption within this general region depends on the degree of hydrogen bonding, and hence upon the physical state of the sample or the polarity of the solvent. Pyrrole and indole in dilute solution in nonpolar solvents show a sharp band near 3495 cm^{-1}; concentrated solutions show a widened band near 3400 cm^{-1}. Both bands may be seen at intermediate concentrations.

2.6.31.3 Ring Stretching Vibrations (Skeletal Bands). Ring stretching vibrations occur in the general region between 1600 cm^{-1} and 1300 cm^{-1}. The absorption involves stretching and contraction of all of the bonds in the ring and interaction between these stretching modes. The band pattern and the relative intensities depend on the substitution pattern and the nature of the substituents.

The IR spectrum of pyridine (Figure 2.40) shows four bands in this region and, in this respect, closely resembles the spectrum of a monosubstituted benzene. Furans, pyrroles, and thiophenes display two to four bands in this region.

2.6.31.4 C—H Out-of-Plane Bending. The C—H out-of-plane bending (γ-CH) absorption pattern of the heteroaromatics is determined by the number of adjacent hydrogen atoms bending in phase. The C—H out-of-plane and ring bending (β ring) absorptions of the alkylpyridines are summarized in Appendix E, Table E.1.

Absorption data for the out-of-phase C—H bending (γ-CH) and ring bending (β ring) modes of three common five-membered heteroaromatic rings are presented in Appendix E, Table E.2. The ranges in Table E.2 include polar and nonpolar substituents on the ring.

REFERENCES

For a list of Chapter References, please visit: www.wiley.com/college/silverstein.

STUDENT EXERCISES

2.1 The hydrogen halides have the following stretching wavenumbers: 4148.3 cm^{-1} (HF); 2988.9 cm^{-1} (HCl); 2649.7 cm^{-1} (HBr); 2309.5 cm^{-1} (HI). Use Hooke's law to calculate the force constants of the hydrogen–halogen bonds. Based on your calculations, predict the corresponding frequencies for the deuterium halides.

2.2 Which of the following molecules may show infrared absorption spectra? Why?

(a) CH_3CH_3, (b) CH_4, (c) CH_3Cl, (d) N_2.

2.3 How many normal modes of vibration are there for each of the following molecules:

(a) C_6H_6, (b) $C_6H_5CH_3$, (c) $HC{\equiv}C{-}C{\equiv}CH$.

2.4 The ATR IR spectra of three xylene isomers (*m-, o-, p*-xylene) are shown below. Examine these spectra and label each with the appropriate structure.

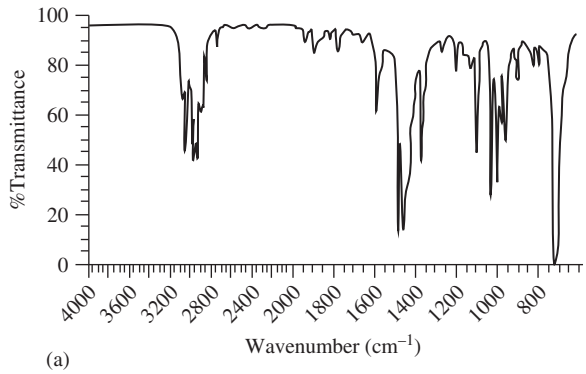

(a)

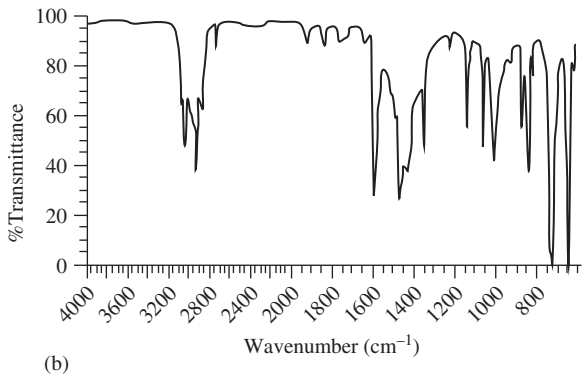

(b)

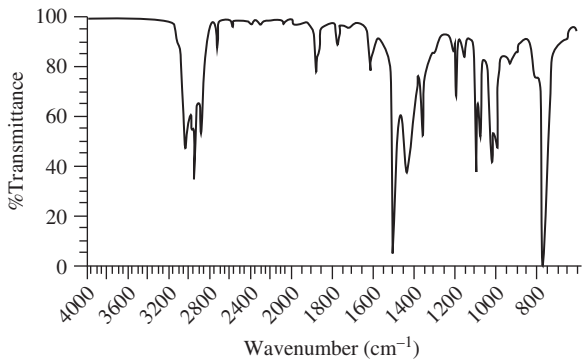

(c)

2.5 Select a compound that best fits each of the following sets of IR bands (in cm^{-1}). Each set corresponds to a list of just a few important bands for each compound.

Benzamide	Diphenyl sulfone
Benzoic acid	Formic acid
Benzonitrile	Isobutylamine
Biphenyl	1-Nitropropane dioxane
	1,4-Dioxane

a. 3080 (w), nothing 3000 to 2800, 2230 (s), 1450 (s), 760 (s), 688 (s)
b. 3380 (m), 3300 (m), nothing 3200 to 3000, 2980 (s), 2870 (m), 1610 (m), ~900 to 700 (b)
c. 3080 (w), nothing 3000 to 2800, 1315 (s), 1300 (s), 1155 (s)
d. 2955 (s), 2850 (5), 1120 (s)
e. 2946 (s), 2930 (m), 1550 (s), 1386 (m)
f. 2900 (b, s), 1720 (b, s)
g. 3030 (m), 730 (s), 690 (s)
h. 3200 to 2400 (5), 1685 (b, s), 705 (s)
i. 3350 (s), 3060 (m), 1635 (s)

s = strong, m = medium, w = weak, b = broad

2.6 The IR spectra of butyric acid and ethyl butyrate show sharp strong singlet absorption at 1725 cm^{-1} and 1740 cm^{-1}, respectively. By contrast, the IR spectrum of butyric anhydride shows a broad, sharp doublet at 1750 cm^{-1} and 1825 cm^{-1}. Why are these so different?

2.7 What are "combination bands"? What are "overtones"? How do each of these contribute to the interpretation of an IR spectrum? Can you give an example?

2.8 Rank the following phosphorus compounds in order of increasing P═O IR stretching frequencies.

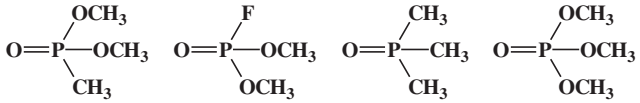

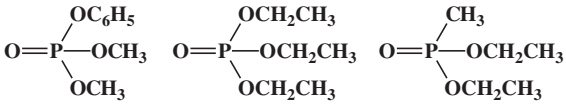

2.9 For each of the following IR spectra (A–W) list functional groups that (a) are present and (b) are absent. The mass spectra of these compounds are in Chapter 1 (Exercise 1.6).

Problem 2.9 Spectrum A

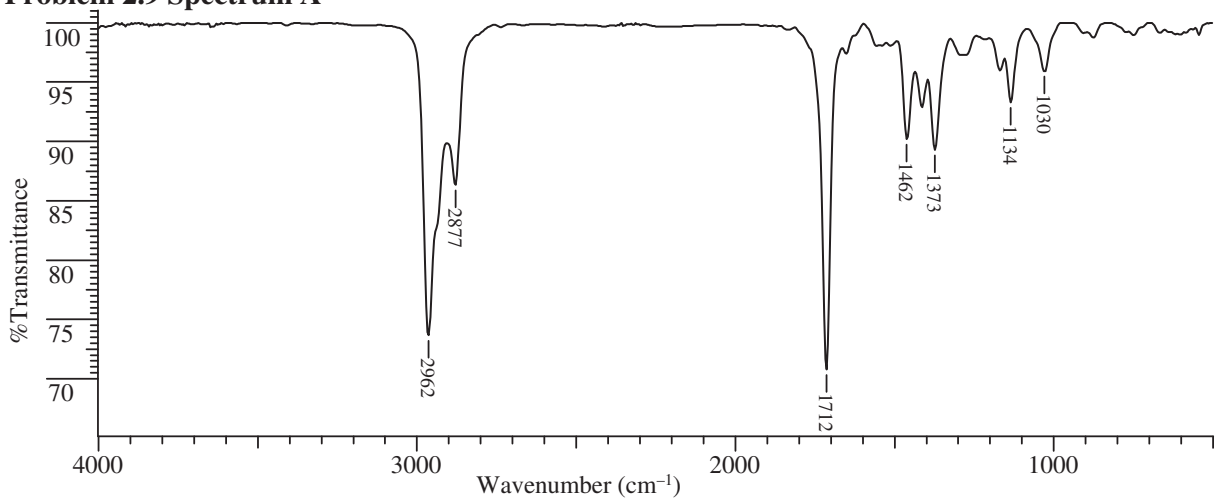

Problem 2.9 Spectrum B

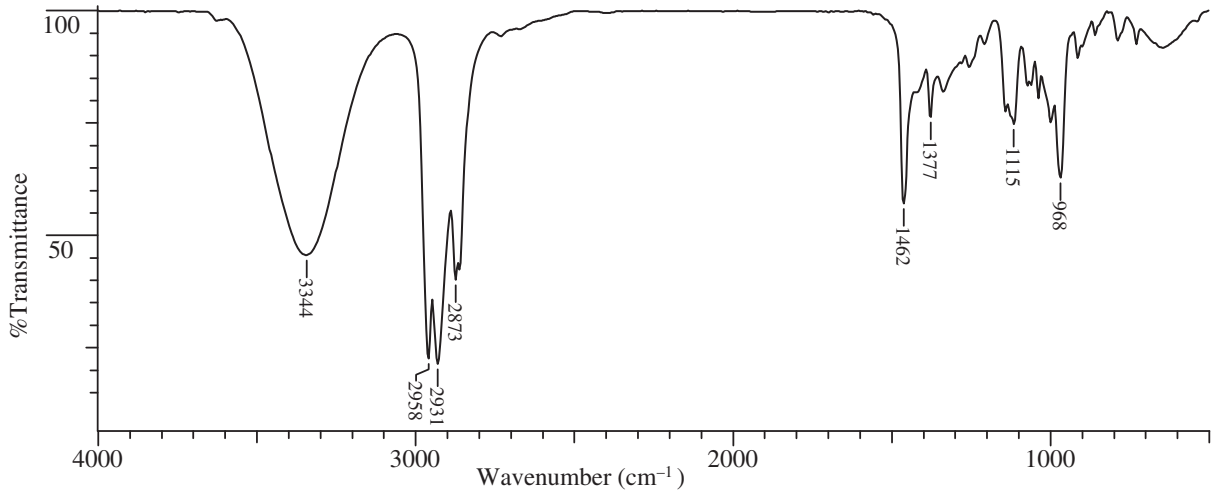

Problem 2.9 Spectrum C

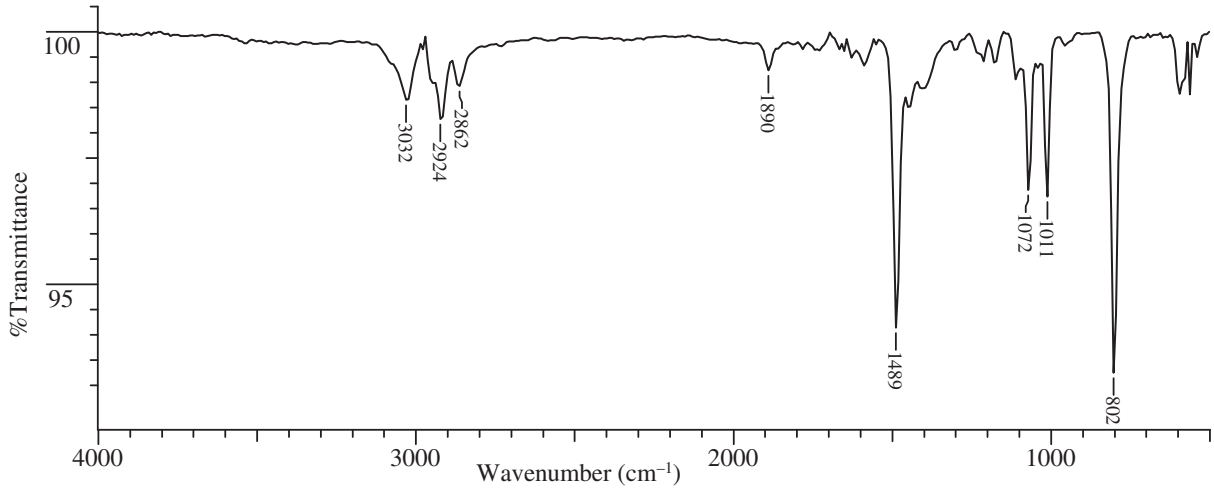

Problem 2.9 Spectrum D

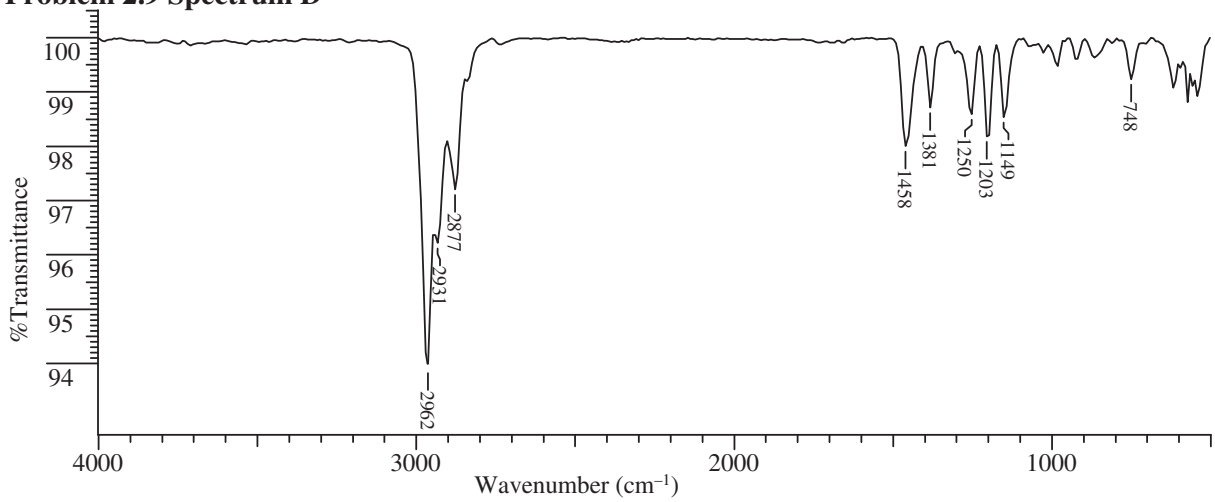

Problem 2.9 Spectrum E

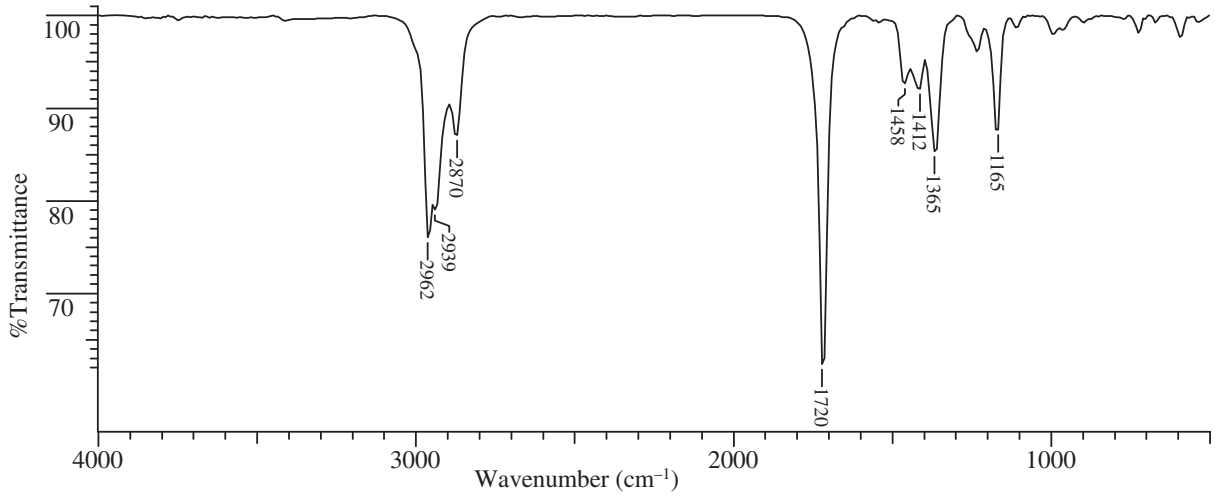

Problem 2.9 Spectrum F

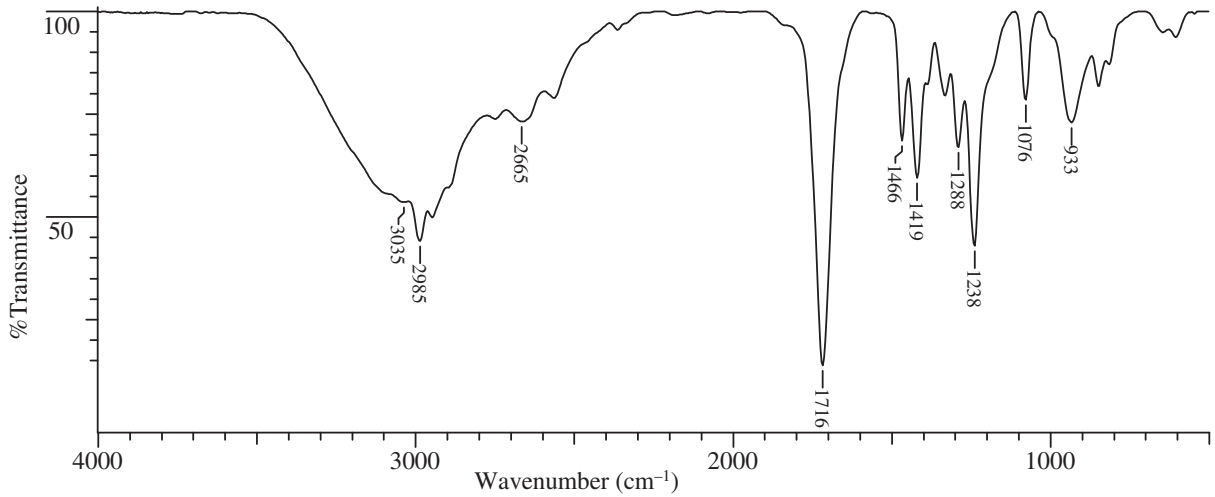

Problem 2.9 Spectrum G

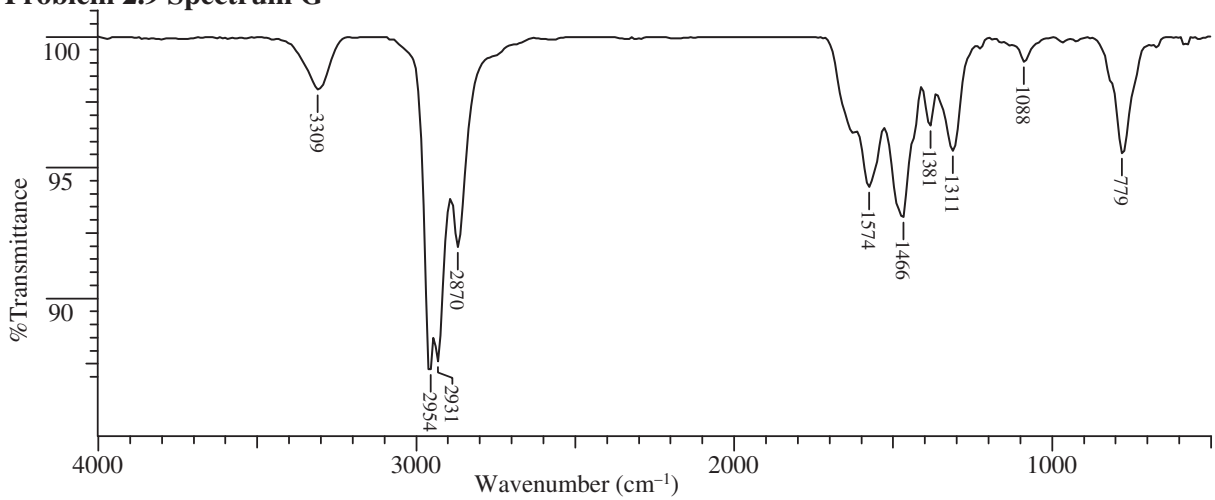

Problem 2.9 Spectrum H

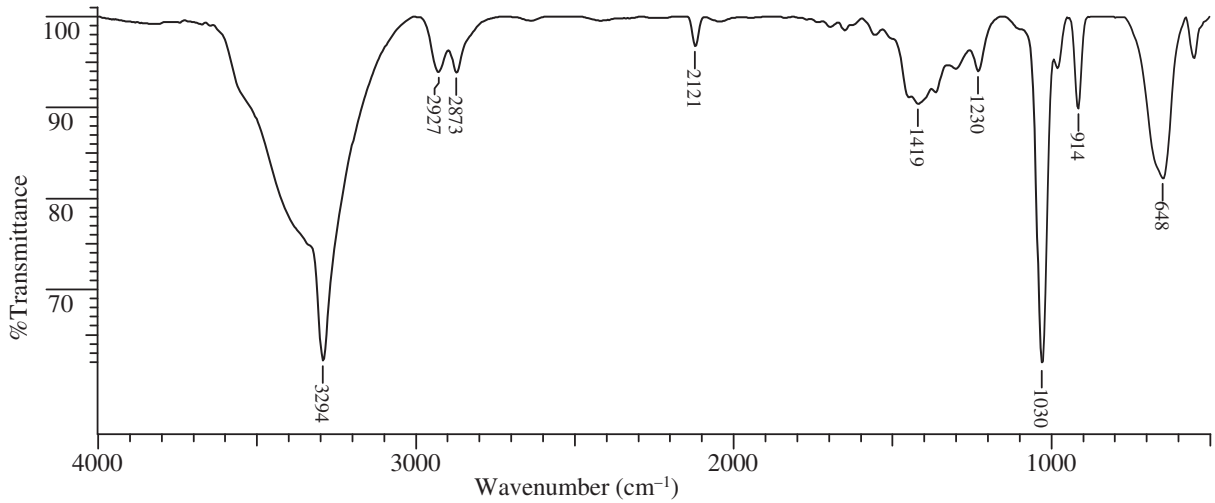

Problem 2.9 Spectrum I

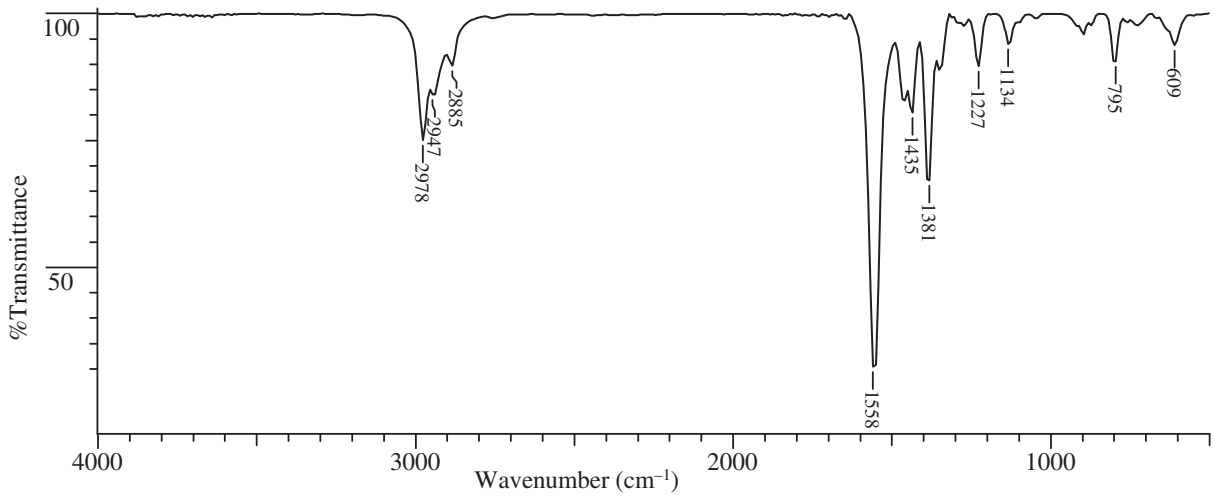

Problem 2.9 Spectrum J

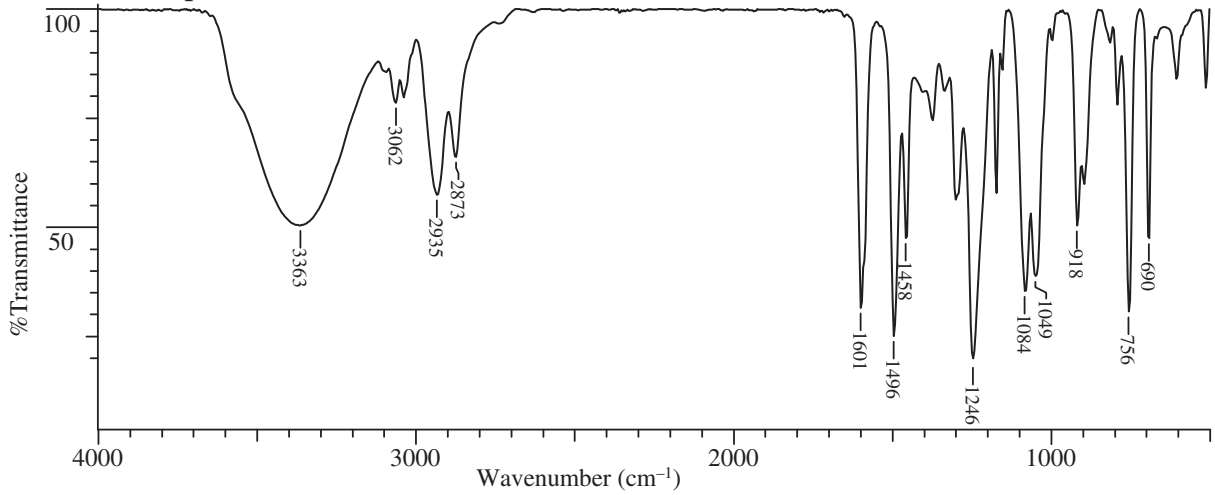

Problem 2.9 Spectrum K

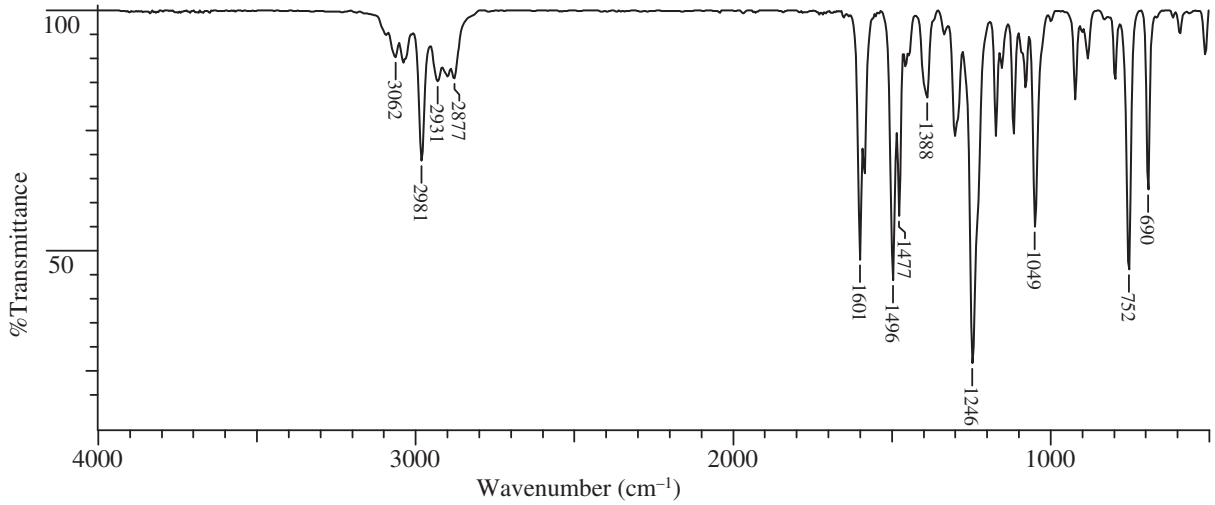

Problem 2.9 Spectrum L

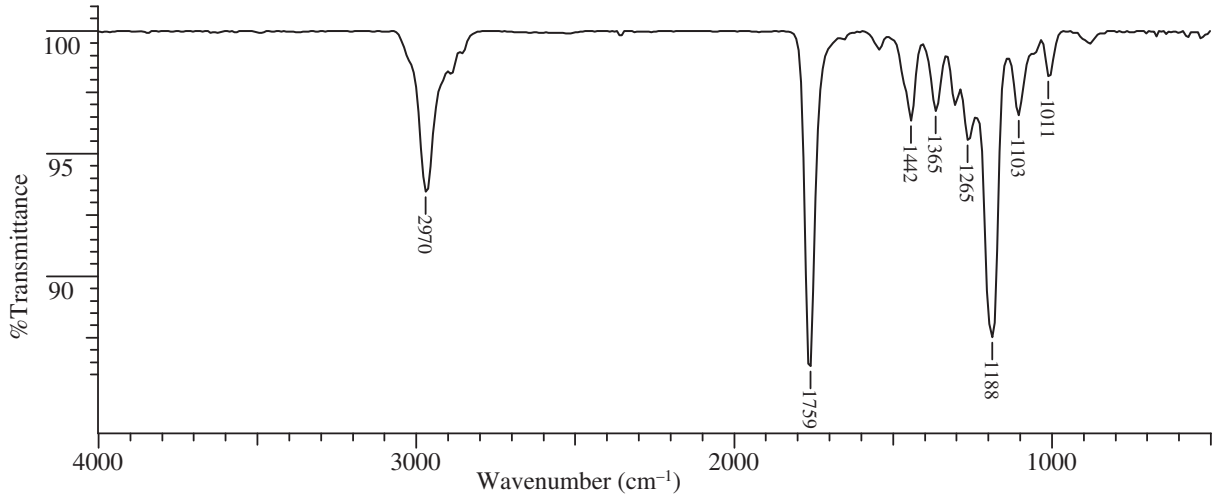

Problem 2.9 Spectrum M

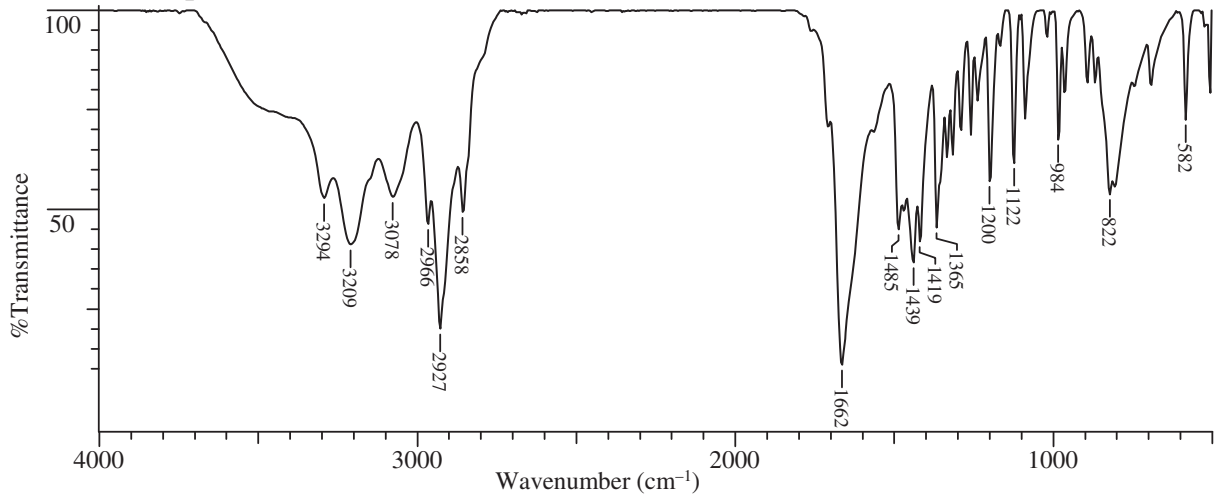

Problem 2.9 Spectrum N

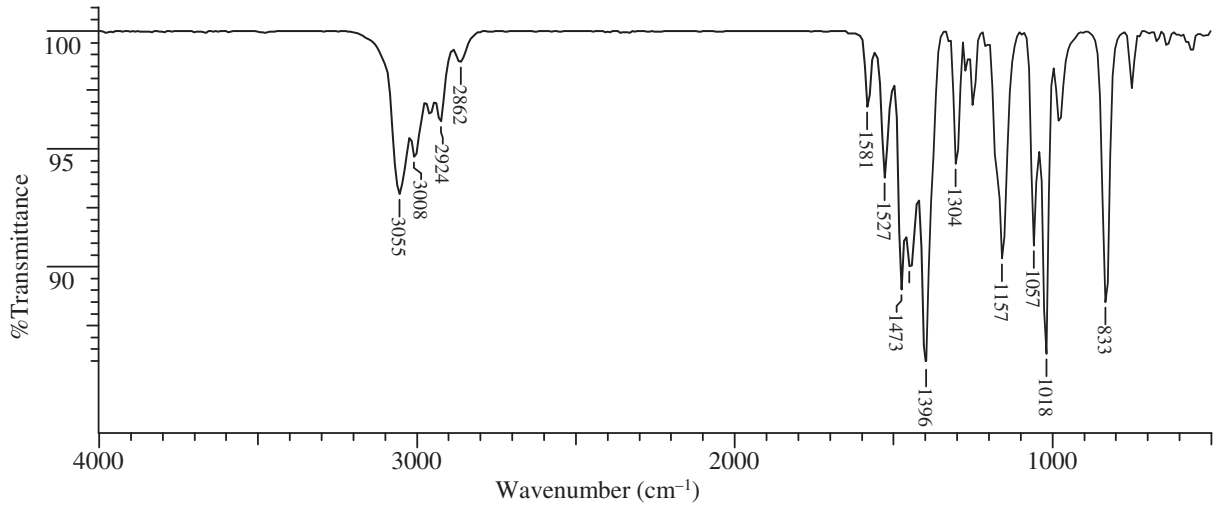

Problem 2.9 Spectrum O

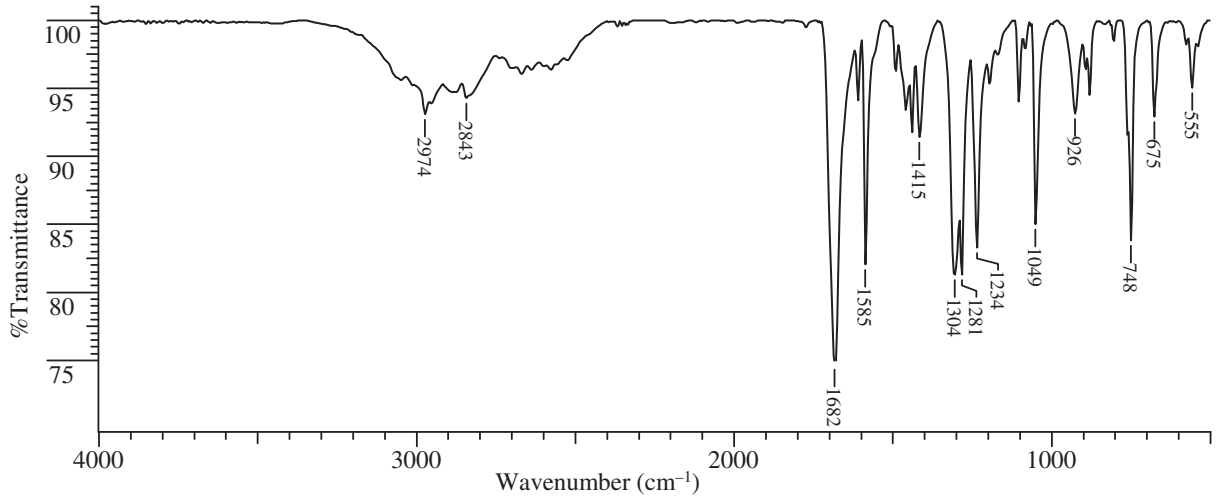

Problem 2.9 Spectrum P

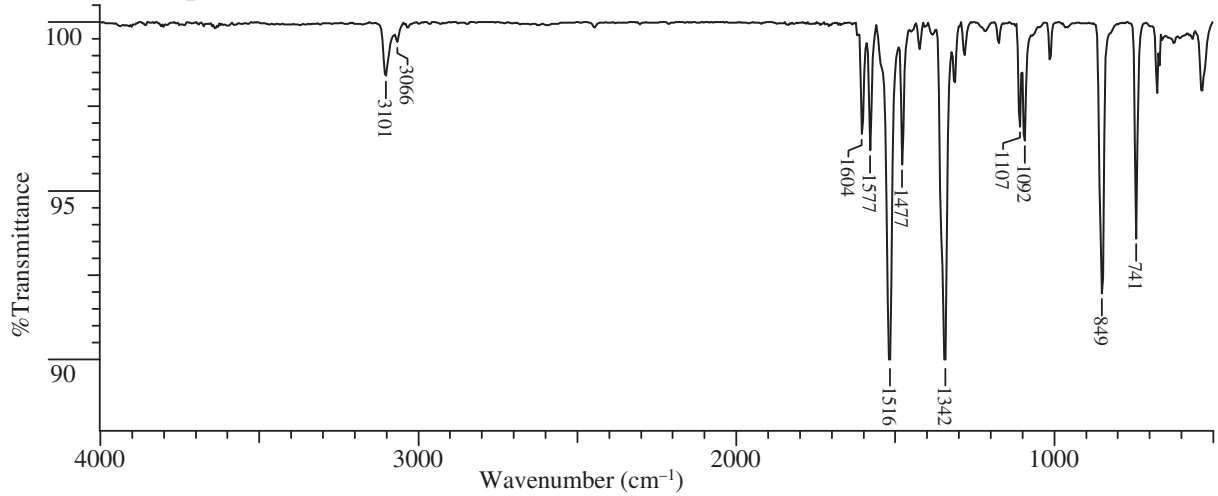

Problem 2.9 Spectrum Q

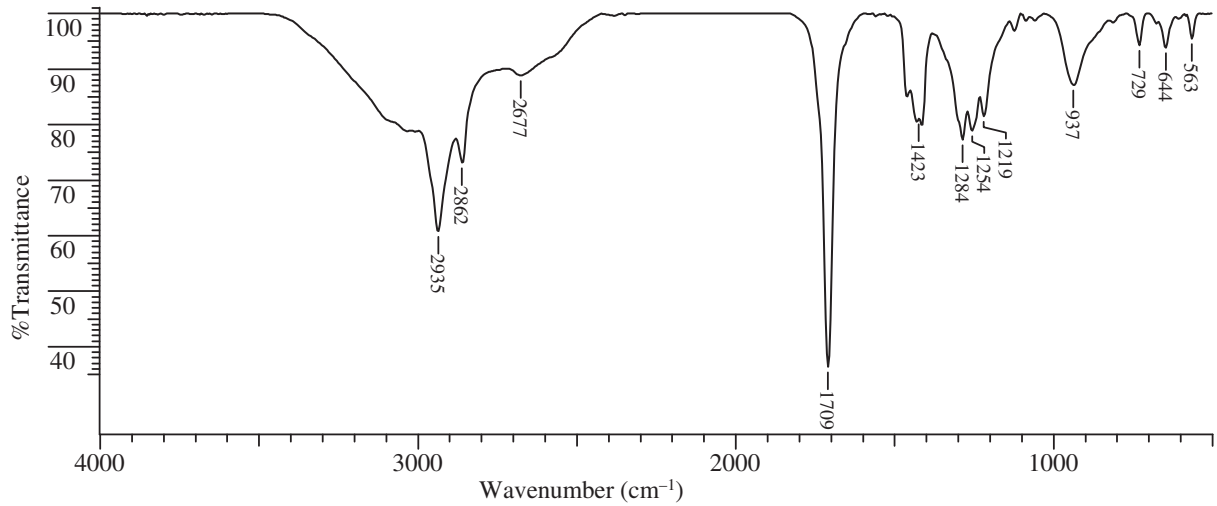

Problem 2.9 Spectrum R

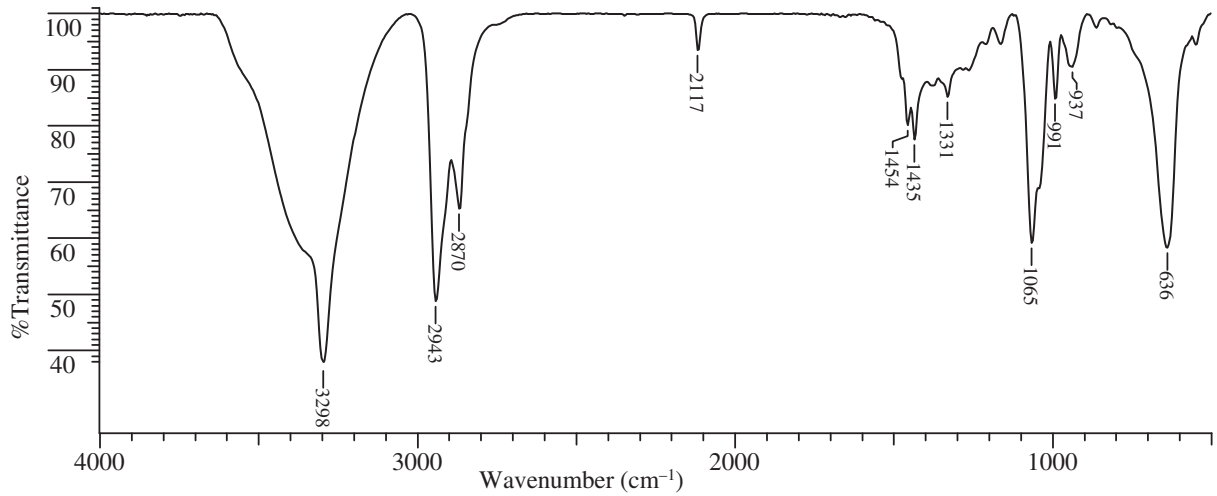

Problem 2.9 Spectrum S

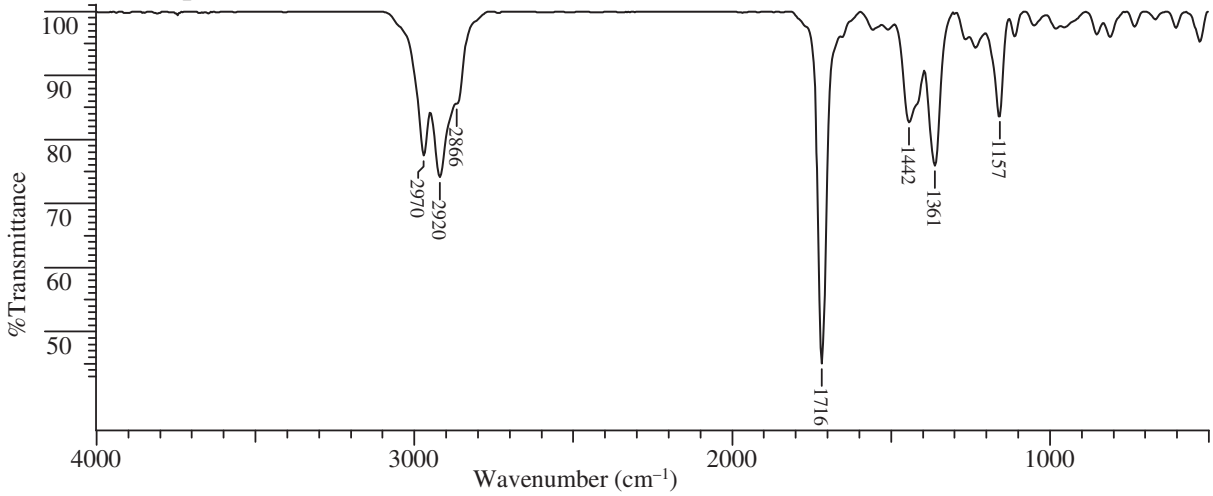

Problem 2.9 Spectrum T

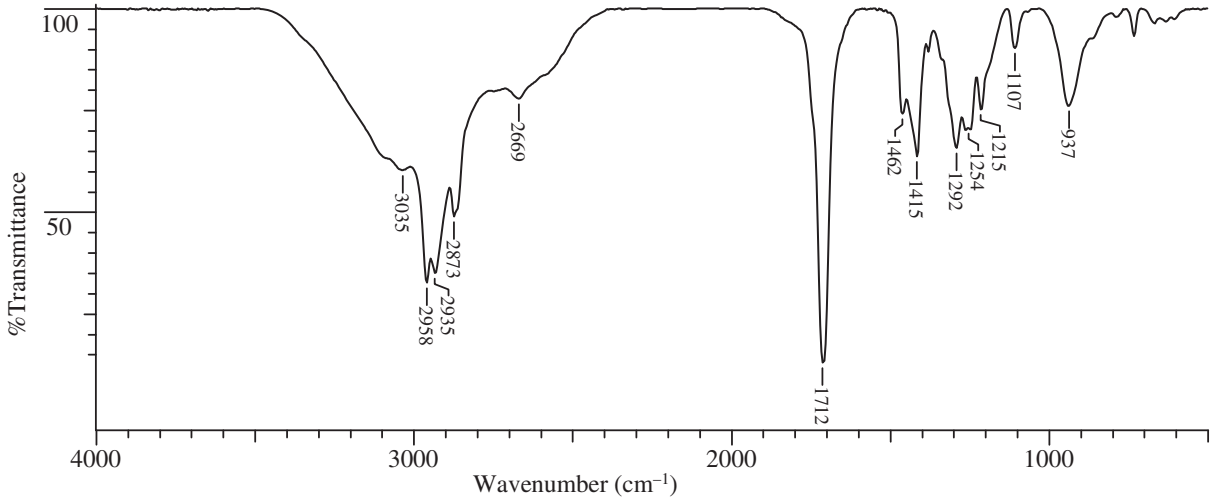

Problem 2.9 Spectrum U

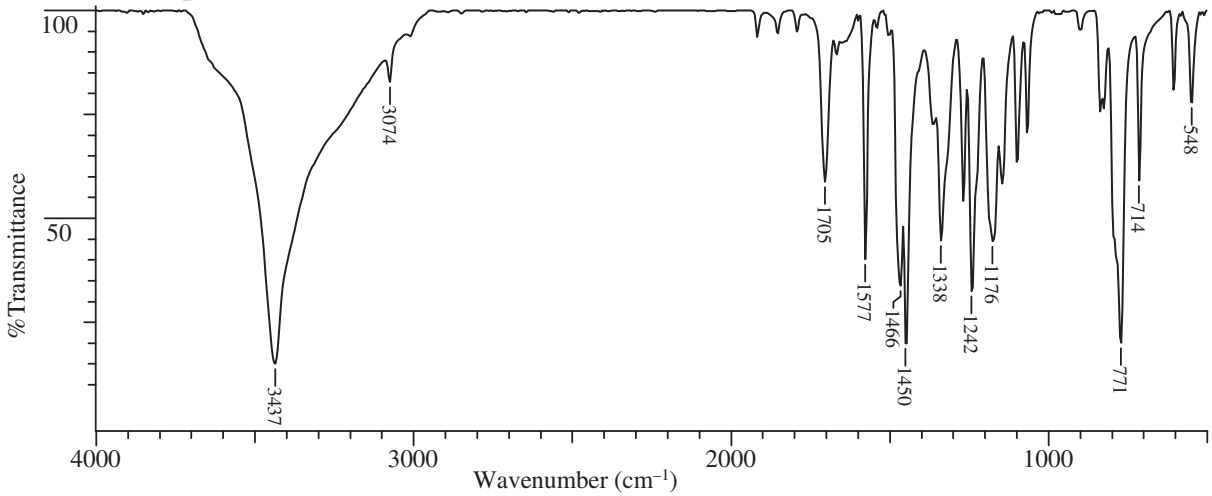

Problem 2.9 Spectrum V

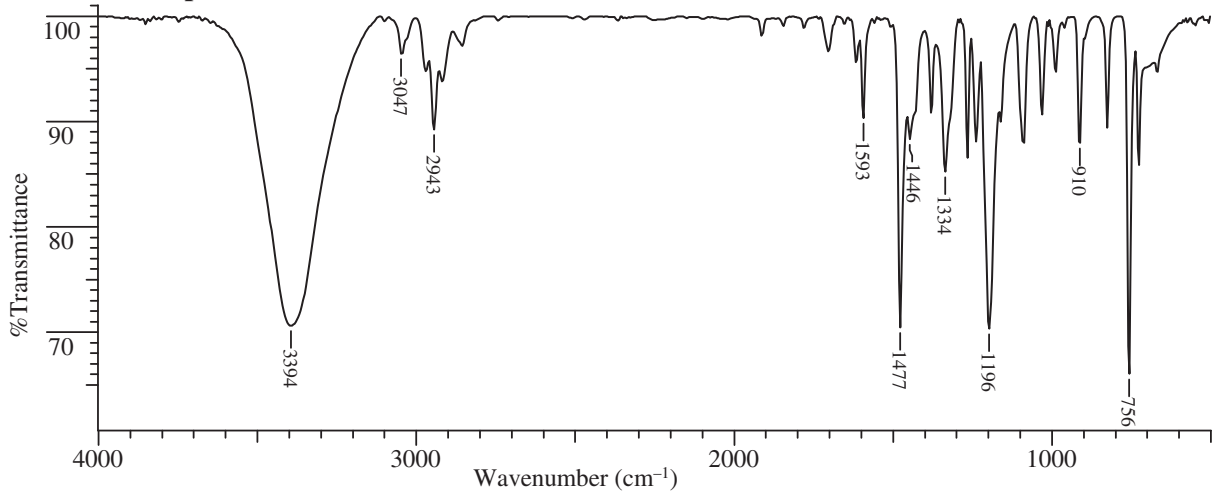

Problem 2.9 Spectrum W

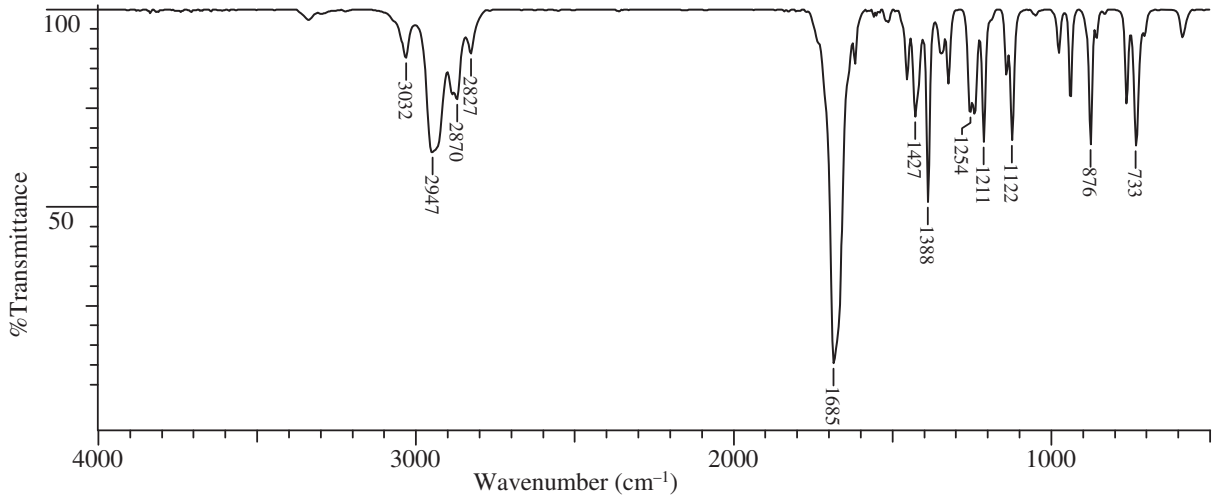

CHART AND SPECTRAL PRESENTATIONS OF ORGANIC SOLVENTS, MULLING OILS, AND OTHER COMMON LABORATORY SUBSTANCES

APPENDIX A TRANSPARENT REGIONS OF SOLVENTS AND MULLING OILS

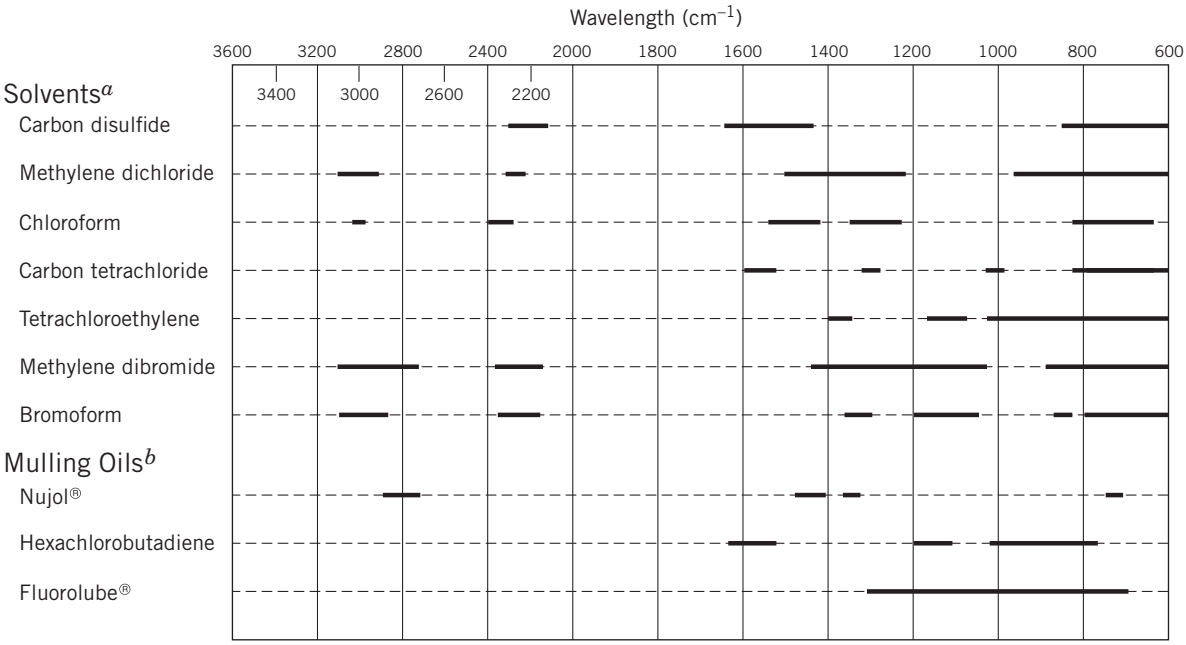

[a] The open regions are those in which the solvent transmits more than 25% of the incident light at 1 mm thickness.
[b] The open regions for mulling oils indicate transparency of thin films.

APPENDIX B CHARACTERISTIC GROUP ABSORPTIONS[a]

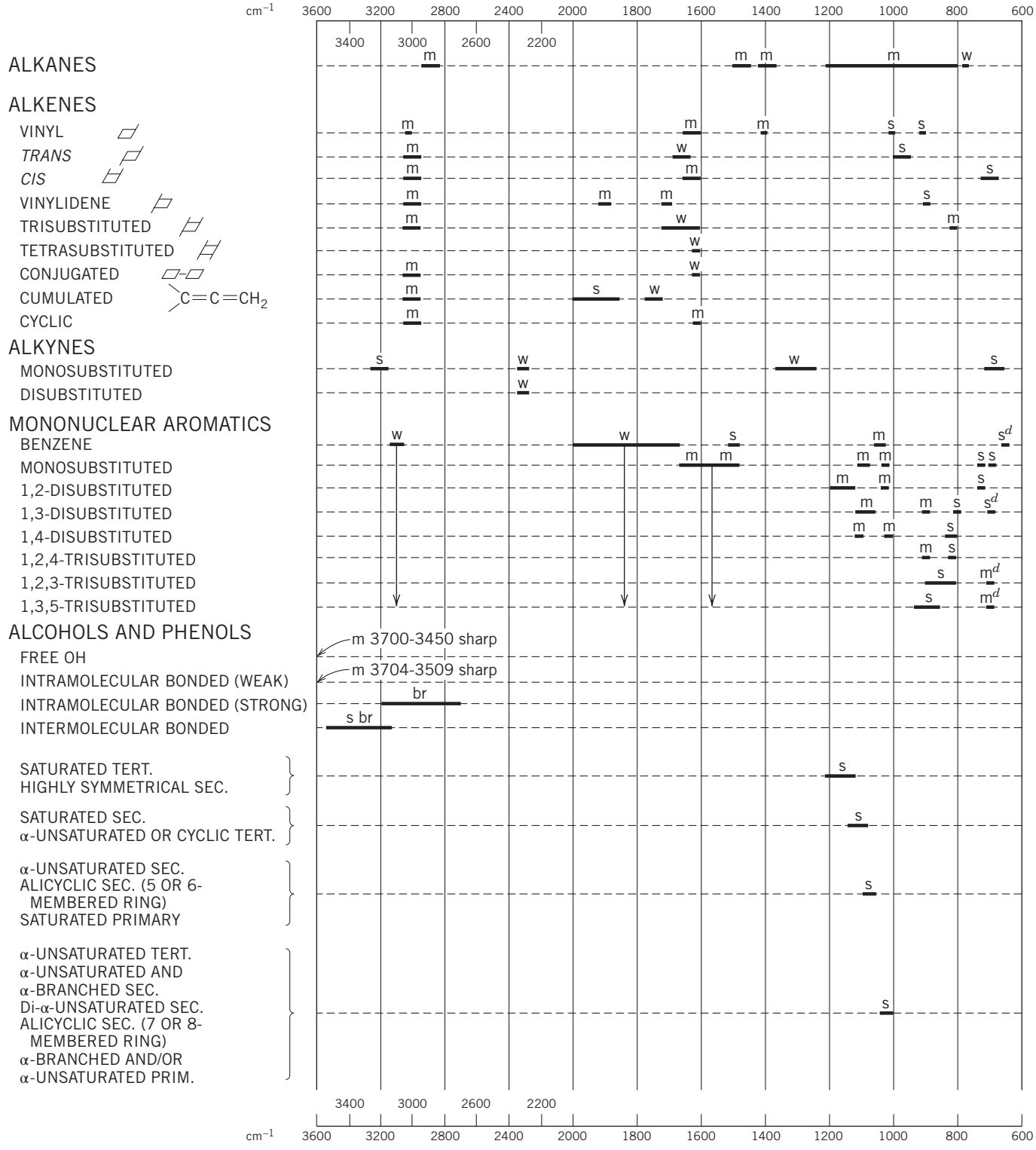

[a] Absorptions are shown by heavy bars. s = strong, m = medium, w = weak, sh = sharp, br = broad. Two intensity designations over a single bar indicate that two peaks may be present.

[b] May be absent.

[c] Frequently a doublet.

[d] Ring bending bands.

APPENDIX B (*continued*)

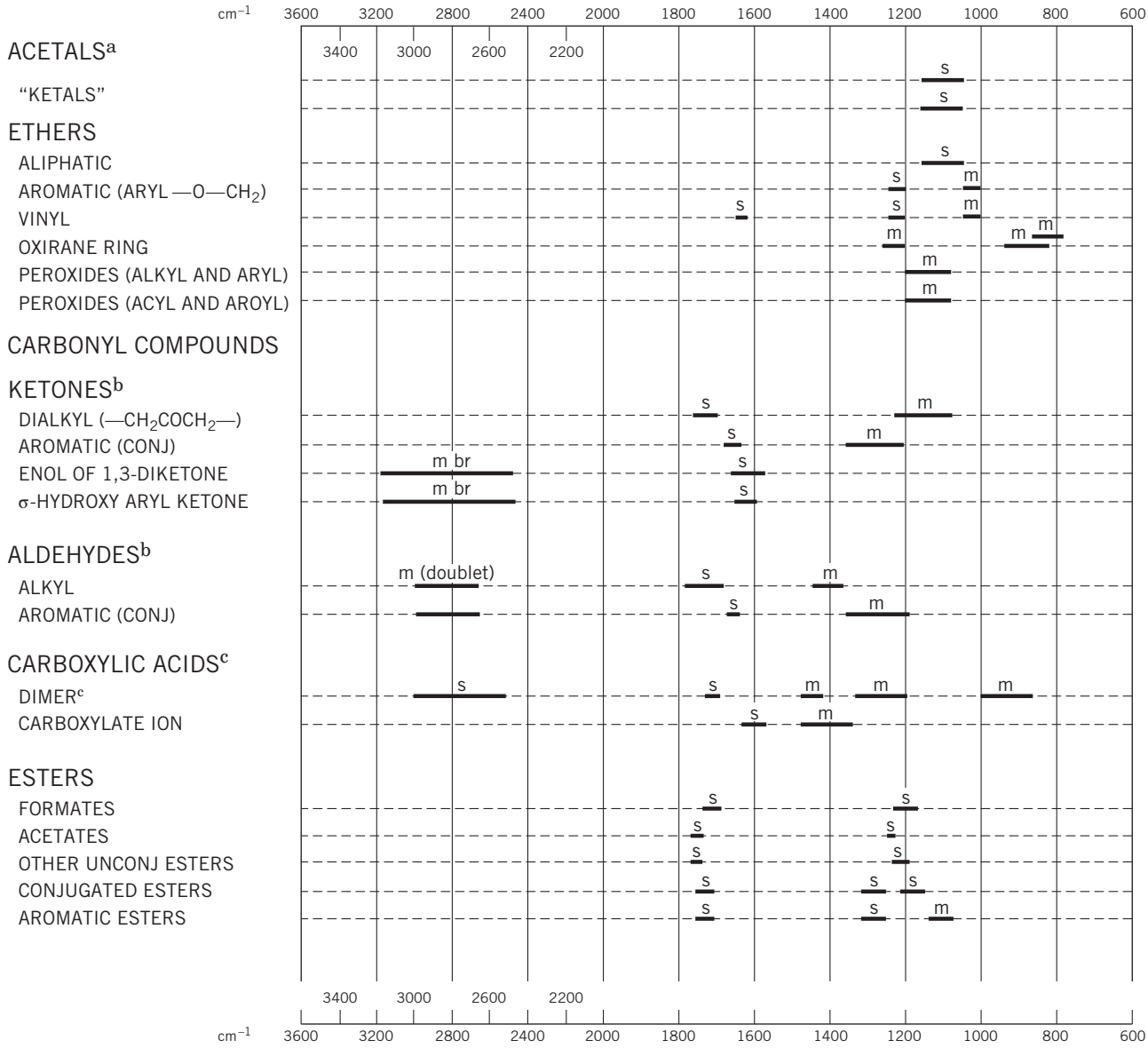

[a] Three bands, sometimes a fourth for ketals, and a fifth band for acetals.
[b] Conjugated aliphatic examples show C═O stretch at virtually the same position as aromatic structures.
[c] Conjugated examples show C═O stretch at lower wavenumbers (1710 cm^{-1} to 1680 cm^{-1}). The O—H stretch (3300 cm^{-1} to 2600 cm^{-1}) is very broad.

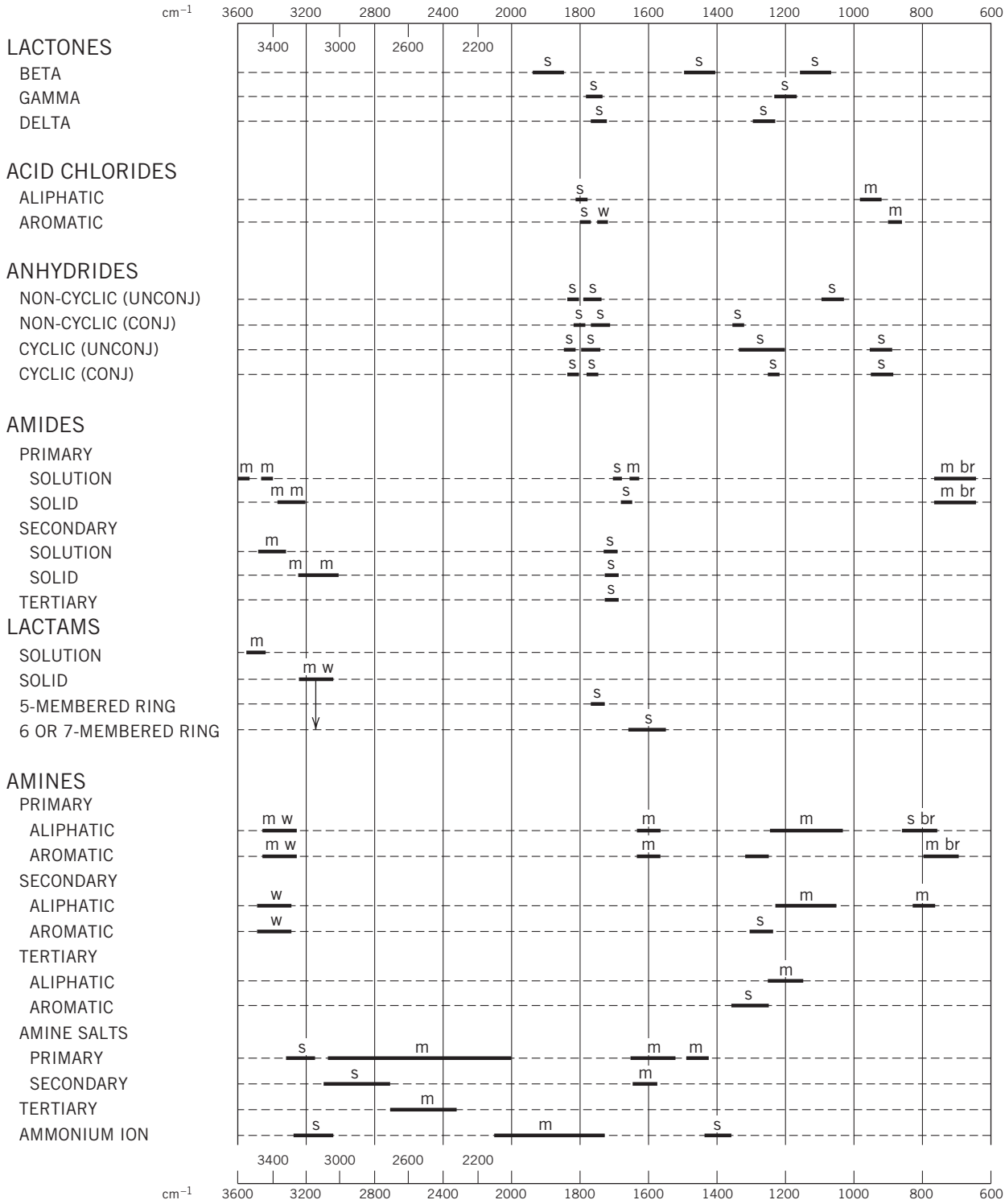
cm⁻¹
3600 3200 2800 2400 2000 1800 1600 1400 1200 1000 800 600
3400 3000 2600 2200
LACTONES
BETA
GAMMA
DELTA
ACID CHLORIDES
ALIPHATIC
AROMATIC
ANHYDRIDES
NON-CYCLIC (UNCONJ)
NON-CYCLIC (CONJ)
CYCLIC (UNCONJ)
CYCLIC (CONJ)
AMIDES
PRIMARY
SOLUTION
SOLID
SECONDARY
SOLUTION
SOLID
TERTIARY
LACTAMS
SOLUTION
SOLID
5-MEMBERED RING
6 OR 7-MEMBERED RING
AMINES
PRIMARY
ALIPHATIC
AROMATIC
SECONDARY
ALIPHATIC
AROMATIC
TERTIARY
ALIPHATIC
AROMATIC
AMINE SALTS
PRIMARY
SECONDARY
TERTIARY
AMMONIUM ION

APPENDIX B (*continued*)

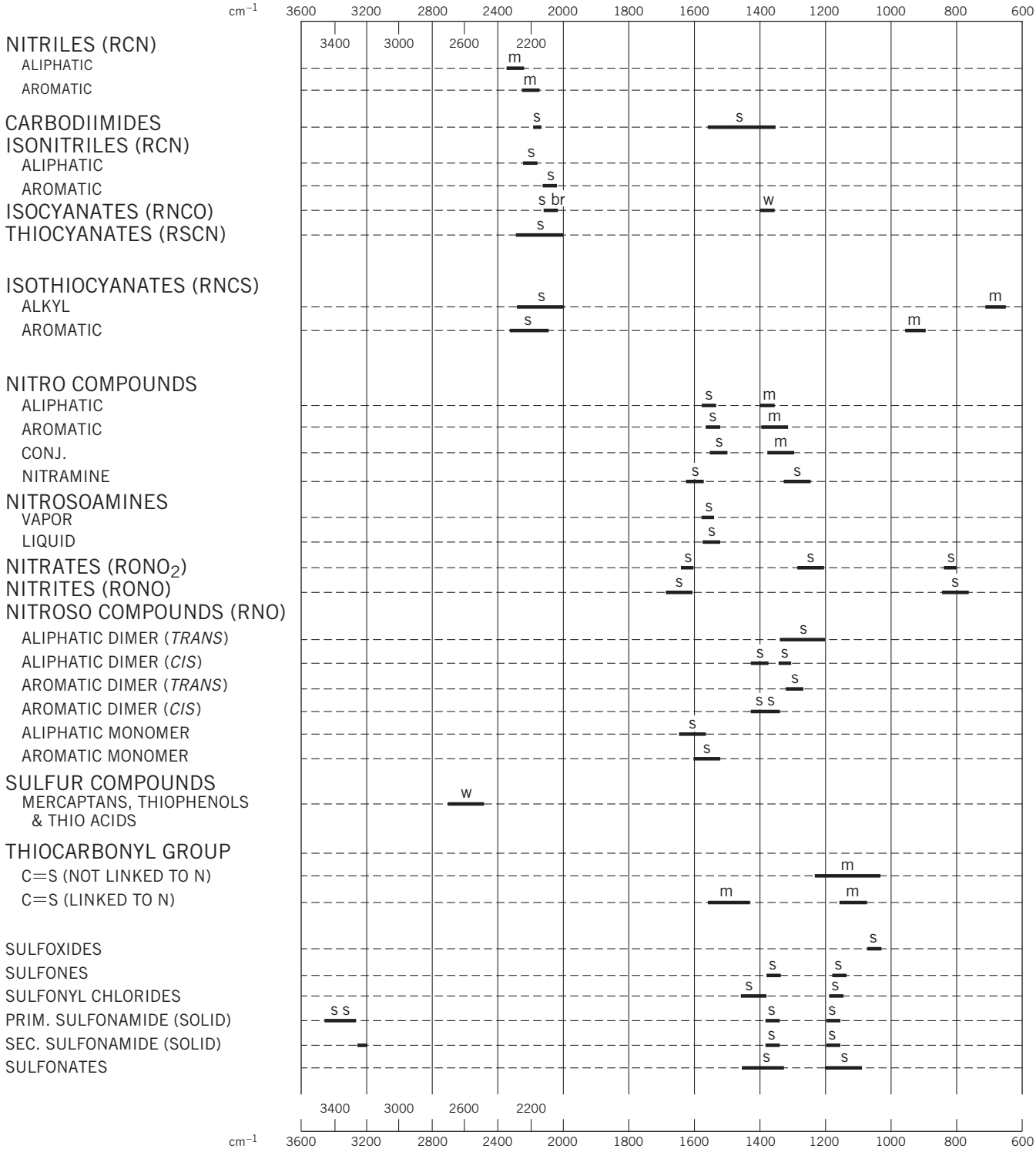

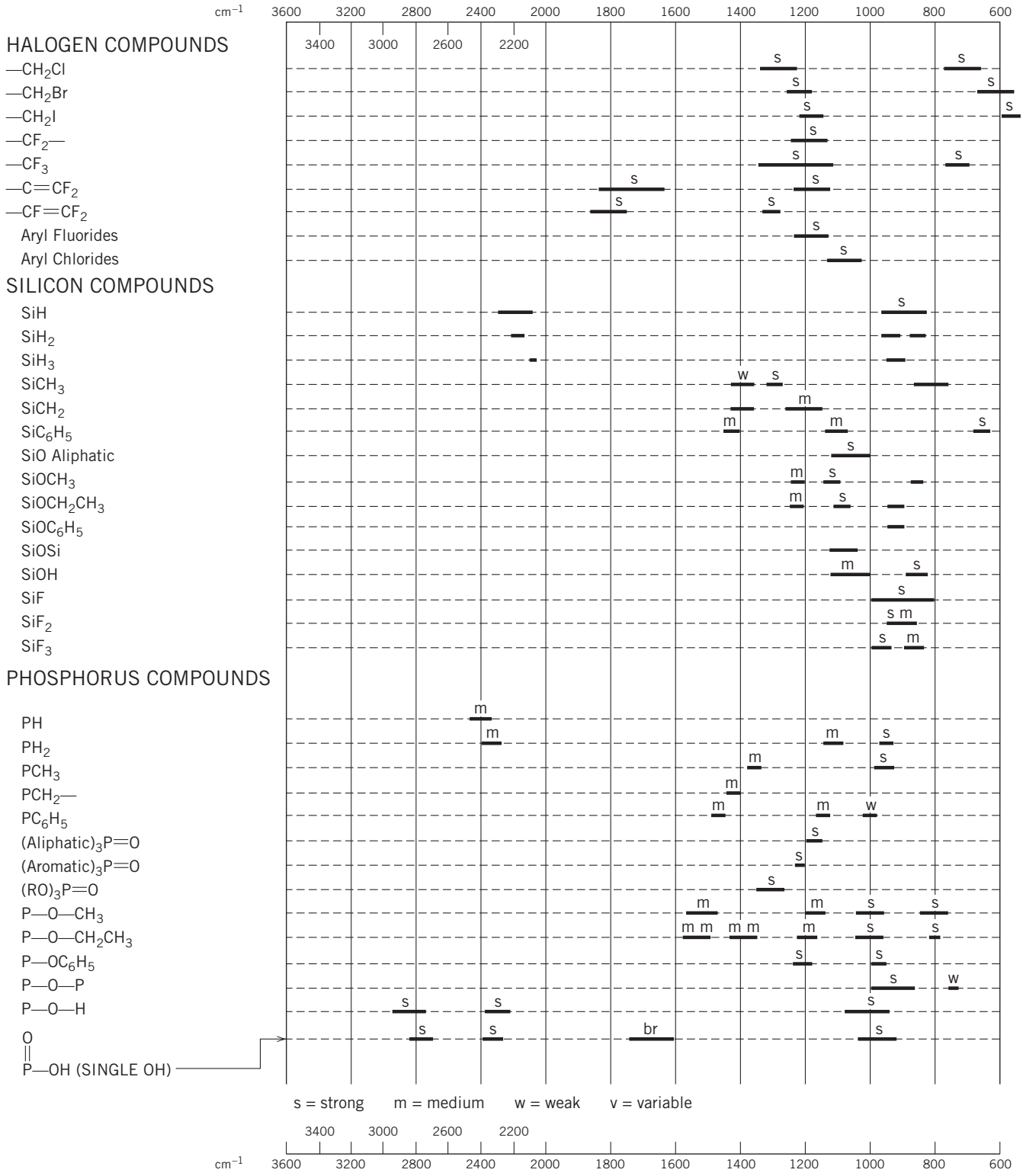
cm⁻¹
3600 3200 2800 2400 2000 1800 1600 1400 1200 1000 800 600
3400 3000 2600 2200
HALOGEN COMPOUNDS
—CH2Cl
—CH2Br
—CH2I
—CF2—
—CF3
—C═CF2
—CF═CF2
Aryl Fluorides
Aryl Chlorides
SILICON COMPOUNDS
SiH
SiH2
SiH3
SiCH3
SiCH2
SiC6H5
SiO Aliphatic
SiOCH3
SiOCH2CH3
SiOC6H5
SiOSi
SiOH
SiF
SiF2
SiF3
PHOSPHORUS COMPOUNDS
PH
PH2
PCH3
PCH2—
PC6H5
(Aliphatic)3P═O
(Aromatic)3P═O
(RO)3P═O
P—O—CH3
P—O—CH2CH3
P—OC6H5
P—O—P
P—O—H
O
||
P—OH (SINGLE OH)
s = strong m = medium w = weak v = variable

APPENDIX C ABSORPTIONS FOR ALKENES

TABLE C-1 Alkene Absorption[a]

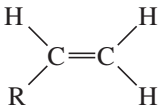	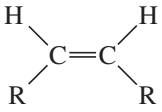	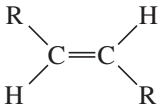
Vinyl 1648 cm^{-1} to 1638 cm^{-1} 995 cm^{-1} to 985 cm^{-1} (s)[b] 915 cm^{-1} to 905 cm^{-1} (s)	*cis* 1662 cm^{-1} to 1626 cm^{-1} (v) 730 cm^{-1} to 665 cm^{-1} (s)	*trans* 1678 cm^{-1} to 1668 cm^{-1} (v) 980 cm^{-1} to 960 cm^{-1} (s)[c]
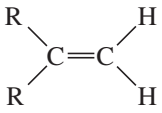	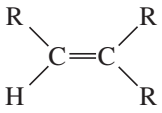	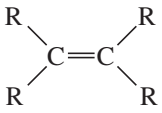
Vinylidene 1658 cm^{-1} to 1648 cm^{-1} (m) 895 cm^{-1} to 885 cm^{-1} (s)	Trisubstituted 1675 cm^{-1} to 1665 cm^{-1} (w) 840 cm^{-1} to 790 cm^{-1} (m)	Tetrasubstituted 1675 cm^{-1} to 1665 cm^{-1} very weak or absent

[a] s = strong, m = medium, w = weak, v = variable.
[b] This band also shows a strong overtone band.
[c] This band occurs near 1000 cm^{-1} in conjugated *trans–trans* systems such as the esters of sorbic acid.

TABLE C-2 C═C Stretching Frequencies in Cyclic and Acyclic Systems (cm^{-1})

Ring[a] or Chain	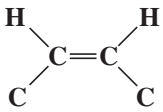	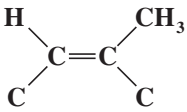	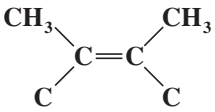	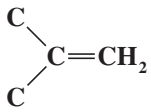
Chain *cis*	1661	1681	1672	1661
Chain *trans*	1676			
Three-membered ring	1641		1890	1780
Four-membered ring	1566		1685	1678
Five-membered ring	1611	1658	1686	1657
Six-membered ring	1649	1678	1685	1651
Seven-membered ring	1651	1673		
Eight-membered ring	1653			

[a] All rings have *cis* double bonds.

APPENDIX D ABSORPTIONS FOR PHOSPHORUS COMPOUNDS

TABLE D-1 P═O and P—O Stretching Vibrations

Group	Wavenumber (cm^{-1})[a]	ν_{P-O} Bands[a] (cm^{-1})
P═O stretch		
Phosphine oxides		
Aliphatic	~1150	
Aromatic	~1190	
Phosphate esters[b]	1299 to 1250	
P—OH	1040 to 910 (s)	
P—O—P	1000 to 870 (s)	~700 (w)
P—O—C (aliph)	1050 to 970 (s)[c]	830 to 740 (s)[d]
P—O—C (arom)	1260 to 1160 (s)	994 to 855 (s)

[a]s = strong; w = weak.
[b]The increase in P═O stretching frequency of the ester, relative to the oxides, results from the electronegativity of the attached alkoxy groups.
[c]May be a doublet.
[d]May be absent.

APPENDIX E ABSORPTIONS FOR HETEROAROMATICS

TABLE E-1 γ-CH and Ring Bending (β-Ring) Bands of Pyridines[a]

Substitution	Number Adjacent H Atoms	γ-CH (cm^{-1})	β-Ring
2-	4	781 to 740	752 to 746
3-	3	810 to 789	715 to 712
4-	2	820 to 794	775 to 709

[a]The γ and β notations are explained in the text and in the book by Katritzky (1963).

TABLE E-2 Characteristic γ-CH or β-Ring Bands of Furans, Thiophenes, and Pyrroles

Ring	Position of Substitution	Phase	γ-CH or β-Ring Modes[a]			
			cm^{-1}	cm^{-1}	cm^{-1}	cm^{-1}
Furan	2-	$CHCl_3$	~925	~884	835 to 780	
	2-	Liquid	960 to 915	890 to 875		780 to 725
	2-	Solid	955 to 906	887 to 860	821 to 793	750 to 723
	3-	Liquid		885 to 870	741	
Thiophene	2-	$CHCl_3$	~925	~853	843 to 803	
	3-	Liquid				755
Pyrrole	2-Acyl	Solid			774 to 740	~755

[a]The γ and β notations are explained in the text and in the book by Katritzky (1963).

CHAPTER 3

PROTON (^{1}H) MAGNETIC RESONANCE SPECTROSCOPY

3.1 INTRODUCTION

Nuclear magnetic resonance (NMR) spectroscopy is the single-most important analytical tool for the organic chemist. It is impossible to overstate the impact that NMR, in all of its forms, has had on advancing organic chemistry and in advancing related fields such as biochemistry and polymer chemistry. In a simple way, NMR spectroscopy can be thought of as another form of absorption spectroscopy, akin to IR or UV spectrometry in that, under appropriate conditions in a magnetic field, a sample can absorb electromagnetic radiation in the radiofrequency (rf) region at frequencies governed by the characteristics of the sample. However, due to the way in which the NMR experiment is performed, we will not discuss the concept of absorption further. We will refer to NMR "peaks" or "resonances." A plot of the peak intensity versus frequency constitutes an NMR spectrum. Our approach will be relatively light on theory and, instead, focus on interpretation. The reader is referred to Levitt (2008) for a more theoretical approach to the basics of NMR. This chapter covers proton nuclear magnetic resonance (^{1}H NMR) spectroscopy as well as some general aspects of NMR.

With some mastery of basic theory, interpretation of NMR spectra merely by inspection is usually feasible in greater detail than is the case for IR or mass spectra. The present account will allow for an in-depth interpretation of proton NMR spectra, which, in conjunction with other spectroscopic information, will enable us to readily identify even moderately complex organic compounds. References are given at the end of this chapter.

3.2 THEORY

3.2.1 Magnetic Properties of Nuclei

We begin by describing the magnetic properties of nuclei that lead to NMR. All nuclei carry a charge. A sometimes useful, though technically inaccurate, picture of spinning charge leads to a magnetic dipole associated with certain nuclei (Figure 3.1). In fact, the nuclei are not spinning. The concept of *nuclear spin* describes the intrinsic angular momentum associated with the magnetic nucleus. Some nuclei have intrinsic spin just as they have other intrinsic properties like mass. Let us remember that nuclear spin is a quantum mechanical phenomenon; our treatment will rely on familiar classical mechanical models. While this approach has an obvious visual appeal, it also has limitations that should be acknowledged from the start.

The nuclear spin angular momentum is described in terms of its nuclear spin quantum number I; these numbers have values of 0, $\frac{1}{2}$, 1, $\frac{3}{2}$, and so on ($I = 0$ denotes no spin). The intrinsic magnitude of the magnetic dipole is expressed in terms of the nuclear magnetic moment, μ.

Relevant properties, including the spin number I, of several nuclei are given in Chapter 6, Appendix A. While we cannot generally predict the exact value of I for every isotope, useful restrictions on their possible values can be determined from the atomic mass and the atomic number as shown in Table 3.1. It is best to simply memorize the values of I for common isotopes such as ^{1}H and ^{13}C ($I = \frac{1}{2}$). In quantum mechanical terms, the spin number I determines the number of quantum mechanical states an isolated spin may assume in an external uniform magnetic field in accordance with the formula $2I + 1$. The possible states may be denoted by a second quantum number, m.

Spectra of several nuclei can be readily obtained (e.g., $^1_1$H, $^{13}_6$C, $^{15}_7$N, $^{19}_9$F, and $^{31}_{15}$P) since they have spin numbers I of $\frac{1}{2}$ and a uniform spherical nuclear charge distribution (Figure 3.1). Of these, the most widely used in NMR spectroscopy are ^{1}H (this chapter) and ^{13}C (Chapter 4). Nuclei with a spin number, I, of one or higher have a nonspherical charge distribution. This is described by an electric quadrupole moment, which, as we shall see later, affects the nuclear spin relaxation time and, consequently, the line width

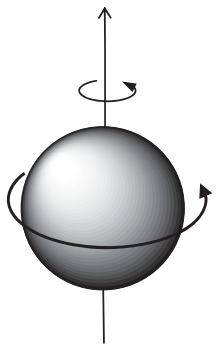

FIGURE 3.1 Several nuclides, including ^{1}H, have intrinsic angular momentum called "spin."

TABLE 3.1 Type of Nuclear Spin Number, I, with Various Combinations of Atomic Mass and Atomic Number

I	Atomic Mass	Atomic Number	Example of Nuclei
Half-integer	Odd	Odd	${}^{1}_{1}\mathrm{H}\left(\frac{1}{2}\right)$, ${}^{3}_{1}\mathrm{H}\left(\frac{1}{2}\right)$, ${}^{15}_{7}\mathrm{N}\left(\frac{1}{2}\right)$, ${}^{19}_{9}\mathrm{F}\left(\frac{1}{2}\right)$, ${}^{31}_{15}\mathrm{P}\left(\frac{1}{2}\right)$
Half-integer	Odd	Even	${}^{13}_{6}\mathrm{C}\left(\frac{1}{2}\right)$, ${}^{17}_{8}\mathrm{O}\left(\frac{5}{2}\right)$, ${}^{29}_{14}\mathrm{Si}\left(\frac{1}{2}\right)$
Integer	Even	Odd	${}^{2}_{1}\mathrm{H}(1)$, ${}^{14}_{7}\mathrm{N}(1)$, ${}^{10}_{5}\mathrm{B}(3)$
Zero	Even	Even	${}^{12}_{6}\mathrm{C}(0)$, ${}^{16}_{8}\mathrm{O}(0)$, ${}^{34}_{16}\mathrm{S}(0)$

of the signal and coupling with neighboring nuclei. We are largely concerned in this chapter with the proton (^{1}H), whose spin number I is $\frac{1}{2}$.

3.2.2 Excitation of Spin $\frac{1}{2}$ Nuclei

For spin $\frac{1}{2}$ nuclei in an external magnetic field (Figure 3.2), there are two energy levels and a slight excess of proton population in the lower energy state ($N_\alpha > N_\beta$) in accordance with the Boltzmann distribution. The states are labeled α and β, or $m = \frac{1}{2}$ and $m = -\frac{1}{2}$ (m is a quantum number); the energy gap between them, ΔE, is given by

$$\Delta E = (h\gamma/2\pi)\boldsymbol{B}_0$$

where h is Planck's constant. The equation simply states that ΔE is proportional to $\boldsymbol{B}_0$ (as shown in Figure 3.2) since h, γ, and π are constants. $\boldsymbol{B}_0$ represents the magnetic field strength.* There is a subtle but important difference here compared to many other forms of spectroscopy such as IR: the energy levels and, therefore, frequencies of peaks in the spectra, depend not only on the molecule itself but also on the strength of the applied magnetic field.

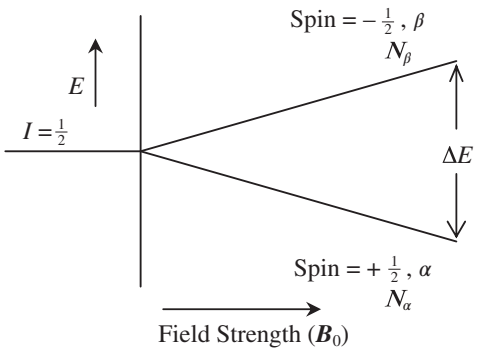

FIGURE 3.2 Two proton energy levels in a magnetic field of magnitude $\boldsymbol{B}_0$. N is the population of spins in the upper (N_β) and lower (N_α) energy states. The direction of the magnetic field ($\boldsymbol{B}_0$) is up, parallel to the ordinate, and field strength increases to the right. Larger magnetic fields increase ΔE.

*The designation $\boldsymbol{B}$ (magnetic induction or flux density) supercedes $\boldsymbol{H}$ (magnetic intensity). The SI term tesla (T), the unit of measurement for $\boldsymbol{B}$, supercedes the term gauss (G); 1 T = 10^4 G. The frequency term hertz (Hz) supercedes cycles per second (cps). MHz is megahertz (10^6 Hz).

A transition from the lower energy state to the higher energy state can be brought about by applying radiation of exactly the required frequency (in the radiofrequency range) for a given stationary magnetic field of strength $\boldsymbol{B}_0$. The fundamental NMR equation correlates a particular value of the applied radiofrequency known as the Larmor frequency, v, with the magnetic field strength:

$$v = (\gamma/2\pi)\boldsymbol{B}_0$$

since

$$\Delta E = hv$$

The radiofrequency v is typically on the order of megahertz (MHz). A frequency of 300 MHz is needed at a magnetic field strength $\boldsymbol{B}_0$ of 7.05 T for the proton (^{1}H) (or any other desired combination of v and $\boldsymbol{B}_0$ such that their ratio is equal to $\gamma/2\pi$; see Chapter 6, Appendix A). At this ratio, the system is in *resonance.* Hence, the name *nuclear magnetic resonance spectroscopy* is applied. The constant, γ, called the magnetogyric ratio, is a fundamental constant specific to each nuclide; it is the proportionality constant between the magnetic moment, μ, and the spin number, I.

$$\gamma = 2\pi\mu/hI$$

The fundamental NMR equation allows us the choice between two methods when describing a given instrument: we could use (i) the magnetic field strength or (ii) the Larmor frequency. Since modern instruments use superconducting magnets whose magnetic fields are extremely constant, it would make sense to refer to an instrument by its field strength in tesla units. This common sense approach is (generally) not used. Instead, the resonance frequency of ^{1}H is used. Thus, an instrument that has a 7.05 T magnet is referred to as a 300 MHz NMR spectrometer.†

The standard method of recording NMR spectra is the pulsed-Fourier transform (FT) method. The sample is placed in an NMR probe in the magnetic field and irradiated with a short pulse (on the order of microseconds) of high-power radiofrequency energy. This pulse simultaneously excites all of the nuclei of a given type (e.g., ^{1}H) in the sample. Immediately following the pulse, the excited spins precess around the external magnetic field together, creating a current in the receiver coil of the NMR probe. The resulting signal, known as the free induction decay (FID), is recorded and digitized by a computer. The information in the FID, a function of time, is converted to a readable spectrum in the frequency domain using a mathematical operation known as the Fourier transform (see Figure 3.9).

Let us consider a large group of identical nuclei (^{1}H, protons) in a strong, stationary magnetic field. The magnetic axis of any single proton precesses about the stationary magnetic field, $\boldsymbol{B}_0$ (along the z-axis), in the same manner in which a spinning top (or a gyroscope) precesses under the influence of gravity (Figure 3.3). The precessional frequency

†Use of the frequency instead of the magnetic field also harkens back to a previous "continuous wave" implementation of NMR where the frequency was held constant and the magnetic field was varied during the experiment.

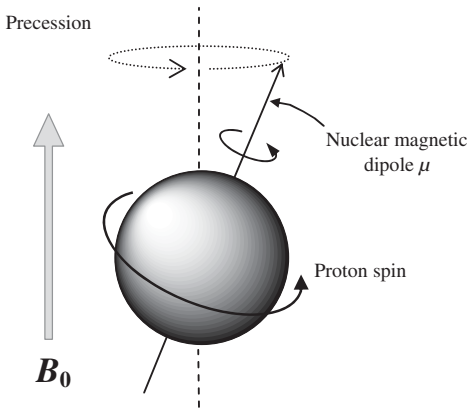

FIGURE 3.3 Classical representation of a proton spin precessing in a magnetic field of magnitude $\boldsymbol{B}_0$ in analogy with a precessing spinning top.

of the nuclear magnetic dipole, μ, about the z-axis is equal to the Larmor frequency, ν.

Before a radiofrequency pulse, the individual members of a large group of nuclear spins will be precessing around the z-axis in a random fashion or in random phase. In Figure 3.4, we see the precessing nuclei represented by their individual spin vectors. Notice that some of the vectors have positive z components (pointing up) and some of them have negative z components (pointing down). These two types of spins represent those in the low-energy (α) and high-energy (β) states, respectively. Notice also that there is a slight excess of spins in the low-energy state (pointing up). In Figure 3.4, there are eight vectors pointing up and six vectors pointing down. If we sum all of these vectors, we obtain a single total vector whose direction is on the positive z-axis and whose magnitude depends on the Boltzmann distribution of spins. Notice that any components in the xy plane cancel out as a result of this summation (see the right-hand side of Figure 3.4). The resulting vector is called the net magnetization vector, $\boldsymbol{M}_0$.

Figure 3.5 shows the fate of the net magnetization vector during a simple pulsed NMR experiment. When a short radiofrequency pulse is applied, a torque is exerted on the net magnetization vector, $\boldsymbol{M}_0$, and it will be tipped away from the z-axis and toward the xy plane (Figure 3.5a). The magnetic component generated in the xy plane (the FID) can be detected as a function of time by a receiver coil mounted in the xy plane (this may be the same coil which generates the initial rf pulse). The torque experienced by the net magnetization vector is more precisely explained as arising from the fact that the oscillating magnetic field associated with the applied radiation is rotating with exactly the same frequency as the individual nuclear spins. This is one way of explaining the concept of resonance; further technical details are beyond the scope of this book.

3.2.3 Relaxation

Relaxation refers to the establishment or re-establishment of the equilibrium state of the nuclear spin magnetization. Equilibrium is achieved when $\boldsymbol{M}_0$ returns to the z-axis after a pulse. Relaxation is not the process which gives rise to an FID. Relaxation is a complex subject, but it is important to have a basic grasp of the fundamentals in order to better understand NMR experiments and NMR spectra.

There are two main types of relaxation which we will briefly discuss here. The first is longitudinal spin relaxation, also known as spin–lattice relaxation, and it is quantified by a time constant T_1. The second is transverse spin relaxation, also known as spin–spin relaxation, and it is quantified by a time constant T_2. The values of these time constants can vary quite a bit depending on the nature of the sample and the type of nucleus studied. For ^{1}H solution NMR studies of small molecules, these values are typically on the order of seconds. For small organic molecules, ^{1}H T_1 and T_2 values are approximately equal to one another. More generally, $T_1 \geq T_2$.

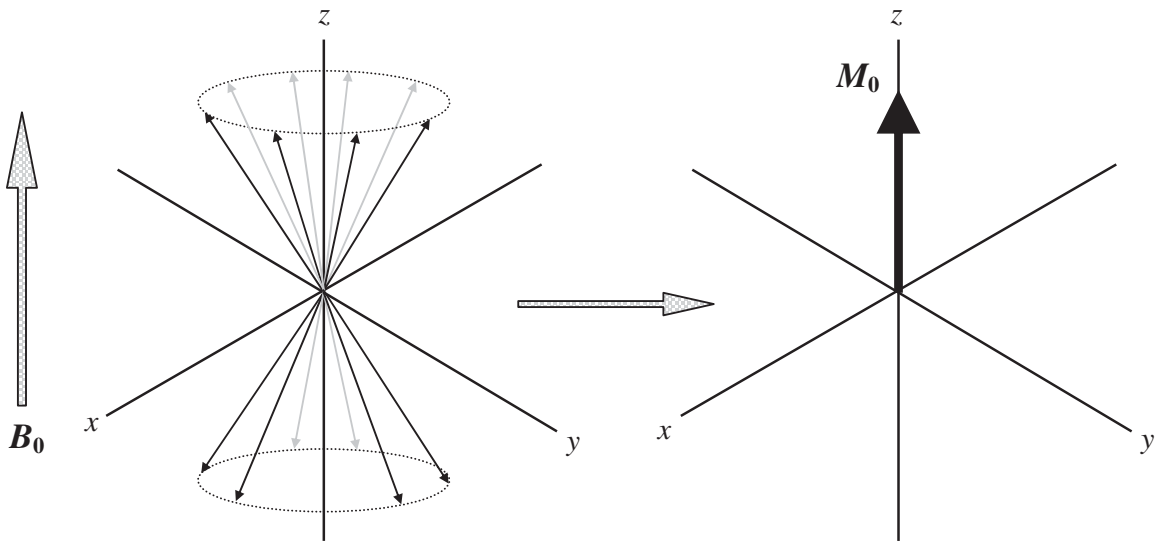

FIGURE 3.4 Assemblage of precessing nuclei with net macroscopic magnetization $\boldsymbol{M}_0$ in the direction of the stationary magnetic field $\boldsymbol{B}_0$ along the z-axis.

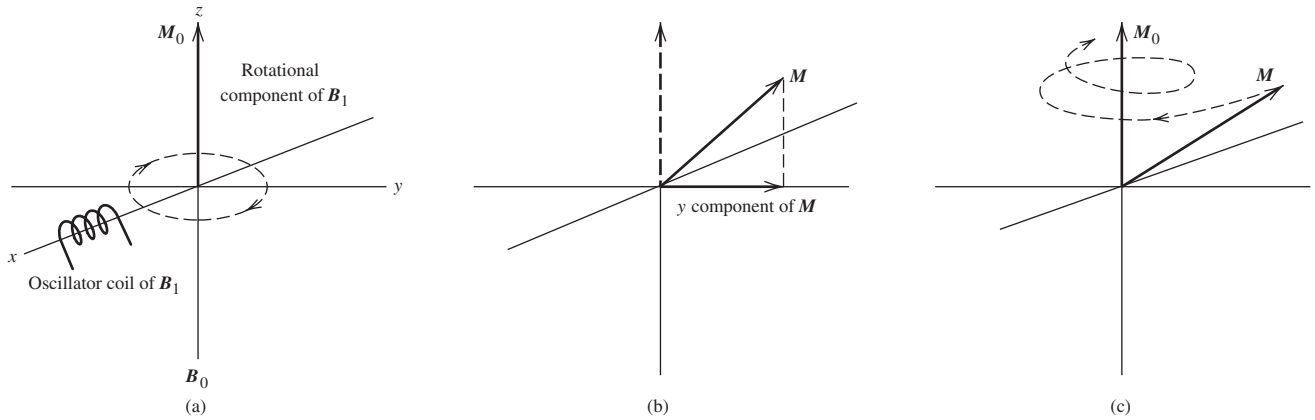

FIGURE 3.5 (a and b) Oscillator generates rotating component of applied magnetic field $\boldsymbol{B}_1$. The net magnetization $\boldsymbol{M}_0$ is tipped toward the *y*-axis to give $\boldsymbol{M}$, which precesses about the *z*-axis generating a component of magnetization in the horizontal plane. (c) Relaxation of $\boldsymbol{M}$ to $\boldsymbol{M}_0$ follows a spiral of decreasing amplitude. The Cartesian frame is stationary.

T_1 relaxation is what allows the *z*-components of the nuclear spin magnetization vectors to re-establish equilibrium according to the Boltzmann distribution. The value of T_1, therefore, typically determines how long the experimentalist must wait after an FID before repeating the process of applying an rf pulse and acquiring another FID. A long T_1 value means that it takes a relatively long time for magnetization along the *z*-axis to be established upon initially placing the sample in the magnet or after pulsing and acquiring a single FID. The role of T_1 relaxation in acquiring and interpreting ^{13}C NMR spectra is discussed in Chapter 4.

T_2 relaxation enables the net magnetization in the *xy* plane to decay to zero, that is, to the equilibrium state, after a radiofrequency pulse. One can see the effects of T_2 relaxation on an FID; the relaxation causes the signal to decay exponentially to zero as it is being acquired (see Figure 3.9). Actually, due to magnetic field inhomogeneities associated with the spectrometer magnet rather than the molecule itself, the typically observed relaxation time constant is smaller than the true T_2 and is denoted T_2^*. The value of T_2^* plays a very practical role in the appearance of NMR spectra (Figure 3.6): it is inversely related to the width of the NMR peak at half-height ($\Delta\nu_{\frac{1}{2}}$):

$$\Delta\nu_{\frac{1}{2}} = 1/(\pi T_2^*)$$

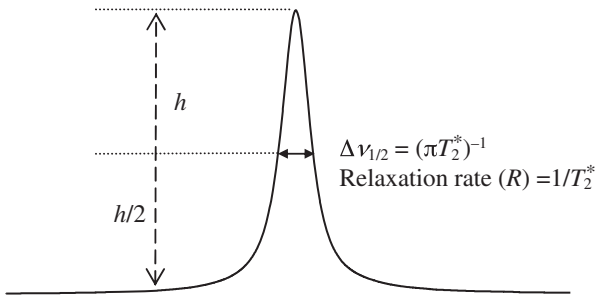

FIGURE 3.6 The peak width at half-height ($h/2$) is inversely related to the transverse relaxation time constant.

Faster spin–spin relaxation leads to shorter FIDs and broader NMR peaks; slower spin–spin relaxation results in longer FIDs and sharper NMR peaks.

3.3 INSTRUMENTATION AND SAMPLE HANDLING

3.3.1 Instrumentation

Beginning in 1953 with the first commercial NMR spectrometer, the early instruments used permanent magnets or electromagnets with fields of 1.41 T, 1.87 T, 2.20 T, or 2.35 T corresponding to 60 MHz, 80 MHz, 90 MHz, or 100 MHz, respectively, for proton magnetic resonance.

The "horsepower race," driven by the need for higher resolution and sensitivity, has resulted in the widespread use of 300 MHz to 800 MHz instruments. Resolution, in general terms, refers to the ability to resolve or differentiate between different spectral peaks along the frequency axis. The most powerful commercial NMR spectrometer is currently 1000 MHz, or 1 GHz, and the development of 1.1 GHz and 1.2 GHz spectrometers is in progress. All of the instruments above 100 MHz are based on helium-cooled superconducting magnets (solenoids) and operate in the pulsed FT mode. The other basic requirements besides high field are frequency-field stability, field homogeneity, and a computer interface (see Figure 3.7). The computer is used to acquire the data, carry out the FT, and further process and analyze the resulting spectra.

The sample (routinely a solution in a deuterated solvent in a 5 mm o.d. glass tube) is placed in the probe, which contains the transmitter and receiver coils and a spinner to spin the tube about its vertical axis in order to average out magnetic field inhomogeneities.

The proton NMR spectrum is shown as a series of peaks whose areas are proportional to the number of protons they represent. Peak areas are determined digitally and are often shown as a series of steps with heights proportional

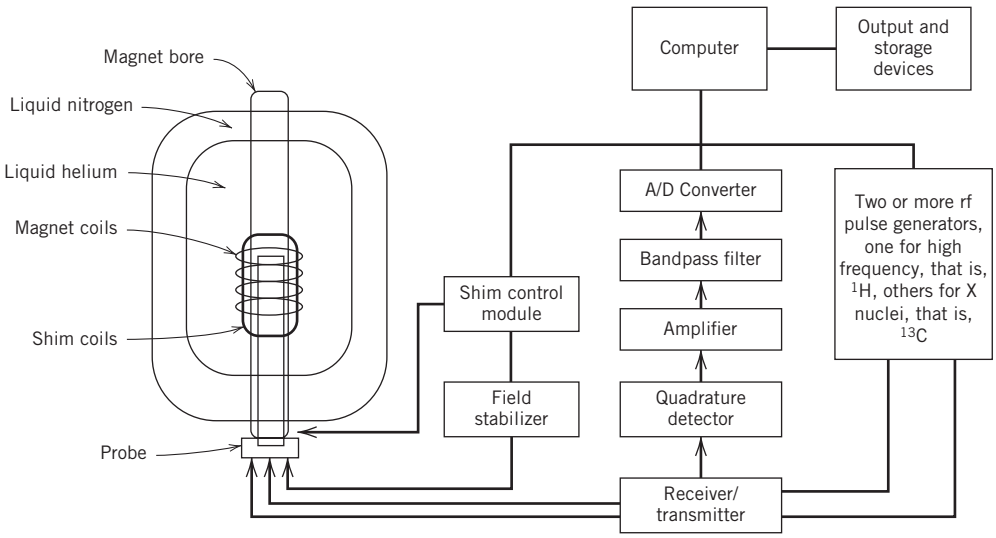

FIGURE 3.7 Schematic diagram of a Fourier transform NMR spectrometer with a superconducting magnet. The probe is parallel with the *z*-axis of the magnet, which is cooled with liquid helium surrounded by liquid nitrogen in a large Dewar flask.

to the peak areas (see Figure 3.8).* A proton count from the integration (area under the peak) is useful to determine or confirm molecular formulas, detect hidden peaks, determine sample purity, and do quantitative analysis. Peak positions (chemical shifts, Section 3.4) are measured in frequency units from a reference peak.

*Chemically different protons resonate at very slightly different frequencies–differences up to around 5000 Hz at a Larmor frequency of 300 MHz. The utility of NMR spectroscopy for the organic chemist dates from the experiment at Varian Associates that obtained three peaks from the chemically different protons in CH_3CH_2OH; the peak areas were in the ratio 3:2:1. [Arnold, J.T., Dharmatti, S.S., and Packard, M.E. (1951) *J. Chem. Phys.*, **19**, 507.]

3.3.2 Sensitivity of NMR Experiments

Sensitivity refers in this context to the signal to noise of the NMR experiment. The signal-to-noise ratio (S/N) of an FID or NMR spectrum depends on many factors, and explicit expressions depend on approximations used and details of the experimental setup. One useful expression is given:

$$\mathrm{S/N} \propto NQ\gamma_{\mathrm{exc}}\gamma_{\mathrm{det}}^{\frac{3}{2}}\boldsymbol{B}_0^{\frac{3}{2}}T_2^{*\frac{1}{2}}T^{\frac{-3}{2}}\,ns^{\frac{1}{2}}$$

where N is the number of spins in the sample; Q is the quality factor of the probe; γ_{exc} and γ_{det} are the magnetogyric ratios of the excited and detected nuclei, respectively; $\boldsymbol{B}_0$ is the external applied magnetic field; T_2^* is the effective spin–spin

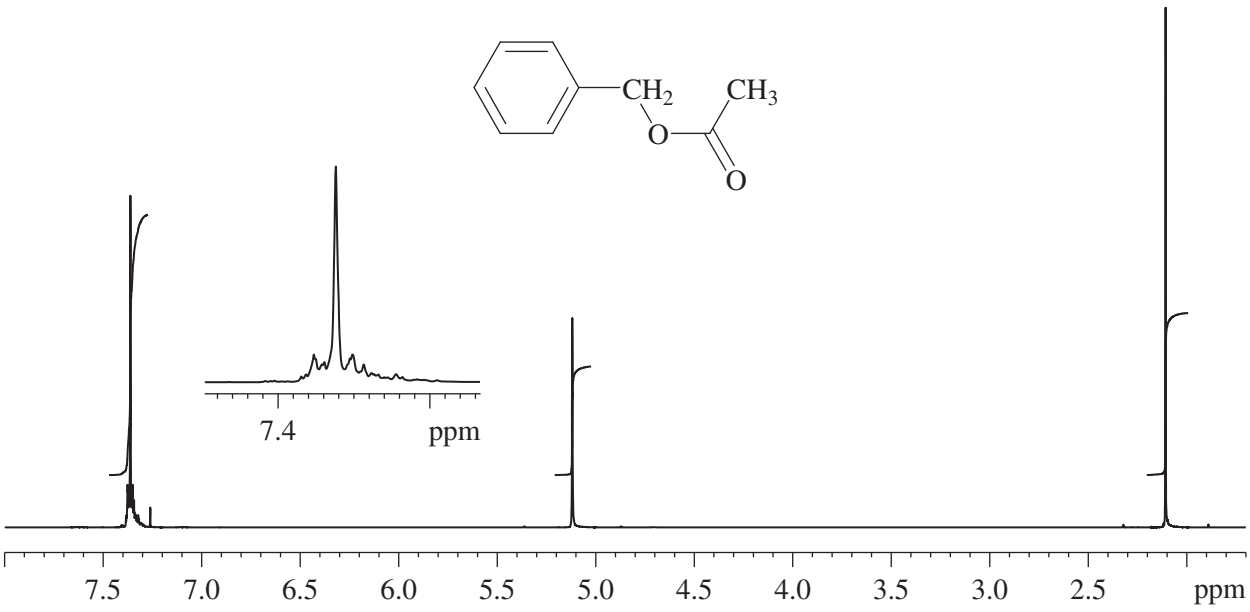

FIGURE 3.8 ^{1}H NMR spectrum of benzyl acetate in $CDCl_3$, 300 MHz.

relaxation time constant; T is the temperature of the sample, and ns is the number of scans. For the ^{1}H NMR spectra discussed in this chapter, γ_{exc} and γ_{det} are the same.

It is important to be aware of the most important factors within the experimentalist's control to increase the signal-to-noise ratio. The conceptually simplest and most effective way for the organic chemist to increase S/N is to increase the number of spins in their sample; that is, to increase the sample concentration. S/N increases linearly with the number of spins in the sample. Conversely, acquiring more scans (signal averaging of the FID) will result in an increase in S/N only proportional to the square root of the number of scans. Decreasing the temperature often affords an increase in S/N due to the reduction of thermal noise in the electronics of the probe, and more obviously due to the greater polarization of the nuclear spins according to the Boltzmann distribution. The Boltzmann distribution may also be altered by increasing the applied magnetic field, $\boldsymbol{B}_0$. It turns out that the overall S/N typically increases with $\boldsymbol{B}_0^{\frac{3}{2}}$. Nuclei with higher magnetogyric ratios also give spectra with higher S/N. Note that the natural abundance of the isotope of interest plays an important role in determining the value of N.

We make brief mention here of three of the more cutting-edge methods in NMR spectroscopy for improving sensitivity. The first two of these work by exploiting an unnatural, large, non-Boltzmann distribution of nuclear spins across their energy levels. For example, dynamic nuclear polarization (DNP) exploits the greater spin polarization of unpaired electrons to enhance the NMR spectrum. The electron spin polarization is transferred to the nuclei, like ^{1}H, giving the latter a large non-Boltzmann nuclear spin polarization and the resulting NMR spectrum is characterized by a concomitantly large S/N. DNP NMR enables the experimentalist to examine chemical species present in very low concentrations and/or in a very short time. Enhancement of ^{1}H NMR can also be achieved using *para*-hydrogen, a nuclear spin isomer of H_2 gas. Reactions of *para*-H_2 with compounds of interest can generate products carrying large non-Boltzmann distributions at particular ^{1}H sites, providing spectra with large S/N. Cryogenically cooled NMR probes can also increase S/N by reducing the noise associated with the electronics in the probe. For further reading on this topic, see Ardenkjær-Larsen (2003) and Duckett (2011).

3.3.3 Solvent Selection and Sample Handling

The sample must be soluble in order to perform NMR measurements in solution.* The ideal solvent should contain no protons and be inert, low boiling, and inexpensive. Deuterated solvents are typically, but not absolutely, necessary for modern instruments because they depend on a deuterium signal to "lock" or stabilize the $\boldsymbol{B}_0$ field of the magnet. Modern instruments have a deuterium channel that constantly monitors and adjusts (locks) the $\boldsymbol{B}_0$ field to the frequency of the deuterated solvent (see Figure 3.7). Typically, ^{1}H NMR signals are on the order of 0.1 to several Hz wide out of 300000000 Hz (for a 300 MHz system), so the $\boldsymbol{B}_0$ field needs to be very stable and homogeneous.

The deuterium signal is also typically used to shim the $\boldsymbol{B}_0$ field. Instruments use small electromagnets (called shims) to adjust the main magnetic field ($\boldsymbol{B}_0$) so that the homogeneity of the field is high at the center of the magnet where the sample resides. Most modern instruments have approximately 20 to 40 electromagnetic shims; they are computer controlled and can be adjusted in an automated manner. Good shimming will increase the value of T_2^* and is essential to obtaining sharp NMR peaks. Shimming is done manually, or with computer automation, each time a new sample is placed in the magnet. Bad shimming will result in short T_2^* values, broad line shapes, and unusable spectra.

Deuterated chloroform ($CDCl_3$) is used as the solvent most of the time for organic compounds. The small sharp proton peak at 7.26 ppm from the $CHCl_3$ impurity present rarely interferes seriously. For very dilute samples, $CDCl_3$ can be obtained in close to 100% isotope purity, thereby reducing even further the intensity of the $CHCl_3$ peak. A list of common, commercially available solvents with the chemical shifts of protonated impurities (e.g., $CHCl_3$ in $CDCl_3$) is given in Appendix G.

A routine sample for ^{1}H NMR on a 300 MHz instrument consists of about 5 mg to 10 mg of the compound in about 0.5 mL of solvent in a 5 mm o.d. glass tube. Microprobes that accept a 1.0 mm, 1.7 mm, 2.5 mm, or 3 mm o.d. tube are available and provide higher sensitivity per unit mass. Under favorable conditions, it is possible to obtain a spectrum on 100 nmol (or less) of a compound of modest molecular weight in a 1.0 mm microtube (volume 5 μL) on a 600 MHz instrument. Of course, one must be aware that it is the concentration of spins which is important, and so the masses required for good spectra will vary depending on the molar mass of the compound.

Traces of ferromagnetic impurities cause severe broadening of NMR peaks because of reduction of relaxation times. Common sources are rust particles from tap water, steel wool, Raney nickel, and particles from metal spatulas or fittings (Figure 3.9). These impurities can be removed by filtration. Dissolved oxygen gas can also broaden NMR lines. The use of freeze–pump–thaw techniques and air-tight NMR tubes (using special caps or by flame sealing) can alleviate this problem.

Traces of common laboratory solvents can be annoying. See Appendix H or Fulmer et al. (2010) for an extensive list of common solvent impurities. Other offenders are greases and plasticizers (phthalates in particular). NMR solvents should be kept in a dessicator.

*If the sample is not soluble, solid-state NMR experiments can be carried out, although there are particular challenges associated with ^{1}H NMR of solids. Solid-state NMR experiments generally require somewhat different spectrometer hardware and sample preparation. See Fyfe, C. A. *Solid State NMR for Chemists*, CFC Press, Guelph, 1983 and Bryce et al., (2001) *Can. J. Anal. Sci. Spectrosc.*, **46**, 46–82.

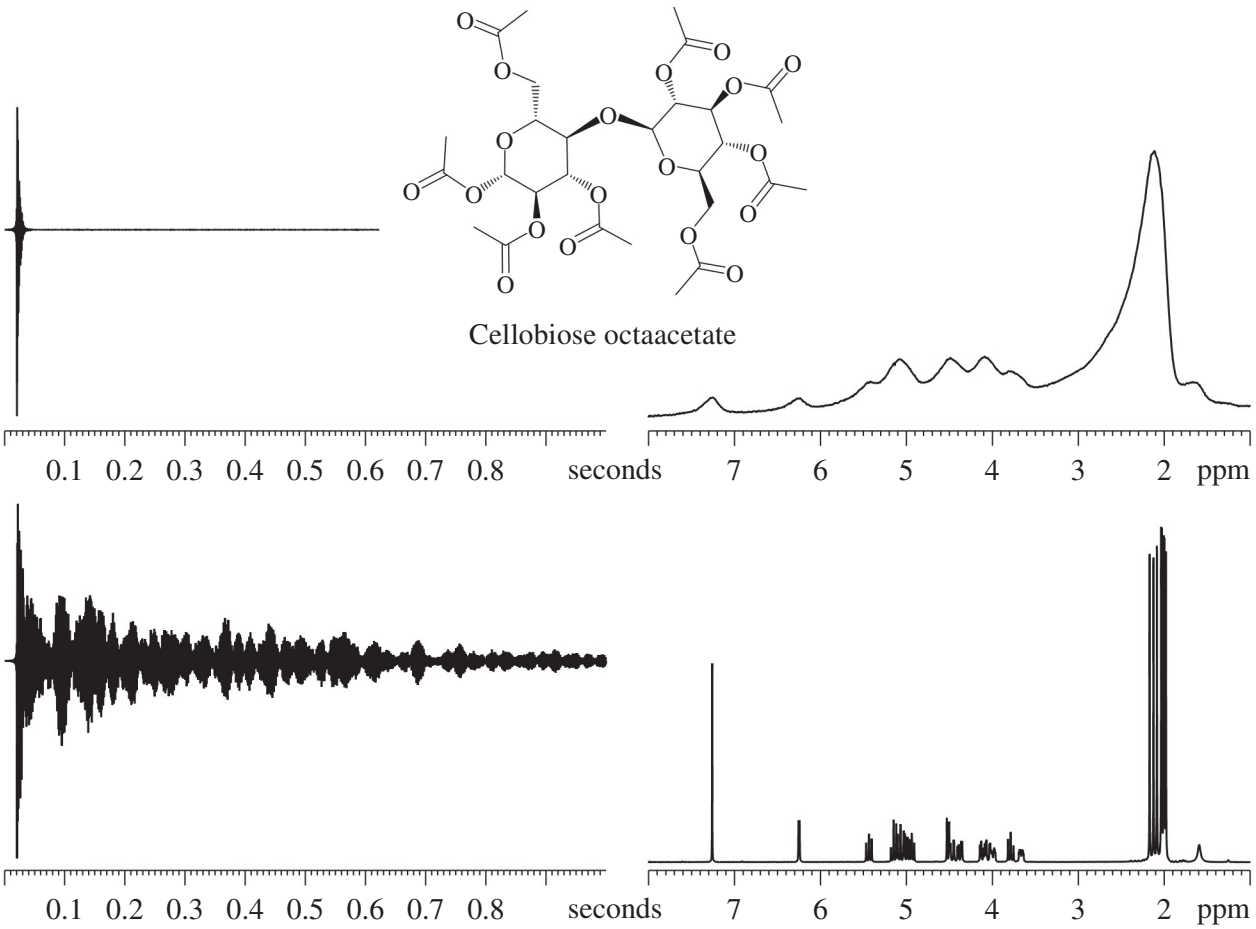

FIGURE 3.9 The effect of a trace amount of ferromagnetic particles on the proton FID and spectrum of cellobiose octaacetate is to speed up T_2 relaxation and give broad spectra (top). The FID and spectrum of a pure sample without ferromagnetic contaminants are shown at the bottom.

3.4 CHEMICAL SHIFT

Our fundamental NMR equation seems insufficient since it states that there is a single resonance frequency (v) for all protons at a given magnetic field strength ($\boldsymbol{B}_0$):

$$v = (\gamma/2\pi)\boldsymbol{B}_0$$

Fortunately, and not surprisingly, the situation is not so simple. A covalently bonded hydrogen atom in a molecule is *shielded* to a very small extent (on the order of parts per million (10^{-6}), or ppm) by the local electronic structure of the molecule; the amount of shielding *varies with the chemical environment*. This variation gives rise to differences in resonance frequencies, which are commonly called *chemical shifts*. The ability to discriminate among the individual spectral resonances (or peaks) describes high-resolution NMR spectroscopy.

The basic NMR equation for all protons is now modified for an ensemble of equivalent protons in the molecule:

$$v_{\text{eff}} = (\gamma/2\pi)\boldsymbol{B}_0(1-\sigma)$$

The symbol σ is the magnetic shielding constant whose value describes the shielding effect of the local electronic structure in the molecule. At a given value of $\boldsymbol{B}_0$, the *effective* frequency at resonance is less than the resonance frequency, v, of a hypothetical "naked" proton, H^+. Note that σ is not a constant in the sense of other fundamental constants; it is a constant only for the particular nucleus we are observing in a particular molecule. Its value varies with the chemical environment.

To visualize this shielding, consider that a pair of electrons under the influence of a magnetic field circulate and, in circulating, generate their own magnetic field opposing the applied field; hence, the shielding effect (Figure 3.10). This effect accounts for the diamagnetism exhibited by organic materials. It should be noted that this description is an approximation and that more detailed theories are required to properly describe and understand shielding constants. In the case of materials with an unpaired electron, the paramagnetism associated with the net electron spin far overrides the diamagnetism of the circulating, paired electrons. We do not consider paramagnetic compounds in our discussion.

The degree of shielding depends on the details of the electronic structure of the molecule and is well described using Ramsey's theory (see References section). However, for the empirical interpretation of ^{1}H NMR spectra, the

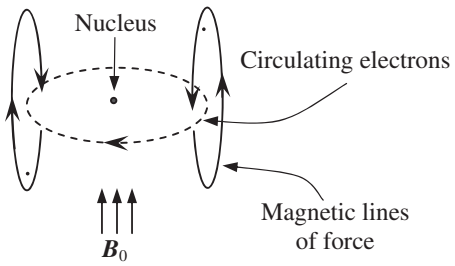

FIGURE 3.10 Diamagnetic shielding of a nucleus by circulating electrons. The arrows, ↑↑↑, represent the direction of the stationary magnetic field of magnitude $\boldsymbol{B}_0$. The circulating electrons comprise the electrical current, but the current direction is shown conventionally as flow of positive charge.

degree of shielding of a hydrogen atom can be roughly rationalized by considering the density of the circulating electrons around the proton. For a proton bonded to a carbon atom, this density will in turn depend on the inductive effect of other groups attached to the carbon atom. At this stage, it is important to understand that *magnetic shielding* is a fundamental physical property, whereas it is the *chemical shift* that one observes in an NMR experiment. The relationship between the two quantities is as follows:

$$\delta = (\sigma_{\text{ref}} - \sigma)/(1 - \sigma_{\text{ref}})$$

where σ_{ref} is the magnetic shielding constant of a reference compound specific to each nuclide under study. Since magnetic shielding constants are on the order of ppm, the above equation is well approximated as $\delta = \sigma_{\text{ref}} - \sigma$ for light nuclides such as ^{1}H and ^{13}C.

We now have the concept that protons in different chemical environments have different chemical shifts. Conversely, protons in the same chemical environment have the same chemical shift. But what do we mean by "different" and "same"? It is intuitively obvious that the chemically different methylene groups of $ClCH_2CH_2OH$ have different chemical shifts and that the protons in either one of the methylene groups have the same chemical shift. But it may not be so obvious, for example, that the individual protons of the methylene group of $C_6H_5CH_2CHBrCl$ do not have the same chemical shift. For the present, we shall deal with obvious cases and postpone a more rigorous treatment of chemical equivalence to Section 3.8.

Tetramethylsilane (TMS), $(CH_3)_4Si$, is the universally accepted reference compound for ^{1}H NMR and ^{13}C NMR (Chapter 4). As proton NMR developed, this material quickly gained in popularity as a chemical shift reference because it has several desirable properties: it is chemically inert, symmetrical, volatile (b.p. 27 °C), and soluble in most organic solvents; it gives a single, intense, sharp, NMR peak, and its protons are more shielded than almost all other protons in organic compounds. When water or deuterium oxide is the solvent, TMS can be used as an external reference in a concentric capillary tube, or the methyl protons of water-soluble sodium 2,2-dimethyl-2-silapentane-5-sulfonate (DSS), $(CH_3)_3SiCH_2CH_2CH_2SO_3Na$, are used as an internal reference ($\delta = 0.015$ ppm). Harris et al. (2008) describe the IUPAC conventions for chemical shift referencing.

Historically, and now by convention, the TMS reference peak is placed at the right-hand edge of the spectrum and designated zero on both the frequency (Hz) and chemical shift (δ) scales (defined below). Positive frequencies and chemical shifts are to the *left* of TMS, negative values are found on the right.* The term "shielded" is a relative one and means toward the right; "deshielded" means toward the left. The strongly deshielded protons of dimethyl ether, for example, are effectively more exposed than those of TMS to the applied field; hence, resonance occurs at higher frequency—that is, to the left—relative to the TMS proton peak.

Let us look at the frequency and chemical shift scales in Figure 3.11 and conventionally set the TMS peak at zero at the right-hand edge. The chemical shifts are dimensionless; they are simply numbers on the order of 10^{-6}; thus, a chemical shift of 2×10^{-6} is reported as 2 ppm. What is the purpose of using chemical shifts instead of simply reporting frequencies in Hz? The chemical shift scale is useful because

*The terms "upfield" and "downfield" are now obsolete and have been replaced, respectively, by shielded (lower δ, or to the right) and deshielded (higher δ, or to the left).

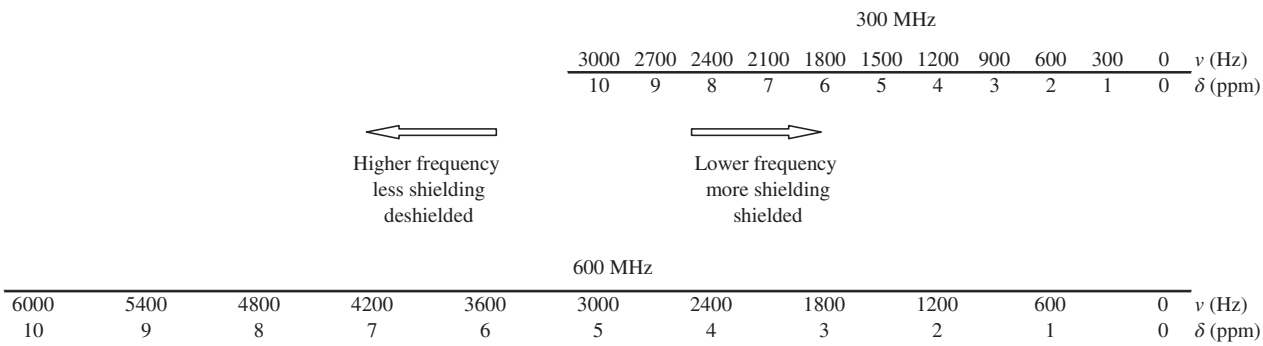

FIGURE 3.11 NMR scale at 300 MHz and 600 MHz ^{1}H Larmor frequency. Relatively few organic compounds show NMR peaks to the right of the TMS peak. These lower frequency signals are designated by negative chemical shifts (not shown in the figure).

chemical shifts are independent of the value of the Larmor frequency (and magnetic field strength) of the spectrometer in use. The frequencies (in Hz) of the various peaks are not independent of these values. Chemical shifts and frequencies are interconverted as follows:

$$\delta = \nu - \nu_{\text{ref}}/\nu_{\text{ref}}$$

where ν is the frequency of the peak of interest in the compound under study, and ν_{ref} is the frequency of the resonance of the reference compound (TMS in the case of ^{1}H). Note that chemical shifts can be positive or negative; however, the reference compound is usually chosen such that the vast majority of chemical shifts of other compounds are positive.

In Figure 3.11, for example, a proton NMR peak at, say, 1200 Hz on the 300 MHz scale gives the following chemical shift relative to TMS (whose frequency, ν_{ref}, is 300 MHz in this example):

$$\frac{(300\text{ MHz} + 1200\text{ Hz}) - (300\text{ MHz})}{300\text{ MHz}} = 4 \times 10^{-6} = 4\text{ ppm}$$

If the same peak is now observed in a spectrum recorded on a 600 MHz spectrometer, its frequency changes but its chemical shift does not. This is one of the advantages of using chemical shifts rather than frequencies. The frequency of the peak relative to TMS ($\nu - \nu_{\text{ref}}$) would now be 2400 Hz:

$$\nu - \nu_{\text{ref}} = (\delta)(\nu_{\text{ref}}) = (4 \times 10^{-6})(600\text{ MHz}) = 2400\text{ Hz}$$

The strongest magnetic field necessary and/or available helps to spread out the various peaks. This increase in resolution is made clear in Figure 3.11 and in Figure 3.12 (see also Figure 3.23) in which increased applied magnetic field in the NMR spectrum of acrylonitrile means increased separation of signals.

The concept of electronegativity (see Table 3.2) of substituents near the proton in question is a dependable guide, up to a point, to chemical shifts. It tells us that the electron density around the protons of TMS is high (silicon is electropositive relative to carbon), and these protons will be shielded (see Table 3.3). C is more electronegative than H, and the sequence of proton NMR peaks in the alkyl series CH_4, RCH_3, R_2CH_2, and R_3CH is from right to left in the

TABLE 3.2 Electronegativity of Selected Elements According to Pauling

H (2.1)						
Li (1.0)	Be (1.5)	B (2.0)	C (2.5)	N (3.0)	O (3.5)	F (4.0)
Na (0.9)	Mg (1.2)	A1 (1.5)	Si (1.8)	P (2.1)	S (2.5)	Cl (3.0)
						Br (2.8)
						I (2.5)

TABLE 3.3 Chemical Shift Trends Guided by Electronegativity

Compound	δ	Compound	δ
$(CH_3)_4Si$	0.00	CH_3F	4.30
$(CH_3)_2O$	3.27	RCO_2H	~ 10.80

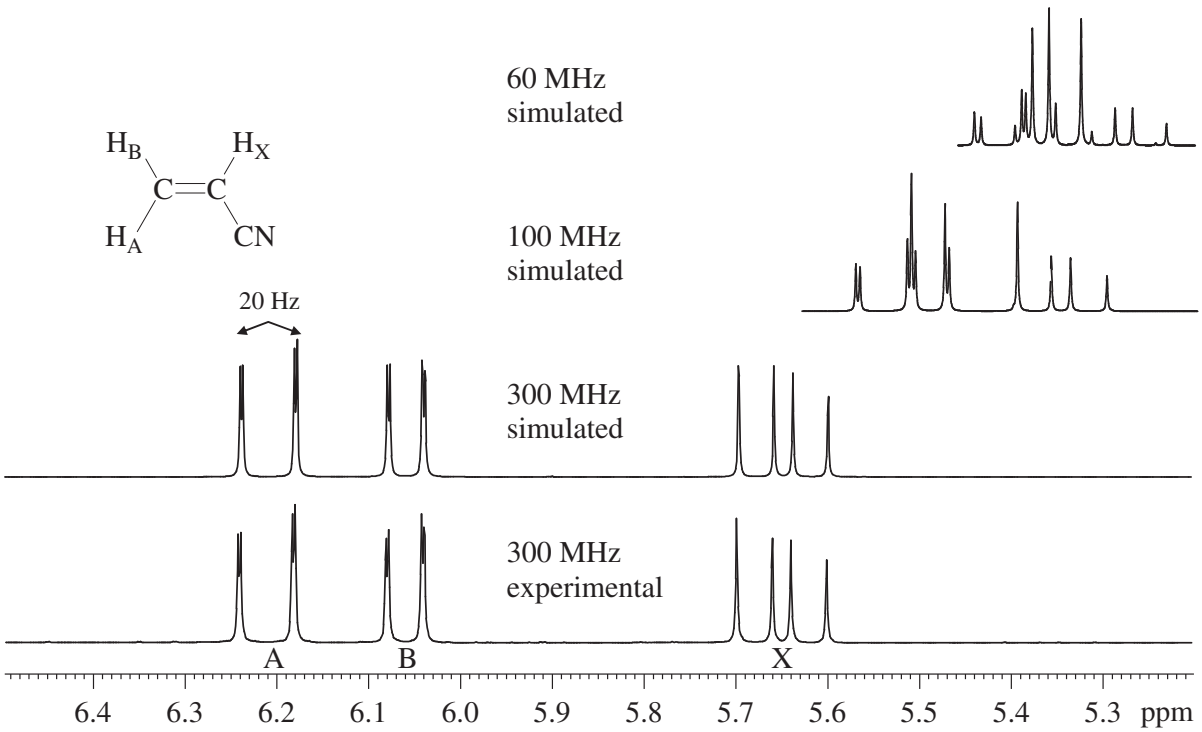

FIGURE 3.12 Simulated 60 MHz, 100 MHz, and 300 MHz ^{1}H NMR spectra of acrylonitrile; 300 MHz experimental spectrum (in $CDCl_3$) for comparison.

spectrum (Appendix A, Chart A.1). Again, it is important to remember that these are empirical arguments.

We could make a number of good estimates as to chemical shifts, using concepts of electronegativity and proton acidity. For example, the values found in Table 3.3 are reasonable solely on the basis of electronegativity.

However, finding the protons of acetylene at 1.80 ppm, that is, more shielded than ethylene protons (5.25 ppm), is perhaps counterintuitive, and finding the aldehydic proton of acetaldehyde at 9.97 ppm demonstrates the caution which must be used in oversimplifying the interpretation of chemical shifts solely in terms of concepts such as electron density or electronegativity. We shall use diamagnetic anisotropy to explain some of these apparent anomalies, such as the unexpectedly large deshielding effect of the benzene ring (7.27 ppm).

Let us begin with acetylene. The molecule is linear, and the triple bond is symmetrical about the axis. If this axis is aligned with the applied magnetic field, the electrons in the triple bond π orbitals can circulate at right angles to the applied field, thus inducing their own magnetic field opposing the applied field. Since the protons lie along the magnetic axis, the magnetic lines of force induced by the circulating electrons act to shield the protons (Figure 3.13), and the NMR peak is found at lower frequency than electronegativity would predict. Of course, only a small number of the rapidly tumbling molecules are aligned at any given moment with the magnetic field, but the overall average shift is affected by these transiently aligned molecules.

This effect is an example of diamagnetic anisotropy, which means that shielding and deshielding depend on the instantaneous orientation of the molecule with respect to the applied magnetic field. Similar arguments can be adduced to rationalize the unexpected deshielded position of the aldehydic proton resonance. In this case, the effect of the applied magnetic field is the greatest along the transverse axis of the C═O bond (i.e., in the plane of the page in Figure 3.14). The geometry is such that the aldehydic proton, which lies in front of the page, is in the deshielding portion of the induced magnetic field. The same argument can be used to account for at least part of the rather large deshielding of alkene protons.

The so-called ring-current effect is another example of diamagnetic anisotropy and accounts for the large deshielding of benzene ring protons. Figure 3.15 helps us visualize this effect. It also indicates that a proton held directly above or below the aromatic ring should be shielded. For example, the methylene protons in 1,4-polymethylenebenzenes (cyclophanes) are about 2.2 ppm more shielded than those of ethylbenzene.

All of the ring protons of acetophenone are deshielded because of the ring-current effect. Moreover, the *ortho* protons are further deshielded (*meta*, *para* ~7.40 ppm; *ortho* ~7.85 ppm) because of the additional deshielding effect of the carbonyl group. The carbonyl bond and the benzene ring are coplanar. If the molecule is oriented so that the applied magnetic field $\boldsymbol{B}_0$ is perpendicular to the plane of the molecule, the circulating π electrons of the C═O bond shield the conical zones above and below them and deshield the lateral zones in which the *ortho* protons are located. Both *ortho* protons are equally deshielded since another, equally populated, conformation can be written in which the other *ortho* proton is deshielded by the anisotropy cone. Nitrobenzene shows a stronger effect.

A spectacular example of shielding and deshielding by ring currents is furnished by some of the annulenes. At about −60 °C, the protons outside the ring of [18]-annulene are strongly deshielded (9.3 ppm) and those inside are strongly shielded (−3.0 ppm, i.e., more shielded than TMS).

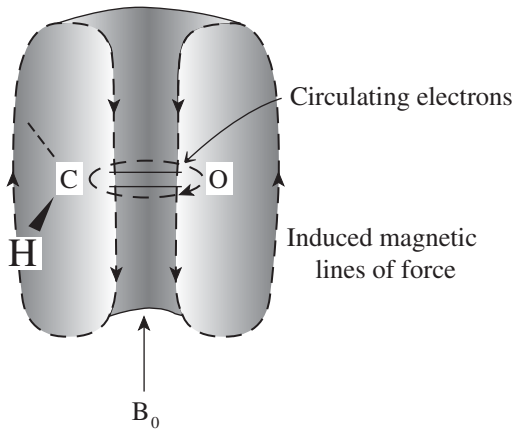

FIGURE 3.14 Deshielding of aldehydic protons.

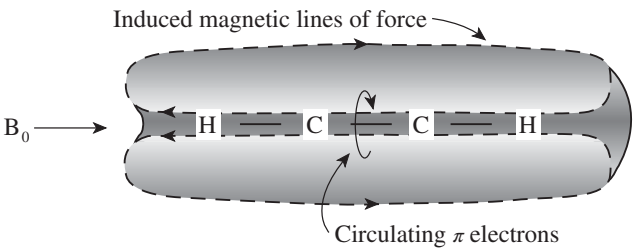

FIGURE 3.13 Shielding of alkyne protons.

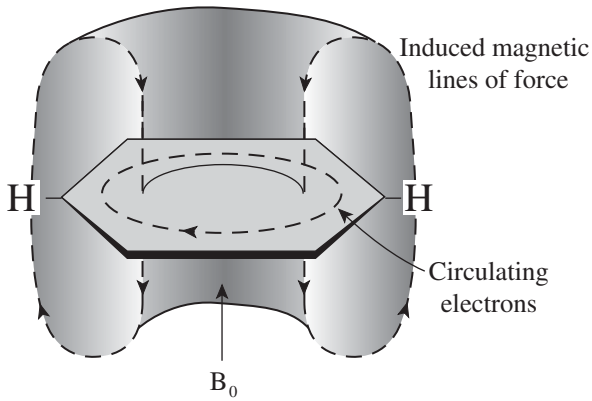

FIGURE 3.15 Ring-current effects in benzene.

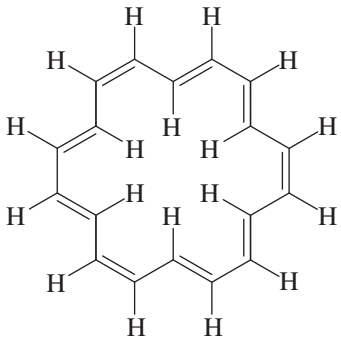

[18]-Annulene

Demonstration of such a ring current is good evidence for planarity and aromaticity, at least at low temperature. As the temperature is raised, the signals broaden because of slow interchanges in ring conformations. At about 110 °C, a single averaged peak appears at approximately 5.3 ppm because of rapid interchanges in ring conformations to give an averaged chemical shift. This hints at the powerful capability of NMR for studying molecular dynamics.

In contrast with the striking anisotropic effects of electrons in π orbitals, those in the σ orbitals of a C—C bond produce a small effect. To a first approximation, one can consider cyclohexane as roughly of the same anisotropic disk shape as an aromatic ring, giving rise to similar effects as observed for aromatic systems. The observation that an equatorial proton is consistently found at higher chemical shifts (by 0.1 ppm to 0.7 ppm) than the axial proton on the same carbon atom in a rigid six-membered ring can thus be rationalized.

Extensive tables and charts of chemical shifts in the Appendices give the useful impression that chemical shifts of protons in organic compounds fall roughly into eight regions as shown in Figure 3.16.

To demonstrate the use of some of the material in the Appendices, we predict the chemical shifts of the protons in benzyl acetate. In Appendix A, Chart A.1, we see that the chemical shift of the CH_3 group is ~2.0 ppm. From Table B.1, we find that the CH_2 group is at ~5.07 ppm. In Appendix D, Chart D.1, the aromatic protons are at ~7.2 ppm. In the spectrum of benzyl acetate (Figure 3.8), we see three sharp peaks from right to left at 1.96 ppm, 5.00 ppm, and 7.22 ppm; the integrations shown are in the ratio 3:2:5, corresponding to CH_3, CH_2, and five ring protons.* The peaks are all singlets, that is, they are simple individual peaks with no additional fine structure or splittings. This means that the CH_3 and CH_2 groups are insulated, that is, there are no protons on the adjacent carbon atoms for coupling (see Section 3.5). However, there is a problem with the apparent singlet representing the ring protons, which are not chemically equivalent (Section 3.8.1) and do couple with one another. At higher resolution, we would see a multiplet rather than an apparent singlet. The expanded inset shows partially resolved peaks.

We point out again that an appreciation of the concepts of electronegativity (inductive effects) and of electron delocalization—combined with an understanding of diamagnetic anisotropy—permits both rationalization and prediction of approximate chemical shift. Several examples make the point:

1. In an α,β-unsaturated ketone, deshielding of the β-proton can be empirically rationalized using resonance:

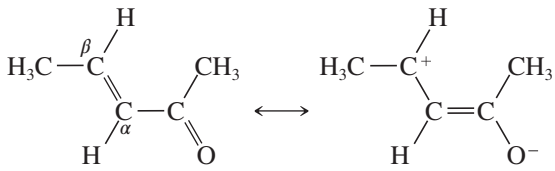

α-proton $\delta \sim 6.2$
β-proton $\delta \sim 6.8$

2. In a substituted vinyl ether, the oxygen atom deshields the α-proton by an inductive effect and shields the β-proton by resonance.

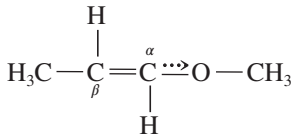

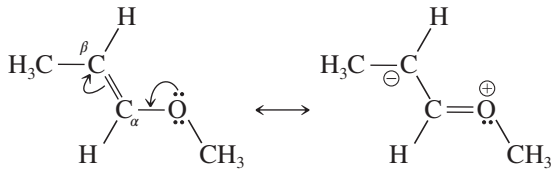

α-proton $\delta \sim 6.2$
β-proton $\delta \sim 4.6$

The above approximate chemical shift values were calculated from Appendix D. In comparison, the alkenyl protons of *trans*-3-hexene are at 5.40 ppm.

Since chemical shift increments are approximately additive, it is possible to calculate the ring proton shifts in polysubstituted benzene rings from the monosubstituted values in Appendix Chart D.1. The chemical shift increments for the ring protons of *m*-diacetylbenzene,

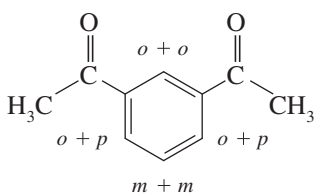

for example, are calculated as follows.

Chemical shift increments are the shifts from that of the protons of benzene (7.27 ppm). Thus for a $CH_3C{=}O$ substituent (line 26, Appendix Chart D.1), the *ortho* increment is +0.63 ppm, and the *meta* and *para* increments are both +0.28 ppm. The C-2 proton has two *ortho* substituents; the C-4 and C-6 protons are equivalent and have *ortho* and

*The "integration step," that is, the vertical distance between the horizontal lines of the integration trace, is proportional to the number of protons represented by the particular peak or multiplet of peaks. These steps give ratios, not absolute numbers of protons. The ratios actually represent areas under the peaks.

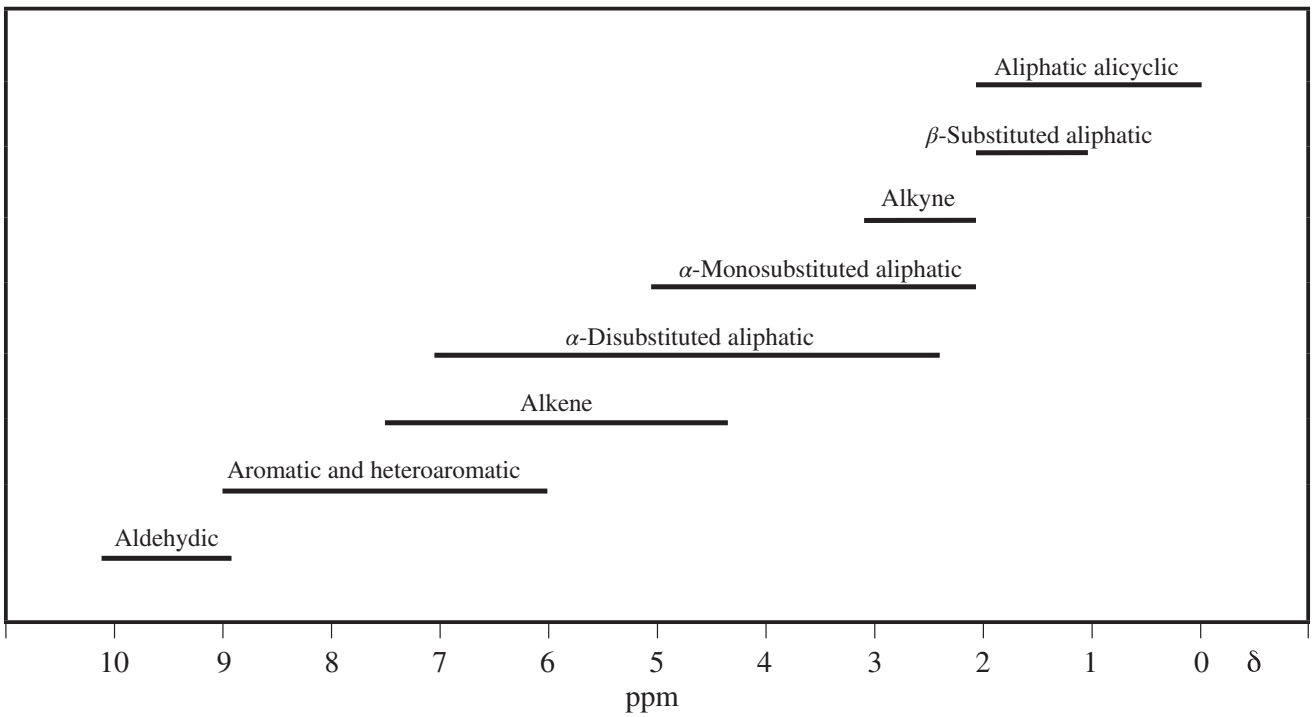

FIGURE 3.16 General regions of proton chemical shifts in organic molecules. Several aldehydes, several enols, and most carboxylic acids resonate at higher chemical shifts than 10 ppm. Metal hydrides can have chemical shifts as low as −50 ppm.

para substituents; the C-5 proton has two *meta* substituents. Thus, the calculated increment for C-2 is +1.26 ppm, for C-4 and C-6 is +0.91 ppm, and for C-5 is +0.56 ppm. The spectrum shows increments of +1.13 ppm, +0.81 ppm, and +0.20 ppm, respectively. This agreement is adequate.* It must be emphasized that these calculations are empirical and that improved understanding of chemical shifts may be obtained using quantum chemical computations.

Obviously, proton NMR spectroscopy is a powerful tool for elucidating aromatic substitution patterns—as is ^{13}C NMR (see Chapter 4). Two-dimensional NMR spectroscopy offers another powerful tool (see Chapter 5).

3.5 SPIN–SPIN COUPLING, MULTIPLETS, AND SPIN SYSTEMS

3.5.1 Simple and Complex First-Order Multiplets

We have obtained a series of NMR peaks representing protons in different chemical environments, with the area under each peak (from integration) being proportional to the number of equivalent protons it represents. We have now to consider one further phenomenon, *spin–spin coupling*. This can be described as the coupling of proton spins through the intervening bonding electrons. In a general sense, "coupling" between a pair of spins means that the energy (and therefore NMR frequency) associated with an individual spin within the pair depends on the state (e.g., α or β) of the other spin. According to the Pauli principle, the bonding electrons between two nuclei are paired so that the electron spins are antiparallel. In a magnetic field, there is some tendency for each nucleus to pair its spin with one of the bonding electrons so that most electron–nuclear spin pairs are aligned in an antiparallel fashion, this being the stable state. Coupling is ordinarily not important beyond three bonds unless there is ring strain as in small rings or bridged systems, delocalization as in aromatic or unsaturated systems, or four connecting bonds in a "W" configuration (Section 3.14). Two-bond coupling is termed *geminal*, three-bond coupling, *vicinal*, and beyond three bonds, *long range*.

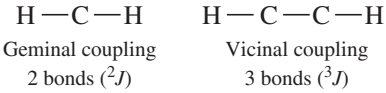

Suppose that two vicinal protons are in very different chemical environments. Each proton will have its own chemical shift, and the corresponding peaks in the NMR spectrum will be widely separated. However, if the two proton spins are coupled, the resonance frequency of each of them is affected slightly by the two possible states (α, β) of the *other* proton through the intervening electrons, so that each peak appears as a doublet (Figure 3.17) with one peak associated with each of the two states of the other spin. The frequency difference, in Hz, between the two peaks of a doublet is proportional to the strength of the coupling and is denoted by a coupling constant, J. Although J is called a coupling "constant," its value varies depending on the molecule being studied. It is a constant with

*Calculations for *ortho*-disubstituted compounds are less satisfactory because of steric or other interactions between the *ortho* substituents.

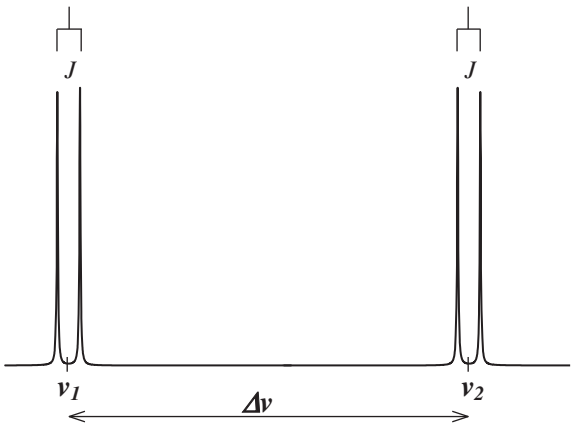

FIGURE 3.17 NMR spectrum of two protons with very different chemical shifts (the frequencies of which are denoted by the tick marks at ν_1 and ν_2) relative to their J coupling constant (an AX spin system).

respect to the strength of the external magnetic field, $\boldsymbol{B}_0$.* Whereas chemical shifts usually range over about 3750 Hz at 300 MHz, coupling constants between protons rarely exceed 20 Hz (see Appendix F). Notice that J coupling constants are reported in frequency units (Hz) whereas chemical shifts are unitless (on the order of ppm). In Figure 3.17, note that while there are four peaks, there are still only two chemical shifts; their positions are at the centers of each of the two doublets.

So long as the chemical shift difference in hertz ($\Delta\nu$) is much larger than the coupling constant (arbitrarily $\Delta\nu/J$ is greater than about 8), the simple pattern of two doublets appears. The value of $\Delta\nu$ may be calculated explicitly from the chemical shifts as follows:

$$\Delta\nu = |(\delta_1 - \delta_2)|(\nu_{\text{ref}})$$

where δ_1 and δ_2 are the chemical shifts of interest and ν_{ref} is the frequency of the chemical shift reference (TMS for ^{1}H NMR).

As the ratio $\Delta\nu/J$ becomes smaller, however, the doublets approach one another, the inner two peaks increase in intensity, and the outer two peaks decrease (Figure 3.18). The shift position of each proton is no longer midway between its two peaks as in Figure 3.17 but is at the center of gravity (Figure 3.19); it can be estimated with fair accuracy by inspection.

The spectrum in Figure 3.18d (and reproduced in Figure 3.19), which consists of two distorted doublets, can readily be mistaken for a quartet. Increasing the applied magnetic field (and therefore the Larmor frequency) would not pull a true quartet apart into two doublets. As the intensities of the outer peaks of spectrum (e) continue to decrease, failure to notice the small outer peaks may lead to mistaking the inner peaks for a doublet. Eventually, as $\Delta\nu/J$ approaches zero,

*The number of bonds between coupled nuclei (protons in this chapter) is designated by J and a left superscript. For example, H—C—H is ^2J, H—C—C—H is ^3J, H—C═C—C—H is ^4J. Double or triple bonds are counted as single bonds.

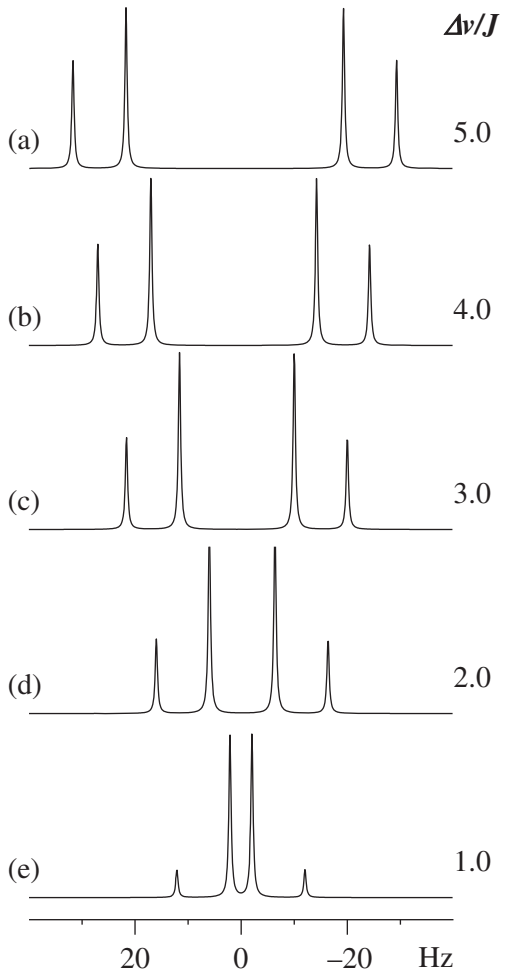

FIGURE 3.18 Spectra for a coupled two-proton system with a decreasing difference in chemical shifts and a large J value (10 Hz); the difference between AB and AX notation is explained in the text.

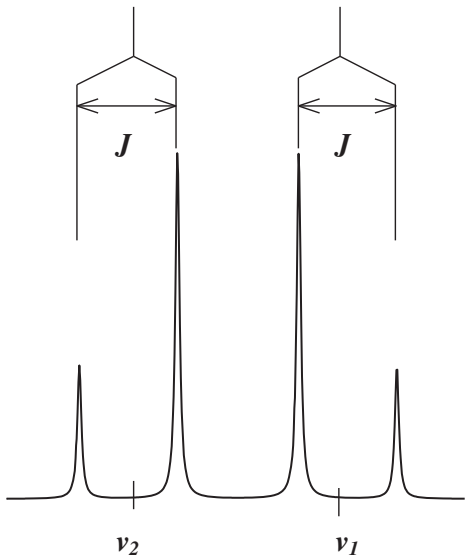

FIGURE 3.19 The horizontal positions of the short vertical lines at the top of the figure denote the centers of gravity, instead of linear midpoints, for shift location in the case of a low $\Delta\nu/J$ ratio.

the outer peaks disappear and the inner peaks merge, producing a two-proton singlet; this is observed for two completely equivalent protons.

The next level of complexity involves three protons. Consider the methylene and methine groups in the hypothetical compound

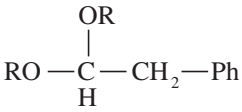

in which the single methine proton is in a very different chemical environment compared with the two methylene protons. Both CH_2 protons couple equally with the methine proton. In Figure 3.20, we see a triplet and a doublet widely separated with an integration ratio of 1:2. The doublet is a result of splitting of the CH_2 resonance by the CH proton. The triplet can be explained as a result of consecutive splitting of the CH resonance by each of the two CH_2 protons; the peaks overlap since the coupling constants are identical (see Figure 3.21).

In a simple first-order multiplet, the number of peaks is determined by the number of coupled, neighboring protons with the same (or negligibly different) coupling constants. Neighboring protons are geminal or vicinal, that is, involving two or three bonds; long-range coupling constants are usually much smaller (see Section 3.14). As we have seen, one neighboring proton induces a doublet, and two equally coupled neighboring protons induce a triplet. The multiplicity (the number of peaks within a multiplet) then is $n + 1$, n being the number of neighboring, equally coupled protons. This is known as the "$n + 1$ rule." The general formula that covers all nuclei is $2nI + 1$, I being the quantum spin number of the nuclei which are coupling to the one being observed (see Section 3.2.1). The relative intensities of the peaks of a simple first-order multiplet also depend on n. For spin $\frac{1}{2}$ nuclei, doublet peaks ($n = 1$) are in the ratio 1:1; triplets ($n = 2$) are 1:2:1; quartets ($n = 3$) are 1:3:3:1; and so forth. The intensities of the peaks in the multiplets are given by the coefficients of the expanded form of the equation

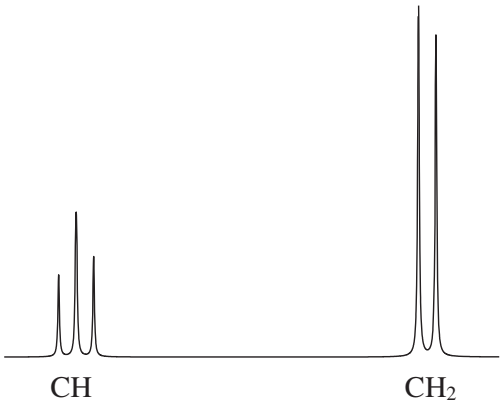

FIGURE 3.20 Proton NMR spectrum showing the effects of spin–spin coupling between CH and CH_2 groups with different chemical shifts.

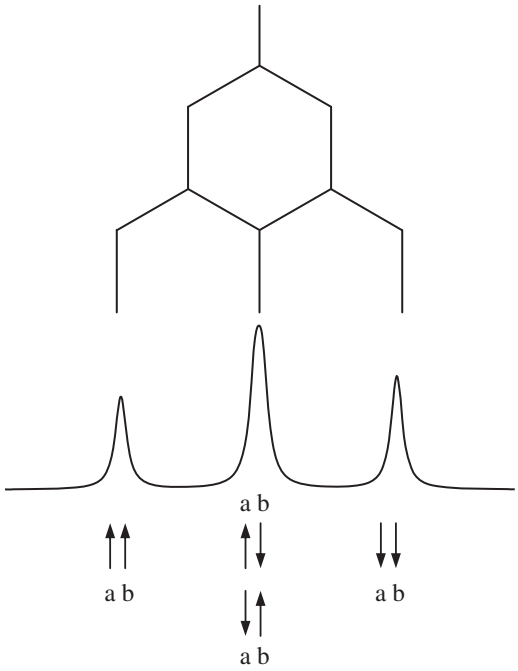

FIGURE 3.21 The appearance of a triplet may be understood by considering, from top to bottom in the diagram, two consecutive splittings of peaks into doublets with equal coupling constants.

$(x + 1)^n$, where n is the number of neighboring protons. Pascal's triangle (see Figure 3.22) gives both the multiplicity and the intensities of a multiplet.

The requirements and appearance for a simple first-order multiplet involving spin $\frac{1}{2}$ nuclei such as ^1H can be summarized as follows:

- The ratio $\Delta\nu/J$ must be larger than about 8; $\Delta\nu$ is the difference in Hz between the midpoints of the coupled multiplets (or the difference in chemical shifts expressed in frequency units). J is the coupling constant.
- The number of peaks in the multiplet is $n + 1$, where n is the number of neighboring protons with the same coupling constant.
- The separation in Hz between the individual peaks of a simple first-order multiplet gives the coupling constant, J.
- A simple first-order multiplet is centrosymmetric, with the most intense peak(s) central (see Pascal's triangle, Figure 3.22).

A complex first-order multiplet differs from a simple first-order multiplet in that several different coupling constants are involved in the complex multiplet. The requirement that $\Delta\nu/J$ be greater than about 8 still holds, but Pascal's triangle (at least not a single Pascal's triangle) does not hold for the complex multiplet. It should become obvious, with some experience, that the ratio $\Delta\nu/J = 8$ is not rigorous, but as the ratio decreases the interpretation gets rougher. The "horsepower race," mentioned in Section 3.3 was (and is) immensely successful in increasing the value of this ratio since $\Delta\nu$ depends directly on the Larmor frequency.

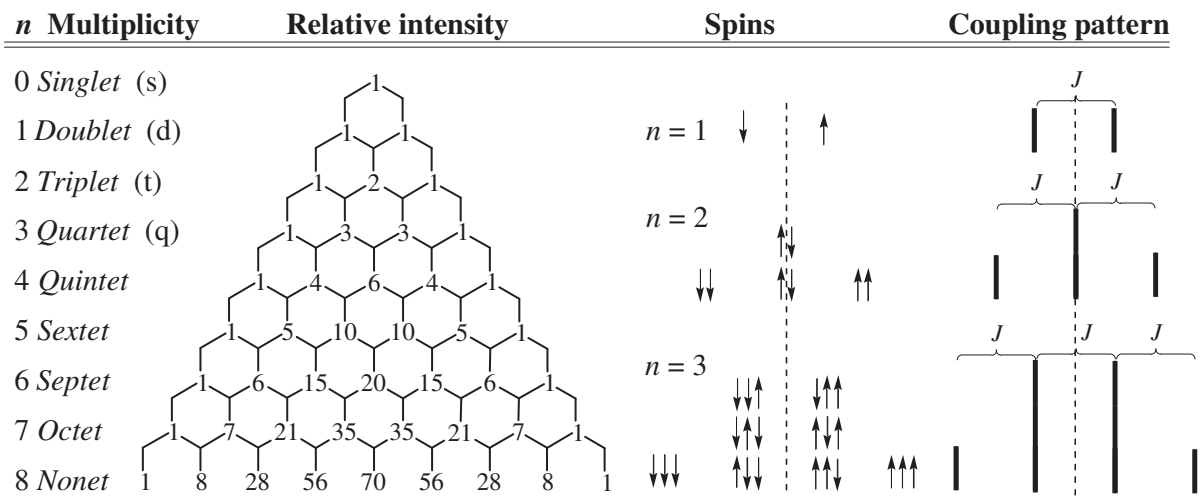

FIGURE 3.22 Relative intensities of the peaks comprising first-order multiplets; n denotes the number of equivalent coupling nuclei of spin $\frac{1}{2}$ (e.g., protons) and the $n + 1$ rule applies. The relative intensities follow the pattern of Pascal's triangle.

The result has been to simplify spectra and thereby permit spectral interpretation for more difficult molecules. It will be useful to get some feeling for this effect at 60 MHz, 300 MHz, and 600 MHz in Figure 3.23. The compound is

$$\mathrm{Cl{-}CH_2{-}CH_2{-}O{-}CH_2{-}CH_2{-}Cl}$$

At 600 MHz, the spectrum consists of two simple first-order triplets. At 300 MHz, the spectrum is slightly distorted, and there are splittings which cannot be explained using first-order rules. At 60 MHz, there is obvious overlap and extraneous peaks. (The expanded multiplets are the result of using the same δ scale for all the spectra.) The $\Delta\nu/J$ ratios are 12 at 600 MHz (certainly first-order) and 6 at 300 MHz (still easily recognized if the additional splitting is ignored). The 60 MHz overlapping multiplets with extraneous peaks are described as "higher order." A glance at Appendix A shows that substituents Cl and OR are almost equally deshielding and suggests that attempting to interpret a 60 MHz spectrum using a simple first-order multiplet analysis would fail. Return to Figure 3.12 for a more complex example.

3.5.2 First-Order Spin Systems

A spin system consists of those spins in a molecule that couple to one another. By definition, it therefore excludes other spins in the molecule. It is not necessary for every spin within the spin system to be directly coupled to every other spin. A spin system is insulated from other spin systems by an absence of coupling due to, for example, heteroatoms or quaternary carbons (atoms without attached hydrogen atoms). The coupling of spins may be described as simple first-order, complex first-order, or higher order. In a given spin system, there may be long-range coupling through the insulating atom, but this usually involves small coupling constants, resulting in peak broadening in a multiplet rather than additional resolved splittings.

The 600 MHz spectrum in Figure 3.23 consists of a simple first-order multiplet. The 60 MHz spectrum consists of a complex multiplet characteristic of a higher order spin system. Importantly, one can realize here that the way we describe and analyze a spin system can change with the strength of the applied magnetic field, and is not always solely related to the structure of the molecule. A spin system may give rise to one or more higher order multiplets, in which case it is difficult to determine all of the chemical shifts, coupling constants,* and multiplicities by inspection. It is notable that ^{1}H chemical shifts are usually reported to two decimal places. But are these numbers always valid? Certainly they are for the almost perfect first-order triplets at 600 MHz in Figure 3.23. At 60 MHz, however, chemical shifts of the overlapping higher order multiplets cannot be measured accurately by inspection. Somewhere between 300 MHz and 60 MHz, attempts to measure the chemical shifts of similar compounds would only yield approximations, but not values accurate to two decimal places.

3.5.3 Pople Notation

Pople notation provides a means for describing spin systems.† Spectral multiplets arise due to various sets of nuclei, and each set is designated by a capital letter. A set refers to a group of equivalent nuclei. Sets may be described as strongly or weakly coupled to each other depending on the ratio $\Delta\nu/J$; the larger this value, the more weakly coupled the spins are relative to their chemical shift difference, and vice

*Coupling constants may be positive or negative. However, the sign of these have no effect in a first-order system, in which we can measure J values by inspection but cannot determine the sign by inspection. Thus, we disregard the sign.

†Pople, J.A., Schneider, W.G., and Bernstein, H.J. (1959). *High Resolution NMR*. McGraw-Hill: New York.

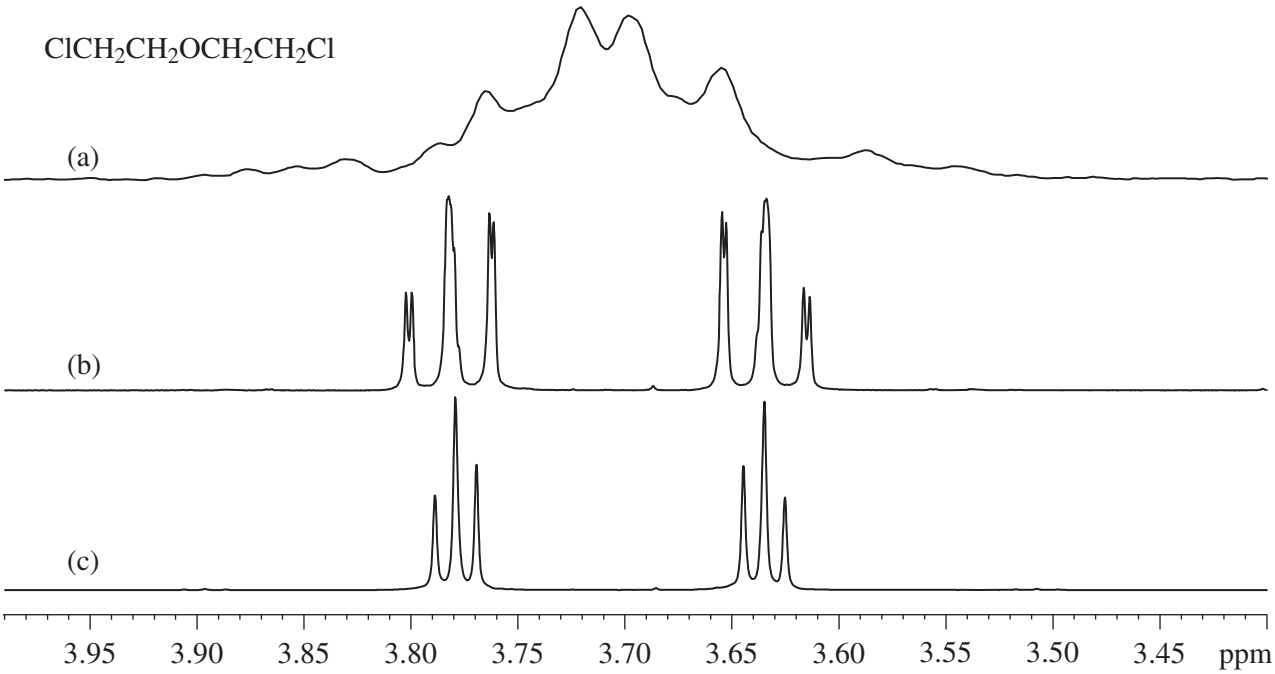

FIGURE 3.23 Proton NMR spectra of chloroethyl ether at Larmor frequencies of (a) 60 MHz, (b) 300 MHz, and (c) 600 MHz, all in $CDCl_3$.

versa. If the $\Delta\nu/J$ ratio is larger than about 8, the coupled sets are considered to weakly coupled, and the resulting spin systems are designated by well-separated letters of the alphabet such as AX. This is because the corresponding chemical shifts of such a system are also well separated. If the ratio is less than 8, letters such as AB are used. If there are three weakly coupled sets, they are designated AMX. If the first two sets are strongly coupled and the last two weakly, ABX is used. The number of magnetically equivalent protons in a set (Section 3.9) is designated by a subscript number; if there is only one proton in a set, no subscript is used.

Any such collection of sets, insulated from all other sets, is a spin system. The following are examples of first-order spin systems: AX (two doublets), A_2X (doublet, triplet), A_2X_2 (two triplets), and A_3X_2 (triplet, quartet). The reasoning is as follows: in A_2X for example, the A_2 set is split into a doublet by the $n + 1$ neighboring protons; in this case there is one proton in the X set; the two protons in the A_2 set account for the triplet.

With two or more sets, there is the complication of several coupling constants; more importantly, one must understand how the various sets are coupled among themselves. Thus, nitropropane can be described as follows since the effect of the NO_2 group is to impart significantly different chemical shifts to each of the three sets of protons:

$$\underset{A_3}{CH_3}—\underset{M_2}{CH_2}—\underset{X_2}{CH_2}—NO_2$$

The A_3 and X_2 groups couple with the M_2 group, but the A_3 group does not couple with the X_2 group. At this point, we note only that the spectrum consists of two triplets with slightly different coupling constants, and a sextet with slightly broadened peaks.

In the styrene molecule,

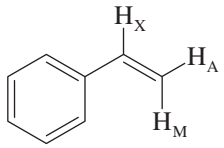

all of the alkenyl protons are weakly coupled with each other at 600 MHz and form an AMX spin system (see Section 3.10).

As mentioned above, letters close together in the alphabet are used to describe spin systems that are not first order: AB, A_2B, ABC, $A_3B_2C_2$, and so on. These strongly coupled spin systems cannot be easily interpreted by inspection. The spectra can, however, be rendered first-order (e.g., AB becomes AX) if a suitably powerful magnetic field is available.

Beyond these spin systems are those containing magnetically nonequivalent but chemically equivalent protons, which are quite common and have an unpleasant aspect: they cannot become first-order systems by increasing the magnetic field. Pople notation for a pair of chemically equivalent (but magnetically inequivalent) spins is AA′. These spin systems are discussed further in subsequent sections.

3.5.4 Further Examples of Simple First-Order Spin Systems

With an understanding of simple first-order spin systems and of Pople notation, we can consider the following example.

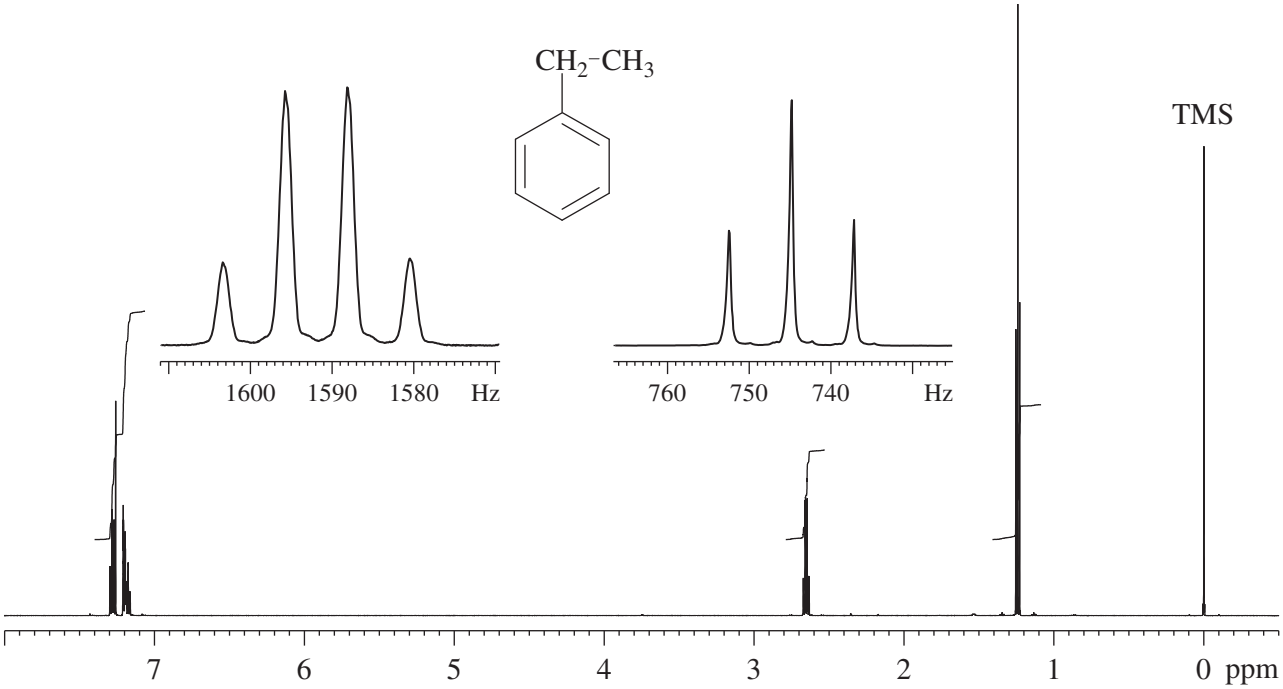

FIGURE 3.24 Proton NMR spectrum of ethylbenzene in $CDCl_3$ at 600 MHz. The ethyl moiety is recognized by the CH_3 triplet and the CH_2 quartet.

The spectrum in Figure 3.24 arises from two spin systems insulated from each other by a carbon atom that has no attached proton. The CH_3—CH_2 spin system consists of a well-resolved triplet and quartet—that is, an A_3X_2 system as suggested by the peak multiplicities and by the 5:2:3 (left to right) ratios of integration.

The ring system, which has a plane of symmetry, consists of two interchangeable *ortho* protons, two interchangeable *meta* protons, and one *para* proton, all in the characteristic region for ring protons. The alert student, having absorbed the concept of Pople notation (Section 3.5.3), would probably write A_2B_2C. The student might go even further and predict that a larger magnet might give a first-order ring system, A_2M_2X. While a larger magnet would separate the chemical shifts of the ring system, we will see in Section 3.9 that a first-order system would not be achieved.

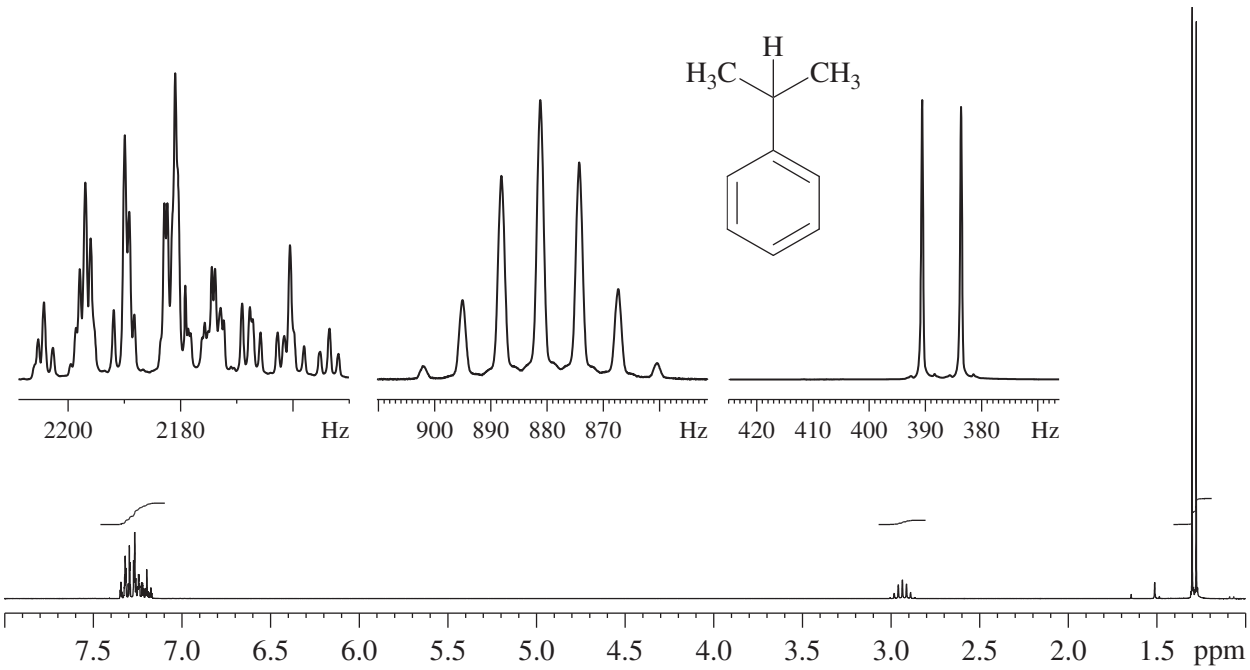

FIGURE 3.25 Proton NMR spectrum of cumene (isopropylbenzene) in $CDCl_3$ at 300 MHz. The isopropyl moiety is recognized by the characteristic six-proton doublet and the one-proton septet.

Briefly, the problem is that neither the *ortho* protons nor the *meta* protons are "magnetically equivalent." They are only chemically equivalent.

One minor but common feature may be pointed out. Note the slight broadening of each of the peaks in the CH_2 quartet. This is the result of a small long-range coupling to the *ortho* protons through the insulating *ipso* carbon atom; as presented here, splittings due to this coupling are not resolved, but instead result in broadening.

The spectrum of isopropylbenzene in Figure 3.25 presents two simple first-order multiplets. The methine proton gives a septet because of coupling with six neighboring identical protons of the two CH_3 groups, all with the same coupling constant. The two chemically equivalent CH_3 groups (because of free rotation) show a six-proton doublet because of coupling with the single methine proton. The ring protons present the same difficulties as those of the ring protons of ethylbenzene (Figure 3.24).

3.5.5 Analysis of First-Order Multiplets

The multiplet arising from one spin (or a set of equivalent spins) coupled to another spin (or a set of equivalent spins) is straightforward and has been explained in Section 3.5.1. There, we saw the familiar doublets, triplets, and quartets. In this section, we explain how to analyze, or deconvolute, spectra arising from a spin (or a set of equivalent spins) coupled to two or more nonequivalent spins (or sets) with two or more different J-coupling constants. As an example, let us consider the spectrum shown in Figure 3.26. It should be noted that NMR software can readily carry out this type of analysis, but for educational purposes it is useful to understand the origins of this type of spectrum.

The following are the general steps to be taken to analyze such a spectrum [see also Hoye et al. (1994) and Mann (1995)]. First, remember that the spectrum we are looking at is only the part of the total ^1H NMR spectrum due to one spin (or a set of equivalent spins).

1. Determine the integration of each peak and normalize the values so that the integrals of the outermost peaks (on each end of the spectra) are equal to 1. Write the integral values under each of the peaks. (If the integration values are not given on the spectrum, a good first approximation is simply to measure the heights of the peaks with a ruler.) As a check, the spectrum and the integral values should be centrosymmetric (i.e., the same on the left side of the spectrum as on the right).
2. Check that the sum of the integral values is 2^n, where n is an integer. The value of n is the total number of spins which are coupled to the one(s) giving rise to the multiplet in Figure 3.26 (e.g., a simple doublet would have intensities of 1:1 and so $2^n = 1 + 1 = 2$ and $n = 1$. This means that one spin ($n = 1$) is coupled to the one we are observing, giving a doublet).
3. Draw a vertical line under each of the peaks in the NMR spectrum (see line b in Figure 3.26). Ensure that these lines are labeled with the integral values you identified in step 1.
4. Look at the integral values associated with the two leftmost lines to determine a multiplicity. Their relative values tell you what type of multiplet is contributing to the spectrum. For example, if the values are 1 and 3, Pascal's triangle (Figure 3.22) tells us we have a quartet. In Figure 3.26, the values are 1 and 1 (line a) and so we have a doublet. Using the $n + 1$ rule, we can conclude that one spin led to the splitting.
5. Measure, along the horizontal frequency axis, the separation between the two peaks you identified in step 4. The value you obtain, in Hz, is the J-coupling constant

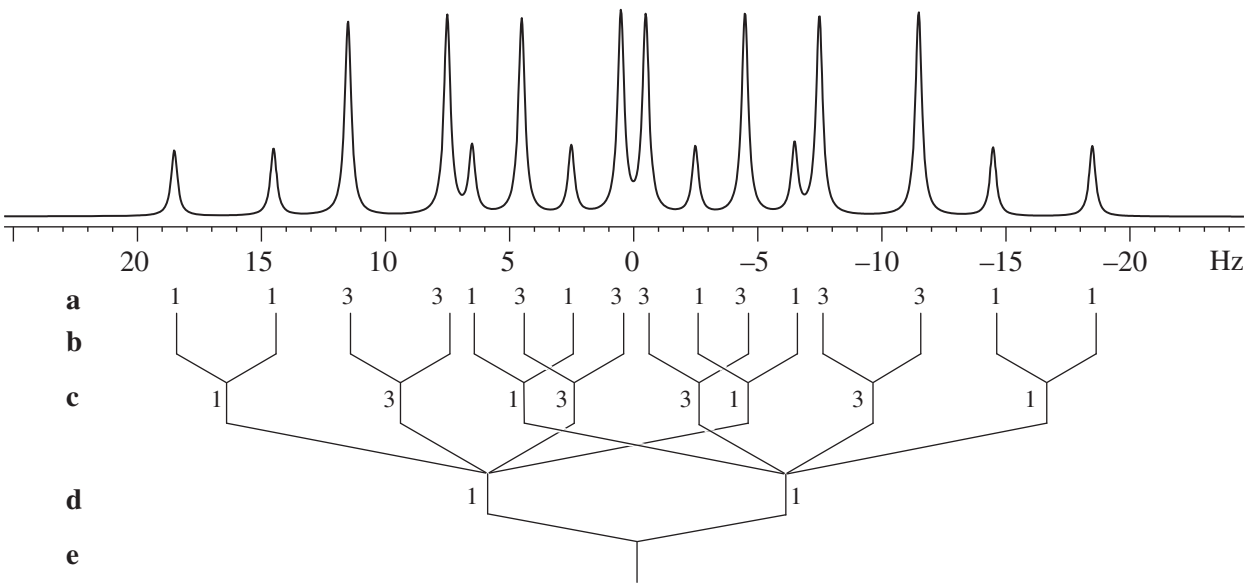

FIGURE 3.26 Analysis of a first-order multiplet. The multiplets and coupling constants are as follows: doublets of 4 Hz and 12 Hz, and two quartets of 7 Hz. The numbers associated with the lines in the stick diagram are relative integration values.

associated with the multiplet you found in step 4. Referring again to line "a" of Figure 3.26, careful measurement of the separation between the two left-most peaks gives a value of $J = 18.5 - 14.5$ Hz $= 4$ Hz.

6. Combine the various vertical lines associated with the multiplet you identified in steps 4 and 5 into one single vertical line. In Figure 3.26, this means in line c we are collapsing all doublets (two lines with equal integrals) with separations of 4 Hz into single lines. In this example, 16 lines are collapsed into 8 lines; we have removed the effect of the 4 Hz J-coupling from the spectrum. The integral values associated with the new lines are those from the left-most peak of the original multiplet (line a).
7. Return to step 4 and repeat the analysis until you are left with only a single line. Each time you repeat the process, you get the following information: the multiplicity (which, because of the $n + 1$ rule, tells you the number of coupled spins) and the J-coupling constant.

The example in Figure 3.26 shows that the multiplet observed is due to (i) coupling to one spin with a J value of 4 Hz, (ii) coupling to three equivalent spins with a J value of 7 Hz, and (iii) coupling to one spin with a J value of 12 Hz. Note that all coupling happens at the same time, even if we analyze their effects on the spectrum sequentially. In this example, one could propose that the proton we are observing is coupled simultaneously to a CH proton, a CH_3 group, and a second nonequivalent CH proton. This combination of functional groups is consistent with the multiplicities determined from the observed spectrum ($n + 1$ rule).

You can help to verify the correctness of your analysis by ensuring that the stick patterns you draw are always centrosymmetric, in terms of both the positions of the lines and their intensities (see Figure 3.26). Remember also that the peaks which you combine into a single peak in step 6 must each be separated from the next by the same amount, that is, the value of J.

It should be noted that accidental overlap of peaks can lead to unexpected integral values. For example, to analyze the spectrum shown in Figure 3.27, one should realize that there is a fortuitous overlap of triplets and extra care must be taken in assigning the integral values and analyzing the multiplet.

3.6 PROTONS ON OXYGEN, NITROGEN, AND SULFUR ATOMS: EXCHANGEABLE PROTONS

Protons directly bonded to an oxygen, nitrogen, or sulfur atom differ from protons on a carbon atom in that:

1. they are exchangeable;
2. they are subject to hydrogen bonding; and
3. those on a nitrogen atom are subject to partial or complete decoupling due to the electric quadrupole moment of the ^{14}N nucleus, whose spin quantum number is one.

Chemical shift ranges for such protons are given in Appendix E. Variations in shift depend on concentration, temperature, and solvent effects.

3.6.1 Protons on an Oxygen Atom

3.6.1.1 Alcohols. Depending on concentration, the hydroxylic peak in alcohols is found between ~0.5 ppm and ~4.0 ppm in $CDCl_3$. A change in temperature or solvent will also shift the peak position.

Intermolecular hydrogen bonding explains why the shift depends on concentration, temperature, and polarity of solvent. Hydrogen bonding decreases the electron density around the hydroxylic proton (deshielding), thus moving the proton peak to higher frequency. Decrease in concentration in a nonpolar solvent disrupts such hydrogen bonding, and the peak appears at lower frequency (shielding), that is, the

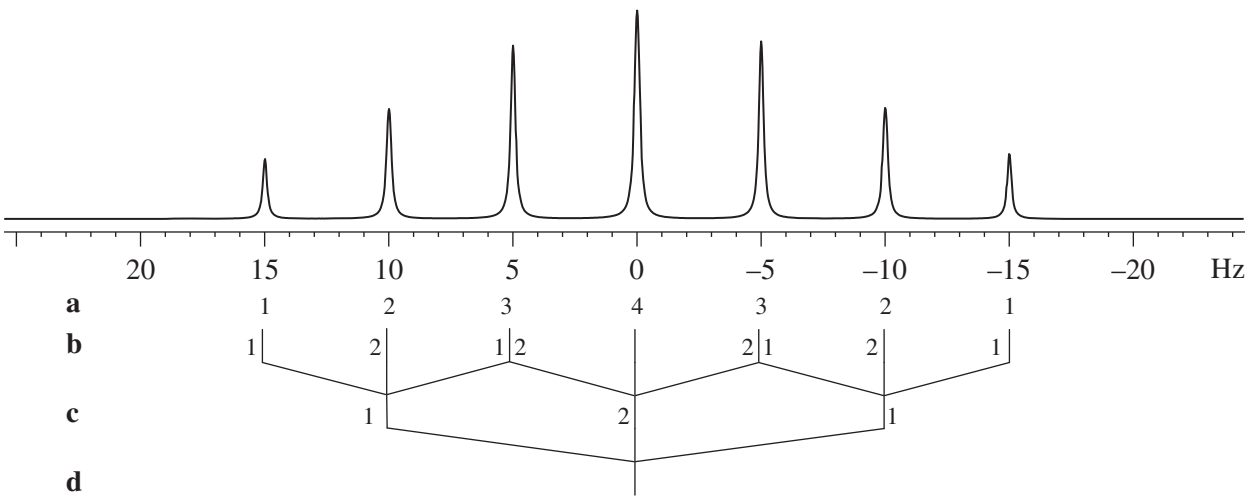

FIGURE 3.27 Peak coincidence arising from a triplet of triplets with coupling constants of 5 Hz and 10 Hz.

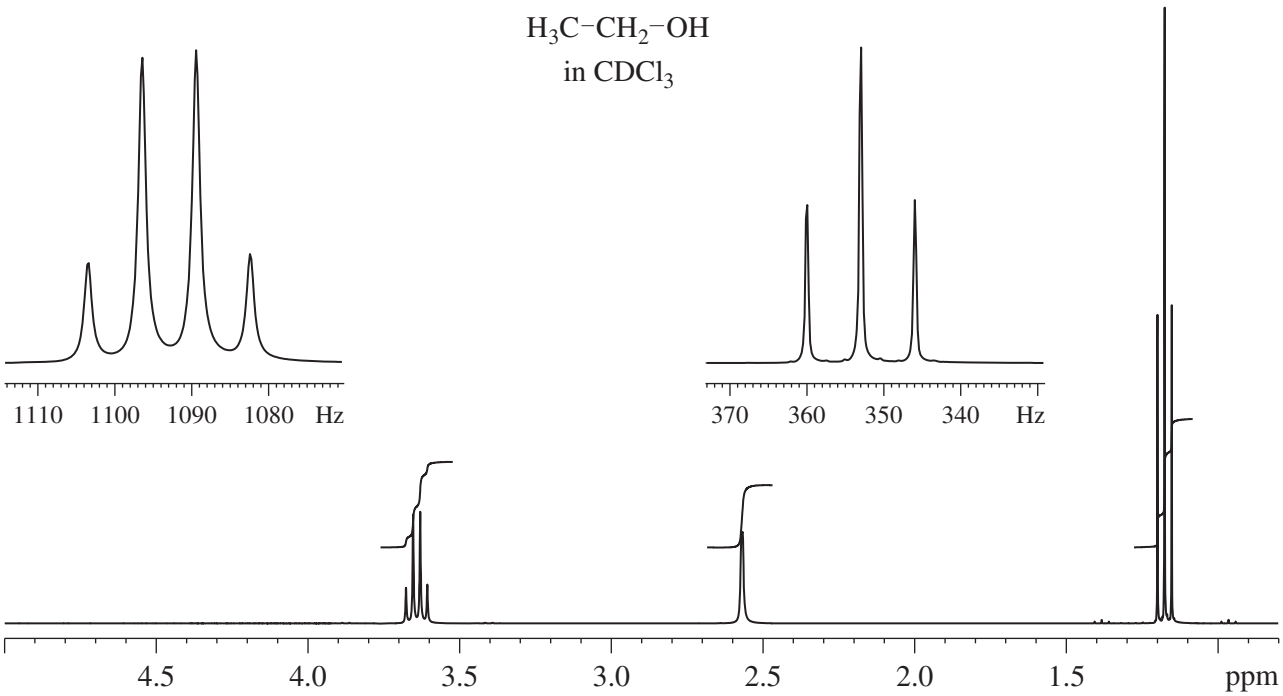

FIGURE 3.28 Proton NMR spectrum of CH_3CH_2OH in $CDCl_3$ at 300 MHz, allowed to stand at room temperature, overnight exposed to air. The CH_2 peaks are broadened by residual coupling to OH, which also shows slight broadening. Absorbed moisture has increased the intensity of the OH signal.

alcohol molecules become less polymeric. Increased temperature has a similar effect.

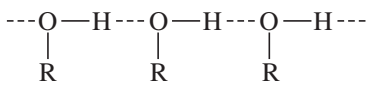

Intramolecular hydrogen bonds are less affected by their environment than are intermolecular hydrogen bonds. In fact, the enolic hydroxylic NMR peak of β-diketones, for example, is hardly affected by change of concentration or solvent, although it can be shifted to a lower frequency by warming. NMR spectroscopy is a powerful tool for studying hydrogen bonding.

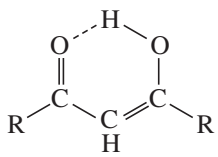

Rapid exchangeability explains why the hydroxylic peak of ethanol is usually seen as a singlet (Figure 3.28). Under ordinary conditions—exposure to air, light, and water vapor—acidic impurities develop in $CDCl_3$ solution and catalyze rapid exchange of the hydroxylic proton.* The proton is not on the oxygen atom of an individual molecule long enough for it to be affected by the methylene protons; therefore, there is no coupling. The OH proton shows a singlet, the CH_2 a quartet, and the CH_3 a triplet.

The rate of exchange can be decreased by lowering the temperature, by using a dilute solution, or by treating the solvent with anhydrous sodium carbonate or anhydrous alumina, then filtering through a pad of dry glass wool in a Pasteur pipette immediately before obtaining the spectrum. Under these conditions, the OH proton is coupled with the CH_2 protons, and useful information is available: an OH singlet indicates a tertiary alcohol, a doublet a secondary alcohol, and a triplet a primary alcohol.

The use of dry, deuterated dimethyl sulfoxide (DMSO-d_6) or deuterated acetone has the same effect as the above treatments. In addition, the OH proton peak is moved to higher frequency by hydrogen bonding between the solute and the solvent, thus providing a useful separation from overlapping peaks of other protons (see Figure 3.29).

In Figure 3.29 and in the following stick diagram, the CH_2 protons of ethanol are coupled to both the hydroxyl proton and the CH_3 protons. The diagram shows a somewhat overlapping quartet of doublets. The OH coupling is 5 Hz, whereas the CH_3 coupling is 7 Hz. It is usually better to start a coupling diagram with the largest coupling constant.

*$CDCl_3$ in small vials from Aldrich is pure enough so that a spectrum of CH_3CH_2OH taken within several hours showed the OH peak as a triplet. On standing for about 24 hours exposed to air, the sample gave a spectrum with the OH peak as a singlet (Figure 3.28). The high dilution used with modern instruments also accounts for the persistence of the vicinal coupling of the OH proton.

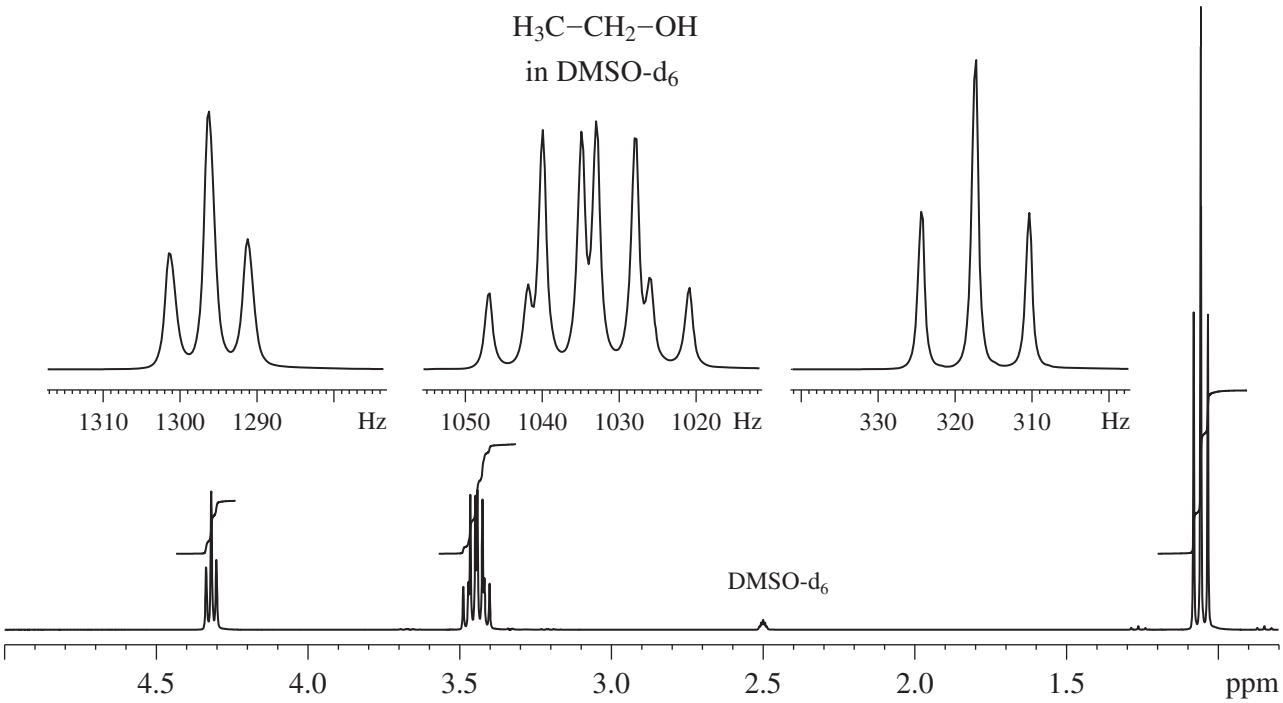

FIGURE 3.29 Proton NMR spectrum of CH_3CH_2OH run in dry deuterated DMSO at 300 MHz. From left to right, the peaks represent OH, CH_2, and CH_3. The small peak at 2.5 ppm represents the protonated impurity in DMSO-d_6 (see Appendix G).

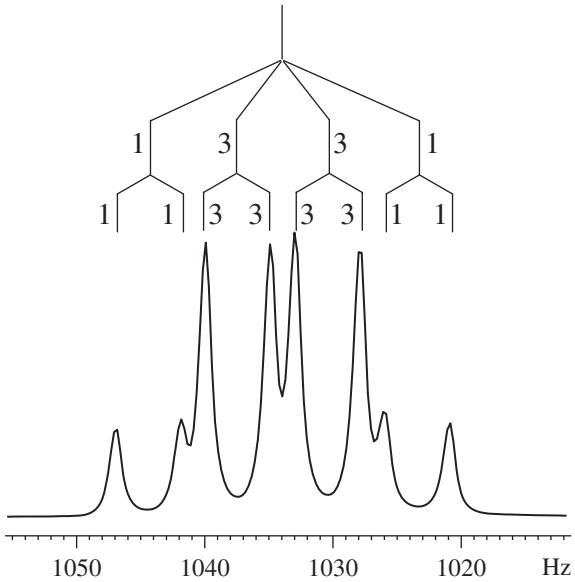

At intermediate rates of exchange, the hydroxylic multiplet merges into a broad band, which progresses to a singlet at higher exchange rates (Figure 3.28).[†]

A diol may show separate peaks for each hydroxylic proton; in this case, the rate of exchange, in hertz, is much less than the difference in hertz between the separate peaks. As the rate increases (due to addition of a trace of acid catalyst), the two peaks broaden and then merge to form a single broad peak; at this point, the exchange rate (k), in hertz, is approximately equal to twice the original signal separation in hertz. As the rate increases, the single peak becomes sharper. The relative position of each peak depends on the extent of hydrogen bonding of each hydroxylic proton.

The spectrum of a compound containing rapidly exchangeable protons can be simplified, and the exchangeable proton peak removed, simply by shaking the solution with excess deuterium oxide or by obtaining a spectrum in deuterium oxide solution if the compound is soluble. A peak resulting from HOD will appear, generally between 5 ppm and 4.5 ppm in nonpolar solvents and near 3.3 ppm in DMSO (see Appendix E). A $CDCl_3$ or CCl_4 solution in a stoppered NMR tube may be shaken vigorously for several seconds with one or two drops of D_2O, and the mixture allowed to stand (or centrifuged) until the layers are clearly separated. The top aqueous layer does not interfere.

Acetylation or benzoylation of a hydroxyl group moves the peak of the CH_2OH protons of a primary alcohol to higher frequency by about 0.5 ppm, and the CHOH proton of a secondary alcohol about 1.0 ppm to 1.2 ppm. Such shifts provide a confirmation of the presence of a primary or secondary alcohol.

3.6.1.2 Water. Aside from the problems of exchangeability, as just discussed, water is a ubiquitous impurity that faithfully obeys Murphy's law by interfering with critically important peaks. Bulk water as suspended droplets or wall films gives a peak at ~4.7 ppm in $CDCl_3$ (HOD occurs in the D_2O exchange experiment mentioned in Section 3.6.1.1).

Dissolved water appears at ~1.55 ppm in $CDCl_3$ and can be a serious interference in a critical region of the spectrum in dilute solutions.[*] Use of C_6D_6 (dissolved H_2O

[†] H_2O as an impurity may exchange protons with other exchangeable protons to form a single peak at an averaged position between the proton peaks involved.

[*] Webster, F.X. and Silverstein, R.M. (1985) *Aldrichimica Acta*, **18** (3), 58. Webster and Silverstein (1985).

at 0.4 ppm) avoids this interference. A table of water peaks in the common deuterated solvents appears in Appendix H.

3.6.1.3 Phenols. The behavior of a phenolic proton resembles that of an alcoholic proton. The phenolic proton peak is usually a sharp singlet (rapid exchange, no coupling), and its range, depending on concentration, solvent, and temperature, is generally to higher frequency (~7.5 ppm to 4.0 ppm) compared with the alcoholic proton. A carbonyl group in the *ortho* position shifts the phenolic proton peak to the range of about 12.0 ppm to 10.0 ppm because of intramolecular hydrogen bonding. Thus, *o*-hydroxyacetophenone shows a peak at about 12.05 ppm almost completely invariant with concentration. The much weaker intramolecular hydrogen bonding in *o*-chlorophenol explains its shift range (~6.3 ppm at 1 M concentration to ~5.6 ppm at infinite dilution), which is broad compared with that of *o*-hydroxyacetophenone but narrow compared with that of phenol.

3.6.1.4 Enols. The familiar tautomeric equilibrium of keto and enol forms of acetylacetone is described in Section 3.8.3.1. The enol form predominates over the keto form under the conditions described.

Ordinarily, we do not write the enol form of acetone or the keto form of phenol, although minuscule amounts do exist at equilibrium. But both forms of acetylacetone are seen in the NMR spectrum because equilibration is slow enough on the NMR scale and the enol form is stabilized by intramolecular hydrogen bonding. The enol form of acetone and the keto form of phenol are not thus stabilized; furthermore, the aromatic resonance stabilization of phenol strongly favors the enol form.

In α-diketones such as 2,3-butanedione, only the keto form is seen in NMR spectra. However, if the enol form of an α-diketone is stabilized by hydrogen bonding—as in the following cyclic α-diketones—only the stabilized enol form appears in the NMR spectra.

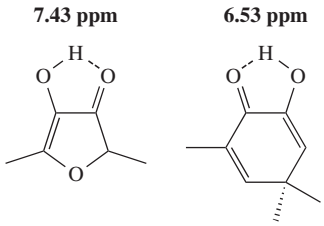

3.6.1.5 Carboxylic Acids. Carboxylic acids exist as stable hydrogen-bonded dimers in nonpolar solvents even at high dilution. The NMR peaks of carboxylic protons therefore appear in a characteristic range of ~13.2 ppm to ~10.0 ppm and are affected only slightly by concentration. Polar solvents partially disrupt the dimer and shift the peak accordingly.

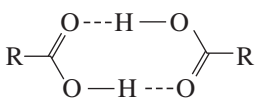

The peak width at room temperature ranges from sharp to broad, depending on the exchange rate of the particular acid. The carboxylic proton exchanges quite rapidly with protons of water and alcohols (or hydroxyl groups of hydroxy acids) to give a single peak whose averaged position depends on concentration. Sulfhydryl or enolic protons do not exchange rapidly with carboxylic protons, and individual peaks are observed.

3.6.2 Protons on Nitrogen

The common ^{14}N nucleus* has a spin quantum number I of 1 and, in accordance with the formula $2nI + 1$, should cause a proton attached to it and a proton on an adjacent carbon atom to show three equally spaced, equally intense peaks. There are two factors, however, that complicate the picture: the rate of exchange of the proton on the nitrogen atom and the electric quadrupole moment of the ^{14}N nucleus (see Section 3.2.1).

The ^{1}H bonded to the nitrogen nucleus may undergo rapid, intermediate, or slow exchange. If the exchange is rapid, the NH proton is decoupled from the N nucleus and from protons on adjacent carbon atoms. The NH proton peak is therefore a sharp singlet, and the adjacent CH protons are not split by the NH proton. Such is the case for most aliphatic amines.†

At an intermediate rate of exchange, the NH proton is partially decoupled, and a broad NH peak results. The adjacent CH protons are not split by the NH proton. Such is the case for *N*-methyl-*p*-nitroaniline.

If the NH exchange rate is slow, the NH peak is still broad because the electric quadrupole interaction at the nitrogen nucleus induces a moderately efficient spin relaxation and, thus, an intermediate lifetime for the spin states of the nitrogen nucleus. The proton thus interacts with three spin states of the nitrogen nucleus which are changing at a moderate rate, and the proton NMR spectrum is a broad peak that may disappear in the baseline. In this case, coupling of the NH proton to the adjacent protons is observed. Such is the case for pyrroles, indoles, secondary and primary amides, and carbamates (Figure 3.30).

Note that H—N—C—H coupling takes place through the C—H, C—N, and N—H bonds, but coupling between nitrogen and protons on adjacent carbon atoms is negligible. The proton–proton coupling is observed in the signal caused by hydrogen on carbon; the N—H proton signal is severely broadened by the ^{14}N quadrupolar interaction.

In the spectrum of ethyl *N*-methylcarbamate (Figure 3.30), the NH proton shows a broad peak centered about 4.70 ppm, and the N—CH_3 peak at 2.78 ppm is split into a doublet ($J \sim 5$ Hz) by the NH proton. The ethoxy protons are represented by the triplet at 1.23 ppm and the quartet at 4.14 ppm.

Aliphatic and cyclic amine NH protons have chemical shifts from ~3.0 ppm to 0.5 ppm; aromatic amines from ~5.0 ppm to 3.0 ppm in $CDCl_3$ (see Appendix E). Because

*^{15}N spectra are discussed in Chapter 6.

†H—C—N—H coupling in several amines was observed following rigorous removal (with Na—K alloy) of traces of water. This effectively stops proton exchange on the NMR time scale. See Henold, K. L. (1970) *J. Chem. Soc. D., Chem. Commun.*, 1340.

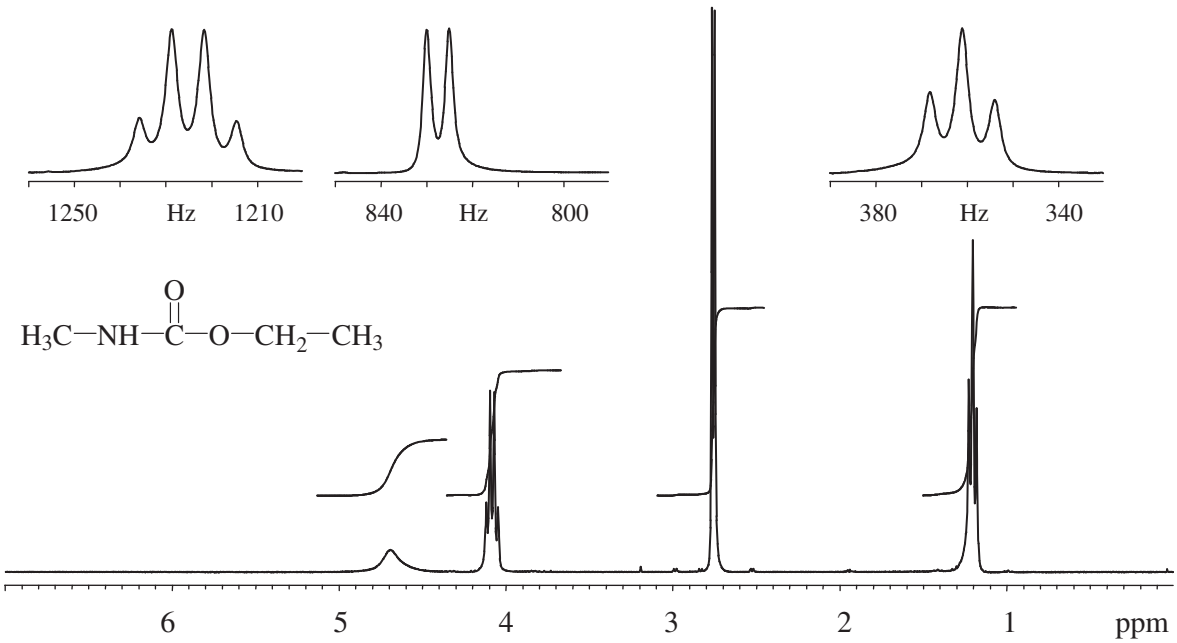

FIGURE 3.30 Proton NMR spectrum of ethyl *N*-methylcarbamate, at 300 MHz in $CDCl_3$.

amines are subject to hydrogen bonding, the shift depends on concentration, solvent, and temperature. Amide, pyrrole, and indole NH groups have chemical shifts from ~8.5 ppm to 5.0 ppm; the effect on the chemical shift of concentration, solvent, and temperature is generally smaller than in the case of amines.

The nonequivalence of the protons on the nitrogen atom of a primary amide and of the methyl groups of *N*, *N*-dimethylamides is caused by slow rotation around the CN bond, as can be rationalized by the contribution of the resonance form $C{=}N^+$ with O^- (Section 3.8.3.2).

Protons on the nitrogen atom of an amine salt exchange at a moderate rate; they are seen as a broad peak (~8.5 ppm to 6.0 ppm), and they are coupled to protons on adjacent carbon atoms ($J \sim 7$ Hz).

The use of trifluoroacetic acid as both a protonating agent and a solvent frequently allows classification of amines as primary, secondary, or tertiary. This is illustrated in Table 3.4, where the number of protons on nitrogen determines the multiplicity of the methylene unit in the salt (Figure 3.31). Sometimes the broad ^+NH, $^+NH_2$, or $^+NH_3$ peak can be seen to consist of three broad humps. These humps are due to *J*-coupling with the ^{14}N nucleus ($J \sim 50$ Hz). The reason that these splittings are observable is due to the high (near tetrahedral) symmetry at the nitrogen atom, which reduces the ^{14}N nuclear quadrupolar interaction. With good resolution, it is sometimes possible to observe splitting of each of the humps by the protons on adjacent carbons ($J \sim 7$ Hz), but it is easier to observe the splitting on the sharper α-CH signals. The behavior of the protons in the H—C—N—H sequence may be summarized as follows in Table 3.5.*

TABLE 3.4 Classification of Amines by NMR of their Ammonium Salts in Trifluoroacetic Acid

Amine Precursor Class	Ammonium Salt Structure	Multiplicity of Methylene unit
Primary	$C_6H_5CH_2NH_3^+$	Quartet (Figure 3.31)
Secondary	$C_6H_5CH_2NH_2R^+$	Triplet
Tertiary	$C_6H_5CH_2NHR_2^+$	Doublet

Source: Anderson, W.R. Jr., and Silverstein R.M. (1965) *Anal. Chem.*, **37**, 1417.

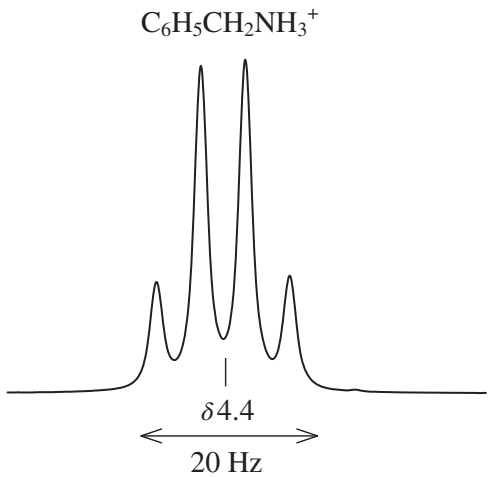

FIGURE 3.31 Proton NMR spectrum of the α-methylene unit of a primary amine at a Larmor frequency of 100 MHz in CF_3CO_2H; corresponds to Table 3.4, first line.

*Courtesy of Dr. Donald C. Dittmer (Syracuse University).

TABLE 3.5 Effect of NH Exchange Rate on Coupling

	Rate of NH Exchange		
	Fast	**Intermediate**	**Slow**
Effect on N—H	Singlet, sharp	Singlet, broad	Singlet, broad
Effect on C—H	No coupling	No coupling	Coupling

Chemical shifts of several classes of protons bonded to nitrogen atoms are available in Appendix E.

3.6.3 Protons on Sulfur

Sulfhydryl protons usually exchange at a low rate so that at room temperature they are coupled to protons on adjacent carbon atoms ($J \sim 8$ Hz). They do not exchange rapidly with hydroxyl, carboxylic, or enolic protons on the same or on other molecules; thus, separate peaks are seen. However, exchange is rapid enough that shaking the solution for a few minutes with deuterium oxide replaces sulfhydryl protons with deuterium. The chemical shift range for aliphatic sulfhydryl protons is 2.5 ppm to 0.9 ppm; for aromatic sulfhydryl protons, 3.6 ppm to 2.8 ppm. Concentration, solvent, and temperature affect the position within these ranges.

3.6.4 Protons on or near Chlorine, Bromine, or Iodine Nuclei

In principle, protons may be weakly coupled to chlorine, bromine, or iodine nuclei, but the effects of such coupling are not observed because of the strong electric quadrupolar relaxation of these halogen nuclei. For example, the proton NMR spectrum of CH_3CH_2Cl is unaffected by the presence of the chlorine nucleus; the triplet and quartet are sharp.

3.7 COUPLING OF PROTONS TO OTHER IMPORTANT NUCLEI (^{19}F, D (^{2}H), ^{31}P, ^{29}Si, AND ^{13}C)

3.7.1 Coupling of Protons to ^{19}F

Since ^{19}F has a nuclear spin quantum number of $\frac{1}{2}$ and 100% natural abundance, H—F coupling and H—H coupling obey the same multiplicity rules; in general, the coupling constants for H—F cover a somewhat larger range than those for H—H (Appendix F), and there is more long-range coupling for H—F pairs.

The spectrum of fluoroacetone, $CH_3—(C{=}O)—CH_2F$, in $CDCl_3$ at 300 MHz (Figure 3.32), shows the CH_3 group as a doublet at 2.2 ppm ($J = 4.3$ Hz) resulting from long-range coupling to the ^{19}F nucleus. The doublet at 4.75 ppm ($J = 48$ Hz) represents the protons of the CH_2 group coupled to the geminal ^{19}F nucleus. The ^{19}F nucleus is about 80% as sensitive as the proton and can be readily observed at the appropriate Larmor frequency for a specific magnetic field (see Chapter 6).

3.7.2 Coupling of Protons to D (^{2}H)

For the purposes of NMR spectroscopy, deuterium (D or ^{2}H) usually is introduced into a molecule to detect a particular functional group or to simplify a spectrum. Deuterium has a nuclear spin quantum number of 1, small coupling constants with protons, and a small electrical quadrupole moment. The ratio of the J values for H—H pairs to those of H—D pairs is about 6.5.

Suppose the protons on the α-carbon atom of a ketone

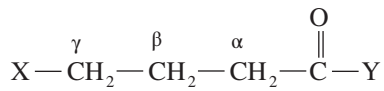

were replaced by deuterium to give

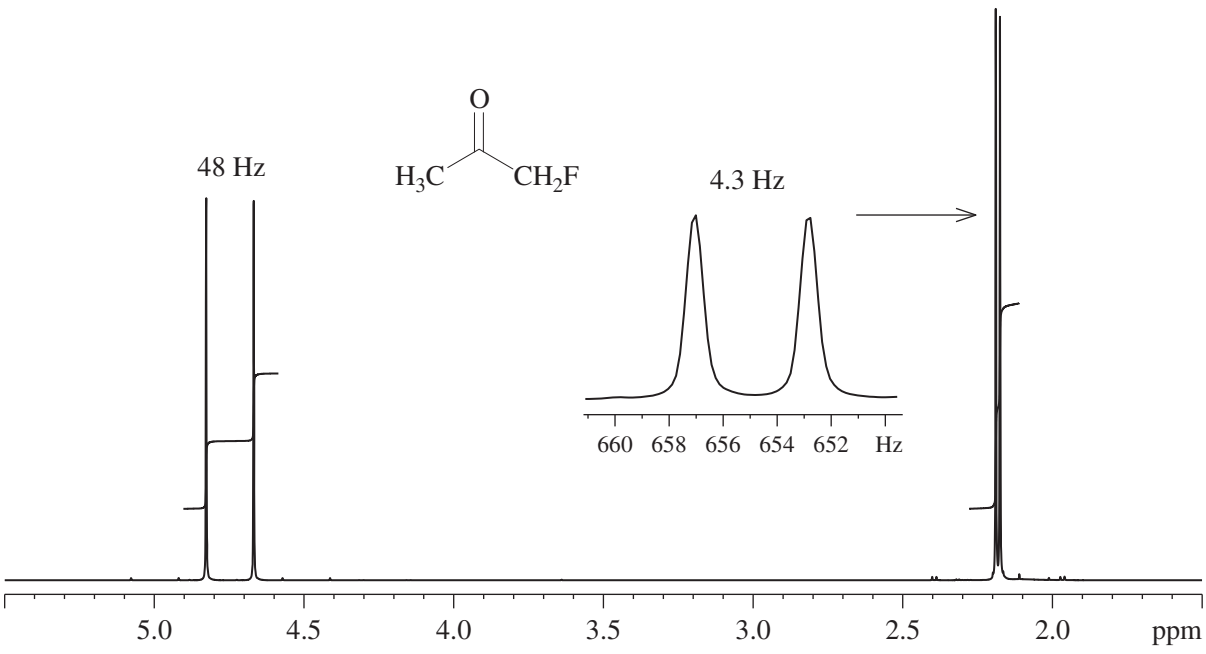

FIGURE 3.32 ^{1}H NMR spectrum of fluoroacetone in $CDCl_3$ at 300 MHz.

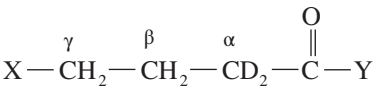

The spectrum of the undeuterated compound consists of a triplet for the α protons, a quintet for the β protons—assuming equal coupling for all protons—and a triplet for the γ protons. For the deuterated compound, the α-proton peak would be absent, the β-proton peak would appear, at modest resolution, as a slightly broadened triplet, and the γ-proton peak would be unaffected. Actually, at very high resolution, each peak of the β-proton triplet would appear as a very closely spaced quintet ($J_{\text{H–C–C–D}} \sim 1$ Hz) since $2nI + 1 = 2 \times 2 \times 1 + 1 = 5$, where n is the number of D nuclei coupled to the β protons.

Most deuterated solvents have residual proton impurities in an otherwise completely deuterated sample; thus, deuterated dimethyl sulfoxide, $(CD_3)_2S{=}O$, contains a few molecules of $CD_2H{-}(S{=}O){-}CD_3$, which show a closely spaced quintet ($J \sim 2$ Hz, intensities 1:2:3:2:1) in accordance with $2nI + 1$ (see Appendix G).

Since deuterium has an electric quadrupole moment, relatively broad peaks are observed in ^{2}H NMR spectra.

3.7.3 Coupling of Protons to ^{31}P

The ^{31}P nucleus has a natural abundance of 100% and a spin number of $\frac{1}{2}$. The multiplicity rules for proton–phosphorus splitting are the same as those for proton–proton splitting. The coupling constants are large ($J_{\text{H—P}} \sim 200$ to 700 Hz, and $J_{\text{HC—P}}$ is 0.5 to 20 Hz) (Appendix F) and are observable through at least four bonds. The ^{31}P nucleus can be observed at the appropriate Larmor frequency for a specific magnetic field (Chapter 6).

3.7.4 Coupling of Protons to ^{29}Si

The NMR-active ^{29}Si isotope has a natural abundance of 4.70% and a nuclear spin quantum number of $\frac{1}{2}$. The value of $J_{^{29}\text{Si—CH}}$ is about 6 Hz. The low-intensity doublet caused by ^{29}Si—CH_3 coupling can often be seen straddling (±3 Hz) the dominant central TMS peak in a ^{1}H NMR spectrum; the low-intensity $^{13}CH_3$ satellite doublet can also be seen at ±59 Hz (Section 3.7.5). ^{29}Si NMR spectra can be obtained at the appropriate Larmor frequency for a specific magnetic field (Chapter 6).

3.7.5 Coupling of Protons to ^{13}C

The ^{13}C isotope has a natural abundance of 1.1% and a nuclear spin quantum number of $\frac{1}{2}$. The peaks due to protons directly bonded to ^{13}C are split into doublets with large coupling constants, about 115 Hz to 270 Hz for ^{13}C—H. The CH_3—CH_2 group, for example, is predominantly $^{12}CH_3$—$^{12}CH_2$ but contains a small amount of $^{13}CH_3$—$^{12}CH_2$ and of $^{12}CH_3$—$^{13}CH_2$. Thus, the $^{13}CH_3$ proton peak is split into a doublet by ^{13}C ($J \sim 120$ Hz), and each peak of the doublet is split into a triplet by the $^{12}CH_2$ protons ($J \sim 7$ Hz) as shown below. These ^{13}C satellite peaks are of low intensity because of the small number of molecules containing the $^{13}CH_3$ group and can usually be seen on both sides of an intense $^{12}CH_3$ peak (e.g., the large $^{12}CH_3$ triplet shown below). The dominant peaks in a ^{1}H NMR spectrum therefore do not show the effects of coupling to ^{13}C. For ^{13}C-labeled compounds, multiplets are of higher intensity depending on the level of isotopic substitution.

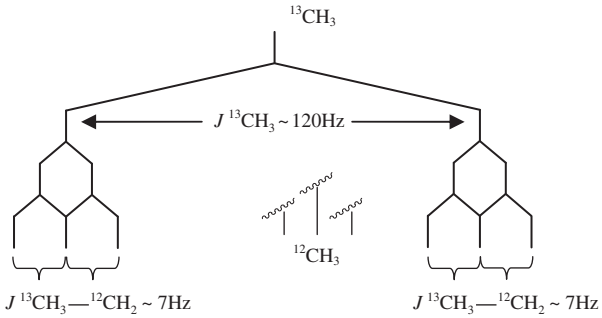

3.8 CHEMICAL EQUIVALENCE

The concept of chemical equivalence is central to NMR spectroscopy. Chemically equivalent nuclei comprise a *set* within a *spin system* (Pople notation, Section 3.5.3). Correct usage of Pople notation, and spectral interpretation, requires one to be able to identify sets of chemically equivalent nuclei.

Nuclei are chemically equivalent *if they are interchangeable through any symmetry operation or by a rapid process*. (This broad definition assumes an achiral environment (solvent or reagent) in the NMR experiment; the common solvents are achiral.)

3.8.1 Determination of Chemical Equivalence by Interchange Through Symmetry Operations

There are three symmetry operations of interest, each involving a symmetry element: rotation about a simple axis of symmetry (C_n), reflection through a plane of symmetry (σ), and inversion through a center of symmetry (i).* More rigorously, symmetry operations may be described under two headings: C_n and S_n. The latter is rotation around an alternating axis of symmetry. It turns out that S_1 is the same as σ, S_2 is the same as i, and higher subscripts for S_n are rare. The subscripts denote the number of such rotations required to make a full 360° rotation. Thus, C_1 is a 360° rotation, C_2 is a 180° rotation, and so on. The designation S_1 requires a 360° rotation followed by a reflection through the plane at a right angle to the axis. S_2 requires a 180° rotation followed by a reflection, and so forth. Students well versed in the use of symmetry operations can use these methods to determine chemical equivalence. A detailed discussion of symmetry

*The symmetry operation must relate to the entire molecule.

operations is beyond the scope of this text, but briefly, if the nuclei are related or exchangeable through a symmetry operation, then they are chemically equivalent. Consider the simple example of the two hydrogen atoms in a water molecule. The positions of these two hydrogen atoms can be exchanged through a C_2 operation (rotation about an axis which passes through the oxygen atom by $\frac{360^\circ}{2} = 180^\circ$) or by reflection through a plane of symmetry (σ) which passes through the oxygen atom and which is perpendicular to the plane of the molecule. As a result, the two hydrogen nuclei in water are chemically equivalent.

3.8.2 Determination of Chemical Equivalence by Tagging (or Substitution)

An alternative, equivalent, means of visualizing whether nuclei are chemically equivalent is through a "tagging" or substitution operation* in which two identical drawings of the same compound are made: one hydrogen atom (or group of hydrogen atoms, e.g., a methyl group) in one of the drawings is tagged (or substituted by a different atom or isotope), and the other hydrogen atom (or group of hydrogen atoms) in the second drawing is also tagged (or substituted) in the same manner. The resulting drawings (or models) are related to each other using the following terms to describe stereochemical and isomeric relationships between molecules: homomers, enantiomers, diastereomers, or constitutional isomers. The H atoms (or groups of atoms) are called, respectively, homotopic, enantiotopic, diastereotopic, or heterotopic. The examples in Figure 3.33 illustrate the process.

In the first example, the models are superimposable (i.e., homomers); in the second, nonsuperimposable mirror images (i.e., enantiomers); and in the third, nonsuperimposable nonmirror images (i.e., diastereomers). Note that the tags are permanent; that is, H and Ⓗ are different kinds of atoms. Alternatively, one proton in each structure may be replaced by Z, representing any nucleus not present in the molecule. From an analysis of symmetry operations, homotopic atoms or groups are chemically equivalent in all chemical environments; enantiotopic atoms or groups are chemically equivalent in an achiral solvent; diastereotopic atoms or groups are not chemically equivalent in any chemical environment; and likewise, heterotopic atoms or groups are not chemically equivalent (usually obvious).

If geminal protons (CH_2) in a molecule cannot be interchanged through a symmetry operation, they are diastereotopic to one another; each has a different chemical shift – except for coincidental overlap (Figure 3.33c). This compound has a stereogenic center, shown by an asterisk. Note, however, that a stereogenic center is not necessary for the occurrence of nonequivalent methylene protons; in this case the term "diastereotopic" is not technically correct but still sometimes used to describe the pair of protons.

3.8.3 Chemical Equivalence by Rapid Interconversion of Structures

If chemical structures can interconvert, the rate of interconversion depends on temperature, catalyst, solvent, and concentration. We assume a given concentration and absence of catalyst, and we treat four systems.

3.8.3.1 Keto–Enol Interconversion. The tautomeric interconversion of acetylacetone (Figure 3.34) at room temperature is slow enough that the NMR peaks of both forms can be observed. The equilibrium keto/enol ratio can be determined from the relative areas of the keto and enol CH_3 peaks, as shown. At higher temperatures, the interconversion rate will be increased so that a single averaged resonance will be obtained. Chemical equivalence for all of the interconverting protons has now been achieved. Note that the NMR time scale is of the same order of magnitude as the chemical shift separation of interchanging signals expressed in hertz, that is, about 10^1 Hz to 10^3 Hz. Processes occurring faster

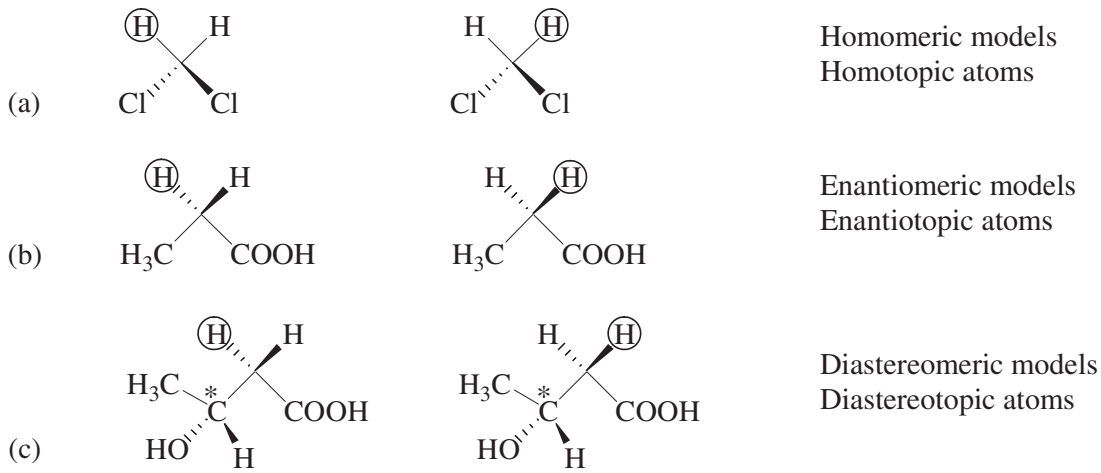

FIGURE 3.33 Tagged molecules: (a) equivalent molecules, (b) enantiomers, and (c) diastereomers.

*Ault, A. (1974) *J. Chem. Educ.*, **51**, 729.

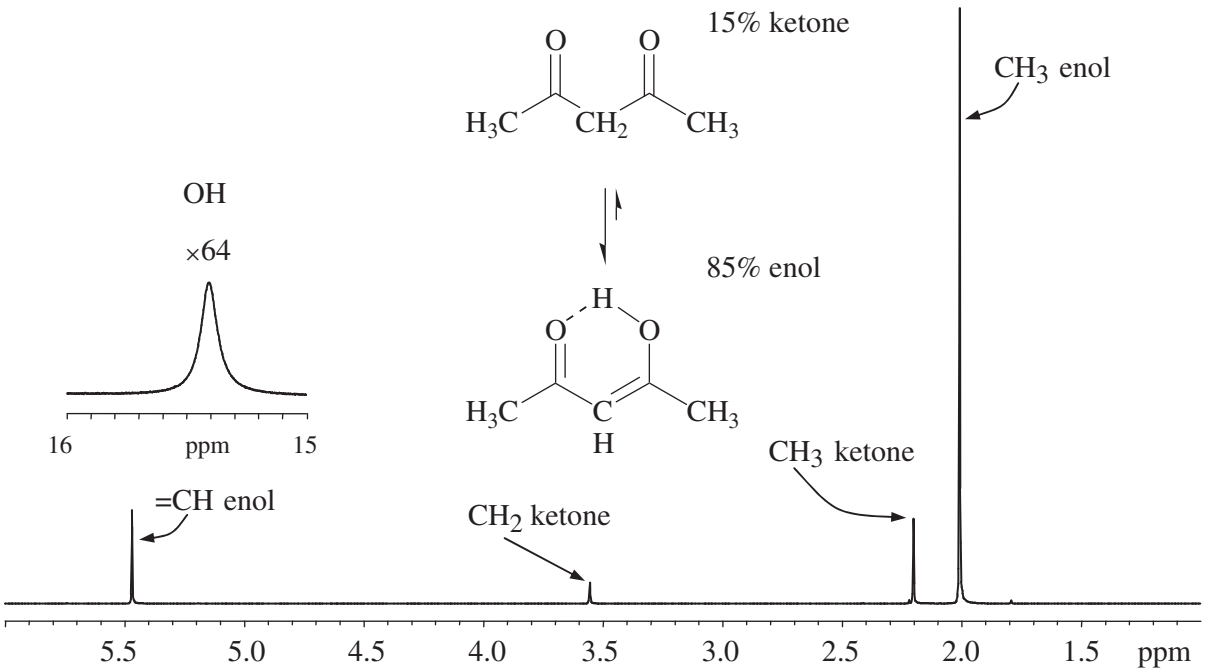

FIGURE 3.34 Proton NMR spectrum of acetylacetone in $CDCl_3$ at 300 MHz and 32 °C. The enol–keto ratio was measured by integration of the CH_3 peaks.

than this will lead to averaged signals. Note also that the enolic OH proton peak is deshielded relative to the OH proton of alcohols because the enolic form is strongly stabilized by intramolecular hydrogen bonding.

3.8.3.2 Interconversion Around a Partial Double Bond (Restricted Rotation). At room temperature, a neat sample of dimethylformamide shows two CH_3 peaks because the rate of rotation around the hindered partial C—N double bond is slow. At ~123 °C, the rate of exchange of the two CH_3 groups is rapid enough so that the two peaks coalesce.

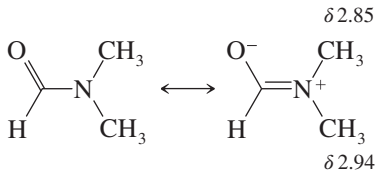

3.8.3.3 Interconversion Around the Single Bonds of Rings. Cyclohexane at room temperature exists in rapidly interconverting, superimposable chair forms.

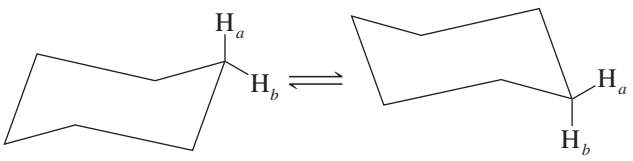

An axial proton becomes an equatorial proton and vice versa in the interconverting structures, and the spectrum consists of a single averaged peak. As the temperature is lowered, the peak broadens and, at a sufficiently low temperature, two peaks appear: one for the axial protons and one for the equatorial protons. In other words, at room temperature, the axial and equatorial protons are chemically equivalent by rapid interchange. At very low temperatures, they are not chemically equivalent; in fact, in each "frozen" chair form, the protons of each CH_2 group are nonequivalent pairs, but at room temperature, the rate of chair interconversion is sufficiently high to average the chemical shifts of these geminal protons.

Methylcyclohexane exists at room temperature as a rapidly interconverting mixture of axial and equatorial conformers. These conformers are not superimposable, and at low temperatures, a spectrum of each conformer exists.

In a fused cyclohexane ring, such as those of steroids, the rings are "frozen" at room temperature and the axial and equatorial protons of each CH_2 group are not chemically equivalent.

3.8.3.4 Interconversion Around the Single Bonds of Chains. Chemical equivalence of protons on a CH_3 group results from rapid rotation around a carbon–carbon single bond even in the absence of a symmetry element. Figure 3.35a shows Newman projections of the three staggered rotamers of a molecule containing a methyl group attached to another sp^3 carbon atom having four different substituents, that is, a stereogenic center. In any single rotamer, none of the CH_3 protons can be interchanged by a symmetry operation. However, the protons are rapidly changing positions. The time spent in any one rotamer is short ($\sim 10^{-6}$ seconds), because the energy barrier for rotation around a C—C single bond is small. The observed chemical shift of the protons in the methyl group is an average of the shifts of the three protons. In other words, each

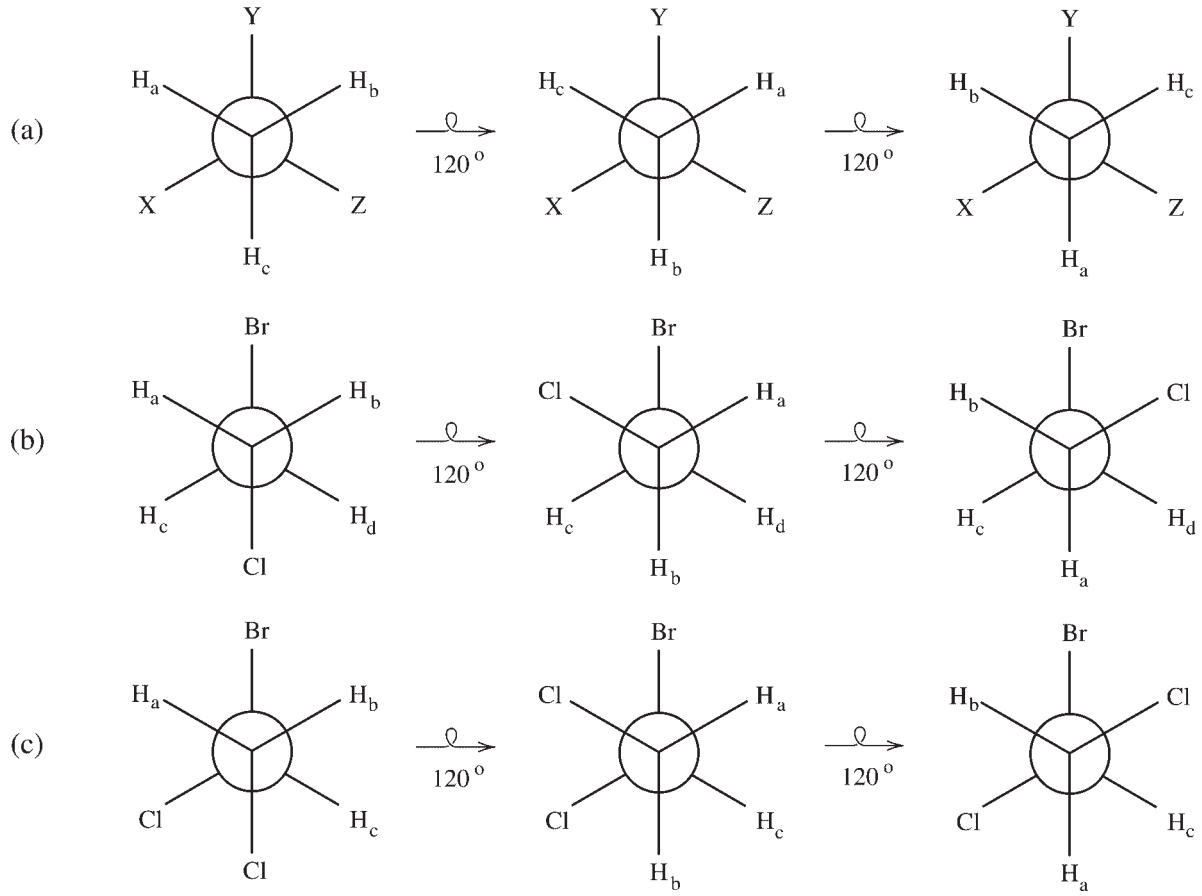

FIGURE 3.35 (a) Newman projection of the staggered rotamers of a molecule with a methyl group attached to a stereogenic sp^3 carbon atom. (b) 1-Bromo-2-chloroethane. (c) 1-Bromo-1, 2-dichloroethane.

proton can be interchanged with the others by a rapid rotational operation. Thus, without the labels on the protons, the rotamers are indistinguishable.

In the same way, the nine protons of the three rotating methyl groups of a *t*-butyl group are all chemically equivalent except in rare cases of steric hindrance. Both the methyl group and the *t*-butyl group are described as symmetrical tops.

The staggered rotamers of 1-bromo-2-chloroethane (Figure 3.35b) are distinguishable. However, in the *anti* rotamer, H_a and H_b are chemically equivalent (enantiotopic) by interchange through a plane of symmetry, as are H_c and H_d; thus, there are two sets of enantiotopic protons. In neither of the gauche rotamers is there a symmetry element, but H_a and H_b, and H_c and H_d, are chemically equivalent by rapid rotational interchange between two enantiomeric rotamers. Now we have one chemical shift for H_a and H_b in the *anti* rotamer, and a different chemical shift for H_a and H_b in the *gauche* rotamers. By rapid averaging of these two chemical shifts, we obtain a single chemical shift (i.e., chemical equivalence) for H_a and H_b, and of course for H_c and H_d. The Pople notation is AA′XX′; it is useful to remember that for any compound of the form X—CH_2CH_2—Y ($X \neq Y$), the four methylene protons will be described by this Pople notation (see Section 3.9). In general, if protons can be interchanged by a symmetry operation (through a plane of symmetry) in one of the rotamers, they are also chemically equivalent (enantiotopic) by rapid rotational interchange.*

Consider a methylene group next to a stereogenic center, as in 1-bromo-1,2-dichloroethane (Figure 3.35c). Protons H_a and H_b are not chemically equivalent since they cannot be interchanged by a symmetry operation in any conformation; the molecule has no simple axis, plane, center, or alternating axis of symmetry. Although there is a rapid rotation around the carbon–carbon single bond, the CH_2 protons are not interchangeable by a rotational operation; the averaged chemical shifts of H_a and H_b are not identical. An observer can detect the difference before and after rotating the methylene group. The protons in this compound are diastereotopic: each has its own chemical shift and they are coupled to each other. The spin system in this molecule is described with the Pople notation ABX. It is useful to remember that any pair of methylene protons in a molecule with a stereogenic center are diastereotopic; if the center is far-enough removed from the CH_2 group (e.g., several bonds away in a different spin

*The discussion of rotamers is taken in part from Silverstein, R.M. and LaLonde, R.T. (1980). *J. Chem. Educ.*, **57**, 343.

system), the protons may, however, appear to behave as if they were chemically equivalent.

3.9 MAGNETIC EQUIVALENCE

In addition to the above requirements for a first-order spin system, we now consider the concept of magnetic equivalence by comparison with the concept of chemical equivalence. In order to consider testing for magnetic equivalence between a set of spins, those spins must have been already identified as being chemically equivalent; that is, chemical equivalence is a prerequisite for magnetic equivalence.

If two chemically equivalent protons each have the same coupling to every other proton in the spin system, then they are also magnetically equivalent, and the following Pople notations apply: A_2, B_2, X_2, and so on. This does not mean that a proton must couple equally to all other protons in the spin system; it means that for any (and all) third proton chosen as a test spin, the two chemically equivalent protons must couple equally to that third proton. As mentioned above, if two protons in a set are only chemically equivalent and not magnetically equivalent, the following notations apply: AA′, BB′, XX′, and so on. To rephrase: two chemically equivalent protons are also magnetically equivalent if they are symmetrically disposed with respect to each and every other proton in the spin system (*excluding those in the chemically equivalent set to which they belong*). For example, to test whether a AA′XX′ system also has magnetic equivalences so that it could be described as A_2X_2, we have to show that the coupling paths from A to X and from A to X′ are equivalent (and also that the coupling path from A′ to X is equivalent to the coupling path from A′ to X′).

The common occurrence of magnetic nonequivalence in aromatic rings depends on the number, kind, and distribution of the substituents.

Consider the protons in *p*-chloronitrobenzene (see Figure 3.36). There is an axis of symmetry (through the substituents) that provides two sets of chemically equivalent protons, AA′XX′. Neither the two A protons nor the two X protons are magnetically equivalent; this is apparent by realizing that the through-bond coupling path traced from proton A to proton X (three bonds) is not the same as the path traced from proton A to proton X′ (five bonds) (important: it is not relevant that the path from A to X is equivalent to the path from A′ to X′). This is not a first-order spin system and the resulting multiplet patterns do not conform to first-order intensity patterns in the Pascal triangle (Figure 3.22) nor do the separations (in Hz) between the peaks correspond to coupling constants. Spectra such as these do not become first-order spectra regardless of the strength of the magnetic field: the experimentalist cannot change the symmetry relationships between the spins in the molecule by increasing the magnetic field. The choice of designating the spectrum as AA′XX′ or AA′BB′, however, does depend on the strength of the applied magnetic field. At lower magnetic field, these spectra become deceptively simple. In the 60 MHz era, students learned to recognize two tight clusters in aromatic region as indicative of *para* disubstitution. The pattern of *o*-dichlorobenzene shows a pattern somewhat resembling that of *p*-chloronitrobenzene for the same reasons (see Figure 3.37). Heteroaromatic rings behave similarly.

Three isomeric difluoroethylenes furnish additional examples of chemically equivalent nuclei that are not magnetically equivalent. The systems are AA′XX′.

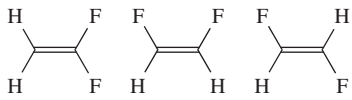

In each system, the protons comprise a set (AA′) and the fluorine nuclei comprise a set (XX′) of chemically equivalent nuclei, but since the nuclei in each set are not magnetically equivalent, the spectra are not first order. One way to quickly see that there cannot be magnetic equivalence is by realizing that each of the two protons do not couple equivalently to a particular fluorine; the *cis* and *trans* coupling constants are not the same.

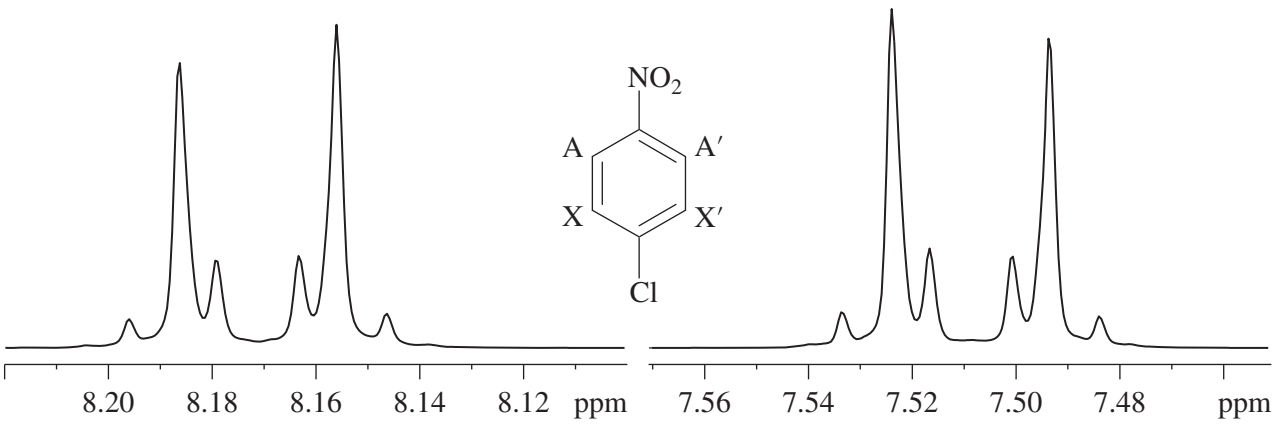

FIGURE 3.36 Proton NMR spectrum of *p*-chloronitrobenzene in $CDCl_3$ at 300 MHz.

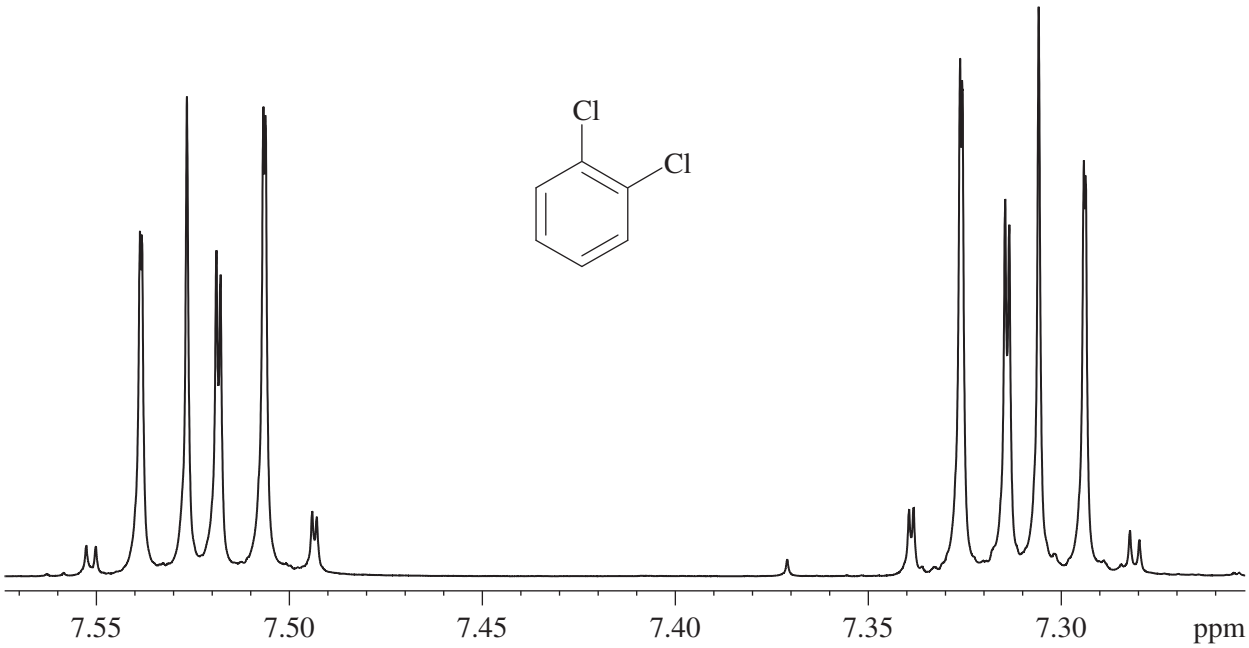

FIGURE 3.37 Proton NMR spectrum of *o*-dichlorobenzene in $CDCl_3$ at 300 MHz.

The open-chain, conformationally mobile compounds of the type:

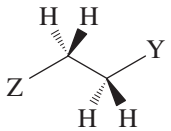

consist of two different sets of proton coupled to each other. The groups Z and Y contain no chiral element and no protons that couple to the two sets shown; Z and Y polarities determine the difference between shifts of the sets (i.e., $\Delta\nu$). Strictly, the protons are described as an AA′XX′ or AA′BB′ system depending on the magnitude of $\Delta\nu/J$ (as described in Section 3.8.3.4). However, in practice for such a molecule undergoing rapid conformational changes (rotation about bonds) at room temperature – barring large conformational preferences – the relevant averaged J values are quite similar, and, in practice, spectra resembling those representative of A_2X_2 or A_2B_2 spin systems result. The "weakly coupled" A_2X_2 system would show two triplets, and a "strongly coupled" A_2B_2 system would show a complex, higher order spectrum.

3.10 AMX, ABX, AND ABC RIGID SYSTEMS WITH THREE COUPLING CONSTANTS

In Section 3.5, we discussed the simple first-order system AX. As the ratio $\Delta\nu/J$ decreases, the two doublets approach each other with a characteristic distortion of peak heights to give an AB system, but no additional peaks appear. However, as an A_2X system – a triplet and a doublet – develops into an A_2B system, additional peaks do appear, and the system presents a higher order spectrum; the J values no longer coincide with the measured differences between peaks [see simulated spectra in Bovey (1988)].

Having considered these systems, we can now examine the systems AMX, ABX, and ABC, starting with a rigid system. Styrene, whose rigid vinylic group furnishes an AMX first-order spectrum at 600 MHz, is a good starting point (see Figure 3.38).

Correlation of the structure of a compound with its spectrum is indeed a gentle approach compared with interpreting the spectrum of an unknown compound, but it is instructive.

Since in styrene there is free rotation around the substituent bond, there are two symmetry planes through the molecule. In one conformation, the vinyl group and the ring are coplanar in the plane of the page with all of the protons in the symmetry plane, hence not interchangeable. In the other conformation, the vinyl group and the benzene ring are perpendicular to one another, and the symmetry plane is perpendicular to the plane of the page. Again, the vinyl protons are in the symmetry plane. The following data for the vinyl group are relevant:

There are three sets in the vinyl system, AMX, each set consisting of one proton.

Chemical shifts: X = 6.73 ppm, M = 5.75 ppm, A = 5.25 ppm.

$\Delta\nu_{XM} = 588$ Hz, $\Delta\nu_{XA} = 888$ Hz, $\Delta\nu_{AM} = 300$ Hz.

$J_{XM} = 17$ Hz, $J_{XA} = 11$ Hz, $J_{AM} = 1.0$ Hz.

The $\Delta\nu/J$ ratios: XM = 35, XA = 88, MA = 300.

Each set gives a doublet of doublets (note the stick diagrams in Figure 3.38). The X proton is the most strongly deshielded by the aromatic ring, and the A proton least so.

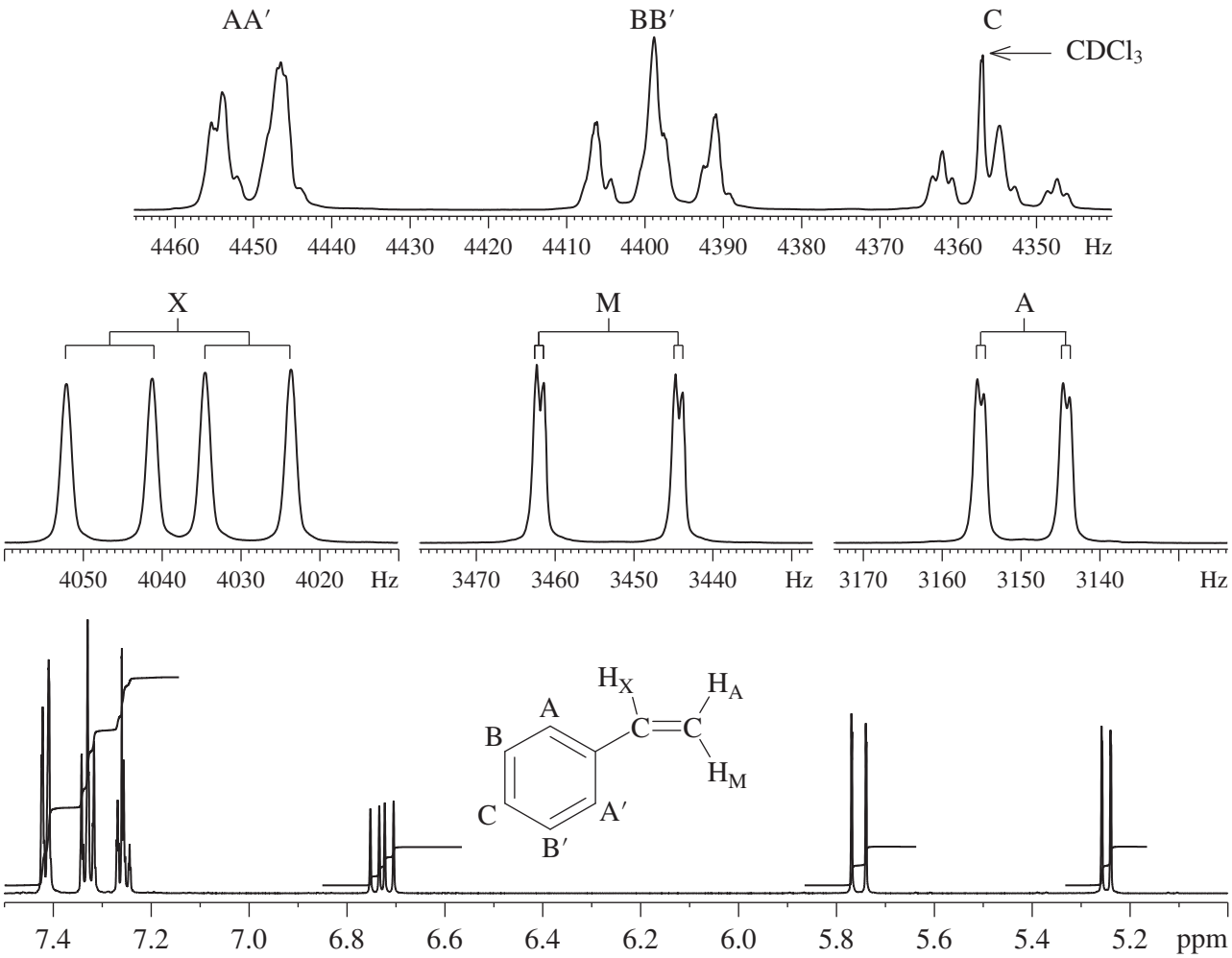

FIGURE 3.38 Proton NMR spectrum of styrene in $CDCl_3$ at 600 MHz.

The X proton is coupled *trans* across the double bond to the M proton with the largest coupling constant, and *cis* across the double bond to the A proton with a slightly smaller coupling constant. The result is the doublet of doublets centered at 6.73 ppm with two large coupling constants.

The M proton is, of course, coupled to the X proton and is coupled geminally to the A proton with a very small coupling constant. The result is a doublet of doublets centered at 5.75 ppm with one large and one very small coupling constant.

The A proton is coupled *cis* across the double bond to the X proton with the slightly smaller coupling constant (as compared with the *trans* coupling). The A proton is coupled geminally to the M proton with the very small coupling constant mentioned above. The result is a doublet of doublets centered at 5.25 ppm with the large coupling constant (smaller than the *trans* coupling) and the very small geminal coupling constant.

In the conformation of the molecule with the perpendicular plane of symmetry, the *ortho* protons of the ring system are interchangeable with each other as are the *meta* protons. However, since the protons in neither set are magnetically equivalent, the aromatic spin system is AA′BB′C. It is a higher order system. At 600 MHz, it is possible to assign approximate chemical shifts (from left to right): ~7.42 ppm, ~7.33 ppm, and ~7.26 ppm.

The ratio of the integrals (2:2:1:1:1:1 from left to right) identifies the proton at 7.26 ppm as *para*. The *ortho* protons are the most deshielded because of the diamagnetic effect of the vinyl double bond.

3.11 WEAKLY AND STRONGLY COUPLED SYSTEMS: VIRTUAL COUPLING

This section compares weakly coupled systems, which are relatively easy to interpret, and strongly coupled systems, which are more complicated.

3.11.1 Weakly Coupled Systems

3.11.1.1 1-Nitropropane. As mentioned in Section 3.9, most open-chain compounds – barring severe steric hindrance – are conformationally mobile at room temperature;

slightly different coupling constants in each set average out and spins become practically magnetically equivalent. Thus, a 300 MHz, room-temperature spectrum of 1-nitropropane is described as $A_3M_2X_2$ rather than $A_3MM'XX'$, and first-order rules apply (see Figure 3.39).

The X_2 protons are strongly deshielded by the NO_2 group, the M_2 protons less so, and the A_3 protons very slightly. There are two coupling constants, J_{AM} and J_{MX}, which are very similar but not exactly equal. In fact, at 300 MHz, the M_2 resonance is a deceptively simple, slightly broadened sextet ($n_A + n_X + 1 = 6$). At sufficient resolution, 12 peaks are possible: $(n_A + 1)\ (n_X + 1) = 12$. The A_3 and X_2 resonances are triplets with slightly different coupling constants.

3.11.2 Strongly Coupled Systems

3.11.2.1 1-Hexanol. In contrast, consider the 300 MHz and 600 MHz spectra of 1-hexanol (Figure 3.40). In the 300 MHz spectrum, the three-proton triplet at 0.87 ppm seems odd for the CH_3 group since the peak intensities deviate from the first-order ratios of 1:2:1. Furthermore, the unusual appearance of the multiplets is obvious despite a reasonable $\Delta\nu/J$ value of 13 for the CH_3—CH_2 (A_3B_2) groups.

The problem is that the B_2, C_2, and D_2 methylene groups are strongly coupled to one another; they appear in the spectrum as a partially resolved band and act as a conglomerate of spins in coupling to the methyl group, which is formally coupled only to the adjoining CH_2 group. This phenomenon is termed "virtual coupling."

At 600 MHz, the CH_2—CH_3 $\Delta\nu/J$ value is 26, and the CH_3 multiplet is now a first-order triplet. The B_2, C_2, and D_2 multiplets remain as a tight conglomerate at 300 MHz but the M_2 multiplet is deshielded enough by the OH group at 300 MHz so that a somewhat distorted quintet (splitting by the D and X protons) is apparent, as are incipient extra peaks; at 600 MHz, we clearly see a first-order quintet. In both spectra, the strongly deshielded triplet represents the X_2 methylene protons split by M_2 methylene protons. The one-proton singlet represents the OH proton. In order to prevent hydrogen bonding of the OH proton to the X proton, a trace of *p*-toluenesulfonic acid was added to the $CDCl_3$ solution. This was necessary because of the high purity of the $CDCl_3$ (see Section 3.6.1.1) and because of the low-solute concentration used when working at high magnetic fields.

3.11.2.2 3-Methylglutaric Acid. Another example of virtual coupling is encountered in 3-methylglutaric acid. Because of the 3-substituent, there is no plane of symmetry through the chain in the plane of the paper, and, as described in Section 3.8, the protons in each methylene group are not interchangeable and are thus diastereotopic.

We can be led astray by a structure that might be expected to give a first-order spectrum, at least at 300 MHz (see Figure 3.41a).

In other words, the $\Delta\nu/J$ ratios for

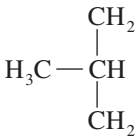

seem adequate, and our expectations of a clean doublet for the CH_3 group seem reasonable.

The difficulty is that the COOH groups deshield the CH_2 groups, thereby decreasing the $\Delta\nu/J$ ratio for CH_2—CH; the

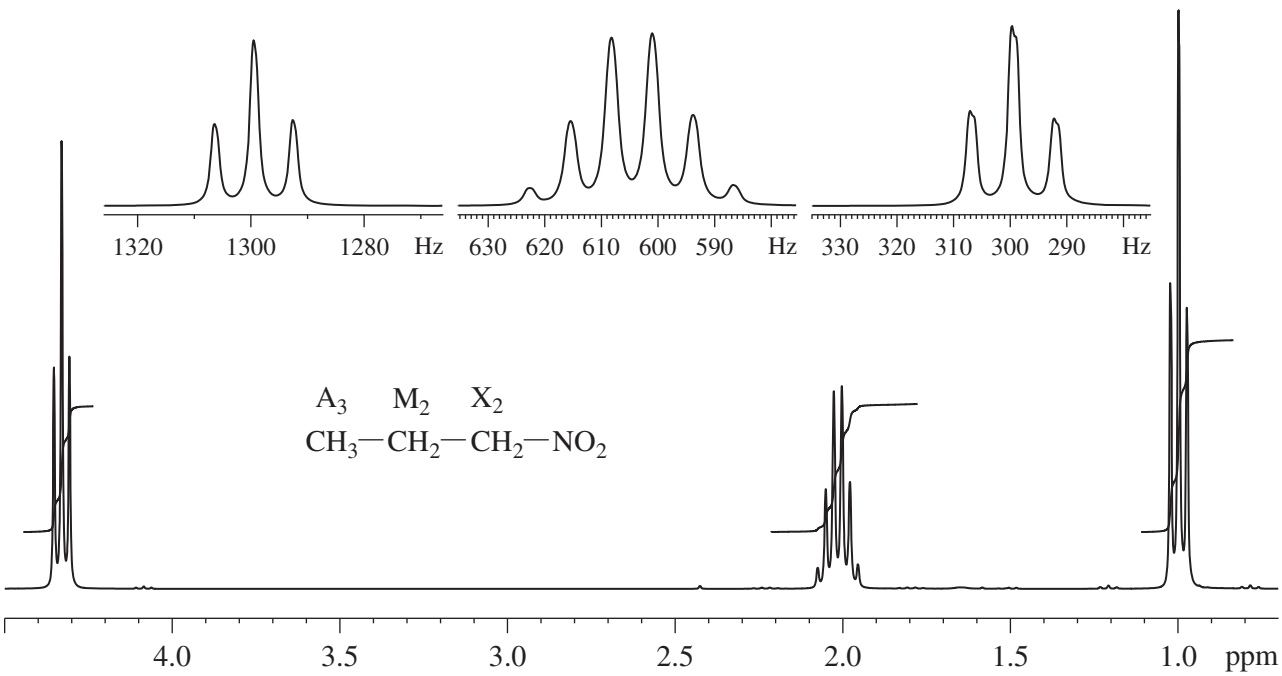

FIGURE 3.39 Proton NMR spectrum of 1-nitropropane in $CDCl_3$ at 300 MHz.

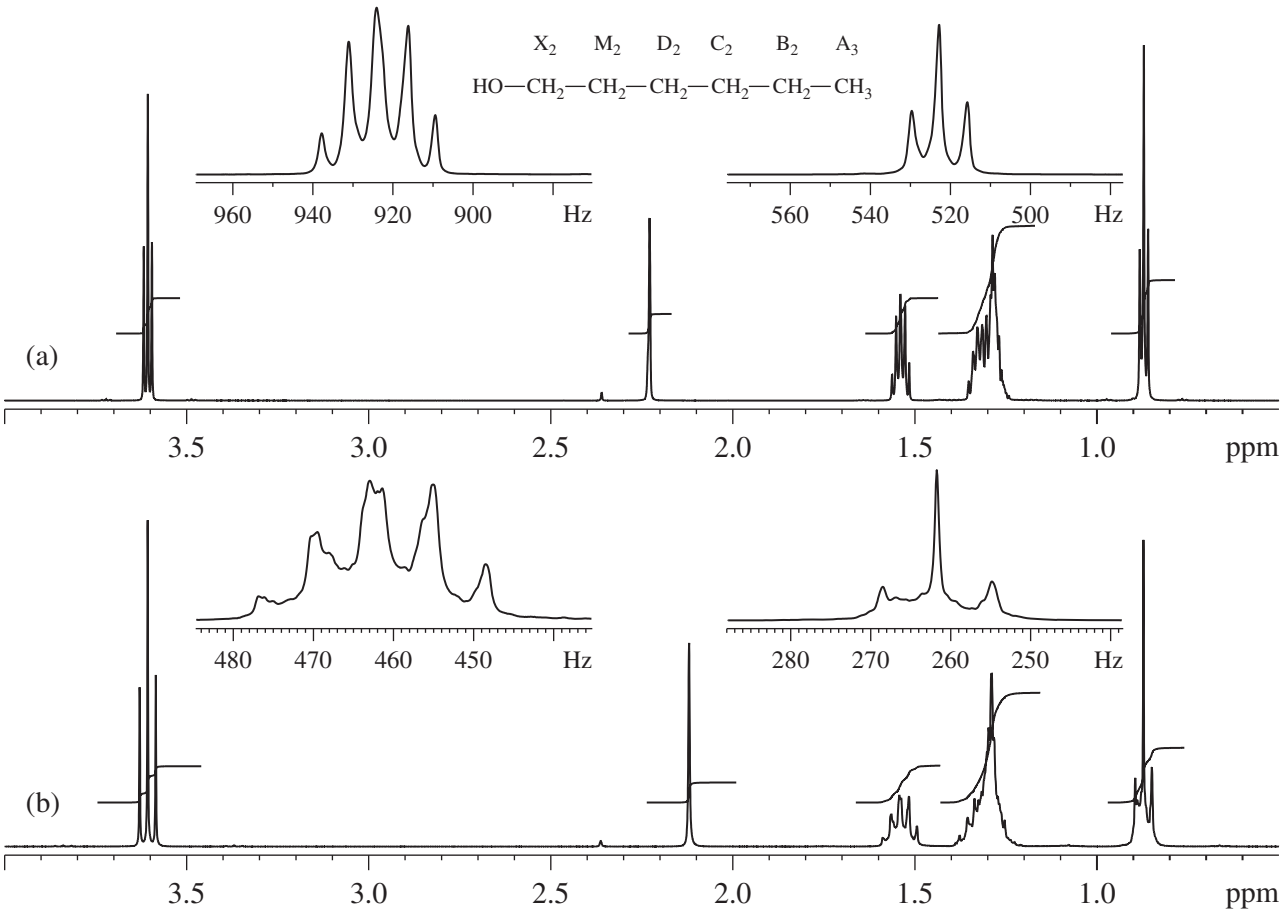

FIGURE 3.40 Proton NMR spectrum of hexanol in $CDCl_3$ at (a) 600 MHz and (b) 300 MHz.

virtual coupling results in a broadened, distorted "doublet" for the CH_3 at 300 MHz. With some experience, such distortions are tolerable. But the overlapping peaks of the CH_2—CH—CH_2 moiety are still beyond interpretation by inspection at 300 MHz.

At 600 MHz (see Figure 3.41b), the CH_3 group is a clean doublet resulting from coupling with the CH proton, which is no longer complicated by the virtual coupling to CH_2 multiplets. The CH proton is coupled, quite equally, to seven neighboring protons; this means that the CH multiplet should consist of eight peaks. And in fact it does, but the eighth peak is buried under the edge of one of the CH_2 multiplets, each of which is a doublet of somewhat distorted doublets. As mentioned above, the protons of each CH_2 group are diastereotopic—meaning that they have two different chemical shifts. The protons of each CH_2 group couple with each other (geminal coupling) and with the CH proton (vicinal coupling); the geminal coupling is larger—hence the two doublets of doublets.

3.12 CHIRALITY

The organic chemist—in particular, the natural products chemist—must always be conscious of chirality when interpreting NMR spectra. An interesting and challenging example is found in the terpene alcohol, 2-methyl-6-methylen-7-octen-4-ol (ipsenol, Figure 3.42). The first thing that we note is that the two methyl groups (part of an isopropyl group) are diastereotopic. Compare this result with isopropylbenzene (Figure 3.25) in which the two methyl groups of the isopropyl group are enantiotopic, and hence, chemically equivalent.

Since the nonequivalent methyl groups are each split by the vicinal CH proton, we expect to see two separate doublets. At 300 MHz, unfortunately, the pattern appears to be a classical triplet, usually an indication of a CH_3–CH_2 moiety—impossible to reconcile with the structural formula and the integration. Higher resolution would pull apart the middle peak to show two doublets.

To remove the coincidence of the inner peaks that caused the apparent triplet, we used the very effective technique of adding deuterated benzene,* which gave convincing evidence of two doublets at 20% C_6D_6/80% $CDCl_3$ and optimal results at about a 50:50 mixture (Figure 3.42). At 600 MHz, two individual doublets are seen.

*Sanders, J.K.M. and Hunter, B.K. (1993). *Modern NMR Spectroscopy*, 2nd ed. Oxford: Oxford University Press, p. 289.

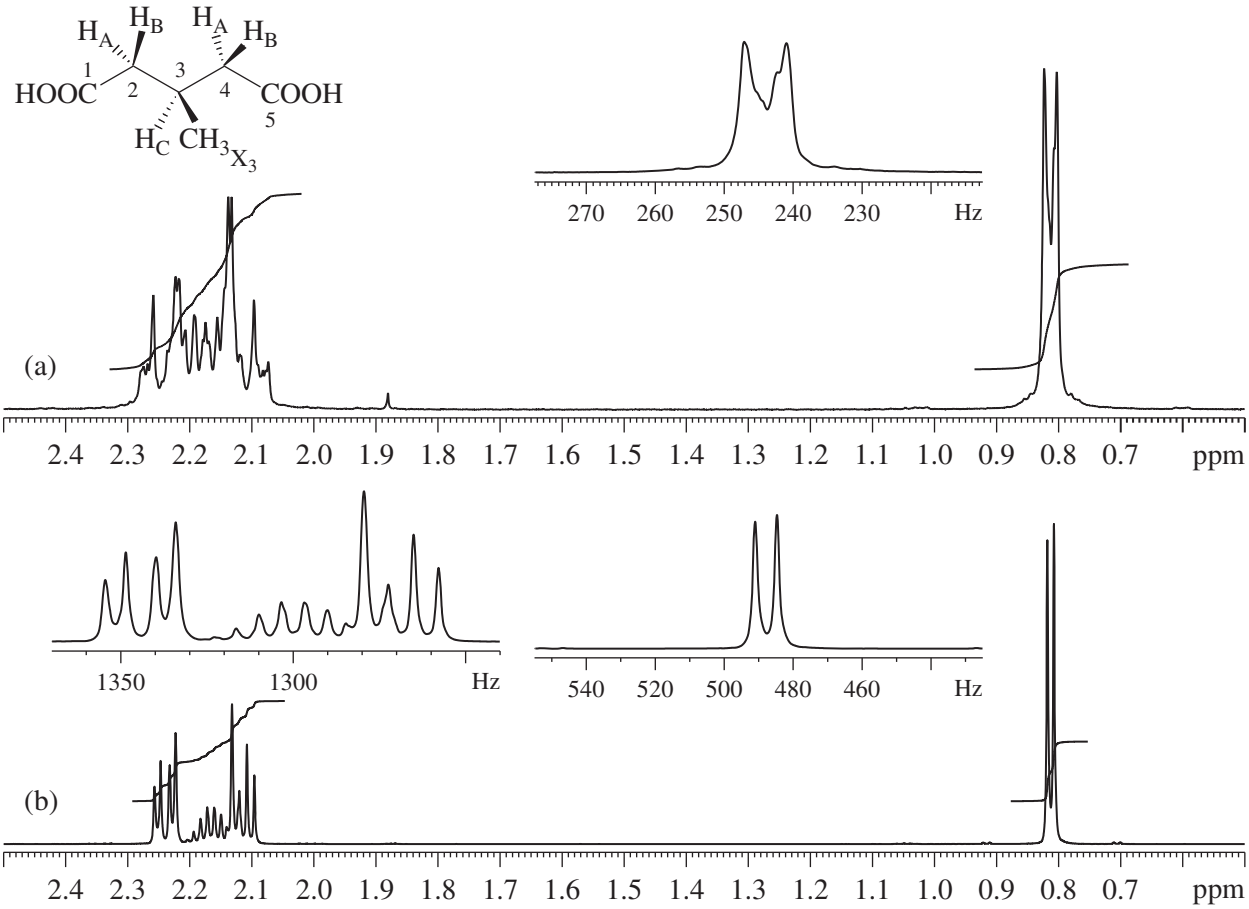

FIGURE 3.41 Proton NMR spectrum of 3-methylglutaric acid in D_2O (a) at 300 MHz and (b) at 600 MHz. The COOH proton exchanges with the D_2O and the corresponding NMR peak is not shown.

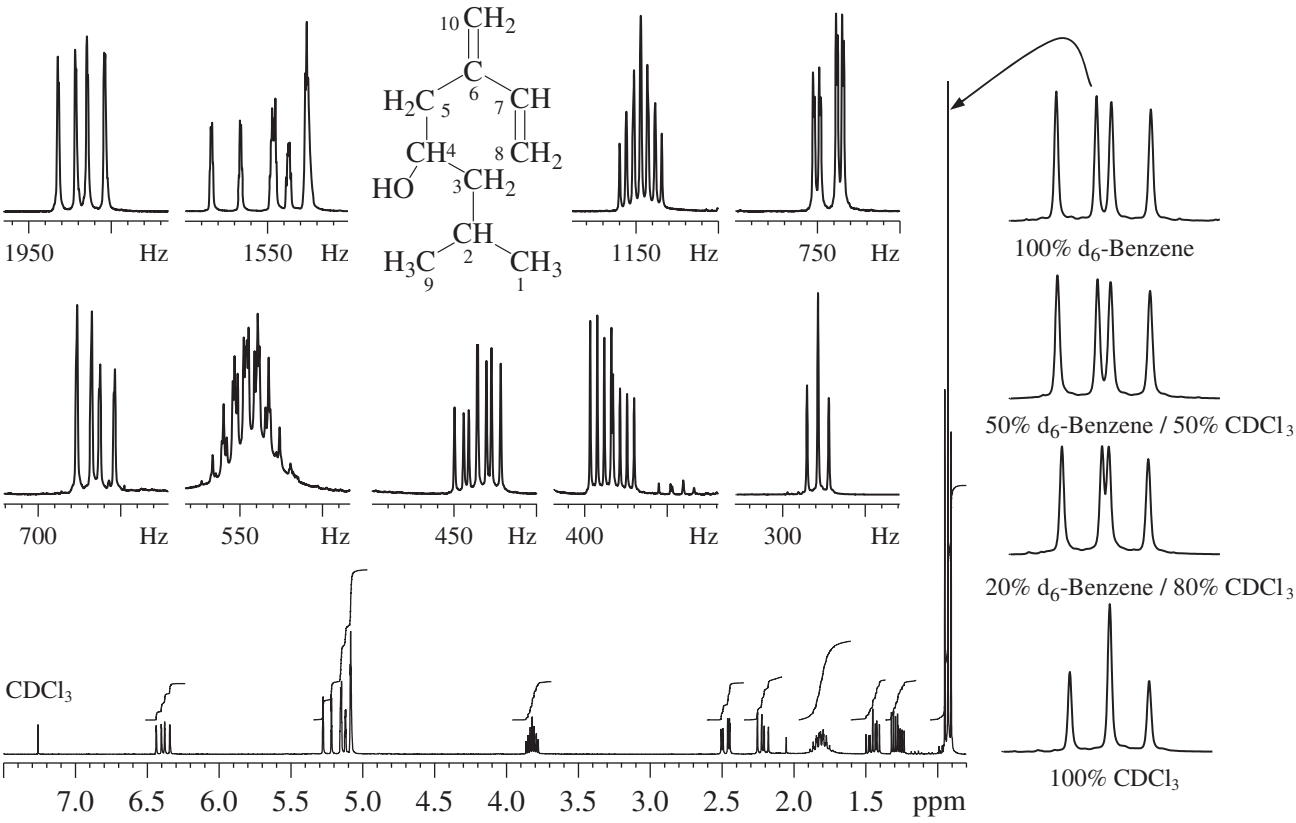

FIGURE 3.42 Proton NMR spectrum of 2-methyl-6-methylen-7-octen-4-ol (ipsenol) in $CDCl_3$ at 300 MHz and effect of titration with benzene. The sample was a gift from Phero Tech, Inc., Vancouver, BC, Canada.

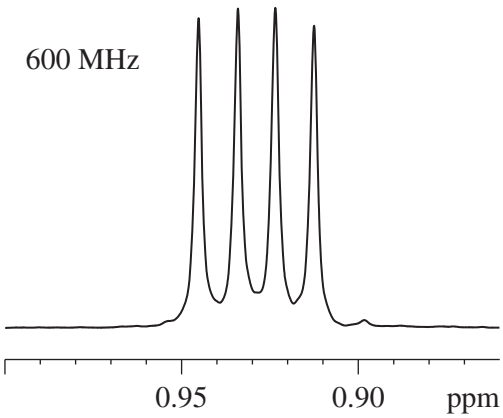

Note that the stereogenic center accounts for the fact that the protons of each of the two aliphatic methylene groups are also diastereotopic. As a result, the rather simple structure presents a challenge in assigning the spectrum.

The proton integration ratios from left to right are 1:4:1:1:1:2:1:1:6, which accounts for 18 protons in accord with the molecular formula $C_{10}H_{18}O$, but there are puzzling discrepancies. The six-proton step at 0.92 ppm in the integration represents the diastereotopic methyl protons described above, and the one-proton integration step at 3.82 ppm with several different coupling constants is a good choice for the C**H**OH proton (see Appendix A, Chart A.1). So far, so good. But there are four CH_2 groups in the structure and apparently only one in the integration ratios — and even this one is misleading.

It will help at this point to realize that the molecule consists of three spin systems with the insulation point at C-6 (see Section 3.5.2). The alkyl system consists of H-1, H-2, H-3, H-4, H-5, and H-9; an alkene system consists of H-7 and H-8; and another alkene system consists of H-10. The alkyl system accounts for the multiplets at the right of the spectrum, and the alkenes account for the multiplets at the left side. It will also help to reiterate that the protons of an alkyl CH_2 group will be diastereotopic in the presence of a stereogenic center. The protons of the alkene $=CH_2$ group will also be nonequivalent.

It should now be apparent that the diastereotopic protons of each alkyl CH_2 group occur as a pair. One pair (H-3) is at 1.28 ppm and 1.42 ppm; the other pair (H-5) is at 2.21 ppm and 2.48 ppm. The two-proton multiplet at 1.80 ppm will be discussed later.

Furthermore, the H-5 protons are at higher frequency because they are deshielded by both the OH group and the $C=CH_2$ group, whereas the H-3 protons are deshielded only by the OH group. The H-5 protons couple geminally and each proton couples once vicinally; thus there is a doublet of doublets (first order) for each C-5 proton. The H-3 protons couple geminally and vicinally to two protons; the result for the H-3 protons (at 300 MHz) is two complex multiplets. Also in favor of the first-order status for the H-5 protons is a larger $\Delta\nu$ value (in Hz) between the two H-5 multiplets.

The mysterious multiplet at 1.80 ppm may now be identified by default as the highly coupled H-2 proton superimposed on the OH peak, which could be confirmed by heating, by a solvent change, or by shaking the solution with D_2O to remove it (see Section 3.6.1.1). Dilution moves it to a lower frequency. The very small peak at about 2.05 ppm is an impurity.

Predictably, the H-7 alkene proton is at the high frequency end of the spectrum. It couples *trans* (J = 18 Hz) and *cis* (J = 10.5 Hz) across the double bond to the H-8 protons to give a doublet of doublets (see Appendix F).

The peaks between about 1585 Hz and 1525 Hz are due to both the H-8 and H-10 protons. At the left side, there is an 18 Hz doublet representing one of the H-8 protons coupled *trans* across the double bond to H-7. These doublet peaks are at 1585 Hz and 1567 Hz.

At 1546 Hz and 1525 Hz are the two individual peaks (not a doublet) of the H-10 protons. The very small geminal coupling results in slight broadening; the jagged edges are evidence of some long-range coupling. Note that the height of the right-hand peak is suspicious.

Having determined the *trans* coupling of one of the H-8 protons, we search for the corresponding doublet of the *cis* coupling. Unfortunately, we seem to be left with only a singlet at about 1538 Hz but quickly assume that the missing peak is buried under the suspiciously large peak at the right edge. Examination at 600 MHz of these diene spin systems clearly shows the (H-8) 10.5 Hz doublet, appropriate for the *cis* coupling, and justifies the above conclusions. The proton NMR spectrum of ipsenol is difficult (though not impossible) to fully understand and assign for us at this point. It is heartening to know that the interpretation becomes much easier with correlation methods that are explained in detail in Chapter 5.

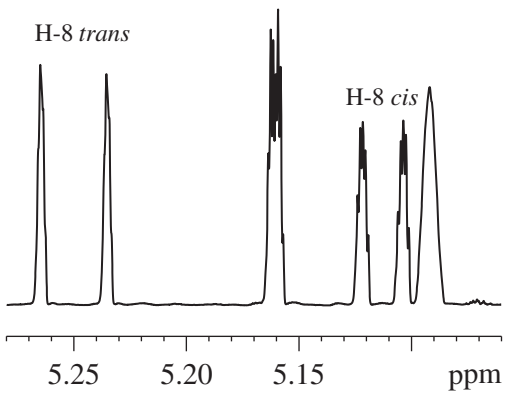

3.13 MAGNITUDE OF VICINAL AND GEMINAL COUPLING CONSTANTS

Coupling between protons on vicinal carbon atoms depends primarily on the dihedral angle ϕ between the H—C—C′ and the C—C′—H′ planes. This angle can be visualized by an end-on view (Newman projection) of the bond between the vicinal carbon atoms and by the perspective in Figure 3.43 in which the relationship between dihedral angle and vicinal coupling constant is graphed.

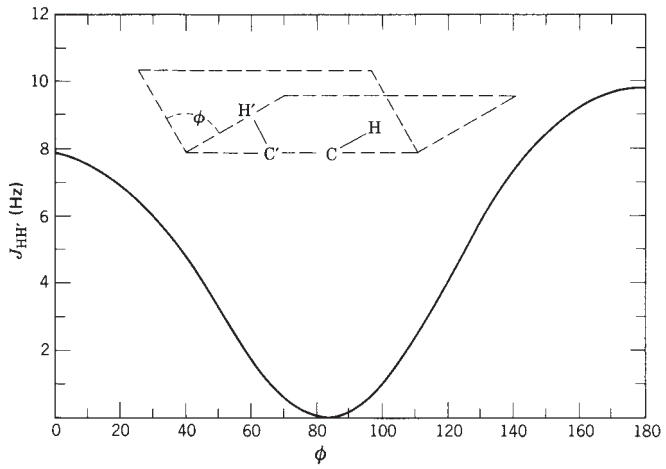

FIGURE 3.43 The vicinal Karplus correlation. Relationship between dihedral angle (ϕ) and coupling constant for vicinal protons.

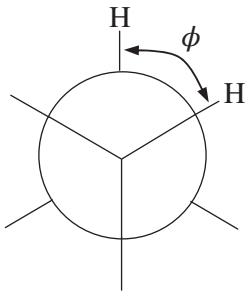

Karplus* emphasized that his calculations are approximations and do not take into account factors such as electronegative substituents, the bond angles θ (<H—C—C′ and the <C—C′—H′), and bond lengths. Deductions of dihedral angles from measured coupling constants are safely made only by comparison with closely related compounds. The correlation has been very useful in cyclopentanes, cyclohexanes, carbohydrates, and polycyclic systems. In cyclopentanes, the observed values of about 8 Hz for vicinal *cis* protons and about 0 Hz for vicinal *trans* protons are in accord with the corresponding angles of about 0° and about 90°, respectively. In substituted cyclohexane or pyranose rings, the chair is the preferred conformation; the following relations in Table 3.6 hold and dihedral angles of substituents follow from these ^3J proton couplings.

Note the near-zero coupling at the 90° dihedral angle. This has been a source of frustration in attempts at fitting proposed structures to the NMR spectra.

A modified Karplus correlation can be applied to vicinal coupling in alkenes. The prediction of a larger *trans* coupling ($\phi = 180°$) than *cis* coupling ($\phi = 0°$) is borne out. The *cis* coupling in unsaturated rings decreases with decreasing ring size (increasing bond angle) as follows: cyclohexenes $^3J = 8.8$ to 10.5 Hz, cyclopentenes $^3J = 5.1$ to 7.0 Hz, cyclobutenes $^3J = 2.5$ Hz to 4.0 Hz, and cyclopropenes $^3J = 0.5$ Hz to 2.0 Hz.

*Karplus, M. (1959) *J. Chem. Phys.*, **30**, 11.

TABLE 3.6 Calculated and Observed Coupling Constants, J, in Cyclohexanes Based on Dihedral Angle

	Dihedral Angle	Calculated J (Hz)	Observed J (Hz)
Axial–axial	180°	9	8 – 14 (usually 8 – 10)
Axial–equatorial	60°	1.8	1 – 7 (usually 2 – 3)
Equatorial–equatorial	60°	1.8	1 – 7 (usually 2 – 3)

Two-bond geminal CH_2 coupling depends on the H—C—H bond angle θ as shown in Figure 3.44. This relationship is quite susceptible to other influences and should be used with due caution. However, it is useful for characterizing methylene groups in a fused cyclohexane ring (approximately tetrahedral, $^2J \sim 12$ Hz to 18 Hz), methylene groups of a cyclopropane ring ($^2J \sim 5$ Hz), or a terminal methylene group, that is, $=CH_2$, ($^2J \sim 0$ Hz to 3 Hz). Electronegative substituents reduce the geminal coupling constant, whereas sp^2 or sp hybridized carbon atoms increase it.

Geminal coupling constants are usually negative in sign, but this can be ignored except for calculations. Note that geminal couplings are seen in routine spectra only when the methylene protons are diastereotopic.

In view of the many factors other than angle dependence that influence coupling constants, it is not surprising that there have been abuses of the Karplus correlation. Attempts to precisely determine angles directly from the magnitude of the ^2J value are risky.

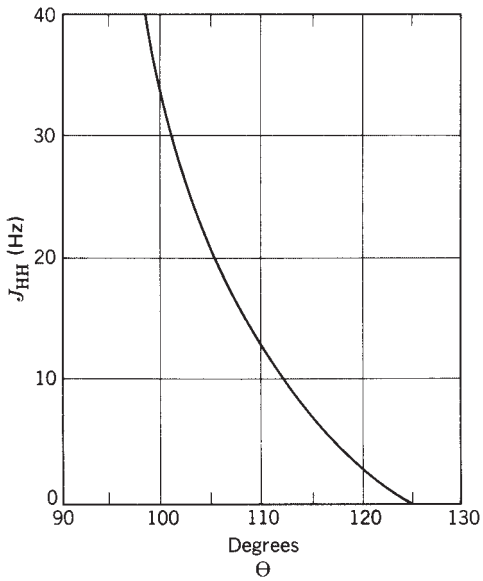

FIGURE 3.44 The geminal Karplus correlation. J_{HH} for CH_2 groups as a function of the H—C—H angle. Note the zero coupling at about 125°.

3.14 LONG-RANGE COUPLING

Proton–proton coupling beyond three bonds (^3J) is usually less than 1 Hz, but appreciable long-range coupling may occur in such rigid structures as alkenes, alkynes, aromatics, and heteroaromatics, and in strained ring systems (small or bridged). Allylic (H—C—C═C—H) couplings are typically about 1.6 Hz. The coupling through five bonds in the conjugated system of butadiene is 1.3 Hz. Coupling through conjugated polyalkyne chains may occur through as many as nine bonds. *Meta* coupling in a benzene ring is 1 Hz to 3 Hz, and *para*, 0 Hz to 1 Hz. In five-membered heteroaromatic rings, coupling between the two and four protons is 0 Hz to 2 Hz. $^4J_{AB}$ in the bicyclo[2.1.1]hexane system is about 7 Hz.

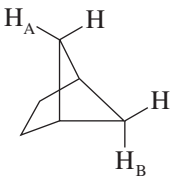

This unusually high long-range coupling constant is attributed to the "W" conformation of the four σ bonds between H_A and H_B.

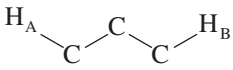

Long-range W coupling

3.15 SELECTIVE SPIN DECOUPLING: DOUBLE RESONANCE

Intense irradiation of a proton (or equivalent protons) at its resonance frequency in a spin-coupled system removes the proton's coupling effect on the neighboring protons to which it has been coupled. Thus, successive irradiation of the protons of 1-propanol, for example, yields the following results:

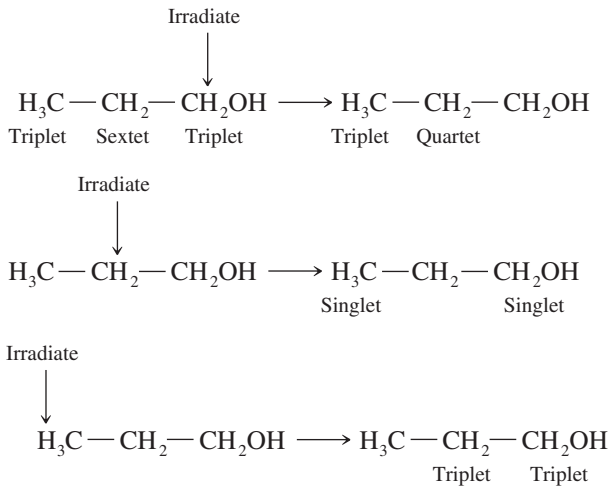

Here, we have a powerful tool for determining the connectivity of protons through bonds and assigning proton peaks. Furthermore, overlapping peaks can be simplified by removing one of the couplings.

Figure 3.45 displays the effect of selective spin decoupling on the neighboring protons of 3-butyne-l-ol.

In spectrum 3.45a from left to right, the H-1 multiplet is a triplet (J = 6 Hz); the H-2 multiplet is a triplet of doublets (J = 6 Hz and 3 Hz); and the H-4 multiplet is a triplet (J = 3 Hz). The OH singlet is at 2.03 ppm. Again from left to right, the integration ratios of the multiplets are 2:2:1:1 (not shown).

In spectrum (b), the H-1 protons are irradiated, and the H-2 triplet of doublets is collapsed to a doublet (J = 3 Hz). This doublet results from long-range coupling with H-4. In spectrum (c), the H-2 triplet of doublets is irradiated, and the H-1 triplet is collapsed to a singlet, and the H-4 is collapsed to a singlet.

In spectrum (d), the H-4 triplet is irradiated, and the H-2 triplet of doublets is collapsed to a triplet (J = 6 Hz).

The overall information obtained from selective spin decoupling is "connectivity" – that is, progressing through the protons of the carbon chain.

It is also possible to simplify two overlapping multiplets by selectively irradiating a neighboring proton, thus disclosing multiplicity and coupling constants in the residual multiplet.

Other methods for establishing ^{1}H—^{1}H relationships are described in Chapter 5 and have certain advantages, although selective spin decoupling methods remain useful.

3.16 NUCLEAR OVERHAUSER EFFECT

The nuclear Overhauser effect (NOE) results from a type of nuclear spin relaxation, involving pairs of spins, called cross-relaxation. The technical details of how the NOE works are beyond the scope of our discussion, but we will see briefly here and in Chapter 4 various applications of the NOE to solving structural problems with NMR. We focus here on the ^{1}H—^{1}H NOE: this is a through-space effect which decreases with the sixth power of the distance between the spins. No intervening chemical bonds or J-coupling between the protons are required; instead, the NOE relies on a dipolar interaction between the spins. One of the useful applications of the NOE is therefore to determine which protons are close in space to which other protons (typically up to ~4 Å). The NOE can be observed by irradiating a peak corresponding to a particular proton in the sample with lower power radiation than is used for decoupling. The NMR peak of a proton that is close in space to the irradiated proton is increased in intensity; this is one manifestation of the NOE. (This is generally true for small molecules; for large molecules such as proteins, the signal may decrease instead of increase.) The usual observable enhancement is less than 20%. To increase sensitivity, we use the NOE *difference* experiment, in which a conventional ^{1}H NMR spectrum is subtracted from a specific

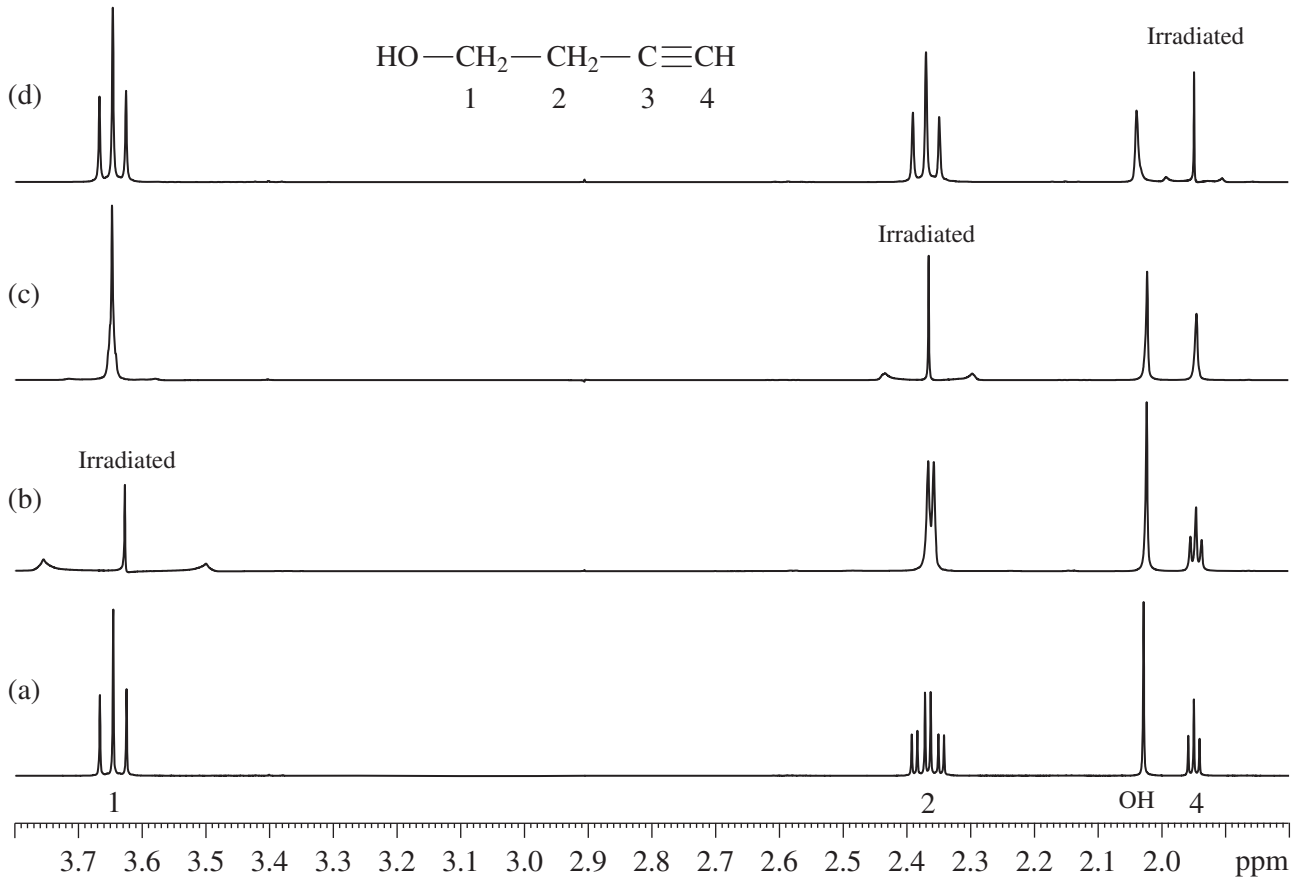

FIGURE 3.45 (a) 300 MHz ^{1}H NMR spectrum of 3-butyn-l-ol in $CDCl_3$. (b) Irradiated protons on C-1. (c) Irradiated protons on C-2. (d) Irradiated protons on C-4. Irradiation may cause a small change in chemical shift of nearby peaks.

proton-irradiated spectrum. The result is a spectrum which only contains the peaks which have been enhanced due to the NOE, that is, it will only show peaks due to protons which are close in space to the protons which have been irradiated.

Consider the example given in Figure 3.46 [see also Charlton et al. (1993)]. The compound is an analog of a sex pheromone natural product of the brownbanded cockroach.

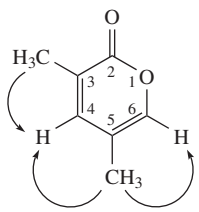

Note that in Figure 3.46, the regular ^{1}H NMR spectrum is shown in (c). Figure 3.46b shows the NOE difference spectrum obtained upon irradiating the peak corresponding to the 3-methyl protons, and Figure 3.46c shows the NOE difference spectrum obtained upon irradiating the peak corresponding to the 5-methyl protons. Recall that peaks which remain in the difference spectra indicate that the corresponding protons are close in space to the protons which have been irradiated. Thus, we see that irradiation of the 5-methyl group results in enhancement of the resonances for both H-4 and H-6, whereas irradiation of the 3-methyl group enhances only the peak for H-4. The 5-methyl group is close to both H-4 and H-6 whereas the 3-methyl group is only close to H-4.

3.17 CONCLUSION

^{1}H NMR spectroscopy is the foundation upon which we will build an understanding of the magnetic resonance of other nuclei, especially ^{13}C, which leads to the important advanced correlation experiments. We began by describing the magnetic properties of nuclei, noting the special importance of spin $\frac{1}{2}$ nuclei. For practical reasons, the historical investigations into the ^{1}H nucleus led to high-resolution NMR and the manufacture of commercial instruments.

Interpretation of ^{1}H NMR spectra is based on consideration of three types of information: integration of signal peaks, chemical shifts, and spin–spin coupling constants. Integration of the signal peaks provides the ratios between the numbers of hydrogen atoms in different equivalent sets in the compound. The concept of chemical shift

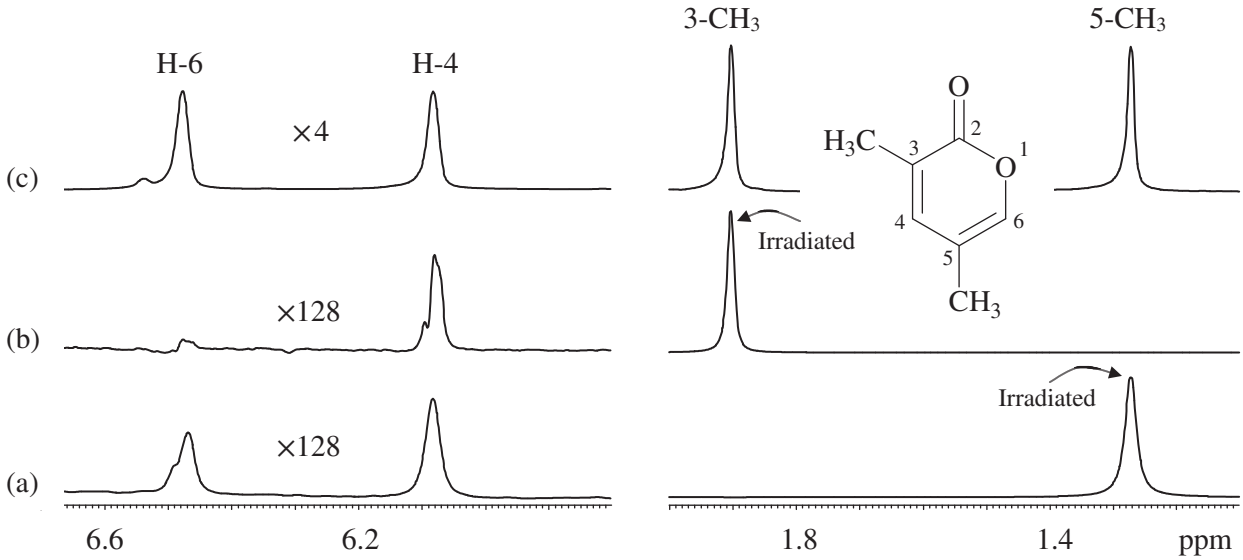

FIGURE 3.46 NOE difference spectroscopy for the compound shown. (a) Enhancement of both protons on irradiation of the 5-methyl group. (b) Enhancement of the H-4 proton on irradiation of the 3-methyl group. (c) The full ^{1}H NMR spectrum. 300 MHz in $CDCl_3$.

relates the frequency of the signal in the spectrum with the chemical environment. Spin–spin coupling explains the interaction of magnetic nuclei within a spin system. Among other things, spin–spin coupling provides information about neighboring nuclei, giving crucial structural insights. The remaining chapters all deal with NMR either entirely (Chapters 4, 5, and 6) or in major part (Chapters 7 and 8).

REFERENCES

For a list of Chapter References, please visit: www.wiley.com/college/silverstein.

STUDENT EXERCISES

3.1 For each compound given below (a–o), describe all spin systems (using Pople notation where appropriate) Label chemically equivalent protons, magnetically equivalent protons, enantiotopic protons, and diastereotopic protons.

3.2 For each compound above, predict the chemical shifts for each proton set. Give the source (table or appendix) that you use for your prediction.

3.3 Sketch the ^{1}H NMR spectrum for each of the compounds in question 3.1. Assume first-order multiplets where possible.

3.4 Determine the structural formula for the compounds whose ^{1}H NMR spectra are given (A – W). They were all run at 300 MHz in $CDCl_3$. The mass spectra were given in Chapter 1 (Question 1.6) and the IR spectra were given in Chapter 2 (Question 2.9).

3.5 After determining the structures in exercise 3.4, calculate $\Delta\nu/J$ for appropriately coupled multiplets where possible in the following spectra: A, E, F, G, H, I, K, L, Q, and U. Use a ruler to measure or estimate J-coupling constants.

3.6 For each structure determined in exercise 3.4, describe all spin systems (using Pople notation where appropriate). Label chemically equivalent protons, magnetically equivalent protons, enantiotopic protons, and diastereotopic protons.

3.7 Sketch spectra for the following spin systems (stick diagrams are sufficient): AX, A_2X, A_3X, A_2X_2, A_3X_2.

3.8 Sketch spectra for the following spin systems (stick diagrams are sufficient): AMX, A_2MX, A_3MX, A_2MX_2, A_2MX_3, A_3MX_3. Assume that A does not couple to X and that $J_{AM} = J_{MX}$.

3.9 Sketch spectra for the following spin systems (stick diagrams are sufficient): AMX, A_2MX, A_3MX, A_2MX_2, A_2MX_3, A_3MX_3. Assume that A does not couple to X, and that $J_{AM} = 10$ Hz and $J_{MX} = 5$ Hz.

3.10 For the following three simulated spin systems (at 300 MHz; see pages 172–174), draw a stick diagram for each first-order multiplet in each spin system. After determining one multiplet in each spin system, the other two multiplets will be useful checks.

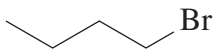

a

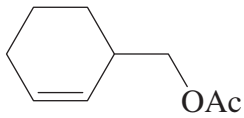

b

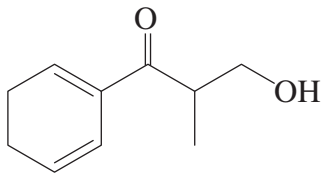

c

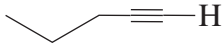

d

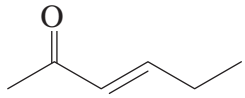

e

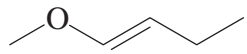

f

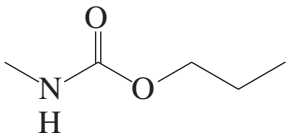

g

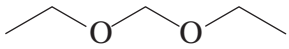

h

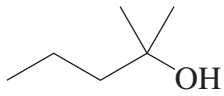

i

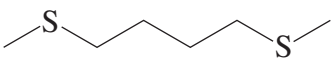

j

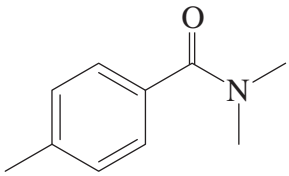

k

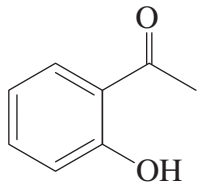

l

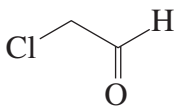

m

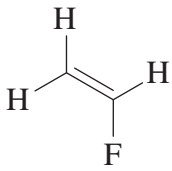

n

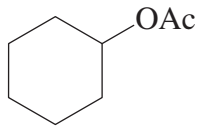

o

Problem 3.4 A

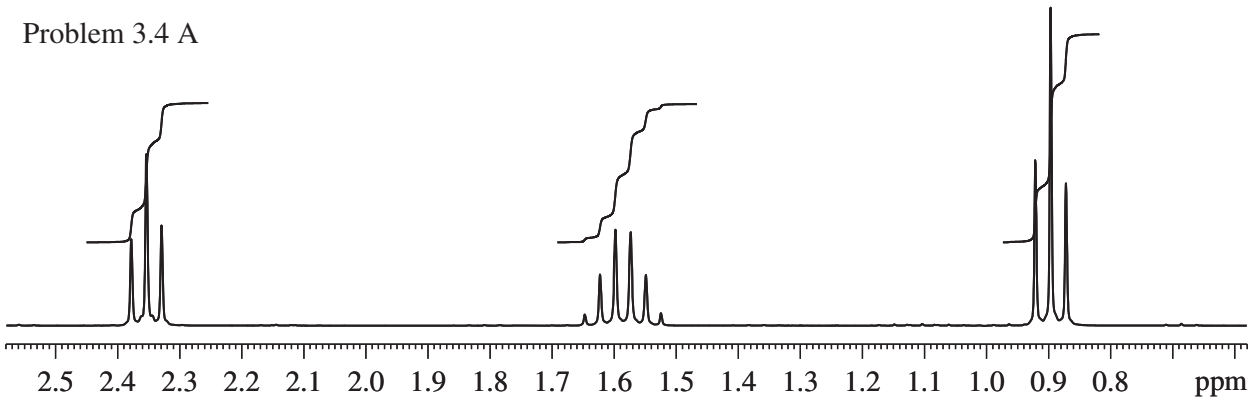

Problem 3.4 B

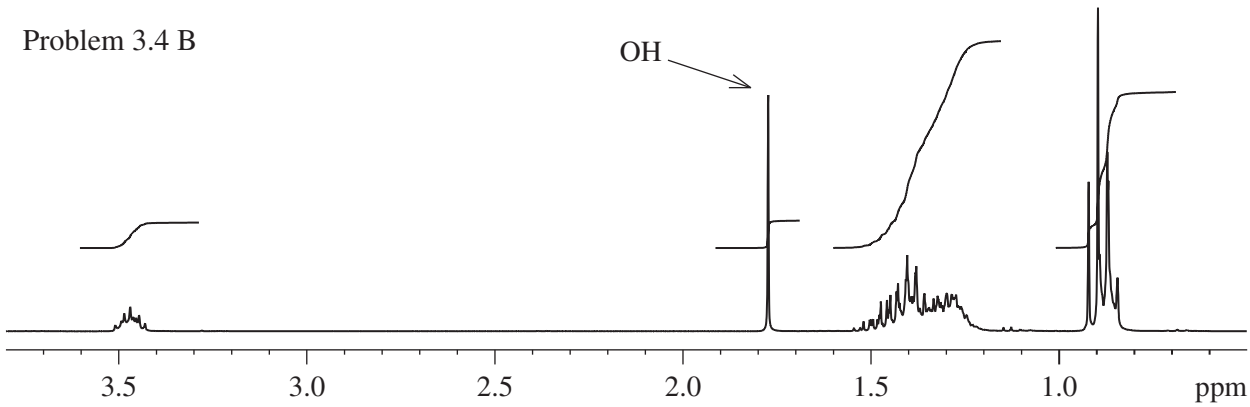

Problem 3.4 C

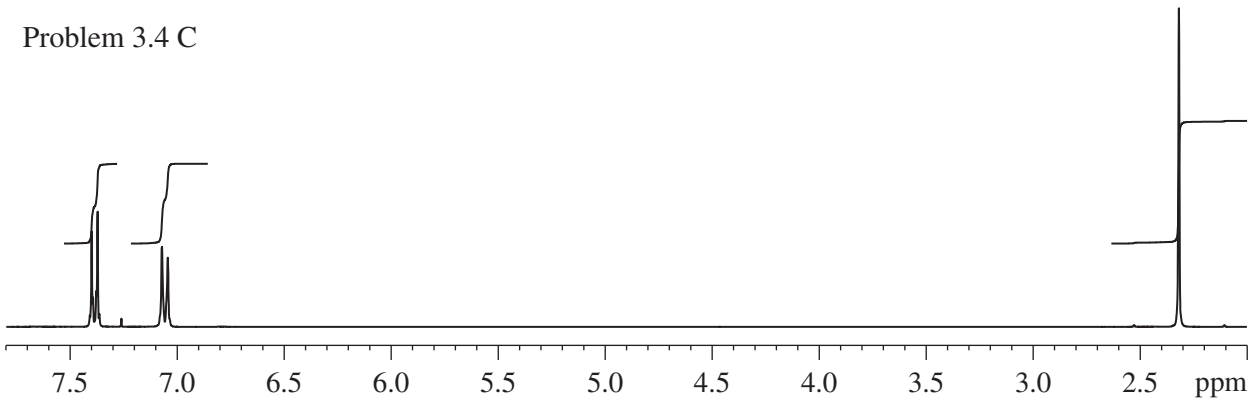

Problem 3.4 D

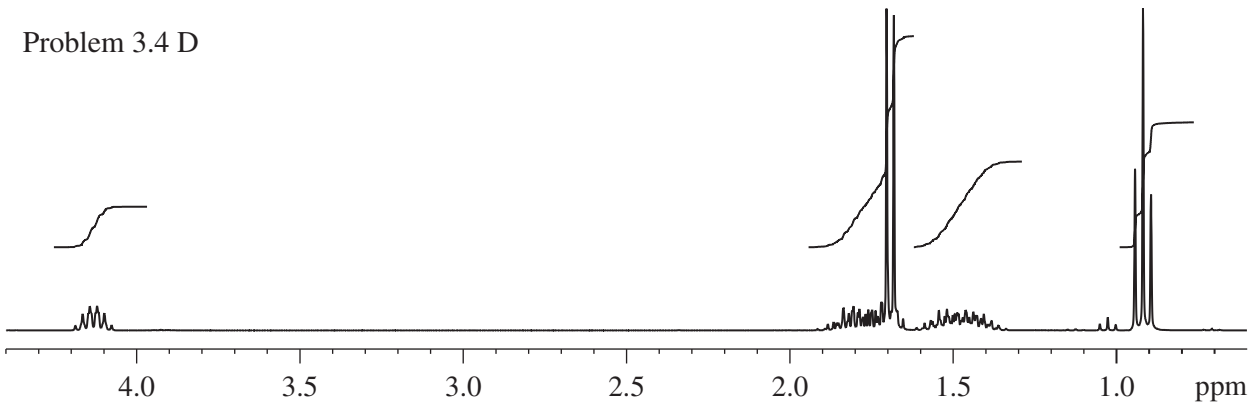

Problem 3.4 E

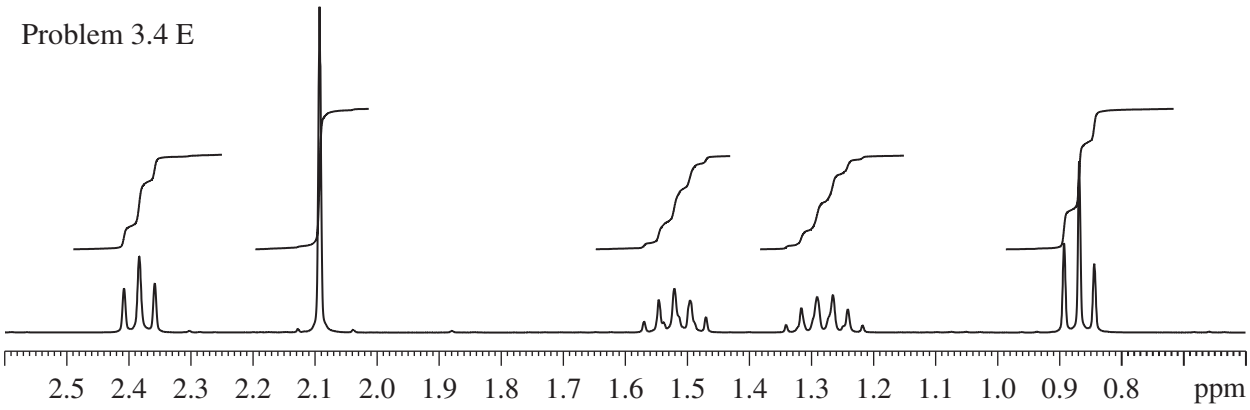

Problem 3.4 F

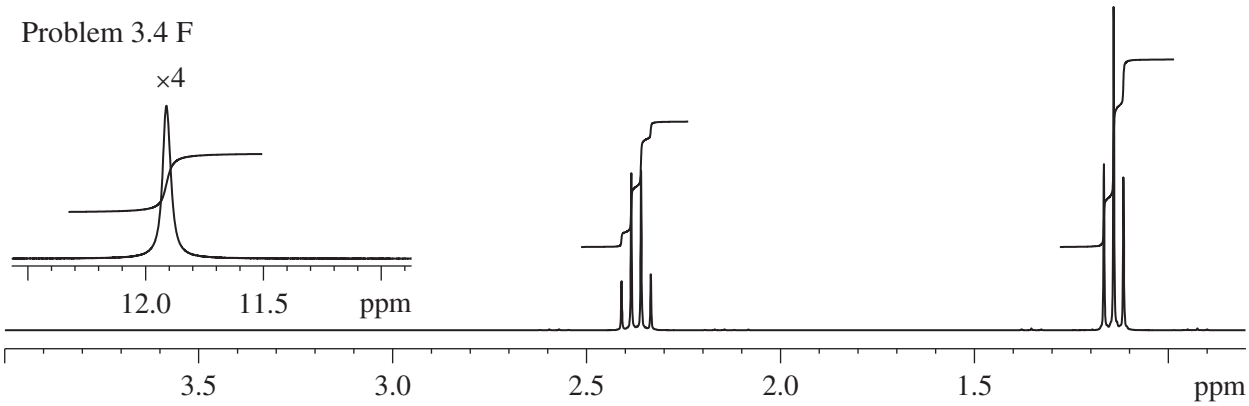

Problem 3.4 G

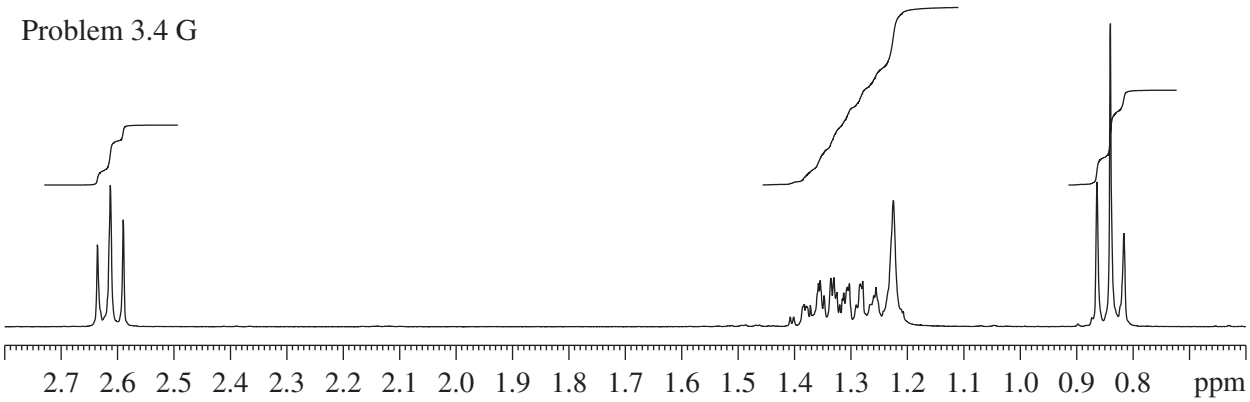

Problem 33.4 H

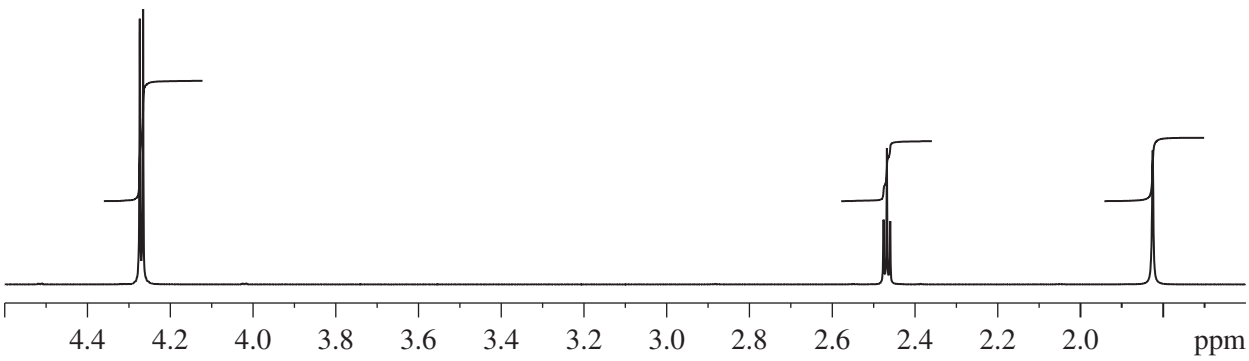

Problem 3.4 I

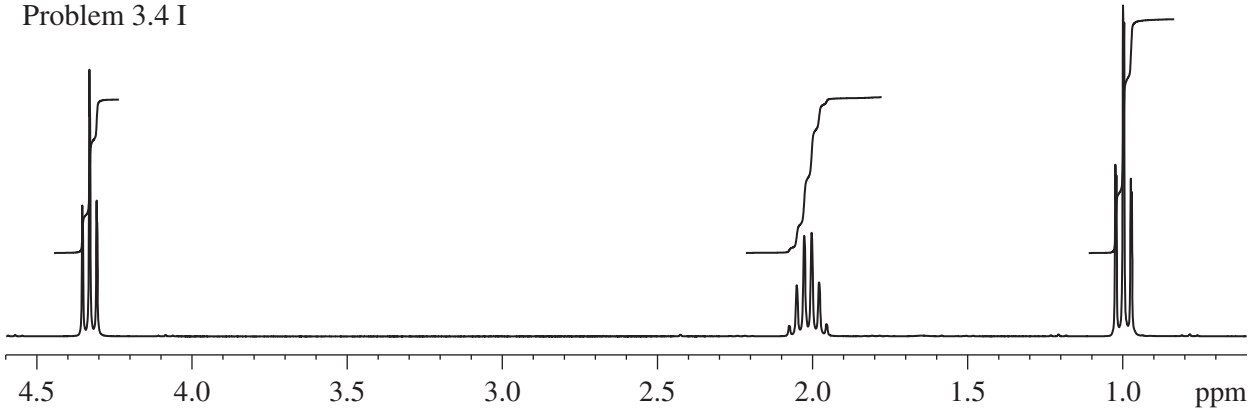

Problem 3.4 J

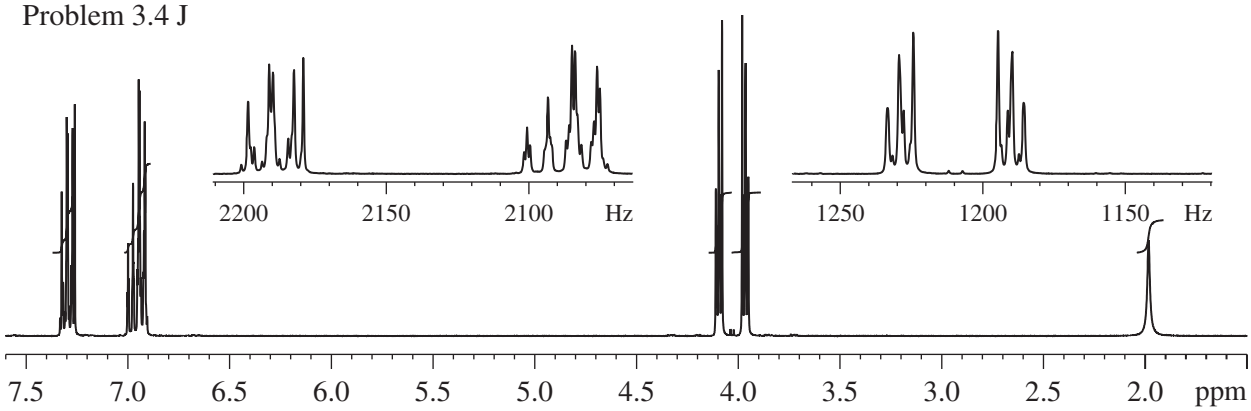

Problem 3.4 K

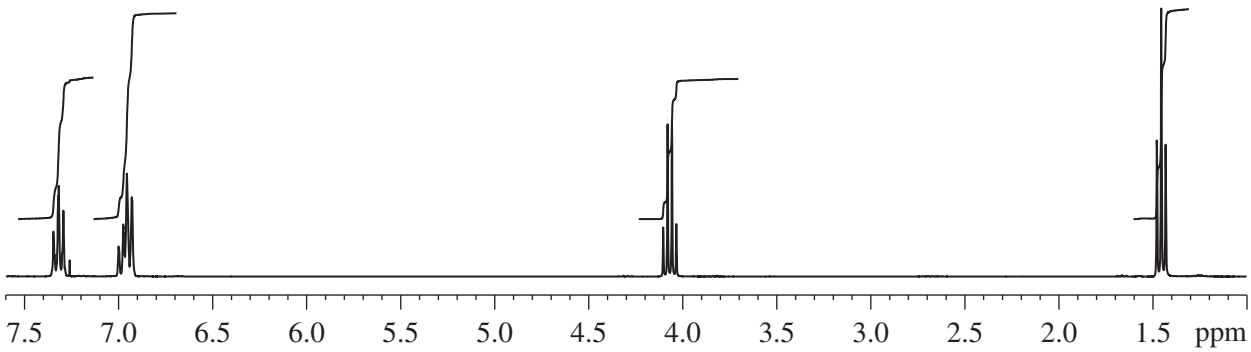

Problem 3.4 L

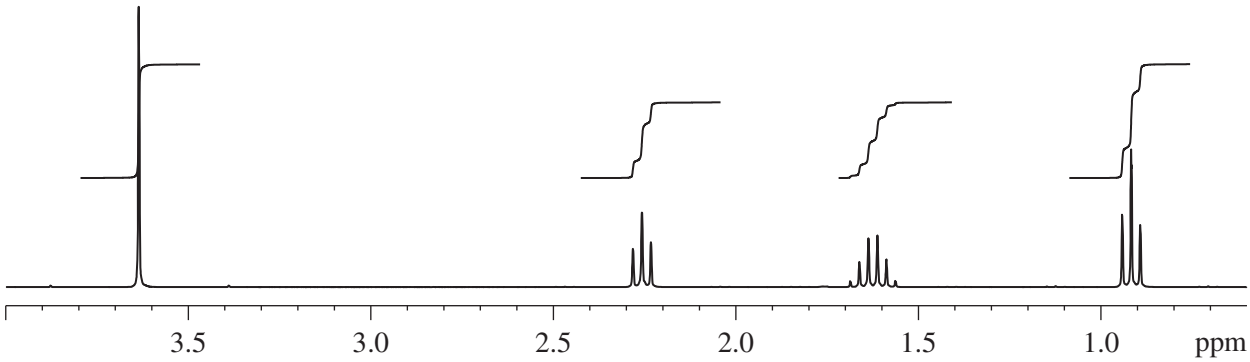

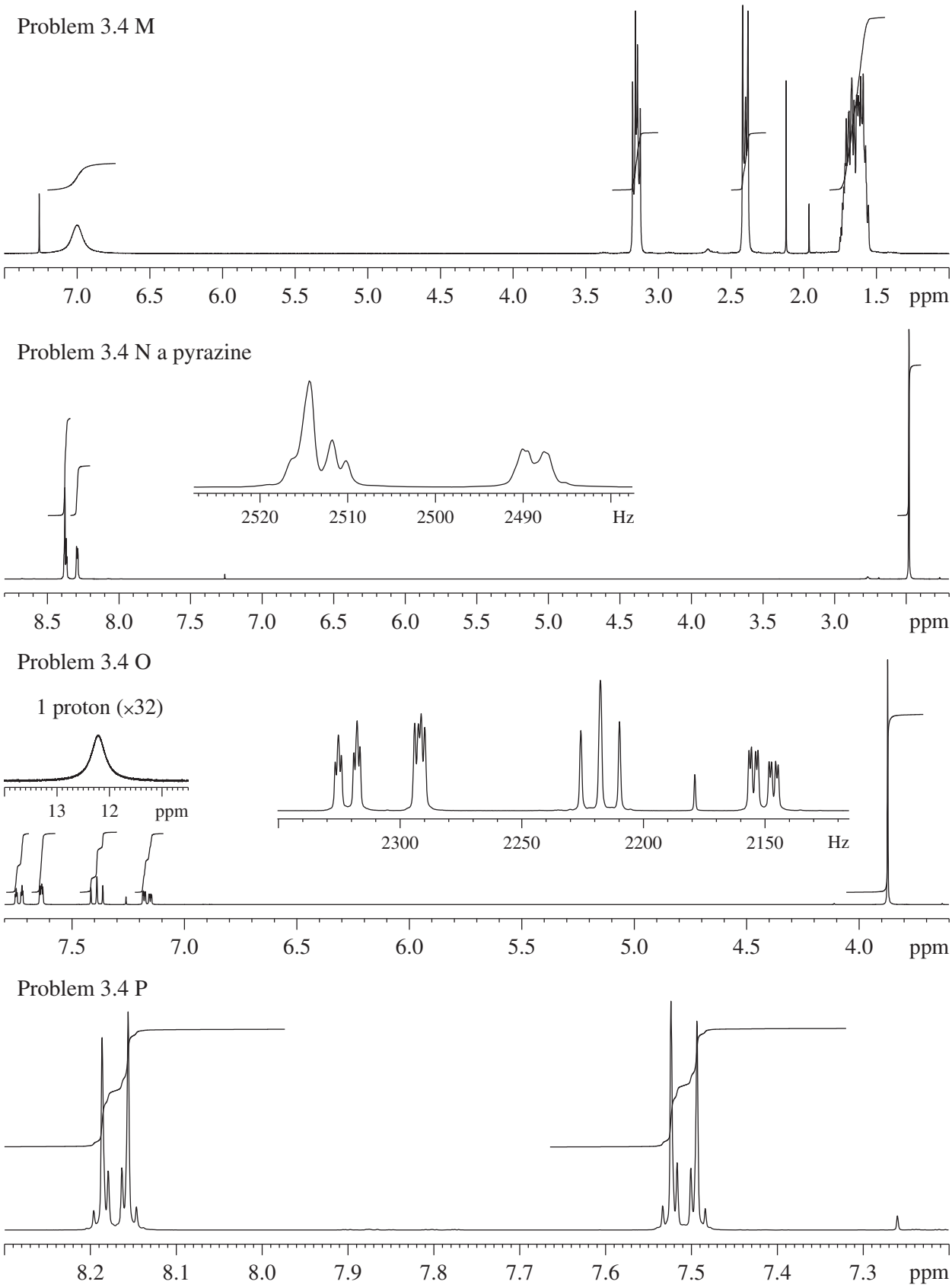
Problem 3.4 M
7.0 6.5 6.0 5.5 5.0 4.5 4.0 3.5 3.0 2.5 2.0 1.5 ppm
Problem 3.4 N a pyrazine
2520 2510 2500 2490 Hz
8.5 8.0 7.5 7.0 6.5 6.0 5.5 5.0 4.5 4.0 3.5 3.0 ppm
Problem 3.4 O
1 proton (×32)
13 12 ppm
2300 2250 2200 2150 Hz
7.5 7.0 6.5 6.0 5.5 5.0 4.5 4.0 ppm
Problem 3.4 P
8.2 8.1 8.0 7.9 7.8 7.7 7.6 7.5 7.4 7.3 ppm

Problem 3.4 Q

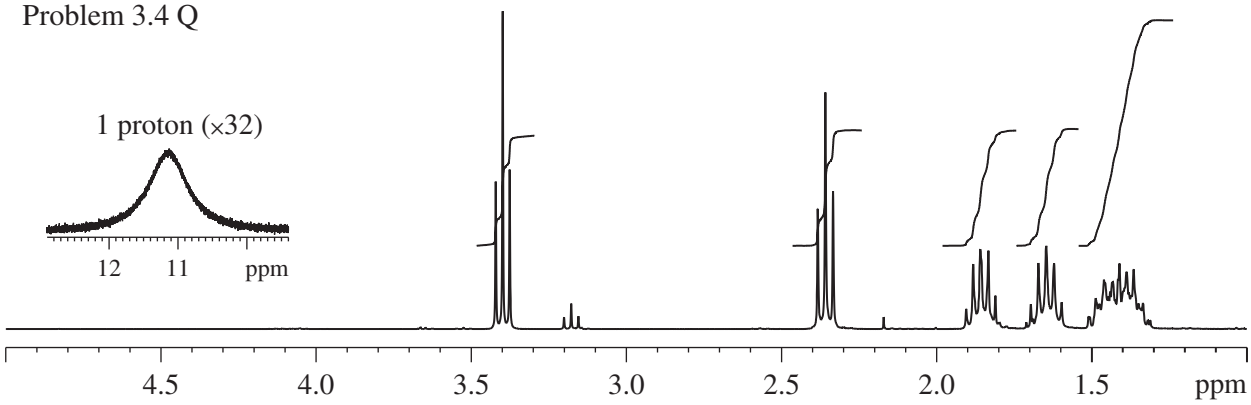

Problem 3.4 R

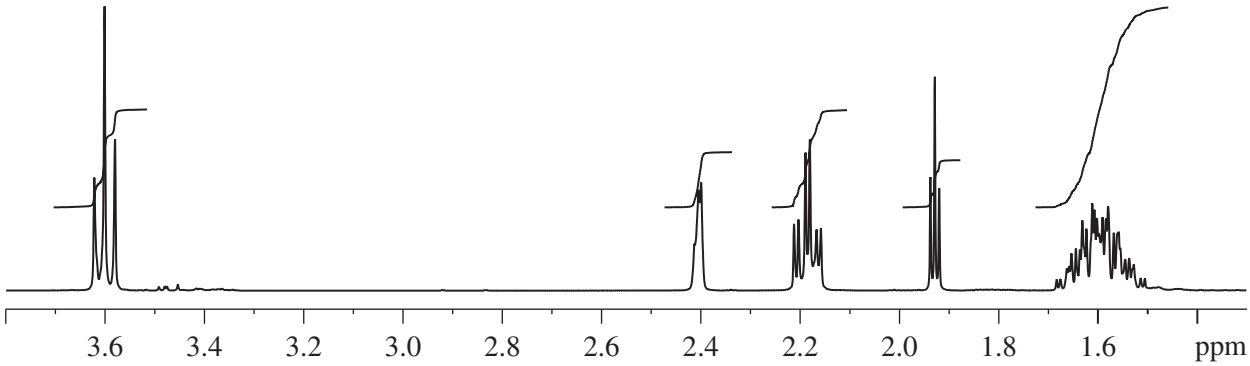

Problem 3.4 S Unsaturated ketone

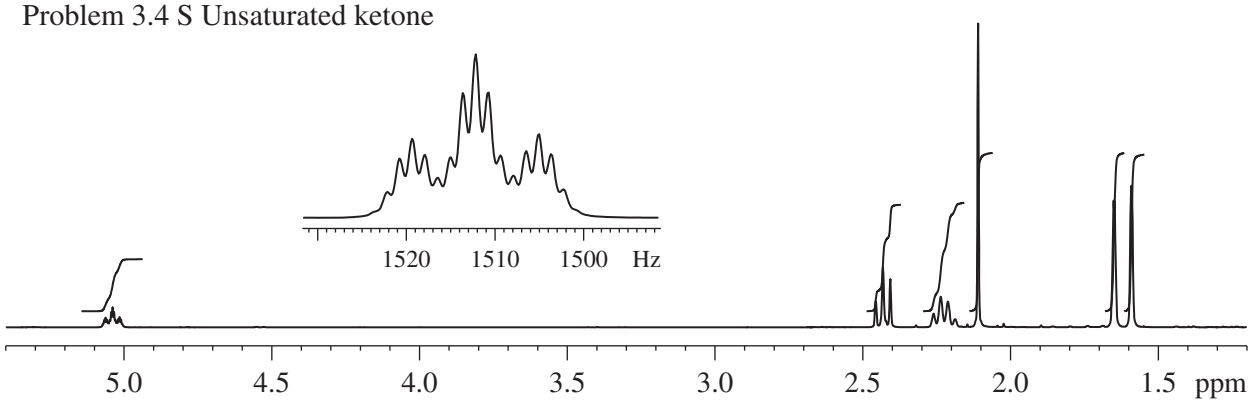

Problem 3.4 T

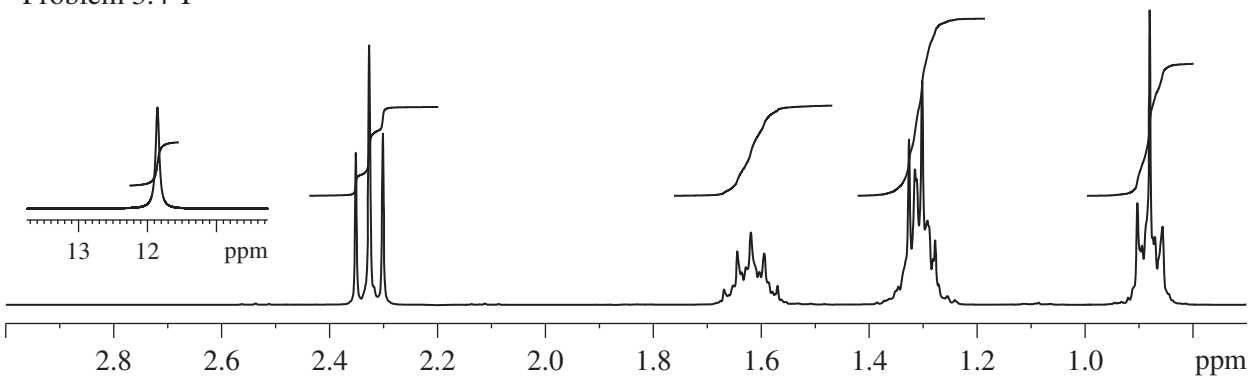

Problem 3.4 U

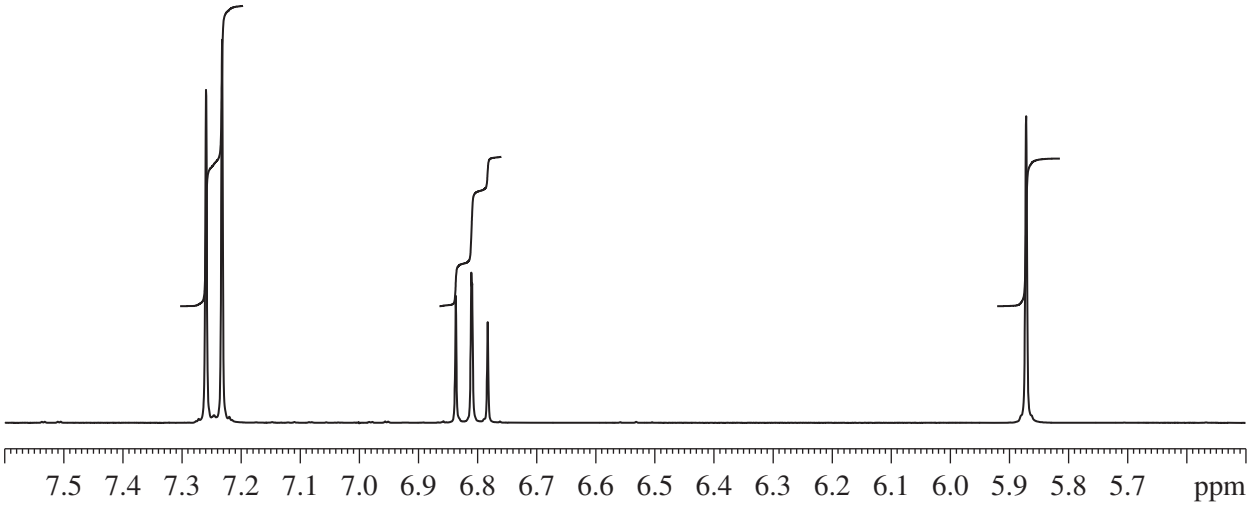

Problem 3.4 V

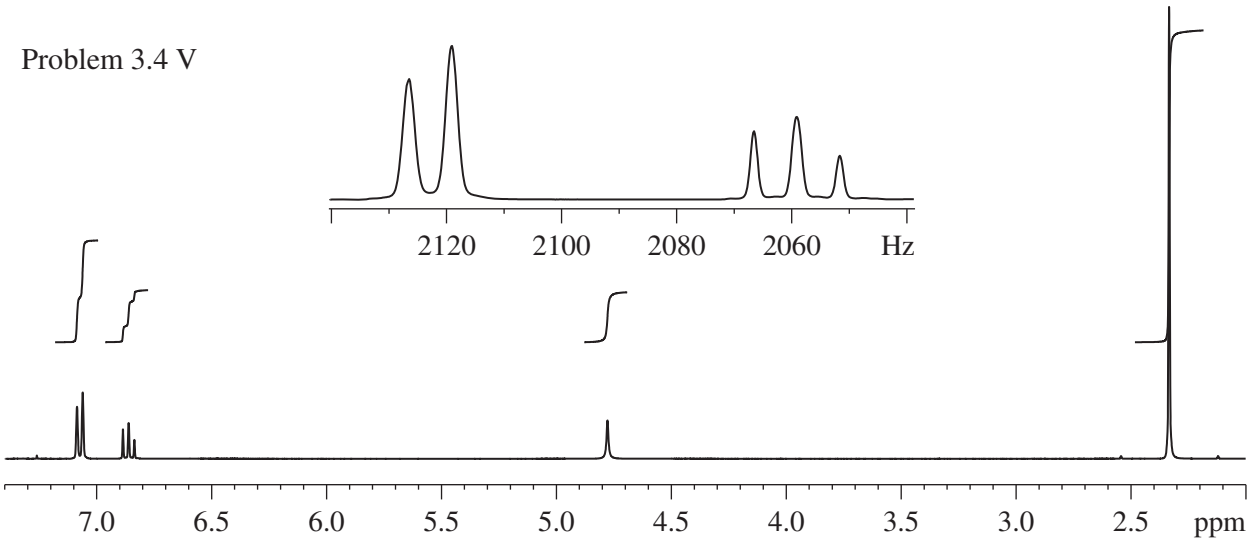

Problem 3.4 W Unsaturated ketone

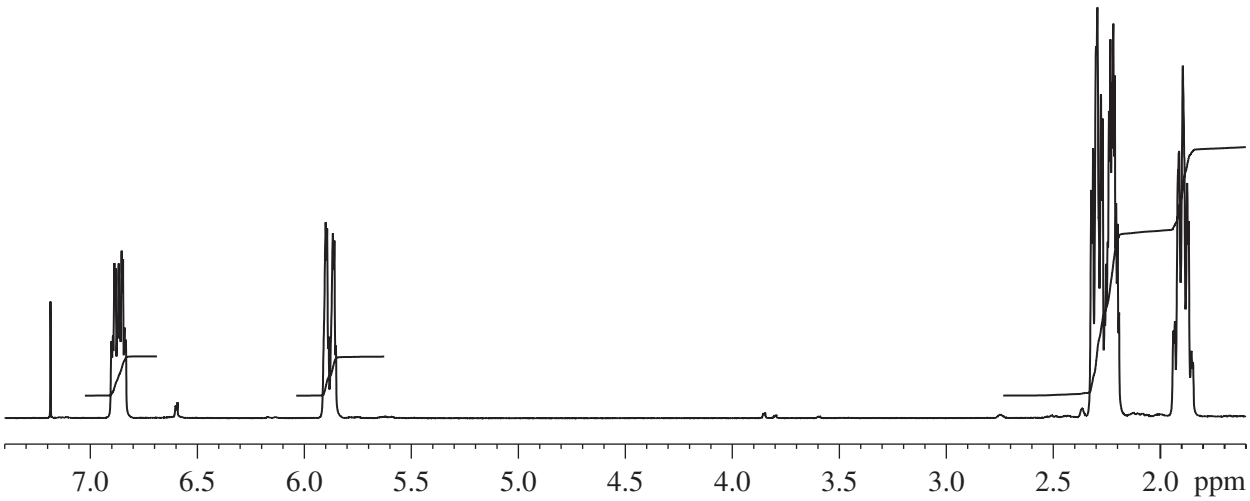

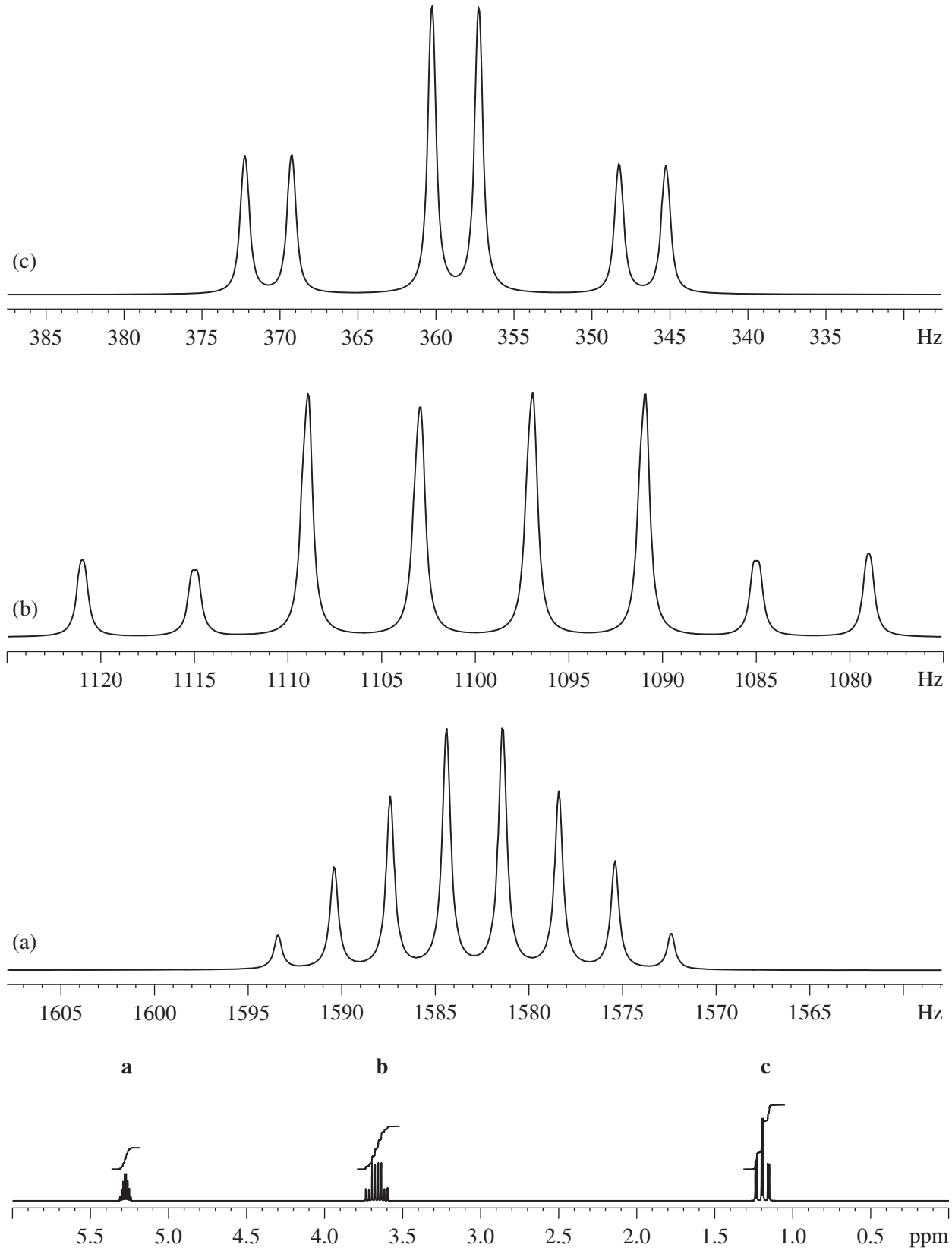
(c)
385 380 375 370 365 360 355 350 345 340 335 Hz
(b)
1120 1115 1110 1105 1100 1095 1090 1085 1080 Hz
(a)
1605 1600 1595 1590 1585 1580 1575 1570 1565 Hz
a
b
c
5.5 5.0 4.5 4.0 3.5 3.0 2.5 2.0 1.5 1.0 0.5 ppm

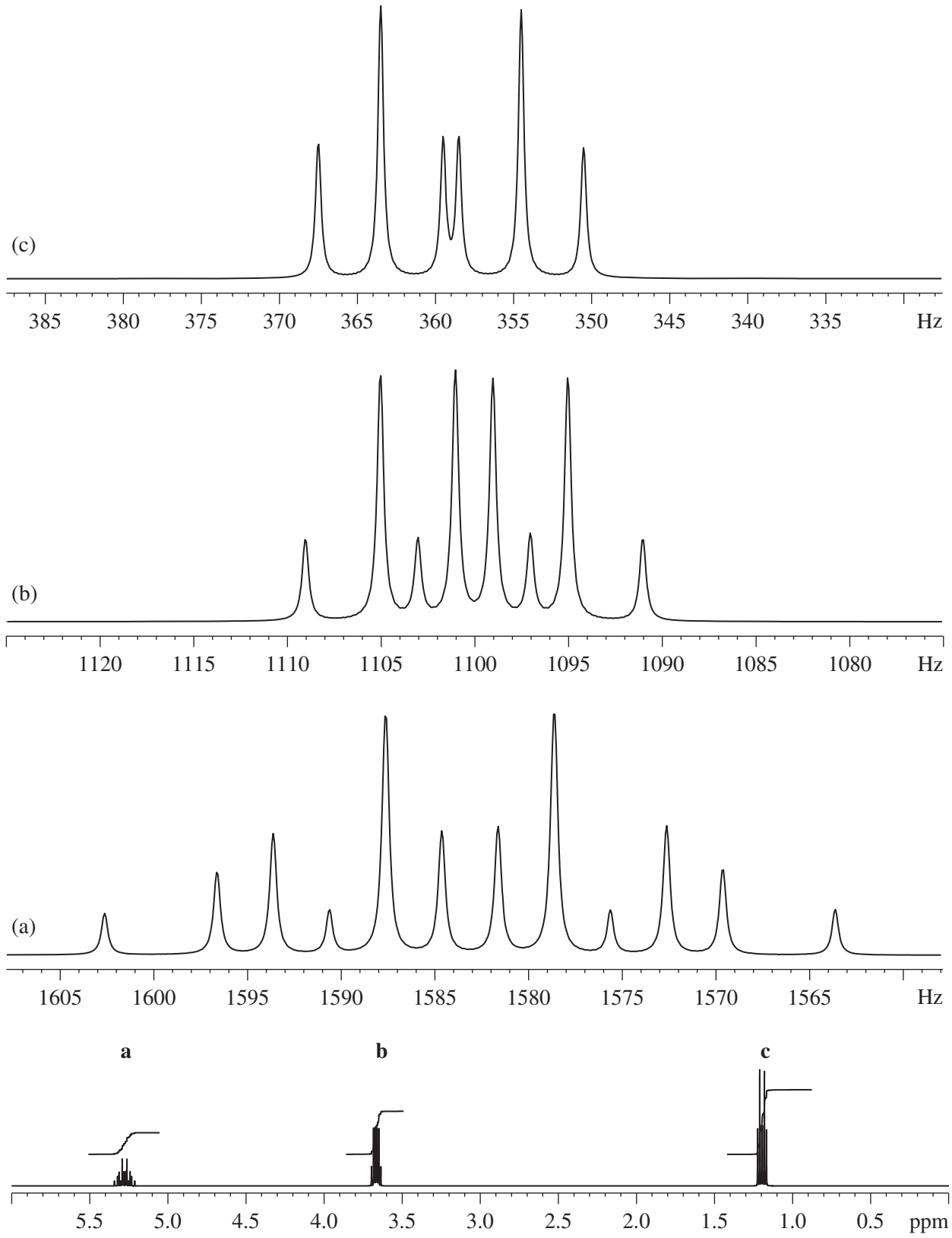
(c)
385 380 375 370 365 360 355 350 345 340 335 Hz
(b)
1120 1115 1110 1105 1100 1095 1090 1085 1080 Hz
(a)
1605 1600 1595 1590 1585 1580 1575 1570 1565 Hz
a
b
c
5.5 5.0 4.5 4.0 3.5 3.0 2.5 2.0 1.5 1.0 0.5 ppm

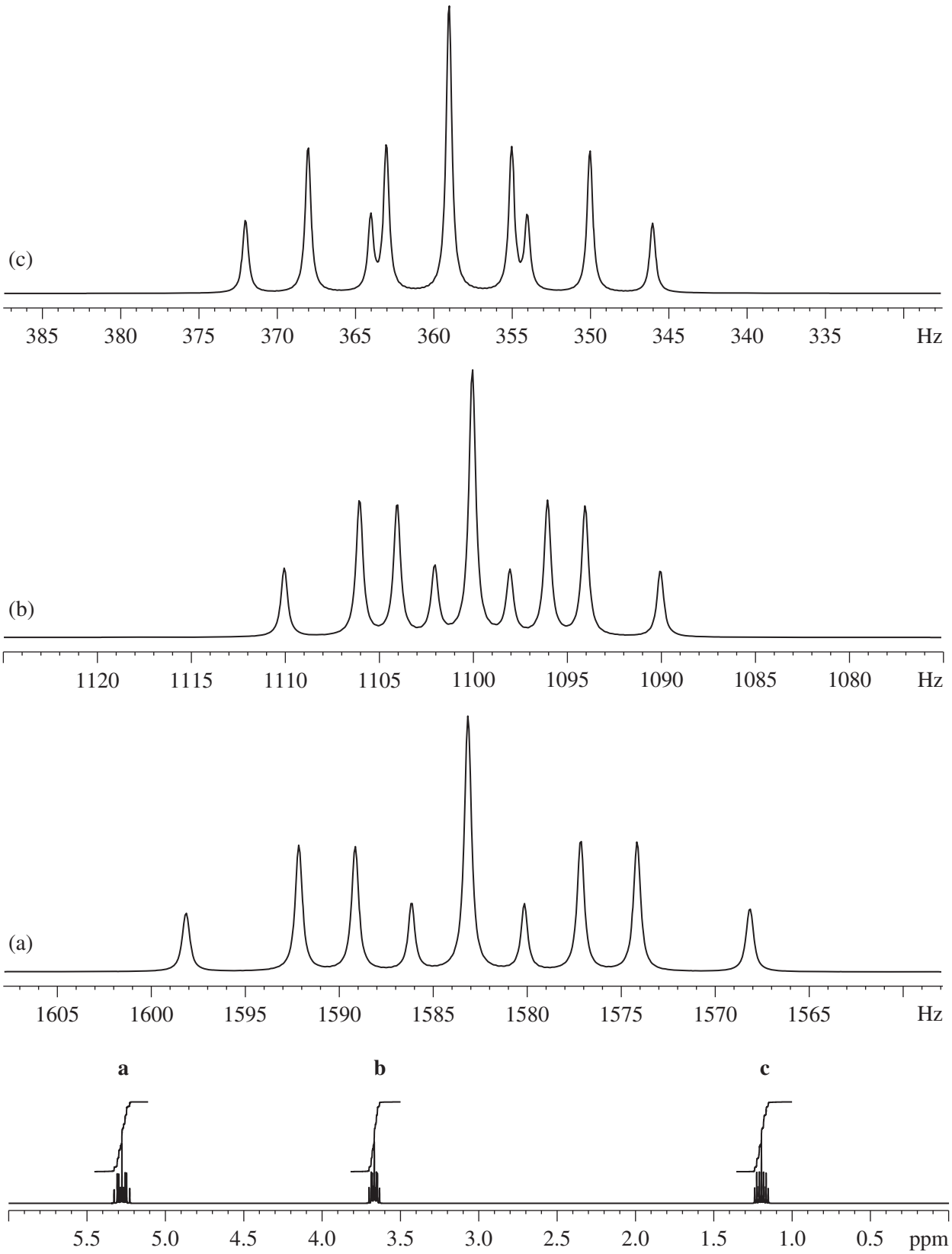
(c)
385 380 375 370 365 360 355 350 345 340 335 Hz
(b)
1120 1115 1110 1105 1100 1095 1090 1085 1080 Hz
(a)
1605 1600 1595 1590 1585 1580 1575 1570 1565 Hz
a
b
c
5.5 5.0 4.5 4.0 3.5 3.0 2.5 2.0 1.5 1.0 0.5 ppm

APPENDIX A

CHART A.1: CHEMICAL SHIFTS OF PROTONS ON A CARBON ATOM ADJACENT (α POSITION) TO A FUNCTIONAL GROUP IN ALIPHATIC COMPOUNDS (M—Y)

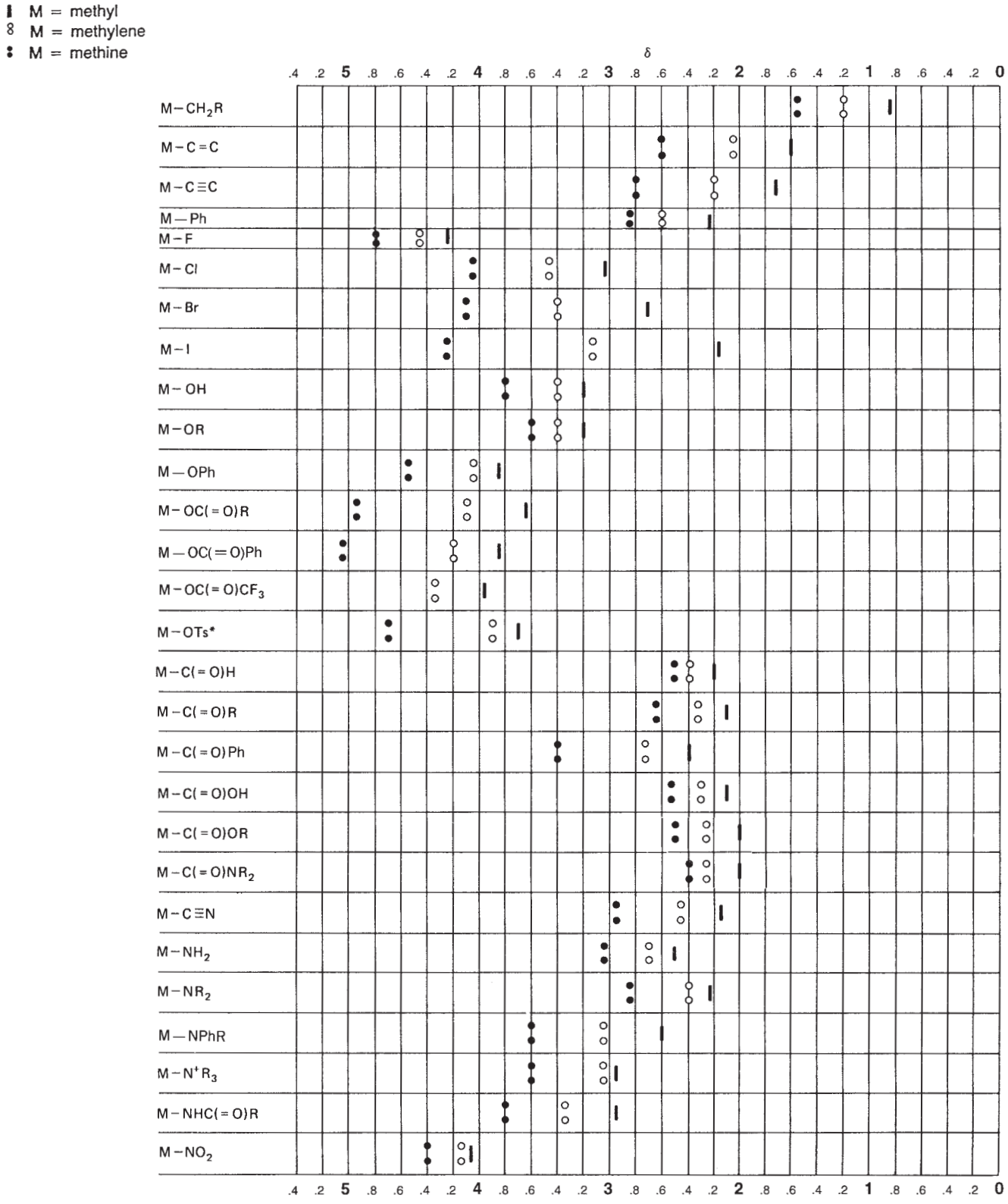

APPENDIX A (*Continued*)

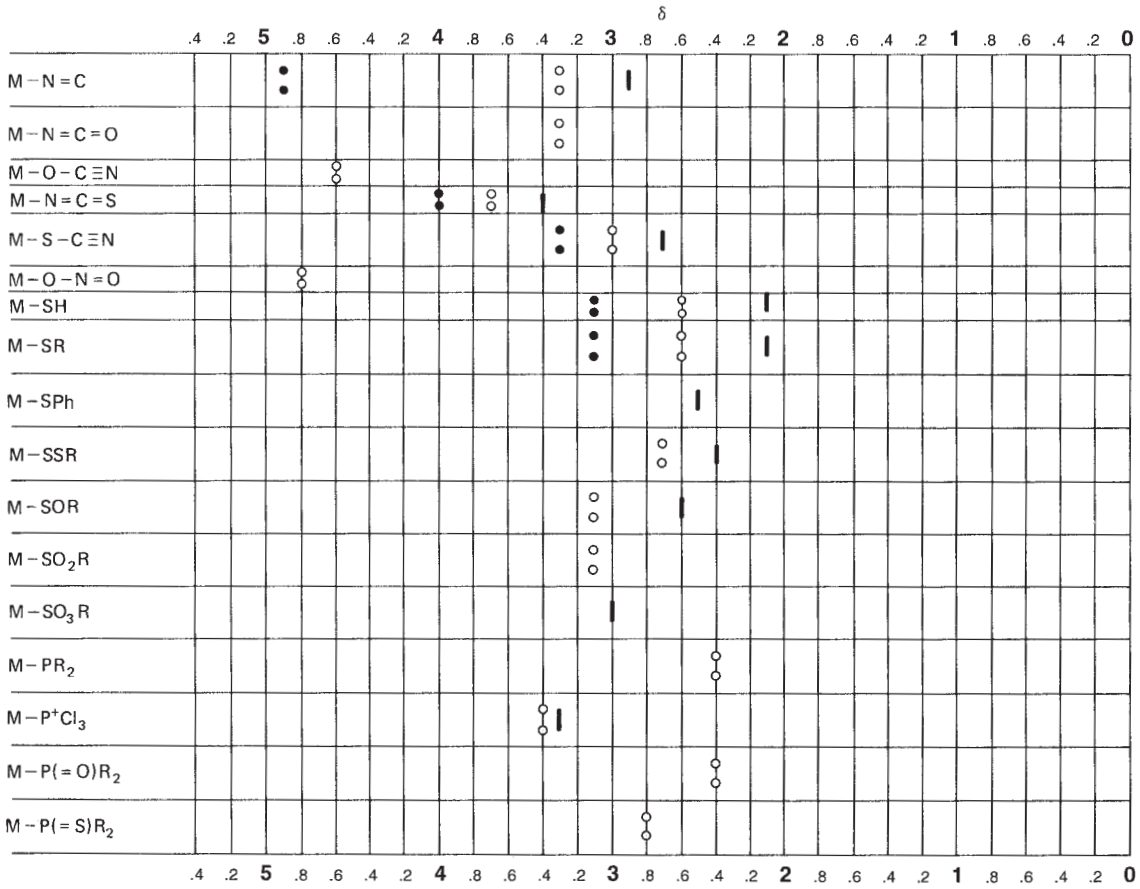

*OTS is 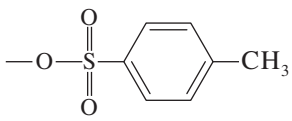

APPENDIX A CHART A.2: CHEMICAL SHIFTS OF PROTONS ON A CARBON ATOM ONCE REMOVED (β POSITION) FROM A FUNCTIONAL GROUP IN ALIPHATIC COMPOUNDS (M—C—Y)

▮ M = methyl
8 M = methylene
⁝ M = methine

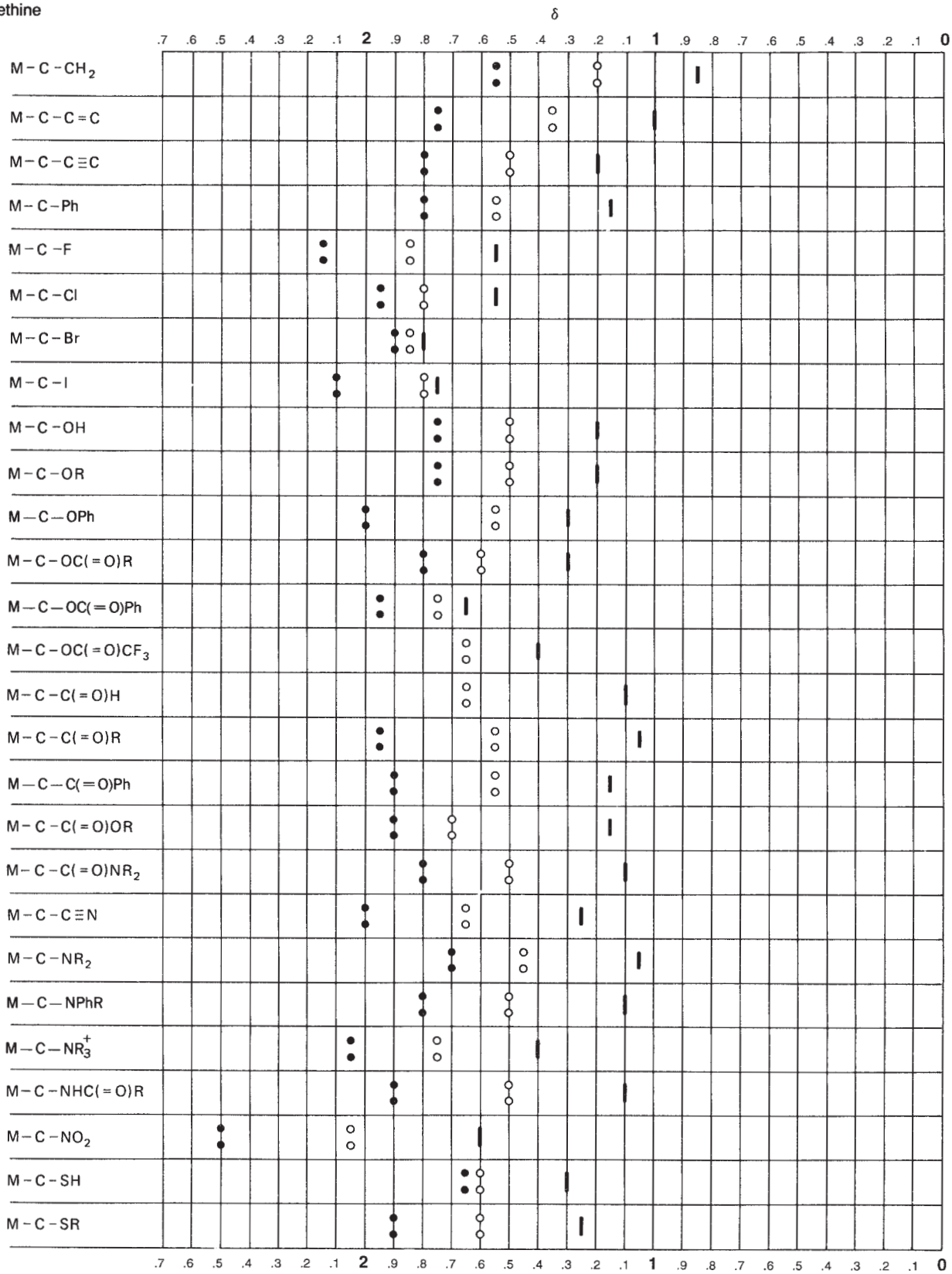

APPENDIX B EFFECT ON CHEMICAL SHIFTS OF TWO OR THREE DIRECTLY ATTACHED FUNCTIONAL GROUPS

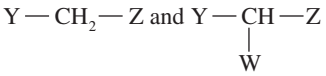

The chemical shift of a methylene group attached to two functional groups can be calculated by means of the substituent constants (σ values) in Table B.1. Shoolery's rule* states that the sum of the constants for the attached functional groups is added to 0.23 ppm, the chemical shift for CH_4:

$$\delta(Y\text{—}CH_2\text{—}Z) = 0.23 + \sigma_Y + \sigma_Z$$

The chemical shift for the methylene protons, of $C_6H_5CH_2Br$, for example, is calculated from the σ values in Table B.1.

	0.23
σ_{Ph}	= 1.85
σ_{Br}	= 2.33
δ	= 4.41 Found, 4.43 ppm

Shoolery's original constants have been revised and extended in Table B.1. The observed and calculated chemical shifts for 62% of the samples tested were within ±0.2 ppm, 92% within ±0.3 ppm, 96% within 0.4 ppm, and 99% within ±0.5 ppm.† Table B.1 contains substituent constants (Friedrich and Runkle, 1984) for the more common functional groups. Note that chemical shifts of methyl protons can be calculated by using the constant for H (0.34). For example H—CH_2—Br is equivalent to CH_3Br.

TABLE B.1 Substituent Constants for Alkyl Methylene (and Methyl) Protons

Y or Z	Substituent Constants (σ)	Y or Z	Substituent Constants (σ)
—H	0.34	—OC(═O)R	3.01
—CH_3	0.68	—OC(═O)Ph	3.27
—C—C	1.32	—C(═O)R	1.50
—C≡C	1.44	—C(═O)Ph	1.90
—Ph	1.83	—C(═O)OR	1.46
—CF_2	1.12	—C(═O)$NR_2(H_2)$	1.47
—CF_3	1.14	—C≡N	1.59
—F	3.30	—$NR_2(H_2)$	1.57
—Cl	2.53	—NHPh	2.04
—Br	2.33	—NHC(═O)R	2.27
—I	2.19	—N_3	1.97
—OH	2.56	—NO_2	3.36
—OR	2.36	—SR(H)	1.64
—OPh	2.94	—OSO_2R	3.13

*Shoolery, J.N. (1959). Varian Technical Information Bulletin, Vol 2, No. 3. Palo Alto, CA: Varian Associates.

†Data from Friedrich, E.C. and Runkle, K.G. (1984). *J. Chem. Educ.* **61** 830; (1986) **63,** 127.

Tables B.2a, B.2b, and B.2c: Chemical Shift Correlations for Methine Protons

Table B.2a gives the substituent constants‡ to be used with the formulation

$$\delta CHXYZ = 2.50 + \sigma_X + \sigma_Y + \sigma_Z$$

which is satisfactory if at least two of the substituents are electron-withdrawing groups. In other words, only a single substituent may be an alkyl group (R). Within these limits, the standard error of estimate is 0.20 ppm. For example, the chemical shift of the methine proton in

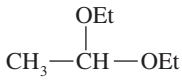

is calculated from Table B.2a as follows:

$$\delta = 2.50 + 1.14 + 1.14 + 0.00 = 4.78 \text{ ppm}$$

The found value is 4.72 ppm.

Tables B.2b and B.2c are used jointly for methine protons that are substituted by at least two alkyl groups (or

TABLE B.2a Substituent Constants for Methine Protons

Group	(σ)
—F	1.59
—Cl	1.56
—Br	1.53
—NO_2	1.84
—NH_2	0.64
—NH_3^+	1.34
—NHCOR	1.80
—OH, —OR	1.14
—OAr	1.79
—OCOR	2.07
—Ar	0.99
—C═C	0.46
—C≡C	0.79
—C≡N	0.66
—COR, —COOR, —COOH	0.47
—$CONH_2$	0.60
—COAr	1.22
—SH, —SR	0.61
—SO_2R	0.94
—R	0

‡Bell, H.M., Bowles, D.B. and Senese, F. (1981). *Org. Magn. Reson.,* (now changed to Magnetic Resonance in Chemistry) **16,** 285. With permission.

TABLE B.2b Observed Methine Proton Chemical Shifts of Isopropyl Derivatives

$(CH_3)_2CHZ$		$(CH_3)_2CHZ$	
Z	δ (ppm) obs	Z	δ (ppm) obs
H	1.33	HO	3.94
H_3C	1.56	RO	3.55
R	1.50	C_6H_5O	4.51
XCH_2	1.85	R(H)C(=O)O	4.94
R(H)C(=O)	2.54	$C_6H_5C(=O)O$	5.22
$C_6H_5C(=O)$	3.58	$F_3CC(=O)O$	5.20
R(H)OC(=O)	2.52	$ArSO_2O$	4.70
$R_2(H_2)NC(=O)$	2.44		
C_6H_5	2.89	R(H)S	3.16
$R_2(H_2)C=CR(H)$	2.62	RSS	2.63
R(H)C≡C	2.59		
N≡C	2.67	F	4.50
		Cl	4.14
$R_2(H_2)N$	3.07	Br	4.21
R(H)C(=O)NH	4.01	I	4.24
O_2N	4.67		

TABLE B.2c Correction Factors for Methine Substituents of Low Polarity

Open-Chain Methine Proton Systems	Δxy	Cyclic Methine Proton Systems	Δxy
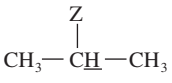	0.00		−1.0
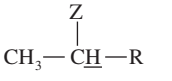	−0.20		+0.40
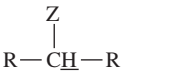	−0.40	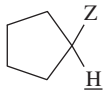	+0.20
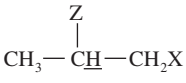	+0.20	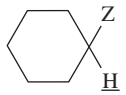	monosub. −0.20
			axial H −0.45
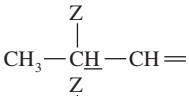	+0.40		equat. H +0.25
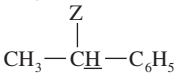	+1.15	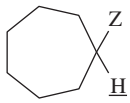	0.00
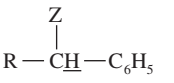	+0.90	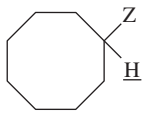	0.00

other groups of low polarity). Friedrich and Runkle proposed the relationship

$$\delta_{CHXYZ} = \delta_{(CH_3)_2CHZ} = \Delta xy$$

in which the X and Y substituents are alkyl groups or other groups of low polarity. The Z substituent covers a range of polarities. Δxy is a correction factor. The relationship states that the chemical shift of a methine proton with at least two low-polarity groups is equivalent to the chemical shift of an isopropyl methine proton plus a correction factor.

The substituent constants for a Z substituent on an isopropyl methine proton are given in Table B.2b. The Δxy correction factors are given in Table B.2c.

The following examples illustrate the joint use of Tables B.2b and B.2c, with CH_3, $CH{=}CH_2$, and C_6H_5 as substituents. The most polar substituent is always designated Z.

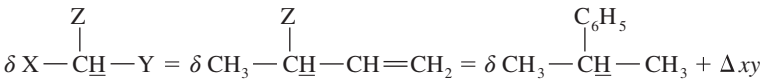

From Table B.2b, $\delta = 2.89$ for  .

From Table B.2c, $\Delta xy = 0.00$ for CH_3 $\Delta xy = 0.40$ for $CH = CH_2$.

Therefore, 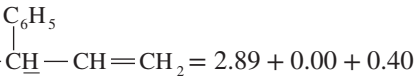 = 2.89 + 0.00 + 0.40 = 3.29 (Found: $\delta = 3.44$).

APPENDIX C CHEMICAL SHIFTS IN ALICYCLIC AND HETEROCYCLIC RINGS

TABLE C.1 Chemicals Shifts in Alicyclic Rings

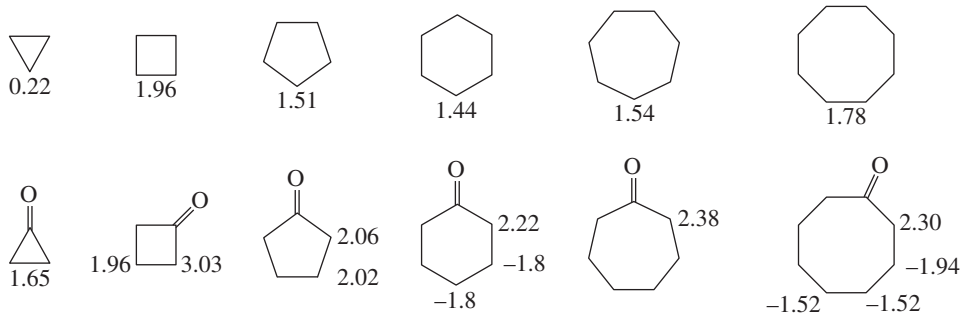

TABLE C.2 Chemical Shifts in Heterocyclic Rings

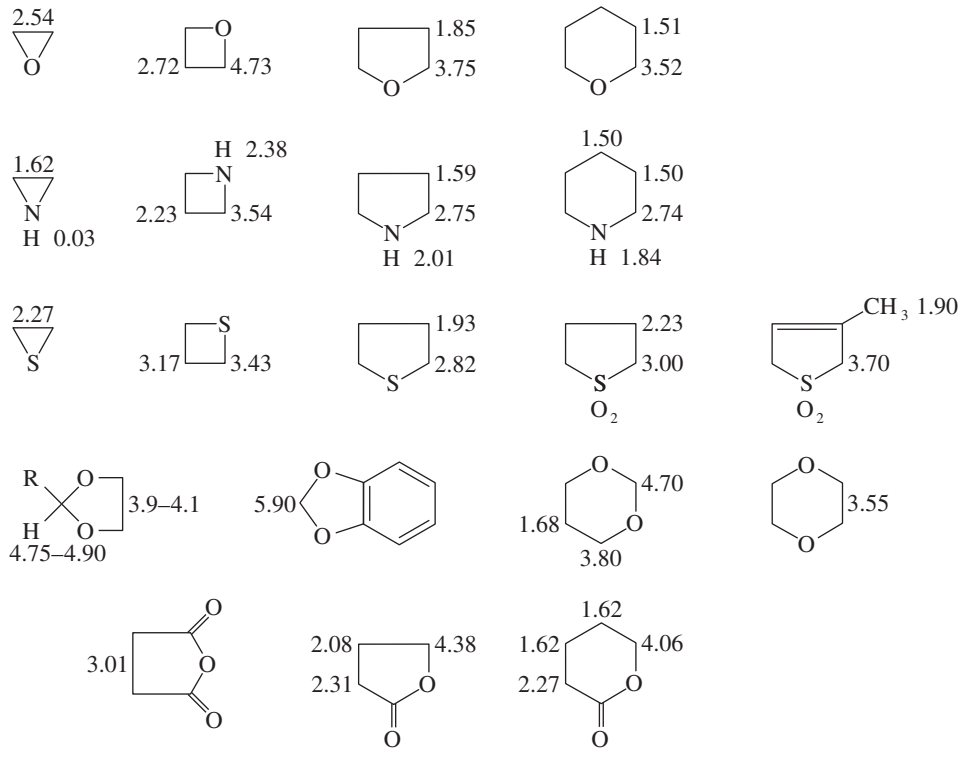

APPENDIX D CHEMICAL SHIFTS IN UNSATURATED AND AROMATIC SYSTEMS

(see Table D.1)

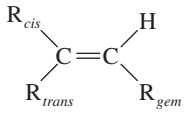

$$\delta_H = 5.25 + Z_{gem} + Z_{cis} + Z_{trans}$$

For example, the chemical shifts of the alkene protons in

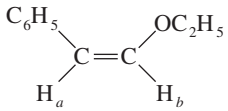

are calculated

H_a	C_6H_5 *gem*	1.35	5.25
	OR_{trans}	−1.28	0.07
		0.07	δ 5.32
H_b	OR_{gem}	1.18	5.25
	C_6H_5 *trans*	−0.10	1.08
		1.08	δ 6.33

TABLE D.1 Substituent Constants (*Z*) for Chemical Shifts of Substituted Ethylenes

	Z				*Z*		
Substituent R	*gem*	*cis*	*trans*	**Substituent R**	*gem*	*cis*	*trans*
—H	0	0	0				
—Alkyl	0.44	−0.26	−0.29		1.03	0.97	1.21
—Alkyl-ring[a]	0.71	−0.33	−0.30				
—CH_2O, —CH_2I	0.67	−0.02	−0.07				
—CH_2S	0.53	−0.15	−0.15		1.37	0.93	0.35
—CH_2Cl, —CH_2Br	0.72	0.12	0.07				
—CH_2N	0.66	−0.05	−0.23		1.10	1.41	0.99
—C≡C	0.50	0.35	0.10				
—C≡N	0.23	0.78	0.58	—OR, R:aliph	1.18	−1.06	−1.28
—C═C	0.98	−0.04	−0.21	—OR, R:conj[b]	1.14	−0.65	−1.05
—C═C conj[b]	1.26	0.08	−0.01	—OCOR	2.09	−0.40	−0.67
—C═O	1.10	1.13	0.81	—Aromatic	1.35	0.37	−0.10
—C═O conj[b]	1.06	1.01	0.95	—Cl	1.00	0.19	0.03
—COOH	1.00	1.35	0.74	—Br	1.04	0.40	0.55
—COOH conj[b]	0.69	0.97	0.39	 R:aliph	0.69	−1.19	−1.31
—COOR	0.84	1.15	0.56	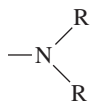 R:conj[b]	2.30	−0.73	−0.81
—COOR conj[b]	0.68	1.02	0.33	—SR	1.00	−0.24	−0.04
				$—SO_2$	1.58	1.15	0.95

[a]Alkyl ring indicates that the double bond is part of the ring  .

[b]The Z factor for the conjugated substituent is used when either the substituent or the double bond is further conjugated with other groups.

Source: Pascual C., Meier, J., and Simon, W. (1966) *Helv. Chim. Acta*, **49**, 164.

TABLE D.2 Chemical Shifts of Miscellaneous Alkenes

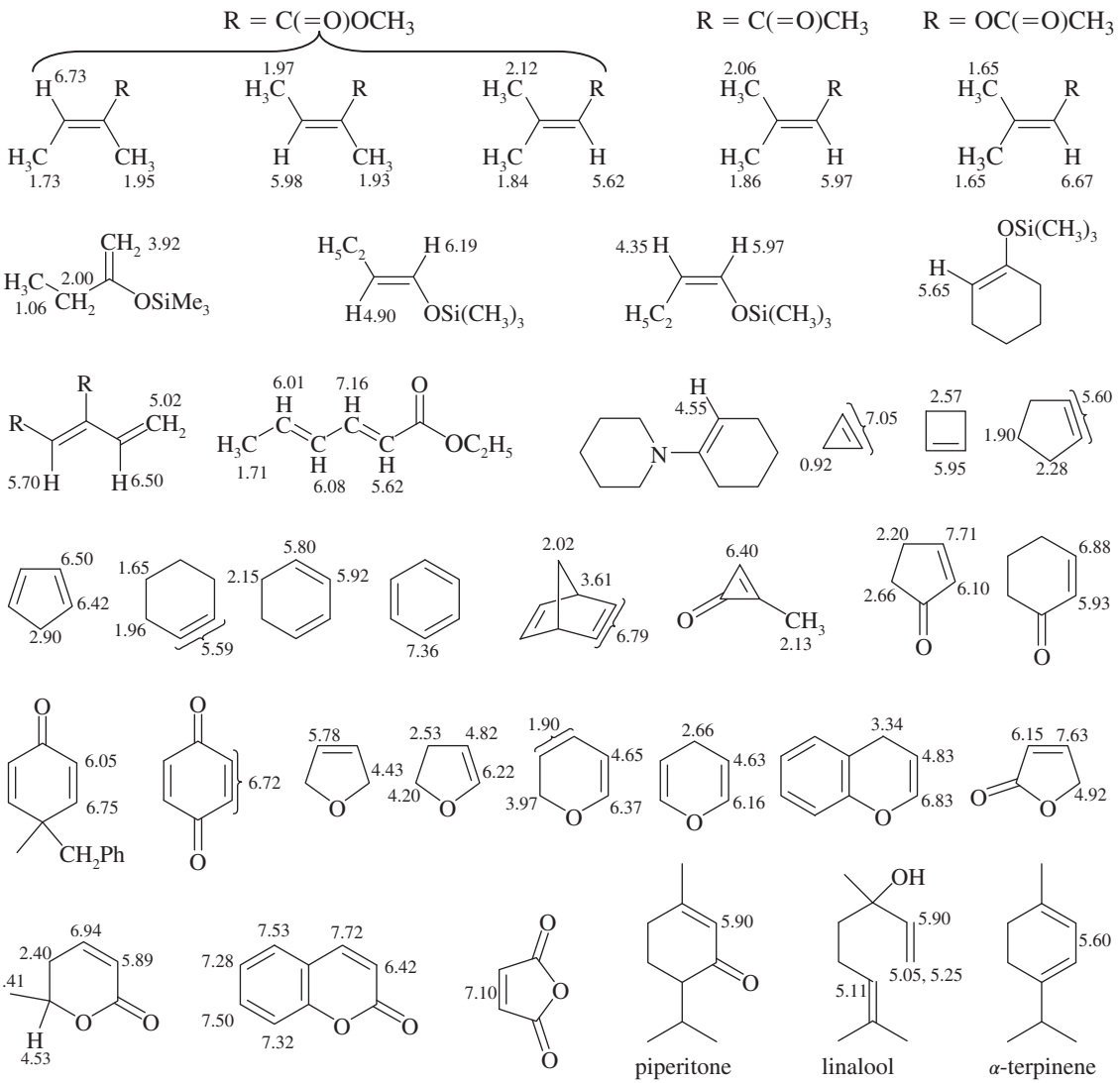

TABLE D.3 Chemical Shifts of Alkyne Protons

HC≡CR	1.73 – 1.88	HC≡C—COH	2.23
HC≡C—C≡CR	1.95	HC≡CH	1.80
HC≡C—Ph	2.71 – 3.37	HC≡C—CH═CR_2	2.60 – 3.10

TABLE D.4 Chemical Shifts of Protons on Fused Aromatic Rings

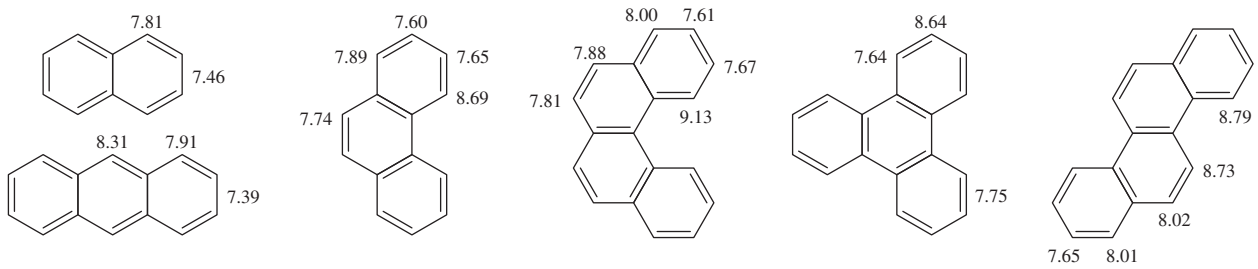

CHART D.1 CHEMICAL SHIFTS OF PROTONS ON MONOSUBSTITUTED BENZENE RINGS

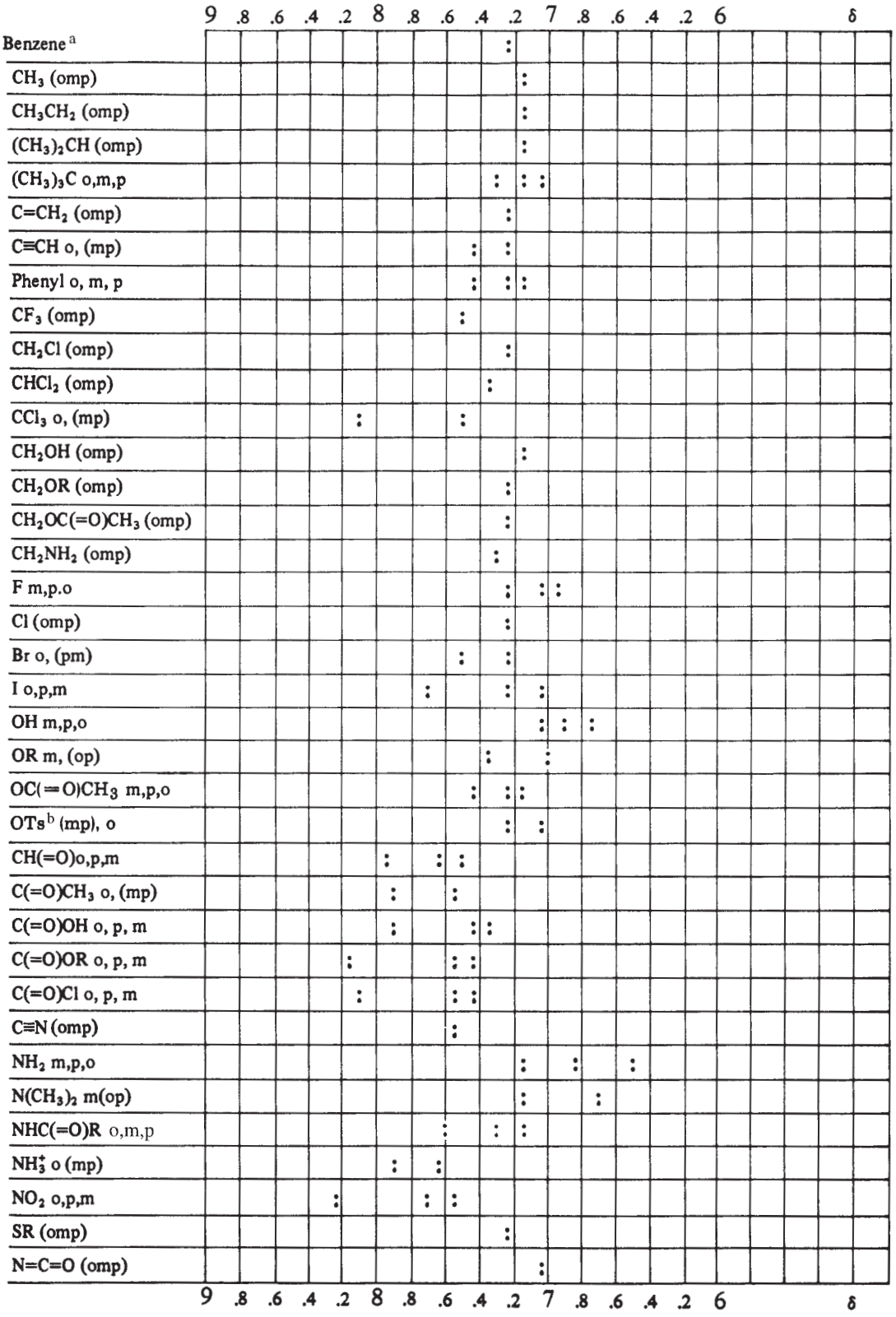

[a]The benzene ring proton is at δ 7.27, from which the shift increments are calculated as shown at the end of Section 3.4.
[b]OTS = *p*-toluenesulfonyloxy group.

TABLE D.5 Chemical Shifts of Protons on Heteroaromatic Rings

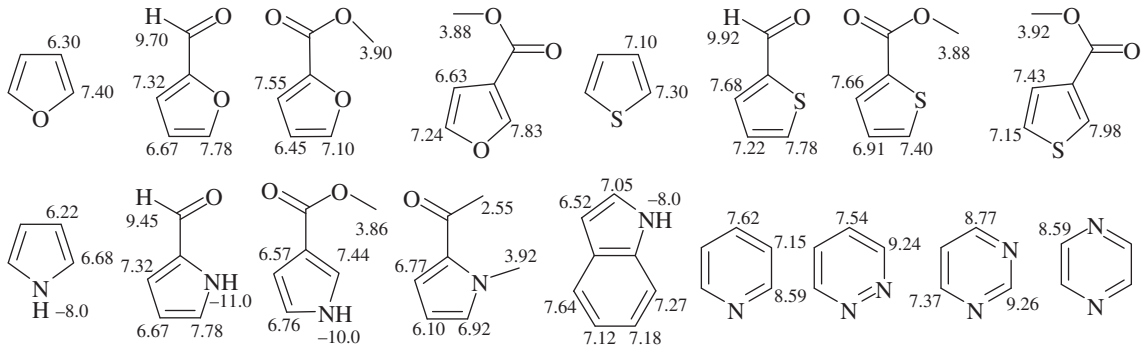

TABLE D.6 Chemical Shifts of HC═O, HC═N, and $HC(O)_3$ Protons

RCH═O	9.70	HC(═O)OR	8.05	RCH═NOH *cis*	7.25
PhCH═O	9.98	$HC(═O)NR_2$	8.05	RCH═NOH *trans*	6.65
RCH═CHCH═O	9.78	$HC(OR)_3$	5.00	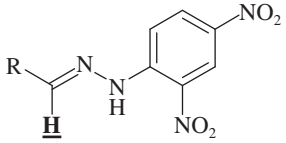	6.05

APPENDIX E PROTONS SUBJECT TO HYDROGEN-BONDING EFFECTS (PROTONS ON HETEROATOMS)[a]

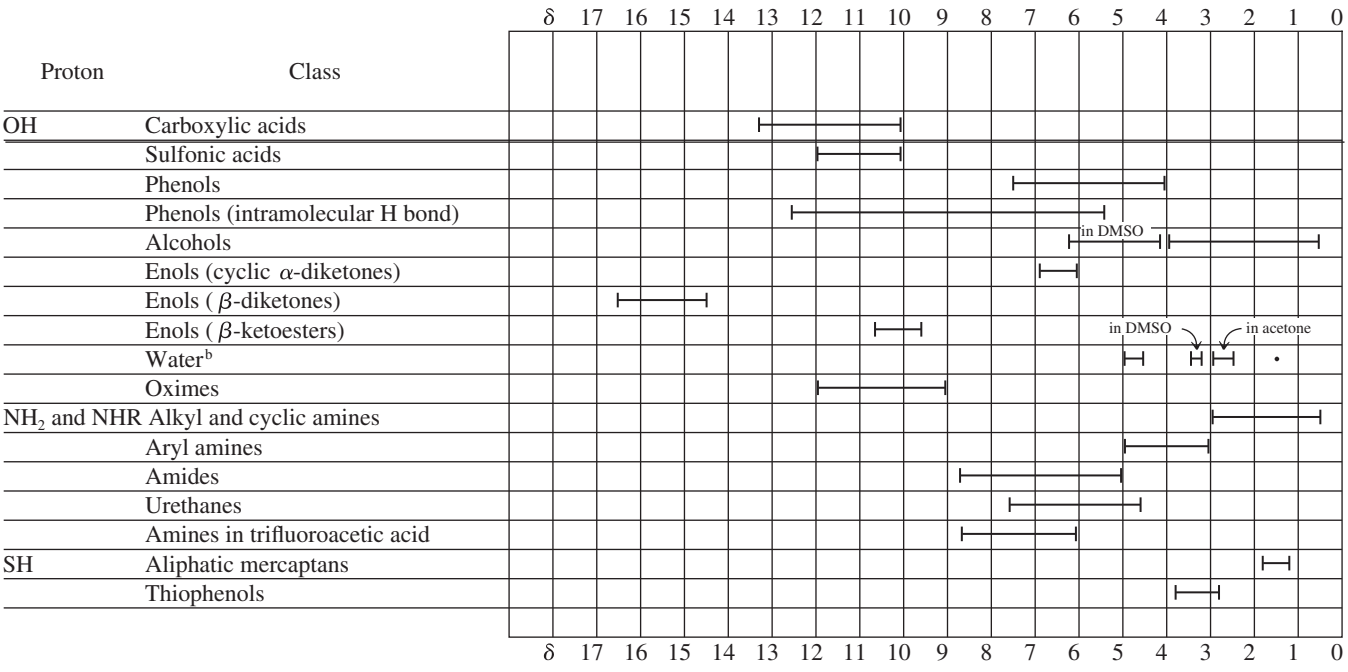

[a]Solvent $CDCl_3$. Chemical shifts within a range are a function of concentration.
[b]See Section 3.6.1.2.

APPENDIX F PROTON SPIN-SPIN COUPLING CONSTANTS

Type	J_{ab} (Hz)	J_{ab} Typical
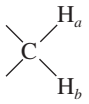	0 – 30	12 – 15
CH_a-CH_b (free rotation)	6 – 8	7
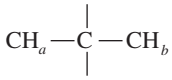	0 – 1	0
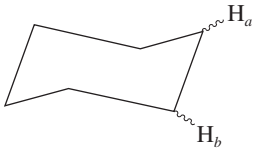		
ax–ax	6 – 14	8 – 10
ax–eq	0 – 5	2 – 3
eq–eq	0 – 5	2 – 3
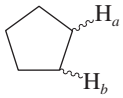 (*cis* or *trans*)	*cis* 5 – 10 *trans* 5 – 10	
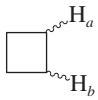 (*cis* or *trans*)	*cis* 4 – 12 *trans* 2 – 10	
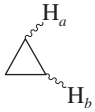 (*cis* or *trans*)	*cis* 7 – 13 *trans* 4 – 9	
CH_a-OH_b (no exchange)	4 – 10	5
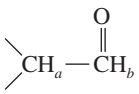	1 – 3	2 – 3
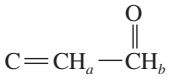	5 – 8	6
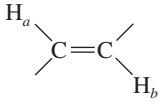	12 – 18	17
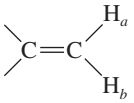	0 – 3	0 – 2

Type	J_{ab} (Hz)	J_{ab} Typical
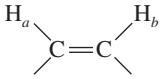	6 – 12	10
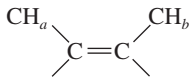	0 – 3	1 – 2
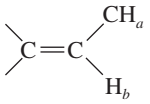	4 – 10	7
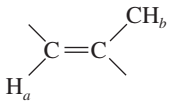	0 – 3	1.5
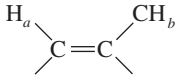	0 – 3	2
$C=CH_a-CH_b=C$	9 – 13	10
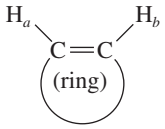	3 member 4 member 5 member 6 member 7 member 8 member	0.5 – 2.0 2.5 – 4.0 5.1 – 7.0 8.8 – 11.0 9 – 13 10 – 13
$CH_a-C\equiv CH_b$	2 – 3	
$-CH_a-C\equiv C-CH_b-$	2 – 3	
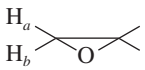		6
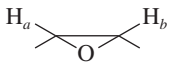		4
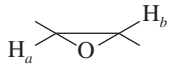		2.5
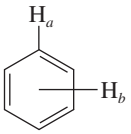	*J (ortho)* *J (meta)* *J (para)*	6 – 10 1 – 3 0 – 1
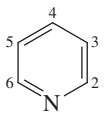	*J* (2 – 3) *J* (3 – 4) *J* (2 – 4) *J* (3 – 5) *J* (2 – 5) *J* (2 – 6)	5 – 6 7 – 9 1 – 2 1 – 2 0 – 1 0 – 1
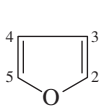	*J* (2 – 3) *J* (3 – 4) *J* (2 – 4) *J* (2 – 5)	1.3 – 2.0 3.1 – 3.8 0 – 1 1 – 2

APPENDIX F (*Continued*)

Type		J_{ab} (Hz)	J_{ab} Typical
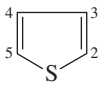	J (2 – 3)	4.9 – 6.2	5.4
	J (3 – 4)	3.4 – 5.0	4.0
	J (2 – 4)	1.2 – 1.7	1.5
	J (2 – 5)	3.2 – 3.7	3.4
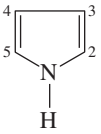	J (1 – 3)	2 – 3	
	J (2 – 3)	2 – 3	
	J (3 – 4)	3 – 4	
	J (2 – 4)	1 – 2	
	J (2 – 5)	1.5 – 2.5	
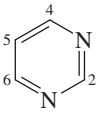	J (4 – 5)	4 – 6	
	J (2 – 5)	1 – 2	
	J (2 – 4)	0 – 1	
	J (4 – 6)	2 – 3	
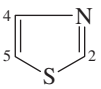	J (4 – 5)	3 – 4	
	J (2 – 4)	~0	
	J (2 – 5)	1 – 2	

Type	J_{ab} (Hz)	J_{ab} Typical
Proton – Fluorine		
	44 – 81	
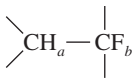	3 – 25	
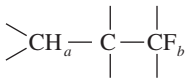	0 – 4	
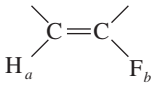	1 – 8	
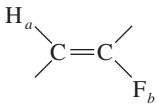	12 – 40	
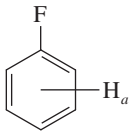	*o* 6 – 10 *m* 5 – 6 *p* 2	
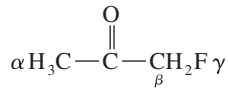	$\alpha\gamma$ 4.3 $\beta\gamma$ 48	

Proton – Phosphorus

	630 – 707
$(CH_3)_3P$	2.7
$(CH_3)_3P{=}O$	13.4
$(CH_3CH_2)_3P$	0.5 (HCCP) 13.7 (HCP)
$(CH_3CH_2)_3P{=}O$	11.9 (HCCP) 16.3 (HCP)
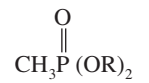	10 – 13
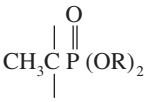	15 – 20
$CH_3OP(OR)_2$	10.5 – 12
$P[N(CH_3)_2]_3$	8.8
$O{=}P[N(CH_3)_2]_3$	9.5

Source: Compiled by Varian Associates. Absolute values. Reproduced with permission.

APPENDIX G CHEMICAL SHIFTS AND MULTIPLICITIES OF RESIDUAL PROTONS IN COMMERCIALLY AVAILABLE DEUTERATED SOLVENTS (MERCK & CO., INC.)

Compound[a] Molecular Weight	δ_H (multiplet)	Compound[a] Molecular Weight	δ_H (multiplet)
Acetic acid-d_4[b]	11.53 (1)	Nitromethane-d_3	4.33 (5)
64.078	2.03 (5)	64.059	
Acetone-d_6	2.04 (5)	Isopropyl alcohol-d_8	5.12 (1)
64.117		68.146	3.89 (br)
Acetonitrile-d_3	1.93 (5)		1.10 (br)
44.071			8.71 (br)
Benzene-d_6	7.15 (br)	Pyridine-d_5	7.55 (br)
84.152		84.133	7.19 (br)
Chloroform-d	7.26 (1)	Tetrahydrofuran-d_8	3.58 (br)
120.384		80.157	1.73 (br)
Cyclohexane-d_{12}	1.38 (br)	Toluene-d_8	7.09 (m)
96.236		100.191	7.00 (br)
Deuterium oxide	4.63 (ref. DSS)[c]		6.98 (m)
20.028	4.67 (ref. TSP)[c]		2.09 (5)
1,2-Dichloroethane-d_4	3.72 (br)	Trifluoroacetic acid-d	11.50 (1)
102.985		115.030	
Diethyl-d_{10} ether	3.34 (m)	2,2,2-Trifluoroethyl alcohol-d_3	5.02 (1)
84.185	1.07 (m)	103.059	3.88 (4×3)
Diglyme-d_{14}	3.49 (br)		
148.263	3.40 (br)		
	3.22 (5)		
N, N-Dimethylformamide-d_7	8.01 (br)		
80.138	2.91 (5)		
	2.74 (5)		
Dimethyl-d_6 sulphoxide	2.49 (5)		
84.170			
p-Dioxane-d_8	3.53 (m)		
96.156			
Ethyl alcohol-d_6 (anh)	5.19 (1)		
52.106	3.55 (br)		
	1.11 (m)		
Glyme-d_{10}	3.40 (m)		
100.184	3.22 (5)		
Hexafluroacetone deuterate	5.26 (1)		
198.067			
HMPT-d_{18}	2.53 (2×5)		
197.314			
Methyl alcohol-d_4	4.78 (1)		
36.067	3.30 (5)		
Methylene chloride-d_2	5.32 (3)		
86.945			
Nitrobenzene-d_5	8.11 (br)		
128.143	7.67 (br)		
	7.50 (br)		

[a]Purity (Atom % D) up to 99.96% ("100%") for several solvents.

[b]The residual proton consists of one proton of each kind in an otherwise completely deuterated molecule. For example, deuterated acetic acid has two different kinds of residual protons: $CD_2H - COOD$ and $CD_3 - COOH$. The CD_2H proton, coupled to two D nuclei is at 2.03 ppm with a multiplicity of 5 (i.e., $2nI + 1 = 2 \times 2 \times 1 + 1 = 5$). The carboxylic proton is a singlet at 11.53 ppm.

[c]DSS is 3-(trimethylsilyl)-1-propane sulfonic acid, sodium salt. TSP is sodium-3-trimethylpropionate-2,2,3,3-d_4. Both are reference standards used in aqueous solutions.

APPENDIX H CHEMICAL SHIFTS OF COMMON LABORATORY SOLVENTS AS TRACE IMPURITIES

	Proton	Mult	$CDCl_3$	$(CD_3)_2CO$	$(CD_3)_2SO$	C_6D_6	CD_3CN	CD_3OD	D_2O
Solvent residual peak			7.26	2.05	2.50	7.16	1.94	3.31	4.79
H_2O		s	1.56	2.84[a]	3.33[a]	0.40	2.13	4.87	
Acetic acid	CH_3	s	2.10	1.96	1.91	1.55	1.96	1.99	2.08
Acetone	CH_3	s	2.17	2.09	2.09	1.55	2.08	2.15	2.22
Acetonitrile	CH_3	s	2.10	2.05	2.07	1.55	1.96	2.03	2.06
Benzene	CH	s	7.36	7.36	7.37	7.15	7.37	7.33	
Tert-Butyl alcohol	CH_3	s	1.28	1.18	1.11	1.05	1.16	1.40	1.24
	OH[c]	s			4.19	1.55	2.18		
tert-Butyl methyl ether	CCH_3	s	1.19	1.13	1.11	1.07	1.14	1.15	1.21
	OCH_3	s	3.22	3.13	3.08	3.04	3.13	3.20	3.22
BHT[b]	ArH	s	6.98	6.96	6.87	7.05	6.97	6.92	
	OH[c]	s	5.01		6.65	4.79	5.20		
	$ArCH_3$	s	2.27	2.22	2.18	2.24	2.22	2.21	
	$ArC(CH_3)_3$	s	1.43	1.41	1.36	1.38	1.39	1.40	
Chloroform	CH	s	7.26	8.02	8.32	6.15	7.58	7.90	
Cyclohexane	CH_2	s	1.43	1.43	1.40	1.40	1.44	1.45	
1,2-Dichloroethane	CH_2	s	3.73	3.87	3.90	2.90	3.81	3.78	
Dichloromethane	CH_2	s	5.30	5.63	5.76	4.27	5.44	5.49	
Diethyl ether	CH_3	t, 7	1.21	1.11	1.09	1.11	1.12	1.18	1.17
	CH_2	q, 7	3.48	3.41	3.38	3.26	3.42	3.49	3.56
Diglyme	CH_2	m	3.65	3.56	3.51	3.46	3.53	3.61	3.67
	CH_2	m	3.57	3.47	3.38	3.34	3.45	3.58	3.61
	OCH_3	s	3.39	3.28	3.24	3.11	3.29	3.35	3.37
1,2-Dimethoxyethane	CH_3	s	3.40	3.28	3.24	3.12	3.28	3.35	3.37
	CH_2	s	3.55	3.46	3.43	3.33	3.45	3.52	3.60
Dimethylacetamide	CH_3CO	s	2.09	1.97	1.96	1.60	1.97	2.07	2.08
	NCH_3	s	3.02	3.00	2.94	2.57	2.96	3.31	3.06
	NCH_3	s	2.94	2.83	2.78	2.05	2.83	2.92	2.90
Dimethylformamide	CH	s	8.02	7.96	7.95	7.63	7.92	7.97	7.92
	CH_3	s	2.96	2.94	2.89	2.36	2.89	2.99	3.01
	CH_3	s	2.88	2.78	2.73	1.86	2.77	2.86	2.85
Dimethyl sulfoxide	CH_3	s	2.62	2.52	2.54	1.68	2.50	2.65	2.71
Dioxane	CH_2	s	3.71	3.59	3.57	3.35	3.60	3.66	3.75
Ethanol	CH_3	t, 7	1.25	1.12	1.06	0.96	1.12	1.19	1.17
	CH_2	q, 7[d]	3.72	3.57	3.44	3.34	3.54	3.60	3.65
	OH	s[c,d]	1.32	3.39	4.63		2.47		
Ethyl acetate	CH_3CO	s	2.05	1.97	1.99	1.65	1.97	2.01	2.07
	CH_2CH_3	q, 7	4.12	4.05	4.03	3.89	4.06	4.09	4.14
	CH_2CH_3	t, 7	1.26	1.20	1.17	0.92	1.20	1.24	1.24
Ethyl methyl ketone	CH_3CO	s	2.14	2.07	2.07	1.58	2.06	2.12	2.19
	CH_2CH_3	q, 7	2.46	2.45	2.43	1.81	2.43	2.50	3.18
	CH_2CH_3	t, 7	1.06	0.96	0.91	0.85	0.96	1.01	1.26
Ethylene glycol	CH	s[e]	3.76	3.28	3.34	3.41	3.51	3.59	3.65
"Grease"[f]	CH_3	m	0.86	0.87		0.92	0.86	0.88	
	CH_2	br s	1.26	1.29		1.36	1.27	1.29	
n-Hexane	CH_3	t	0.88	0.88	0.86	0.89	0.89	0.90	
	CH_2	m	1.26	1.28	1.25	1.24	1.28	1.29	
HMPA[g]	CH_3	d, 9.5	2.85	2.59	2.53	2.40	2.57	2.64	2.61
Methanol	CH_3	s[h]	3.49	3.31	3.16	3.07	3.28	3.34	3.34
	OH	s[g,h]	1.09	3.12	4.01		2.16		
Nitromethane	CH_3	s	4.33	4.43	4.42	2.94	4.31	4.34	4.40
n-Pentane	CH_3	t, 7	0.88	0.88	0.86	0.87	0.89	0.90	
	CH_2	m	1.27	1.27	1.27	1.23	1.29	1.29	

APPENDIX H (*Continued*)

	Proton	Mult	$CDCl_3$	$(CD_3)_2CO$	$(CD_3)_2SO$	C_6D_6	CD_3CN	CD_3OD	D_2O
2-Propanol	CH_3	d, 6	1.22	1.10	1.04	0.95	1.09	1.50	1.17
	CH	sep, 6	4.04	3.90	3.78	3.67	3.87	3.92	4.02
Pyridine	CH(2)	m	8.62	8.58	8.58	8.53	8.57	8.53	8.52
	CH(3)	m	7.29	7.35	7.39	6.66	7.33	7.44	7.45
	CH(4)	m	7.68	7.76	7.79	6.98	7.73	7.85	7.87
Silicone grease[i]	CH_3	s	0.07	0.13		0.29	0.08	0.10	
Tetrahydrofuran	CH_2	m	1.85	1.79	1.76	1.40	1.80	1.87	1.88
	CH_2O	m	3.76	3.63	3.60	3.57	3.64	3.71	3.74
Toluene	CH_3	s	2.36	2.32	2.30	2.11	2.33	2.32	
	CH (*o*/*p*)	m	7.17	7.1 – 7.2	7.18	7.02	7.1 – 7.3	7.16	
	CH (*m*)	m	7.25	7.1 – 7.2	7.25	7.13	7.1 – 7.3	7.16	
Triethylamine	CH_3	t, 7	1.03	0.96	0.93	0.96	0.96	1.05	0.99
	CH_2	q, 7	2.53	2.45	2.43	2.40	2.45	2.58	2.57

[a] In these solvents the intermolecular rate of exchange is slow enough that a peak due to HDO is usually also observed; it appears at 2.81 and 3.30 ppm in acetone and DMSO, respectively. In the former solvent, it is often seen as a 1:1:1 triplet, with $^2J_{H,D} = 1$ Hz.

[b] 2,6-Dimethyl-4-*tert*-butylphenol.

[c] The signals from exchangeable protons were not always identified.

[d] In some cases (see note *a*), the coupling interaction between the CH_2 and the OH protons may be observed ($J = 5$ Hz).

[e] In CD_3CN, the OH proton was seen as a multiplet at 2.69 ppm, and extra coupling was also apparent on the methylene peak.

[f] Long-chain, linear aliphatic hydrocarbons. Their solubility in DMSO was too low to give visible peaks.

[g] Hexamethylphosphoramide.

[h] In some cases (see notes *a*, *d*), the coupling interaction between the CH_3 and the OH protons may be observed ($J = 5.5$ Hz).

[i] Poly(dimethylsiloxane). Its solubility in DMSO was too low to give visible peaks.

APPENDIX I PROTON NMR CHEMICAL SHIFTS OF AMINO ACIDS IN D_2O

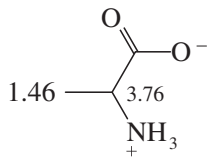

Alanine (Ala) (A)

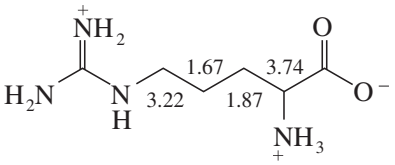

Arginine (Arg) (R)

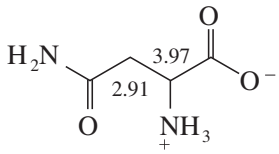

Asparagine (Asn) (N)

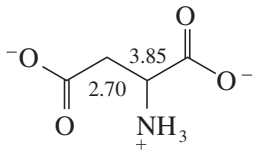

Aspartic Acid (Asp) (D)

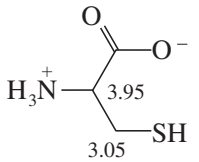

Cysteine (Cys) (C)

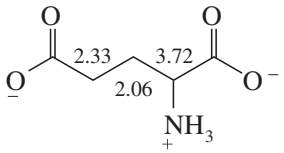

Glutamic Acid (Glu) (E)

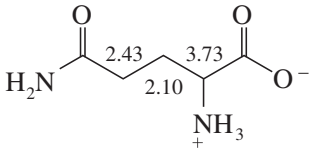

Glutamine (Gln) (Q)

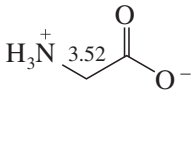

Glycine (Gly) (G)

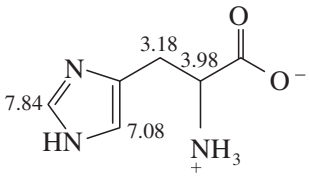

Histidine (His) (H)

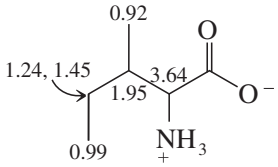

Isoleucine (Ilue) (I)

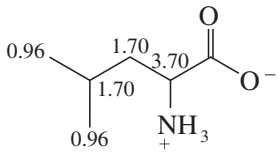

Leucine (Leu) (L)

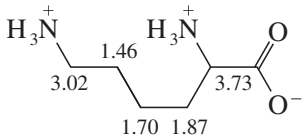

Lysine (Lys) (K)

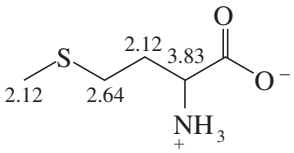

Methionine (Met) (M)

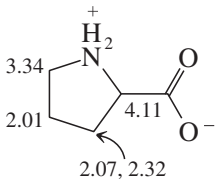

Proline (Pro) (P)

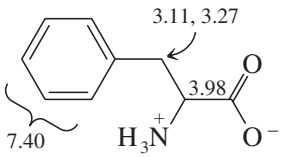

Phenylalanine (Phe) (F)

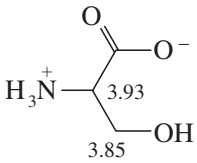

Serine (Ser) (S)

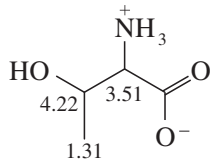

Threonine (Thr) (T)

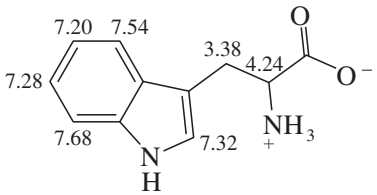

Tryptophan (Trp) (W)

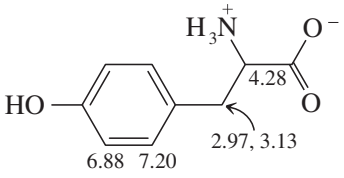

Tyrosine (Tyr) (Y)

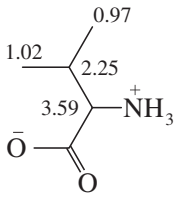

Valine (Val) (V)

CHAPTER 4

CARBON-13 NMR SPECTROSCOPY*

4.1 INTRODUCTION

Faced with a choice during the early development of nuclear magnetic resonance spectroscopy, most organic chemists would certainly have selected the carbon nucleus over the hydrogen nucleus for immediate investigation. After all, the carbon skeletons of rings and chains are central to organic chemistry. The problem, of course, is that the carbon skeleton consists almost completely of the ^{12}C nucleus, which is not accessible to NMR spectroscopy. The spectroscopist is left to cope with the very small amount of the ^{13}C nucleus.

There are enough differences between ^{13}C and ^{1}H NMR to justify separate chapters on pedagogical grounds. With an understanding of the basic concepts of NMR in Chapter 3, mastery of ^{13}C spectroscopy will be rapid.

The ^{12}C nucleus is not magnetically active (spin number, I, is zero), but the ^{13}C nucleus, like the ^{1}H nucleus, has a spin number of $\frac{1}{2}$. However, since the natural abundance of ^{13}C is only 1.1% and its magnetogyric ratio is only about a quarter that of ^{1}H, the overall sensitivity of ^{13}C compared with ^{1}H is about $\frac{1}{5870}$. Because of the low natural abundance of ^{13}C, the occurrence of adjacent ^{13}C atoms has a low probability; thus, we are free of the complication of ^{13}C—^{13}C coupling.

4.2 THEORY

The theoretical background for NMR has already been presented in Chapter 3. Some of the principal aspects of ^{13}C NMR to consider that differ from ^{1}H NMR are as follows:

- In the commonly used proton-decoupled ^{13}C spectrum (see Section 4.2.1), the peaks are singlets unless the molecule contains other magnetically active nuclei such as ^{2}H, ^{31}P, or ^{19}F.
- The ^{13}C peaks are distributed over a larger chemical shift range in comparison with the proton range.
- ^{13}C peak intensities do not correlate with the number of carbon atoms associated with a given peak in routine spectra, due to variable T_1 values and the NOE.
- The ^{13}C nuclei are much less abundant and much less sensitive than protons. More concentrated samples and longer times are needed.
- For a given deuterated solvent, the ^{13}C and ^{1}H solvent peaks differ in multiplicities.

*Familiarity with Chapter 3 is assumed.

At first glance, some of the above summary would seem to discourage the use of ^{13}C spectra. However, the ingenious remedies for these difficulties have made ^{13}C NMR spectroscopy a powerful tool, as this chapter will confirm. In fact, side-by-side interpretation of ^{13}C and ^{1}H spectra provides complementary information.

4.2.1 ^{1}H Decoupling Techniques

In ^{1}H NMR spectra, the main peaks do not show the effects of J coupling with carbon because 98.9% of the carbon atoms are the ^{12}C isotope ($I = 0$). Protons that are coupled to the 1.1% of carbon atoms, which are ^{13}C isotopes, *do* show J coupling multiplets in the ^{1}H NMR spectra, but these weak "satellites" of the main peaks only account for 1.1% of the total spectral intensity. Conversely, because the ^{1}H isotope is nearly 100% abundant, ^{13}C NMR peaks clearly show the effects of J coupling with ^{1}H. Because of the large $^{1}J_{CH}$ values for ^{13}C—^{1}H (~110–320 Hz) and appreciable $^{2}J_{CH}$, $^{3}J_{CH}$ values for ^{13}C—C—^{1}H and ^{13}C—C—C—^{1}H (~0–60 Hz) couplings, proton-coupled ^{13}C spectra usually show complex overlapping multiplets that are difficult to interpret (Figure 4.1a); the proton-coupled ^{13}C NMR spectrum of cholesterol is hopelessly overlapped and difficult to decipher.

To alleviate this problem, an important development was the simultaneous use of proton broadband decoupling—irradiation and saturation of the attached protons—and detection of ^{13}C signals. Irradiation of the protons over a broad frequency range with composite pulse decoupling† (CPD) removes these couplings. In Figure 4.1b, the proton-decoupled ^{13}C spectrum of cholesterol shows 27 single peaks, each representing one of the carbon atoms. Before we get too far ahead of ourselves, we defer our discussions of actual interpretation of ^{13}C spectra until Sections 4.3 and 4.7.

The standard pulse program for acquiring a proton-decoupled ^{13}C NMR spectrum is shown in Figure 4.2a. The sequence consists of a relaxation delay (R_d) (see Section 4.2.3), rf pulse of tip angle θ, and signal acquisition (t). The proton channel has the decoupler on to remove the ^{1}H—^{13}C coupling, while a short, powerful rf pulse (of the order of a few microseconds) excites all the ^{13}C nuclei simultaneously. Since the transmitter frequency is slightly off

†Composite pulse decoupling relies on a continuous sequence of individual rf pulses. See Claridge (1999) in references for details.

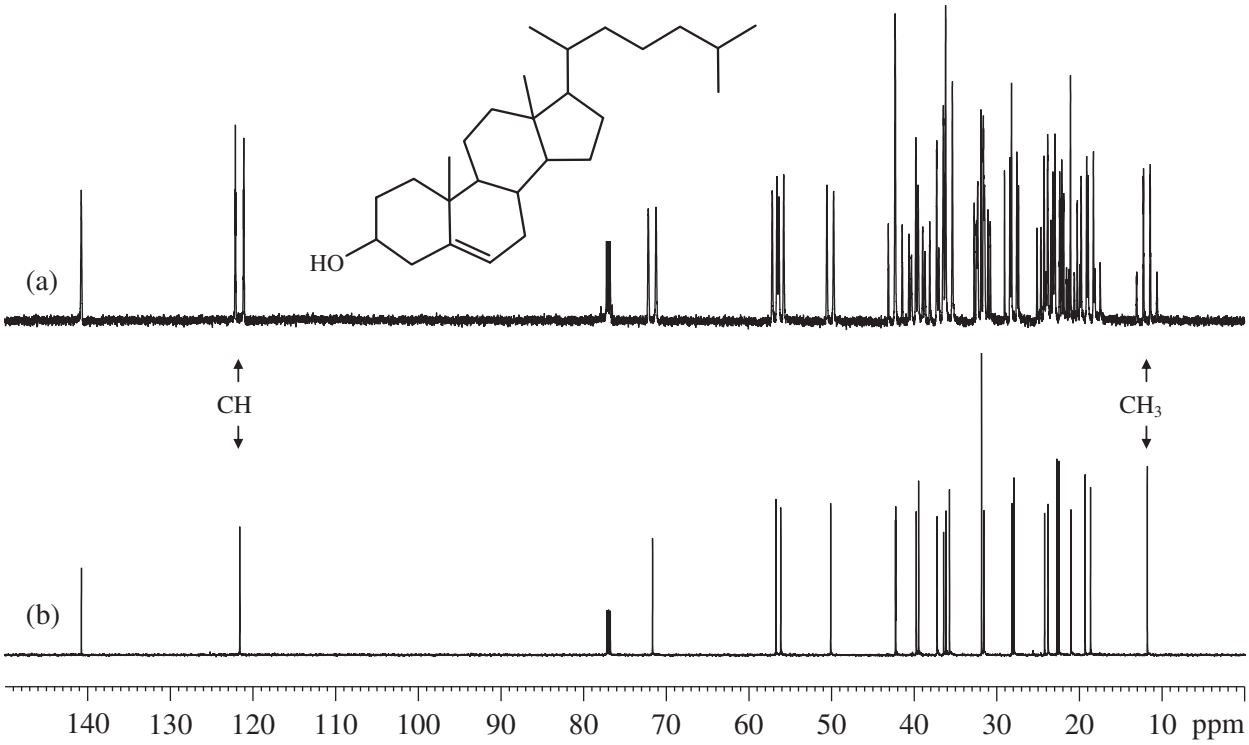

FIGURE 4.1 (a) Proton-coupled ^{13}C NMR spectrum of cholesterol. (b) Proton-decoupled ^{13}C NMR spectrum of cholesterol. Both were acquired using $CDCl_3$ as the solvent at a ^{13}C Larmor frequency of 150.9 MHz.

resonance for all the ^{13}C frequencies, each ^{13}C nucleus shows a FID, which is an exponentially decaying sine wave. The frequencies of the sine waves lead directly to the various frequencies of the peaks in the NMR spectrum.

Figure 4.2b is a presentation of the FID of the proton-decoupled ^{13}C NMR spectrum of cholesterol. Figure 4.2c is an expanded, small section of the beginning of the FID from Figure 4.2b. The complex FID is the result of a number of overlapping sine waves and interfering (beat) patterns. A series of repetitive pulses, signal acquisitions, and relaxation delays builds the signal through a process known as signal averaging. Fourier transform by the computer converts the accumulated FID (a time domain signal) to the decoupled, frequency-domain spectrum of cholesterol (at 150.9 MHz in $CDCl_3$). See Figure 4.1b.

The result, in the absence of other nuclei such as ^{2}H, ^{31}P, or ^{19}F, is a sharp peak for each chemically nonequivalent carbon in the compound, except for the infrequent coincidence of ^{13}C chemical shifts. See Figure 4.1b for the ^{1}H-decoupled ^{13}C spectrum of cholesterol and compare its simplicity with the ^{1}H-coupled spectrum in Figure 4.1a. Note that, when ^{13}C is decoupled from ^{1}H, useful information on the multiplicity of the carbon resonances is lost ($n + 1$ rule). For example, in Figure 4.1a, a methyl group is a quartet ($3 + 1$) and a methine group is a doublet ($1 + 1$). A more complete discussion of multiplets can be found in Sections 4.2.5 and 4.3. There are techniques, however, such as the DEPT sequence (Section 4.6) that supplies this information in a much simpler way.

4.2.2 Chemical Shift Scale and Range

As with ^{1}H NMR, the ^{13}C NMR frequency axis is converted to a unitless scale; this is the familiar chemical shift (δ) scale. The chemical shifts in routine ^{13}C NMR spectra range over about 220 ppm from TMS—about 20 times that of routine ^{1}H NMR spectra ($\sim$10 ppm). As a result of the large range and the sharpness of the decoupled peaks, coincidences of ^{13}C chemical shifts are uncommon, and impurities are readily detected. Often, even mixtures provide useful information. (See Appendix B for an extensive list of common impurities.) For example, diastereomers that are difficult to analyze by means of ^{1}H spectroscopy usually show distinct ^{13}C NMR spectra.

The fundamental NMR equation [$\nu = (\gamma/2\pi)\boldsymbol{B}_0$] is used to calculate the resonance frequency for the ^{13}C nucleus at a given magnetic field strength. For example, a 600 MHz instrument (for ^{1}H) is used at 150.9 MHz to produce a ^{13}C spectrum—that is, the ratio is about 4:1. The ratio of frequencies is directly related to the ratio of γ's, the magnetogyric ratios, which are (in units of 10^7 rad $T^{-1}s^{-1}$) 26.753 and 6.728 for ^{1}H and ^{13}C, respectively (see Appendix A in Chapter 6). As a quirk of history, an instrument is often referred to by its proton resonance frequency regardless of the nucleus under investigation.

Figure 4.3 gives credence to the statement that ^{13}C chemical shifts somewhat parallel to those of ^{1}H, but we note some divergences that are not readily explainable and require development of another set of interpretive skills

(see Section 4.7). In general, in comparison with ^{1}H NMR spectra, it is less advisable to attempt to correlate ^{13}C shifts with substituent electronegativity.

4.2.3 T_1 Relaxation

Unlike ^{1}H NMR spectra, the integration of which provides information on the relative numbers of protons in different chemical environments, integrations of ^{13}C peaks do not correlate with the relative number of each type of carbon atom in routine spectra. There are two major factors that account for the problem of peak intensities in ^{13}C NMR spectra:

- The spin-lattice relaxation process, quantified by a time constant, T_1 (also termed longitudinal relaxation), varies widely for carbon atoms in different functional groups and chemical environments.
- The strongest NOEs are observed for carbons with directly bonded protons (Section 4.2.4).

As discussed in Section 3.2.3, T_1 and T_2 relaxation times are short for protons resulting in intensities that are proportional to the number of protons involved and sharp peaks. In proton-decoupled ^{13}C NMR spectra, large T_1 values for quaternary carbons, caused by an absence of dipole-dipole interaction with directly attached protons, may result in detection of only a part of the possible signal, which can be overcome by inserting a longer delay interval R_d between the individual pulses (see Figure 4.2a). The relaxation delay needs to be carefully considered when acquiring ^{13}C data because signals can be missed completely if this delay is too short. For most samples, we strike a compromise between instrument time and sensitivity. Typically, a 45° pulse angle (θ) and a delay of a few seconds may be used for small molecules. For larger molecules, which usually have much shorter T_1 values, shorter relaxation delays can be used.

It may sometimes be of interest to measure T_1 values so that weak signals are not lost in the noise or in order to obtain quantitative results. The inversion-recovery method to determine T_1 is demonstrated in Figure 4.4. Generally, T_1 values decrease as the number of protons directly bonded to the ^{13}C nucleus increases. In other words, a quaternary ^{13}C nucleus gives a peak of lowest intensity as shown in Figure 4.4d; it also gives the slowest recovery in the inversion-recovery method. However, it is often difficult to differentiate between CH_3, CH_2, and CH functional groups on the basis of T_1 values alone since other factors are involved. T_1 values cover a range of several seconds for a CH_3 group to well over a minute for some quaternary ^{13}C nuclei. As a point of reference, T_1 values measured for the various carbon functional groups in 3,5-dimethyl-cyclohex-2-ene-1-one are 2 to 6 seconds for the methyls, about 3 seconds for the methylenes, 5 seconds for the methines, and 30 to 40 seconds for the quaternary carbons (Freeman and Hill, 1970). A delay between pulses of approximately $5T_1$ is recommended for a ^{13}C nucleus without an attached proton, and this appreciable delay must be tolerated (for quantitative purposes).

The overall pulse sequence in Figure 4.4a consists of the following: Relaxation—180° pulse—variable time interval—90° pulse—acquire while decoupling.

In Figure 4.4b, the net magnetization $\boldsymbol{M}_0$ is represented by the upright, boldface vector. The first pulse inverts the vector clockwise 180° to the $-z$ axis. After a short time ($\Delta\tau$), during which the arrow shows a slight recovery toward its original, upright position, a 90° pulse rotates the vector clockwise and places it along the $-y$ axis, which is toward the left at 270°. At this point, the receiver along the y axis reads the signal as slightly diminished and negative—that is, pointed down in the spectrum. The receiver accepts the usual 90° signal along the $+y$ axis as positive, hence pointing up in the phased spectrum.

In Figure 4.4c, $\Delta\tau$ has been increased so that the inverted vector was allowed to proceed further toward recovery—in fact past the null point; it is again slightly diminished and pointing up. The 90° pulse rotates it clockwise and it is recorded as a positive signal.

In Figure 4.4d, the inversion-recovery sequence is repeated eight times on diethyl phthalate (see Section 4.4 for a complete assignment of diethyl phthalate) with increasingly longer $\Delta\tau$ time increments. It is apparent that most signals have different null points indicating that they have different T_1 values. As implied above, the C═O signal at ~167 ppm has the slowest recovery in the inversion-recovery experiment. Its signal inverts between the seventh and eighth spectra, whereas the methyl signal at ~13 ppm inverts between the fourth and fifth spectra. T_1 values can be calculated with the following formula: $T_1 = t_{null}/\ln(2)$, which yields approximate values that suffice for most purposes.

4.2.4 Nuclear Overhauser Effect (NOE)

We described the nuclear Overhauser effect (NOE) involving protons in Section 3.16; we now discuss the heteronuclear NOE, which results from broadband proton decoupling in ^{13}C NMR spectra (see Figure 4.1b). The net effect of NOE on ^{13}C NMR spectra is the enhancement of peaks whose carbon atoms have directly bonded protons. This enhancement is due to the reversal of spin populations from the normal Boltzmann distribution. The total amount of enhancement depends on the theoretical maximum and the mode of relaxation. The maximum possible enhancement is equal to one-half the ratio of the nuclei's magnetogyric ratios (γ), while the actual enhancement is also proportional to the extent of $^{13}C—^{1}H$ dipolar relaxation. For a proton-decoupled ^{13}C experiment, the maximum NOE enhancement is $\gamma_H/(2)\gamma_C$ or 26.753/(2)6.728 which equals 1.98. The total sensitivity increase is therefore nearly *threefold* because the NOE enhancement is added to the original intensity.

The actual enhancement for the $^{13}C—^{1}H$ system can be anywhere from 0 to 1.98 depending on the mechanism of relaxation for each individual nucleus. In practice, for carbons with no directly bonded protons, the enhancement is

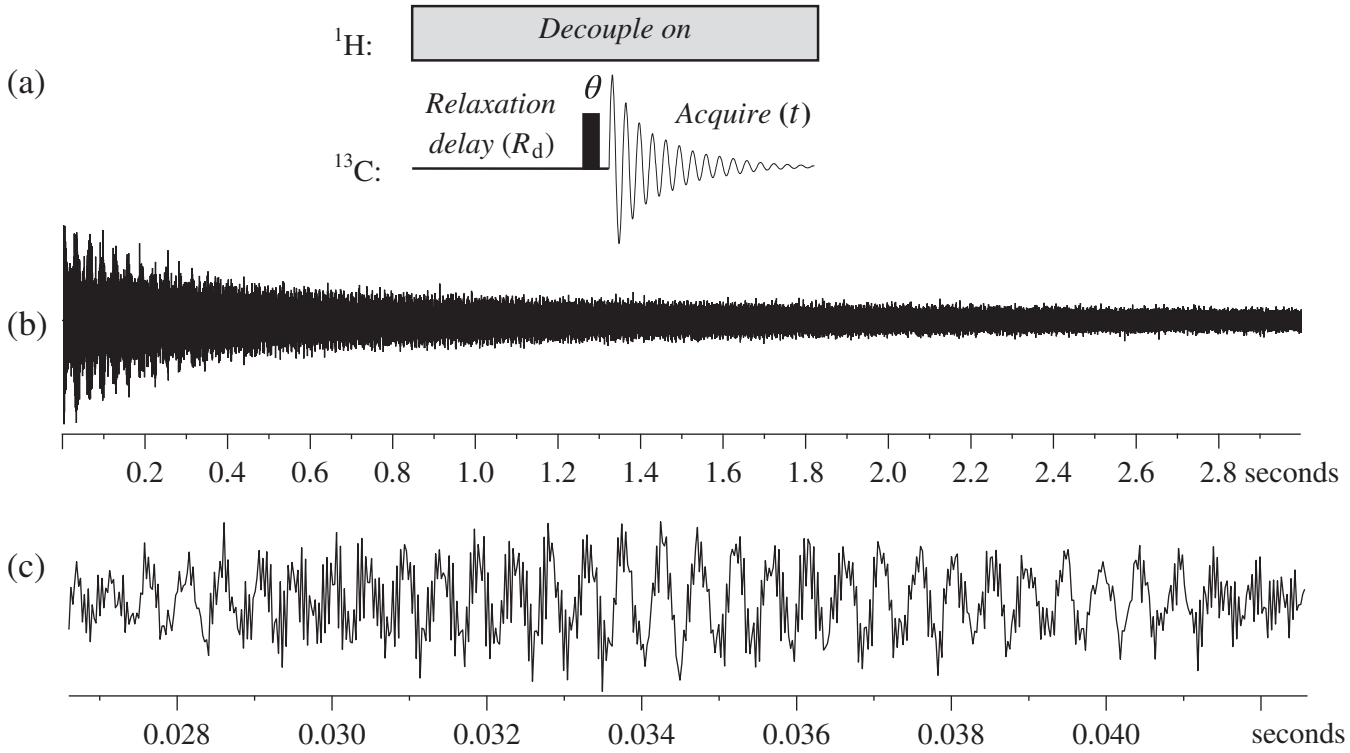

FIGURE 4.2 (a) Standard ^{13}C rf pulse sequence with proton decoupling. R_d is the relaxation delay, θ is a variable pulse angle, and t is the acquisition time. (b) FID resulting from the pulse sequence shown in (a), for cholesterol at 150.9 MHz in $CDCl_3$. (c) Expanded small section of the FID.

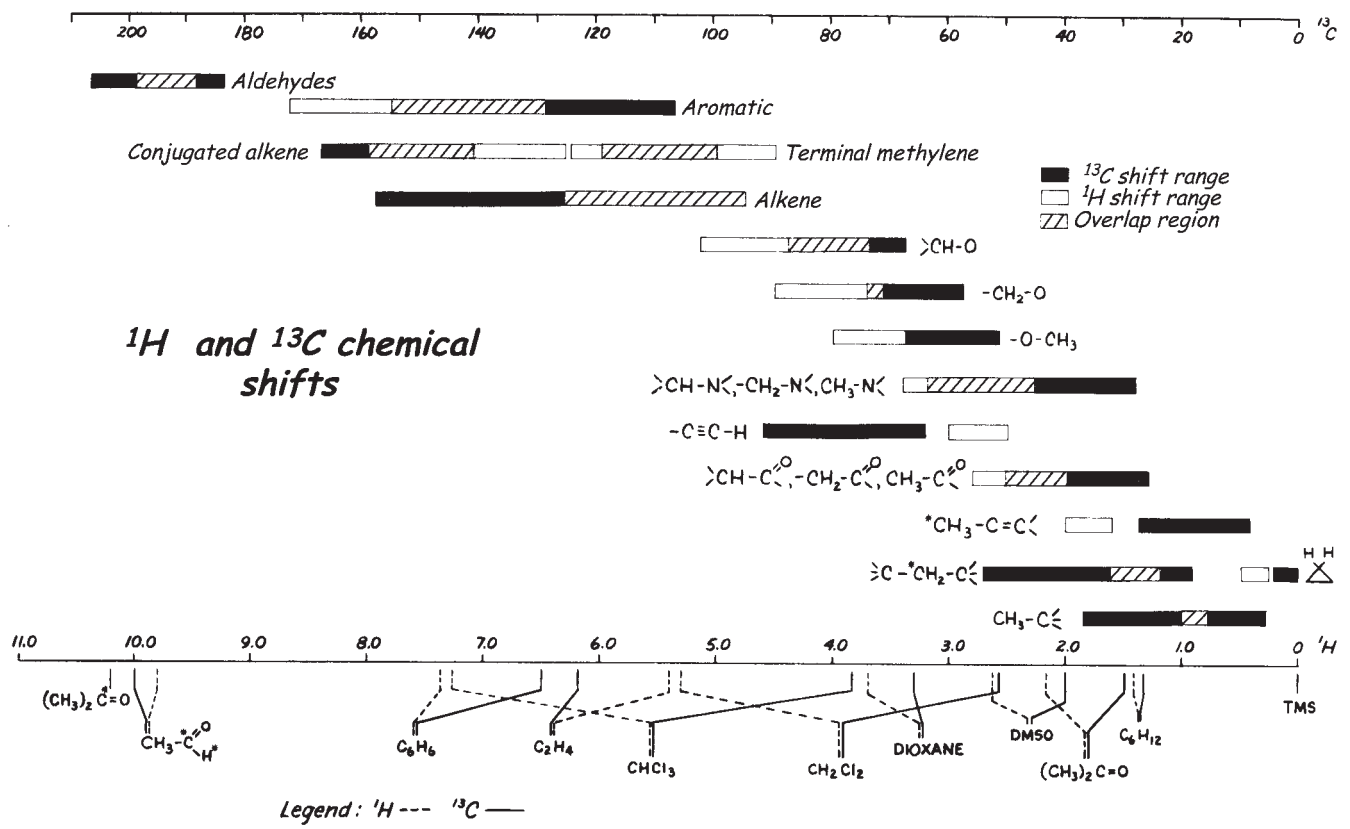

FIGURE 4.3 Comparison of ^{1}H and ^{13}C chemical shift scales.

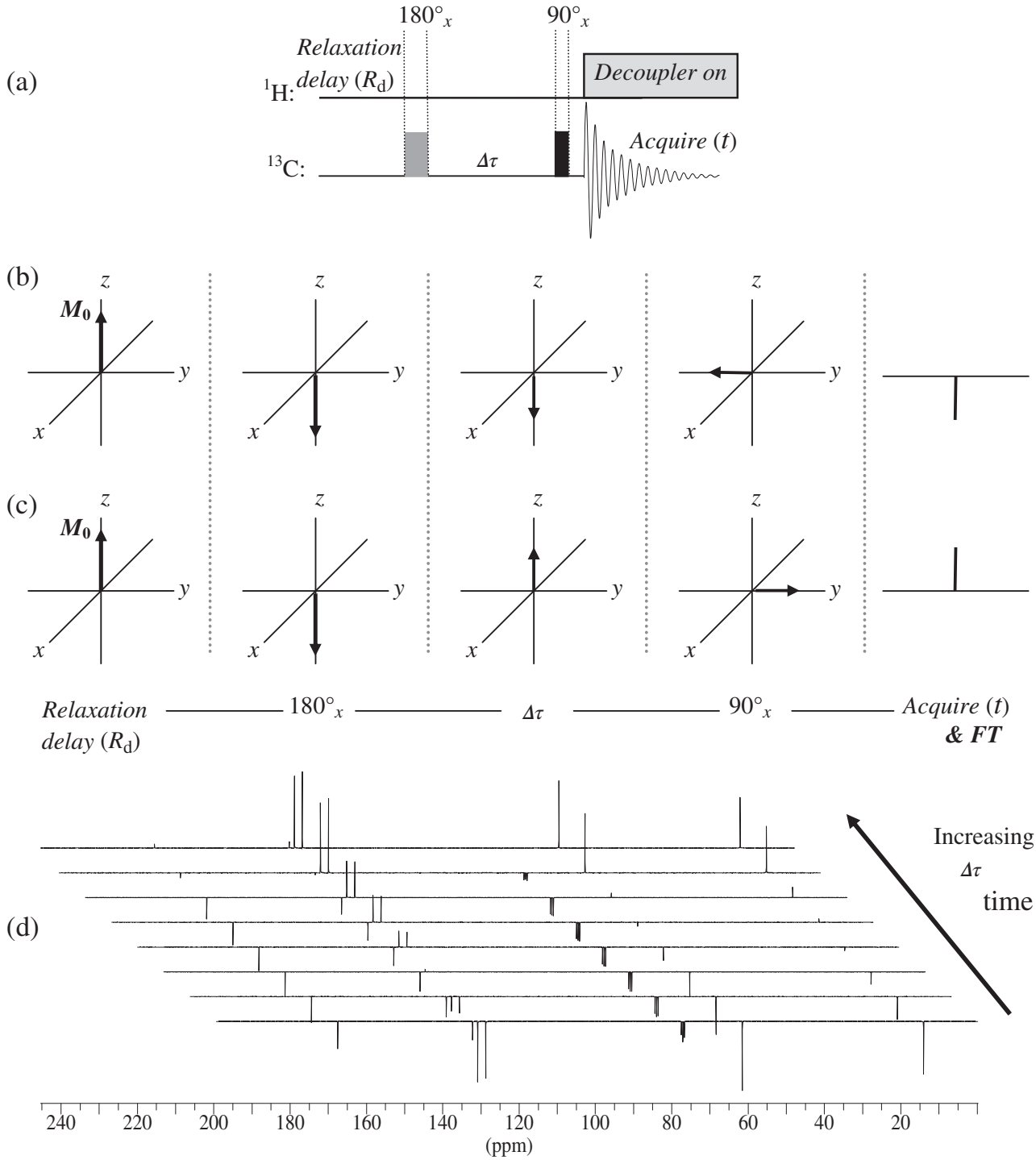

FIGURE 4.4 (a) Inversion-recovery pulse sequence with inverse-gated proton decoupling for T_1 measurement. (b) Short $\Delta\tau$ time. (c) Long $\Delta\tau$ time. (d) Example of a ^{13}C T_1 data set for diethyl phthalate at 75.5 MHz. See Section 4.3 for complete assignment of diethyl phthalate.

essentially zero since there is practically no $^{13}C—^{1}H$ dipolar relaxation. For small- to medium-sized organic molecules, $^{13}C—^{1}H$ dipolar relaxation for carbons with directly bonded protons is very efficient, yielding close to the full threefold increase in signal.

The net effect is a large reduction in the time needed to obtain a decoupled spectrum as compared with a coupled spectrum. Furthermore, this contribution to intensity increase is a nonlinear function of the number of protons directly bonded to the particular ^{13}C nucleus. ^{13}C nuclei without directly bonded protons – are characterized by peaks of distinctly low intensities (see Figure 4.1b). These erratic contributions make peak intensities unrelated to the number of ^{13}C nuclei that they should represent.

4.2.5 ^{13}C—^{1}H Spin-Spin Coupling (*J* Coupling)

Spin-spin (J) coupling constants—at least as an initial consideration—are less important in ^{13}C NMR than in ^{1}H NMR. Since routine ^{13}C NMR spectra are usually proton-decoupled, ^{13}C—^{1}H coupling values are discarded in the interest of obtaining a spectrum in a short time or on small samples—a spectrum, furthermore, free of complex, overlapping multiplets.

For the spectrum of cholesterol in Figure 4.1a, the J couplings were retained using the gated proton-decoupling technique rather than the usual, continuous, broadband decoupling. The gated proton-decoupling technique allows us to retain part of the NOE (Section 4.2.3) and still maintain C—H coupling (Figure 4.5). Briefly, the broadband proton decoupler is gated (switched) "on" during the relaxation delay period, then gated "off" during the brief acquisition period. The NOE (a slow process) builds up during the lengthy delay period (on the order of seconds). Coupling is in effect throughout the acquisition period. The result is a coupled spectrum, in which part of the NOE has been retained; thus time has been saved compared to the direct acquisition of a proton-coupled ^{13}C spectrum acquired without gated decoupling.

We demonstrated the utility of spin-spin coupling in Figure 4.1a in which the $^{1}J_{CH}$ coupling values are of interest. Table 4.1 gives some representative $^{1}J_{CH}$ values.

One-bond ^{13}C—^{1}H coupling ($^{1}J_{CH}$) ranges from about 110 Hz to 320 Hz, increasing with increased *s* character of the ^{13}C—^{1}H bond, with substitution on the carbon atom of electron-withdrawing groups, and with angular distortion. Appreciable ^{13}C—^{1}H coupling also extends over two or more (n) bonds ($^{n}J_{CH}$). Table 4.2 gives some representative $^{2}J_{CH}$ values, which range from about 5 Hz to 60 Hz.

The $^{3}J_{CH}$ values are roughly comparable to $^{2}J_{CH}$ values for sp^3 carbon atoms. In aromatic rings, however, the $^{3}J_{CH}$ values are characteristically larger than $^{2}J_{CH}$ values. In benzene itself, $^{3}J_{CH} = 7.6$ Hz and $^{2}J_{CH} = 1.0$ Hz (see Table 4.2).

Coupling of ^{13}C to several other nuclei, the most important of which are ^{31}P, ^{19}F, and ^{2}D, may be observed in proton-decoupled spectra. Representative coupling constants are given in Table 4.3.

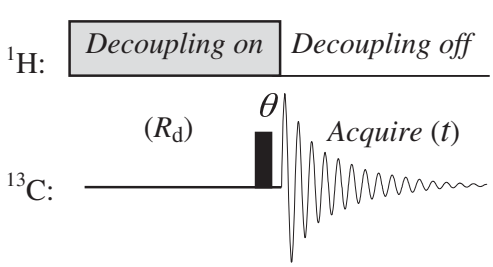

FIGURE 4.5 Gated proton-decoupling pulse sequence. R_d is the relaxation delay, θ is a variable pulse angle, and t is the acquisition time.

TABLE 4.1 Some $^{1}J_{CH}$ Values

Compound	J(Hz)
sp^3	
CH_4	125.0
CH_3CH_3	124.9
$CH_3\underline{C}H_2CH_3$	119.2
$(CH_3)_3CH$	114.2
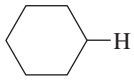	123
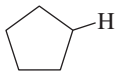	128
$PhCH_3$	129
CH_3NH_2	133
	134
$ROCH_3$	140
CH_3OH	141
CH_3Cl	150
CH_3Br	151
	161
$(CH_3O)_2C\underline{H}_2$	162
CH_2Cl_2	178
	180
	205
$CHCl_3$	209
sp^2	
$CH_3\underline{C}H{=}C(CH_3)_2$	148
$CH_2{=}CH_2$	156
C_6H_6	159
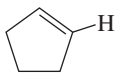	160
$C{=}C{=}C{-}H$	168
	170
$CH_3\underline{C}H{=}O$	172
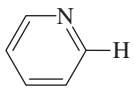	178
$NH_2\underline{C}H{=}O$	188
$=COH(OR)$	195
$CH_3\underline{C}HX$, X = halogen	198
	238
sp	
$CH{\equiv}CH$	249
$C_6H_5C{\equiv}CH$	251
$HC{\equiv}N$	269

TABLE 4.2 Some $^2J_{CH}$ Values

Compound	J(Hz)
sp^3	
$C\underline{H}_3CH_3$	−4.5
$C\underline{H}_3\underline{C}Cl_3$	5.9
$R\underline{C}(=O)C\underline{H}_3$	6.0
$\underline{C}H_3C\underline{H}=O$	26.7
sp^2	
$^*C_6H_6$	1.0
$C\underline{H}_2=\underline{C}H_2$	2.4
$C=C(\underline{C}H_3)\underline{H}$	5.0
$(C\underline{H}_3)_2\underline{C}=O$	5.5
$CH_2=\underline{C}HC\underline{H}=O$	26.9
sp	
$C\underline{H}\equiv\underline{C}H$	49.3
$C_6H_5O\underline{C}\equiv C\underline{H}$	61.0

* ^3J = 7.6 Hz (> ^2J).

TABLE 4.3 Coupling Constants for ^{19}F, ^{31}P, and ^{2}D Coupled to ^{13}C

Compound	^1J(Hz)	^2J(Hz)	^3J(Hz)	^4J(Hz)
CH_3CF_3	271			
CF_2H_2	235			
CF_3CO_2H	284	43.7		
C_6H_5F	245	21.0	7.7	3.3
$(C_4H_9)_3P$	10.9	11.7	12.5	
$(CH_3CH_2)_4P^+Br^-$	49.0	4.3		
$(C_6H_5)_3P^+CH_3I^-$	88.0	10.9		
	^1J(Hz) of CH_3 = 52			
$C_2H_5(P=O)(OC_2H_5)_2$	143	7.1 (J_{COP})	6.9 (J_{CCOP})	
$(C_6H_5)_3P$	12.4	19.6	6.7	
$CDCl_3$	31.5			
$CD_3(C=O)CD_3$	19.5			
$(CD_3)_2SO$	22.0			
C_6D_6	25.5			

4.2.6 Sensitivity

^{13}C nuclei are much less abundant and much less sensitive than protons. More concentrated samples and longer times are needed to acquire spectra with sufficient signal-to-noise ratios. Let us turn once again to the sensitivity of pulsed FT NMR experiments in which the signal-to-noise ratio (S/N) is proportional to various factors within the control of the experimentalist (see the equation given in Section 3.3.2).

S/N grows proportionately to $\sqrt{ns}$, where ns is the number of scans or repetitions of the pulse program. This relationship is not typically a problem with ^{1}H experiments, where only a few μg to a mg of material is enough to get good S/N in a few scans. As mentioned previously, ^{13}C is ~6000 times less sensitive than ^{1}H, and therefore requires either more sample (N), higher field strengths $\boldsymbol{B}_0$ (or better probe technology, i.e., a cryo-probe), or an increase in the number of scans (ns).

In most labs, the only alternative is to increase *ns,* but to double the S/N you need to take four times the number of scans, which rapidly escalates into long experiment times due to 1, 4, 16, 64, 256, 1024(1k), 2k, 4k, 16k, 64k,… scans. Another solution is presented in Section 5.4.2, in which it describes an experiment that takes advantage of the higher sensitivity of one nucleus (^{1}H) and transfers the magnetization to another less sensitive nucleus (^{13}C).

A routine ^{13}C NMR spectrum at a Larmor frequency of 75.5 MHz normally requires about 10 mg of sample in 0.5 mL of deuterated solvent in a 5 mm o.d. tube. Samples on the order of 100 μg can be handled in a probe that accepts a 2.5-mm o.d. tube, which gives higher sensitivity (see Section 3.3).

4.2.7 Solvents

Organic compounds are typically dissolved in $CDCl_3$ for ^{13}C NMR experiments, and the ^{13}C peak of the solvent is used as an internal secondary reference (77.0 ppm relative to TMS). Internal TMS may also be set to 0 ppm, if present in the solvent. A list of the common deuterated solvents is given in Appendix A.

For a given deuterated solvent, the ^{13}C and ^{1}H solvent peaks differ in multiplicities. It is worth noting the difference in appearance between the solvent peaks in a proton spectrum and a ^{13}C spectrum. For example, the familiar singlet at 7.26 ppm in a proton spectrum is the result of a small amount of $CHCl_3$ in the solvent $CDCl_3$. The ^{1}H peak is not split since ^{12}C is magnetically inactive, and the $^{35/37}$Cl nuclei have strong electric quadrupole moments. The small amount of ^{13}C present is insufficient to produce a visible doublet (see Section 3.7). In the case of another useful solvent, dimethyl-d_6 sulfoxide, the quintet at 2.49 ppm in a proton spectrum is a result of the proton in the impurity split by D_2: $\mathbf{H}CD_2—S(=O)—CD_3$. The proton peak is split by two deuterium nuclei with nuclear spin quantum numbers (I) of one. The multiplicity can be calculated by the familiar formula $2nI + 1$; thus $2 \times 2 \times 1 + 1 = 5$. The $—CD_3$ group does not interfere because it comprises a different spin system.

In a typical ^{13}C NMR spectrum, $CDCl_3$ gives a triplet centered at 77.0 ppm. But now the presence of small amount of $CHCl_3$ is irrelevant since all protons are decoupled by the usual broadband decoupling and because the signal from $CDCl_3$ is much stronger. The triplet results from splitting of the ^{13}C peak by the D nucleus. The formula $2nI + 1$ gives $2 \times 1 \times 1 + 1 = 3$. The intensity ratios are 1:1:1. In the case of $\mathbf{C}D_3S(=O)CD_3$, the formula gives $2 \times 3 \times 1 + 1 = 7$. The multiplet at 39.7 ppm is a septet with a coupling constant of 21 Hz; the intensity ratios are 1:3:6:7:6:3:1 (see Appendix A). The following diagram is the deuterium analogue of Pascal's triangle for protons (see Figure 3.22 for ^{1}H equivalent).

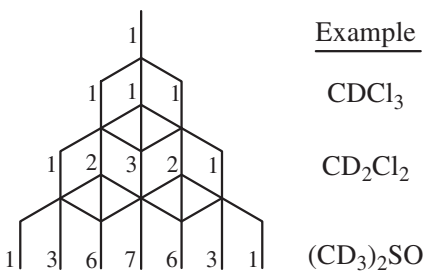

Substitution of D for H on a carbon atom results in a dramatic diminution of the height of the ^{13}C signal in a proton-decoupled spectrum for the following reasons. Since deuterium has a spin number of 1 and a magnetogyric ratio $\frac{1}{6.5}$ that of ^{1}H, it will split the ^{13}C peak into three lines (ratio 1:1:1) with a J value equal to $0.154 \times J_{CH}$. Furthermore, T_1 for $^{13}C—D$ is longer than that for $^{13}C—^{1}H$ because of decreased dipole-dipole relaxation. Finally, the NOE is lost, since there is no irradiation of deuterium.* A separate peak may also be seen for any residual $^{13}C—^{1}H$ since the isotope effect usually results in a slight shift to lower frequency of the $^{13}C—D$ peak (~0.2 ppm per D atom). The isotope effect may also slightly shift the ^{13}C peak positions relative to those in the same nondeuterated solvent. As an example, pure deuterated benzene, a common NMR solvent, gives a 1:1:1 triplet centered at 128.0 ppm in a decoupled spectrum; J is 25 Hz. Under the same conditions, pure benzene (C_6H_6) gives a singlet at 128.5 ppm (see Table 4.12 and Appendix A).

4.3 INTERPRETATION OF A SIMPLE ^{13}C NMR SPECTRUM: DIETHYL PHTHALATE

Even though we have not discussed the chemical shifts of the different functional groups (Section 4.7), it is possible to discuss the peak assignments of diethyl phthalate from what we do know: peak intensities, $^{13}C—^{1}H$ coupling, and an expectation of chemical shifts relative to what we know for ^{1}H. The T_1 and NOE affect the peak intensities and the latter are therefore not representative of the relative number of different types of carbon atoms: this, however, results in an advantage. It is usually possible by inspection of the ^{13}C spectrum to recognize the nuclei that do not bear protons by their low intensity (Figure 4.6a, C═O and the peak labeled 1). The common spin-lattice relaxation mechanism for ^{13}C results from dipole-dipole interaction with directly bonded protons. Thus, nonprotonated carbon atoms have longer T_1 relaxation times, which together with little or no NOE, results in low-intensity peaks. It is therefore often possible to recognize carbonyl groups (except formyl), nitriles, nonprotonated alkene and alkyne carbon atoms, and other quaternary carbon atoms readily.

Since diethyl phthalate ($C_{12}H_{14}O_4$) has an axis of symmetry (and a plane of symmetry), the proton-decoupled ^{13}C NMR spectrum in Figure 4.6a consists of six peaks. Since there is no coupling, the peaks are singlets, and there is no overlap. We examine the chemical shifts and observe similarities with ^{1}H chemical shifts (see Figure 4.3 and Appendix C). For example, we can place the alkyl groups on the right-hand side of the ^{13}C NMR spectrum with the deshielded CH_2 group to the left of the CH_3 group. It seems safe to designate the strongly deshielded cluster of three peaks as aromatic. The C═O group is on the far left. We also note that the ^{13}C aromatic nucleus (labeled 1) without an attached proton gives a peak that is distinctly decreased in height relative to the protonated aromatic carbon atoms. The same applies to the C═O group.

The ^{1}J coupling in Figure 4.6b provides the multiplicities; that is, the number of protons that are directly bonded to each carbon atom. These couplings confirm our chemical shift assignments. Thus, from right to left, we see the quartet of the CH_3 group (the $n + 1$ rule) and triplet of the CH_2 group. Then there is a cluster of the two doublets of the two aromatic CH groups and the singlet of the carbon atom to which no proton is directly bonded (labeled 1). Finally, there is the C═O singlet at higher frequency.

In Figure 4.6c, we see the expansion of the quartet shown in Figure 4.6b, each peak of which is a triplet resulting from ^{2}J coupling of the methyl ^{13}C nucleus with the protons of the adjacent CH_2 group. These ^{2}J couplings are much smaller than the ^{1}J couplings.

In Figure 4.6d, we see the expansion of the CH_2 triplet shown in Figure 4.6b, each peak of which is a quartet resulting from ^{2}J coupling with the CH_3 protons. In Figure 4.6e, we see the expansion of the right-hand doublet of the aromatic cluster labeled 2 in Figure 4.6b. Each peak of this doublet is split by ^{2}J and ^{3}J coupling of the neighboring protons.

The expansion shown in Figure 4.6f is the other aromatic doublet shown in Figure 4.6b labeled 3. Each peak of the doublet is split by either ^{2}J or ^{3}J coupling. Also in the same panel is the expansion of the singlet remaining in the aromatic cluster of Figure 4.6b. The singlet is not split by a large coupling since there is no attached proton. It is split only by the small ^{2}J and ^{3}J couplings and is readily assigned to the carbon nucleus labeled 1.

Carbon atom 2 is *ortho* and *meta* to the substituents, and carbon atom 3 is *meta* and *para.* Use of Table 4.12 (Section 4.7.4) gives 129.6 ppm for peak 2 and 133.2 ppm for peak 3. Measurements of peaks in Figure 4.6 give 128.5 ppm for peak 2 and 131.2 ppm for peak 3. Reasonable, but perhaps unexpected to some who recall from Chapter 3 that a carbonyl substituent deshields the *ortho* position of protons more so than the *para* position. Chart D.1 in Chapter 3 confirms this impression, at least for a single carbonyl substituent. And the result of comparing *ortho* and *meta* with *meta* and *para* gives the expected results for the ^{1}H chemical shifts: 8.0 ppm for peak 2 and 7.60 ppm for peak 3.

4.4 QUANTITATIVE ^{13}C ANALYSIS

Quantitative ^{13}C NMR is desirable in two situations. First, in structure determinations, it is clearly useful to know whether a signal results from more than one chemically equivalent

*The same explanation also accounts for the relatively weak ^{13}C signal shown by deuterated solvents. In addition, small solvent molecules tumble rapidly; this rapid movement makes for a longer T_1, hence for less intense peaks in the absence of complete ^{13}C relaxation. Deuterated chloroform, $CDCl_3$, shows a 1:1:1 triplet, deuterated *p*-dioxane a 1:2:3:2:1 quintet, and deuterated DMSO a 1:3:6:7:6:3:1 septet in accordance with the $2nI + 1$ rule (Chapter 3). The chemical shifts, coupling constants, and multiplicities associated with the ^{13}C atoms of common NMR solvents are given in Appendix A.

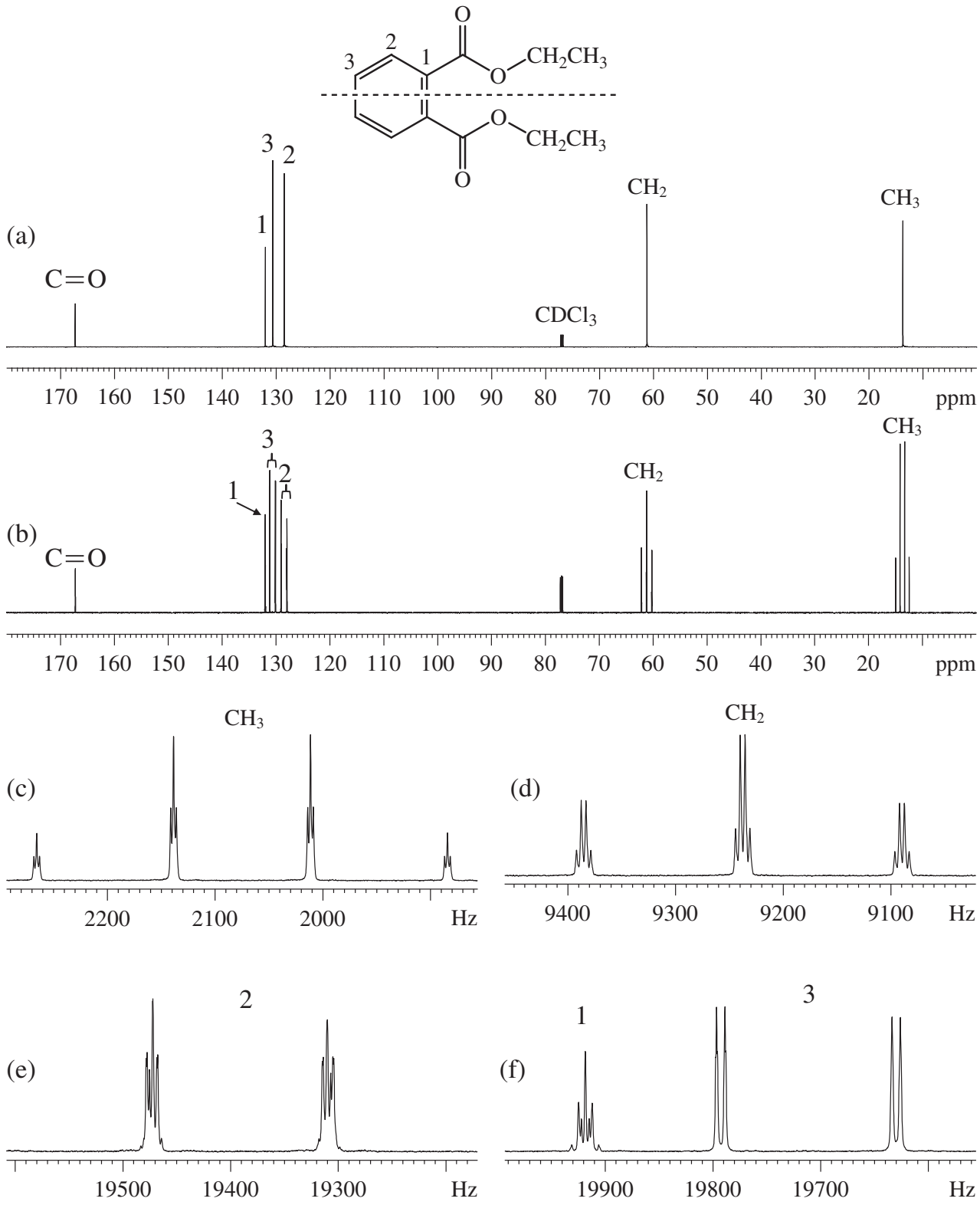

FIGURE 4.6 (a) Proton-decoupled ^{13}C NMR spectrum of diethyl phthalate at a Larmor frequency of 150.9 MHz in $CDCl_3$, (b) proton-coupled ^{13}C NMR spectrum, and (c–f) expansions of the proton-coupled ^{13}C NMR spectrum.

carbon. Second, quantitative analysis of a mixture of two or more components requires that the area of the peaks be proportional to the number of carbons atoms causing that signal.

There are two reasons that broadband-decoupled ^{13}C NMR spectra are usually not susceptible to quantitative analysis:

- ^{13}C nuclei with long T_1 relaxation times may not return to the equilibrium Boltzmann distribution between pulses. Thus, the signals do not achieve full amplitude (see Section 4.2.3).
- The enhancement due to the NOE (see Section 4.2.4) varies among ^{13}C nuclei, and the signal intensities vary accordingly.

In Section 4.2.5, we discussed the gated proton-decoupling technique. The purpose was to develop a high level of the nuclear Overhauser effect so that a coupled spectrum could be achieved in the least time. In the present section, we deal with the inverse-gated proton-decoupling technique. The proton decoupler is gated off at the beginning of the relaxation delay and gated on at the beginning of the acquisition period (see Figure 4.7). The purpose is to maintain a low, constant level of NOE (ideally zero). This is feasible because the NOE builds up slowly during the relatively brief time of the signal-acquisition period (t). The overall result is a spectrum consisting of singlets whose intensities correspond to the number of ^{13}C nuclei they represent. Lest we forget, we must still allow for the T_1 relaxation delay (R_d).

Figure 4.8 demonstrates the effects of T_1 and NOE on the peak intensities. Figure 4.8a is a standard proton-decoupled ^{13}C NMR spectrum with R_d set to $<T_1$; notice that the integrated intensity of the peak due to the methyl carbon is set to one and the rest of the integrals are labeled above the peaks. The spectrum is not quantitative due to NOE and T_1 effects. In Figure 4.4d (Section 4.2.3), the protonated aromatic carbons showed the shortest T_1 values, which explains the larger integrals of those peaks. The spectrum in Figure 4.8b was obtained using the inverse-gated proton-decoupling technique. Notice that by removing the NOE, the intensities of the peaks due to carbon atoms with directly bonded hydrogens are more quantitative than the ones that are quaternary. R_d is still less than T_1. Figure 4.8c illustrates that, by using long relaxation delays ($R_d > 5T_1$) and by minimizing the NOE by using the inverse-gated proton-decoupling technique, ^{13}C data can be quantitative. The drawback is that it takes a long time to acquire the data because the relaxation delay has to be set to at least five times the expected T_1 and the loss of the NOE means many more repetitions are needed to build up the signal intensity. The time required can be reduced by addition of a paramagnetic relaxation reagent. A common procedure is to add a trace amount of chromium (III) acetylacetonate ($Cr(acac)_3$), a paramagnetic substance, whose unpaired electrons efficiently reduce the T_1 and T_2 relaxation times.

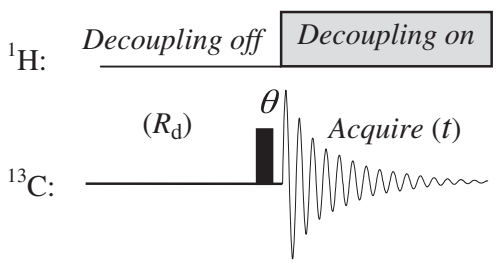

FIGURE 4.7 Inverse-gated proton-decoupling pulse sequence. R_d is relaxation delay, θ is a variable pulse angle, and t is the acquisition time.

4.5 CHEMICAL EQUIVALENCE

The definition of chemical equivalence given for protons also applies to carbon atoms: interchangeability by a symmetry operation or by a rapid mechanism. The presence of equivalent carbon atoms (or coincidence of shift) in a molecule results in a discrepancy between the apparent number of peaks and the actual number of carbon atoms in the molecule.

Thus the three ^{13}C nuclei of the methyl groups in *t*-butyl alcohol (Figure 4.9) are chemically equivalent by rapid rotation in the same sense in which the protons of a methyl group are chemically equivalent. The ^{13}C NMR spectrum of *t*-butyl alcohol shows two peaks, one much more intense than the other; the carbinyl carbon peak (quaternary) is much less intense than the peak representing the carbon atoms of the methyl groups.

In the chiral molecule 2,2,4-trimethyl-1,3-pentanediol (Figure 4.10) at 75.5 MHz, we note that CH_3(a) and CH_3(b) are not chemically equivalent and two peaks are seen. Even though the two methyl groups labeled c and c′ are not chemically equivalent, they coincidently show only one peak. Two peaks are seen at higher field strength (150.9 MHz). Note that the lowercase letters used to label the atoms are not related to their Pople notation.

In Section 3.8.3.2, we noted that the CH_3 protons of $(CH_3)_2NCH{=}O$ gave separate peaks at room temperature, but became chemically equivalent at about 123°. Of course, the ^{13}C peaks show similar behavior.

4.6 DEPT

Broadband proton decoupling of ^{13}C NMR spectra is a mixed blessing. On the one hand, the simplicity of a spectrum with a single peak for each unique carbon atom in the molecule is extremely attractive. On the other hand, $^1H{-}^{13}C$ coupling information is valuable and clearly useful in determining structure. There have been many experiments developed over the years attempting to usefully tap this information and still maintain the simplicity of the completely decoupled spectrum. Two are worth mentioning because both were popular at one time and both are common in older literature.

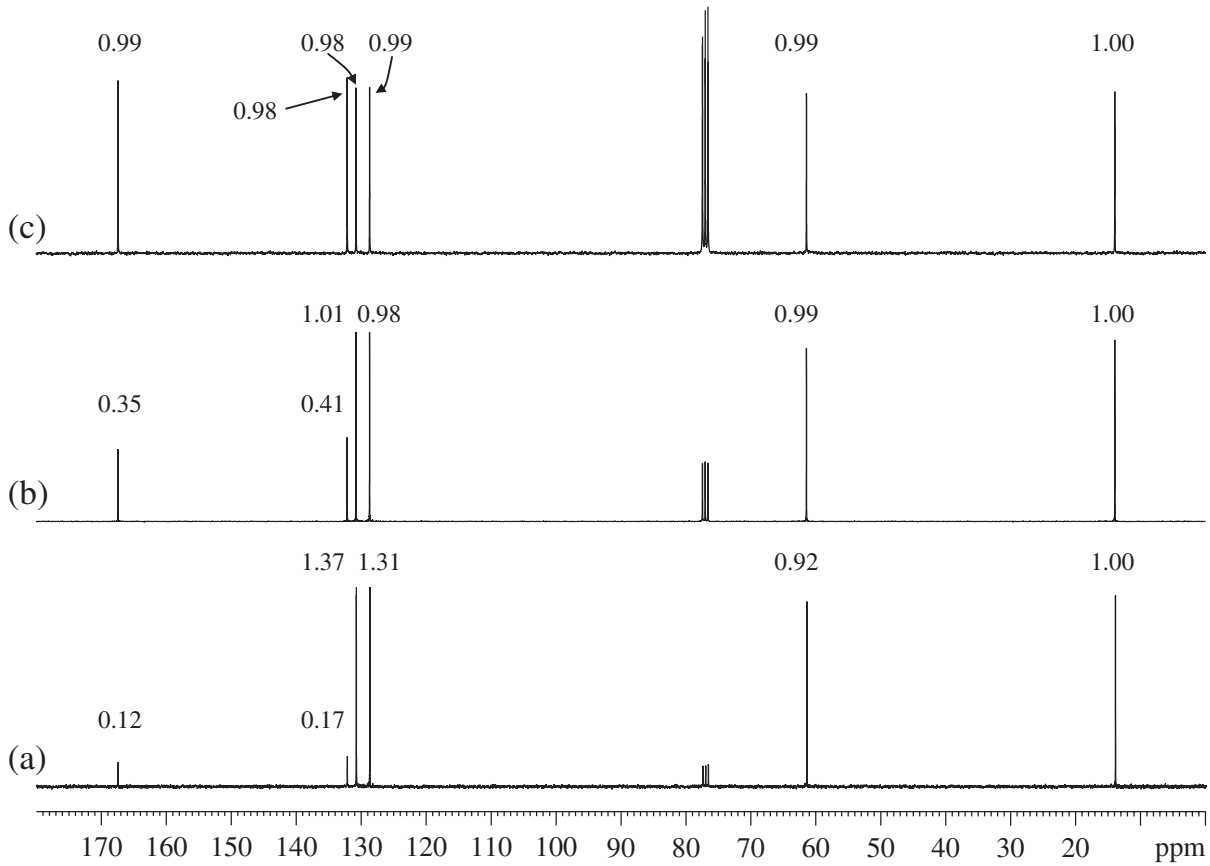

FIGURE 4.8 (a) Standard ^{1}H-decoupled ^{13}C NMR spectrum of diethyl phthalate with relaxation delay (R_d) < T_1, (b) inverse-gated proton-decoupling technique with $R_d < T_1$ and (c) $R_d > 5T_1$ and inverse-gated decoupling to compensate for NOE. The number above each peak represents its integrated value. Spectra recorded at 150.9 MHz in $CDCl_3$.

Also, some of the terminology that we use today grew from one of these experiments.

The first of these now obsolete experiments is called the off-resonance ^{1}H-decoupled spectrum. In this experiment, the ^{1}H—^{13}C coupling is restricted to one bond (i.e., each carbon only shows coupling to its directly bonded protons) by moving the broadband decoupler "off-resonance" or away from the middle of the proton chemical shift range. Note that the apparent value of the one-bond J_{CH} coupling constant is reduced from its true value as a result of this off-resonance decoupling. Thus, each carbon resonance gives a singlet (no attached protons), a doublet (one attached proton), a triplet (two attached protons), or a quartet (three attached protons). Note that these patterns are an application of first-order coupling rules and the $n + 1$ rule. This experiment also gave rise to the common practice (still used today) of referring to a

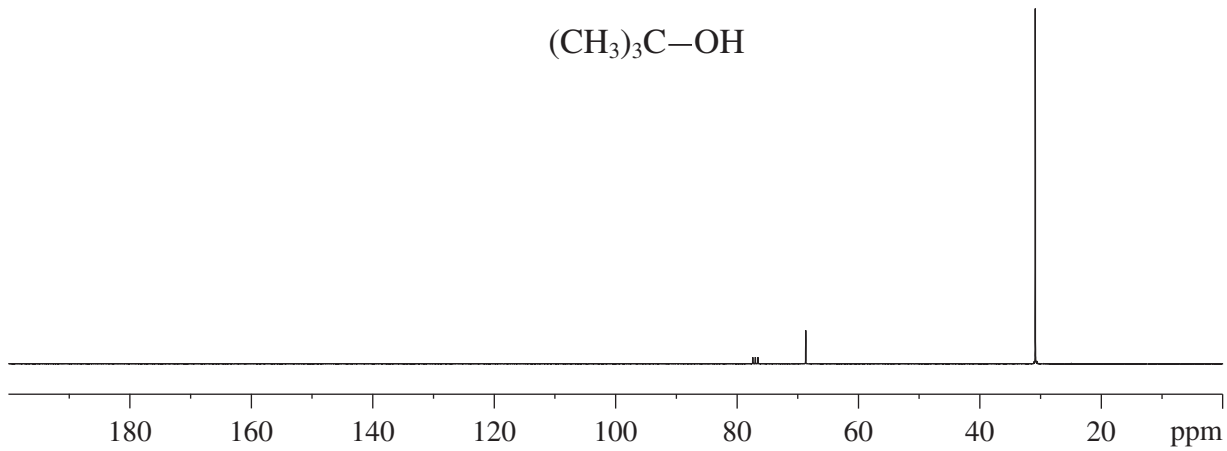

FIGURE 4.9 ^{1}H-decoupled ^{13}C NMR spectrum of *t*-butanol at 75.5 MHz, in $CDCl_3$.

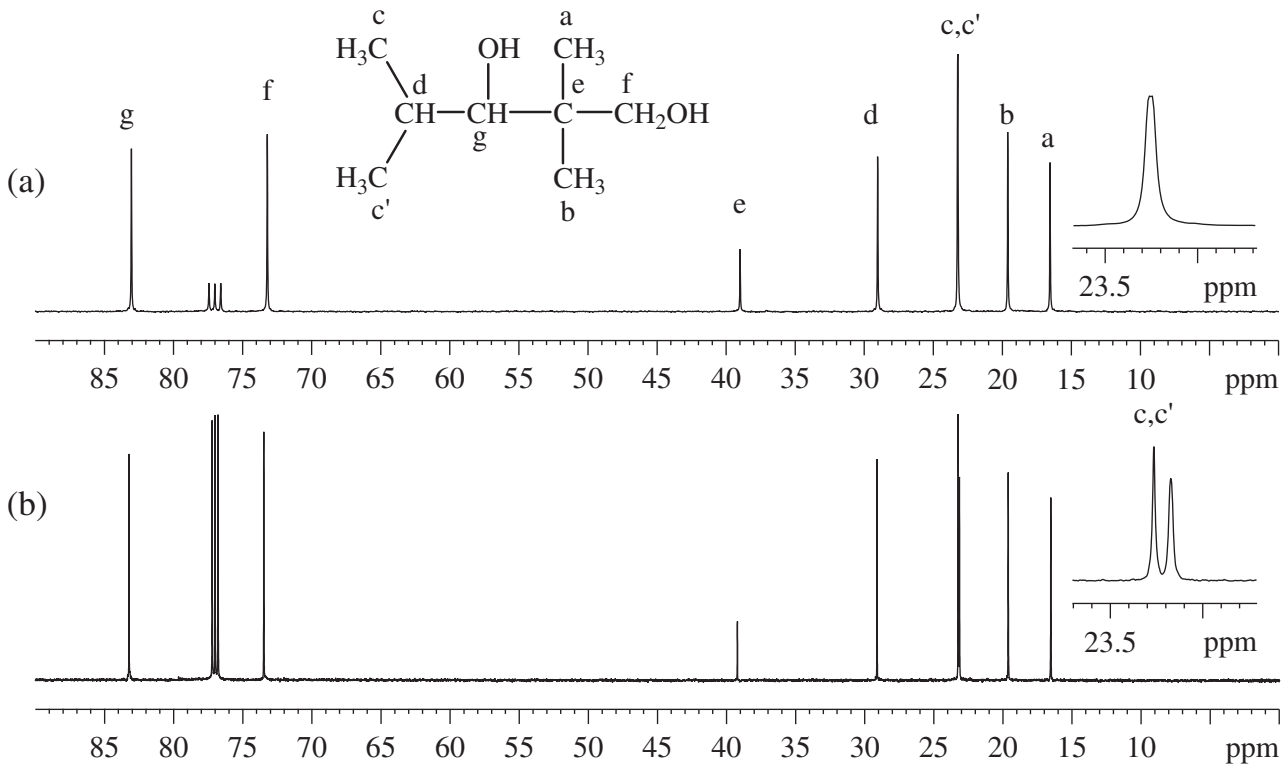

FIGURE 4.10 (a) ^{1}H-decoupled ^{13}C NMR spectrum of 2,2,4-trimethyl-1-3-pentanediol in $CDCl_3$ at a Larmor frequency of 75.5 MHz. (b) Same as (a) but at a Larmor frequency of 150.9 MHz.

carbon resonance by its "multiplicity" ("s," "d," "t," or "q"). We use these descriptions of multiplicity whether or not we use this experiment.

The other experiment worth mentioning, which, by the way, is also obsolete, is the attached proton test or APT. This experiment is based on the different values of the ^{1}H—^{13}C J coupling constant for methine, methylene, and methyl groups. By adjusting certain delays in the pulse sequence (not shown), quaternary and methylene carbons could be phased up, and methine and methyl carbons could be phased down. Since phase is arbitrary, this order could be reversed. This ability to distinguish of carbon types by the magnitude of their respective coupling constants led to the now popular DEPT experiment.

The DEPT (distortionless enhancement by polarization transfer) sequence has developed into the preferred procedure for determining the number of protons directly bonded to various ^{13}C nuclei. The DEPT experiment can be done in a reasonable time and on small samples; in fact, it is several times more sensitive than the usual ^{13}C procedure. DEPT is now routine in many laboratories and is widely used in the Student Exercises in this textbook. The novel feature in the DEPT sequence is a variable proton pulse angle θ (see Figure 4.11) that is set at 90° for one subspectrum, and 135° for a second, separate experiment.

The DEPT spectra of ipsenol are shown in Figure 4.12. We see in Figure 4.12a a standard ^{1}H-decoupled ^{13}C spectrum; the middle spectrum, Figure 4.12b, is a DEPT 135 where the peaks associated with CH_3 and CH groups are phased up, whereas the peaks due to CH_2 groups are phased down. The top spectrum, Figure 4.12c, is a DEPT 90, where only CH carbons are detected. Quaternary ^{13}C atoms are not detected in the DEPT subspectra. We can now interpret the ^{13}C peaks in the main spectrum as CH_3, CH_2, CH, or C by examining the two subspectra peaks along with the main spectrum. The easiest way to approach the interpretation of the ^{13}C-DEPT spectra is to first look for peaks that are in the ^{1}H-decoupled ^{13}C spectrum and not in either of the other two DEPT spectra. These are identified as being quaternary (no protons attached). Next, look at the DEPT 135 and label all the CH_2 peaks; they are easily identified because they are phased down. Finally, identifying CH_3 peaks versus CH peaks is accomplished by inspection of the DEPT 135 versus

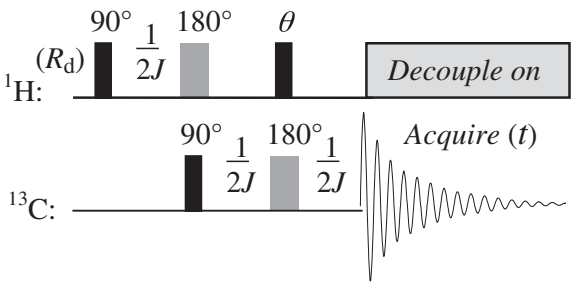

FIGURE 4.11 DEPT pulse sequence. Based on an approximate average J_{CH} value of 145 Hz, $\frac{1}{(2J)}$ is 3.45 ms. R_d is the relaxation delay, θ is a variable pulse angle, and t is the acquisition time.

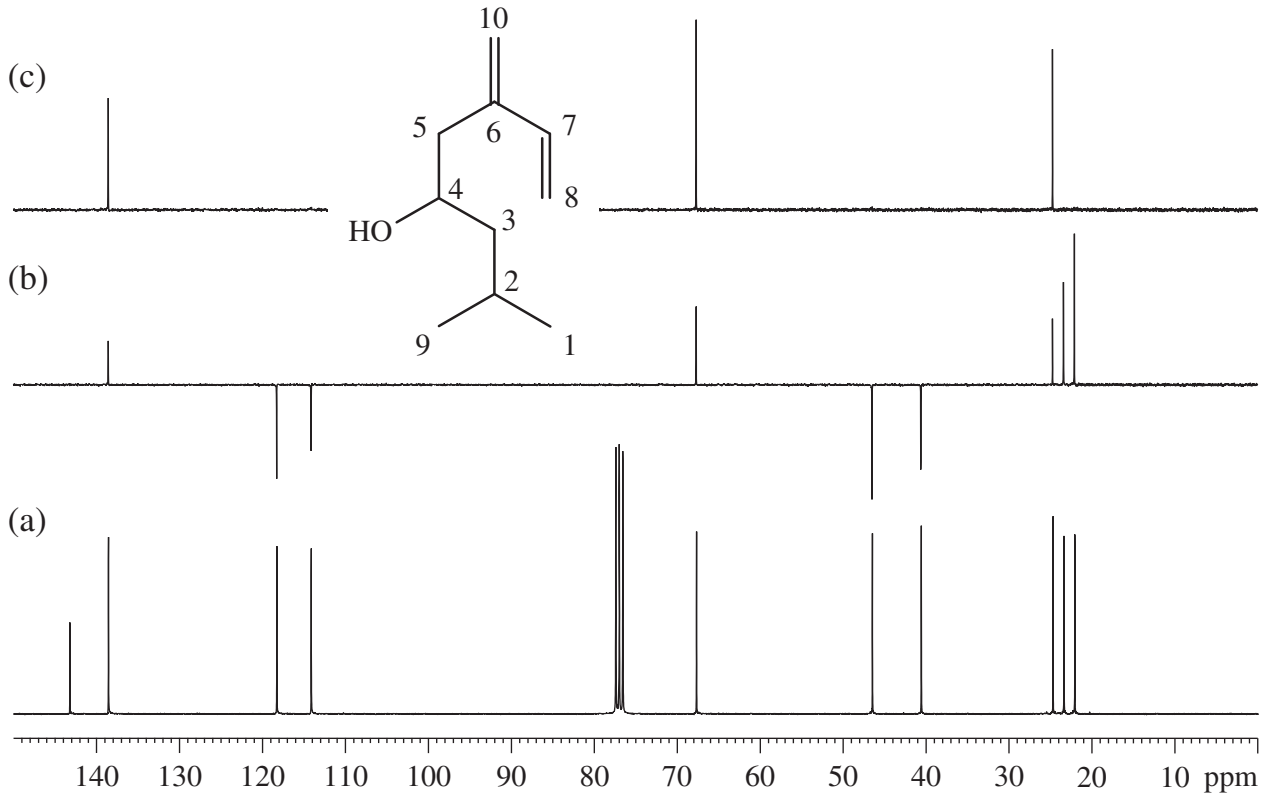

FIGURE 4.12 (a) Standard proton-decoupled ^{13}C NMR spectrum of ipsenol in $CDCl_3$ at 75.5 MHz. DEPT subspectra: (b) DEPT 135° (CH and CH_3 up, CH_2 down); (c) DEPT 90° (CH only).

the DEPT 90. The DEPT 90 has only CH carbons, so by difference the rest that are phased up in the DEPT 135 are due to CH_3 groups.

To illustrate the simplicity of interpreting ^{13}C-DEPT spectra, we return to ipsenol in Figure 4.12, starting at the high-frequency peak at the left end of the main spectrum. We note that there are no peaks directly aligned above in the subspectra; therefore, this peak in the main spectrum is due to a quaternary carbon atom, that is, no directly bonded protons. The next peak to the right in the main spectrum is a CH peak, since the peak aligned in the lower subspectrum is pointed up, as is the aligned peak in the upper subspectrum. The next two peaks in the main spectrum are CH_2 peaks, since the aligned peaks in the lower subspectrum are pointed down. The next peak to the right of the solvent peak (a triplet for $CDCl_3$) is another CH peak. The next two peaks are CH_2 peaks. The next peak is again associated with a CH group. The next two are due to CH_3 groups since the aligned peaks in the lower subspectrum are pointed up, and there are no aligned peaks in the upper subspectrum. Summing up, we have (in order of decreasing frequency)

6	7	8	10		4	5	3	2	1	9
C,	CH,	CH_2,	CH_2,	solvent,	CH,	CH_2,	CH_2,	CH,	CH_3,	CH_3

Interpretation of the various DEPT spectra takes a bit of practice, but the results are most instructive. Not only do we have the number of carbon and hydrogen atoms, but now we have the chemical shifts of the carbon atoms and the number of hydrogen atoms attached to each carbon. However, there is a discrepancy between the proton count (see Figure 3.42 for ^1H spectrum for confirmation) in the proton spectrum and in the DEPT spectrum, since the OH is not accounted for in the DEPT spectrum nor are protons that are attached to other atoms such as nitrogen, sulfur, silicon, or phosphorus. It is not difficult to correlate the DEPT spectrum with the ^1H spectrum. In fact, it is striking to observe how resonances due to the alkenyl and alkyl groups are widely separated in both spectra.

4.7 CHEMICAL CLASSES AND CHEMICAL SHIFTS

In this section, chemical shifts will be discussed under the headings of the common chemical classes of organic compounds. As noted earlier, the range of shifts generally encountered in routine ^{13}C NMR studies is about 220 ppm.

Trends in ^{13}C chemical shifts somewhat parallel those of ^1H, so some of the empirical rules developed for assigning ^1H NMR spectra may carry over to ^{13}C NMR spectra. Furthermore, the concept of additivity of substituent effects (see Sections 4.7.1 and 4.7.6) is useful for both nuclides. In some case, the ^{13}C shifts may be rationalized by considering

hybridization, substituent electronegativity, and diamagnetic anisotropy (to a lesser extent); solvent effects are important in both spectra. As for ^{1}H chemical shifts, it is important to remember that such rationalizations are empirical and will not work in every case. Chemical shifts for ^{13}C are affected by substitutions as far removed as the δ position; in the benzene ring, pronounced shifts for ^{13}C are caused by substituents at the point of attachment and at the *ortho, meta,* and *para* positions. The ^{13}C chemical shifts are also decreased significantly by the *γ-gauche* effect (see Section 4.7.1). Decreases in the chemical shift by as much as several ppm may occur on dilution. Hydrogen bonding effects with polar solvents may result in increased chemical shifts.

As with other types of spectroscopy, peak assignments are facilitated by comparison with those of reference compounds. Reference material for many classes of compounds has accumulated in the literature. The starting point is a general correlation chart for ^{13}C chemical shifts of the major chemical classes (see Figure 4.3 and Appendix C); then, minor changes within these regions are correlated with structure variations in the particular chemical class. The chemical shift values in the following tables must not be taken too literally because of their variation with solvent and concentration. For example, the C═O peak of acetophenone in $CDCl_3$ appears 2.4 ppm higher than that in CCl_4; the effect on the other carbon atoms of acetophenone ranges from 0.0 to 1.1 ppm. Furthermore, much of the early work used various reference compounds, and the values were corrected to give parts per million from TMS.

A ^{13}C NMR spectrum will often distinguish substitution patterns on an aromatic ring. If, for example, there are two identical (achiral) substituents, the symmetry elements alone will distinguish among the *para, ortho,* and *meta* isomers if the chemical shifts of the ring carbon atoms are sufficiently different. The *para* isomer has two rotational symmetry axes and two mirror planes. The *ortho* and *meta* isomers have one rotational axis and one mirror plane, but in the *meta* isomer the elements pass through two atoms. There is also a symmetry plane in the plane of the ring in each compound, which does not affect the ring carbon atoms.

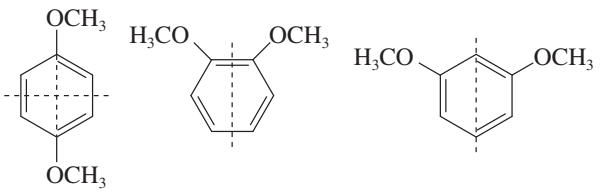

The aromatic region of the ^{13}C NMR spectrum for the *para* isomer shows two peaks; for the *ortho* isomer, three peaks; and for the *meta* isomer, four peaks. The quaternary carbon peaks are much less intense than the unsubstituted carbon peaks.

The additivity of shift increments is demonstrated in the following sections.

4.7.1 Alkanes

4.7.1.1 Linear and Branched Alkanes. We know from the general correlation chart (Appendix C) that alkane groups unsubstituted by heteroatoms have ^{13}C chemical shifts of about 60 ppm. (Methane has a ^{13}C chemical shift of −2.5 ppm.) Within this range, we can predict the chemical shifts of individual ^{13}C atoms in a straight-chain or branched-chain hydrocarbon from the data in Table 4.4 and the empirical formula given below.

This table shows the additive shift parameters (A) in hydrocarbons: the α effect of +9.1, the β effect of +9.4 ppm, the γ effect of −2.5, the δ effect of +0.3, the ϵ effect of +0.1, and the corrections for branching effects. The empirical (and observed) shifts for the carbon atoms of 3-methylpentane are

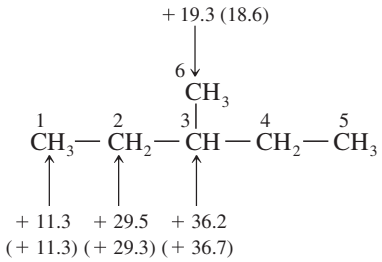

Calculations of the chemical shifts are made from the formula: $\delta = -2.5 + \Sigma nA$, where δ is the predicted shift for a carbon atom, A is the additive shift parameter, and n is the number of carbon atoms for each shift parameter (−2.5 is the shift of the ^{13}C of methane). Thus, for carbon atom 1, we have 1α-, 1β-, 2γ-, and 1δ-carbon atoms.

$$\delta_1 = -2.5 + (9.1 \times 1) + (9.4 \times 1) + (-2.5 \times 2) + (0.3 \times 1) = 11.3$$

Carbon atom 2 has 2α-, 2β-, and 1γ-carbon atoms. Carbon atom 2 is a 2° carbon with a 3° carbon attached [2°(3°) = −2.5].

TABLE 4.4 Empirical ^{13}C Chemical Shift Parameters in Some Linear and Branched Hydrocarbons

^{13}C Atoms	Shift (ppm) (A)
α	9.1
β	9.4
γ	−2.5
δ	0.3
ϵ	0.1
1°(3°)[a]	−1.1
1°(4°)[a]	−3.4
2°(3°)[a]	−2.5
2°(4°)	−7.2
3°(2°)	−3.7
3°(3°)	−9.5
4°(1°)	−1.5
4°(2°)	−8.4

[a]The notations 1°(3°) and 1°(4°) denote a CH_3 group bonded to a R_2CH group and to a R_3C group, respectively. The notation 2°(3°) denotes a RCH_2 group bonded to a R_2CH group, and so on.

$$\delta_2 = -2.5 + (9.1 \times 2) + (9.4 \times 2) + (-2.5 \times 1) + (-2.5 \times 1) = 29.5$$

Carbon atom 3 has 3α- and 2β-carbon atoms, and it is a 3° atom with two 2° atoms attached [3°(2°) = −3.7]. Thus,

$$\delta_3 = -2.5 + (9.1 \times 3) + (9.4 \times 2) + (-3.7 \times 2) = 36.2.$$

Carbon atom 6 has 1α-, 2β-, and 2γ-carbon atoms, and it is a 1° atom with a 3° atom attached [1°(3°) = −1.1]. Thus,

$$\delta_6 = -2.5 + (9.1 \times 1) + (9.4 \times 2) + (-2.5 \times 2) + (-1.1 \times 1) = 19.3$$

The agreement with the determined values for such calculations is very good. Another useful calculation has been given.* The ^{13}C γ shift to lower frequency resulting from the γ carbon has been attributed to the steric compression of a γ *gauche* interaction but has no counterpart in ^{1}H spectra. It accounts, for example, for the decreased chemical shift of an axial methyl substituent on a conformationally rigid cyclohexane ring, relative to an equatorial methyl, and for the decreased chemical shift of the γ carbon atoms of the ring. Table 4.5 lists the shifts in some linear and branched alkanes.

TABLE 4-5 The ^{13}C Chemical Shifts for Some Linear and Branched-Chain Alkanes (ppm from TMS)

Compound	C-1	C-2	C-3	C-4	C-5
Methane	−2.5				
Ethane	5.7				
Propane	15.8	16.3			
Butane	13.4	25.2			
Pentane	13.9	22.8	34.7		
Hexane	14.1	23.1	32.2		
Heptane	14.1	23.2	32.6	29.7	
Octane	14.2	23.2	32.6	29.9	
Nonane	14.2	23.3	32.6	30.0	30.3
Decane	14.2	23.2	32.6	31.1	30.5
Isobutane	24.5	25.4			
Isopentane	22.2	31.1	32.0	11.7	
Isohexane	22.7	28.0	42.0	20.9	14.3
Neopentane	31.7	28.1			
2,2-Dimethylbutane	29.1	30.6	36.9	8.9	
3-Methylpentane	11.5	29.5	36.9	(18.8, 3-CH_3)	
2,3-Dimethylbutane	19.5	34.3			
2,2,3-Trimethylbutane	27.4	33.1	38.3	16.1	
2,3-Dimethylpentane	7.0	25.3	36.3	(14.6, 3-CH_3)	

4.7.1.2 Effect of Substituents on Alkanes. Table 4.6 shows the effects of a substituent on linear and branched alkanes. The effect on the α-carbon parallels the electronegativity of the substituent except for bromine and iodine.† This demonstrates again that these empirical computations will not always provide numbers in agreement with experimental shifts. The effect at the β-carbon seems fairly constant for all the substituents except for the carbonyl, cyano, and nitro groups. The decreased chemical shift at the γ carbon results (as above) from steric compression of a *gauche* interaction. For Y = N, O, and F, there is a decrease in chemical shift with Y in the *anti* conformation, attributed to hyperconjugation.

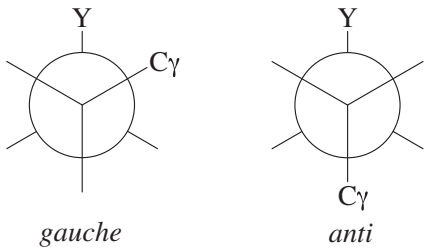

gauche *anti*

Table 4.6 provides the functional group increments that must be added to the appropriate shift values for alkanes given in Table 4.5. For example, we can calculate the ^{13}C shifts for 3-pentanol.

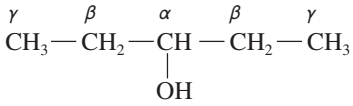

The OH substituent is attached "internally" (rather than "terminally") to the linear alkane chain of pentane; the point of attachment is labeled α, which corresponds to C-3 of pentane, for which the shift value of 34.7 is given in Table 4.6. To this value is added the increment +41, this being the increment for an OH group attached internally to the α-carbon of 3-pentanol (see line 12, 2nd column of numbers). The shift, therefore, for the point of attachment (the α-carbon) is calculated as 75.7. The β and γ shifts are calculated as shown below. All of the calculated shifts are in reasonable agreement with the experimental values (Table 4.14).

	Calculated	Experimental (See Table 4.14)
C_α	34.7 + 41 = 75.7	73.8
C_β	22.8 + 8 = 30.8	29.7
C_γ	13.9 − 5 = 8.9	9.8

1-Pentanol would be treated similarly but as a "terminal" alcohol, and the carbon atom to which the OH group is attached would again be labeled α.

4.7.1.3 Cycloalkanes and Saturated Heterocyclics. The chemical shifts of the CH_2 groups in monocyclic alkanes are given in Table 4.7. The striking feature here is the negative ^{13}C chemical shift of cyclopropane, analogous to its ^{1}H chemical shift.

Each ring skeleton has its own set of empirical shift parameters, but a detailed listing of these is beyond the scope

*Lindeman, L.P., and Adams, J.Q. (1971). *Anal. Chem.,* **43**, 1245.

†See Section 3.4, Table 3.2 (Pauling table of electronegativity).

TABLE 4.6 Incremental Substituent Effects (ppm) on Replacement of H by Y in Alkanes. Y is Terminal or Internal[a]

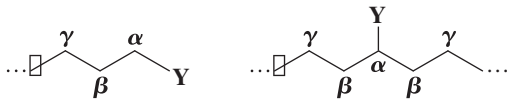

	α		β		
Y	Terminal	Internal	Terminal	Internal	γ
CH_3	9	6	10	8	−2
$CH{=}CH_2$	20		6		−0.5
$C{\equiv}CH$	4.5		5.5		−3.5
COOH	21	16	3	2	−2
COO^-	25	20	5	3	−2
COOR	20	17	3	2	−2
COCl	33	28		2	
$CONH_2$	22		2.5		−0.5
COR	30	24	1	1	−2
CHO	31				−2
Phenyl	23	17	9	7	−2
OH	48	41	10	8	−5
OR	58	51	8	5	−4
OCOR	51	45	6	5	−3
NH_2	29	24	11	10	
NH_3^+	26	24	8	6	−5
NHR	37	31	8	6	−4
NR_2	42		6		−3
NR_3^+	31		5		−7
NO_2	63	57	4	4	
CN	4	1	3	3	−3
SH	11	11	12	11	−4
SR	20		7		−3
F	68	63	9	6	−4
Cl	31	32	11	10	−4
Br	20	25	11	10	−3
I	−6	4	11	12	−1

[a]Add these increments to the shift values of the appropriate carbon atom in Table 4.5 or to the shift value calculated from Table 4.4.

Source: Wehrli et al. (1983).

of this text. Rough estimates for substituted rings can be made with the substitution increments in Table 4.6. One of the striking effects in rigid cyclohexane rings is the shielding caused by the *γ-gauche* steric compression. Thus, an axial methyl group at C-1 causes a decrease of several ppm of the chemical shifts of C-3 and C-5.

Table 4.8 presents chemical shifts for several saturated heterocyclics.

TABLE 4.7 ^{13}C Chemical Shifts of Cycloalkanes (ppm from TMS)

C_3H_6	−2.9	C_7H_{14}	28.4
C_4H_8	22.4	C_8H_{16}	26.9
C_5H_{10}	25.6	C_9H_{18}	26.1
C_6H_{12}	26.9	$C_{10}H_{20}$	25.3

TABLE 4.8 ^{13}C Chemical Shifts for Saturated Heterocyclics (ppm from TMS, neat)

Unsubstituted

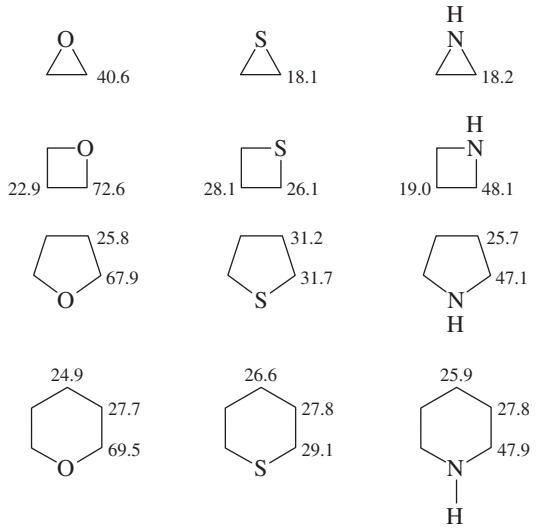

Substituted

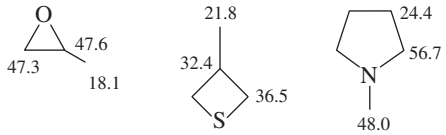

4.7.2 Alkenes

The sp^2 carbon atoms of alkenes substituted only by alkyl groups resonate in the range of about 110 ppm to 150 ppm. The double bond has a rather small effect on the shifts of the sp^3 carbons in the molecule as the following comparisons demonstrate:

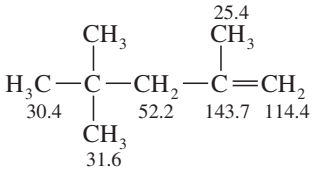

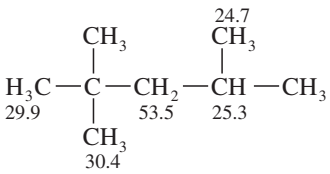

The methyl signal of propene is at 18.7 ppm and that of propane is at 15.8 ppm. In (*Z*)-2-butene, the methyl signals are at 12.1 ppm, compared with 17.6 ppm in (*E*)-2-butene, because of the γ effect. (For comparison, the methyl signals of butane are at 13.4 ppm.) Note the γ effect on one of the geminal methyl groups in 2-methyl-2-butene (Table 4.9).

In general, the terminal $=CH_2$ group has a lower ^{13}C chemical shift than an internal =CH— group, and (*Z*)—CH=CH— ^{13}C chemical shifts are lower than those of corresponding *E* groups. Calculations of approximate shifts can be made from the following parameters, where

TABLE 4.9 Alkene and Cycloalkene ^{13}C Chemical Shifts (ppm from TMS)

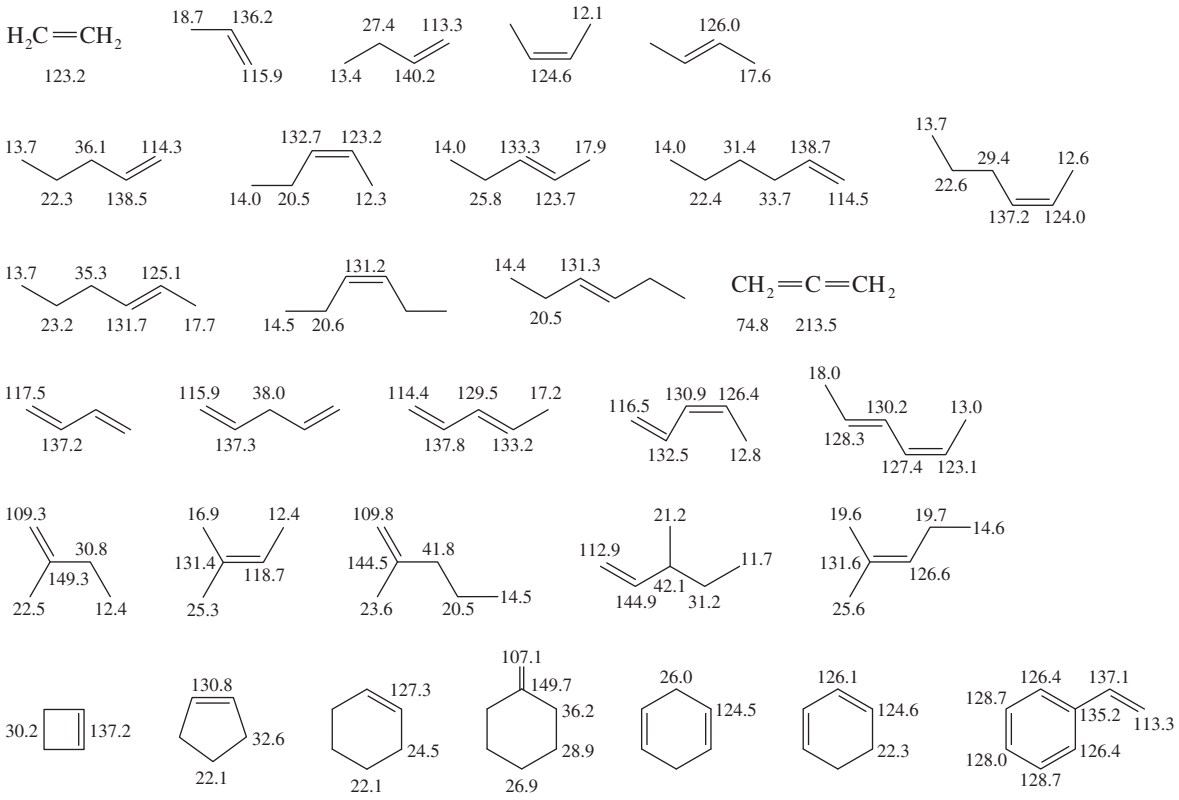

α, β, and γ represent substituents on the same end of the double bond as the alkene carbon of interest, and α', β', and γ' represent substituents on the far side.

α	10.6
β	7.2
γ	−1.5
α'	−7.9
β'	−1.8
γ'	−1.5
Z(*cis*) correction	−1.1

These parameters are added to 123.3 ppm, the shift for ethylene. We can calculate the values of C-3 and C-2 for (*Z*)-3-methyl-2-pentene as follows:

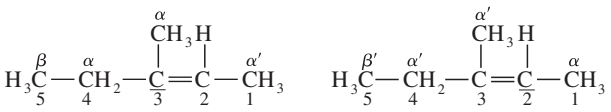

$$\delta_3 = 123.3 + (10.6 \times 2) + (7.2 \times 1) + (-7.9 \times 1) - 1.1 = 142.7 \text{ ppm}$$

$$\delta_2 = 123.3 + (10.6 \times 1) + (-7.9 \times 2) + (-1.8 \times 1) - 1.1 = 115.2 \text{ ppm}$$

The measured values are 137.2 ppm for C-3 and 116.8 ppm for C-2. The agreement is fair.

Carbon atoms directly attached to a (*Z*) C=C group are more shielded than those attached to the stereoisomeric (*E*) group by 4 to 6 ppm (Table 4.9). Alkene carbon atoms in polyenes are treated as though they were alkane carbon substituents on one of the double bonds. Thus, in calculating the shift of C-2 in 1,4-pentadiene, C-4 is treated like a β-sp^3 carbon atom.

Representative alkenes are presented in Table 4.9. There are no simple rules to handle polar substituents on an alkene carbon. The shifts for vinyl ethers can be rationalized using the following resonance structures

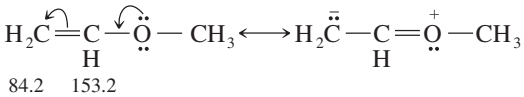

as can the shifts for α, β-unsaturated ketones.

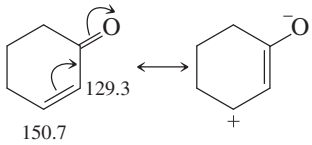

The same rationalization applies to the proton shifts in these compounds. Shifts for several substituted alkenes are presented in Table 4.10.

The chemical shift of the central carbon atom (=C=) of alkyl-substituted allenes is about 200 ppm to 215 ppm, whereas those of the terminal atoms (C=C=C) are about 75 ppm to 97 ppm.

TABLE 4.10 ^{13}C Chemical Shifts of Substituted Alkenes (ppm from TMS)

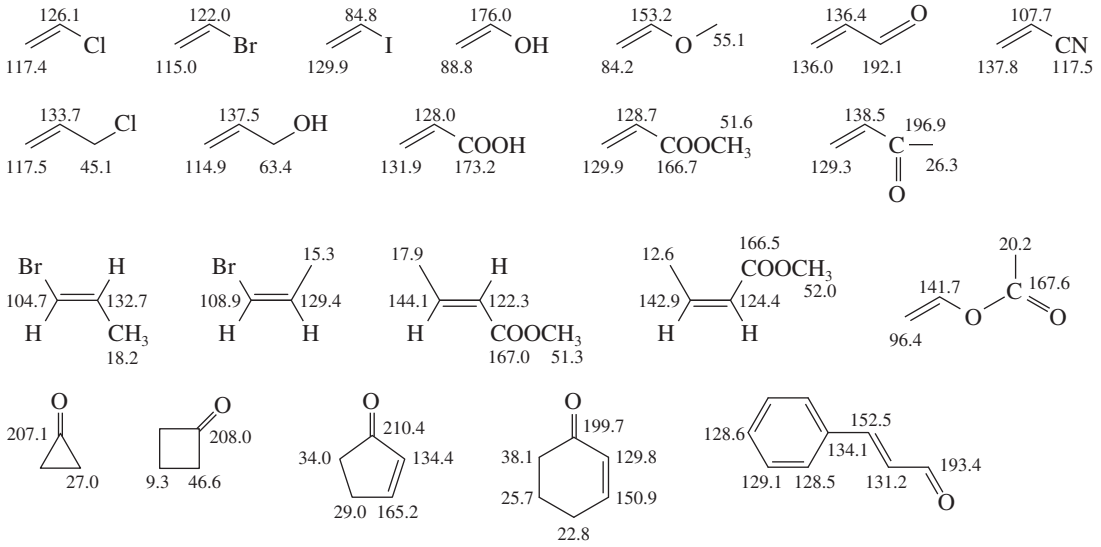

4.7.3 Alkynes

The ^{13}C chemical shifts of alkynes substituted only by alkyl groups range from approximately 65 ppm to 90 ppm (Table 4.11). The triple bond shields the directly attached sp^3 carbon atoms by about 5 ppm to 15 ppm relative to the corresponding alkane. The ^{13}C chemical shifts of terminal ≡CH are lower than those of internal ≡CR groups. Alkyne carbon atoms to which a polar group is directly bonded have chemical shifts of about 20 ppm to 95 ppm.

Polar resonance structures may be used to rationalize these shifts for alkynyl ethers, which are analogous to the shifts for vinyl ethers (Section 3.4).

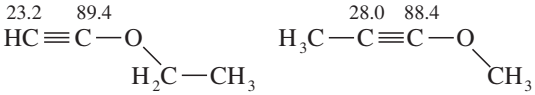

4.7.4 Aromatic Compounds

Benzene carbon atoms resonate at 128.5 ppm, neat or as a solution in $CDCl_3$. Substituents shift the attached aromatic carbon atom as much as ±35 ppm. Fused-ring chemical shifts are as follows:

TABLE 4-11 Alkyne ^{13}C Chemical Shifts (ppm)

Compound	C-1	C-2	C-3	C-4	C-5	C-6
1-Butyne	71.9	86.0	12.3	13.8		
2-Butyne	3.3	73.6				
1-Hexyne	68.1	84.5	18.1	30.7	21.9	13.5
2-Hexyne	2.7	73.7	76.9	19.6	21.6	12.1
3-Hexyne	15.4	13.0	80.9			

Naphthalene: C-1, 128.1; C-2, 125.9; C-4a, 133.7 ppm.
Anthracene: C-1, 130.1; C-2, 125.4; C-4a, 132.2; C-9, 132.6 ppm.
Phenanthrene: C-1, 128.3; C-2, 126.3; C-3, 126.3; C-4, 122.2; C-4a, 131.9*; C-9, 126.6; C-10a, 130.1 ppm.*

Shifts of the aromatic carbon atom directly attached to the substituent have been correlated with substituent electronegativity after correcting for magnetic anisotropy effects; shifts at the *para* aromatic carbon have been correlated with the Hammett σ constant. *Ortho* shifts are not readily predictable and range over about 15 ppm. *Meta* shifts are generally up to several ppm for a single substituent.

The resonances due to substituted aromatic carbon atoms can be distinguished from those due to protonated aromatic carbon atoms by the lower integrated intensities of the former; that is, they lack directly bonded protons and thus suffer from a longer T_1 and a diminished NOE.

Incremental shifts from the carbon atoms of benzene for the aromatic carbon atoms of representative monosubstituted benzene rings (and shifts from TMS of carbon-containing substituents) are given in Table 4.12. Shifts from benzene for polysubstituted benzene ring carbon atoms can be approximated by applying the principle of increment additivity. For example, the shift from benzene for C-2 of the disubstituted compound 4-chlorobenzonitrile is

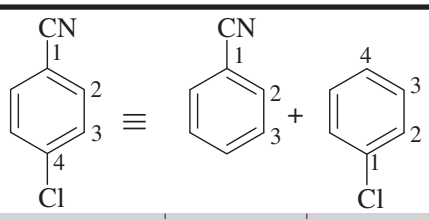

I			II		III	
C #	Cal	Obs	C #	Obs	C #	Obs
1	–18.0	–16.6	1	–16.0	4	–2.0
2	4.6	5.1	2	3.6	3	1.0
3	0.8	1.3	3	0.6	2	0.2
4	10.7	10.8	4	4.3	1	6.4

*Assignment uncertain.

TABLE 4.12 Incremental Shifts for the Aromatic Carbon Atoms of Monosubstituted Benzenes (ppm from benzene at 128.5 ppm). ^{13}C Chemical Shifts of Substituents in ppm from TMS[a]

Substituent	C-1 (Attachment)	C-2	C-3	C-4	C of Substituent (ppm from TMS)
H	0.0	0.0	0.0	0.0	
CH_3	9.3	0.7	−0.1	−2.9	21.3
CH_2CH_3	15.6	−0.5	0.0	−2.6	29.2 (CH_2), 15.8 (CH_3)
$CH(CH_3)_2$	20.1	−2.0	0.0	−2.5	34.4 (CH), 24.1 (CH_3)
$C(CH_3)_3$	22.2	−3.4	−0.4	−3.1	34.5 (C), 31.4 (CH_3)
$CH{=}CH_2$	9.1	−2.4	0.2	−0.5	137.1 (CH), 113.3 (CH_2)
$C{\equiv}CH$	−5.8	6.9	0.1	0.4	84.0 (C), 77.8 (CH)
C_6H_5	12.1	−1.8	−0.1	−1.6	
CH_2OH	13.3	−0.8	−0.6	−0.4	64.5
$CH_2O(C{=}O)CH_3$	7.7	∼0.0	∼0.0	∼0.0	20.7 (CH_3), 66.1 (CH_2), 170.5 (C=O)
OH	26.6	−12.7	1.6	−7.3	
OCH_3	31.4	−14.4	1.0	−7.7	54.1
OC_6H_5	29.0	−9.4	1.6	−5.3	
$O(C{=}O)CH_3$	22.4	−7.1	−0.4	−3.2	23.9 (CH_3), 169.7 (C=O)
$(C{=}O)H$	8.2	1.2	0.6	5.8	192
$(C{=}O)CH_3$	7.8	−0.4	−0.4	2.8	24.6 (CH_3), 195.7 (C=O)
$(C{=}O)C_6H_5$	9.1	1.5	−0.2	3.8	196.4 (C=O)
$(C{=}O)F_3$	−5.6	1.8	0.7	6.7	
(C=O)OH	2.9	1.3	0.4	4.3	168
$(C{=}O)OCH_3$	2.0	1.2	−0.1	4.8	51.0 (CH_3), 166.8 (C=O)
(C=O)Cl	4.6	2.9	0.6	7.0	168.5
$(C{=}O)NH_2$	5.0	−1.2	0.0	3.4	
$C{\equiv}N$	−16	3.6	0.6	4.3	119.5
NH_2	19.2	−12.4	1.3	−9.5	
$N(CH_3)_2$	22.4	−15.7	0.8	−11.8	40.3
$NH(C{=}O)CH_3$	11.1	−9.9	0.2	−5.6	
NO_2	19.6	−5.3	0.9	6.0	
$N{=}C{=}O$	5.7	−3.6	1.2	−2.8	129.5
F	35.1	−14.3	0.9	−4.5	
Cl	6.4	0.2	1.0	−2.0	
Br	−5.4	3.4	2.2	−1.0	
I	−32.2	9.9	2.6	−7.3	
CF_3	2.6	−3.1	0.4	3.4	
SH	2.3	0.6	0.2	−3.3	
SCH_3	10.2	−1.8	0.4	−3.6	15.9
SO_2NH_2	15.3	−2.9	0.4	3.3	
$Si(CH_3)_3$	13.4	4.4	−1.1	−1.1	

[a]See Ewing, D.E. (1979). *Org. Magn. Reson.*, **12**, 499, for 709 chemical shifts of monosubstituted benzenes.

calculated by adding the effect for an *ortho* CN group (+3.6) to that for a *meta* Cl group (+1.0): 128.5 + 3.6 + 1.0 = 133.1 ppm.

4.7.5 Heteroaromatic Compounds

Complex empirical rationalizations have been offered for the shifts of carbon atoms in heteroaromatic compounds. As a general rule, the chemical shift of C-2 of oxygen- and nitrogen-containing rings is higher than that for C-3. Large solvent and pH effects have been recorded. Table 4.13 gives values for neat samples of several five- and six-membered heterocyclic compounds.

4.7.6 Alcohols

Substitution of H in an alkane by an OH group changes the chemical shift of the directly bonded carbon atom by 35 ppm to 52 ppm for C-1, 5 ppm to 12 ppm for C-2, and up to −6 ppm for C-3. Shifts for several acyclic and alicyclic alcohols are given in Table 4.14. Acetylation provides a useful diagnostic test for an alcohol. The C-1 chemical shift increases by about 2.5 ppm to 4.5 ppm, and the C-2 chemical shift decreases by a similar amount; a 1,3-diaxial interaction may cause a slight (∼1 ppm) increase in shift for C-3. Table 4.14 may be used to empirically predict shifts for alcohols as described earlier.

4.7.7 Ethers, Acetals, and Epoxides

An alkoxy substituent causes a somewhat larger shift at C-1 (∼11 ppm larger) than that of a hydroxy substituent. This is attributed to the C-1′ of the alkoxy group having the same effect as a β-C relative to C-1. The O atom is regarded here as an "α-C" to C-1.

TABLE 4.13 ^{13}C Chemical Shifts of Heteroaromatics (ppm from neat TMS)

Compound	C-2	C-3	C-4	C-5	C-6	Substituent
Furan	142.7	109.6				
2-Methylfuran	152.2	106.2	110.9	141.2		13.4
Furan-2-carboxaldehyde	153.3	121.7	112.9	148.5		178.2
Methyl 2-furoate	144.8	117.9	111.9	146.4		159.1 (C═O), 51.8 (CH_3)
Pyrrole	118.4	108.0				
2-Methylpyrrole	127.2	105.9	108.1	116.7		12.4
Pyrrole-2-carboxaldehyde	134.0	123.0	112.0	129.0		178.9
Thiophene	124.4	126.2				
2-Methylthiophene	139.0	124.7	126.4	122.6		14.8
Thiophene-2-carboxaldehyde	143.3	136.4	128.1	134.6		182.8
Thiazole	152.2		142.4	118.5		
Imidazole	136.2		122.3	122.3		
Pyridine	150.2	123.9	135.9			
Pyrimidine	159.5		157.4	122.1	157.4	
Pyrazine	145.6					
2-Methylpyrazine	154.0	141.8[a]	143.8[a]	144.7[a]		21.6

[a]Assignment not certain.

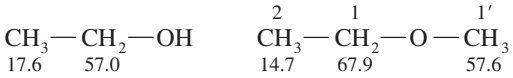

Note also that the "γ effect" (decreased shift) on C-2 is explainable by similar reasoning. Conversely, the ethoxy group affects the OCH_3 group (compare CH_3OH). Table 4.15 gives ^{13}C chemical shifts of several ethers.

The dioxygenated carbon of acetals resonates in the range of about 88 ppm to 112 ppm. Oxirane (an epoxide) has a ^{13}C chemical shift of 40.6 ppm.

The alkyl carbon atoms of arylalkyl ethers have shifts similar to those of dialkyl ethers. Note the large shielding of the ring *ortho* carbon.

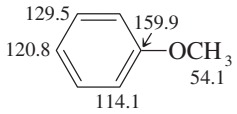

TABLE 4.14 ^{13}C Chemical Shifts of Alcohols (ppm from TMS)

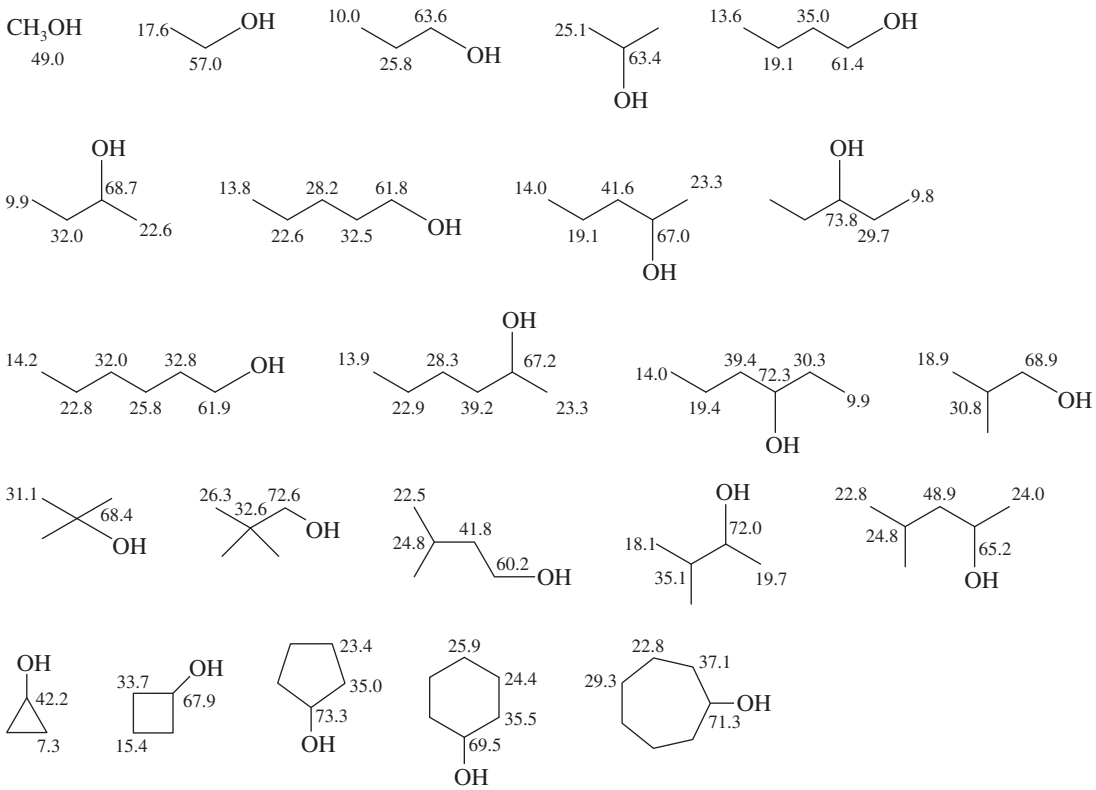

TABLE 4.15 ^{13}C Chemical Shifts of Ethers, Acetals, and Epoxides (ppm from TMS)

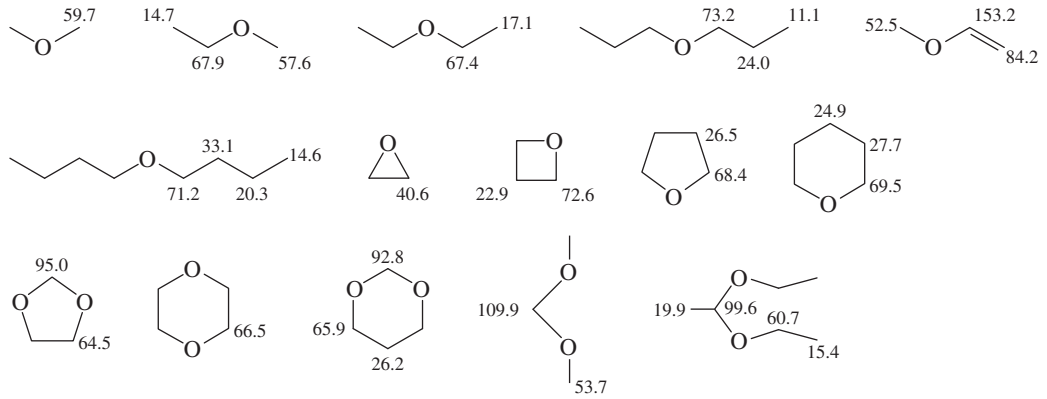

4.7.8 Halides

The effect of halide substitution is complex. A single fluorine atom (in CH_3F) causes a large increase in the ^{13}C chemical shift relative to CH_4 as electronegativity considerations would suggest. Successive geminal substitution by Cl ($CH_3Cl, CH_2Cl_2, CHCl_3, CCl_4$) results in increasing shifts, again expected on the basis of electronegativity. But with Br and I, the heavy atom effect prevails. The carbon resonances of CH_3Br and CH_2Br_2 become progressively more shielded. A strong deshielding of the ^{13}C peaks due to directly bonded iodine commences with CH_3I, which is shielded relative to CH_4. There is a progressive deshielding of C-2 in the order I > Br > F. Cl and Br show *γ-gauche* shielding at C-3, but I does not, presumably because of the low population of the hindered gauche rotamer. Relativistic effects can also play a role in determining the ^{13}C chemical shift when carbon is bonded to a heavy atom such as iodine. Table 4.16 shows these trends. These examples demonstrate clearly that simple electronegativity or electron density interpretations of chemical shifts can fail spectacularly and that caution must always be exercised when attempting to interpret shifts in this manner.

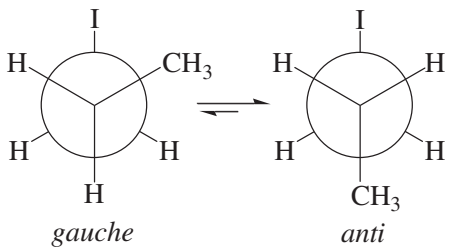

gauche *anti*

Halides may show large solvent effects, for example, C-1 for iodoethane is at −6.6 ppm in cyclohexane and at −0.4 ppm in DMF.

4.7.9 Amines

A terminal NH_2 group attached to an alkyl chain causes a deshielding of about 30 ppm at C-1, a deshielding of about 11 ppm at C-2, and a shielding of about 4.0 ppm at C-3. The NH_3^+ group shows a somewhat smaller effect. *N*-alkylation increases the shift at C-1. Chemical shifts for selected acyclic and alicyclic amines are given in Table 4.17 (see Table 4.8 for heterocyclic amines).

TABLE 4.16 ^{13}C Chemical Shifts of Alkyl Halides (neat, ppm from TMS)

Compound	C-1	C-2	C-3
CH_4	−2.5		
CH_3F	75.4		
CH_3Cl	24.9		
CH_2Cl_2	54.0		
$CHCl_3$	77.5		
CCl_4	96.5		
CH_3Br	10.0		
CH_2Br_2	21.4		
$CHBr_3$	12.1		
CBr_4	−28.5		
CH_3I	−20.7		
CH_2I_2	−54.0		
CHI_3	−139.9		
CI_4	−292.5		
CH_3CH_2F	79.3	14.6	
CH_3CH_2Cl	39.9	18.7	
CH_3CH_2Br	28.3	20.3	
CH_3CH_2I	−0.2	21.6	
$CH_3CH_2CH_2Cl$	46.7	26.5	11.5
$CH_3CH_2CH_2Br$	35.7	26.8	13.2
$CH_3CH_2CH_2I$	10.0	27.6	16.2

4.7.10 Thiols, Sulfides, and Disulfides

Substitution with sulfur generally has less of an effect on ^{13}C chemical shifts than does substitution with oxygen. Examples of thiols, sulfides, and disulfides are given in Table 4.18.

4.7.11 Functional Groups Containing Carbon

Carbon-13 NMR spectroscopy permits direct observation of carbon-containing functional groups; the shift ranges for these are given in Appendix C. With the exception of

TABLE 4.17 ^{13}C Chemical Shifts of Acyclic and Alicyclic Amines (in $CDCl_3$, ppm from TMS)

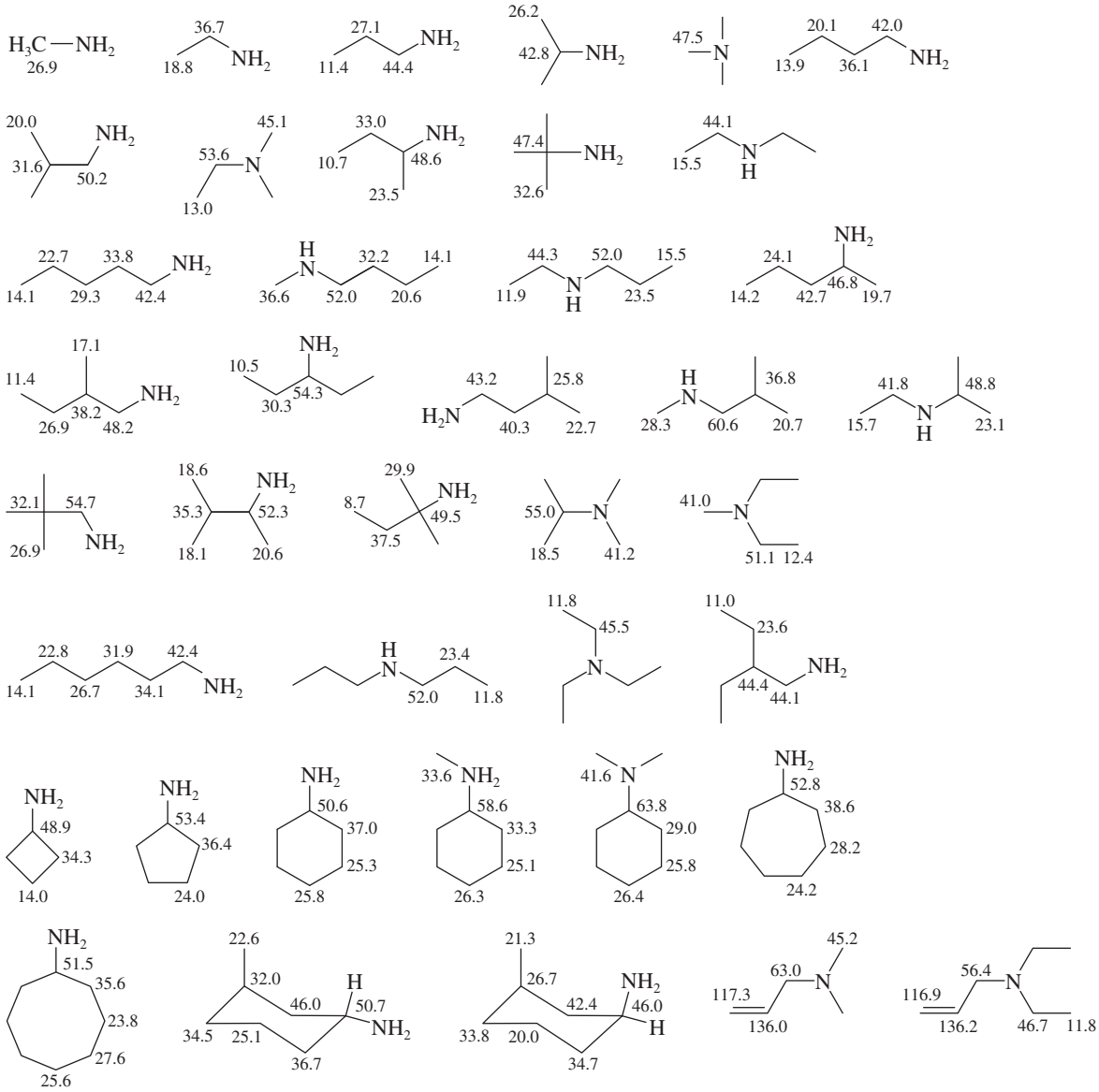

CH═O, the presence of these groups could not be directly ascertained by ^{1}H NMR.

TABLE 4.18 ^{13}C Chemical Shifts of Thiols, Sulfides, and Disulfides (ppm from TMS)

Compound	C-1	C-2	C-3
CH_3SH	6.5		
CH_3CH_2SH	19.8	17.3	
$CH_3CH_2CH_2SH$	26.4	27.6	12.6
$CH_3CH_2CH_2CH_2SH$	23.7	35.7	21.0
$(CH_3)_2S$	19.3		
$(CH_3CH_2)_2S$	25.5	14.8	
$(CH_3CH_2CH_2)_2S$	34.3	23.2	13.7
$(CH_3CH_2CH_2CH_2)_2S$	34.1	31.4	22.0
CH_3SSCH_3	22.0		
$CH_3CH_2SSCH_2CH_3$	32.8	14.5	

4.7.11.1 Ketones and Aldehydes. The R_2C═O and the RCH═O carbon nuclei resonate in a characteristic region. Acetone resonates at 203.3 ppm, and acetaldehyde at 199.3 ppm. Alkyl substitution on the α-carbon causes an increase in the C═O chemical shift of 2 ppm to 3 ppm, although steric effects can reverse this trend. Replacement of the CH_3 of acetone or acetaldehyde by a phenyl group causes a deshielding of the C═O resonance (acetophenone, 195.7 ppm; benzaldehyde, 190.7 ppm); similarly, α,β-unsaturation causes deshielding (acrolein, 192.1 ppm, compared with propionaldehyde, 201.5 ppm).

Of the cycloalkanones, cyclopentanone has a particularly high ^{13}C chemical shift. Table 4.19 presents chemical shifts of the C═O group of some ketones and aldehydes. Because of rather large solvent effects, there are differences of several ppm from different literature sources. Replacement of CH_2 of alkanes by C═O causes a deshielding of the

TABLE 4.19 ^{13}C Chemical Shifts of the C═O Group and Other Carbon Atoms of Ketones and Aldehydes (ppm from TMS)

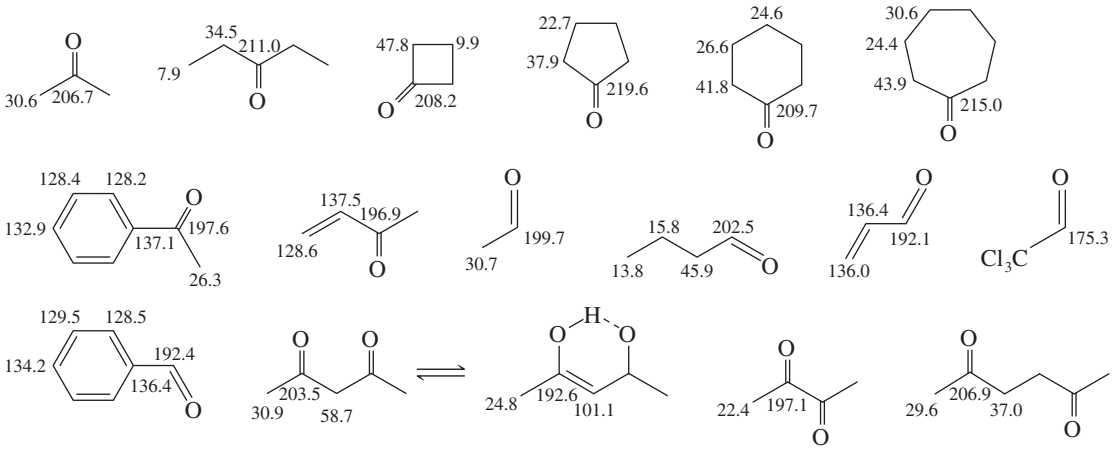

TABLE 4.20 ^{13}C Chemical Shifts of the C═O Group and other Carbon Atoms of Carboxylic Acids: Esters, Lactones, Chlorides Anhydrides, Carbamates, and Nitriles (ppm from TMS)

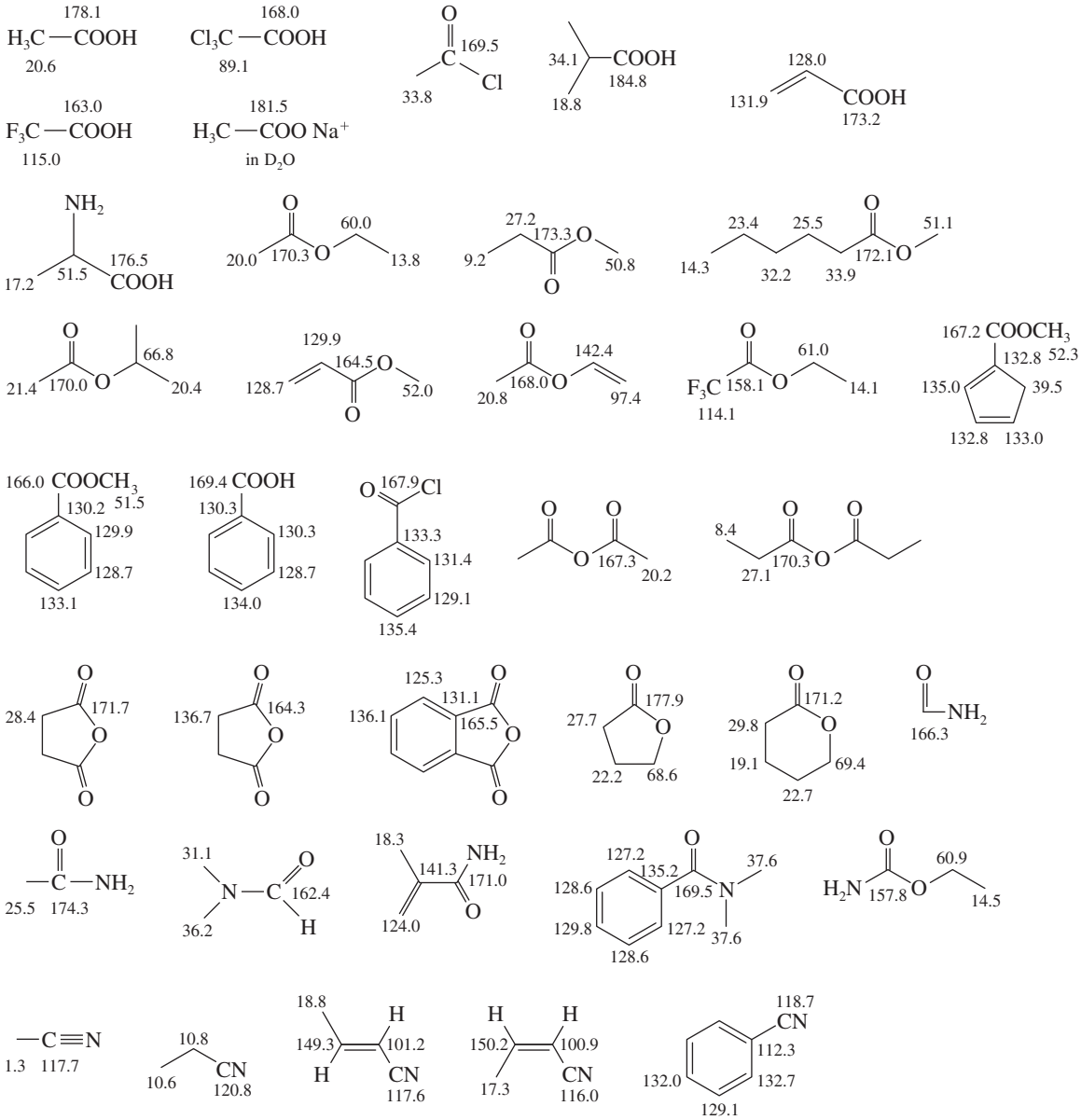

α-carbon (~10 – 14 ppm) and a shielding of the β-carbon (several ppm in acyclic compounds). In a proton-coupled ^{13}C NMR spectrum, the aldehyde CH═O resonance is a doublet.

4.7.11.2 Carboxylic Acids, Esters, Chlorides, Anhydrides, Amides, and Nitriles. Carbon-13 chemical shifts of the C═O groups of carboxylic acids and derivatives are in the range of 150 ppm to 185 ppm. Dilution and solvent effects are marked for carboxylic acids; anions have higher chemical shifts. The effects of substituents and electron delocalization are generally similar to those for ketones. Nitriles resonate in the range of 115 ppm to 125 ppm. Alkyl substituents on the nitrogen of amides cause a small (up to several ppm) shielding of the C═O group (see Table 4.20).

4.7.11.3 Oximes. The quaternary carbon atom of simple oximes resonates in the range of 145 ppm to 165 ppm. It is possible to distinguish between *E* and *Z* isomers since the C═O shift is smaller in the sterically more compressed *E* form, and the shift of the more hindered substituent (*syn* to the OH) is less than that of the less hindered.

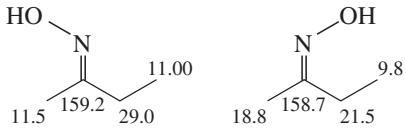

REFERENCES

For a list of Chapter References, please visit: www.wiley.com/college/silverstein.

STUDENT EXERCISES

4.1 For each compound given below (a – o), identify all chemically equivalent carbons.

4.2 For each compound below, predict the chemical shifts for each carbon. Give the source (Table or Appendix) that you use for your prediction.

4.3 Sketch the proton-decoupled ^{13}C NMR spectrum and DEPT spectra for each of the compounds in question 4.1.

4.4 Confirm the structure and assign all the ^{13}C resonances in spectra A–W for the compounds whose structures were determined in Problem 3.4 ^{1}H NMR. They were all run at 75.5 MHz in $CDCl_3$. The mass spectra were given in Chapter 1 (Question 1.6) and the IR spectra were given in Chapter 2 (Question 2.9).

4.5 Predict the number of lines in ^{13}C spectra for the following compounds:

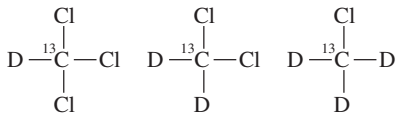

4.6 Interpret the following ^{13}C/DEPT spectra (4.6A to 4.6F). Confirm the structure and assign all the ^{13}C resonances. Give the source (Table or Appendix) that you use for your prediction.

4.7 What are the symmetry elements in *ortho, meta, para*-diethyl phthalates? How many nonequivalent carbon atoms and hydrogen atoms are there for each compound? Draw the proton-decoupled ^{13}C spectrum and DEPT spectra for each compound.

The workbook of Forrest et al. (2011) provides numerous additional exercises.

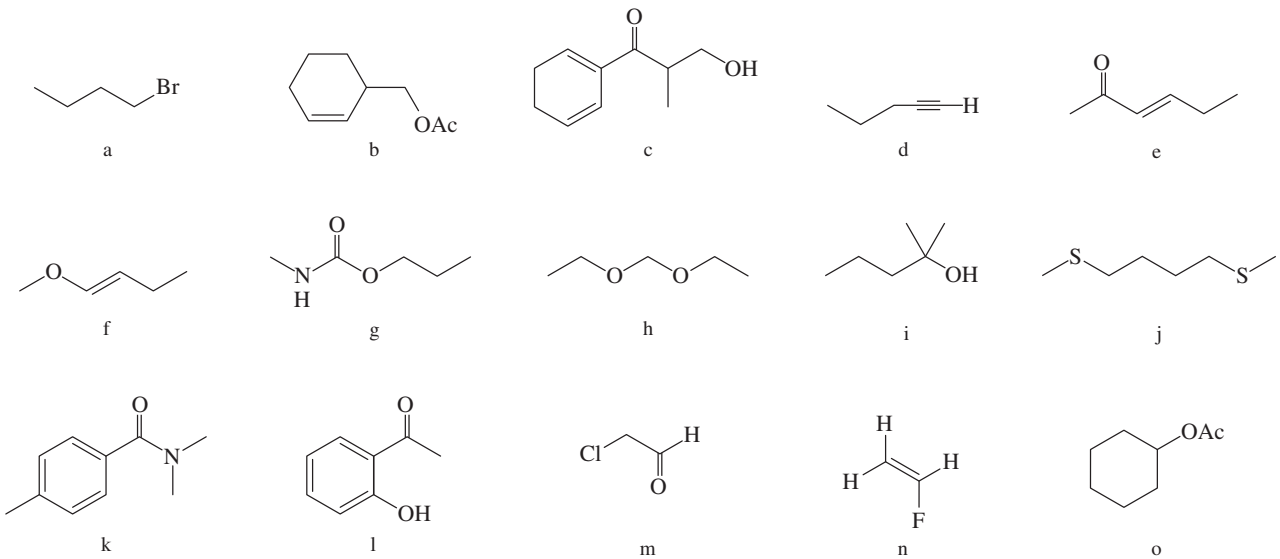

Problem 4.4 A

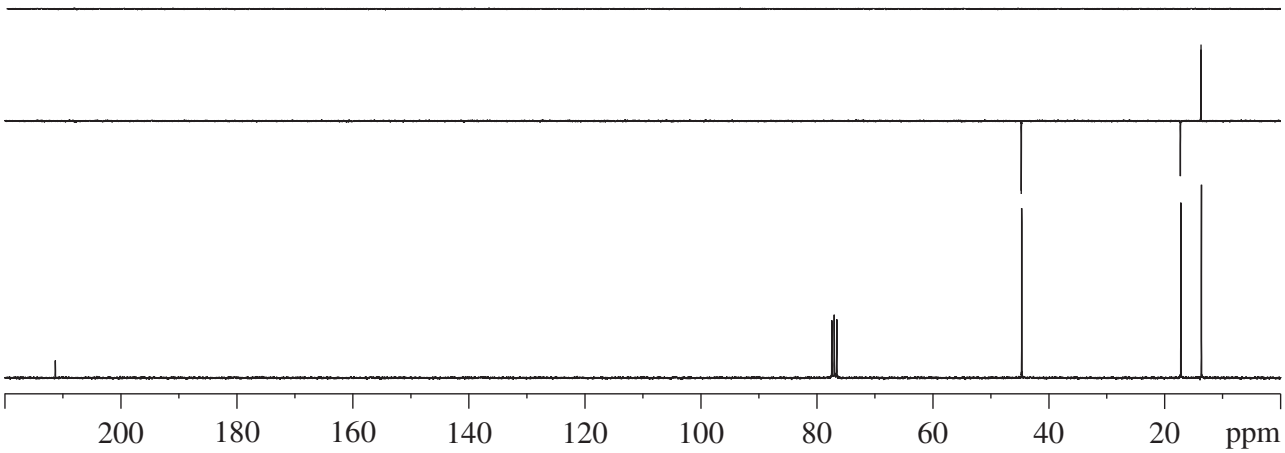

Problem 4.4 B

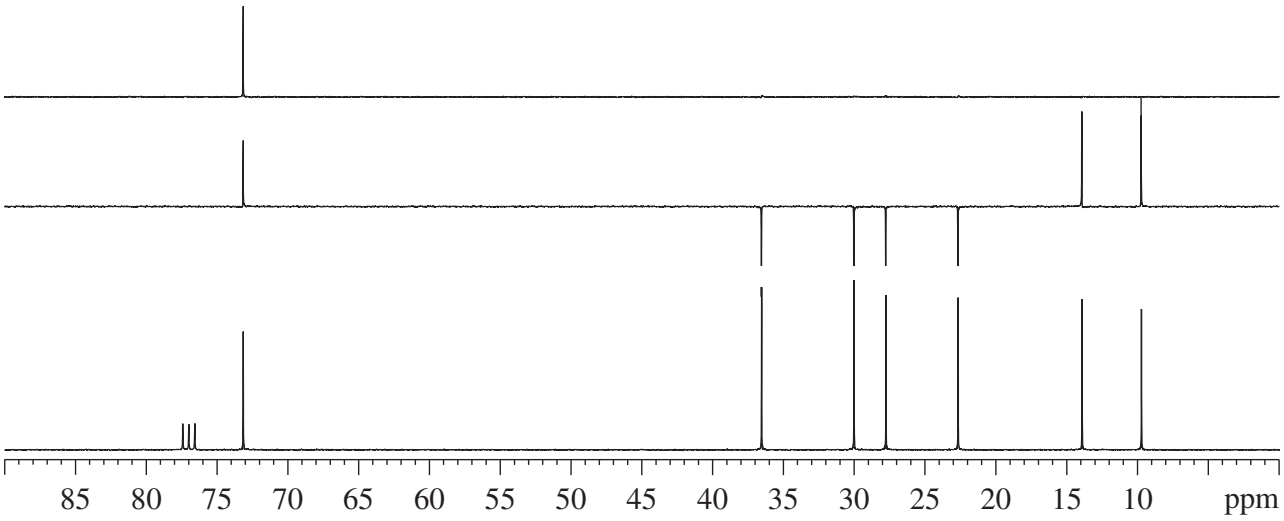

Problem 4.4 C

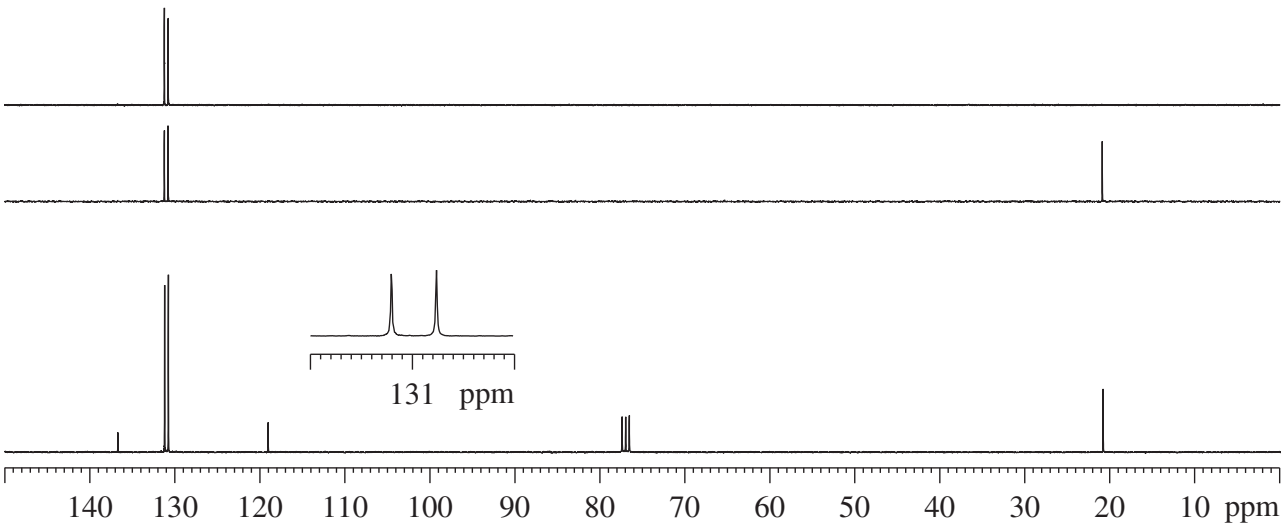

Problem 4.4 D

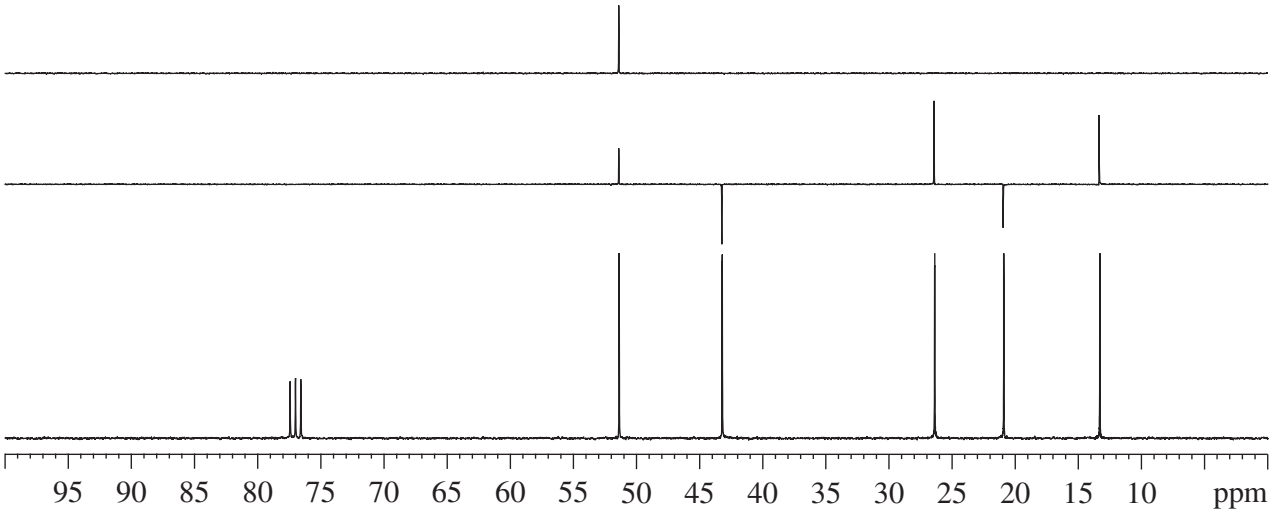

Problem 4.4 E

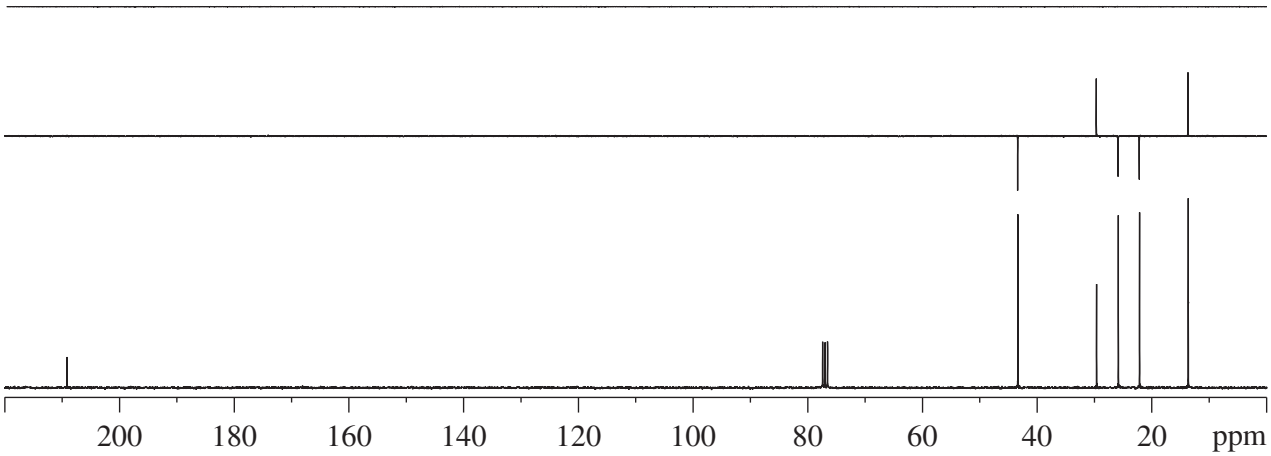

Problem 4.4 F

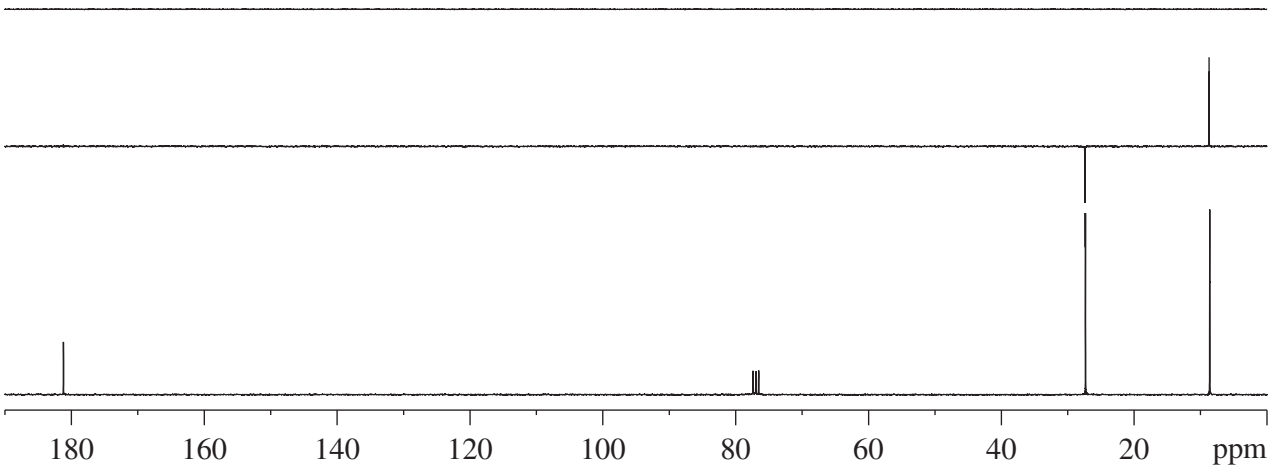

Problem 4.4 G

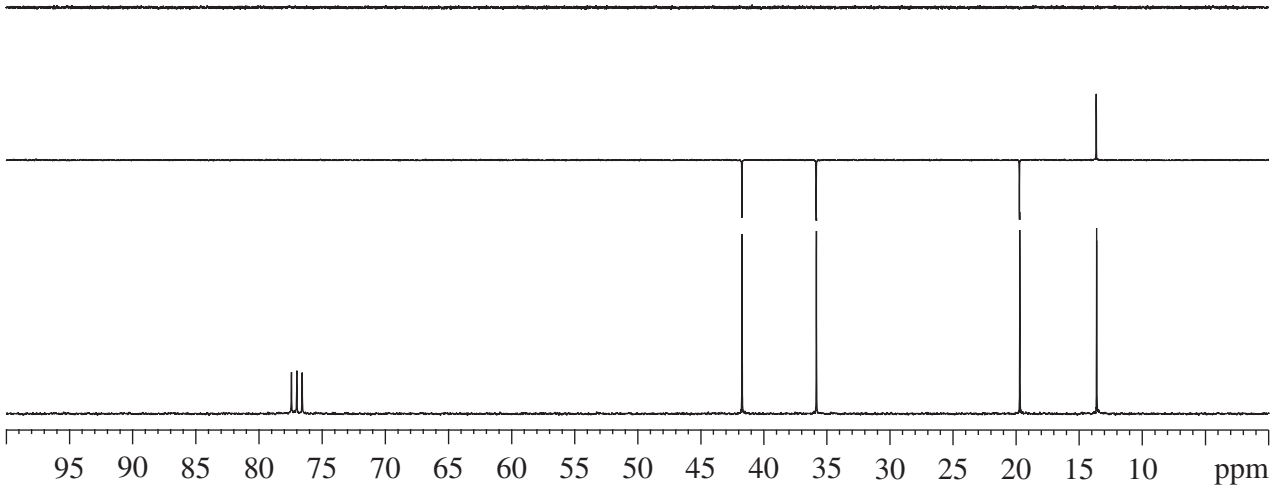

Problem 4.4 H

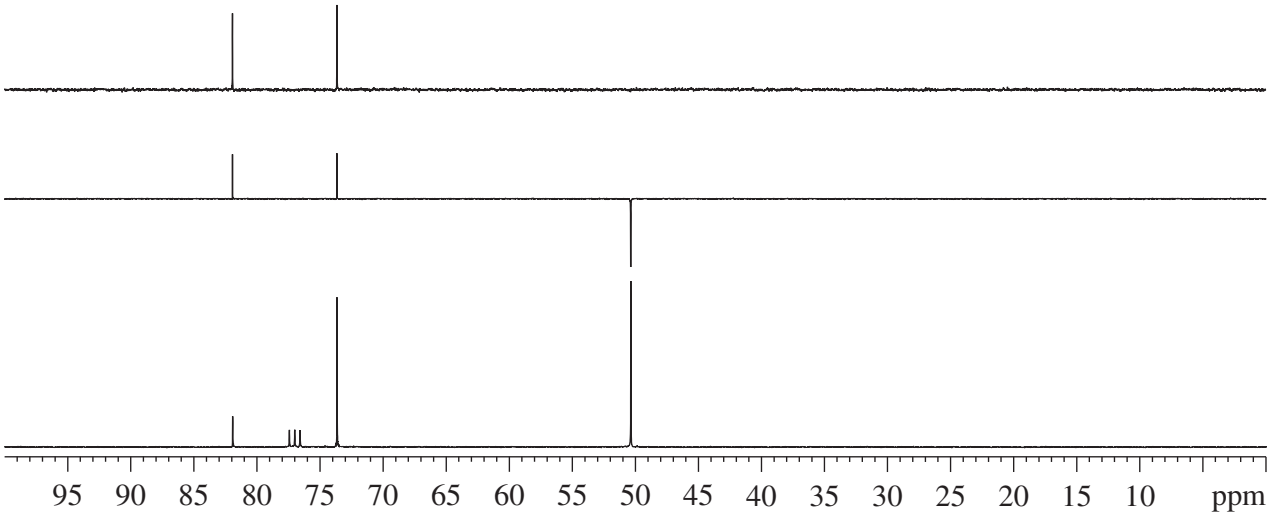

Problem 4.4 I

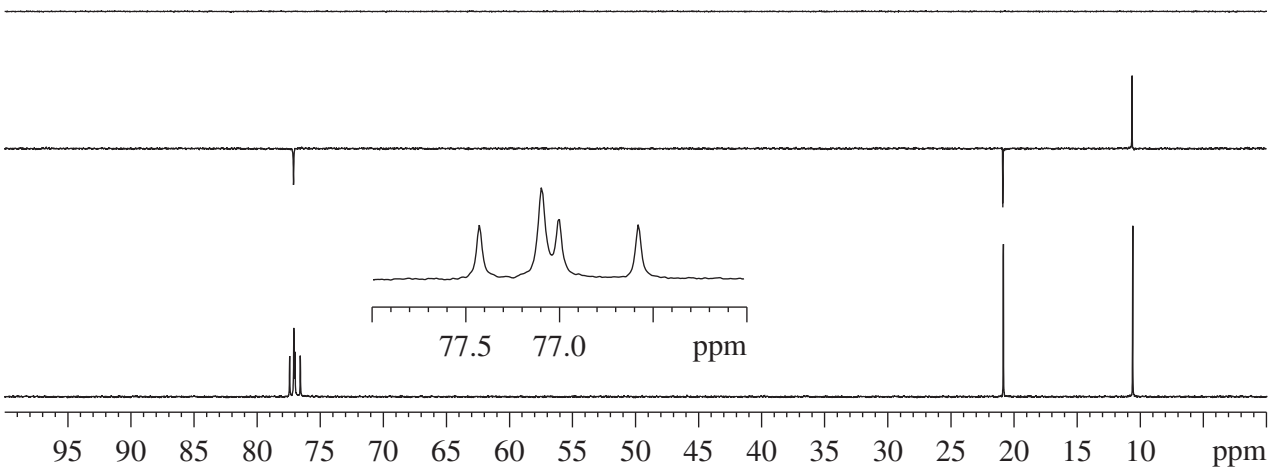

Problem 4.4 J

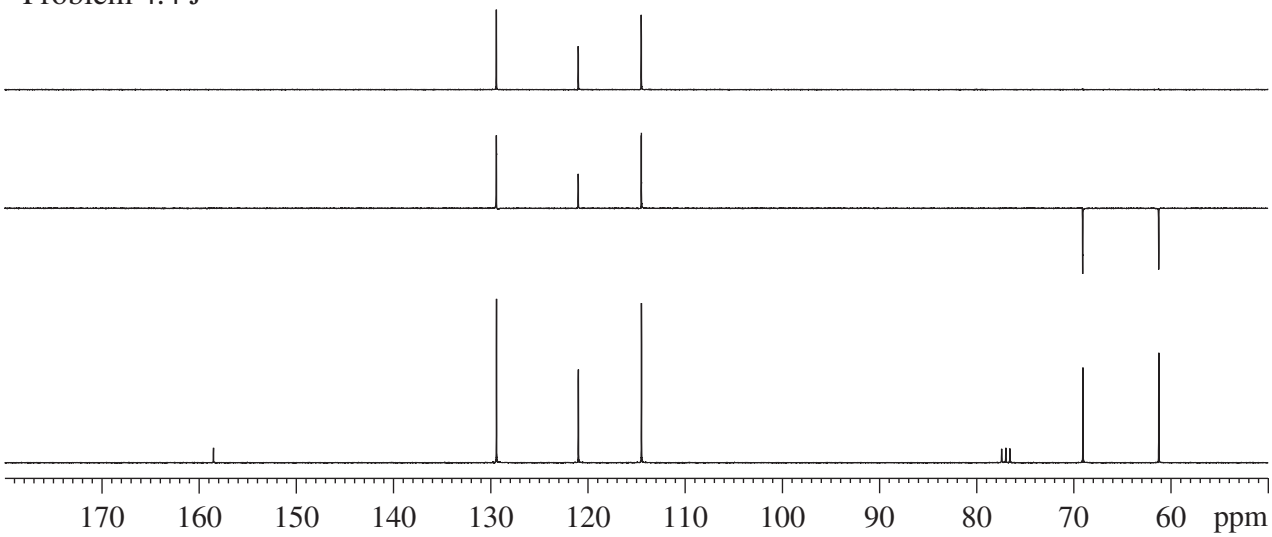

Problem 4.4 K

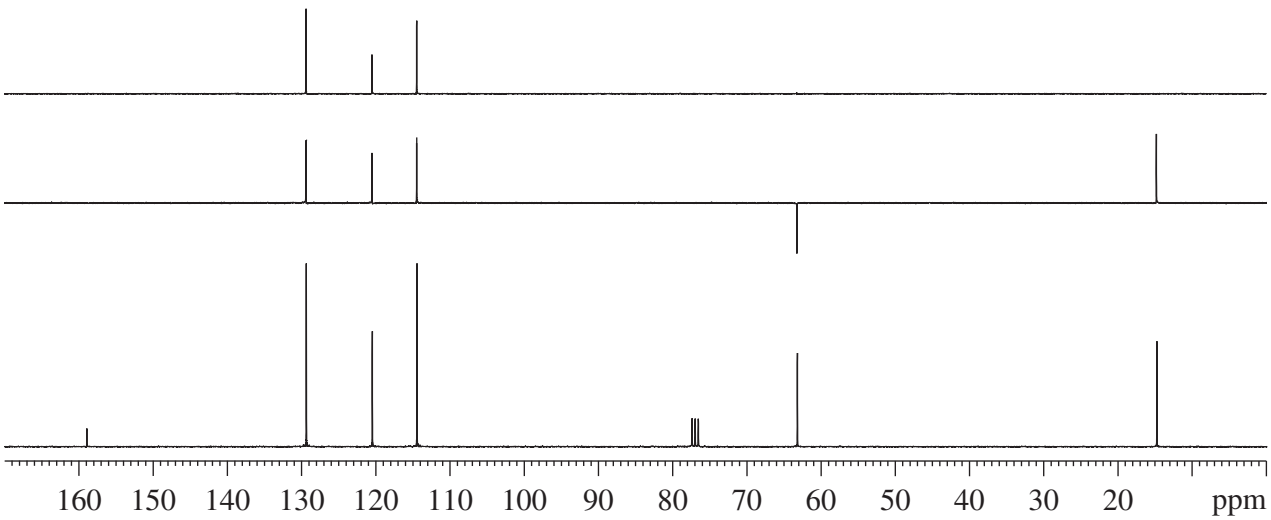

Problem 4.4 L

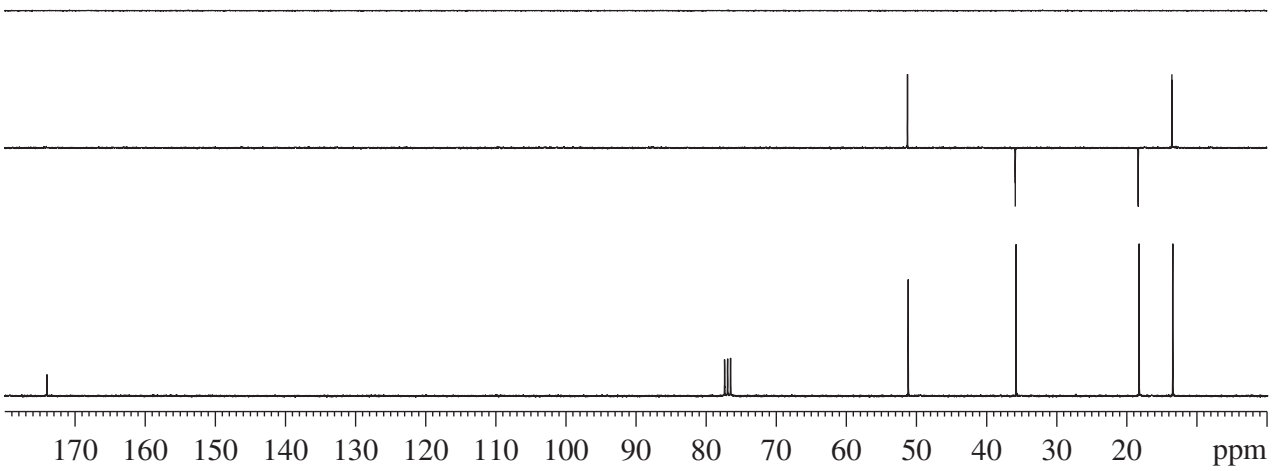

Problem 4.4 M

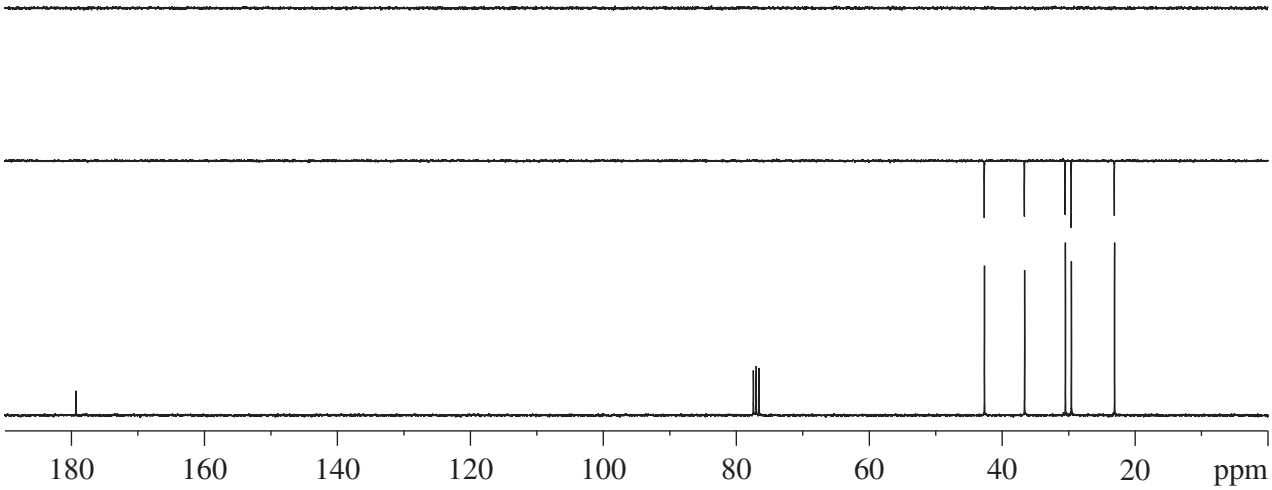

Problem 4.4 N

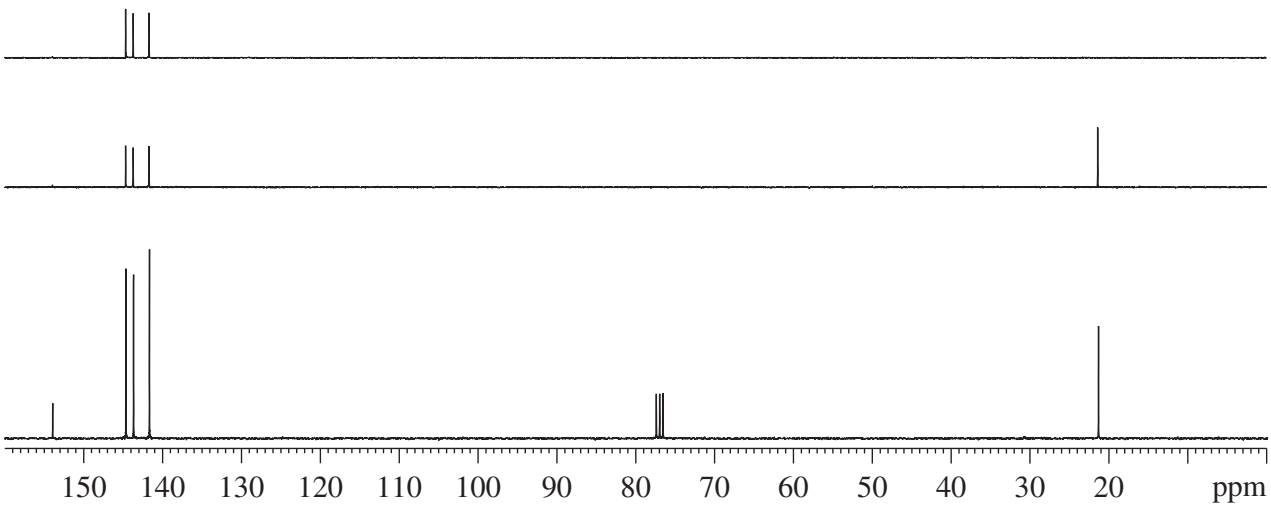

Problem 4.4 O

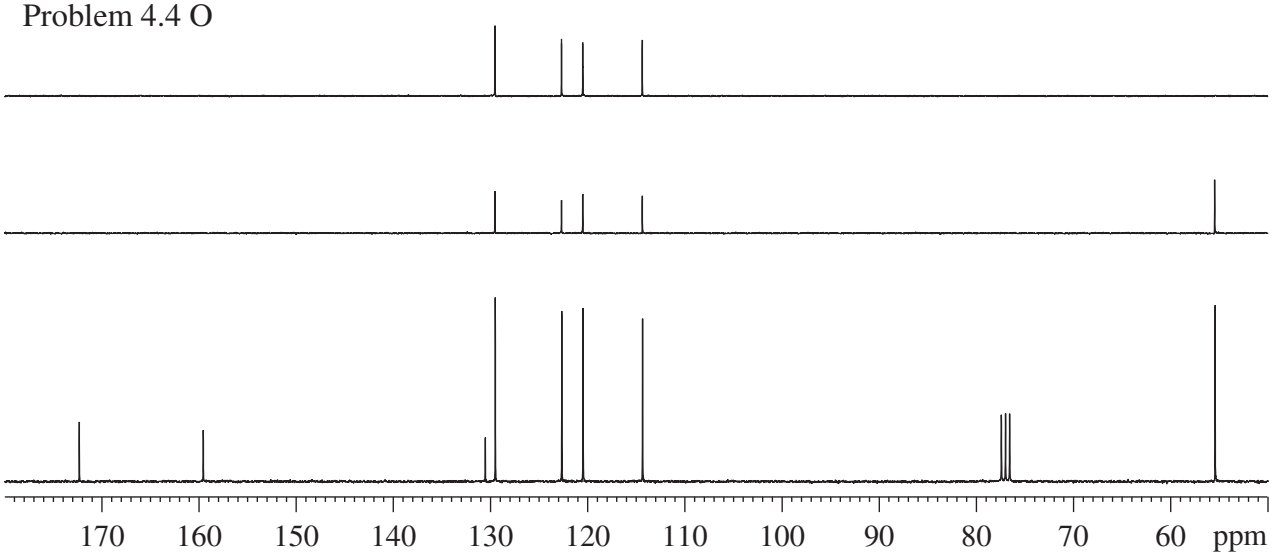

Problem 4.4 P

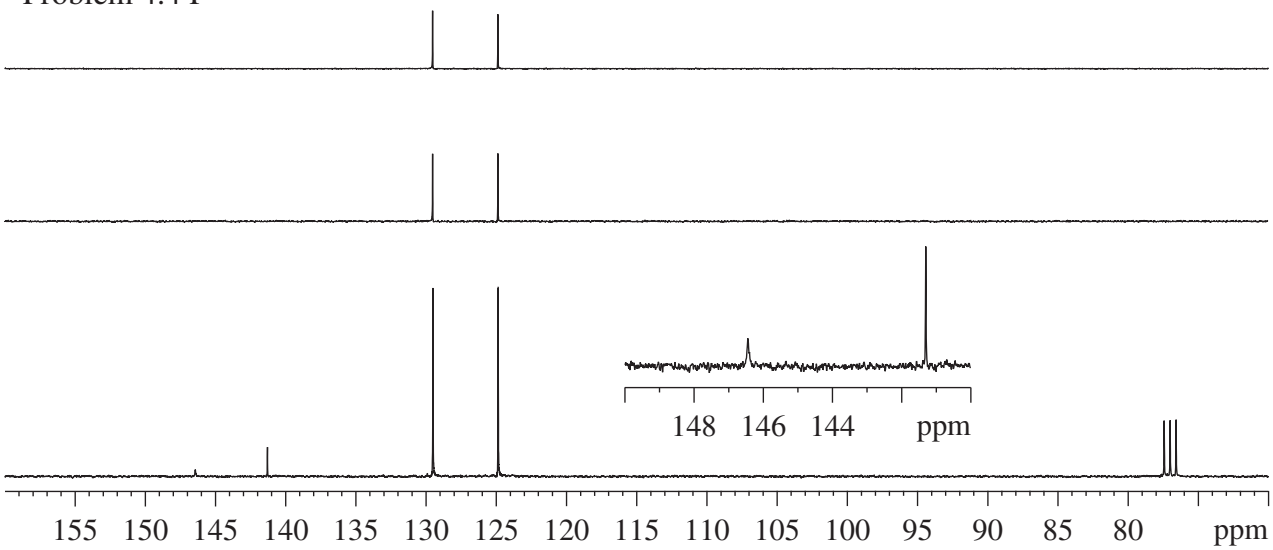

Problem 4.4 Q

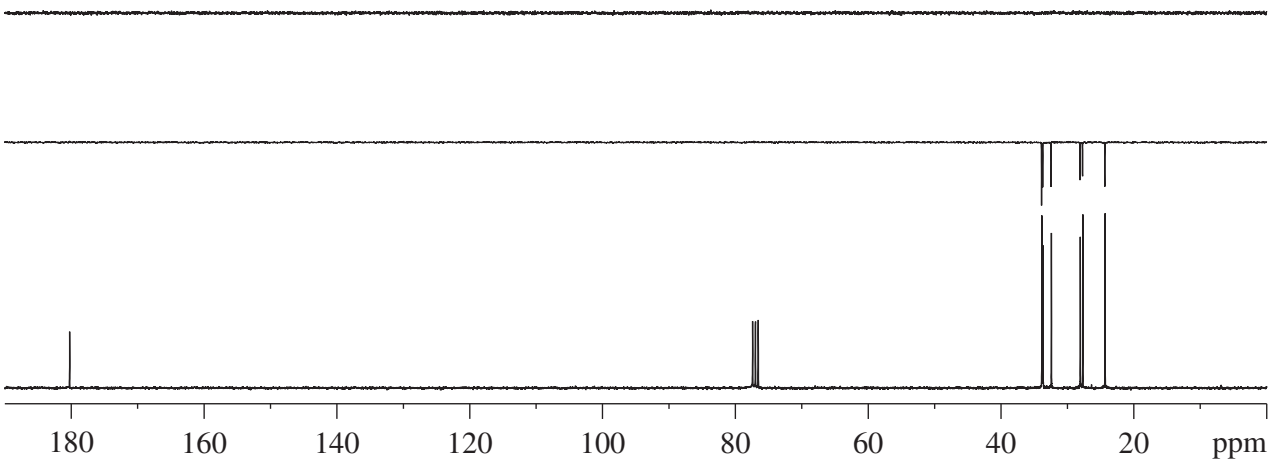

Problem 4.4 R

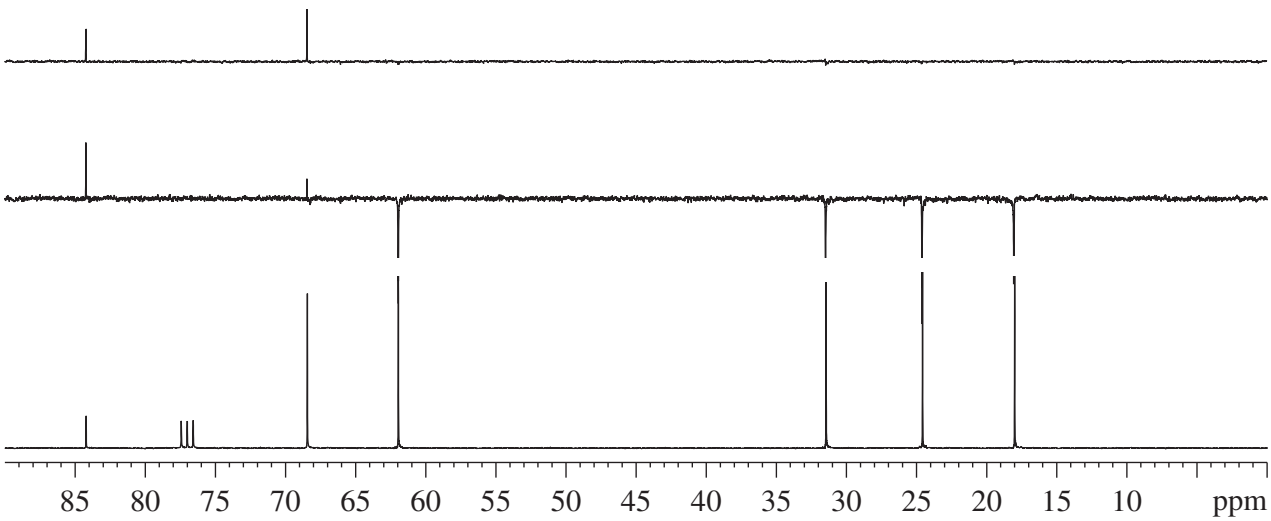

Problem 4.4 S

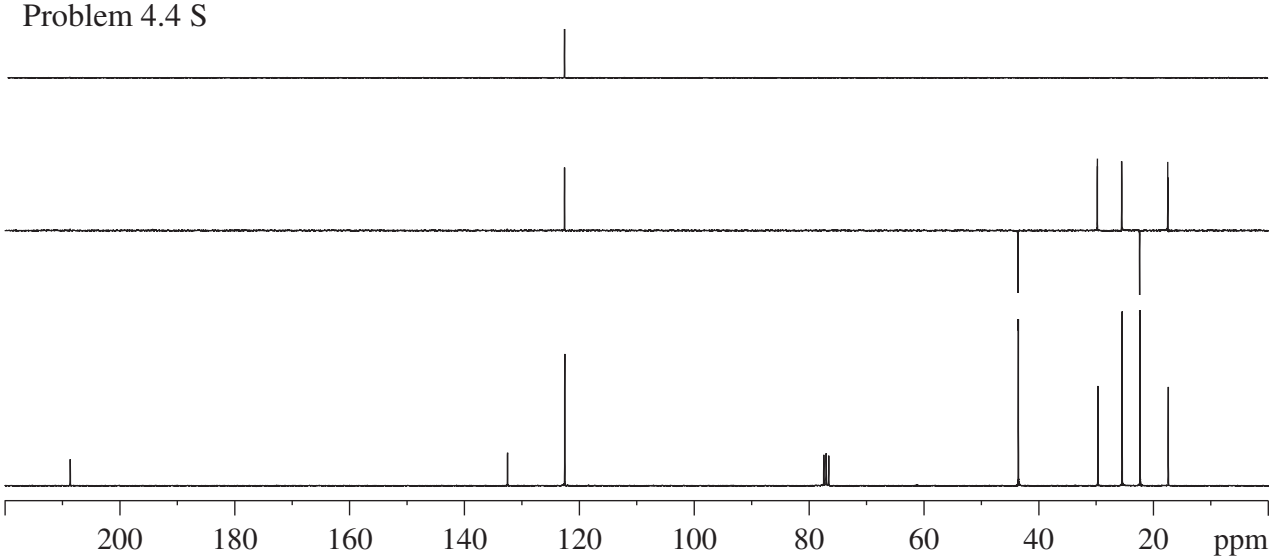

Problem 4.4 T

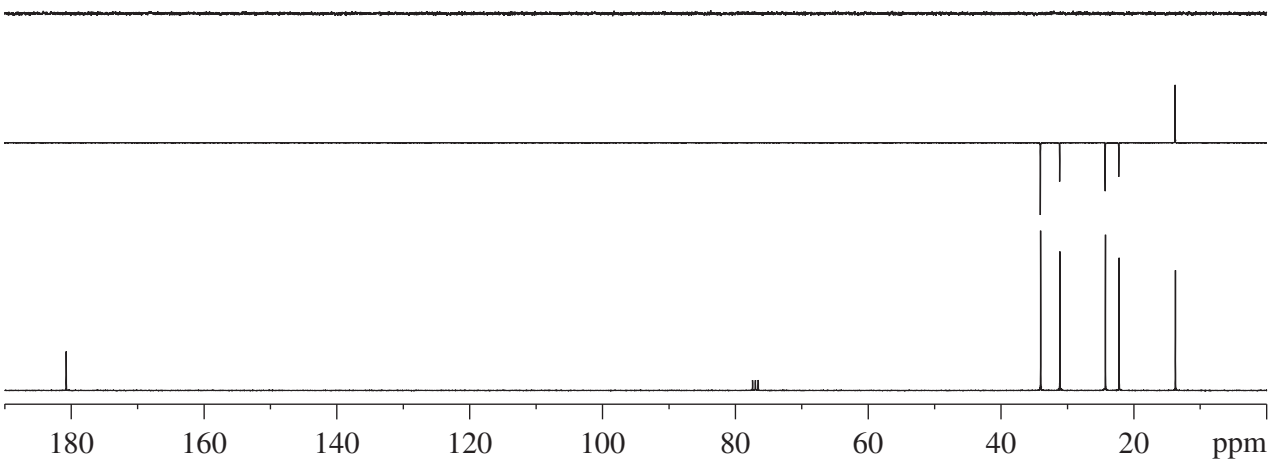

Problem 4.4 U

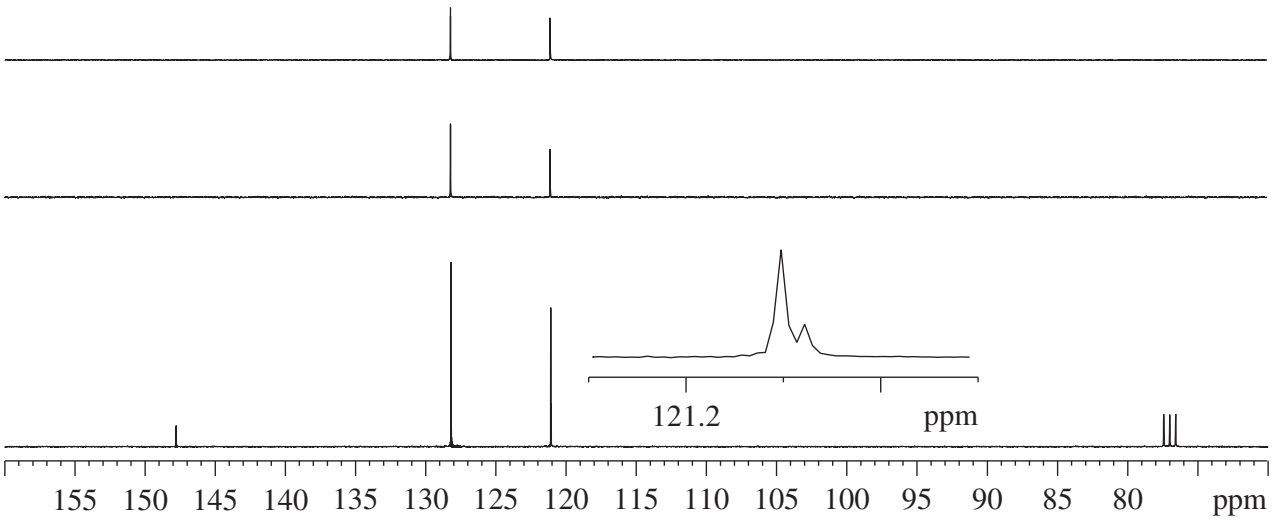

Problem 4.4 V

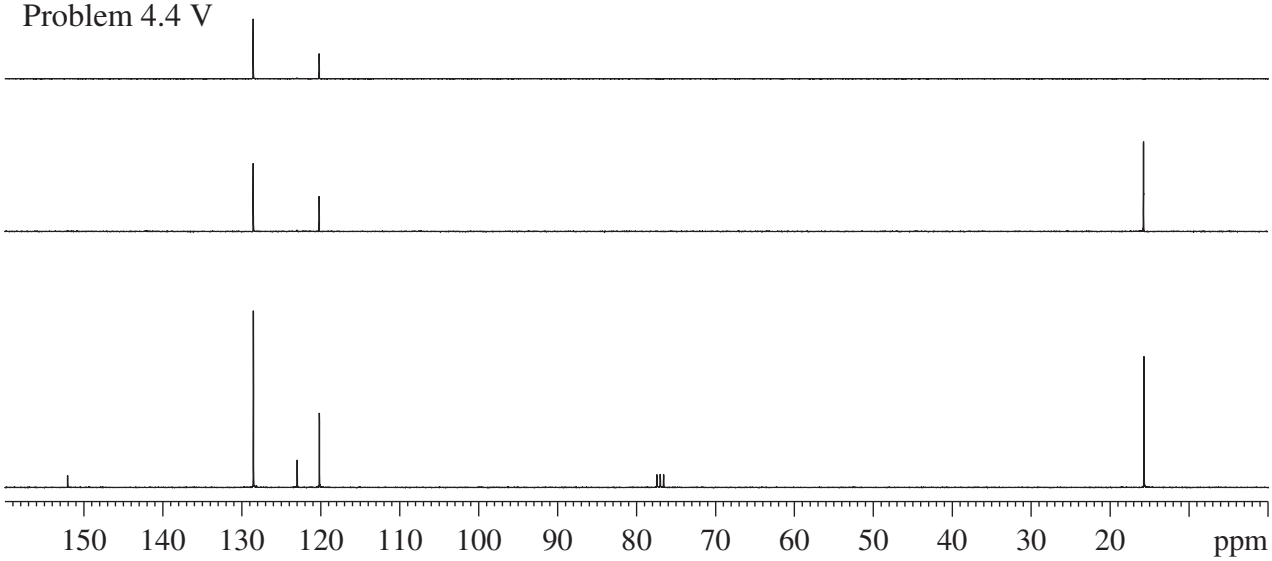

Problem 4.4 W

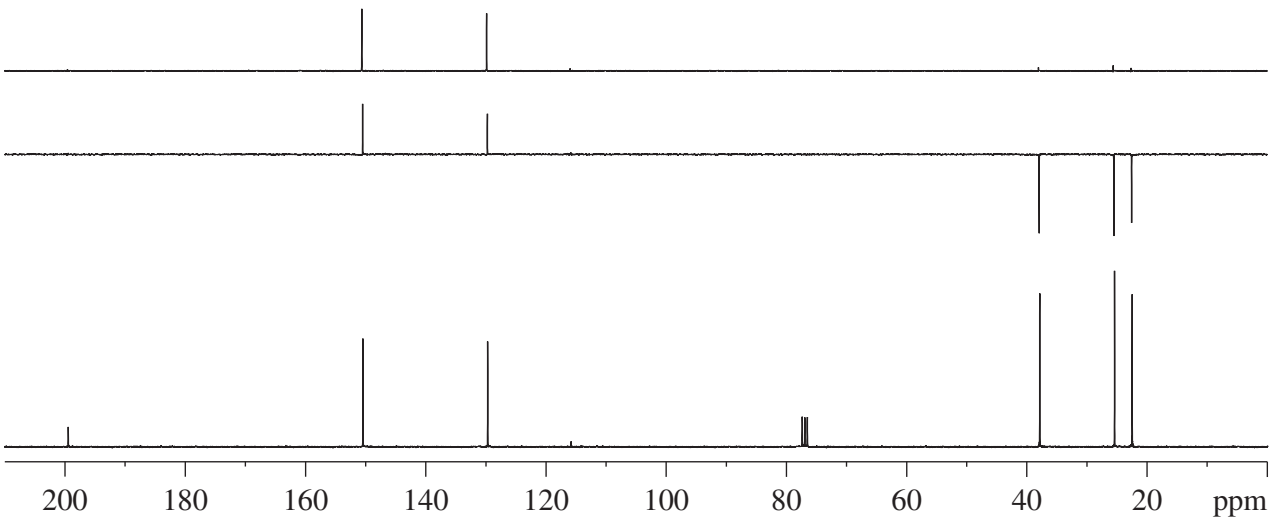

Problem 4.6 A

$C_5H_{10}Br_2$

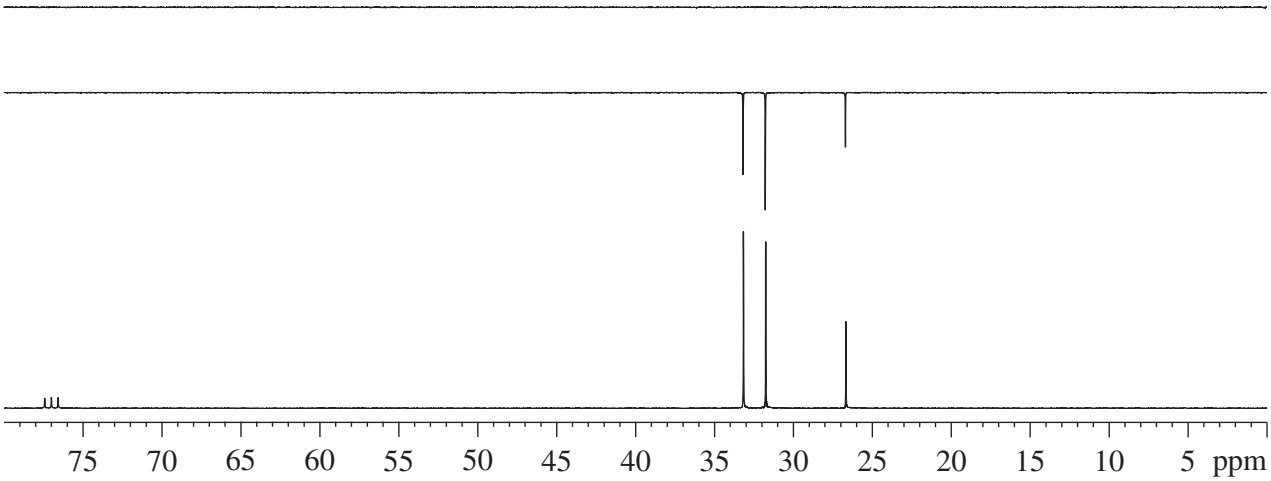

Problem 4.6 B

$C_8H_8O_2$

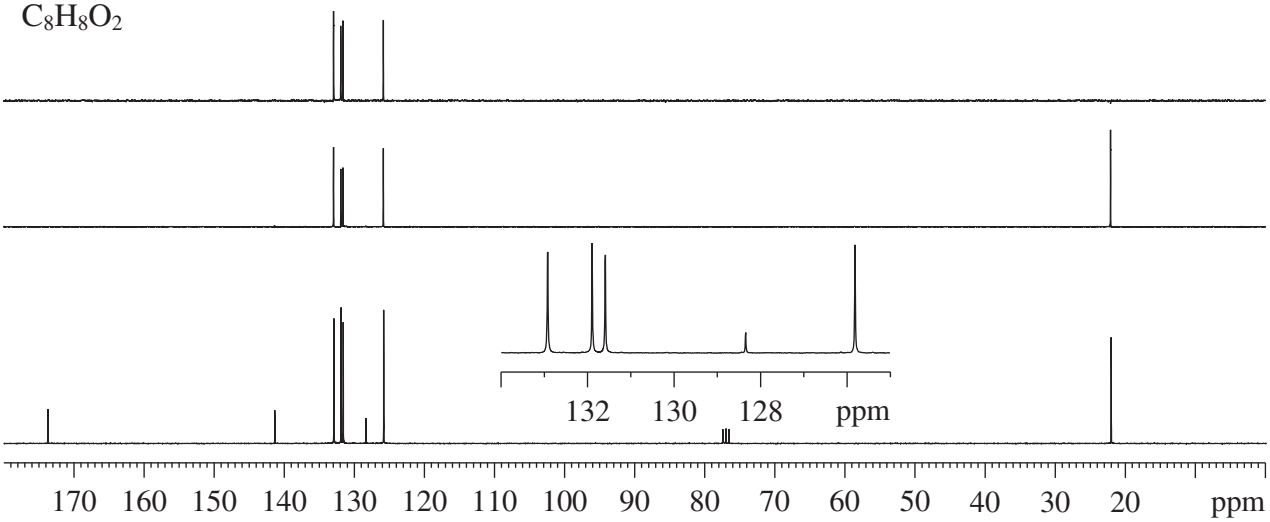

Problem 4.6 C

$C_{12}H_{27}N$

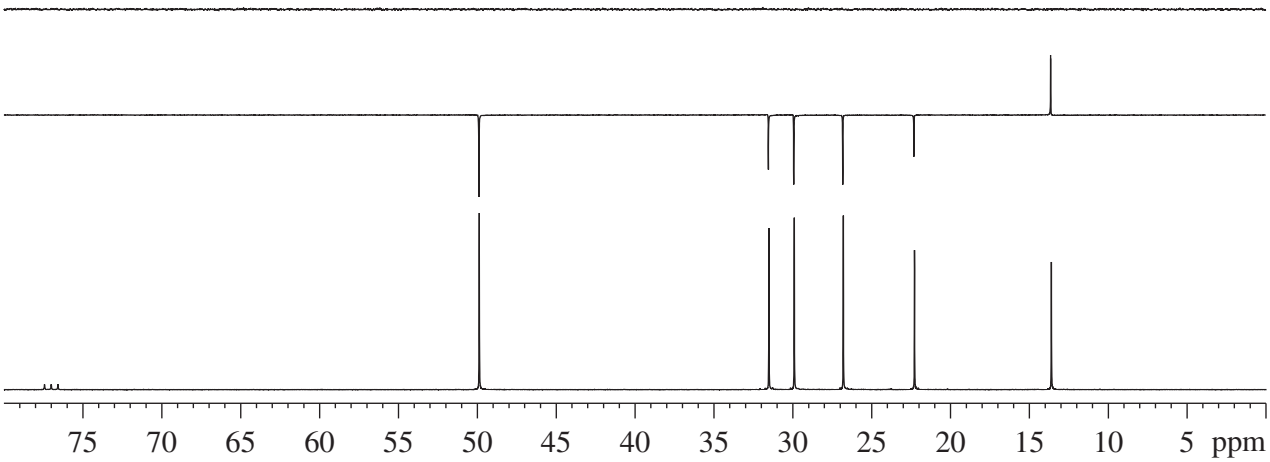

Problem 4.6 D

$C_{16}H_{22}O_4$

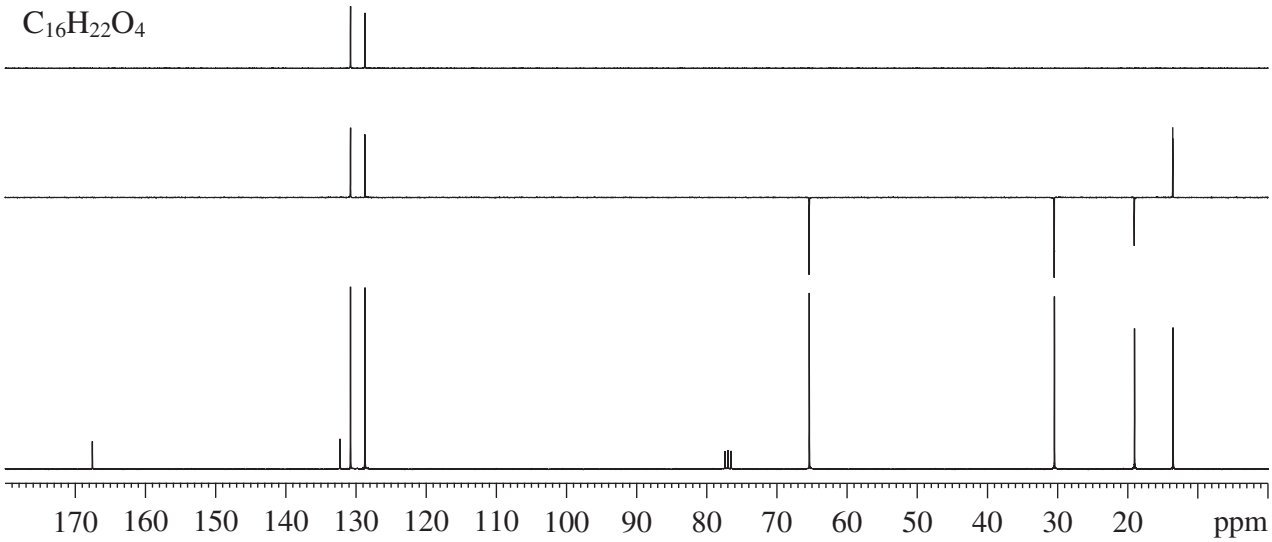

Problem 4.6 E

$C_7H_{12}O$

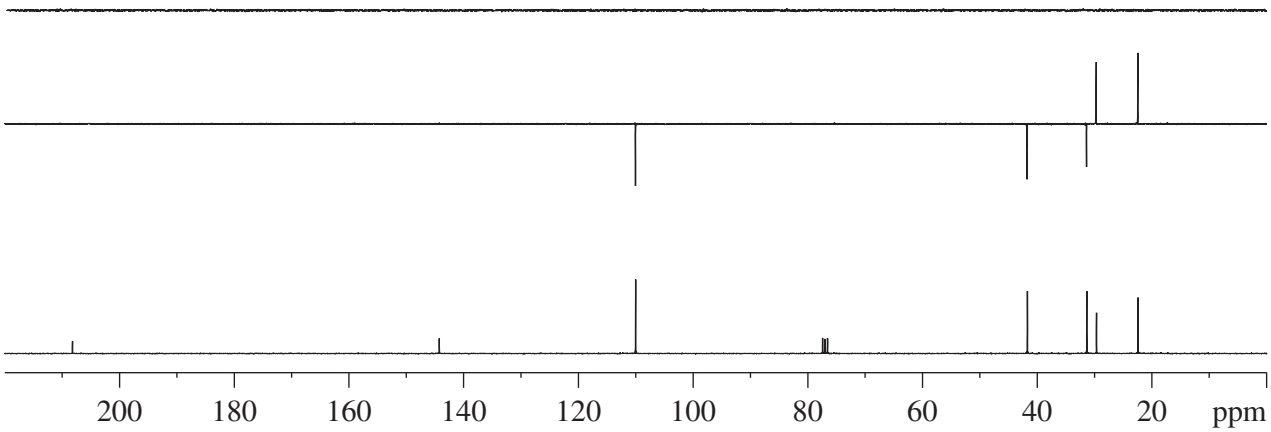

Problem 4.6 F

$C_8H_{14}O$

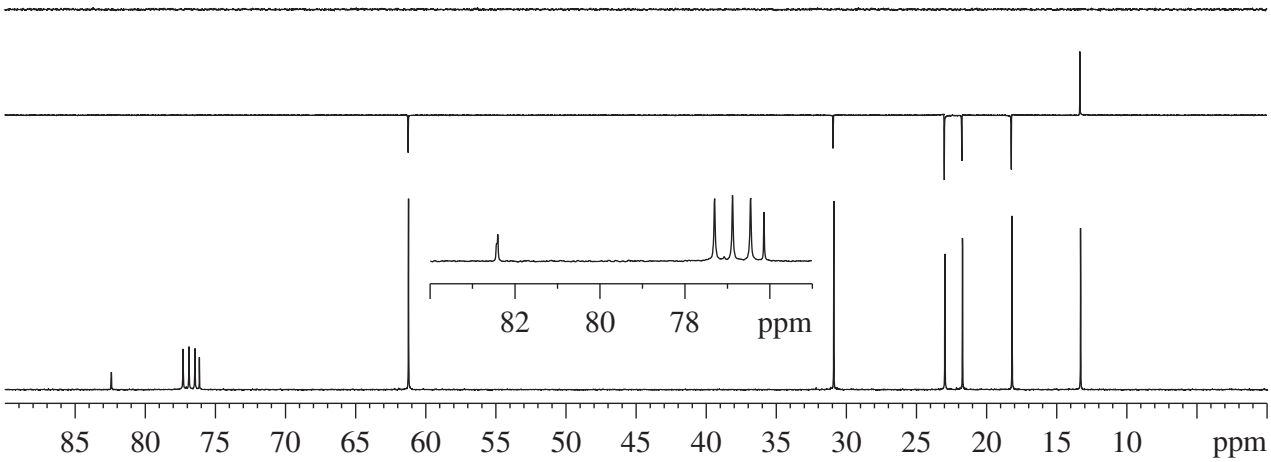

APPENDIX A THE ^{13}C CHEMICAL SHIFTS, COUPLING CONSTANTS, AND PEAK MULTIPLICITIES OF COMMON DEUTERATED NMR SOLVENTS

Formula	Name	δ (ppm)	J_{C-D} (Hz)	Multiplicity[a]
$CDCl_3$	Chloroform-d_1	77.0	32	Triplet
CD_3OD	Methanol-d_4	49.0	21.5	Septet
CD_3SOCD_3	DMSO-d_6	39.7	21	Septet
	DMF-d_7	30.1	21	Septet
		35.2	21	Septet
		167.7	30	Triplet
C_6D_6	Benzene-d_6	128.0	24	Triplet
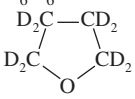	THF-d_8	25.2	20.5	Quintet
		67.4	22	Quintet
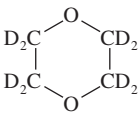	Dioxane-d_8	66.5	22	Quintet
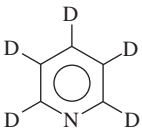	Pyridine-d_5	123.5 (C-3,5)	25	Triplet
		135.5 (C-4)	24.5	Triplet
		149.2 (C-2,6)	27.5	Triplet
		29.8 (methyl)	20	Septet
	Acetone-d_6	206.5 (carbonyl)	<1	Septet[b]
CD_3CN	Acetonitrile-d_3	1.3 (methyl)	32	Septet
		118.2 (CN)	<1	Septet[b]
CD_3NO_2	Nitromethane-d_3	60.5	23.5	Septet
CD_3CD_2OD	Ethanol-d_6	15.8 (C-2)	19.5	Septet
		55.4 (C-1)	22	Quintet
$(CD_3CD_2)_2O$	Ether-d_{10}	13.4 (C-2)	19	Septet
		64.3 (C-1)	21	Quintet
$[(CD_3)_2N]_3P{=}O$	HMPA-d_{18}	35.8	21	Septet
CD_3CO_2D	Acetic acid-d_4	20.2 (C-2)	20	Septet
		178.4 (C-1)	<1	Septet[b]
CD_2Cl_2	Dichloromethane-d_2 (Methylene chloride-d_2)	53.1	29	Quintet

[a]Triplet intensities = 1:1:1, quintet = 1:2:3:2:1, septet = 1:3:6:7:6:3:1.
[b]Unresolved, long-range coupling.

Source: Breitmaier, and Voelter (1987) p. 109; used with permission. Also Merck & Co., Inc.

APPENDIX B ^{13}C CHEMICAL SHIFTS OF COMMON LABORATORY SOLVENTS AS TRACE IMPURITIES IN SELECTED DEUTERATED NMR SOLVENTS

		$CDCl_3$	$(CD_3)_2CO$	$(CD_3)_2SO$	C_6D_6	CD_3CN	CD_3OD	D_2O
Solvent signals		77.16 ± 0.06	29.84 ± 0.01 206.26 ± 0.13	39.52 ± 0.06	128.06 ± 0.02	1.32 ± 0.02 118.26 ± 0.02	49.00 ± 0.01	
Acetic acid	CO	175.99	172.31	171.93	175.82	173.21	175.11	177.21
	CH_3	20.81	20.51	20.95	20.37	20.73	20.56	21.03
Acetone	CO	207.07	205.87	206.31	204.43	207.43	209.67	215.94
	CH_3	30.92	30.60	30.56	30.14	30.91	30.67	30.89
Acetonitrile	CN	116.43	117.60	117.91	116.02	118.26	118.06	119.68
	CH_3	1.89	1.12	1.03	0.20	1.79	0.85	1.47
Benzene	CH	128.37	129.15	128.30	128.62	129.32	129.34	
tert-Butyl alcohol	C	69.15	68.13	66.88	68.19	68.74	69.40	70.36
	CH_3	31.25	30.72	30.38	30.47	30.68	30.91	30.29
tert-Butyl methyl	OCH_3	49.45	49.35	48.70	49.19	49.52	49.66	49.37
Ether	C	72.87	72.81	72.04	72.40	73.17	74.32	75.62
	CCH_3	26.99	27.24	26.79	27.09	27.28	27.22	26.60
BHT	C(1)	151.55	152.51	151.47	152.05	152.42	152.85	
	C(2)	135.87	138.19	139.12	136.08	138.13	139.09	
	CH(3)	125.55	129.05	127.97	128.52	129.61	129.49	
	C(4)	128.27	126.03	124.85	125.83	126.38	126.11	
	CH_3Ar	21.20	21.31	20.97	21.40	21.23	21.38	
	CH_3C	30.33	31.61	31.25	31.34	31.50	31.15	
	C	34.25	35.00	34.33	34.35	35.05	35.36	
Chloroform	CH	77.36	79.19	79.16	77.79	79.17	79.44	
Cyclohexane	CH_2	26.94	27.51	26.33	27.23	27.63	27.96	
1,2-Dichloroethane	CH_2	43.50	45.25	45.02	43.59	45.54	45.11	
Dichloromethane	CH_2	53.52	54.95	54.84	53.46	55.32	54.78	
Diethyl ether	CH_3	15.20	15.78	15.12	15.46	15.63	15.46	14.77
	CH_2	65.91	66.12	62.05	65.94	66.32	66.88	66.42
Diglyme	CH_3	59.01	58.77	57.98	58.66	58.90	59.06	58.67
	CH_2	70.51	71.03	69.54	70.87	70.99	71.33	70.05
	CH_2	71.90	72.63	71.25	72.35	72.63	72.92	71.63
1,2-Dimethoxyethane	CH_3	59.08	58.45	58.01	58.68	58.89	59.06	58.67
	CH_2	71.84	72.47	71.17	72.21	72.47	72.72	71.49
Dimethylacetamide	CH_3	21.53	21.51	21.29	21.16	21.76	21.32	21.09
	CO	171.07	170.61	169.54	169.95	171.31	173.32	174.57
	NCH_3	35.28	34.89	37.38	34.67	35.17	35.50	35.03
	NCH_3	38.13	37.92	34.42	37.03	38.26	38.43	38.76
Dimethylformamide	CH	162.62	162.79	162.29	162.13	163.31	164.73	165.53
	CH_3	36.50	36.15	35.73	35.25	36.57	36.89	37.54
	CH_3	31.45	31.03	30.73	30.72	31.32	31.61	32.03
Dimethyl sulfoxide	CH_3	40.76	41.23	40.45	40.03	41.31	40.45	39.39
Dioxane	CH_2	67.14	67.60	66.36	67.16	67.72	68.11	67.19
Ethanol	CH_3	18.41	18.89	18.51	18.72	18.80	18.40	17.47
	CH_2	58.28	57.72	56.07	57.86	57.96	58.26	58.05
Ethyl acetate	CH_3CO	21.04	20.83	20.68	20.56	21.16	20.88	21.15
	CO	171.36	170.96	170.31	170.44	171.68	172.89	175.26
	CH_2	60.49	60.56	59.74	60.21	60.98	61.50	62.32
	CH_3	14.19	14.50	14.40	14.19	14.54	14.49	13.92
Ethyl methyl ketone	CH_3CO	29.49	29.30	29.26	28.56	29.60	29.39	29.49
	CO	209.56	208.30	208.72	206.55	209.88	212.16	218.43
	CH_2CH_3	36.89	36.75	35.83	36.36	37.09	37.34	37.27
	CH_2CH_3	7.86	8.03	7.61	7.91	8.14	8.09	7.87
Ethylene glycol	CH_2	63.79	64.26	62.76	64.34	64.22	64.30	63.17
"Grease"	CH_2	29.76	30.73	29.20	30.21	30.86	31.29	

APPENDIX B *(Continued)*

n-Hexane	CH_3	14.14	14.34	13.88	14.32	14.43	14.45	
	$CH_2(2)$	22.70	23.28	22.05	23.04	23.40	23.68	
	$CH_2(3)$	31.64	32.30	30.95	31.96	32.36	32.73	
HMPA	CH_3	36.87	37.04	36.42	36.88	37.10	37.00	36.46
Methanol	CH_3	50.41	49.77	48.59	49.97	49.90	49.86	49.50
Nitromethane	CH_3	62.50	63.21	63.28	61.16	63.66	63.08	63.22
n-Pentane	CH_3	14.08	14.29	13.28	14.25	14.37	14.39	
	$CH_2(2)$	22.38	22.98	21.70	22.72	23.08	23.38	
	$CH_2(3)$	34.16	34.83	33.48	34.45	34.89	35.30	
2-Propanol	CH_3	25.14	25.67	25.43	25.18	25.55	25.27	24.38
	CH	64.50	63.85	64.92	64.23	64.30	64.71	64.88
Pyridine	CH(2)	149.90	150.67	149.58	150.27	150.76	150.07	149.18
	CH(3)	123.75	124.57	123.84	123.58	127.76	125.53	125.12
	CH(4)	135.96	136.56	136.05	135.28	136.89	138.35	138.27
Silicone grease	CH_3	1.04	1.40		1.38		2.10	
Tetrahydrofuran	CH_2	25.62	26.15	25.14	25.72	26.27	26.48	25.67
	CH_2O	67.97	68.07	67.03	67.80	68.33	68.83	68.68
Toluene	CH_3	21.46	21.46	20.99	21.10	21.50	21.50	
	C(*i*)	137.89	138.48	137.35	137.91	138.90	138.85	
	CH(*o*)	129.07	129.76	128.88	129.33	129.94	129.91	
	CH(*m*)	128.26	129.03	128.18	128.56	129.23	129.20	
	CH(*p*)	125.33	126.12	125.29	125.68	126.28	126.29	
Triethylamine	CH_3	11.61	12.49	11.74	12.35	12.38	11.09	9.07
	CH_2	46.25	47.07	45.74	46.77	47.10	46.96	47.19

APPENDIX C ^{13}C CHEMICAL SHIFT RANGES FOR CHEMICAL CLASSES

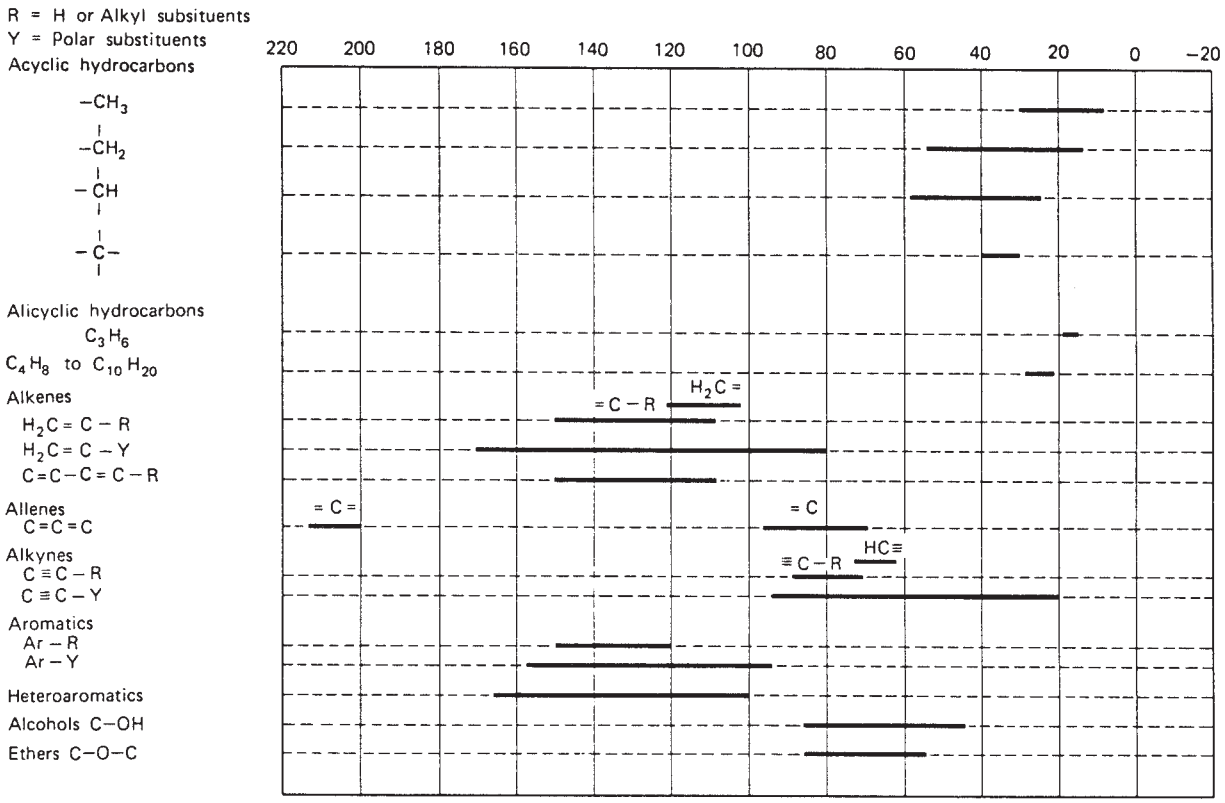

APPENDIX C *(Continued)*

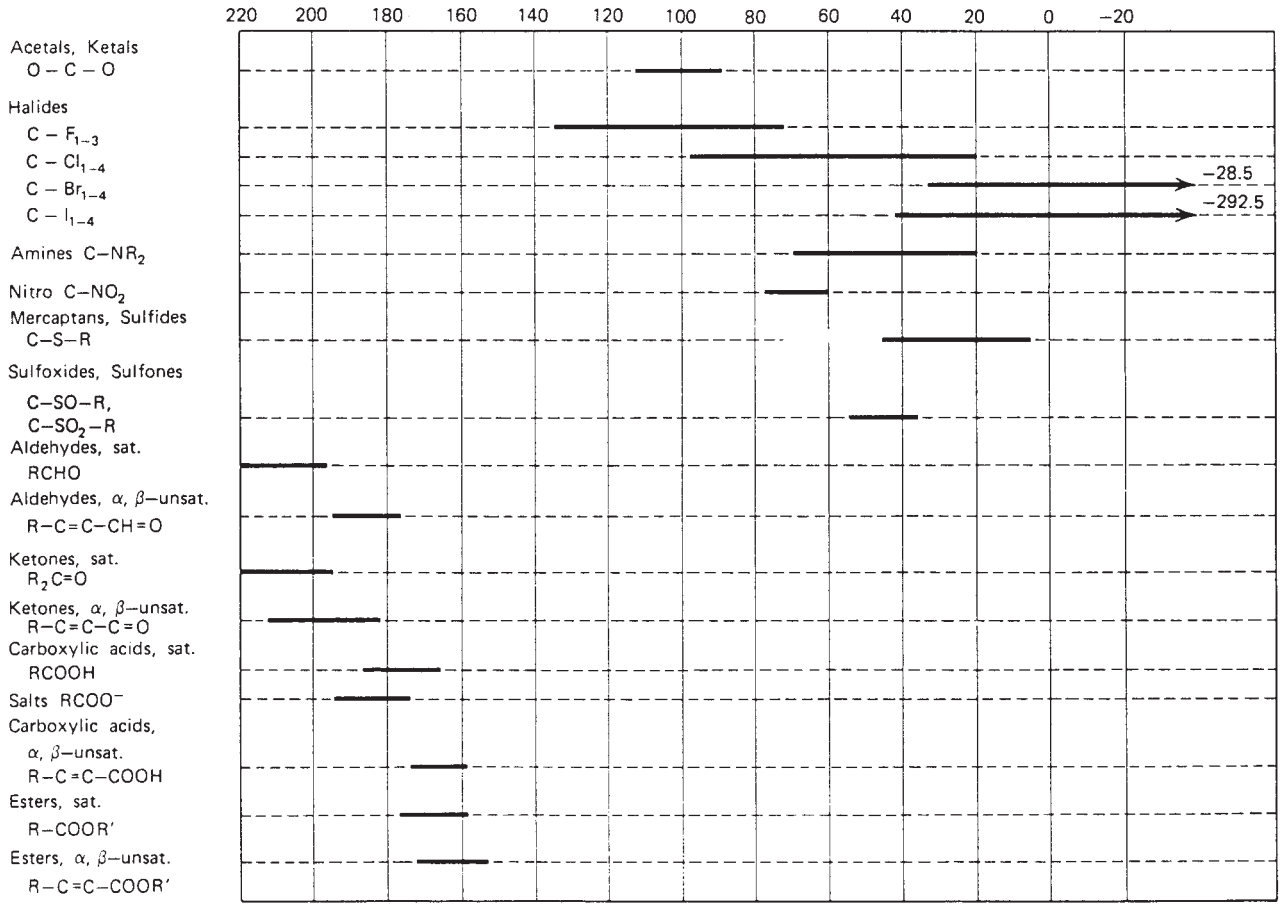

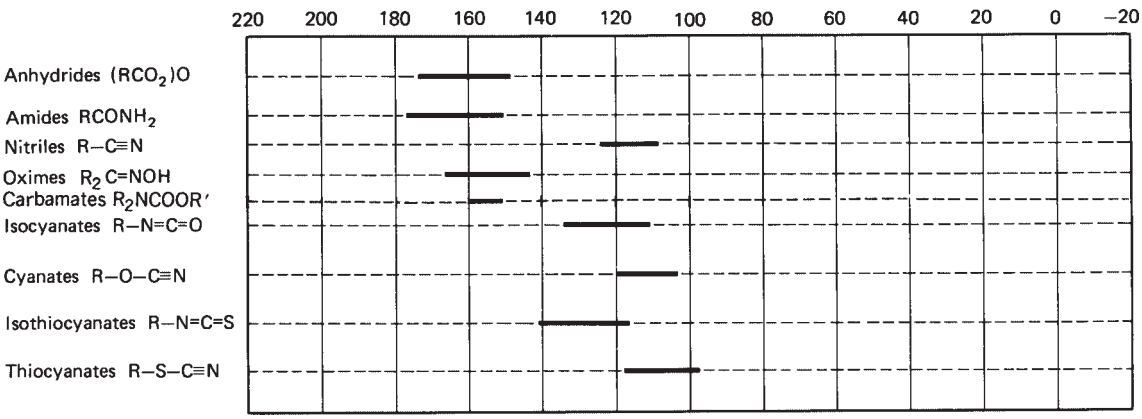

APPENDIX D ^{13}C CHEMICAL SHIFTS (ppm) FOR SEVERAL NATURAL PRODUCTS

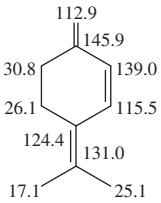

Myrcene

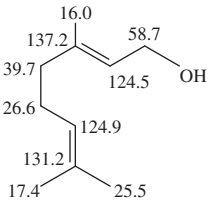

Geraniol

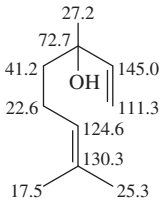

Linalool

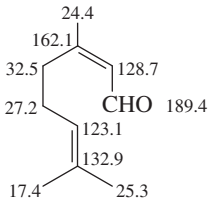

cis-Citral
(Neral, Citral b)

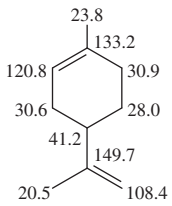

Limonene

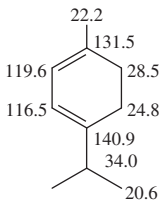

α-Terpinene

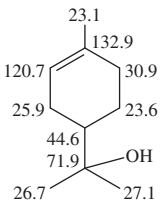

α-Terpineol

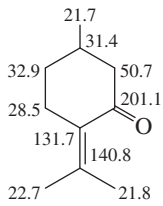

Pulegone

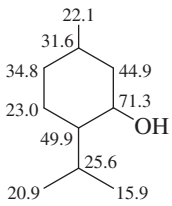

Menthol

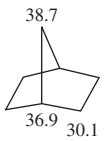

Norbornane

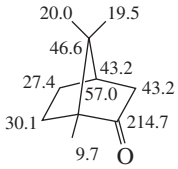

Camphor

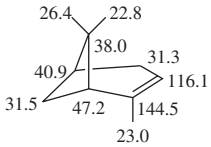

α-Pinene

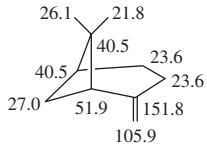

β-Pinene

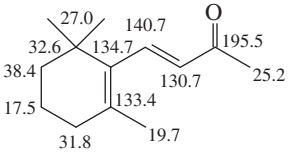

β-Ionone

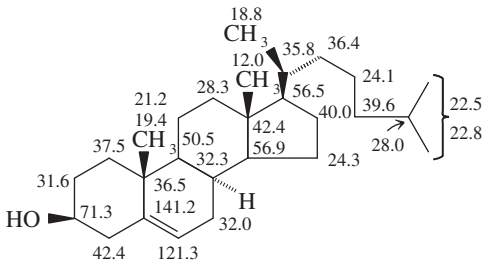

Cholesterol

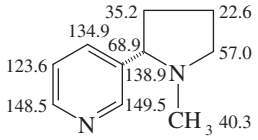

Nicotine

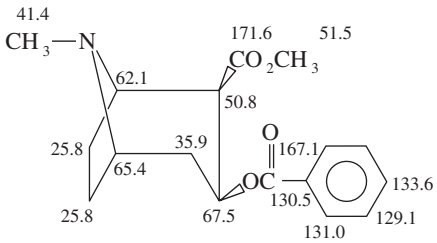

Cocaine

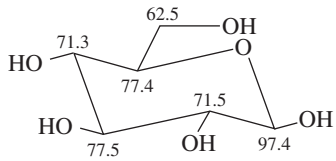

β-D-Glucose

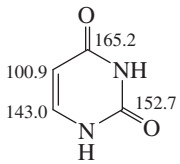

Uracil

CHAPTER 5

TWO-DIMENSIONAL NMR SPECTROSCOPY

5.1 INTRODUCTION

Chapters 3 and 4 (familiarity with which is assumed) provide us with powerful techniques and methods to elucidate the structures of organic compounds, especially when combined with information derived from IR and mass spectrometry. These NMR methods are collectively referred to as one-dimensional techniques. To extend our capabilities, we turn once more to NMR. We will use four compounds as examples: ipsenol (see Chapter 3), caryophyllene oxide (a sesquiterpene epoxide), lactose (a β-linked disaccharide), and a small peptide (valine-glycine-serine-glutamate, VGSE). The structures of these compounds are shown in Figure 5.1.

These compounds provide a rich variety of structural types and features. The two terpenoids possess the typical branched carbon skeletons of isoprenoids; both compounds have diastereotopic methylene and methyl groups. Lactose is a β-1,4-linked disaccharide of galactose and glucose; glucose is the reducing residue, which at equilibrium in aqueous solution shows both anomers. The tetrapeptide, VGSE, contains four different amino acid residues and is a reasonable model for some of the spectroscopic properties of a small protein. The NMR signals associated with these compounds can sometimes be difficult to interpret using simple one-dimensional ^{1}H and ^{13}C NMR spectra.

In this chapter, using these four compounds as examples, we turn our attention to correlation NMR spectroscopy; most (but not all) of the useful experiments fall into the category of two-dimensional NMR. Our approach in this chapter is to present the spectra for each compound independently as a logical set. Most of the general aspects of each experiment are given in the discussion of ipsenol; others are only introduced with the more complicated compounds. The material for ipsenol should be thoroughly covered first. The other compounds can be covered independently.

Correlation in NMR is not a new concept to us. For instance, the ^{1}H NMR spectrum of ethylbenzene (Figure 3.24) shows a clean triplet and quartet for the methyl and methylene groups, respectively. These two groups are correlated to each other because the spins within each group are coupled to the spins within the other group. First-order rules helped us to interpret these interactions among neighboring nuclei. Coupling among protons is only one type of correlation that we will be considering.

We did a reasonable job interpreting the relationship between the structure of ipsenol and its ^{1}H NMR spectra in Chapter 3; however, better, less ambiguous information

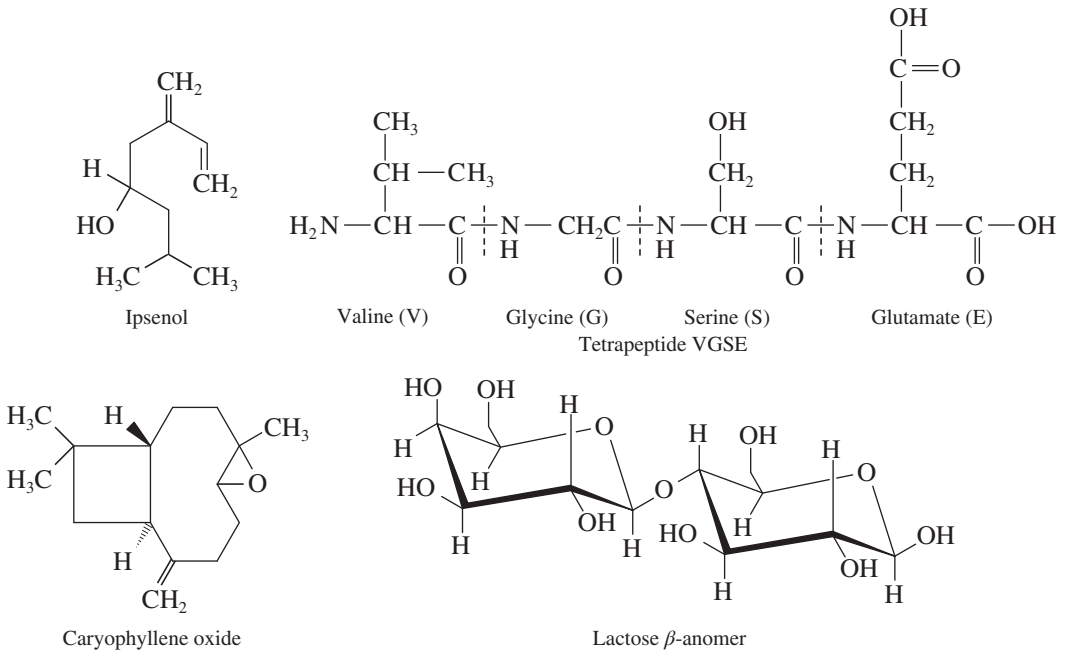

FIGURE 5.1 Structures of the four compounds used as examples in this chapter.

can be obtained more quickly with two-dimensional NMR correlation spectroscopy. On the other hand, caryophyllene oxide, lactose, and VGSE are too complex to fully analyze using one-dimensional ^{1}H and ^{13}C NMR alone. Before turning our attention to the description of specific experiments and their interpretation, we will first take a closer look at radiofrequency pulse sequences and Fourier transformation.

5.2 THEORY

We recall that in order to obtain a routine ^{1}H or ^{13}C NMR spectrum, the pulse sequence (Figure 5.2) involves an equilibration in the magnetic field, an rf pulse, and signal acquisition. This sequence is repeated until a satisfactory signal/noise ratio is obtained; Fourier transformation of the FID results in the familiar frequency-domain spectrum.

Figure 5.2 reveals a number of interesting features. We note that there is a separate line for the ^{1}H channel and one for the ^{13}C channel. These channels represent the hardware associated with the irradiation and signal acquisition of each relevant nucleus in our experiments. Following equilibration, the pulse sequence used to obtain a one-dimensional (1D) proton NMR spectrum consists of a $(\pi/2)_x$ pulse, delay, and signal acquisition of the order of seconds (Figure 5.2a). We also notice that the ^{13}C channel (not shown) is inactive during a simple proton experiment. Normally, we will not show a given channel unless there is some activity in that channel.

Shown in Figure 5.2b is the pulse sequence for a 1D ^{13}C NMR experiment. The sequence in the ^{13}C channel is exactly the same as the sequence in the ^{1}H channel in Figure 5.2a. The protons are decoupled from the ^{13}C nuclei

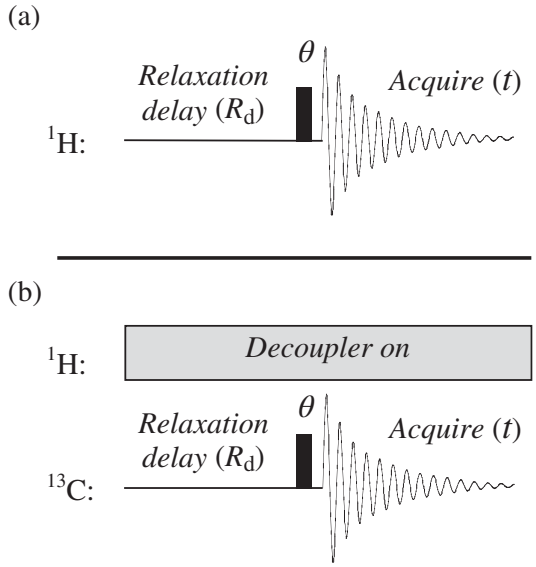

FIGURE 5.2 (a) Pulse sequence for a standard one-dimensional ^{1}H NMR spectrum. (b) Pulse sequence for a standard (proton-decoupled) ^{13}C NMR spectrum. θ is normally a $(\pi/2)_x$ pulse along the x-axis. R_d (known as the relaxation delay) is an equilibration period in the magnetic field before the pulse.

by irradiating the protons during the experiment; that is, the proton decoupler is turned on during the entire experiment. In other experiments, the decoupler for a given nucleus can be turned on and off to coincide with pulses and delays in another channel (i.e., for another nucleus). This process is termed gated decoupling. (See Sections 4.2.5 and 4.4.)

It is worthwhile to review here (see Chapters 3 and 4) what is happening to the net magnetization vector, $\mathbf{M_0}$, during this pulse sequence. In a frame of reference rotating at the Larmor frequency, $\mathbf{M_0}$ is stationary on the z-axis (equilibration period in Figure 5.2). A $\pi/2$ $(\theta, 90°)$ pulse brings $\mathbf{M_0}$ onto the y-axis; when viewed in this rotating frame, the magnetization vector appears to remain stationary after the pulse, although the component of the vector along the y-axis is decreasing with time (T_1 and T_2 relaxation). Returning for a moment to the static laboratory frame, we see that the net magnetization vector is actually not static; it is rotating in the xy-plane about the z-axis at the Larmor frequency. This rotating magnetization generates an rf signal that is detected as an FID in an NMR experiment. The net magnetization vector soon returns to the z-axis, relaxation is complete, and the sequence can be repeated. In this example, the detector records the component of the magnetization which lies along the y-axis. In a simple one-pulse experiment, a $\pi/2$ pulse is used because it produces the strongest signal.* A pulse (θ) less than (or greater than) $\pi/2$ leaves some of the possible signal on the z (or $-z$) -axis; only the component of the vector on the y-axis generates a signal.

We now consider multiple-pulse experiments and two-dimensional (2D) NMR. Exactly what does the term "dimension" in NMR mean? The familiar proton spectrum is a plot of frequency versus intensity—obviously two dimensions but called a "1D" NMR experiment, the relevant dimension being the frequency axis. It is important to remember that the frequency axis, with which we are comfortable, is derived from the time axis (the acquisition time) of the FID through the mathematical process of Fourier transformation. Thus, *experimentally,* the variable of the abscissa of a 1D experiment is in time units.

The so-called 2D NMR spectrum is actually a three-dimensional plot; the omitted dimension when describing all NMR experiments (1D, 2D, 3D, etc.) is the intensity. The two dimensions referred to in a 2D NMR spectrum are the two frequency axes. It requires two Fourier transformations at right angles to each other on two independent time axes to arrive at two orthogonal frequency axes.

When the simple one-pulse experiment is again considered, there is only one time variable that affects the spectrum, namely the acquisition time, t. We now consider a multiple-pulse sequence in which the equilibration period is followed by two pulses with an intervening time interval, the final pulse being the $\pi/2$ acquisition pulse. Thus, we have inserted an "evolution" period between the pulses.

*This is true in the absence of relaxation considerations. The Ernst angle ($\cos\theta = \exp(-T_r/T_1)$) may be used to determine the repetition time (T_r) and pulse angle (θ) to optimize S/N; the angle thus determined is less than 90°, e.g., ~45°.

If we now systematically increase this evolution time interval (t_1) over many different 1D experiments and collect the resulting FIDs into one overall dataset, we have the basis for a 2D NMR spectrum. For example, t_1 is increased 15 times, meaning that 16 FIDs will have been recorded, each with a different t_1 value. Sequential Fourier transformation of each of these FIDs yields a set of one-dimensional spectra whose peak intensities vary sinusoidally from one spectrum to the next (see Figure 5.5). This first series of Fourier transformations results in what is labeled as the second frequency axis, ν_2, derived from the acquisition time, t_2, of each FID. The data are now turned by 90°, and a second Fourier transformation is carried out at right angles to the first series of transformations. This second series of Fourier transformations results in what is labeled as the first frequency axis, ν_1, a function of the evolution time, t_1, which we recall was incremented in the pulse sequence for each successive FID acquired in t_2.

A simple prototype of a 2D experiment should clarify some of these ideas while serving as a template for other more useful 2D experiments. In this simple case, the pulse sequence (Figure 5.3) consists of a relaxation delay (R_d), a $\pi/2$ pulse, a variable time interval (t_1, the evolution period), a second $\pi/2$ acquisition pulse, and acquisition (t_2). This pulse sequence (individual experiment) is repeated a number of times (each time resulting in a *separate* FID) with an increased t_1 interval.

We choose for this experiment a simple compound, acetone (CH_3—(C═O)—CH_3), to avoid the complication (for now) of spin-spin coupling. In Figure 5.4, we see that, after the first $\pi/2$ pulse along the x-axis, the magnetization $\mathbf{M_0}$ has rotated onto the y-axis (the magnetization is now labeled $\mathbf{M}$). The evolution of $\mathbf{M}$ for the equivalent protons of acetone during t_1 is shown in a rotating frame. In this treatment, we ignore spin-lattice relaxation but include transverse relaxation with time constant T_2. If the Larmor frequency (ν_2) is at higher frequency than that of the rotating frame, $\mathbf{M}$ precesses clockwise in the xy plane during the time interval t_1 through the angle $2\pi\nu t_1$. From trigonometry, the y component of $\mathbf{M}$ is $\mathbf{M}\cos(2\pi\nu t_1)$, and the x component is $\mathbf{M}\sin(2\pi\nu t_1)$.

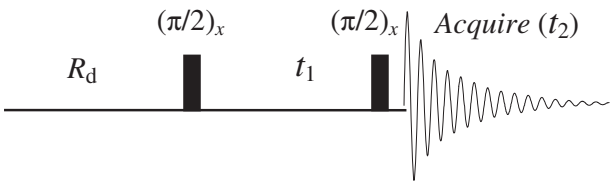

FIGURE 5.3 Traditional prototypical pulse sequence for two-dimensional NMR. Data associated with the incremental delay, t_1, and the acquisition time, t_2, are Fourier transformed into frequencies ν_1 and ν_2, respectively. $(\pi/2)_x$ represents a 90° pulse along the x-axis. The interval t_1 is of the order of microseconds to milliseconds; t_2 is of the order of seconds.

After time t_1, the acquisition pulse $(\pi/2)_x$ rotates the y component of $\mathbf{M}$ downward onto the $-z$-axis; this component therefore contributes no signal to the FID acquired during t_2. The x component, on the other hand, remains unchanged (in the xy-plane) and this magnetization is recorded as the FID. When this FID is Fourier transformed, it gives a peak with frequency ν_2 and amplitude $\mathbf{M}\sin(2\pi\nu t_1)$. If we repeat this experiment many times (e.g., 1024), each time increasing t_1 in a regular way, we obtain 1024 FIDs. Successive Fourier transformation of each of these FIDs gives a series of 1D spectra each with a single peak of frequency ν_2 and amplitude $\mathbf{M}\sin(2\pi\nu t_1)$. In Figure 5.5a, 22 of the 1024 spectra are plotted; we see that the amplitude of the acetone peak varies sinusoidally as a function of t_1. We have now established one of the frequency axes (ν_2) for our prototypical 2D NMR spectrum.

Before we establish our second axis, let us do a little bookkeeping. Remember that each of these spectra that we now have is actually a digitized collection of points. Let us assume that each of these 1024 spectra is composed of 1024 data points. Thus, we have a square matrix of data. If we mentally rotate this collection of spectra, we can perform a second series of Fourier transformations on the data orthogonal to the first. Before we perform these transformations though, let us take a closer look at the data in Figure 5.5a.

By physically rotating the spectra of Figure 5.5a so that we are looking along the ν_2 axis, the data appear as the projections shown in Figure 5.5b. Small circles are drawn at the maxima of the first seven rows of data of Figure 5.5a.

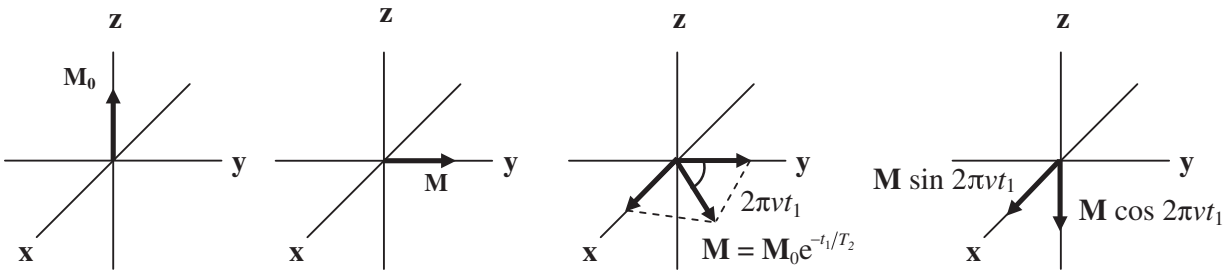

FIGURE 5.4 Evolution in a rotating frame of the magnetization of the acetone protons is shown during time interval t_1 following the first pulse. The second pulse and acquisition give a signal resulting only from the x component of $\mathbf{M}$; this signal amplitude varies sinusoidally with t_1. Interval t_1 is in the range of microseconds to milliseconds; t_2 is of the order of seconds. The precessional frequency of the protons is higher than that of the rotating frame in this example.

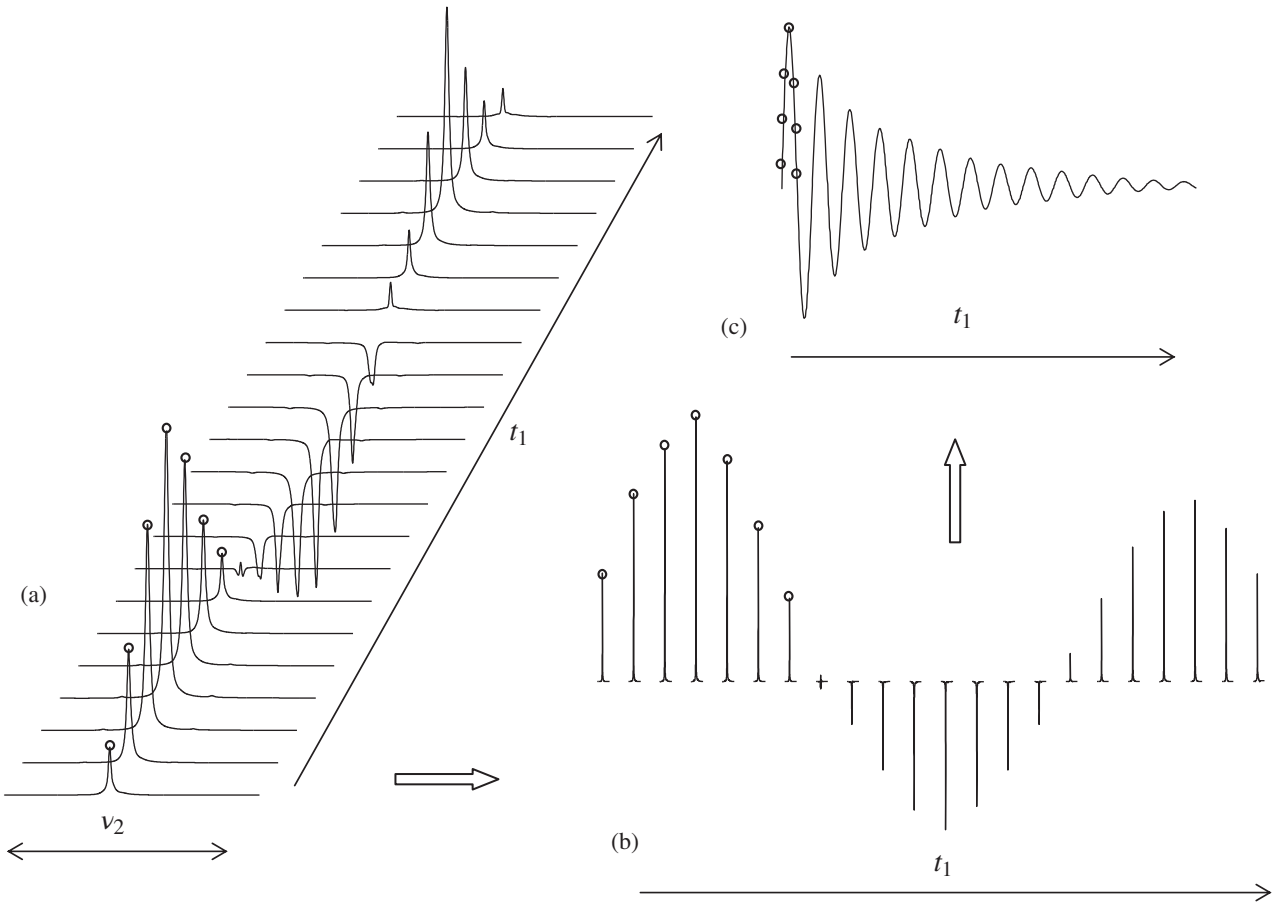

FIGURE 5.5 (a) Stacked plot of 22 ^{1}H NMR spectra from acetone in which t_1 is varied incrementally in 22 consecutive experiments. (b) Projection of (a) showing the sinusoidal behavior of the peak intensity as a function of t_1. In this projection, the frequency axis, ν_2, is perpendicular to the plane of the page. (c) Resulting interferogram which is simply a plot of the intensities of the peaks in (b) as a function of t_1. The frequency of the sinusoidal oscillation is related to the peak position along the indirect dimension (ν_1) in the final two-dimensional NMR spectrum.

These circles of the seven maxima are again drawn in Figure 5.5b (and Figure 5.5c) so that you can follow the rotation and projection. If we replot one column of data from Figure 5.5a (let us choose the column that corresponds to the maximum (and minimum) for the acetone peak), the data we obtain (Figure 5.5c) look like an FID. In fact, it is a time domain spectrum, now a function of the interval t_1 from our pulse sequence. To distinguish, we refer to data obtained in real time (a function of t_2) as an FID and data constructed point by point as a function of t_1 as an interferogram.

We now perform our second series of Fourier transformations on each of the 1024 interferograms. The end result is a 2D spectrum. We are now faced, however, with the challenge of visualizing our results. One way to present the data is as a stack plot similar to the plot that we have already seen in Figure 5.5a. This type of plot, shown in the left part of Figure 5.6, gives a sense of three dimensions. Note that the two frequency axes are now labeled F2 and F1 (same as ν_2 and ν_1), which is consistent with the rest of the text and is commonly used. For this spectrum, this type of plot is satisfactory because there are no peaks being blocked. Thus, one perspective is sufficient.

For more complex spectra, the data are usually presented as a series of contours just as hills and valleys are represented on a topographical map. We see this representation of the data in the right part of Figure 5.6. Projections of the data are often included in 2D spectra, which is equivalent to "shining a light" on the peak to reveal its "shadow." Often these projections are replaced with actual 1D spectra that have been acquired separately. So long as there are no negative peaks (e.g., phase sensitive COSY, not covered in this book), we use this method without comment.

5.3 CORRELATION SPECTROSCOPY

The observant reader will have realized by now that the above experiment, which is a type of frequency modulation, provides no additional information beyond the simple ^{1}H NMR spectrum of acetone. Actually, that is the beauty of that experiment; it has all of the elements of a 2D correlation experiment *and* we can completely follow the activity of the net magnetization vector for acetone using simple vectorial models. Let us generalize the prototypical 2D NMR pulse

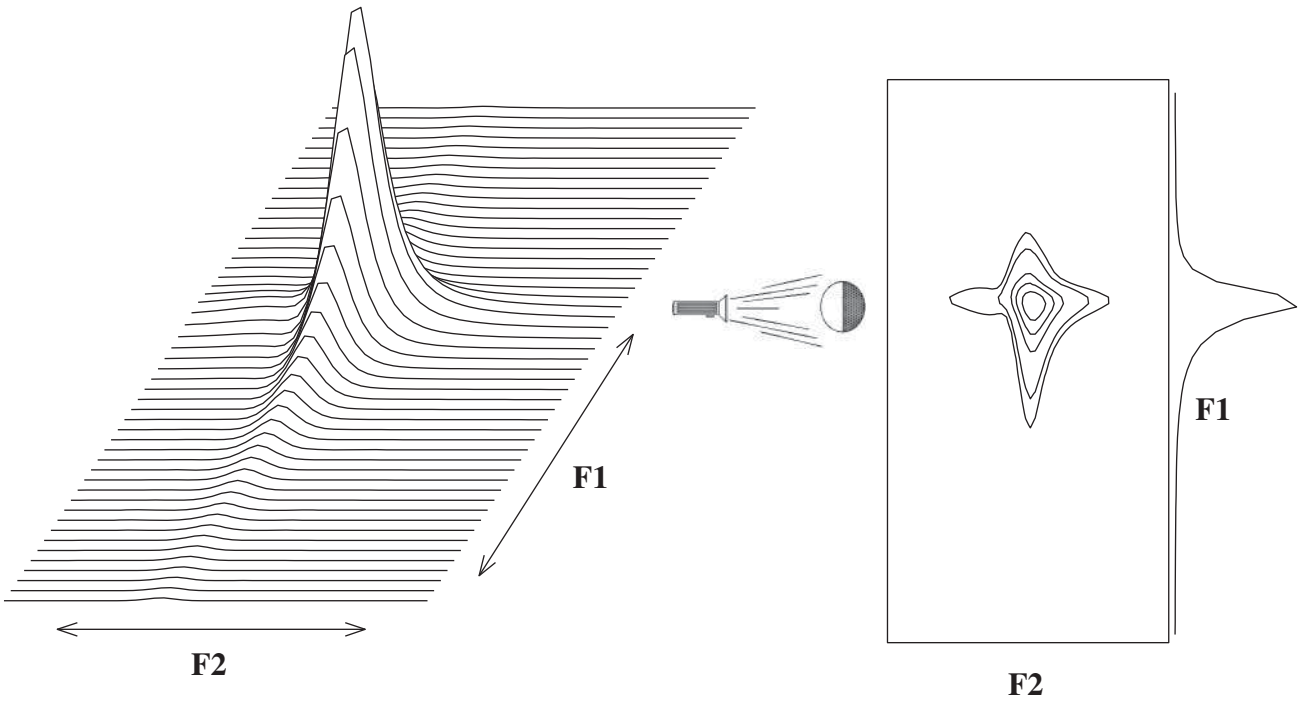

FIGURE 5.6 Fourier transformation of a series of interferograms like the ones in Figure 5.5c to give the frequency-domain spectrum as both a peak and as contours. The contour plot also shows a projection parallel to **F1**.

sequence. If we replace the first $\pi/2$ pulse with a generalized pulse or block of pulses and delays and replace the second acquisition $\pi/2$ pulse with a generalized acquisition pulse or block of pulses and delays, we arrive at the general pulse sequence for 2D correlation experiments, shown in Figure 5.7. Unlike 1D NMR, we typically cannot describe, using simple vector models and trigonometry, the result of what is happening inside the boxes. For the time being, let us ignore the details of what is occurring inside the boxes and concentrate on what is happening during t_1 and t_2.

In all 2D experiments, we detect a signal (during acquisition) as a function of t_2; *this signal, however, has been* ***modulated*** *as a function of* t_1. The acetone experiment above is simple because the magnetization experiences identical modulation during t_1 and t_2. In an experiment in which the magnetization is identically modulated during t_1 and t_2, the resulting peaks will be such that ν_1 equals ν_2; in the parlance of 2D NMR, the experiment gives rise to diagonal peaks. For useful 2D information, we are interested in experiments in which the magnetization evolves with one frequency during t_1 and a different frequency during t_2. In this case, our experiment will give rise to peaks in which ν_1 and ν_2 are different; this time we call the peaks off-diagonal or cross peaks. In order to interpret a 2D NMR spectrum, there are two things that we need to know. First, what frequencies do the axes represent? One axis (ν_2) always

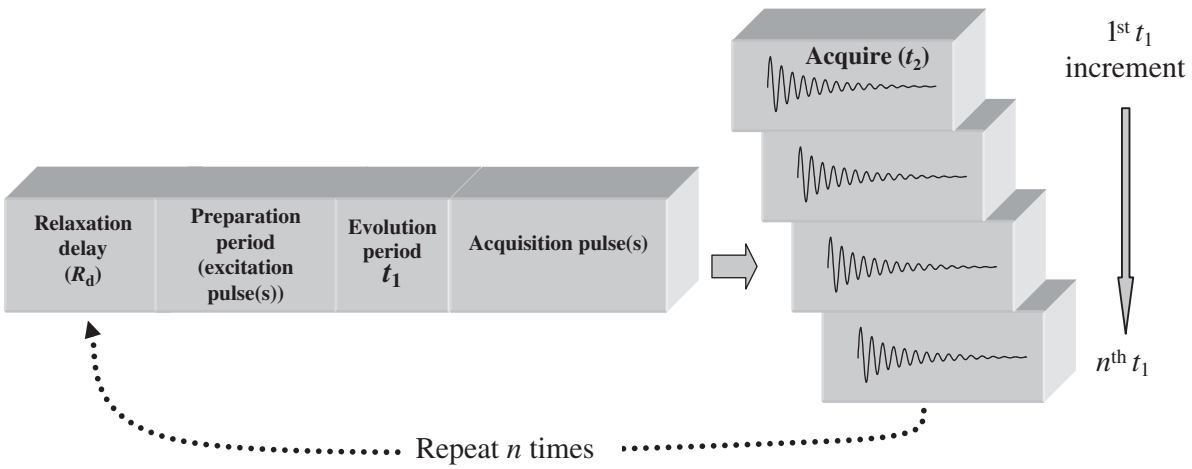

FIGURE 5.7 Classical Jeener–Ernst style generalized pulse sequence for 2D NMR. The signal detected during acquisition, t_2, is modulated during the incremented time, t_1, thus giving rise to cross peaks in the 2D spectrum.

represents the nucleus detected during acquisition (t_2). The other axis (ν_1, which obviously depends on t_1) can represent the same nucleus (e.g., ^{1}H—^{1}H COSY), a different nucleus (e.g., ^{1}H—^{13}C COSY also called HMQC or HETCOR), or a coupling constant (e.g., *J*-resolved spectroscopy, not covered in this chapter). Second, we need to know how the magnetizations are related during t_1 and t_2; in this way, we can account for and interpret the cross peaks.

If we return to our prototype 2D experiment and apply this pulse sequence to an AX spin system, we will be in a better position to appreciate the incremented time, t_1. While we can describe mathematically precisely how the spins evolve during this time, we cannot show this evolution pictorially with vector diagrams. (The mathematical description for this system requires quantum mechanics and solution of the density matrix, well beyond the scope of this text. See Levitt (2008) or Cavanagh et al. (1996) for further reading.) After the first $\pi/2$ pulse, the system can be described as a sum of two terms; each term contains the spin of only one of the two protons. During the time t_1, the spins precess (evolve) under the influences of both chemical shifts *and their mutual spin-spin coupling*. The mutual coupling has the effect of changing some of the individual spin terms into products containing magnetization components of both nuclei. Next, the second $\pi/2$ pulse causes the spins that were precessing under both chemical shift and coupling influences to redistribute magnetization among all spins (there is only one other spin in this case) with which it is associated (coupled). This redistribution of magnetization is detected in t_2; thus, a frequency detected in t_2 has its amplitude modulated as a function of other spins (again, only one here), with which it is coupled during t_1, leading to cross peaks connecting the coupled nuclei. Because the magnetization is redistributed equally in both directions (i.e., from A to X and from X to A), the cross peaks (at least for this experiment) will be symmetrically disposed about the diagonal. This description of spins precessing and mixing during t_1 and their redistribution during the acquisition pulse (and detection during t_2) is admittedly difficult to follow without pictures. The pulse sequences are not given detailed explanations in this text because of this difficulty.

5.3.1 ^{1}H—^{1}H Correlation: COSY

Our simple 2D experiment is actually a very important experiment sometimes simply called **COSY** (**CO**rrelation **S**pectroscop**Y**), and which we will call ^{1}H—^{1}H COSY for the time being in order to clearly indicate what is being correlated.* The pulse sequence for ^{1}H—^{1}H COSY is none other than the one we have already described above in Figure 5.3: two $\pi/2$ proton pulses separated by the required evolution period, t_1, which is systematically incremented, and the acquisition period, t_2.

The actual pulse sequences used by all modern spectrometers are more complicated than the idealized ones given in this text. Many spectrometers employ a technique known as phase cycling in which the phase of the rf pulse is changed in a regular manner (through a cycle) for each t_1 increment. These phase cycles are extremely important *experimental factors* that help remove artifacts and other peculiarities of quadrature detection. We will ignore phase cycling in our pulse sequences and discussions because they do not affect our understanding and interpretation of these experiments. The interested reader is referred to Claridge (see References) for these and other experimental parameters important for 2D experiments. Another factor that is ignored in our discussion is the use of gradients. A short description of them and their purpose is given at the end of this chapter.

In the description of the 2D experiment above for an AX spin system, we found that during t_1, spins which are mutually coupled precess under the influence of the chemical shifts of both nuclei and thus give rise to peaks in which ν_1 does not equal ν_2. In the general case, ^{1}H—^{1}H COSY spectra are interpreted as giving rise to off-diagonal or cross peaks for all protons that have spin-spin coupling; put simply, the cross peaks correlate coupled protons. In a sense, the experiment can be thought of as simultaneously doing all pertinent decoupling experiments to see which protons are coupled to which other protons. Of course, no protons are being decoupled in an ^{1}H—^{1}H COSY and this experiment should not be thought of as replacing homonuclear decoupling experiments (see Section 3.15).

5.4 IPSENOL: ^{1}H—^{1}H COSY

Let us continue our discussion of 2D NMR by considering the ^{1}H—^{1}H COSY spectrum of ipsenol, the monoterpene alcohol considered in some detail in Sections 3.12 and 4.6. For reference and as a reminder, the typical 1D NMR data at 300 MHz for ipsenol, and its structure, are provided in Figure 5.8.

The contour display of the simple COSY spectrum for ipsenol is shown in the top part of Figure 5.9. The presentation shown here is typical; F2 is found on the bottom (or top) with the proton scale as usual (from right to left). F1 is displayed on the right (or left) with the proton scale running from top to bottom. A proton spectrum is displayed opposite the F1 scale as a convenience instead of the poorly resolved projection; this 1D spectrum is not part of the ^{1}H—^{1}H COSY spectrum but added later. From the upper right to the lower left runs the "diagonal," a series of peaks for which ν_1 equals ν_2; these diagonal peaks provide nothing in the way of useful information beyond the simple 1D ^{1}H spectrum. On either side of the diagonal and symmetrically disposed (at least theoretically) are the cross peaks. The symmetry in this type of spectrum is oftentimes imperfect.

*Many readers will already be aware that acronyms for 2D NMR experiments have proliferated along with available experiments. This chapter attempts neither an encyclopedic approach to describing these acronyms nor their experimental counterparts. This chapter does, however, cover enough important experiments to enable the reader to interpret nearly any 2D experiment that one is likely to encounter. Acronyms are listed in the index.

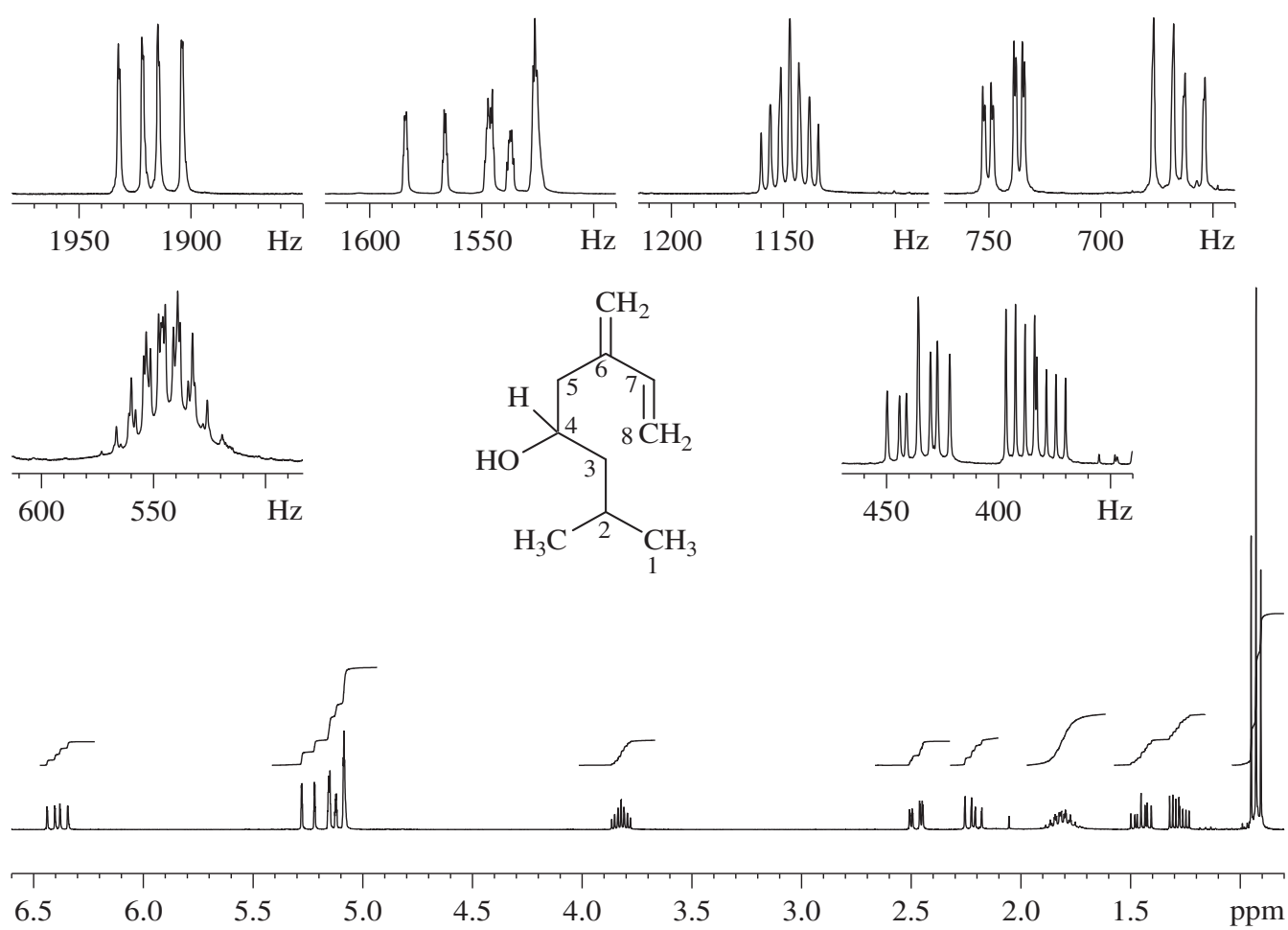

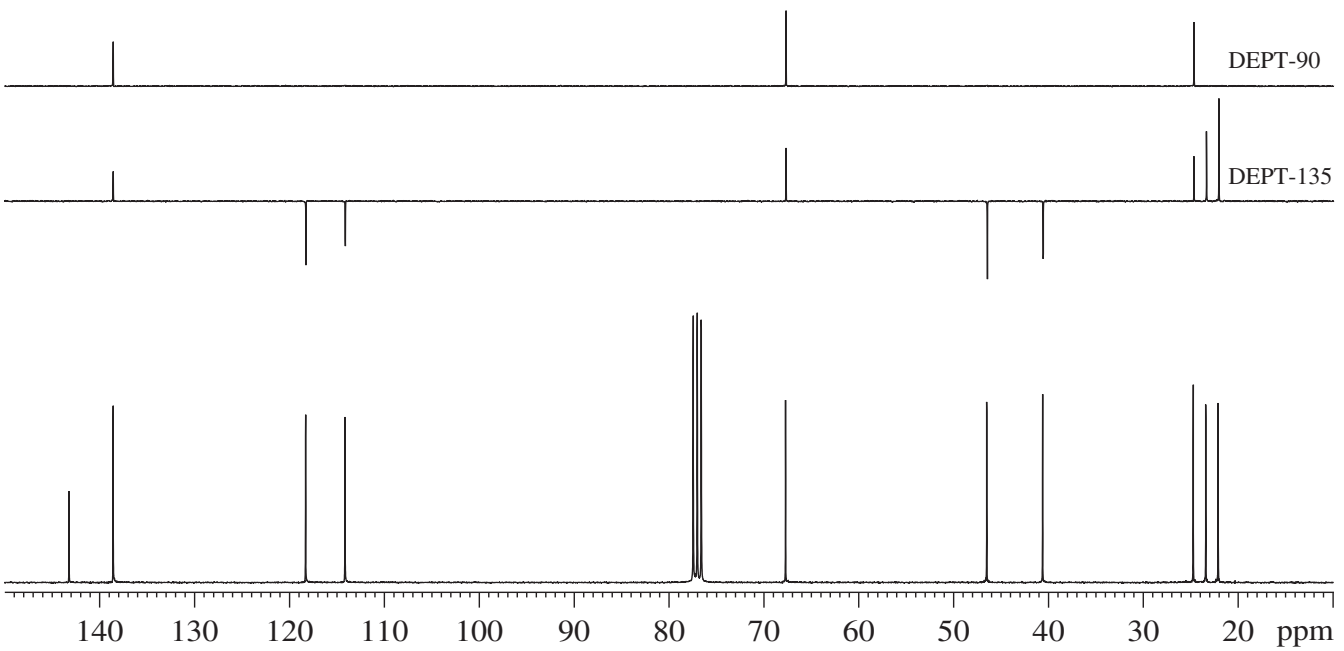

FIGURE 5.8 300 MHz ^{1}H, ^{13}C, and DEPT spectra for ipsenol in $CDCl_3$. The structure of ipsenol is given with the numbering used in the text.

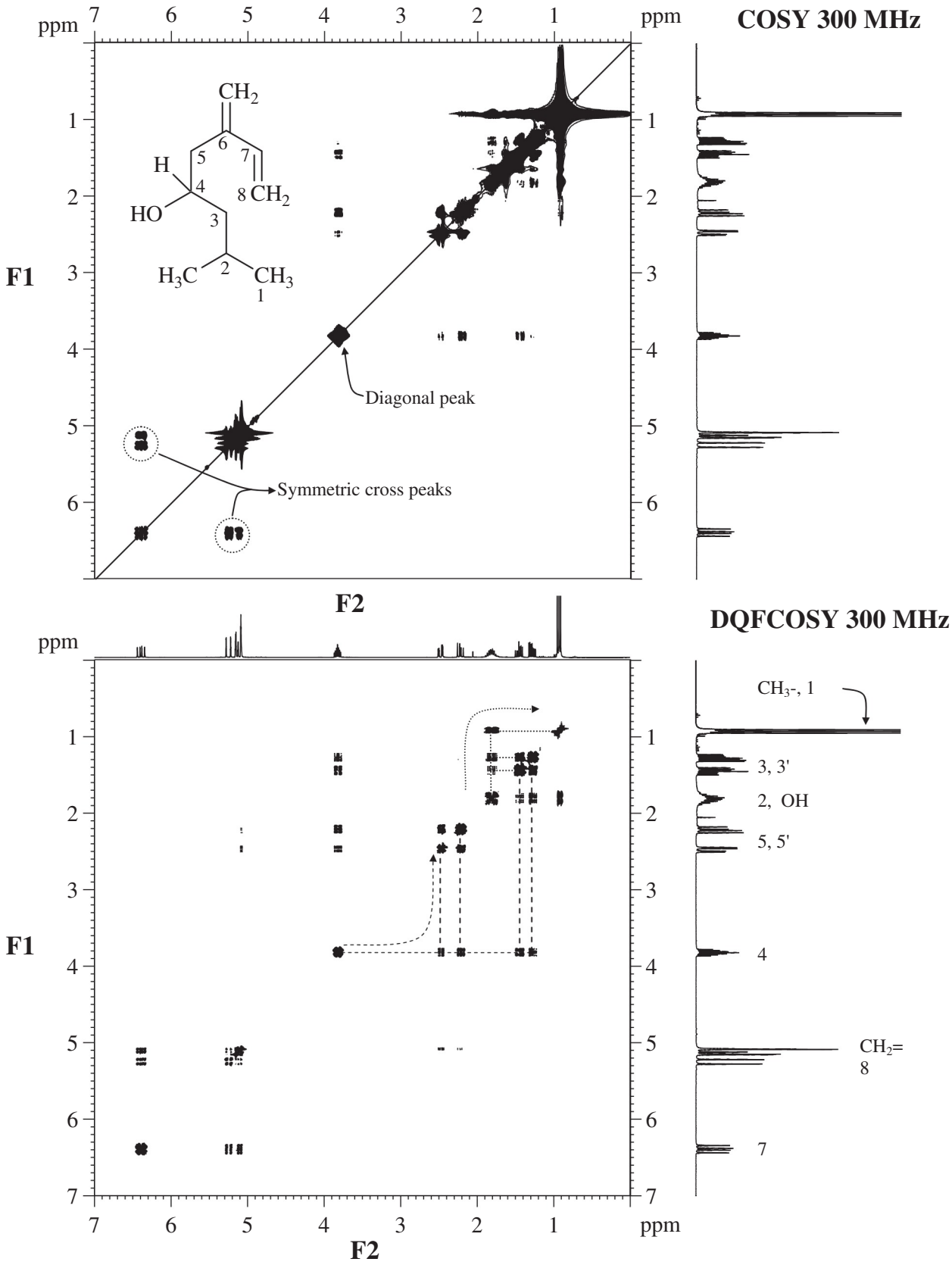

FIGURE 5.9 The top part is the 300 MHz simple COSY spectrum for ipsenol; the bottom part is the 300 MHz DQF COSY spectrum for ipsenol.

Before undertaking detailed discussions of ^{1}H—^{1}H COSY and the structure of ipsenol, there is one further experimental refinement that decreases the clutter along the diagonal. Although we can interpret this spectrum without this refinement, there are instances (e.g., caryophyllene oxide) when this improvement makes a great deal of difference.

5.4.1 Ipsenol: Double Quantum Filtered ^{1}H—^{1}H COSY

By simply adding a third $\pi/2$ pulse immediately following the second $\pi/2$ pulse in our simple COSY pulse sequence and changing nothing else, we have the pulse sequence for the very popular **D**ouble-**Q**uantum **F**iltered ^{1}H—^{1}H COSY (**DQF-COSY**) experiment (Figure 5.10). The purpose of the third $\pi/2$ pulse is to remove or "filter" single-quantum transitions so that only double-quantum or higher transitions remain. In practical terms, the double quantum filter will select only those systems with at least two spins (minimum AB or AX); thus, methyl singlets (noncoupled) will be greatly reduced. Higher quantum filtering is possible but is generally not used. For instance, in a triple-quantum filtered COSY, only systems with three spins or more are selected so that AB and AX spin systems as well as noncoupled systems will be eliminated.

The DQF ^{1}H—^{1}H COSY spectrum of ipsenol can be found at the bottom of Figure 5.9. Note that the spectrum seems cleaner, especially along the diagonal, making the task of interpretation significantly easier. Because of the greatly improved appearance of DQF-COSY spectra, all COSYs in this book are double-quantum filtered.

As we begin our interpretation of the DQF-COSY spectrum in Figure 5.9, let us recall that this spectrum shows correlation between coupled protons. A point of entry (i.e., a distinctive peak) into a COSY spectrum (and other types of correlation spectra as well) is one of the keys to successfully gleaning information from it. The structure of ipsenol allows for more than one useful entry point, so let us select the carbinol methine resonance at 3.83 ppm. If we begin at the diagonal and trace either directly to the right or directly up (we obtain the same result because the spectrum is symmetric), we intersect four off-diagonal or cross peaks. By drawing lines through these cross peaks at right angles to the one we just traced, we find the chemical shifts of the four coupled resonances. A quick check of the structure of ipsenol finds the carbinol methine adjacent to two pairs of diastereotopic methylene groups;* in other words, the proton at 3.83 ppm is coupled to four protons, and the four protons correspond to two adjacent methylene groups.

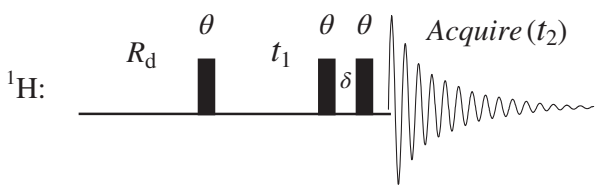

FIGURE 5.10 Pulse sequence for double-quantum filtered ^{1}H—^{1}H COSY (DQF-COSY). $\theta = 90°$ and δ is a fixed delay of the order of a few microseconds (it is unrelated to the chemical shift).

We could continue to trace correlation paths from these four protons and the reader is invited to do so at the end of this section. Let us instead select another equally useful entry point: the isopropyl methine at 1.81 ppm. We again begin at the diagonal and this time we find that the isopropyl methine is correlated with three distinct resonances. Two of the correlations correspond to the two protons of one of the diastereotopic methylenes that also correlated with the carbinol methine above. In addition, we find a correlation to the two overlapping methyl doublets at 0.93 ppm. These correlations of course make perfect sense with the structure; in fact, by only considering these two protons (i.e., at 3.83 and 1.81 ppm) we have established correlations (also called "connectivities") through three-fifths of the molecule. A correlation implies a connectivity because the COSY spectrum will typically only show strong cross peaks for coupled protons which are on adjacent (bonded) carbon atoms.

Next we consider the two protons on the C-5 methylene at 2.48 and 2.22 ppm. We have already seen that they are coupled to the carbinol methine (you can and should verify this from the methylene protons' perspective) and we see that they are also coupled to each other.† In addition, we see weaker cross peaks from both methylene protons correlating to an olefinic proton at 5.08 ppm. This correlation is due to long range coupling ($^4J_{HH}$ or four-bond coupling) of the methylene protons to the *cis*-proton of the adjacent double bond. This is a nice correlation to find because it provides H—H connectivity to the otherwise isolated diene spin system. In the absence of these long-range correlations, such isolated spin systems can be connected to each other by either HMBC or INADEQUATE sequences, which are described below. At this point, the reader is invited to complete the correlations for ipsenol in this DQF-COSY spectrum. Correlations can be found for all protons except the hydroxylic proton, which is rapidly exchanging.

5.4.2 Carbon Detected ^{13}C—^{1}H COSY: HETCOR

The ^{13}C—^{1}H COSY (HETCOR) experiment correlates ^{13}C nuclei with directly bonded (i.e., coupled) protons through one-bond ($^1J_{CH}$) couplings. The frequency domains of F1 (ν_1) and F2 (ν_2) are of different nuclei, and so there is no apparent diagonal or symmetry.

The pulse sequence for this experiment, commonly called **HETCOR** (**HET**eronuclear **COR**relation), is shown

*We will reserve further discussion of diastereotopic methylene groups until the next section on ^{1}H—^{13}C HMQC.

†Geminal methylene protons (sp^3 hybridized carbon) are always coupled to each other and their coupling constant ($^2J_{HH}$) is always rather large (see Appendices, Chapter 3).

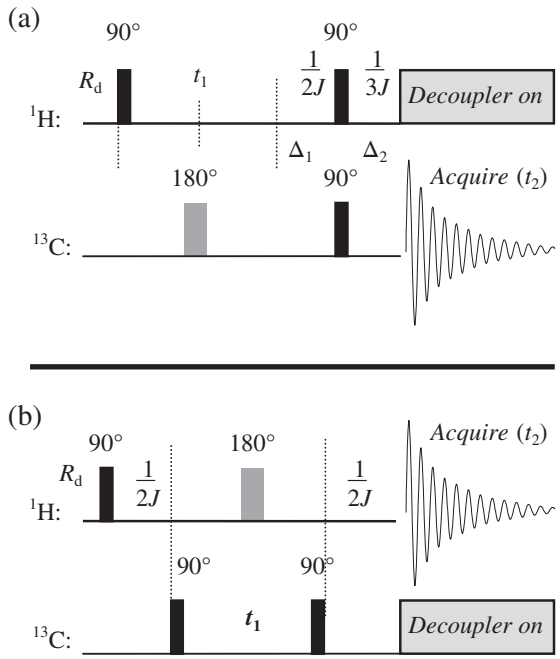

FIGURE 5.11 (a) The pulse sequence for HETCOR. (b) The pulse sequence for HMQC. The value for $^1J_{CH}$ is typically 145 Hz.

in Figure 5.11a. During the evolution time (t_1), the large one-bond heteronuclear J-coupling (J_{CH}) is used for polarization transfer, and thus only ^{13}C's bonded directly to ^{1}H's are detected. To realize maximum polarization transfer, a fixed delay $\Delta_1 = 1/(2J_{CH})$ is added after t_1. The short delay (Δ_2) between the final ^{13}C pulse and the start of acquisition is a refocusing period so that the ^{13}C lines do not have opposite phase and thus do not cancel one another when ^{1}H-decoupling is applied. The optimal refocusing time (Δ_2) depends on whether the ^{13}C belongs to a CH, CH_2, or CH_3 group. Typically, a compromise value of $\Delta_2 = 1/(3J_{CH})$ is chosen.

The F1 axis (ν_1), which is derived from the incremented delay, t_1, is the proton axis. The F2 axis (ν_2), obtained during t_2, is the carbon axis. Thus, our $\pi/2$ read pulse is on the ^{13}C channel, and the FID acquired during t_2 represents the ^{13}C nucleus. Lastly, in an ideal experiment, the carbon resonances should be singlets rather than multiplets, as composite pulse (broadband) decoupling (CPD) is applied on the proton channel during acquisition. Remember, in a 2D experiment, correlation occurs during t_1 and, hence, the proton decoupler is not turned on during this period.

5.4.3 Proton Detected ^{1}H—^{13}C COSY: HMQC

Historically, the **HMQC** (**H**eteronuclear **M**ultiple **Q**uantum **C**oherence) experiment was preceded by the HETCOR experiment. Although experimentally there are many differences, the essential difference is that, while the HETCOR experiment is carbon detected, the HMQC experiment is proton detected. Since there are great discrepancies between proton and carbon in their relative abundances and sensitivities, the HMQC sequence is greatly preferred today. The advantage of inverse experiments over direct detection experiments is that with inverse experiments the nucleus with the highest γ (usually ^{1}H) is detected, yielding the highest sensitivity.

As mentioned in Chapter 3, the sensitivity of an NMR experiment depends on the magnetogyric ratios of the excited nucleus (γ_{exc}) and of the detected nucleus to the power of $\frac{3}{2}$ ($\gamma_{det}^{\frac{3}{2}}$). For the HETCOR experiment, ^{1}H is the excited nucleus and ^{13}C is the detected nucleus; the sensitivity is therefore proportional to $\gamma_{1H}\gamma_{13C}^{\frac{3}{2}}$. For the inversely detected HMQC experiment, ^{1}H is both the excited and the detected nucleus and so the sensitivity is proportional to $\gamma_{1H}^{\frac{5}{2}}$. The associated improvement in sensitivity for the HMQC experiment compared to the HETCOR experiment is therefore $(\gamma_{1H}/\gamma_{13C})^{\frac{3}{2}}$. Keep in mind that even though the HMQC experiment excites and detects ^{1}H, magnetization must still pass through a ^{13}C nucleus and so the low natural abundance of ^{13}C adversely affects the overall S/N compared to a one-dimensional ^{1}H NMR spectrum. One of the challenges of an inverse-detected chemical shift correlation experiment is that the large signals from ^{1}H not coupled directly to a ^{13}C nucleus must be suppressed, which poses a dynamic range problem, and usually requires additional phase cycling. The introduction of pulsed field gradients in high-resolution NMR greatly improved the problem of suppressing signals from ^{1}H bonded to ^{12}C. The suppression is almost perfect without additional phase cycling, which significantly improves the quality of the spectrum and requires much less time.

The pulse sequence for the HMQC experiment is shown in Figure 5.11b. Three details in this pulse sequence are worth discussing. The F1 axis (ν_1), which is derived from the incremented delay, t_1, is the carbon axis. The F2 axis (ν_2), obtained during t_2, is the proton axis. Thus, our $\pi/2$ read pulse is on the ^{1}H channel, and the FID acquired during t_2 represents the ^{1}H nucleus. Lastly, GARP decoupling—which is a low power, CPD routine—is used to decouple nuclei with large chemical shift ranges. This **GARP** (**G**lobally optimized, **A**lternating phase, **R**ectangular **P**ulses) CPD technique is applied on the carbon channel during acquisition so that the proton signals obtained are not split into doublets by the ^{13}C nuclei. Recall that the HMQC experiment works through ^{1}H–^{13}C J coupling, so only ~1.1% of the directly bonded C—H pairs will contribute to the spectrum. These same pairs give rise to ^{13}C satellite signals in a normal 1D ^{1}H NMR spectrum.

5.4.4 Ipsenol: HETCOR and HMQC

The upper portion in Figure 5.12 is the HETCOR spectrum of ipsenol, and the lower portion is a HMQC spectrum of ipsenol. The presentation of the two spectra is the same except that the axes have been switched. Thus, in the HETCOR spectrum, the F2 axis on the bottom has the carbon

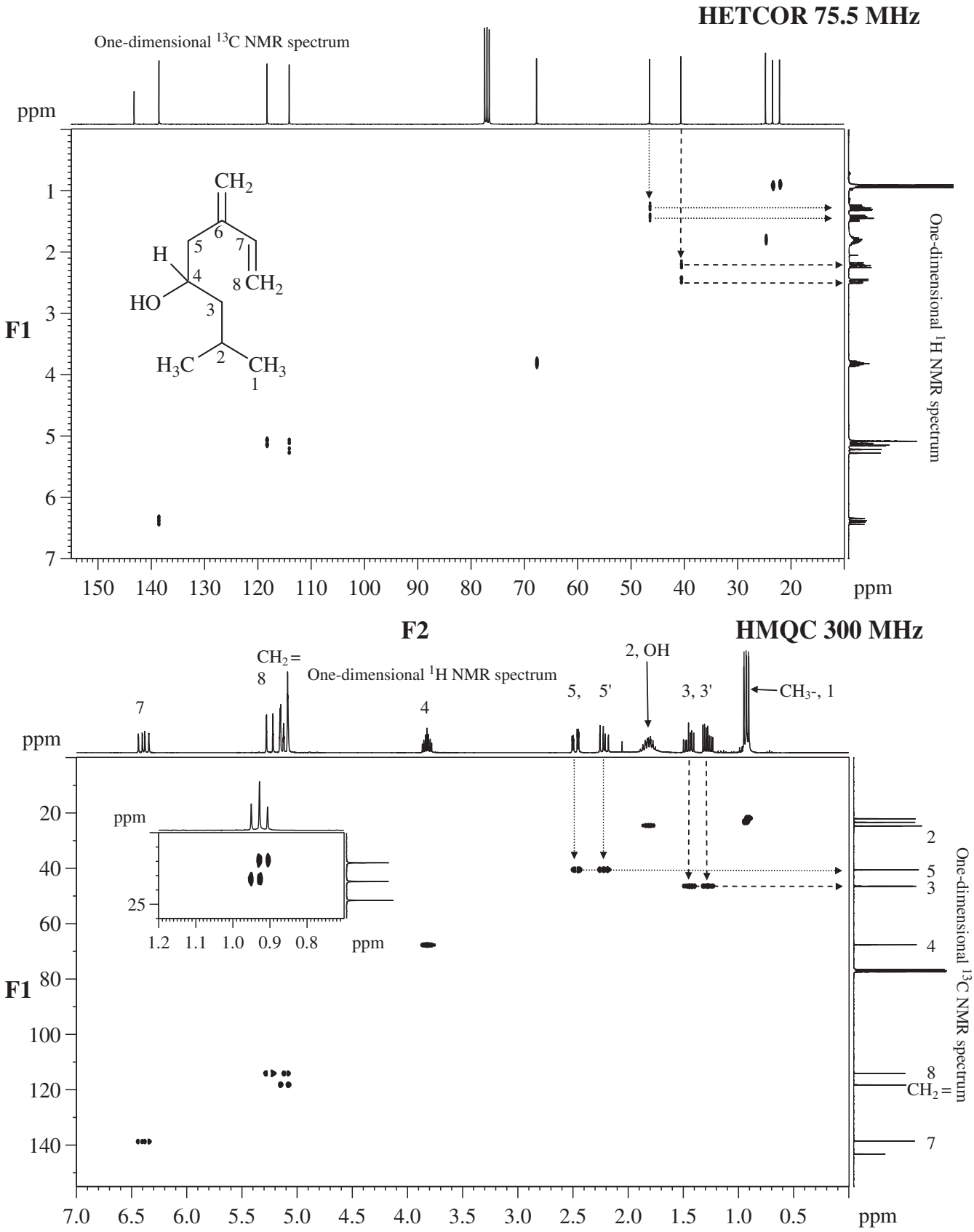

FIGURE 5.12 The bottom part of the figure is the HMQC spectrum for ipsenol while the top part of the figure is the HETCOR spectrum of ipsenol. Note that by convention, the spectrum of the directly detected nucleus (during t_2) is plotted on the *x*-axis and so the nuclei represented on the axes of the HMQC spectrum are transposed relative to the HETCOR spectrum.

scale and the F1 axis on the side has the proton scale, whereas in the HMQC spectrum these axes are reversed. The reason for this is simply that by convention the data for the directly detected nucleus (F2) are plotted in the *x*-dimension. In theory, the information content of the two spectra is identical; in fact, we find exactly the same correlations for ipsenol. The only real practical consideration when comparing the data of the two experiments is the difference in the digital resolution of the carbon axis.

Let us familiarize ourselves with HMQC spectra by considering the HMQC spectrum of ipsenol (Figure 5.12. bottom part). Immediately obvious is the fact that there is no diagonal and no symmetry; this will be true whenever F1 and F2 represent different nuclei. In this presentation, the F1 axis (carbon) is along the left side and the F2 axis (proton) is along the bottom. Opposite these axes we find the corresponding 1D spectra, which are given as a convenience and are not part of the actual 2D spectrum. Interpretation of this spectrum is straightforward. We begin with any carbon resonance and mentally draw a line horizontally until a cross peak is encountered.* Another line is mentally drawn perpendicular to the first to find the proton resonance with which the carbon resonance correlates.

There are only three cases possible for each carbon atom. If a line drawn encounters no cross peaks, then the carbon has no attached hydrogens. If the drawn line encounters only one cross peak, then the carbon may have either 1, 2, or 3 protons attached; if 2 protons are attached, then they are either chemically equivalent or their chemical shifts fortuitously overlap. If the horizontal line encounters two cross peaks, then we have the special case of diastereotopic protons attached to a methylene group. Much of this information will already be available to us from DEPT spectra (see Section 4.6); indeed, the HMQC spectrum should, whenever possible, be considered along with the DEPT. The reader should also be aware that there are numerous additional two-dimensional correlation experiments which can give the same sort of information (e.g., variants of the heteronuclear single-quantum coherence (HSQC) experiment), many of which rely on pulsed field gradients (see Section 5.12).

In ipsenol, there are four methylene groups, all of which possess diastereotopic pairs of protons. Resonances for two of these methylene groups occur in the carbon spectrum at 41 ppm and 47 ppm. Note with which protons these carbon atoms are correlated and compare these results with what we found with COSY. As we expect, the results here confirm our assignments from COSY and help build an ever-strengthening basis for our assignments. The other two methylene carbon atoms are found at higher frequency in the alkenyl region, and the HMQC cross peaks for these carbon resonances help clarify the overlapping proton resonances that we find in the proton spectrum.

*We could just as well start on the proton axis and in this case we would obtain exactly the same result. In cases of overlap in the proton spectrum, we will not always be able to find all of the proper starting points. Overlap is usually not a problem on the carbon axis.

Ipsenol has two methyl groups that appear as a "triplet" at 0.93 ppm in the proton spectrum. A closer look, however, at the inset in the HMQC spectrum reveals that it is a pair of coincidental doublets. Before moving on to the next section, consider the following question: can the alkenyl methylene carbon resonances be assigned on the basis of combined information from COSY and HMQC?

5.4.5 Ipsenol: Proton-Detected, Long-Range ^{1}H—^{13}C Heteronuclear Correlation: HMBC

For the HMQC sequence described above, we wanted an experiment that eliminated long-range (i.e., two and three bond) proton-carbon couplings while preserving the directly attached (i.e., one-bond) couplings, which we correlated in a 2D experiment. The **HMBC** (**H**eteronuclear **M**ultiple **B**ond **C**oherence) experiment, on the other hand, which is also proton detected, capitalizes on these two- and-three-bond couplings, providing us with an extremely powerful (although sometimes cluttered) spectrum. In essence, we indirectly obtain carbon-carbon (although not ^{13}C—^{13}C) correlations, and, in addition, we are able to correlate quaternary carbons with nearby protons. Since both $^2J_{CH}$ and $^3J_{CH}$ couplings are present, interpretation can be tedious; we must be methodical in our approach and keep in mind the HMQC correlations.

Interpretation of HMBC spectra requires a degree of flexibility because we do not always find what we expect to find. In particular, depending on the hybridization of carbon and other factors, some of the expected two-bond correlations ($^2J_{CH}$) or three-bond ($^3J_{CH}$) correlations are occasionally absent. To add to the confusion, infrequently we find four-bond ($^4J_{CH}$) correlations! The variations in correlations that we find are due to the variations in the magnitude of $^2J_{CH}$, $^3J_{CH}$, and $^4J_{CH}$ coupling constants.

The pulse sequence for HMBC is given in Figure 5.13 for interested readers. The time delay, $1/(2J)$, can be optimized for different coupling constants. A typical value for J assumes an average long-range coupling constant of 8 Hz.

The HMBC spectrum for ipsenol (Figure 5.14) looks like the HMQC spectrum for ipsenol with two obvious differences: there are considerably more cross peaks and the one-bond correlations (HMQC) are gone. (The spectrum

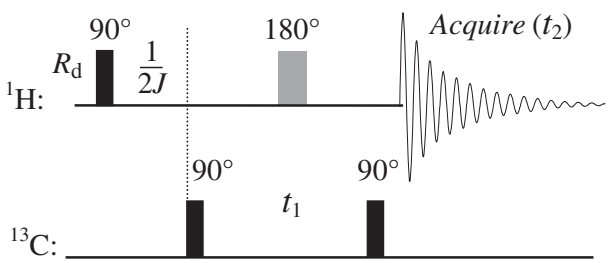

FIGURE 5.13 Pulse sequence for HMBC. J is chosen for long-range CH coupling ($^2J_{HC}$ and $^3J_{HC}$), typically 8 Hz.

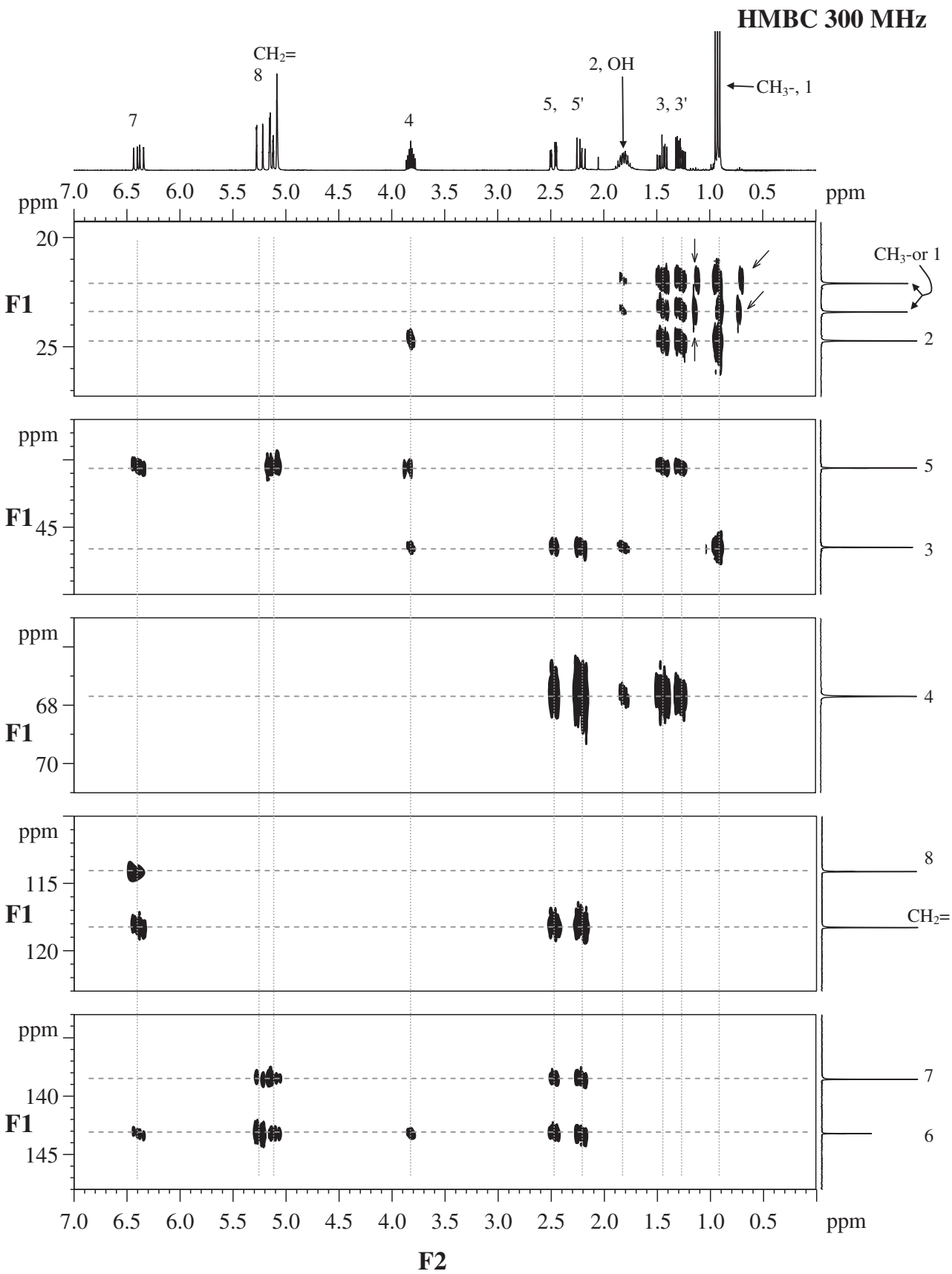

FIGURE 5.14 The HMBC spectrum for ipsenol. The spectrum is split into five sections for clarity. The arrows in the top section point to ^{13}C satellites. Lines are drawn to show correlations.

is broken into five sections so that there is sufficient resolution to see all of the correlations.) Interpretation for ipsenol is straightforward. But first, let us note a common artifact: ^{13}C satellites of intense proton peaks, especially methyl groups. If we trace parallel to the proton axis (F2) at about 23 ppm on the carbon axis (F1), we find a cross peak at about 0.93 ppm (proton), which is real. On either side, we find two additional cross peaks that do not line up (correlate) with any proton resonances in F2. These are ^{13}C satellites and may be ignored. The other methyl carbon resonance shows the same phenomenon; the satellite peaks are marked with arrows in the figure.

We can begin with either a carbon or a proton resonance and obtain equivalent results. We will use the carbon axis as our starting point because we usually have less overlap there. For example, a line drawn parallel to the proton axis at about 68 ppm on the carbon axis (the carbinol carbon) intersects five cross peaks; none of the five correlations corresponds to the directly bonded proton ($^1J_{CH}$) at 3.8 ppm. Four of the cross peaks correspond to the two pairs of diastereotopic methylene protons (2.48 ppm, 2.22 ppm, 1.45 ppm, and 1.28 ppm) and these arise due to two-bond couplings. The fifth cross peak (arising due to $^3J_{CH}$) correlates this carbon atom (68 ppm) to the isopropyl methine proton (1.81 ppm), which is bonded to a carbon atom in the β-position. The other carbon atom in a β-position has no attached protons so we do not have a correlation to it from the carbinol carbon atom. Thus, we have indirect carbon connectivities to two α-carbons and to one of two β-carbons.

Another useful example can be found by drawing a line from the carbon resonance at 41 ppm. This carbon is the C-5 methylene and we first note that correlations to the directly bonded protons at 2.48 ppm and 2.22 ppm are absent. There is only one α-carbon that has one or more attached protons; its corresponding correlation is found to the C-4 carbinol methine proton at 3.83 ppm.* There are three β-carbons and they all have directly bonded protons. The C-3 methylene carbon shows indirect correlation through both of its diastereotopic protons at 1.45 ppm and 1.28 ppm. The C-7 alkenyl methine proton gives a cross peak at 6.39 ppm as do the protons of the alkenyl methylene group attached to C-6 at 5.16 ppm and 5.09 ppm. Since C-6 is a quaternary carbon, the HMBC experiment enables us to "see through" these normally insulating points in a molecule. Other assignments are left to the reader as an exercise; the quaternary carbon at about 143 ppm (C-6) is a good place to start.

5.5 CARYOPHYLLENE OXIDE

The structure of caryophyllene oxide is significantly more complicated and is a worthy challenge for the methods that we introduced with ipsenol. For use here and for future reference, the ^1H, ^{13}C, and DEPT NMR spectra are given in Figure 5.15. As an aid in discussing the DQF-COSY spectrum of caryophyllene oxide, note the following description of the proton spectrum: there are three methyl singlets (at 0.98 ppm, 1.01 ppm, and 1.19 ppm), two alkenyl doublets (small geminal coupling) at 4.86 ppm and 4.97 ppm, and resonances from 13 other protons giving multiplets between 0.9 ppm and 3.0 ppm. Even though we know the structure, it is impossible to assign any of these protons unless we make one or more unreasonable assumptions.†

5.5.1 Caryophyllene Oxide: DQF-COSY

The DQF-COSY spectrum of caryophyllene oxide can be found in Figure 5.16. The problem here is that *there is no good entry point*. The previous statement is not trivial. Without an entry point, it is impossible to relate the many obvious correlations (drawn in for convenience) that we see to a structural formula. Our approach therefore will be to record some of the correlations that we do see and wait until we have other information (i.e., HMQC) before we try to translate these correlations into a structure.

The exocyclic alkenyl methylene protons show obvious COSY correlations to one another. In addition, we note weak cross peaks between the alkenyl protons at 4.86 ppm and 4.97 ppm and an apparent diastereotopic methylene group (2.11 ppm and 2.37 ppm) and a quartet at 2.60 ppm, respectively. These interactions are reminiscent of the long-range allylic coupling that we saw in ipsenol; we could assign these correlations to the diastereotopic methylene C-7 and the methine at C-9. For now, we will be cautious and conservative, and return to this point later in the chapter.

A look at the extreme low-frequency portion of this COSY spectrum reveals an unexpected interaction. It seems that either one or both of the methyl singlets shows coupling to resonances at 1.65 ppm and at 2.09 ppm. This apparent conflict can be resolved by a close examination of the methyl singlets at about 0.98 ppm. There is an unusually low-frequency multiplet (labeled 3′), partially buried by the methyl singlets, which we had initially overlooked. This type of unexpected dividend is common in correlation spectra; both partially and completely obscured resonances usually reveal themselves in 2D spectra (see HMQC below). Before continuing our discussion of caryophyllene oxide, let us consider ^1H—^{13}C correlations and how ^1H—^1H correlations interplay with ^1H—^{13}C correlations.

5.5.2 Caryophyllene Oxide: HMQC

The COSY spectrum for caryophyllene oxide can be understood more clearly when interpreted in conjunction with the information from an HMQC spectrum (Figure 5.17).

*The other α-carbon at C-6, which was a β-carbon in our first example, also shows no correlation in the HMQC. The reader should show that there are useful correlations to this carbon atom in Figure 5.14.

†If pressed, we might assume that the allylic bridgehead methine would be the most deshielded and assign the doublet of doublets at 2.86 ppm to this proton (wrong). The methods in this chapter will allow us to make these assignments without making unsubstantiated assumptions.

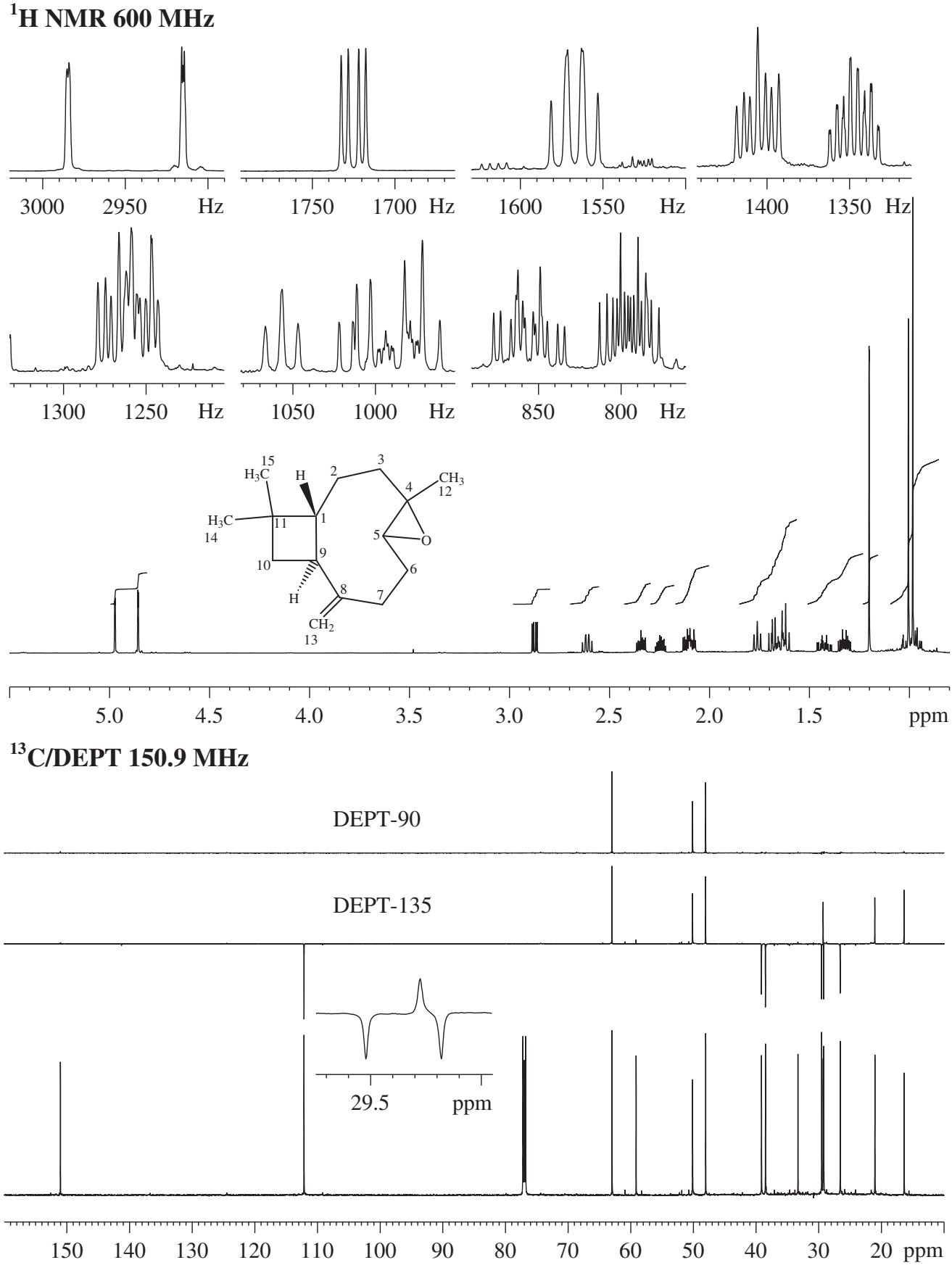

FIGURE 5.15 The ^{1}H, ^{13}C, and DEPT NMR spectra for caryophyllene oxide. The numbering for this structure is used in the text.

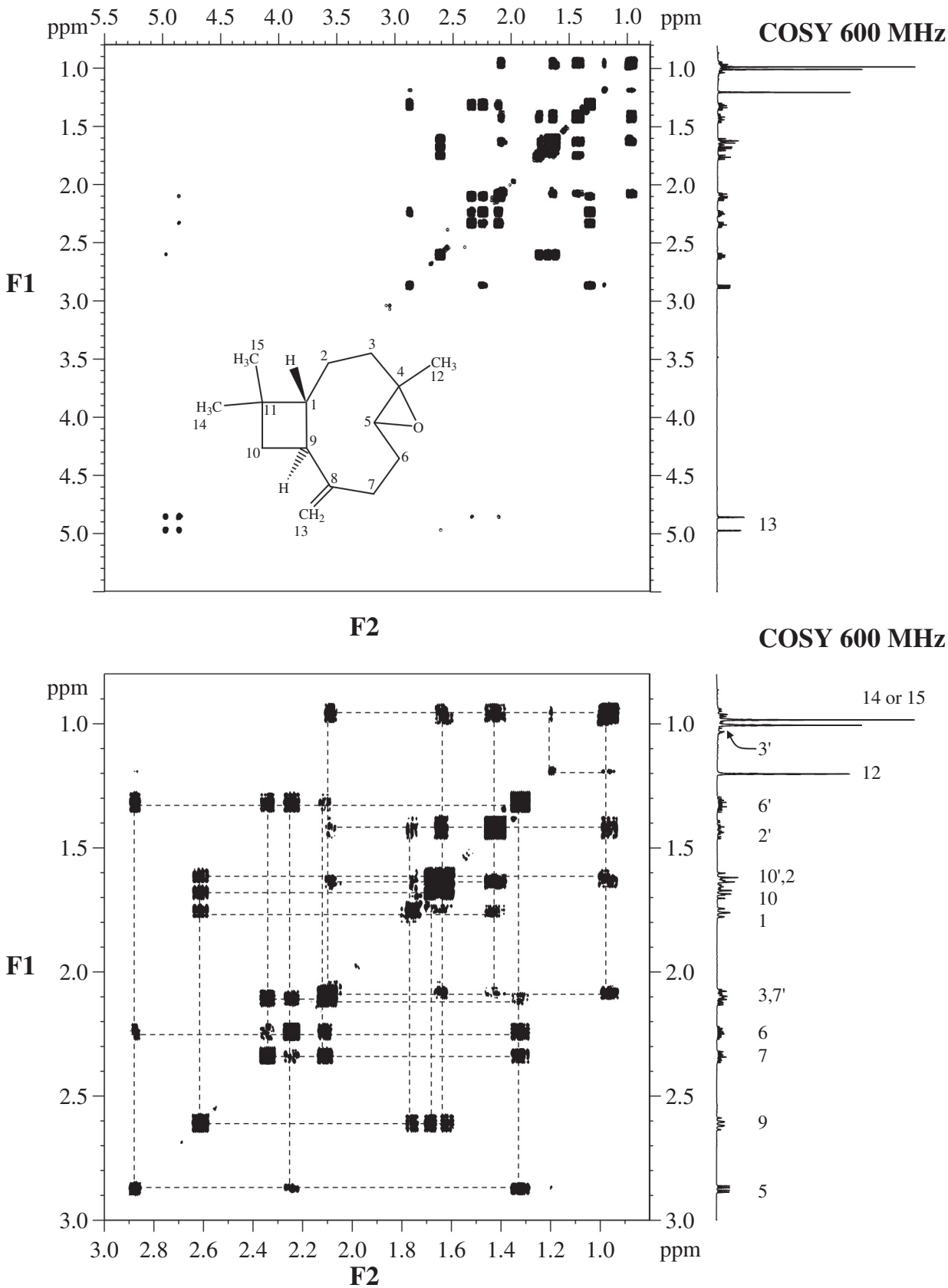

FIGURE 5.16 The DQF COSY spectrum for caryophyllene oxide. The lower portion is an expanded view with correlation lines drawn in and assignments are given as an aid.

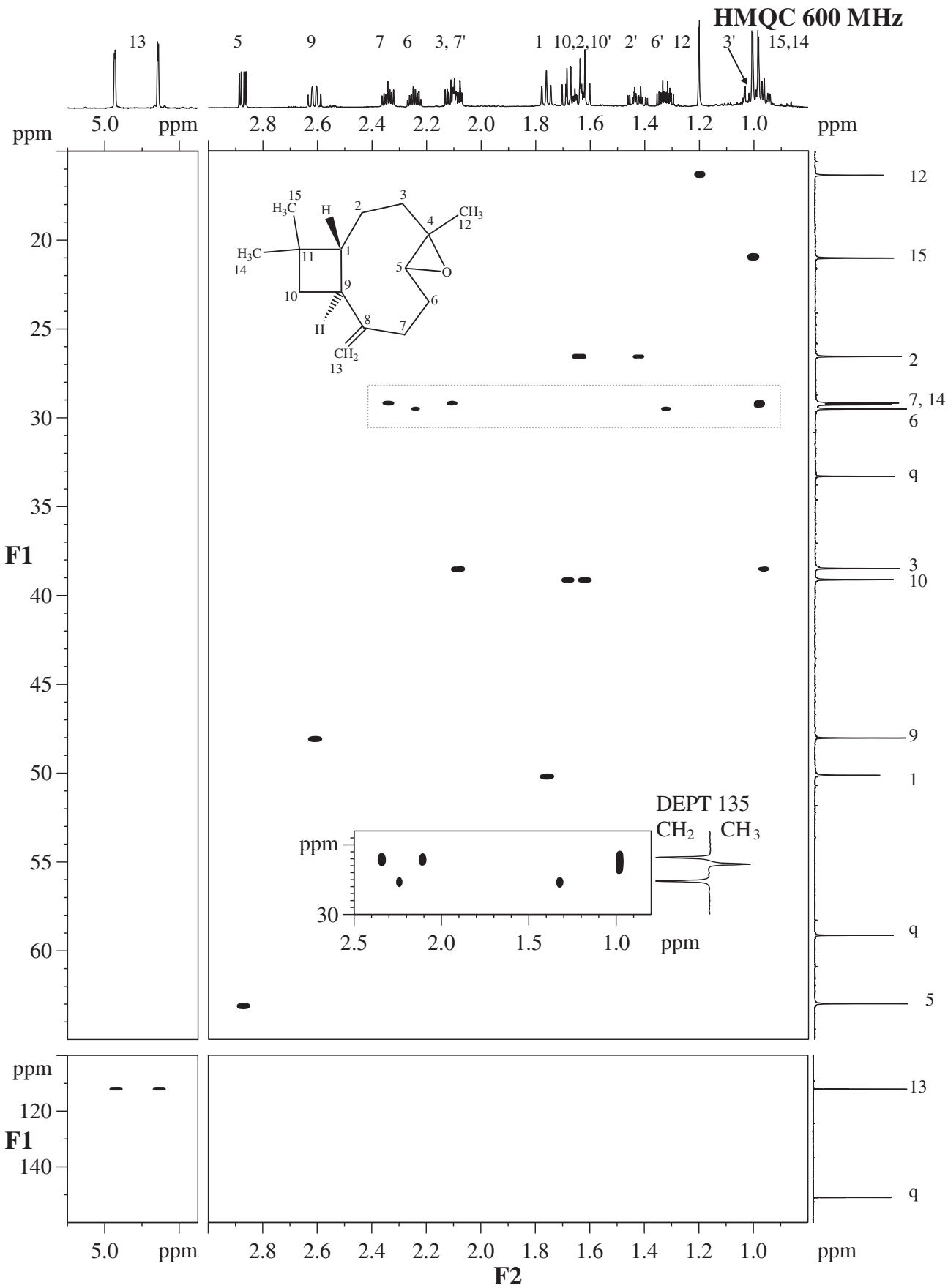

FIGURE 5.17 The HMQC spectrum for caryophyllene oxide. In place of the usual ^{13}C NMR spectrum, the inset uses the DEPT 135 spectrum for better clarity.

From the DEPT spectrum (see Figure 5.15), we already know that caryophyllene oxide has three methyl carbon resonances (16.4 ppm, 22.6 ppm, and 29.3 ppm), six methylene carbon resonances (26.6 ppm, 29.2 ppm, 29.5 ppm, 38.4 ppm, 39.1 ppm, and 112.0 ppm), three methine carbon resonances (48.1 ppm, 50.1 ppm, and 63.0 ppm) and three quaternary carbon resonances (33.3 ppm, 59.1 ppm, and 151.0 ppm).

The alkenyl methylene group (protons and carbon) and the three methyl groups (protons and carbons) are trivial assignments, and they correspond with our previous discussion. Of more interest and of greater utility, we assign the three methine protons: the doublet of doublets at 2.86 ppm (correlates with the carbon resonance at 63.0 ppm), the apparent quartet at 2.60 ppm (correlates with the carbon resonance at 48.0 ppm), and an apparent triplet at 1.76 ppm (correlates with the carbon resonance at 50.1 ppm). From the COSY spectrum and from the known structure, we are now able to assign all three methine resonances and feed this information back into the COSY to establish other correlations.

From the long-range, allylic correlation that we found in the COSY, we now confirm our cautious assignments that we made earlier. The doublet of doublets at 2.86 ppm is assigned to the methine proton of the epoxide ring, and its chemical shift is rationalized on the basis of the deshielding effect of the epoxide oxygen. The other bridgehead methine (adjacent to the *gem*-dimethyl group) is assigned to the multiplet at 1.76 ppm. With these assignments in hand, we could return to the COSY spectrum, but instead we will restrain our enthusiasm for now and assign the methylene protons first. Knowing these assignments first will help speed our way through the COSY.

Beginning from the low-frequency end of the ^{13}C spectrum, the following assignments can be made: the methylene carbon peak at 26.6 ppm correlates with proton resonances at 1.45 ppm and 1.63 ppm, the methylene carbon peak at 29.2 ppm correlates with proton resonances at 2.11 ppm and 2.37 ppm, the methylene carbon at 29.5 ppm correlates with proton resonances at 1.33 ppm and 2.23 ppm, the methylene carbon at 38.4 ppm correlates with proton resonances at 0.96 ppm and 2.09 ppm, the methylene carbon at 39.1 ppm correlates with proton resonances at 1.62 ppm and 1.68 ppm, and we have already assigned the alkenyl methylene group above. Thus, with little effort we have assigned a chemical shift for all of the protons in caryophyllene oxide and correlated them with a resonance from the ^{13}C NMR spectrum; we have grouped the diastereotopic protons together for each of the methylene groups, and we have obtained three separate entry points for the COSY spectrum when before we had none. We are now ready to return to the analysis of the COSY spectrum of caryophyllene oxide and assign the correlations in light of the structure.

An expanded section from 0.8 ppm to 3.0 ppm of the DQF-COSY spectrum of caryophyllene oxide can be found in the bottom part of Figure 5.16. Included in this portion of the figure are lines connecting proton-proton correlations to aid our discussion. The COSY connectivities allow us to construct structure fragments, or in this case, confirm structural segments. To correlate C-5, C-6, and C-7, we start with H-5 at 2.87 ppm. This proton shows cross peaks with two resonances at 1.32 ppm and 2.24 ppm. From the HMQC, we know that these are diastereotopic and assign them as H-6 and H-6′. The protons attached to C-6 give correlations with protons at 2.11 ppm and 2.37 ppm; we assign these protons, which also are diastereotopic, to C-7 at 29.2 ppm. The C-7 protons are coupled to each other, as certainly are the C-6 protons.

Other correlations are also straightforward. The C-5, C-6, and C-7 spin system is isolated so we must select another entry point. We can start again with the allylic bridgehead methine (H-9) at 2.60 ppm. We have noted already the long-range allylic interaction. In addition, we find three other interactions that the HMQC helps us to assign. One of the correlations is to a methine proton at 1.76 ppm, which we assign to H-1. The other two correlations find two diastereotopic protons (again, from HMQC) at 1.62 ppm and 1.68 ppm; we assign them as H-10 and H-10′. The C-10 protons are a dead end, and we find no other correlations to them.

H-1 shows coupling to both C-2 protons at 1.45 ppm and 1.63 ppm. The interaction is weak between H-1 and H-2′ at 1.63 ppm. Both C-2 protons are coupled to both C-3 protons at 0.95 ppm and 2.06 ppm and the appropriate cross peaks can be found. Thus, we have shown indirect connectivities from C-10 through C-9, C-1, and C-2 all the way to C-3. The HMQC has been invaluable in our interpretation. However, many questions still remain. We neither have correlations to the three quaternary carbons nor to the three methyl groups. The HMQC and the COSY together *support* the structure for caryophyllene oxide, but they do not preclude other possible structures.

5.5.3 Caryophyllene Oxide: HMBC

The HMBC spectrum of caryophyllene oxide (Figure 5.18) allows us to completely confirm its structure by giving us the required indirect carbon-carbon connectivities. An analysis of the structure of caryophyllene oxide reveals that there should be 87 cross peaks; this number is derived from considering each of the 15 carbon atoms and counting the number of chemically distinct protons at the α-positions and the number of chemically distinct protons at the β-positions. In order to keep track of all of those interactions, one must be methodical indeed.

One way to keep track of these data is to construct a table listing the carbon resonances in one direction and the proton resonances in the other. In Table 5.1, the carbons are given across the top and protons along the side. The numbering for caryophyllene oxide is the same in Table 5.1 as in all the figures.

Our approach for this spectrum is no different from any other spectrum. In this case, it is easier to start on the proton axis and look for the required cross peaks to the carbons as listed in Table 5.1. If we wished to start on the carbon axis, we would, of course, obtain the same results. If we begin

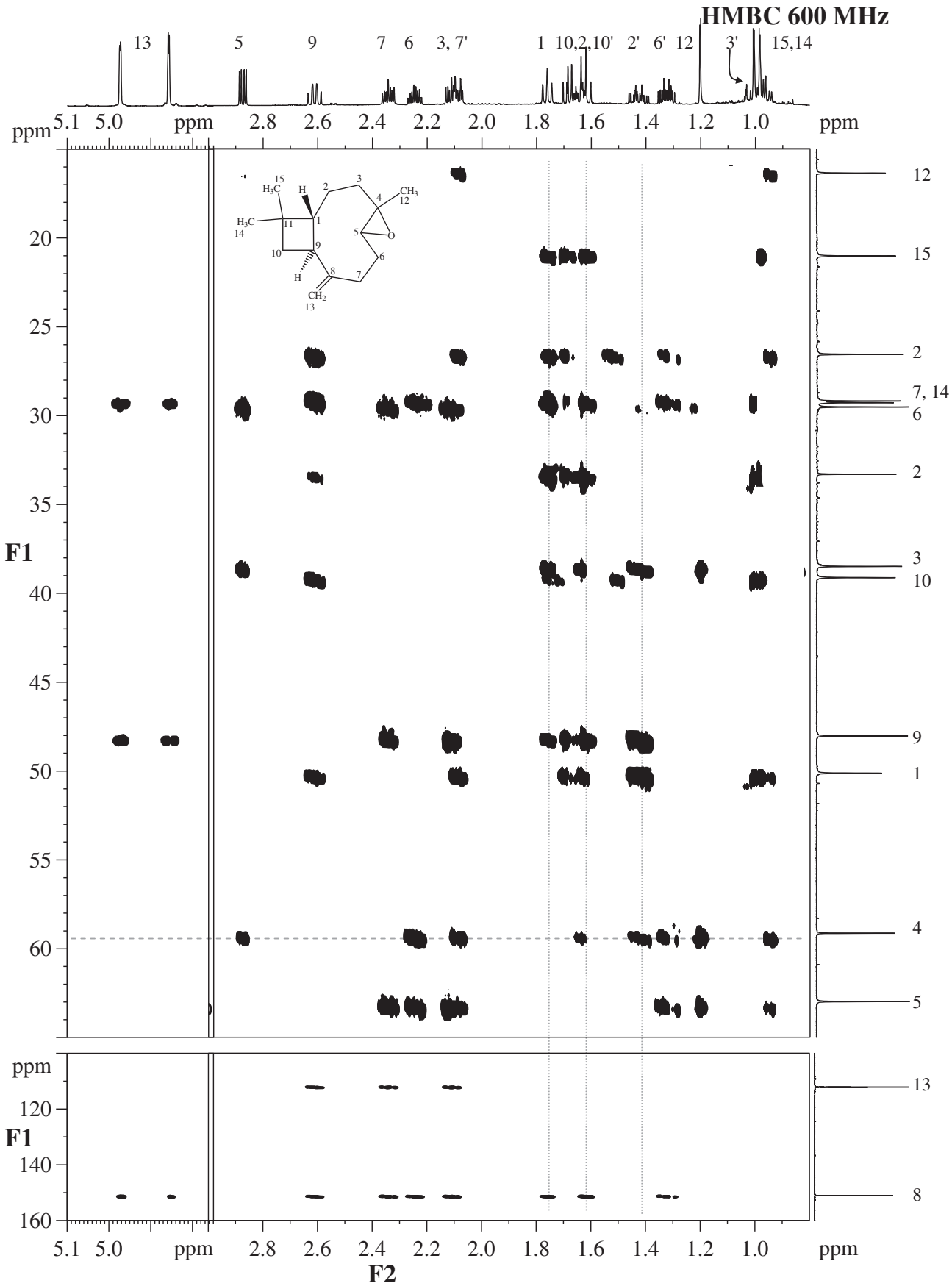

FIGURE 5.18 The HMBC spectrum for caryophyllene oxide.

TABLE 5.1 HMBC Correlations for Caryophyllene Oxide

	Carbon	C-1	C-2	C-3	C-4	C-12	C-5	C-6	C-7	C-8	C-13	C-9	C-10	C-11	C-15	C-14
Proton	**δ/ppm**	**50.1**	**26.6**	**38.4**	**59.1**	**16.4**	**63.0**	**29.5**	**29.2**	**151**	**112**	**48.0**	**39.1**	**33.3**	**22.6**	**29.3**
H-1	1.76	DB*	α	β						β		α	β	α	β	β
H-2	1.45	α	DB	α	β	β						β		β		
H-2′	1.63	α	DB	α	β	β						β		β		
H-3	0.95	β	α	DB	α	β	β									
H-3′	2.06	β	α	DB	α	β	β									
H-12	1.19			β	α	DB	β									
H-5	2.86			β	α	β	DB	α	β							
H-6	1.28				β		α	DB	α	β						
H-6′	2.23				β		α	DB	α	β						
H-7	2.11						β	α	DB	α	β	β				
H-7′	2.37						β	α	DB	α	β	β				
H-13	4.86								β	α	DB	β				
H-13′	4.97								β	α	DB	β				
H-9	2.6	α	β						β	α	β	DB	α	β		
H-10	1.43	β								β		α	DB	α	β	β
H-10′	1.47	β								β		α	DB	α	β	β
H-15	0.98	β											β	α	DB	β
H-14	1.01	β											β	α	β	DB

*Directly bonded proton-carbon pairs, which are not seen in the HMBC spectrum.

at the top left of the table with H-1 at 1.76 ppm, we see first that H-1 is bonded to C-1 at 50.1, a result that we have already determined with HMQC. Going across the row, we find a total of eight interactions are expected. In the table, each interaction is labeled either α or β depending upon whether it is due to a two-bond coupling ($^2J_{CH}$) or a three-bond coupling ($^3J_{CH}$). Of course, in the spectrum itself, there is no differentiation of the two types of interactions; we label them that way for our own bookkeeping efforts. Each of the interactions for H-1 designated in the table is found in the spectrum.

There are two protons on C-2, which are labeled H-2 and H-2′; these protons have different chemical shifts. Thus, we have a useful independent check of our HMBC assignments for each pair of diastereotopic protons in caryophyllene oxide. For H-2 at 1.45 ppm, we have the same five correlations that we have for H-2′ at 1.63 ppm. As we study the spectrum and the table more closely, we find that we have exquisitely detailed structural information that can be deciphered with a methodical approach.

An important point about quaternary carbons requires comment. Until now, we have had no direct correlations for carbons without protons, nor have we been able to establish connectivities through heteroatoms such as oxygen, nitrogen, sulfur, etc. Both the two- and three-bond coupling correlations of HMBC provide us with both types of critical information. For example, C-4 of caryophyllene oxide at 59.1 ppm has no directly-bonded protons, so far it has only appeared in the ^{13}C spectrum of the compound, and we know that it is quaternary from DEPT. If we look in Table 5.1 at the C-4 column, we find four two-bond correlations and four three-bond correlations. The HMBC spectrum bears out these expectations fairly well and gives us direct evidence of the C-4 position in the molecule.

5.6 ^{13}C—^{13}C CORRELATIONS: INADEQUATE

The HMBC experiment allows us to trace the skeleton of organic compounds by way of indirect carbon-carbon connectivities, but the process is tedious because we do not know whether the correlations are due to two- or to three-bond couplings. The 2D **INADEQUATE** (**I**ncredible **N**atural **A**bundance **D**oubl**E** **QUA**ntum **T**ransfer **E**xperiment) spectrum completes our set of basic through-bond correlations; we have COSY for proton-proton coupling, HMQC (or HETCOR) for one-bond and HMBC for two- and three-bond proton-carbon coupling, and now INADEQUATE for directly attached (one-bond) carbon-carbon couplings. For elucidation of the structure of organic compounds, this experiment is, without question and without exception, the most powerful and the least ambiguous available, and, to top it off, the experiment is easy to interpret. After reading that last statement, the naturally pessimistic among us inevitably will ask: what's the catch? Indeed, the catch is plain and simple: sensitivity. Recall from Chapter 4 that the probability of any one carbon atom being a ^{13}C atom is about 0.01. Thus, the probability that any two adjacent carbon atoms will both be ^{13}C atoms (independent events) is 0.01×0.01 or 0.0001; in rounded whole numbers, that is about 1 molecule in 10,000!

These long odds are overcome with the aid of double quantum filtering. We recall from our DQF-COSY experiment that double quantum filtering removes all single spin transitions, which in this case corresponds to isolated ^{13}C atoms; only those transitions from systems with two spins (AB and AX systems) and higher* are detected

*Following the same reasoning as above, the probability of a three-spin system in an unenriched sample is 1 in 1,000,000.

during acquisition. The main problem facing us experimentally is sample size, assuming that the compound has the required solubility in an appropriate lock solvent. For low molecular weight compounds (atomic weight <500 Da) run on a modern high field spectrometer, about 50–100 mg dissolved in 0.5 mL of a deuterated solvent is appropriate.

One way to imagine this experiment is as a carbon analogue of DQF-COSY in which both F1 and F2 would be carbon axes, and theoretically this experiment is possible. For practical considerations related to obtaining complete double quantum filtration, the INADEQUATE experiment is run slightly differently. In the display of the INADEQUATE spectrum of caryophyllene oxide (Figure 5.19), we find that the F2 axis is the familiar carbon axis, which we can, of course, relate to t_2 acquisition. The F1 axis looks unfamiliar and requires further explanation.

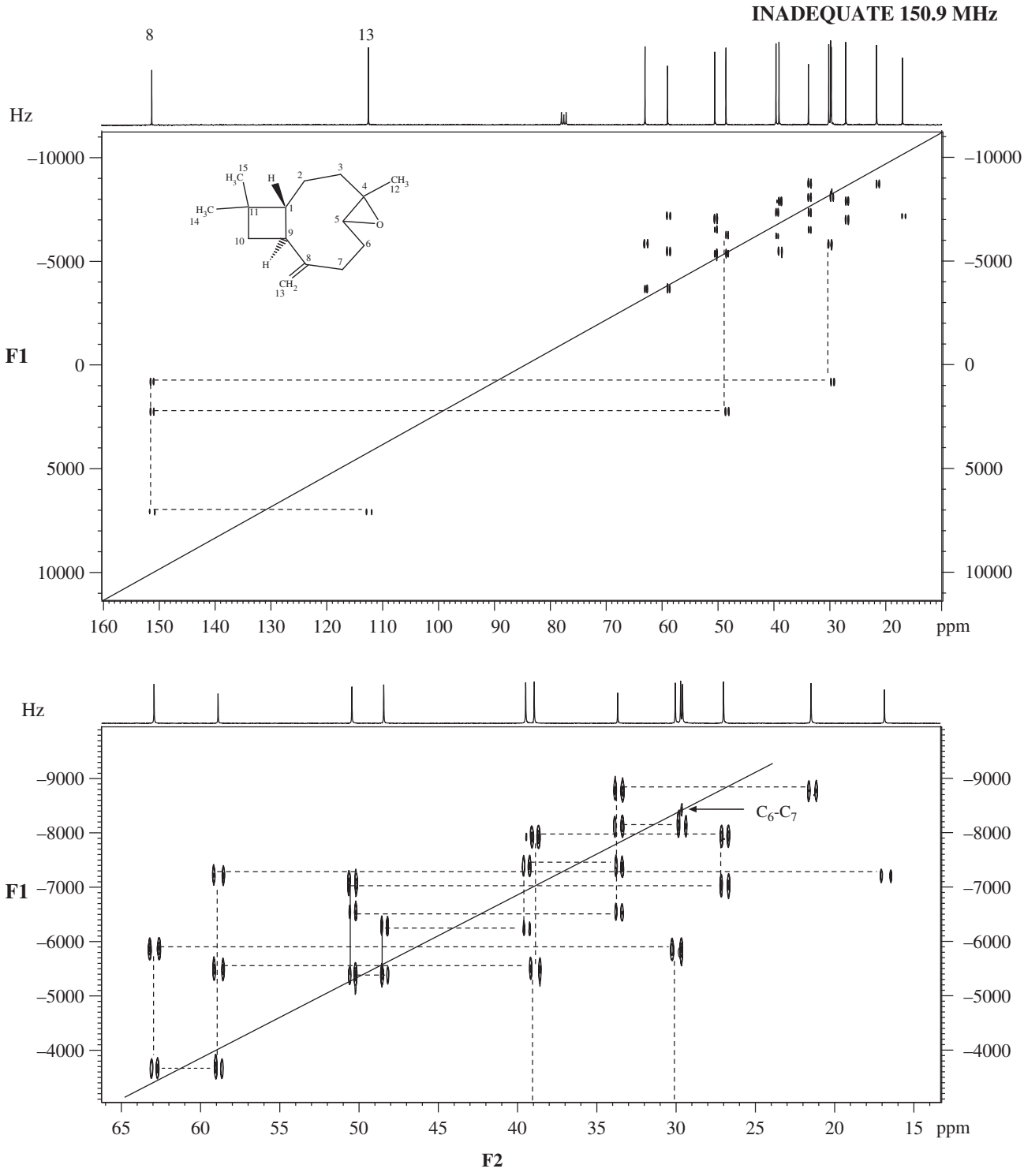

FIGURE 5.19 The INADEQUATE spectrum of caryophyllene oxide. Correlation lines are drawn as an aid.

During t_1, the frequencies that evolve are not the chemical shifts of the coupled nuclei as they are in a typical DQF-COSY. Instead, it is the *sum* of the offsets from the transmitter frequency of the coupled nuclei that evolve during t_1, and, because they are double quantum filtered, it is only the two-spin AB and AX systems that contribute significantly to the intensity of cross peaks in the INADEQUATE spectrum. This is why the cross peaks appear as doublets in the F2 dimension. Proper selection of experimental parameters in the pulse sequence allows us to select the larger one-bond couplings ($^1J_{CC}$), thus ensuring that we are only looking at directly bonded carbon-carbon correlations. The F1 axis is usually given in Hz and it is two times the range in F2, whose units are ppm.

5.6.1 INADEQUATE: Caryophyllene Oxide

The 2D INADEQUATE spectrum of caryophyllene oxide is presented in Figure 5.19. Cross peaks or correlations are found at $(\nu_A + \nu_X, \nu_A)$ and at $(\nu_A + \nu_X, \nu_X)$ in the (F1, F2) coordinate system for a given AX system. The actual cross peaks themselves are doublets (see the expanded portion of the spectrum, bottom of Figure 5.19) with a spacing equal to the ($^1J_{CC}$) coupling constant. The midpoint of the line connecting the two sets of doublets is $(\nu_A + \nu_X)/2, (\nu_A + \nu_X)$; thus, the collection of midpoints for all of the pairs of doublets lie on a line running along the diagonal. This is an important observation because it can be used to distinguish genuine cross peaks from spurious peaks and other artifacts.

With a better understanding of the F1 axis and the diagonal, we can proceed with interpretation of the spectrum. Table 5.1 lists carbon chemical shifts and carbon numbers based on the structure given earlier; we refer to these numbers in the present discussion. From Figure 5.19, we can make the high-frequency connections quite easily. The carbon at highest frequency is C-8 at 151.0 ppm; by tracing vertically down from this peak on the F2 axis, we intersect three cross peak doublets. These cross peaks connect horizontally with C-7 at 29.2 ppm, C-9 at 48.0 ppm, and C-13 at 112.0 ppm. Toward lower frequencies, C-13 at 112.0 ppm comes next, and it has only one cross peak, namely the reciprocal connection to C-8 at 151.0 ppm.

In order to present the low-frequency section more clearly, the lower portion of Figure 5.19 shows an expanded view of that area. The higher resolution of this figure enables us to see the doublet fine structure more readily. Let us trace one carbon's connectivities from this expanded view. C-11, at 33.3 ppm, is a quaternary carbon, and it accordingly shows four cross peaks. We have connectivities from C-11 to C-15 at 22.6 ppm, C-14 at 29.3 ppm, C-10 at 39.1 ppm, and C-1 at 50.1 ppm.

Before we conclude our discussion, we note that the INADEQUATE spectrum of caryophyllene oxide contains an uncommon phenomenon worth exploring. Carbons 6 and 7 of caryophyllene oxide nearly overlap in the ^{13}C spectrum with each other and with the C-15 methyl; we list their chemical shifts from Table 5.1 as 29.5 ppm and 29.2 ppm. Because they are bonded to one another in caryophyllene oxide, they should show correlation in the INADEQUATE spectrum, but, instead of an AX system, we have an AB system with $\Delta\nu/J$ being much less than eight. For this special case, we no longer expect two doublets whose midpoint lies on the diagonal; instead, we predict that an AB multiplet (see Chapter 3) should fall on the diagonal line itself. This prediction is borne out in Figure 5.19 where we find a cross peak directly below C-6 and C-7, and this cross peak intersects the diagonal line.

The other connectivities found in the expanded spectrum are left to the reader as an exercise. We summarize this section with two points:

- 2D INADEQUATE provides direct carbon-carbon connectivities enabling us to sketch the carbon skeleton unambiguously.
- In practice, 2D INADEQUATE has limited applicability due to its low sensitivity and concomitant long experimental times.

5.7 LACTOSE

The structure of the β-anomer of lactose is given in Figure 5.1. The challenges that lactose presents in the interpretation of its ^1H and ^{13}C NMR spectra (Figure 5.20) are obvious, but the opportunities for correlation NMR are irresistible. In solution, lactose is an equilibrium mixture of α- and β-anomers. The two diastereomers are epimeric at only 1 stereocenter out of 10. In addition, the protons of the two sugar residues in each diastereomer are insulated from each other by the glycosidic oxygen atom, forming isolated spin systems. This situation is common to all oligo- and polysaccharides.

We are not going to spend too much time discussing the 1D spectra except to note some of the obvious features. The anomeric proton resonances can be found at 4.45 ppm, 4.67 ppm, and 5.23 ppm and the anomeric carbon resonances at 91.7 ppm, 95.6 ppm, and 102.8 ppm. The reason for three anomeric protons and carbons is that the α- and β-anomers of glucose give two sets of resonances while the galactose residue, which exists only in the β-form, gives a single set of resonances in both the proton and carbon spectra. The other portions of both spectra, especially the proton spectrum, are quite complicated and show considerable overlap.

5.7.1 DQF-COSY: Lactose

The DQF-COSY spectrum for lactose (Figure 5.21) is rich with correlations, and entry points are easy to find. This figure and others use a simplified notation in which galactose resonances are labeled G*n*, where *n* is the proton or carbon position, and either αn or βn for positions in the α-glucose residue and the β-glucose residue, respectively. Each of the anomeric protons, which are the protons attached to C-1 for

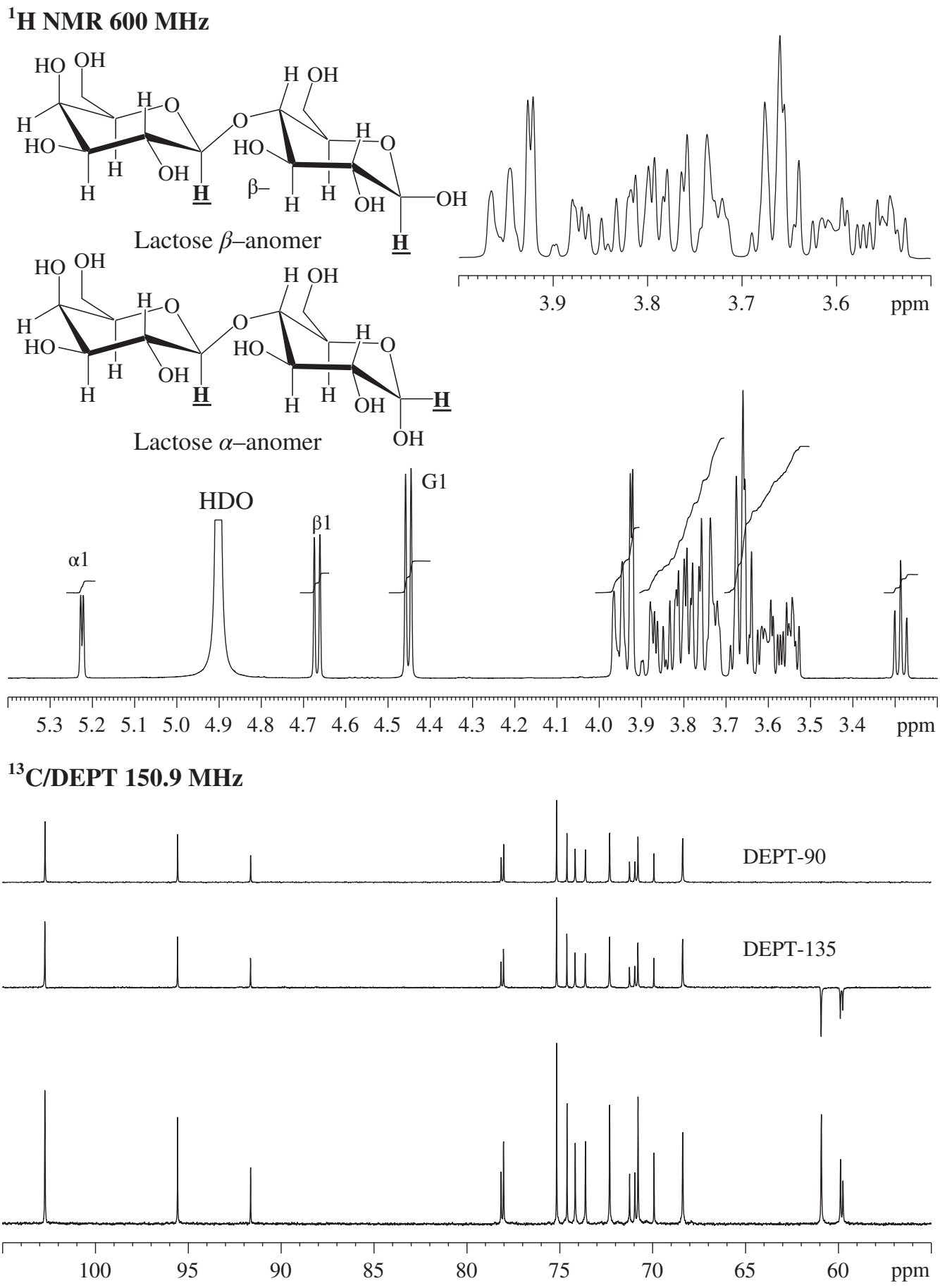

FIGURE 5.20 The ^{1}H, ^{13}C, and DEPT NMR spectra of lactose. In solution, lactose is an equilibrium mixture of anomers.

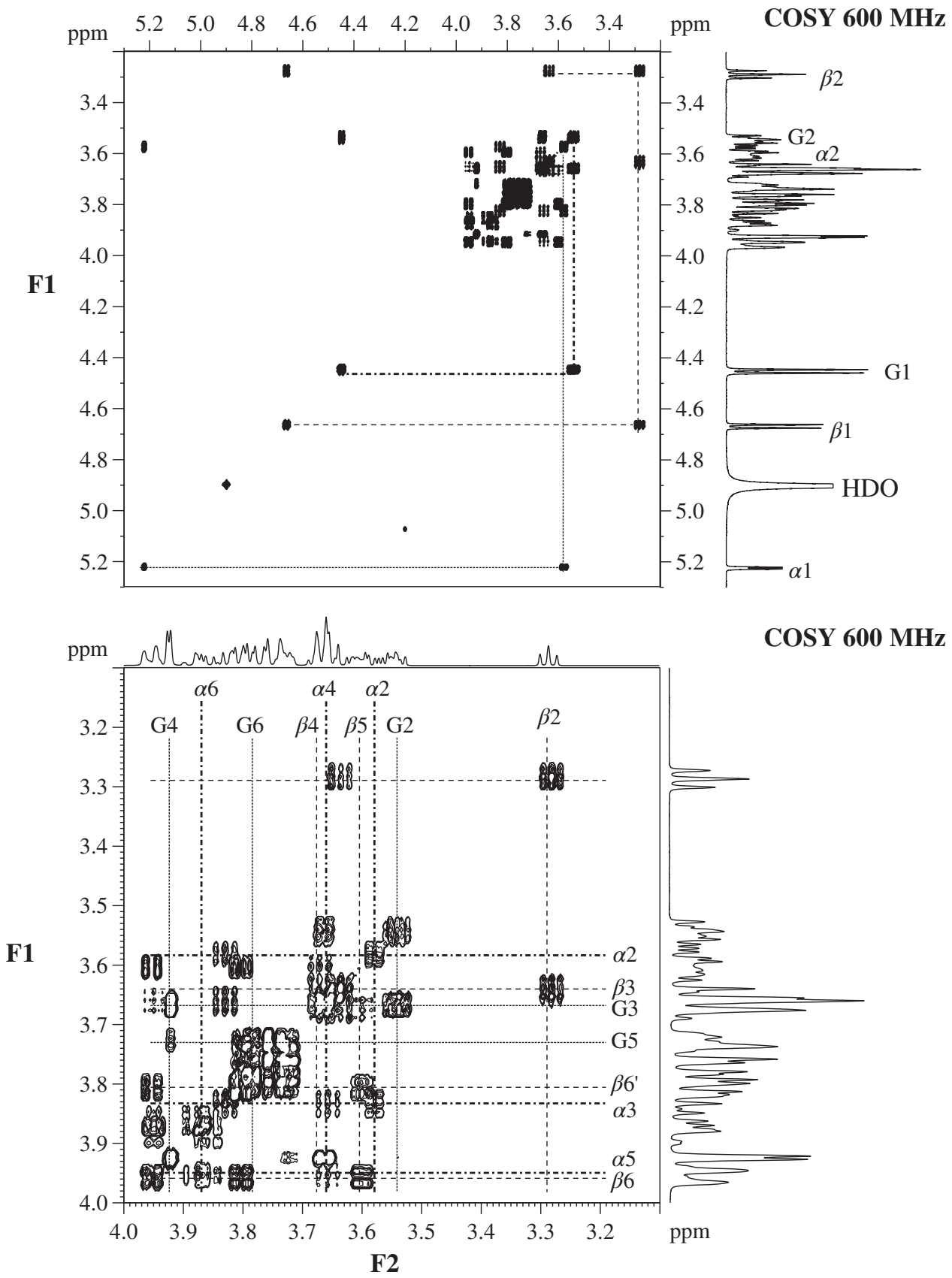

FIGURE 5.21 The DQF COSY spectrum for lactose. See the text for an explanation of the shorthand notation for proton resonances. Correlation lines are drawn in and assignments are given as an aid.

each sugar residue, show one and only one correlation to their respective C-2 protons. For instance, the anomeric proton at 4.67 ppm shows a correlation to a proton (obviously attached to C-2) at 3.29 ppm. This C-2 proton at 3.29 ppm shows a correlation to a C-3 proton at 3.64 ppm.

Continuation of this process quickly becomes dreadfully complicated because of the severe overlap of signals. Many of the correlations have been drawn in with different types of lines for each of the different residues in the expanded view. The reader is invited to trace some of these correlations but cautioned to be wary of frustration. Below, lactose will again be analyzed in light of other experiments that will literally remove the overlap.

5.7.2 HMQC: Lactose

The HMQC spectrum of lactose is shown in Figure 5.23 in three sections to minimize overlap and to show good resolution on the carbon axis. As with the COSY spectrum, this figure is labeled with assignments. These assignments were made with information beyond what we have seen so far. (By the end of our discussion of lactose, it will be clear that these assignments are correct, and it should be obvious how these assignments were made.) Overlap is less severe so that some of the assignments can be made quite easily. This spectrum is useful in that it allows us to find the chemical shift of most of the protons, many of which are overlapping in the 1D spectrum.

5.7.3 HMBC: Lactose

Considering the complexity of lactose, a complex and overlapping HMBC spectrum is expected. The spectrum found in Figure 5.24 measures up to this expectation. Students are encouraged to analyze this spectrum, which is facilitated by the labeling.

An important correlation in this spectrum is highlighted in the expanded inset that shows the correlation between C-4 of glucose (from both α- and β-anomers) and the C-1 proton of galactose. This three-bond coupling is extremely important because it shows that the glycosidic linkage is indeed from galactose C-1 to glucose C-4. Because there is no overlap in this part of the spectrum, our conclusion is unambiguous. The reciprocal correlation between the C-1 carbon of galactose and the C-4 protons of glucose (both anomers) is most likely there, but, because there is overlap among G3 (which also has a correlation to C-1 of galactose), α4, and β4 protons, it is not possible to observe this correlation conclusively.

5.8 RELAYED COHERENCE TRANSFER: TOCSY

The common theme so far in our correlation experiments has been to allow spins to evolve during t_1 under the influence of J couplings between the spins of interest. We have seen the power of COSY, HMQC, HMBC, and INADEQUATE to provide us with detailed structural information for ipsenol, caryophyllene oxide, and lactose. In this section, we will develop another method for showing correlations and apply it to molecules with distinct, isolated proton spin systems such as carbohydrates, peptides, and nucleic acids.

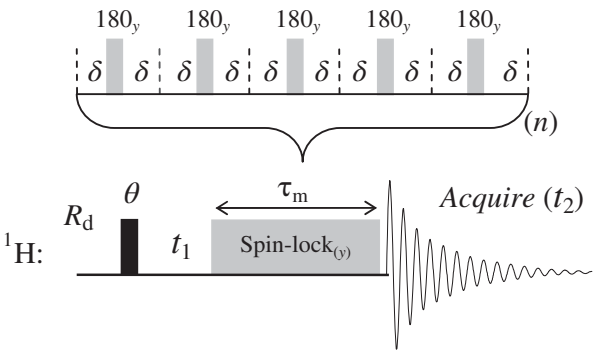

FIGURE 5.22 The pulse sequence for a 2D TOCSY experiment. Note that the delays (δ) are unrelated to chemical shifts.

Our goal is to relay or transfer magnetization beyond directly coupled spins, thus enabling us to see correlations among nuclei that are not directly coupled to each other but within the same spin system. The experiment is called **TOCSY** (**TO**tal **C**orrelation **S**pectroscop**Y**) and we will consider both the 2D and 1D versions. The pulse sequence for a 2D TOCSY experiment resembles our prototype 2D experiment, but, instead of a second $\pi/2$ pulse, we insert a mixing period during which the magnetization is spin locked on the y-axis (Figure 5.22). To understand the outcome of the experiment, we can ignore the particulars of spin locking and concentrate on the consequences of the mixing period. During this mixing period, magnetization is relayed from one spin to its neighbor and then to its next neighbor and so on. The longer the mixing period, the further the transfer of magnetization can propagate, traveling, in favorable cases, throughout an entire spin system.

The appearance of a 2D TOCSY spectrum resembles in all aspects a COSY spectrum. The F1 and F2 axes are for proton, the diagonal contains 1D information, and even the cross peaks have the same appearance. The difference here is that the cross peaks in a COSY spectrum are due to coupled spins while the cross peaks in the TOCSY spectrum arise from relayed coherence transfer. For long mixing times in a TOCSY spectrum, all spins within a spin system appear to be coupled. To appreciate the advantages of TOCSY, we continue with the disaccharide lactose, which has three distinct (i.e., separate) spin systems.

5.8.1 2D TOCSY: Lactose

The 2D TOCSY spectrum of lactose is given in Figure 5.25. The mixing time for this 2D spectrum was sufficiently long that magnetic coherence has been transferred more or less throughout each sugar residue's spin system. Compare this

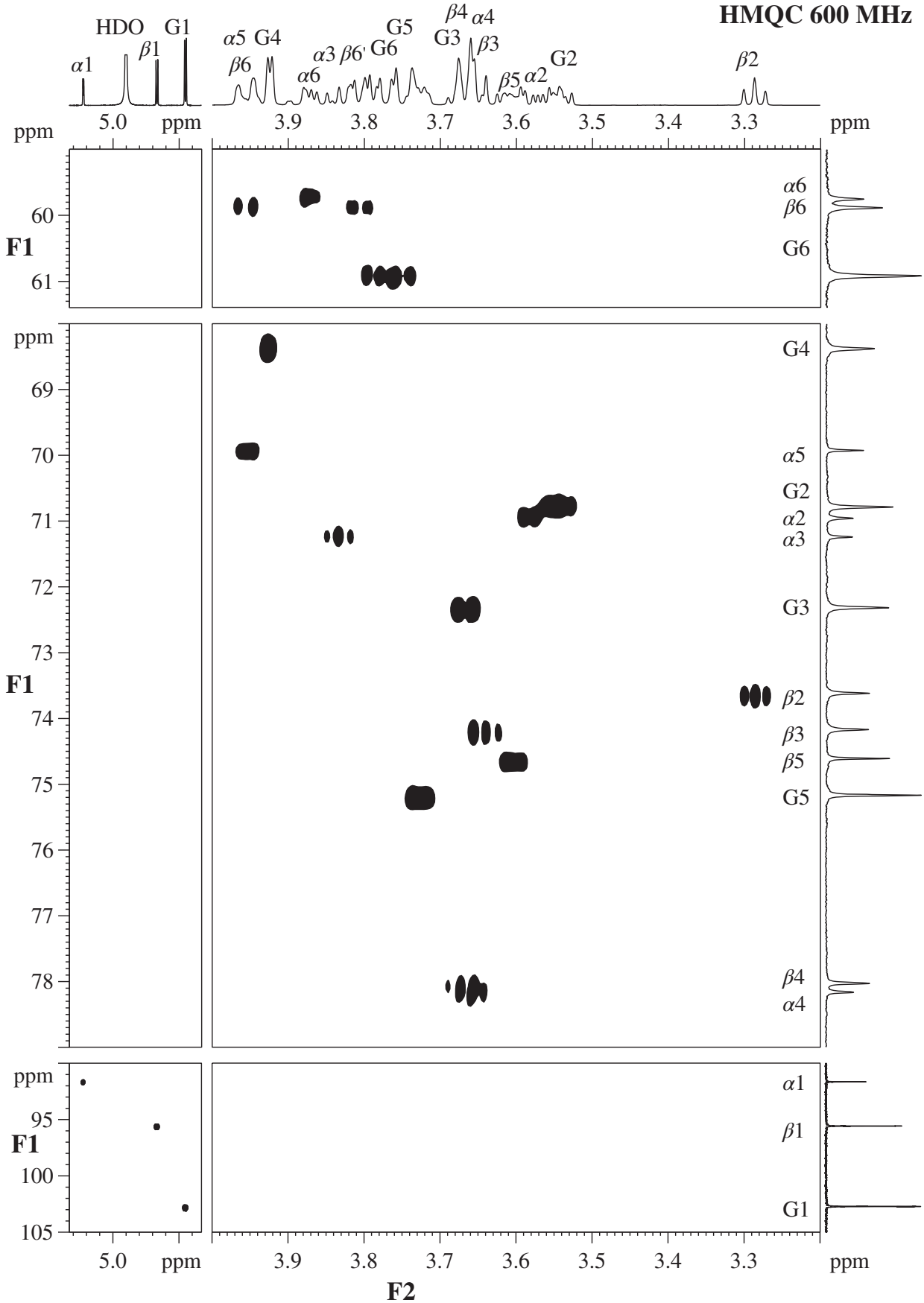

FIGURE 5.23 The HMQC spectrum for lactose. See text for an explanation of the notation. Assignments are given as an aid.

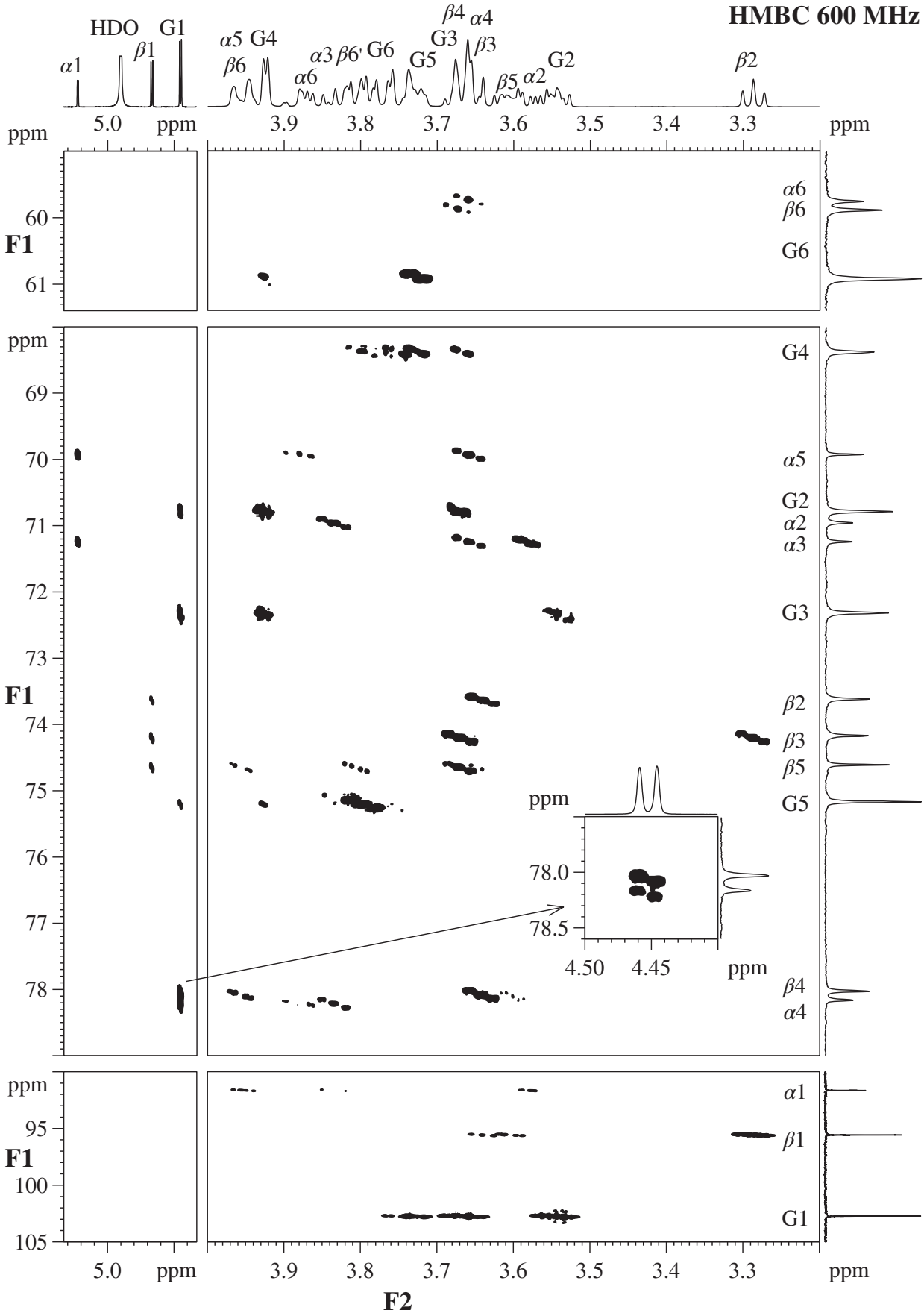

FIGURE 5.24 The HMBC spectrum for lactose. See text for an explanation of the inset.

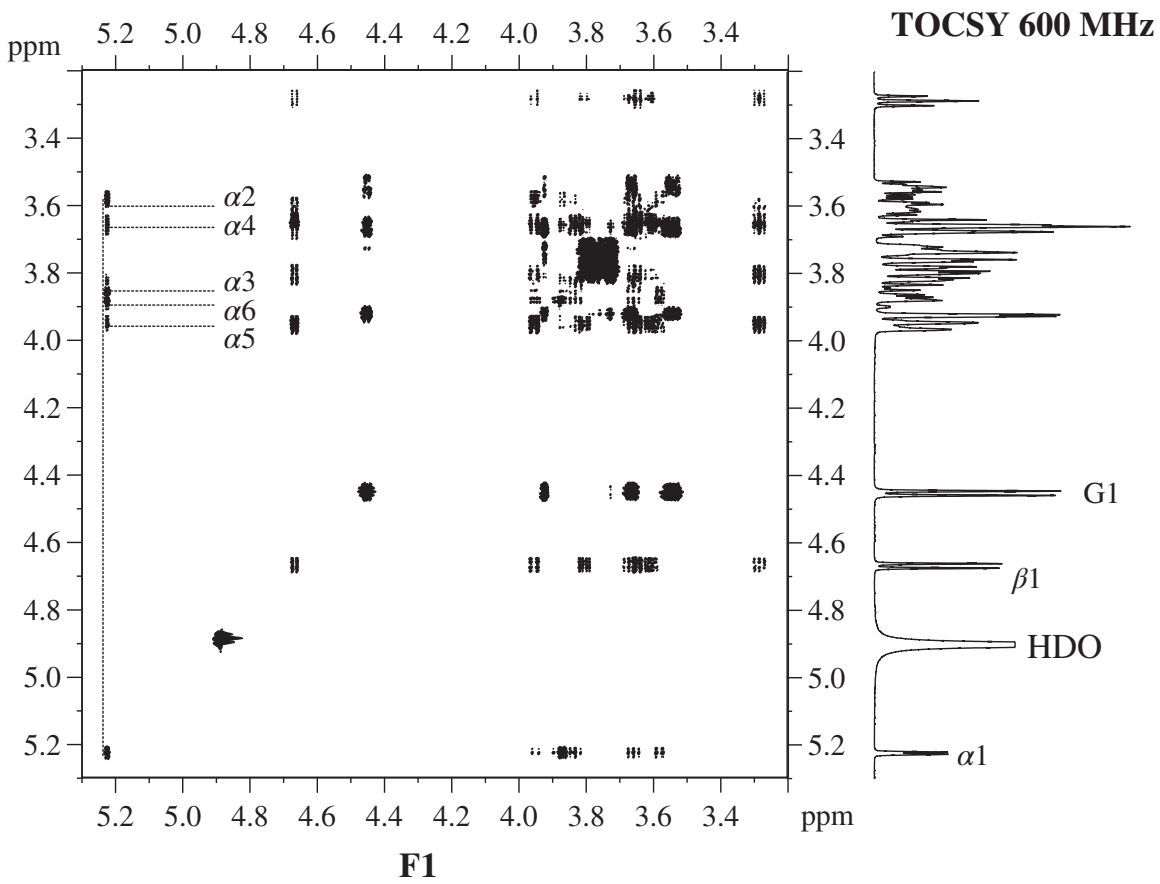

FIGURE 5.25 The 2D TOCSY spectrum of β-lactose. Correlation lines are drawn in and some assignments are given as an aid.

figure to the COSY spectrum for lactose in Figure 5.21 and note the similarities and differences.

As an example, we can find all of the proton resonances (and determine their chemical shifts) for the α-anomer of glucose by starting at its anomeric proton resonance at 5.23 ppm. These correlations have been marked in the figure. Assignment of the proton resonances (which are shown in the figure) cannot be made on the basis of this spectrum alone, but could be made in conjunction with the COSY spectrum. The same exercise can be carried out for the other two anomeric resonances, but these are left for the student.

5.8.2 1D TOCSY: Lactose

Every 2D experiment has a 1D analogue and we tend to think that these 1D experiments are less efficient or informative, which they usually are. If we think again about our COSY experiment, we have said that homonuclear decoupling would give us the same type of information. We select a proton resonance, irradiate it, and compare the result with the original 1D proton spectrum. In similar fashion for a 1D TOCSY experiment, often called HOHAHA (Homonuclear Hartmann-Hahn), we select a proton resonance and irradiate it; we allow for an appropriate mixing time for the magnetization to be relayed during which we apply spin locking, and we acquire the 1D spectrum. The only signals that will be recorded in this spectrum are those to which magnetization has been transferred. Put another way, all other signals that are outside the spin system do not appear.

An even better scenario is to run a series of 1D TOCSY experiments in which the mixing time is systematically increased while the proton being irradiated is kept constant. To illustrate these experiments, we irradiated the anomeric proton from the β-anomer of the glucose ring in lactose at 4.67 ppm and ran a series of experiments with mixing times ranging from 20 ms to 400 ms. The results of these experiments are shown in a series of stacked plots in Figure 5.26.

At a mixing time of 20 ms, we find only the $\beta 2$ resonance, which is seen clearly as an apparent triplet at 3.29 ppm. After 40 ms of mixing time, transfer to $\beta 3$ is readily discernable (another apparent triplet) and the $\beta 4$ proton is just barely visible. A plot of the experiment with a mixing time of 80 ms reveals the $\beta 4$ resonance a little better, while, after 120 ms, the signal from $\beta 5$ has sprouted from the baseline. After 400 ms, transfer throughout the entire spin system is evident; the H-5 signal is robust as that from the diastereotopic $\beta 6$ methylene group. This part of the figure shows the $\beta 6$ and $\beta 6'$ resonances with clearly different coupling constants to $\beta 5$. One negative aspect of long mixing times is that both resolution and signal are lost.

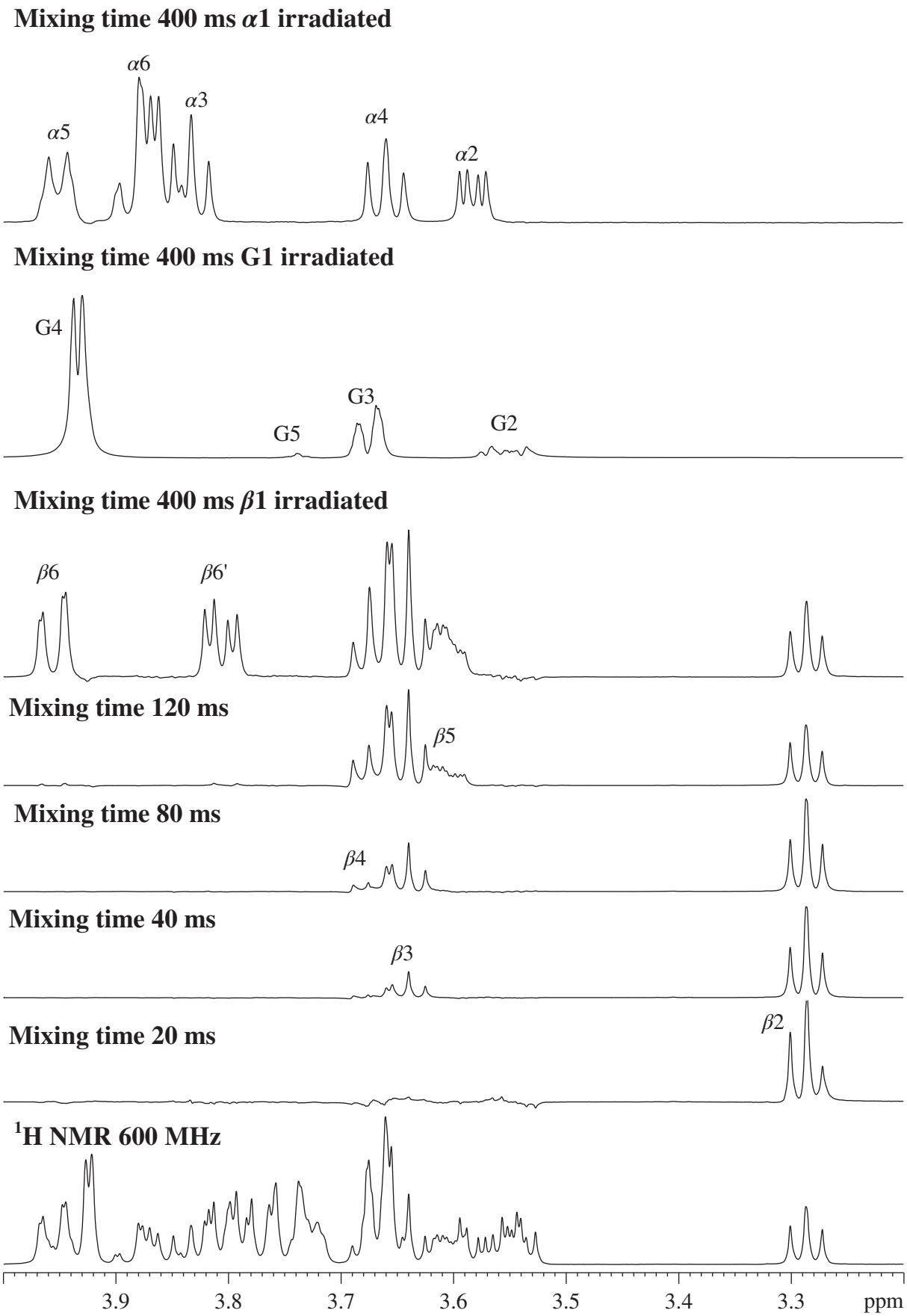

FIGURE 5.26 Stacked plots of a series of 1D TOCSY experiments on β-lactose with increasing mixing times. See text for an explanation. A portion of the ^{1}H NMR spectrum is reproduced for reference in the bottom plot.

We can usually offset signal loss by acquiring and summing more FIDs. Also shown in this figure are the 400 ms (longest mixing time) experiments for the galactose anomeric proton and the α-anomeric proton for glucose.

Both the 1D and 2D versions of TOCSY find wide application in deciphering overlapping signals that originate from different spin systems. The 1D version is particularly exciting as it enables us to "walk" through a spin system as we systematically increase the mixing time.

5.9 HMQC–TOCSY

There are various hybrid 2D correlation experiments that combine features of two simpler 2D experiments. A popular and useful example is the HMQC–TOCSY spectrum that correlates one-bond $^{1}H—^{13}C$ couplings (HMQC) but shows these correlations throughout an entire spin system (TOCSY). This experiment simplifies the analysis of complex carbohydrate and peptide systems and allows ready assignments of systems of protons and carbons.

5.9.1 HMQC–TOCSY: Lactose

The HMQC–TOCSY spectrum for lactose is given in Figure 5.28 with all of the proton and carbon resonances labeled. The overall appearance of this spectrum is reminiscent of an HMBC but the correlations are quite different. It is equally interesting and useful to start on the proton axis (F2) or the carbon axis (F1). If we start on the proton axis at 5.23 ppm, the anomeric proton for the α-anomer of glucose (α1), and proceed downward vertically, we find six correlations to the six carbons of this glucose residue. If we refer back to the simple HMQC spectrum for lactose, we find only one correlation for this proton. Likewise, the anomeric proton of the β-anomer of glucose at 4.67 ppm also shows six correlations to the carbons of its respective glucose residue.

Correlations to the anomeric proton of galactose (4.46 ppm), however, only show four interactions along the carbon axis. This result is consistent with the 1D TOCSY spectrum of the galactose anomeric proton shown in Figure 5.26, where we find that coherence transfer does not travel beyond H-4 (G4). All six correlations are found if we start at H-4 (G4, 3.93 ppm) instead. As an exercise, try a similar process by starting on the carbon axis and tracing horizontally to the left to find HMQC–TOCSY correlations to protons. The anomeric carbon resonances are the easiest to try, but it is worthwhile to try others as well.

5.10 ROESY

The ROESY experiment, rotating-frame Overhauser effect spectroscopy, is a useful 2D analogue of the nuclear Overhauser effect difference experiment. This experiment is useful for molecules of all sizes whereas the related

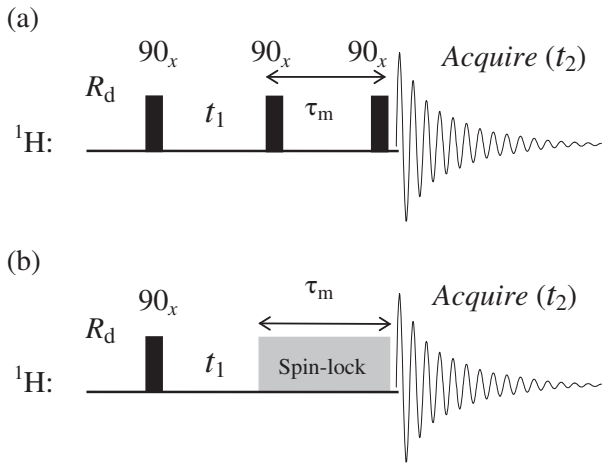

FIGURE 5.27 Pulse sequences for (a) 2D NOESY and (b) 2D ROESY.

experiment, NOESY (nuclear Overhauser effect spectroscopy), is not very useful for small molecules. NOESY is used primarily with biological macromolecules. Both NOESY and ROESY experiments correlate protons that are close to each other in space, typically 4.5 Å or less.

Because ROESY provides through-space proton-proton correlations, its appearance and presentation resembles COSY. In fact, COSY peaks (generated through J coupling) are present in ROESY spectra; these COSY peaks are superfluous and should be ignored. Occasionally, another complication arises from TOCSY-like transfer of magnetic coherence among J-coupled spins. The pulse sequences for 2D NOESY and 2D ROESY experiments are given in Figure 5.27. The only difference between the two experiments is that ROESY uses a spin lock during the mixing time τ_m.

5.10.1 ROESY: Lactose

The ROESY spectrum of lactose is given in Figure 5.29. Note the overall appearance in the upper part of the figure. In the lower part, the anomeric region is shown as expanded insets. The two glucose residues are straightforward to interpret. The α-anomeric proton shows only one correlation and this is the expected COSY interaction. Recall that by definition, the α-anomer has its C-1 hydroxyl in the axial position and its C-1 proton (α1) in the equatorial position. In the equatorial position, there are no through space interactions likely and none are seen.

The other anomer of glucose, in contrast, has its anomeric proton (β1) in the axial position. In the preferred chair conformation of glucose, protons occupy all of the other axial positions leading to presumed diaxial interactions between H-1 (β1) and H-3 (β3) and between H-1 (β1) and H-5 (β5). The ROESY spectrum reveals three interactions with the anomeric proton, β1, at 4.67 ppm. The H-2 COSY interaction is, of course, present, and the two diaxial NOE interactions with H-3 (β3) and H-5 (β5) are quite evident.

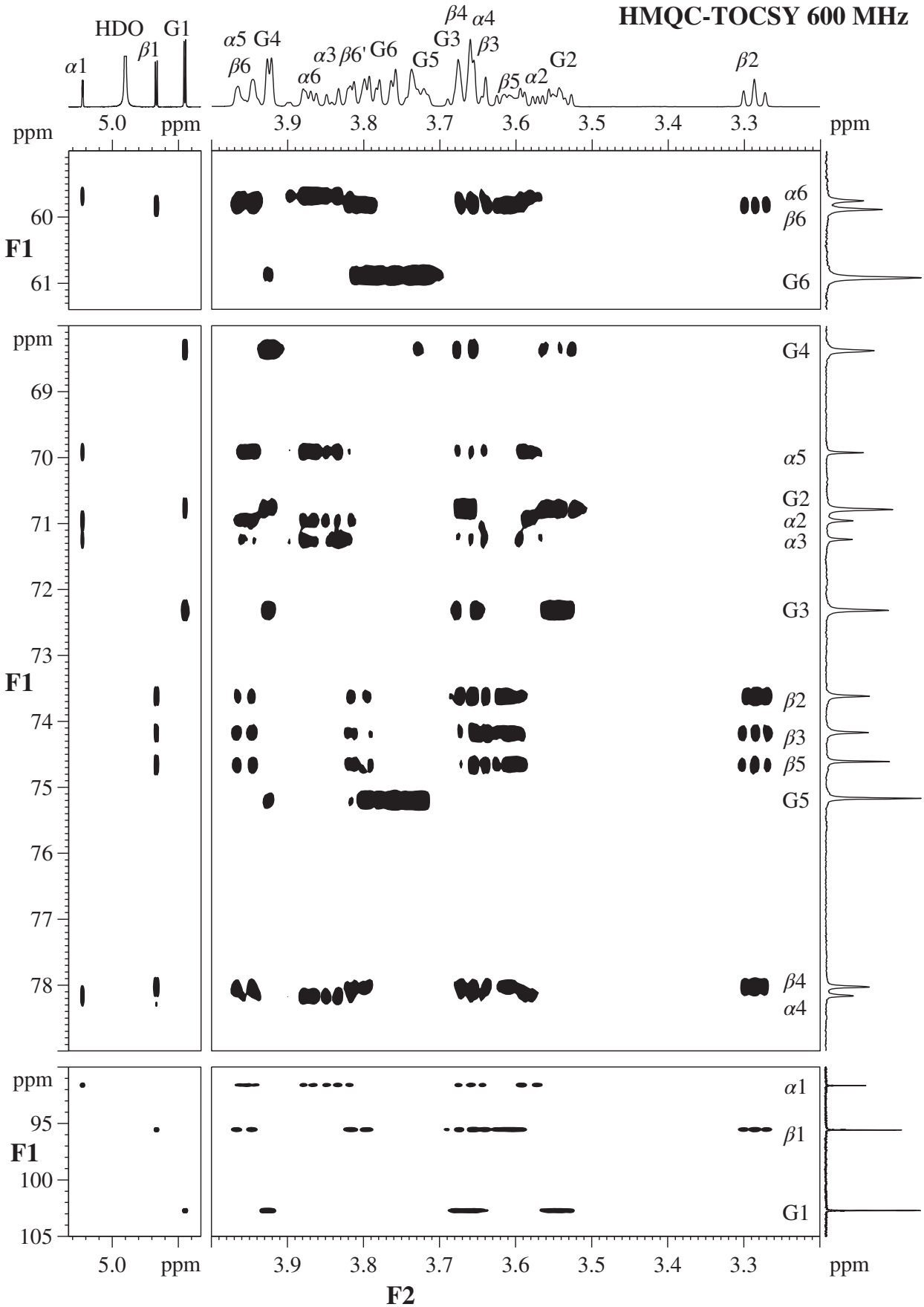

FIGURE 5.28 The HMQC–TOCSY spectrum of lactose. Assignments are given as an aid.

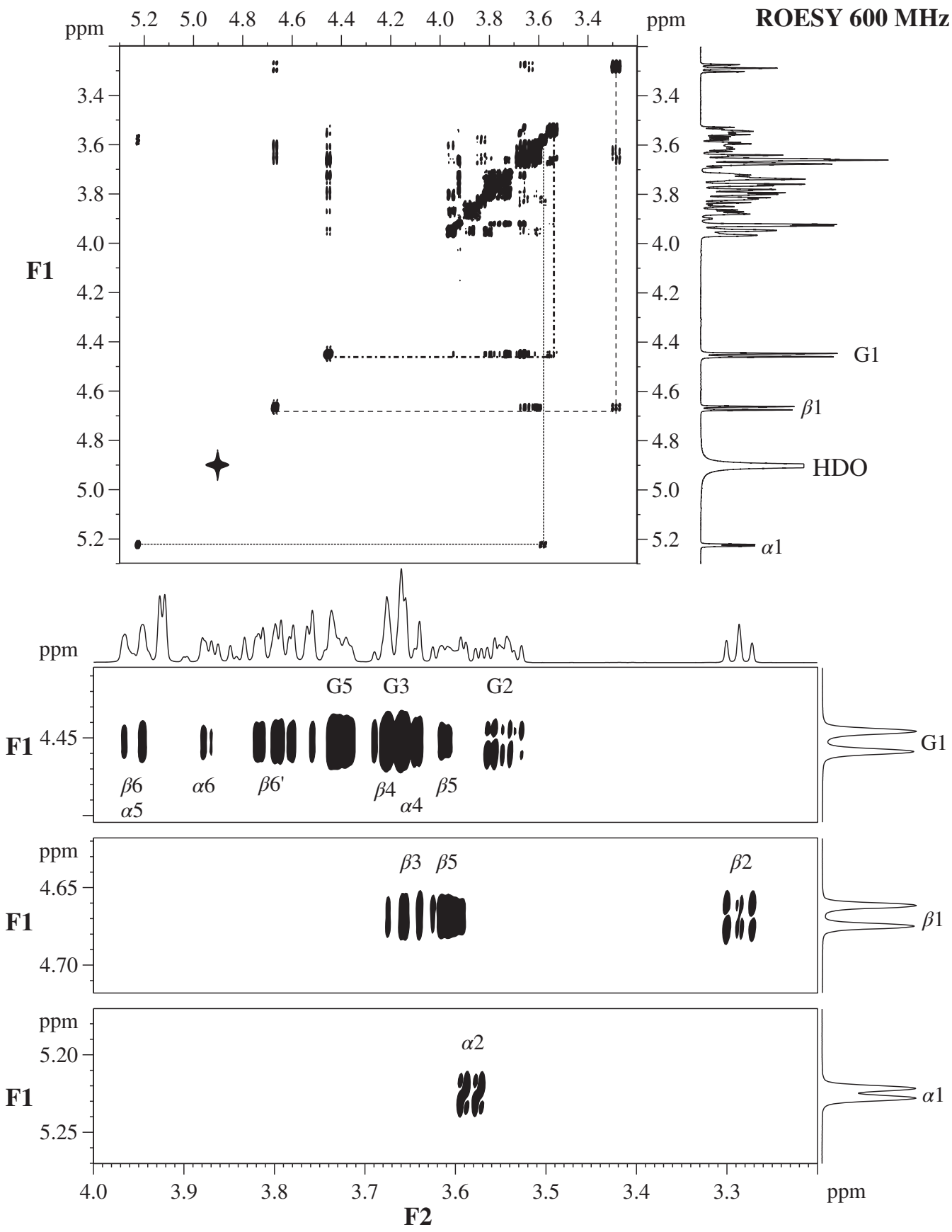

FIGURE 5.29 Top: the 2D ROESY spectrum of lactose. Bottom: expansions of the three anomeric correlations.

5.11 VGSE

Proteins or polypeptides are polymers or oligomers made from a limited number of (mostly) α-amino acids linked by amide or peptide bonds. A polypeptide example would be too difficult an undertaking at this point, but a tetrapeptide, on the other hand, is quite manageable while still illustrating many of the important features of a true polypeptide. Although many small oligopeptides are found in nature, a plethora of small peptides are now manmade utilizing automated synthesis equipment.

The structure of the small peptide being used as an example in this chapter is given in Figure 5.1. Starting with the N-terminus, the peptide contains the amino acids valine, glycine, serine, and glutamic acid (VGSE) linked in the usual way. The 1D NMR spectra for this compound are shown in Figure 5.30. The positions in each amino acid have been labeled and assignments of the protons and carbons have been made. The assignments have been given in this figure to facilitate discussion; they cannot be made from these data alone.

One aspect of the experimental conditions under which these spectra were obtained is important to understand so that the spectra can be rationally interpreted. For solubility and stability purposes, peptides are generally dissolved in buffered water. Recall from Chapter 3 that compounds prepared for NMR experiments are almost always dissolved in deuterated solvents. The need for deuterated solvents is so that the spectrometer can remain stable for the duration of the experiment by way of the field/frequency lock. The lock signal comes from the deuterium NMR signal of the solvent. However, if the peptide sample were dissolved in buffered D_2O, all of the exchangeable protons, including the amide protons, would be replaced with deuterons and not seen in a ^1H NMR spectrum. A compromise is necessary; the sample was dissolved in 95% buffered H_2O containing 5% D_2O. Note the presence of the three amide proton resonances between 8.0 ppm and 9.0 ppm. These amide resonances, as we shall see, are extremely important and they would be absent if the sample were dissolved in pure D_2O.

5.11.1 COSY: VGSE

The DQF-COSY spectrum of VGSE can be found in Figure 5.31. As with lactose, there are several good entry points, especially the resonances of the three amide protons. Three of the four amino acid residues can be traced using these as starting points. The fourth amino acid can be traced starting with the methyl groups (the only ones in the molecule) at 1.0 ppm. Verify the correlations that have been drawn in Figure 5.31. Watch out for confusion between valine and serine.

5.11.2 TOCSY: VGSE

The 2D TOCSY spectrum for VGSE is given in Figure 5.32. Like lactose, VGSE is composed of several isolated spin systems of protons; in this case there are four moieties. As an example of "total correlation," the correlations among the glutamic acid protons are drawn in the figure. As with the COSY spectrum, the amide protons are expedient entry points to initiate the process. Can you find an appropriate entry point for the valine, which has no amide proton?

In some ways, the information from the COSY spectrum of VGSE is complementary to its TOCSY spectrum, and in other ways the information is redundant. Both spectra allow us to individually assign all of the proton signals of VGSE in different ways. In this case, which spectrum furnishes the information more easily or more clearly?

5.11.3 HMQC: VGSE

Compared to caryophyllene oxide and lactose, the HMQC spectrum for the tetrapeptide appears relatively simple (Figure 5.33). Indeed, VGSE has only 10 carbon atoms with attached protons and the spectrum shows correlations to nine carbons. Actually, there are 10 correlations as can be seen in the inset of the shielded methyl portion of the spectrum. Let us summarize the complementary information up to and including the HMQC spectrum.

Let us start our analysis with the carbon resonance at 43 ppm in the HMQC spectrum, which is a $—CH_2—$ group from the DEPT spectra, and note that it correlates with a diastereotopic methylene group centered at 4.04 ppm. From the DQF-COSY spectrum (see Figure 5.31), the multiplet at 4.04 ppm shows only one correlation to an amide proton at 8.75 ppm. Thus, the methylene group must belong to the glycine residue, and furthermore, the glycine residue cannot be the N-terminus, since the N-terminal amino acid must have a free amino group.

The serine residue can be accounted for by starting with the carbon resonance at 62 ppm. DEPT indicates another methylene group, and the HMQC spectrum shows that it correlates with coincident protons resonating at 3.85 ppm. These protons overlap with another proton. Careful line drawing in the DQF-COSY spectrum (or more easily in the TOCSY spectrum) suggests correlation with a proton at 4.48 ppm. This proton shows a correlation to a carbon atom at 56 ppm in the HMQC spectrum. That proton also shows a correlation to an amide proton at 8.40 ppm in the COSY spectrum. Like glycine, the serine residue cannot be the N-terminus.

Since valine is the only amino acid in the tetrapeptide that has methyl groups, and since the DEPT spectra show two methyl groups at about 17 ppm and 18 ppm, we can safely start with those in the HMQC. Both methyl carbons fortuitously correlate with the same doublet at 1.01 ppm, even though they are obviously diastereotopic. (Note that the integration of this doublet in the proton spectrum [Figure 5.30] corresponds to six protons.) The methyl groups are coupled to a methine proton at 2.20 ppm (COSY). In turn, the HMQC reveals a correlation from the methine proton to a carbon resonance at 31.5 ppm. The isopropyl methine (2.20 ppm) shows a further correlation in the COSY to a methine in the

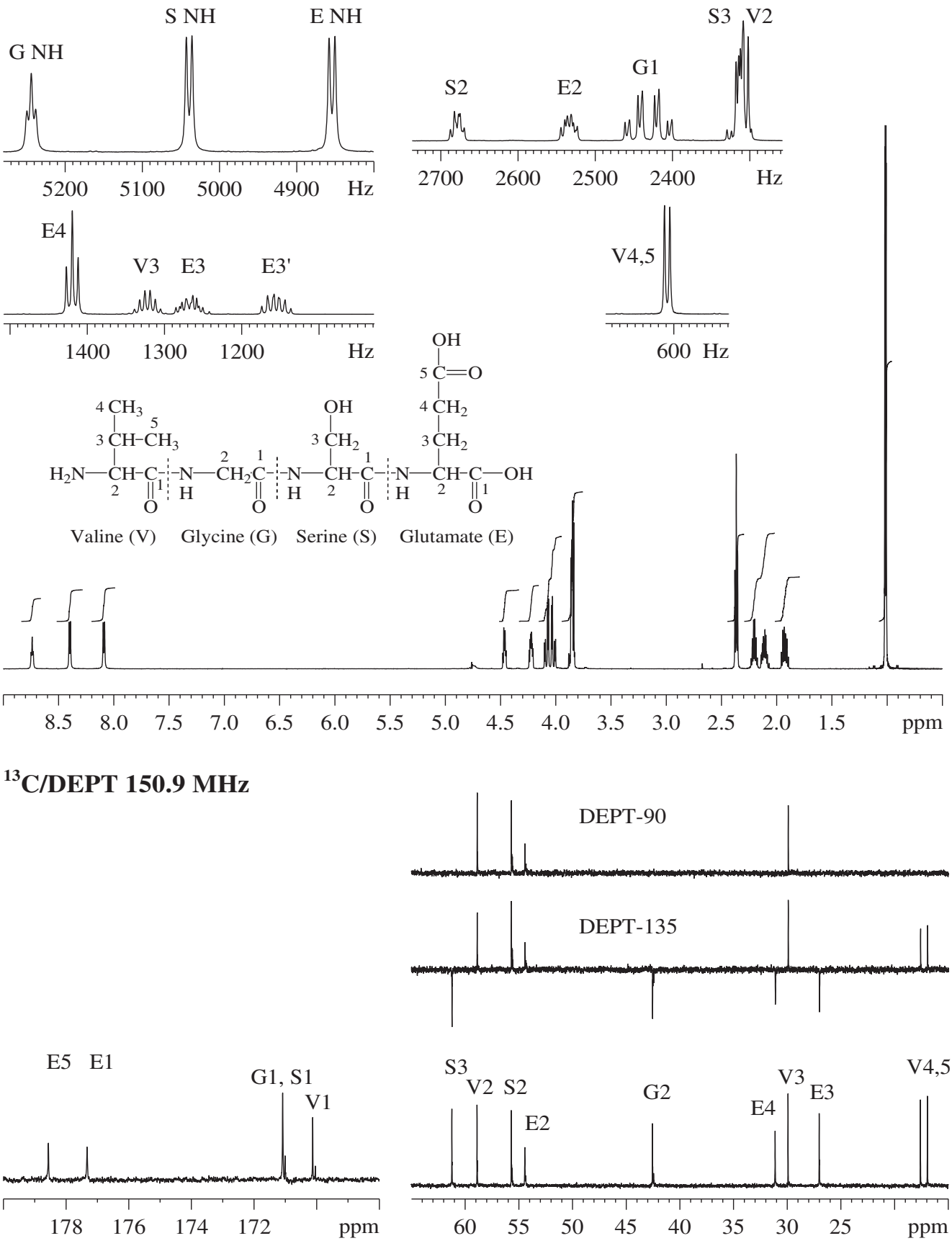

FIGURE 5.30 The ^{1}H, ^{13}C, and DEPT NMR spectra for the tetrapeptide, VGSE, in 95% H_2O and 5% D_2O.

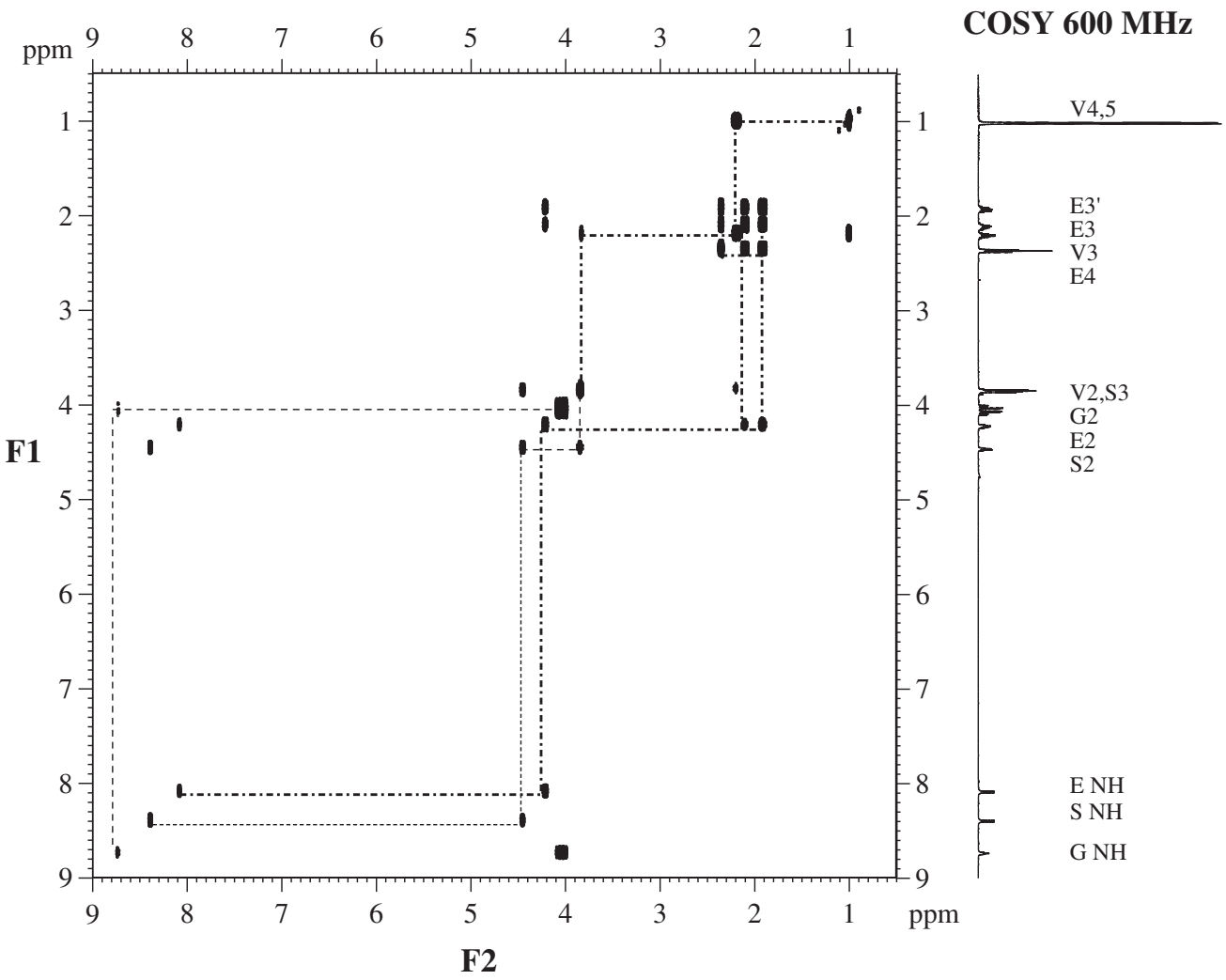

FIGURE 5.31 The DQF COSY spectrum of VGSE. Correlation lines are drawn in and some assignments are given as an aid.

overlapping multiplet at 3.85 ppm. This proton shows a correlation in the HMQC to the carbon at 59 ppm. Although it is difficult to see, this methine does not correlate any further (i.e., it does not couple with any of the amide protons), making valine the N-terminus.

Assignments for the final amino acid (glutamic acid) logically can begin with the unassigned carbon at 54 ppm. The HMQC spectrum provides us with its proton partner, a multiplet at 4.21 ppm. Correlations in the COSY spectrum are found for proton resonances at 1.93 ppm and 2.11 ppm. These two protons are readily seen as being diastereotopic because they correlate to the same carbon atom (27 ppm) in the HMQC spectrum. Both of the diastereotopic protons correlate (COSY) with a triplet at 2.37 ppm, which represents the protons of the second methylene group of glutamic acid. The carbon resonance for this methylene group is revealed in the HMQC spectrum at 31 ppm. It is worth noting from the COSY spectrum that the methine proton at 4.21 ppm is coupled to the amide proton at 8.10 ppm.

For VGSE, the HMQC spectrum is the perfect accompaniment to the DQF-COSY and TOCSY spectra for assigning all of the protons and nearly all of the carbons (except the carbonyls). This collection of spectra, however, does not allow us to assign or confirm the order of amino acids in the peptide, an immensely important task.

5.11.4 HMBC: VGSE

The HMBC spectrum of VGSE is given in Figure 5.34; to improve the resolution of the cross peaks, the spectrum has been split into four parts. In order to assign the carbonyl carbon resonances and to completely sequence the amino acids, we can start at either end of the molecule. We have previously stated that valine is the N-terminal amino acid because its α-amino group is not part of a peptide bond. A logical place to start within the valine residue is to assign its carbonyl. This assignment can be made to the peak at 170.1 ppm, as there are obvious correlations to the valine C-2 proton (V2) and the valine C-3 proton (V3). In addition, there are correlations to the glycine methylene group (G2) and to the glycine amide proton (G NH).

These two correlations (and generally, ones like them) are extremely important in the process of sequencing the amino acids. Until now, all of the correlations have been

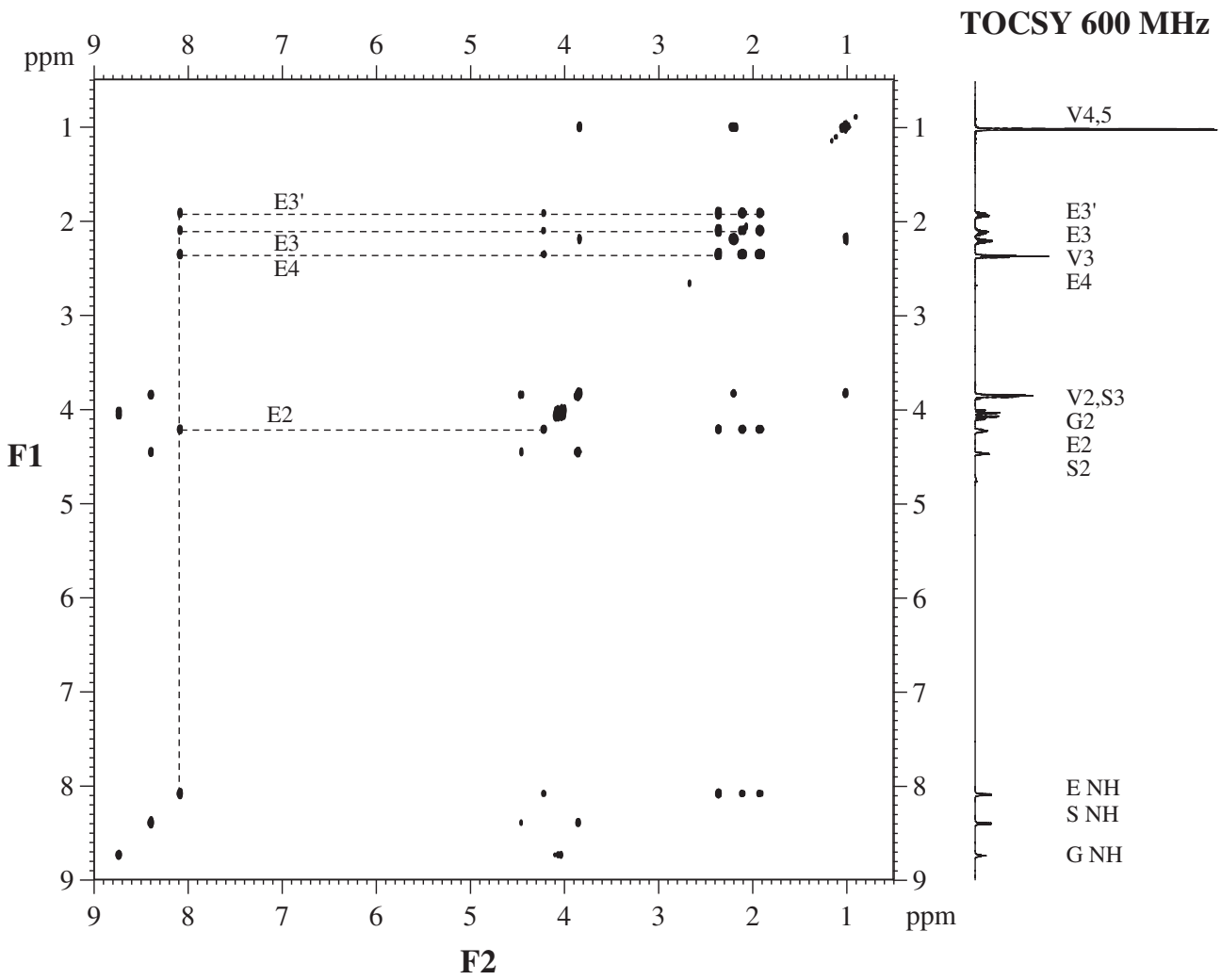

FIGURE 5.32 The 2D TOCSY spectrum of VGSE. Some correlation lines are drawn in and assignments are given as an aid.

intra-residue, but the HMBC experiment allows generally for inter-residue correlations. Develop a line of reasoning to sequence the remaining two amino acids (serine and glutamic acid). Note that the carbonyl carbons for glycine and serine overlap in the carbon spectrum.

5.11.5 ROESY: VGSE

We end our discussion of VGSE by comparing the ROESY correlations of the amide protons with the corresponding interactions in COSY and TOCSY. Figure 5.35 shows comparable sections of each spectrum. We have seen the COSY and TOCSY portions earlier and showed how these spectra, along with the HMQC spectrum, can be used for intra-residue assignments. The ROESY correlations, on the other hand, reinforce the HMBC information and help to confirm the sequence of amino acids with inter-residue correlations.

The boxed cross peaks illustrate the through space interaction of the amide proton of one amino acid with the adjacent amino acid's C-2 proton. Thus, the amide proton of glycine (G NH) correlates with the C-2 proton of valine (V2), the amide proton of serine (S NH) correlates with the C-2 protons of glycine (G2), the amide proton of glutamic acid (E NH) correlates with the C-2 proton (and C-3 protons as well) of serine (S2 and S3). The manner in which the data are presented in Figure 5.35 greatly simplifies our interpretation and makes comparisons more meaningful.

5.12 PULSED FIELD GRADIENT NMR

A well-established area in the field of NMR is the use of pulsed field gradients, or **PFG** NMR. It is ironic to consider that so much effort has been expended over so many years to provide a homogeneous or stable magnetic field. Today, most modern high field NMR spectrometers are routinely equipped with hardware (coils) that rapidly ramps the magnetic field along one of three mutually orthogonal axes. These magnetic field gradients are incorporated into the pulse sequence in a large range of applications.

We include a brief discussion of gradients here because there are many applications to correlation experiments. We treat gradients in a general manner; for a more technical

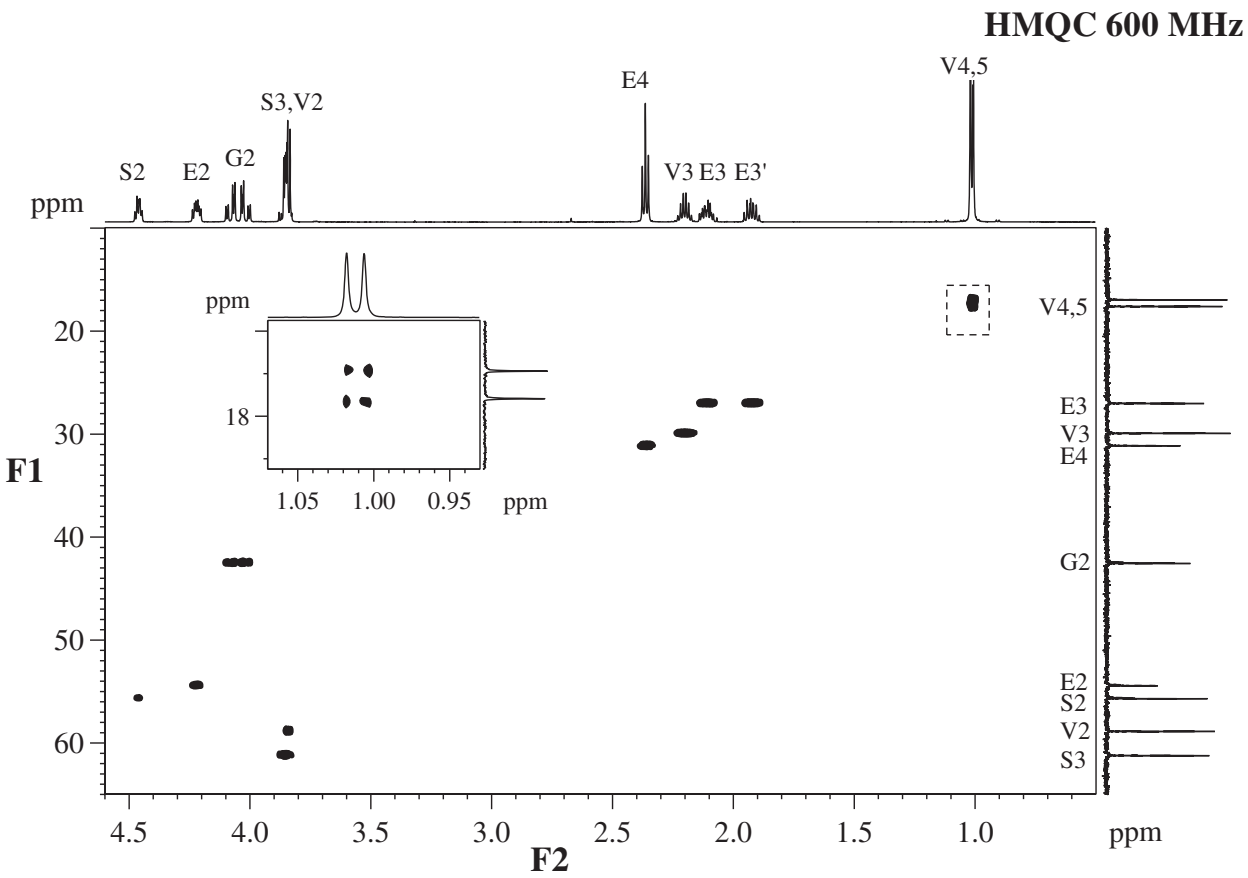

FIGURE 5.33 The HMQC spectrum for VGSE. Assignments are given as an aid.

treatment and for a myriad of other applications, consult the review by Price (1996).

In Section 5.3.1, we mention phase cycling as an important part of any pulse sequence. The details of phase cycling are still beyond our treatment (see Claridge, 1999), but we can easily appreciate one of their negative aspects: time. In correlation experiments, anywhere from 4 to 64 phase cycles must be summed in order to produce one usable FID. If signal-to-noise is poor, then the identical cycle is repeated until sufficient signal is acquired. Particularly if signal-to-noise is not an issue, these phase cycles can be wasteful of spectrometer time and account for at least one reason why 2D experiments take so long.

In a PFG experiment, the pulse sequence can be rewritten so that phase cycling can be greatly reduced or eliminated altogether. Thus, if signal-to-noise is sufficient, each run through the pulse sequence can generate one FID in a 2D experiment. The saving in instrument time is enormous; experiments that previously took several hours to an entire day can now be run in a matter of minutes. One reassuring point for us to realize is that, even though the experiment is run differently, the results, and hence, the interpretation remain the same. One should be aware that the use of gradients typically reduces the S/N compared to using phase cycles. Therefore, for dilute samples where extensive signal averaging is needed anyways, it may be advantageous to avoid gradients.

Dynamic nuclear polarization (DNP), mentioned in Chapter 3, is an alternative emerging method which can also provide even more substantial time savings for multidimensional NMR experiments.

While our initial interest in gradient NMR stems from the fact that familiar experiments can be run more quickly and more efficiently, the most exciting uses of gradients are the novel experiments that cannot be run without them. We find that gradients allow for improved magnetic resonance imaging (MRI), improved magnetic resonance microscopy, better solvent suppression (especially water), and entirely new areas of inquiry such as diffusion measurements.

Gradients are also used in a new class of so-called ultrafast multidimensional NMR experiments. A detailed discussion of these is beyond the scope of this text. However, the reader should be aware that these methods can speed up multidimensional NMR experiments by orders of magnitude. Alternatives to the standard method of systematically incrementing t_1 and carrying out two sets of Fourier transforms also offer new opportunities in multidimensional NMR. Even single-scan multidimensional NMR is now possible (see Tal and Frydman, 2010 and Freeman, 2011); one can envisage real-time two-dimensional NMR monitoring of chemical reactions and dynamic processes. These methods are particularly beneficial when one is not sample limited. If the concentration of the sample is too low, signal averaging will still be required to get spectra with good signal-to-noise ratios.

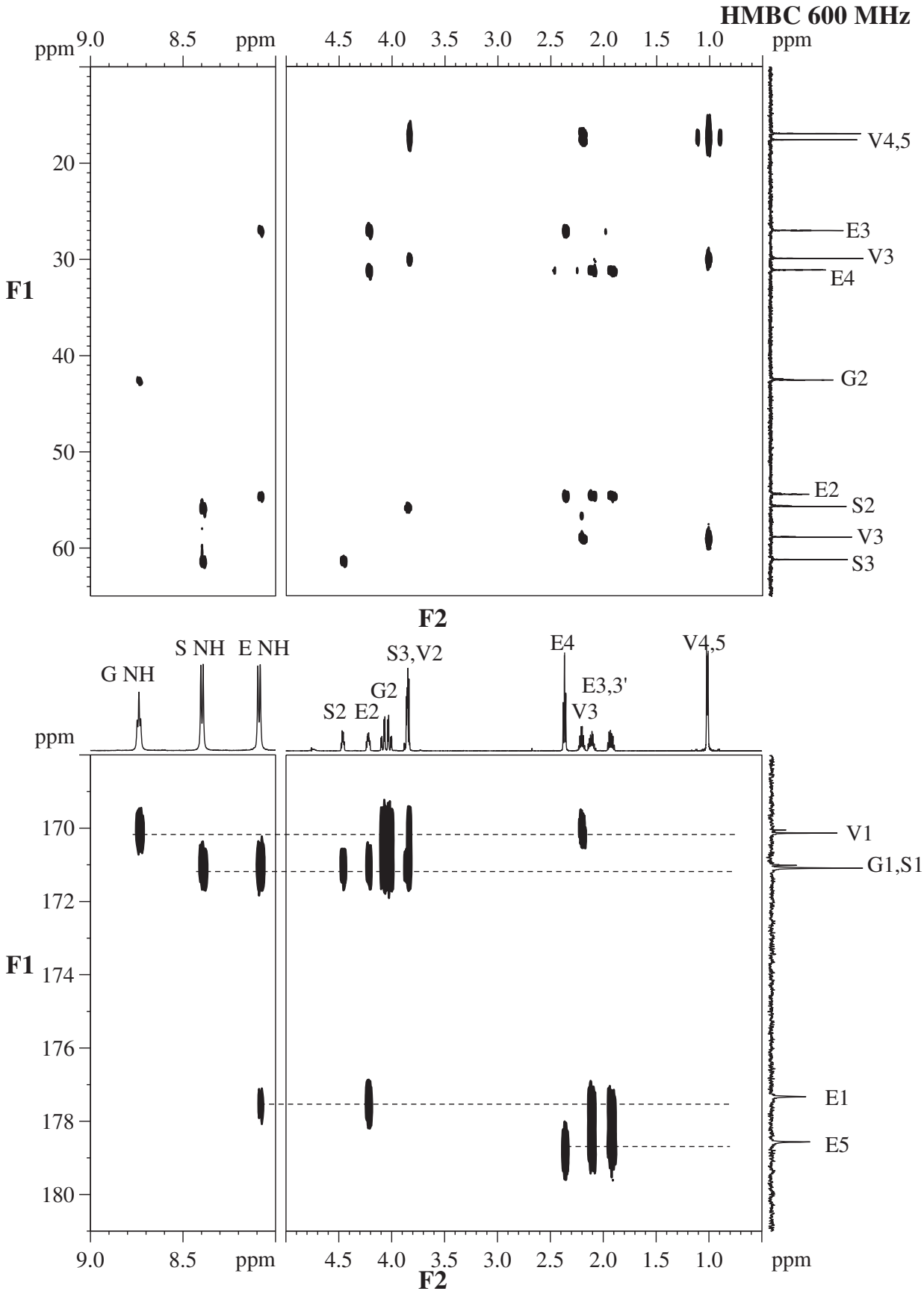

FIGURE 5.34 The HMBC spectrum for VGSE. Important correlation lines are drawn in and assignments are given as an aid.

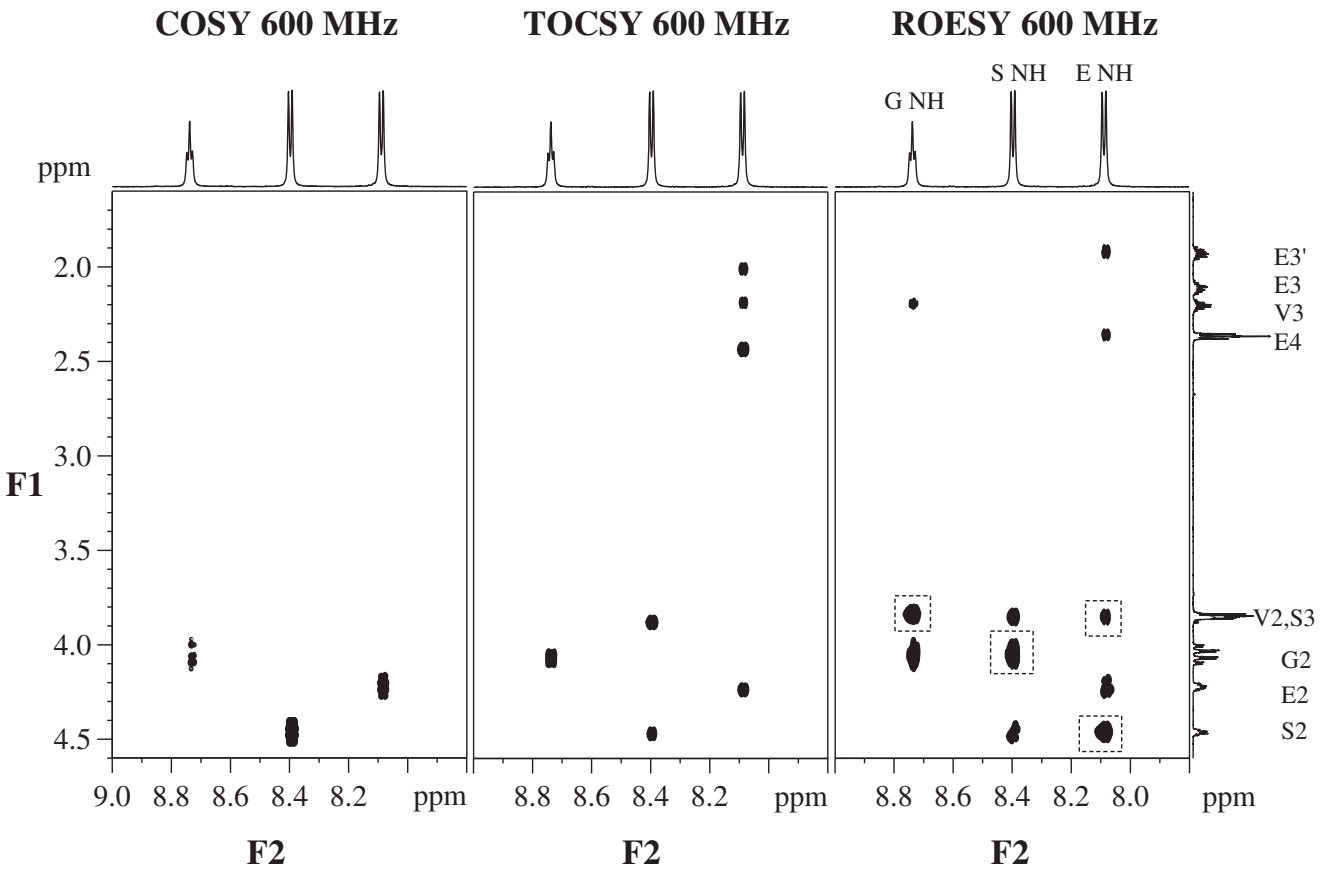

FIGURE 5.35 A comparison of the DQF COSY, 2-D TOCSY, and ROESY spectra showing the interactions of the amide protons.

REFERENCES

For a list of Chapter References, please visit: www.wiley.com/college/silverstein.

STUDENT EXERCISES

5.1 For the compounds of Problem 3.3 a-o, draw the following spectra: COSY, HMQC, HMBC, and INADEQUATE. Be sure to label the F1 and F2 axes. Assume experimental conditions are the same as in Problem 3.3.

5.2 Assign all of the correlations for ipsenol in the DQF COSY spectrum found in Figure 5.9. Indicate each type of coupling as geminal, vicinal, or long range.

5.3 Complete the assignments for ipsenol for the HMBC spectrum found in Figure 5.14. To aid in bookkeeping, you may want to construct a table similar to Table 5.1.

5.4 Identify the compound $C_6H_{10}O$ from its ^1H, ^{13}C/DEPT, COSY, and HMQC spectra and show all correlations.

5.5 Identify the compound $C_{10}H_{10}O$ from its ^1H, ^{13}C/DEPT, COSY, and HMQC spectra and show all correlations.

5.6 Identify the compound $C_8H_9NO_2$ from its ^1H, ^{13}C/DEPT, COSY, HMQC, and INADEQUATE spectra and show all correlations.

5.7 Assign all of the carbon connectivities for caryophyllene oxide using the INADEQUATE spectrum found in Figure 5.19.

5.8 Identify compound $C_{10}H_{18}O$ from its ^1H, ^{13}C/DEPT, HMQC, HMBC, and INADEQUATE spectra.

5.9 Make as many correlations as possible for lactose using the 2D TOCSY spectrum found in Figure 5.25. Compare your results for the glucose residue to the results that were found in the 1D HOHAHA in Figure 5.26.

5.10 Given are the structure and ^1H, ^{13}C/DEPT, COSY, 1D TOCSY, 2D TOCSY, HMQC, HMQC–TOCSY, HMBC, and ROESY spectra for raffinose. Confirm the structure, assign all protons and carbons, and show as many correlations as possible.

5.11 Given are the structure and ^1H, ^{13}C/DEPT, COSY, HMQC, and HMBC spectra for stigmasterol. Confirm the structure, assign all protons and carbons, and show as many correlations as possible.

5.12 The ^1H, ^{13}C/DEPT, COSY, 2D TOCSY, HMQC, HMBC, and ROESY spectra for a tri-peptide containing the amino acids lysine, serine, and threonine. Sequence the peptide and assign all protons and carbons. Show as many correlations as possible.

In all exercises, the ^{13}C NMR spectra shown are, from top to bottom, the DEPT-90, DEPT-135, and full proton-decoupled ^{13}C NMR spectra.

^{1}H NMR 600 MHz

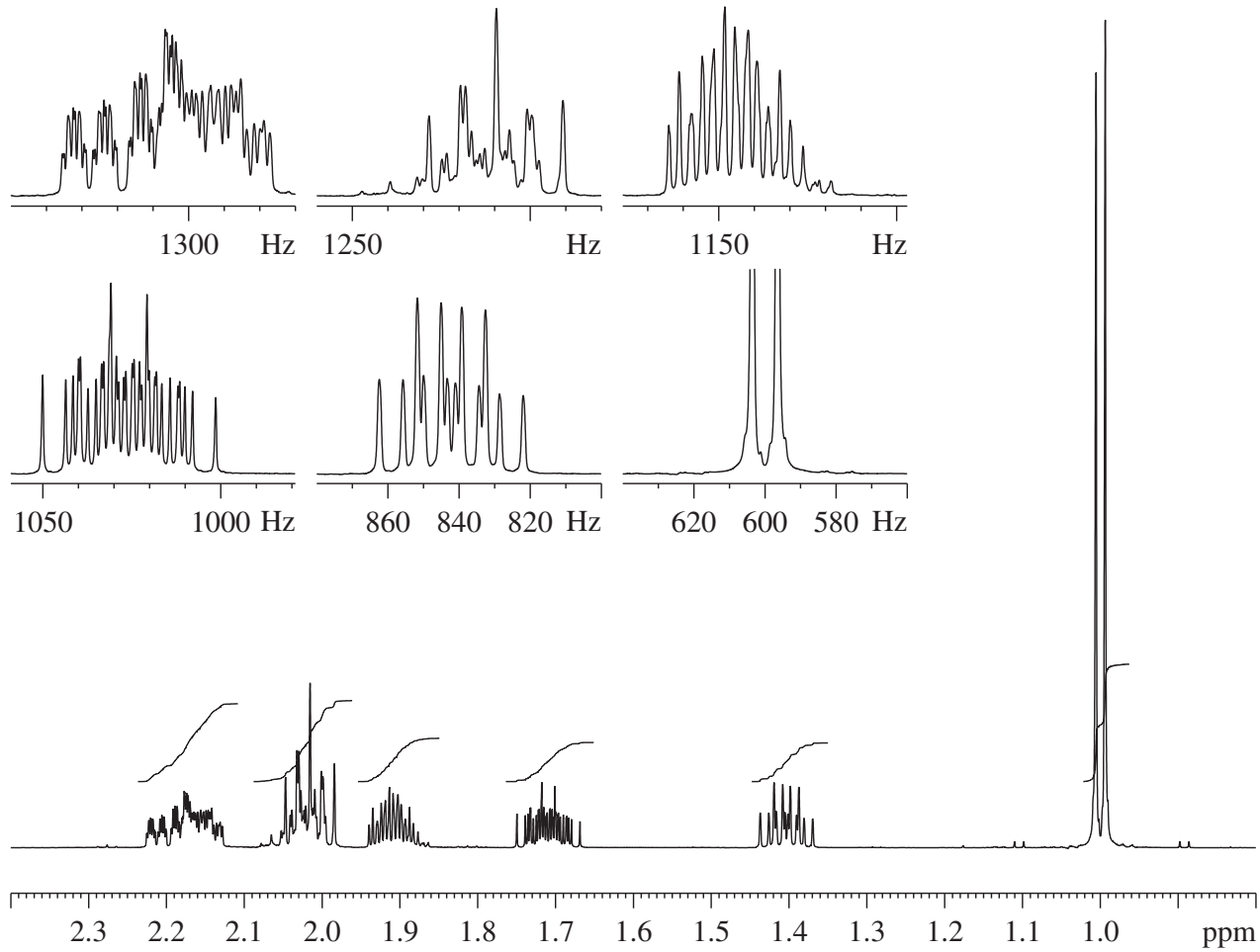

^{13}C/DEPT 150.9 MHz

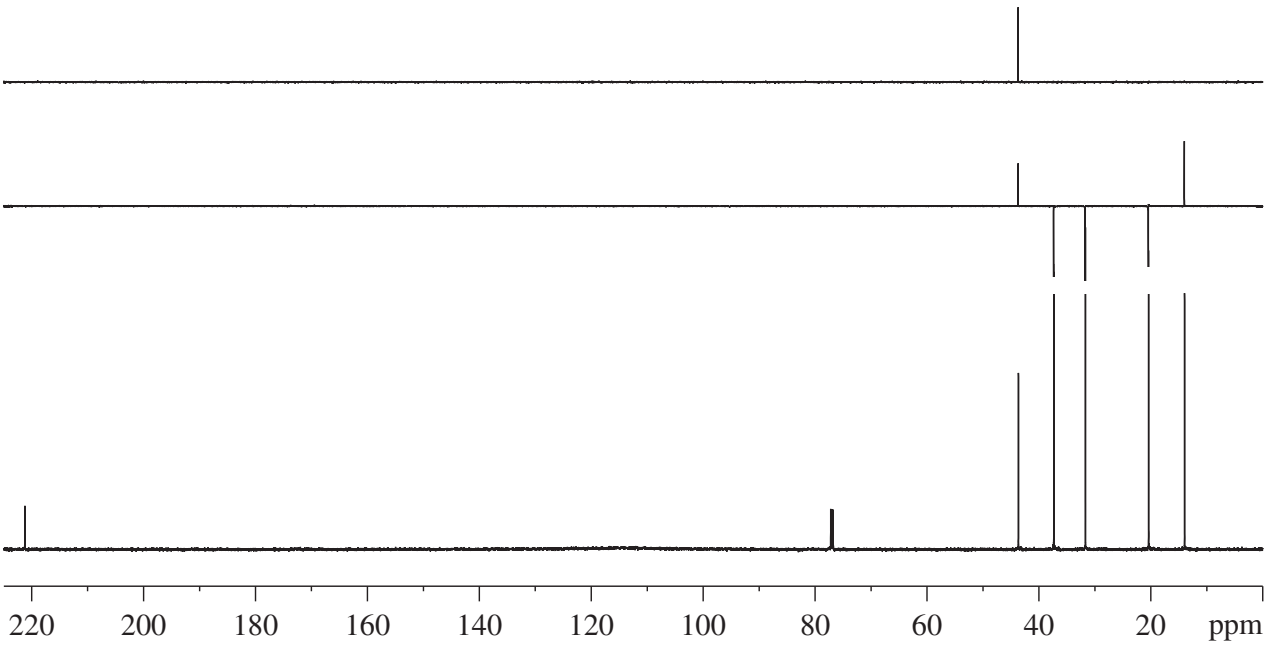

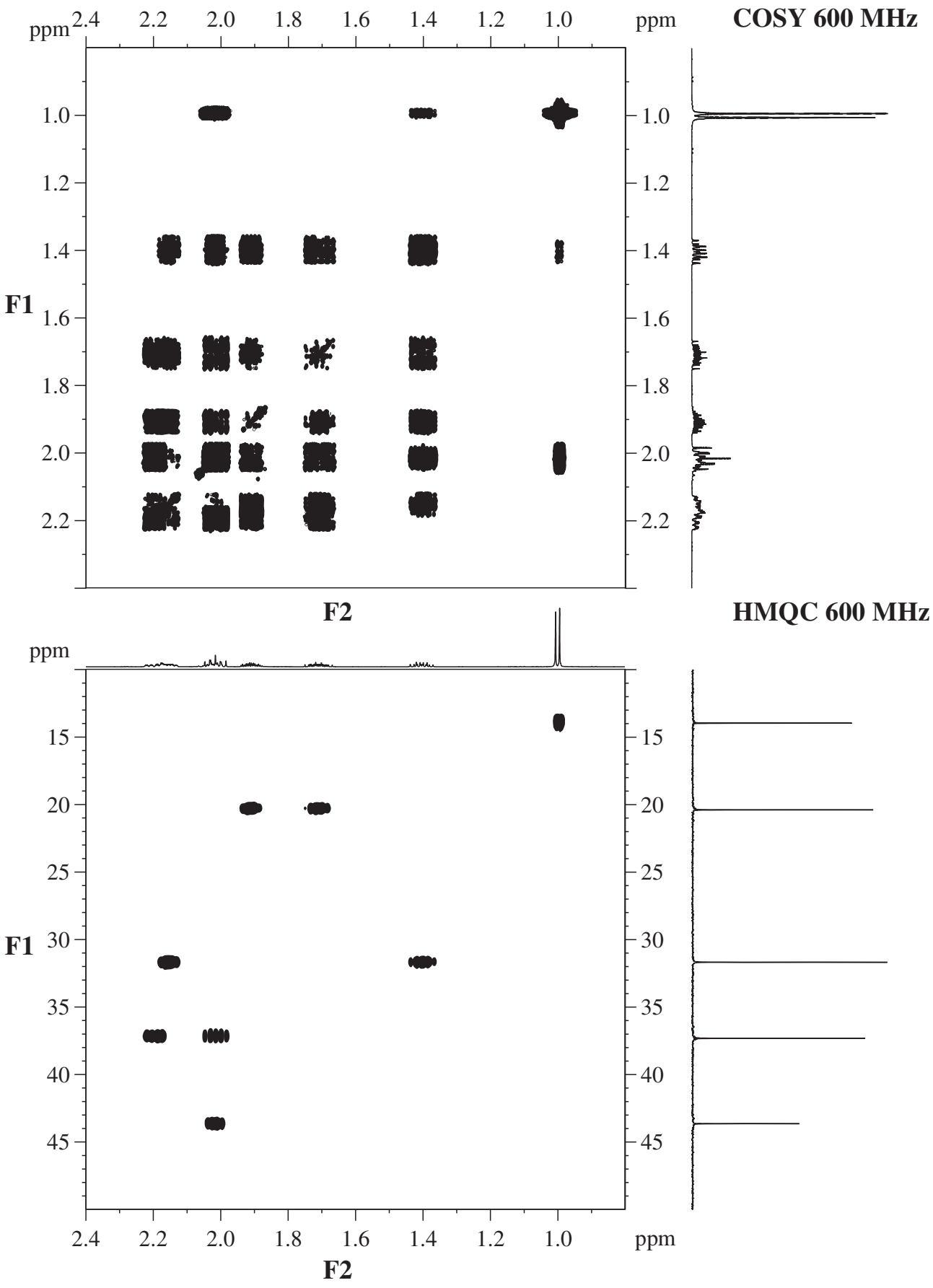
COSY 600 MHz
ppm
2.4
2.2
2.0
1.8
1.6
1.4
1.2
1.0
F1
F2
HMQC 600 MHz
15
20
25
30
35
40
45

^{1}H NMR 600 MHz

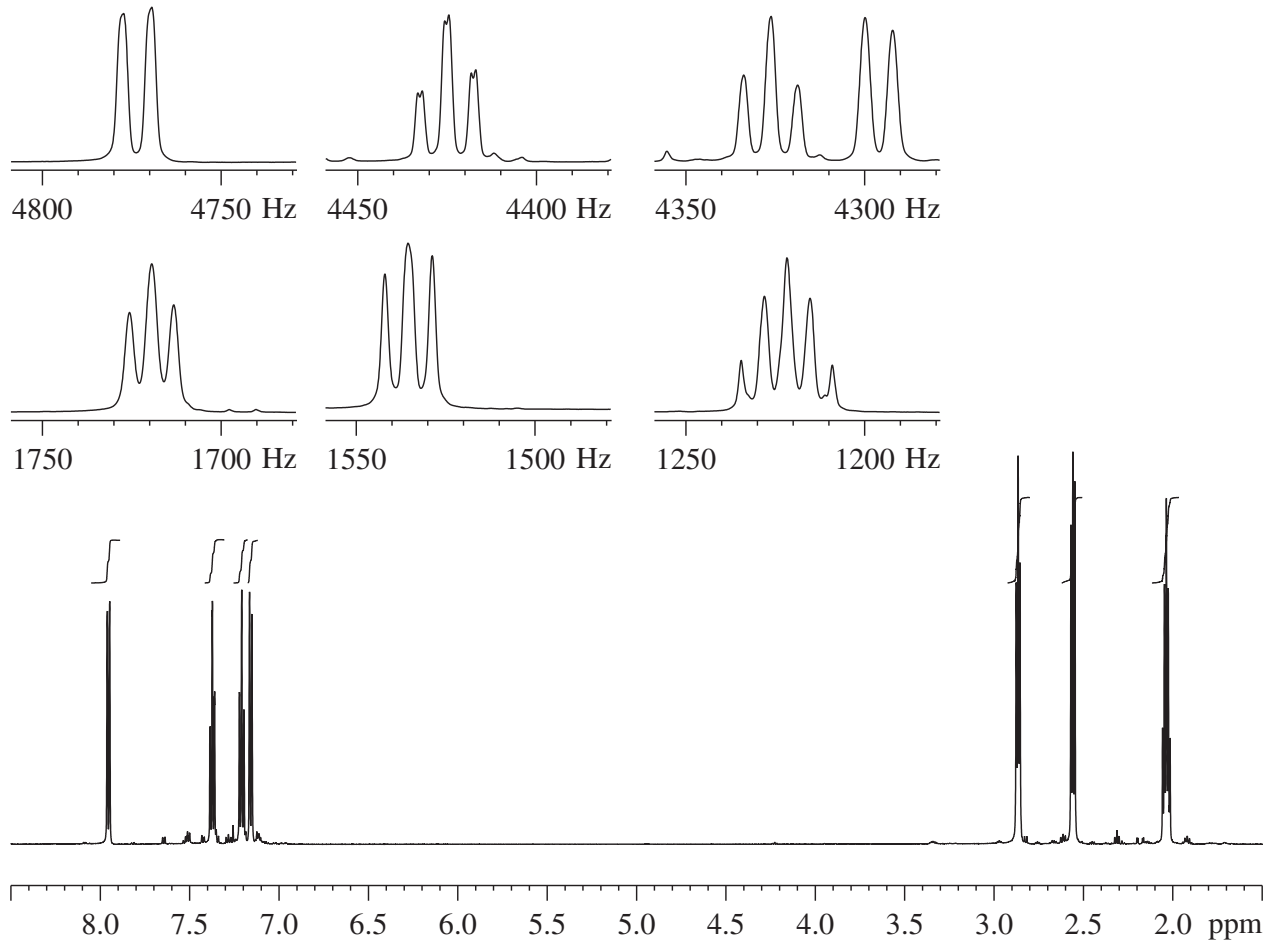

^{13}C/DEPT 150.9 MHz

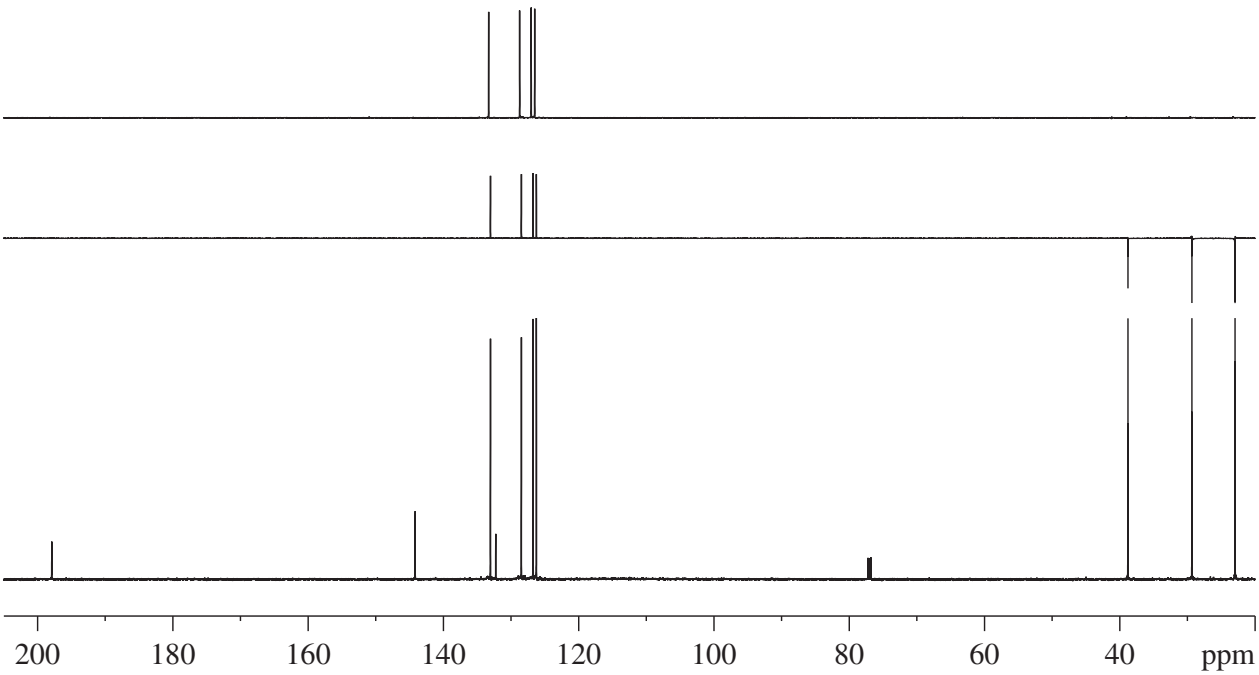

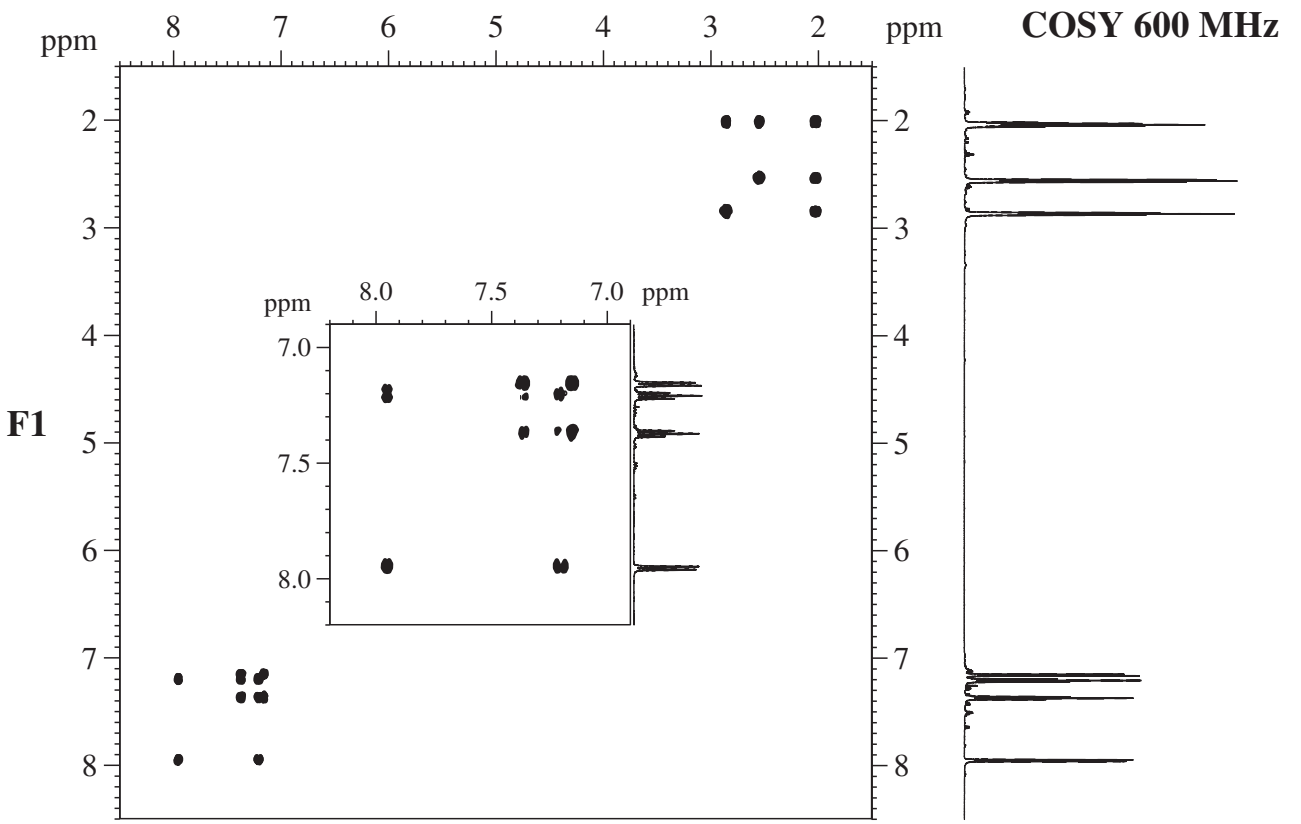
COSY 600 MHz
ppm
8 7 6 5 4 3 2 ppm
2 3 4 5 6 7 8
F1
F2
ppm
8.0 7.5 7.0 ppm
7.0 7.5 8.0

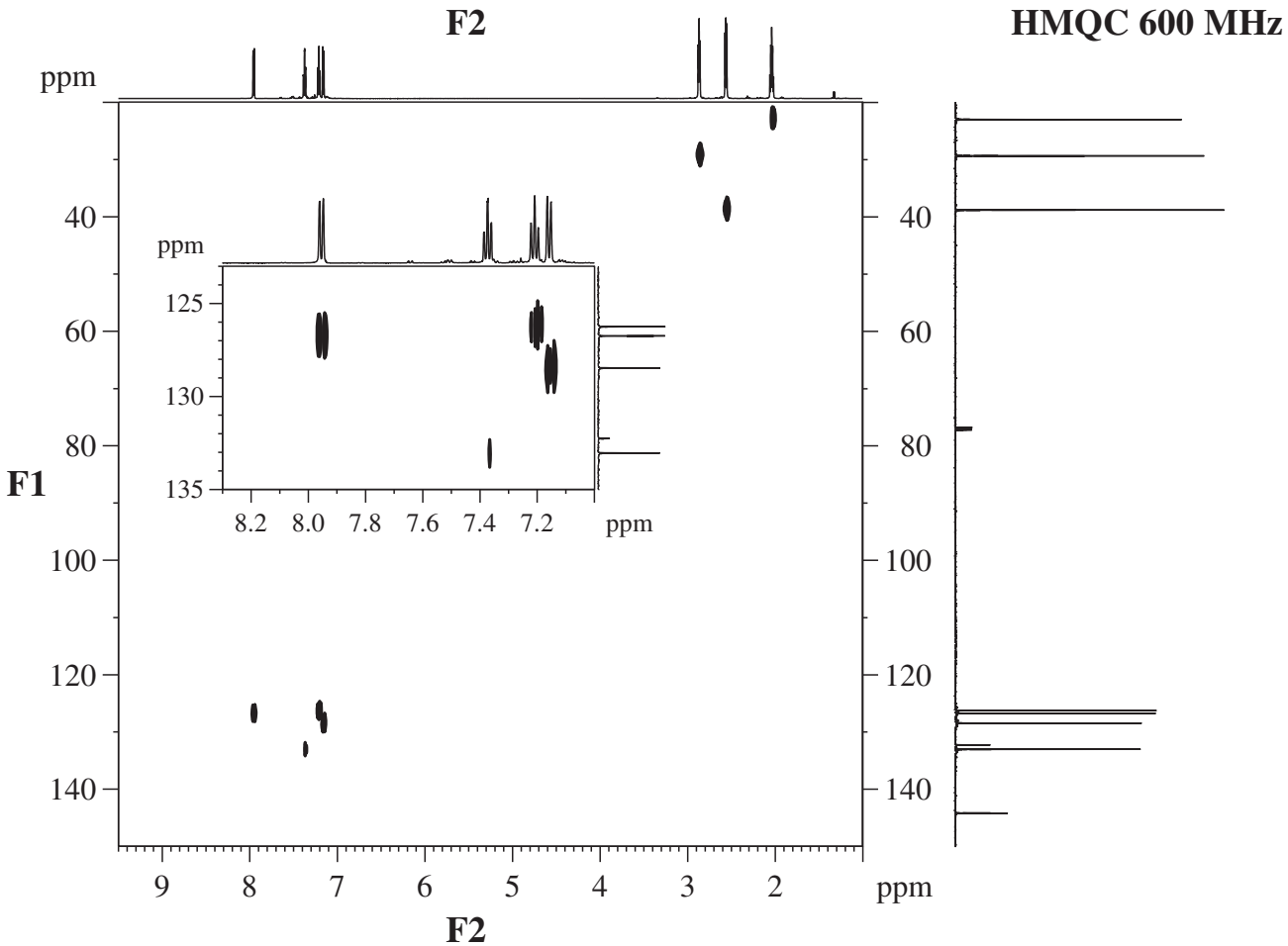
HMQC 600 MHz
ppm
40 60 80 100 120 140
F1
F2
9 8 7 6 5 4 3 2 ppm
ppm
125 130 135
8.2 8.0 7.8 7.6 7.4 7.2 ppm

^{1}H NMR 600 MHz

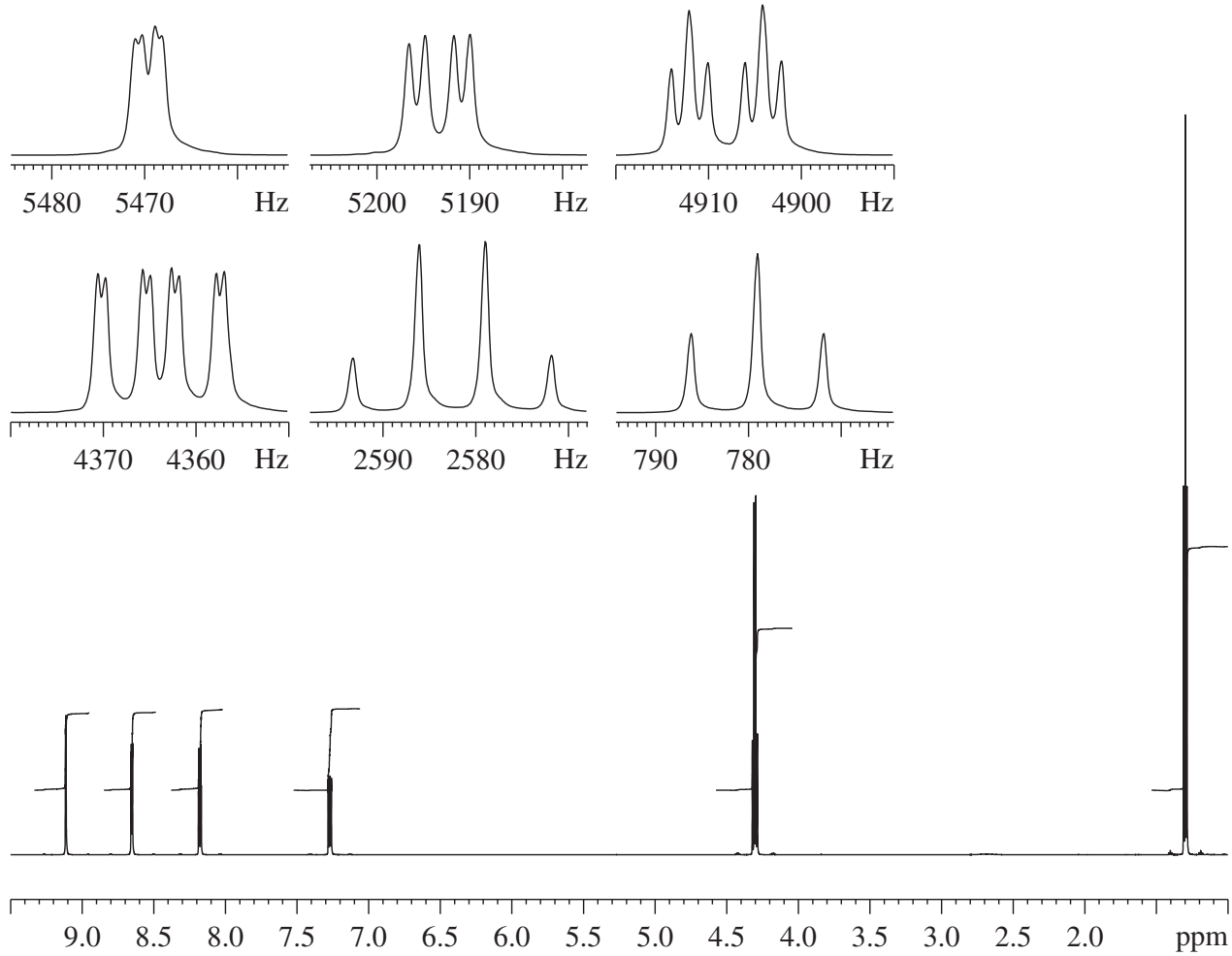

^{13}C/DEPT 150.9 MHz

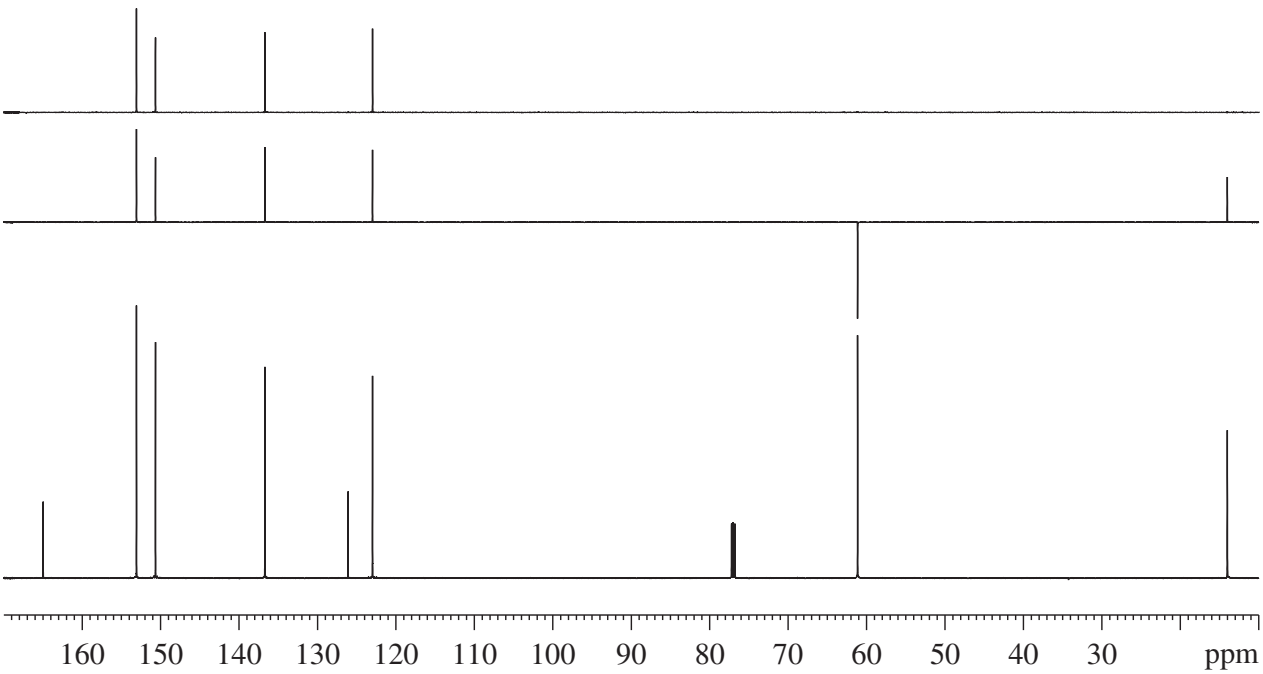

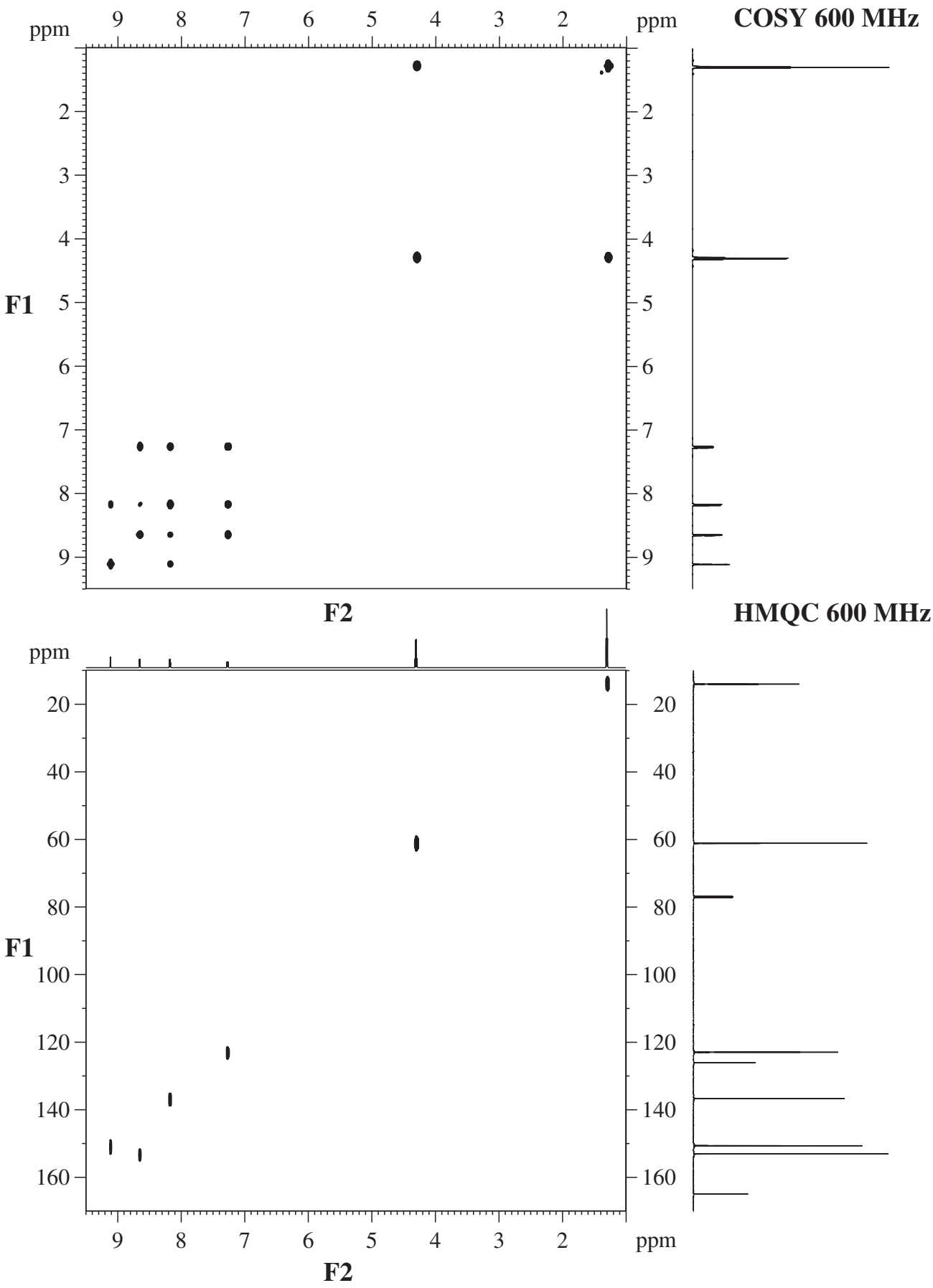
COSY 600 MHz
ppm
9 8 7 6 5 4 3 2
F1
F2
HMQC 600 MHz
20 40 60 80 100 120 140 160

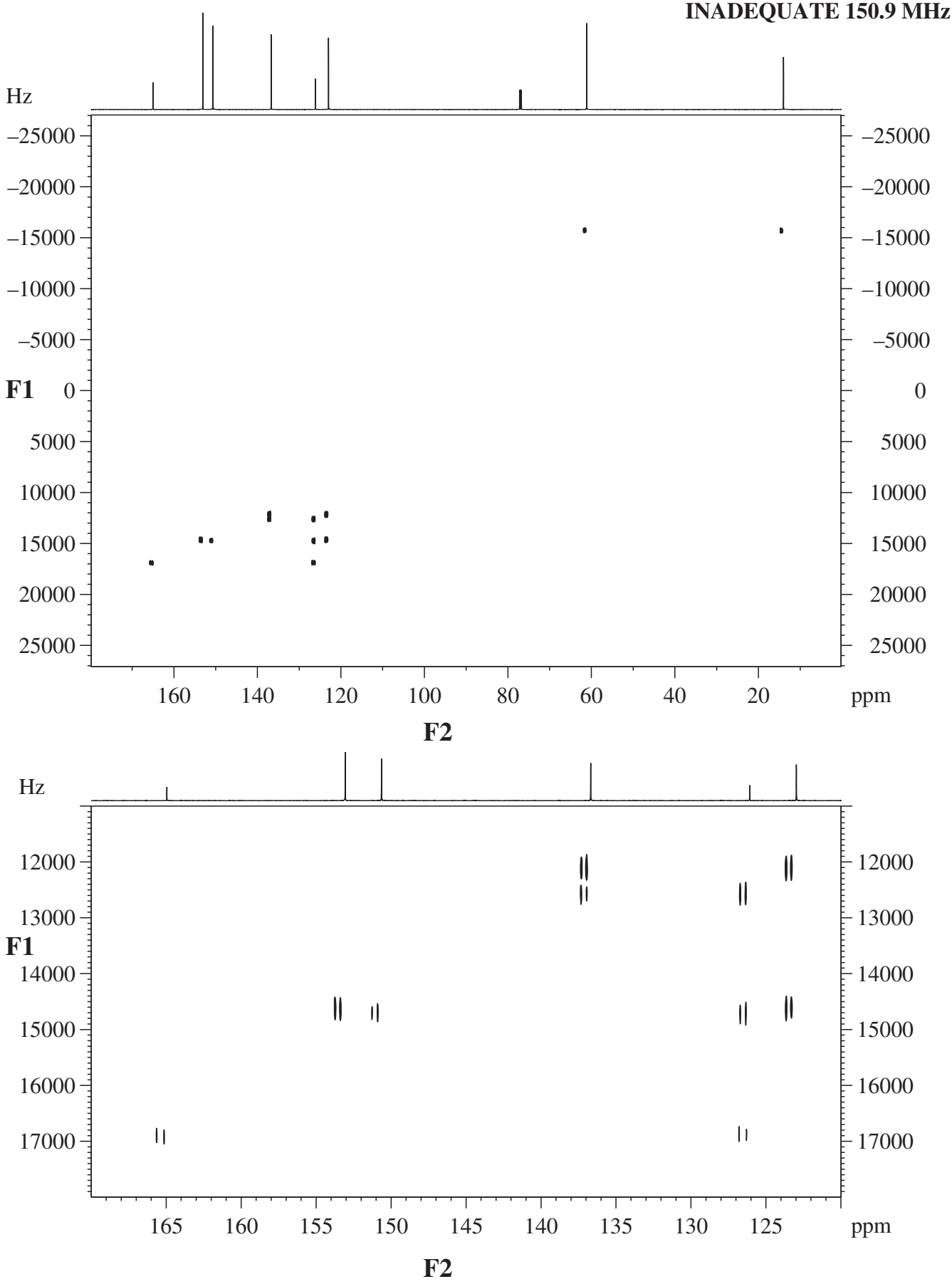
INADEQUATE 150.9 MHz
Hz
–25000
–20000
–15000
–10000
–5000
F1
0
5000
10000
15000
20000
25000
160
140
120
100
80
60
40
20
ppm
F2
Hz
12000
13000
F1
14000
15000
16000
17000
165
160
155
150
145
140
135
130
125
ppm
F2

^{1}H NMR 600 MHz

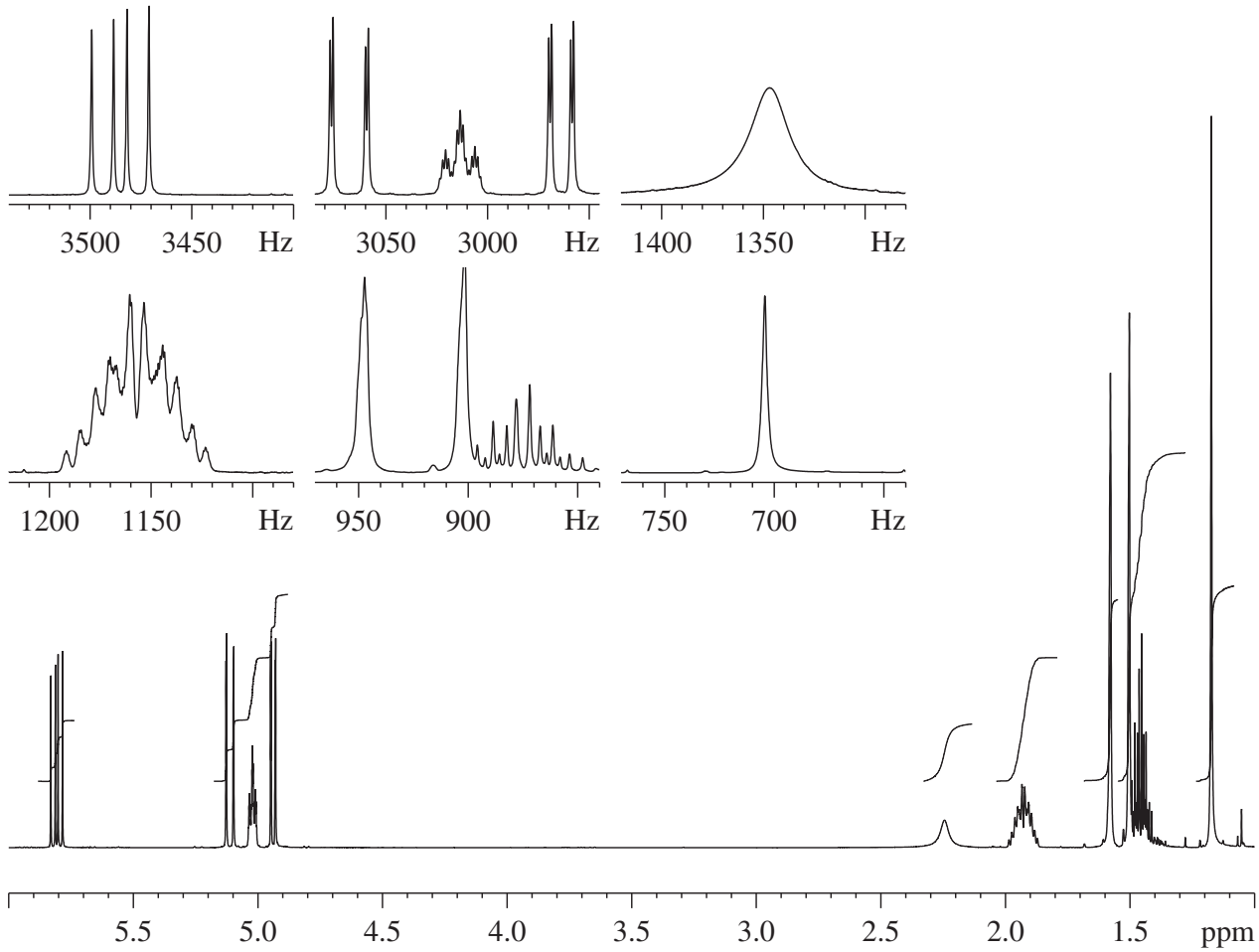

^{13}C/DEPT 150.9 MHz

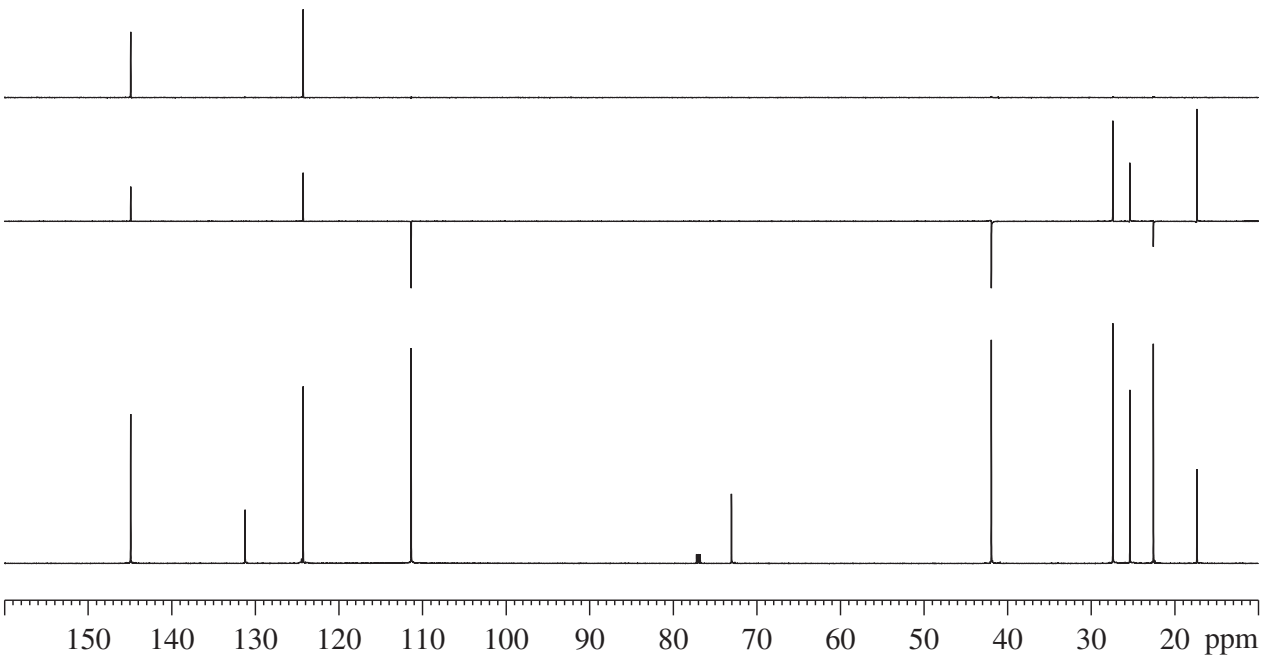

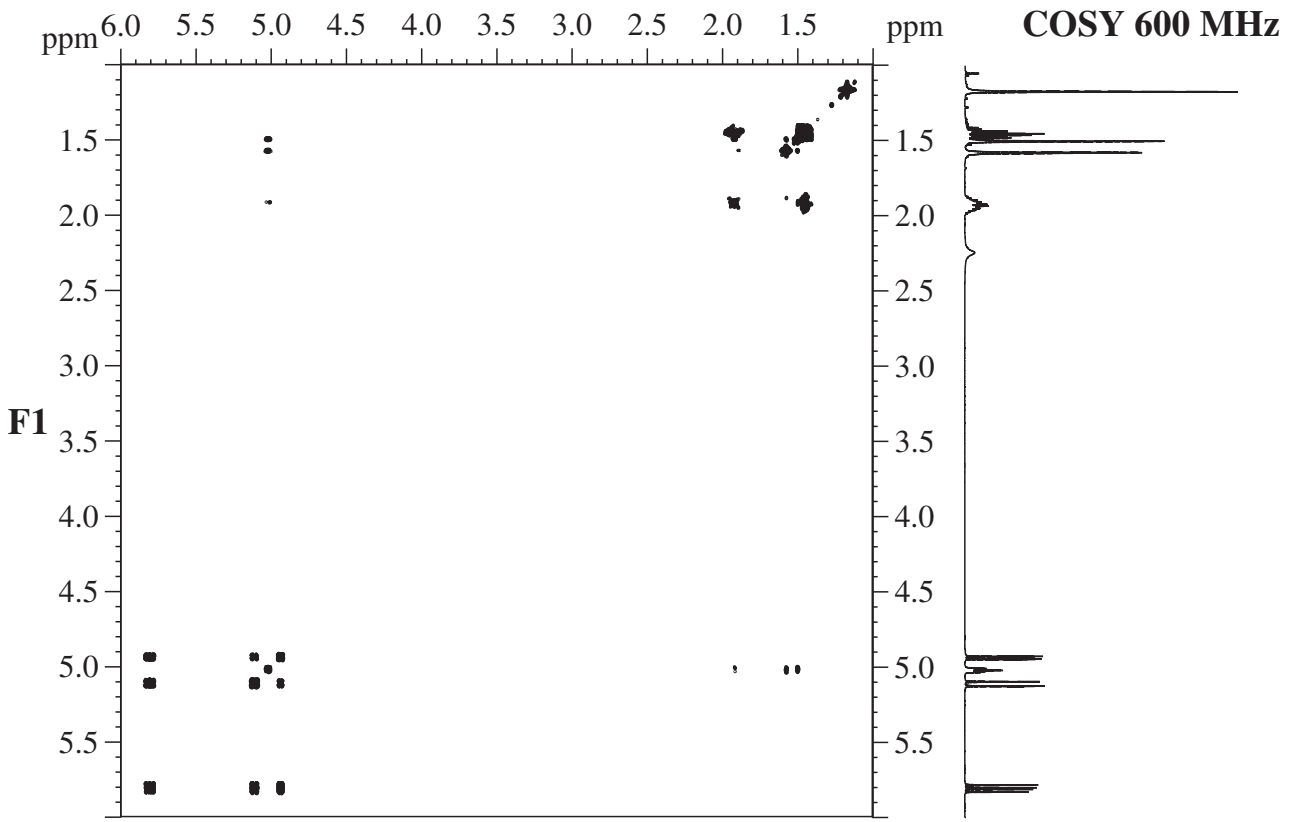
COSY 600 MHz
ppm
6.0 5.5 5.0 4.5 4.0 3.5 3.0 2.5 2.0 1.5
ppm
F1
F2

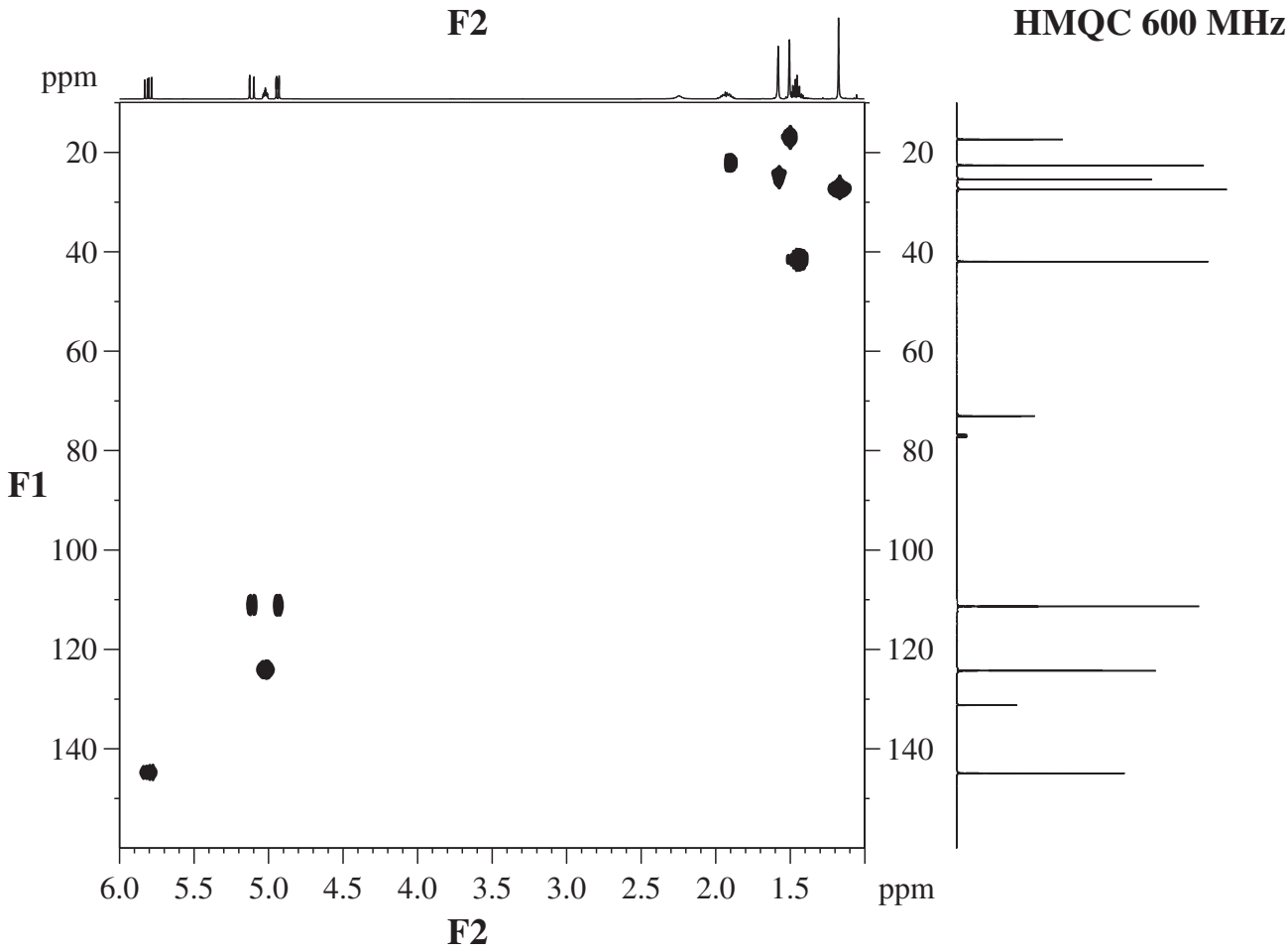
HMQC 600 MHz
ppm
20 40 60 80 100 120 140
F1
6.0 5.5 5.0 4.5 4.0 3.5 3.0 2.5 2.0 1.5
ppm
F2

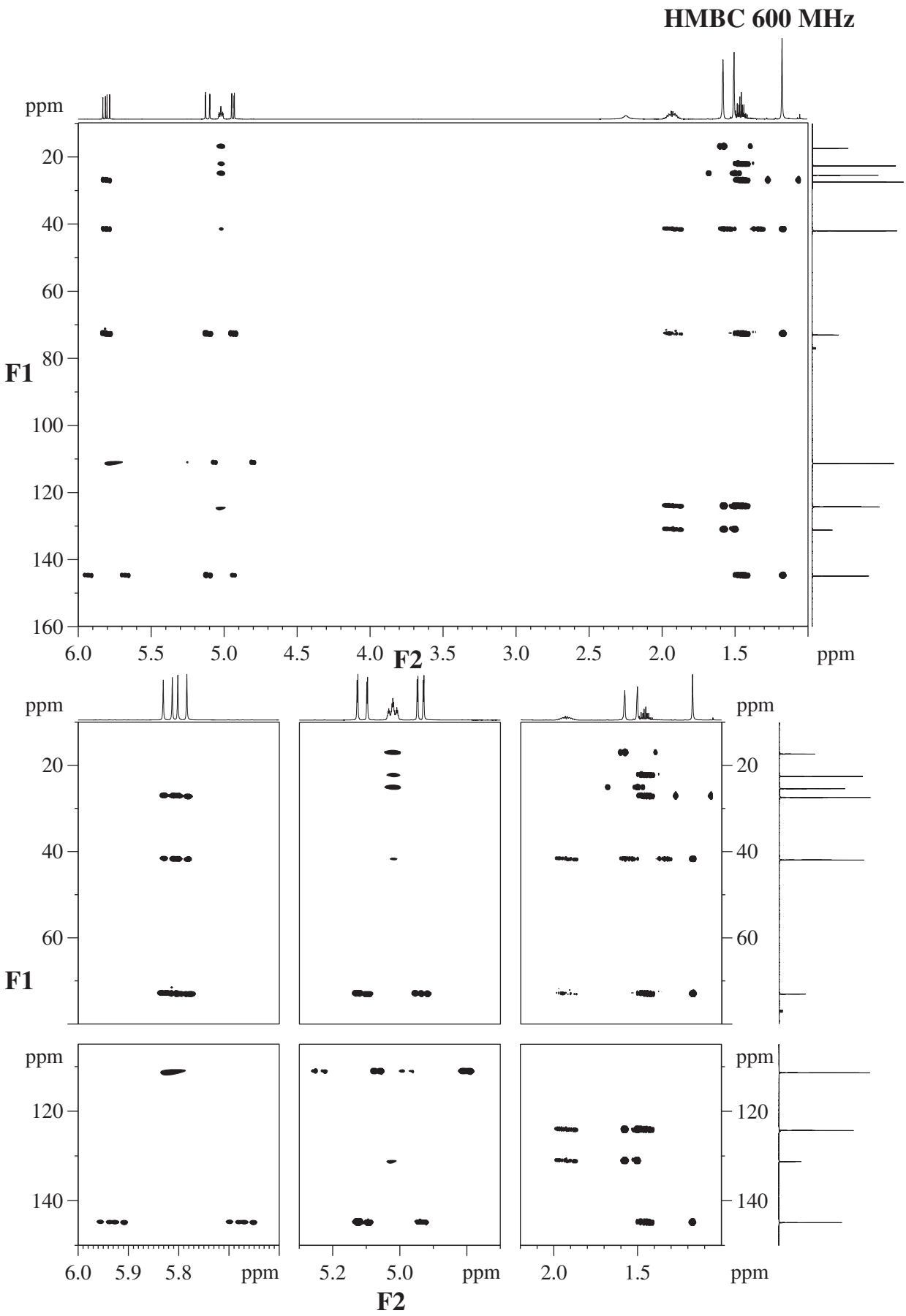
HMBC 600 MHz
ppm
20
40
60
80
100
120
140
160
F1
6.0
5.5
5.0
4.5
4.0
3.5
3.0
2.5
2.0
1.5
ppm
F2
ppm
20
40
60
F1
ppm
20
40
60
ppm
120
140
120
140
6.0
5.9
5.8
ppm
5.2
5.0
ppm
2.0
1.5
ppm
F2

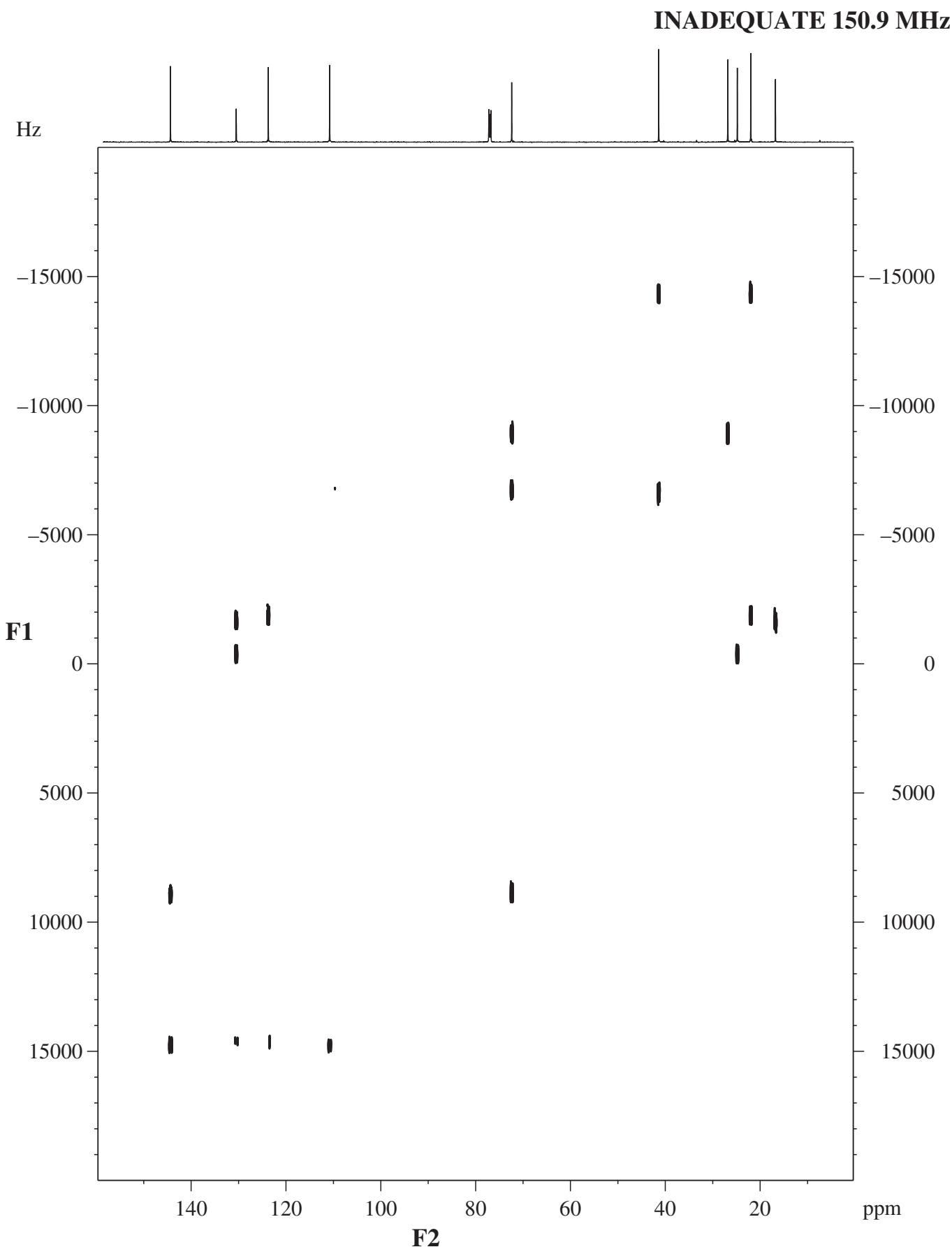
INADEQUATE 150.9 MHz
Hz
–15000
–10000
–5000
0
5000
10000
15000
F1
140
120
100
80
60
40
20
ppm
F2

^{1}H NMR 600 MHz

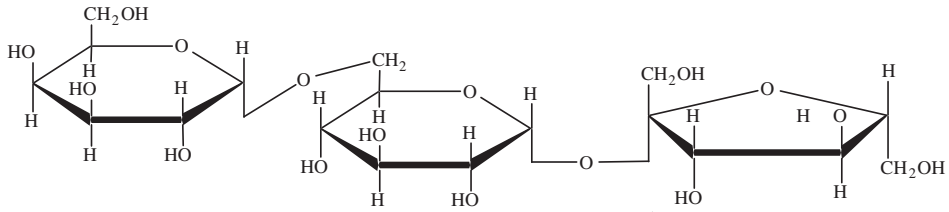

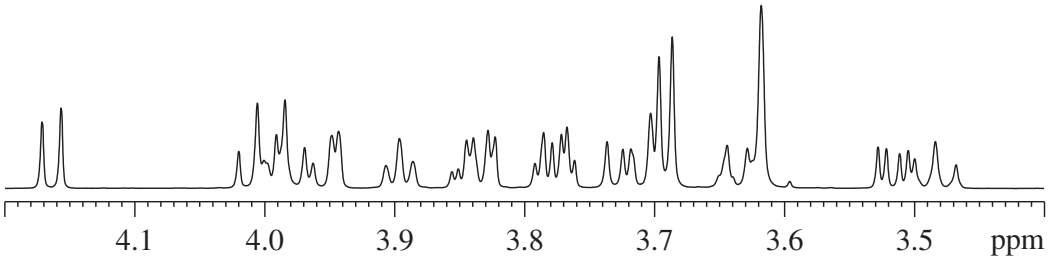

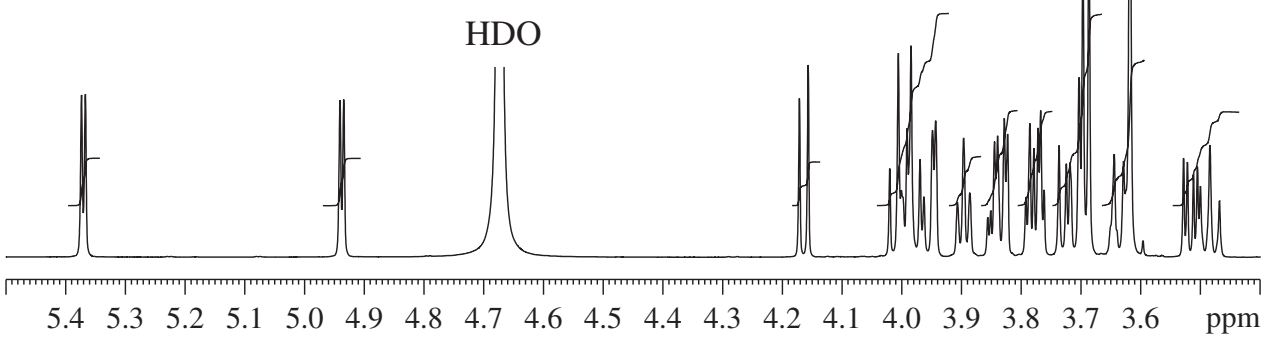

^{13}C/DEPT 150.9 MHz

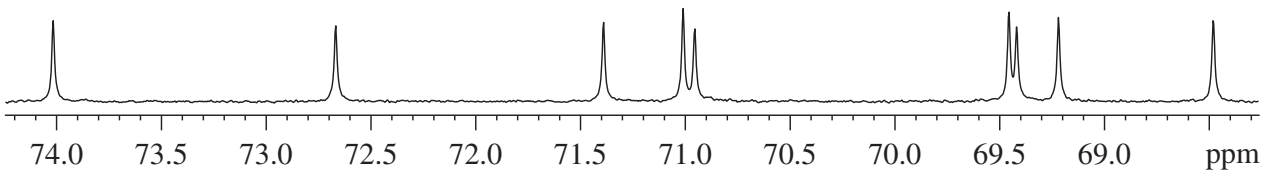

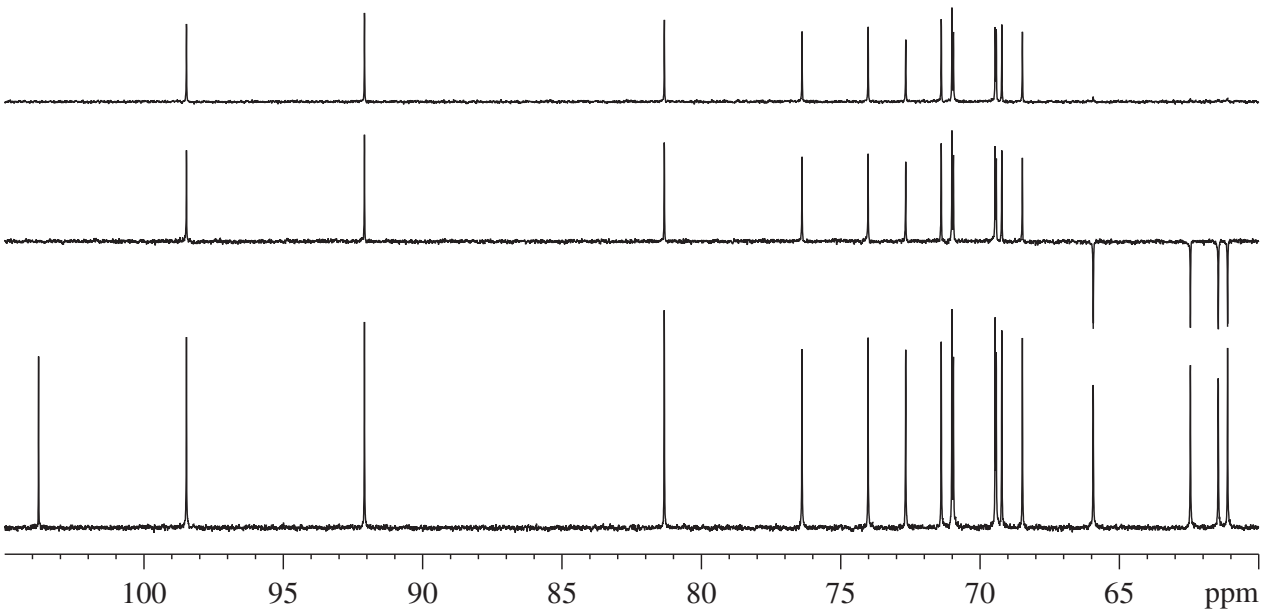

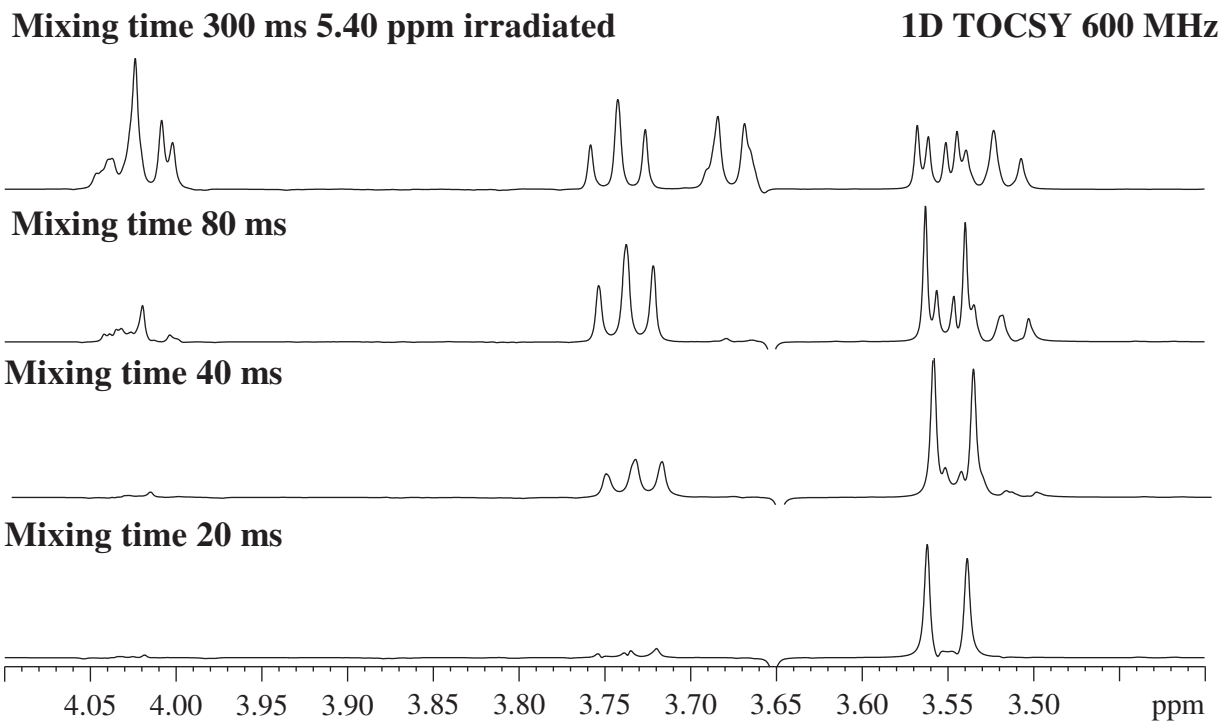
Mixing time 300 ms 5.40 ppm irradiated
1D TOCSY 600 MHz
Mixing time 80 ms
Mixing time 40 ms
Mixing time 20 ms
4.05 4.00 3.95 3.90 3.85 3.80 3.75 3.70 3.65 3.60 3.55 3.50 ppm

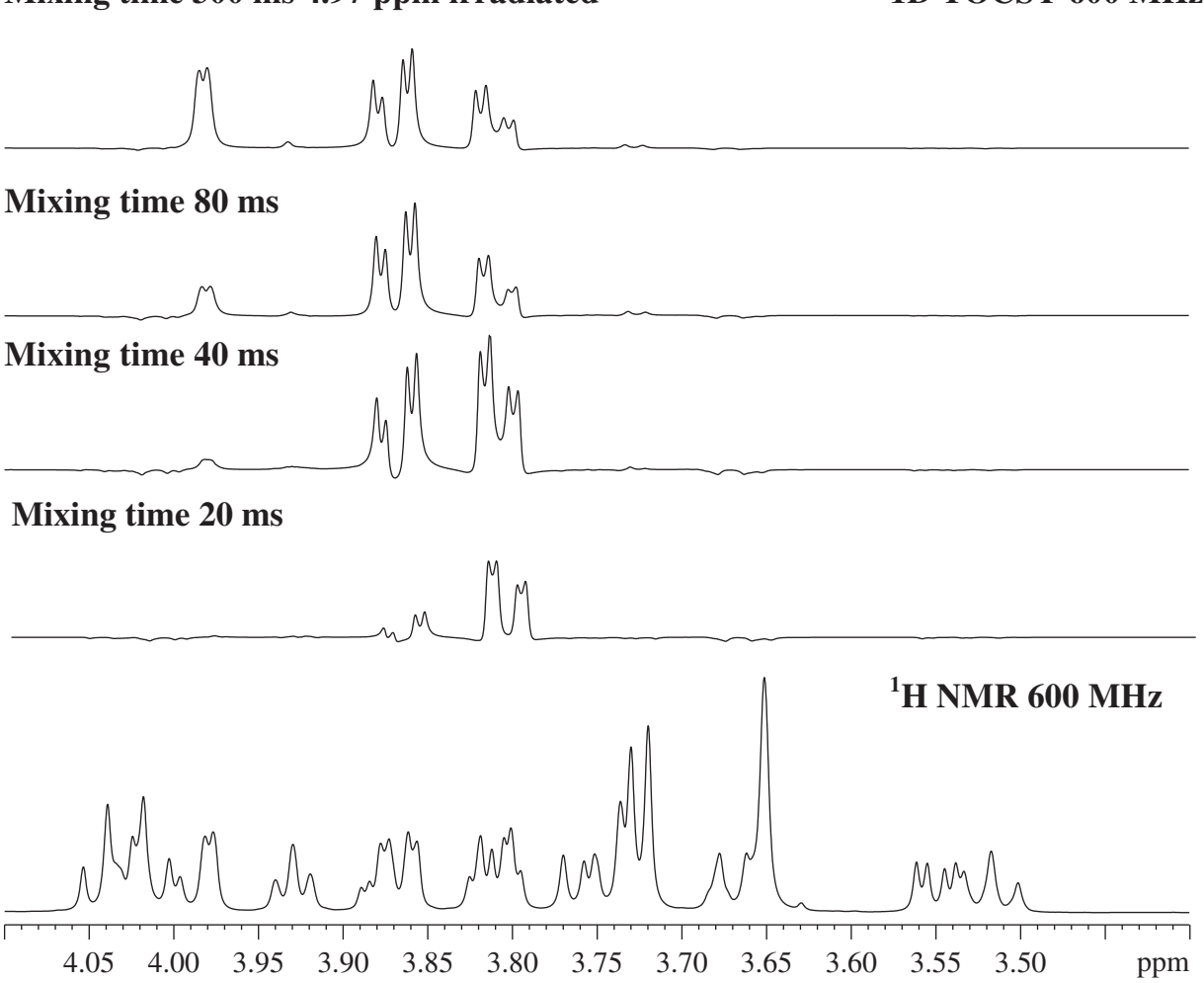
Mixing time 300 ms 4.97 ppm irradiated
1D TOCSY 600 MHz
Mixing time 80 ms
Mixing time 40 ms
Mixing time 20 ms
^{1}H NMR 600 MHz
4.05 4.00 3.95 3.90 3.85 3.80 3.75 3.70 3.65 3.60 3.55 3.50 ppm

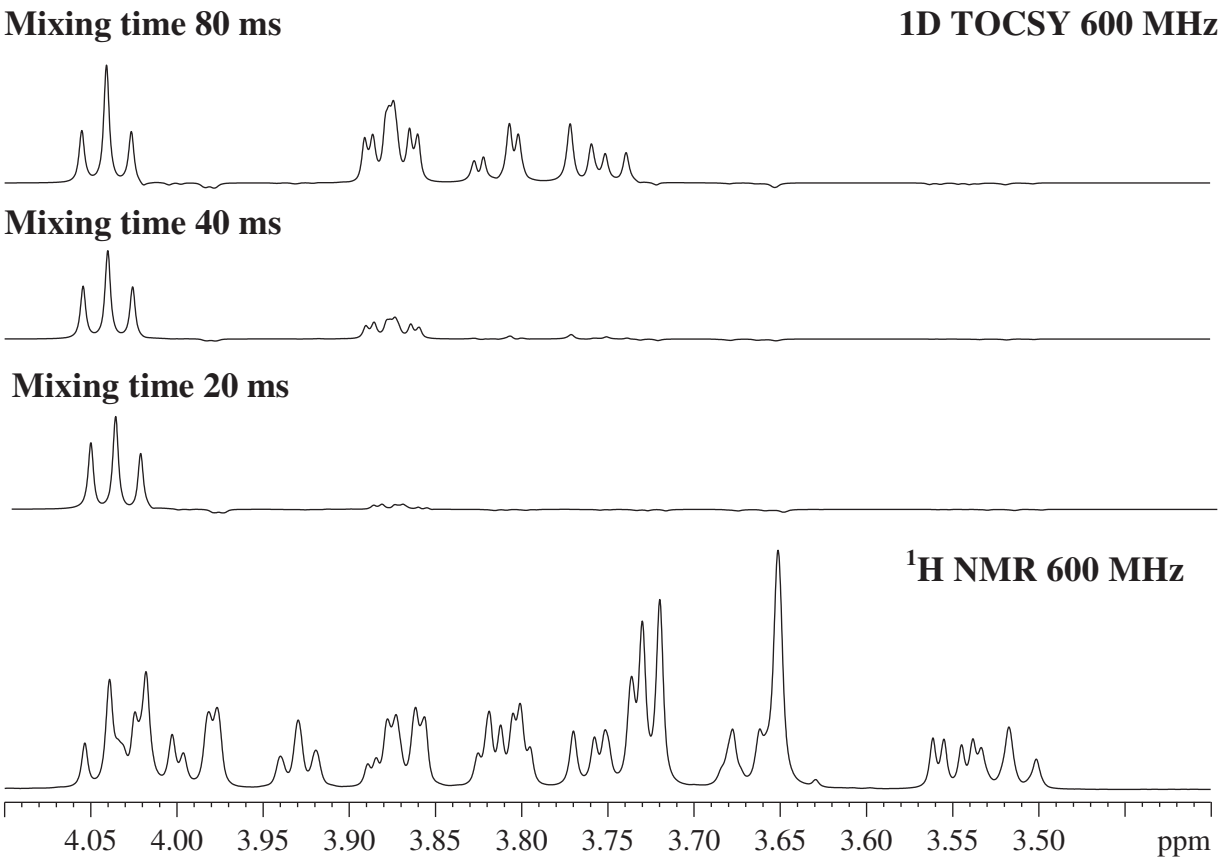
Mixing time 80 ms
1D TOCSY 600 MHz
Mixing time 40 ms
Mixing time 20 ms
^{1}H NMR 600 MHz
4.05
4.00
3.95
3.90
3.85
3.80
3.75
3.70
3.65
3.60
3.55
3.50
ppm

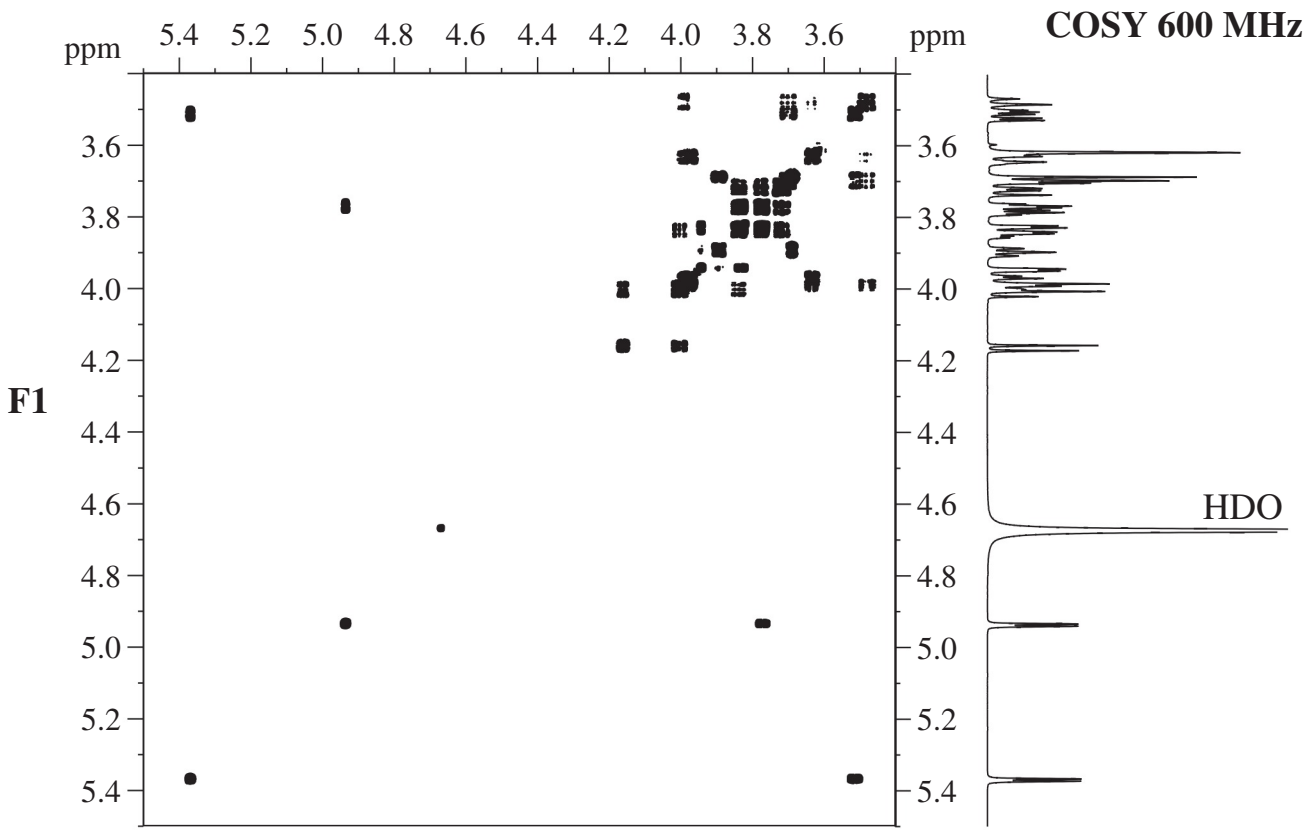
COSY 600 MHz
ppm
5.4 5.2 5.0 4.8 4.6 4.4 4.2 4.0 3.8 3.6
ppm
F1
3.6 3.8 4.0 4.2 4.4 4.6 4.8 5.0 5.2 5.4
HDO

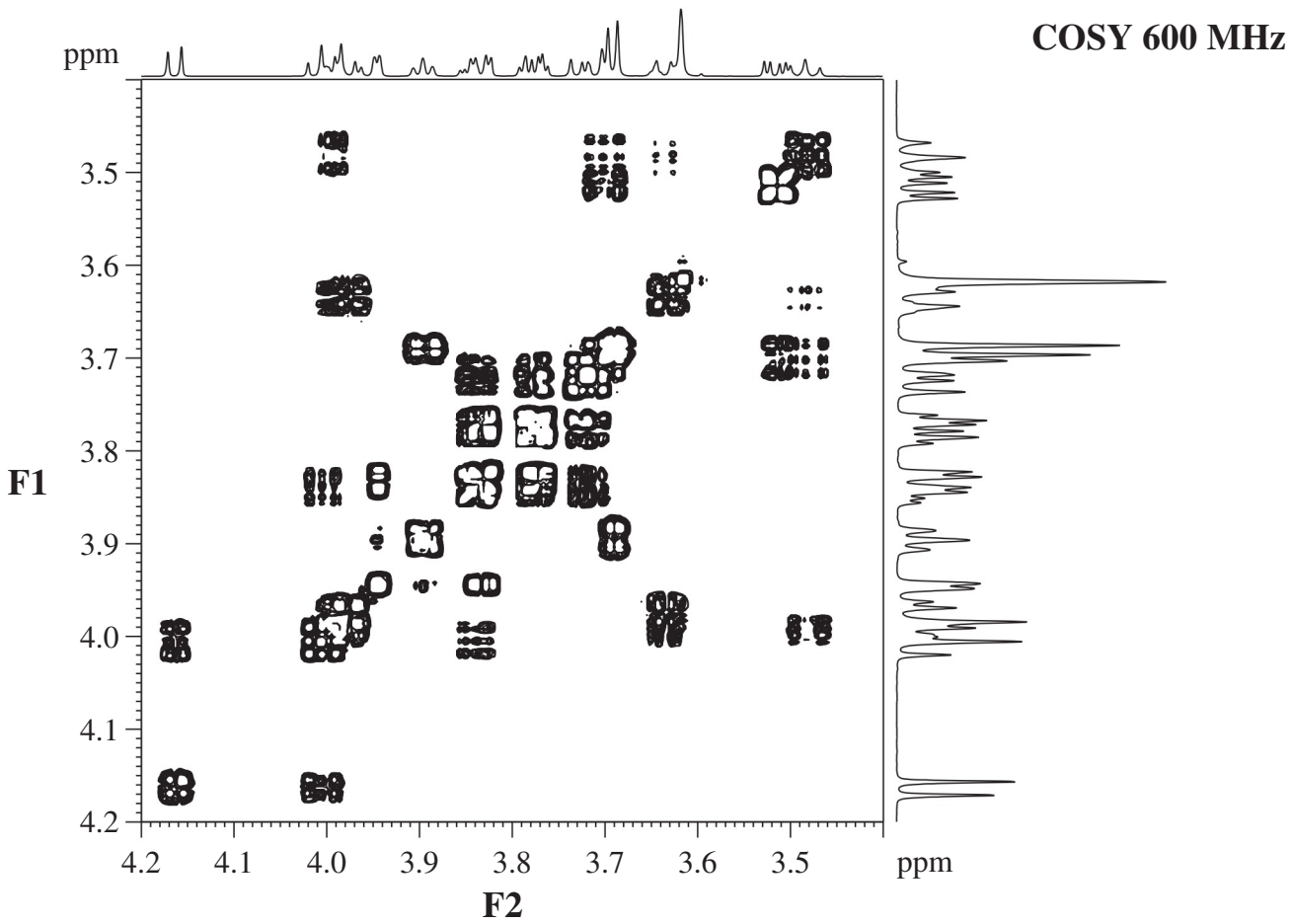
COSY 600 MHz
ppm
F1
3.5 3.6 3.7 3.8 3.9 4.0 4.1 4.2
4.2 4.1 4.0 3.9 3.8 3.7 3.6 3.5
ppm
F2

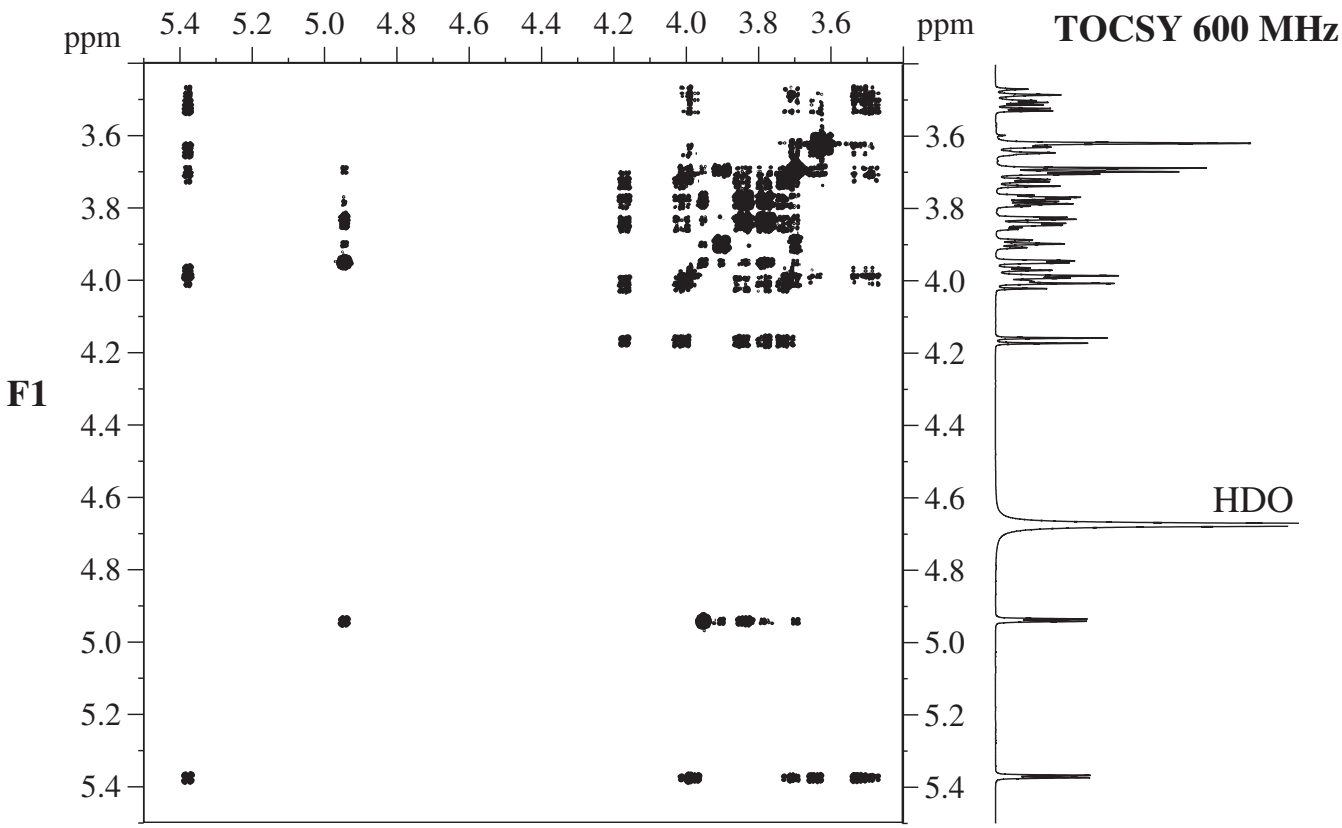
TOCSY 600 MHz
ppm
5.4 5.2 5.0 4.8 4.6 4.4 4.2 4.0 3.8 3.6
F1
HDO

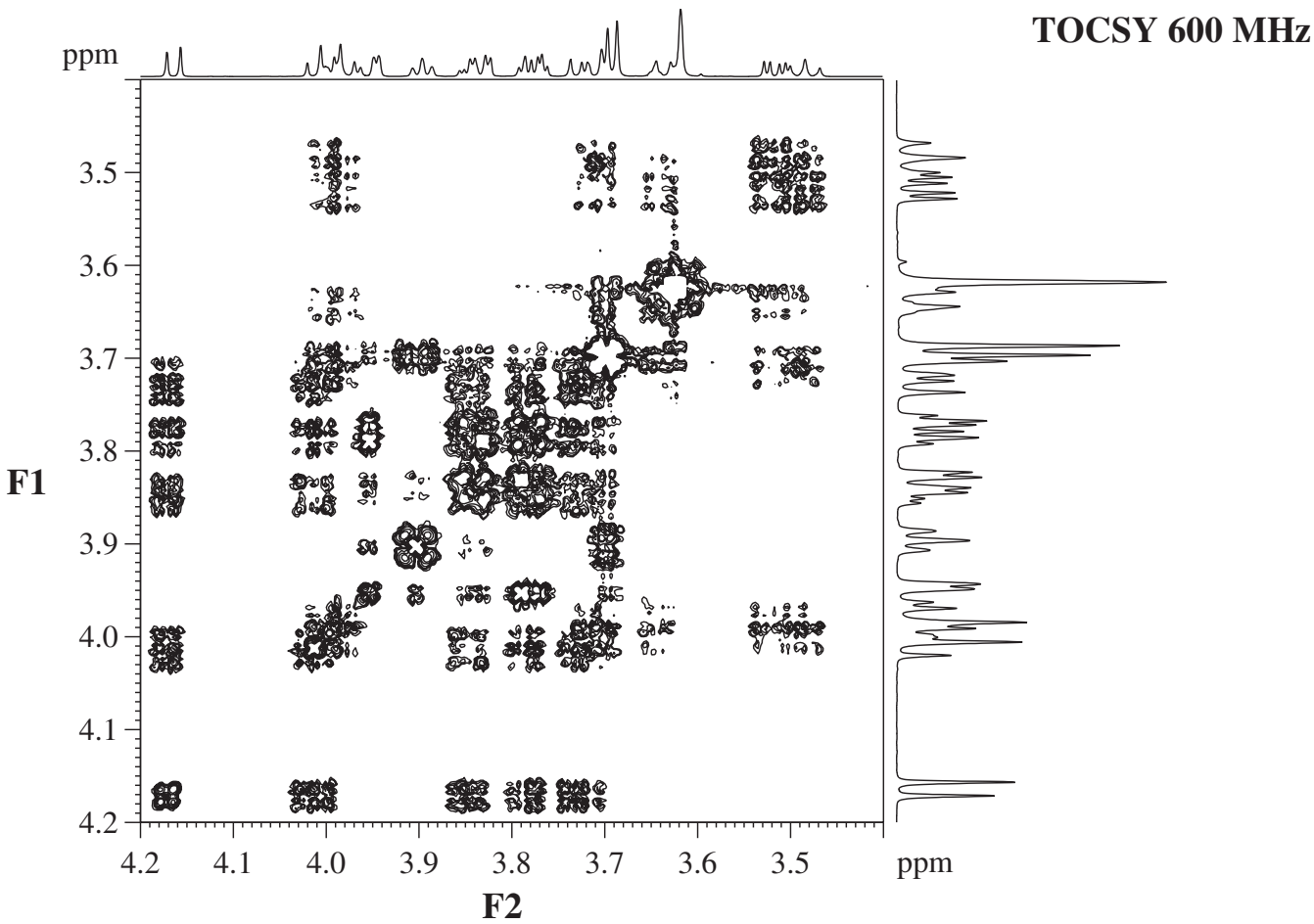
TOCSY 600 MHz
ppm
3.5 3.6 3.7 3.8 3.9 4.0 4.1 4.2
F1
F2

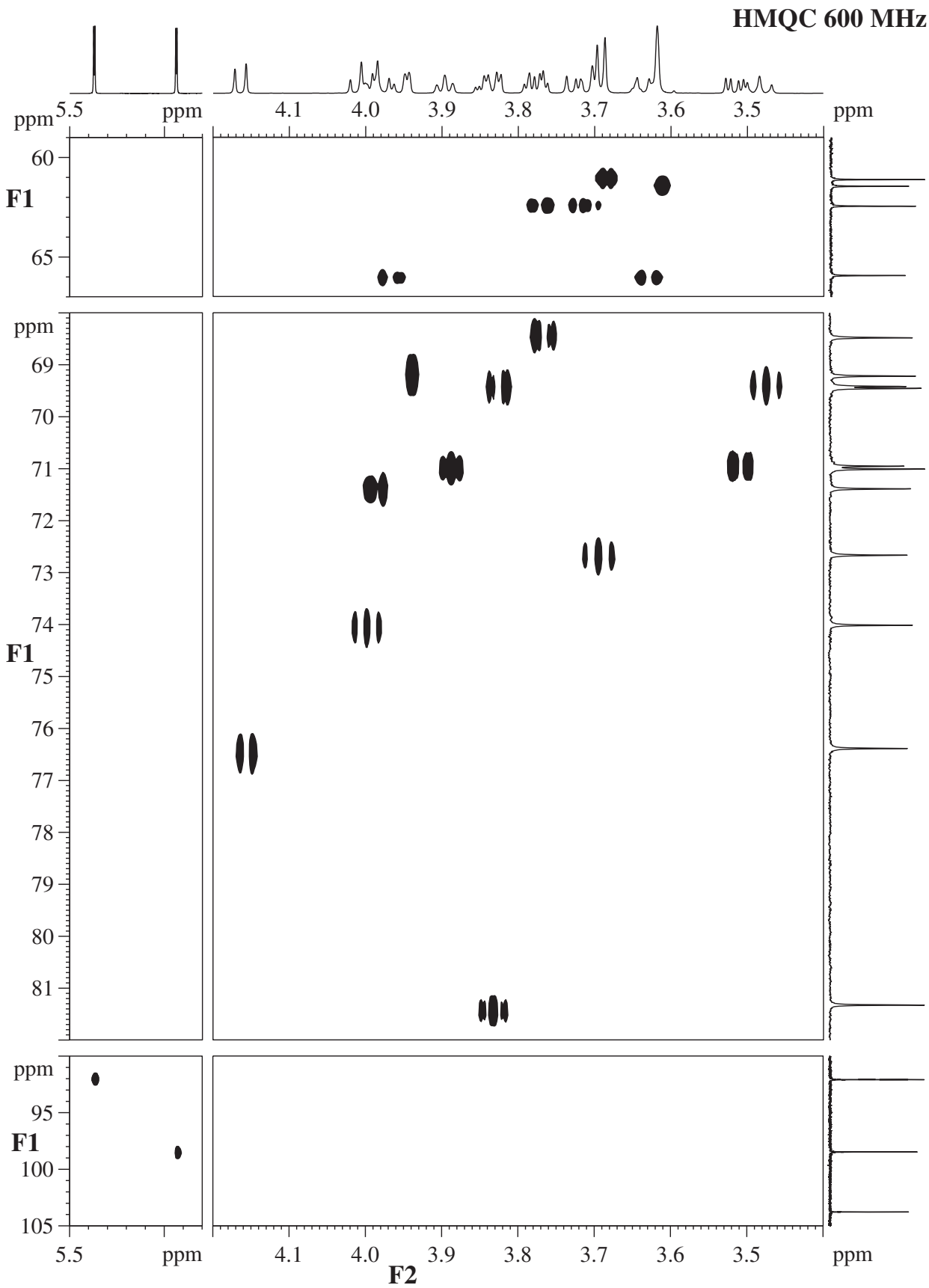
HMQC 600 MHz
ppm
5.5
ppm
4.1
4.0
3.9
3.8
3.7
3.6
3.5
ppm
F1
60
65
ppm
69
70
71
72
73
74
F1
75
76
77
78
79
80
81
ppm
95
F1
100
105
5.5
ppm
4.1
4.0
3.9
3.8
3.7
3.6
3.5
ppm
F2

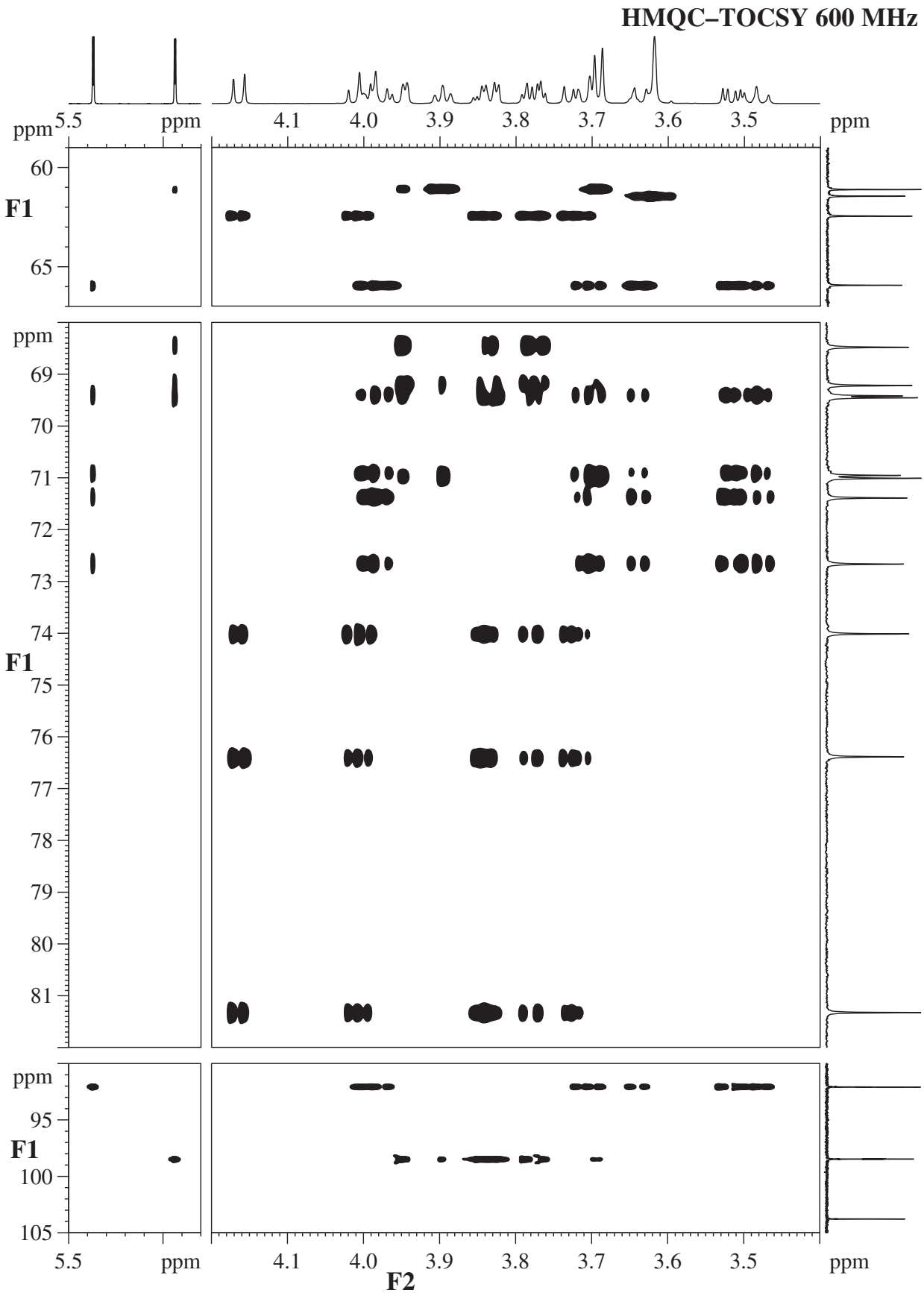
HMQC–TOCSY 600 MHz
ppm
5.5
ppm
4.1
4.0
3.9
3.8
3.7
3.6
3.5
ppm
F1
60
65
ppm
69
70
71
72
73
74
75
76
77
78
79
80
81
F1
ppm
95
100
105
F1
5.5
ppm
4.1
4.0
3.9
3.8
3.7
3.6
3.5
ppm
F2

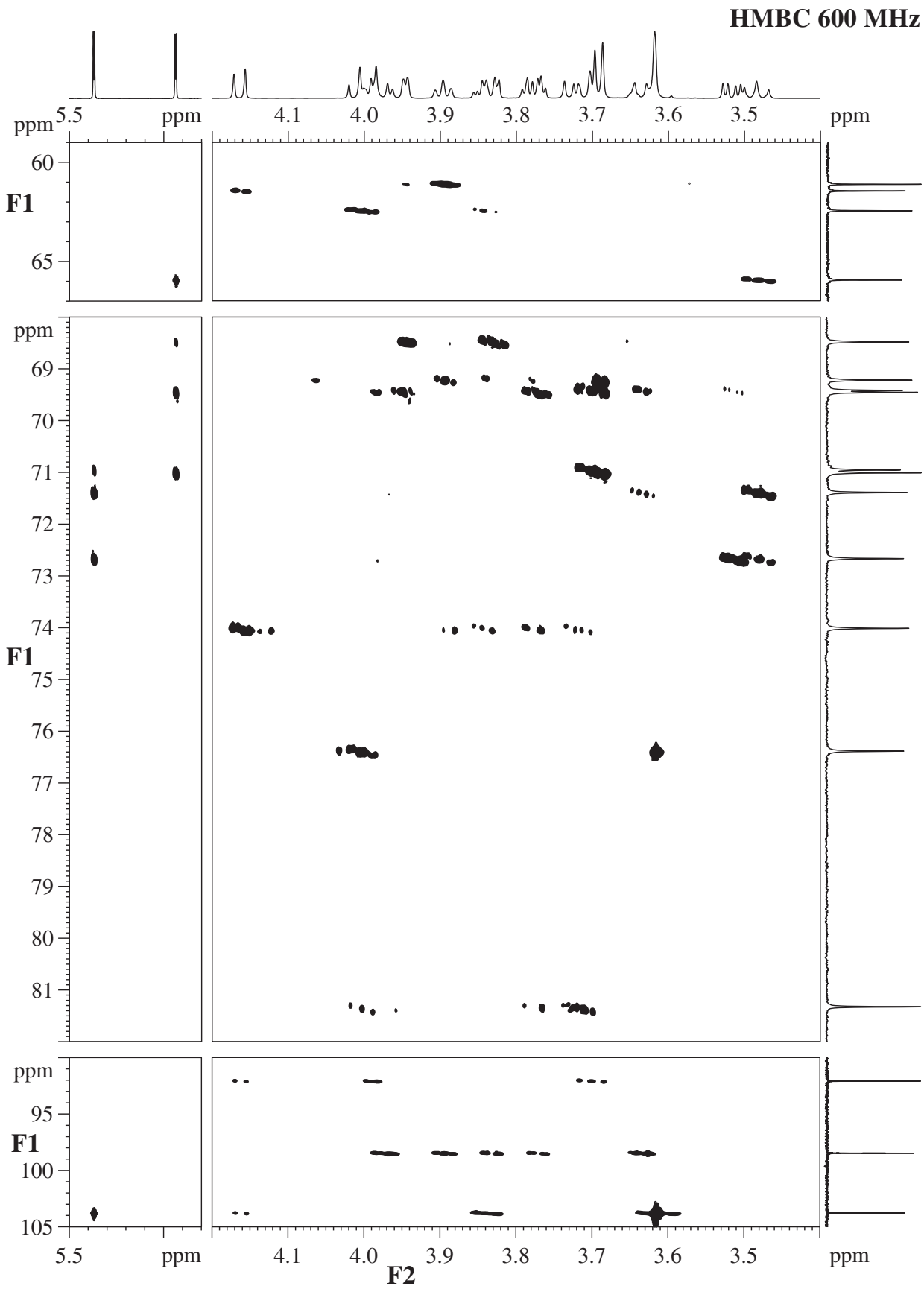
HMBC 600 MHz
ppm
5.5
4.1
4.0
3.9
3.8
3.7
3.6
3.5
F1
60
65
69
70
71
72
73
74
75
76
77
78
79
80
81
95
100
105
F2

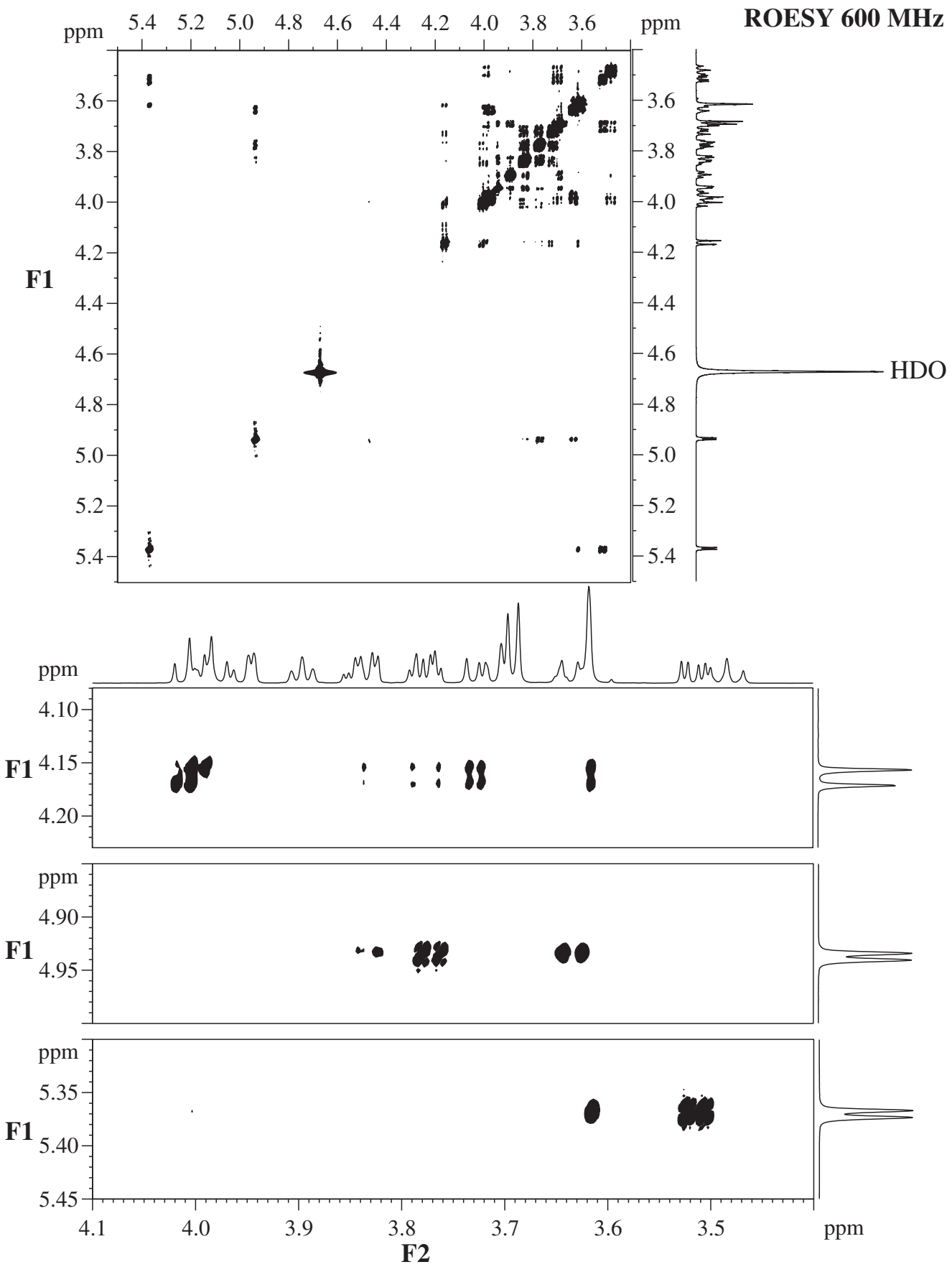
ROESY 600 MHz
ppm
5.4 5.2 5.0 4.8 4.6 4.4 4.2 4.0 3.8 3.6
F1
HDO
4.10
4.15
4.20
4.90
4.95
5.35
5.40
5.45
4.1 4.0 3.9 3.8 3.7 3.6 3.5
F2

^{1}H NMR 600 MHz

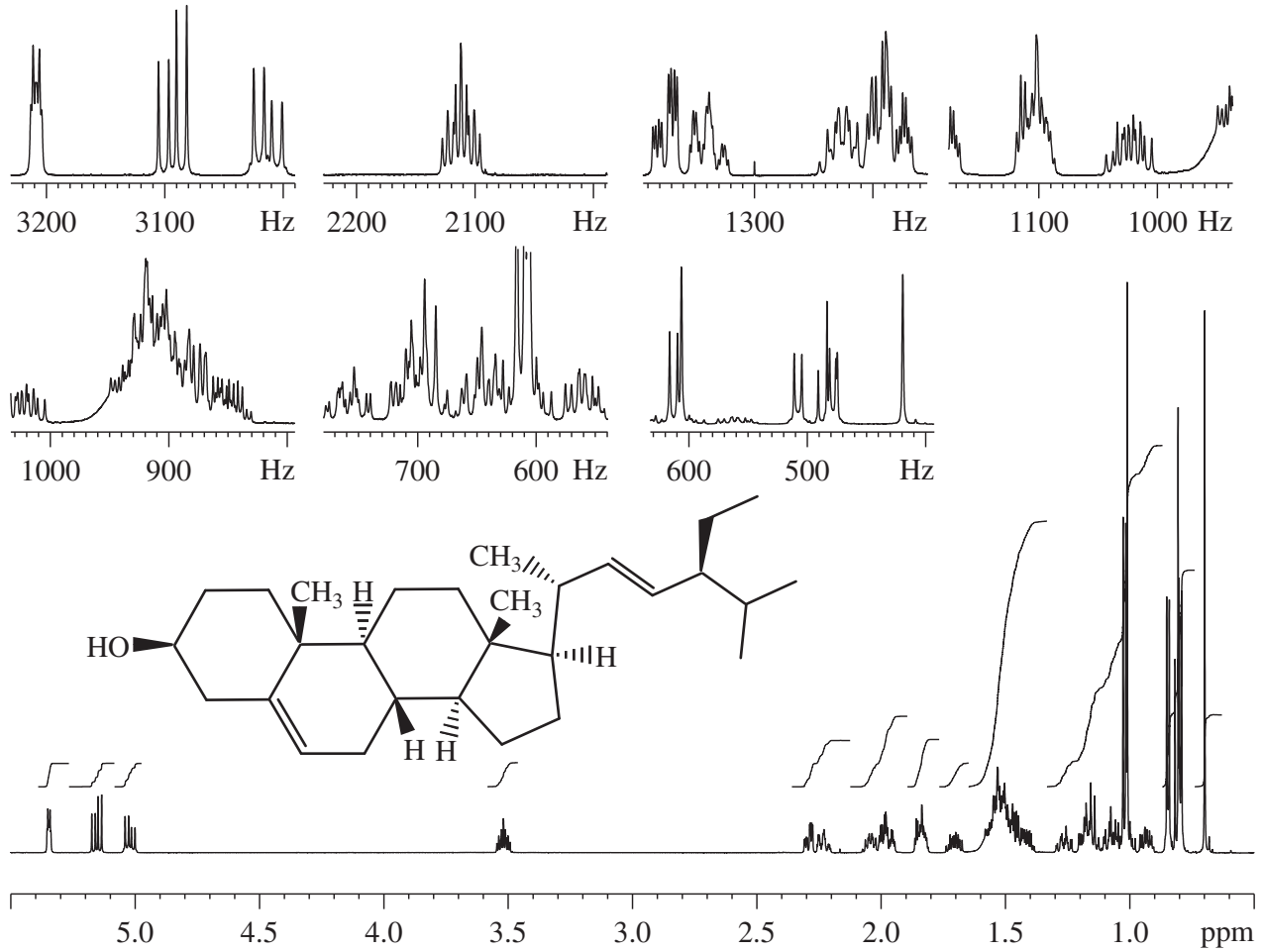

^{13}C/DEPT 600 MHz

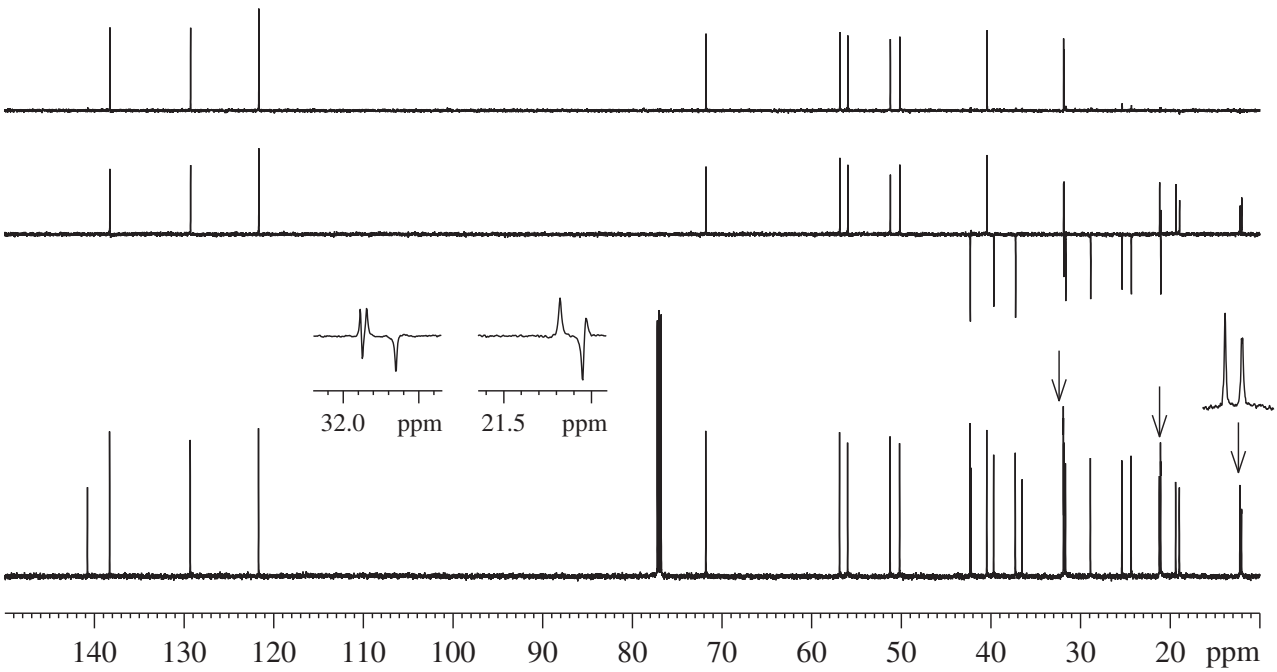

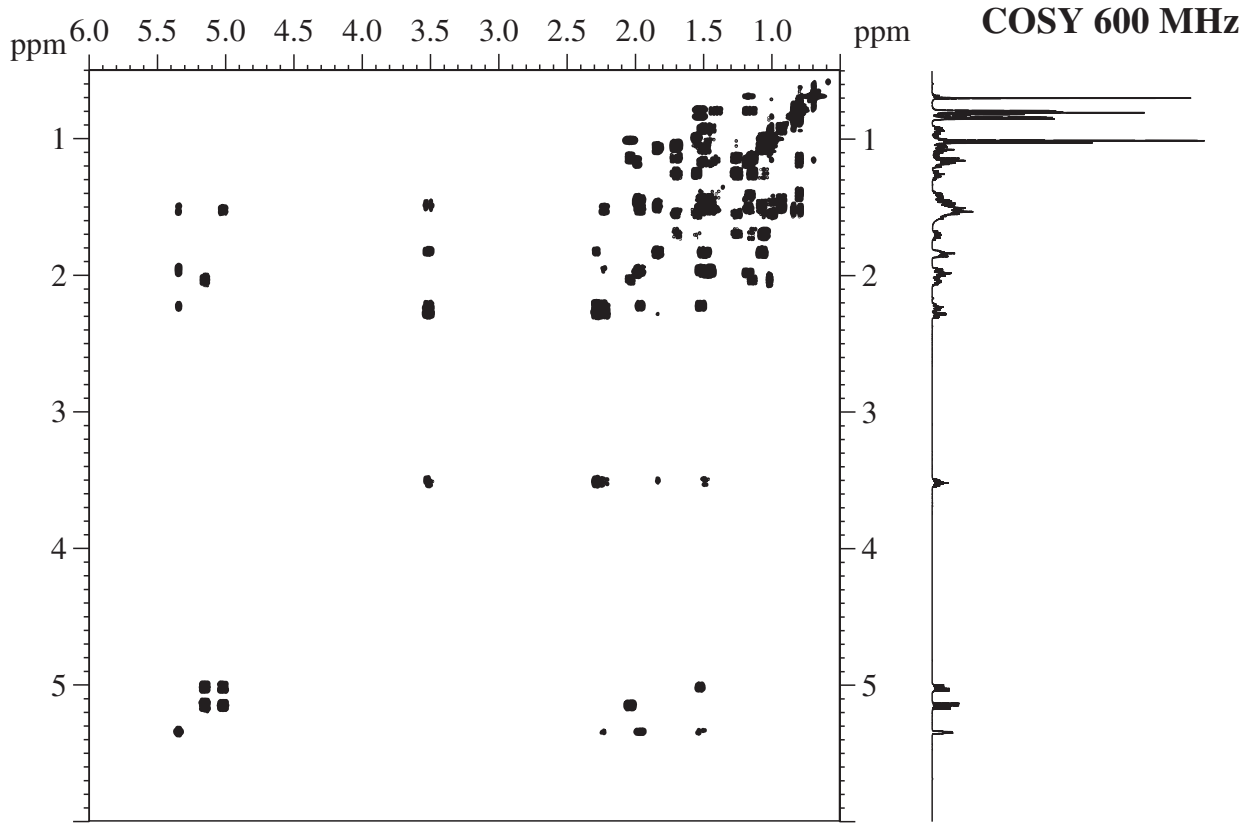
COSY 600 MHz
ppm
6.0 5.5 5.0 4.5 4.0 3.5 3.0 2.5 2.0 1.5 1.0
ppm
1
2
3
4
5

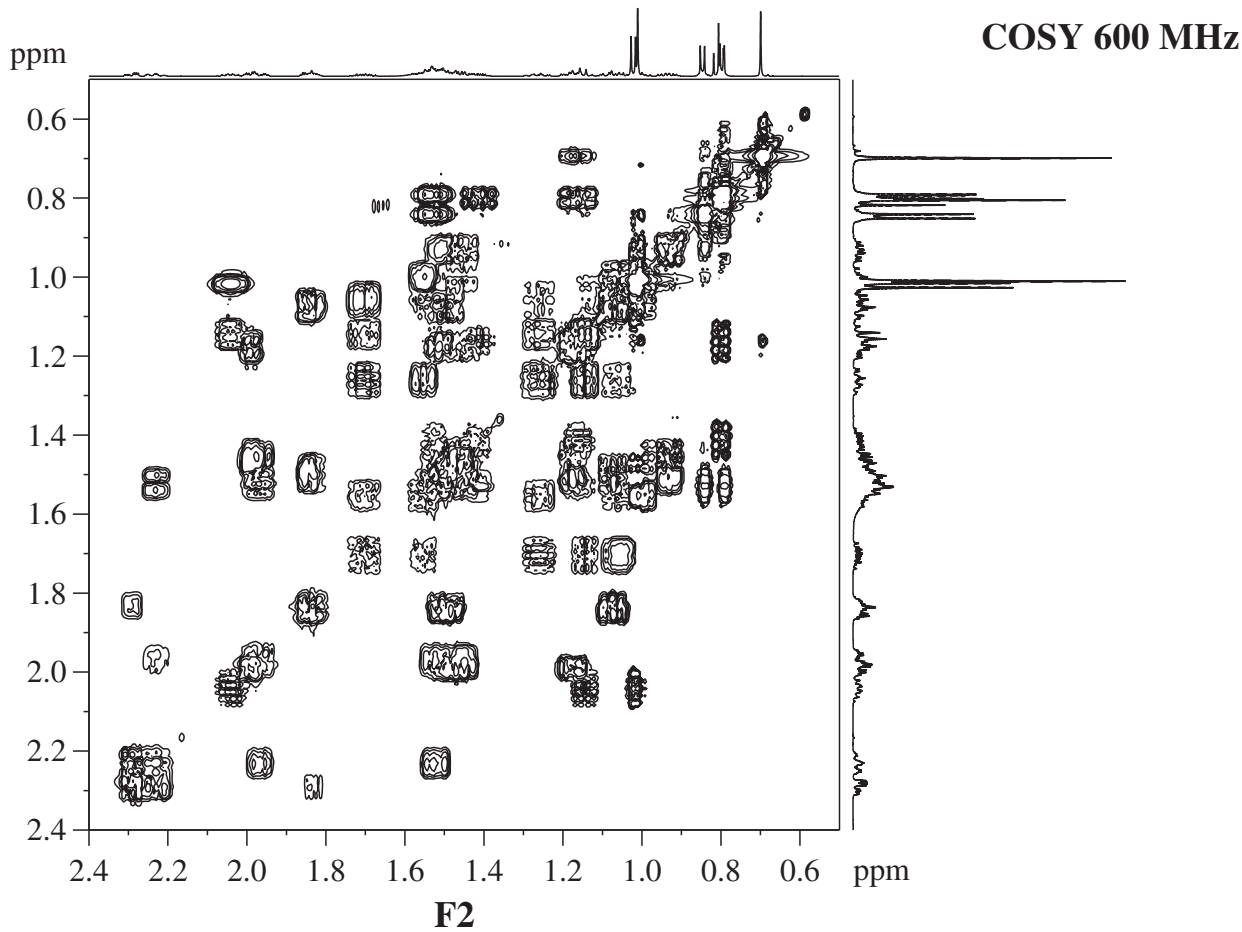
COSY 600 MHz
ppm
0.6
0.8
1.0
1.2
1.4
1.6
1.8
2.0
2.2
2.4
2.4 2.2 2.0 1.8 1.6 1.4 1.2 1.0 0.8 0.6
ppm
F1
F2

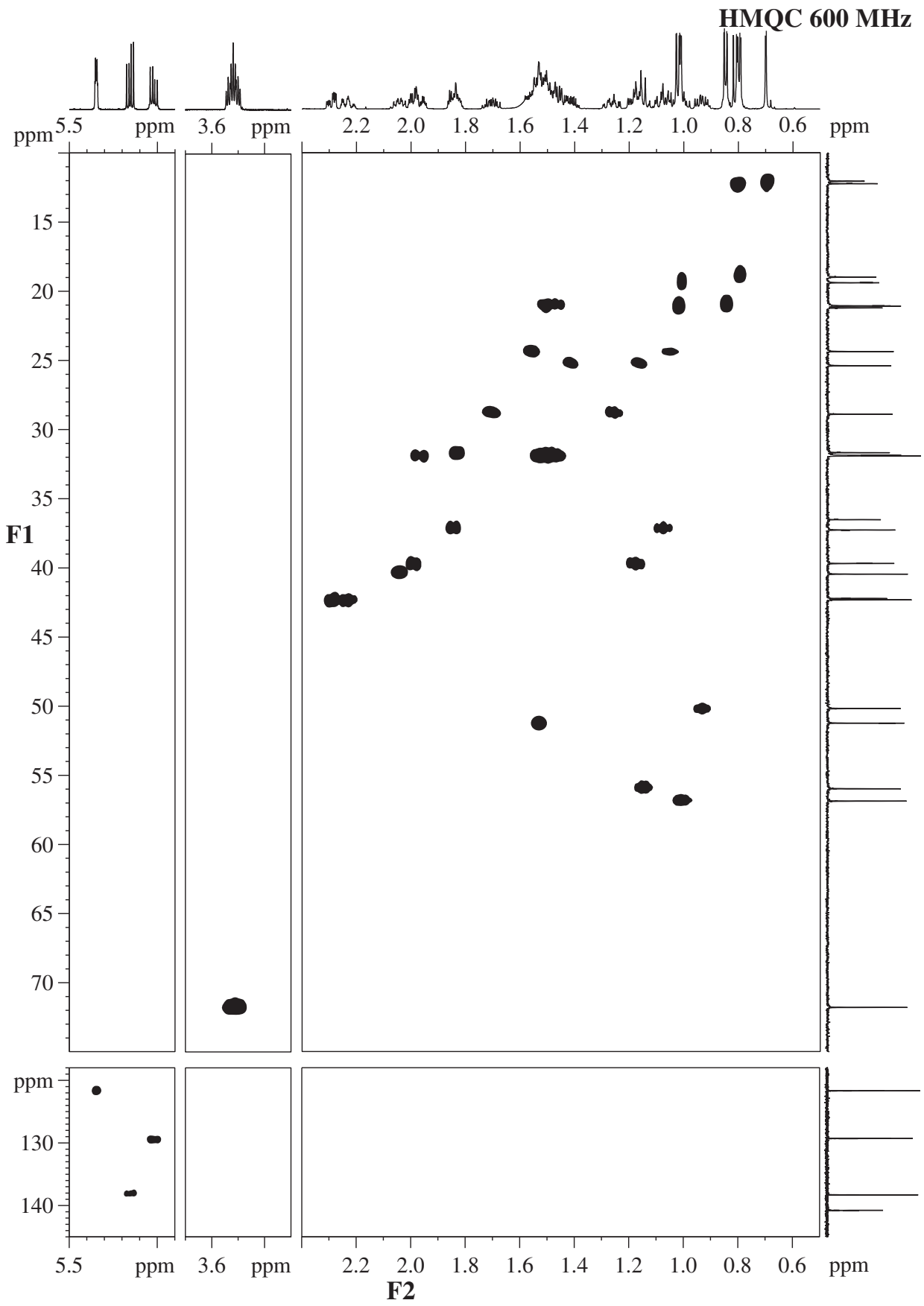
HMQC 600 MHz
ppm
5.5
ppm
3.6
ppm
2.2
2.0
1.8
1.6
1.4
1.2
1.0
0.8
0.6
ppm
15
20
25
30
35
F1
40
45
50
55
60
65
70
ppm
130
140
5.5
ppm
3.6
ppm
2.2
2.0
1.8
1.6
1.4
1.2
1.0
0.8
0.6
ppm
F2

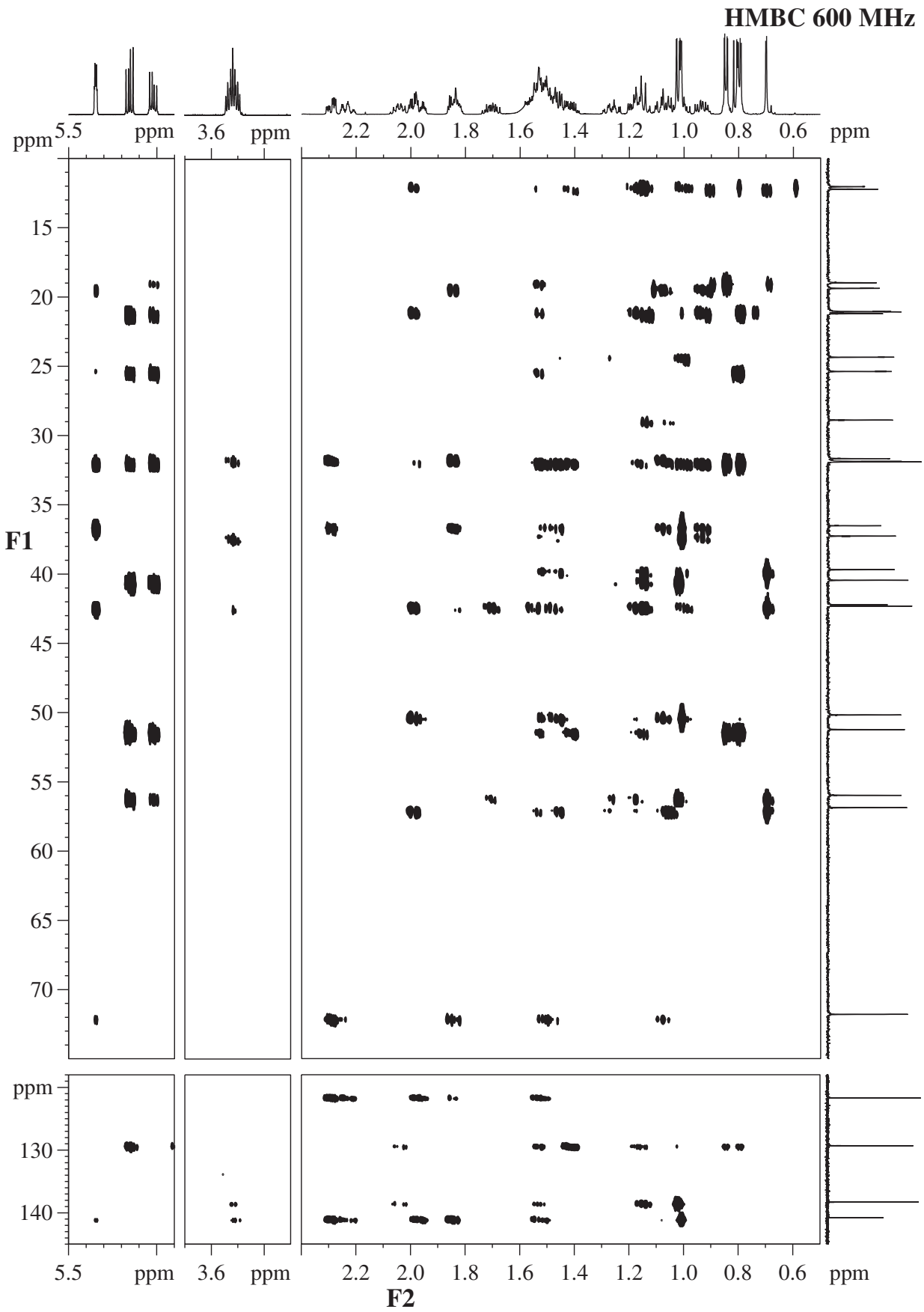
HMBC 600 MHz
ppm
5.5
ppm
3.6
ppm
2.2
2.0
1.8
1.6
1.4
1.2
1.0
0.8
0.6
ppm
15
20
25
30
35
F1
40
45
50
55
60
65
70
ppm
130
140
5.5
ppm
3.6
ppm
2.2
2.0
1.8
1.6
1.4
1.2
1.0
0.8
0.6
ppm
F2

^{1}H NMR 600 MHz

0° C in 5%/95% D_2O/H_2O

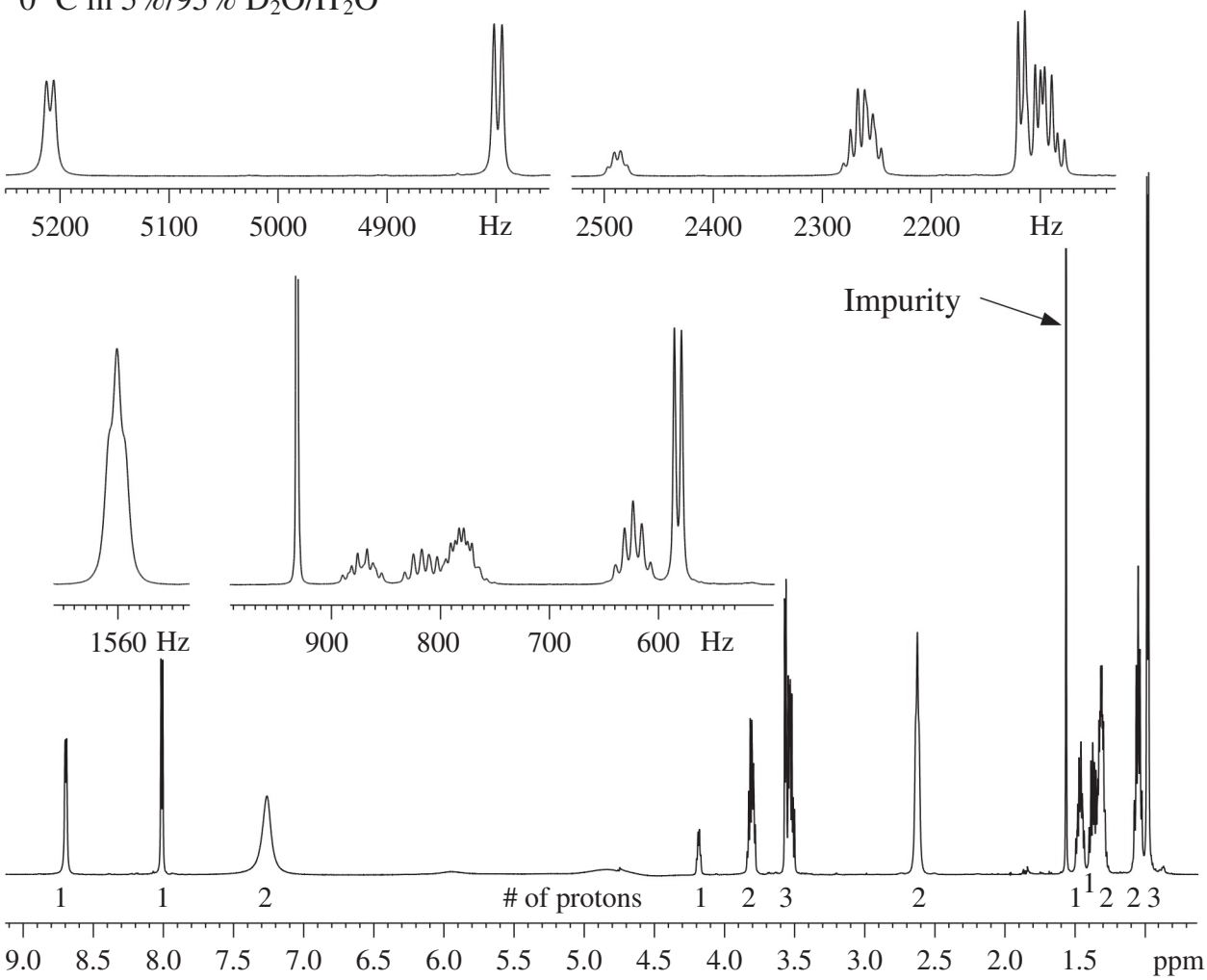

^{13}C/DEPT 150.9 MHz

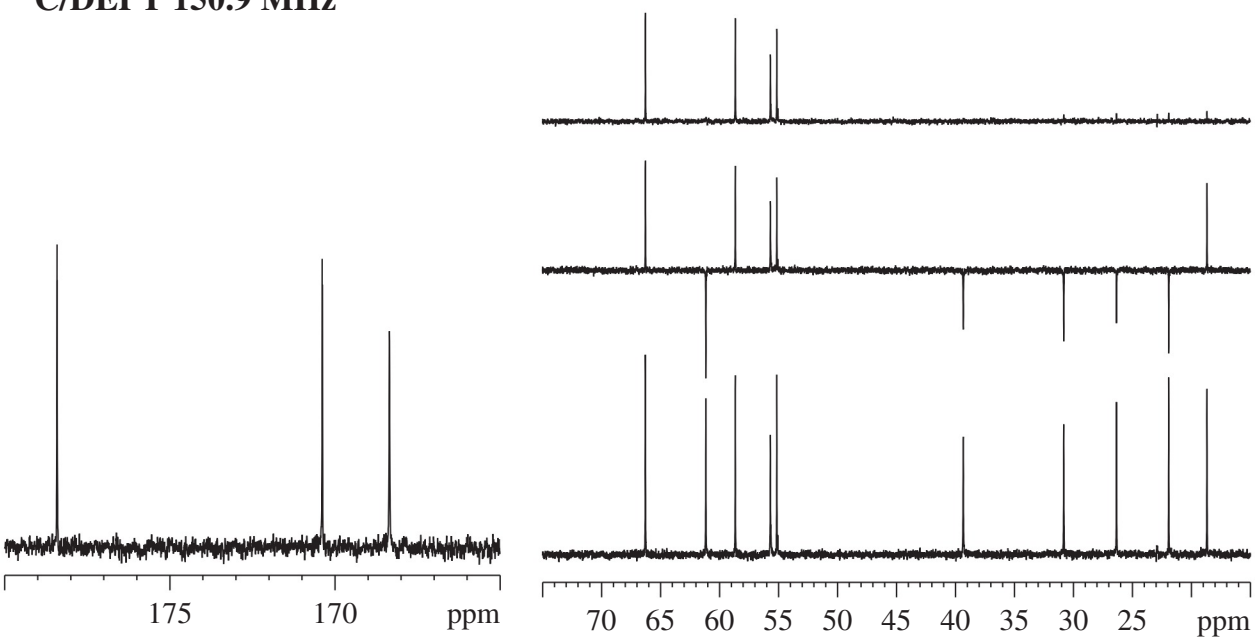

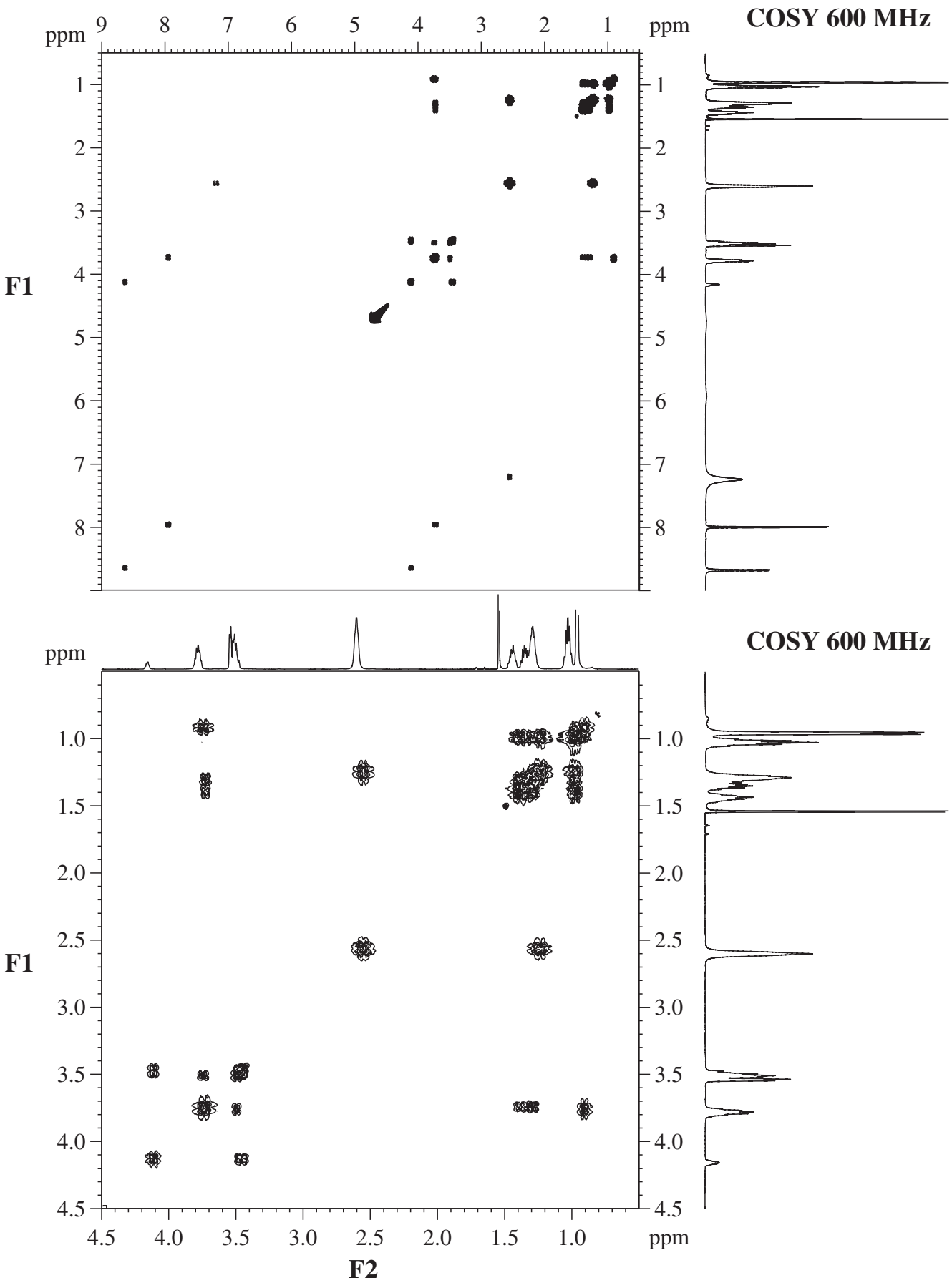
COSY 600 MHz
ppm
9 8 7 6 5 4 3 2 1
F1
COSY 600 MHz
ppm
1.0 1.5 2.0 2.5 3.0 3.5 4.0 4.5
F1
4.5 4.0 3.5 3.0 2.5 2.0 1.5 1.0 ppm
F2

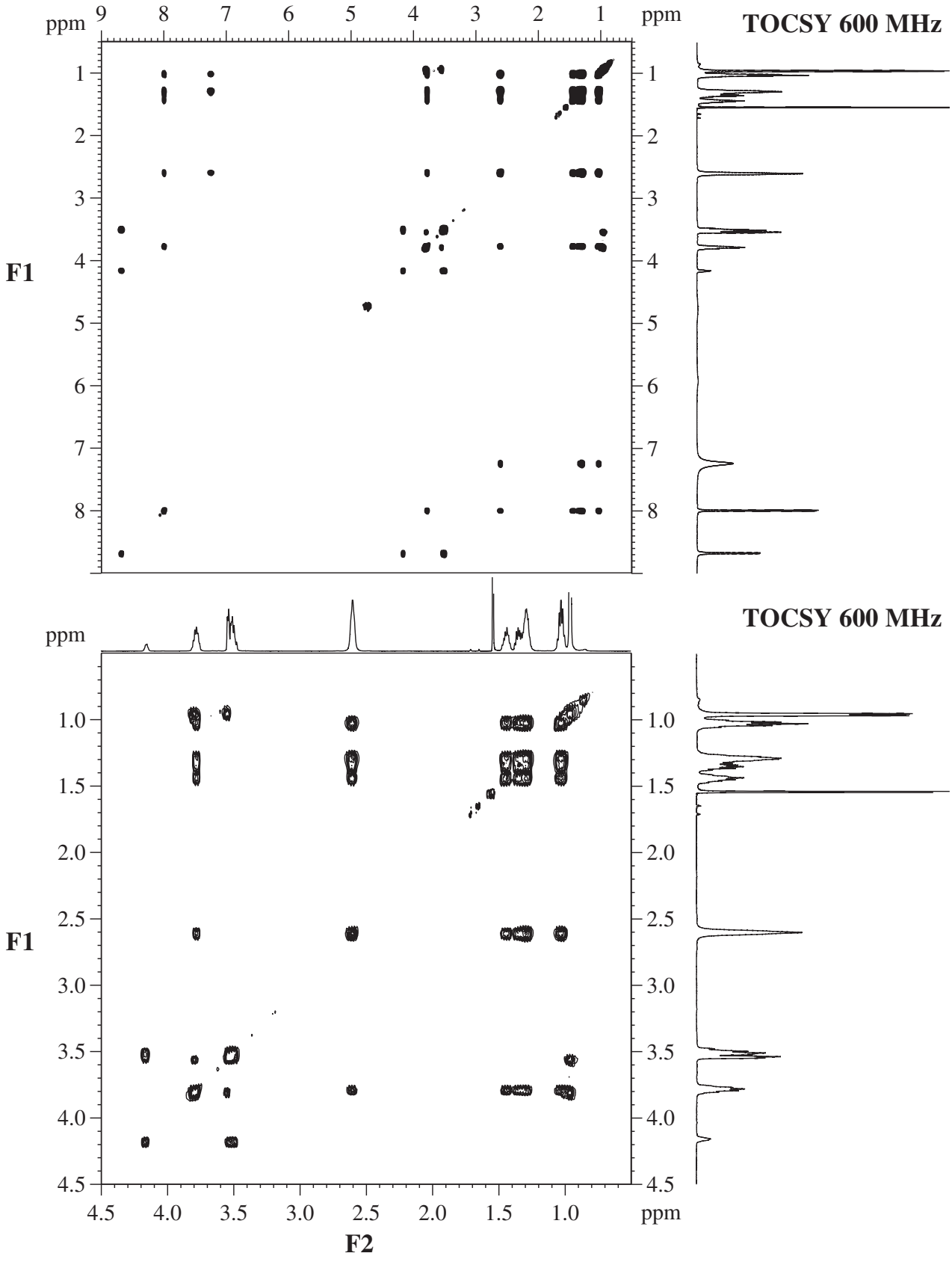
TOCSY 600 MHz
ppm
F1
TOCSY 600 MHz
ppm
F1
F2
ppm

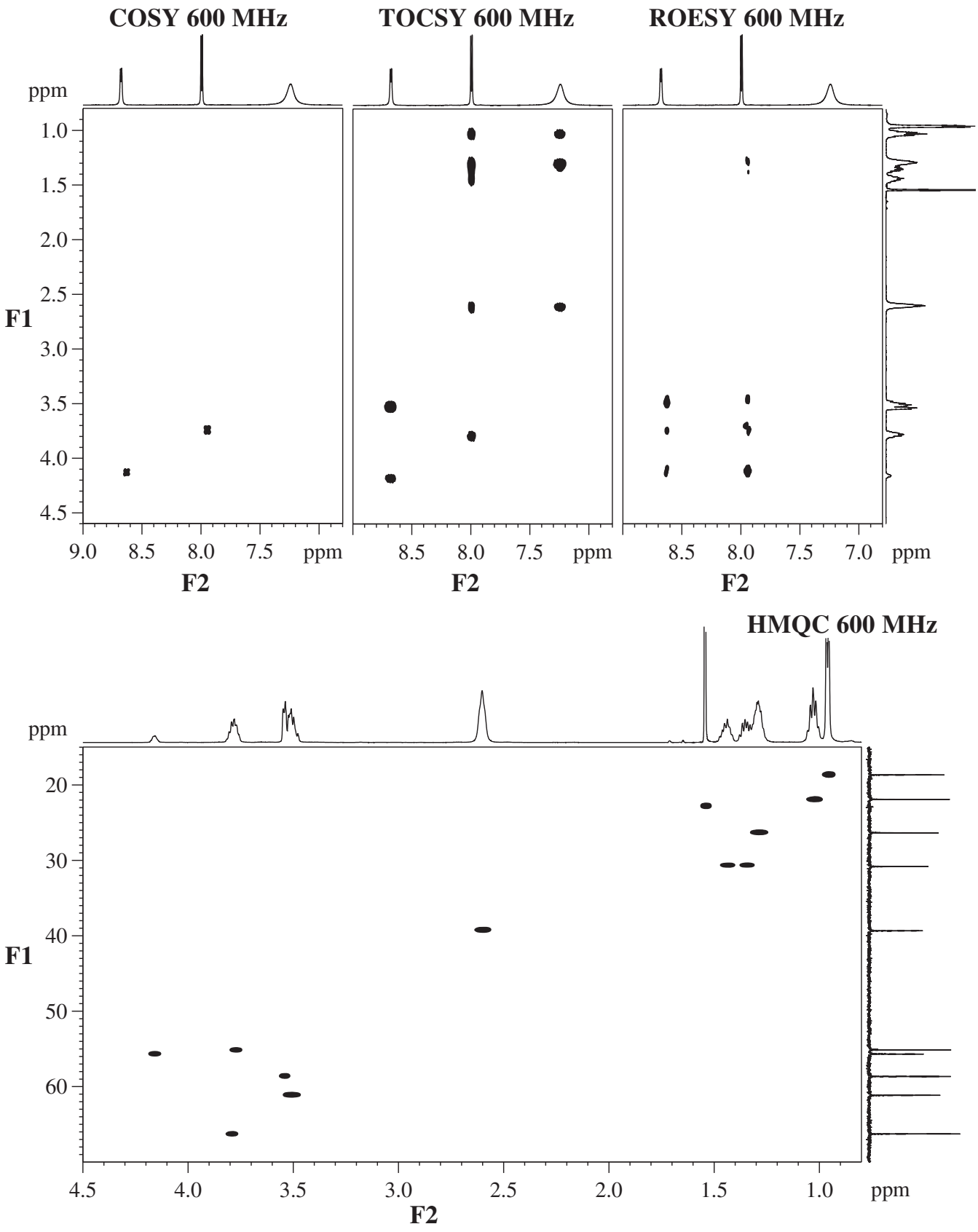
COSY 600 MHz
TOCSY 600 MHz
ROESY 600 MHz
ppm
1.0
1.5
2.0
2.5
3.0
3.5
4.0
4.5
F1
9.0
8.5
8.0
7.5
7.0
ppm
F2
HMQC 600 MHz
20
30
40
50
60
4.5
4.0
3.5
3.0
2.5
2.0
1.5
1.0

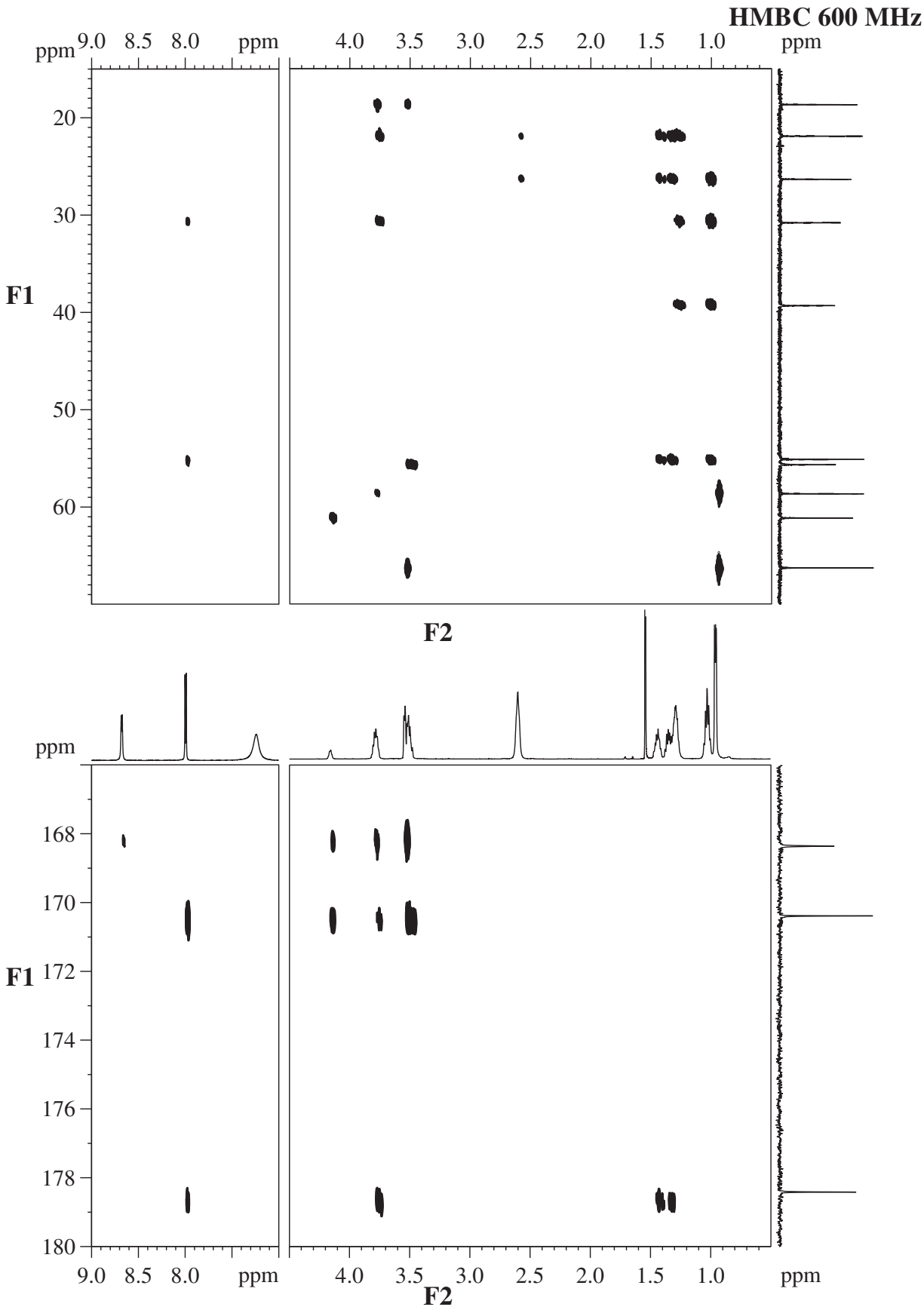
HMBC 600 MHz
ppm
9.0 8.5 8.0 ppm
4.0 3.5 3.0 2.5 2.0 1.5 1.0 ppm
20
30
40
50
60
F1
F2
ppm
168
170
172
174
176
178
180
F1
9.0 8.5 8.0 ppm
4.0 3.5 3.0 2.5 2.0 1.5 1.0 ppm
F2

CHAPTER 6

MULTINUCLEAR MAGNETIC RESONANCE SPECTROSCOPY

6.1 INTRODUCTION AND GENERAL CONSIDERATIONS

The previous three chapters have shown that nuclear magnetic resonance experiments with ^{1}H and ^{13}C nuclei are enormously useful to the chemist working with organic compounds. There is no need, however, to limit ourselves to these two important nuclei. Indeed, there are about 130 different stable isotopes whose spin quantum number, I, is greater than zero and, therefore, theoretically observable in an NMR experiment. Of these nuclides, 33 have a spin quantum number of $\frac{1}{2}$.

Listed in Appendix A are all magnetically active nuclei along with some of their properties. It is worthwhile to spend some time exploring Appendix A and to compare some of the nuclides listed there with ^{1}H and ^{13}C (also listed). First, we find that many elements have more than one magnetically active isotope. A small portion of Appendix A is reproduced in Table 6.1, with the addition of typical chemical shift ranges. Generally, the range of chemical shifts observed for various elements increases from left to right across the periodic table, and from top to bottom. (Although a detailed discussion is beyond the scope of this text, the main factor that contributes to typical chemical shift ranges is the paramagnetic contribution to magnetic shielding, which in turn depends on the average of the inverse cubed valence electron–nuclear distance.) Compare, for example, the ranges for ^{1}H (~10 ppm), ^{13}C (~220 ppm), and ^{195}Pt (over 10000 ppm).

Recall that chemical shift data are only useful if properly referenced. In fact, excluding ^{1}H and ^{13}C data, we must exercise extreme caution when comparing chemical shifts from different sources because many other nuclei have seen more than one compound used as a reference. To attempt to standardize chemical shifts, IUPAC has proposed a unified scale for referencing chemical shifts of any nuclei in any sample relative to an established primary reference. With modern instruments, at a given magnetic field, all resonance frequencies are derived from a single source: the magnet. It is therefore possible to relate the observed frequencies of all nuclides in a particular sample to a single primary reference and, for the sake of simplicity, the proton resonance of TMS (0.00 ppm) has been chosen as this primary standard. Using a suitable secondary reference compound is no longer the officially recommended method for reporting chemical shifts, although it is still widely done that way in practice. Implementation of the IUPAC referencing procedure can be straightforward, depending on the spectrometer software used.

The IUPAC method uses the proton resonance of tetramethylsilane (TMS) for organic solvents, and 2,2-dimethyl silapentane-5-sulfonic acid (DSS) for aqueous samples to get the primary frequency of the spectrometer. This frequency is then used to reference all X nuclei using the following equation:

$$\Xi = 100\left(\nu_X/\nu_{TMSobs}\right)$$

where Ξ is the frequency ratio (Appendix A), ν_X is the absolute frequency for the 0.00 ppm position in the X spectrum, and ν_{TMSobs} is the absolute frequency for ^{1}H of TMS that is a measured value on the specific instrument. The advantage of this method is that once the ^{1}H frequency is calibrated, the entire periodic table of spin-active nuclei can be analyzed without running the typical external or internal standard for that nucleus.

Let us return to Table 6.1 that lists the nuclides discussed in some detail in this chapter. To determine the suitability of a particular nuclide for an NMR experiment, we must consider several factors such as the natural abundance, receptivity, and spin quantum number. Consider the element hydrogen as an example. Hydrogen has three isotopes: ^{1}H (protium), ^{2}H (deuterium), and ^{3}H (tritium). Each isotope has been used in NMR studies, and each has different advantages to offer. ^{1}H and ^{3}H both have a spin quantum number of $\frac{1}{2}$ and they both have high receptivities (proportional to $\gamma^3(I(I+1))$, but ^{3}H has zero natural abundance and is radioactive. Tritium can therefore only be observed if we intentionally put it into a molecule synthetically, while protium is ubiquitous and we are already familiar with its uses. Deuterium has a spin of one and a very low natural abundance of 0.0115%; it is not radioactive. It is a useful isotope for mechanistic studies in organic chemistry and biochemistry. Its low natural abundance allows us to effectively ignore it when we observe other nuclei (couplings to ^{2}H will not be evident in the spectra), yet with modern instruments we are able to directly record natural abundance ^{2}H NMR spectra.

Besides deuterium, ^{11}B and ^{27}Al are two other nuclides listed in Table 6.1 that have spin quantum numbers greater than $\frac{1}{2}$. Most of the elements of the periodic table have quadrupolar nuclei ($I > \frac{1}{2}$). These so-called quadrupolar

TABLE 6.1 Useful Magnetic Resonance Data for Some of the Nuclides Discussed in This Chapter

Isotope	Spin Quantum Number	Natural Abundance %	Relative[a] Receptivity	Frequency (MHz) at 7.046 T	Primary Reference Compound	Typical Chemical Shift Range (ppm)
^{1}H	$\frac{1}{2}$	99.9885	1.000	300.000	$Si(CH_3)_4$	10 to 0
^{2}H	1	0.0115	1.11×10^{-6}	46.052	$Si(CD_3)_4$	10 to 0
^{3}H	$\frac{1}{2}$	0	0	319.993	$Si(CT_3)_4$	10 to 0
^{11}B	$\frac{3}{2}$	80.1	0.132	96.269	$BF_3 \cdot Et_2O$ in $CDCl_3$	135 to −130
^{13}C	$\frac{1}{2}$	1.07	1.70×10^{-4}	75.451	$Si(CH_3)_4$	220 to 0
^{14}N	1	99.632	1.00×10^{-3}	21.686	$^{14}NH_3(l)$[b]	900 to 0
^{15}N	$\frac{1}{2}$	0.368	3.84×10^{-6}	30.419	$^{15}NH_3(l)$[b]	900 to 0
^{17}O	$\frac{5}{2}$	3.7×10^{-2}	2.91×10^{-2}	40.670	H_2O	1700 to −50
^{19}F	$\frac{1}{2}$	100	0.834	282.387	$CFCl_3$	276 to −280
^{27}Al	$\frac{5}{2}$	100	0.207	78.232	$Al(NO_3)_3$ (aq)	250 to −200
^{29}Si	$\frac{1}{2}$	4.6832	3.68×10^{-4}	59.648	$Si(CH_3)_4$	175 to −380
^{31}P	$\frac{1}{2}$	100	6.65×10^{-2}	121.554	85% H_3PO_4 (aq)	270 to −480
^{195}Pt	$\frac{1}{2}$	33.832	3.51×10^{-3}	65.473	Na_2PtCl_6 (aq)	7500 to −6500

[a]Relative to ^{1}H.
[b]At 25°C.

nuclei can often be observed in NMR experiments; however, there are also many examples where rapid quadrupolar relaxation broadens the signals beyond detection. ^{11}B and ^{27}Al have good spectroscopic properties in that they have high natural abundances and good receptivities relative to ^{1}H. In addition to the general considerations of natural abundance and receptivity, the quadrupole moment of a particular nuclide as well as its environment in the molecule of interest will determine the rate of quadrupolar relaxation, which is inversely proportional to the line width in the NMR spectrum. Quadrupolar nuclei with good natural abundances and which are found in symmetric environments (e.g., tetrahedral or octahedral) can give sharp NMR lines and even give rise to splittings due to J couplings in some cases. Note that the $2nI + 1$ rule applies for predicting J multiplets for all nuclei, where n is the number of equivalent nuclei coupled to the observed nucleus. Conversely, nuclides such as ^{63}Cu, ^{105}Pd, ^{127}I, or ^{187}Re will almost invariably give extremely broad lines, and it is not generally practical to acquire their spectra. Without isotopic enrichment, the NMR spectroscopy of nuclei such as ^{17}O, ^{33}S, and ^{43}Ca is also often impractical due to their very low natural abundances.

Our goals for the remainder of this chapter are modest as we confront such a vast field as multinuclear magnetic resonance. In Section 3.7, we have seen the impact of other nuclei that possess a magnetic moment (especially those with spin $\frac{1}{2}$) on proton NMR spectra. We will briefly examine below the NMR spectroscopy of four spin $\frac{1}{2}$ nuclides, which were selected for their historic importance in organic chemistry (and related natural products and pharmaceutical fields), biochemistry, and polymer chemistry. These four nuclides, ^{15}N, ^{19}F, ^{29}Si, and ^{31}P, are presented with a few simple examples and a brief consideration of important experimental factors and limitations.

The theoretical background for understanding the NMR spectroscopy of these four nuclides is analogous to that which has been presented for ^{1}H and ^{13}C in Chapters 3 and 4. Our treatment of spin, coupling constants, the NOE, Fourier transformation, etc. can be applied to these nuclides without modification. We also use the concept of chemical shift without modification, but we must avoid exercising the predictive skills that we have developed for ^{1}H and ^{13}C chemical shifts for these nuclei. The use of NMR spectroscopy of nuclei other than ^{1}H and ^{13}C to characterize and identify organic compounds is now commonplace. The use of other nuclei in NMR experiments ranges from diverse areas such as simply determining whether an unknown compound contains nitrogen to more complex questions of stereochemistry and reaction mechanisms.

6.2 ^{15}N NUCLEAR MAGNETIC RESONANCE

After carbon and hydrogen, oxygen and nitrogen are the next two most important elements in organic compounds. In the mind of the organic chemist, the presence of either of these elements represents the presence of one or more functional groups and the use of IR spectroscopy may be invoked. Without detracting in any way from IR, this line of reasoning is nonetheless too restrictive, especially with

respect to nitrogen. Inspection of Table 6.1 reveals that in the case of oxygen, we have but a single choice of a nucleus on which NMR is possible; ^{17}O has a spin of $\frac{5}{2}$ and it is not used much in NMR studies due to its low natural abundance, while ^{16}O has a spin of 0 and is thus not NMR-active (not listed in Table 6.1).

Nitrogen, on the other hand, has two magnetically active isotopes, ^{14}N and ^{15}N. Because nitrogen compounds are so important in organic chemistry, natural products chemistry, pharmacology, and biochemistry, both of these isotopes have been the subject of intensive NMR investigation. Aside from the various classes of nitrogen containing functional groups with which we are familiar, entire fields of study have developed based on nitrogen-containing compounds. These include alkaloids, peptides and/or proteins, and nucleic acids. For purposes of study by NMR, nucleic acids are a favorite subject because not only is nitrogen ubiquitous in these compounds but so is phosphorus (see Section 6.5). If we again refer to Table 6.1, we find that neither of the two isotopes of nitrogen is ideal for NMR. The most abundant isotope of nitrogen, ^{14}N, which represents greater than 99% of nitrogen's natural abundance, possesses a spin of 1 and hence an electric quadrupole moment. This nucleus has a low Larmor frequency and typically gives broad NMR peaks due to quadrupolar relaxation. We shall not consider it any further.

The other isotope of nitrogen, ^{15}N, also has a low Larmor frequency, which, when multiplied by a very low natural abundance, leads to an extremely low absolute sensitivity. Modern methods have largely overcome the problem of sensitivity (by isotopically enriching samples or by indirect ^{1}H detection) and we focus our attention on ^{15}N largely because its spin quantum number is $\frac{1}{2}$ and the NMR line widths are quite narrow.

There are two important experimental factors that must be accounted for if we are to be successful in running ^{15}N NMR experiments. The ^{15}N nucleus tends to relax very slowly; T_1's of greater than 80 seconds have been measured. Thus, either long recycle delays must be incorporated into our pulse sequence or, alternatively, we could provide another route for spin relaxation. A common procedure is to add a trace amount of chromium (III) acetylacetonate, a paramagnetic substance, whose unpaired electrons can efficiently decrease the T_1 of ^{15}N. In cases where T_1 values are not known (and not intended to be measured), recycle delays and pulse angles must be considered carefully because the signal from one (or more) ^{15}N resonance can accrue too slowly or be missed altogether.

We consider the other experimental factor, the NOE, which has already been discussed in Chapters 3 and 4, now in more detail. Recall that we routinely run ^{13}C NMR experiments with irradiation of the protons (i.e., proton decoupled) that, aside from producing the desired effect of singlets for all ^{13}C signals, also enhances the signal for carbons with directly bonded protons. This enhancement is due to the NOE; the changes in signal intensity arise from polarization of spin populations away from the natural Boltzmann distribution. The amount of enhancement depends on two factors: (i) the fixed value of one-half the ratio of the proton's magnetogyric ratio (γ) relative to that of the other nuclide is the maximum possible enhancement, while the actual enhancement is also proportional to (ii) the extent of ^{13}C—^{1}H dipolar relaxation. For a proton-decoupled ^{13}C NMR experiment, the maximum NOE enhancement is $\gamma_H/(2)\gamma_C$ or 26.753/(2)6.728, which equals 1.98. The total sensitivity increase is therefore nearly threefold because the NOE enhancement is added to the original intensity.

The actual enhancement for the ^{13}C—^{1}H system can be anywhere from 0 to 1.98 depending on the mechanism of relaxation for each individual nucleus. In practice, for carbons with no attached protons, the enhancement is essentially zero since there is practically no ^{13}C—^{1}H dipolar relaxation. For small- to medium-sized organic molecules, ^{13}C—^{1}H dipolar relaxation for carbons with attached protons is very efficient, yielding close to the full 200% increase in signal. If we apply the same reasoning to the ^{15}N nucleus, we arrive at a very different situation. The magnetogyric ratio for ^{15}N is small and negative ($\gamma = -2.713 \times 10^7$ rad T^{-1} s^{-1}). A quick calculation shows that the maximum NOE enhancement for ^{15}N is $\gamma_H/(2)\gamma_N = (26.753/(2) \times (-2.713))$ which is equal to -4.93. Generally, a spin $\frac{1}{2}$ nucleus with a positive magnetogyric ratio gives positive NOE enhancement with proton decoupling, while a spin $\frac{1}{2}$ nucleus with a negative magnetogyric ratio gives negative NOE enhancement.

For the ^{15}N nucleus, the maximum enhancement is $-4.93 + 1$, or -3.93. In the case where ^{15}N—^{1}H dipolar relaxation dominates, the signal is inverted (negative) and its intensity is nearly four times what it would be in the absence of ^{1}H irradiation. However, since ^{15}N dipolar relaxation is one of many relaxation mechanisms for ^{15}N, proton decoupling can lead to NOEs ranging from 0 to -4.93 or a signal ranging from $+1$ to -3.93. The experimental downside to this situation is that any NOE between 0 and -2.0 lowers the absolute intensity of the observed signal. In fact, an NOE of exactly -1.0 produces no signal at all. In general, as we saw for carbon and now for nitrogen, proton decoupling is commonly practiced for routine heteronuclear NMR experiments. In so doing, we must always bear in mind the practical outcome of NOE enhancement. It is important to note that inverse-gated proton decoupling, discussed in Chapter 4, can be used to overcome the problem of the NOE potentially lowering signal intensity for ^{15}N.

Let us turn our attention to ^{15}N NMR spectra. As we have already mentioned, natural-abundance ^{15}N NMR spectra can be obtained on modern instruments even though ^{15}N is about an order of magnitude less sensitive than ^{13}C. Today, there is general agreement that liquid ammonia* is the standard primary reference compound for ^{15}N (used

*Nitromethane was used occasionally as an internal reference and set to 0 ppm, but the resulting ^{15}N chemical shifts for nitrogen-containing organic compounds are generally negative. The use of liquid ammonia as an external reference precludes the need for negative numbers because virtually all ^{15}N atoms are deshielded by comparison, but handling liquid ammonia is awkward. The usual procedure is to add 380 ppm to the shift obtained by reference to nitromethane in order to report the shift relative to liquid ammonia.

externally), although, in the past, many compounds such as ammonium nitrate, nitric acid, and nitromethane have been used. When consulting the literature, reliable chemical shifts can usually be obtained after correcting for their reported standard.

We are by now familiar with the construction of the chemical shift scale and need not consider the details here. Nitrogen, like carbon, is a second-row element and in many ways experiences similar electronic influences. To a first approximation, the chemical shifts of nitrogen-containing organic compounds closely parallel carbon chemical shifts. The chemical shift range for nitrogen in common organic compounds is just over 500 ppm, which is about twice that for carbon chemical shifts. Figure 6.1 shows the chemical shift ranges for many types of nitrogen-containing compounds. The relatively large chemical shift range taken together with the very narrow lines for ^{15}N resonances means that the chances of fortuitous overlap in an ^{15}N NMR spectrum are even smaller than in a ^{13}C NMR spectrum. Beyond a simple comparison of ^{15}N chemical shifts against a list of tabulated values, prediction and interpretation of ^{15}N chemical shifts are best carried out using modern quantum chemistry methods, as empirical models can fail.

Lest we take this analogy with carbon too far, we must remember that nitrogen is unique and has peculiar chemical shift features. The two most important ones are both due largely to the unshared pair of electrons found on nitrogen. Just as this electron pair has a large impact on the chemistry of these compounds, it also has a great influence on the chemical shifts of the nitrogen in certain environments. We find quite often that chemical shift positions are more sensitive to the solvent than are structurally similar carbon resonances. The other way that the lone pair on nitrogen influences chemical shift is through protonation. Protonation can have either a shielding or deshielding effect on the nitrogen chemical shift depending on the functional group. For example, strong shielding on the order of 100 ppm due to protonation is observed for nitrogen atoms in conjugated heterocycles, while slight deshielding can be observed for alkyl amines. Solvent effects can be as large as 45 ppm;

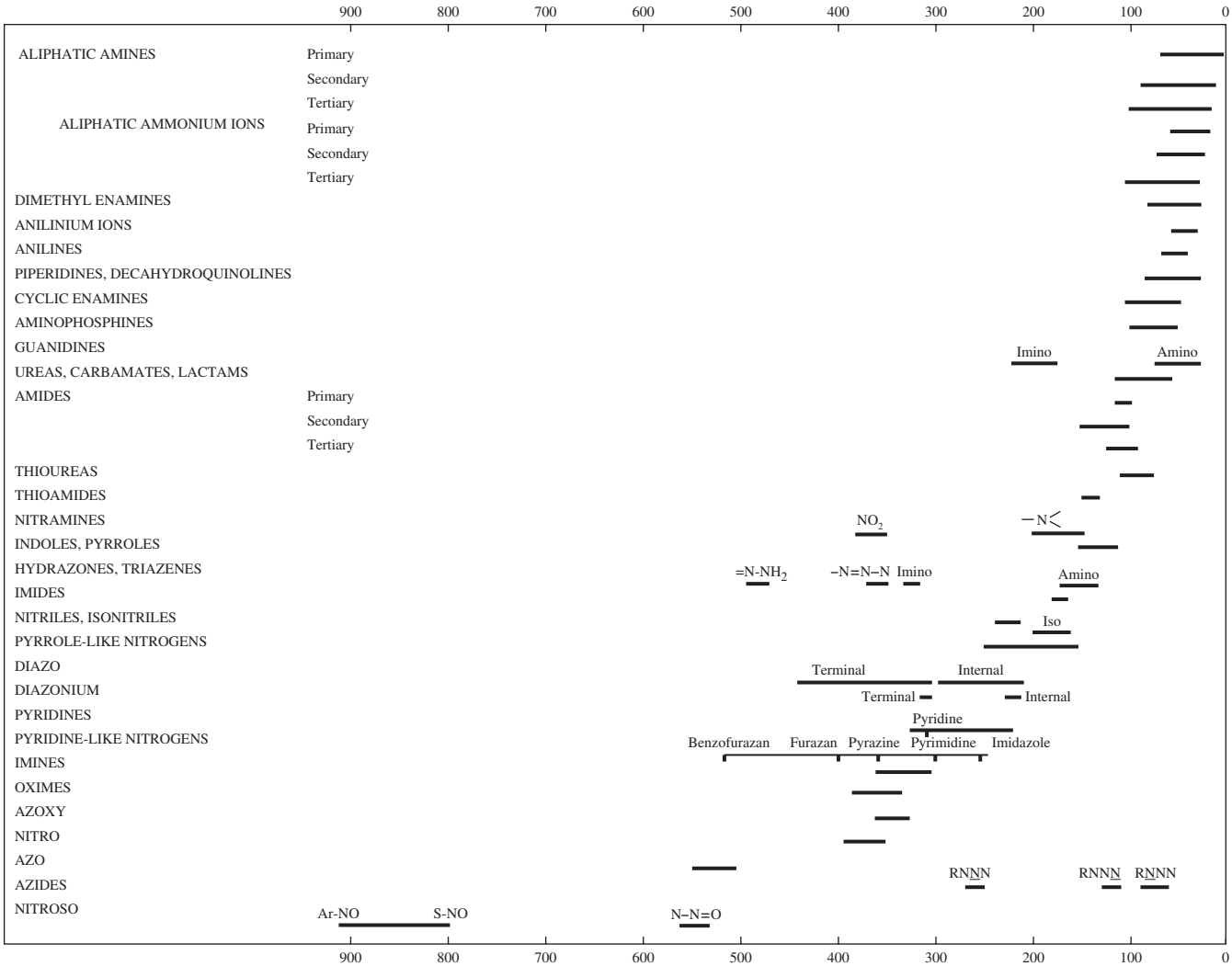

FIGURE 6.1 Chemical shift ranges for various nitrogen-containing compounds and functional groups. Adapted from Levy and Lichter (1979).

TABLE 6.2 Typical *J*-Coupling Constants Involving ^{15}N[a]

Coupling Constant	Typical Range of Values (Hz)
$^{1}J_{NH}$	−40 to −136
$^{2}J_{NH}$	−15 to +15
$^{1}J_{NC}$	−77.5 to +36
$^{1}J_{NN}$	−25 to +15
$^{1}J_{NP}$	−82 to +92
$^{1}J_{NSi}$	<20

[a]See Witanowski et al. (1986, 1993) and Berger et al. (1997).

pyridine, for example, shows a range of 33 ppm in different solvents. These effects are larger than those observed for ^{13}C in large part due to the participation of the nitrogen atom in a hydrogen bond with the solvent. Shifts due to aprotic solvents are typically smaller. The reviews by Witanowski et al. (1986, 1993) summarize the effects of protonation, solvent, temperature, and hydrogen bonding on the nitrogen chemical shifts of various functional groups.

Nitrogen-15 will *J* couple to other spins as we have seen for ^{1}H and ^{13}C. Typical ranges of various coupling constants are summarized in Table 6.2. Note that, due to the low natural abundance of ^{15}N, couplings to ^{15}N are not observed in ^{1}H NMR spectra; however, the converse is not true because in an N—H bond, for example, practically every ^{15}N spin is bonded to a ^{1}H spin. Splittings due to ^{19}F or ^{31}P are similarly readily observed in ^{15}N NMR spectra due to the high natural abundances of the former nuclei. However, couplings between ^{13}C and ^{15}N will not be observed in the NMR spectra of either nucleus unless isotopic enrichment is used.

The proton-decoupled ^{15}N NMR spectrum of formamide is shown in Figure 6.2. This spectrum looks remarkably like a ^{13}C NMR spectrum with a single resonance. This ^{13}C-like appearance as opposed to a ^{1}H-like appearance will be the norm throughout this chapter as long as we apply proton decoupling. The other feature worth noting is the phase of the peak. With proton decoupling, formamide experiences negative NOE enhancement and therefore the peak should be negative.* When processing an FID, however, peaks may be phased either up or down; the phase of a single peak may be manually phased in an arbitrary manner and the sign only has meaning if peaks of differing phase are found in the same spectrum.† The nitrogen in formamide has partial double bond character and is shifted accordingly (deshielding effect).

The proton-coupled and proton-decoupled ^{15}N NMR spectra of ethylenediamine are shown in Figure 6.3. First, we note the relatively shielded position of the nitrogen resonance here compared to formamide. The other noteworthy feature of these spectra is the inset showing proton coupling. Before we discuss this part of the figure, a few general comments are in order. One-, two-, and three-bond ^{15}N—^{1}H couplings are common while long-range couplings usually require intervening π bonds. The magnitude and sign of the coupling constants have been compiled but detailed consideration here is beyond our goal. We note that the magnitude of $^{1}J_{NH}$ varies from about 40 Hz to 135 Hz, $^{2}J_{NH}$ between 0 Hz and 15 Hz, and $^{3}J_{NH}$ between 0 Hz and 10 Hz. If we again consider the inset in Figure 6.3, we note an apparent quintet with a relatively small coupling constant of about 2 Hz to 3 Hz. Our interpretation is that we see no $^{1}J_{NH}$ coupling because of rapid exchange and that the two- and three-bond coupling constants are about the same. In a heteronuclear system (e.g., $^{n}J_{XH}$), first-order rules always apply because $\Delta\nu$ is of the order of millions of hertz.

The proton-decoupled ^{15}N NMR spectrum of pyridine, which has an aromatic nitrogen, is shown in Figure 6.4. A comfortable pattern is now emerging and, in fact, we can safely say that there is nothing extraordinary about this or

*Note that, in general, the phase of the peak could depend on various experimental parameters including the relaxation delay, pulse angle, T_1, etc. The discussion here considers only theoretical magnitude of the NOE.

†Although the origin of the positive and negative peaks in the DEPT experiment is different from that discussed here, DEPT spectra are a useful example of a scenario where peaks of opposite phase are observed in a single spectrum.

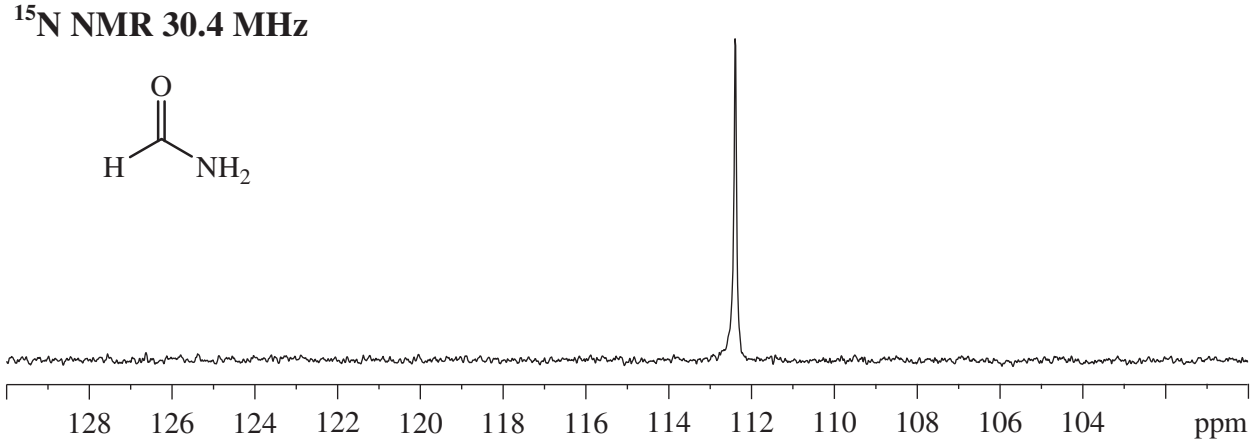

FIGURE 6.2 The proton-decoupled ^{15}N NMR spectrum of formamide in $CDCl_3$, referenced to external $NH_3(l)$.

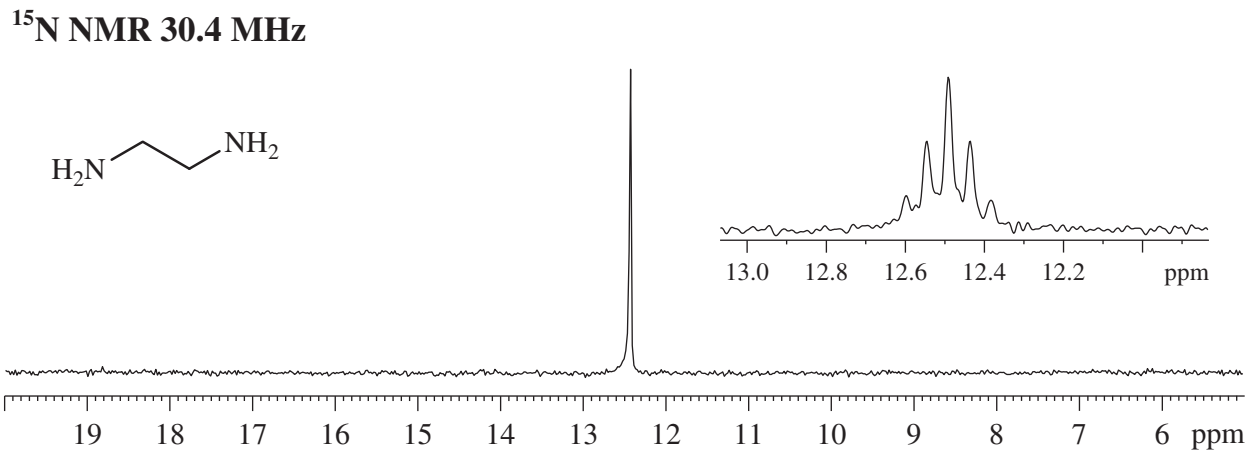

FIGURE 6.3 The proton-decoupled ^{15}N NMR spectrum of ethylene diamine in $CDCl_3$, referenced to external NH_3(l). The proton-coupled ^{15}N NMR spectrum is shown in the inset.

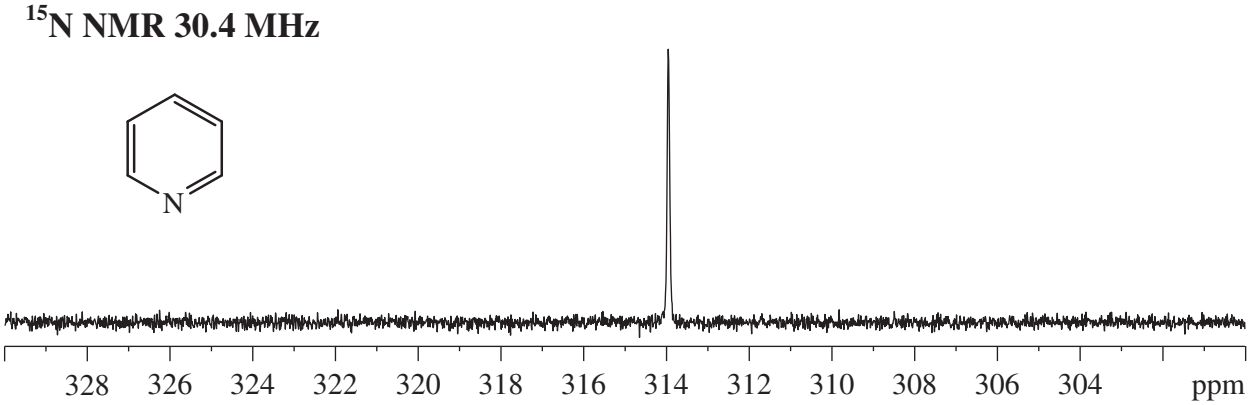

FIGURE 6.4 The proton-decoupled ^{15}N NMR spectrum of pyridine in $CDCl_3$, referenced to external NH_3(l).

any of the spectra that we have seen thus far. Since our goal in this chapter is not to catalog the literally thousands of chemical shifts that have been reported but to introduce the NMR of other nuclei besides ^{13}C and ^{1}H, let us conclude our survey of one-dimensional ^{15}N NMR spectra by briefly considering the proton-decoupled ^{15}N NMR spectrum of quinine (Figure 6.5), a well-studied, naturally occurring alkaloid.

Both nitrogen atoms of quinine are evident and, without hesitation, we can make assignments. If, instead, we

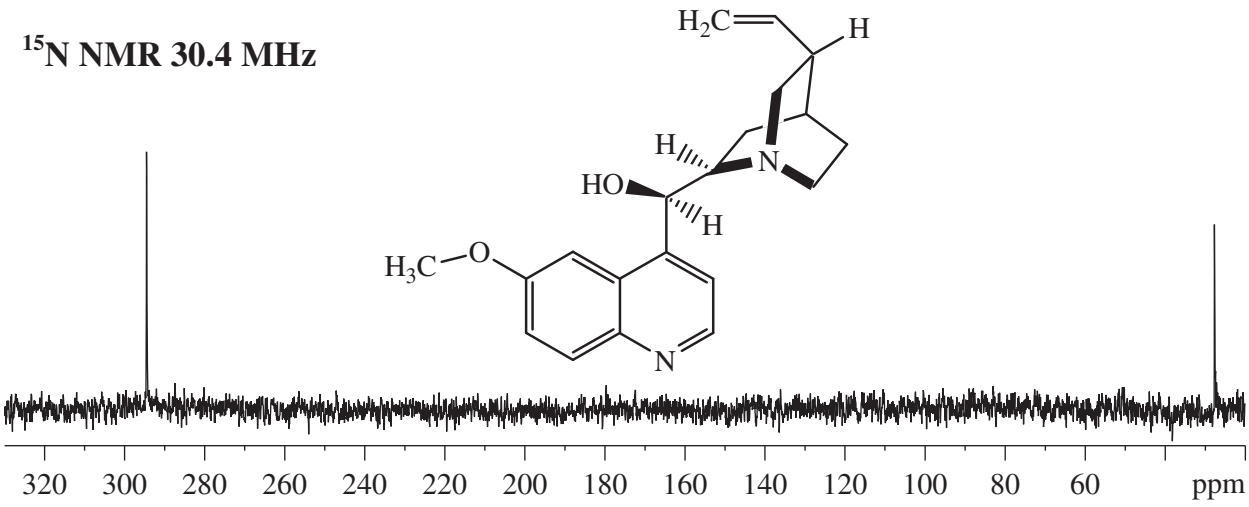

FIGURE 6.5 The proton-decoupled ^{15}N NMR spectrum of quinine in $CDCl_3$, referenced to external NH_3(l).

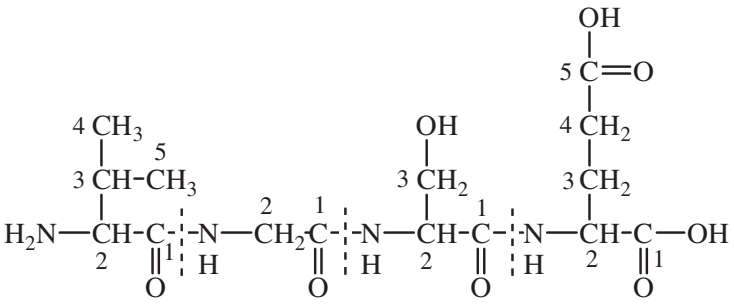

^{1}H–^{15}N HSQC 600 MHz

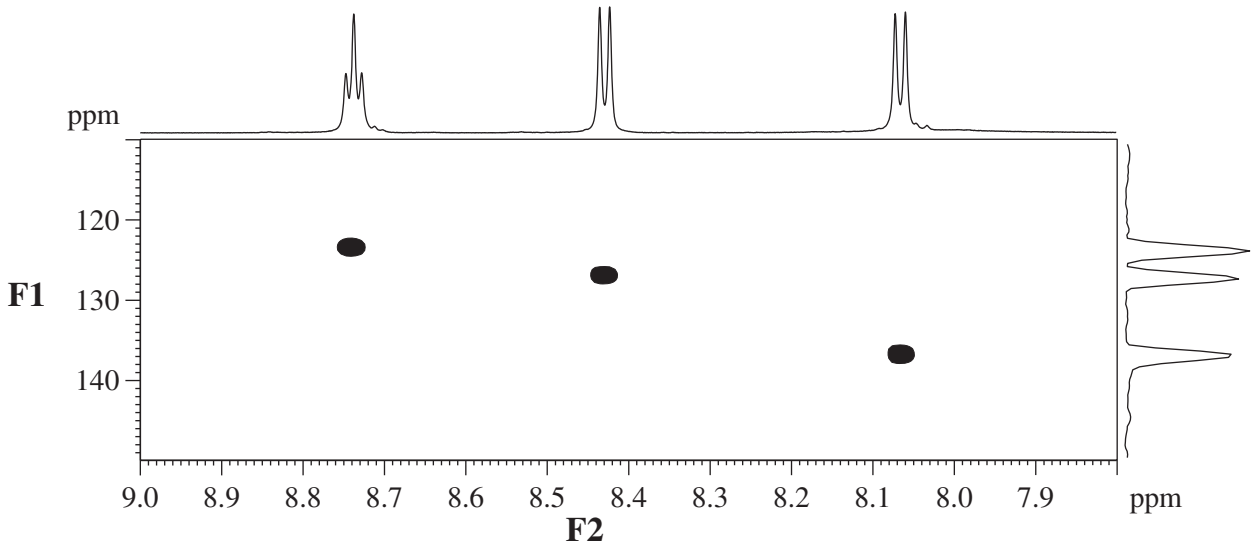

^{15}N Projection from ^{1}H–^{15}N HSQC 600 MHz (1 hour)

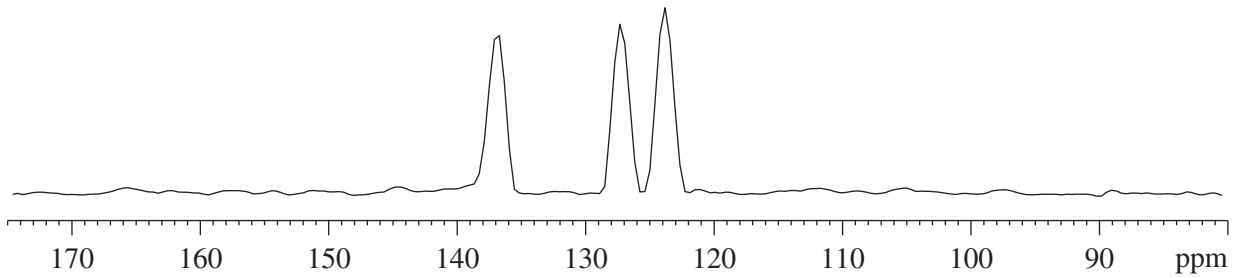

^{15}N NMR 60.8 MHz (15 hours)

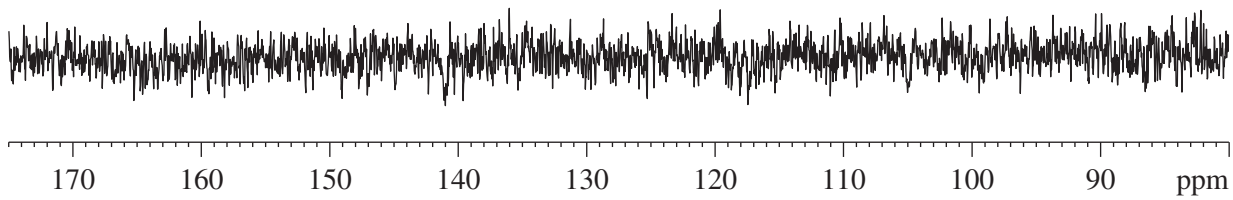

FIGURE 6.6 The ^{1}H—^{15}N HSQC NMR spectrum and its projection of a tetrapeptide (see the structure) in dilute solution. The 2D spectrum required 1 hour of instrument time. The bottom spectrum shows an attempt to obtain a 1D ^{15}N NMR spectrum for 15 hours.

had isolated quinine as a new unknown, natural compound, we could envision a procedure in which we extend the concept of identifying compounds from a combination of spectra to include heteronuclear NMR; ^{15}N NMR would assume a natural place alongside mass spectrometry, IR, and other NMR spectroscopy experiments. Furthermore, as we made the transition from simple ^{1}H and ^{13}C spectra to correlation spectroscopy in Chapter 5, we raise the question: Is there more to ^{15}N NMR than proton-decoupled (and proton-coupled) one-dimensional spectra? The question is rhetorical; it is obvious that correlation experiments are possible and indeed many are commonplace. A good example is the two-dimensional ^{1}H—^{15}N heteronuclear single-quantum coherence (HSQC) experiment, which is illustrated in Figure 6.6 using the tetrapeptide example (valine–glycine–serine–glutamate) used in Chapter 5. (HSQC yields the same type of information as the HMQC; the HSQC has less line broadening in the F1 dimension and therefore provides better resolution in F1.) The experiment was conducted on a dilute solution (5 mg in 0.5 ml of 95% H_2O/5% D_2O) of the compound. This spectrum gives us the chemical shifts of all three amide nitrogens indirectly. At the bottom of this figure is a comparison of the projection from the 2D spectrum onto the ^{15}N axis, which took 1 hour of instrument time to obtain, with an attempt to obtain the ^{15}N spectrum directly, which showed no signal even after 15 hours. As discussed in Chapter 5, inverse-detected experiments give a sensitivity increase of $\left(\gamma^{1}\mathrm{H}/\gamma^{15}\mathrm{N}\right)^{\frac{3}{2}}$, which is about 310-fold for ^{1}H—^{15}N HSQC compared to directly detected methods. In the field of biomolecular NMR, proteins are prepared for NMR analysis by expressing them with ^{15}N-labeled amino acid residues. Since ^{15}N has a natural abundance of 0.368%, labeling to 99% increases the sensitivity of the experiment by a factor of about 270, which, when combined with the HSQC type experiment, yields about an 84000-fold sensitivity increase over natural abundance directly detected methods. Thus, it is possible to obtain good quality spectra on proteins up to 50 kDa (and beyond under favorable conditions). As an illustration of the power of this technique, the 600 MHz ^{1}H—^{15}N HSQC NMR spectrum of myoglobin is shown in Figure 6.7; a complete analysis of this spectrum is beyond the scope of this text. Note that the 1D ^{1}H NMR spectrum of myoglobin, which has 153 amino acid residues, is hopelessly overlapped in the amide region (see the spectrum along the F2 axis). However, by separating these resonances in the ^{15}N dimension (F1), most of the ^{1}H—^{15}N correlations are clearly resolved. This is a nice demonstration of the resolving power of two-dimensional correlation spectroscopy. The amide ^{15}N chemical shift range for peptides covers a 40 ppm window from about 110 ppm to 150 ppm. It should be noted that with modern instrumentation, it is possible to acquire ^{15}N—^{1}H HSQC and HMBC NMR spectra for small molecules with ^{15}N in natural abundance. Two-dimensional correlation experiments with ^{15}N open up many possibilities for structural characterization, with spectral interpretation being generally analogous to what we have seen for ^{13}C in Chapter 5.

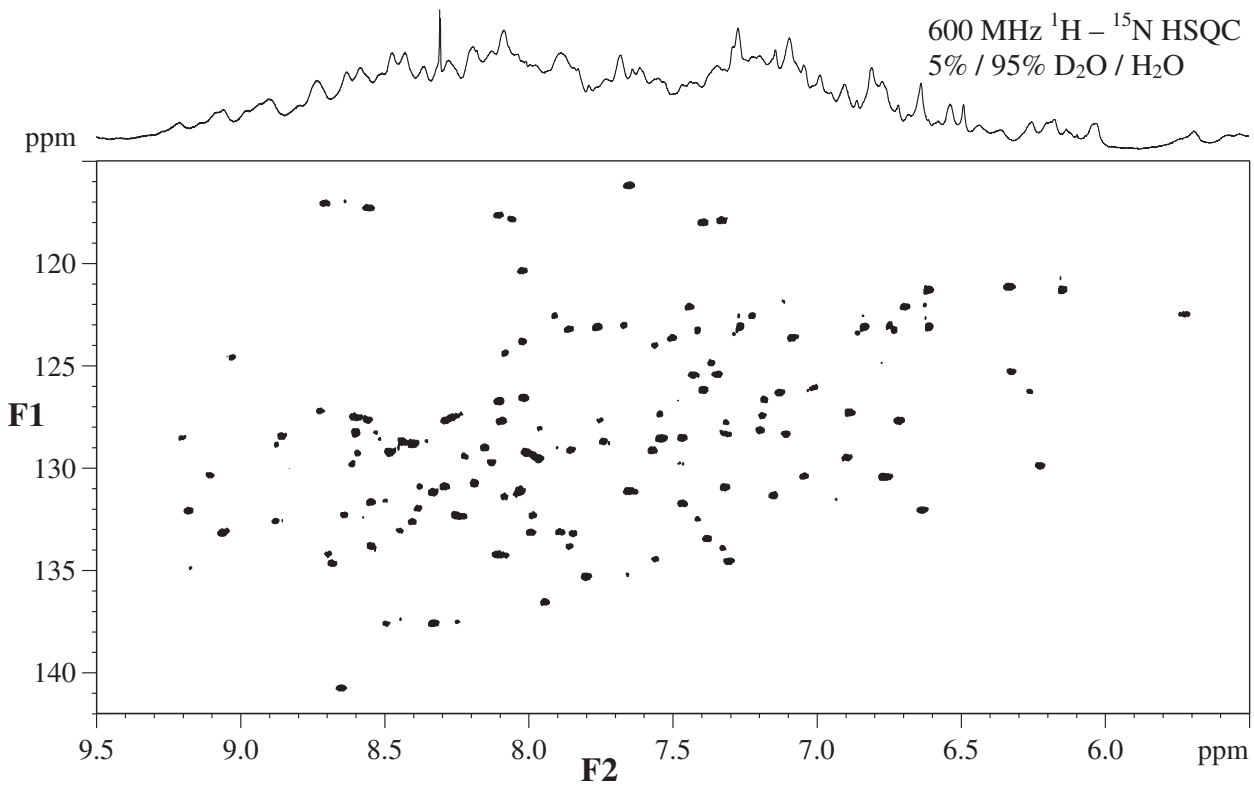

FIGURE 6.7 The ^{1}H—^{15}N HSQC spectrum of ^{15}N-labeled myoglobin.

6.3 ^{19}F NUCLEAR MAGNETIC RESONANCE

The NMR of ^{19}F has great historic importance. Fluorine has only one naturally occurring isotope, ^{19}F, and Table 6.1 shows that it is an ideal nucleus for study by NMR. The sensitivity of ^{19}F is about 0.83 that of ^{1}H; this is the main reason why ^{19}F NMR developed contemporaneously with ^{1}H NMR. The literature on chemical shifts and coupling constants is now old, and, again, some caution is needed when comparing older chemical shifts with newer literature because much of it is referenced to external CF_3COOH. Today, trichlorofluoromethane, $CFCl_3$, is the standard ^{19}F reference compound (0.00 ppm compared to CF_3COOH at −78.5 ppm), which is generally inert, volatile, and gives rise to a single ^{19}F resonance.

Our approach to ^{19}F NMR is different than was our approach to ^{15}N NMR and this section is brief. Fluorine is monovalent and can be thought of as a substitute for hydrogen in organic compounds. Fluorine is virtually unknown in naturally occurring organic compounds; our interest in fluorine NMR involves synthetic compounds. Proton decoupling in ^{19}F NMR experiments does not involve NOE enhancement in a critical way, and there are no other experimental factors out of the ordinary. Much of the original chemical shift and coupling constant data for ^{19}F were published contemporaneously with those of ^{1}H. Figure 6.8 gives chemical shift ranges for various fluorine-containing compounds.

The ^{1}H NMR spectrum of fluoroacetone was given in Chapter 3 to show the effect of fluorine on ^{1}H spectra. Recall that resonances from both the methylene group and the methyl group were split by coupling to the ^{19}F nucleus, each into doublets with different coupling constants. In Figure 6.9, we have an opportunity to see the reciprocal effect of the protons on the ^{19}F nucleus in fluoroacetone. This figure shows a complete set of ^{19}F, ^{1}H, and ^{13}C NMR spectra. In the proton-decoupled ^{19}F spectrum, we see only a singlet for the fluorine atom, reminding us again of a ^{13}C spectrum. In the proton-coupled spectrum, however, we see that the fluorine is coupled to two sets of hydrogens, producing a triplet with a large coupling constant; the triplet is further split into three quartets by a four-bond coupling with the protons of the methyl group. The coupling constants are listed on each spectrum for convenience. We emphasize again that the combination of ^{1}H, ^{13}C, and ^{19}F spectra is more convincing and more informative than any one spectrum is by itself.

An example of an aromatic fluorine-containing compound can be found in Figure 6.10, where we have recorded the ^{19}F NMR spectra (both proton-coupled and decoupled) of fluorobenzene along with the ^{1}H and ^{13}C NMR spectra. Once again, we find a singlet for the fluorine atom in the proton-decoupled spectrum and a complex multiplet for the fluorine atom in the proton-coupled spectrum. The fluorine atom couples differently to the ortho-, meta-, and para-protons in this mono-substituted compound. Proton–fluorine coupling constants can be found in Appendix F of Chapter 3. It is notable that all of the aromatic ^{13}C resonances appear as doublets due to coupling with the fluorine, even though the fluorine is up to four bonds away. Such two-, three-, and four-bond couplings to fluorine are not unusual in rigid systems.

It is tempting to treat the proton NMR spectrum in a similar fashion to our treatment of fluoroacetone. What we have, however, is a higher order system, described by the Pople notation AA′GG′MX, where X is the fluorine nucleus. The A and A′ protons are not magnetically equivalent since they do not couple equally with the G proton or the G′ proton. Nor are the G and G′ protons magnetically equivalent since they do not couple equally with the A proton or the A′ proton. The fluorine resonance is deceptively simple and appears to be described by first-order rules. However, because the fluorine is part of a higher order spin system, it is *not* properly described by first-order rules and very complicated spectra are obtained depending on the strength of the applied magnetic field [see Page Jr. (1967)].

Chemical shifts for ^{19}F are difficult to predict empirically and we will make no attempt to offer a predictive model. Table 6.3 presents a compilation of ^{19}F chemical shifts for various fluorine-containing compounds. One reason that the chemical shifts for ^{19}F are difficult to predict and rationalize is that less than 1% of the shielding of the ^{19}F nucleus in organic compounds is due to diamagnetic shielding. Rather, paramagnetic shielding is the predominant factor and is difficult to predict using empirical models. Quantum chemical calculations are more useful in this context. A selection of *J*-coupling constants involving ^{19}F is presented in Table 6.4.

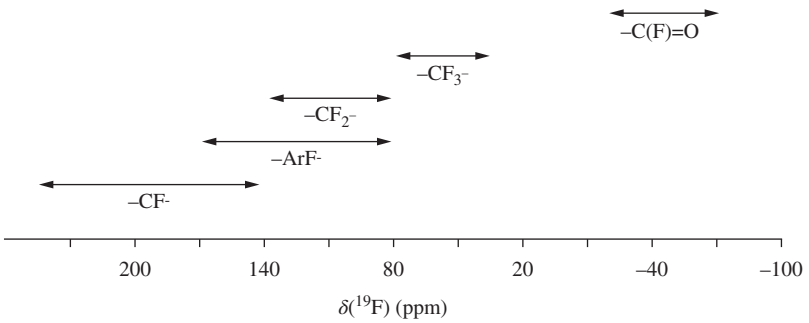

FIGURE 6.8 Fluorine-19 chemical shift ranges for compounds with various fluorine-containing functional groups.

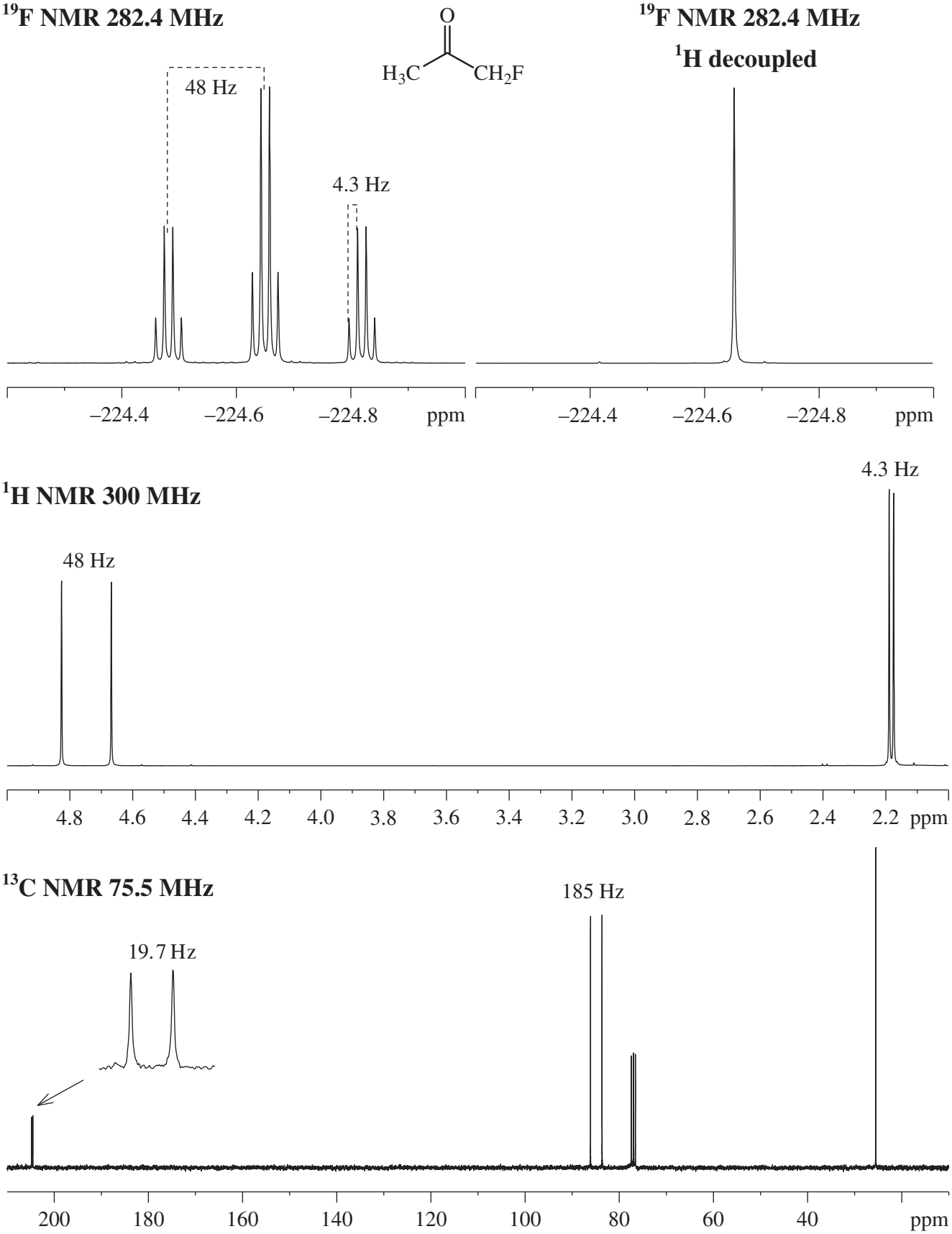

FIGURE 6.9 NMR spectra of fluoroacetone in $CDCl_3$.Top left: the proton-coupled ^{19}F NMR spectrum. Top right: the proton-decoupled version of the same spectrum. Middle: ^{1}H NMR spectrum showing doublet splittings due to coupling with ^{19}F. Bottom: ^{13}C NMR spectrum showing doublet splittings due to coupling with ^{19}F.

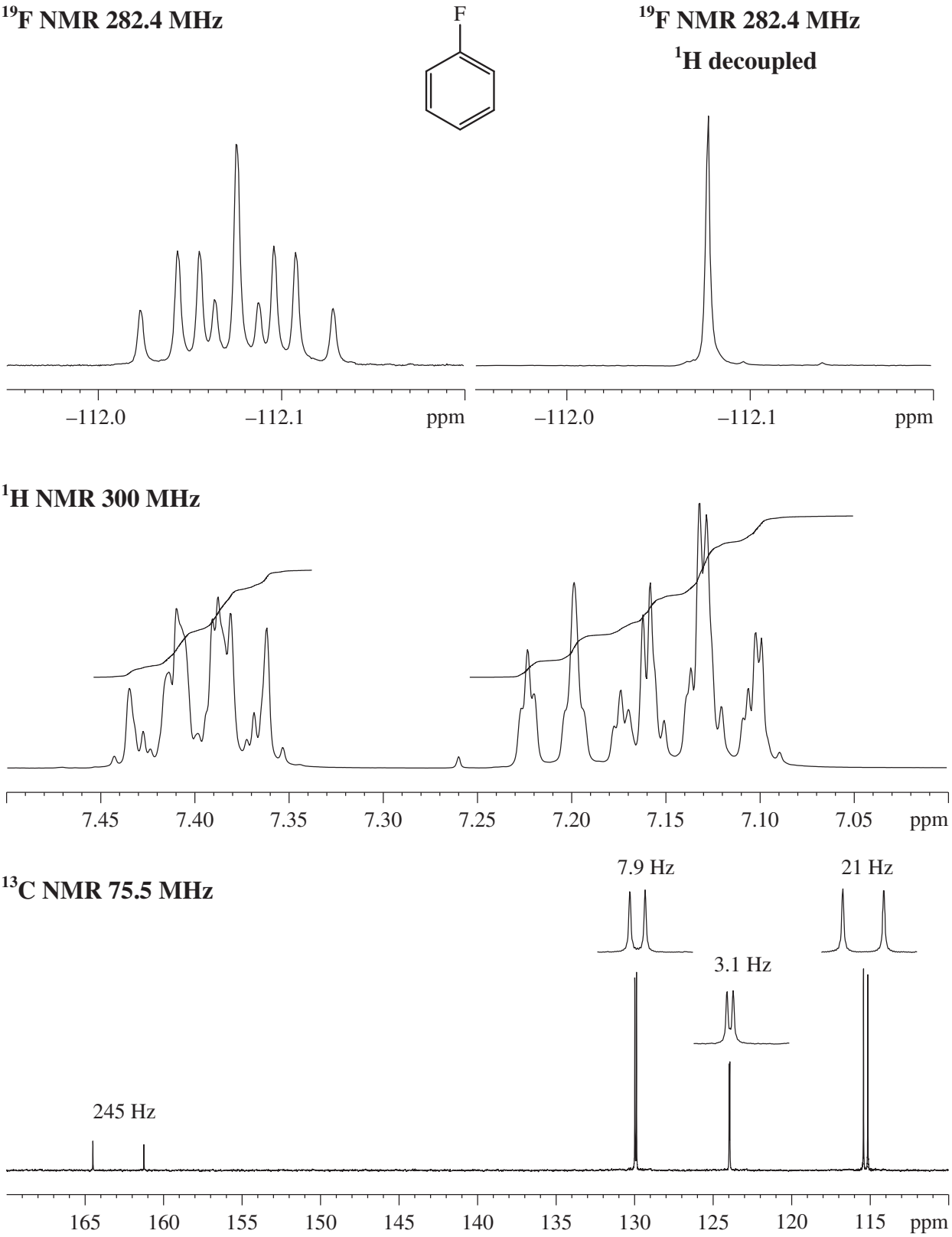

FIGURE 6.10 Top: the proton-decoupled and proton-coupled ^{19}F NMR spectra (282.4 MHz) of fluorobenzene in $CDCl_3$. Middle: ^{1}H NMR spectrum. Bottom: ^{1}H-decoupled ^{13}C NMR spectrum. There is long-range coupling to ^{19}F evident in the ^{1}H and ^{13}C NMR spectra (see text for explanation).

TABLE 6.3 Chemical Shifts for Various Fluorine-Containing Compounds

Compound	$\delta(^{19}F)$ (ppm)
$CFCl_3$	0
CF_2Cl_2	8
CF_3Cl	28.6
$CFBr_3$	7.4
CF_2Br_2	7
$CFBr_3$	7
CFH_3	271.9
CF_2H_2	1436
CF_3H	78.6
CF_4	62.3
C_4F_8	135.15
C_5F_{10}	132.9
$(CF_3)_2CO$	84.6
$CF_3C(O)OH$	76.5
$CF_3C(O)OCH_3$	74.2
CF_3COOEt	78.7
$(CF_3)_3N$	56
CH_2FCN	251
$FCH{=}CH_2$	114
$F_2C{=}CH_2$	81.3
$F_2C{=}CF_2$	135
C_6F_6	164.9
C_6H_5F	113.5
p-$C_6H_4F_2$	106
$C_6H_5CFH_2$	207
$C_6H_5C(O)OCF_3$	73.9
$C_6H_5C(CF_3)_2OH$	74.7
$C_6H_5CF_3$	63.7
F_2 (elemental)	422.9
SF_6	57.4
SiF_4	163.3
HF (aqueous)	204
KF (aqueous)	125.3

In closing this section, we mention that beyond routine organic chemistry applications, ^{19}F NMR has in addition found widespread applications in various specialized areas of research including polymer chemistry, metabolism studies, biopharmaceutical sciences, magnetic resonance imaging, and in studies of fluorine-labeled proteins. The interested reader is referred to recent reviews by Kitevski-LeBlanc and Prosser (2012) and Yu et al. (2013).

TABLE 6.4 Typical *J*-Coupling Constants Involving ^{19}F[a]

Structure	
	$^2J_{HF}$ (Hz)
FCH_2CH_2Cl	46
CFH_3	46
CF_2H_2	50
CF_3H	79
cis-$C_2F_2H_2$	72.7
trans-$C_2F_2H_2$	74.3
	$^3J_{HF}$ (Hz)
p-fluorobromobenzene	8.62
FCH_2CH_2Cl	23
F_3CCH_3	12.8
cis-$C_2F_2H_2$	20.4
trans-$C_2F_2H_2$	4.4
$FC{\equiv}CH$	21
	$^4J_{HF}$ (Hz)
$(CH_3)_3NBF_3$	0.8
p-fluorobromobenzene	4.90
$CF_3C(CH_3){=}CHNO_2$	1.45
$CF_3C{\equiv}CF$	4.3
	$^2J_{FF}$ (Hz)
$CF_2BrCHBrCl$	154
CF_2ClCH_2Cl	170
$CF_2{=}CBrCl$	30
o-difluorobenzene	$^3J_{FF} = -21$ Hz
m-difluorobenzene	$^4J_{FF} = 6$ Hz
p-difluorobenzene	$^5J_{FF} = 18$ Hz
	$^1J_{CF}$ (Hz)
$CFBr_3$	372
$CFCl_3$	337
CF_2H_2	235
CF_4	257
$FClC{=}CCl_2$	303
p-hydroxyfluorobenzene	$^1J_{CF} = 237$ Hz $^2J_{CF} = 23$ Hz $^3J_{CF} = 7.9$ Hz $^4J_{CF} = 2.1$ Hz
NF_3	$^1J_{NF} = 160$ Hz
CH_3SiF_3	$^1J_{SiF} = 267$ Hz
$ClCH_2PF_2$	$^1J_{PF} = -1203$ Hz

[a]See Emsley et al. (1976) *Prog. Nucl. Magn. Reson. Spectrosc.*, **10**, 83–756.

6.4 ^{29}SI NUCLEAR MAGNETIC RESONANCE

Silicon-containing organic compounds are increasingly used by synthetic organic chemists and by polymer chemists. The ^{29}Si nucleus is the only isotope of silicon with a magnetic moment and has a natural abundance of 4.7%. We have already come across the ^{29}Si nucleus in the ^{1}H NMR spectrum of TMS; a small doublet, characterized by a coupling constant ($^2J_{SiH}$) of about 6 Hz, with an intensity of 2% to 3% straddles the sharp, intense TMS singlet (Section 3.7.4). This small doublet represents the 4.7% of spin $\frac{1}{2}$ ^{29}Si, which naturally occurs in all silicon compounds.

Table 6.1 reveals that the receptivity of the ^{29}Si nucleus is about two times that of the ^{13}C nucleus when both are recorded at natural abundance. The magnetogyric ratio for ^{29}Si (γ_{Si}) is negative (-5.319×10^7 rad T^{-1} s^{-1}) so, for routine proton-decoupled spectra, we again have the possibility of negative ^{29}Si NOE enhancement depending, on the

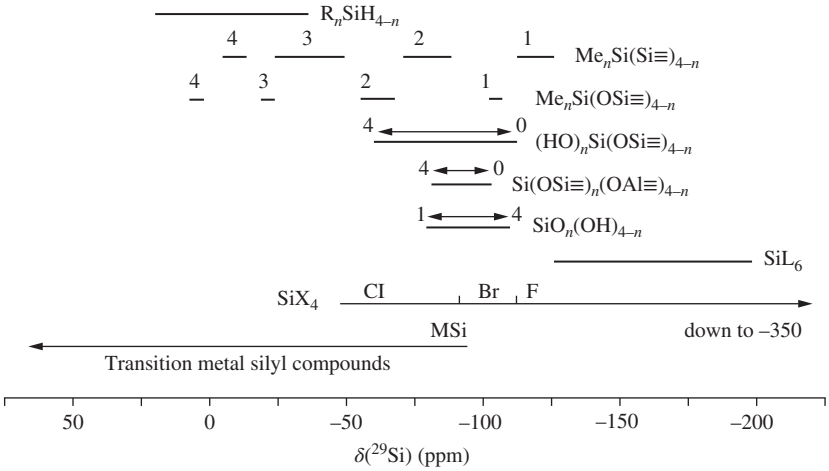

FIGURE 6.11 Silicon-29 chemical shift ranges for various silicon-containing compounds and functional groups. Adapted from Bruker Almanac 1995.

relative importance of dipolar spin relaxation. In this case, the maximum NOE is −2.51. This situation is much worse than with ^{15}N NOEs because only NOEs between −2.01 and the maximum, −2.51, actually result in an enhancement. All other values result in a net decrease in signal intensity compared to no proton decoupling. Thus, experimental conditions must be carefully controlled if we are to realize the maximum signal, especially because the ^{29}Si nucleus can have long relaxation time constants. As mentioned for ^{15}N, such intensity problems can be largely overcome with the use of inverse-gated proton decoupling. Two-dimensional correlation experiments involving ^{29}Si (e.g., HMBC) can be used in many applications, including, for example, to monitor silyl-protecting group migration in organic compounds.

The chemical shifts for ^{29}Si in common organic compounds are much smaller than for ^{13}C shifts in common compounds. This smaller shift range is probably due to the lack of multiple bonds to silicon in common functional groups. Figure 6.11 gives chemical shift ranges for various silicon-containing compounds, and some specific values are given in Table 6.5. Typical coupling constants that involve ^{29}Si are presented in Table 6.6.

The proton-decoupled ^{29}Si NMR spectrum of TMS is shown at the top of Figure 6.12 with the proton-coupled spectrum for comparison as an inset. TMS is the obvious choice for a ^{29}Si reference compound and we set it at 0 ppm. The proton-coupled spectrum is quite interesting because the ^{29}Si nucleus is coupled to 12 equivalent protons in TMS. First-order rules predict a multiplet with 13 peaks. There are 9 peaks clearly visible and 11 with a little imagination; we do not see the full 13 peaks because the outer peaks are too weak and are lost in the noise.

The ^{29}Si NMR spectra of triethylsilane in both proton-decoupled and proton-coupled modes are presented in Figure 6.12. The proton-decoupled spectrum gives a singlet that is only slightly shifted from TMS. In triethylsilane, there is a proton directly attached to silicon, resulting in a large one-bond coupling ($^1J_{SiH}$) of about 175 Hz. There are

TABLE 6.5 Some Representative ^{29}Si Chemical Shifts[a]

Compound	$\delta(^{29}Si)$ (ppm)
$(CH_3)_3Si$ (TMS)	0.00
$(((CH_3)_3)Si)_2O$	6.53
$(EtO)_4Si$ (TEOS)	−82.04
Silicon oil or silicone grease	−22.0
Ph_4Si	−14
SiF_4	−112
$SiCl_4$	−18
$SiBr_4$	−92
SiI_4	−350
SiH_4	−91.9
$Me_3SiSiMe_3$	−19.7
$Me_3SiMn(CO)_5$	17.95
Me_3SiOMe	20.72
Me_3SiOH	14.84
TBDMS-OMe	21.02
TBDMS-OEt	18.52

[a]See Williams, E.A. (1983) *Ann. Rep. Nucl. Magn. Reson. Spectrosc.*, **15**, 235–289.

TABLE 6.6 Typical *J*-Coupling Constants Involving ^{29}Si[a]

Compound	Coupling Constant (Hz)
$(EtO)_3SiH$	$^1J_{SiH} = -287$
H_4Si	$^1J_{SiH} = -202.5$
Me_3SiH	$^1J_{SiH} = -184.0$
F_3SiSiF_3	$^1J_{SiF} = 321.8$
F_3SiNMe_2	$^1J_{SiF} = 201.4$
$CH_2{=}CHSiCl_3$	$^1J_{SiC} = 113$
$MeSiCl_3$	$^1J_{SiC} = 86.6$
Me_3SiH	$^1J_{SiC} = 50.8$
$(Cl_3Si)_2SiCl_2$	$^1J_{SiSi} = 186$
$Me_3SiSiMe_2F$	$^1J_{SiSi} = 98.7$
$(Me_3Si)_4Si$	$^1J_{SiSi} = 52.5$
$(H_3Si)_3P$	$^1J_{SiP} = 42.2$
Me_3SiPH_2	$^1J_{SiP} = 16.2$

[a]See Williams, E.A. (1983) *Ann. Rep. Nucl. Magn. Reson. Spectrosc.*, **15**, 235–289.

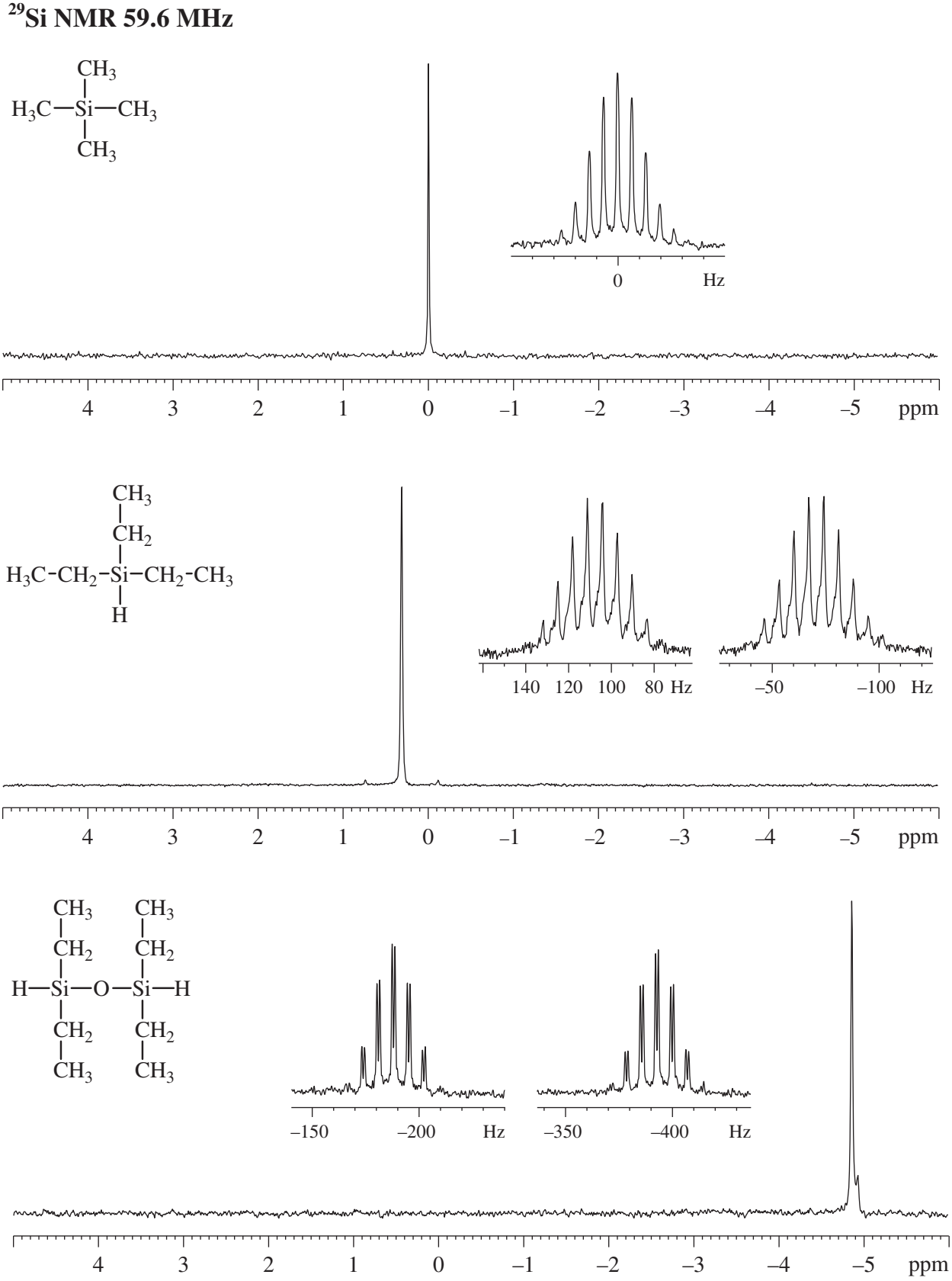

FIGURE 6.12 (a) The proton-decoupled and proton-coupled (inset) ^{29}Si NMR spectra (59.6 MHz) of tetramethylsilane (TMS) in $CDCl_3$. The outer peaks of the multiplet are not discernible because of an insufficient signal-to-noise ratio. (b) The proton-decoupled and proton-coupled (inset) ^{29}Si NMR spectra (59.6 MHz) of triethylsilane in $CDCl_3$. (c) Bottom, the proton-decoupled and proton-coupled (inset) ^{29}Si NMR spectra (59.6 MHz) of 1,1,3,3-tetraethyldisiloxane in $CDCl_3$.

smaller two- and three-bond couplings that lead to identical complex multiplets.

A final example of ^{29}Si NMR is presented at the bottom of Figure 6.12, where we find the proton-decoupled and proton-coupled ^{29}Si NMR spectra of 1,1,3,3-tetraethyldisiloxane. This compound is commercially available and is widely used to make various silicon-containing polymers. Before using the sample, a conscientious chemist might analyze it using various methods, which we now imagine might include ^{29}Si NMR. In this case, one would find that there are two types of silicon in the sample (i.e., an unwanted impurity) because we find a peak with an intensity of about 5% to 10% on the shoulder of the main peak in the proton-decoupled spectrum. The chemical shifts of both peaks are negative, a common feature for silicon bonded to oxygen.

The proton-coupled spectrum reveals a large one-bond coupling constant ($^1J_{SiH}$) of about 215 Hz. The coupling pattern derived from the two- and three-bond coupling is complex but the pattern might serve as a starting point in the interpretation of ^{29}Si NMR spectra of reaction products.

TABLE 6.7 Phosphorus-31 Chemical Shifts for Various Phosphorus-Containing Compounds[a]

Phosphorus (III) Compounds	δ (ppm)	Phosphorus (V) Compounds	δ (ppm)
PMe_3	62	Me_3PO	36.2
PEt_3	20	Et_3PO	48.3
$P(n\text{-}Pr)_3$	33	$[Me_4P]^+$	24.4
$P(i\text{-}Pr)_3$	19.4	$[PO_4]^{3-}$	6
$P(n\text{-}Bu)_3$	32.5	PF_5	80.3
$P(i\text{-}Bu)_3$	45.3	PCl_5	80
$P(s\text{-}Bu)_3$	7.9	$MePF_4$	29.9
$P(t\text{-}Bu)_3$	63	Me_3PF_2	158
$PMeF_2$	245	Me_3PS	59.1
$PMeH_2$	163.5	Et_3PS	54.5
$PMeCl_2$	192	$[Et_4P]^+$	40.1
$PMeBr_2$	184	$[PS_4]^{3-}$	87
PMe_2F	186	$[PF_6]^-$	145
PMe_2H	99	$[PCl_4]^+$	86
PMe_2Cl	96.5	$[PCl_6]^-$	295
PMe_2Br	90.5	Me_2PF_3	8

Adapted from Bruker Almanac (1995).
[a]Referenced to 85% H_3PO_4 (aq) at 0 ppm.

6.5 ^{31}P NUCLEAR MAGNETIC RESONANCE

The last of the four nuclides that we treat briefly in this chapter is ^{31}P, the only naturally occurring isotope of phosphorus. Phosphorus is of great interest to the organic chemist because reagents containing phosphorus, which range from various inorganic forms of phosphorus to the organic phosphines, phosphites, phosphonium salts, phosphorus ylides, etc., have long been used by organic chemists; the nucleus is of great interest to the biochemists primarily because of the nucleic acids that contain phosphate esters and also smaller molecules such as ADP and ATP.

NMR experiments with ^{31}P are rather straightforward; ^{31}P is a spin $\frac{1}{2}$ nucleus with a positive magnetogyric ratio (10.840×10^7 rad T^{-1} s^{-1}). ^{31}P NOE enhancement from proton decoupling is positive with a maximum of 1.23. There has been a long history and therefore a rich literature of ^{31}P NMR. ^{31}P chemical shift data are reliable because 85% H_3PO_4(aq) is virtually the only ^{31}P primary reference compound used (external) and it remains the preferred reference today (the top spectrum in Figure 6.13). The chemical shift range for ^{31}P is rather large and generalizations are dangerous. In fact, even chemical shifts of compounds where phosphorus is in different oxidation states are not diagnostic of this state. All is not lost, however, since there are many reliable published studies of ^{31}P chemical shifts. Typical values are shown in Table 6.7. Recall that chemical shift values can be positive or negative. Representative proton–phosphorus coupling constants can be found in Appendix F of Chapter 3, and a summary of coupling constant ranges due to coupling of ^{31}P with protons and various other nuclides is given in Table 6.8. Shown in Figure 6.13 is the proton-decoupled ^{31}P NMR spectrum of triphenylphosphine, a common reagent in organic synthesis. The spectrum itself is unremarkable in that we see a single resonance for the single phosphorus atom in triphenylphosphine. What is remarkable is the fact that there is a chemical shift range of less than 10 ppm for three different compounds (the first two in Figures 6.13 and 6.14, respectively) and yet the phosphorus atoms differ widely with respect to oxidation state, attached groups, and so on. We would have a very difficult job trying to rationalize these ^{31}P chemical shifts empirically.

The bottom two spectra in Figure 6.13 are the proton-decoupled ^{31}P NMR spectra of triphenylphosphite and triethylphosphite. Both compounds give a sharp single peak as expected. The point here is to illustrate that even without a set of predictive rules for chemical shift, we can nonetheless expect useful information with little chance of overlap. By themselves, these spectra might not provide much information but when combined with other spectra, they give one more perspective on composition, structure, and stereochemistry.

TABLE 6.8 Typical J-Couplings Involving ^{31}P[a]

Coupling Constant	Typical Range of Values (Hz)
$^1J_{PH}$	140 to 1115
$^1J_{PP}$	−620 to +766
$^1J_{PB}$	13 to 175
$^1J_{PC}$	−43 to 448
$^1J_{PF}$	−550 to −1441
$^1J_{PN}$	−82 to +92
$^1J_{PHg}$	140 to 17500
$^1J_{PAg}$	210 to 1100

[a]See Verkade and Quin (1987) and Berger et al. (1997).

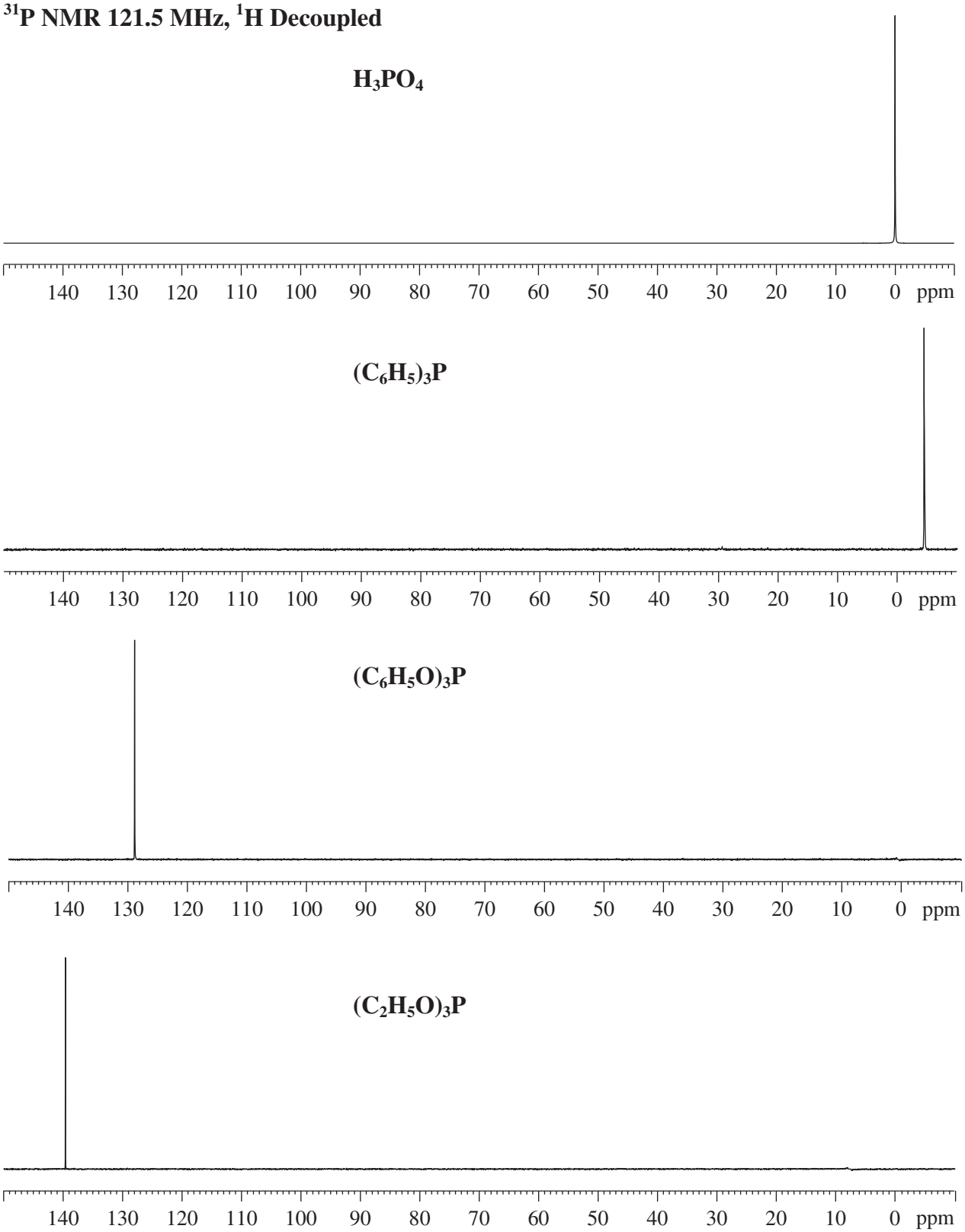

FIGURE 6.13 From top to bottom, the proton-decoupled ^{31}P NMR spectrum (121.5 MHz) of 85% phosphoric acid with a small amount of D_2O, of triphenylphosphine in $CDCl_3$, of triphenylphosphite in $CDCl_3$, and of triethylphosphite in $CDCl_3$.

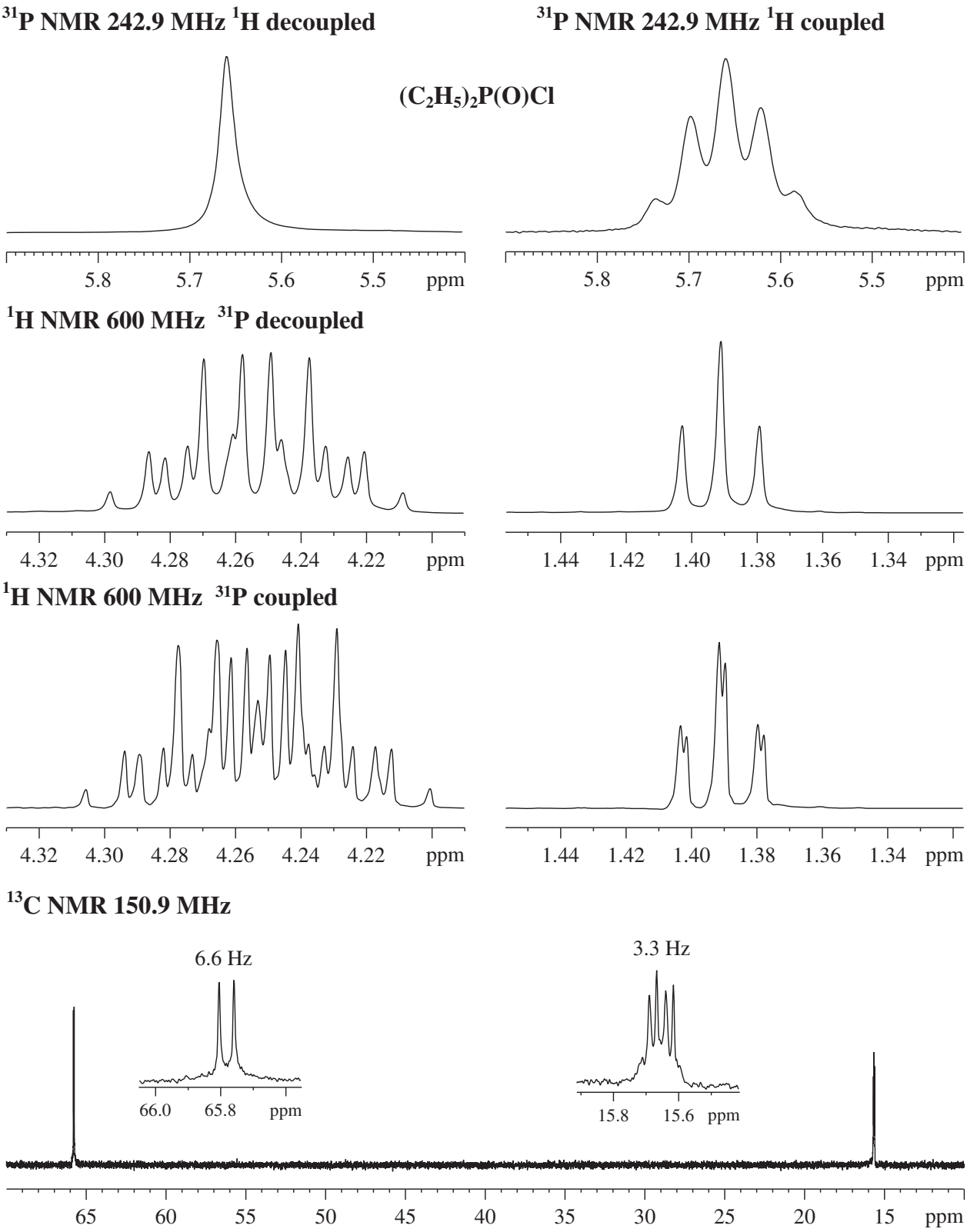

FIGURE 6.14 (a–d) From top to bottom, the proton-decoupled and proton-coupled ^{31}P NMR spectra (242.9 MHz), the ^{31}P-decoupled ^{1}H NMR spectrum, the ^{31}P-coupled ^{1}H NMR spectrum, and the ^{31}P-coupled ^{13}C NMR spectrum of diethyl chlorophosphate in $CDCl_3$.

The proton-decoupled ^{31}P NMR spectrum of diethyl chlorophosphate is found in Figure 6.14 along with the proton-coupled spectrum. Also included with this figure are the ^{1}H and ^{13}C NMR spectra for a complete set. The proton-coupled ^{31}P NMR spectrum shows an apparent quintet, suggesting that there is no appreciable coupling of the phosphorus nucleus to the protons of the methyl groups. Inspection of the corresponding proton NMR spectrum reveals, however, that the methyl resonance is actually a triplet of doublets with a four-bond $^{31}P—^{1}H$ coupling constant of ca. 1 Hz. Thus, we conclude that the 1 Hz coupling is not resolved in the ^{31}P NMR spectrum but simply results in line broadening. The four protons of the two methylene groups couple equally (approximately) to the phosphorus atom to give the observed quintet. The methylene proton resonances in the ^{1}H NMR spectrum may at first seem too complex. The matter is resolved by noting that the methylene protons in diethyl chlorophosphate are diastereotopic (see Figure 3.42), and therefore they are not chemically equivalent and show strong coupling. First-order analysis is impossible.

In this brief chapter, it is not possible to cover all areas of application of ^{31}P NMR. Phosphorus-31 NMR spectroscopy has broad application in the study of metal–phosphine complexes and related compounds, and the role of these in catalysis, for example. The interested reader is referred to Berger et al. (1997) and Nelson (2002). It is also important to note that, as for the other nuclei we have discussed, ^{31}P can be observed to great effect in two-dimensional HSQC and HMQC correlation experiments to gain additional structural insights.

6.6 CONCLUSIONS

We have introduced in this chapter a few other useful nuclei and some examples of their spectra. The discussion has intentionally largely been centered on organic compounds. It is useful to be aware of the possibilities as well as the limitations associated with NMR spectroscopy of less common nuclei. Multinuclear magnetic resonance is a very broad field of research with diverse applications. For the organic chemist, many of the nuclei that potentially will be of interest in addition to ^{1}H and ^{13}C have been discussed in this chapter. The interested reader is encouraged to further consult the references as well as the general NMR literature for additional applications in inorganic chemistry, materials science, polymer chemistry, and beyond.

REFERENCES

For a list of Chapter References, please visit: www.wiley.com/college/silverstein.

STUDENT EXERCISES

6.1 Deduce the structure of the compound whose molecular formula is $C_5H_{12}N_2$ from the combined information from the ^{1}H, ^{13}C, DEPT, and ^{15}N NMR spectra. There is no proton-coupled ^{15}N NMR spectrum provided because it provides no useful information.

6.2 The compound for this exercise is a reagent commonly used in organic synthesis; its molecular formula is $C_6H_{15}SiCl$. Provided are the ^{1}H, ^{13}C, DEPT, and ^{29}Si (proton-decoupled) spectra.

6.3 Determine the structure of the phosphorus-containing compound whose molecular formula is $C_{19}H_{18}PBr$ from the ^{1}H, ^{13}C, DEPT, and ^{31}P (both proton-coupled and proton-decoupled) NMR spectra.

6.4 Determine the structure of the fluorine-containing compound for which the mass, IR, ^{1}H NMR, ^{13}C/DEPT NMR, and ^{19}F NMR spectra are given.

6.5 Using the information in Appendix A, calculate the Larmor frequencies of ^{7}Li, ^{23}Na, and ^{207}Pb in a magnetic field of 21.1 T.

6.6 When the NMR spectra of heteronuclei show *J* couplings to protons, why are these couplings essentially never "strong" in the sense of Pople (AB)?

^{1}H NMR 300 MHz

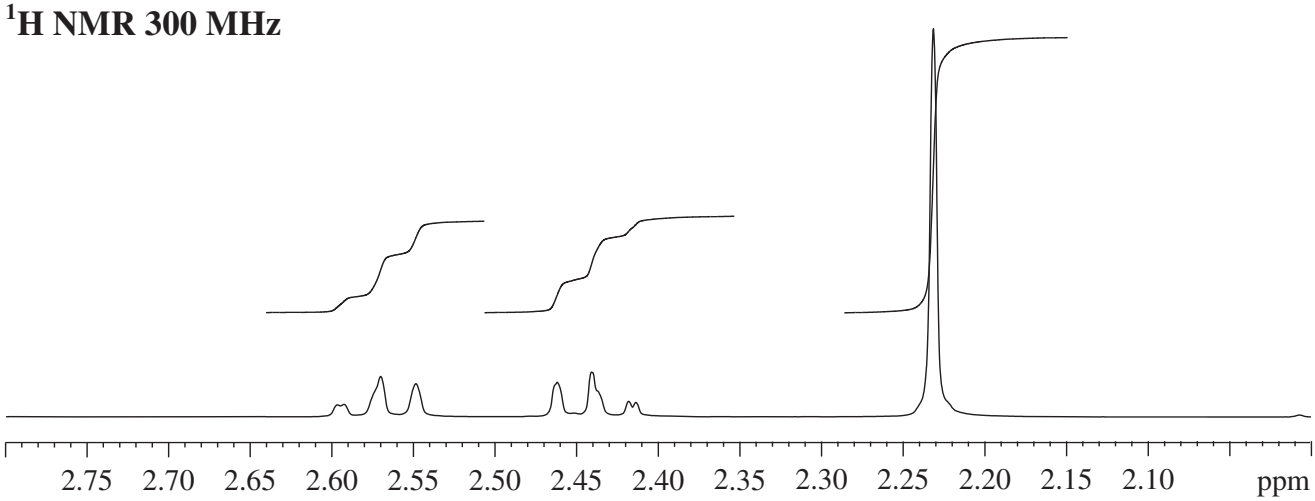

^{13}C/DEPT NMR 75.5 MHz

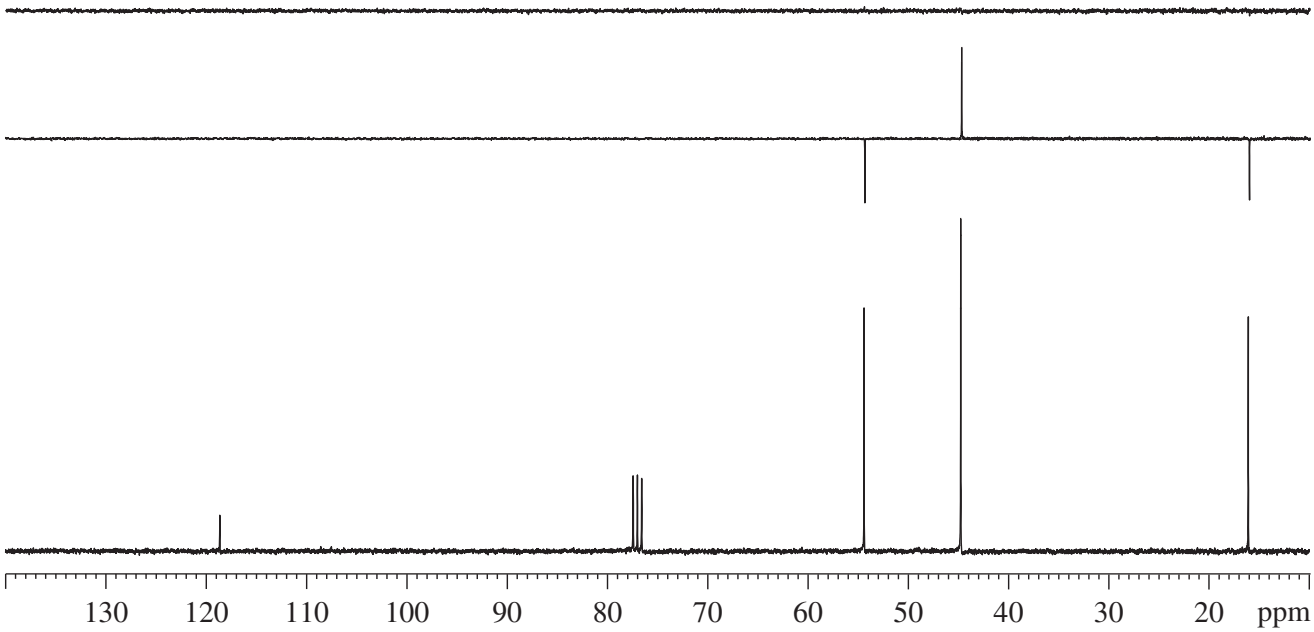

^{15}N NMR 30.4 MHz

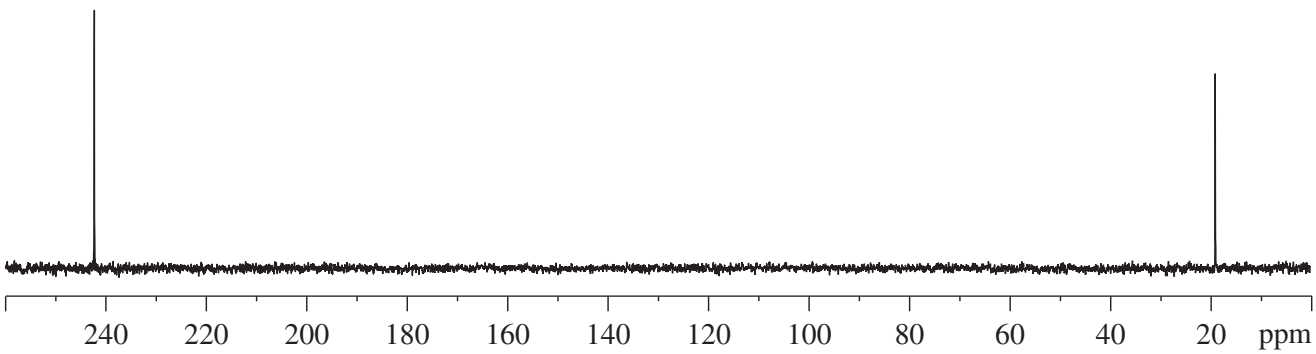

^{1}H NMR 300 MHz

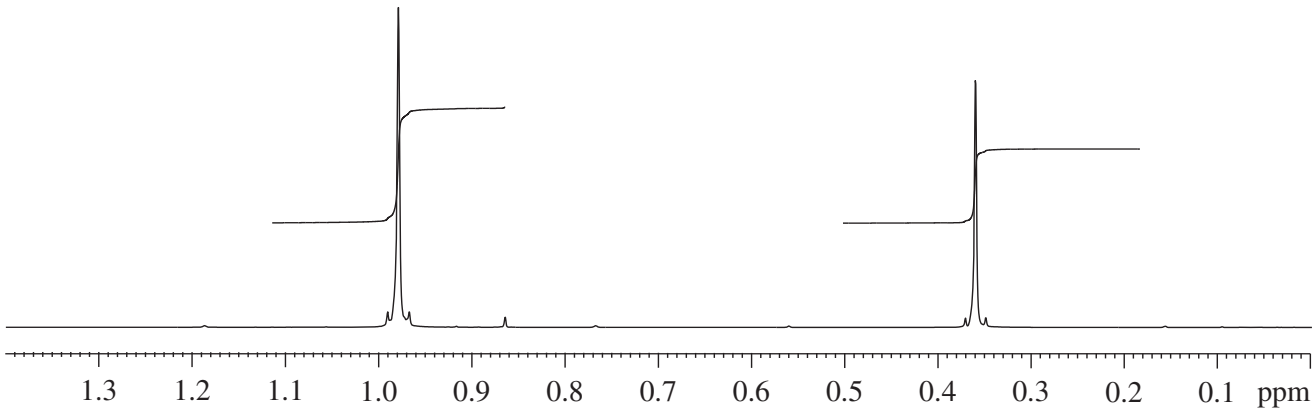

^{13}C/DEPT NMR 75.5 MHz

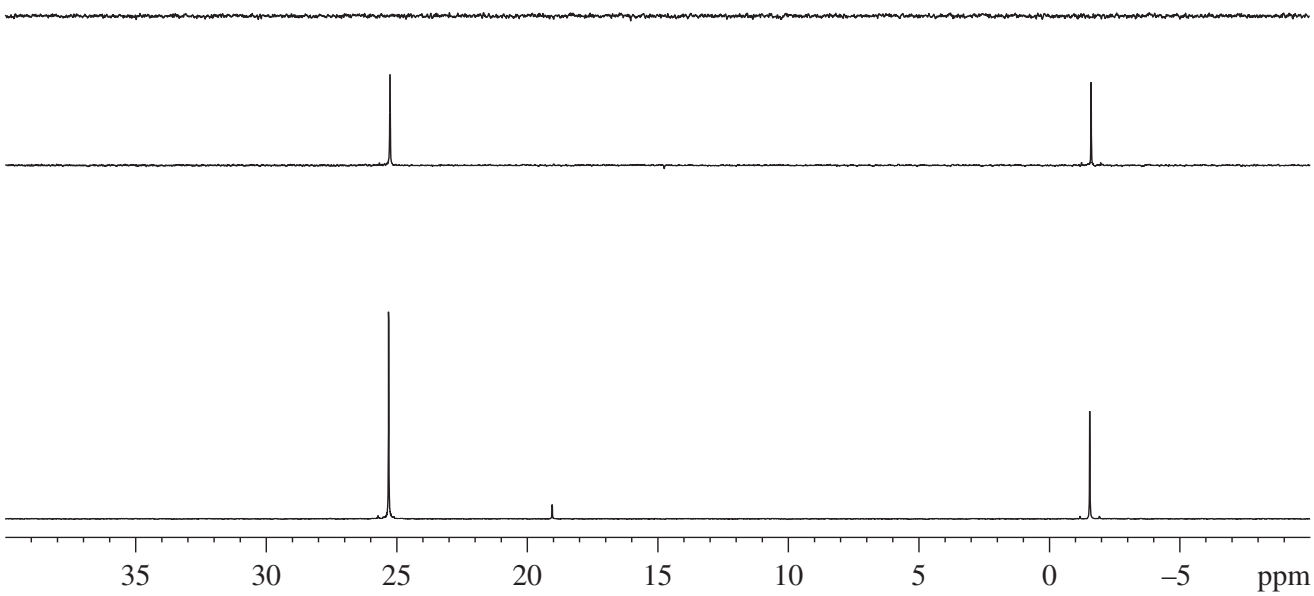

^{29}Si NMR 59.6 MHz

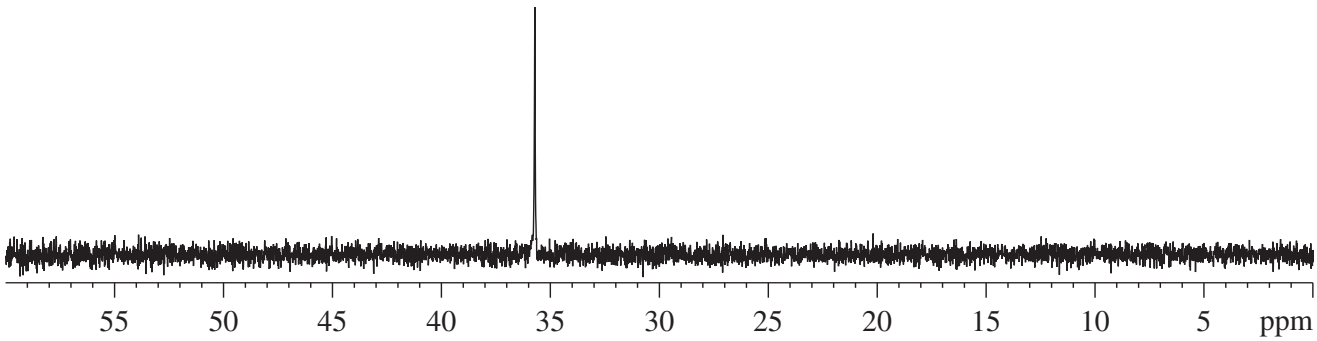

^{1}H NMR 300 MHz

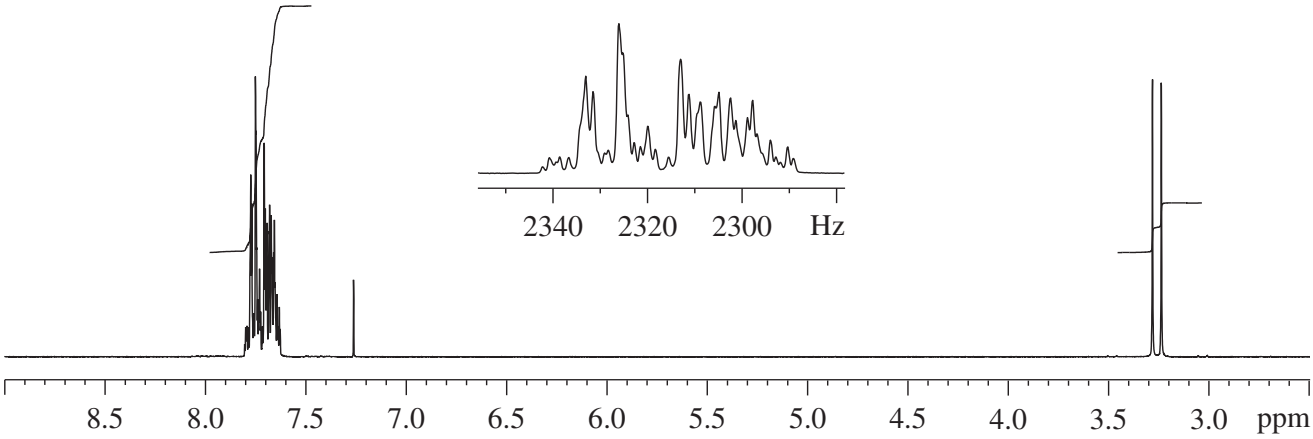

^{13}C/DEPT NMR 75.5 MHz

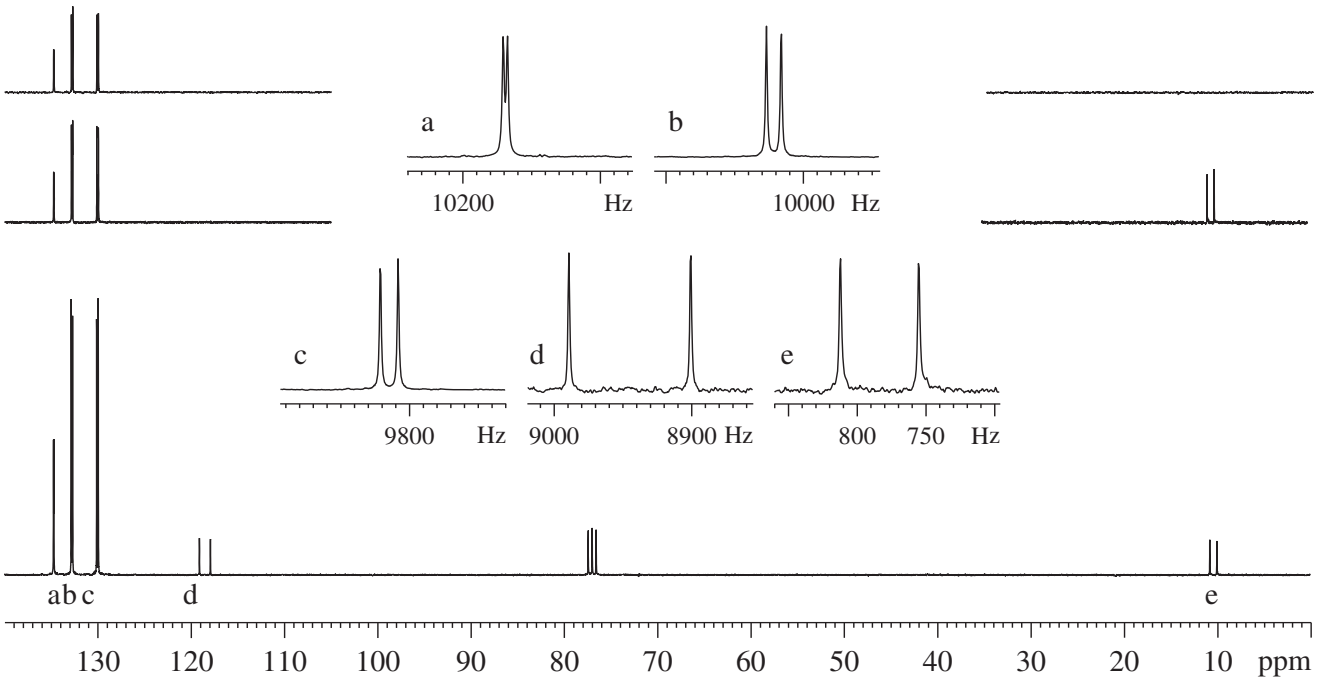

^{31}P NMR 121.5 MHz, ^{1}H decoupled

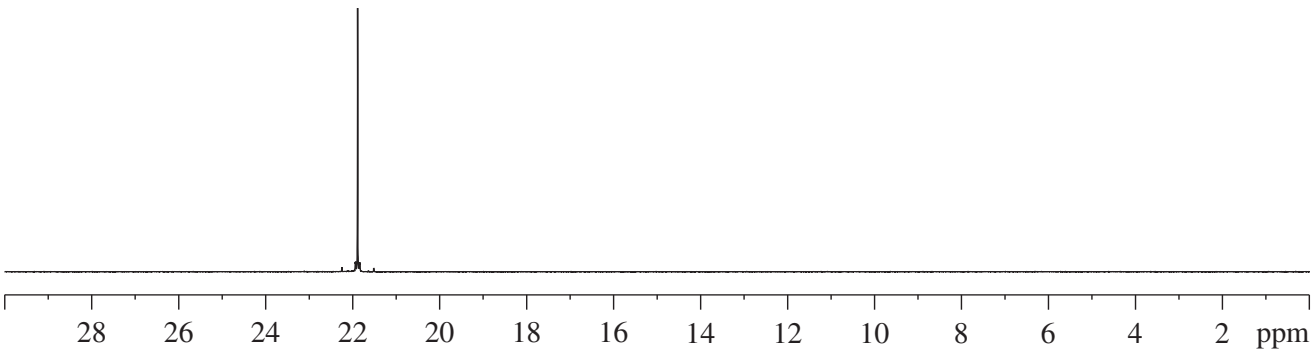

MASS

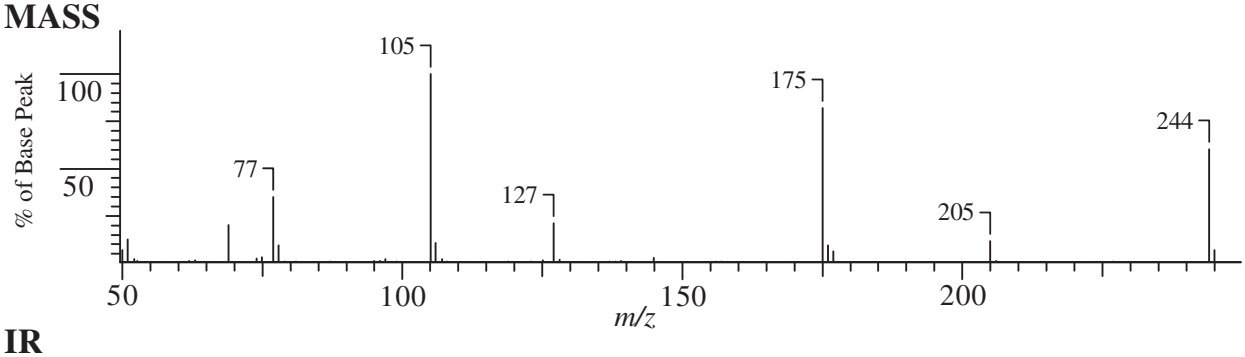

IR

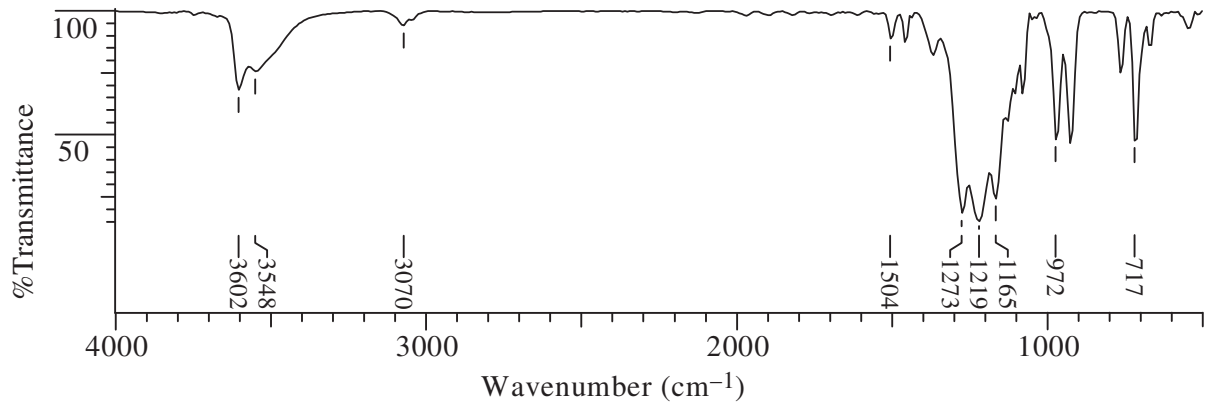

^{1}H NMR 300 MHz

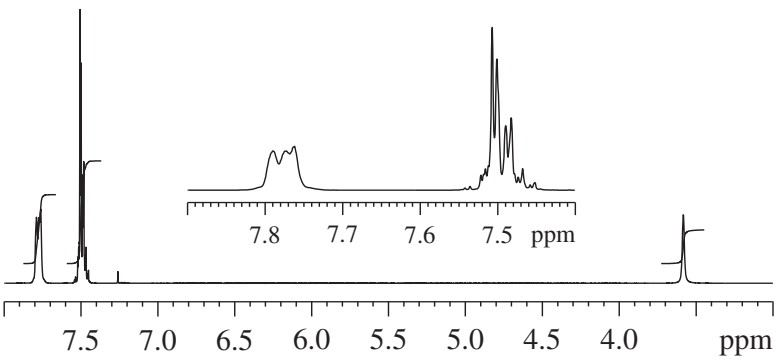

^{19}F NMR 282.4 MHz

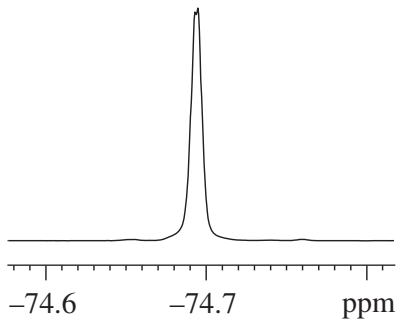

^{13}C/DEPT 75.5 MHz

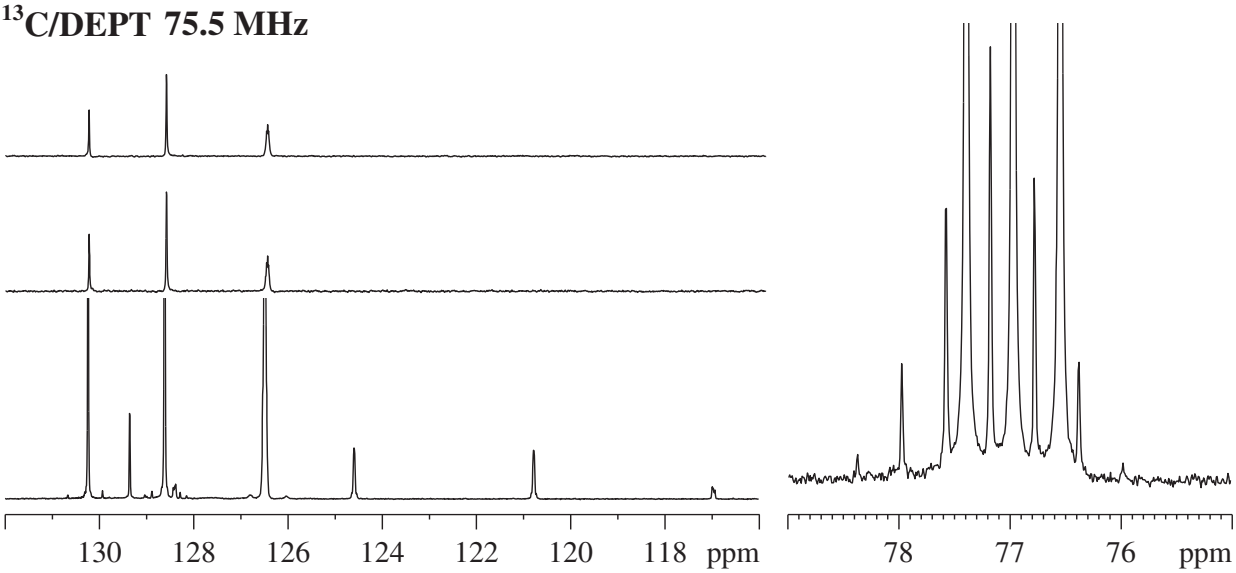

APPENDIX A PROPERTIES OF MAGNETICALLY ACTIVE NUCLEI

Isotope	Spin	Natural Abundance (%)	Magnetic Moment μ/μ_N	Magnetogyric Ratio $\gamma/10^7$ rad T^{-1} s^{-1}	Quadrupole Moment Q/fm^2	Frequency Ratio (Ξ)	Reference Compound	Relative Receptivity	
								D^{Proton}	D^{Carbon}
^{1}H	$\frac{1}{2}$	99.9885	4.837353570	26.7522128	–	100.000000	Me_4Si	1	5.87×10^{3}
^{2}H	1	0.0115	1.21260077	4.106 62791	0.286	15.350609	$(CD_3)_3Si$	1.11×10^{-6}	6.52×10^{-3}
^{3}H	$\frac{1}{2}$	–	5.159714367	28.5349779	–	106.663974	Me_4Si	–	–
^{3}He	$\frac{1}{2}$	1.37×10^{-4}	−3.685154336	−20.3801587	–	76.179437	He(gas)	6.06×10^{-7}	3.56×10^{-3}
^{6}Li	1	7.59	1.1625637	3.9371709	−0.0808	14.716086	LiCl	6.45×10^{-4}	3.79
^{7}Li	$\frac{3}{2}$	92.41	4.20407505	10.3977013	−4.01	38.863797	LiCl	0.271	1.59×10^{3}
^{9}Be	$\frac{3}{2}$	100	−1.520136	−3.759666	5.288	14.051813	$BeSO_4$	1.39×10^{-2}	81.5
^{10}B	3	19.9	2.0792055	2.8746786	8.459	10.743658	$BF_3 \cdot Et_2O$	3.95×10^{-3}	23.2
^{11}B	$\frac{3}{2}$	80.1	3.4710308	8.5847044	4.059	32.083974	$BF_3 \cdot Et_2O$	0.132	7.77×10^{2}
^{13}C	$\frac{1}{2}$	1.07	1.216613	6.728284	–	25.145020	Me_4Si	1.70×10^{-4}	1
^{14}N	1	99.632	0.57100428	1.9337792	2.044	7.226317	CH_3NO_2 or NH_3(l)	1.00×10^{-3}	5.9
^{15}N	$\frac{1}{2}$	0.368	−0.49049746	−2.71261804	–	10.132912	CH_3NO_2 or NH_3(l)	3.84×10^{-6}	2.25×10^{-2}
^{17}O	$\frac{5}{2}$	0.038	−2.24077	−3.62808	−2.56	13.556457	D_2O	1.11×10^{-5}	6.50×10^{-2}
^{19}F	$\frac{1}{2}$	100	4.553333	25.18148	–	94.094011	CCl_3F	0.834	4.90×10^{3}
^{21}Ne	$\frac{3}{2}$	0.27	−0.854376	−2.11308	10.155	7.894296	Ne (gas)	6.65×10^{-6}	3.91×10^{-2}
^{23}Na	$\frac{3}{2}$	100	2.8629811	7.0808493	10.40	26.451900	NaCl	9.27×10^{-2}	5.45×10^{2}
^{25}Mg	$\frac{5}{2}$	10.00	−1.01220	−1.63887	19.94	6.121635	$MgCl_2$	2.68×10^{-4}	1.58
^{27}Al	$\frac{5}{2}$	100	4.3086865	6.9762715	14.66	26.056859	$Al(NO_3)_3$	0.207	1.22×10^{3}
^{29}Si	$\frac{1}{2}$	4.6832	−0.96179	−5.3190	–	19.867187	Me_4Si	3.68×10^{-4}	2.16
^{31}P	$\frac{1}{2}$	100	1.95999	10.8394	–	40.480742	H_3PO_4	6.65×10^{-2}	3.91×10^{2}
^{33}S	$\frac{3}{2}$	0.76	0.8311696	2.055685	−6.78	7.676000	$(NH_4)_2SO_4$	1.72×10^{-5}	0.101
^{35}Cl	$\frac{3}{2}$	75.78	1.061035	2.624198	−8.165	9.797909	NaCl	3.58×10^{-3}	21
^{37}Cl	$\frac{3}{2}$	24.22	0.8831998	2.184368	−6.435	8.155725	NaCl	6.59×10^{-4}	3.87
^{39}K	$\frac{3}{2}$	93.2581	0.50543376	1.2500608	5.85	4.666373	KCl	4.76×10^{-4}	2.79

(^{40}K)	4	0.0117	−1.4513203	−1.5542854	−7.30	5.802018	KCl	6.12×10^{-7}	3.59×10^{-3}
(^{41}K)	$\frac{3}{2}$	6.7302	0.2773961	0.68606808	7.11	2.561305	KCl	5.68×10^{-6}	3.33×10^{-2}
^{43}Ca	$\frac{7}{2}$	0.135	−1.494067	−1.803069	−4.44	6.730029	$CaCl_2$	8.68×10^{-6}	5.10×10^{-2}
^{45}Sc	$\frac{7}{2}$	100	5.3933489	6.5087973	−22.0	24.291747	$Sc(NO_3)_3$	0.302	1.78×10^{3}
^{47}Ti	$\frac{5}{2}$	7.44	−0.93294	−1.5105	30.2	5.637534	$TiCl_4$	1.56×10^{-4}	0.918
^{49}Ti	$\frac{7}{2}$	5.41	−1.25201	−1.51095	24.7	5.639037	$TiCl_4$	2.05×10^{-4}	1.2
(^{50}V)	6	0.25	3.6137570	2.6706490	21.0	9.970309	$VOCl_3$	1.39×10^{-4}	0.818
^{51}V	$\frac{7}{2}$	99.75	5.8380835	7.0455117	−5.2	26.302948	$VOCl_3$	0.383	2.25×10^{3}
^{53}Cr	$\frac{3}{2}$	9.501	−0.61263	−1.5152	−15.0	5.652496	K_2CrO_4	8.63×10^{-5}	0.507
^{55}Mn	$\frac{5}{2}$	100	4.1042437	6.645 2546	33.0	24.789218	$KMnO_4$	0.179	1.05×10^{3}
^{57}Fe	$\frac{1}{2}$	2.119	0.1569636	0.8680624	–	3.237778	$Fe(CO)_5$	7.24×10^{-7}	4.25×10^{-3}
^{59}Co	$\frac{7}{2}$	100	5.247	6.332	42.0	23.727074	$K_3[Co(CN)_6]$	0.278	1.64×10^{3}
^{61}Ni	$\frac{3}{2}$	1.1399	−0.96827	−2.3948	16.2	8.936051	$Ni(CO)_4$	4.09×10^{-5}	0.24
^{63}Cu	$\frac{3}{2}$	69.17	2.8754908	7.1117890	−22.0	26.515473	$[Cu(CH_3CN)_4][ClO_4]$	6.50×10^{-2}	3.82×10^{2}
^{65}Cu	$\frac{3}{2}$	30.83	3.07465	7.60435	−20.4	28.403693	$[Cu(CH_3CN)_4][ClO_4]$	3.54×10^{-2}	2.08×10^{2}
^{67}Zn	$\frac{5}{2}$	4.10	1.035556	1.676688	15.0	6.256803	$Zn(NO_3)_2$	1.18×10^{-4}	0.692
(^{69}Ga)	$\frac{3}{2}$	60.108	2.603405	6.438855	17.1	24.001354	$Ga(NO_3)_3$	4.19×10^{-2}	2.46×10^{2}
^{71}Ga	$\frac{3}{2}$	39.892	3.307871	8.181171	10.7	30.496704	$Ga(NO_3)_3$	5.71×10^{-2}	3.35×10^{2}
^{73}Ge	$\frac{9}{2}$	7.73	−0.9722881	−0.9360303	−19.6	3.488315	$(CH_3)_4Ge$	1.09×10^{-4}	0.642
^{75}As	$\frac{3}{2}$	100	1.858354	4.596163	31.4	17.122614	$NaAsF_6$	2.54×10^{-2}	1.49×10^{2}
^{77}Se	$\frac{1}{2}$	7.63	0.92677577	5.1253857	–	19.071513	Me_2Se	5.37×10^{-4}	3.15
(^{79}Br)	$\frac{3}{2}$	50.69	2.719351	6.725616	31.3	25.053980	NaBr	4.03×10^{-2}	2.37×10^{2}
^{81}Br	$\frac{3}{2}$	49.31	2.931283	7.249776	26.2	27.006518	NaBr	4.91×10^{-2}	2.88×10^{2}
^{83}Kr	$\frac{9}{2}$	11.49	−1.07311	−1.03310	25.9	3.847600	Kr(gas)	2.18×10^{-4}	1.28
(^{85}Rb)	$\frac{5}{2}$	72.17	1.6013071	2.5927050	27.6	9.654943	RbCl	7.67×10^{-3}	45
^{87}Rb	$\frac{3}{2}$	27.83	3.552582	8.786400	13.35	32.720454	RbCl	4.93×10^{-2}	2.90×10^{2}
^{87}Sr	$\frac{9}{2}$	7.00	−1.2090236	−1.1639376	33.5	4.333822	$SrCl_2$	1.90×10^{-4}	1.12
^{89}Y	$\frac{1}{2}$	100	−0.23801049	−1.3162791	–	4.900198	$Y(NO_3)_3$	1.19×10^{-4}	0.7

(*Continued*)

APPENDIX A (*Continued*)

Isotope	Spin	Natural Abundance (%)	Magnetic Moment μ/μ_N	Magnetogyric Ratio $\gamma/10^7$ rad T^{-1} s^{-1}	Quadrupole Moment Q/fm^2	Frequency Ratio (Ξ)	Reference Compound	Relative Receptivity	
								D^{Proton}	D^{Carbon}
^{91}Zr	$\frac{5}{2}$	11.22	−1.54246	−2.49743	−17.6	9.296298	$Zr(C_5H_5)_2Cl_2$	1.07×10^{-3}	6.26
^{93}Nb	$\frac{9}{2}$	100	6.8217	6.5674	−32.0	24.476170	$K[NbCl_6]$	0.488	2.87×10^{3}
^{95}Mo	$\frac{5}{2}$	15.92	−1.0820	−1.7510	−2.2	6.516926	Na_2MoO_4	5.21×10^{-4}	3.06
(^{97}Mo)	$\frac{5}{2}$	9.55	−1.1050	−1.7880	25.5	6.653695	Na_2MoO_4	5.33×10^{-4}	1.95
^{99}Tc	$\frac{9}{2}$	–	6.2810	6.0460	−12.9	22.508326	NH_4TcO_4	–	–
^{99}Ru	$\frac{5}{2}$	12.76	−0.7588	−1.2290	7.9	4.605151	$K_4[Ru(CN)_6]$	1.44×10^{-4}	0.848
^{101}Ru	$\frac{5}{2}$	17.06	−0.8505	−1.3770	45.7	5.161369	$K_4[Ru(CN)_6]$	2.71×10^{-4}	1.59
^{103}Rh	$\frac{1}{2}$	100	−0.1531	−0.8468	–	3.186447	$Rh(acac)_3$	3.17×10^{-5}	0.186
^{105}Pd	$\frac{5}{2}$	22.33	−0.7600	−1.2300	66.0	4.576100	K_2PdCl_6	2.53×10^{-4}	1.49
(^{107}Ag)	$\frac{1}{2}$	51.839	−0.19689893	−1.0889181	–	4.047819	$AgNO_3$	3.50×10^{-5}	0.205
^{109}Ag	$\frac{1}{2}$	48.161	−0.22636279	−1.2518634	–	4.653533	$AgNO_3$	4.94×10^{-5}	0.290
(^{111}Cd)	$\frac{1}{2}$	12.80	−1.0303729	−5.6983131	–	21.215480	Me_2Cd	1.24×10^{-3}	7.27
^{113}Cd	$\frac{1}{2}$	12.22	−1.0778568	−5.9609155	–	22.193175	Me_2Cd	1.35×10^{-3}	7.94
(^{113}In)	$\frac{9}{2}$	4.29	6.1124	5.8845	79.9	21.865755	$In(NO_3)_3$	1.51×10^{-2}	88.50
^{115}In	$\frac{9}{2}$	95.71	6.1256	5.8972	81.0	21.912629	$In(NO_3)_3$	0.338	1.98×10^{3}
(^{115}Sn)	$\frac{1}{2}$	0.34	−1.5915	−8.8013	–	32.718749	Me_4Sn	1.21×10^{-4}	0.711
(^{117}Sn)	$\frac{1}{2}$	7.68	−1.73385	−9.58879	–	35.632259	Me_4Sn	3.54×10^{-3}	20.8
^{119}Sn	$\frac{1}{2}$	8.59	−1.81394	−10.0317	–	37.290632	Me_4Sn	4.53×10^{-3}	26.6
^{121}Sb	$\frac{5}{2}$	57.21	3.9796	6.4435	−36.0	23.930577	$KSbCl_6$	9.33×10^{-2}	5.48×10^{2}
(^{123}Sb)	$\frac{7}{2}$	42.79	2.8912	3.4892	−49.0	12.959217	$KSbCl_6$	1.99×10^{-2}	1.17×10^{2}
(^{123}Te)	$\frac{1}{2}$	0.89	−1.276431	−7.059098	–	26.169742	Me_2Te	1.64×10^{-4}	0.961
^{125}Te	$\frac{1}{2}$	7.07	−1.5389360	−8.5108404	–	31.549769	Me_2Te	2.28×10^{-3}	13.40
^{127}I	$\frac{5}{2}$	100	3.328710	5.389573	−69.6	20.007486	KI	9.54×10^{-2}	5.60×10^{2}

^{129}Xe	$\frac{1}{2}$	26.44	−1.347494	−7.452103	–	27.810186	$XeOF_4$	5.72×10^{-3}	33.60
^{131}Xe	$\frac{3}{2}$	21.18	0.8931899	2.209076	−11.4	8.243921	$XeOF_4$	5.96×10^{-4}	3.50
^{133}Cs	$\frac{7}{2}$	100	2.9277407	3.5332539	−0.343	13.116142	$CsNO_3$	4.84×10^{-2}	2.84×10^{2}
(^{135}Ba)	$\frac{3}{2}$	6.592	1.08178	2.67550	16.0	9.934457	$BaCl_2$	3.30×10^{-4}	1.93
^{137}Ba	$\frac{3}{2}$	11.232	1.21013	2.99295	24.5	11.112928	$BaCl_2$	7.87×10^{-4}	4.62
^{138}La	5	0.09	4.068095	3.557239	45.0	13.19430	$LaCl_3$	8.46×10^{-5}	0.497
^{139}La	$\frac{7}{2}$	99.91	3.155677	3.8083318	20.0	14.125641	$LaCl_3$	6.05×10^{-2}	3.56×10^{2}
^{141}Pr	$\frac{5}{2}$	100	5.0587	8.1907	−5.89	30.62	–	–	–
^{143}Nd	$\frac{7}{2}$	12.2	−1.208	−1.4570	−63.0	5.45	–	–	–
^{145}Nd	$\frac{7}{2}$	8.3	−0.7440	−0.8980	−33.0	3.36	–	–	–
^{147}Sm	$\frac{7}{2}$	14.99	−0.9239	−1.1150	−25.9	4.17	–	–	–
^{149}Sm	$\frac{7}{2}$	13.82	−0.7616	−0.9192	7.4	3.44	–	–	–
^{151}Eu	$\frac{5}{2}$	47.81	4.1078	6.6510	90.3	24.86	–	–	–
^{153}Eu	$\frac{5}{2}$	52.19	1.8139	2.9369	241.2	10.98	–	–	–
^{155}Gd	$\frac{3}{2}$	14.80	−0.33208	−0.82132	127.0	3.07	–	–	–
^{157}Gd	$\frac{3}{2}$	15.65	−0.4354	−1.0769	135.0	4.03	–	–	–
^{159}Tb	$\frac{3}{2}$	100	2.6000	6.4310	143.2	24.04	–	–	–
^{161}Dy	$\frac{5}{2}$	18.91	−0.5683	−0.9201	250.7	3.44	–	–	–
^{163}Dy	$\frac{5}{2}$	24.90	0.7958	1.2890	264.8	4.82	–	–	–
^{165}Ho	$\frac{7}{2}$	100	4.7320	5.7100	358.0	21.34	–	–	–
^{167}Er	$\frac{7}{2}$	22.93	−0.63935	−0.77157	356.5	2.88	–	–	–
^{169}Tm	$\frac{1}{2}$	100	−0.4011	−2.2180	–	8.29	–	–	–
^{171}Yb	$\frac{1}{2}$	14.28	0.85506	4.7288	–	17.499306	–	–	–
^{173}Yb	$\frac{5}{2}$	16.13	−0.80446	−1.3025	280.0	4.821	–	–	–
^{175}Lu	$\frac{7}{2}$	97.41	2.5316	3.0552	349.0	11.404	–	–	–
^{176}Lu	7	2.59	3.3880	2.16844	497.0	8.131	–	–	–
^{177}Hf	$\frac{7}{2}$	18.60	0.8997	1.0860	336.5	4.007	–	2.61×10^{-4}	1.54
^{179}Hf	$\frac{9}{2}$	13.62	−0.7085	−0.6821	379.3	2.517	–	7.45×10^{-5}	0.438

(*Continued*)

APPENDIX A (*Continued*)

Isotope	Spin	Natural Abundance (%)	Magnetic Moment μ/μ_N	Magnetogyric Ratio $\gamma/10^7$ rad T^{-1} s^{-1}	Quadrupole Moment Q/fm^2	Frequency Ratio (Ξ)	Reference Compound	Relative Receptivity	
								D^{Proton}	D^{Carbon}
^{181}Ta	$\frac{7}{2}$	99.988	2.6879	3.2438	317.0	11.989600	$KTaCl_6$	3.74×10^{-2}	2.20×10^{2}
^{183}W	$\frac{1}{2}$	14.31	0.20400919	1.1282403	–	4.166387	Na_2WO_4	1.07×10^{-5}	6.31×10^{-2}
(^{185}Re)	$\frac{5}{2}$	37.4	3.7710	6.1057	218.0	22.524600	$KReO_4$	5.19×10^{-2}	3.05×10^{2}
^{187}Re	$\frac{5}{2}$	62.6	3.8096	6.1682	207.0	22.751600	$KReO_4$	8.95×10^{-2}	5.26×10^{2}
^{187}Os	$\frac{1}{2}$	1.96	0.1119804	0.6192895	–	2.282331	OsO_4	2.43×10^{-7}	1.43×10^{-3}
^{189}Os	$\frac{3}{2}$	16.15	0.851970	2.10713	85.6	7.765400	OsO_4	3.95×10^{-4}	2.32
(^{191}Ir)	$\frac{3}{2}$	37.3	0.1946	0.4812	81.6	−1.718	–	1.09×10^{-5}	6.38×10^{-2}
^{193}Ir	$\frac{3}{2}$	62.7	0.2113	0.5227	75.1	−1.871	–	2.34×10^{-5}	0.137
^{195}Pt	$\frac{1}{2}$	33.832	1.0557	5.8385	–	21.496784	Na_2PtCl_6	3.51×10^{-3}	20.7
^{199}Hg	$\frac{1}{2}$	16.87	0.87621937	4.8457916	–	17.910822	Me_2Hg	1.00×10^{-3}	5.89
^{197}Au	$\frac{3}{2}$	100	0.191271	0.473060	54.7	−1.729	–	2.77×10^{-5}	0.162
^{201}Hg	$\frac{3}{2}$	13.18	−0.7232483	−1.788769	38.6	6.611583	$(CH_3)_2Hg$	1.97×10^{-4}	1.16
(^{203}Tl)	$\frac{1}{2}$	29.524	2.80983305	15.5393338	–	57.123200	$Tl(NO_3)_3$	5.79×10^{-2}	3.40×10^{2}
^{205}Tl	$\frac{1}{2}$	70.476	2.8374709	15.6921808	–	57.683838	$Tl(NO_3)_3$	0.142	8.36×10^{2}
^{207}Pb	$\frac{1}{2}$	22.1	1.00906	5.58046	–	20.920599	Me_4Pb	2.01×10^{-3}	11.8
^{209}Bi	$\frac{9}{2}$	100	4.5444	4.3750	−51.6	16.069288	$Bi(NO_3)_2$	0.144	8.48×10^{2}
^{235}U	$\frac{7}{2}$	0.72	−0.4300	−0.5200	493.6	1.8414	–	–	–

Nuclei in parentheses are not considered the most favorable for NMR.

Adapted in part from Harris, R.K, Becker, E.D., Cabral de Menezes, S.M., Goodfellow, R., and Granger, P. (2001). NMR nomenclature. Nuclear spin properties and conventions for chemical shifts. *Pure Appl. Chem.*, **73**, 1795–1818.

CHAPTER 7

SOLVED PROBLEMS

7.1 INTRODUCTION

The perennial student question: Where do we start? The instructor will be sympathetic but not rigidly prescriptive. There are, however, guidelines that do start with the prescriptive statement: *Go for the molecular formula.* Why? Simply because it is the single most useful bit of information available to the chemist and is worth the effort sometimes necessary. It provides an overall impression of the molecule (i.e., the number and kinds of atoms), and it provides the *index of hydrogen deficiency*—in other words, the sum of the number of rings and of double and triple bonds (Section 1.5.3).

Development of the molecular formula starts with recognition of the molecular ion peak (Section 1.5). We assume the usual situation: high-resolution MS instrumentation is not readily available. Let us also assume for now that the peak of highest m/z (except for its isotope peaks) is the molecular ion peak and is intense enough so that the isotope peak intensities can be determined accurately and the presence and number of S, Br, and Cl atoms can be ascertained. Look also at the fragmentation pattern of the mass spectrum for recognizable fragments. If the molecular ion peak is an odd number, an odd number of N atoms is present.

Difficulty often starts with uncertainty in the choice of a molecular ion peak. Many laboratories use chemical ionization as a routine supplement to electron impact, and of course, access to a high-resolution instrument is desirable for more difficult problems.

Next, a search of the infrared spectrum for absorptions indicative of particular functional groups is in order. Note in particular C—H stretching, O—H and/or N—H absorptions, and the presence (or absence) of absorptions indicative of unsaturated functional groups.

With this information in hand, search the proton NMR spectrum for confirmation and further leads. If the spectrum allows, determine the total number of protons and ratios of groups of chemically equivalent protons from the integration. Look for first-order coupling patterns and for characteristic chemical shifts. Look at the ^{13}C/DEPT spectra; determine the carbon and proton counts and the numbers of CH_3, CH_2, CH, and quaternary C groups. A discrepancy between the proton integration and the number of protons represented in the ^{13}C/DEPT spectra suggests the presence of protons bonded to heteroatoms.

Overlap of proton resonances in the one-dimensional spectrum is common, but absolute coincidence of nonequivalent ^{13}C peaks is quite rare with a high-resolution instrument. Now, select the most likely molecular formula(s) from Appendix A of Chapter 1 for comparison and determine the index of hydrogen deficiency for each. In addition to difficulties caused by unresolved or overlapping peaks, discrepancies may appear between the selected molecular formula(s) and the ^{1}H and ^{13}C counts because of the presence of elements of symmetry. Although identifying these elements may initially require some additional effort, such symmetry information is very valuable in the structure determination process.

Students are urged to develop their own approaches. To provide practice, we have sometimes presented more information than needed, but other Problems should provide compensatory frustration to simulate the real world. Remember the overall strategy: Play the spectra against one another, focusing on the more obvious features. Develop a hypothesis from one spectrum: look to the other spectra for confirmation or contradictions; modify the hypothesis if necessary. *The effect is synergistic,* the total information being greater than the sum of the individual parts.

With the high magnetic fields now available, many *J* coupling multiplets are first order, or nearly so, and can be interpreted by inspection with the leads furnished by the mass and infrared spectra. Nevertheless, a rereading of Sections 3.8 through 3.12 may engender caution.

As an example, consider two similar compounds:

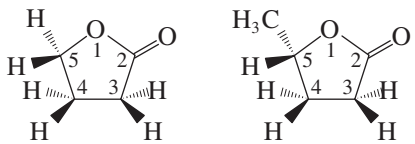

Both rings exist in rapidly flexing ring conformations, but only in compound A do the protons of each CH_2 group interchange to become chemically equivalent (enantiotopes). Only compound A has a plane of symmetry in the plane of the page through which the protons interchange.

From high frequency to low frequency in the ^{1}H NMR spectrum, we predict for compound A: H-5, a two-proton triplet; H-3, a two-proton triplet; H-4, a two-proton quintet (assuming nearly equal coupling constants). In a moderately high magnetic field, the spectrum is first order.

Compound B has no symmetry element in the planar conformation. C-5 is a stereogenic center and the protons of each CH_2 group are diastereotopic pairs. Each proton of the pair has its own chemical shift. The resonances due to the H-4 protons adjacent to the stereogenic center are distinctly separated, but those of the H-3 protons are not, at 300 MHz.

Each proton of a diastereotopic pair couples geminally with the other and independently (different coupling constants) with the vicinal protons to give complex multiplets.

The possibility of a stereogenic center should always be kept in mind; *toujours la stereochimie*.

The power of 2D spectra will become more evident as we work through the problems in Chapters 7 and 8. It is often not necessary to examine all of the spectra in detail before proposing—tentatively—possible structures or fragments. Spectral features predicted for the postulated structures or fragments are compared with the observed spectra, and structural modifications are made to accommodate discrepancies.

These suggestions are illustrated by the following solved problems presented in increasing order of difficulty. The assigned problems in this Chapter and the end of Chapter 8, again in increasing order of difficulty, will provide essential practice.

Most students enjoy problem solving and rise to the challenge. They also begin to appreciate the elegance of chemical structure as they interpret spectra. Good sleuthing! Be wary of chirality, diastereotopes, virtual coupling, dihedral angles of about 90°, and the concepts of chemical and magnetic equivalence.

Finally, what are the requirements for proof of structure? Ultimately, it is congruence of all available spectra with those of a pure, authentic sample obtained under the same conditions and on the same instruments. Obviously, some compromises are acceptable. Congruence with published spectra or spectral data is considered acceptable for publication, but this cannot apply to a new compound, which must then be synthesized.

Computer programs for simulating NMR spectra are available.* If accurate measurements of chemical shifts and coupling constants for all of the protons can be obtained, the simulated spectrum will be congruent with the actual spectrum. In many cases, at least some of the spin systems will be first order. If not, reasonable estimates of shifts and coupling constants may be made, and the iterative computer program will adjust the values until the simulation matches the actual spectrum—assuming, of course, that the identification is valid. Such simulations are nowadays quite reliable for proton NMR spectra and continue to improve for ^{13}C NMR spectra. The user should keep in mind that while simulation software can be useful, it is based in part on empirical trends and/or databases, and therefore may not always provide reliable spectral simulations, particularly for unusual structures. Quantum chemical calculations can provide more reliable predictions of NMR parameters but are much more time consuming.

Checklist for logical and pedagogical completeness, not necessarily in order:

1. Show how the molecular formula was derived.
2. Calculate the index of hydrogen deficiency.
3. ***Assign*** diagnostic bands in the IR spectrum.
4. ***Assign all*** resonances in the ^{1}H NMR spectrum.
5. ***Assign all*** resonances in the ^{13}C/DEPT NMR spectra. (Note that the ^{13}C/DEPT NMR spectra in this book are always displayed in the following order, from top to bottom: DEPT-90, DEPT-135, regular proton-decoupled ^{13}C NMR spectrum.)
6. Calculate or estimate $\Delta\nu/J$ where appropriate.
7. Explain multiplicity where appropriate. Use J coupling values wherever possible to provide structural insights (e.g., *cis* vs *trans* stereochemistry, vicinal vs geminal couplings, etc.)
8. Assign all correlations in 2D spectra.
9. Show how the EI mass spectrum supports the structure.
10. Consider possible isomers.

Each problem in this chapter is organized so that the molecular structure and the spectra appear first and are followed by the discussion. The molecular structure is displayed on most of the individual spectra to minimize back-and-forth page turning. The purpose of this arrangement is to encourage students to make their own tentative connections between the molecule and familiar features in the spectra. With this preparation, the subsequent discussions will be more helpful.

*Spectra can be simulated on most modern computers. Companies such as Bruker Biospin (Billerica, MA, USA), Mestrelab (Santiago de Compostela, Spain), and ACD Labs (Toronto, Canada) offer software to simulate NMR spectra.

MASS EI

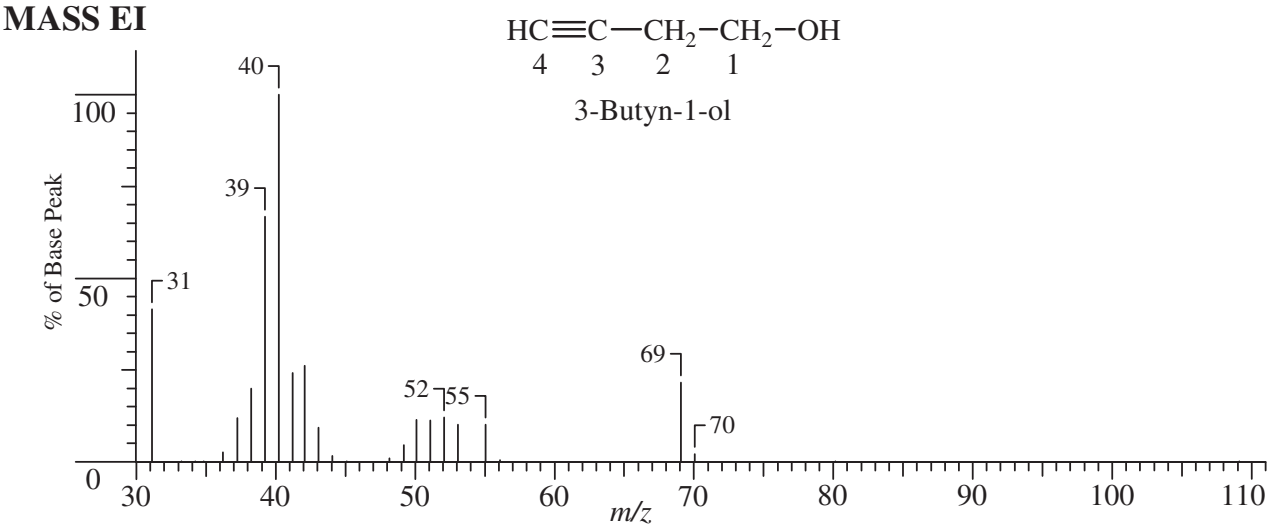

MASS CI reagent gas methane

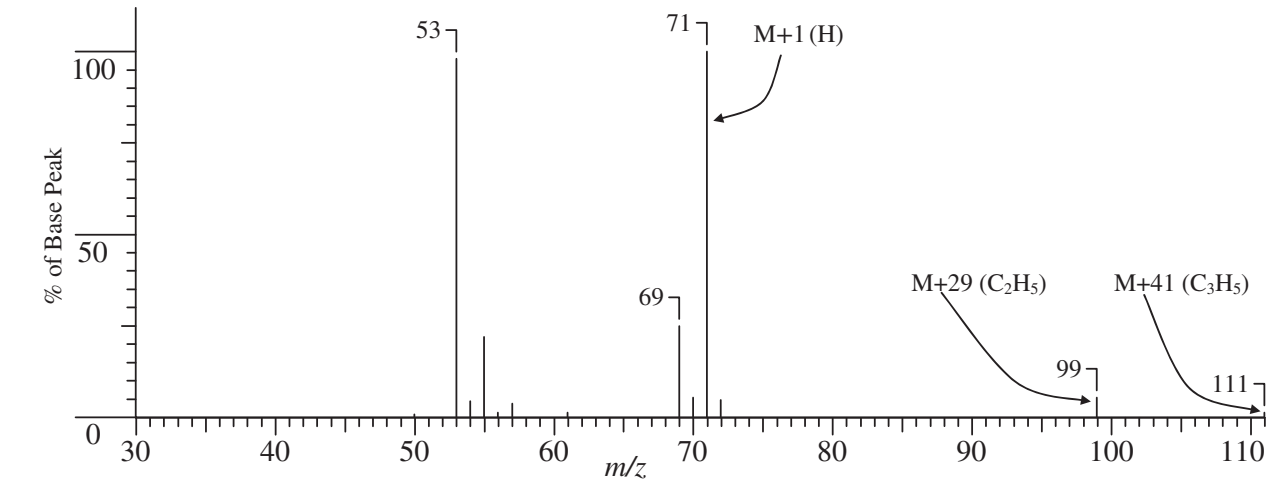

IR

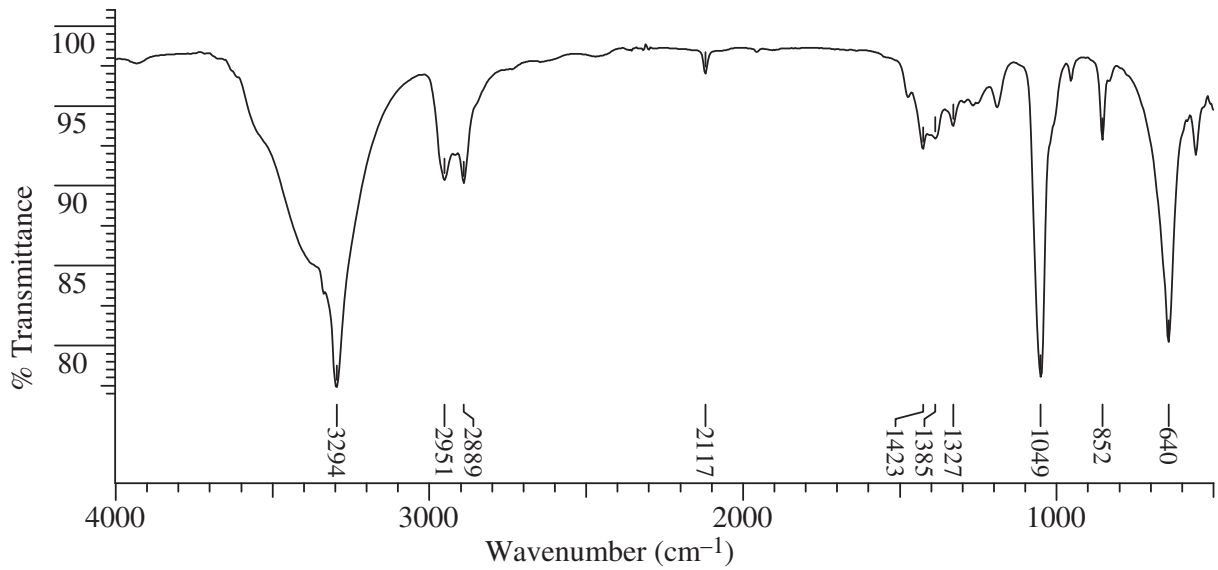

Problem 7.1B

^{1}H NMR 600 MHz

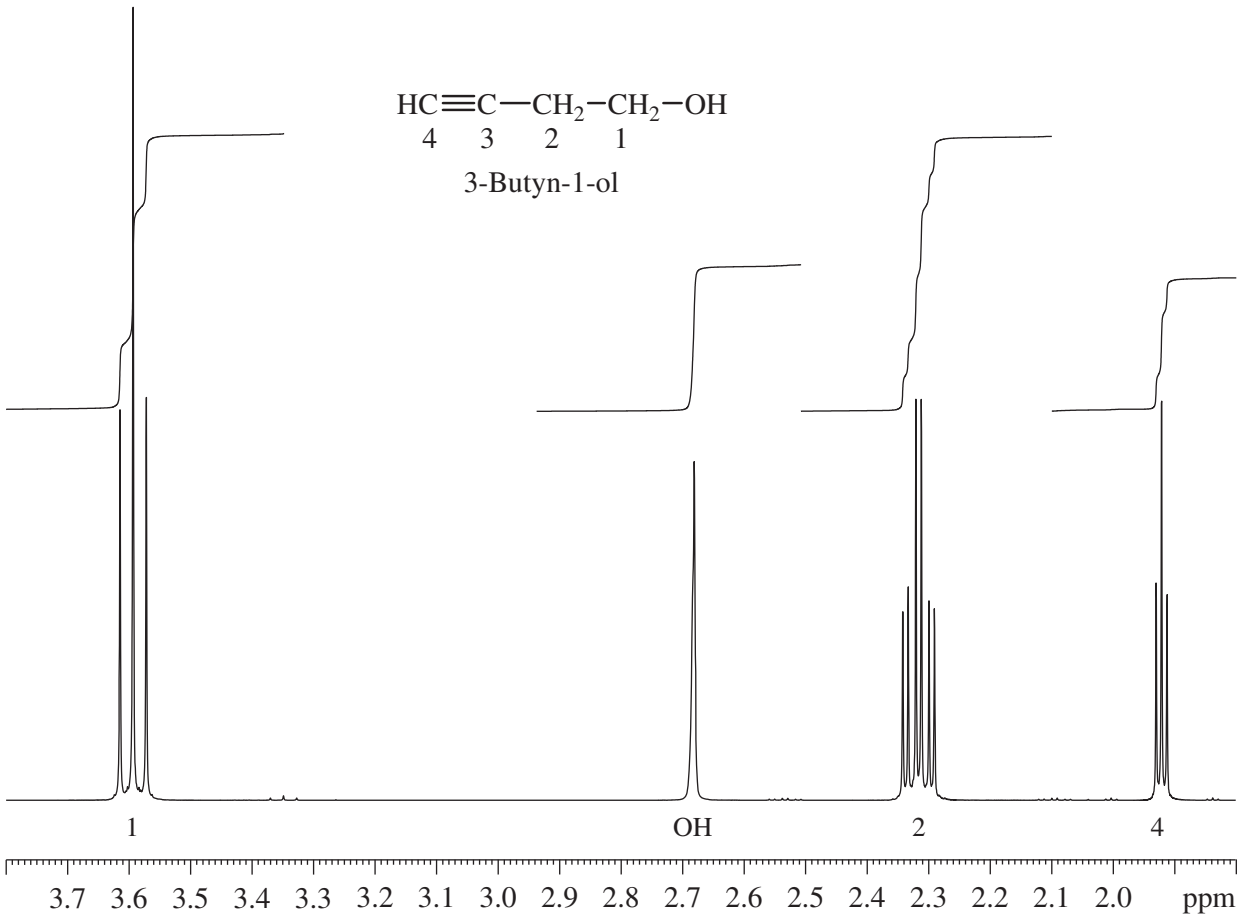

^{13}C/DEPT NMR 150.9 MHz

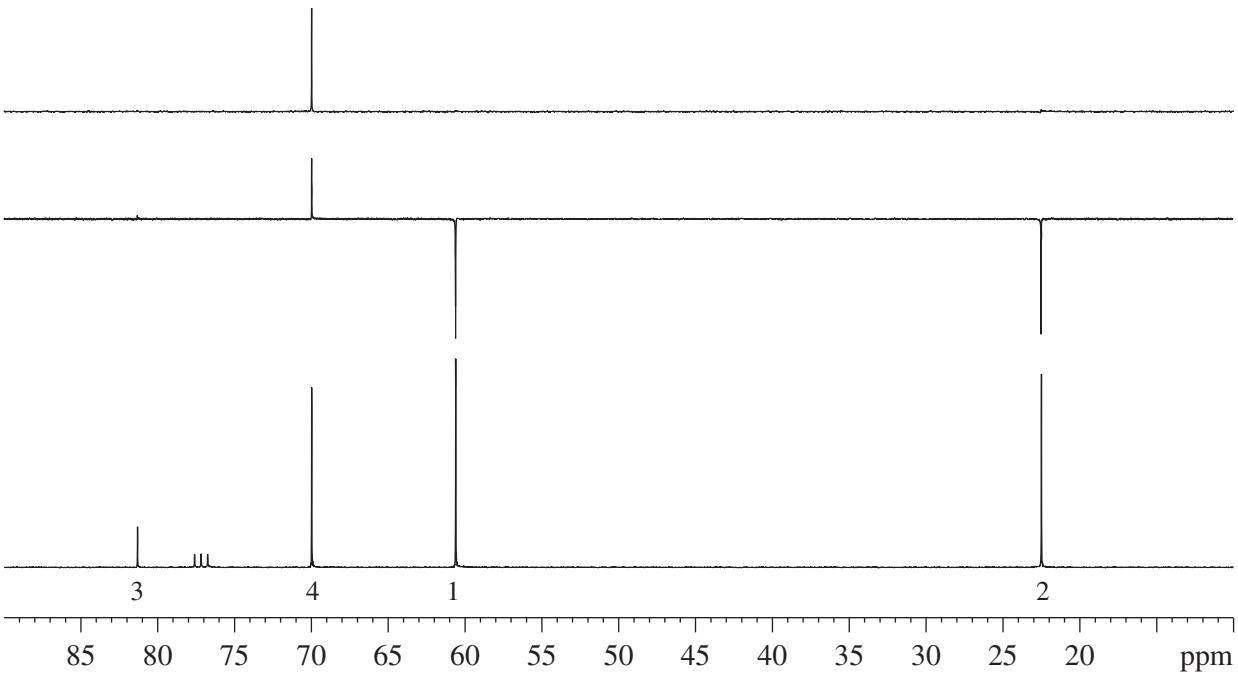

PROBLEM 7.1 DISCUSSION

Everything points to a small molecule. There appear to be no further peaks in the mass spectrum beyond m/z 69, but it is rejected as the molecular ion because the next peak is found at m/z 55, a putative loss of 14 mass units. The CI mass spectrum possesses a base peak of m/z 71, which represents an M + 1 pseudomolecular ion. The molecular weight of this compound is thus taken as 70 amu. The IR spectrum suggests an alcohol with a broad O—H stretching band at about 3350 cm^{-1} and a strong C—O stretching at 1049 cm^{-1}.

The proton NMR spectrum consists of classical first-order multiplets. From high frequency to low frequency, the multiplicities and integrations are triplet (2), singlet (1), triplet of doublets (2), triplet (1), which yields six hydrogen atoms. The ^{13}C/DEPT spectra show four carbon resonances which indicate, from high frequency to low frequency: C, CH, CH_2, CH_2. This discrepancy implies that one of the protons is bonded to a heteroatom. The OH proton at 2.68 ppm in the ^1H spectrum accounts for the difference in proton count between the ^1H spectrum and the ^{13}C/DEPT spectra.

The assumption of m/z 70 as the molecular ion is now quite valid. The molecular formula is now assumed to be C_4H_6O with an index of hydrogen deficiency of two. The options are: two double bonds, one double bond and a ring, two rings, or a triple bond. We can consider these options seriatim.

Consider two double bonds. Do any of the proton or carbon peaks fall in the usual ranges for alkenes? Perusal of Chapters 3 and 4 eliminates the possibility. This leaves us with rings or a triple bond.

Rings are often difficult to rule out on the basis of chemical shifts alone, but the spin-spin couplings would be difficult to explain. Let us consider a triple bond.

Yes, a triple bound would qualify on the basis of chemical shifts for both protons and carbons. The first question is whether the triple bond is terminal or internal; in other words, is there an alkyne proton?

$$\text{H—C}\equiv\text{C—R} \quad \text{or} \quad \text{R—C}\equiv\text{C—R}'$$

The ^{13}C NMR spectrum is unequivocal. It shows two peaks in the range for alkyne carbons. The peak at 70 ppm is about the same intensity as each of the two CH_2 peaks, but the peak at about 81.2 ppm is distinctly less intense, suggesting that it has no attached proton. Furthermore, the ^{13}C/DEPT subspectra show that the peak at about 70 ppm represents a CH group. We can now write two fragments or substructures:

$$\text{H—C}\equiv\text{C—} \quad \text{and} \quad \text{—CH}_2\text{—OH}$$

Insertion of the missing CH_2 group gives a complete molecule:

$$\text{H—C}\equiv\text{C—CH}_2\text{—CH}_2\text{—OH}$$

This structure is completely in accord with the ^1H and ^{13}C/DEPT NMR spectra. The ^1H spectrum provides a nice demonstration of long-range coupling through the triple bond (from H-4 to H-2), splitting the triplet further into doublets.

Returning with hindsight to the infrared spectrum, we may note the strong H—C≡ stretching band at 3294 cm^{-1} superposed on the O—H band. There is also a strong ≡C—H band at 640 cm^{-1}. Furthermore, there is a weak but distinctive C≡C stretching band at 2117 cm^{-1}.

Several of the major peaks in the mass spectrum are difficult to assign since there are two functional groups of similar mass. Although trivial, verification of the assignments of the proton resonances and their multiplicities are left as an exercise for the student. Likewise, verification of the assignments of the resonances in the ^{13}C/DEPT spectra are left for the student.

Problem 7.2A

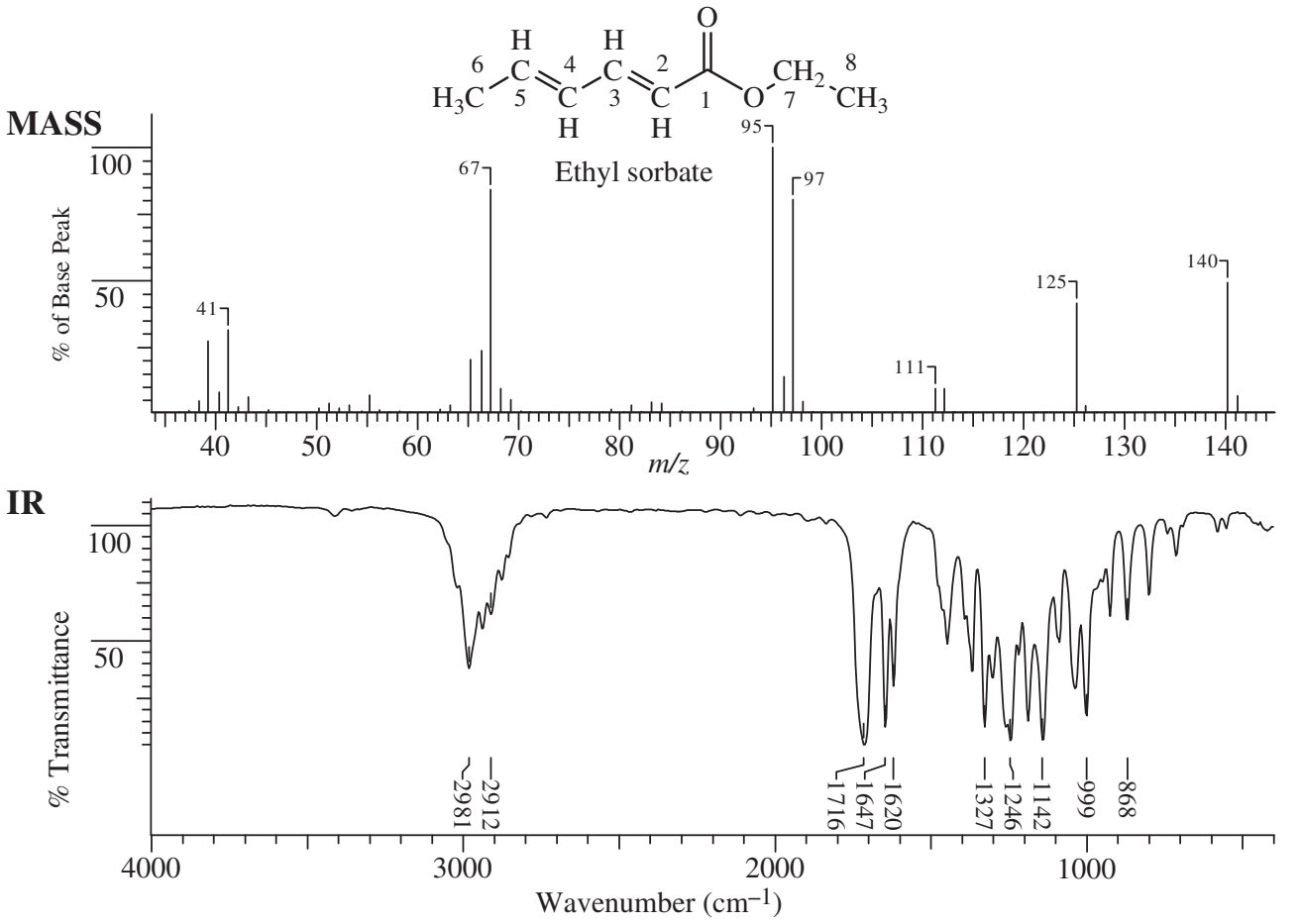
MASS
Ethyl sorbate
% of Base Peak
m/z
IR
% Transmittance
Wavenumber (cm−1)
2981
2912
1716
1647
1620
1327
1246
1142
999
868

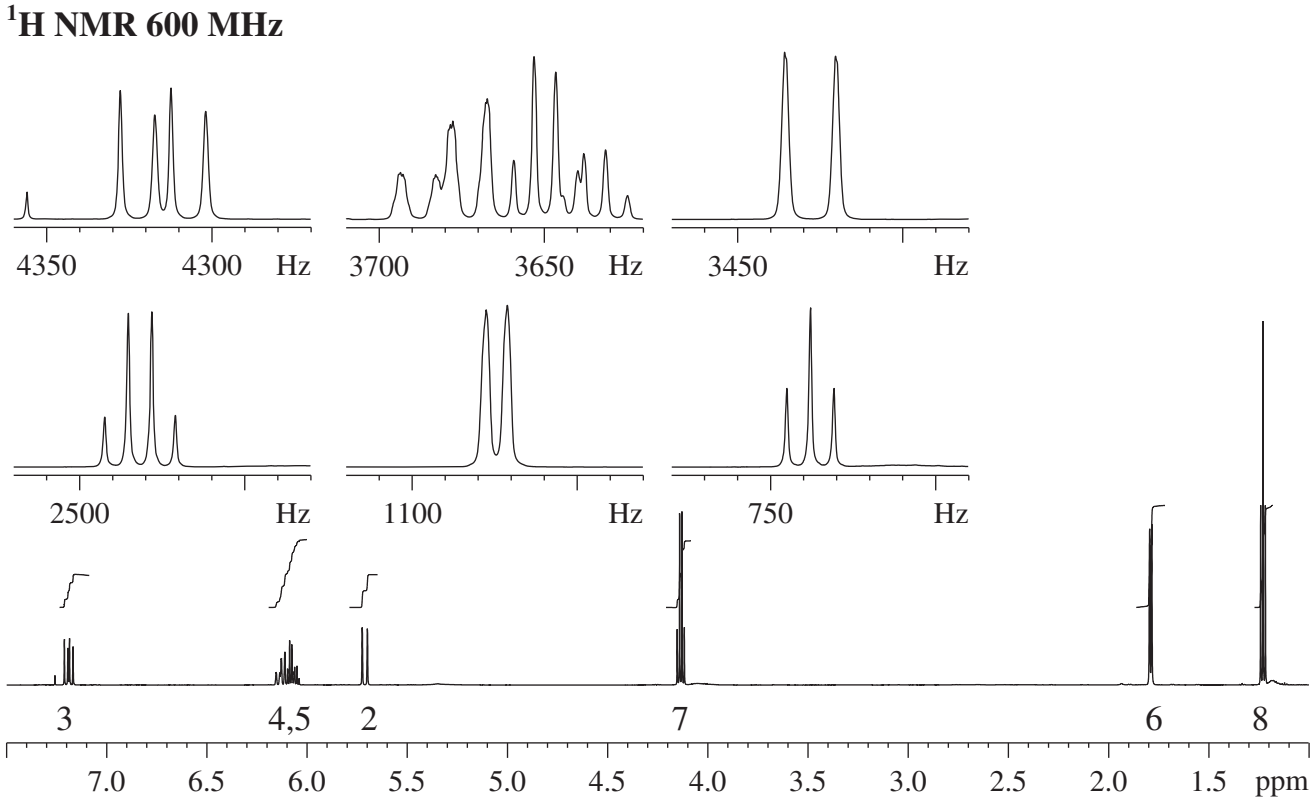
1H NMR 600 MHz
4350
4300 Hz
3700
3650 Hz
3450 Hz
2500 Hz
1100 Hz
750 Hz
3
4,5
2
7
6
8
ppm

^{1}H Homodecoupled 600 MHz

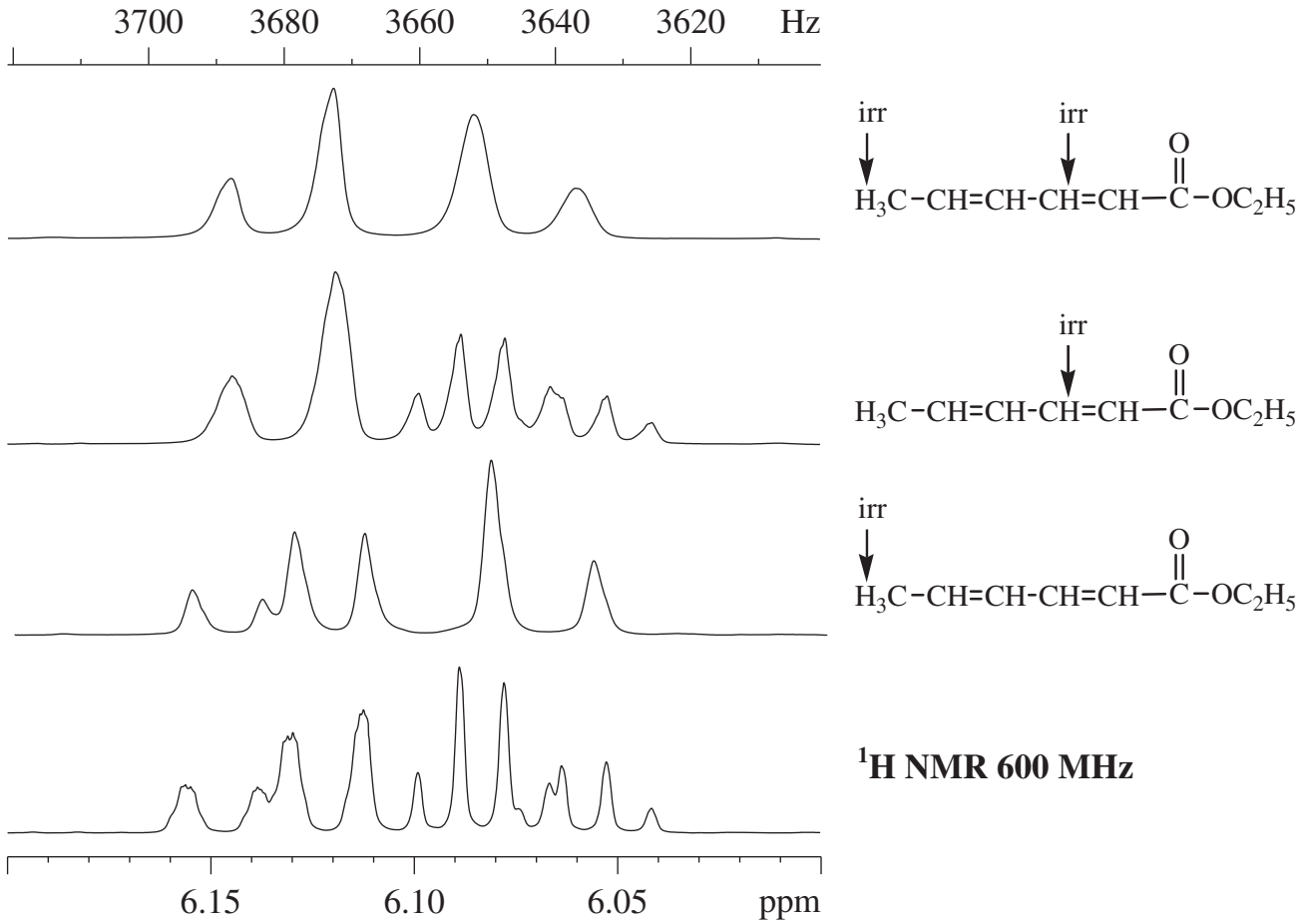

^{1}H NMR 600 MHz

^{13}C/DEPT NMR 150.9 MHz

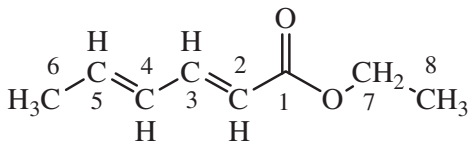

Ethyl sorbate

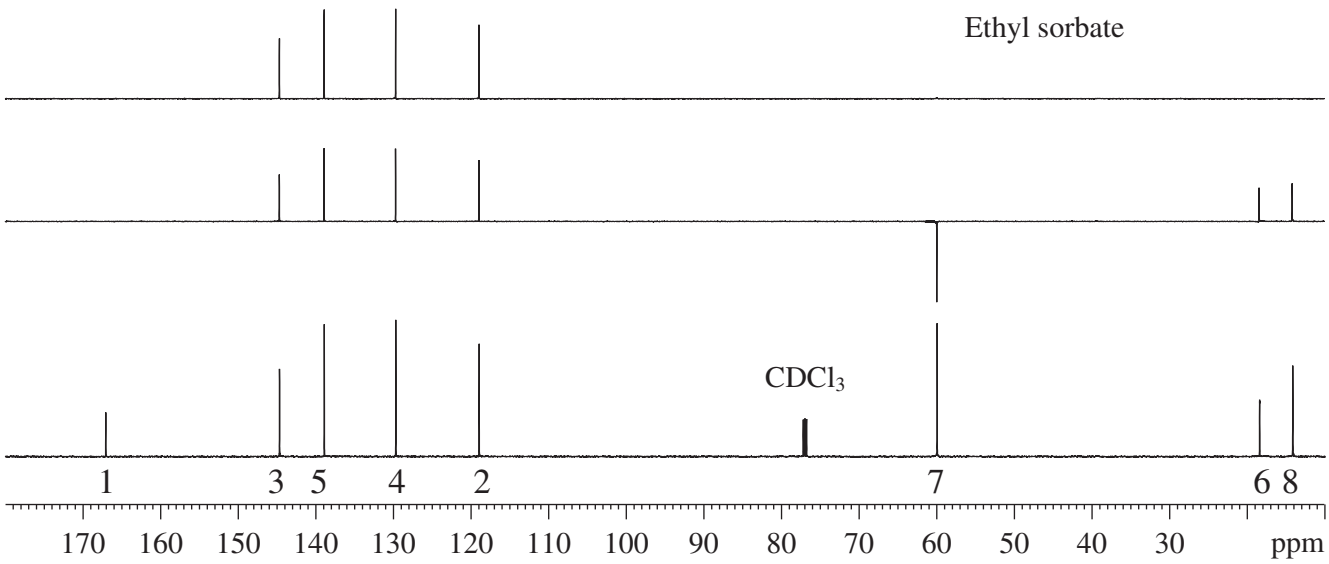

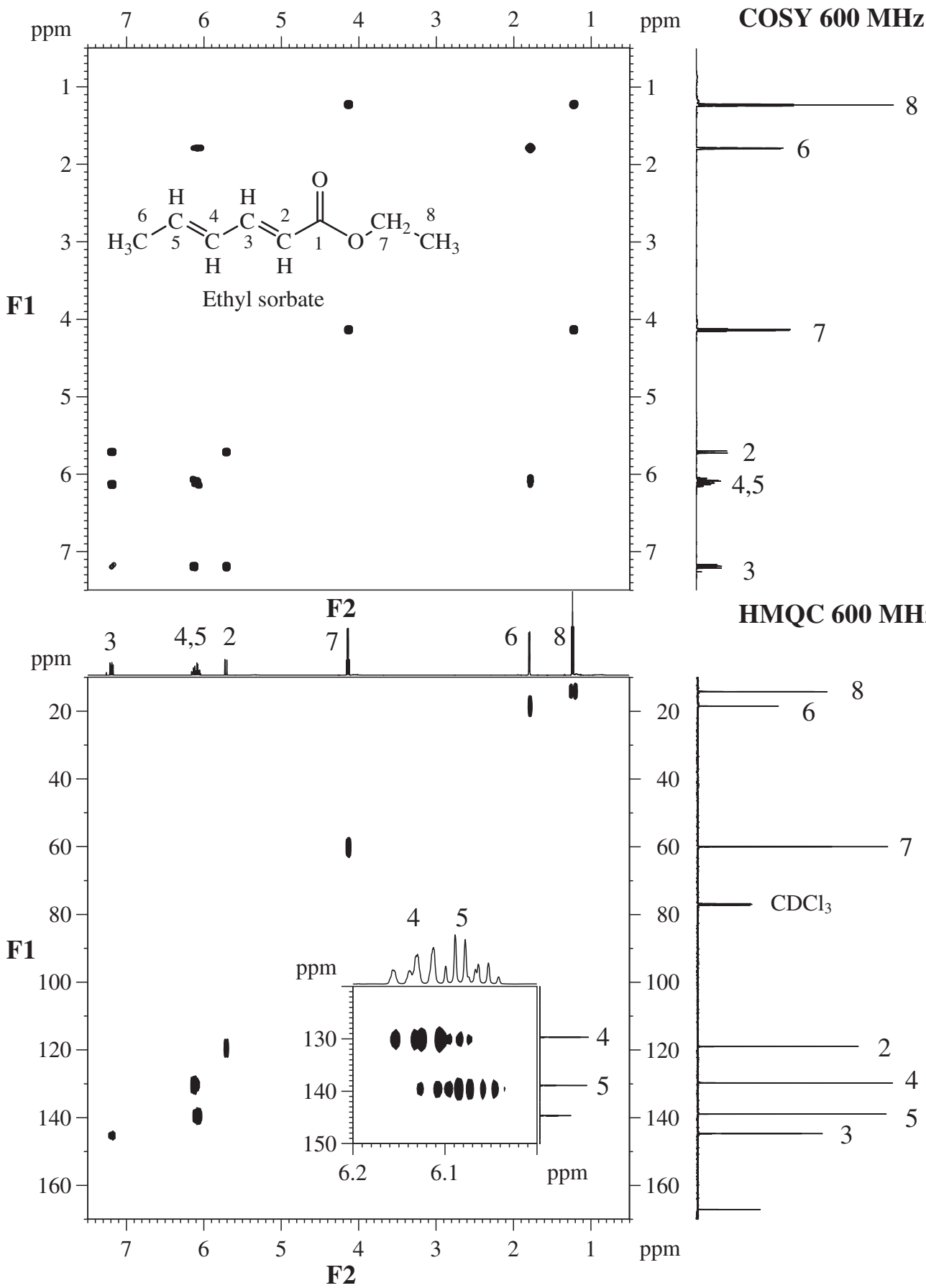
COSY 600 MHz
ppm
F1
F2
Ethyl sorbate
8
6
7
2
4,5
3
HMQC 600 MHz
CDCl3
4
5

PROBLEM 7.2 DISCUSSION

The relatively intense peak at m/z 140 in the mass spectrum is a reasonable choice for the molecular ion peak, since there are no further peaks, and the fragment at m/z 125 represents loss of CH_3. Since 140 is an even number, there are an even number of N atoms, and we assume 0 as a starting point. The very small M + 1 and M + 2 peaks preclude S, Cl, and Br.

The strong IR band at 1716 cm^{-1} indicates a carbonyl (C═O) group. The two sharp bands at 1647 cm^{-1} and 1620 cm^{-1} indicate one or more carbon—carbon double bonds (C═C) that may be conjugated (see Section 2.6.4.1).

There are six different kinds of protons in the ^1H spectrum in the ratios, from high frequency to low frequency, 1:2:1:2:3:3, for a total of 12 protons. We now count eight peaks in the ^{13}C NMR spectrum (assuming one carbon atom per peak), and from the ^{13}C/DEPT subspectra we read (from high frequency): (C═O) (from IR), CH, CH, CH, CH, CH_2, CH_3, CH_3. With the present information, we write $C_8H_{12}O$ with unit mass 124, which is 16 units less than a molecular ion peak at m/z 140. Is there another oxygen atom in the molecular ion?

Indeed so. The chemical shift of the CH_2 group at 60 ppm suggests a —(C═O)OCH_2— sequence (see Table 4.20). Also, the ^{13}C chemical shift of the carbonyl carbon (168 ppm) suggests a carboxylic acid derivative such as an ester. The partial molecular formula can now be revised to $C_8H_{12}O_2$ with a hydrogen deficiency of three.

The proton NMR spectrum immediately shows that the CH_3 triplet at 1.2 ppm is directly attached to the deshielded CH_2 group (quartet) at 4.1 ppm. The COSY spectrum confirms this correlation. The sequence, above, is now one end of the molecule: —(C═O)OCH_2CH_3.

In the ^{13}C/DEPT spectra, there are four CH alkene peaks between ~119 ppm and ~145 ppm. There is also the remaining CH_3 group at ~18.5 ppm, which appears in the proton spectrum at ~1.8 ppm as a doublet—obviously attached to one of the four CH groups.

It may seem presumptuous to formulate a molecular structure at this early stage, but we do have one end of the structure, four CH groups with an attached CH_3 group, no possibility for branching, and do not forget the two remaining sites of unsaturation. With some trepidation, we offer the following structure:

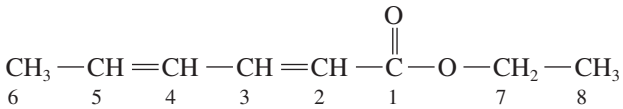

The synergism between the ^{13}C/DEPT spectra and the proton spectrum should be explored. There are two aspects to a proton spectrum: The first-order multiplets can usually be resolved, whereas the higher order multiplets are frustrating. In the present proton spectrum, there are five first-order multiplets and two overlapping multiplets that are not first order.

The ethyl protons are represented by the triplet at ~1.2 ppm coupled to the deshielded quartet at ~4.1 ppm. The other CH_3 group is represented by the doublet at ~1.8 ppm, coupled to one of four alkene CH protons. Rather than attempting to interpret the higher order multiplets, we turn to the 2D spectra.

In the COSY spectrum, one of the two overlapping CH resonances, which are centered at ~6.1 ppm (labeled H-5 and H-4), couples to the CH_3 doublet at ~1.8 ppm; this coupling confirms the earlier assumption that the CH_3 group is terminal. The proton-labeled H-5 also couples with the other overlapping CH group (labeled H-4), which in turn couples with the neighboring CH group at ~7.2 ppm (labeled H-3). The slightly broadened doublet at ~5.7 ppm (labeled H-2) is a result of coupling to H-3 and long-range coupling. We can summarize as follows:

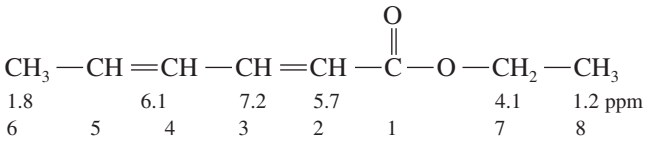

With the complete proton assignments and the direct correlations between carbons and attached protons from the HMQC spectrum, we are able to assign all of the carbon resonances, except for the quaternary carbon, which is a trivial assignment in this case. An interesting example is found in the inset of the HMQC spectrum, which shows the correlations of the two overlapped protons, H-4 and H-5. Even though they are overlapped in the one-dimensional proton spectrum, they are well resolved in the HMQC spectrum because the carbon resonances are not overlapped.

One important question still remains: Are the double bonds *E* (*trans*) or *Z* (*cis*)? This question can be answered if the alkenyl proton *J* values can be determined. One obvious starting point is the H-2 doublet, which is the result of coupling to H-3. The *J* value is about 16 Hz; this coupling constant falls within the range given for *E*-double bonds given in Appendix F, Chapter 3.

The complex, overlapping multiplets of H-4 and H-2 are not inviting. However, H-3 shows a pair of doublets as a result of the 16 Hz (*trans*) coupling to H-2 and a 10 Hz single bond coupling to H-4. Unfortunately, the coupling constant for the 4,5-double bond is not readily accessible. But spin decoupling (homodecoupling) is worth investigating (see Section 3.15). Irradiation of the H-6 resonance simplifies the overlapping H-5, H-4 multiplet considerably; in fact, there is a 16 Hz doublet (somewhat distorted) at the lower-frequency edge. Irradiation of H-3, individually, simplifies the complex multiplet and shows a 16 Hz doublet at the high-frequency edge. Simultaneous irradiation of the H-6 and H-3 resonances results in a pair of 16 Hz doublets. The doublet intensities are not ideal because of the small $\Delta\nu/J$ ratio. There is now no doubt that both double bonds are *E*.

Problem 7.3A

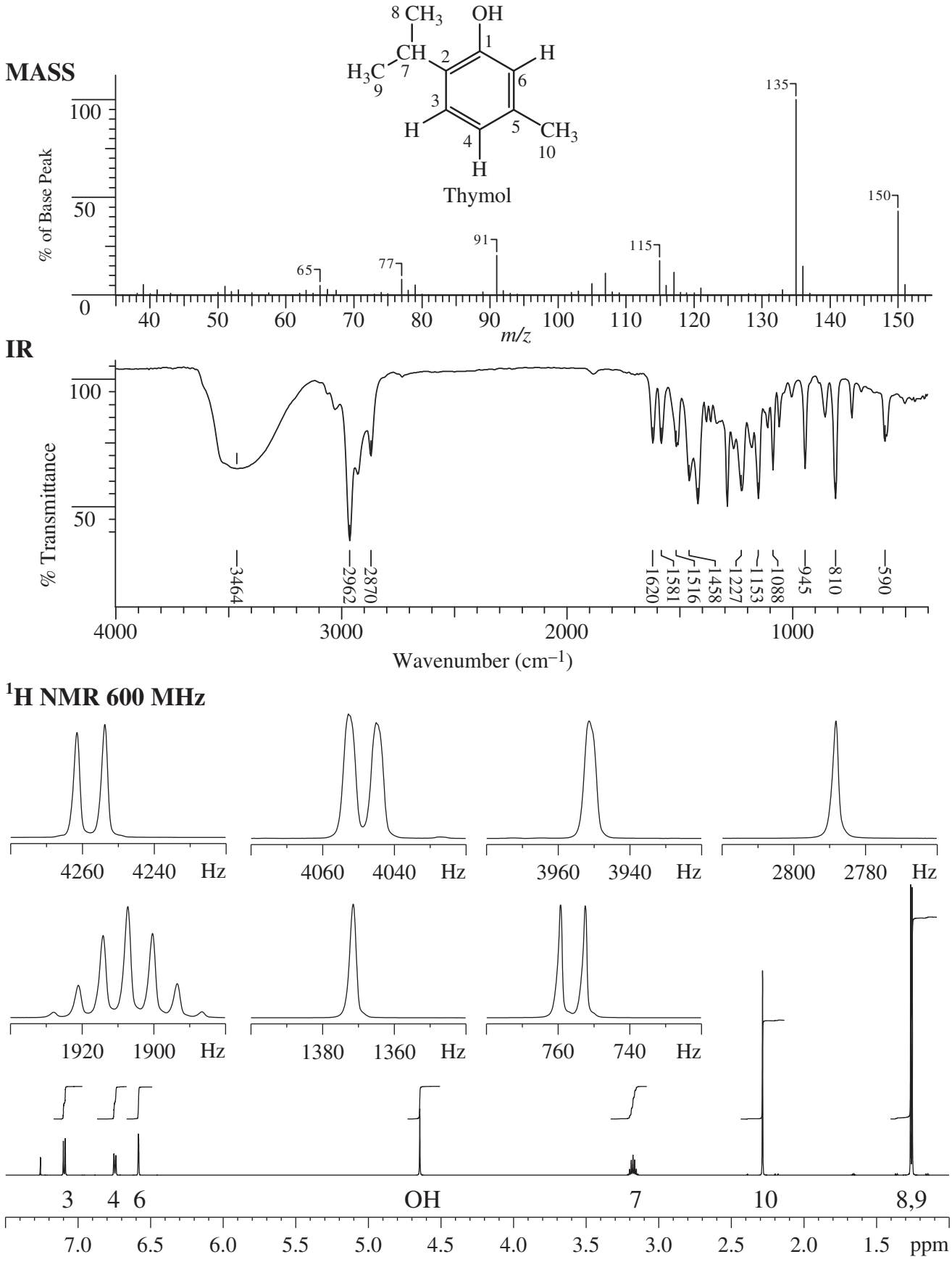
MASS
Thymol
% of Base Peak
m/z
IR
% Transmittance
Wavenumber (cm–1)
3464
2962
2870
1620
1581
1516
1458
1227
1153
1088
945
810
590
1H NMR 600 MHz
Hz
3 4 6
OH
7
10
8,9
ppm

DQFCOSY 600 MHz

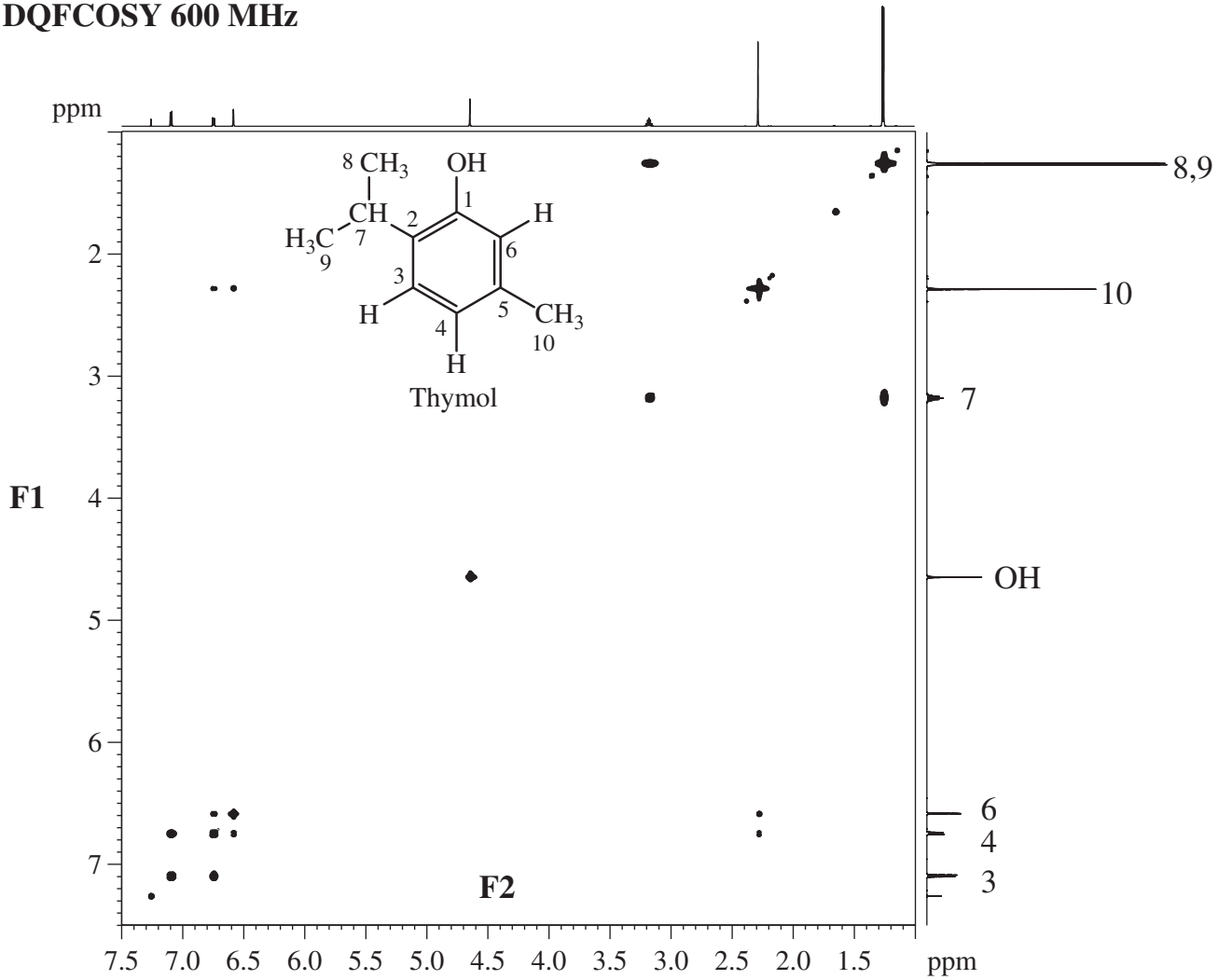

^{13}C/DEPT NMR 150.9 MHz

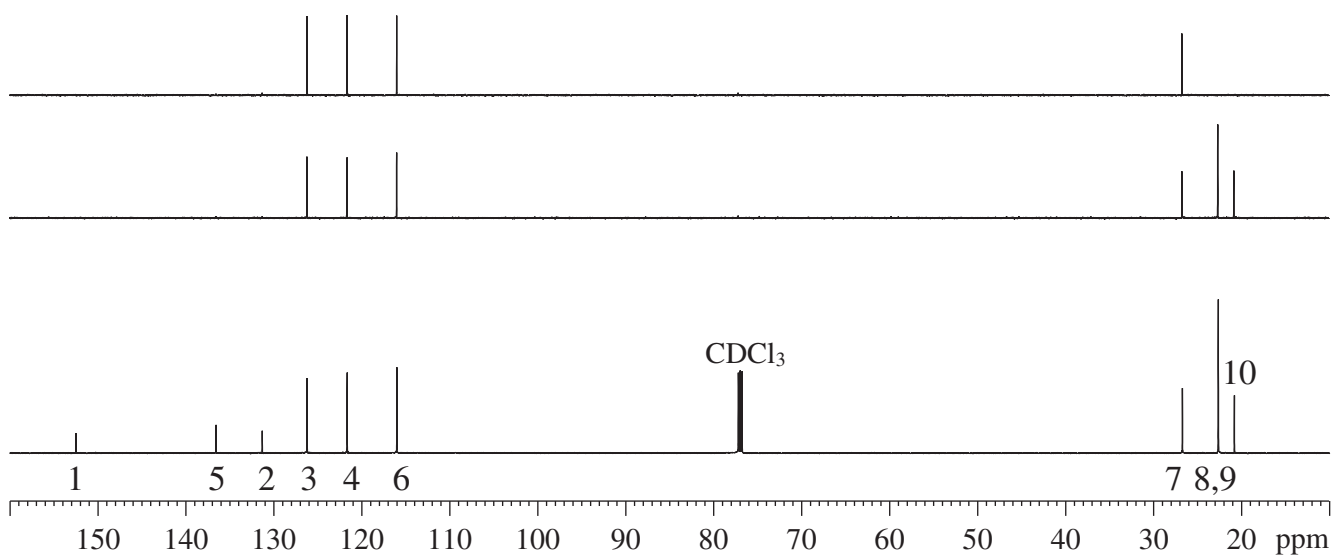

HMQC 600 MHz

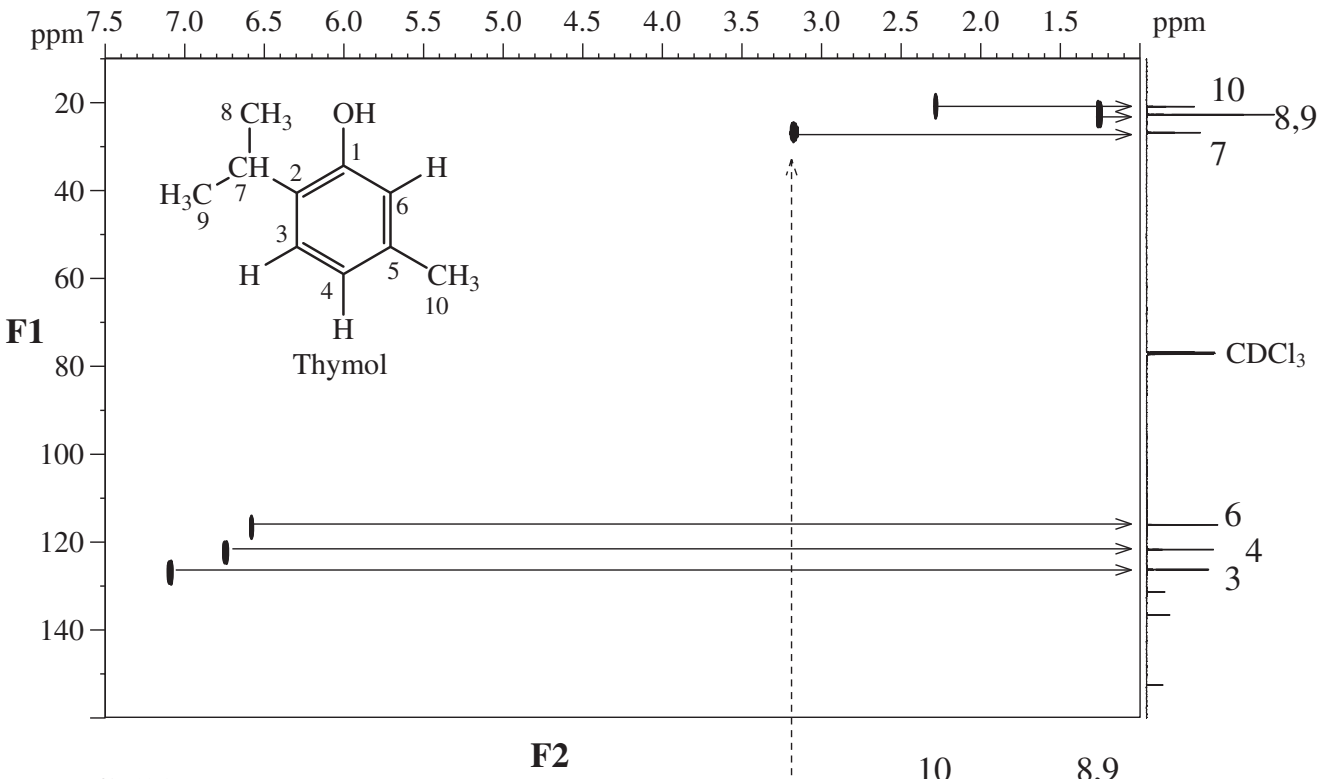

HMBC 600 MHz

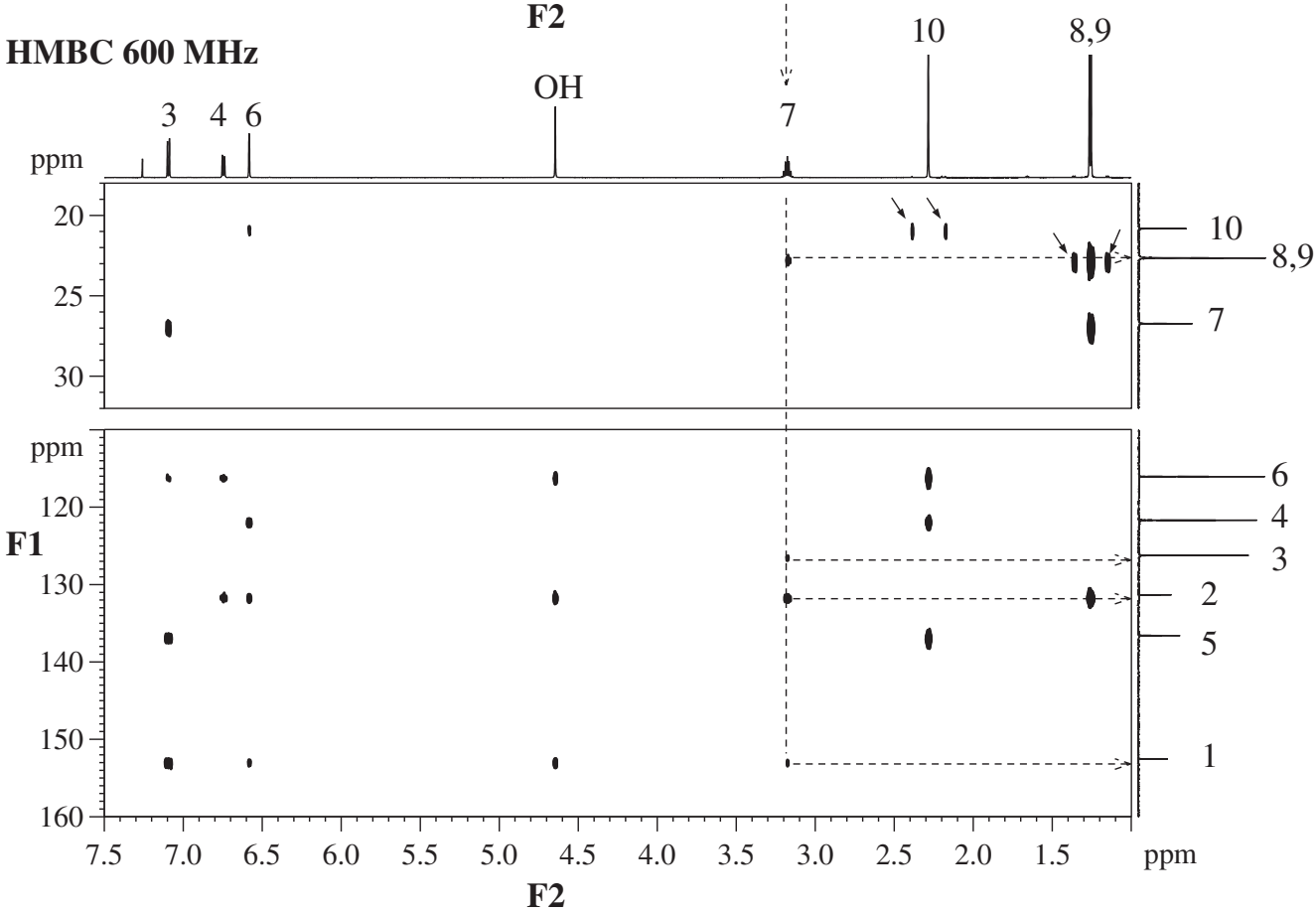

PROBLEM 7.3 DISCUSSION

The molecular ion is certainly the medium-intensity peak in the mass spectrum at m/z 150; there is a rational loss of a CH_3 group to give the base peak at m/z 135. The isotope peaks for the molecular ion do not permit the presence of S, Cl, or Br. Let us assume, tentatively, that the even-numbered molecular ion peak indicates the absence of N. If so, with the help of Appendix A (Chapter 1), the molecular formula can be limited to these possibilities: $C_6H_{14}O_4$, $C_8H_6O_3$, $C_9H_{10}O_2$, or $C_{10}H_{14}O$. The IR spectrum is notable for the intense OH peak at 3464 cm^{-1}. The immediate question is the presence or absence of aromaticity. If an aromatic ring is present, is it attached directly to the OH group to give a phenol? The ^1H and ^{13}C NMR spectra provide answers with peaks in the aromatic regions. The strong IR peaks between 1600 and 600 wavenumbers suggest aromaticity and ions at 77 m/z and 91 m/z serve to confirm our conclusion.

There are seven different kinds of protons in the ^1H NMR spectrum in the ratios, from high frequency to low frequency, of 1:1:1:1:1:3:6 giving a total of 14 protons. The six-proton doublet at 1.25 ppm probably represents two equivalent CH_3 groups of an isopropyl moiety; the one-proton septet at 3.2 ppm is the resonance of the corresponding methine group of the isopropyl group.

The ^{13}C NMR spectrum shows nine peaks, but one of them (at 23 ppm) is suspiciously intense and since it correlates with the six-proton doublet in the HMQC spectrum, we conclude that there are two superposed CH_3 groups, which makes a total of 10 carbon atoms. The ^{13}C/DEPT spectra specify, from high to low frequency, C, C, C, CH, CH, CH, CH, CH_3(×2), CH_3, to which we add the OH group. For a total mass of 150, the most reasonable molecular formula is $C_{10}H_{14}O$, which has an index of hydrogen deficiency of four. This degree of unsaturation fully accounts for a benzene ring, that is, three double bonds and one ring. Furthermore, the ^{13}C NMR spectrum consists of peaks in the aromatic region and the aliphatic region.

In the aromatic region, the three weak peaks represent three quaternary carbon atoms, and the three more intense peaks represent the carbon atoms with directly bonded hydrogen atoms. The most deshielded weak peak at 153 ppm represents the carbon atom to which the OH group is attached (see Table 4.12).

The substituents in the aliphatic region must be a methyl group and an isopropyl group. For confirmation, the aliphatic region in the proton spectrum shows (from high to low frequency) a one-proton septet (i.e., CH), a three-proton singlet (i.e., CH_3), and a six-proton doublet. It is a doublet because it consists of two identical CH_3 groups coupled to the CH group—hence an isopropyl substituent.

At this point, we distribute the two alkyl substituents with reference to the OH group and do so somewhat indirectly by considering the chemical shifts and coupling constants of the three ring protons. We can assume that the proton peak at 6.6 ppm represents the hydrogen atom which is *ortho* to the OH group (see Chart D.1, Chapter 3). Since this peak is a broadened singlet, there is no adjacent hydrogen atom, but there is a hydrogen atom *meta* to it with a coupling constant too small to resolve. Furthermore, since the spectrum shows only one proton *ortho* to the OH substituent, the other *ortho* position must be attached to either the methyl or the isopropyl group.

The sharp doublet at 7.1 ppm with a J value of about 8 Hz represents an aromatic hydrogen atom with one *ortho* coupling. Since the peaks are sharp, there is no *meta* coupling. Its chemical shift places it *meta* to the OH group, the alkyl groups having little effect on the chemical shift (see Chart D.1, Chapter 3). The broad doublet at 6.75 ppm is due to the proton which is *para* to the OH group, the coupling being *ortho* and weakly *meta.* The choice is between **I** and **II**.

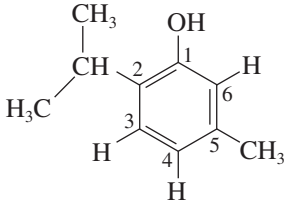

Thymol

I

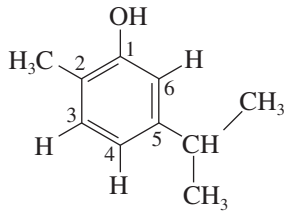

II

The COSY spectrum confirms the previous findings and shows that the protons of the methyl substituent are long-range coupled (^4J) to H-4 and H-6. Interestingly, the isopropyl CH proton does not show long-range coupling to H-3, possibly due to the high multiplicity of the CH peak, which would produce a very diffuse (not visible) cross peak. As expected, the aromatic protons show meta coupling (^4J) between H-6 and H-4, and ortho (^3J) coupling between H-4 and H-3. Structure I (thymol) is now heavily favored. Note that the definitive long-range coupling between the CH_3 substituent and H-4 and H-6 was not resolved in the one-dimensional ^1H spectrum.

The HMQC spectrum shows $^1J_{CH}$ coupling. Table 4.12 in Chapter 4 allows us to arrange the aromatic unsubstituted carbon atoms as C-6, C-4, C-3 from top to bottom. The HMQC spectrum confirms the same sequence for H-6, H-4, and H-3. The aromatic, unsubstituted carbon atoms can now be correlated with the firmly assigned aliphatic protons. The substituted aromatic carbon atoms cannot yet be assigned.

The HMBC spectrum permits correlation between isolated proton spin systems—that is, bridging such "insulating" atoms as O, S, N, and quaternary carbon atoms.

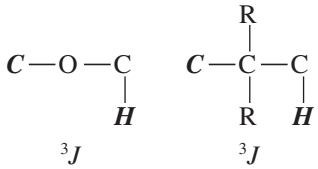

Even in a molecule of modest size, the number of $^2J_{CH}$ and $^3J_{CH}$ couplings can be daunting. Where to start?

Well, simply pose an important question: How do we fully confirm the positions of alkyl substituents? The COSY spectrum did detect the long-range coupling for the methyl substituent but not for the isopropyl substituent. Confirmation can be found by looking down from the CH isopropyl septet in the HMBC spectrum and observing four cross peaks that correlate this CH proton with C-8, 9 (^2J), C-2 (^2J), C-3 (^3J) and C-1 (^3J) in the thymol structure. Certainly convincing. As overkill, note that in the HMBC spectrum, the protons of the methyl substituent correlate with C-6 (^3J), C-4 (^3J), and C-5 (^2J). Further, note that the six methyl protons of the isopropyl group correlate with C-7 (^2J) and with C-2 (^3J). It is interesting to note that the correlations of H-8 to C-9 (^3J) and H-9 to C-8 (^3J) are also observed.

The utility of HMBC in correlating quaternary carbon atoms with assigned protons can be shown by working out the correlations of C-1, C-5, and C-2. The assignment earlier of C-1 on the basis of its chemical shift is sound, but the assignment of C-5 and C-2 on the basis of chemical shift alone should be affirmed by correlations. This exercise is left to the student.

Bridging across quaternary carbon atoms has been demonstrated in the course of the above correlations. Two final points: (1) There are four contours, designated by arrows, that represent $^1J_{CH}$ couplings (large) that have not been completely suppressed. These CH doublets are obvious since they straddle the proton peaks. They can be ignored. (2) The correlations of the OH proton with C-6, C-2, and C-1 should be noted. Correlations to OH protons can be very useful, but are rarely seen in an HMBC spectrum because they are typically too broad to detect.

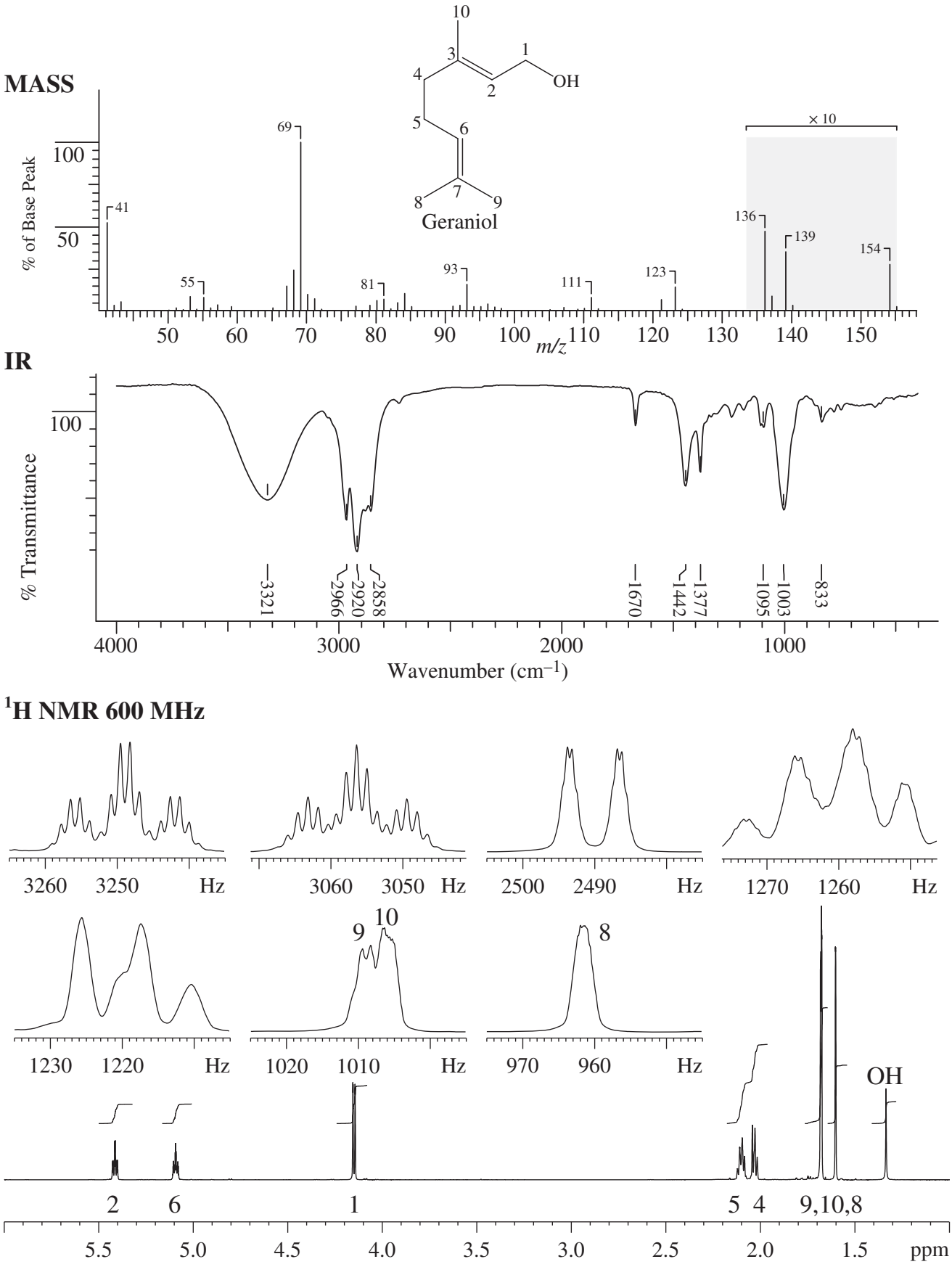
MASS
Geraniol
% of Base Peak
m/z
IR
% Transmittance
Wavenumber (cm−1)
3321
2966
2920
2858
1670
1442
1377
1095
1003
833
1H NMR 600 MHz
Hz
ppm
OH
2
6
1
5 4
9,10,8

Problem 7.4B

DQFCOSY 600 MHz

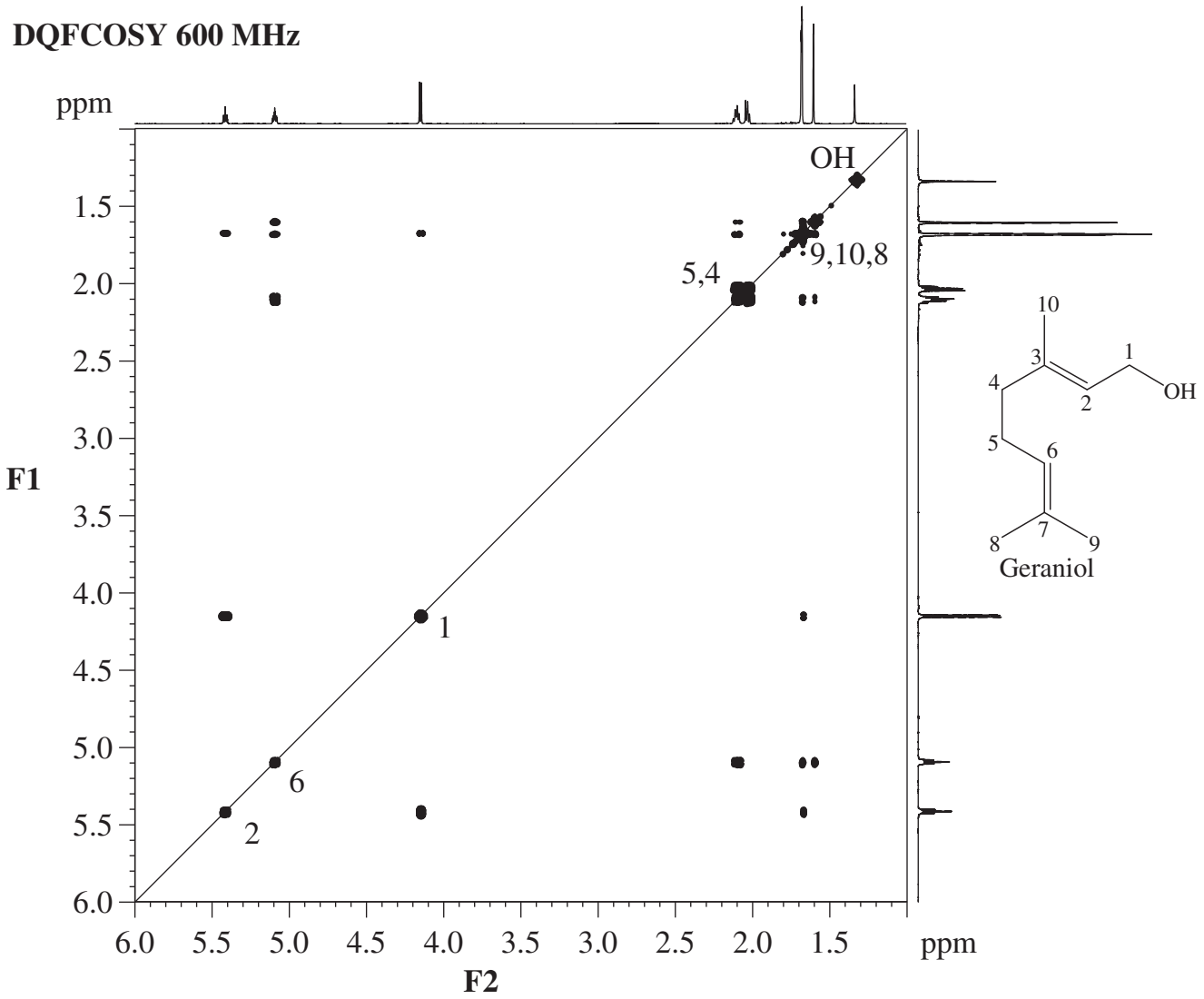

^{13}C/DEPT NMR 150.9 MHz

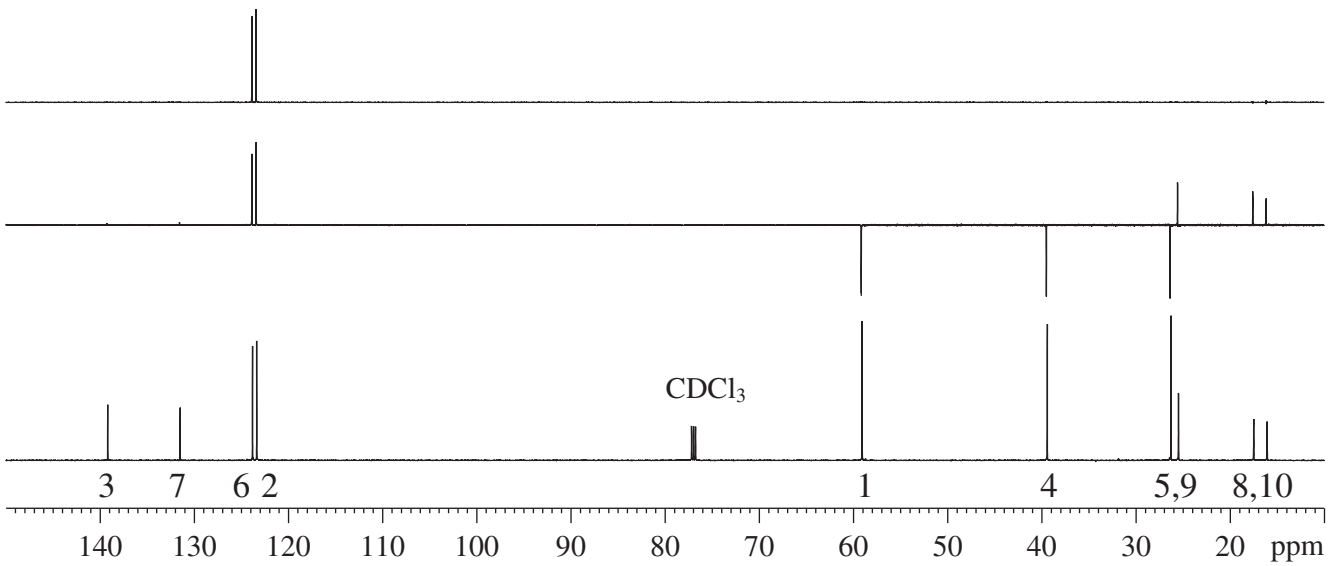

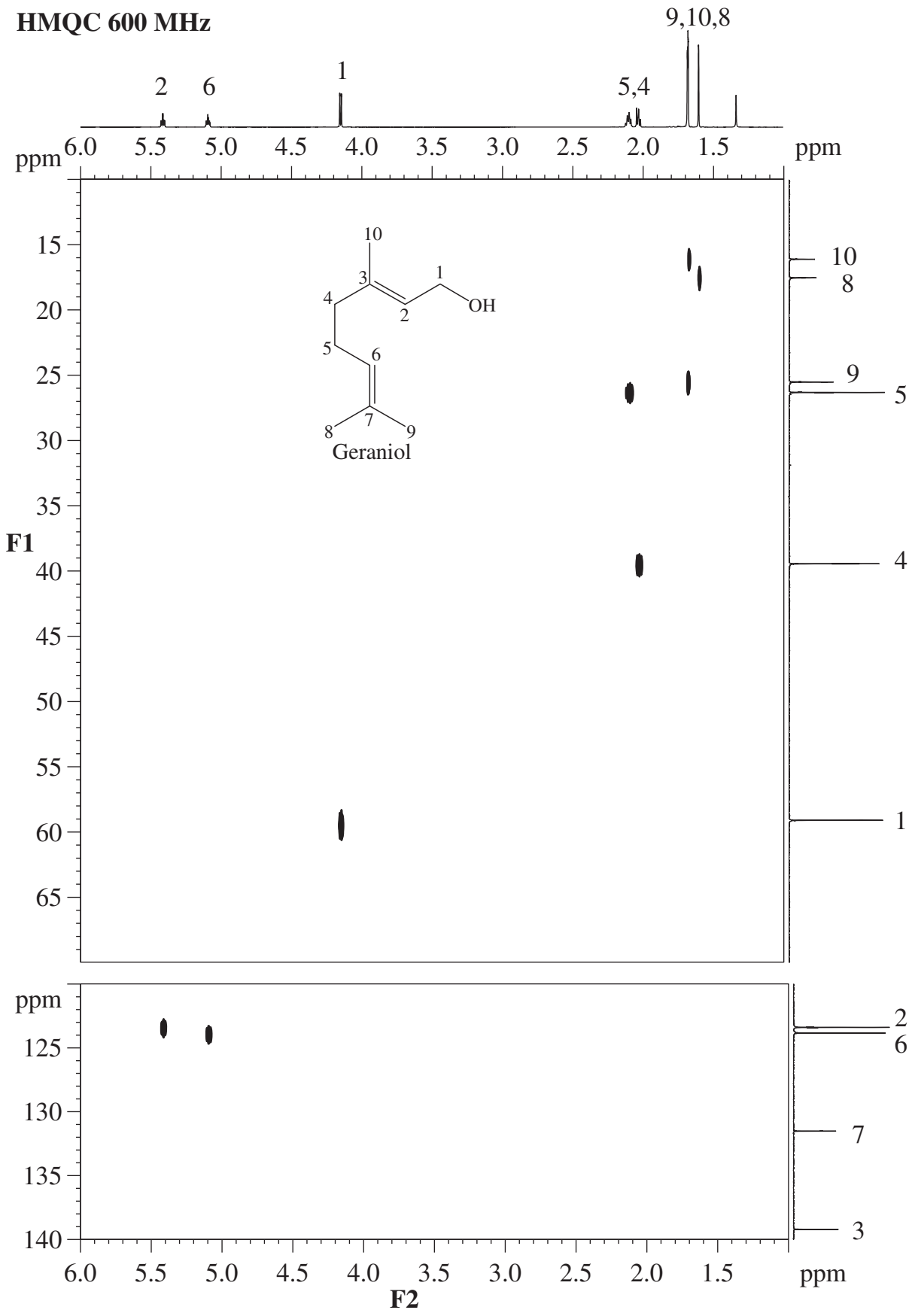
HMQC 600 MHz
9,10,8
2
6
1
5,4
ppm
6.0
5.5
5.0
4.5
4.0
3.5
3.0
2.5
2.0
1.5
ppm
10
3
1
4
2
OH
5
6
8
7
9
Geraniol
F1
15
20
25
30
35
40
45
50
55
60
65
10
8
9
5
4
1
ppm
125
130
135
140
2
6
7
3
6.0
5.5
5.0
4.5
4.0
3.5
3.0
2.5
2.0
1.5
ppm
F2

Problem 7.4D

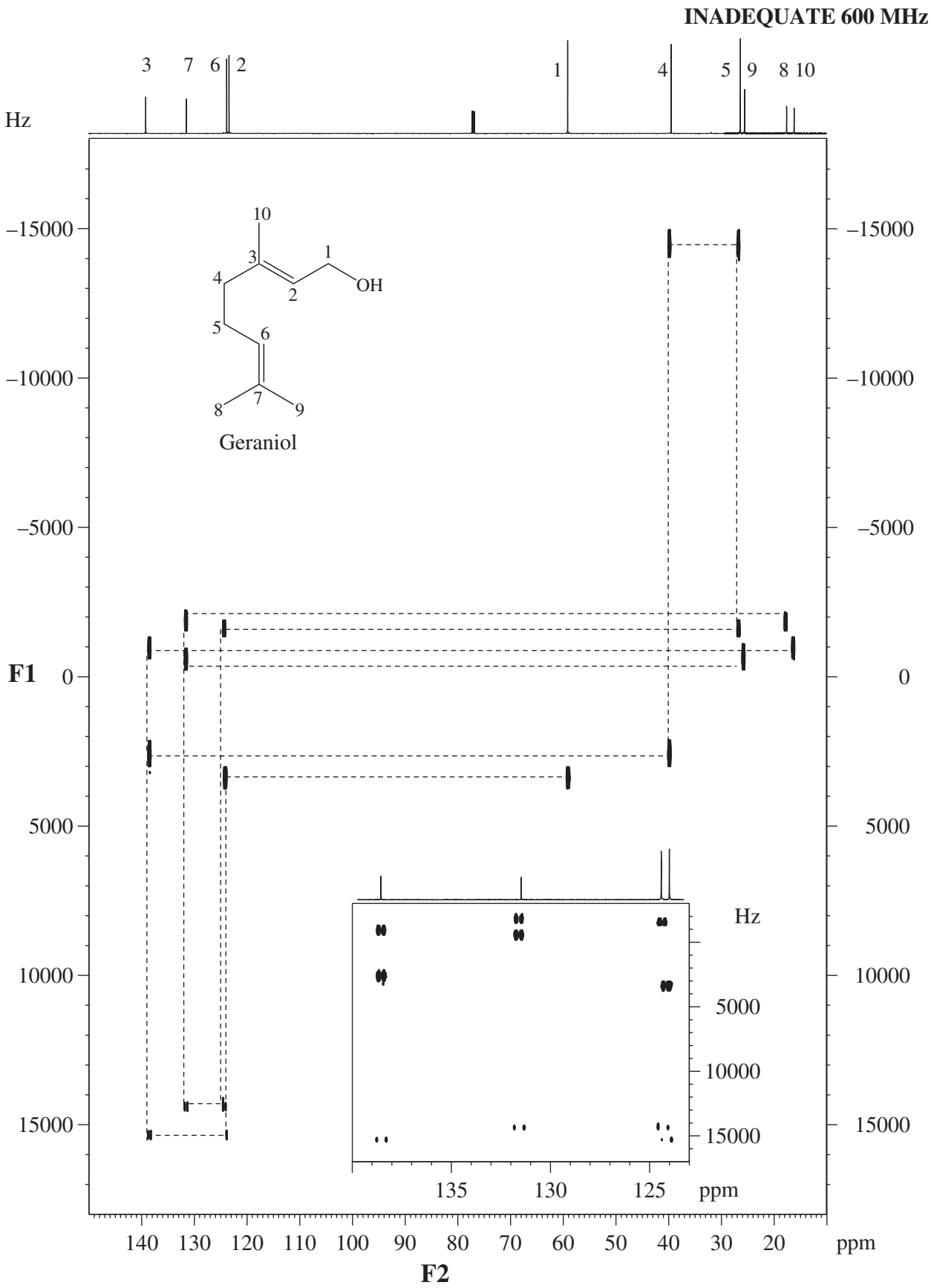
INADEQUATE 600 MHz
3 7 6 2 1 4 5 9 8 10
Hz
10
3
1
4
2
OH
5
6
8
7
9
Geraniol
–15000
–10000
–5000
0
5000
10000
15000
F1
Hz
135 130 125 ppm
140 130 120 110 100 90 80 70 60 50 40 30 20 ppm
F2

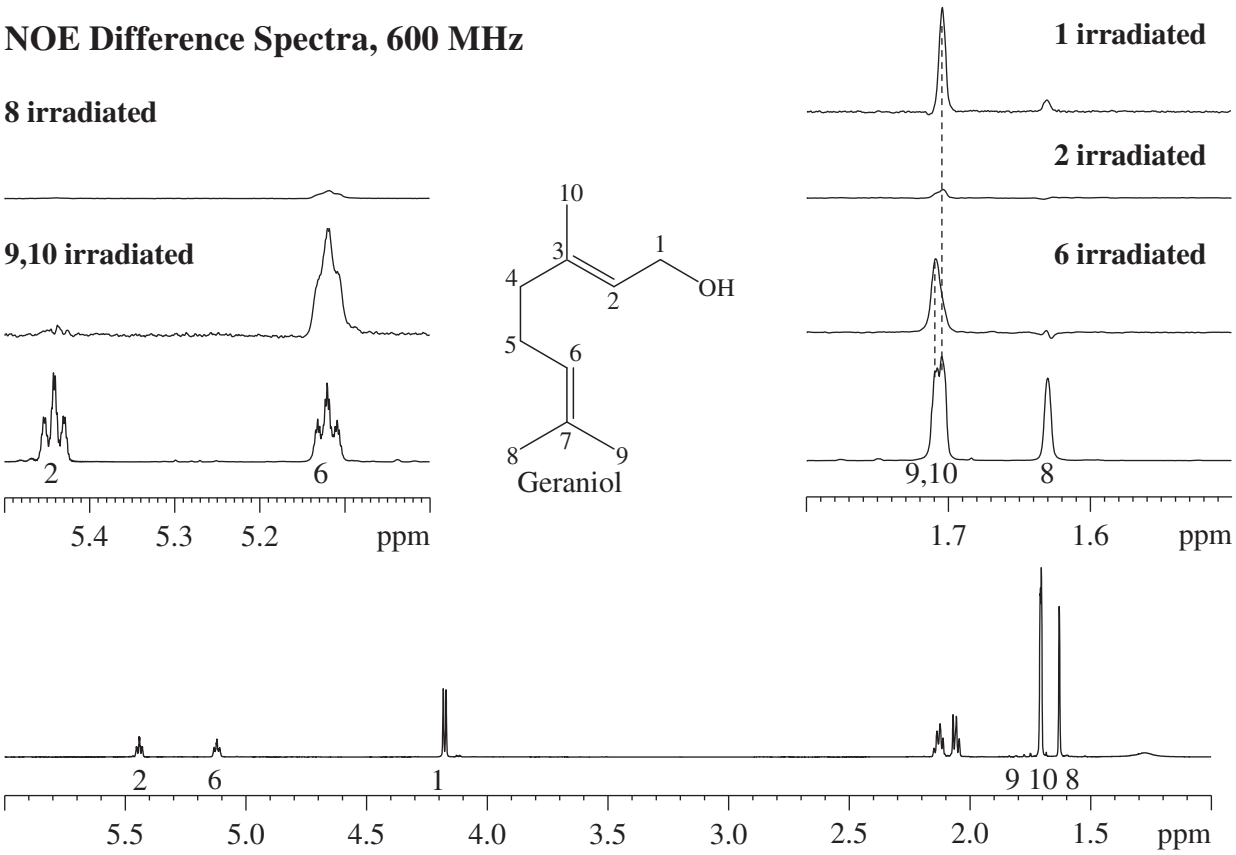
NOE Difference Spectra, 600 MHz
8 irradiated
9,10 irradiated
1 irradiated
2 irradiated
6 irradiated
10
3
1
4
2
OH
5
6
8
7
9
Geraniol
2
6
9,10
8
5.4
5.3
5.2
ppm
1.7
1.6
ppm
2
6
1
9 10 8
5.5
5.0
4.5
4.0
3.5
3.0
2.5
2.0
1.5
ppm

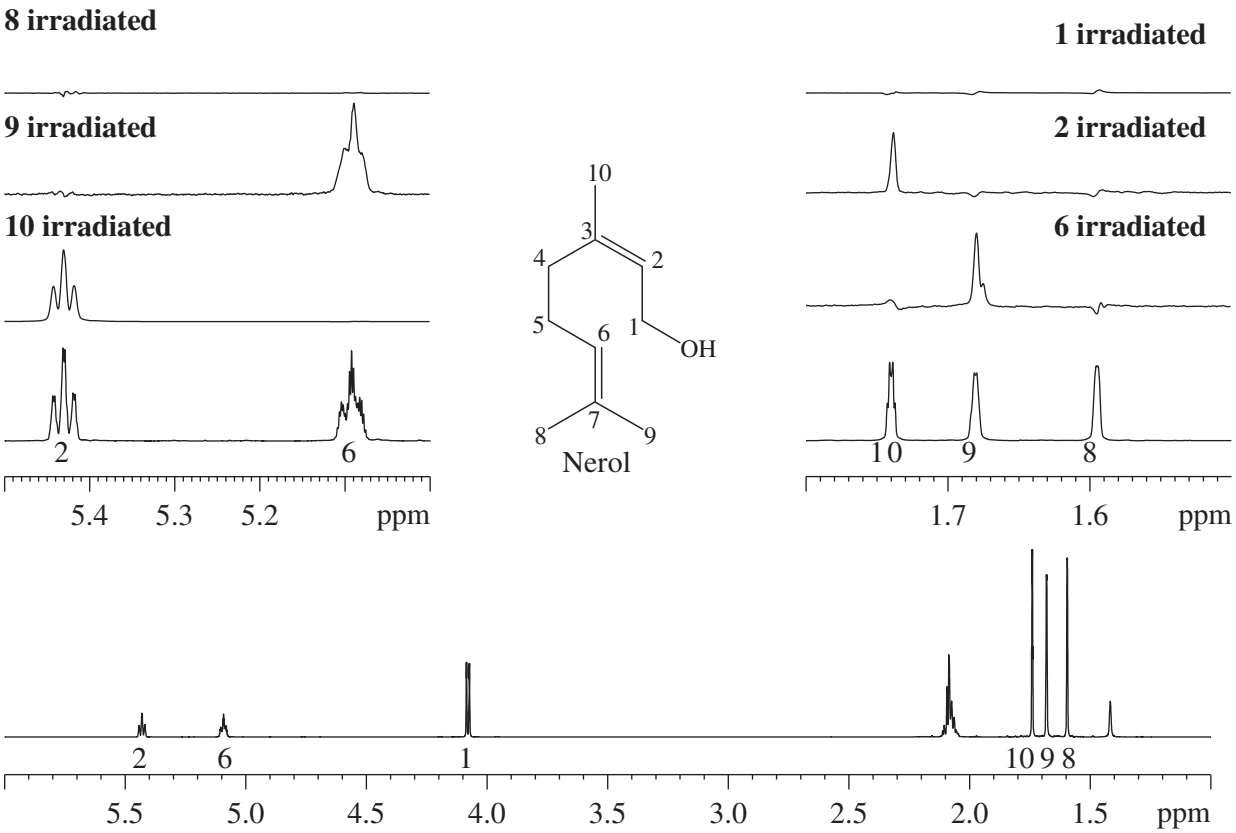
8 irradiated
9 irradiated
10 irradiated
1 irradiated
2 irradiated
6 irradiated
10
3
4
2
5
6
1
OH
8
7
9
Nerol
2
6
10
9
8
5.4
5.3
5.2
ppm
1.7
1.6
ppm
2
6
1
10 9 8
5.5
5.0
4.5
4.0
3.5
3.0
2.5
2.0
1.5
ppm

PROBLEM 7.4 DISCUSSION

It is quite likely that the m/z 154 peak, though small (the gray area is multiplied by 10), is the molecular ion peak. The m/z 139 peak, also small, results from rational loss of a methyl group. The alert interpreter also notes the M-18 peak at m/z 136 and promptly finds the intense, broad OH peak in the "neat" IR spectrum at 3321 cm^{-1} for confirmation; the intense band at 1003 cm^{-1} is probably due to C—O stretching. Again, as in Problem 7.3 we ask: alcohol or phenol; aromatic or not?

The very weak molecular ion peak in the present problem, together with loss of H_2O, suggests, but does not prove, an alcohol rather than a phenol. It may be worthwhile at this point to entertain the possibility that the base peak (m/z 69) represents the fragment $C_5H_9^+$ and results directly from the molecular ion peak by a strongly favored mechanism. If so, the intact molecule probably contains at least one double bond.

The ^{13}C/DEPT spectra provide 10 distinct carbons and 17 hydrogen atoms arranged thus from high to low frequency: C, C, CH, CH, CH_2, CH_2, CH_2, CH_3, CH_3, CH_3. The first four are very likely alkenyl. If the hydroxylic hydrogen atom is added, the tentative molecular formula is $C_{10}H_{18}O$, in accord with the molecular ion, m/z 154. The index of hydrogen deficiency is two, which would allow two double bonds, supported by the four alkenyl carbon atoms.

At this point, it is possible to solve the overall structure by using the wealth of information in the one-dimensional NMR spectra. This limited approach will be explored first, followed by an approach which also makes use of the 2D NMR spectra. Let us note at this time that the stereochemistry of this molecule cannot be ***proved*** using simple ^1H and ^{13}C NMR spectra.

Beginning with the ^1H NMR spectrum, the integration from high to low frequency reads: 1:1:2:2:2:6:3:1, in conformity with the 18 hydrogen atoms in the molecular formula. It can also be read: (CH, CH alkenyl), (CH_2, deshielded by OH), CH_2, CH_2, CH_3, CH_3, (almost superposed), CH_3, OH. Recall from the ^{13}C/DEPT spectra that there are two carbon atoms that have no attached hydrogen atoms. Recall also that the ^{13}C/DEPT spectra showed three distinct CH_3 groups, whereas the ^1H NMR spectrum showed H-9 and H-10 peaks apparently superposed even at 600 MHz. However, they are not completely superposed when expanded; they are partially overlapped with some long-range coupling.

A methylene group (from the ^{13}C/DEPT) is represented by a doublet (with some long-range coupling from H-10) at 4.15 ppm in the ^1H NMR spectrum. Since the only methine groups in the structure are alkenyl (also from the ^{13}C/DEPT), the compound must be an allylic alcohol. The three methyl groups are relatively deshielded and show no vicinal coupling, forcing us to place them on alkenyl carbon atoms. We consider two possible resulting allylic alcohol structures:

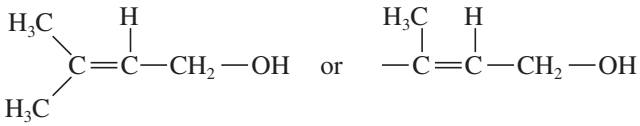

The structure on the left is in fact a complete molecule with no open valences; hence, it is rejected as the alcohol "fragment." The fragment on the right however seems plausible.

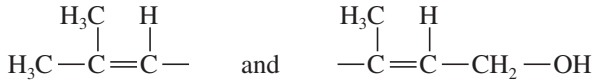

Another "fragment" can be constructed by considering that we have another double bond with two methyl groups that have no vicinal coupling (i.e., they are geminal) and an alkenyl methine, shown at left above. If we consider the two fragments that we now have and realize that the two remaining pieces that have not been used are methylene groups, it is a simple matter of inserting them between the two fragments shown above to arrive at the structure below:

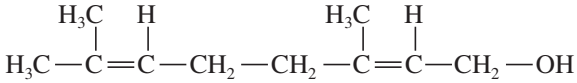

This is a doubly unsaturated terpene alcohol. The *cis/trans* stereochemistry is more accessible (and more obvious) in the following representation:

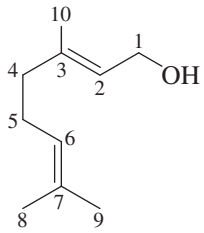

The structure has no stereogenic center. There is a plane of symmetry in the plane of the page; thus, the protons of each methylene group are interchangeable (enantiotopic). The H-4 protons give rise to a distorted triplet by coupling to the H-5 protons, which give a distorted quartet by coupling to the H-4 protons and to the H-6 proton with a slightly different coupling constant. The small $\Delta\nu/J$ ratio for H-4, H-5 also contributes to the distortion. The methyl groups, H-8 and H-9, are in the symmetry plane and are thus not interchangeable. The three methyl proton groups have distinct chemical shift.

Certainly the story is convincing, but the evidence is based only on the chemical shifts and on coupling patterns. It is unwarranted to base an analysis on chemical shifts and coupling patterns when a detailed analysis can be done unambiguously with 2D experiments.

A better approach for solving structures relies less on the 1D spectra and taps the wealth of information in the

2D spectra. We obtain the molecular formula as we did above, noting also the presence of the alcohol functionality from the IR spectrum with confirmation in the ^{13}C/DEPT and ^{1}H NMR spectra. Next, we turn to the 2D NMR data. Evidence of diastereotopic protons is quickly ascertained in the HMQC spectrum by noting if there are two protons with different chemical shifts that show correlations to the same ^{13}C peak. No such diastereotopic correlations are seen.

The connectivity data of the COSY spectrum are most reassuring and a good place to start. The peaks along the diagonal are numbered for convenience. A good entry point for the COSY data is the methylene resonance at 4.15 ppm (H-1). (If you need convincing that this peak is CH_2 number 1, confirmation can be found in the HMQC and ^{13}C/DEPT spectra.) Correlation by way of vicinal coupling is found to the alkenyl methine (H-2) at 5.41 ppm and correlation to a methyl group at 1.68 ppm (H-10) by way of long-range coupling is also evident. How do we know that the proton multiplet at 5.41 ppm is associated with a methine functionality? By using the natural interplay of spectra, the proton multiplet at 5.41 ppm correlates with a carbon resonance at 123 ppm in the HMQC spectrum; this information is fed back into the ^{13}C/DEPT spectra and we find that the carbon resonance at 123 ppm is due to a methine carbon. Likewise, the proton resonance at 1.68 ppm is correlated to a methyl carbon atom in the HMQC spectrum.

We can continue the connectivity pattern with the COSY to H-4 because there is a weak long-range coupling from methyl H-10 to methylene H-4 at 2.11 ppm. (The student is encouraged to confirm that the multiplet at 2.11 ppm is a methylene group by examining and comparing the COSY, HMQC, and ^{13}C/DEPT spectra.) The only other correlation to H-4 is to H-5; this correlation is seen, but difficult to discern because the cross peaks are nearly on the diagonal. The H-5 methylene group shows a correlation to H-6 (the other alkenyl methine) at 2.03 ppm. H-6 shows two other correlations, both long range, to the methyl groups H-8 and H-9. There are no other correlations in this COSY spectrum. The OH proton shows no cross peak because of rapid exchange.

At this point, we have assigned all of the protons but still cannot differentiate between the methyl groups at H-8 and H-9. Since we know all the ^{1}H assignments, it is a trivial task to transfer assignments to the ^{13}C signals through the HMQC spectrum. The quaternary carbons C-3 and C-7 have no attached protons and do not show up in the HMQC spectrum. An HMBC spectrum could be used to correlate the quaternary carbon atoms, but for this example we use carbon connectivities instead.

The INADEQUATE spectrum provides the connectivities between adjacent ^{13}C atoms. It is a most powerful tool; after all, organic molecules consist mainly of chains and rings of carbon atoms. Lines showing connectivities between and among correlated carbons have been added to the INADEQUATE spectrum. As a starting point, consider the three methyl carbons C-8, C-9, and C-10. We note that C-10 is bonded to C-3 whereas C-8 and C-9 are both bonded to an alkenyl carbon (C-7). These connectivities confirm our assignment of C-10; however, we are unable to distinguish between C-8 and C-9. These assignments are made in the next section. If we continue from C-3, we see two more connectivities, one to an alkenyl carbon (C-2) (see inset) and the other to an aliphatic carbon (C-4). The rest of the connectivities are left as an exercise for the student to transform the correlations into a carbon skeleton.

There are still two remaining tasks: assignment of stereochemistry of the C-2, C-3 double bond and assignment of the C-8 and C-9 methyl groups. NOE difference spectroscopy reveals $^{1}H—^{1}H$ proximities through space because of enhancement by the nuclear Overhauser effect. The "difference" spectrum is obtained by subtracting a standard ^{1}H spectrum from the NOE spectrum; this leaves only the enhanced peak(s).

The task we face with the present molecule—distinguishing between a trisubstituted (*E*) double bond and the corresponding (*Z*) double bond—is not a trivial assignment. Nor is the task of distinguishing between the H-8 and H-9 methyl groups, as has been mentioned earlier. For conclusive results, we examine both the (*E*) isomer (geraniol) and the (*Z*) isomer (nerol) at the C-2 double bond.

In the top half of the NOE difference spectra, the ^{1}H NMR spectrum of geraniol, along with the NOE difference subspectra resulting from irradiation of key proton groups, are given and, in the bottom half of the page, the ^{1}H NMR spectrum of nerol (the geometric isomer of geraniol) along with the corresponding NOE difference subspectra are given. In geraniol, irradiation of alkenyl methine H-2 shows no NOE enhancement of the H-10 methyl group; the reciprocal irradiation of the H-10 methyl group shows no NOE enhancement of the H-2 methine group. We conclude that these two groups are on opposite sides of the double bond and assign geraniol an *E*-double bond. This assignment is confirmed by irradiation of the H-1 allylic methylene group and the concomitant NOE enhancement of the H-10 methyl group, thereby proving their disposition on the same side of the double bond. Since methyl groups H-9 and H-10 overlap in the proton spectrum, they are irradiated together and we see an NOE enhancement of alkenyl methine H-6. Check the result of irradiation of methine H-6.

Quite often in "real life" problems, especially those involving natural products, the geometric isomer is not available (although, in principle, it could be synthesized). For pedagogical purposes, the results from nerol are presented. In this case, irradiation of alkenyl proton H-2 does result in NOE enhancement of methyl group H-10, and we conclude that nerol has a Z-double bond. The assignments of methyl groups H-8 and H-9 are left to the student.

With hindsight, we can now recognize the fragment peak at m/z 69 (the base peak) as the result of the allylic cleavage of an alkene. Ordinarily, reliance on this cleavage for location of a double bond is dubious, but in geraniol, cleavage of the bis-allylic bond between C-4 and C-5 results in the stabilized fragment, m/z 69. See Section 1.6.1.2 for the analogous allylic cleavage of β-myrcene into fragments m/z 69 and 67.

Problem 7.5A

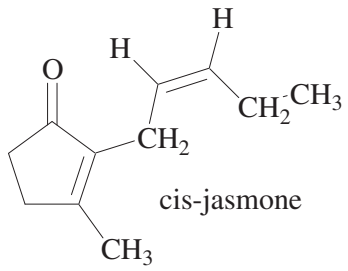

cis-jasmone

MASS

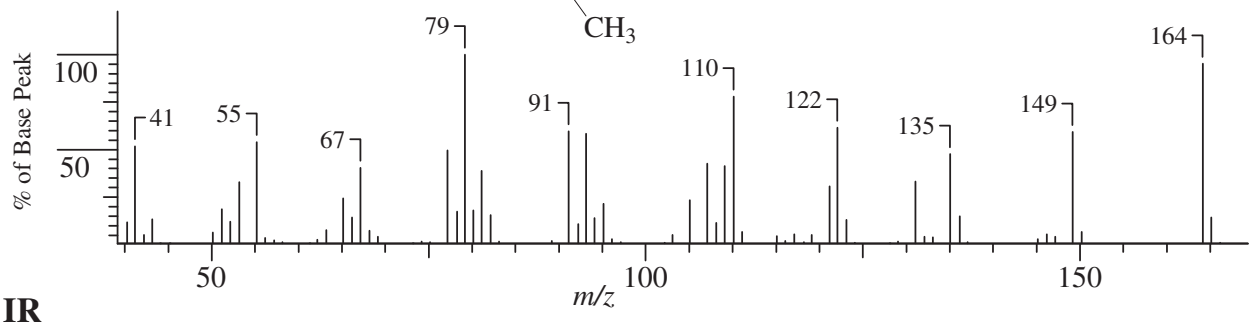

IR

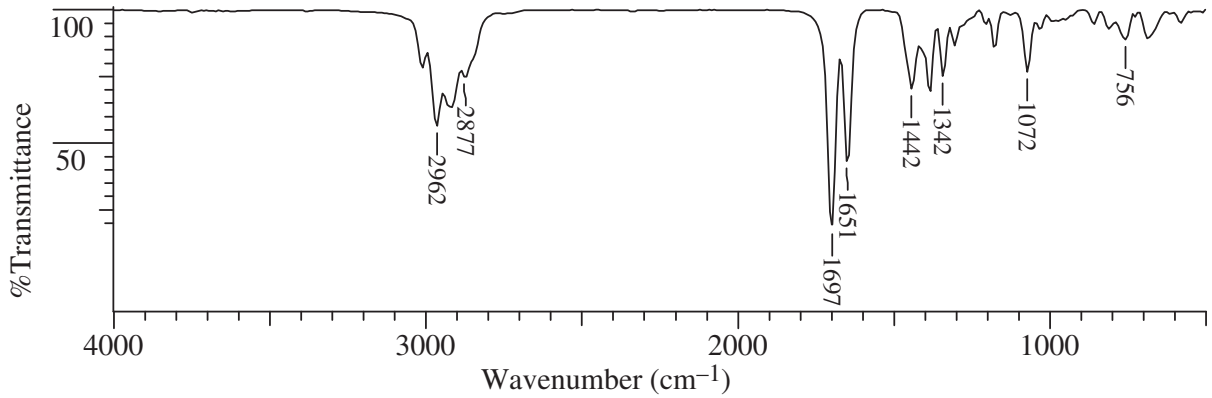

^{1}H NMR 600 MHz

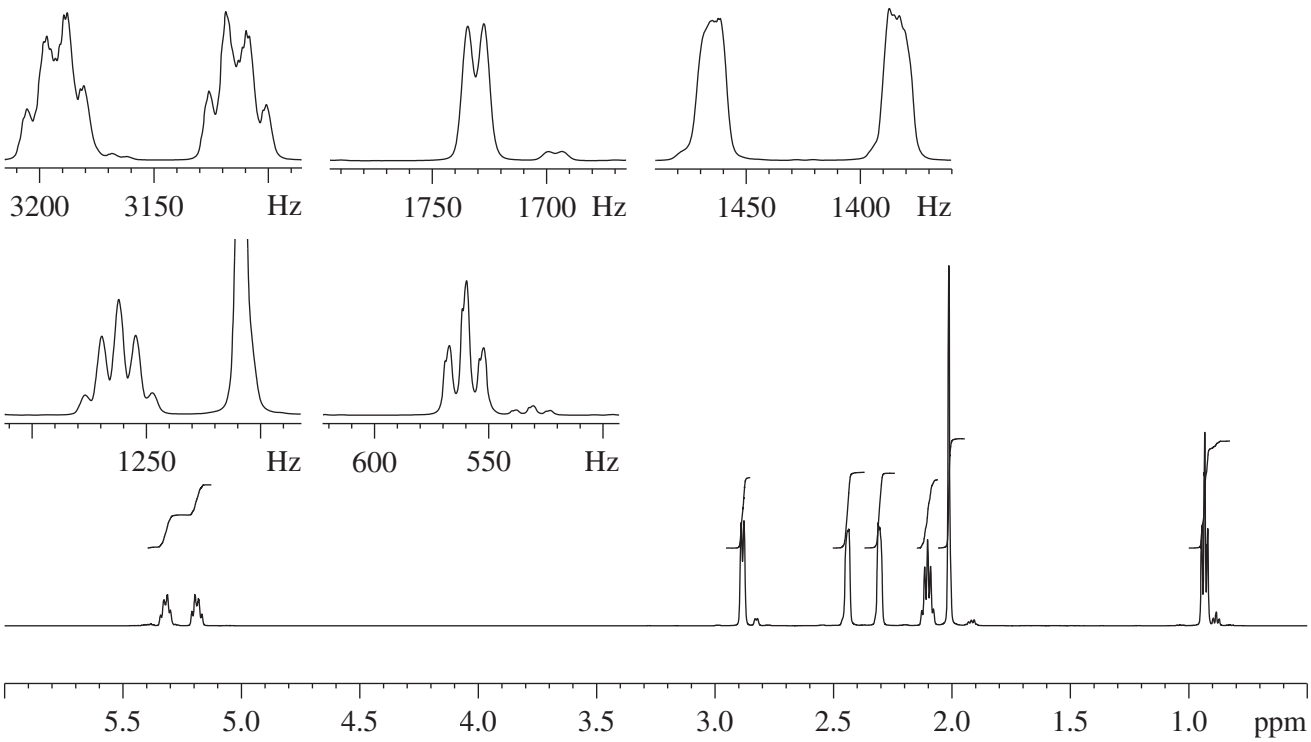

DQFCOSY 600 MHz

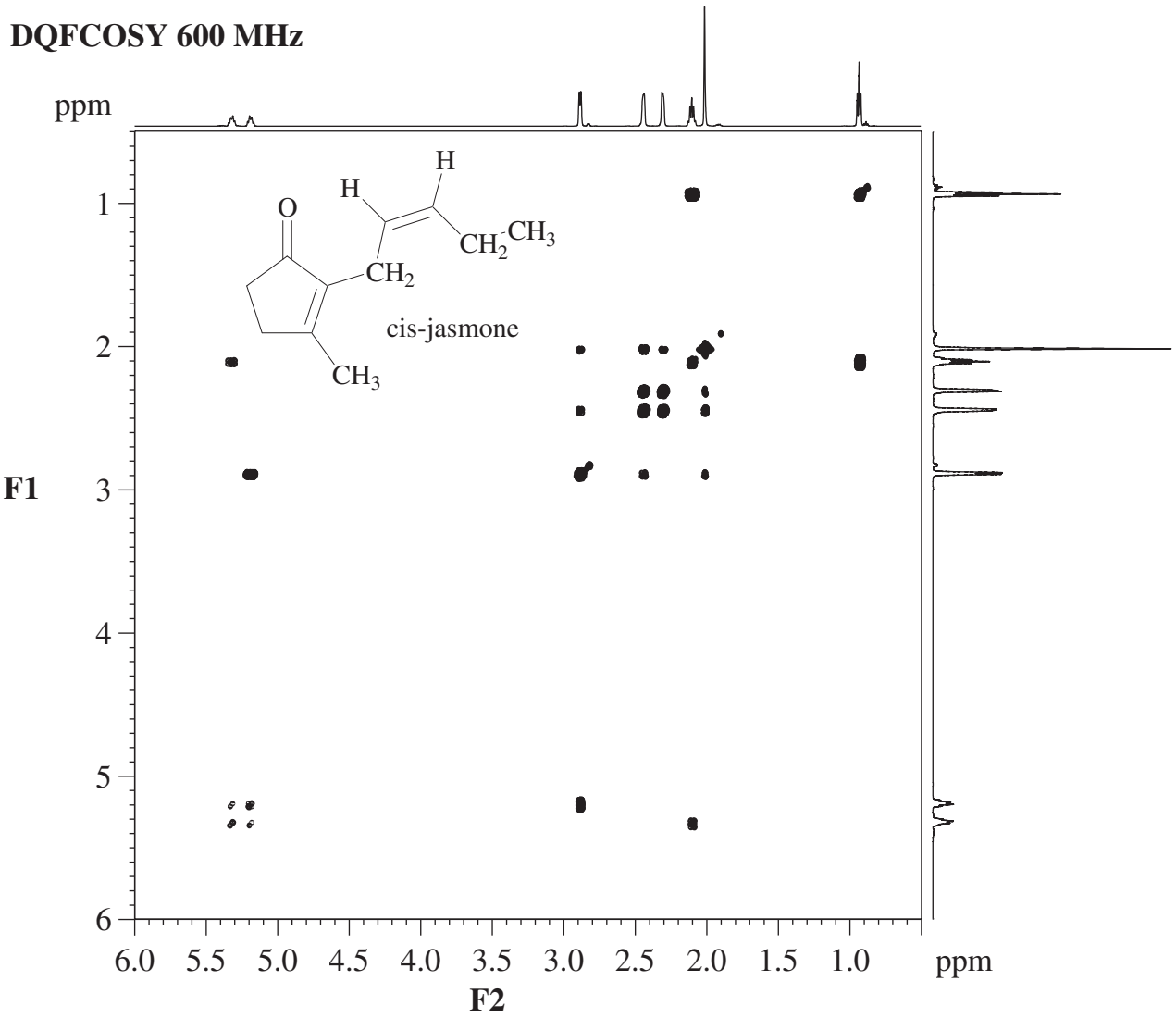

^{13}C/DEPT NMR 150.9 MHz

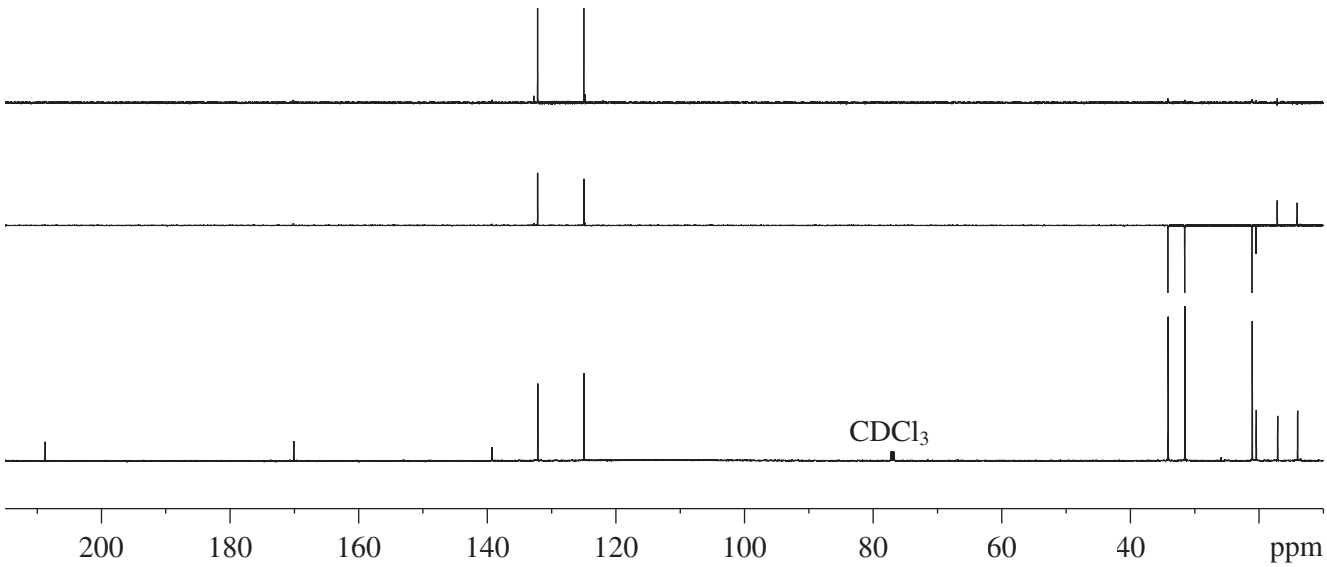

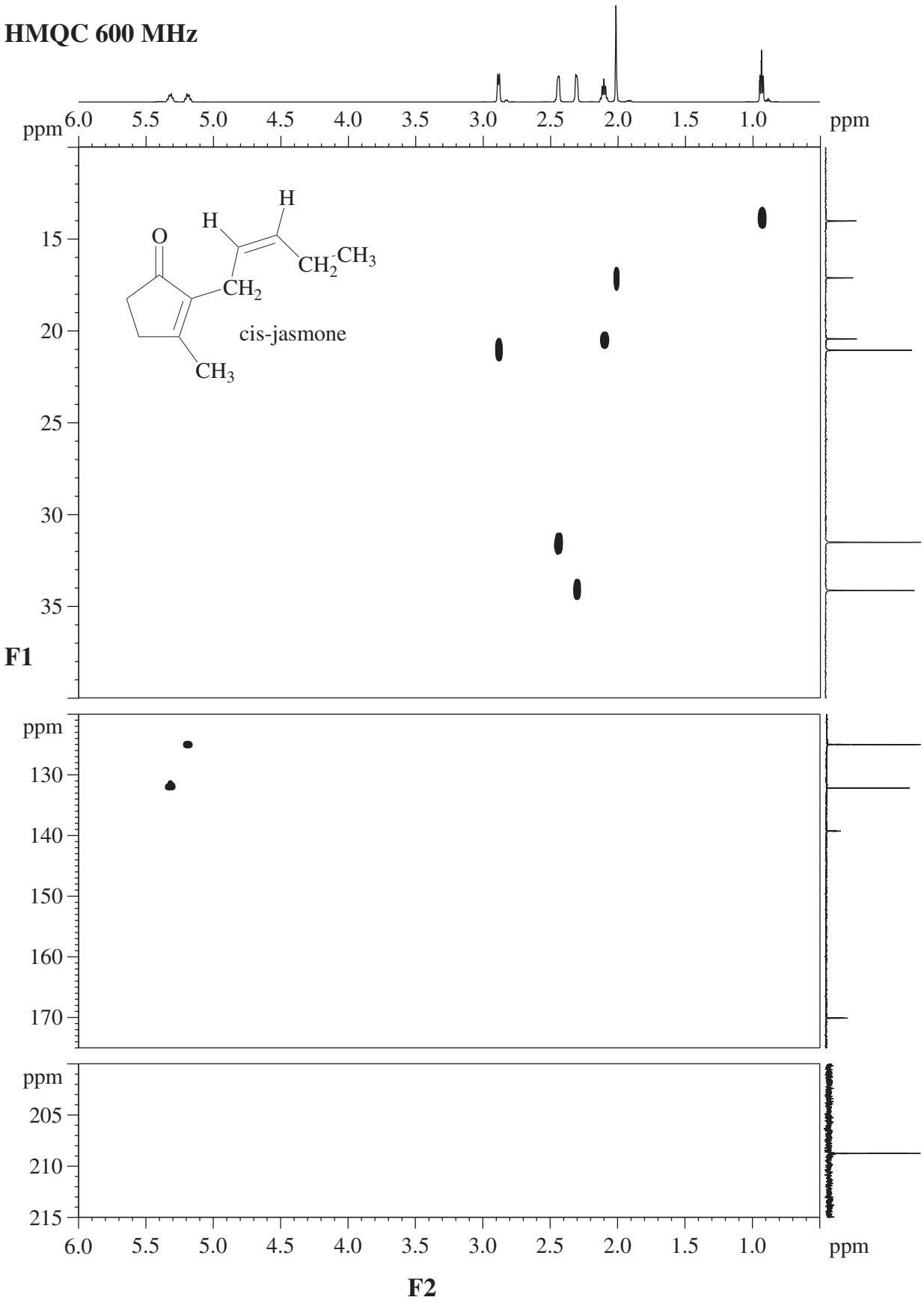
HMQC 600 MHz
ppm
6.0
5.5
5.0
4.5
4.0
3.5
3.0
2.5
2.0
1.5
1.0
ppm
15
20
25
30
35
F1
H
H
O
CH2
CH2
CH3
cis-jasmone
CH3
ppm
130
140
150
160
170
ppm
205
210
215
6.0
5.5
5.0
4.5
4.0
3.5
3.0
2.5
2.0
1.5
1.0
ppm
F2

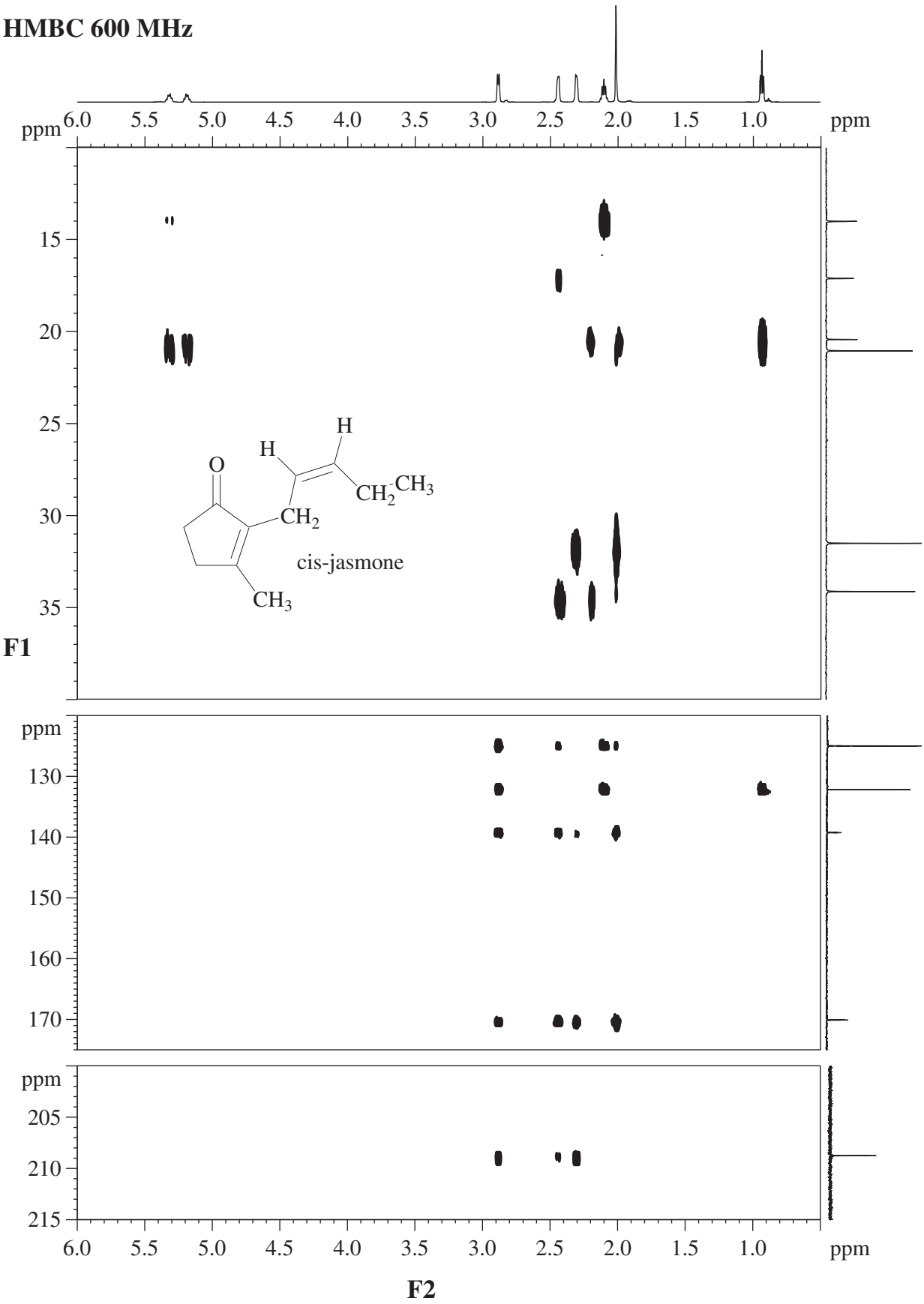
HMBC 600 MHz
ppm
6.0
5.5
5.0
4.5
4.0
3.5
3.0
2.5
2.0
1.5
1.0
ppm
15
20
25
30
35
F1
O
H
H
CH2
CH2
CH3
cis-jasmone
CH3
ppm
130
140
150
160
170
ppm
205
210
215
6.0
5.5
5.0
4.5
4.0
3.5
3.0
2.5
2.0
1.5
1.0
ppm
F2

PROBLEM 7.5 DISCUSSION

In the mass spectrum, the peak at m/z 149 represents a rational loss of a CH_3 group (M-15) and indicates that the m/z 164 peak is the molecular ion peak. The lack of an M + 2 peak indicates the absence of Cl, Br, and S. The IR spectrum shows an intense peak at 1697 cm^{-1}, suggestive of a C═O group, which is confirmed by the peak in the ^{13}C NMR spectrum at 208 ppm (in the range of ketones). In the ^{1}H NMR spectrum, the integrals are: 1:1:2:2:2:2:3:3 (16 protons). The ^{13}C NMR spectrum indicates 11 carbon atoms. Thus, the tentative molecular formula is $C_{11}H_{16}O$, which agrees with the molecular ion peak of m/z 164. The index of hydrogen deficiency is four. From high to low frequency in the ^{13}C/DEPT spectra, the following functionalities are identified: C, C, C, CH, CH, CH_2, CH_2, CH_2, CH_2, CH_3, CH_3.

Three of the four degrees of unsaturation can be dealt with directly from the ^{13}C NMR spectrum. We have already noted the carbonyl peak and because of its chemical shift we associate it with a ketone. There are four alkenyl carbon resonances, which account for two more degrees of unsaturation. By inference, the fourth degree of unsaturation is attributed to a ring.

The ^{13}C/DEPT spectra have provided the various molecular fragments, which is a large step toward deciphering the structure. We turn to the 2D NMR spectra to assemble the pieces. As needed, we will jump from one spectrum to another. The more shielded of the two methyl groups at 0.93 ppm, which correlates with the methyl carbon resonance at 15 ppm in the HMQC, is a good place to start. This methyl group is coupled to a methylene group at 2.12 ppm, as evidenced by the strong cross peak in the COSY spectrum. The carbon resonance associated with this group is found at 21 ppm in the HMQC spectrum. This methylene group also correlates with one of the alkenyl methines in the COSY spectrum at 5.33 ppm. The methylene group at 2.12 ppm shows a nearly first-order quintet.

The other alkenyl methine resonance at 5.18 ppm shows a correlation in the COSY spectrum to the first methine (at 5.33 ppm) strongly suggesting a disubstituted double bond. In addition, the methine resonance at 5.18 ppm is coupled to a rather deshielded methylene group at 2.88 ppm. This methylene resonance is a broadened doublet and shows no other vicinal coupling. According to the COSY spectrum, this methylene group shows long-range coupling to two other groups not yet used (one of the two unused methylene groups and the other methyl group.) So far, we have a 2-pentenyl group, which must be attached to one of the quaternary alkenyl carbon atoms. The broadened singlet at 2.01 ppm must be due to a methyl group attached to the other quaternary alkenyl methine carbon.

If we take stock of the remaining molecular fragments from the ^{13}C/DEPT spectra (a ketone carbonyl, two methylene groups, and two quaternary alkenyl carbons) and the fact that there is still the unused degree of unsaturation for a ring, we realize that we must draw an unsaturated five-membered ring ketone with these pieces. Further evidence allows us to order these pieces. First, the COSY spectrum tells us that the two methylene groups (at 2.30 ppm and 2.45 ppm) are vicinally coupled and therefore adjacent. Second, the ^{13}C chemical shift of one of the quaternary alkenyl carbons is 170 ppm; such deshielding can only be explained by conjugation with the ketone carbonyl. One obvious structure is shown below. The HMBC spectrum (see the correlations to the carbonyl carbon) confirms the ring structure and the lack of a stereogenic carbon atom (there is a plane symmetry in the plane of the page) explains the absence of diastereotopic methylene protons.

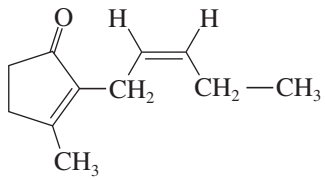

Before we finish, we ask ourselves if there are any constitutional isomers that we need to consider. Yes, if we switch the two substituents (i.e., the 2-pentenyl group and the methyl group), the resulting structure also fits the data so far. Again, the complex HMBC spectrum resolves the issue. For instance, the ring substituted methyl resonance at 17 ppm shows only one correlation to the methylene group at 2.45 ppm. This methylene group is in the β-position relative to the carbonyl, thereby confirming the structure given above. Are there other correlations in the HMBC that can confirm the structure? The student can finish the assignments.

LCMS ES

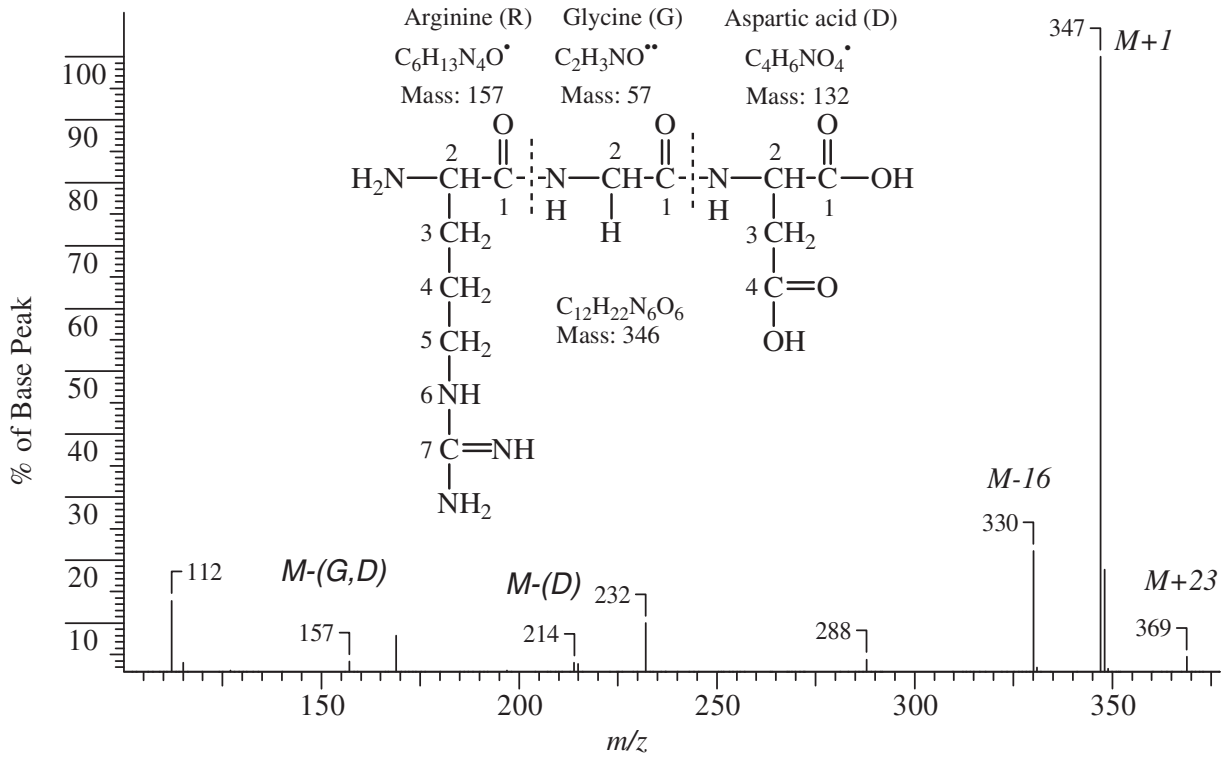

HMQC 600 MHz

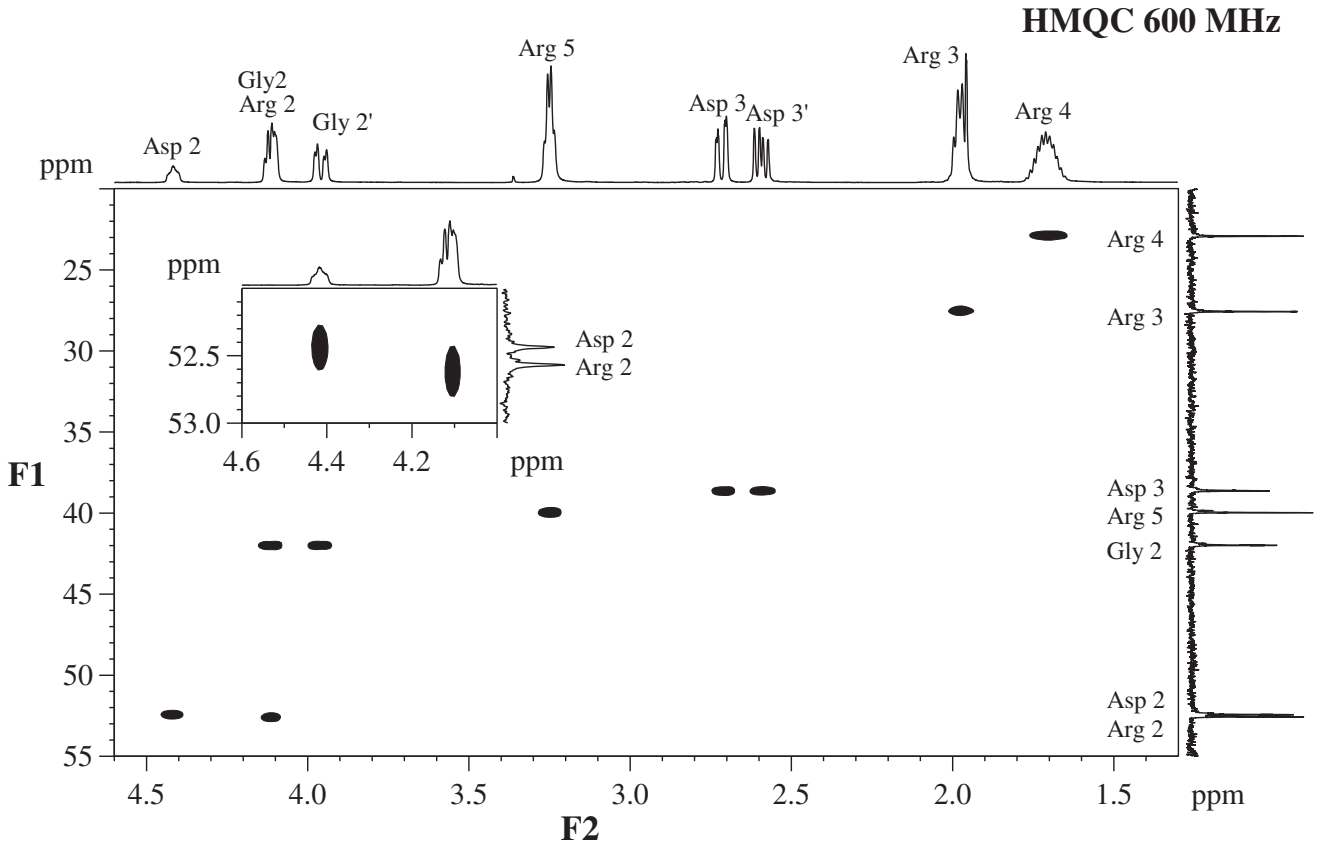

^{1}H NMR 600 MHz

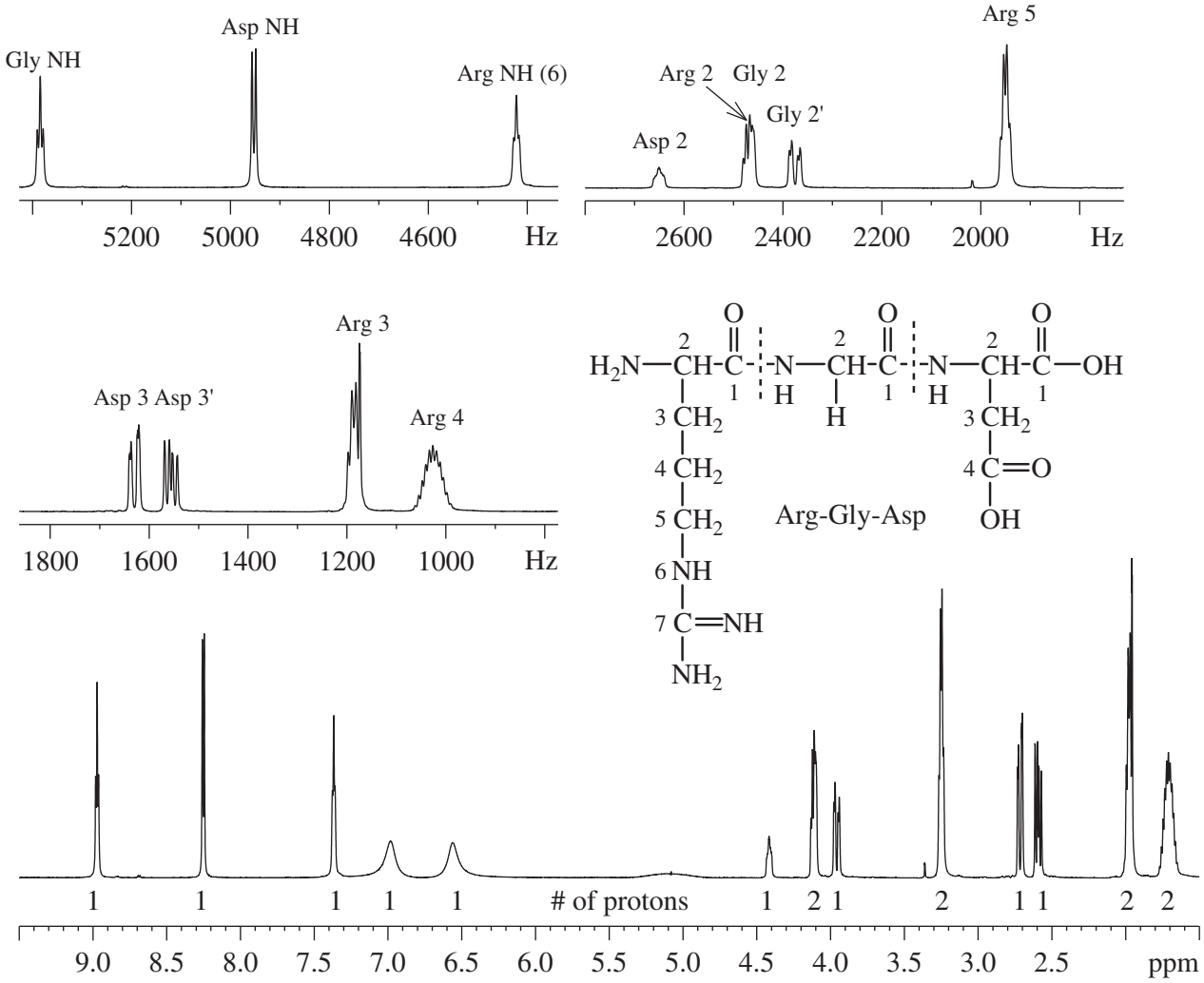

^{13}C/DEPT NMR 150.9 MHz

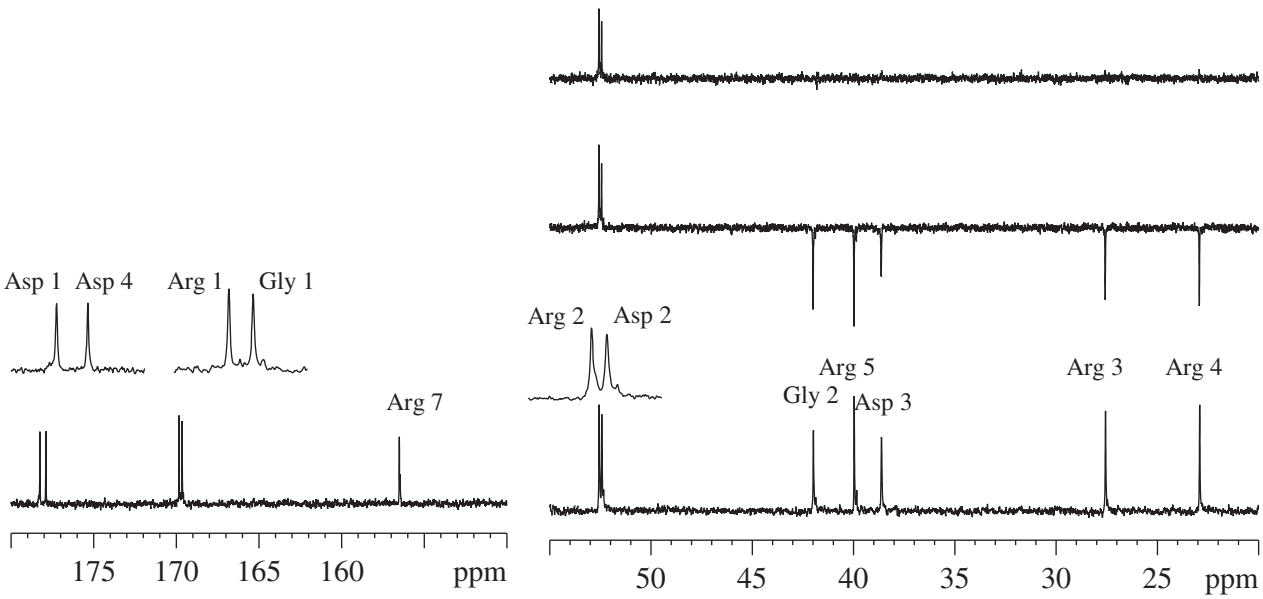

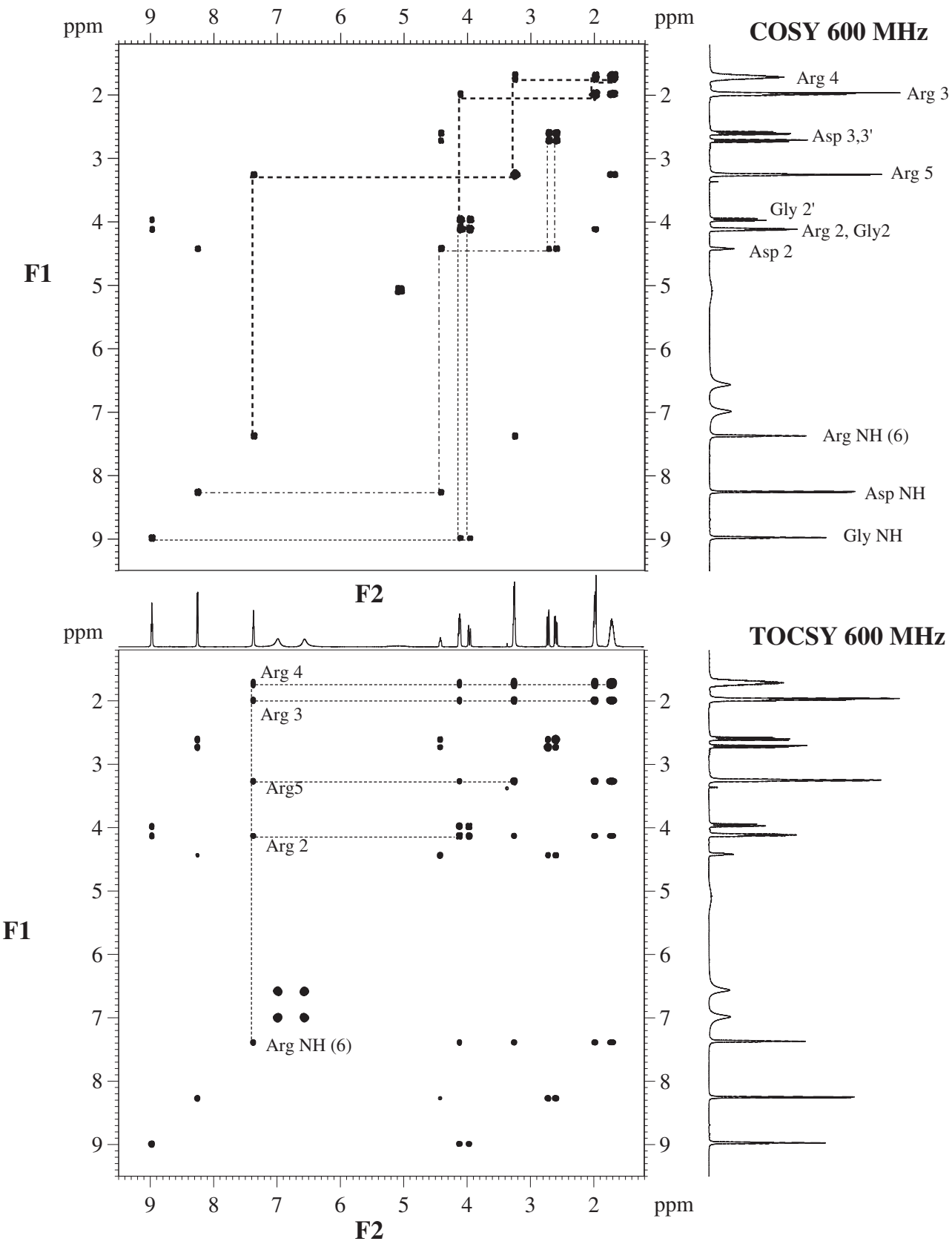
COSY 600 MHz
ppm
F1
F2
Arg 4
Arg 3
Asp 3,3'
Arg 5
Gly 2'
Arg 2, Gly2
Asp 2
Arg NH (6)
Asp NH
Gly NH
TOCSY 600 MHz
Arg 4
Arg 3
Arg5
Arg 2
Arg NH (6)

Problem 7.6D

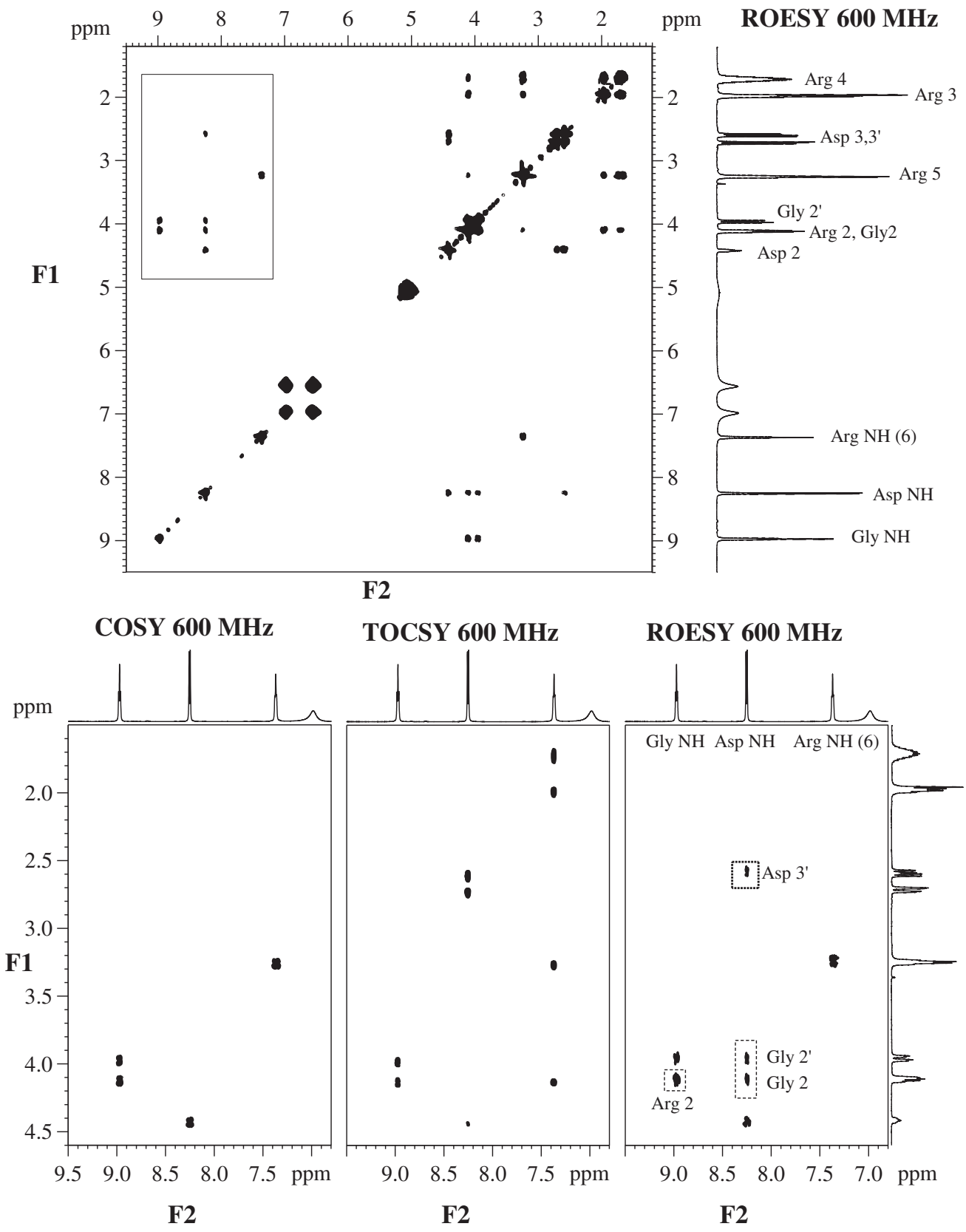
ROESY 600 MHz
ppm
F1
F2
Arg 4
Arg 3
Asp 3,3'
Arg 5
Gly 2'
Arg 2, Gly2
Asp 2
Arg NH (6)
Asp NH
Gly NH
COSY 600 MHz
TOCSY 600 MHz
ROESY 600 MHz
Gly NH Asp NH Arg NH (6)
Asp 3'
Gly 2'
Gly 2
Arg 2

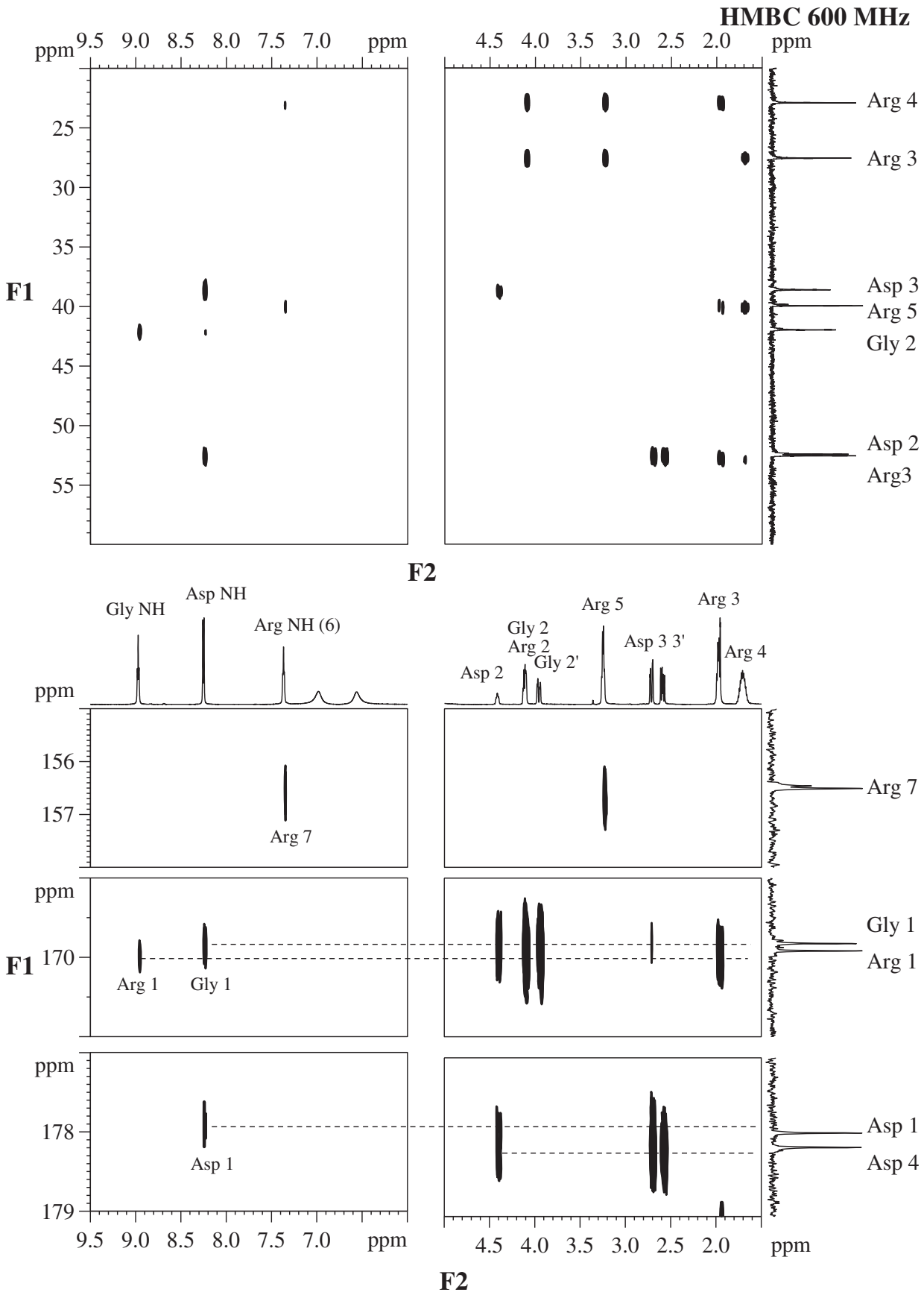
HMBC 600 MHz
ppm
9.5 9.0 8.5 8.0 7.5 7.0 ppm
4.5 4.0 3.5 3.0 2.5 2.0 ppm
F1
25
30
35
40
45
50
55
Arg 4
Arg 3
Asp 3
Arg 5
Gly 2
Asp 2
Arg3
F2
Gly NH
Asp NH
Arg NH (6)
Asp 2
Gly 2
Arg 2
Gly 2'
Arg 5
Asp 3 3'
Arg 3
Arg 4
156
157
Arg 7
Arg 7
170
Arg 1
Gly 1
Gly 1
Arg 1
178
179
Asp 1
Asp 1
Asp 4

PROBLEM 7.6 DISCUSSION

The last of the solved problems in this chapter is quite different from the other problems presented above, and our approach takes a different tack as well. The compound is a tripeptide, and structure elucidation of peptides requires two distinct solutions. First, the individual amino acids (and their number) are determined and second, the amino acid units are put in order (sequenced). Neither of these exercises is trivial since there are more than 20 common amino acids, and the nature of the peptide bond means that they can be arranged in any order.

Before discussing the actual data, some discussion of sample handling is worthwhile. The mass spectrum of the tripeptide was obtained using an electrospray LCMS (see Chapter 1). Electrospray (ES) is a "soft" method of ionization (a type of chemical ionization), which suppresses or limits fragmentation and enhances pseudomolecular ions (depends on the number of charges on the ion, z). The NMR experiments were carried out in 95% H_2O and 5% D_2O at 0°C. The reasoning for using these solvents and the details are given in Section 5.11.

The LCMS ES gives an M + 1 peak of m/z 347, which corresponds to a molecular formula of $C_{12}H_{22}N_6O_6$. Derivation of this formula is not considered in detail since Appendix A in Chapter 1 only goes up to 250 amu. The small peak at m/z 369 (M + 23) is due to the presence of sodium ions, which are ubiquitous in aqueous solutions. Although there is only limited fragmentation, the fragments that do appear can be quite useful to an experienced interpreter, and some of the cleavages are shown as insets in the mass spectrum.

To ascertain the three amino acids, we use information from the ^{1}H NMR spectrum, the ^{13}C/DEPT spectra, the COSY spectrum, the TOCSY spectrum, and the HMQC spectrum. Chemical shifts for protons of amino acids are given in Appendix I of Chapter 3. Peptides are chiral molecules, and all methylene protons are diastereotopic, even those of glycine. (The methylene protons of free glycine are enantiotopic.) A starting point for peptides (and other compounds made of distinct units such as oligo- and polysaccharides) is the TOCSY spectrum. The 2D TOCSY spectrum shows correlations among all spins in a spin system, but no correlations to spins outside the system. For a tripeptide, there are three distinct spin systems, and they are easy to find in the TOCSY spectrum (Problem 7.6C). The N—H resonance at 8.95 ppm reveals one spin system showing correlations to two resonances at 3.96 ppm and 4.13 ppm. If we feed this information into the HMQC spectrum, we find that these two proton-resonances correlate to the same carbon atom at 41.9 ppm (i.e., the two methylene protons are diastereotopic). This amino acid is identified as a glycine residue, and since there is correlation to an amide N—H group, we conclude that the glycine is not the N-terminus. (This point will be confirmed using other methods.)

Another spin system may be easily identified through a convenient starting point with the N—H resonance at 8.26 ppm. There are three correlations to this resonance, giving a total of four moieties in this spin system. If we again take this information directly to the HMQC spectrum, we can find the corresponding carbon resonances. Of course, there is no correlation to the N—H resonance. The proton resonance at 4.41 ppm correlates to a carbon resonance at 52.4 ppm, and the ^{13}C/DEPT spectra confirm that this is a methine group. The remaining spins in the system are proton resonances at 2.58 ppm and 2.72 ppm, which correlate to a single carbon resonance at 38.6 ppm. The ^{13}C/DEPT spectra confirm that this is a methylene group. This residue is identified as aspartic acid, and again we conclude that it is not the N-terminus.

A starting point for the final spin system is the N—H resonance at 7.35 ppm. There are four other proton resonances in this spin system; the HMQC spectrum and the ^{13}C/DEPT spectra indicate that these resonances represent one methine group and three methylene groups. Thus, this amino acid residue is arginine.

The COSY spectrum could be used to confirm our analysis thus far but it has not been necessary. However, the COSY and TOCSY are not redundant, and, in fact, they are complementary in at least one important aspect. While the TOCSY shows all of the spins in a spin system, it does not reveal which spins are actually coupled to one another. For instance, the N—H proton at 8.26 ppm (from aspartic acid) shows only a correlation to a methine group in the COSY; we can safely conclude that this N—H group is involved in a peptide linkage and that the methine group is the α- or asymmetric carbon of the amino acid. (Glycine is a trivial case and not considered here.) The N—H proton at 7.35 ppm, which we assigned to an aspartic acid residue, correlates with all of the spins in the TOCSY, but only shows coupling to a methylene group at 2.24 ppm in the COSY. This information allows us to draw two conclusions that were not available from the TOCSY. First, the N—H resonance is not coupled to the α-carbon of arginine and therefore must represent the N—H from the guanadino group and not α-amino group. Second, the arginine residue must be the N-terminal residue because there is no correlation between the methine proton at 4.13 ppm and an N—H proton in either the COSY or the TOCSY. In the discussion of the sequence of the amino acids, we will confirm this second point.

The combined information from the ^{13}C/DEPT, COSY, TOCSY, and HMQC spectra enables us to assign all protons in the ^{1}H spectrum except those that are exchanging rapidly (i.e., the carboxyl and free amino protons) and all of the non quaternary carbon resonances in the ^{13}C spectrum. There is no need to assign the rapidly exchanging protons, and the non-quaternary carbons will be assigned during the sequencing discussion.

The second main objective is to "sequence" the peptide or place the amino acids in their proper order. Two powerful tools from our NMR experimental repertoire are HMBC and ROESY (or NOESY). Recall that the HMBC shows long range ^{1}H—^{13}C coupling (generally 2-bond, $^2J_{CH}$, and 3-bond, $^3J_{CH}$ couplings). For sequencing purposes, this

experiment shows correlation between adjacent amino acids, as it were, "seeing through" the amide (peptide) carbonyl to the amide N—H. This exercise will also enable us to assign the carbonyls.

The ROESY experiment facilitates sequencing utilizing the inevitable through space correlations between adjoining amino acids. We expect to find through space connectivities from one amino acid's N—H to the adjoining amino acid's α- or C-2 proton(s). The data from either experiment should be sufficient; together they provide strong confirmatory evidence.

The full ROESY spectrum is shown in Problem 7.6D (top part). ROESY cross peaks show both COSY correlations and NOE correlations. For easy comparison, therefore, the area of interest for sequencing (the boxed area) is shown along with the corresponding COSY and TOCSY (bottom part of Problem 7.6D). The glycine N—H, which correlates with the adjacent methylene group in both the COSY and TOCSY spectra, gives an additional correlation in the ROESY spectrum to H-2 of arginine. This correlation shows a linkage between glycine and arginine. Some might consider this correlation inconclusive because of the overlap between H-2 of arginine and one of the H-2's of glycine. In this case, confirmation is desirable (see below).

The other connectivity can be established by way of the NOE interaction between the aspartic acid N—H and the two glycine H-2's. There is no ambiguity or overlap in this correlation, thus proving the sequence given in Problem 7.6A. An interesting aside worth noting is the NOE correlation between the aspartic acid N—H and only one of the two diastereotopic methylene protons of aspartic acid (H-3). This selective interaction suggests restricted rotation and allows differentiation and assignment of the diastereotopic protons.

Confirmation of this sequence and assignment of the quaternary carbons is accomplished with the HMBC spectrum, which is shown in Problem 7.6E. The bottom part of this page is pertinent. Before confirming the sequence, a simple assignment of a quaternary carbon is made. The assignment of the C-7 carbon of arginine can be made by noting the correlation between the arginine N—H (H-6) and the quaternary carbon at 156.5 ppm.

The analysis of the HMBC spectrum in the region of the carbonyl carbons is hampered by the lack of digital resolution along the F1 axis. Recall that the HMBC experiment is proton detected, which gives good resolution in the proton (F2) dimension. The only way to improve resolution along the F1 axis is to increase the number of t_1 increments in the experiment, which has serious practical limitations. The lines drawn in the insets help clarify the correlations.

The glycine N—H correlates with the arginine carbonyl (C-1), thereby confirming the arginine–glycine linkage. The assignment of the arginine carbonyl resonance is accomplished by noting the correlation of the carbonyl resonance at about 170 ppm with the arginine methine H-2. The other linkage is established by the correlation of the aspartic acid N—H and the glycine carbonyl (C-1) resonances; the glycine carbonyl is pinpointed from its correlations with the diastereotopic methylene protons of glycine. The sequence of the tripeptide is thus confirmed by two independent methods.

STUDENT EXERCISES

The following exercises are given for the student to work through. The structures and spectra for two compounds are shown on the following pages. The student should use all available data to prove to themselves the correctness of the structures shown, and assign all proton and carbon resonances.

MASS

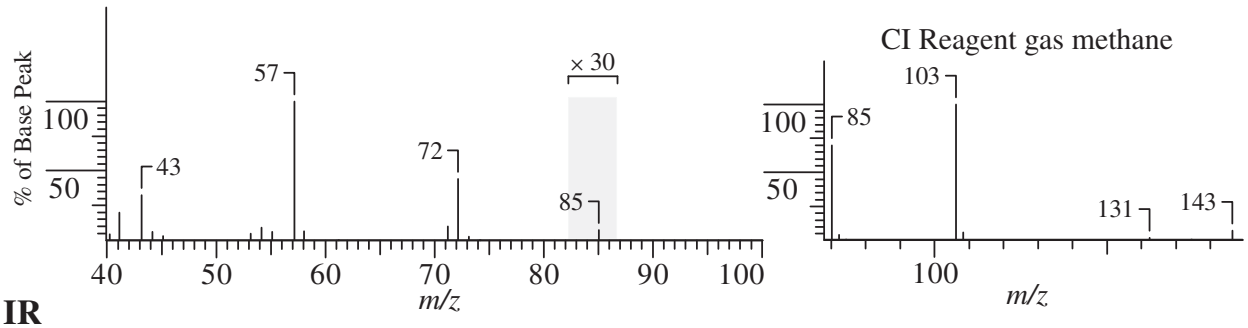

IR

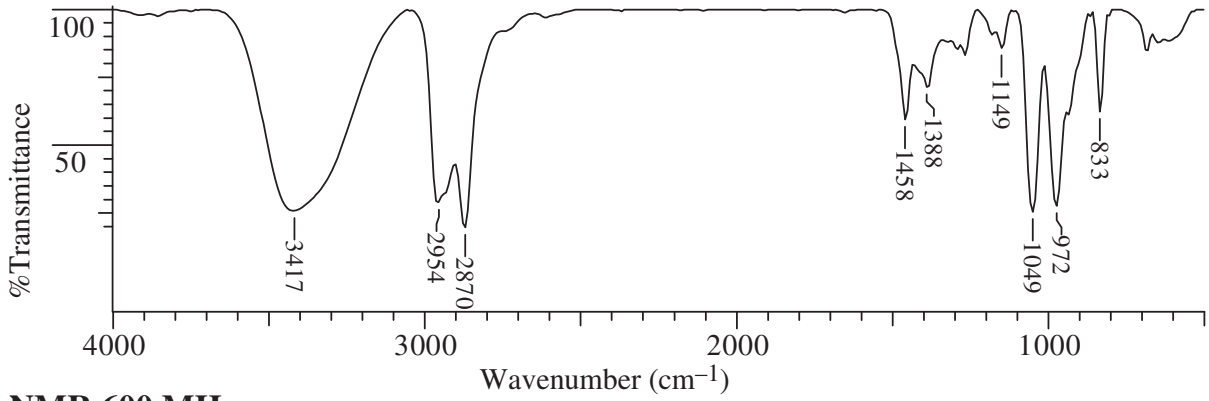

^{1}H NMR 600 MHz

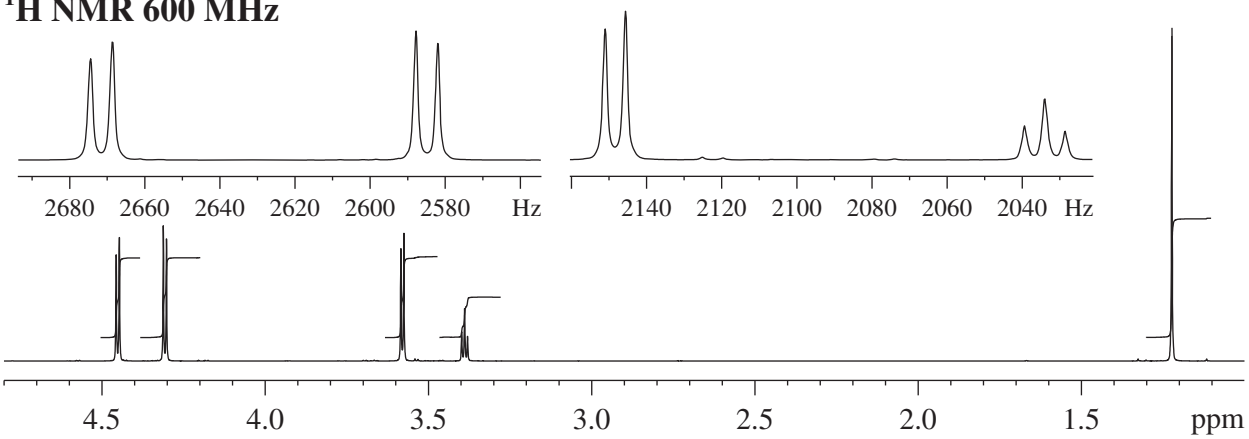

^{13}C/DEPT NMR 150.9 MHz

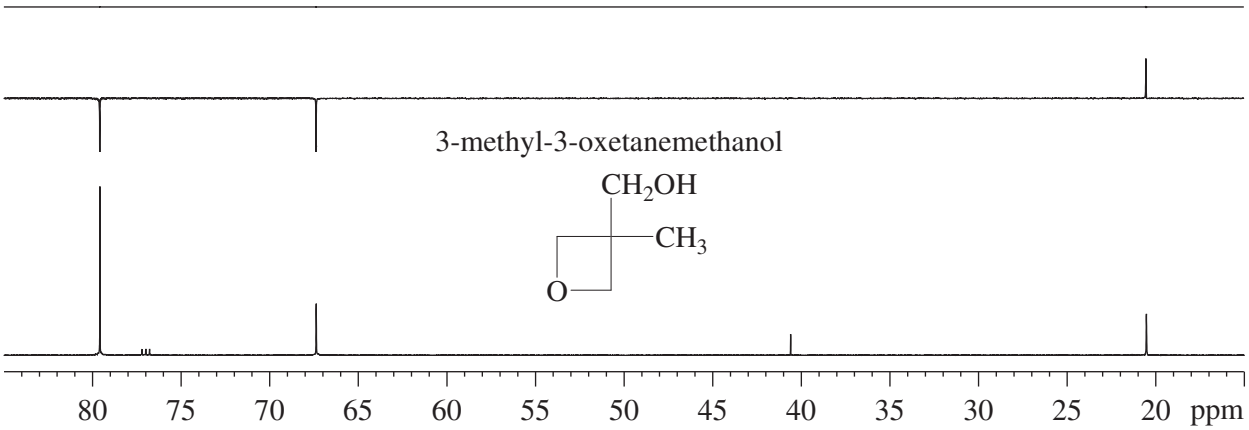

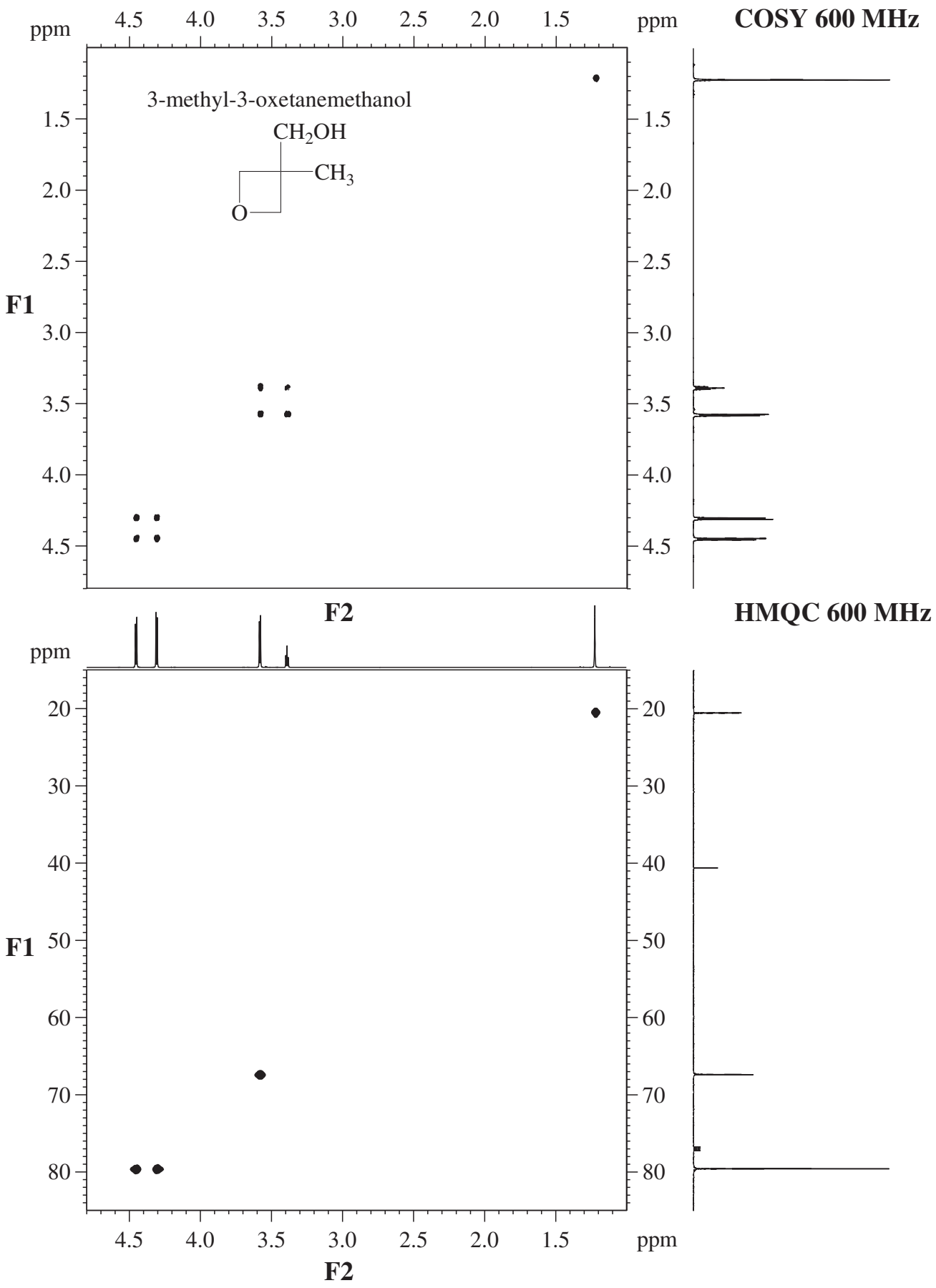
COSY 600 MHz
ppm
4.5 4.0 3.5 3.0 2.5 2.0 1.5
3-methyl-3-oxetanemethanol
CH2OH
CH3
O
F1
F2
HMQC 600 MHz
20 30 40 50 60 70 80

MASS

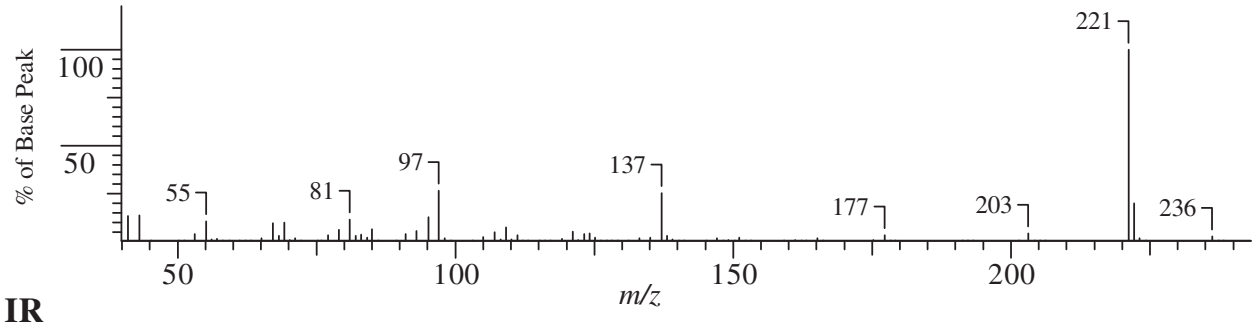

IR

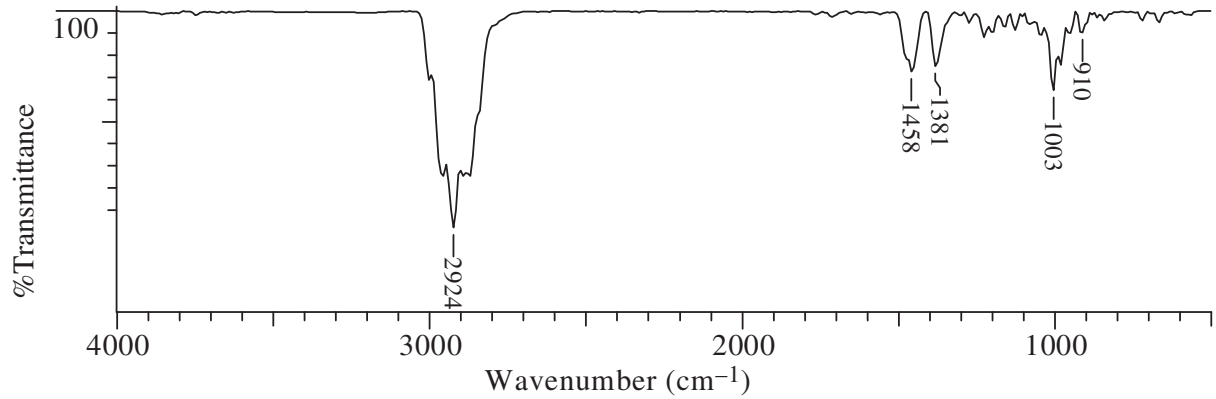

^{1}H NMR 600 MHz

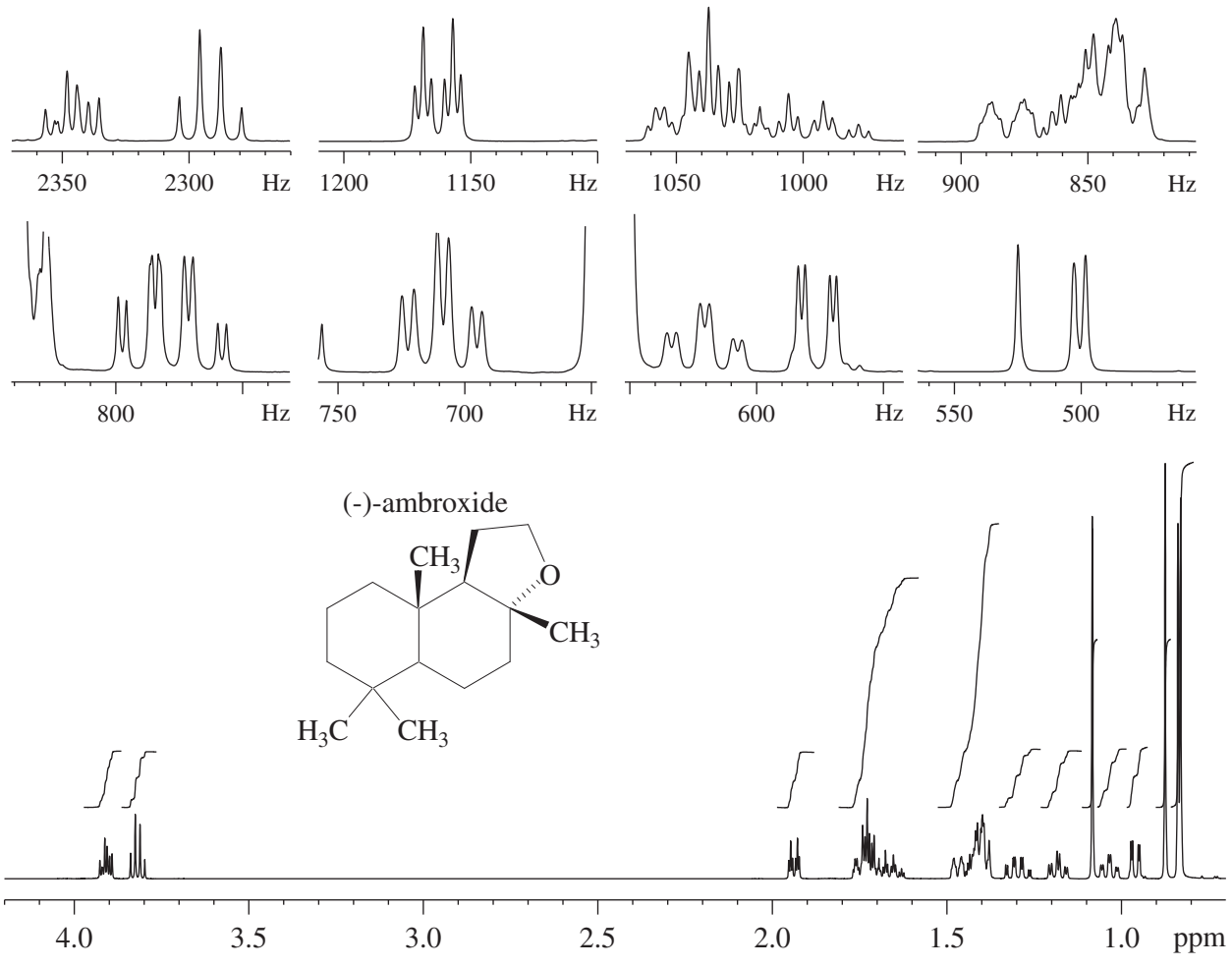

^{13}C/DEPT NMR 150.9 MHz

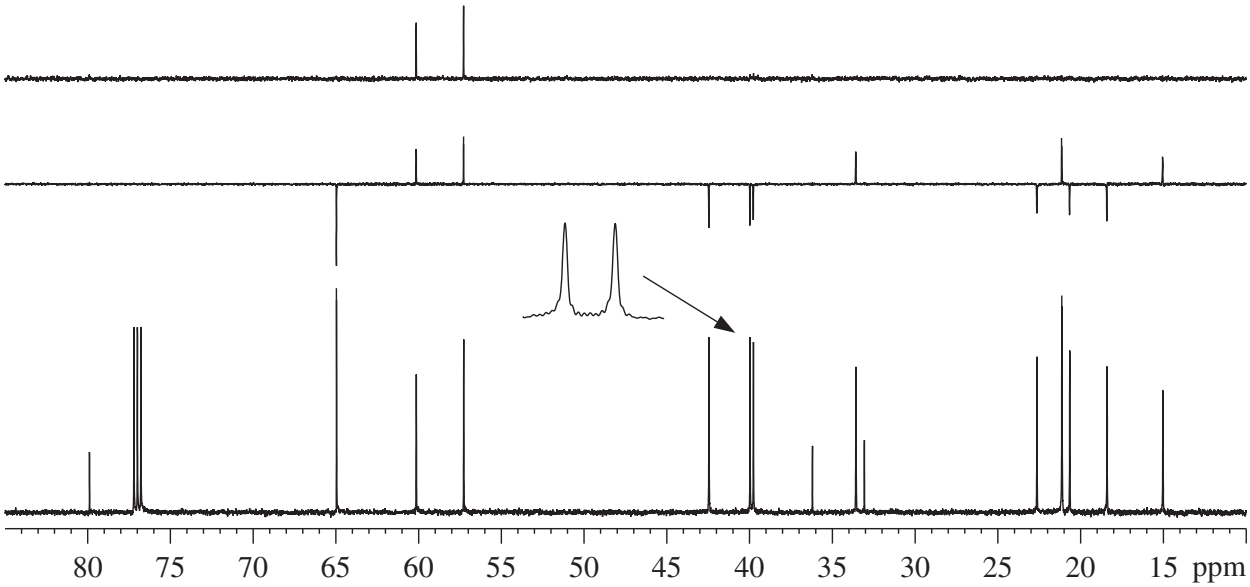

HMQC 600 MHz

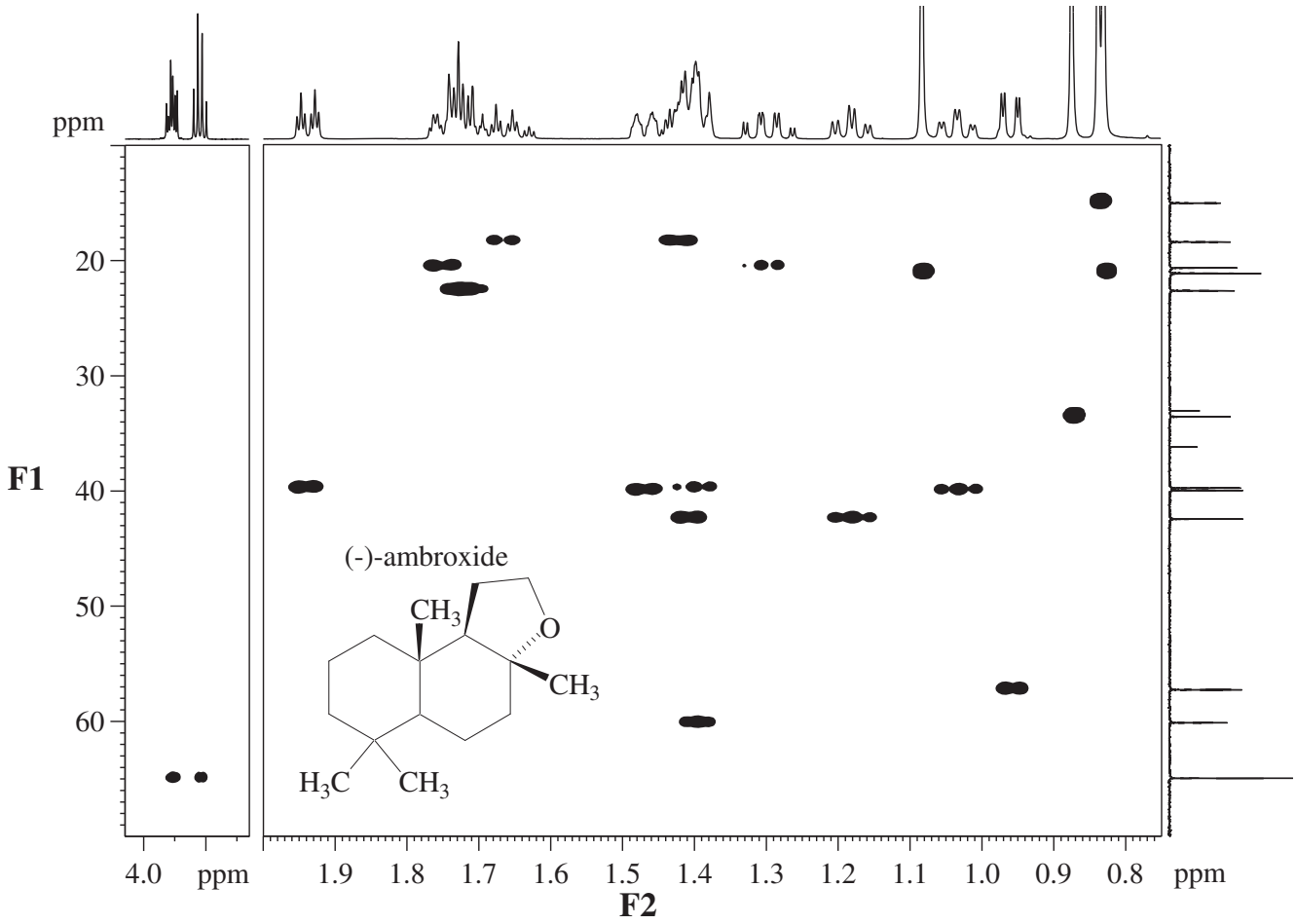

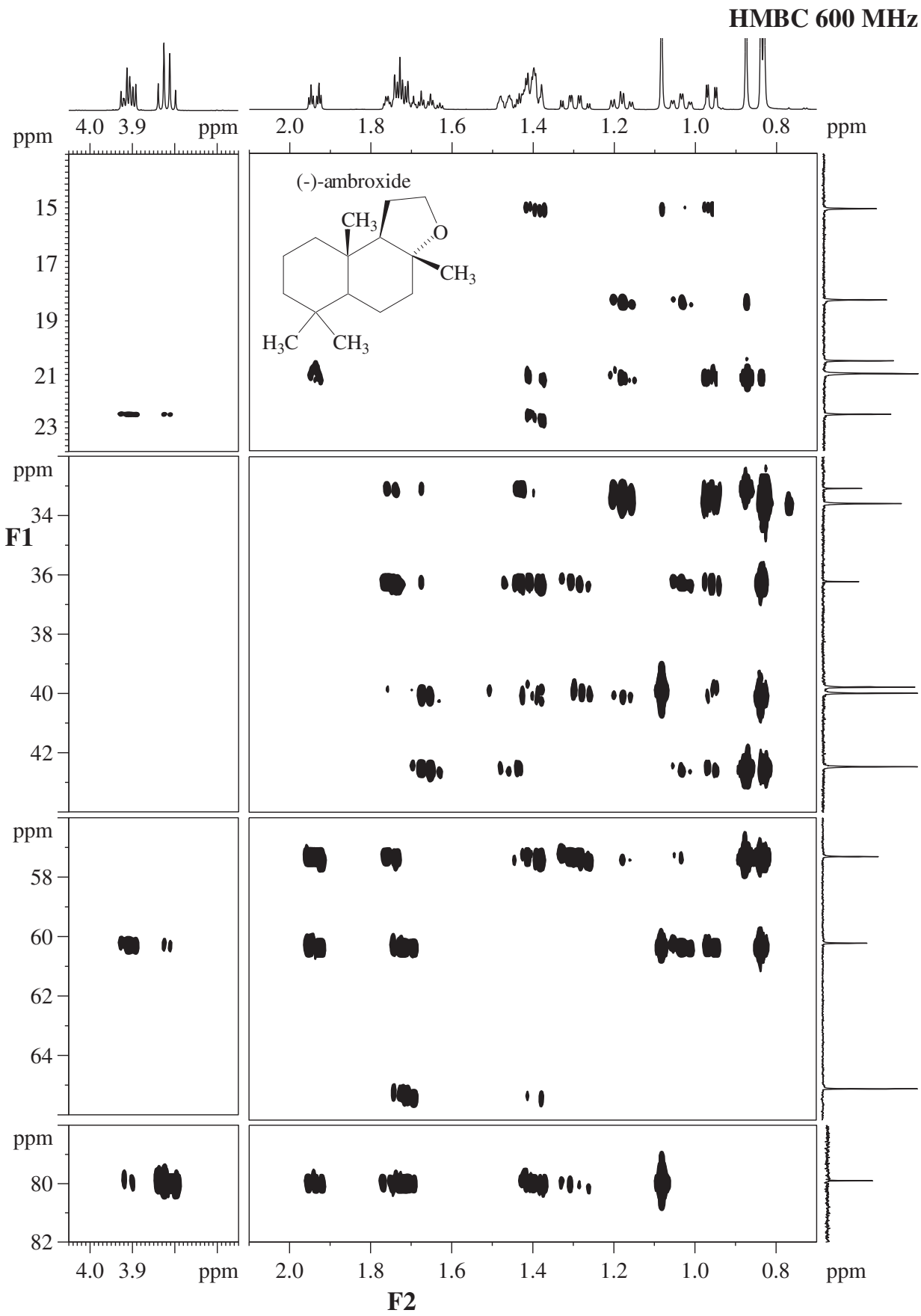
HMBC 600 MHz
(-)-ambroxide
CH3
O
CH3
H3C
CH3
ppm
4.0 3.9 ppm
2.0 1.8 1.6 1.4 1.2 1.0 0.8 ppm
15
17
19
21
23
34
36
38
40
42
58
60
62
64
80
82
F1
F2

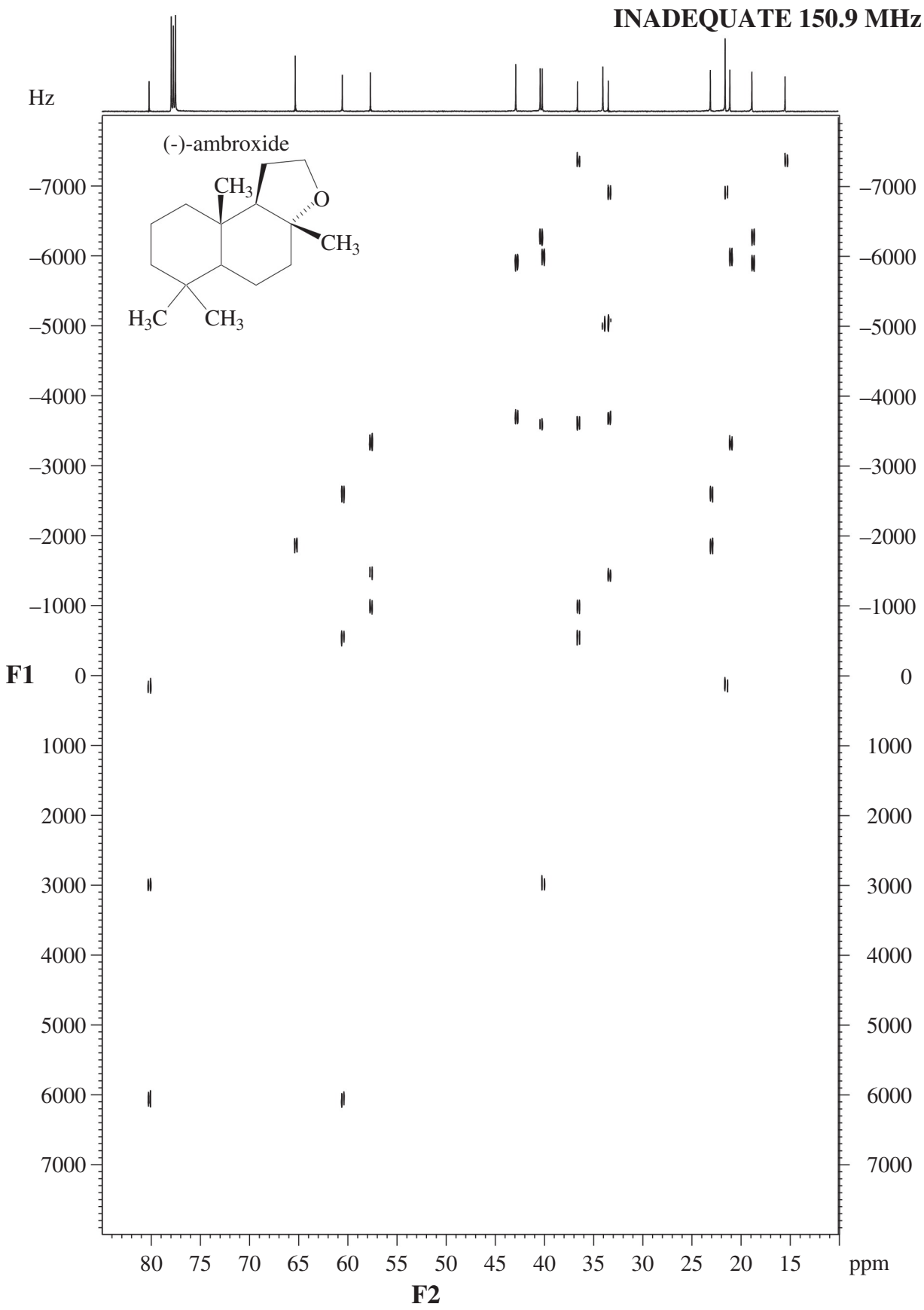
INADEQUATE 150.9 MHz
Hz
(-)-ambroxide
CH3
O
CH3
H3C
CH3
–7000
–6000
–5000
–4000
–3000
–2000
–1000
F1
0
1000
2000
3000
4000
5000
6000
7000
80 75 70 65 60 55 50 45 40 35 30 25 20 15
ppm
F2

CHAPTER 8

ASSIGNED PROBLEMS

8.1 INTRODUCTION

Chapter 7 has been propounded as though unknown problems were being resolved by the authors. Not so. It was inevitable that the authors knew the structures. The students inevitably consulted the structures as they worked through the explanations. The experience, therefore, has been more rationalization of the given structures than analysis of spectra. Nonetheless, the experience was worthwhile.

Chapter 8 will be an experience in foresight rather than hindsight (except for the final group of problems), but the first few modest problems should provide encouragement, as did the problems at the end of each chapter. Admittedly, difficulties will be encountered further along, but satisfactions also.

The NMR spectra were obtained at either 300 MHz or 600 MHz for protons and 75.5 MHz or 150.9 MHz for carbon; $CDCl_3$ was the solvent unless otherwise indicated. At 600 MHz, all 2D spectra were obtained with gradients except the INADEQUATE spectra. The IR spectra were obtained neat (i.e., no solvent) unless otherwise indicated. The mass spectra were obtained by EI GC-MS unless otherwise noted. Methane was used to obtain the chemical ionization mass spectra.

The problems that follow cover a wide array of compound types and range from easy to moderate to difficult. Clearly, these terms are relative; for a beginning student, none of these problems are truly easy. With experience, many of the moderately difficult problems will seem easier especially with 2D spectra. The first group of problems has a mass spectrum, an IR spectrum, and a ^{1}H and ^{13}C/DEPT NMR spectra. In all cases, the ^{13}C/DEPT NMR spectra are displayed in the following order, from top to bottom: DEPT-90, DEPT-135, and regular proton-decoupled ^{13}C NMR spectrum. The second group of problems has, in addition to these spectra, some 2D NMR spectra. Many of these problems can be completed without recourse to the information available in the 2D spectra. The third group of problems is presented with the compounds' structures and generally has more 2D spectra.

The problems in the third group are intended as exercises so that the student can work with more complicated structures. These problems can be assigned with the objective of verifying the structure and making assignments.

For most of the problems, there is more than enough information to fully solve the problem, including stereochemistry, except, of course, absolute stereochemistry. There are, however, a few problems that lack enough information to determine stereochemistry. In these cases, the student should indicate the possible stereoisomers and suggest ways to distinguish among them. Additional Student Exercises can be found at http://www.wiley.com/college/silverstein.

At this point, we may all enjoy a more literary statement: "It is easy to be wise in retrospect, uncommonly difficult in the event."*

*Stegner, W. (1954). *Beyond the Hundredth Meridian.* Boston, MA: Houghton Mifflin. Reprint, Penguin Books, 1992, Chapter 3.

MASS

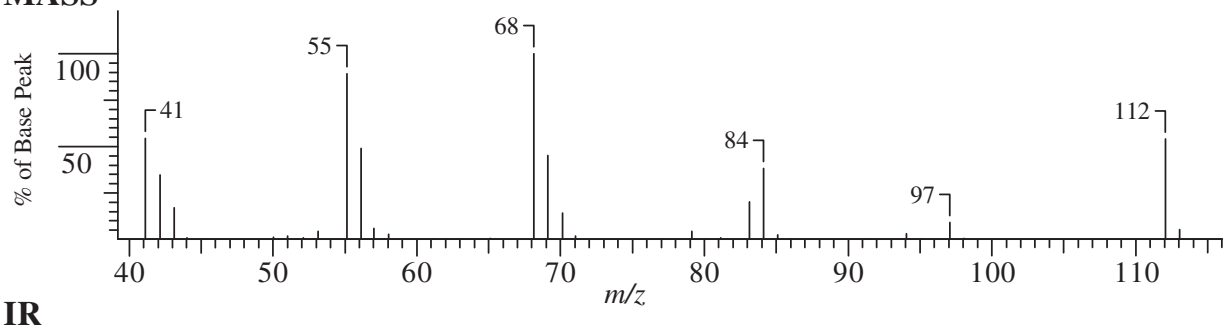

IR

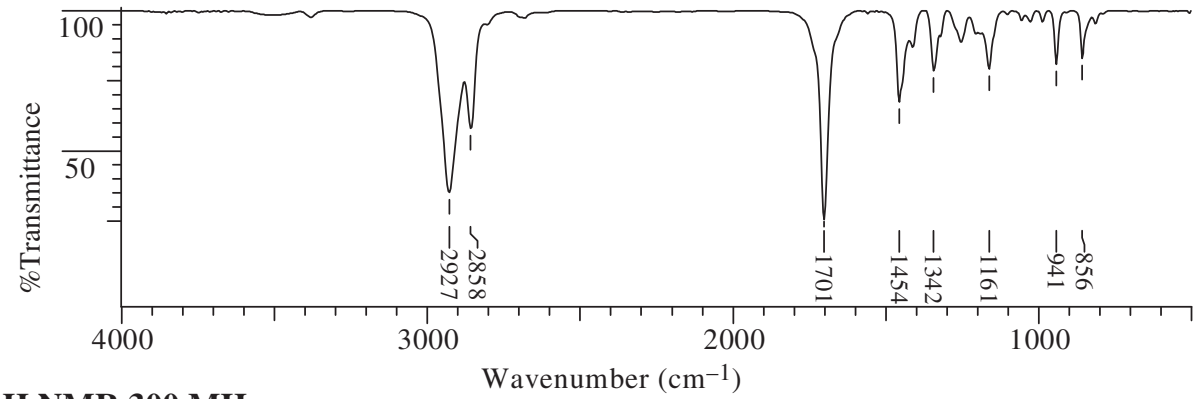

^{1}H NMR 300 MHz

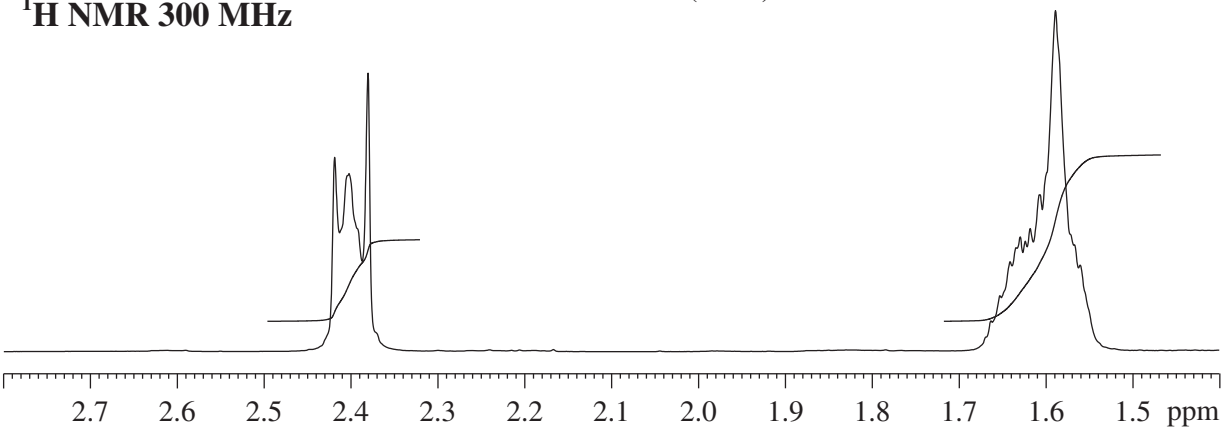

^{13}C/DEPT NMR 75.5 MHz

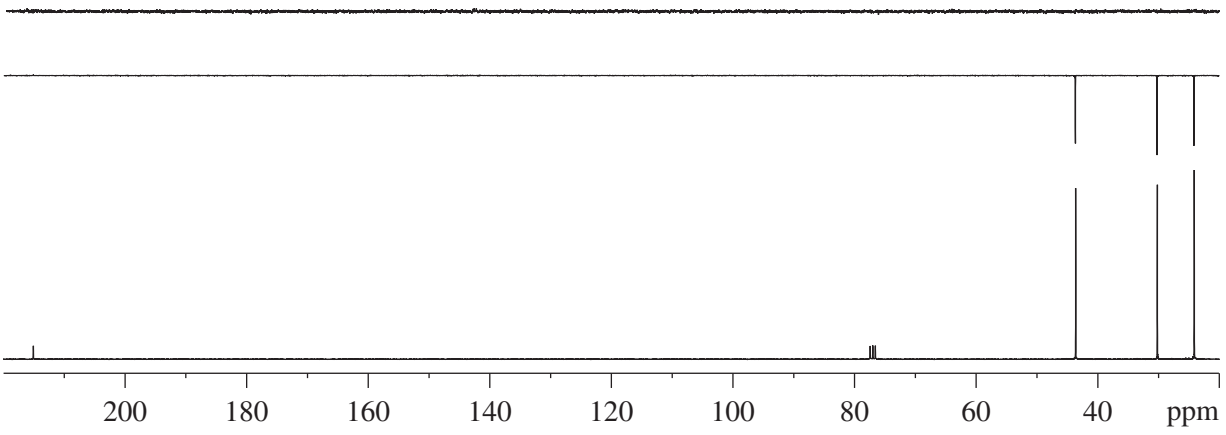

MASS

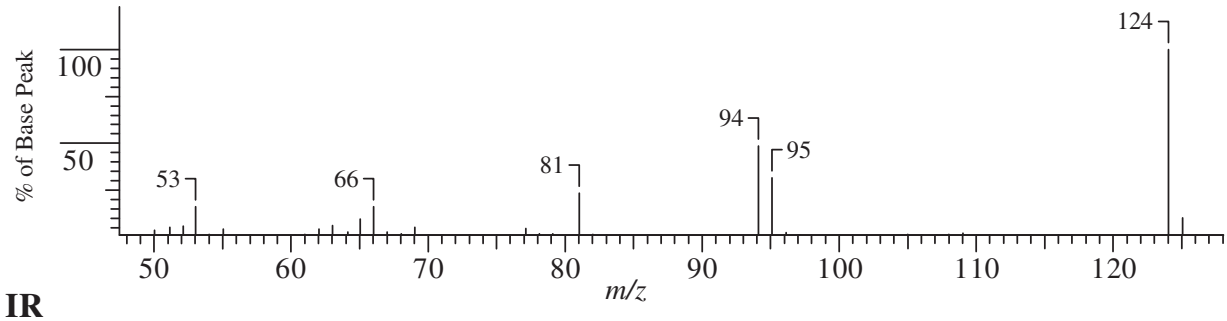

IR

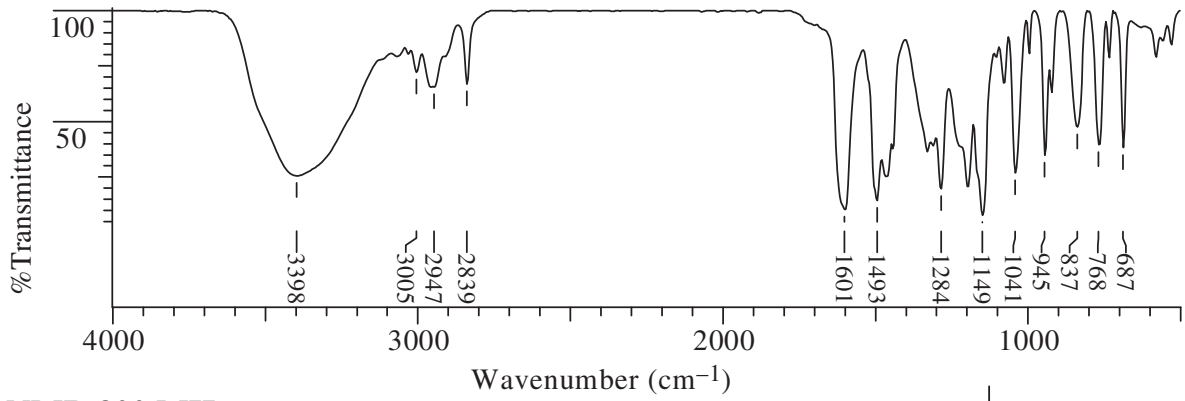

^{1}H NMR 300 MHz

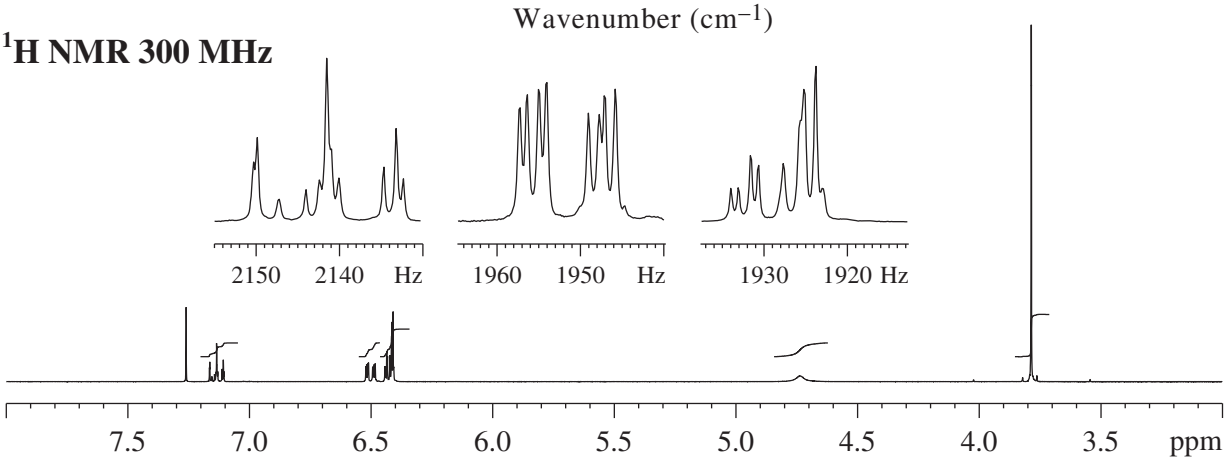

^{13}C/DEPT NMR 75.5 MHz

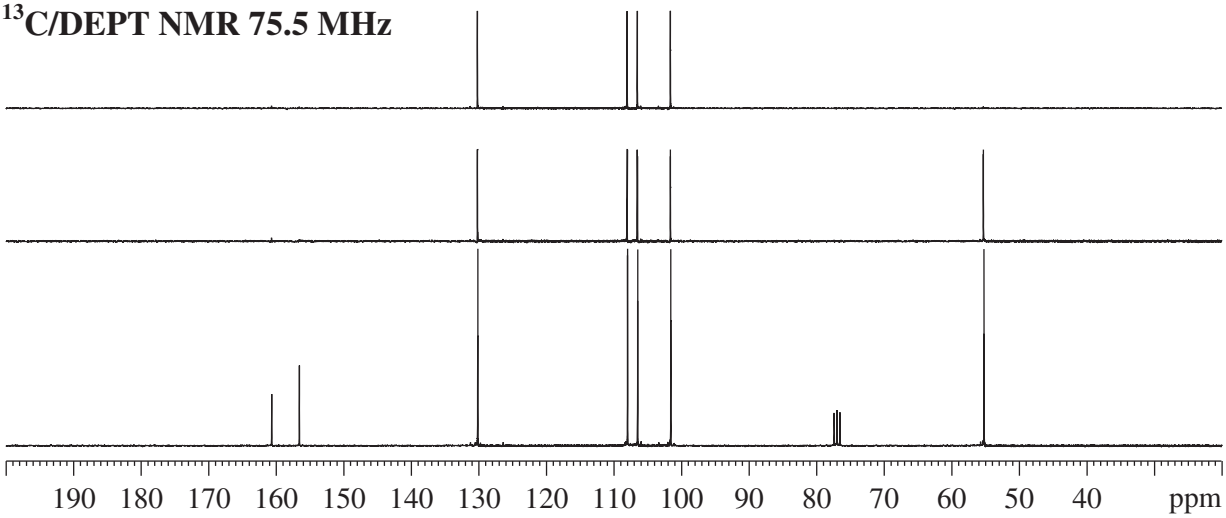

MASS

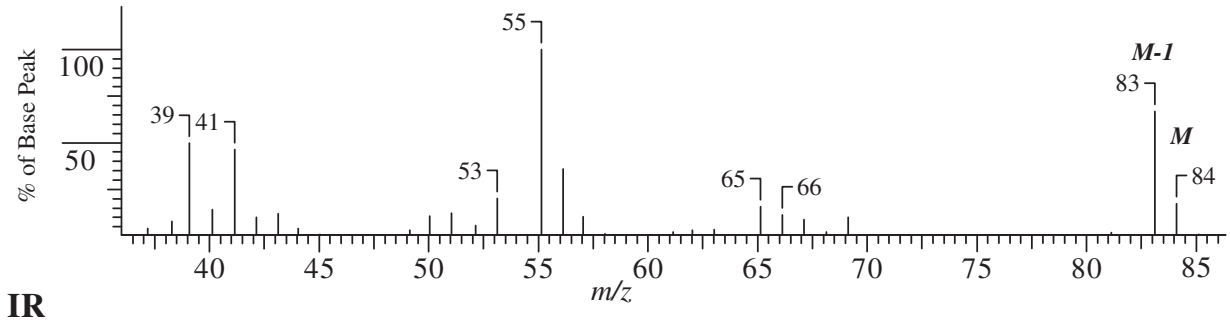

IR

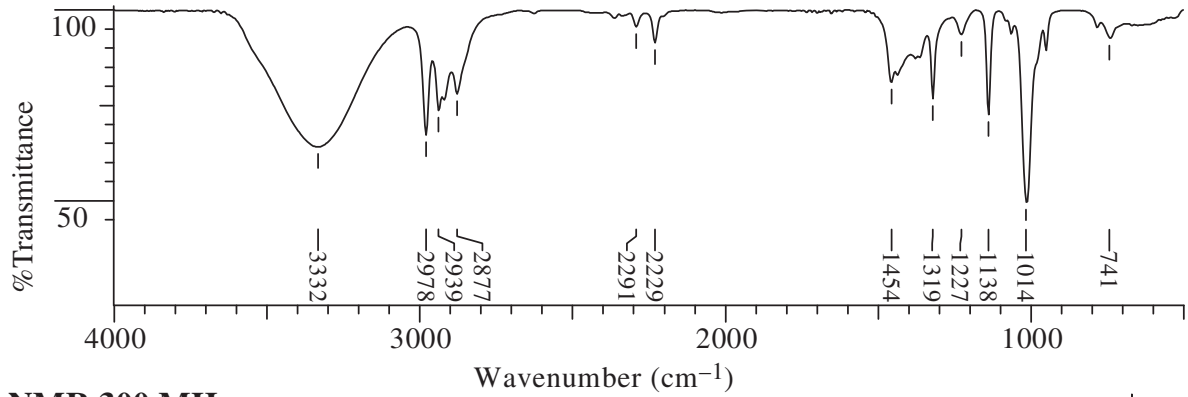

^{1}H NMR 300 MHz

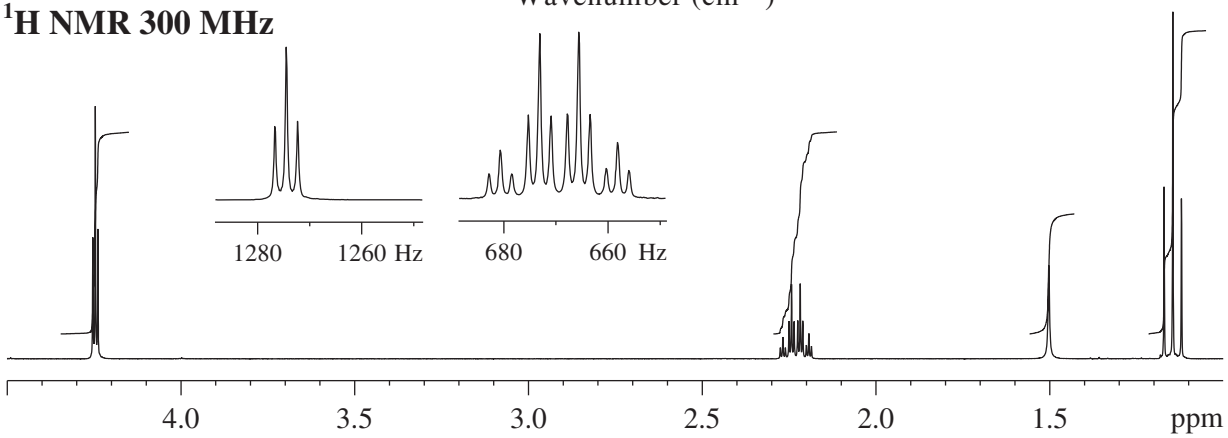

^{13}C/DEPT NMR 75.5 MHz

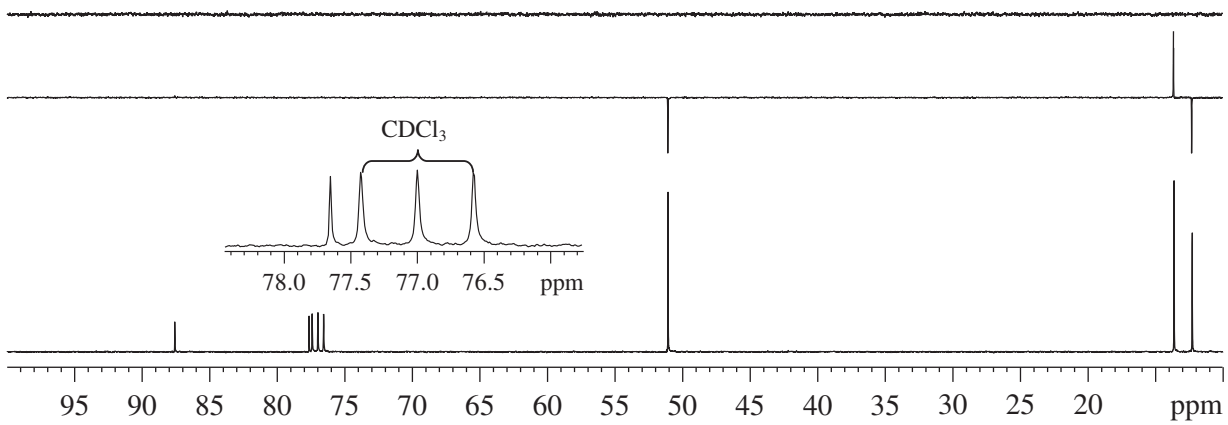

MASS

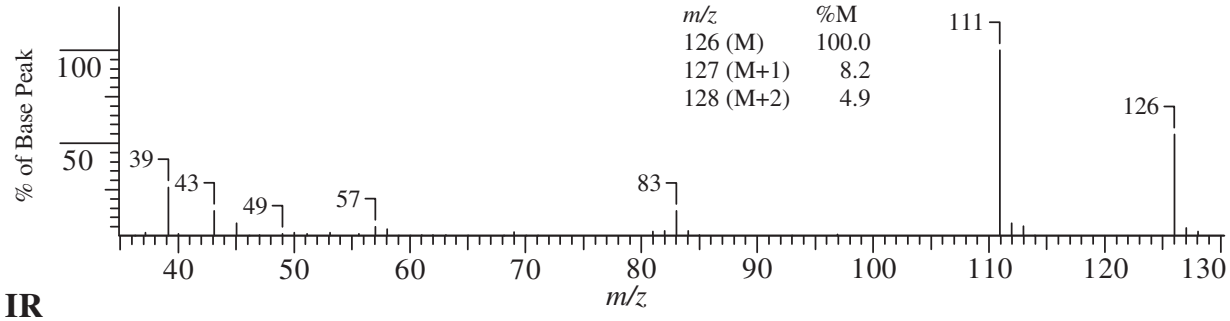

IR

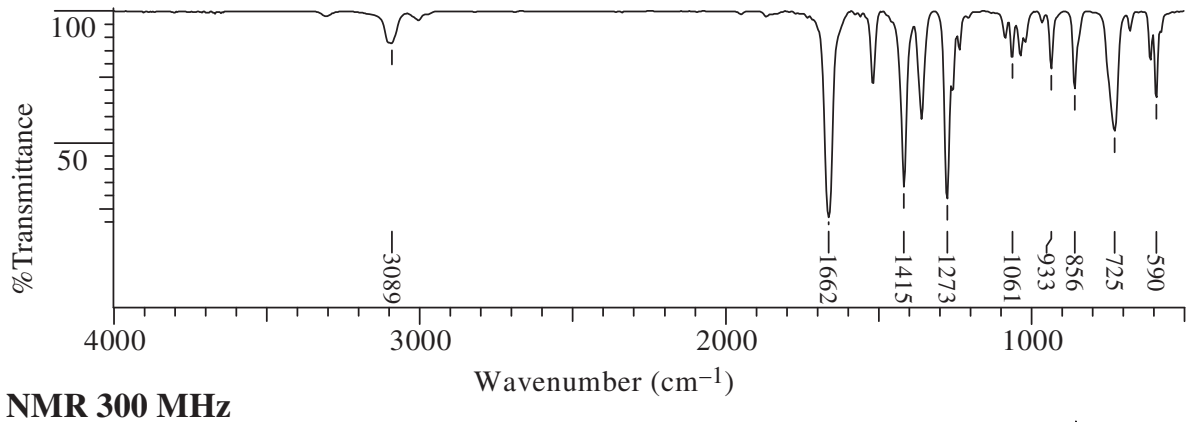

^{1}H NMR 300 MHz

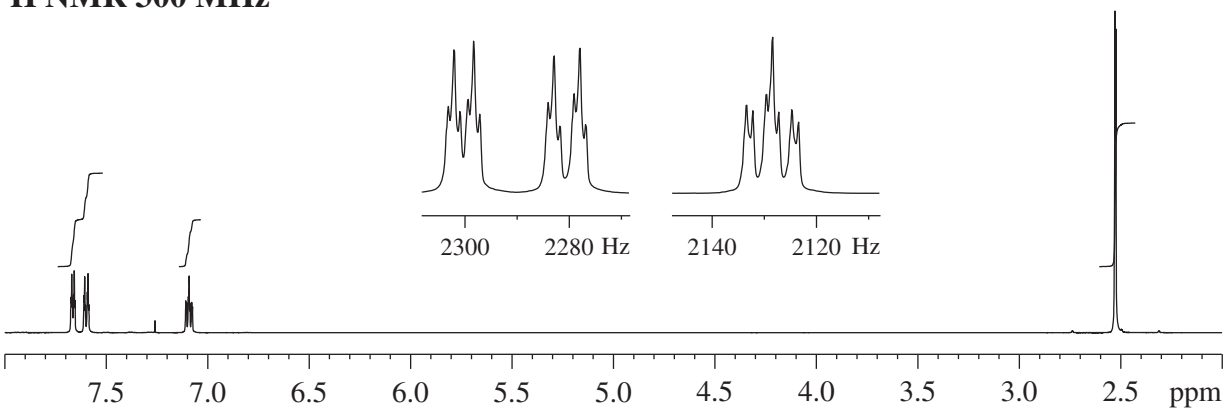

^{13}C/DEPT NMR 75.5 MHz

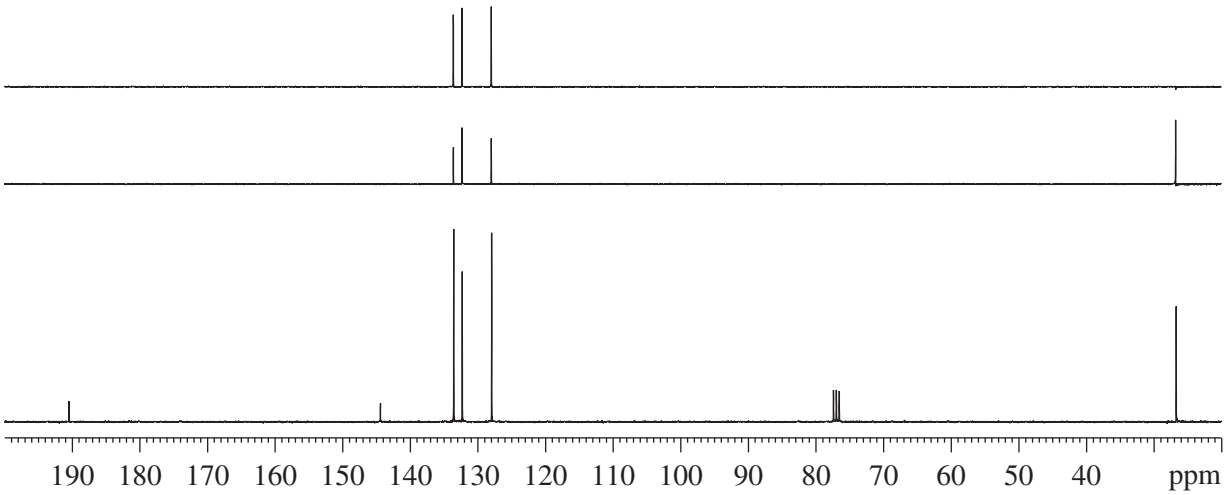

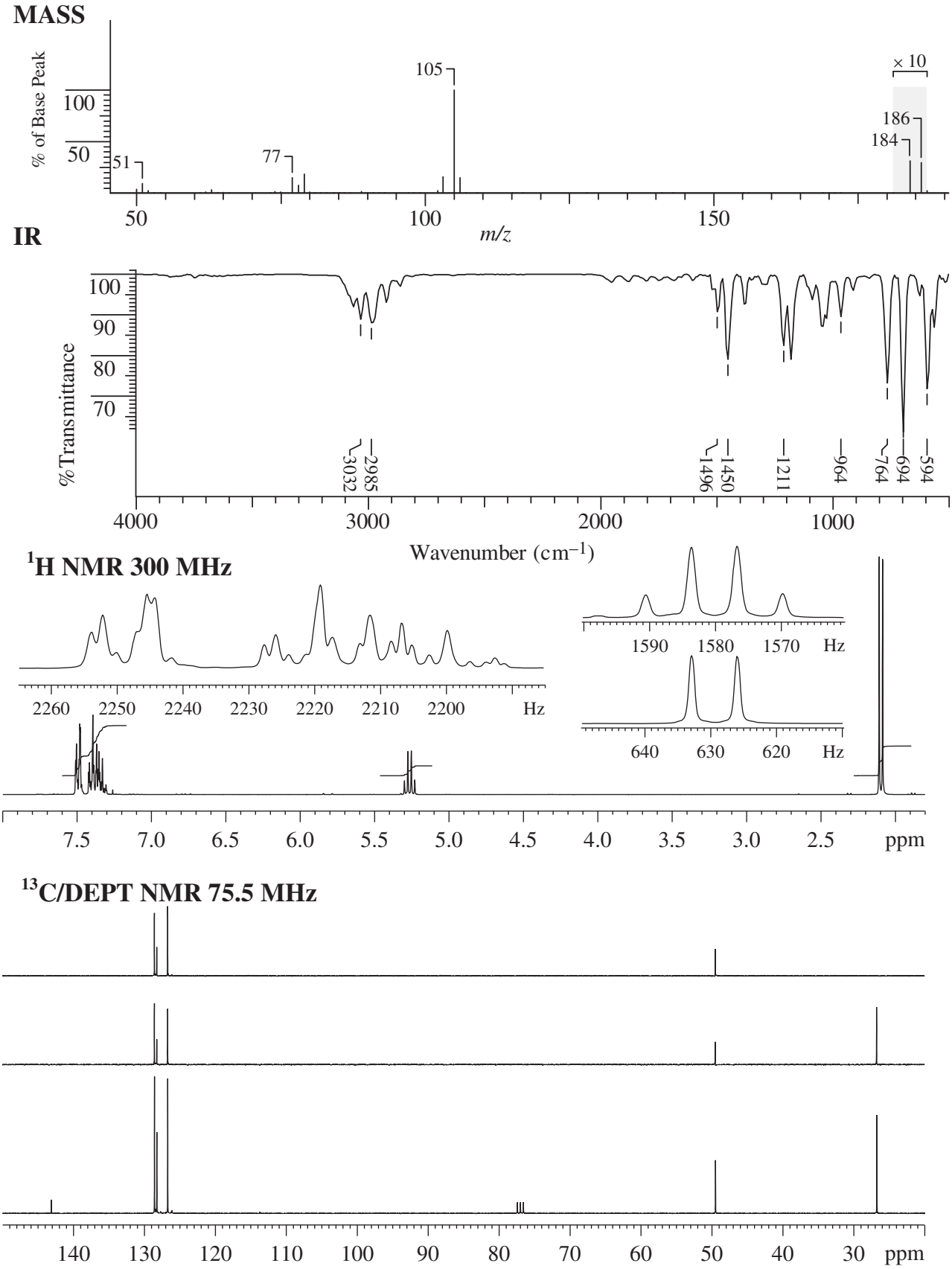
MASS
% of Base Peak
100
50
51
77
105
× 10
186
184
50
100
150
m/z
IR
%Transmittance
100
90
80
70
3032
2985
1496
1450
1211
964
764
694
594
4000
3000
2000
1000
Wavenumber (cm−1)
1H NMR 300 MHz
2260 2250 2240 2230 2220 2210 2200 Hz
1590 1580 1570 Hz
640 630 620 Hz
7.5 7.0 6.5 6.0 5.5 5.0 4.5 4.0 3.5 3.0 2.5 ppm
13C/DEPT NMR 75.5 MHz
140 130 120 110 100 90 80 70 60 50 40 30 ppm

MASS

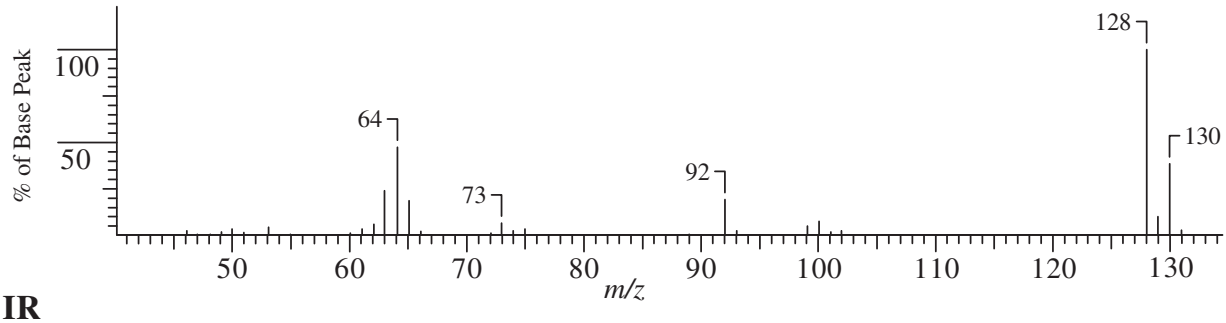

IR

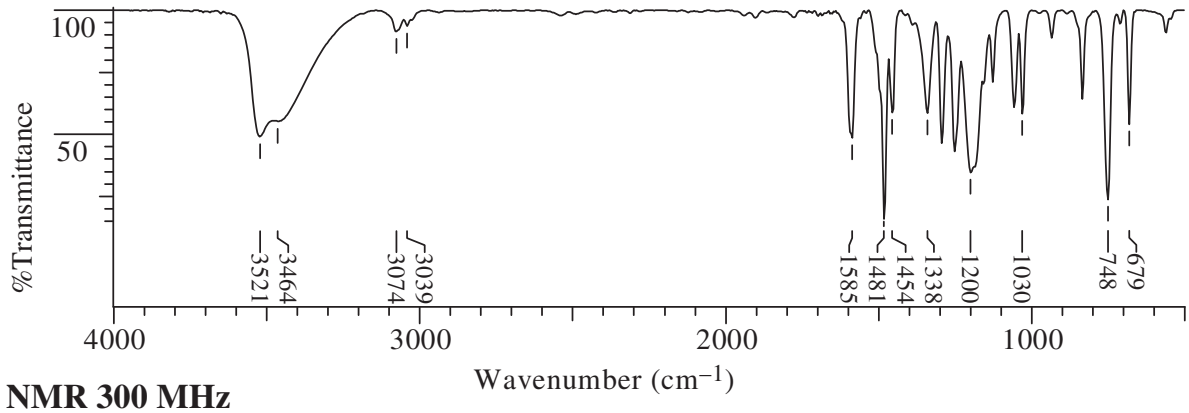

^{1}H NMR 300 MHz

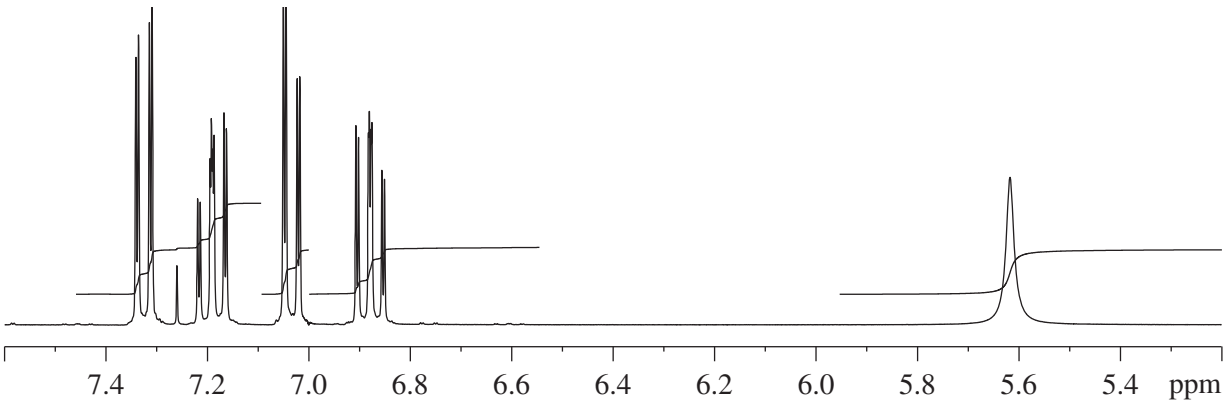

^{13}C/DEPT NMR 75.5 MHz

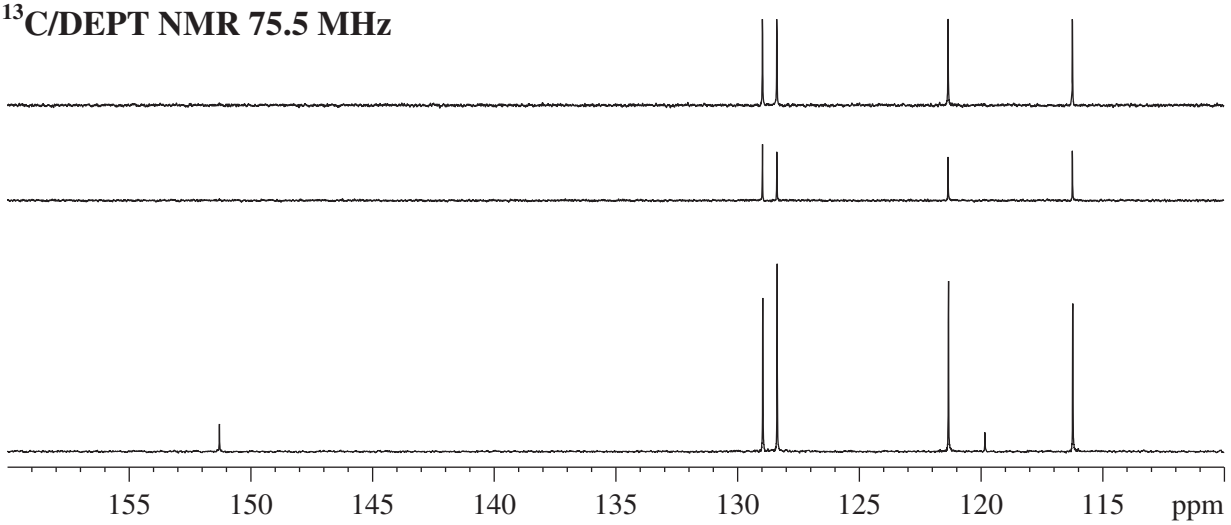

MASS

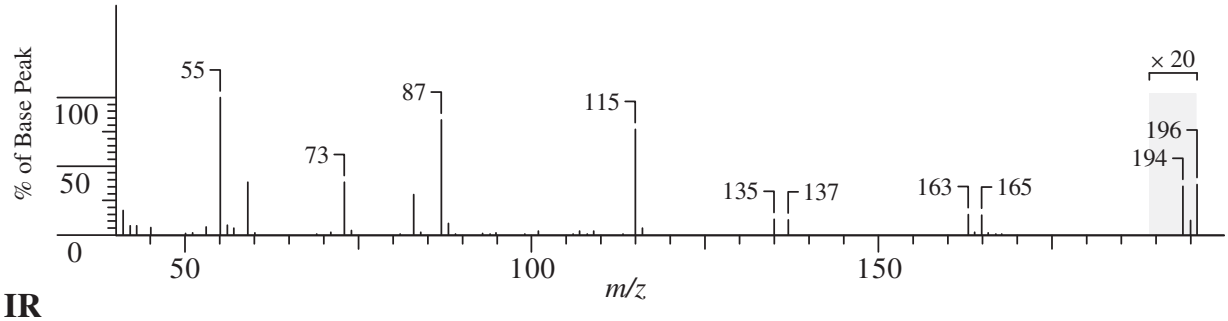

IR

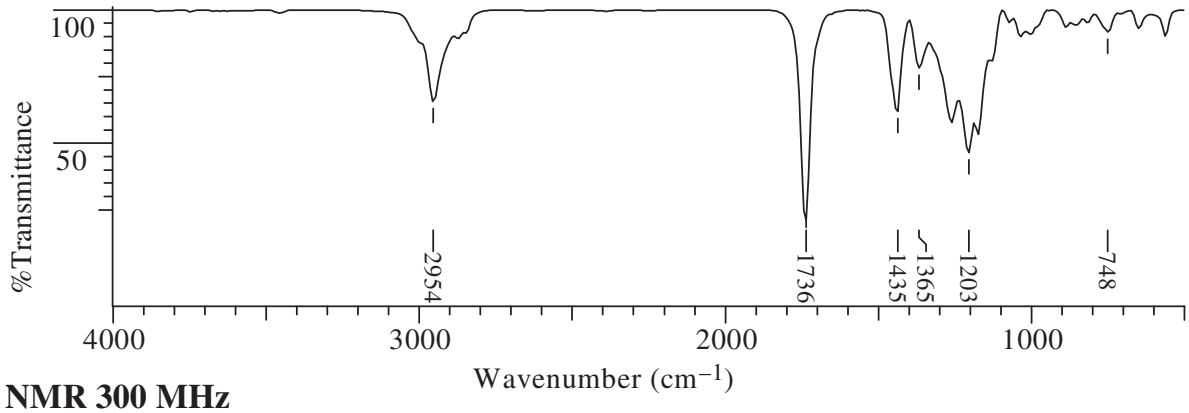

^{1}H NMR 300 MHz

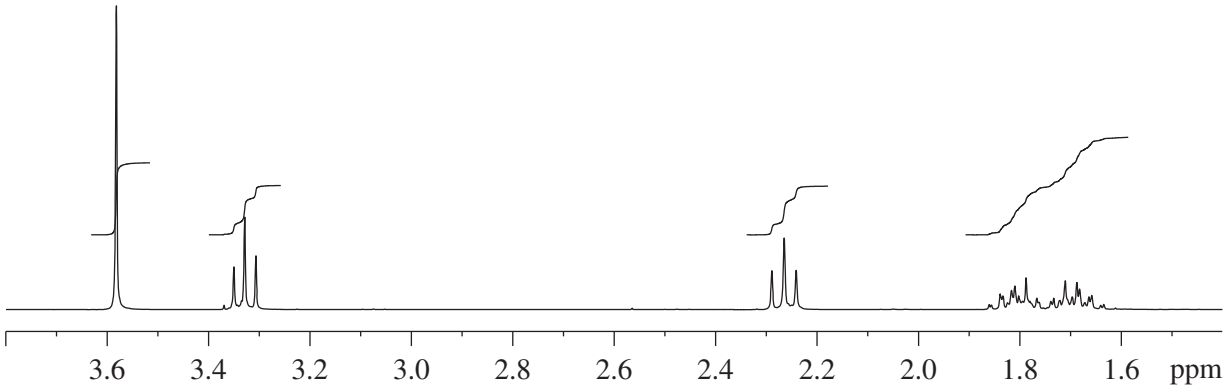

^{13}C/DEPT NMR 75.5 MHz

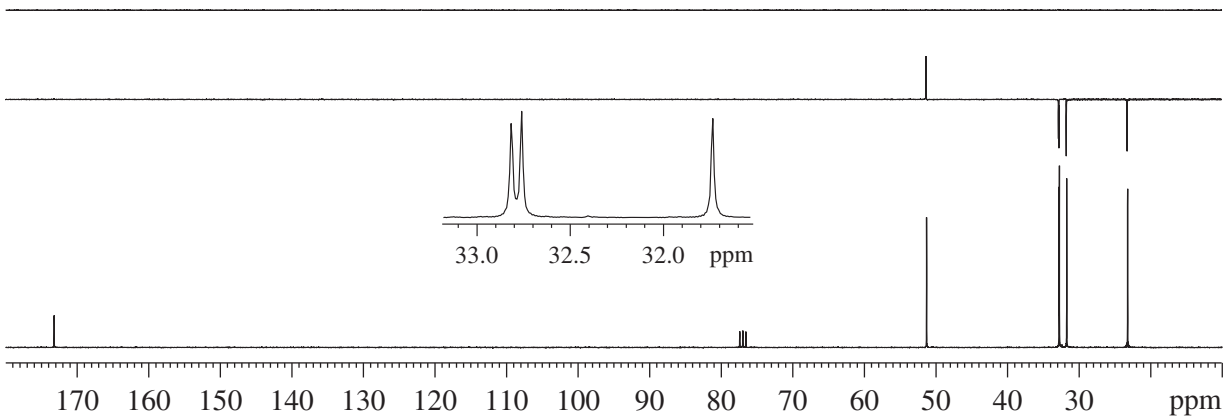

MASS

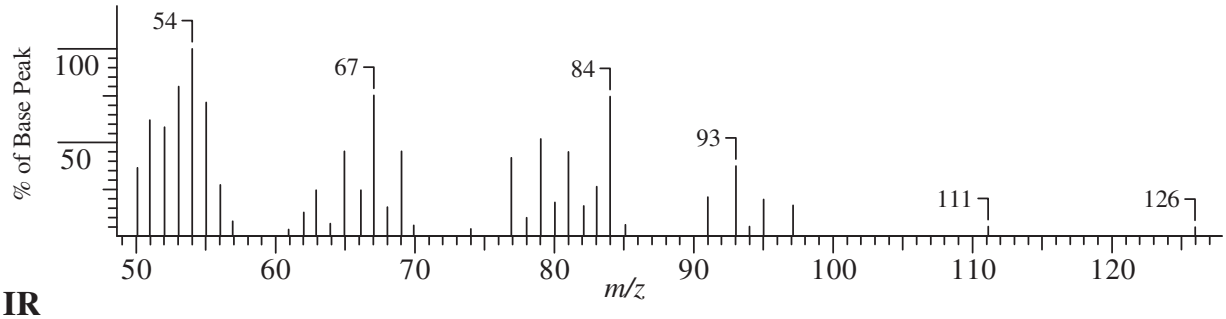

IR

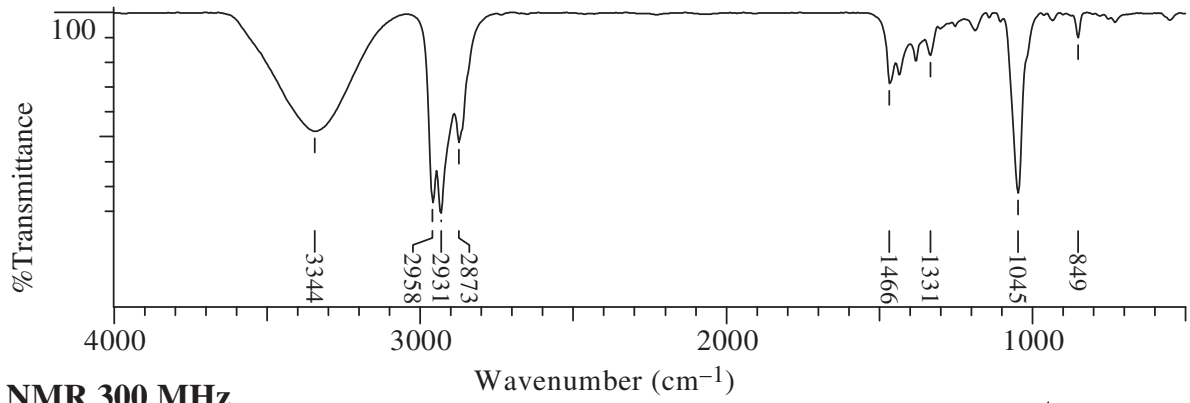

^{1}H NMR 300 MHz

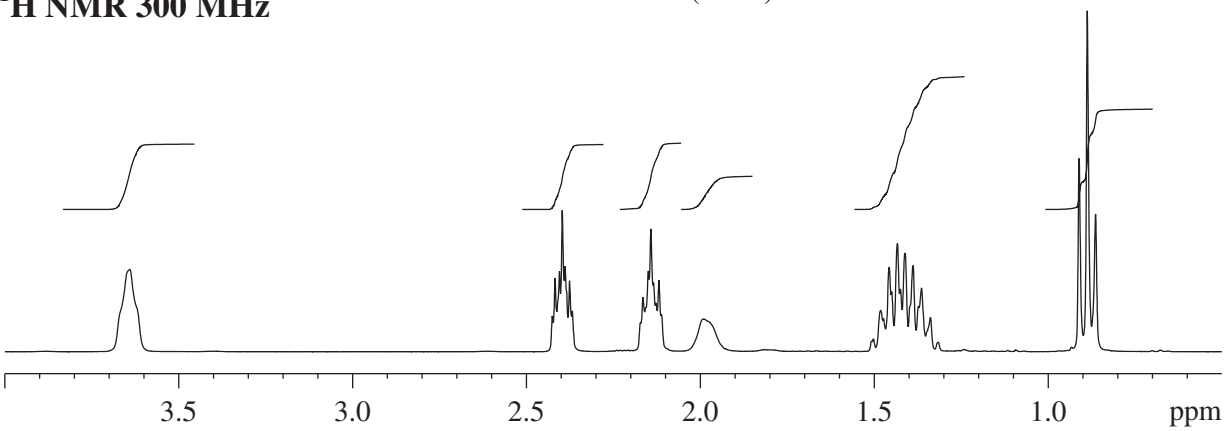

^{13}C/DEPT NMR 75.5 MHz

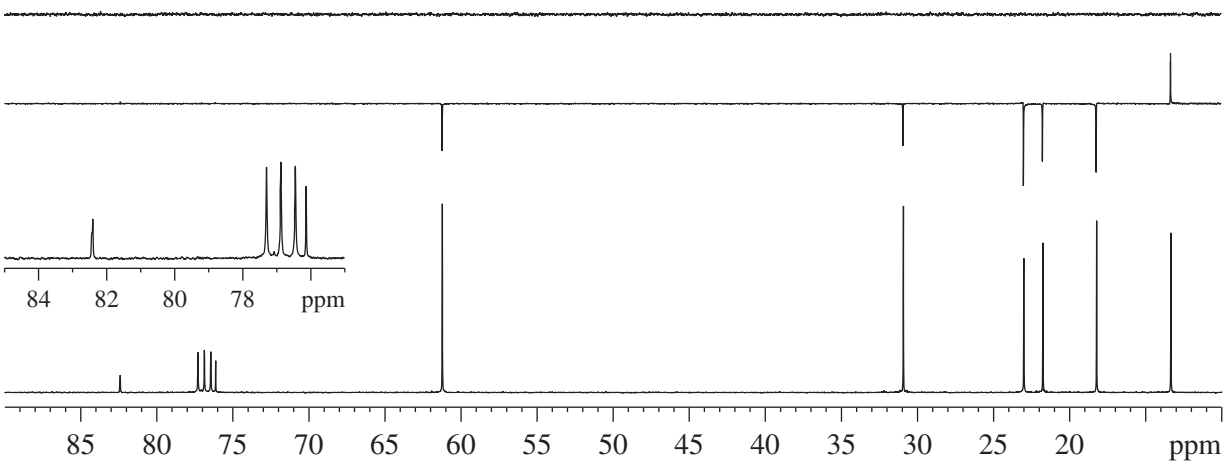

MASS

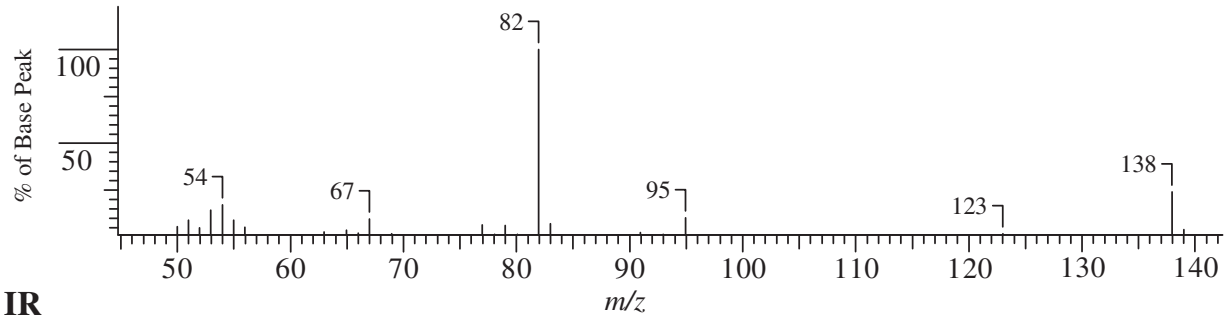

IR

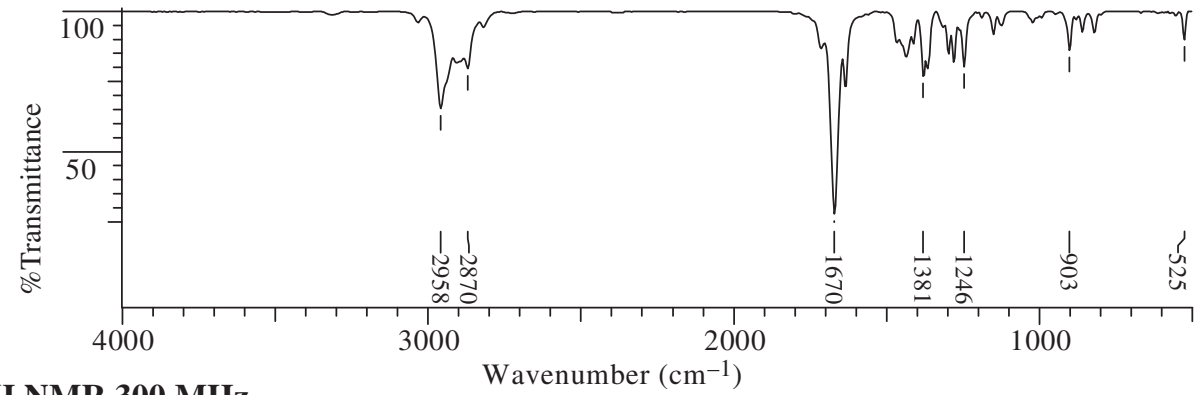

^{1}H NMR 300 MHz

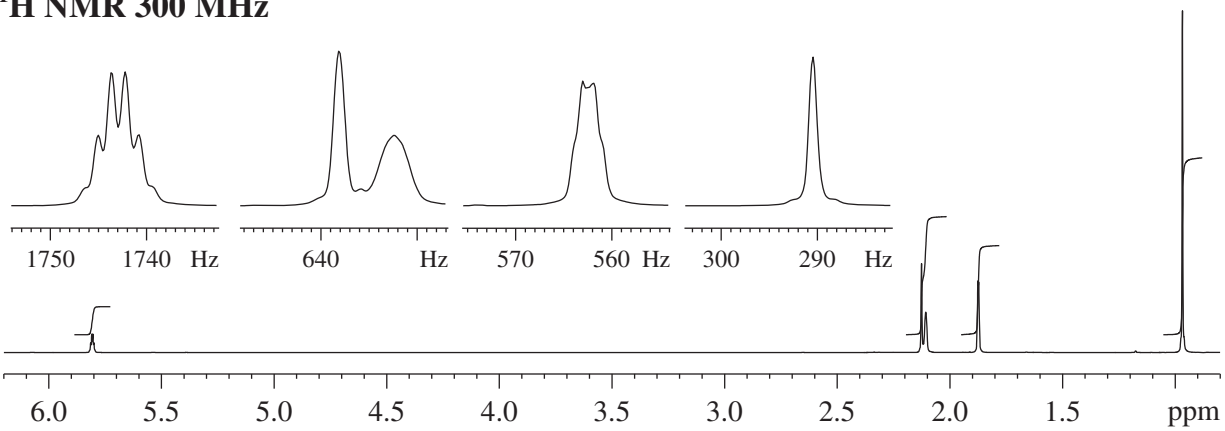

^{13}C/DEPT NMR 75.5 MHz

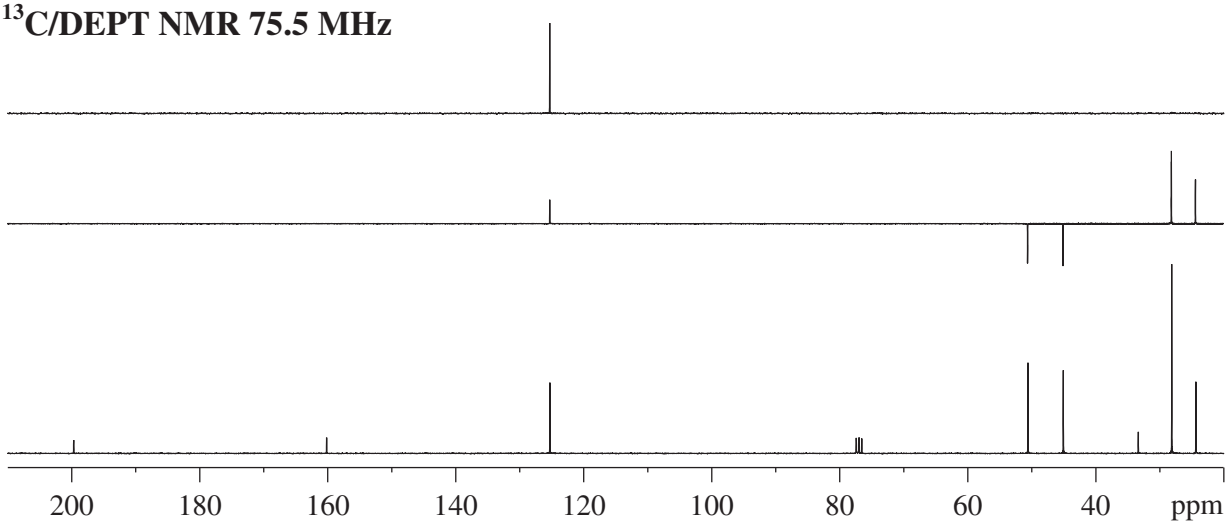

MASS

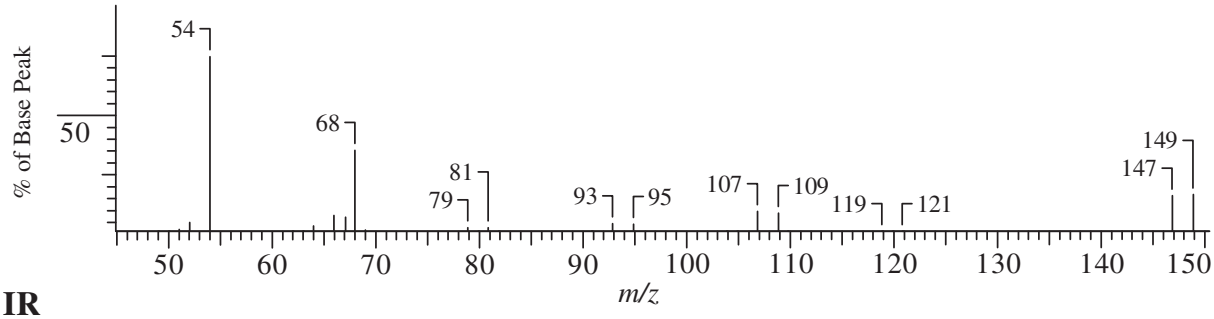

IR

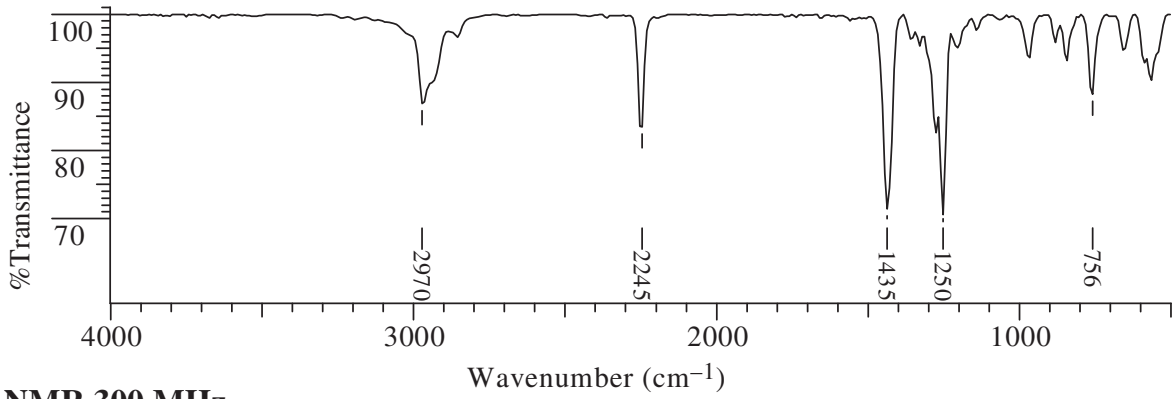

^{1}H NMR 300 MHz

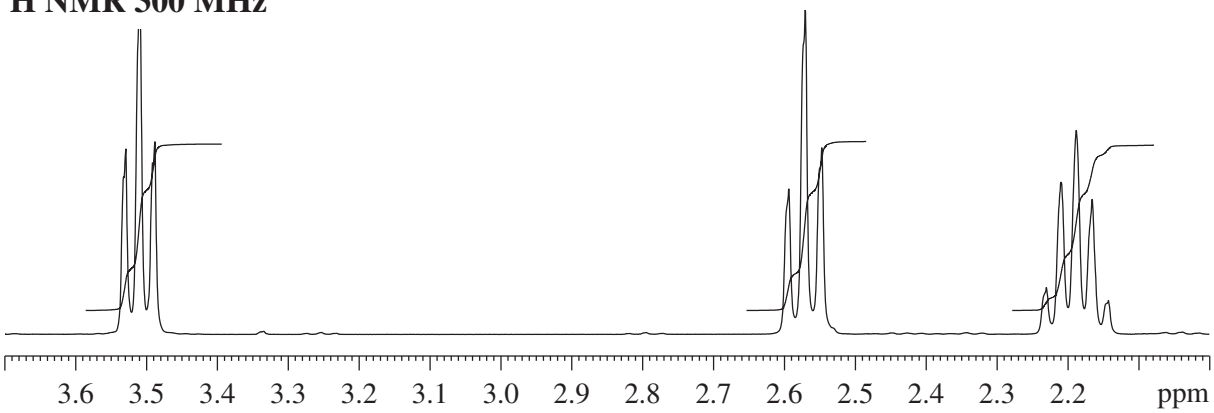

^{13}C/DEPT NMR 75.5 MHz

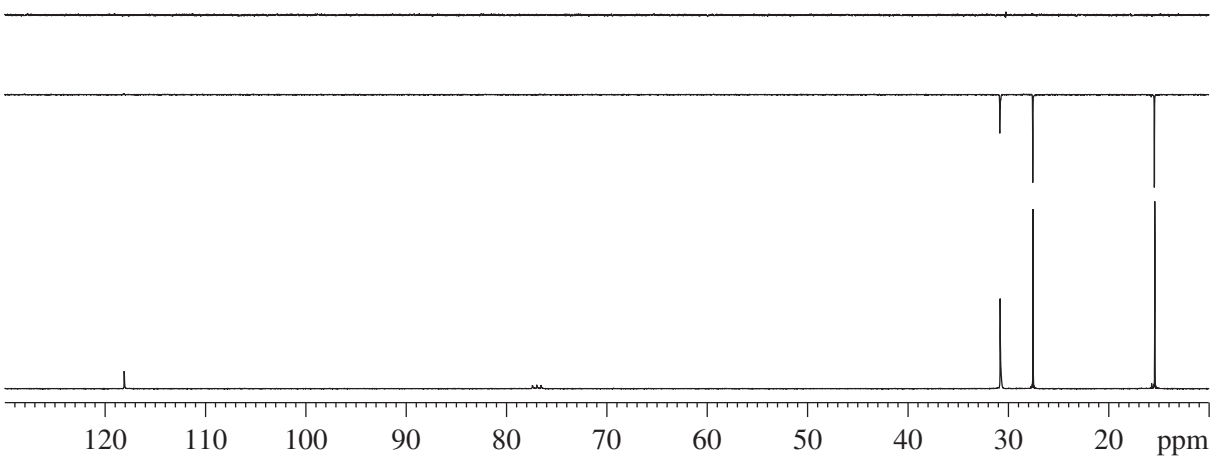

MASS

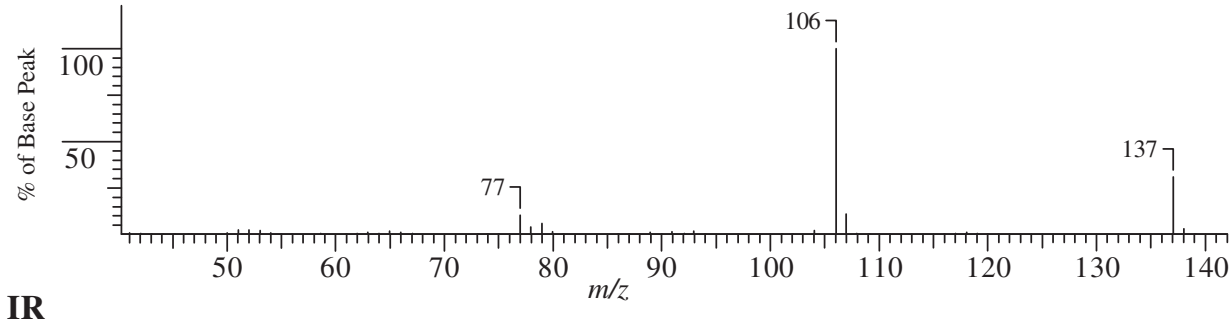

IR

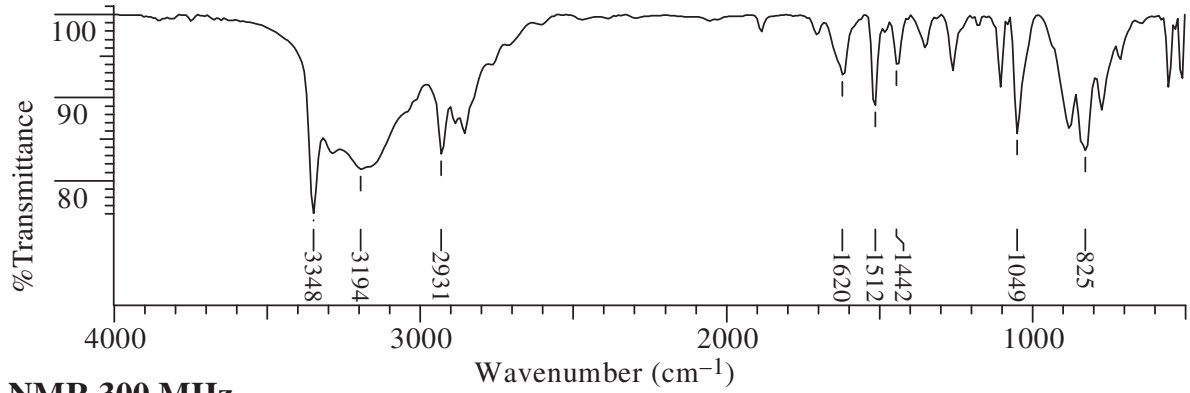

^{1}H NMR 300 MHz

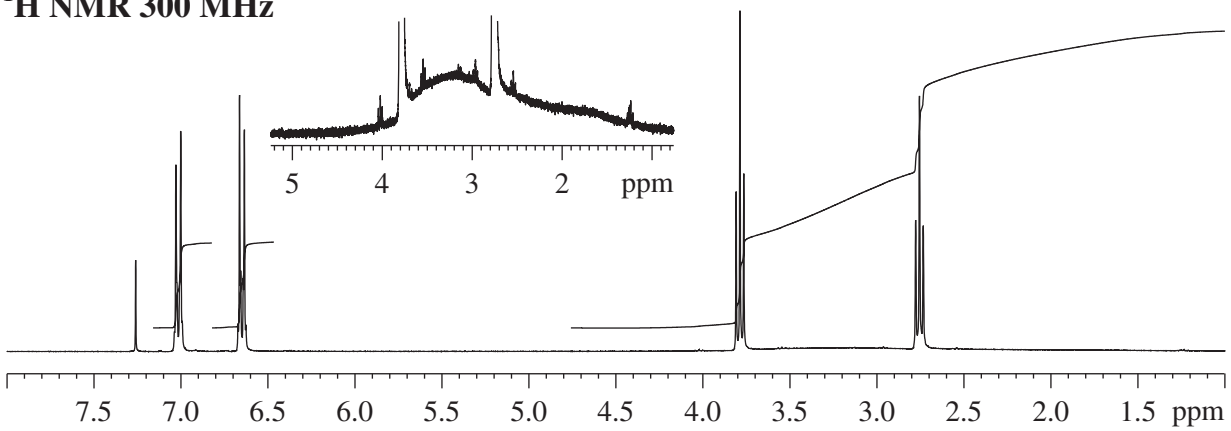

^{13}C/DEPT NMR 75.5 MHz

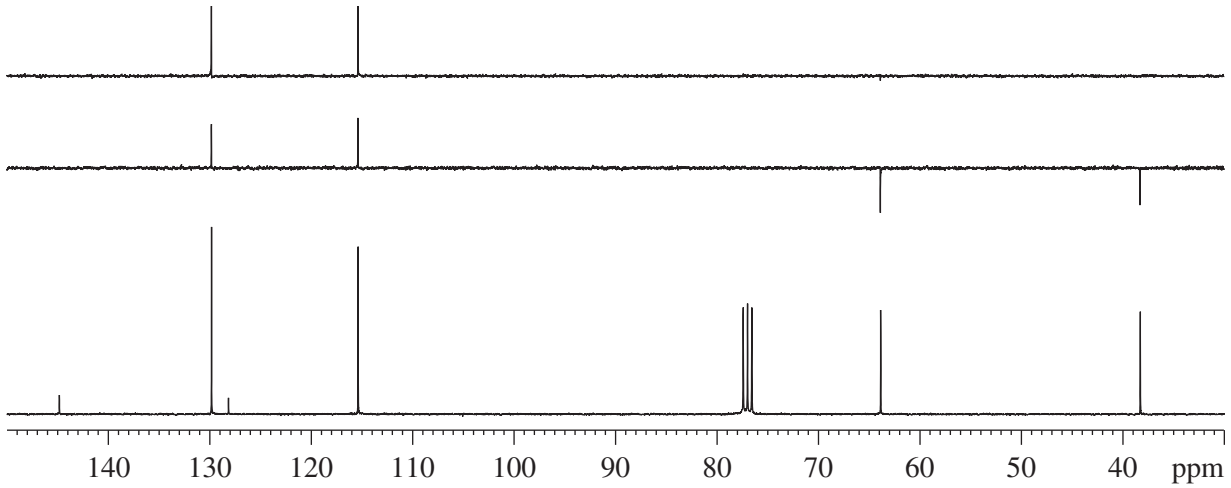

MASS

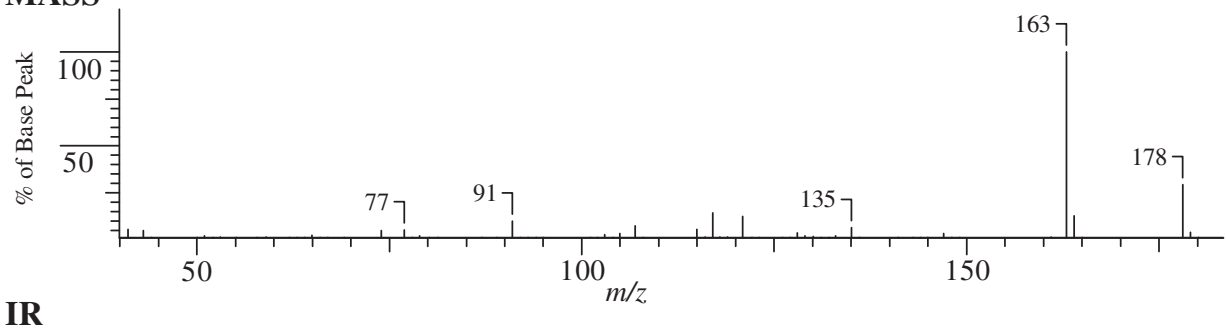

IR

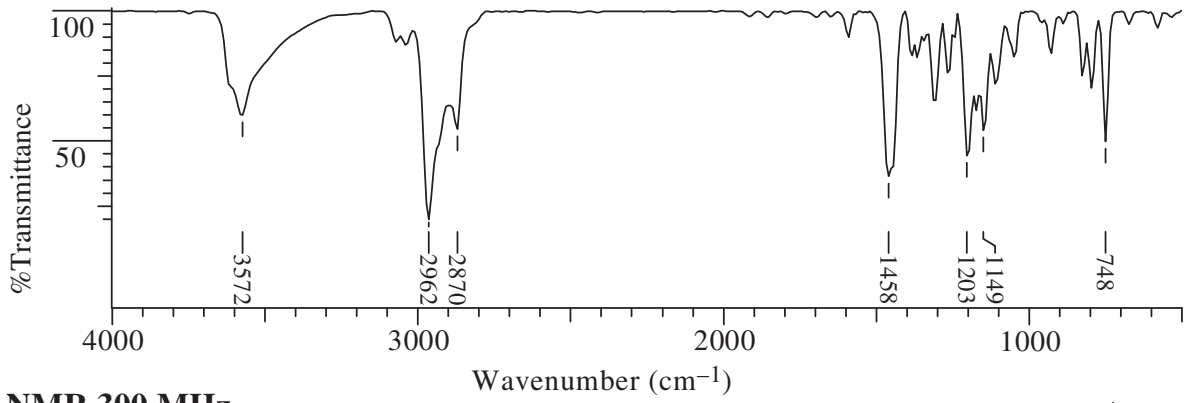

^{1}H NMR 300 MHz

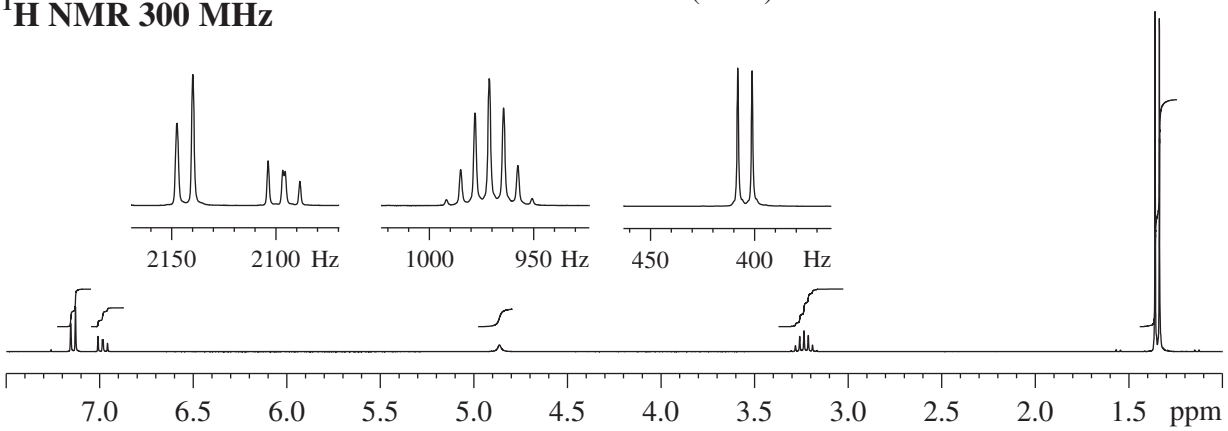

^{13}C/DEPT NMR 75.5 MHz

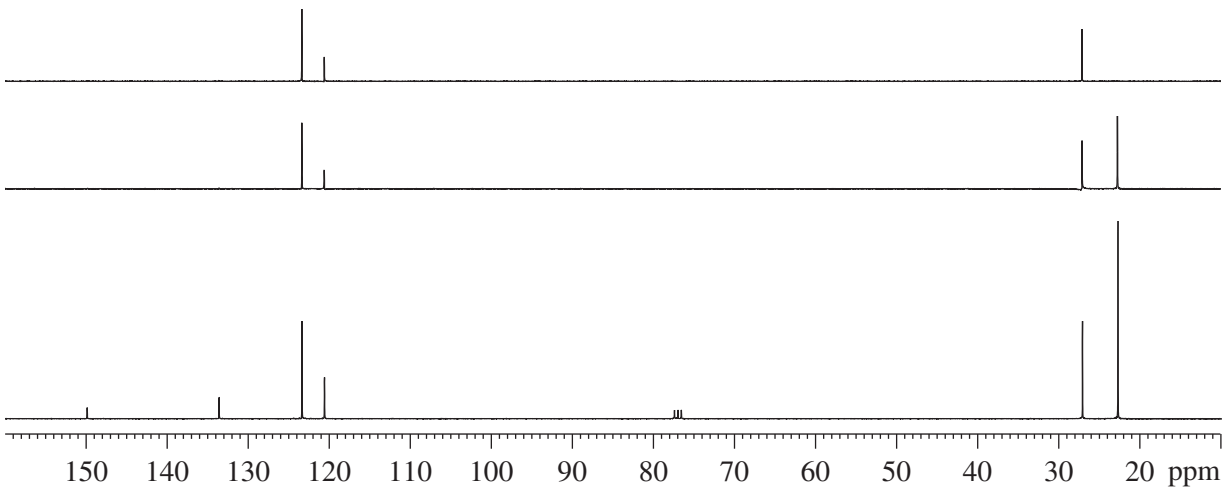

MASS

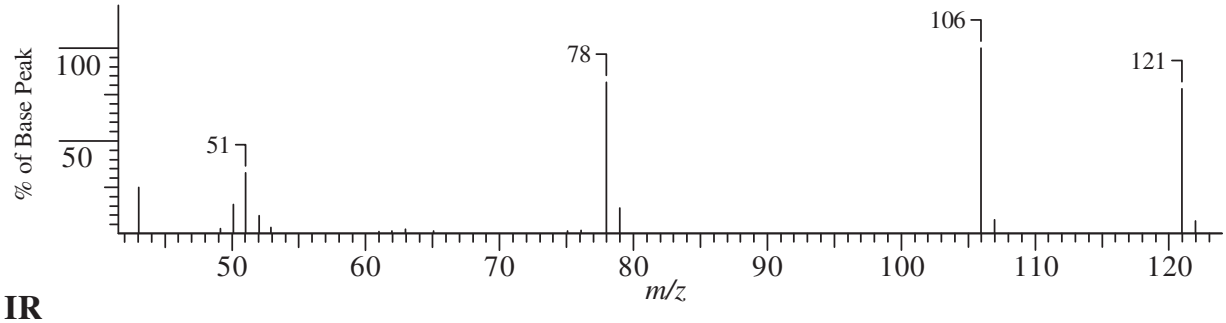

IR

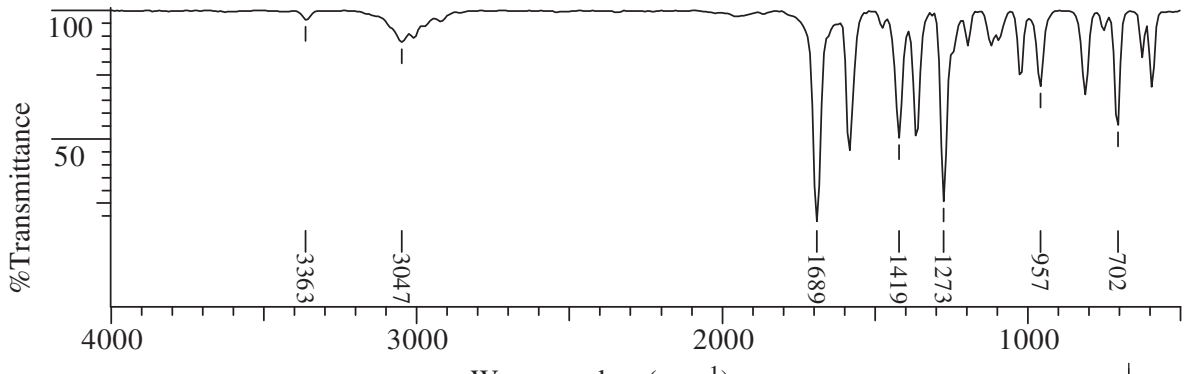

^{1}H NMR 300 MHz

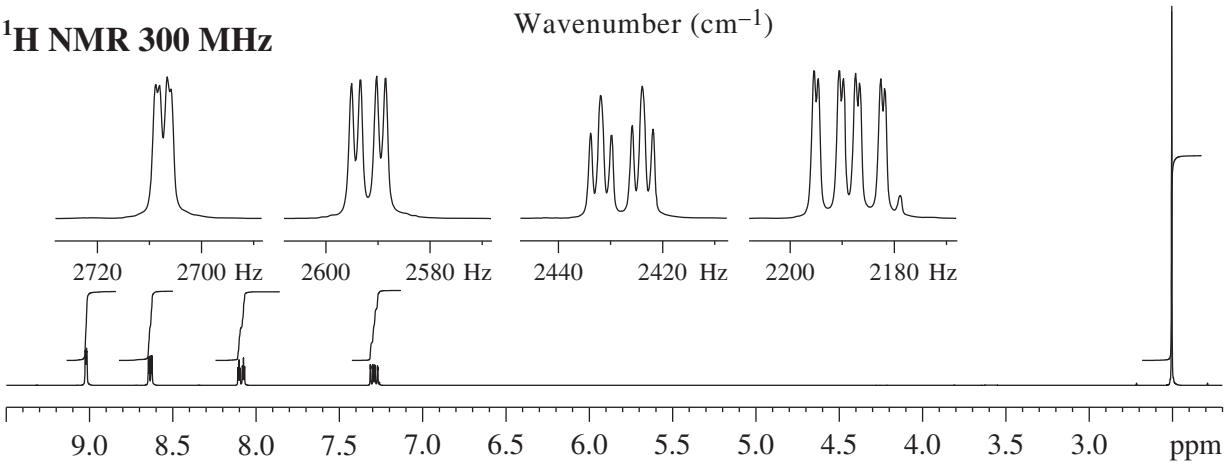

^{13}C/DEPT NMR 75.5 MHz

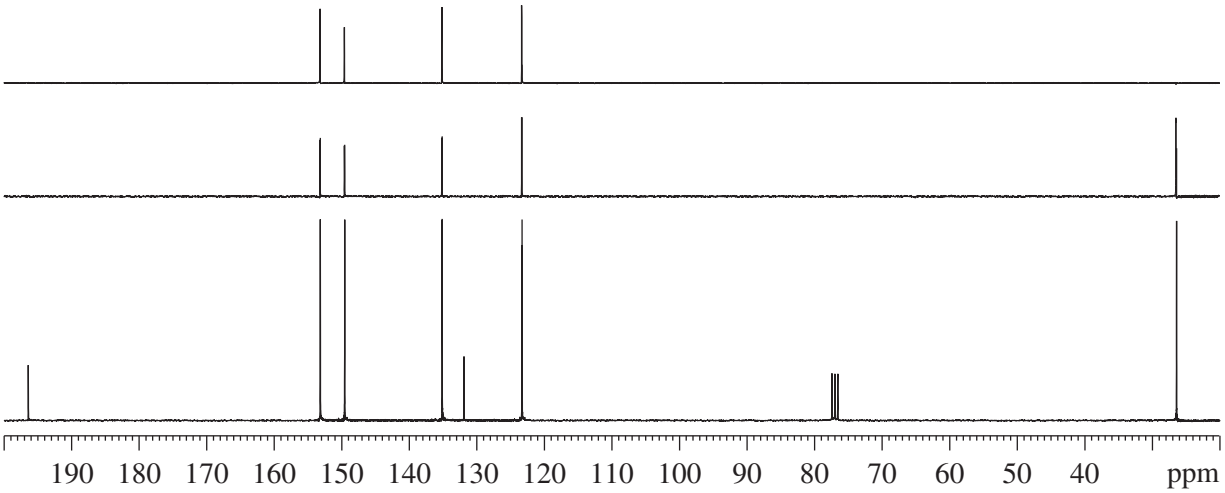

MASS

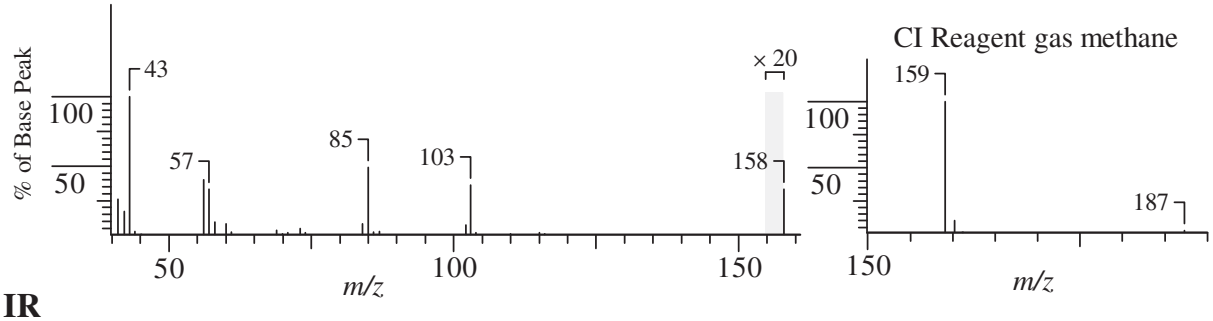

IR

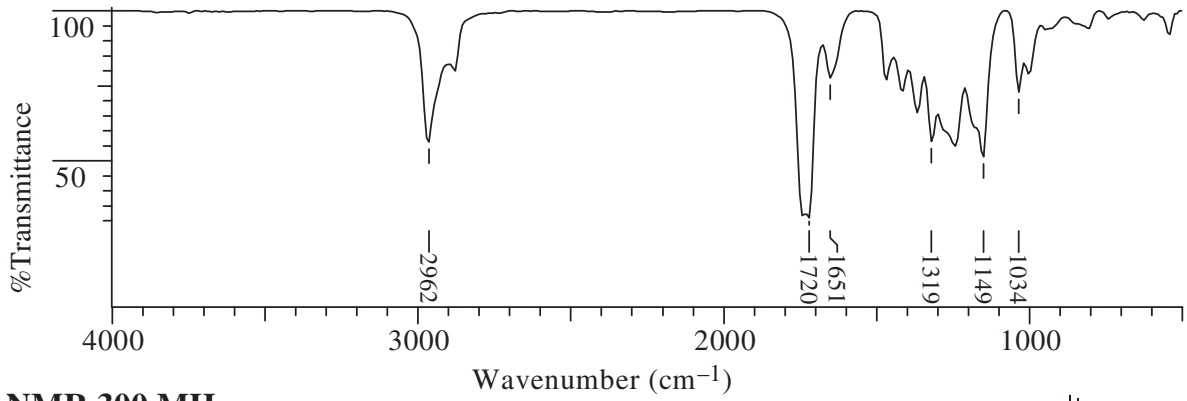

^{1}H NMR 300 MHz

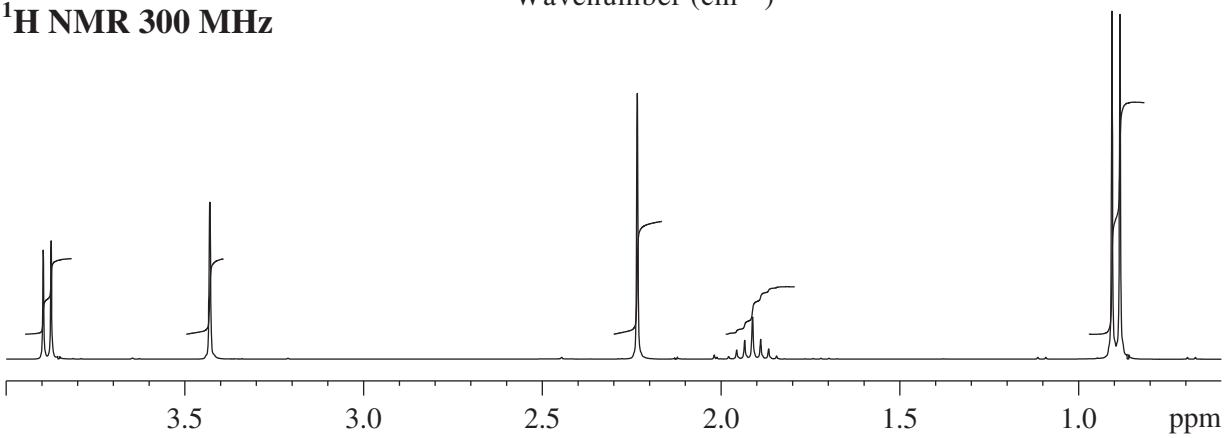

^{13}C/DEPT NMR 75.5 MHz

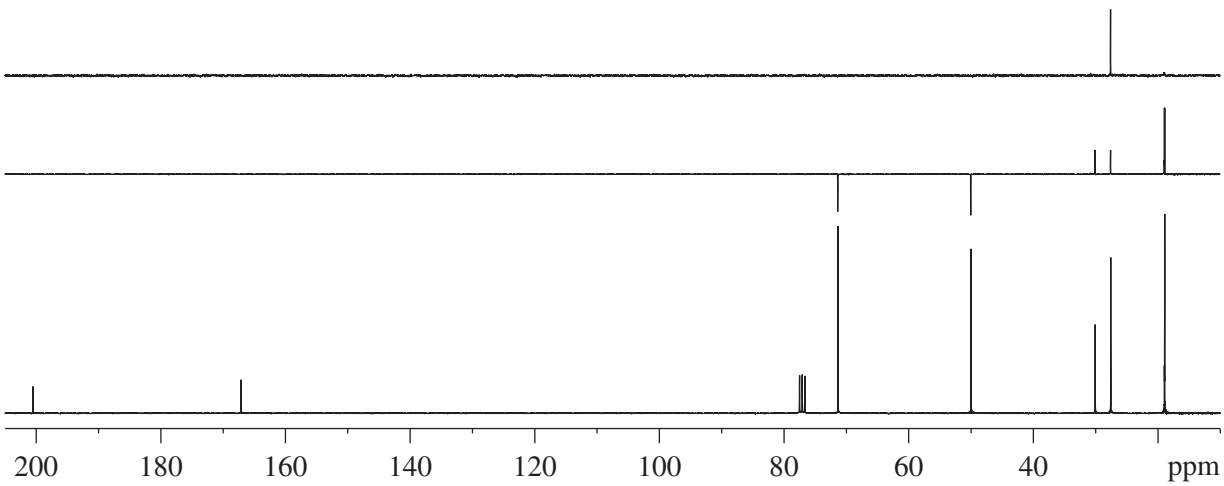

MASS

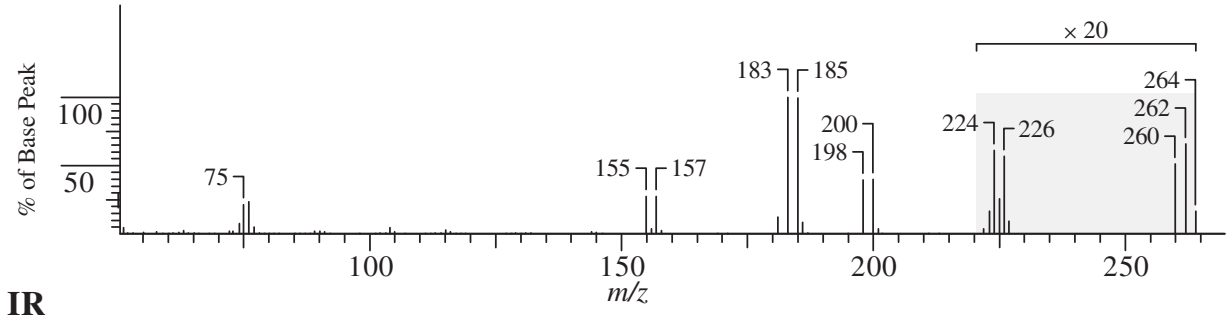

IR

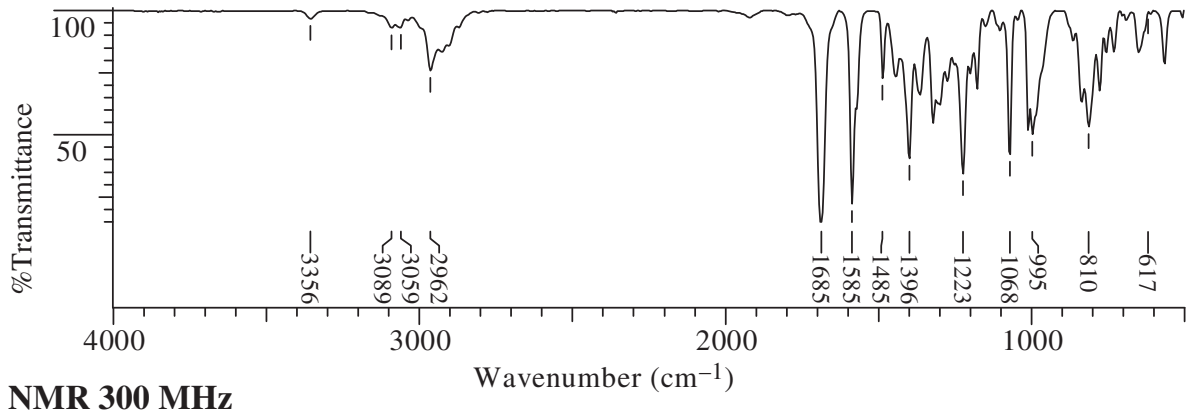

^{1}H NMR 300 MHz

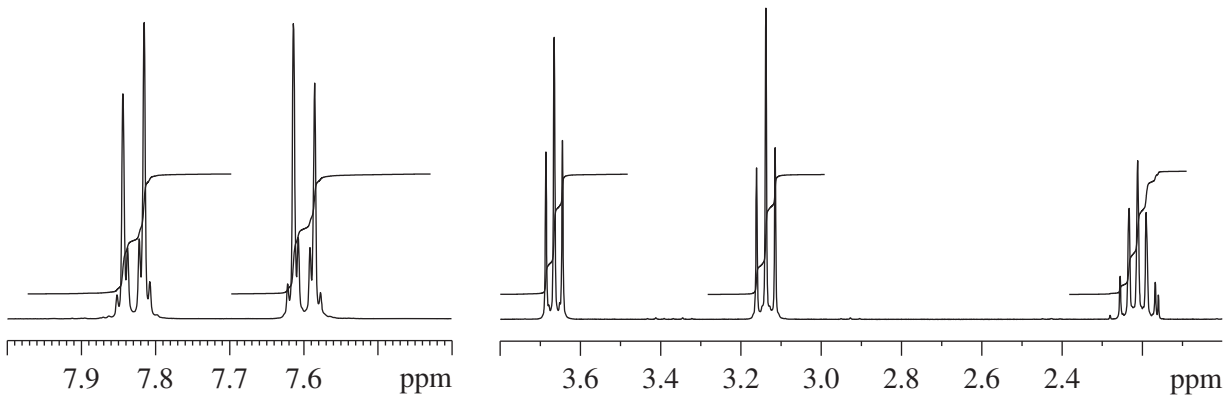

^{13}C/DEPT NMR 75.5 MHz

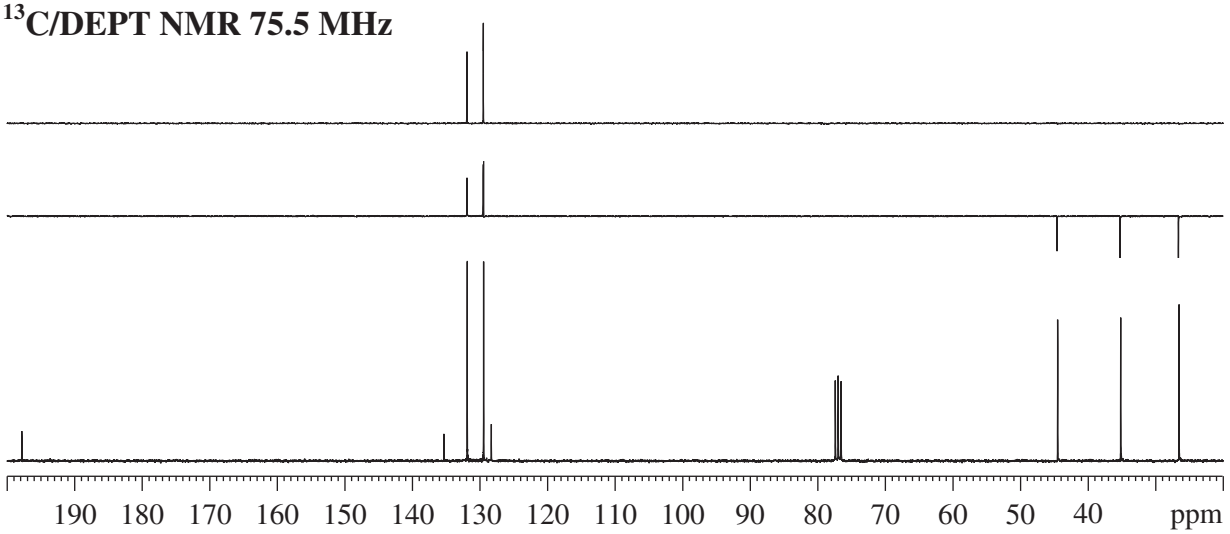

MASS

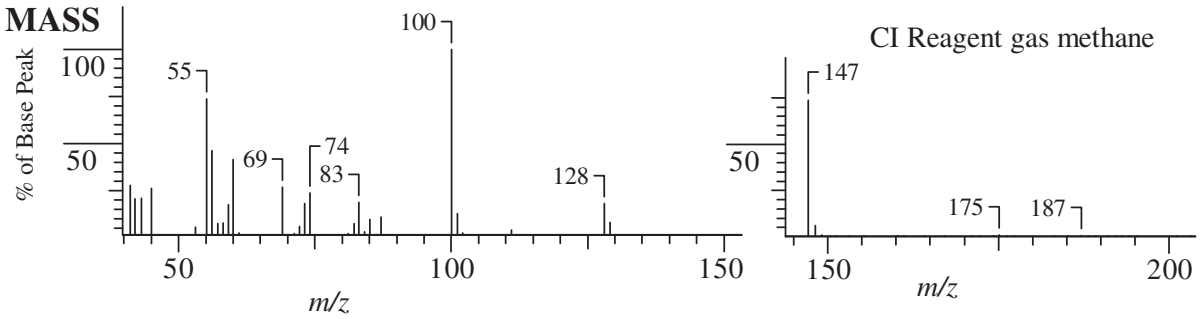

IR

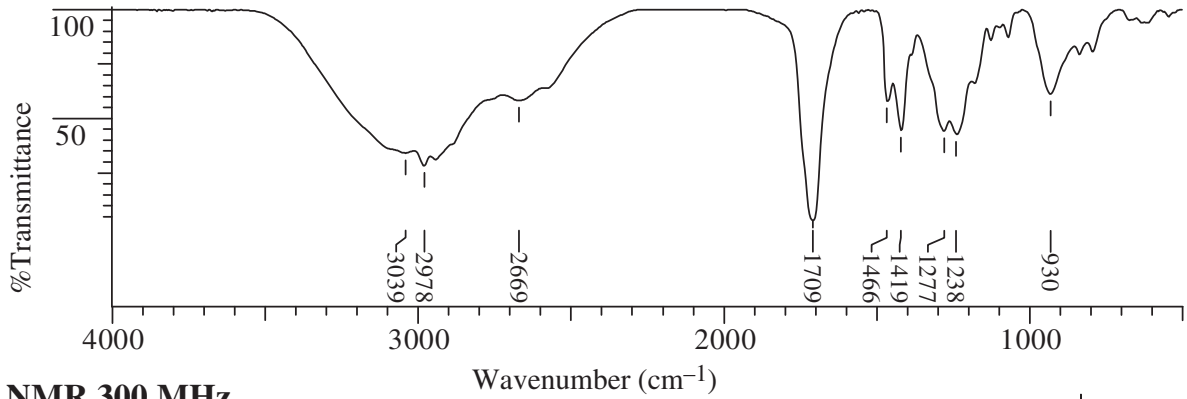

^{1}H NMR 300 MHz

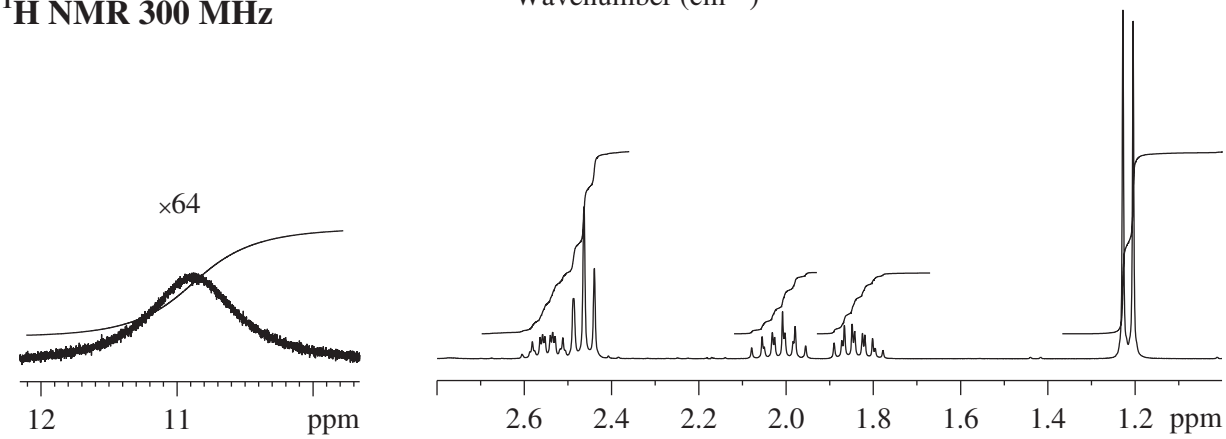

^{13}C/DEPT NMR 75.5 MHz

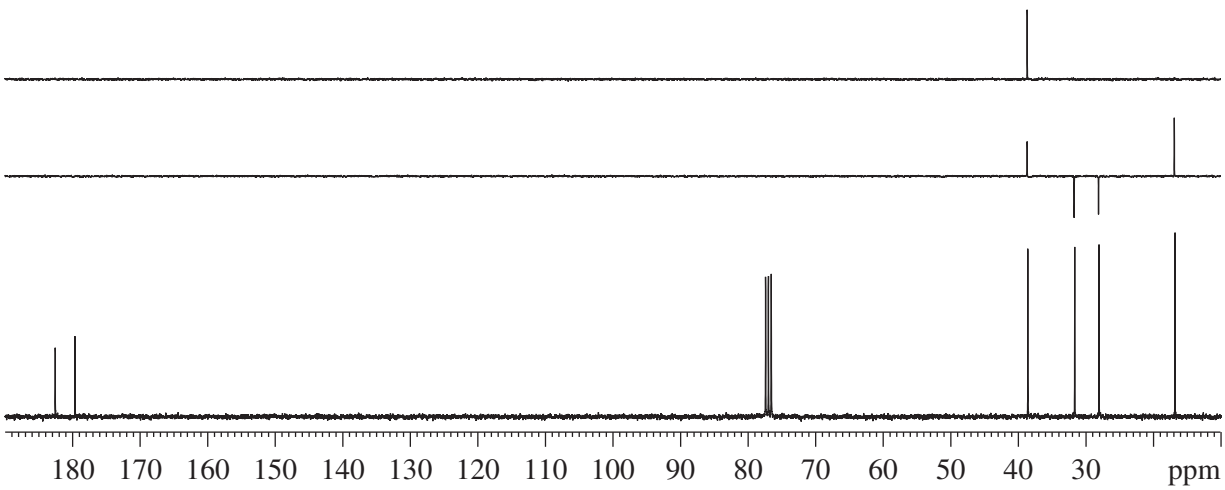

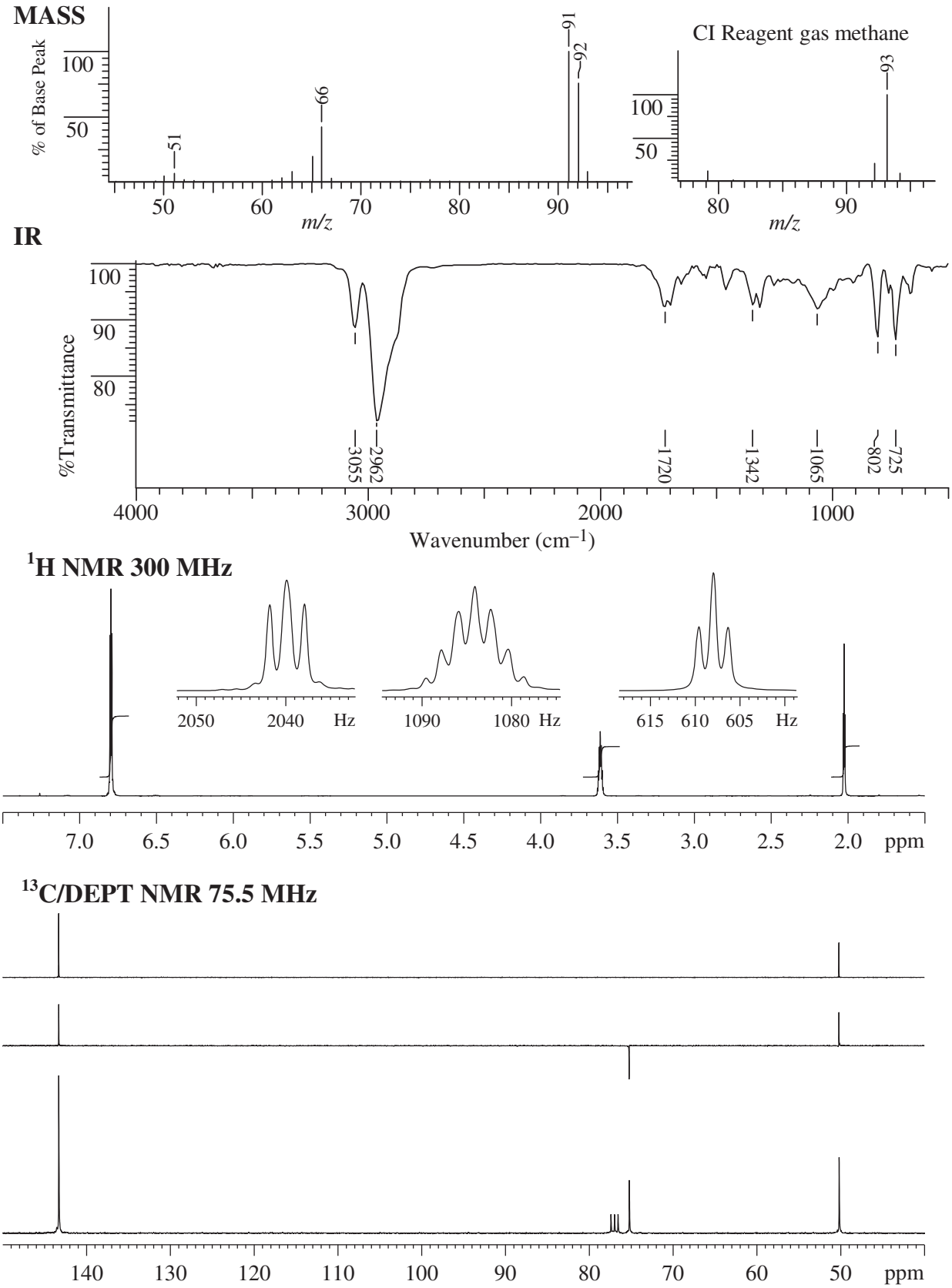
MASS
% of Base Peak
100
50
51
69
91
92
50
60
70
80
90
m/z
CI Reagent gas methane
93
100
50
80
90
m/z
IR
%Transmittance
100
90
80
3055
2962
1720
1342
1065
802
725
4000
3000
2000
1000
Wavenumber (cm−1)
1H NMR 300 MHz
2050
2040
Hz
1090
1080
Hz
615
610
605
Hz
7.0
6.5
6.0
5.5
5.0
4.5
4.0
3.5
3.0
2.5
2.0
ppm
13C/DEPT NMR 75.5 MHz
140
130
120
110
100
90
80
70
60
50
ppm

MASS

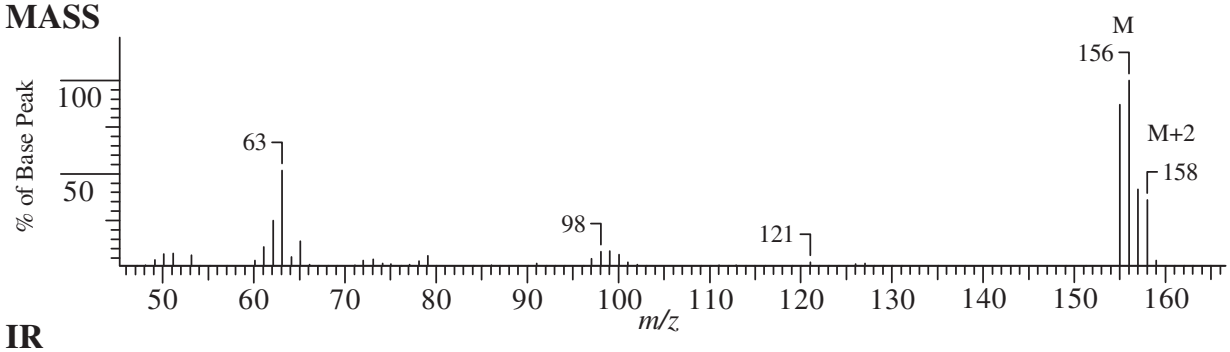

IR

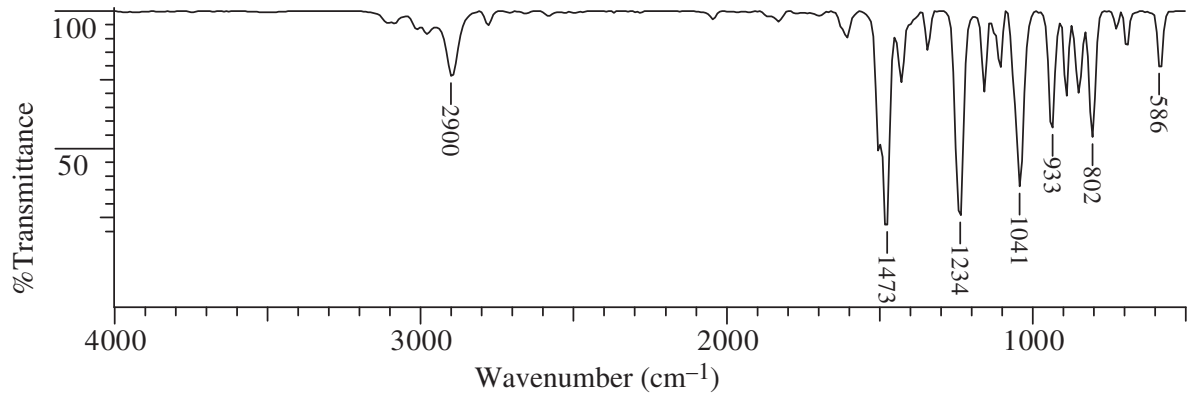

^{1}H NMR 600 MHz

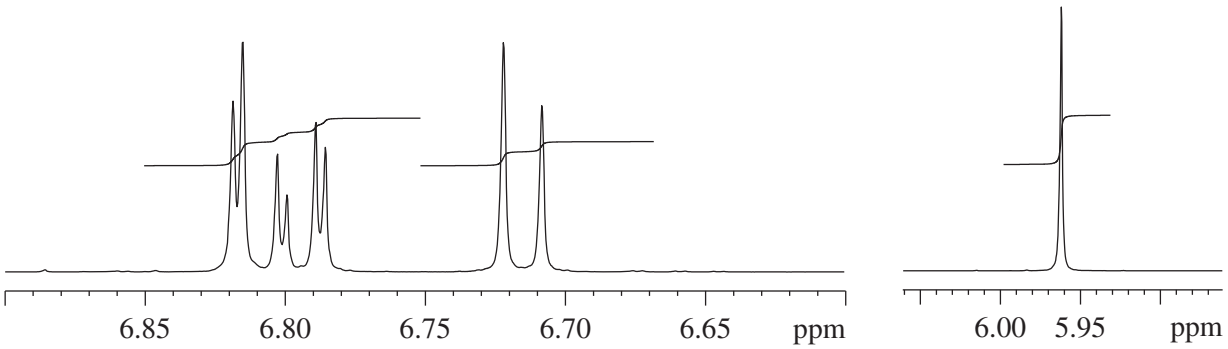

^{13}C/DEPT NMR 150.9 MHz

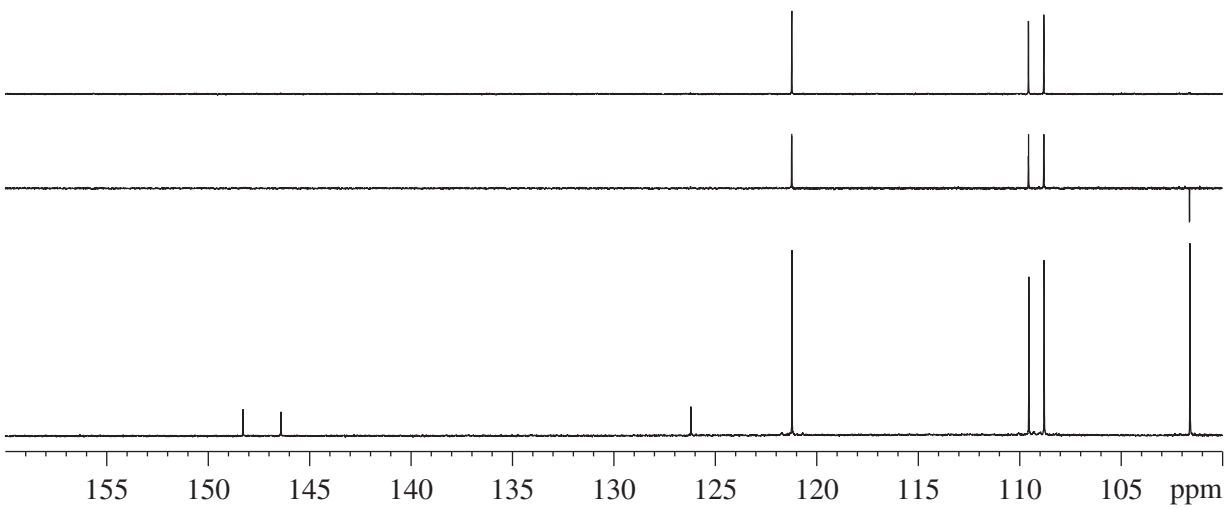

MASS

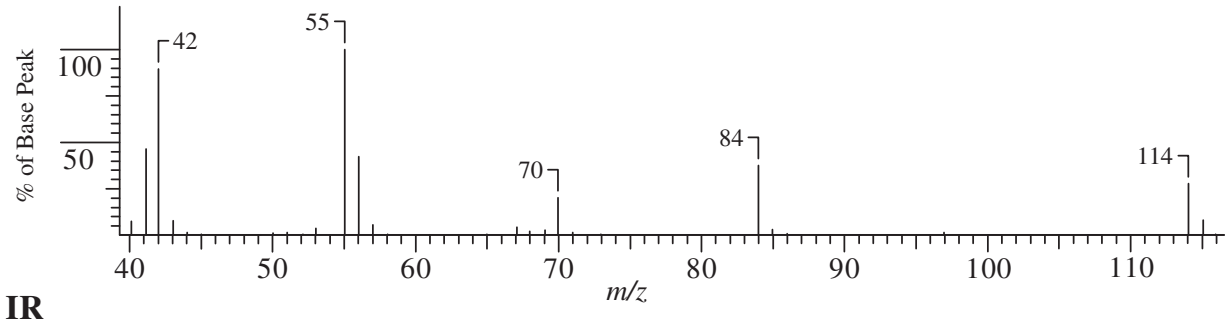

IR

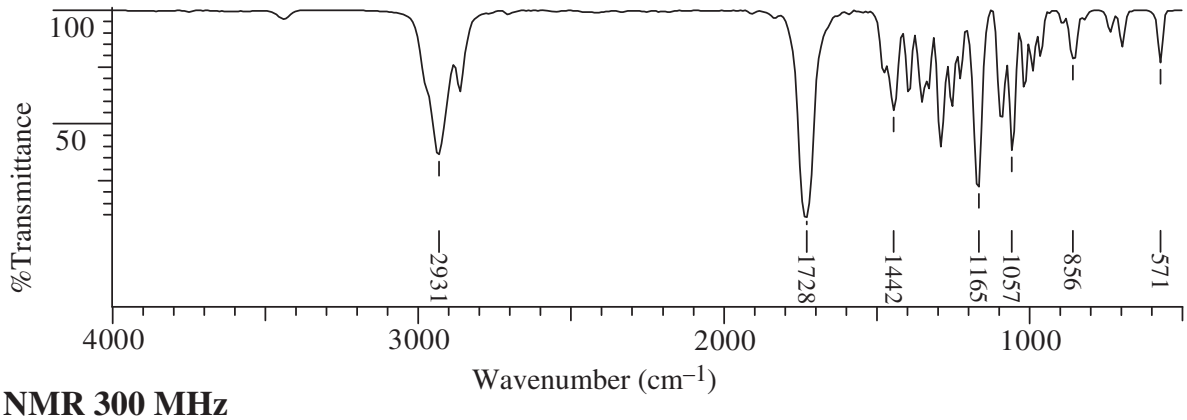

^{1}H NMR 300 MHz

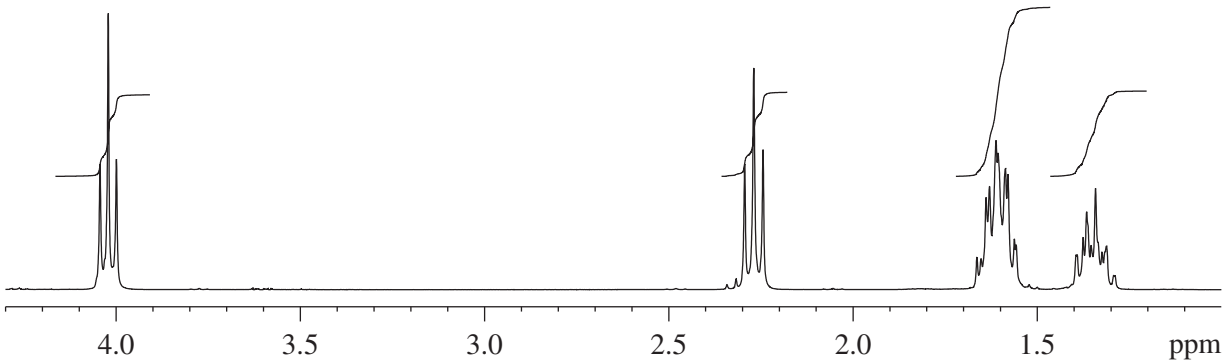

^{13}C/DEPT NMR 75.5 MHz

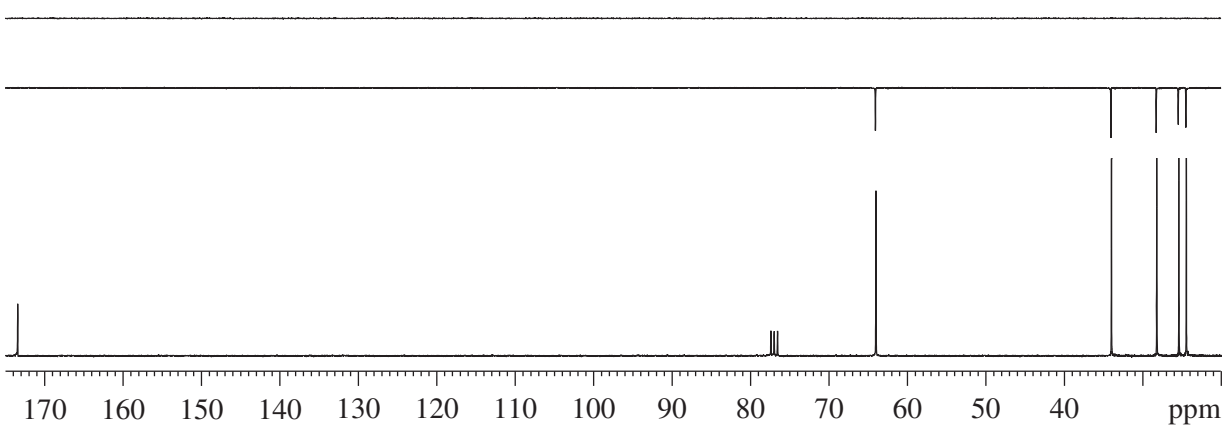

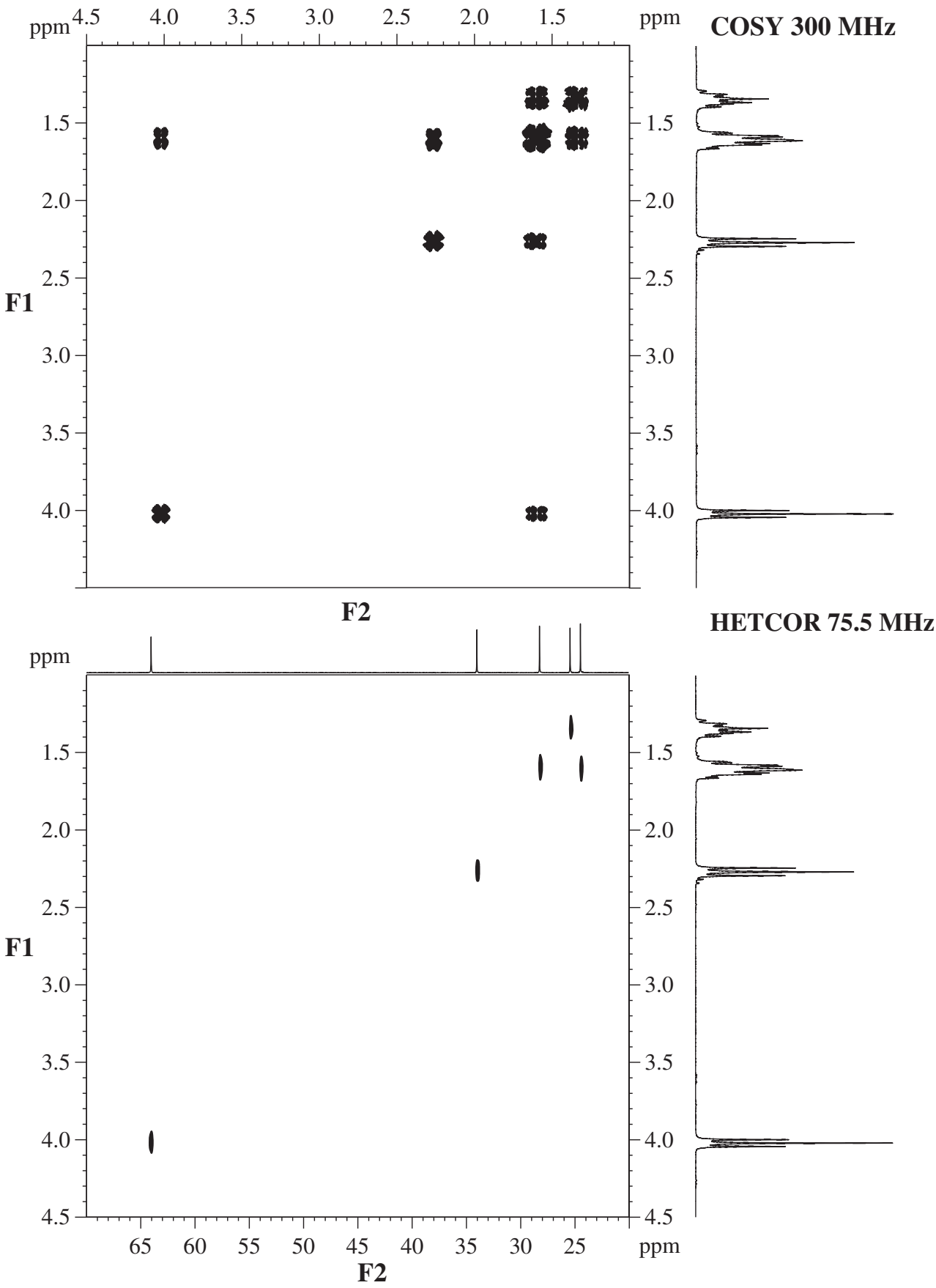
COSY 300 MHz
ppm
4.5
4.0
3.5
3.0
2.5
2.0
1.5
ppm
F1
F2
HETCOR 75.5 MHz
ppm
65
60
55
50
45
40
35
30
25
ppm
F1
F2

MASS

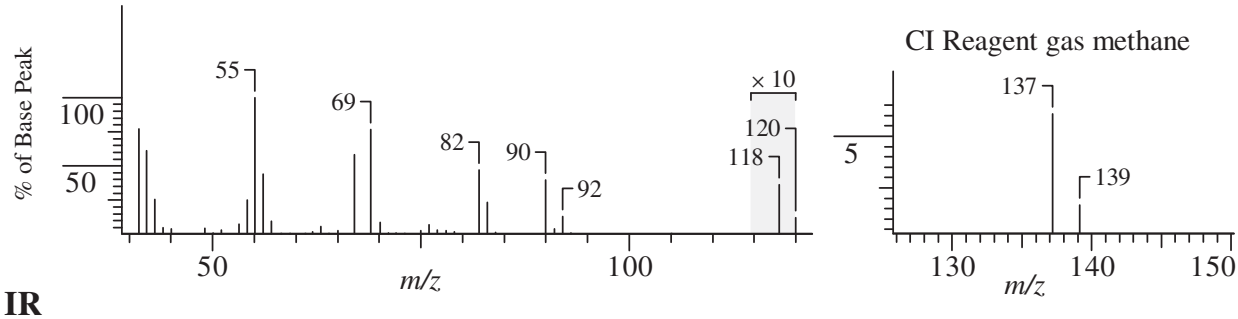

IR

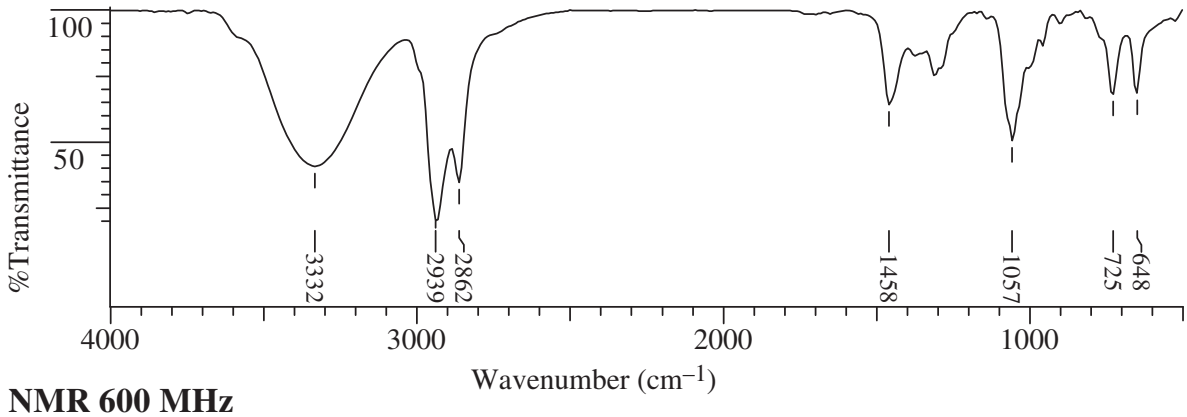

^{1}H NMR 600 MHz

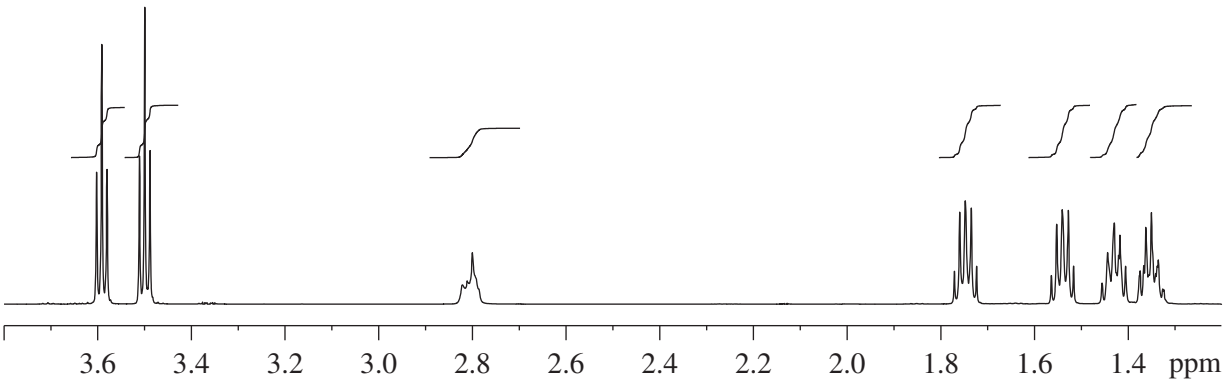

^{13}C/DEPT NMR 150.9 MHz

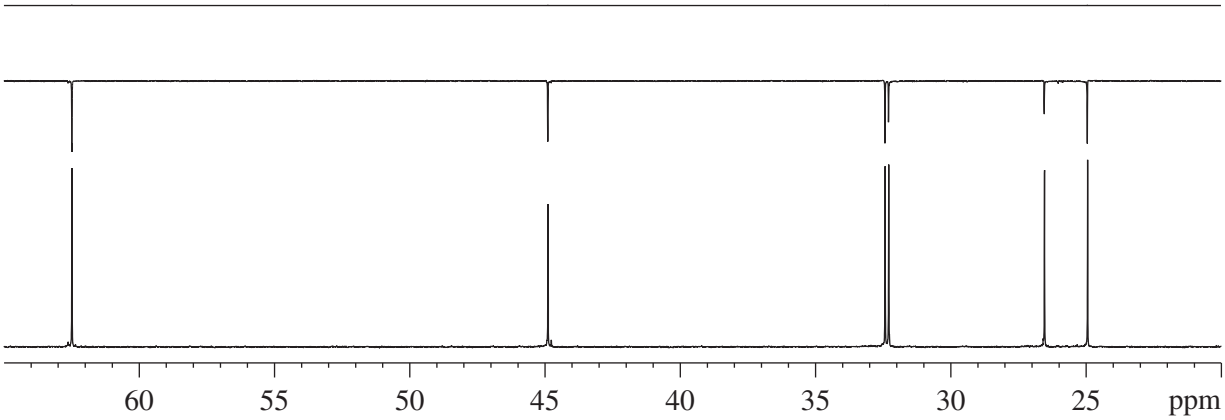

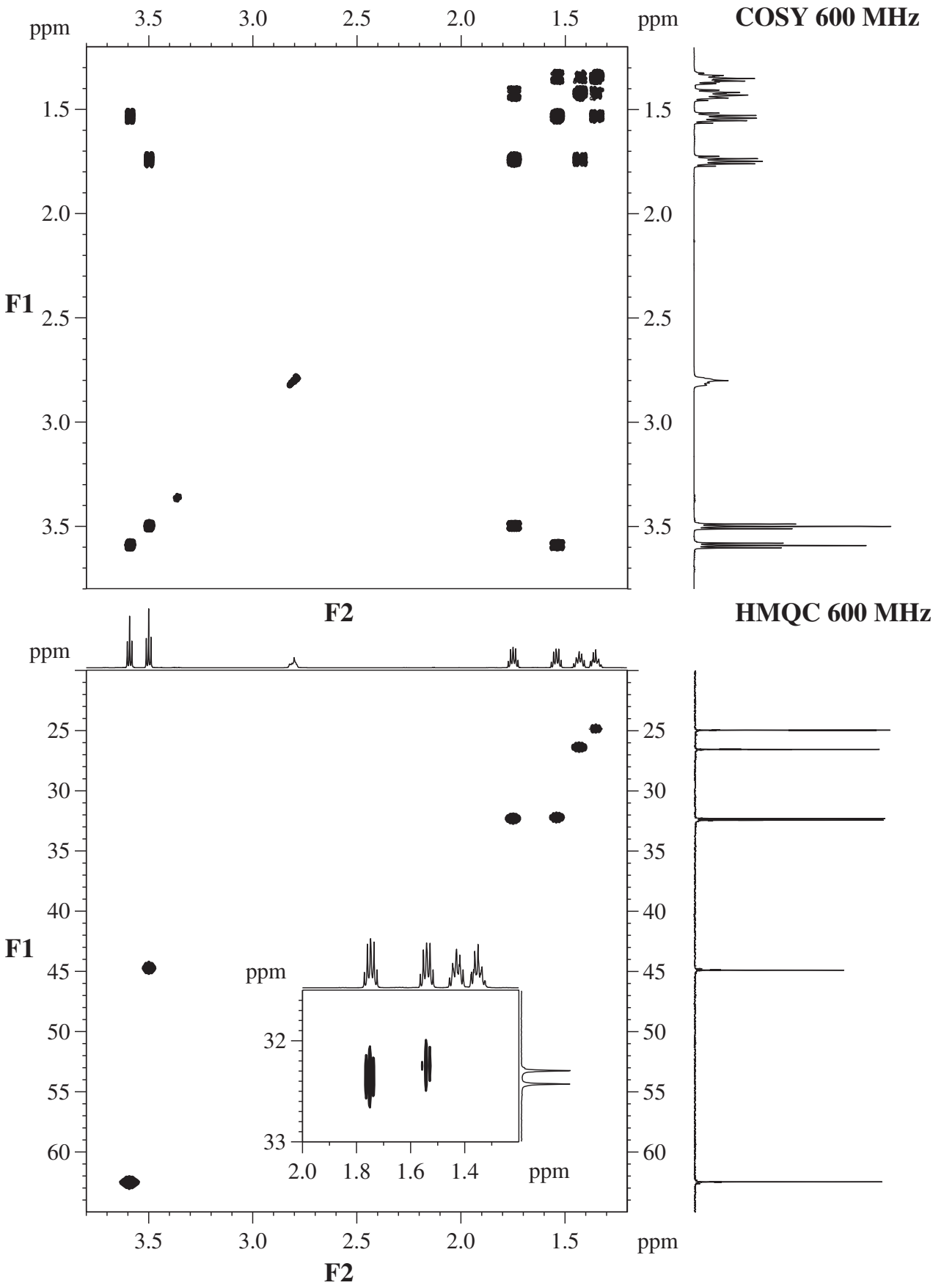
COSY 600 MHz
ppm
3.5
3.0
2.5
2.0
1.5
F1
F2
HMQC 600 MHz
25
30
35
40
45
50
55
60
32
33
1.8
1.6
1.4

MASS

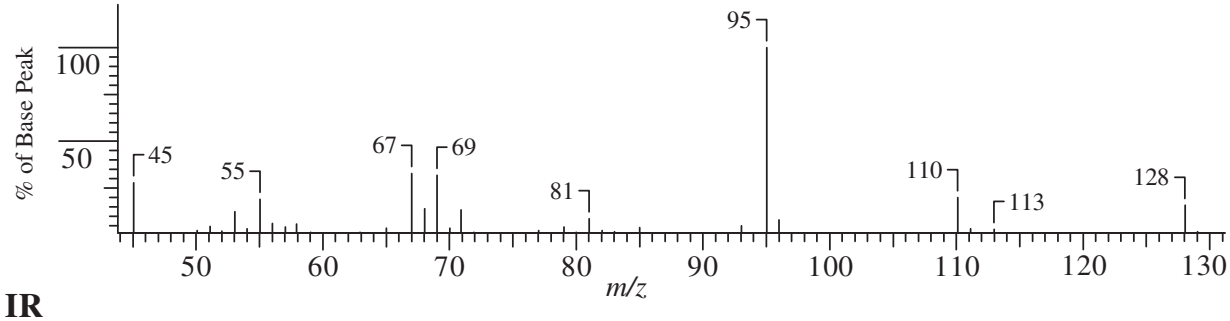

IR

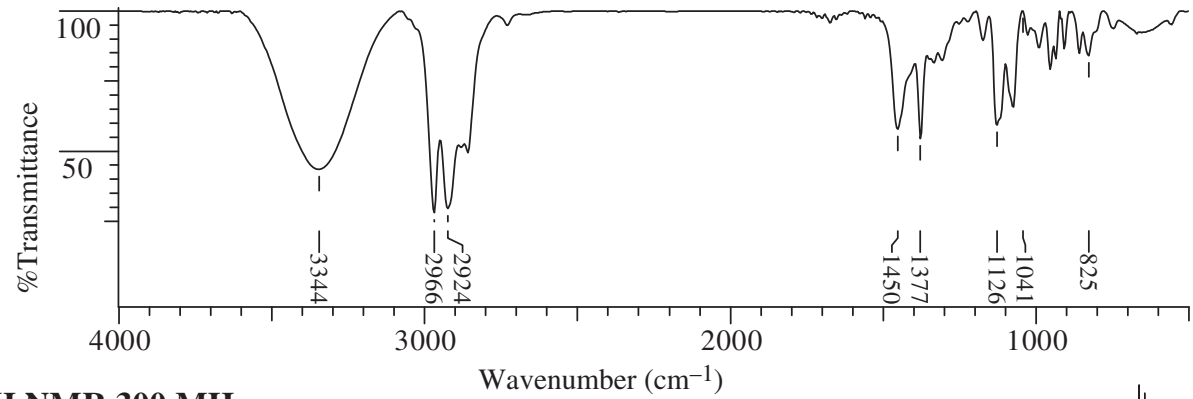

^{1}H NMR 300 MHz

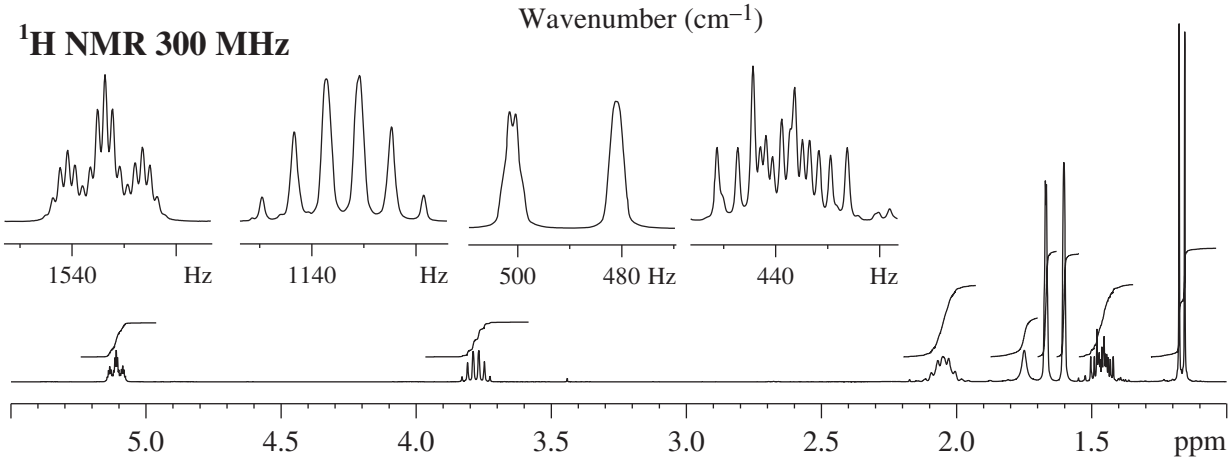

^{13}C/DEPT NMR 75.5 MHz

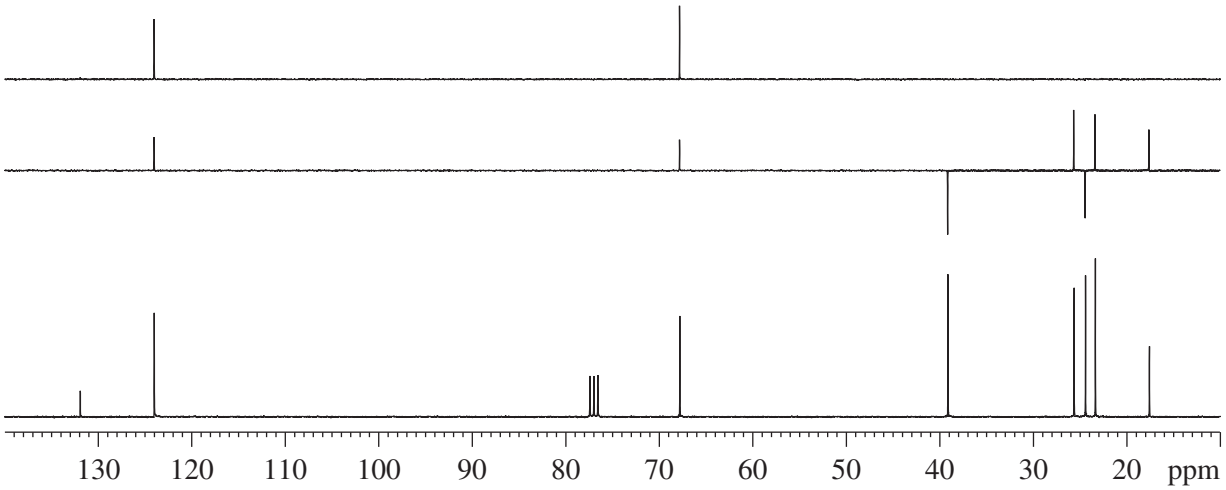

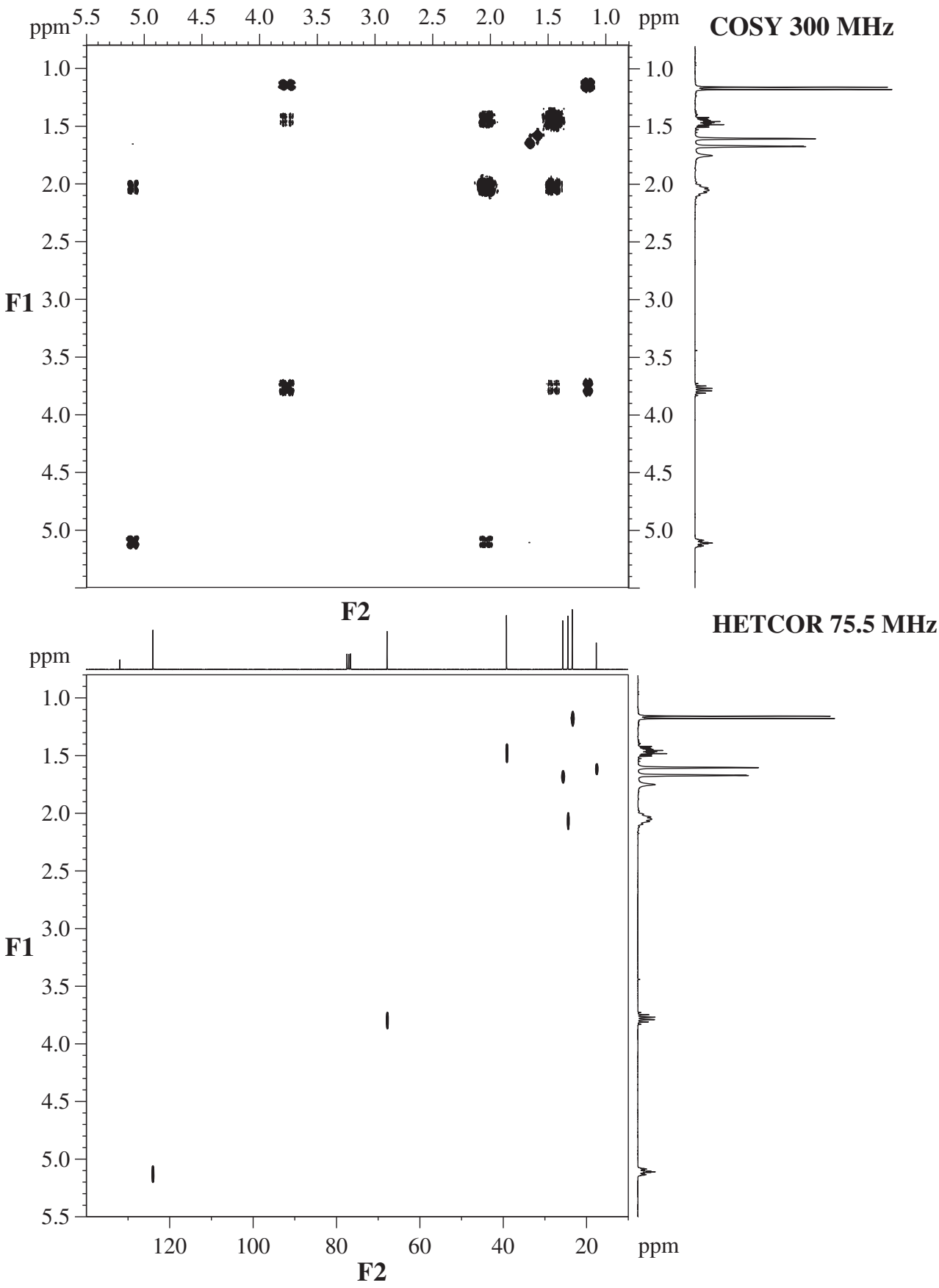
COSY 300 MHz
ppm
5.5 5.0 4.5 4.0 3.5 3.0 2.5 2.0 1.5 1.0 ppm
1.0
1.5
2.0
2.5
F1 3.0
3.5
4.0
4.5
5.0
F2
HETCOR 75.5 MHz
ppm
1.0
1.5
2.0
2.5
F1 3.0
3.5
4.0
4.5
5.0
5.5
120 100 80 60 40 20 ppm
F2

MASS

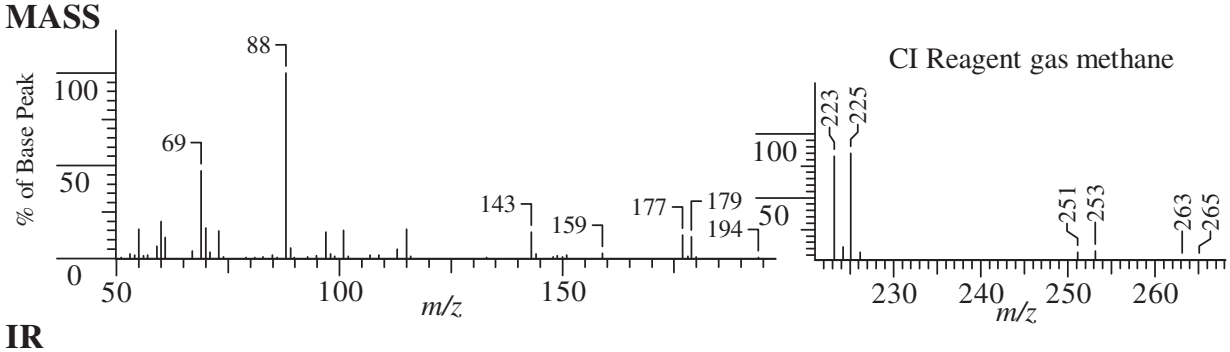

IR

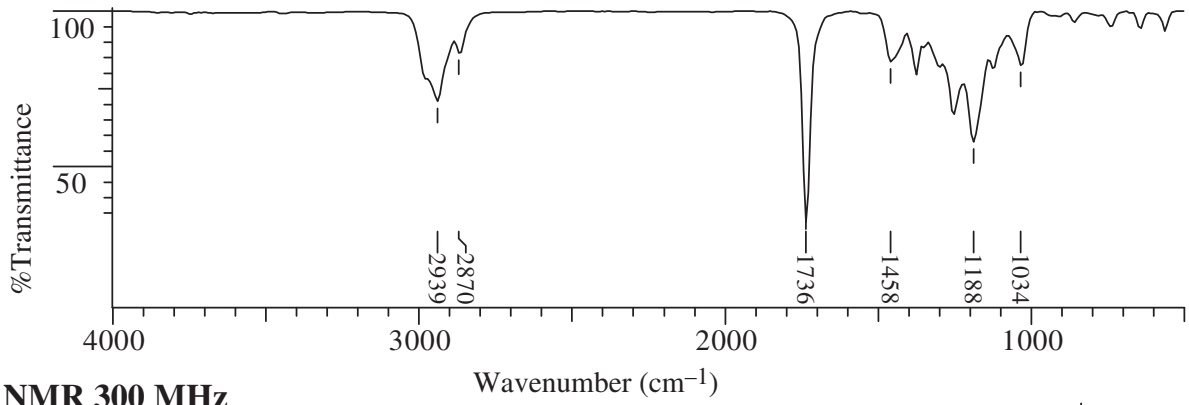

^{1}H NMR 300 MHz

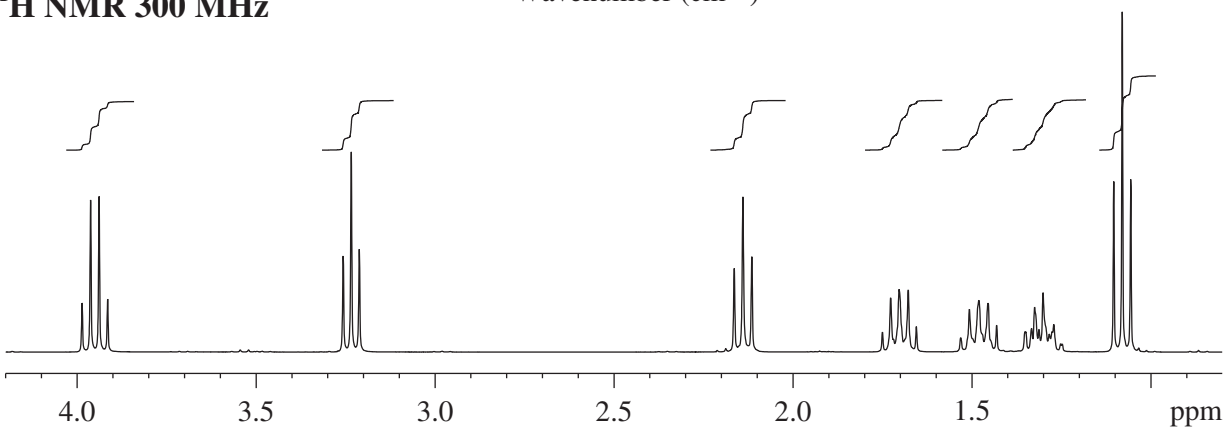

^{13}C/DEPT NMR 75.5 MHz

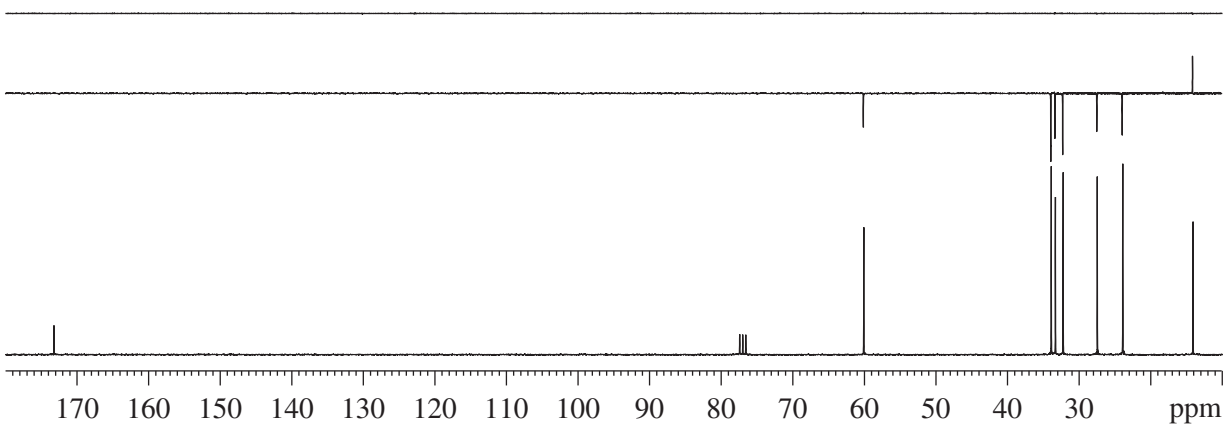

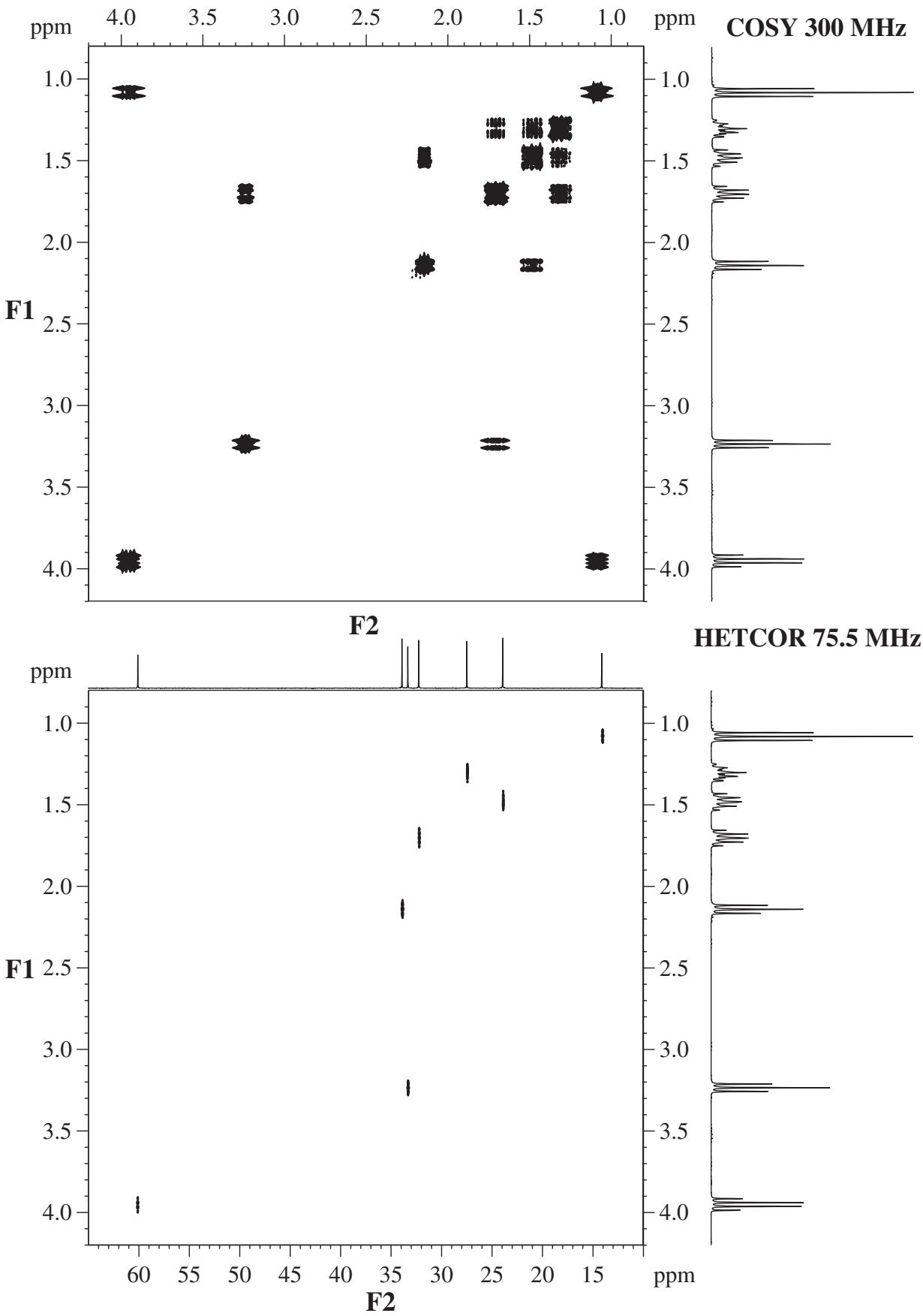
COSY 300 MHz
ppm
4.0
3.5
3.0
2.5
2.0
1.5
1.0
F1
F2
HETCOR 75.5 MHz
60
55
50
45
40
35
30
25
20
15

MASS

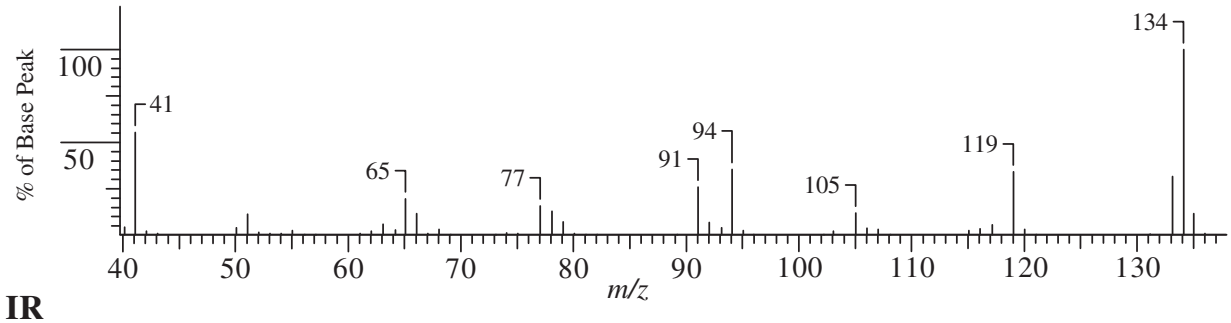

IR

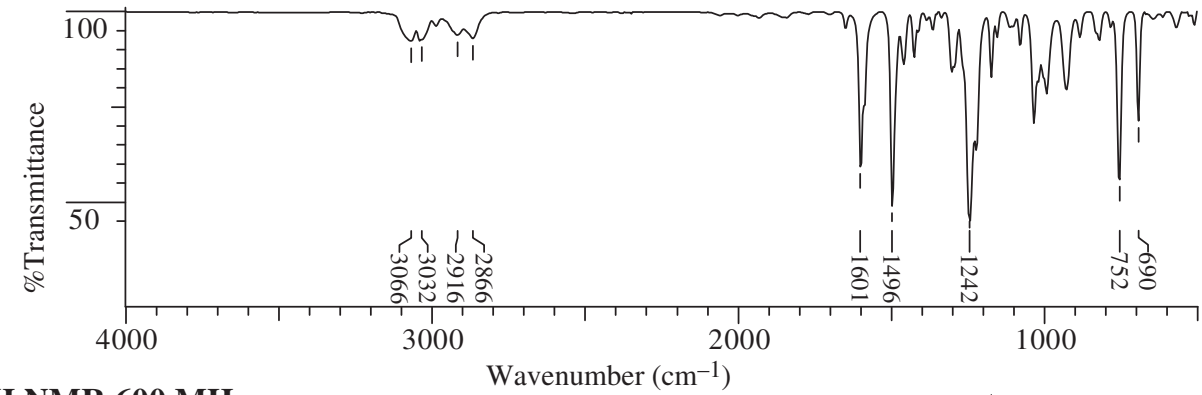

^{1}H NMR 600 MHz

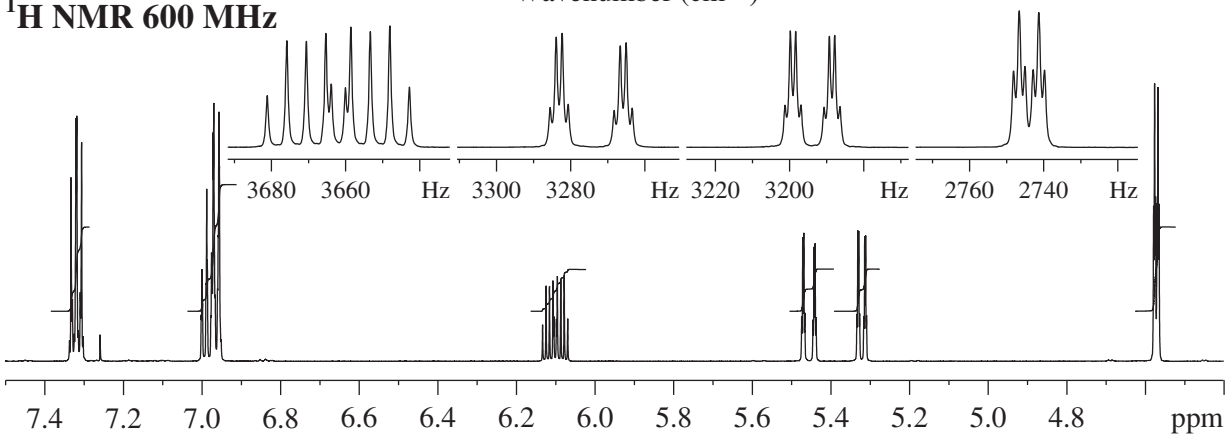

^{13}C/DEPT NMR 150.9 MHz

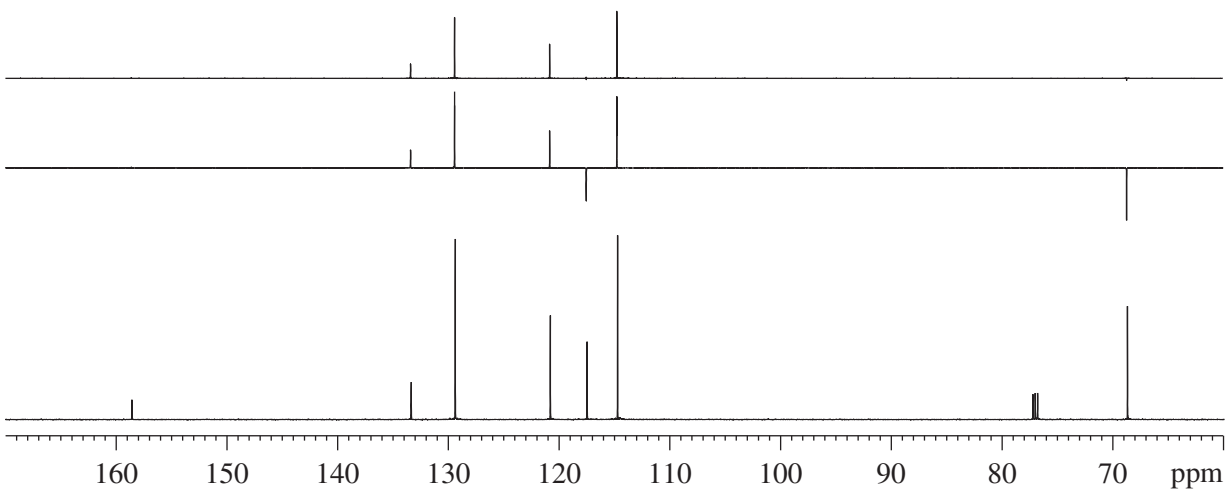

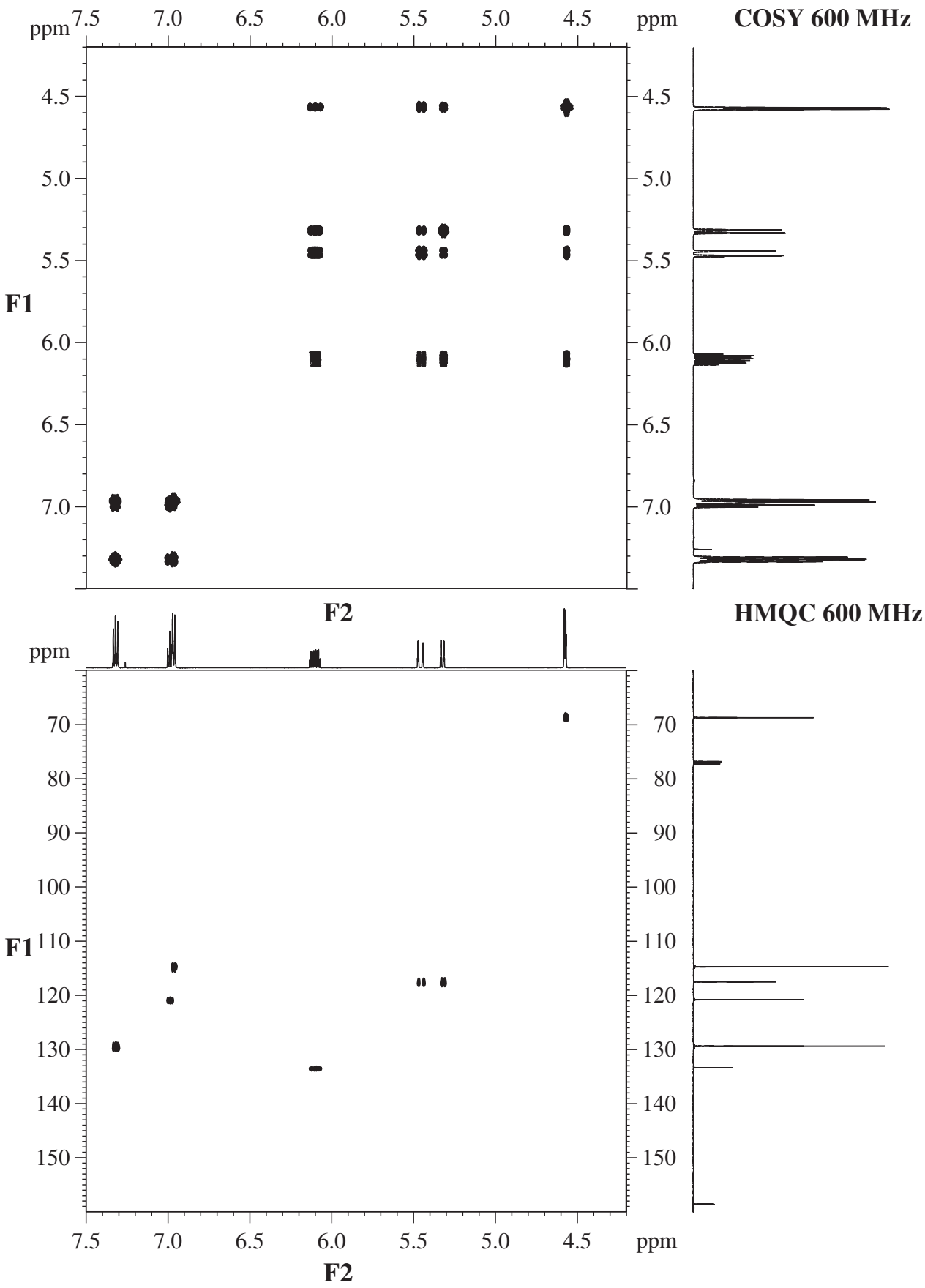
COSY 600 MHz
ppm
7.5
7.0
6.5
6.0
5.5
5.0
4.5
F1
F2
HMQC 600 MHz
70
80
90
100
110
120
130
140
150

MASS

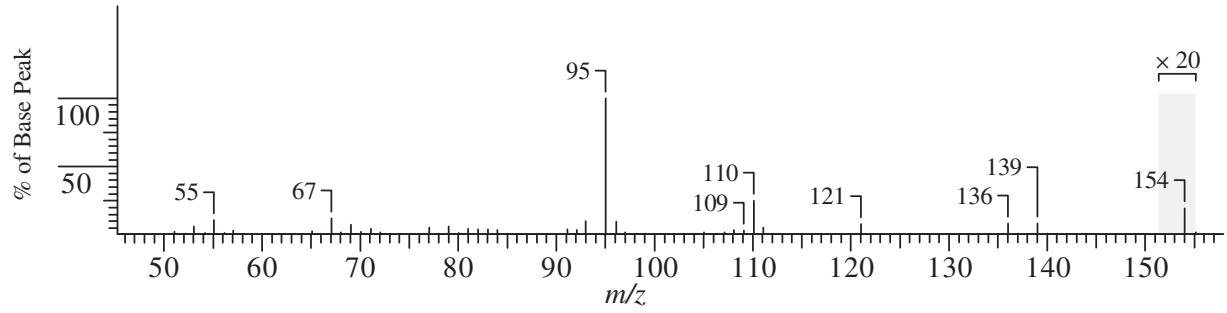

^{1}H NMR 600 MHz

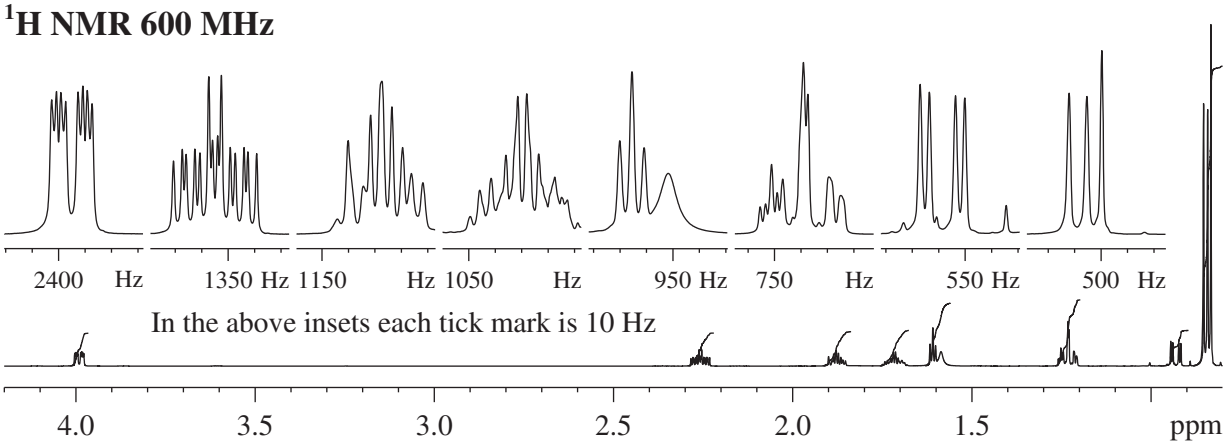

^{13}C/DEPT NMR 150.9 MHz

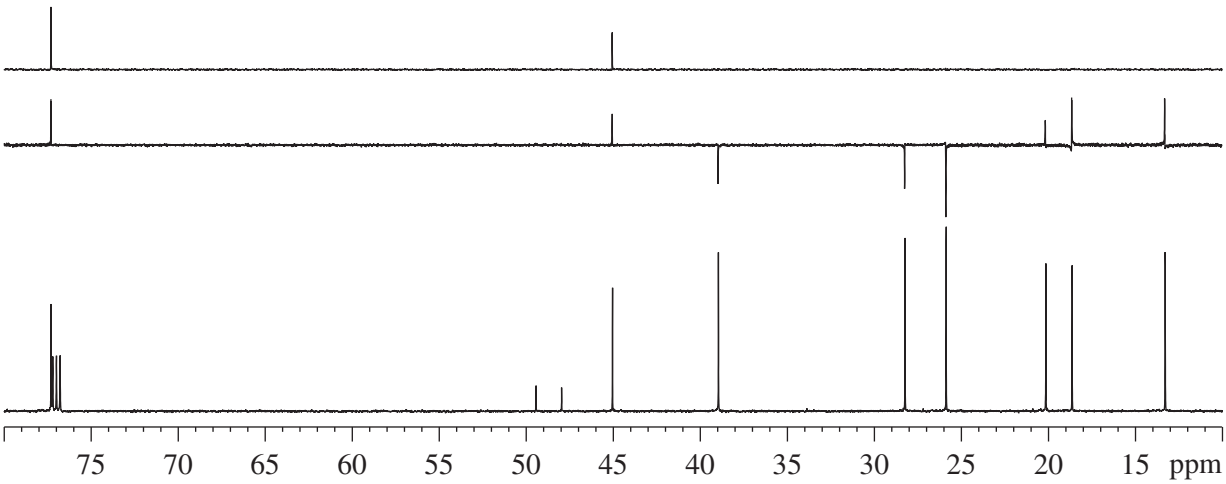

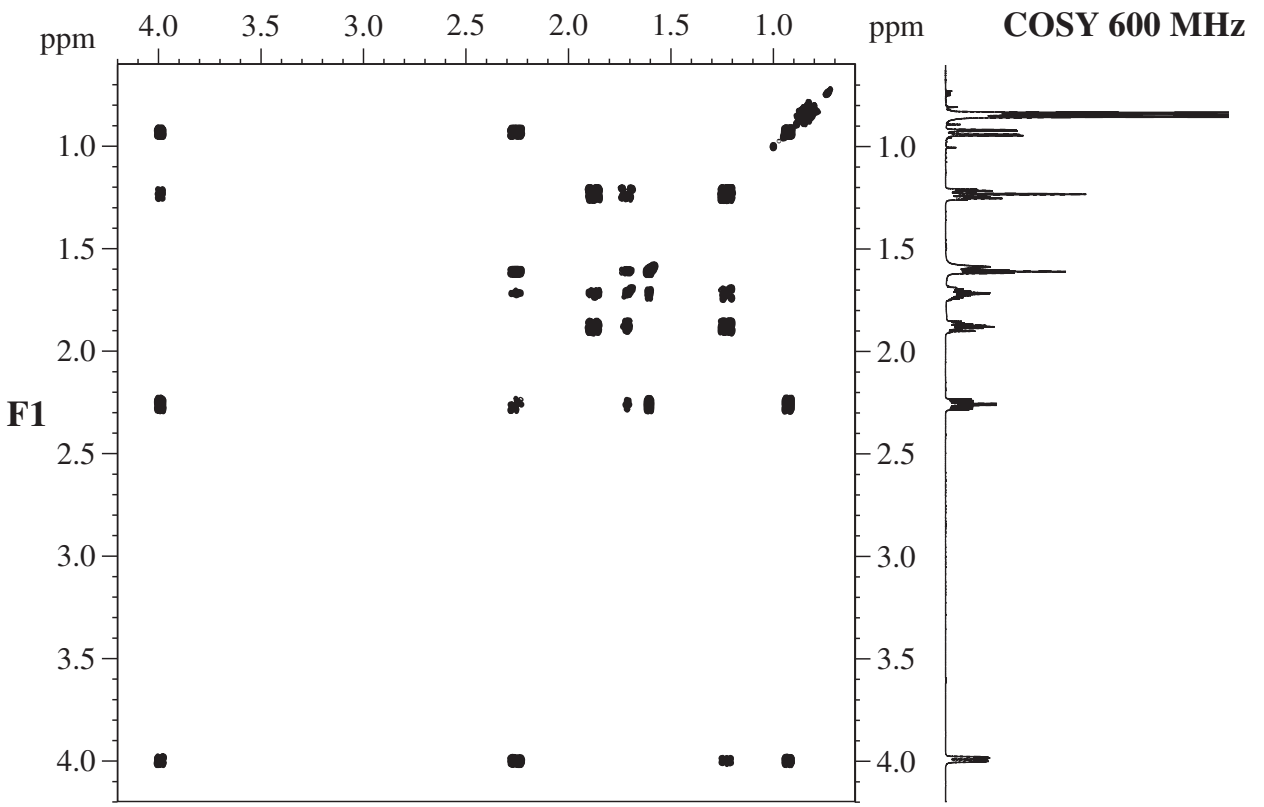
COSY 600 MHz
ppm
4.0
3.5
3.0
2.5
2.0
1.5
1.0
F1
F2

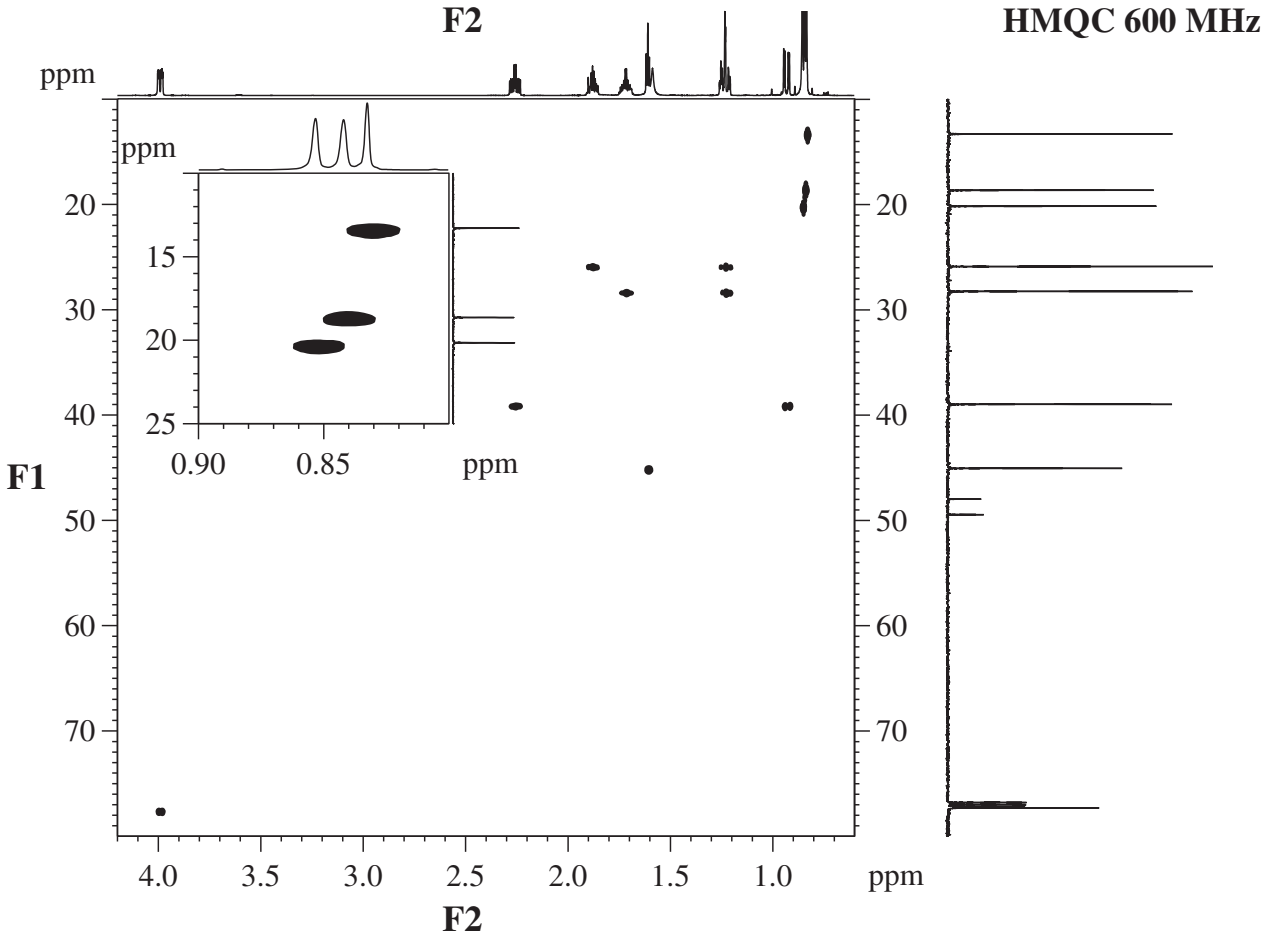
HMQC 600 MHz
ppm
20
30
40
50
60
70
15
25
0.90
0.85
F1
F2

MASS

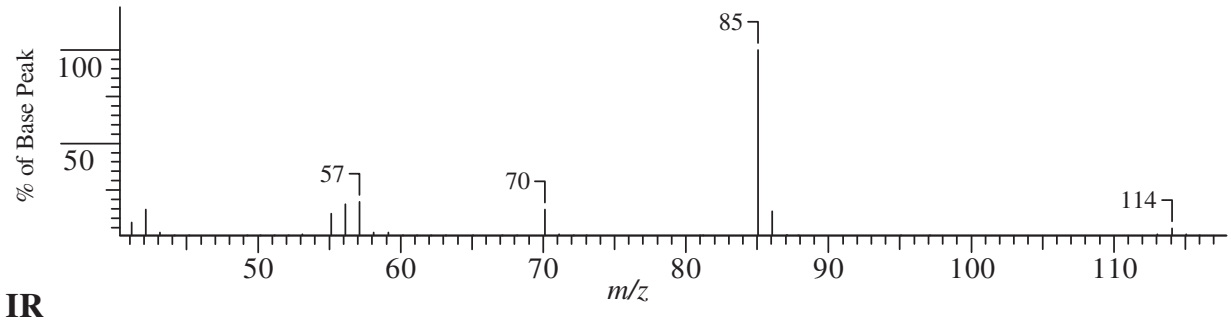

IR

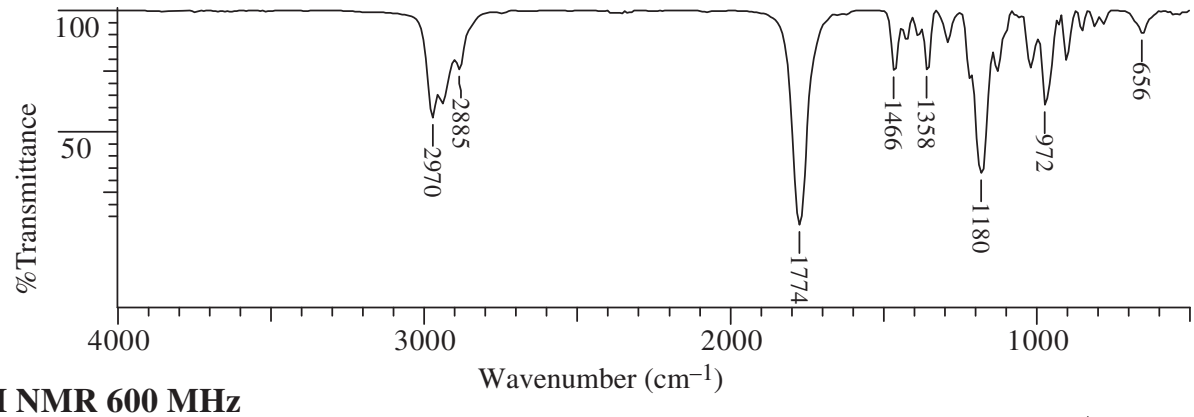

^{1}H NMR 600 MHz

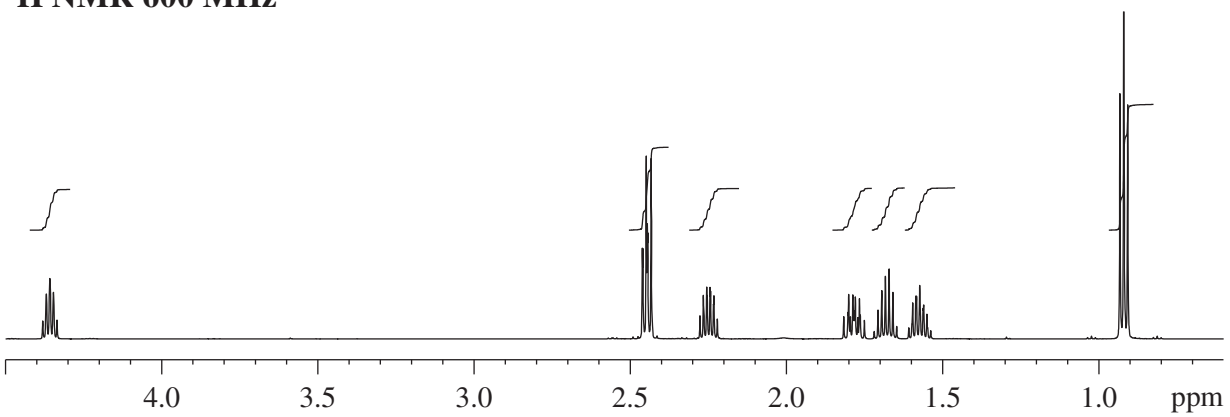

^{13}C/DEPT NMR 150.9 MHz

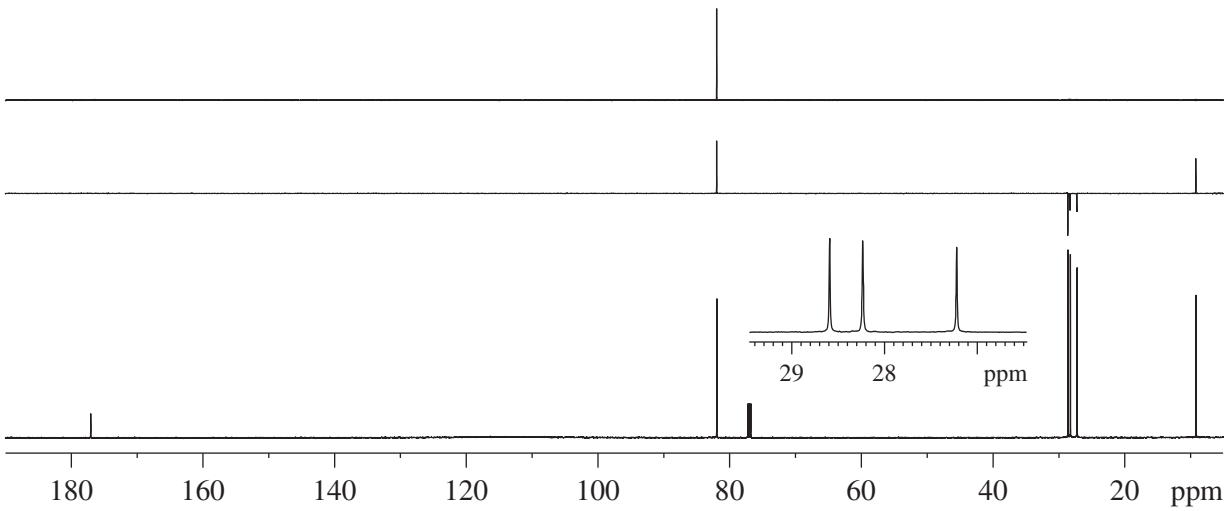

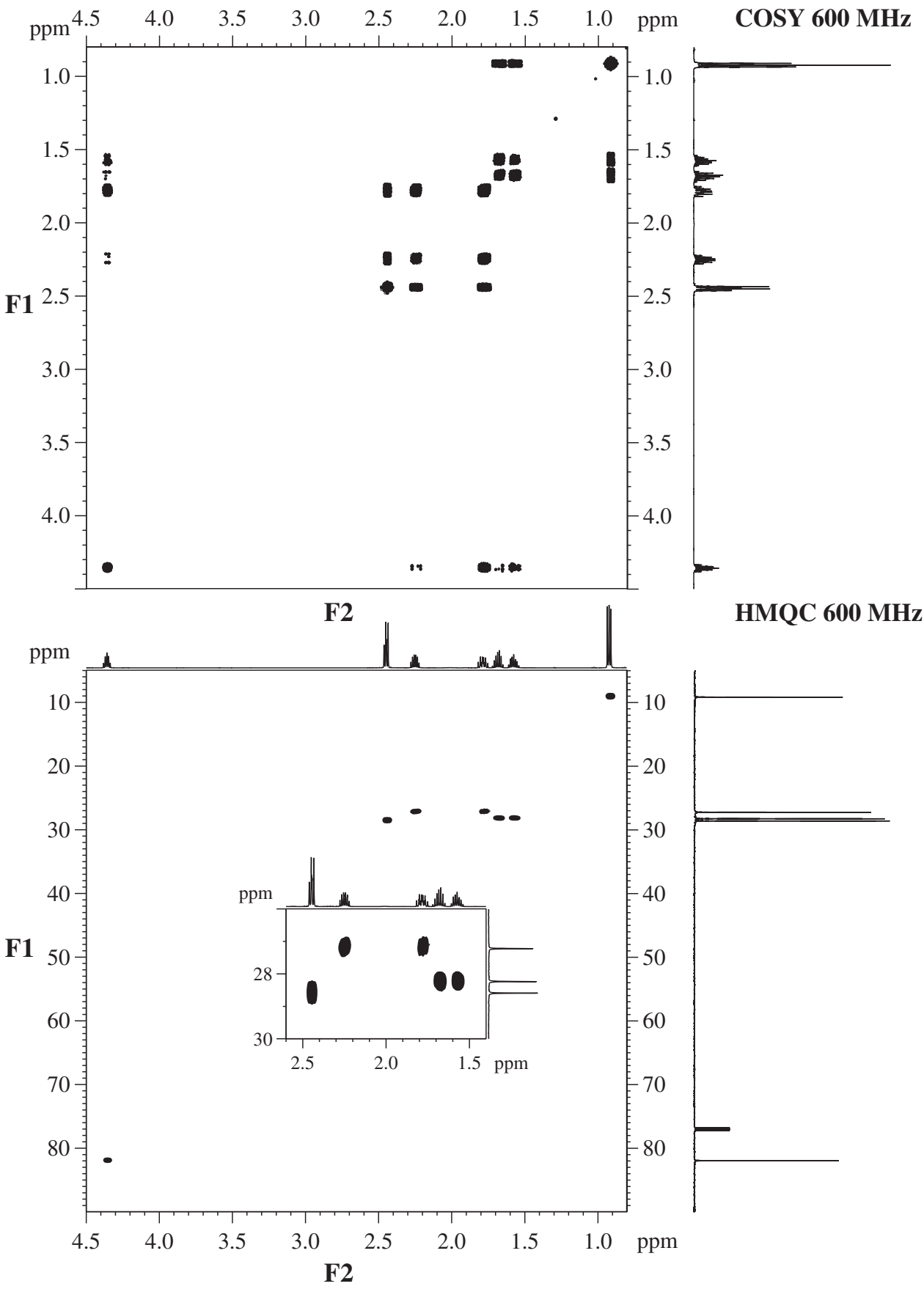
COSY 600 MHz
ppm
4.5
4.0
3.5
3.0
2.5
2.0
1.5
1.0
F1
F2
HMQC 600 MHz
10
20
30
40
50
60
70
80
28
2.5
2.0
1.5

MASS

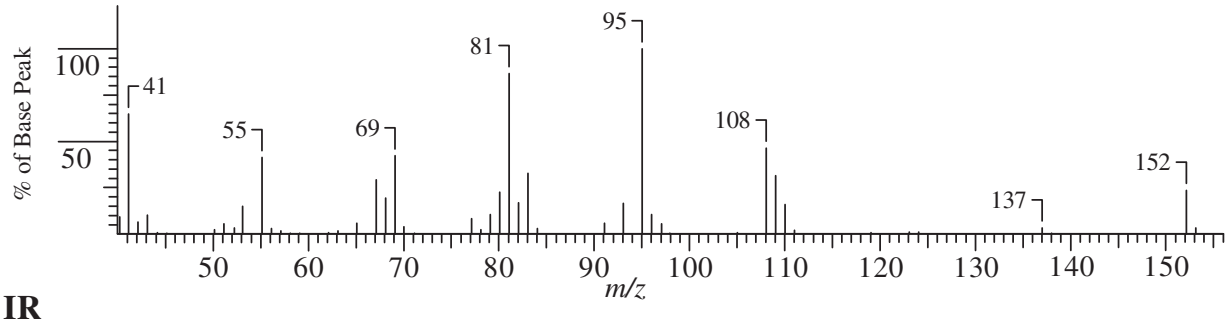

IR

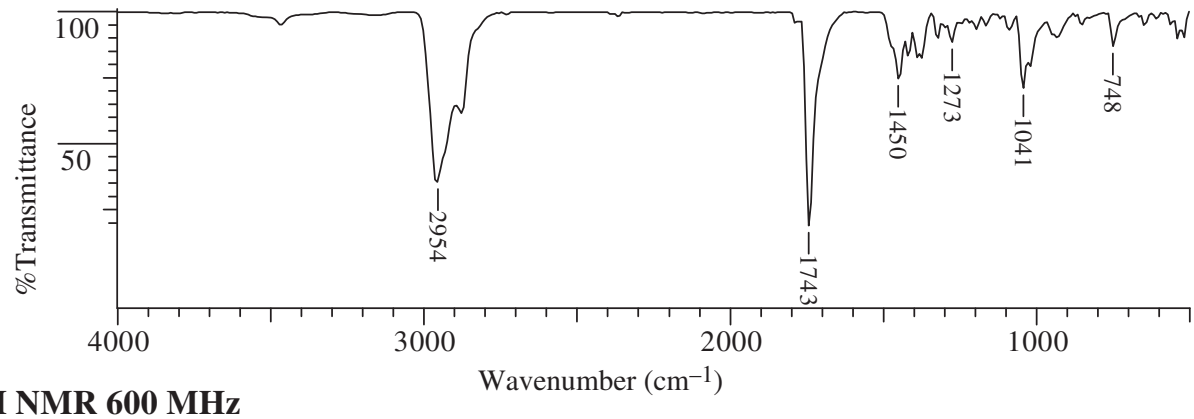

^{1}H NMR 600 MHz

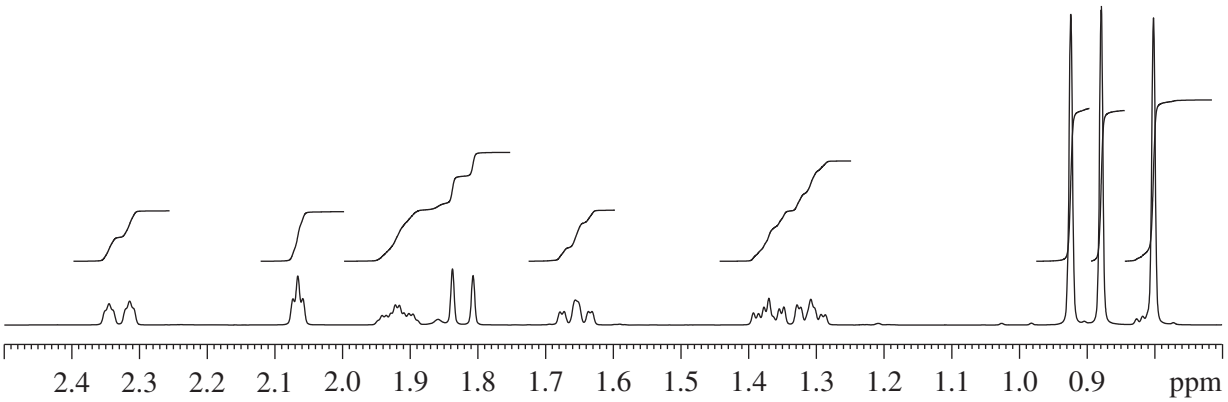

^{13}C/DEPT NMR 150.9 MHz

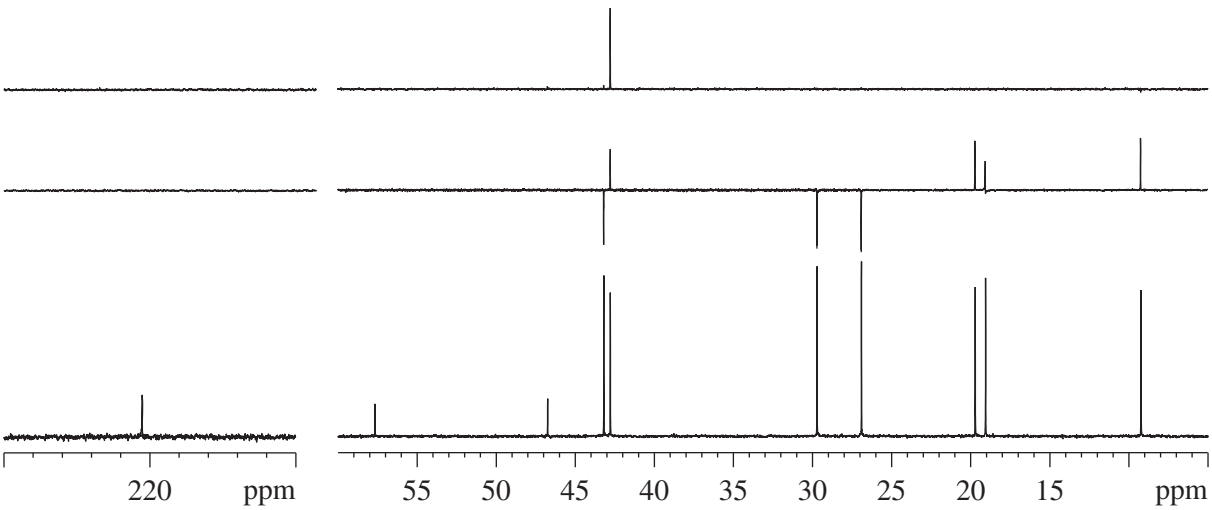

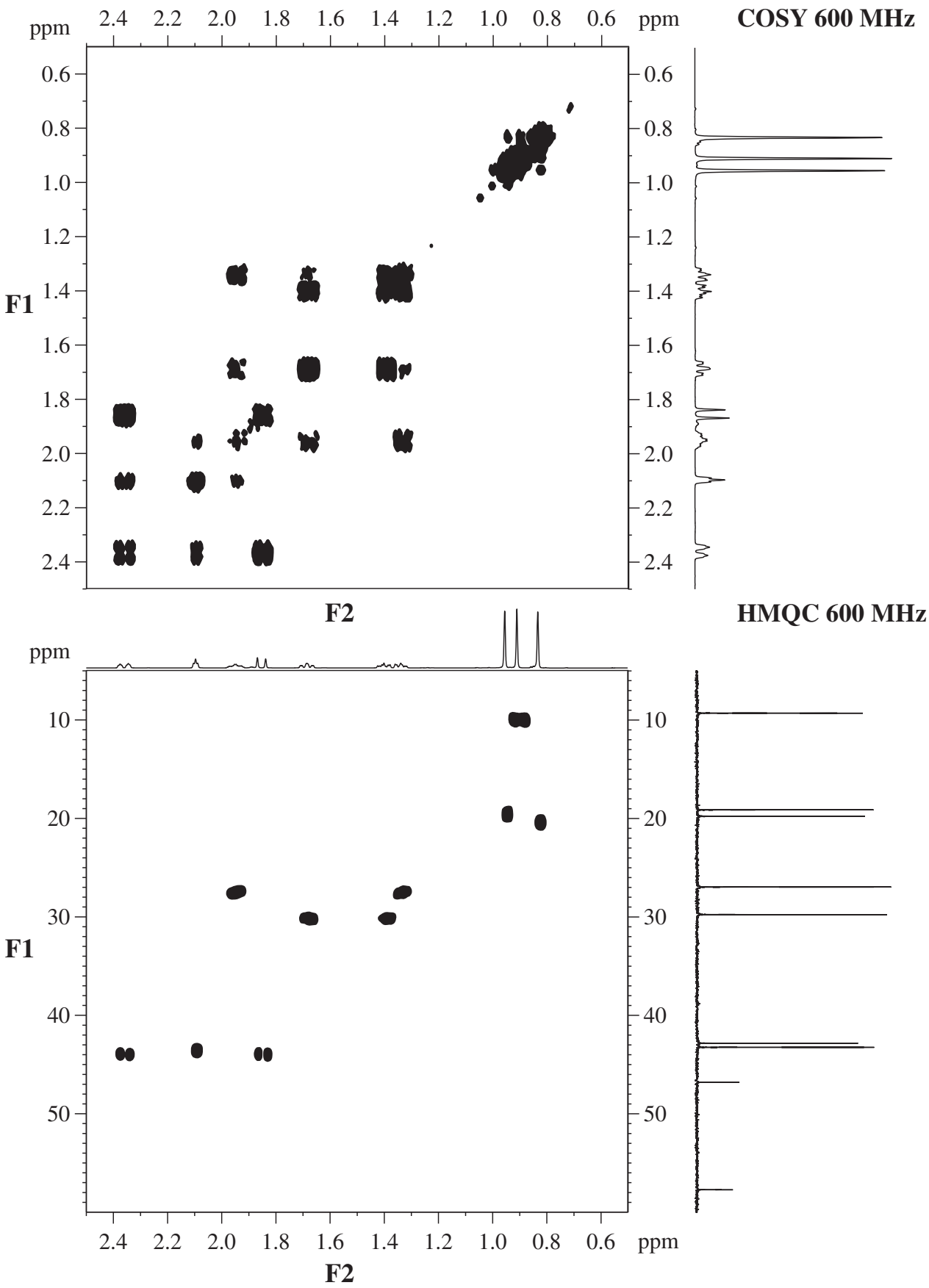
COSY 600 MHz
ppm
2.4 2.2 2.0 1.8 1.6 1.4 1.2 1.0 0.8 0.6
F1
F2
HMQC 600 MHz
10 20 30 40 50

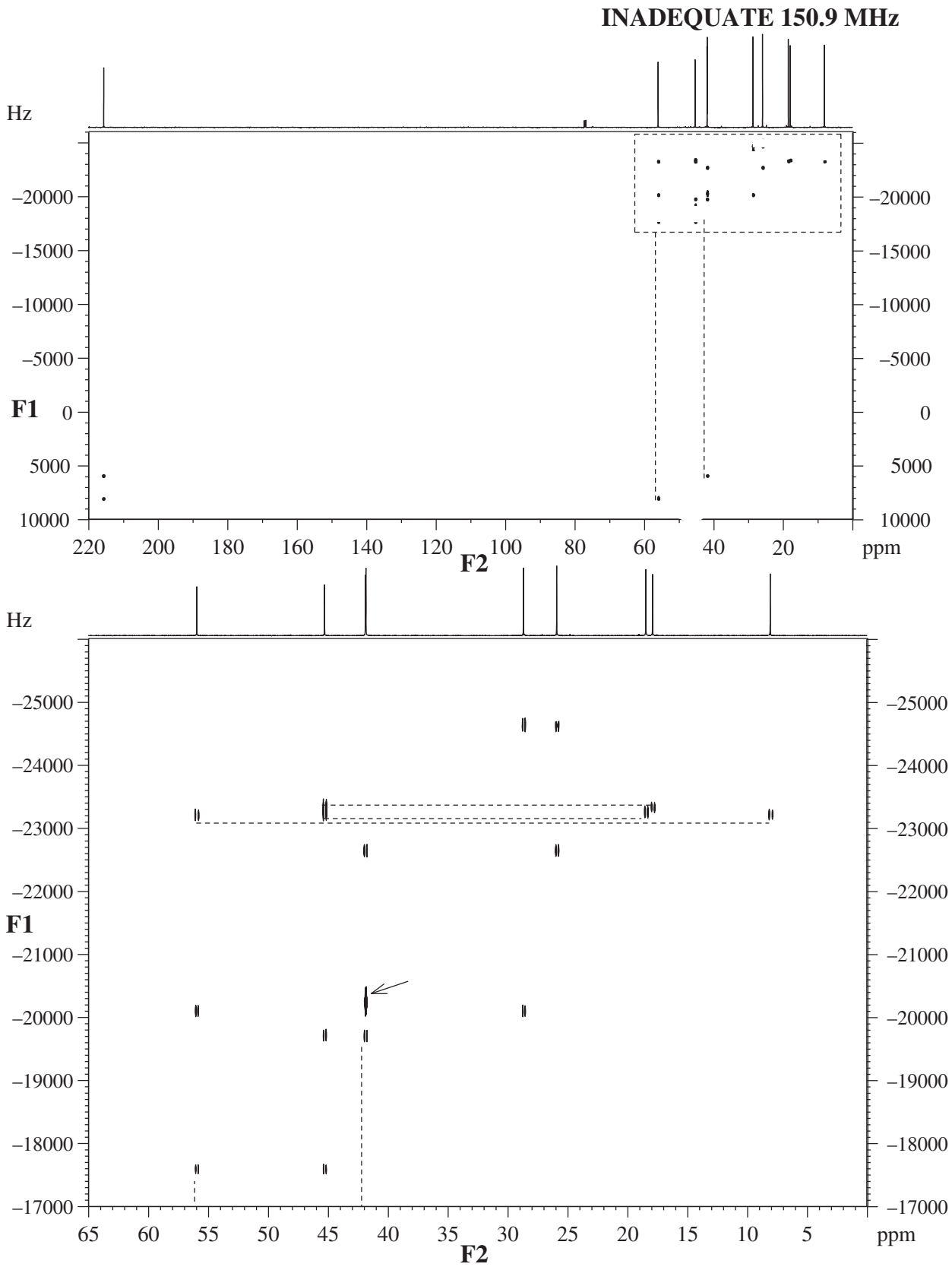
INADEQUATE 150.9 MHz
Hz
–20000
–15000
–10000
–5000
F1
0
5000
10000
220
200
180
160
140
120
100
80
60
40
20
ppm
F2
Hz
–25000
–24000
–23000
–22000
F1
–21000
–20000
–19000
–18000
–17000
65
60
55
50
45
40
35
30
25
20
15
10
5
ppm
F2

MASS

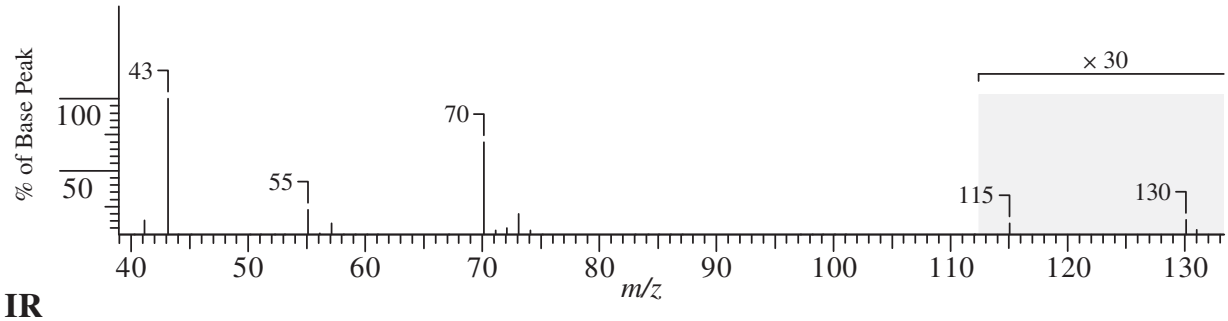

IR

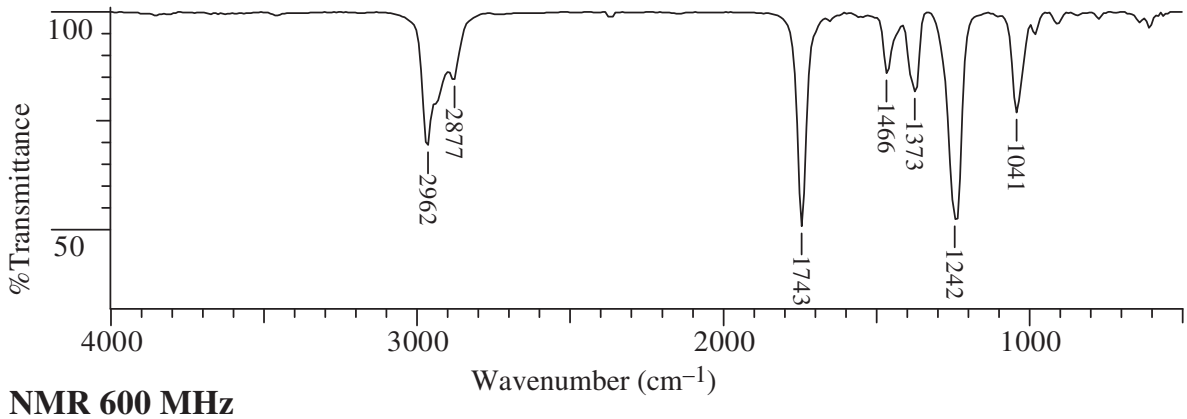

^{1}H NMR 600 MHz

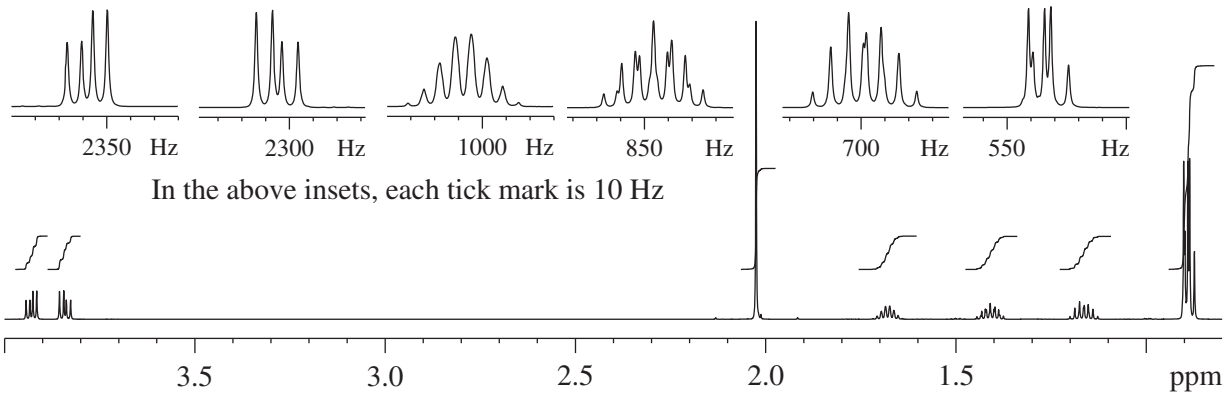

^{13}C/DEPT NMR 150.9 MHz

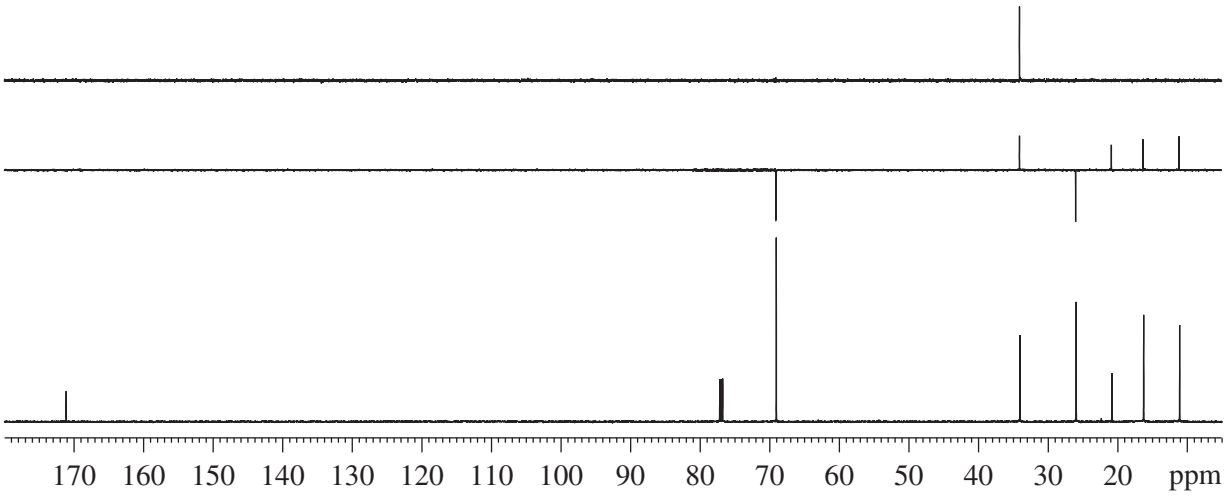

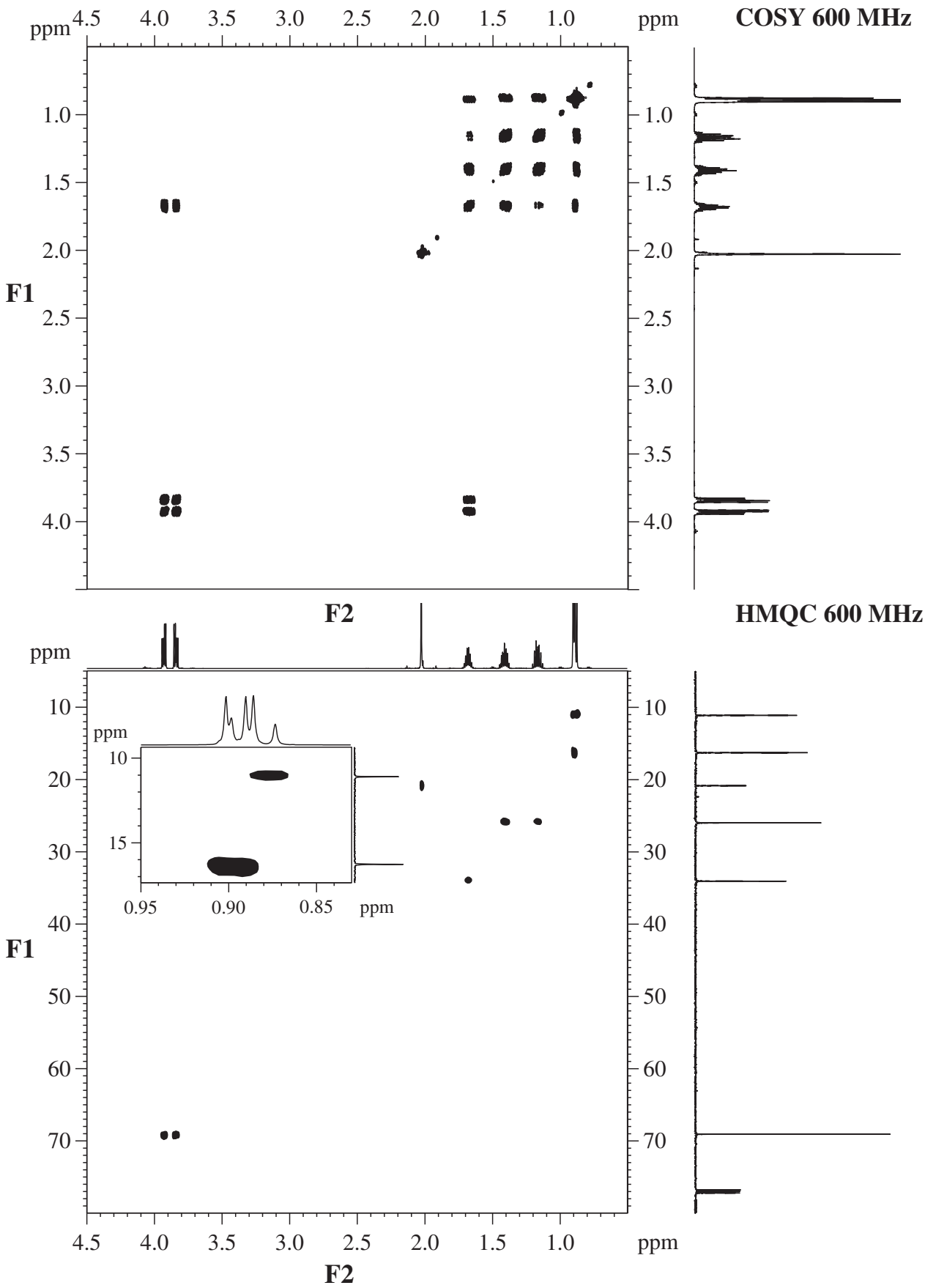
COSY 600 MHz
ppm
4.5 4.0 3.5 3.0 2.5 2.0 1.5 1.0
F1
F2
HMQC 600 MHz
10 20 30 40 50 60 70
0.95 0.90 0.85 ppm
15

MASS

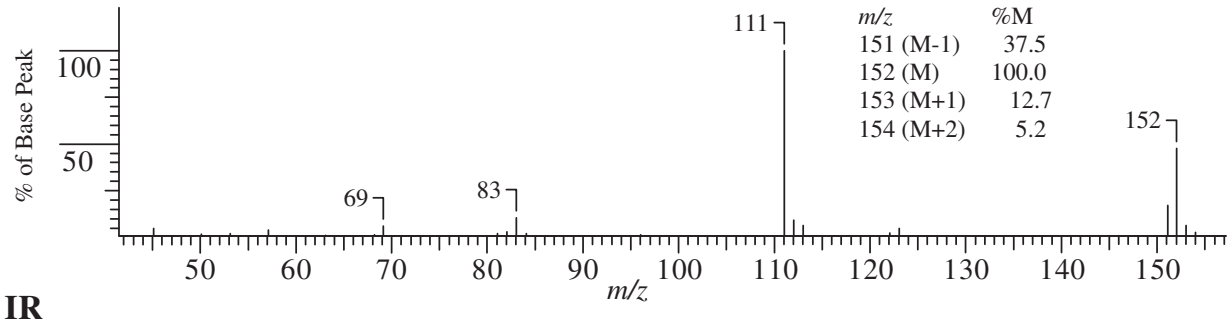

IR

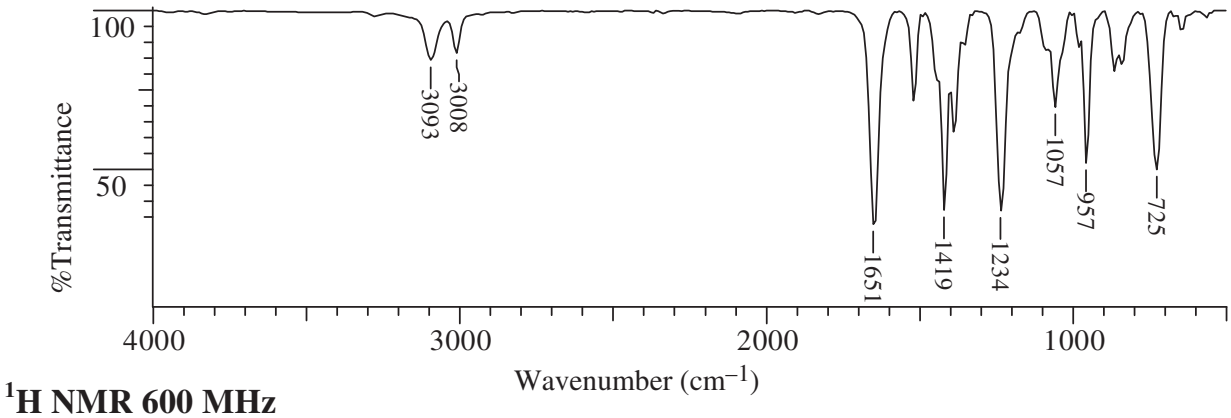

^{1}H NMR 600 MHz

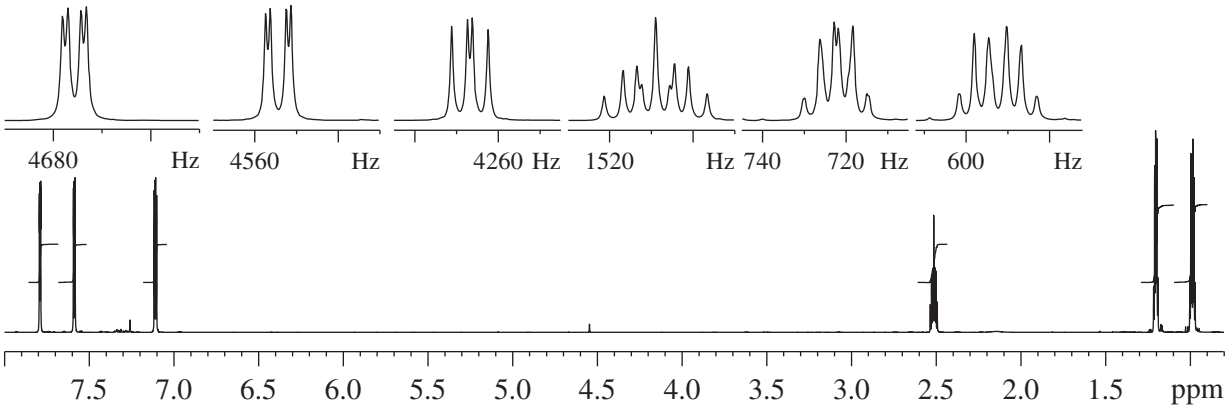

^{13}C/DEPT NMR 150.9 MHz

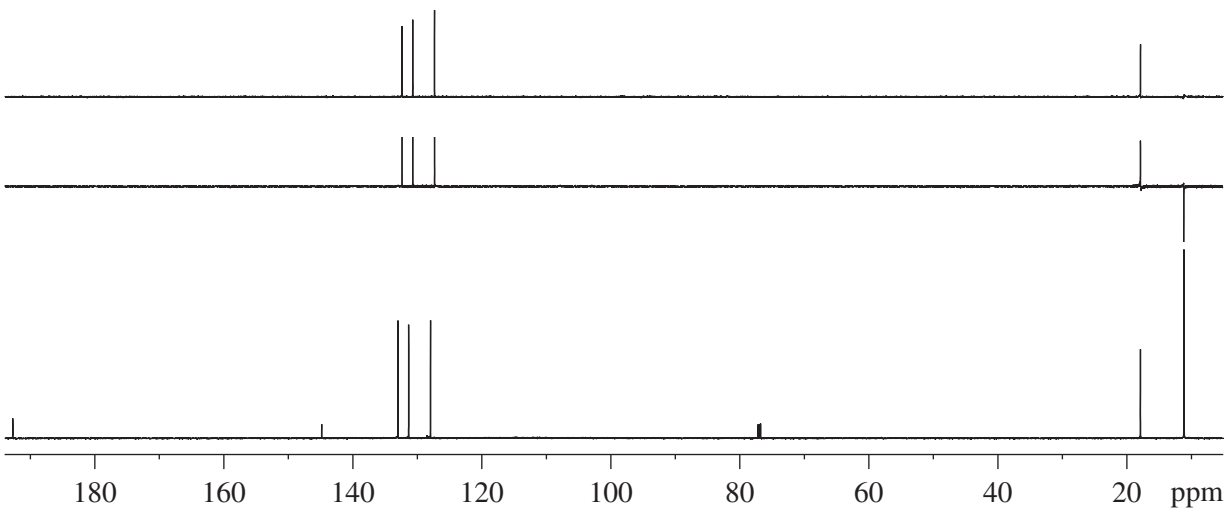

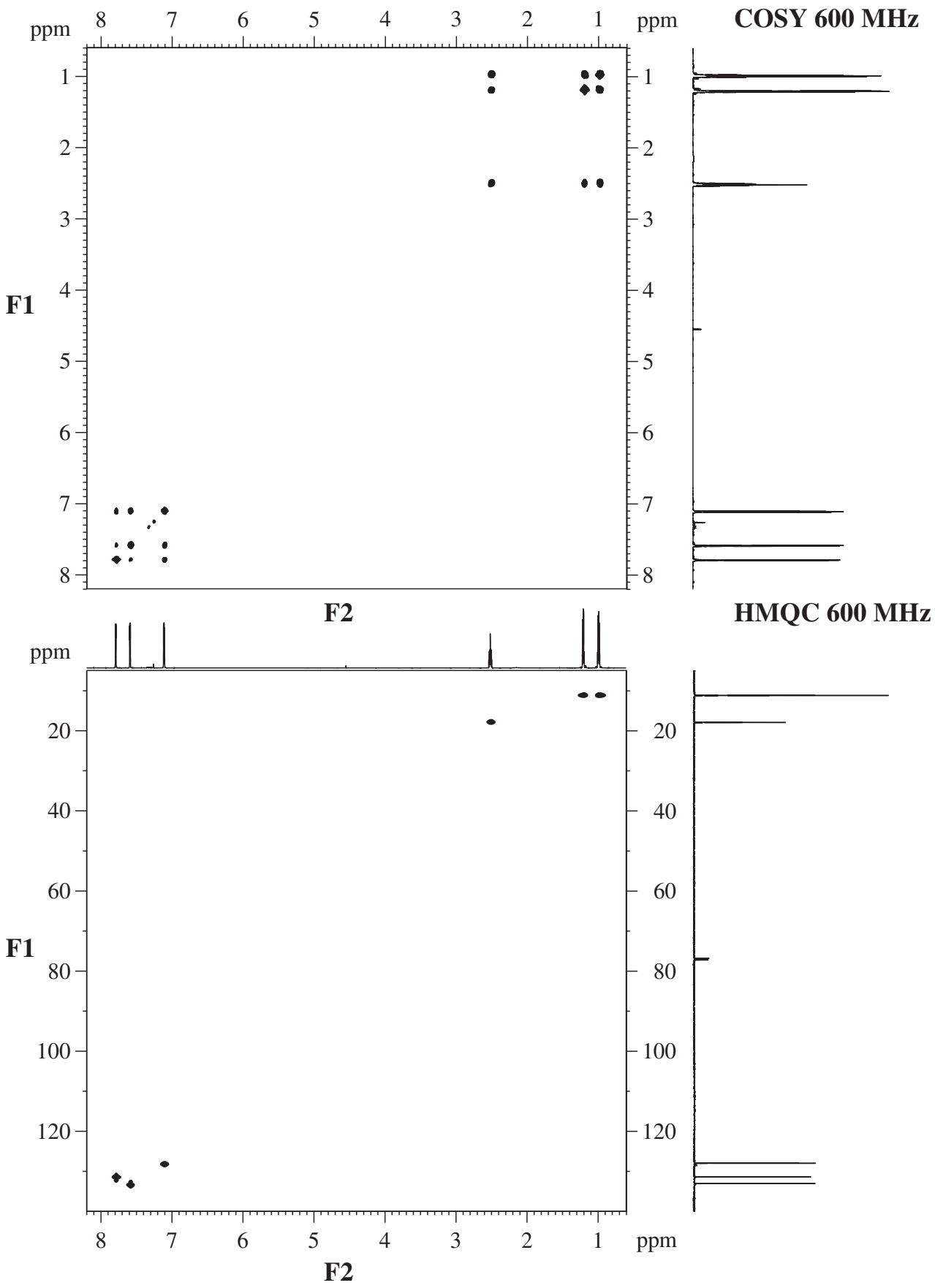
COSY 600 MHz
ppm
8 7 6 5 4 3 2 1 ppm
F1
F2
HMQC 600 MHz
ppm
20 40 60 80 100 120
F1
F2
8 7 6 5 4 3 2 1 ppm

MASS

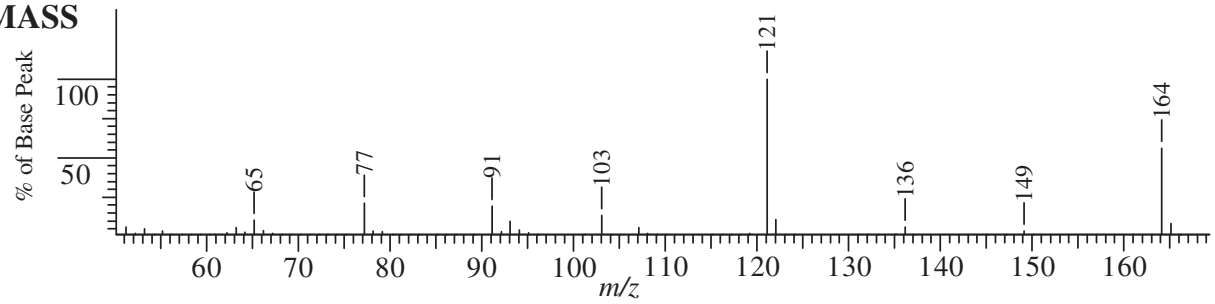

IR

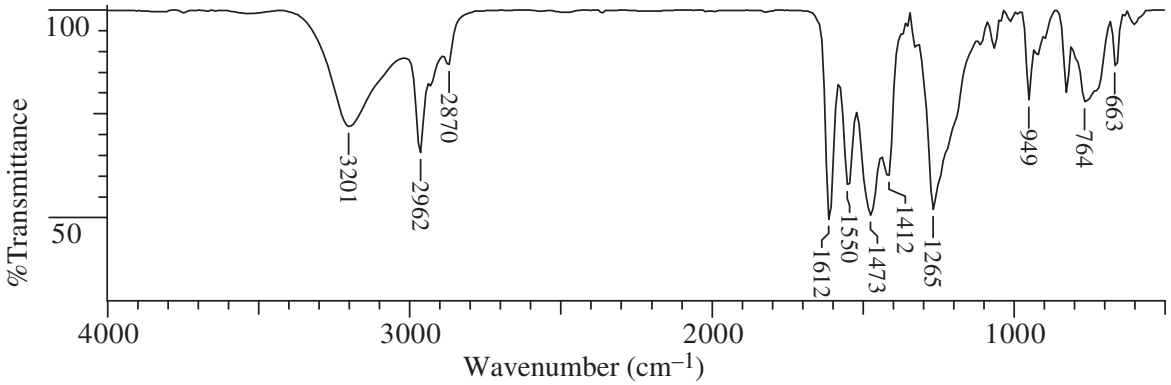

^{1}H NMR 600 MHz

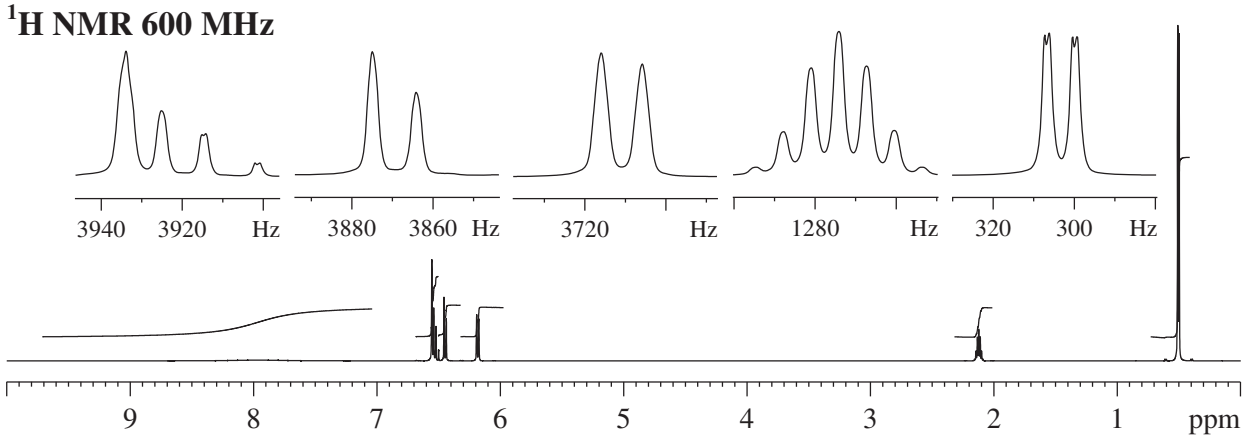

^{13}C/DEPT NMR 150.9 MHz

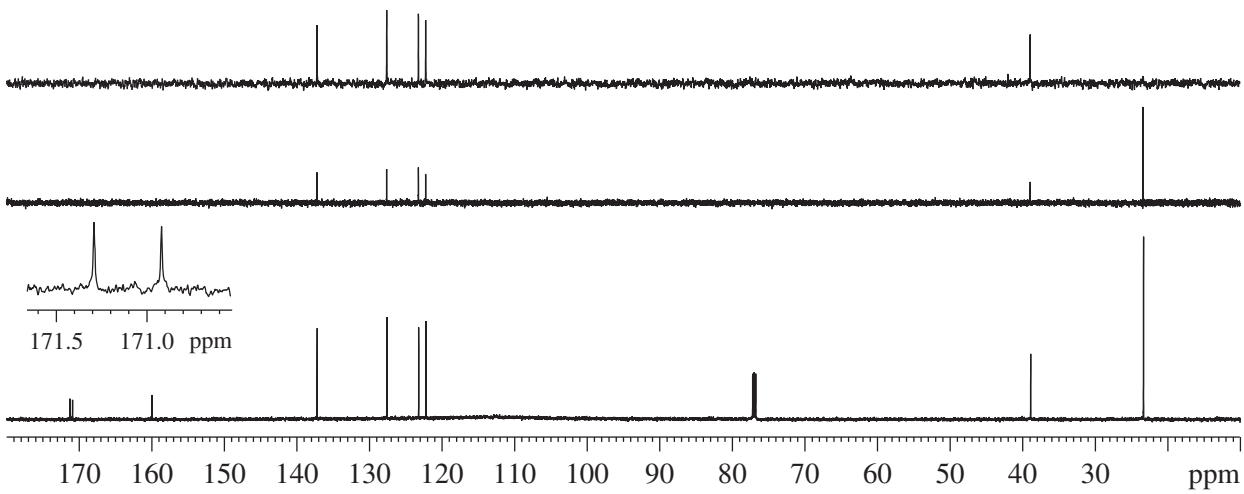

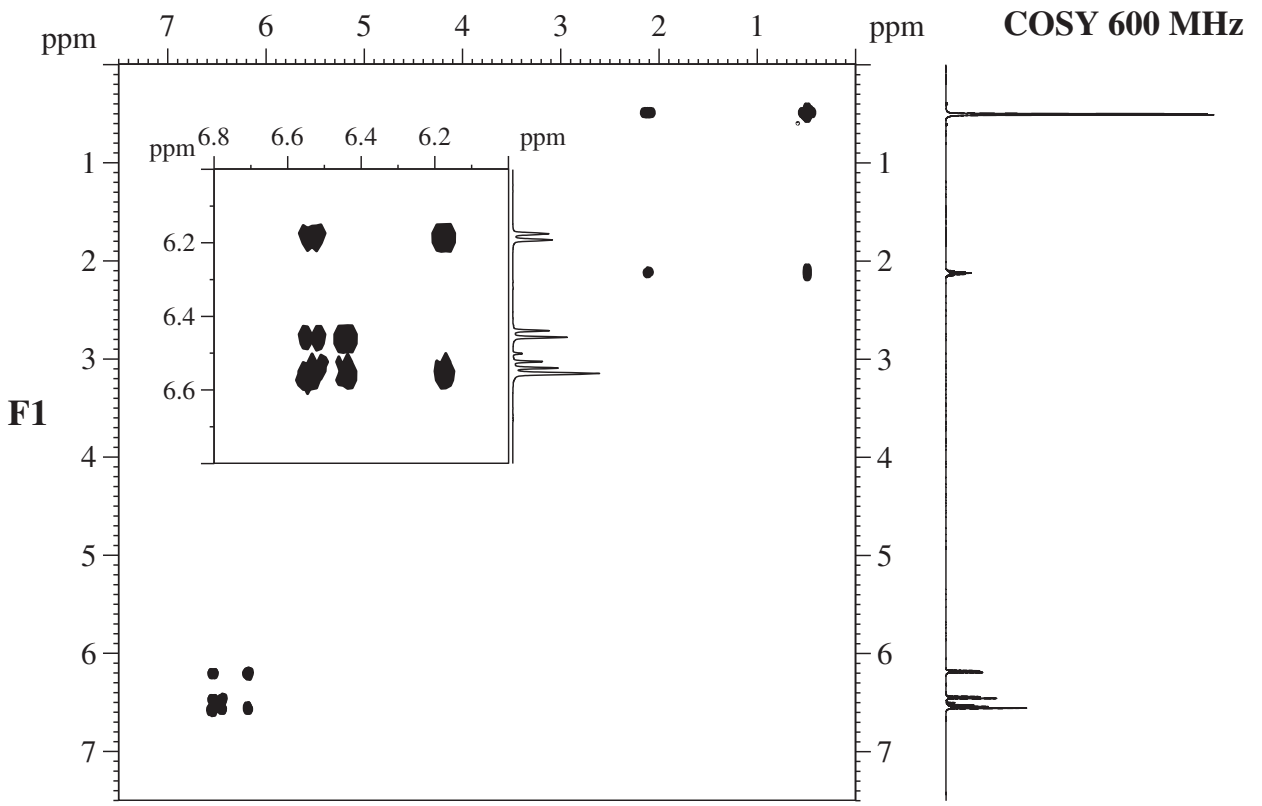
COSY 600 MHz
ppm
7 6 5 4 3 2 1
ppm
6.8 6.6 6.4 6.2
ppm
6.2
6.4
6.6
F1
1 2 3 4 5 6 7
F2

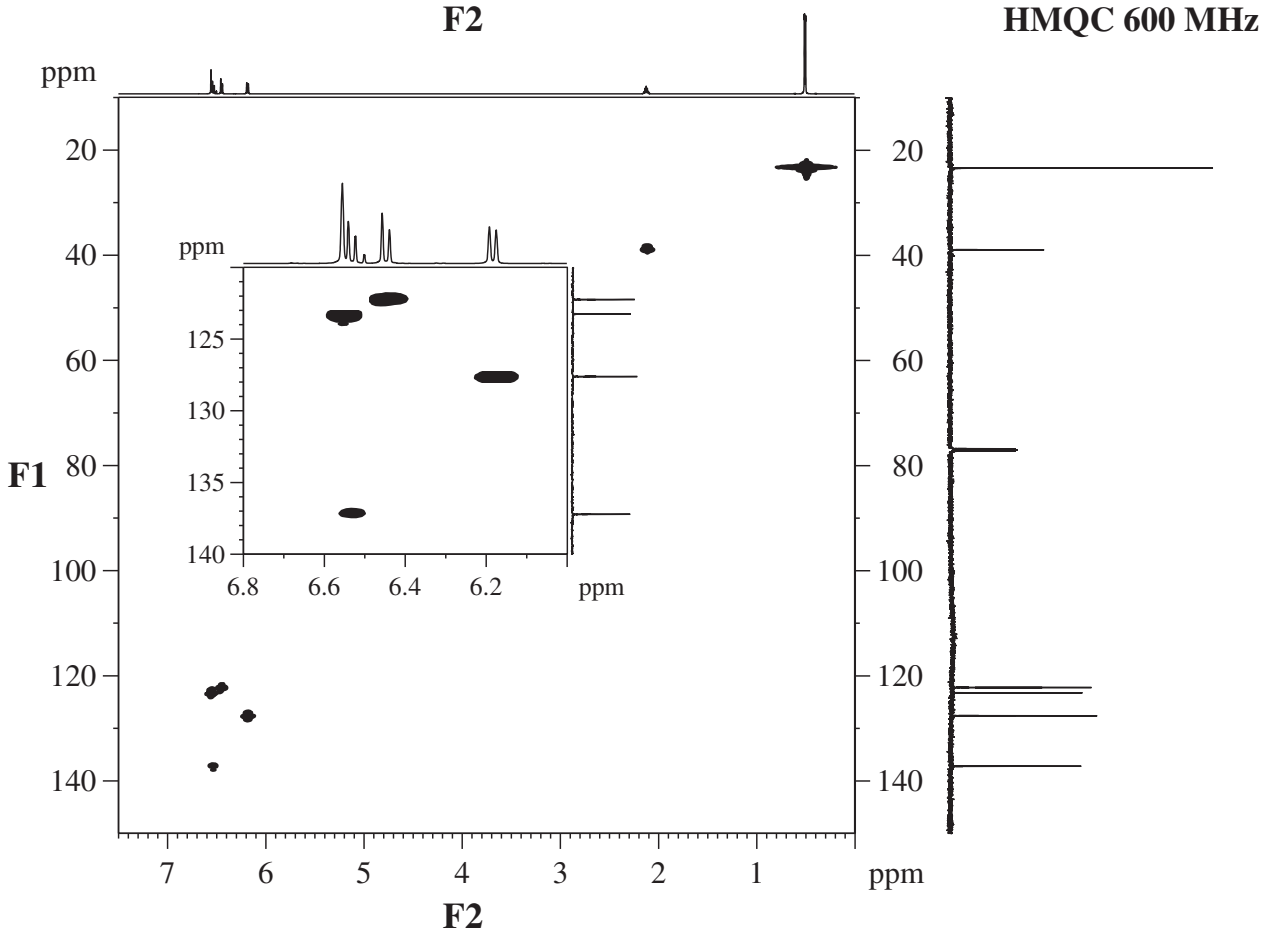
HMQC 600 MHz
ppm
20 40 60 80 100 120 140
ppm
125 130 135 140
6.8 6.6 6.4 6.2
ppm
F1
7 6 5 4 3 2 1
ppm
F2

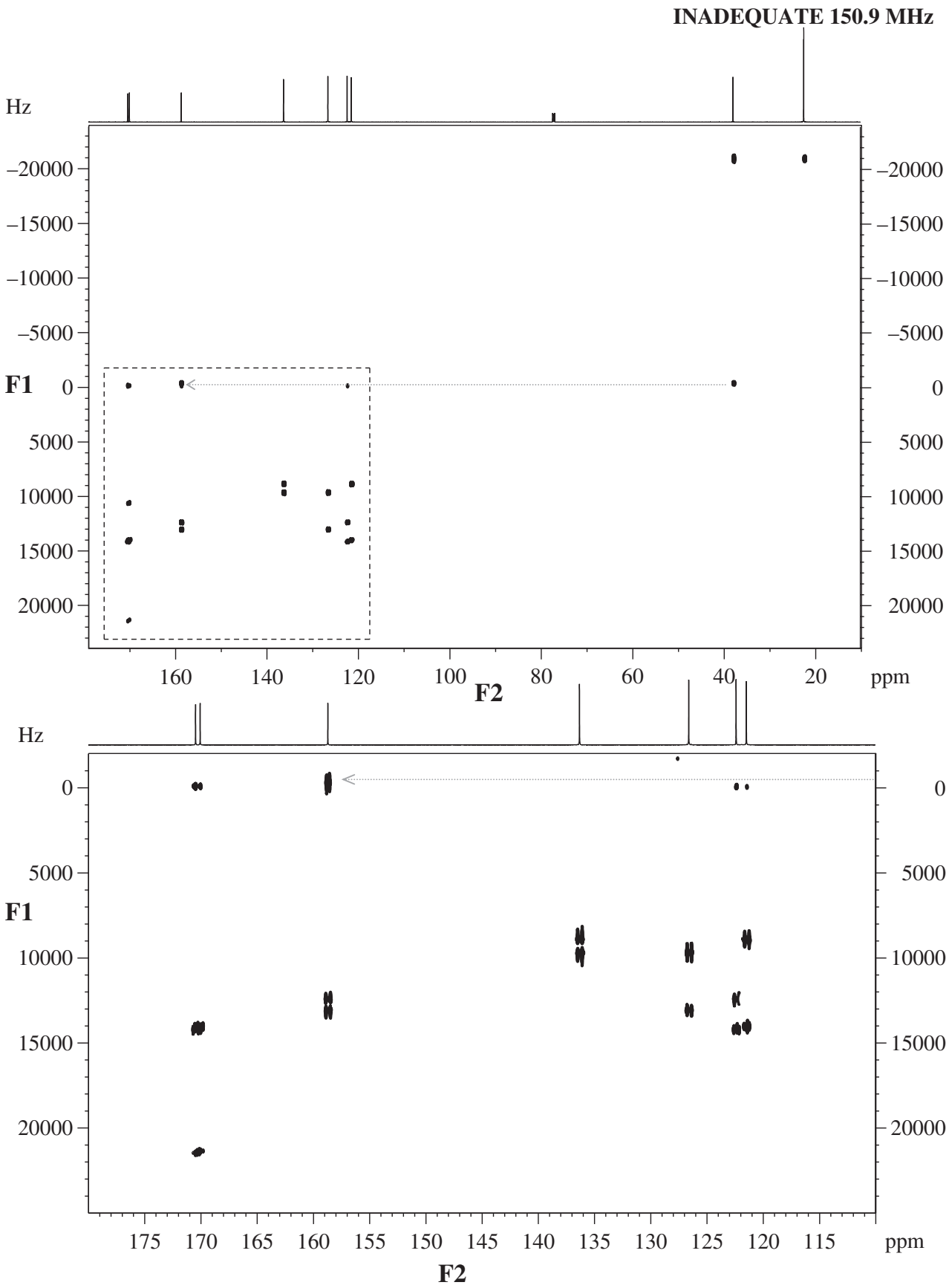
INADEQUATE 150.9 MHz
Hz
–20000
–15000
–10000
–5000
F1
0
5000
10000
15000
20000
160
140
120
100
80
60
40
20
ppm
F2
Hz
0
5000
F1
10000
15000
20000
175
170
165
160
155
150
145
140
135
130
125
120
115
ppm
F2

MASS

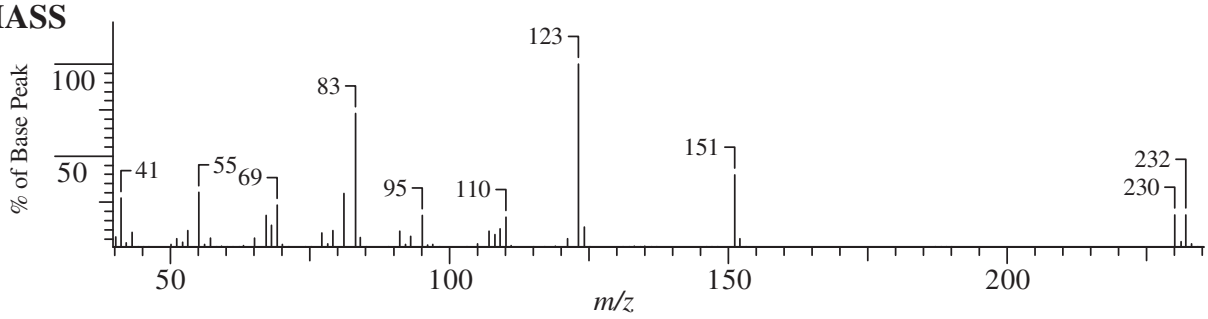

IR

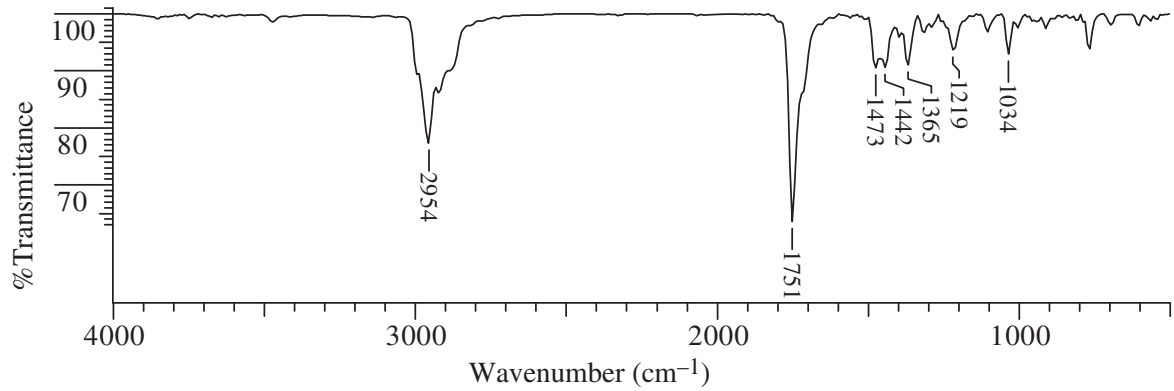

^{1}H NMR 600 MHz

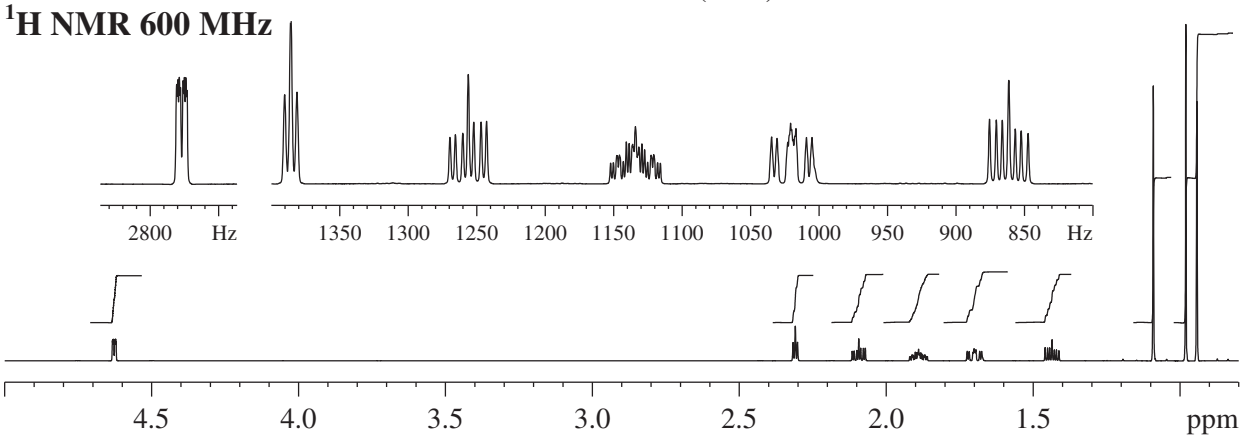

^{13}C/DEPT NMR 150.9 MHz

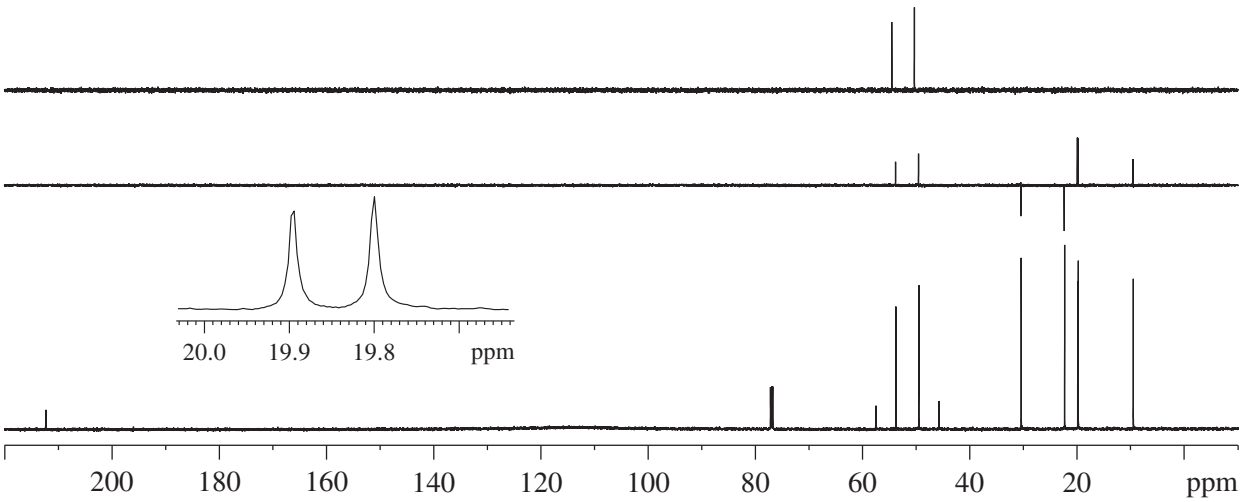

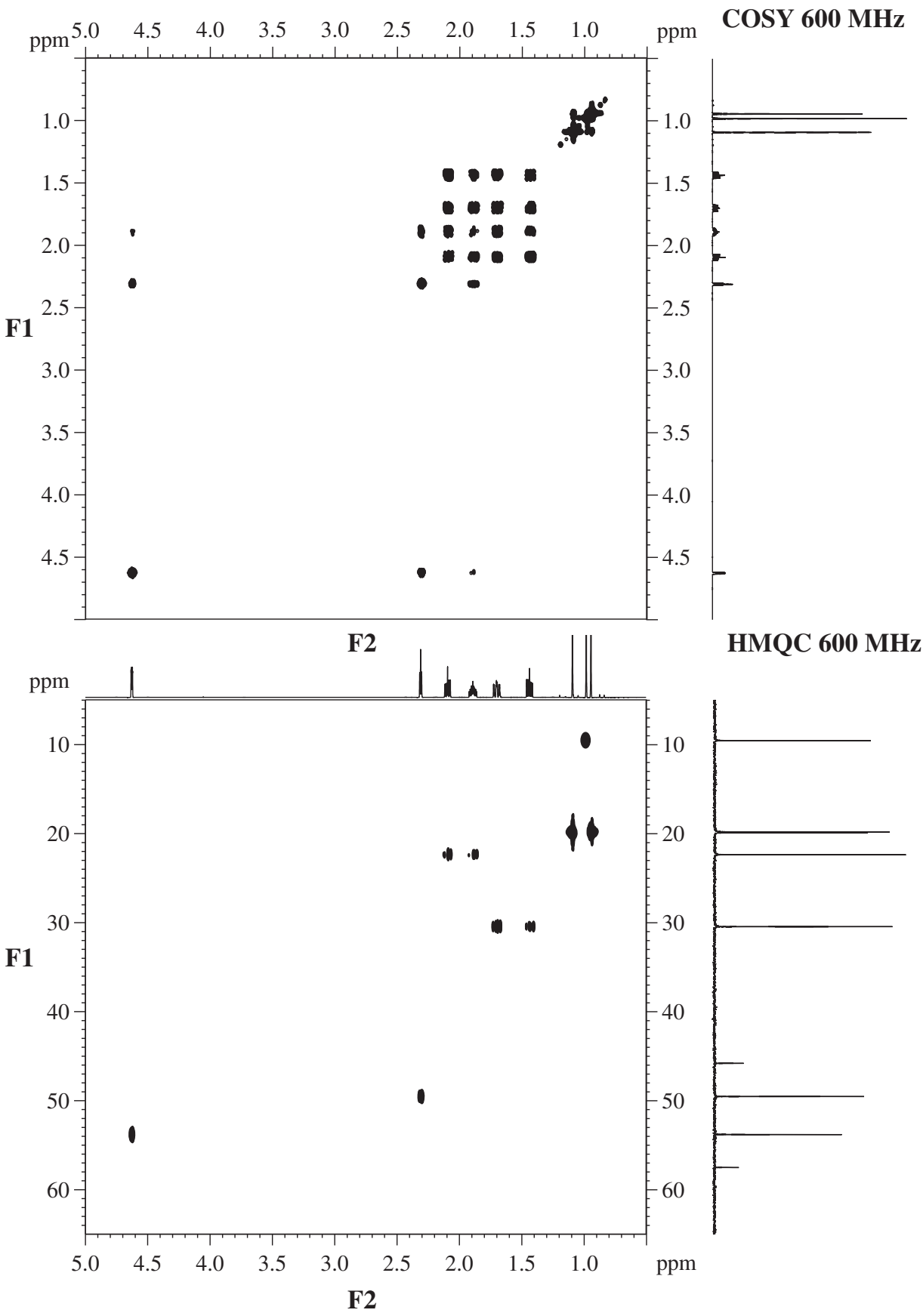
COSY 600 MHz
ppm
5.0 4.5 4.0 3.5 3.0 2.5 2.0 1.5 1.0
F1
F2
HMQC 600 MHz
10 20 30 40 50 60
F1
F2

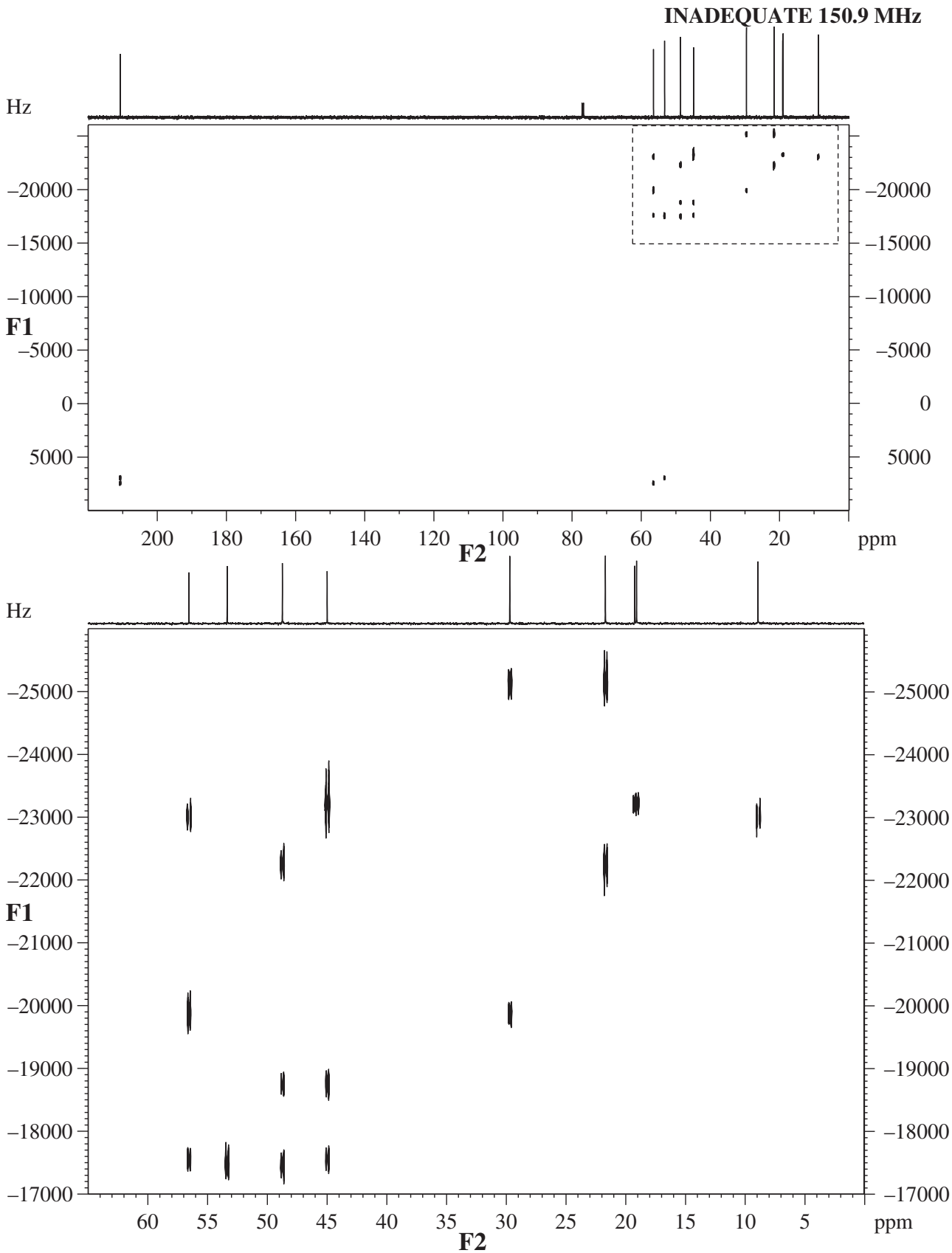
INADEQUATE 150.9 MHz
Hz
–20000
–15000
–10000
F1
–5000
0
5000
200
180
160
140
120
100
80
60
40
20
ppm
F2
Hz
–25000
–24000
–23000
–22000
F1
–21000
–20000
–19000
–18000
–17000
60
55
50
45
40
35
30
25
20
15
10
5
ppm
F2

MASS

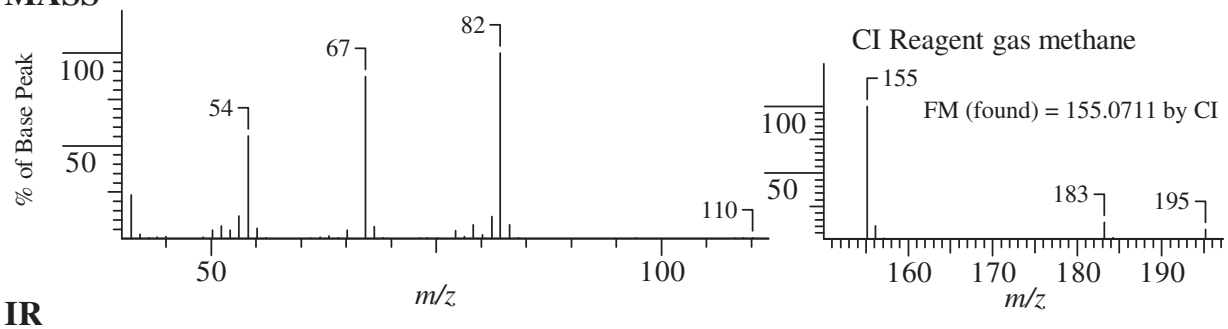

IR

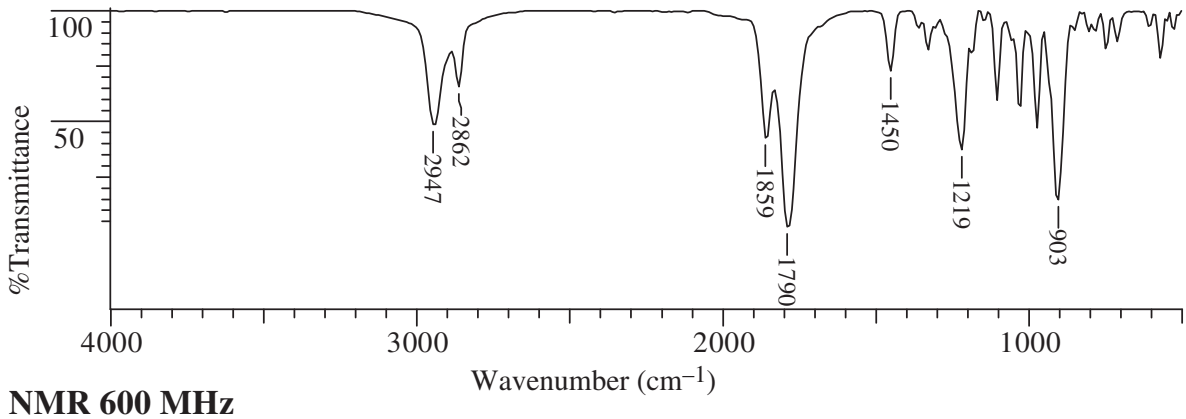

^{1}H NMR 600 MHz

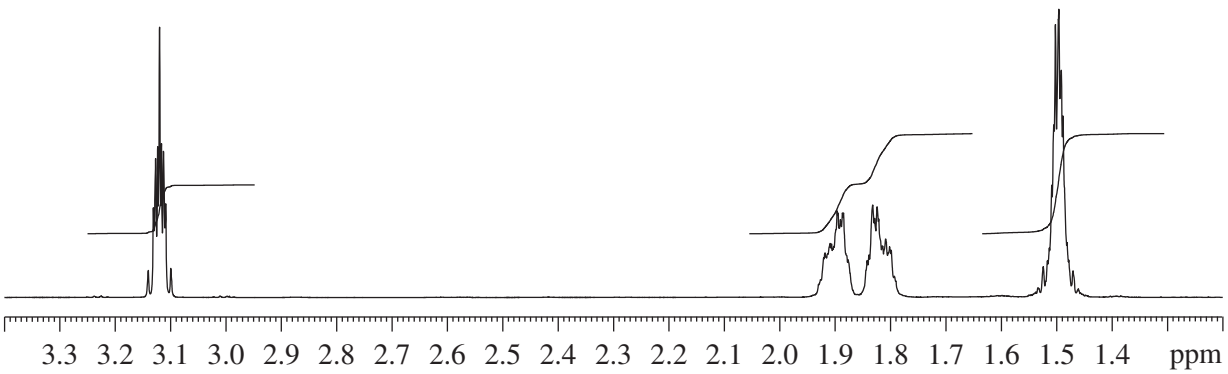

^{13}C/DEPT NMR 150.9 MHz

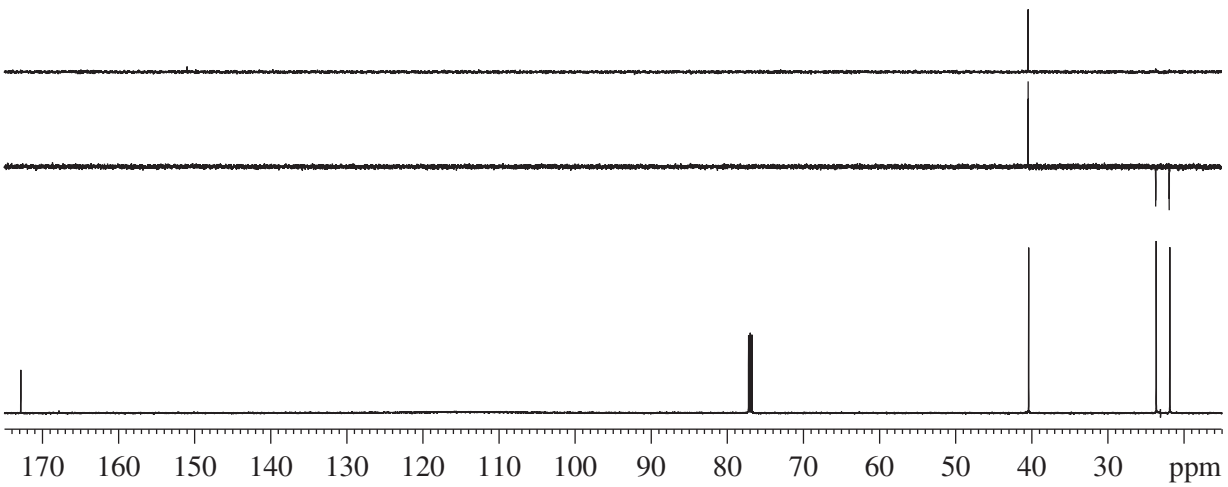

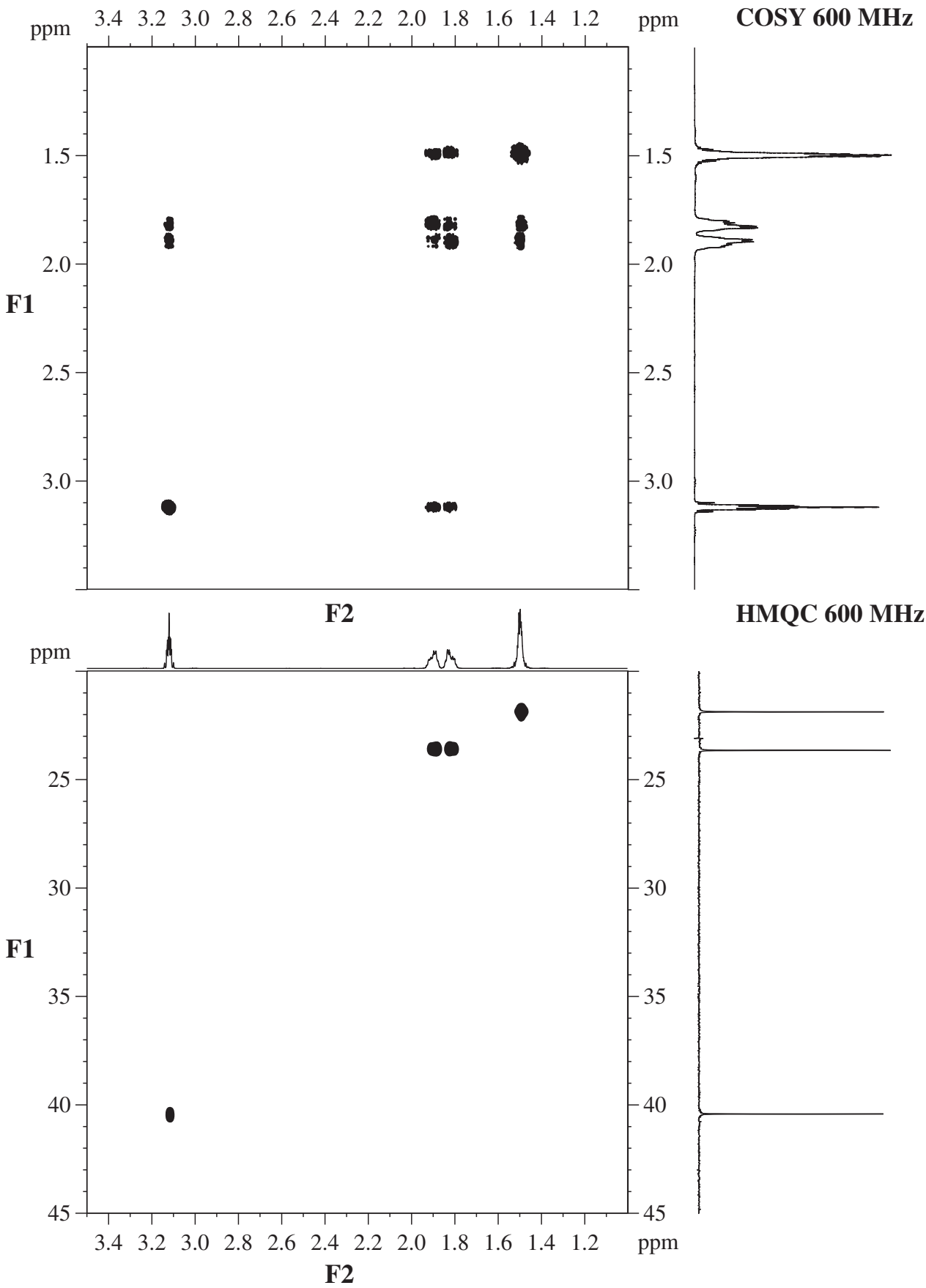
COSY 600 MHz
ppm
3.4 3.2 3.0 2.8 2.6 2.4 2.2 2.0 1.8 1.6 1.4 1.2
ppm
1.5
2.0
2.5
3.0
F1
F2
HMQC 600 MHz
ppm
25
30
35
40
45
F1
3.4 3.2 3.0 2.8 2.6 2.4 2.2 2.0 1.8 1.6 1.4 1.2
ppm
F2

MASS

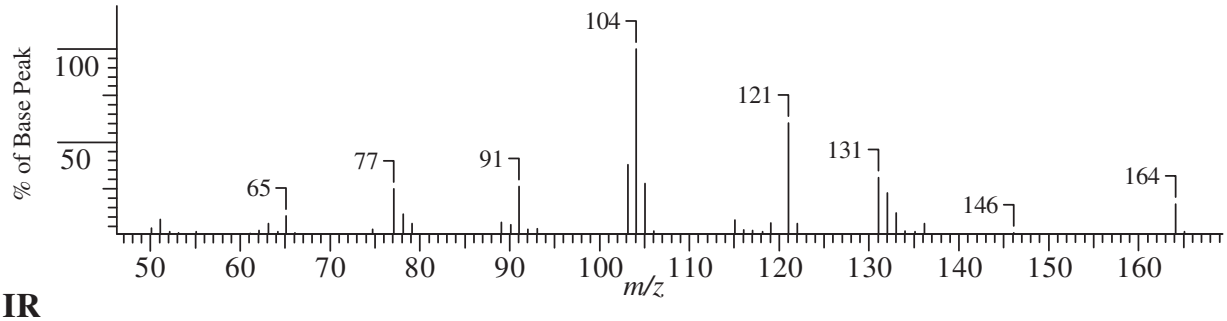

IR

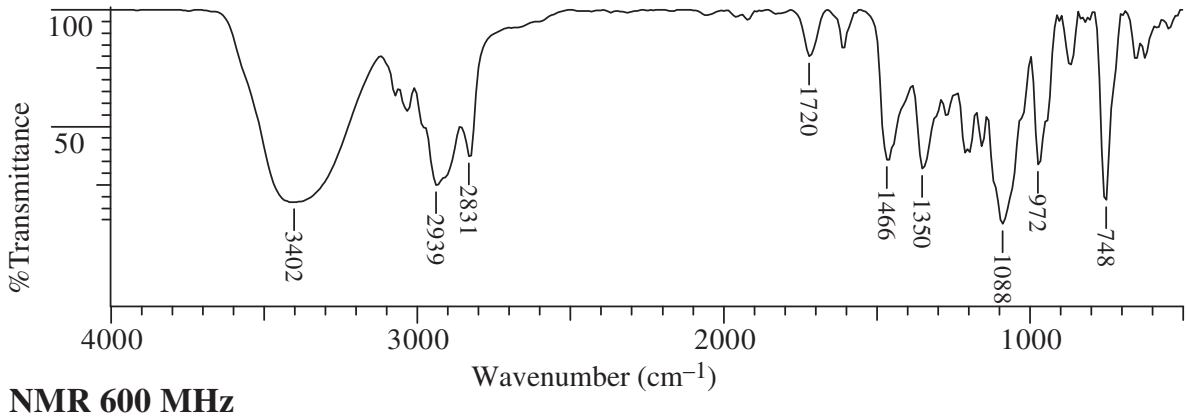

^{1}H NMR 600 MHz

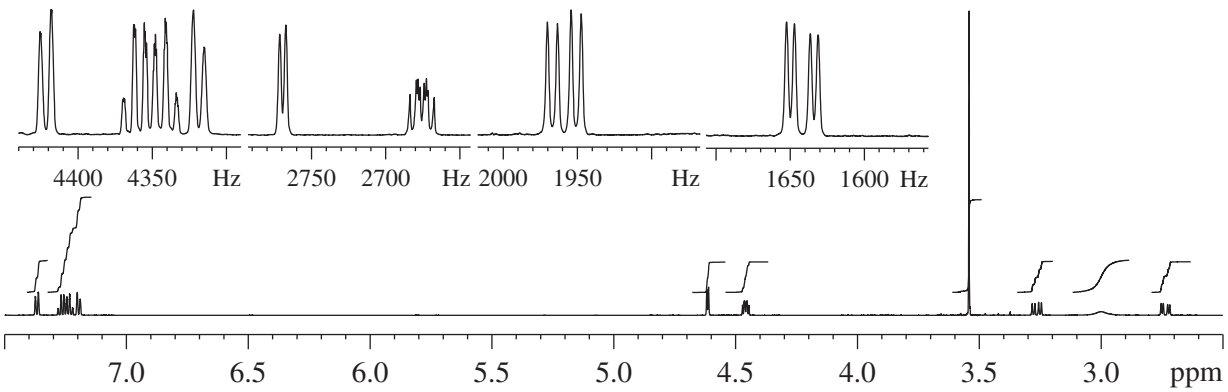

^{13}C/DEPT NMR 150.9 MHz

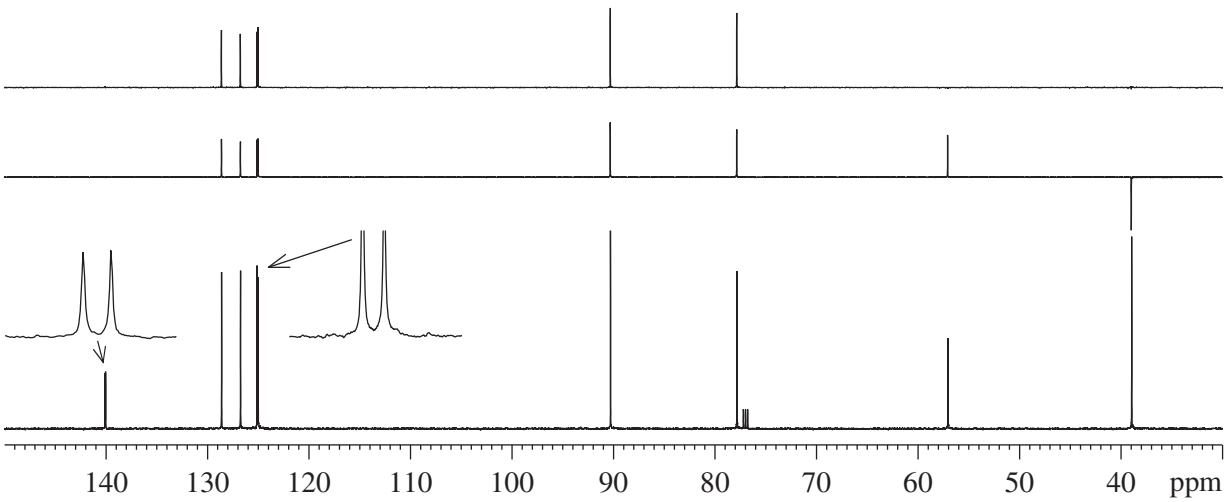

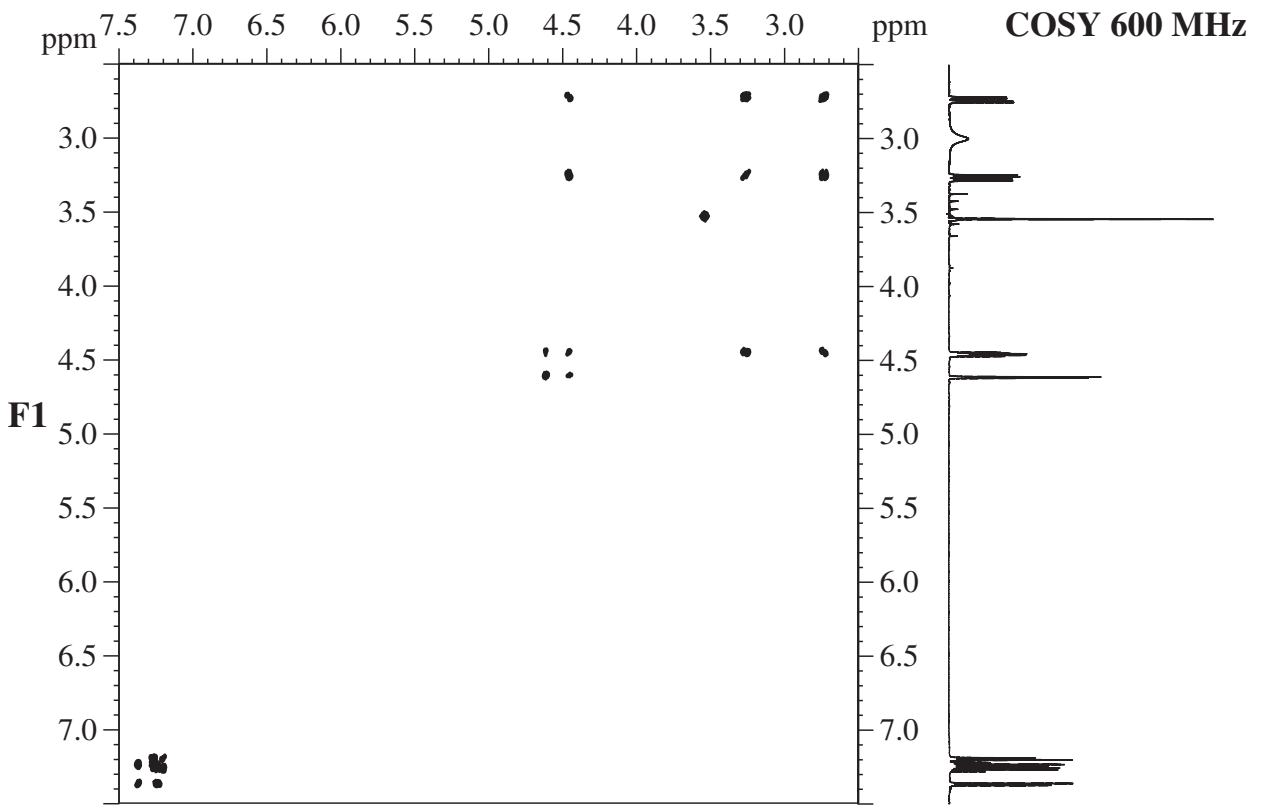
COSY 600 MHz
ppm
7.5 7.0 6.5 6.0 5.5 5.0 4.5 4.0 3.5 3.0
F1
F2

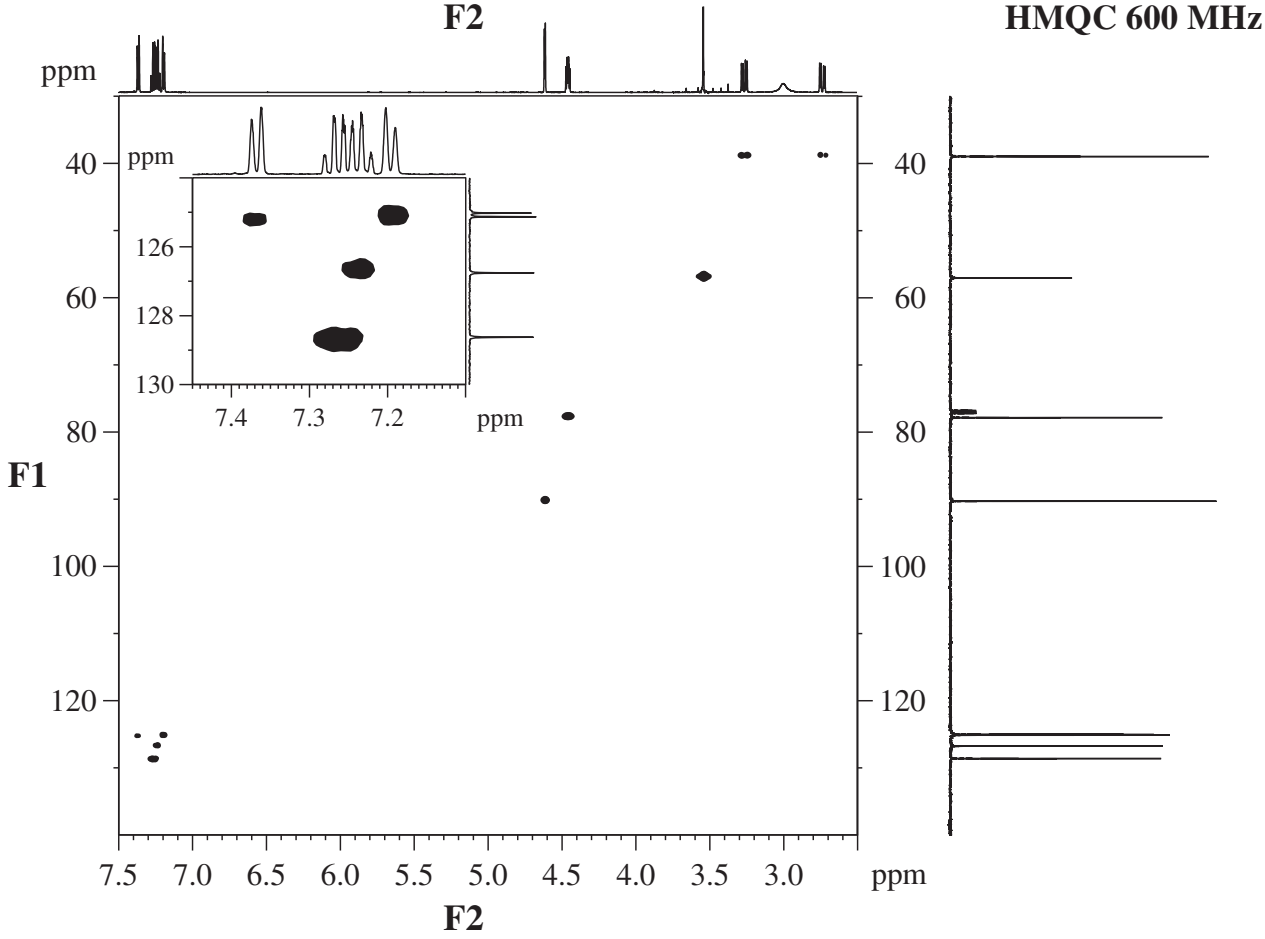
HMQC 600 MHz
ppm
40
60
80
100
120
126
128
130
7.4 7.3 7.2
F1
F2

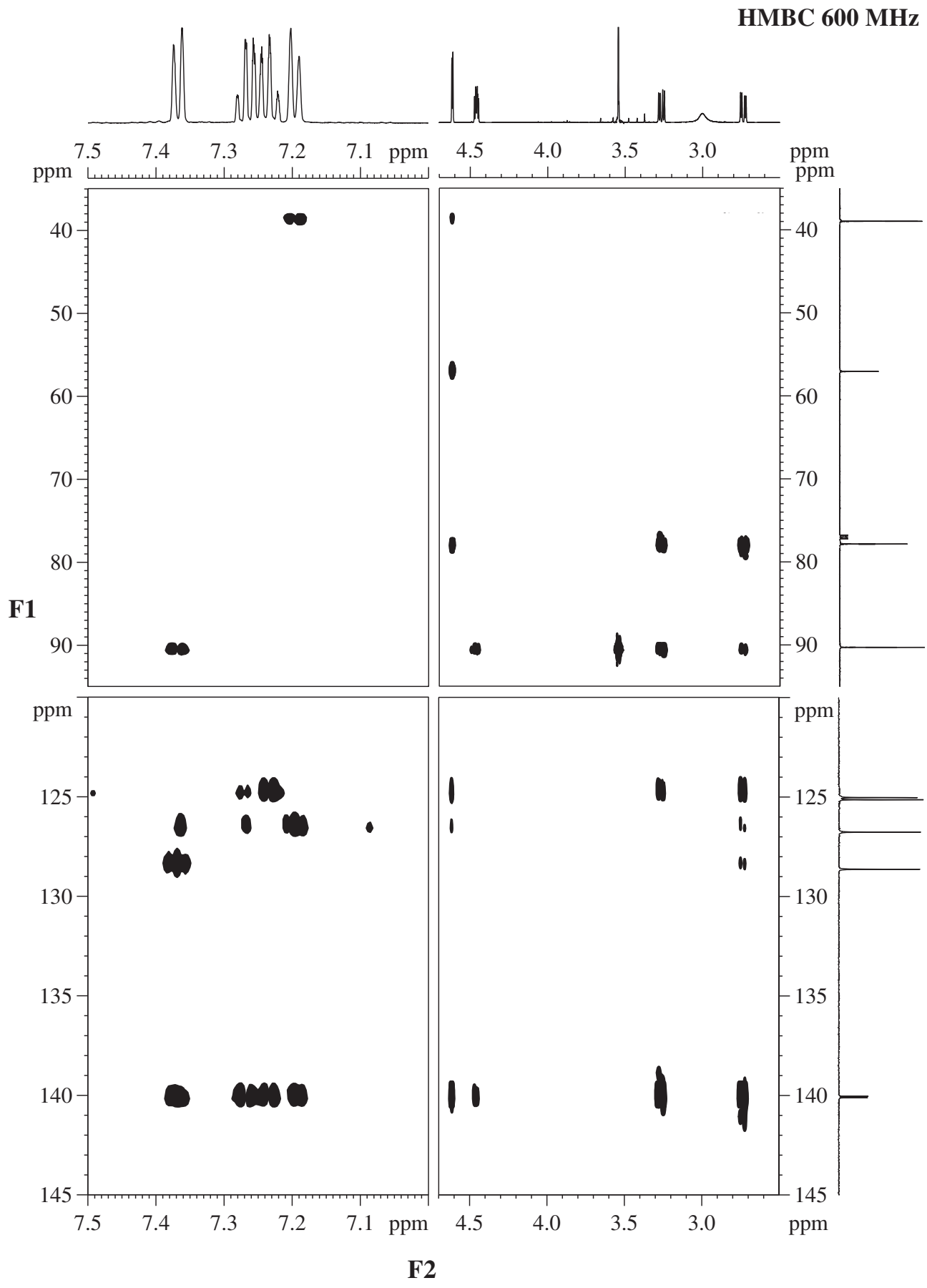
HMBC 600 MHz
7.5
7.4
7.3
7.2
7.1
ppm
4.5
4.0
3.5
3.0
40
50
60
70
80
90
125
130
135
140
145
F1
F2

MASS

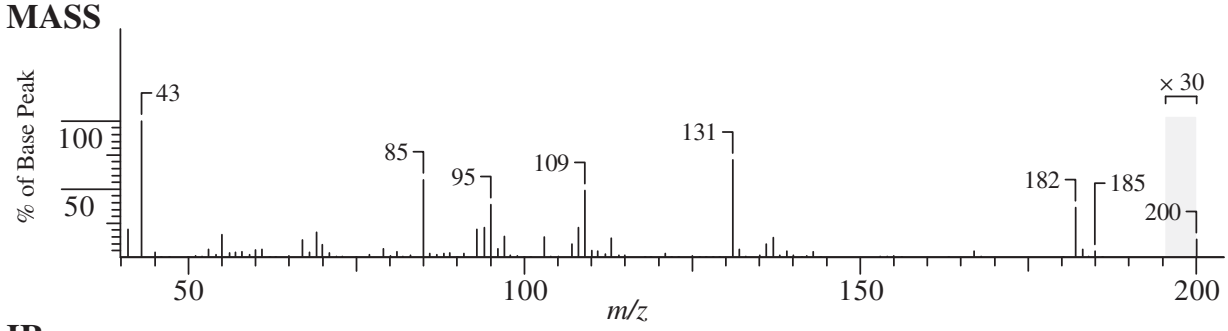

IR

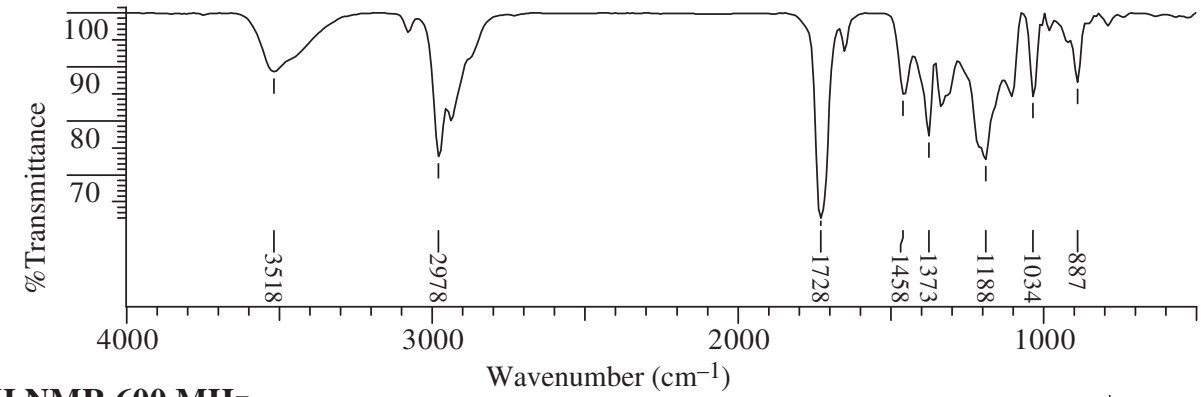

^{1}H NMR 600 MHz

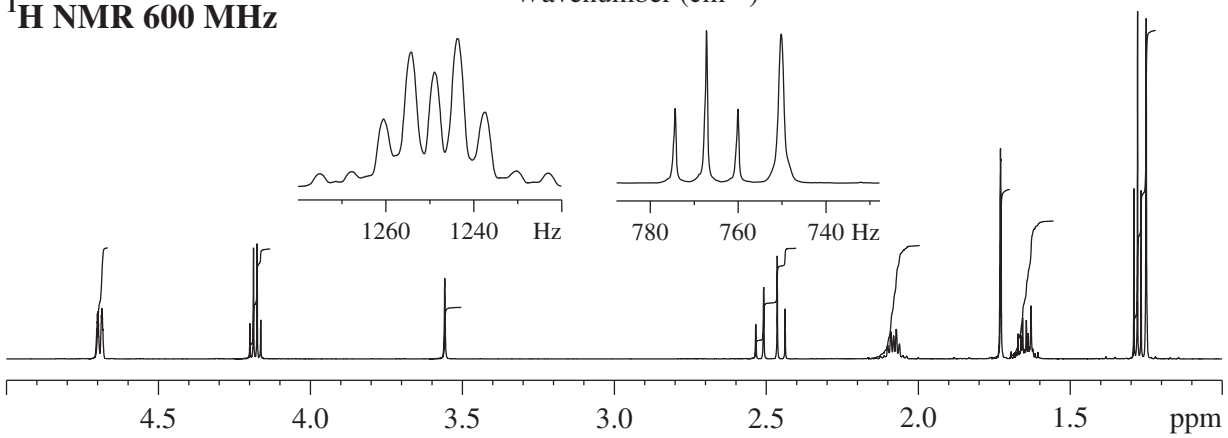

^{13}C/DEPT NMR 150.9 MHz

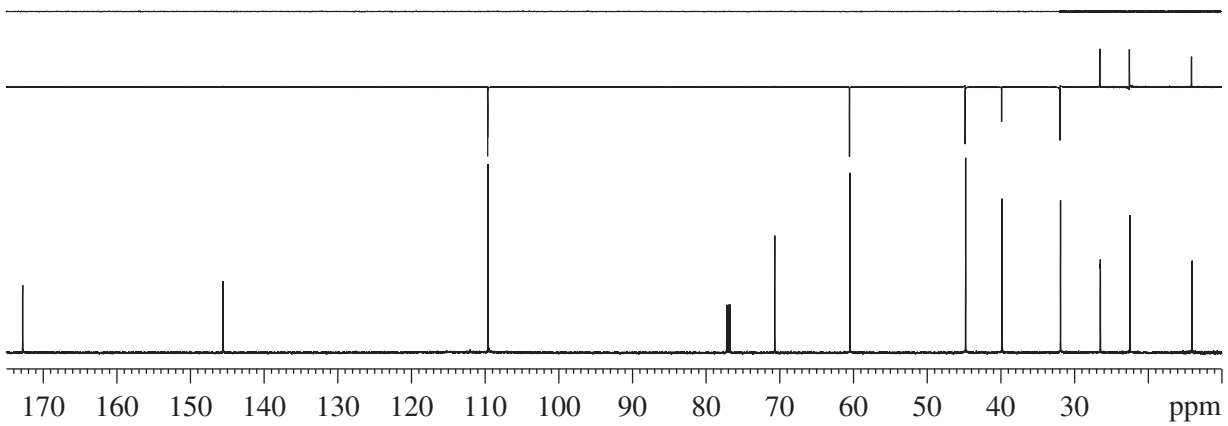

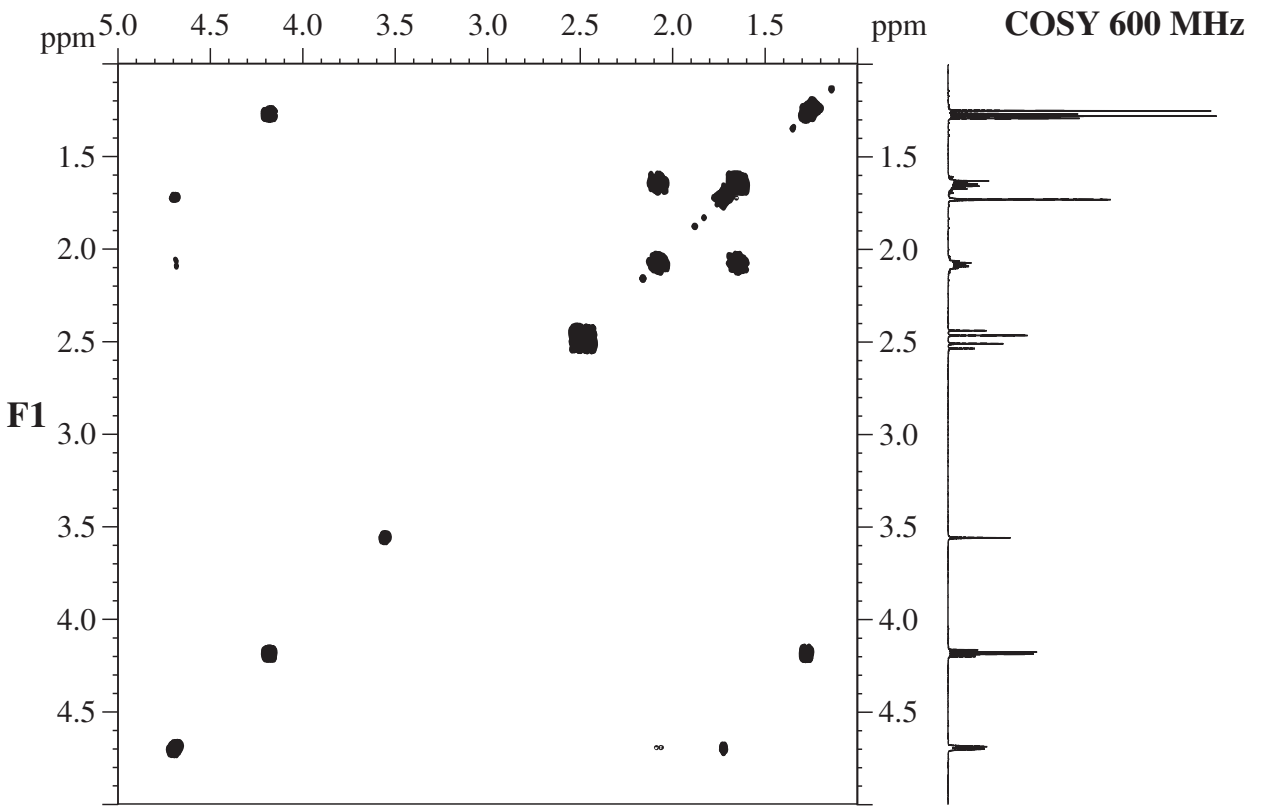
COSY 600 MHz
ppm
5.0 4.5 4.0 3.5 3.0 2.5 2.0 1.5
ppm
1.5
2.0
2.5
3.0
3.5
4.0
4.5
F1
F2

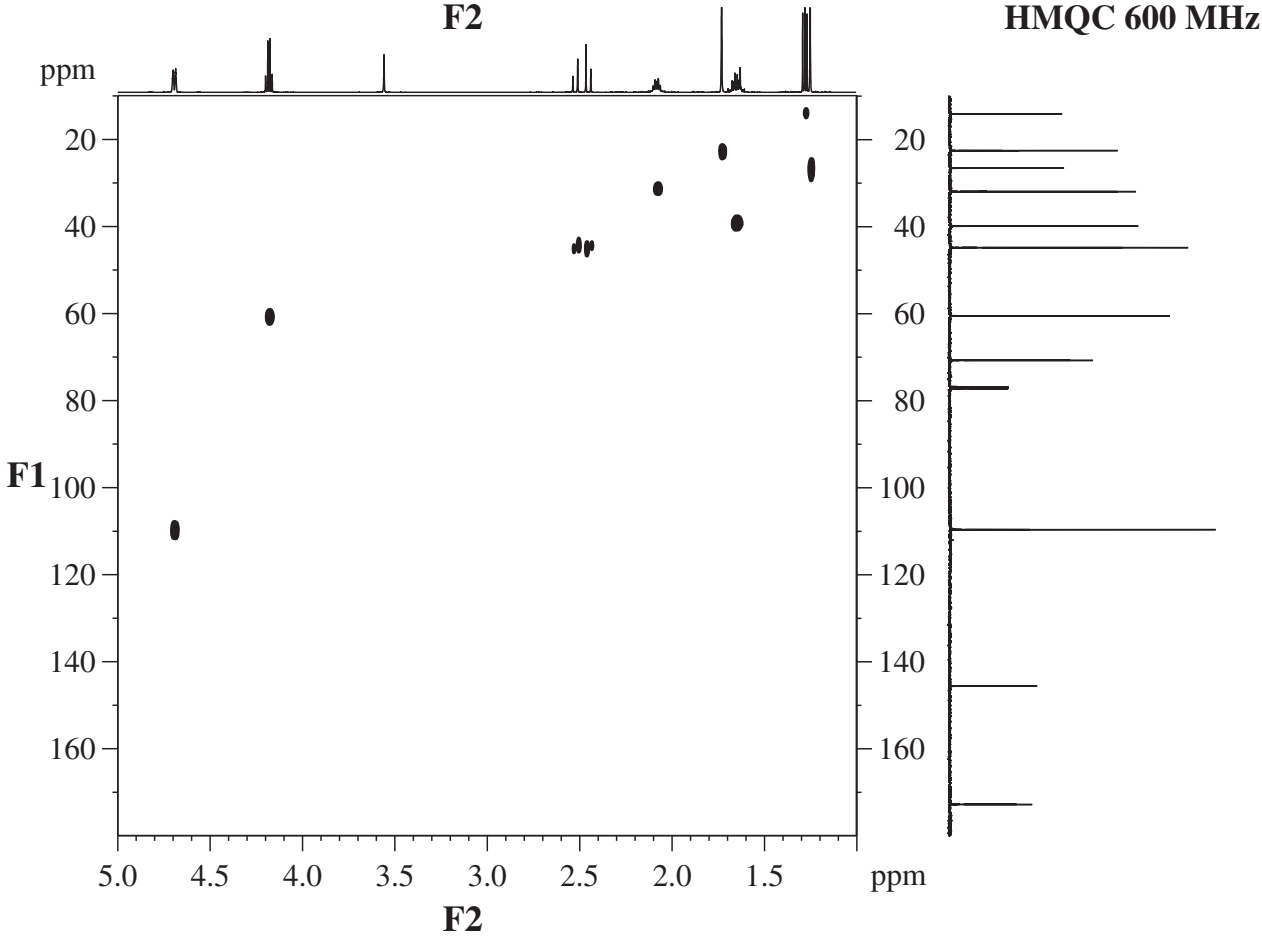
HMQC 600 MHz
ppm
20
40
60
80
100
120
140
160
F1
5.0 4.5 4.0 3.5 3.0 2.5 2.0 1.5
ppm
F2

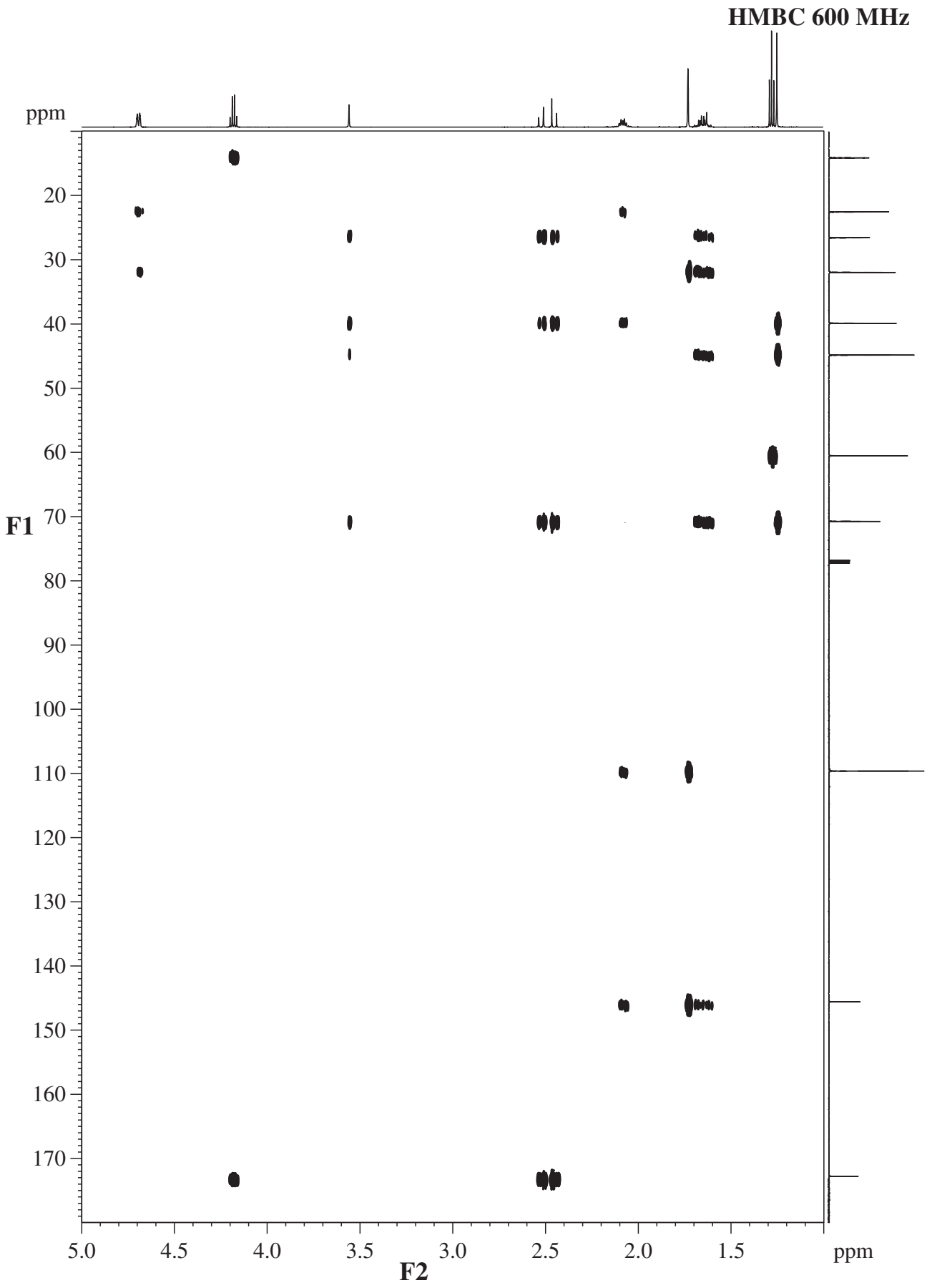
HMBC 600 MHz
ppm
20
30
40
50
60
70
80
90
100
110
120
130
140
150
160
170
F1
5.0
4.5
4.0
3.5
3.0
2.5
2.0
1.5
ppm
F2

MASS

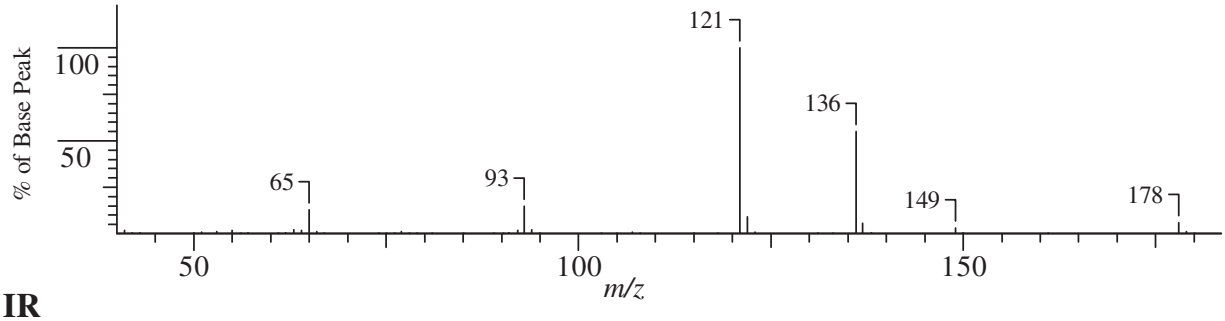

IR

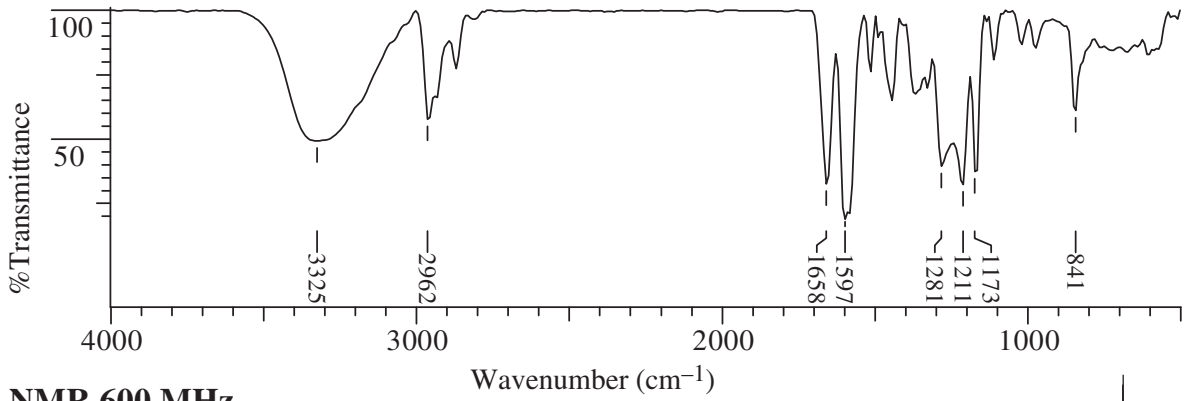

^{1}H NMR 600 MHz

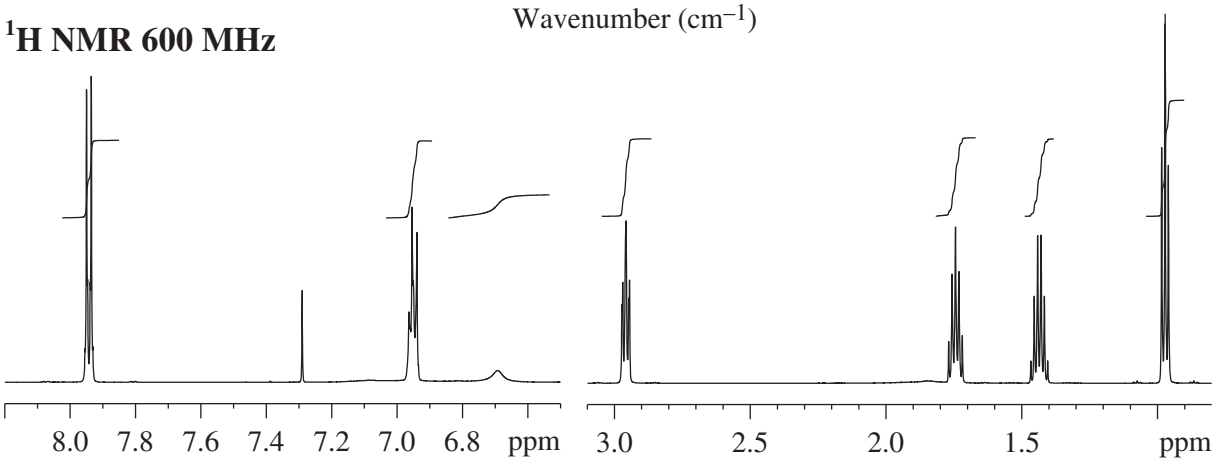

^{13}C/DEPT NMR 150.9 MHz

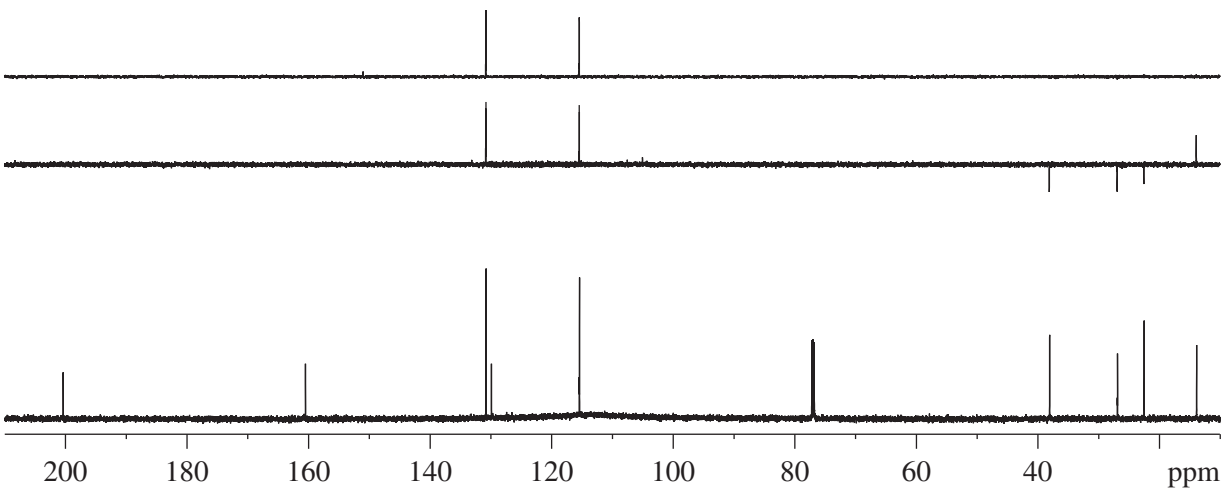

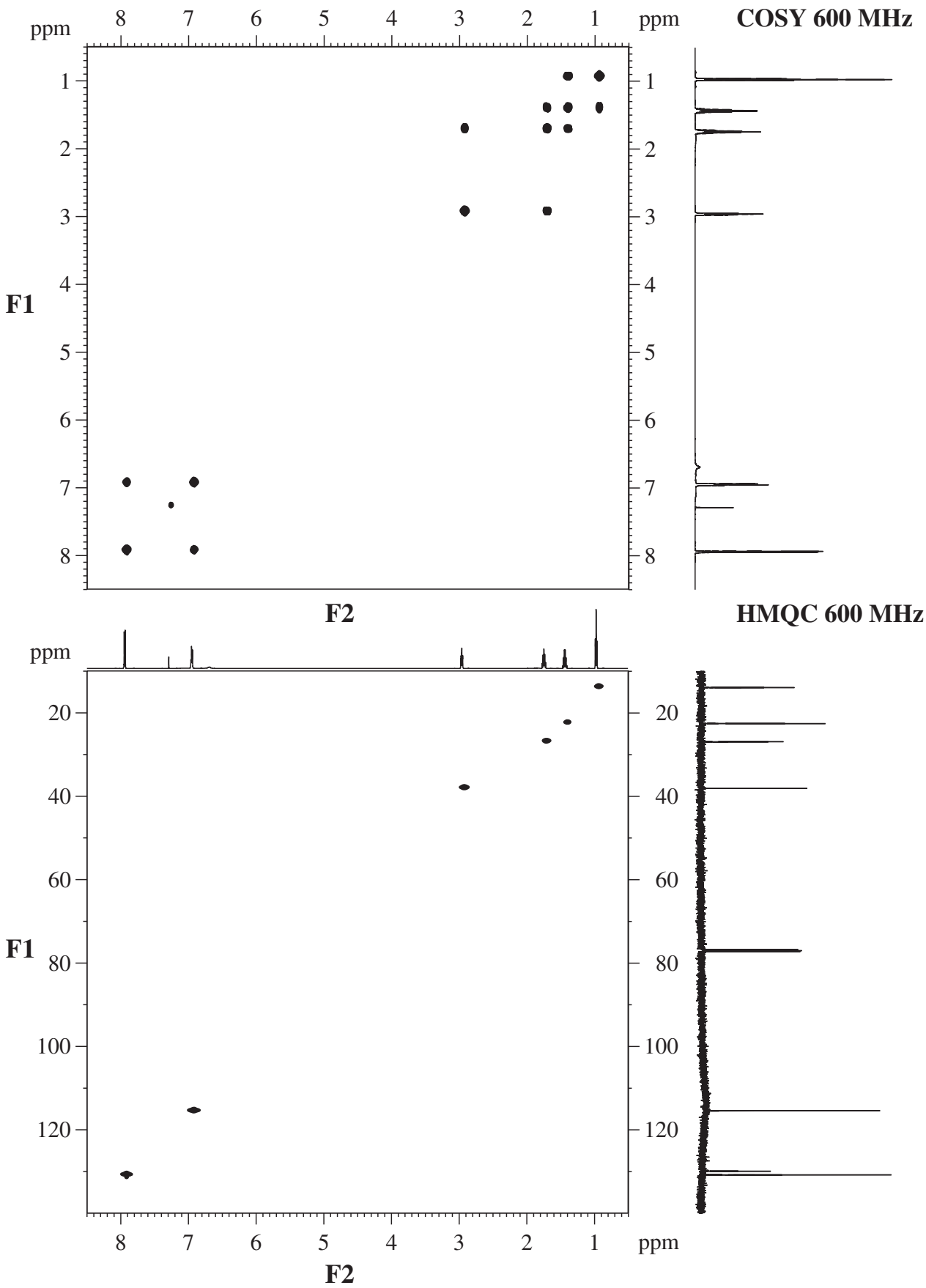
COSY 600 MHz
ppm
8 7 6 5 4 3 2 1
F1
F2
HMQC 600 MHz
20 40 60 80 100 120

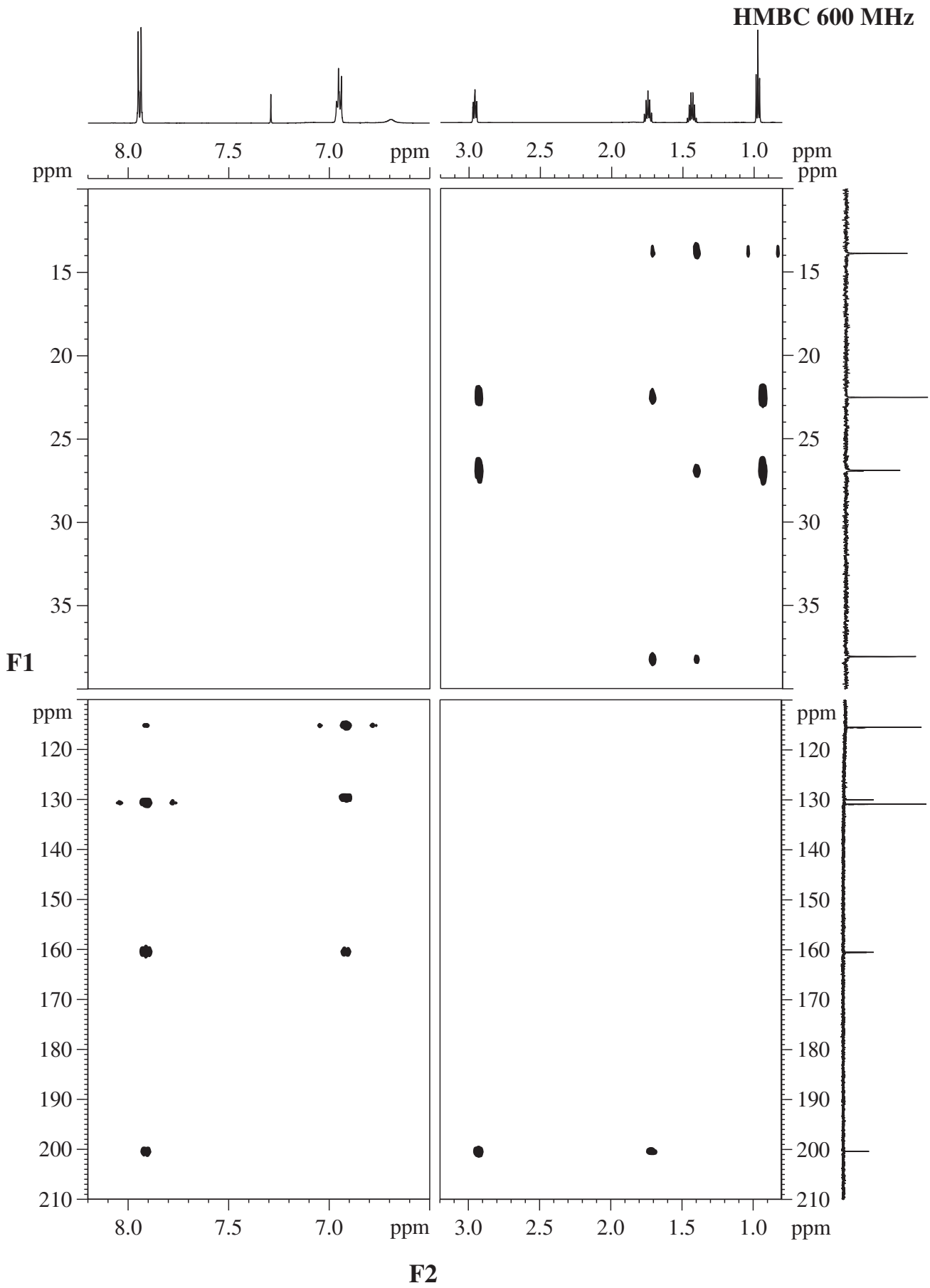
HMBC 600 MHz
8.0
7.5
7.0
ppm
3.0
2.5
2.0
1.5
1.0
ppm
15
20
25
30
35
F1
120
130
140
150
160
170
180
190
200
210
F2

MASS

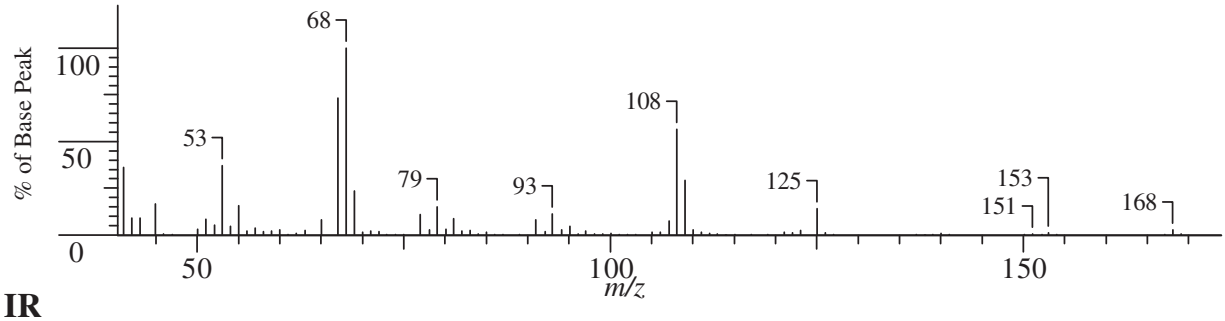

IR

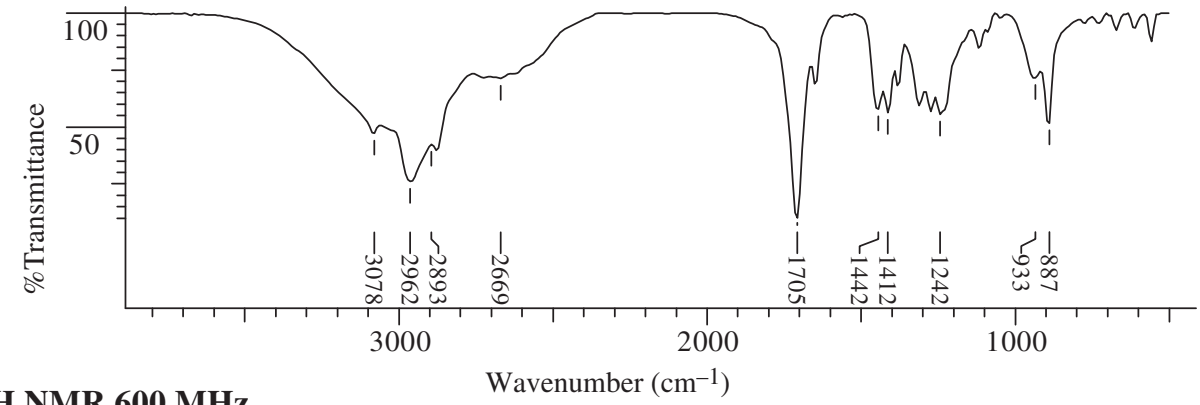

^{1}H NMR 600 MHz

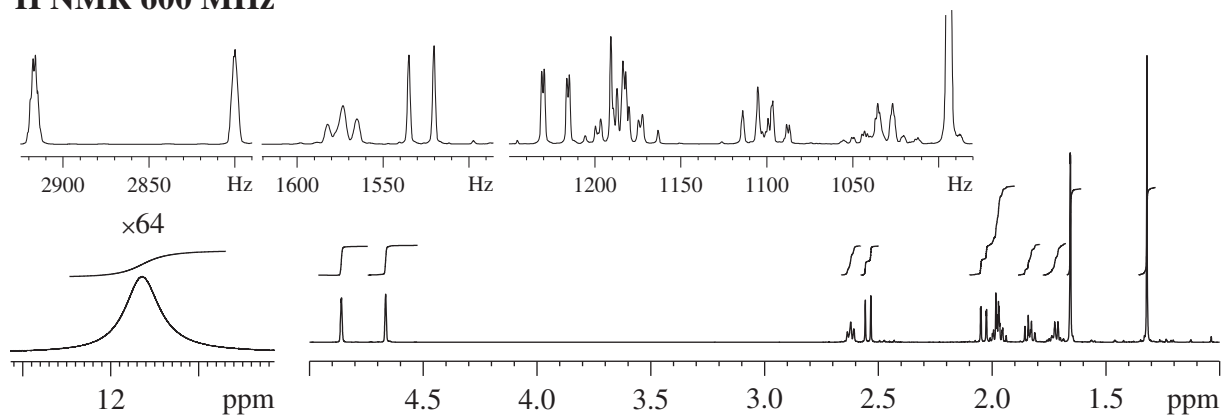

^{13}C/DEPT NMR 150.9 MHz

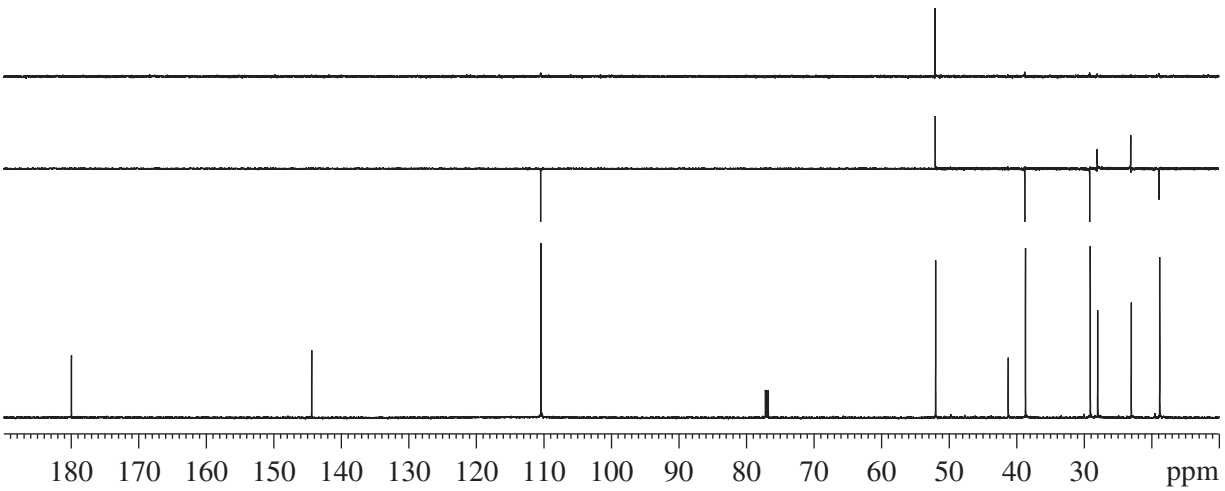

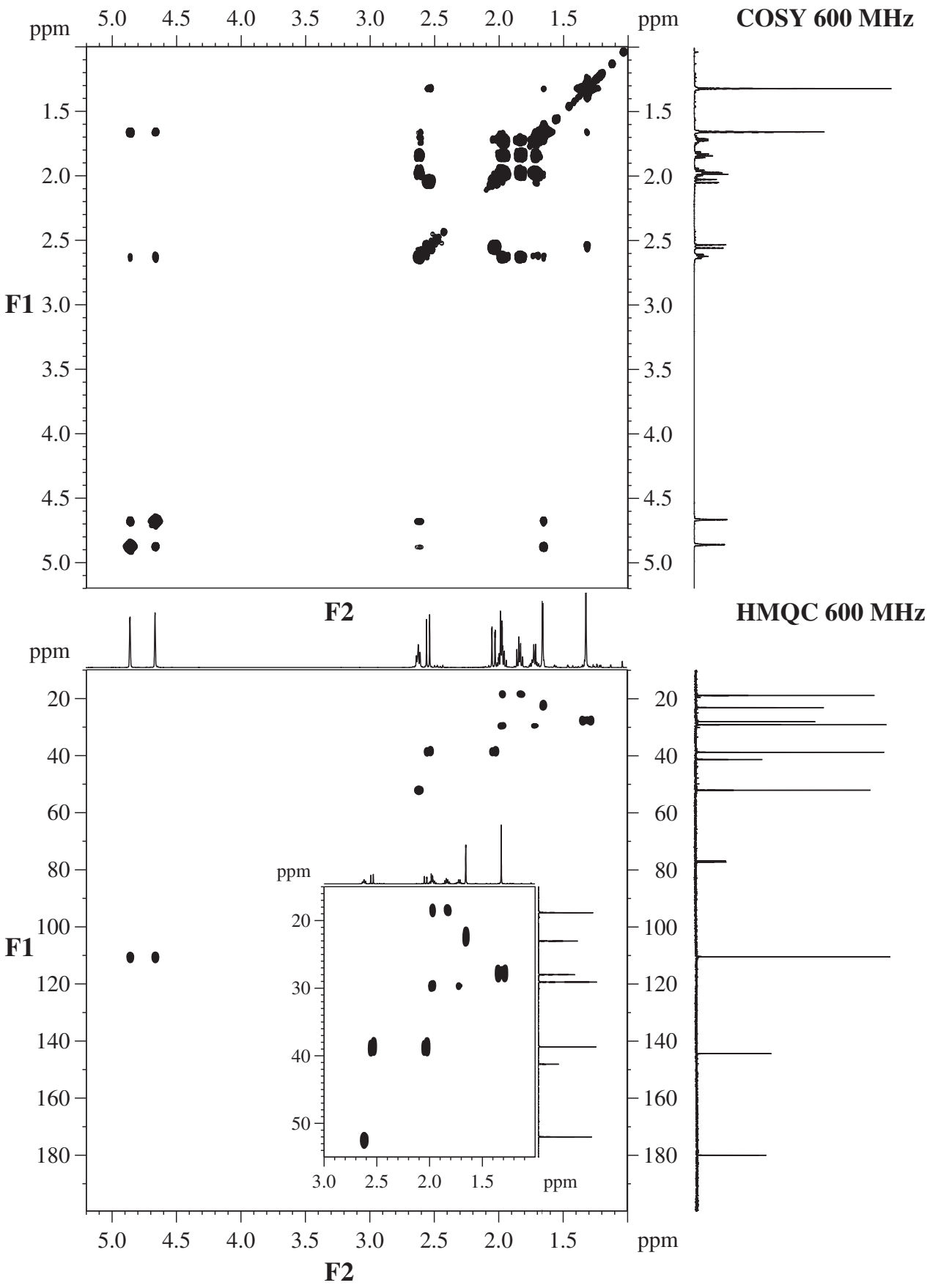
COSY 600 MHz
ppm
5.0 4.5 4.0 3.5 3.0 2.5 2.0 1.5
F1
F2
HMQC 600 MHz
20 40 60 80 100 120 140 160 180
3.0 2.5 2.0 1.5 ppm

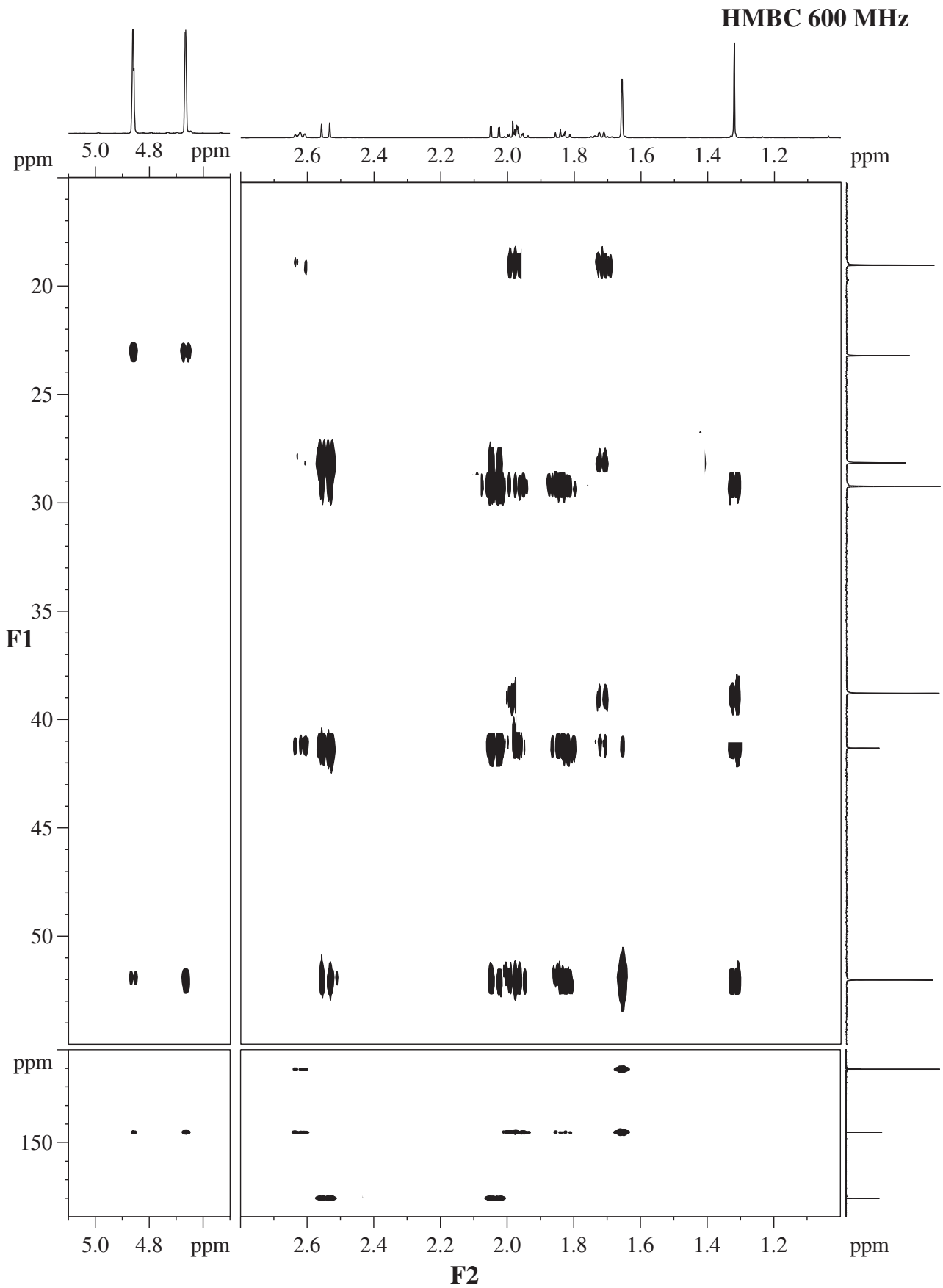
HMBC 600 MHz
ppm
5.0
4.8
ppm
2.6
2.4
2.2
2.0
1.8
1.6
1.4
1.2
ppm
20
25
30
35
F1
40
45
50
ppm
150
5.0
4.8
ppm
2.6
2.4
2.2
2.0
1.8
1.6
1.4
1.2
ppm
F2

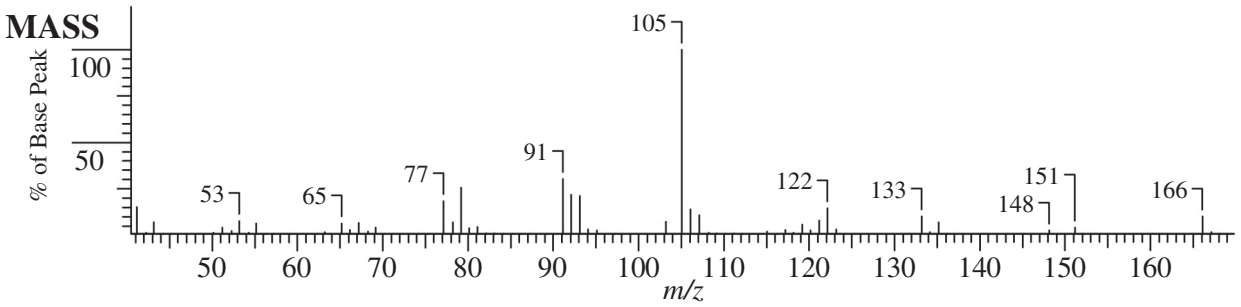
MASS
% of Base Peak
100
50
105
91
77
53
65
122
133
151
148
166
50 60 70 80 90 100 110 120 130 140 150 160
m/z

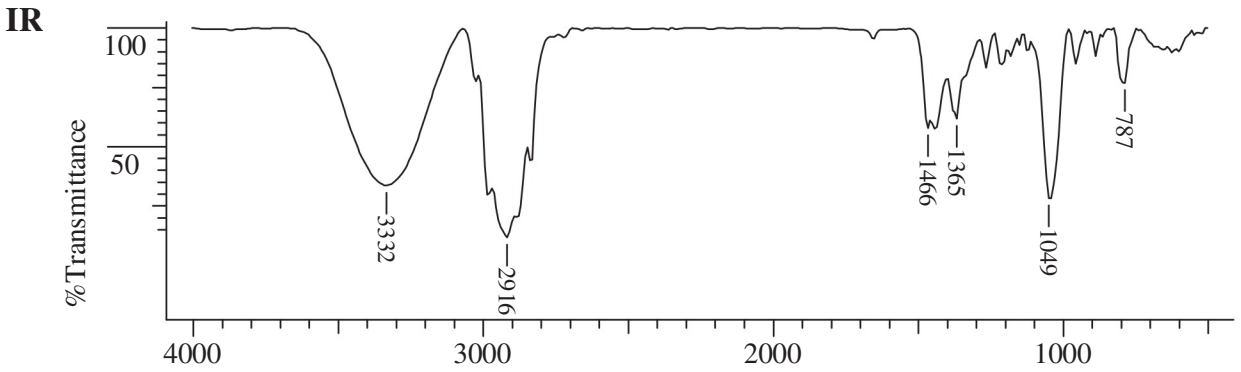
IR
100
50
%Transmittance
3332
2916
1466
1365
1049
787
4000 3000 2000 1000
Wavenumber (cm−1)

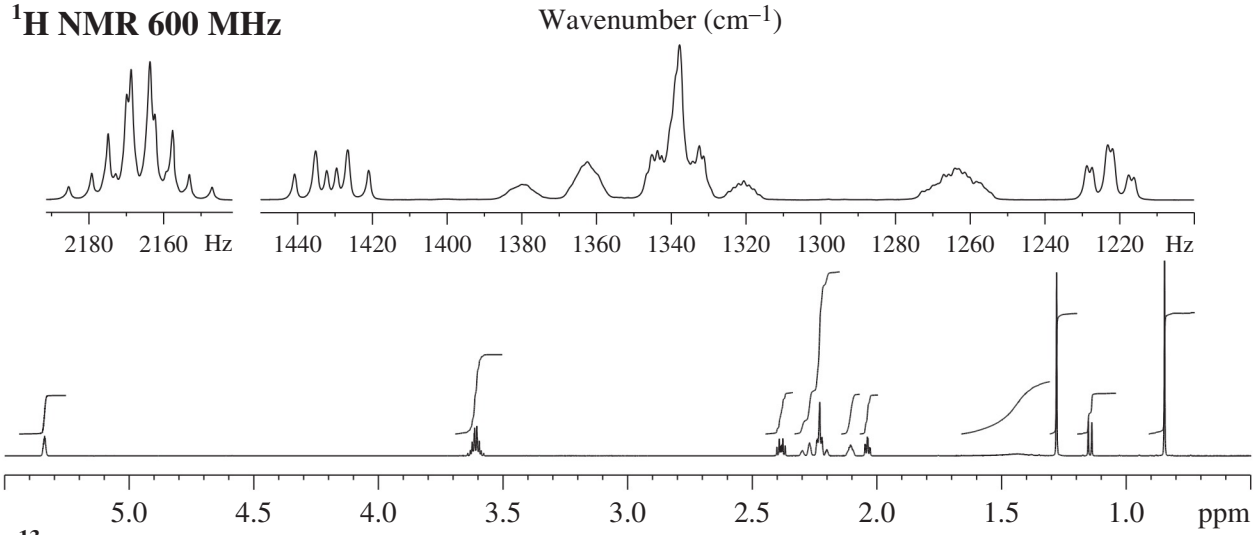
1H NMR 600 MHz
2180 2160 Hz
1440 1420 1400 1380 1360 1340 1320 1300 1280 1260 1240 1220 Hz
5.0 4.5 4.0 3.5 3.0 2.5 2.0 1.5 1.0 ppm

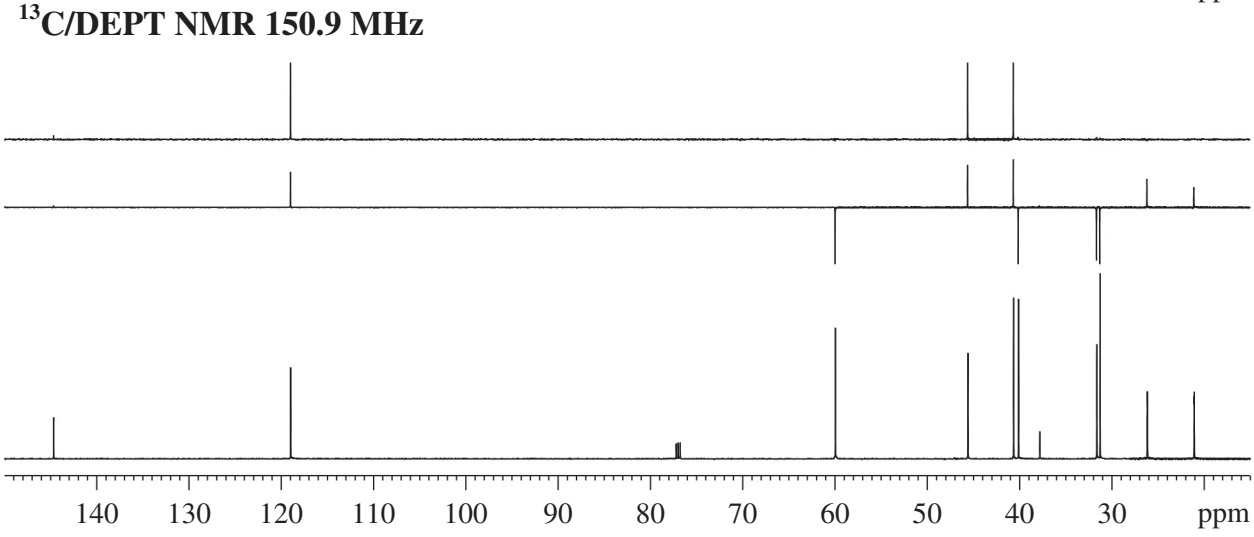
13C/DEPT NMR 150.9 MHz
140 130 120 110 100 90 80 70 60 50 40 30 ppm

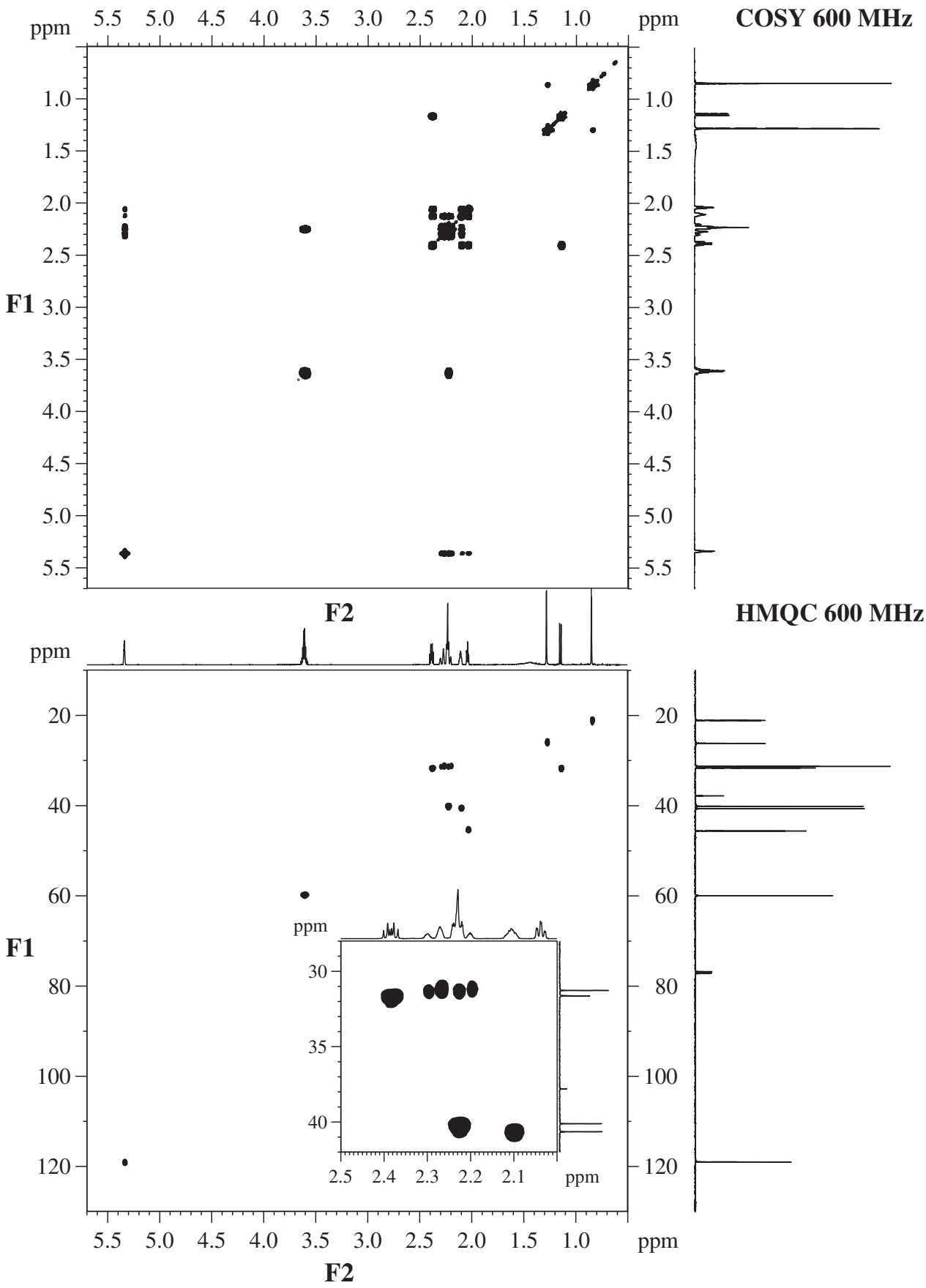
COSY 600 MHz
ppm
5.5 5.0 4.5 4.0 3.5 3.0 2.5 2.0 1.5 1.0
F1
F2
HMQC 600 MHz
20
40
60
80
100
120
30
35
40
2.5 2.4 2.3 2.2 2.1

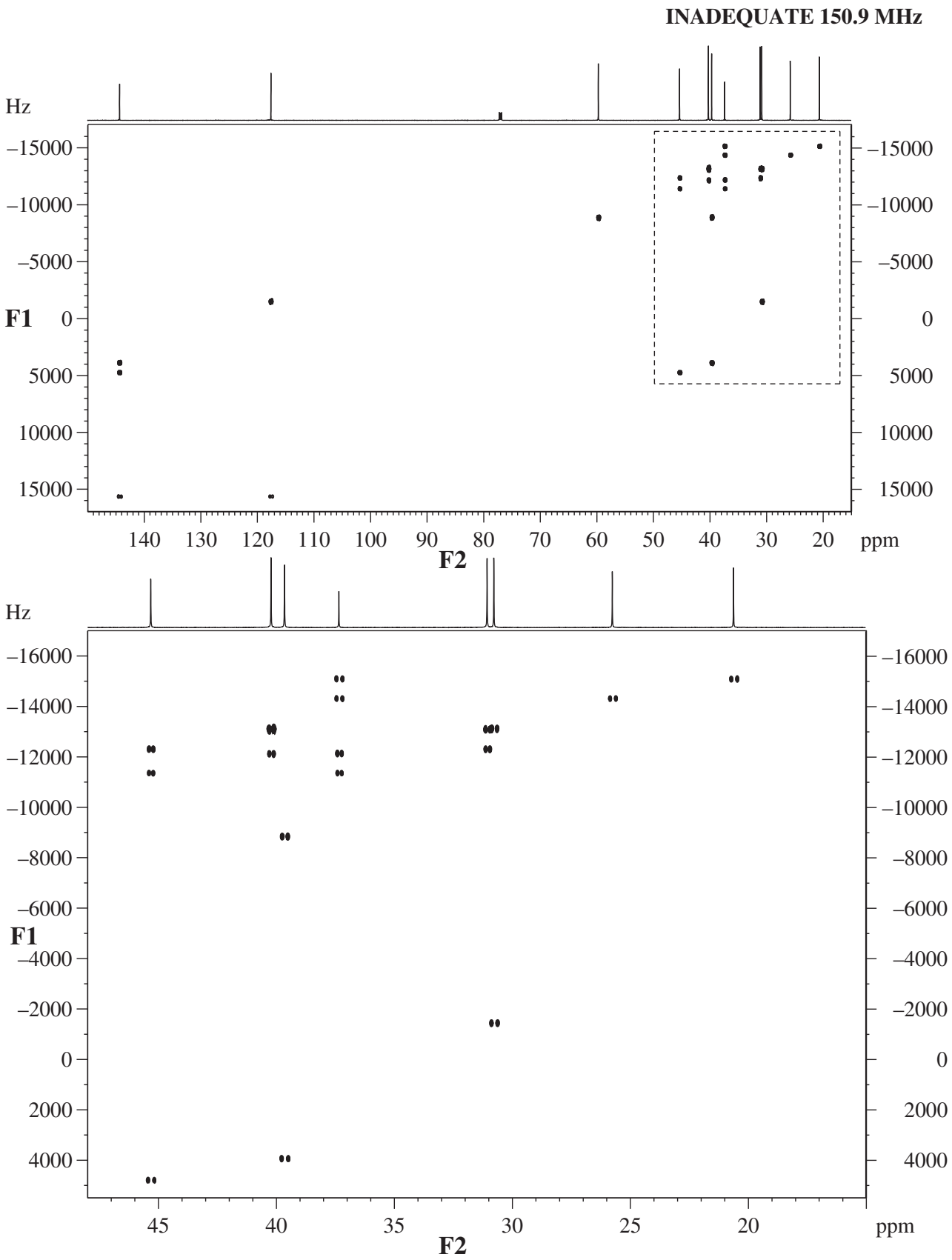
INADEQUATE 150.9 MHz
Hz
–15000
–10000
–5000
F1
0
5000
10000
15000
140 130 120 110 100 90 80 70 60 50 40 30 20 ppm
F2
Hz
–16000
–14000
–12000
–10000
–8000
–6000
F1
–4000
–2000
0
2000
4000
45 40 35 30 25 20 ppm
F2

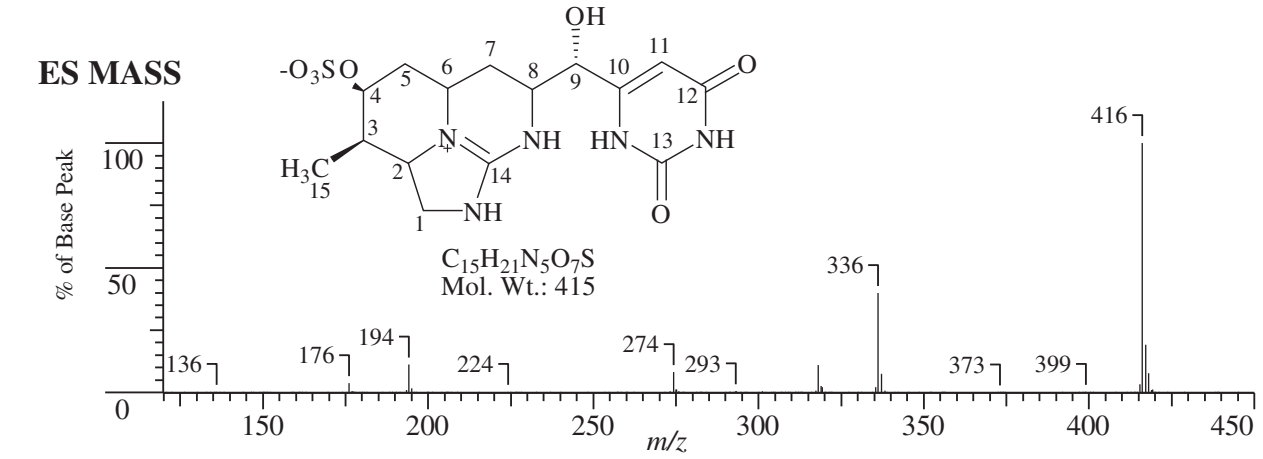

^{1}H NMR 600 MHz in D_2O

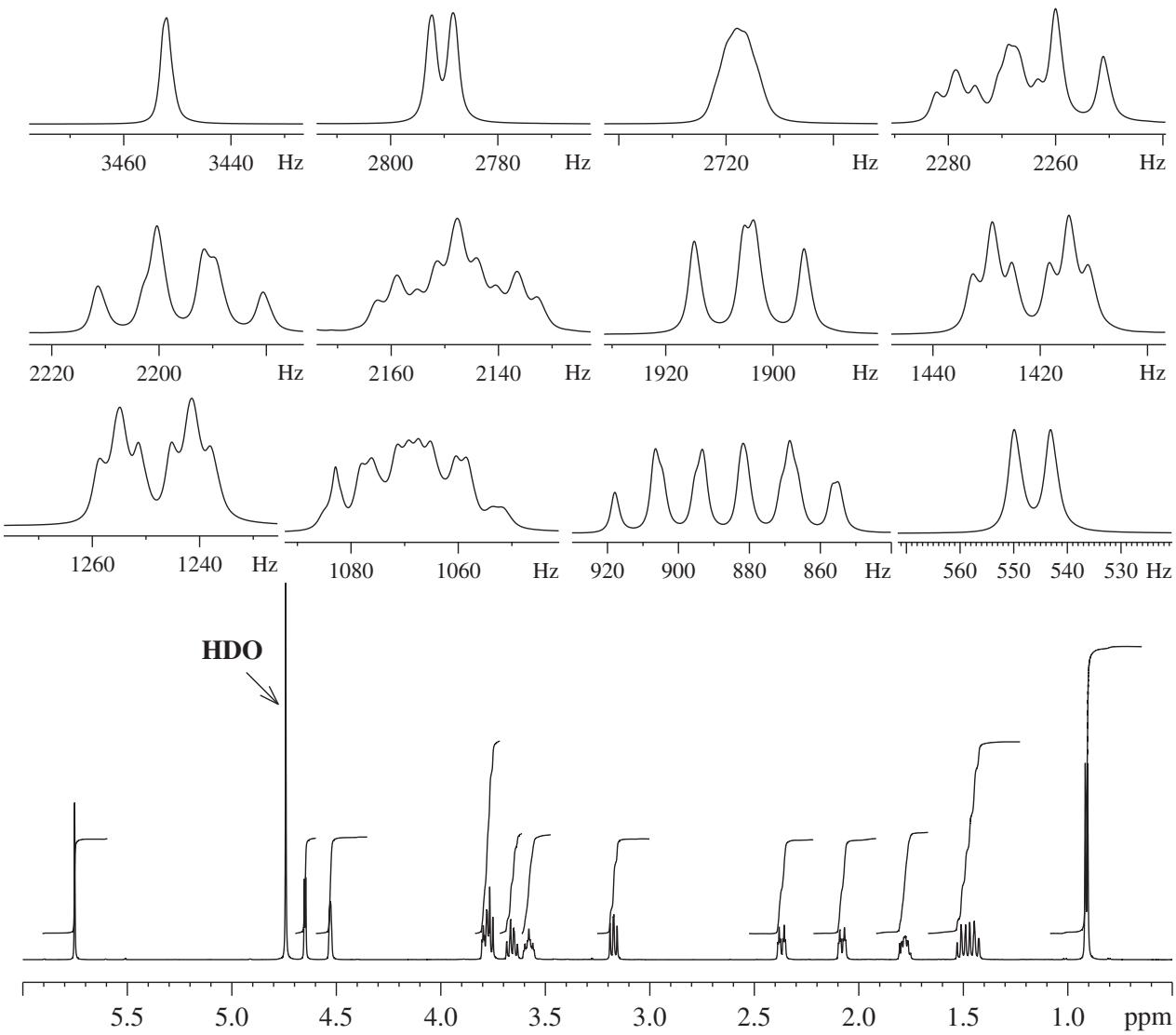

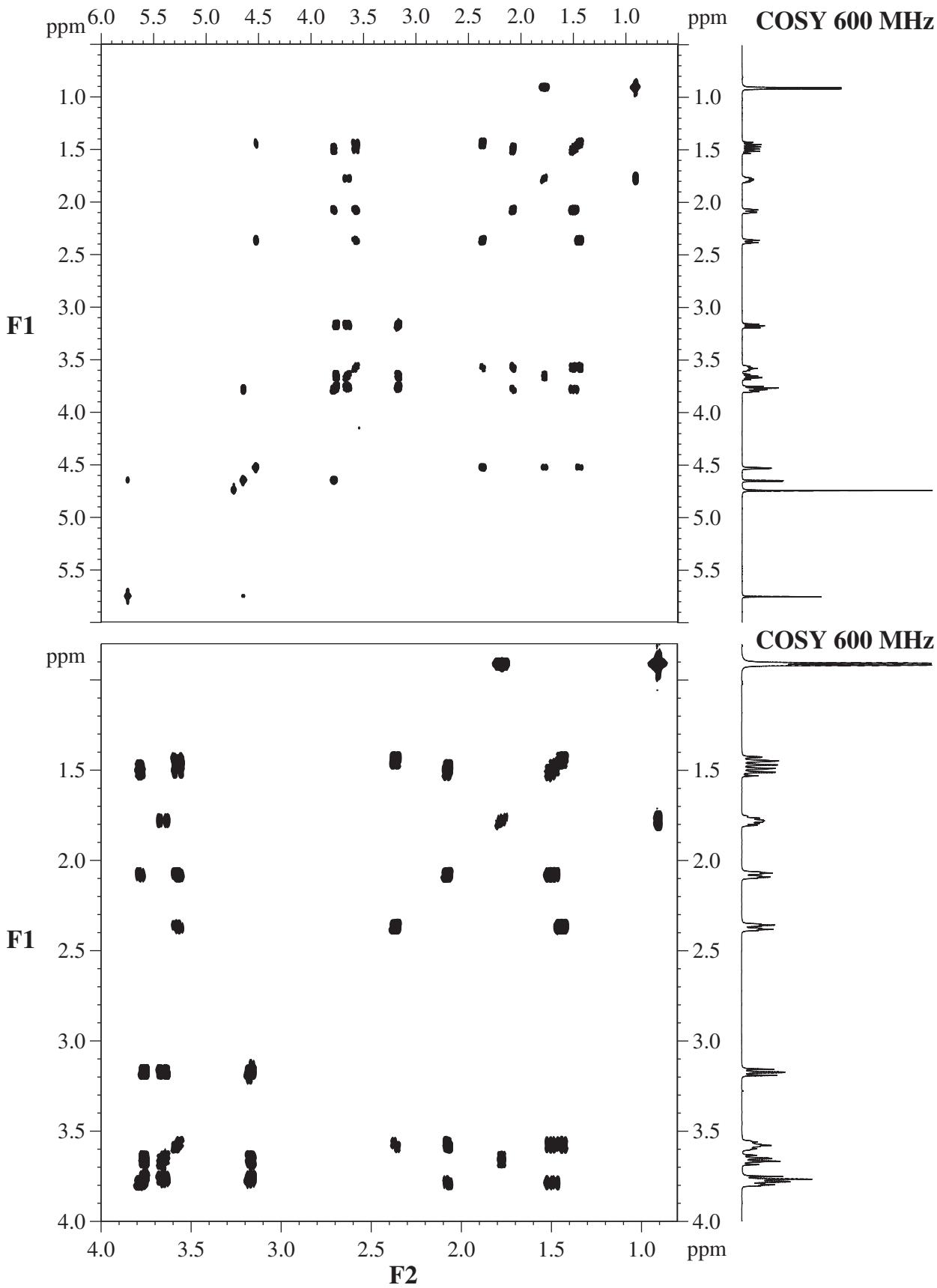
COSY 600 MHz
COSY 600 MHz
F1
F1
F2
ppm
6.0 5.5 5.0 4.5 4.0 3.5 3.0 2.5 2.0 1.5 1.0
1.0 1.5 2.0 2.5 3.0 3.5 4.0 4.5 5.0 5.5
4.0 3.5 3.0 2.5 2.0 1.5 1.0

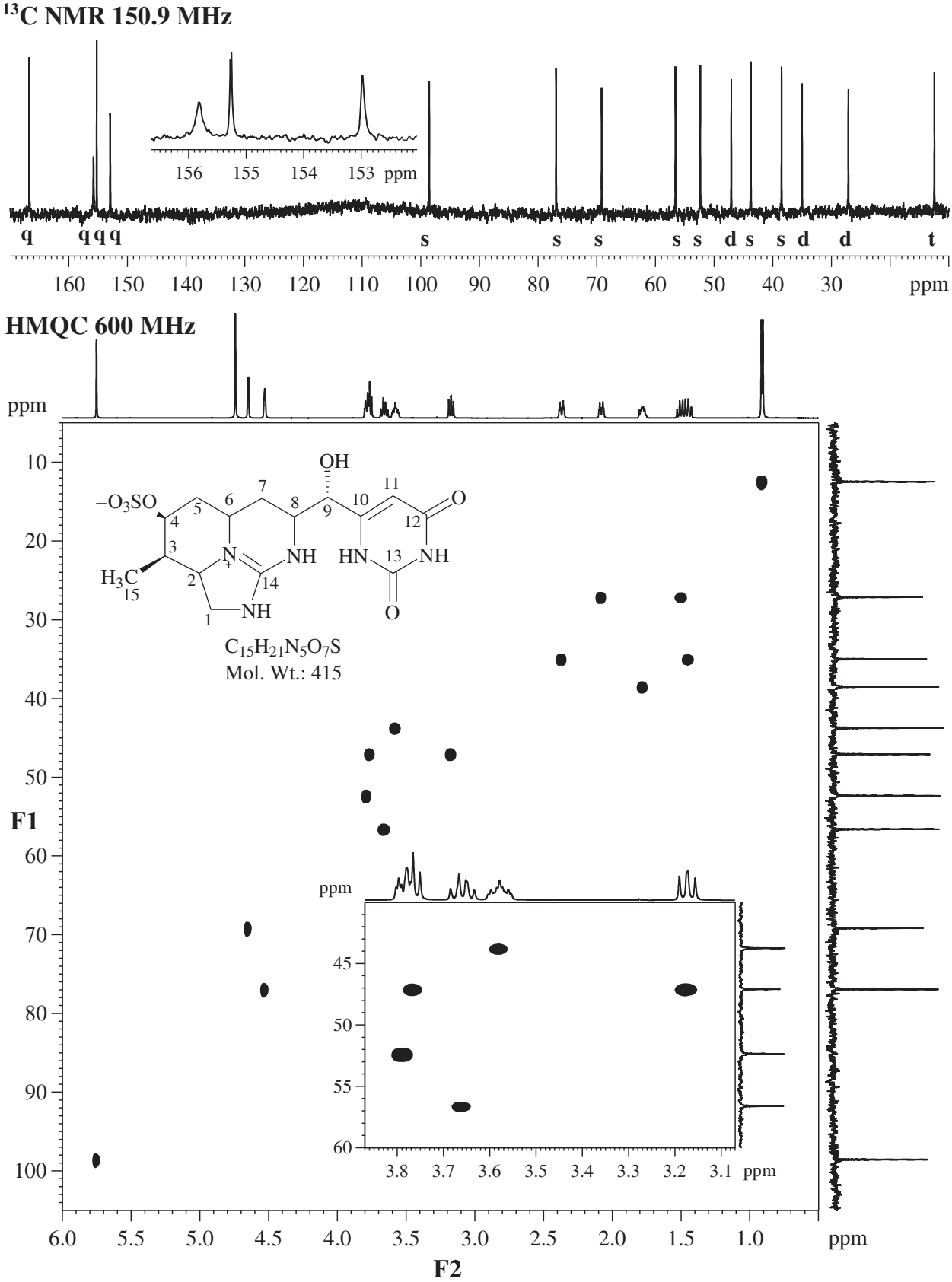
13C NMR 150.9 MHz
q q q q s s s s s d s s d d t
160 150 140 130 120 110 100 90 80 70 60 50 40 30 ppm
156 155 154 153 ppm
HMQC 600 MHz
ppm
OH
−O3SO
H3C
15
N
NH
HN
NH
O
C15H21N5O7S
Mol. Wt.: 415
F1
F2
6.0 5.5 5.0 4.5 4.0 3.5 3.0 2.5 2.0 1.5 1.0 ppm
3.8 3.7 3.6 3.5 3.4 3.3 3.2 3.1 ppm

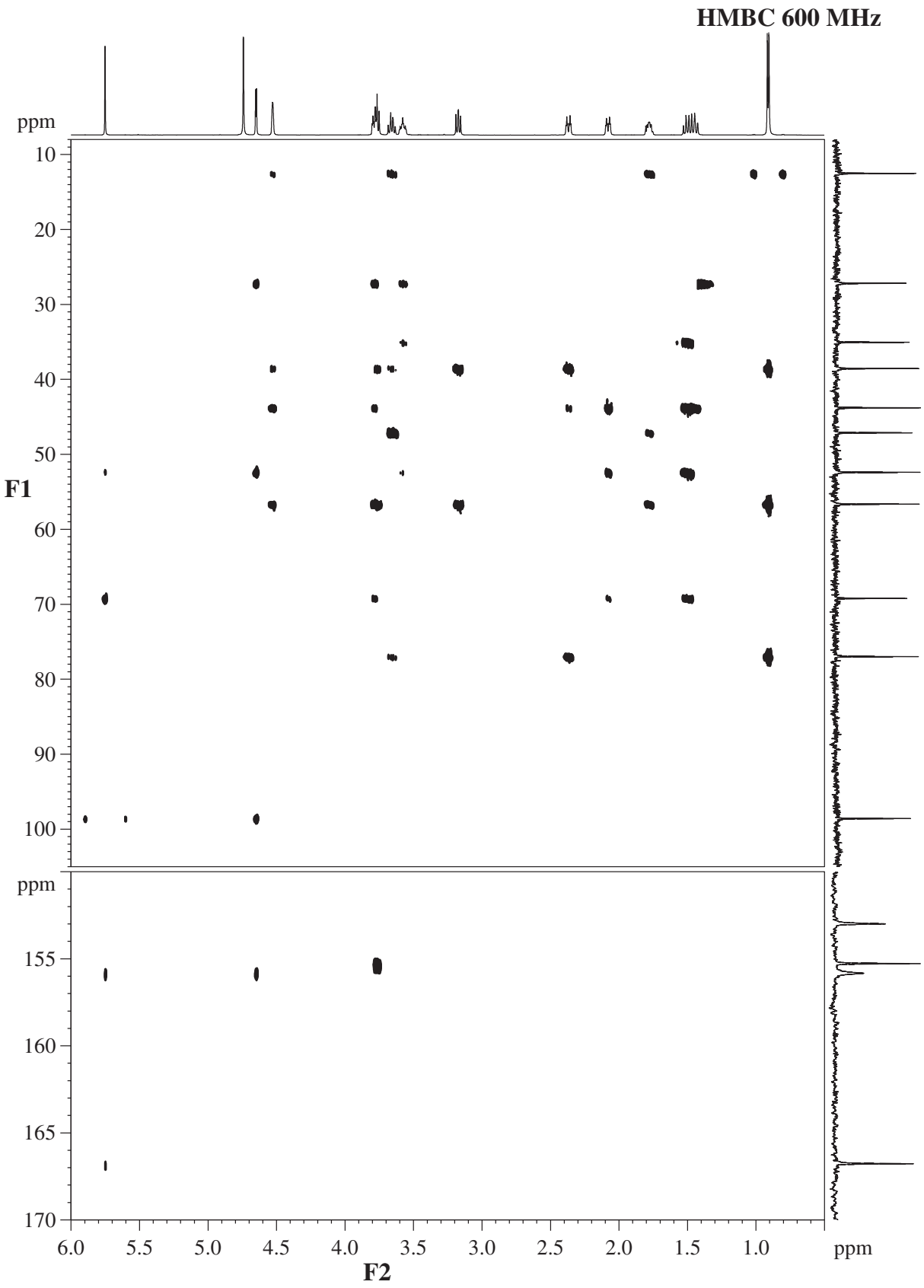
HMBC 600 MHz
ppm
10
20
30
40
50
F1
60
70
80
90
100
ppm
155
160
165
170
6.0
5.5
5.0
4.5
4.0
3.5
3.0
2.5
2.0
1.5
1.0
ppm
F2

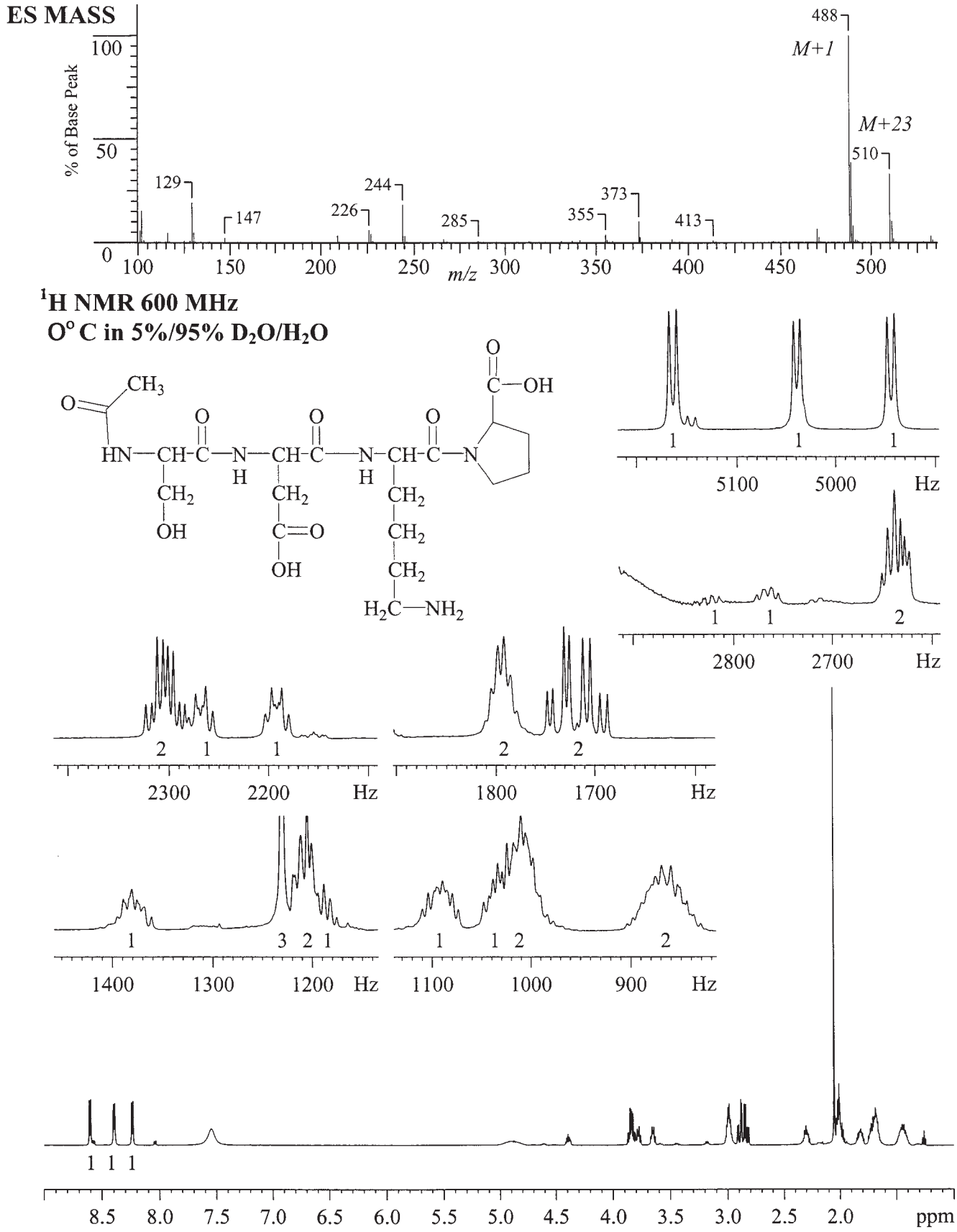
ES MASS
% of Base Peak
100
50
0
488
M+1
M+23
510
129
147
226
244
285
355
373
413
100
150
200
250
m/z
300
350
400
450
500
1H NMR 600 MHz
O° C in 5%/95% D2O/H2O
1 1 1
5100
5000
Hz
1 1 2
2800
2700
Hz
2 1 1
2300
2200
Hz
2 2
1800
1700
Hz
1 3 2 1
1400
1300
1200
Hz
1 1 2 2
1100
1000
900
Hz
1 1 1
8.5
8.0
7.5
7.0
6.5
6.0
5.5
5.0
4.5
4.0
3.5
3.0
2.5
2.0
ppm

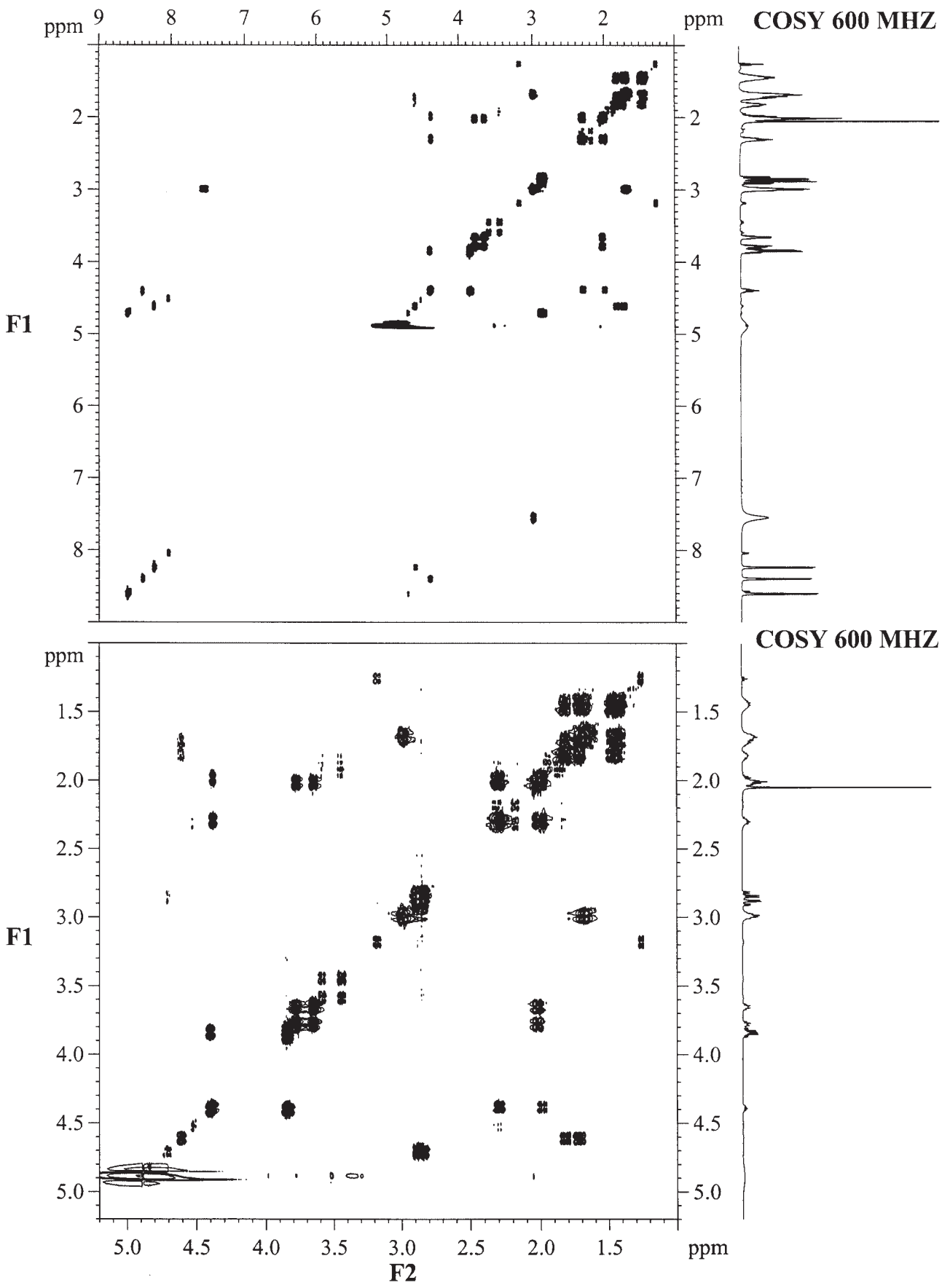
COSY 600 MHZ
ppm
9
8
7
6
5
4
3
2
F1
COSY 600 MHZ
1.5
2.0
2.5
3.0
3.5
4.0
4.5
5.0
F2

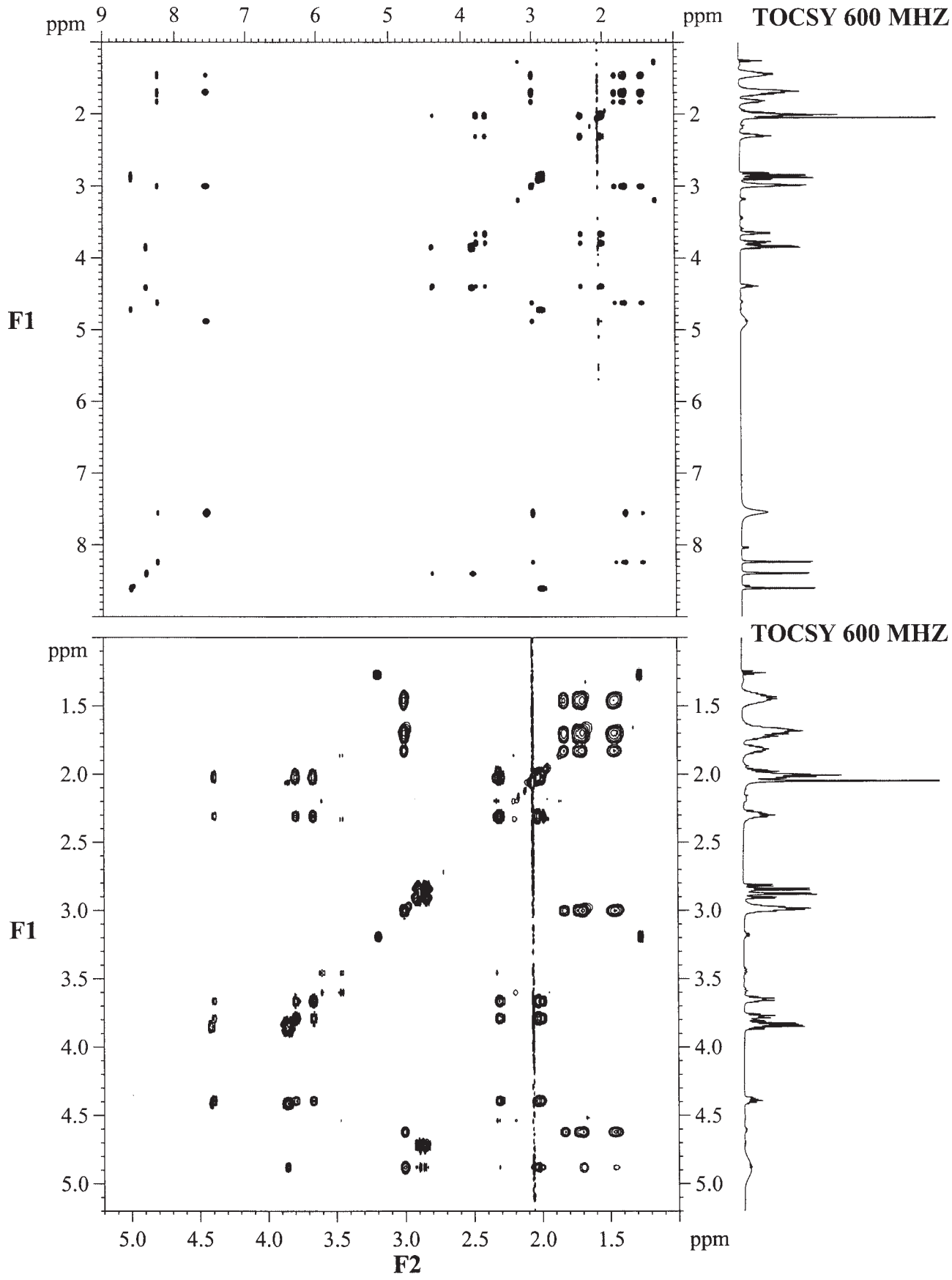
TOCSY 600 MHZ
ppm
F1
F2
TOCSY 600 MHZ

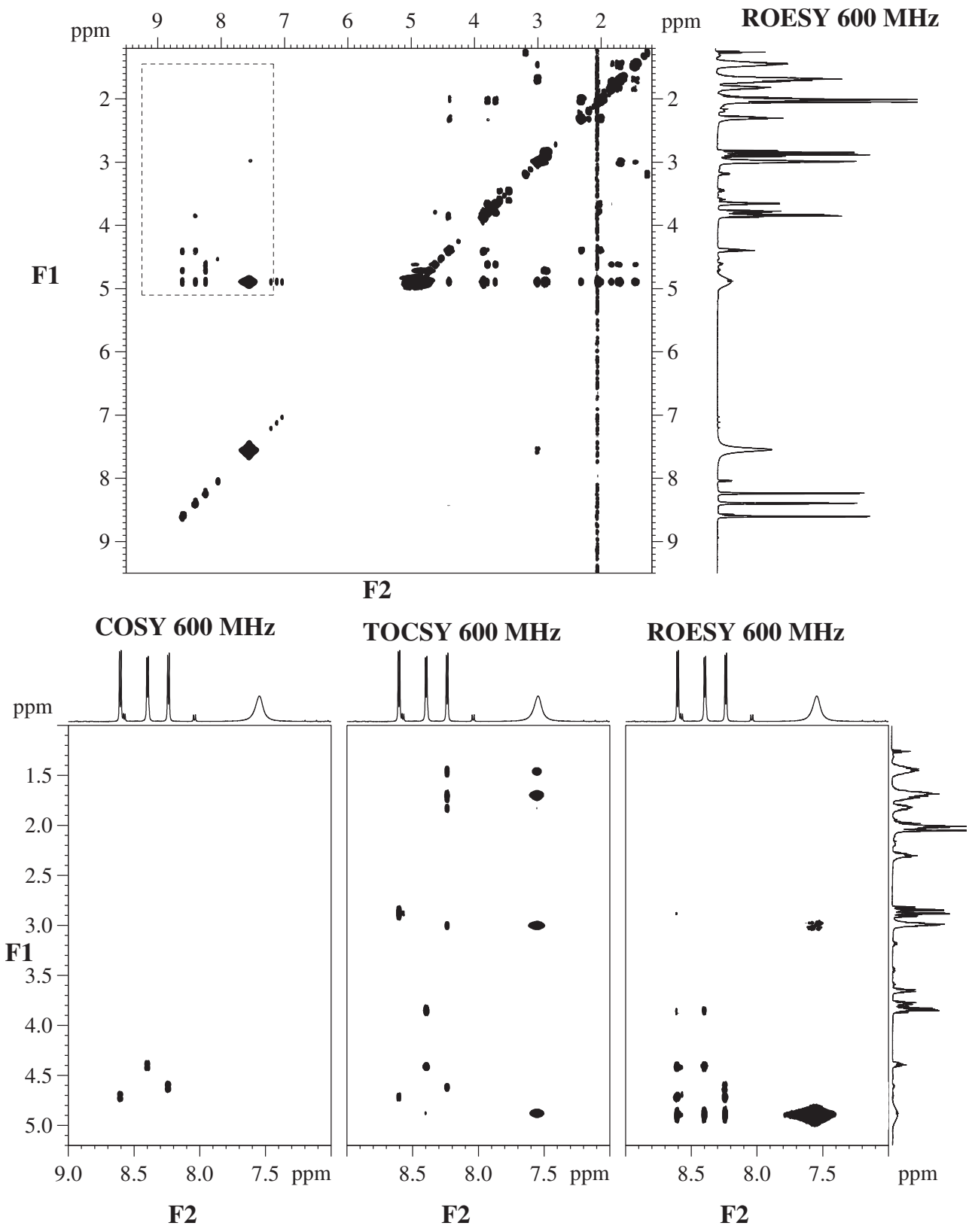
ROESY 600 MHz
ppm
F1
F2
COSY 600 MHz
TOCSY 600 MHz
ROESY 600 MHz
ppm
F1
F2
F2
F2

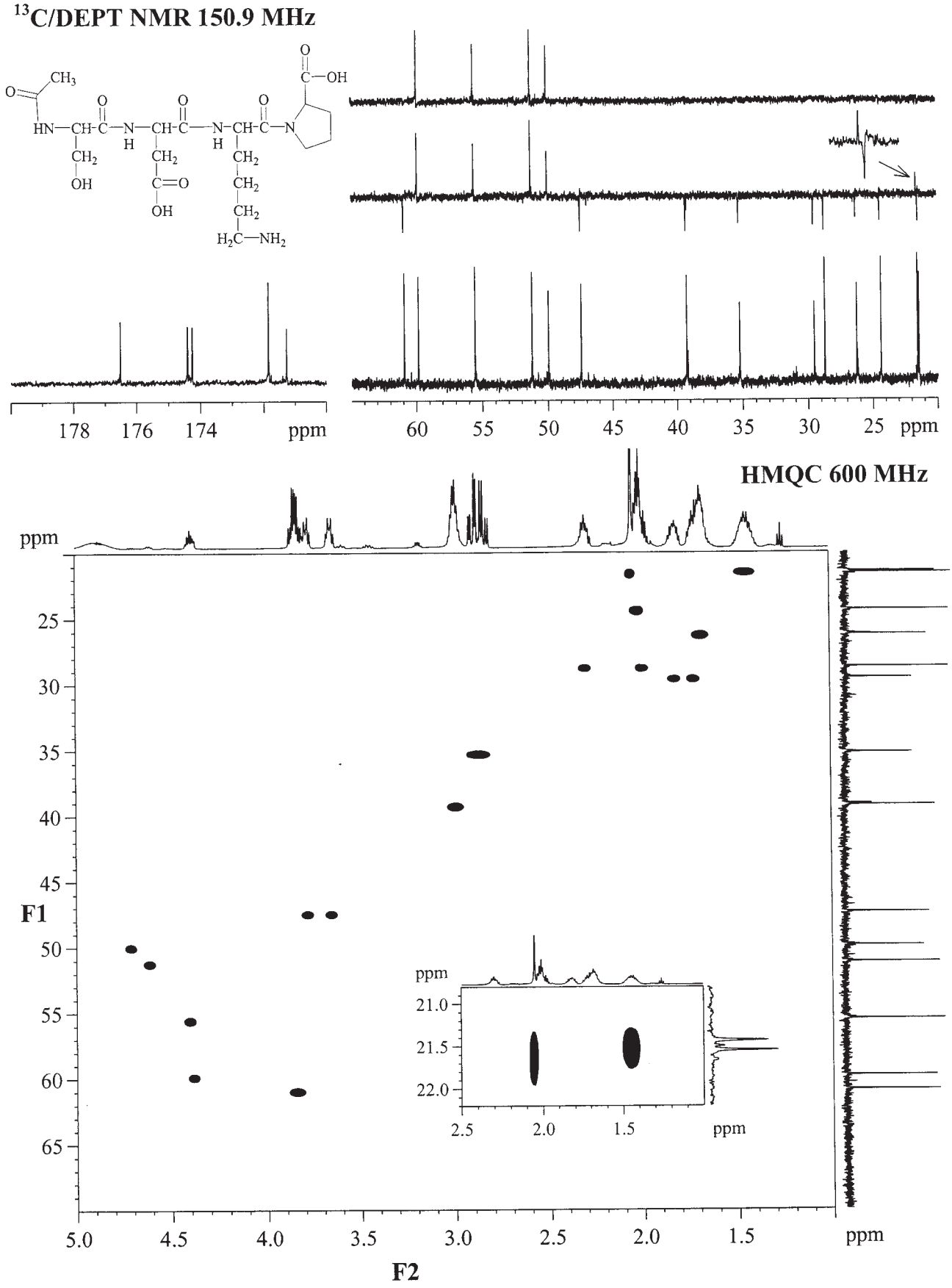
13C/DEPT NMR 150.9 MHz
178 176 174 ppm
60 55 50 45 40 35 30 25 ppm
HMQC 600 MHz
ppm
25
30
35
40
45
F1
50
55
60
65
5.0 4.5 4.0 3.5 3.0 2.5 2.0 1.5 ppm
F2
ppm
21.0
21.5
22.0
2.5 2.0 1.5 ppm

MASS

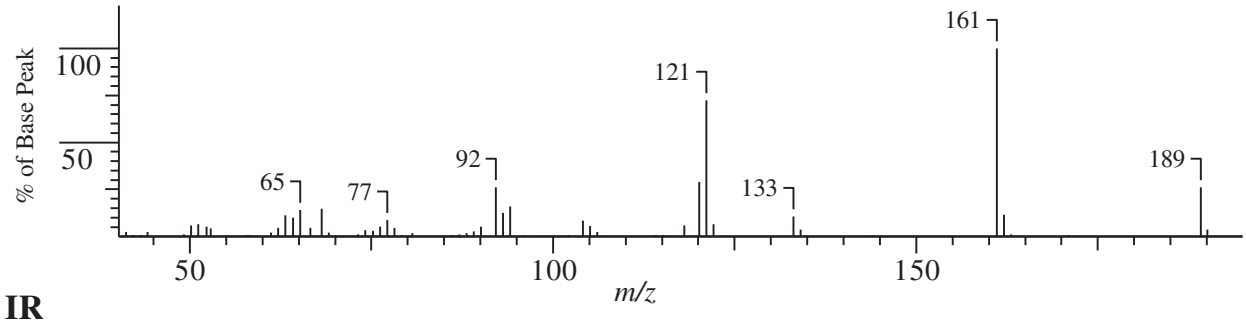

IR

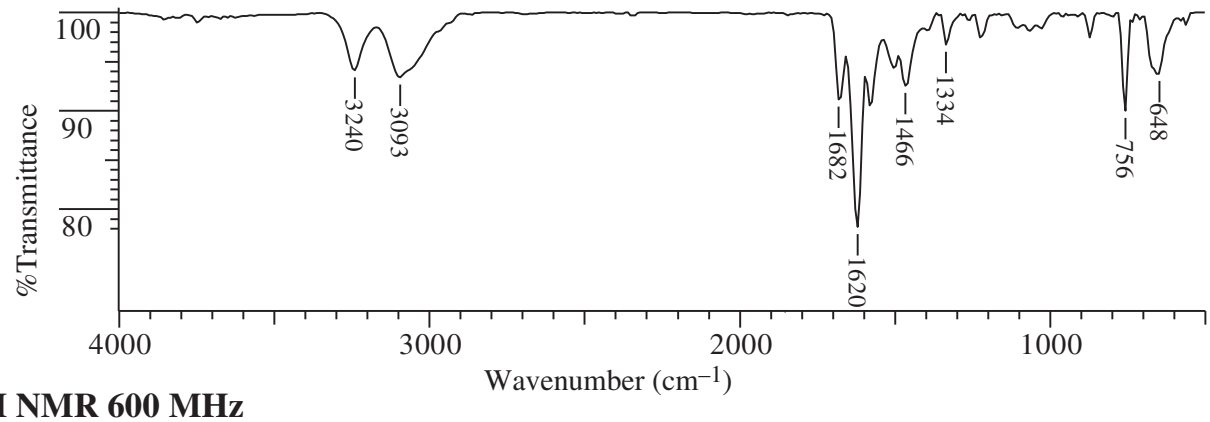

^{1}H NMR 600 MHz

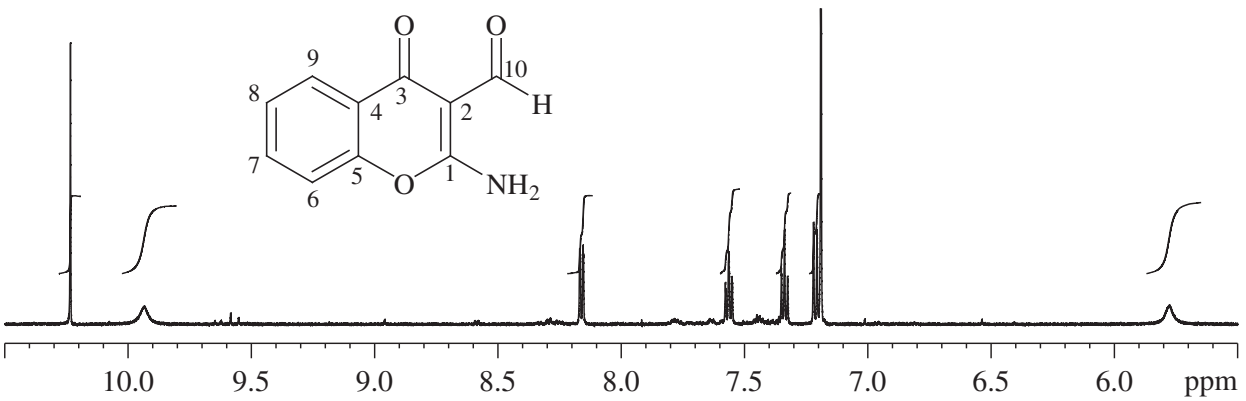

^{13}C/DEPT NMR 600 MHz

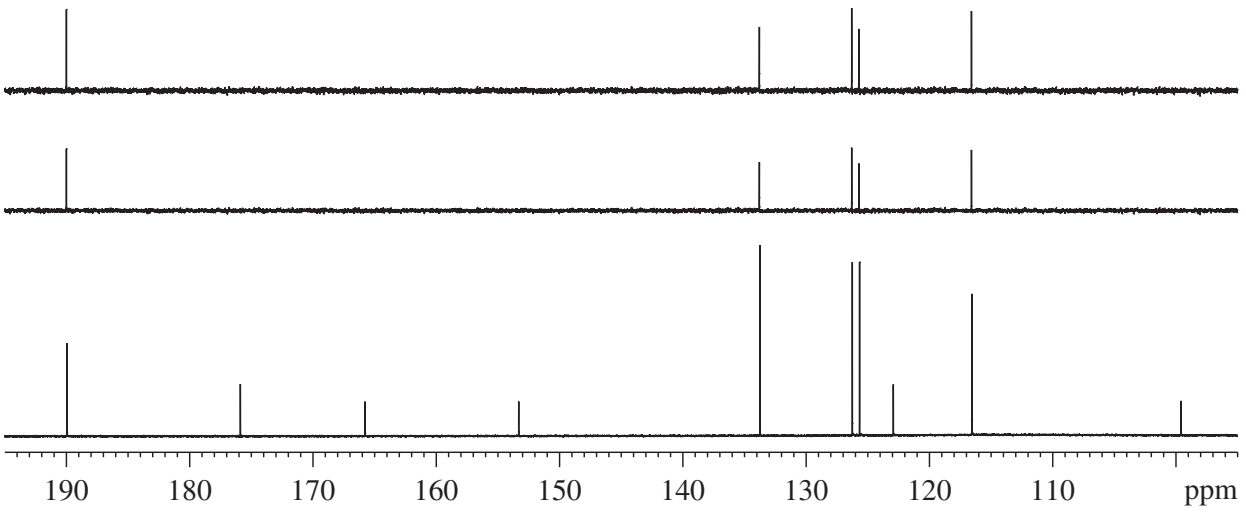

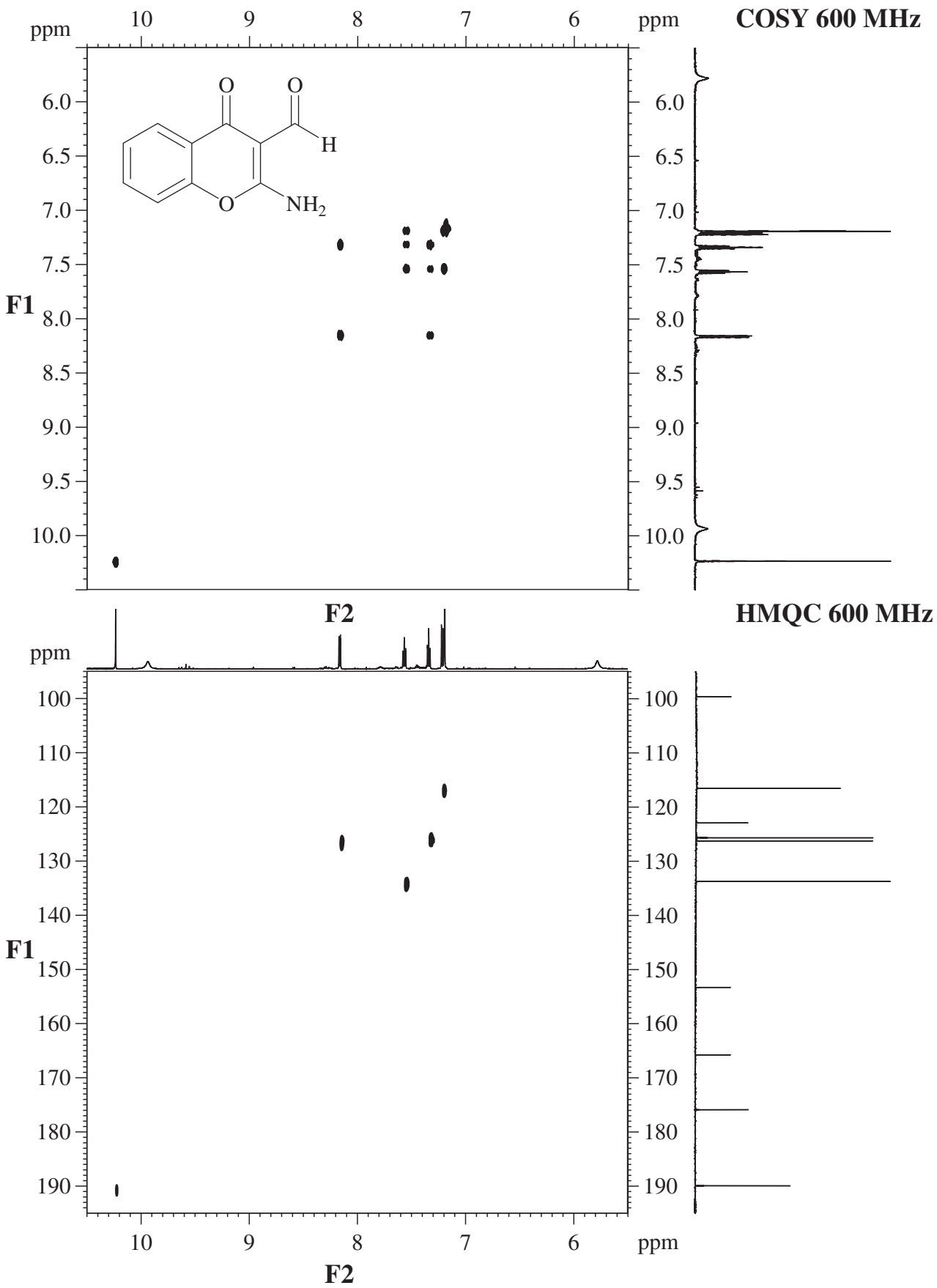
COSY 600 MHz
ppm
10
9
8
7
6
ppm
6.0
6.5
7.0
7.5
8.0
8.5
9.0
9.5
10.0
F1
O
O
H
O
NH2
F2
HMQC 600 MHz
ppm
100
110
120
130
140
150
160
170
180
190
F1
10
9
8
7
6
ppm
F2

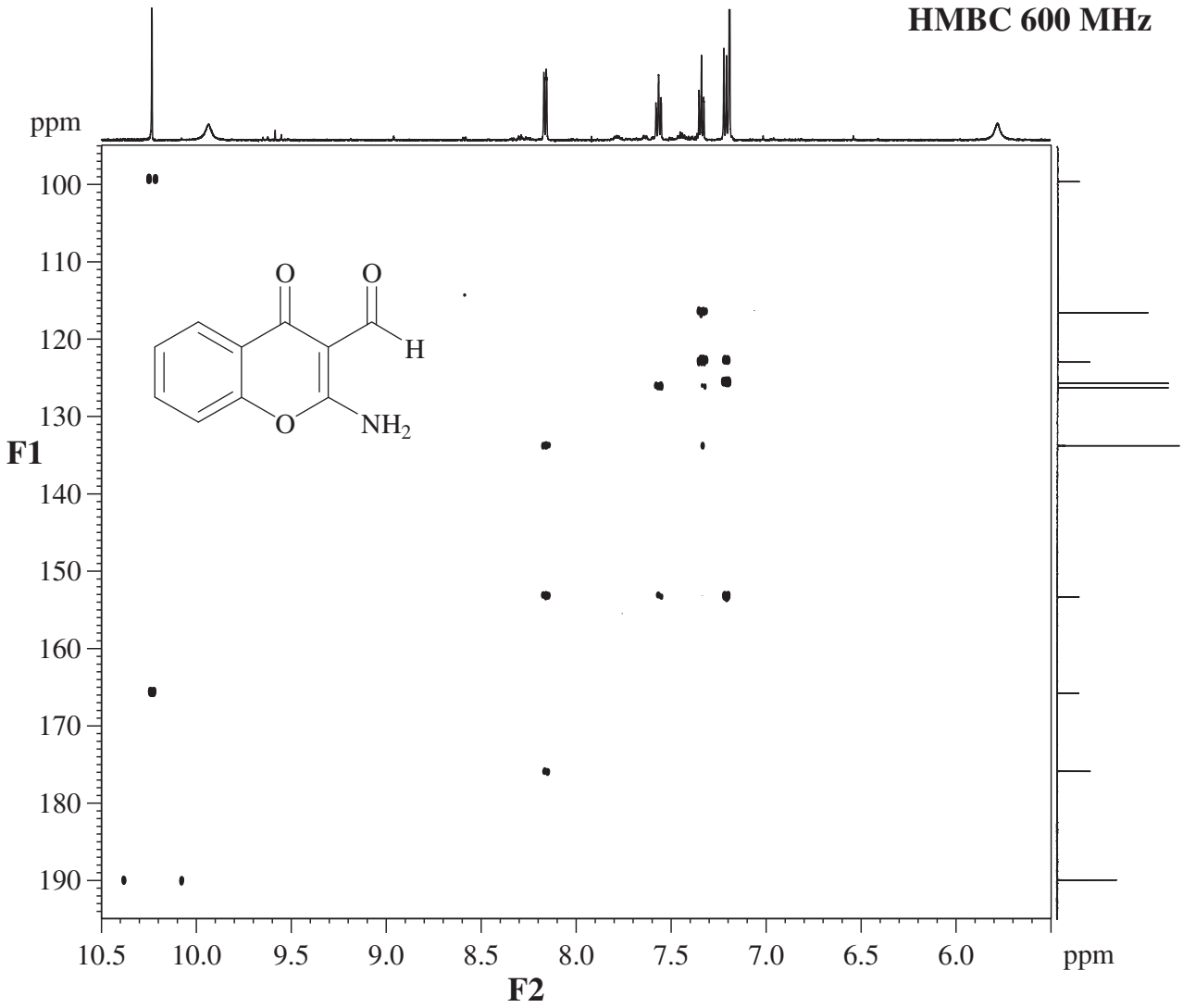
HMBC 600 MHz
ppm
100
110
120
130
140
150
160
170
180
190
F1
O
O
H
O
NH2
10.5
10.0
9.5
9.0
8.5
8.0
7.5
7.0
6.5
6.0
ppm
F2

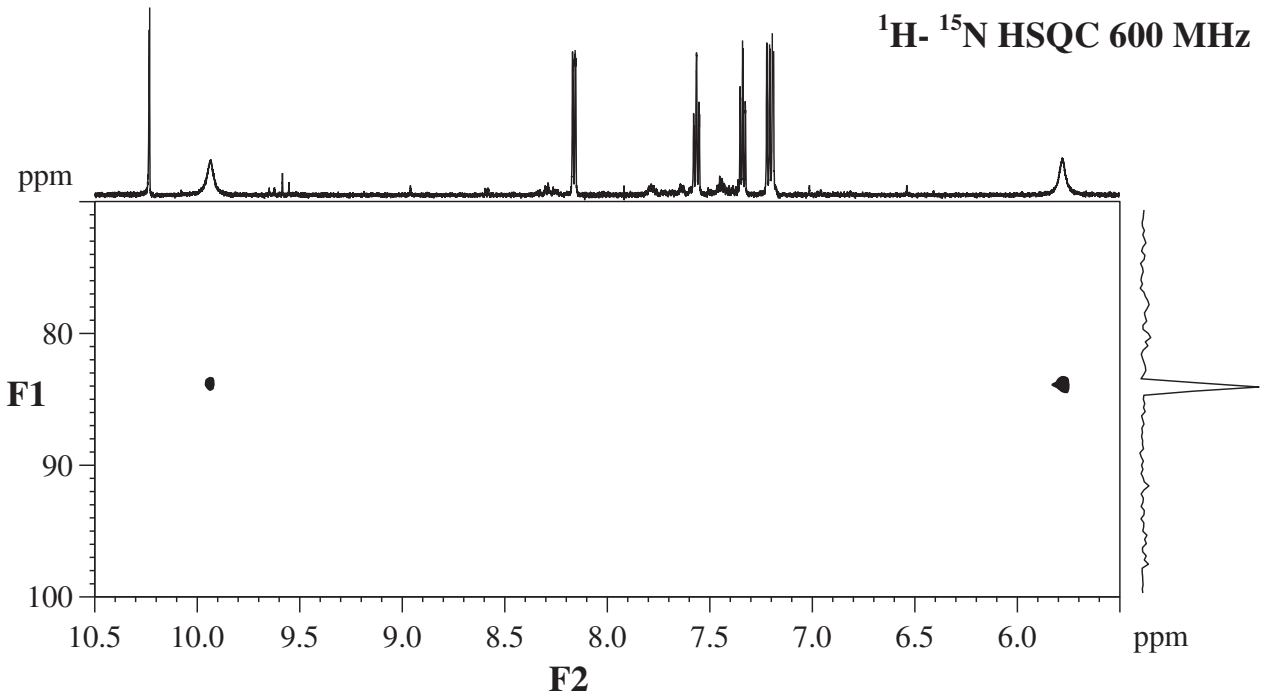
1H- 15N HSQC 600 MHz
ppm
80
90
100
F1
10.5
10.0
9.5
9.0
8.5
8.0
7.5
7.0
6.5
6.0
ppm
F2

MASS

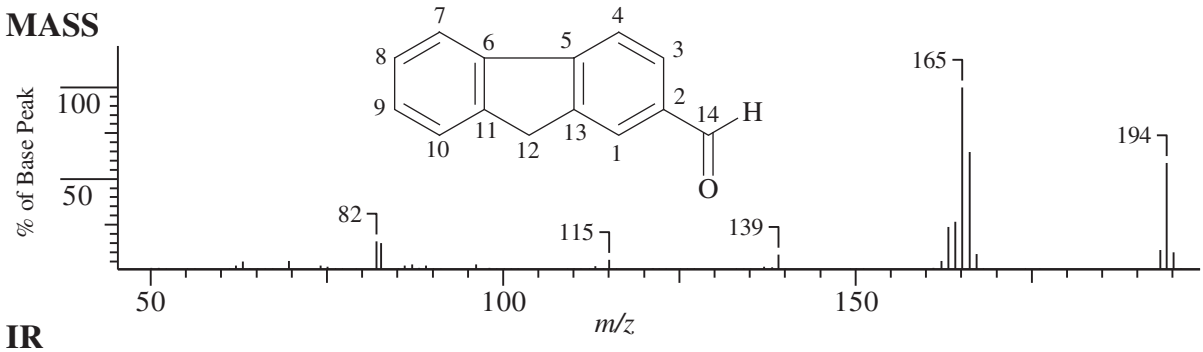

IR

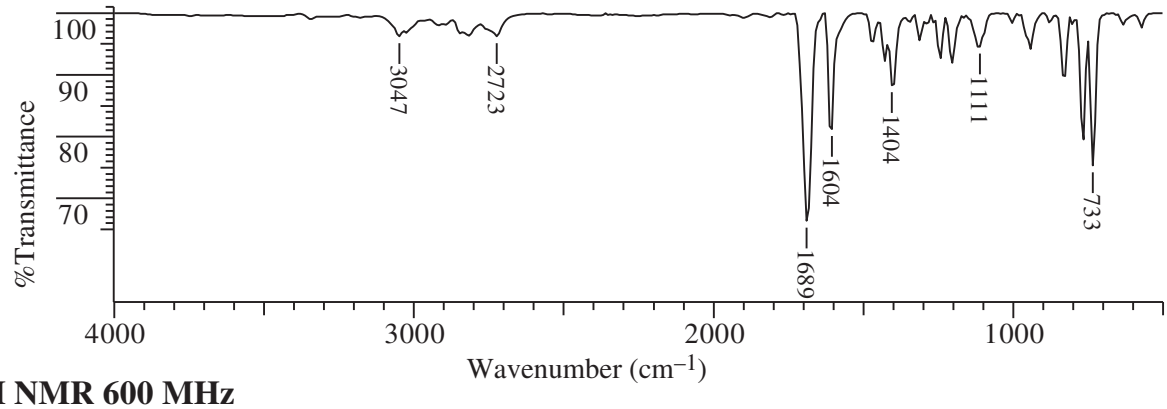

^{1}H NMR 600 MHz

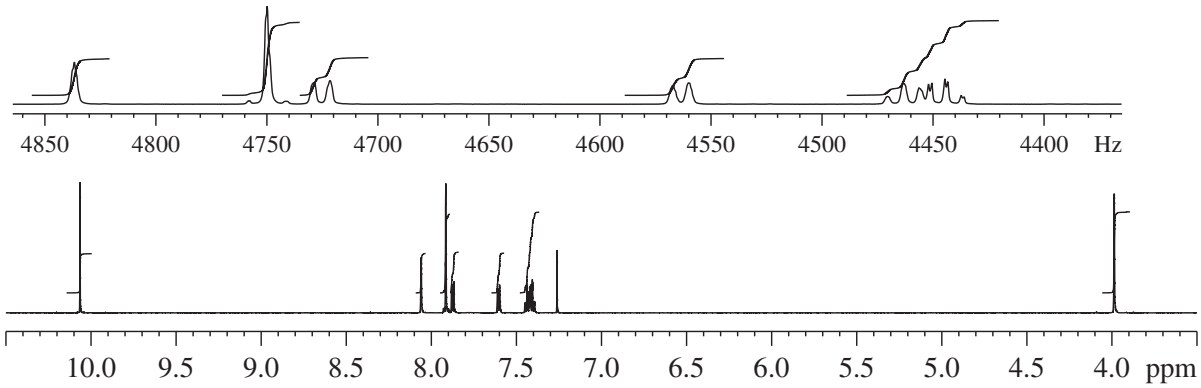

^{13}C/DEPT NMR 150.9 MHz

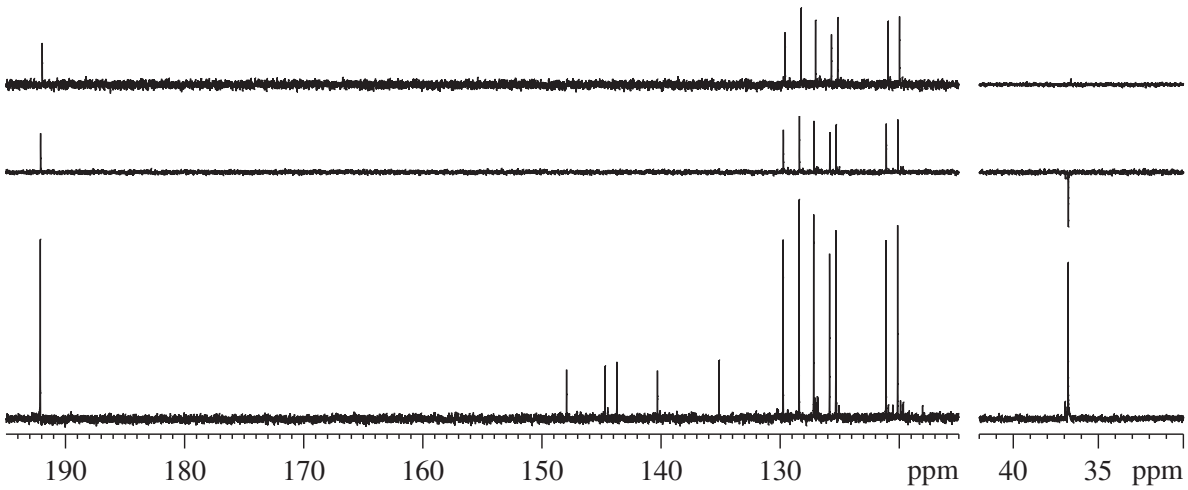

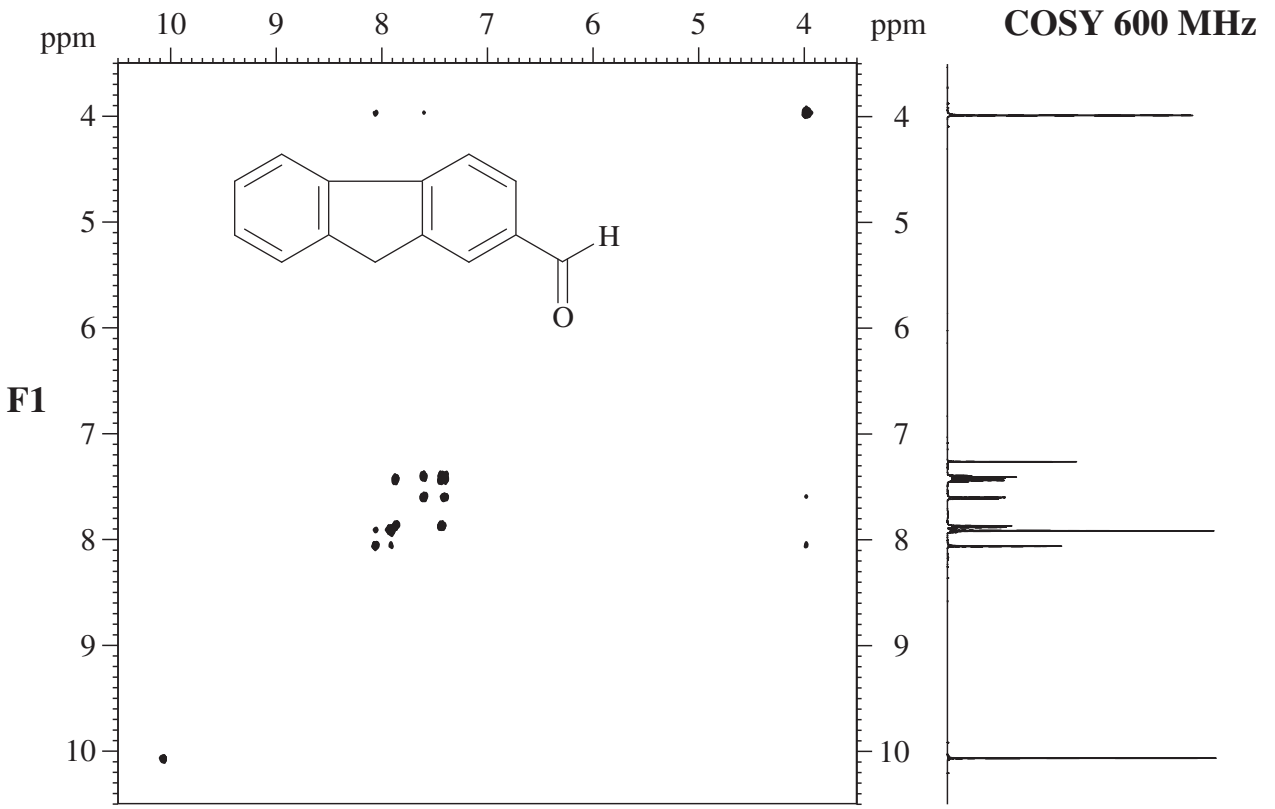
COSY 600 MHz
ppm
10 9 8 7 6 5 4
F1
F2
H
O

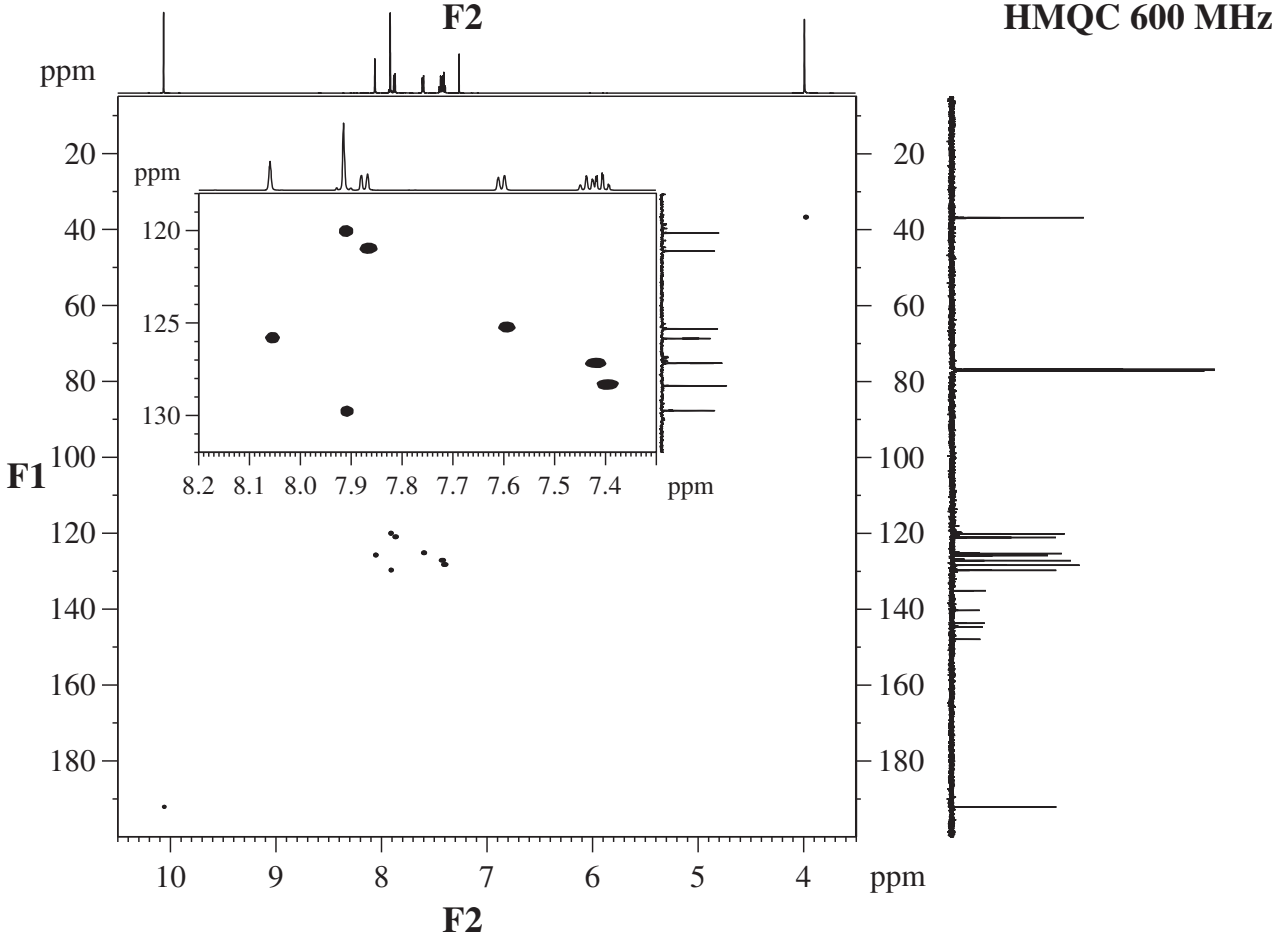
HMQC 600 MHz
ppm
20 40 60 80 100 120 140 160 180
F1
F2
120 125 130
8.2 8.1 8.0 7.9 7.8 7.7 7.6 7.5 7.4

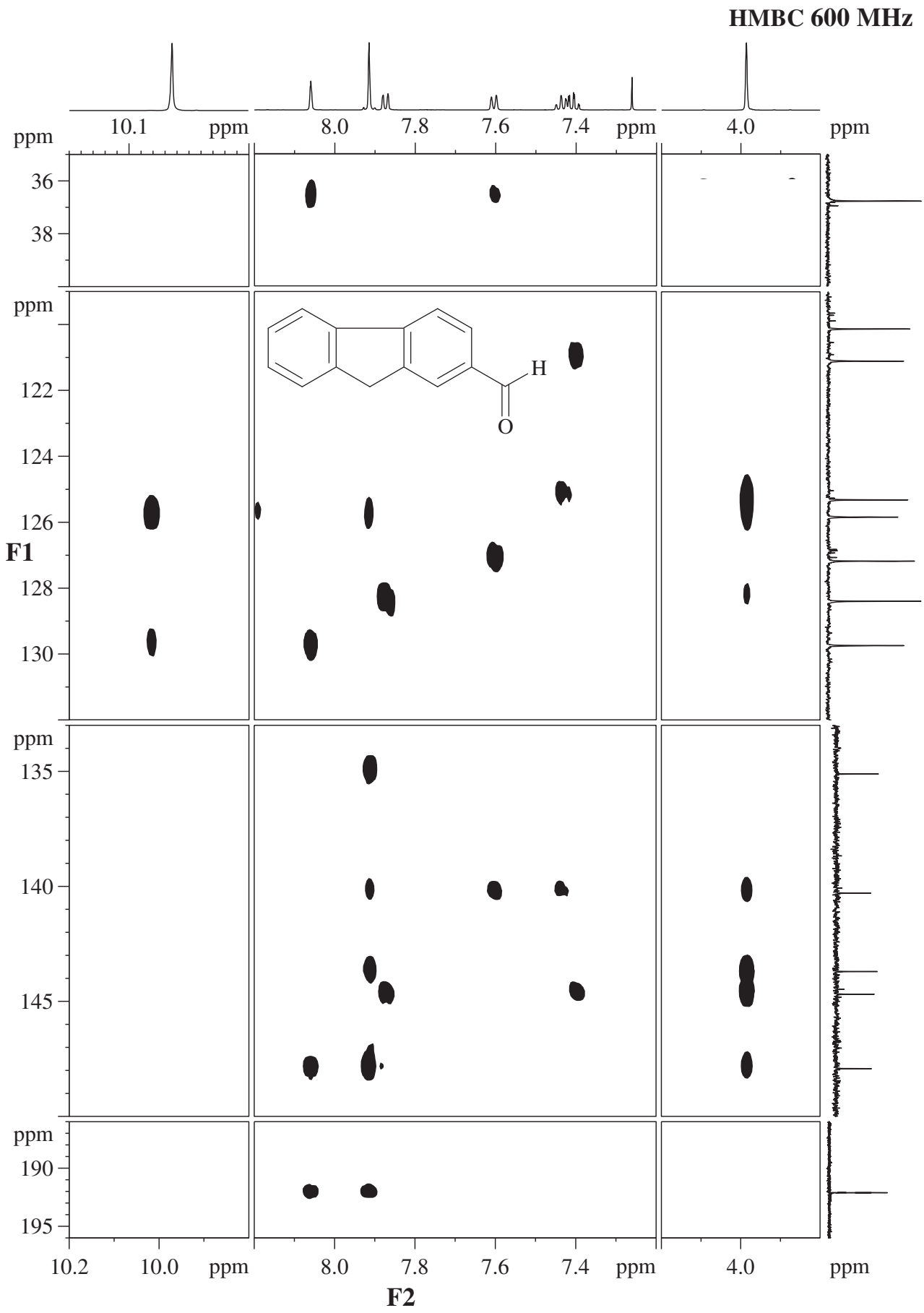
HMBC 600 MHz
10.1
ppm
8.0
7.8
7.6
7.4
ppm
4.0
ppm
36
38
122
124
126
128
130
135
140
145
190
195
F1
H
O
10.2
10.0
ppm
F2

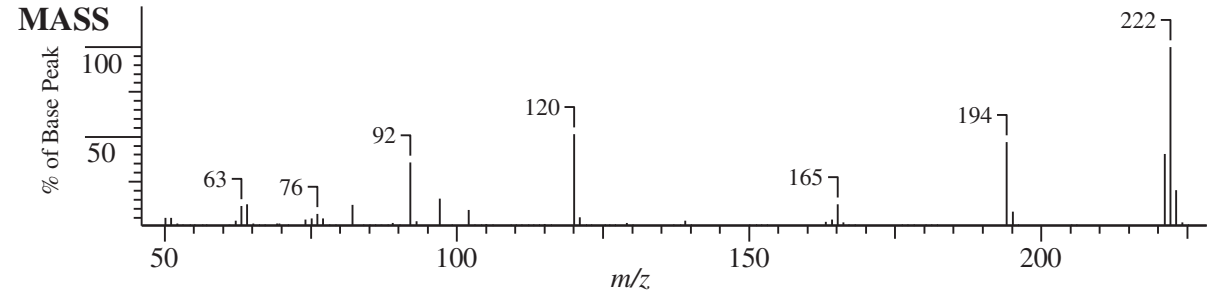
MASS
% of Base Peak
100
50
63
76
92
120
165
194
222
50
100
150
200
m/z

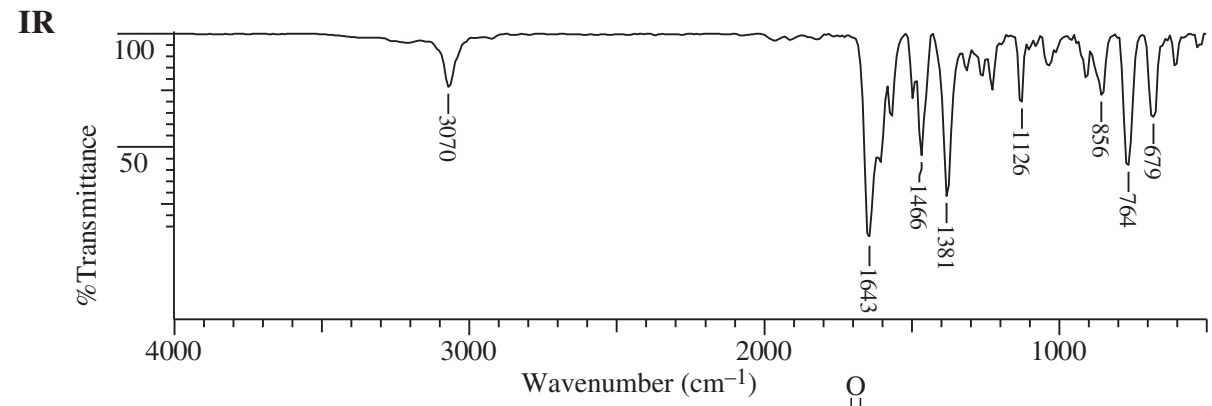
IR
100
50
%Transmittance
3070
1643
1466
1381
1126
856
764
679
4000
3000
2000
1000
Wavenumber (cm−1)

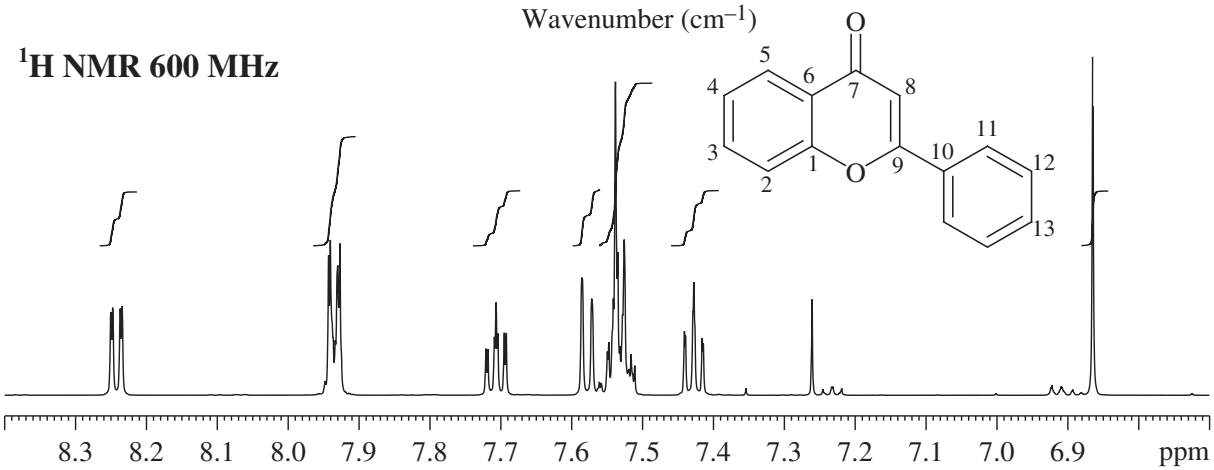
1H NMR 600 MHz
O
5
6
7
8
4
3
2
1
O
9
10
11
12
13
8.3
8.2
8.1
8.0
7.9
7.8
7.7
7.6
7.5
7.4
7.3
7.2
7.1
7.0
6.9
ppm

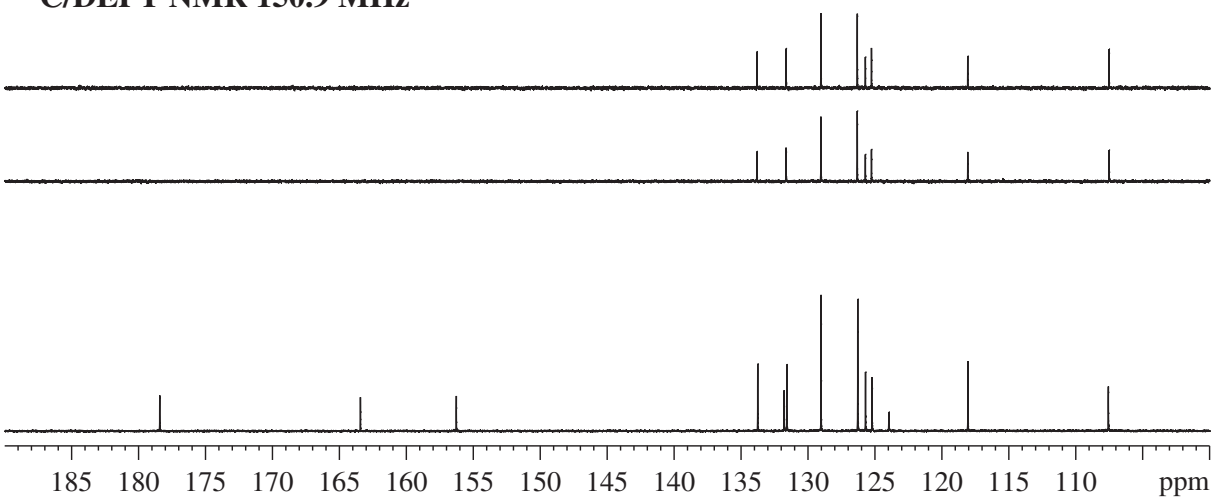
13C/DEPT NMR 150.9 MHz
185
180
175
170
165
160
155
150
145
140
135
130
125
120
115
110
ppm

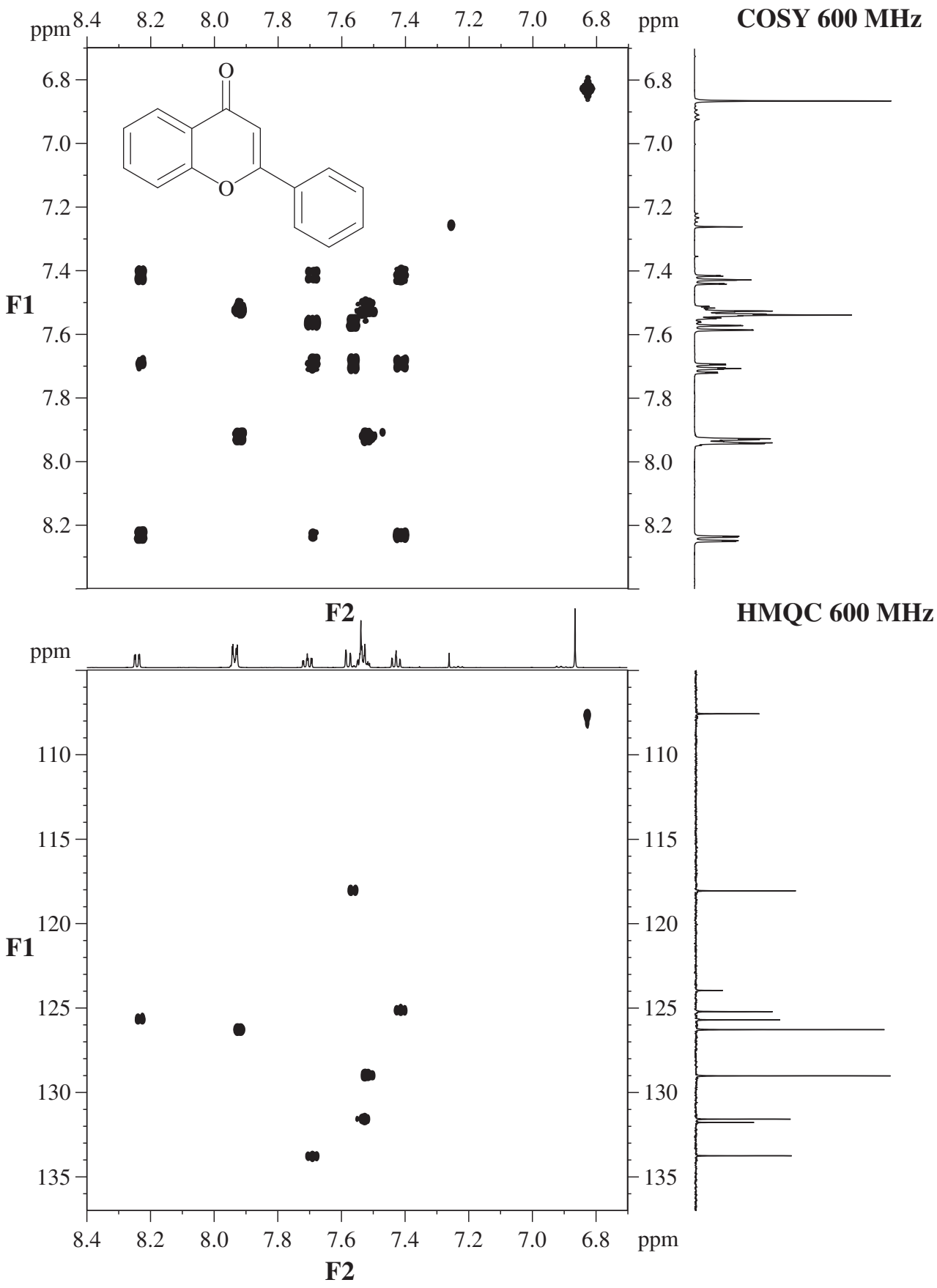
COSY 600 MHz
ppm
8.4 8.2 8.0 7.8 7.6 7.4 7.2 7.0 6.8
6.8 7.0 7.2 7.4 7.6 7.8 8.0 8.2
F1
F2
HMQC 600 MHz
110 115 120 125 130 135

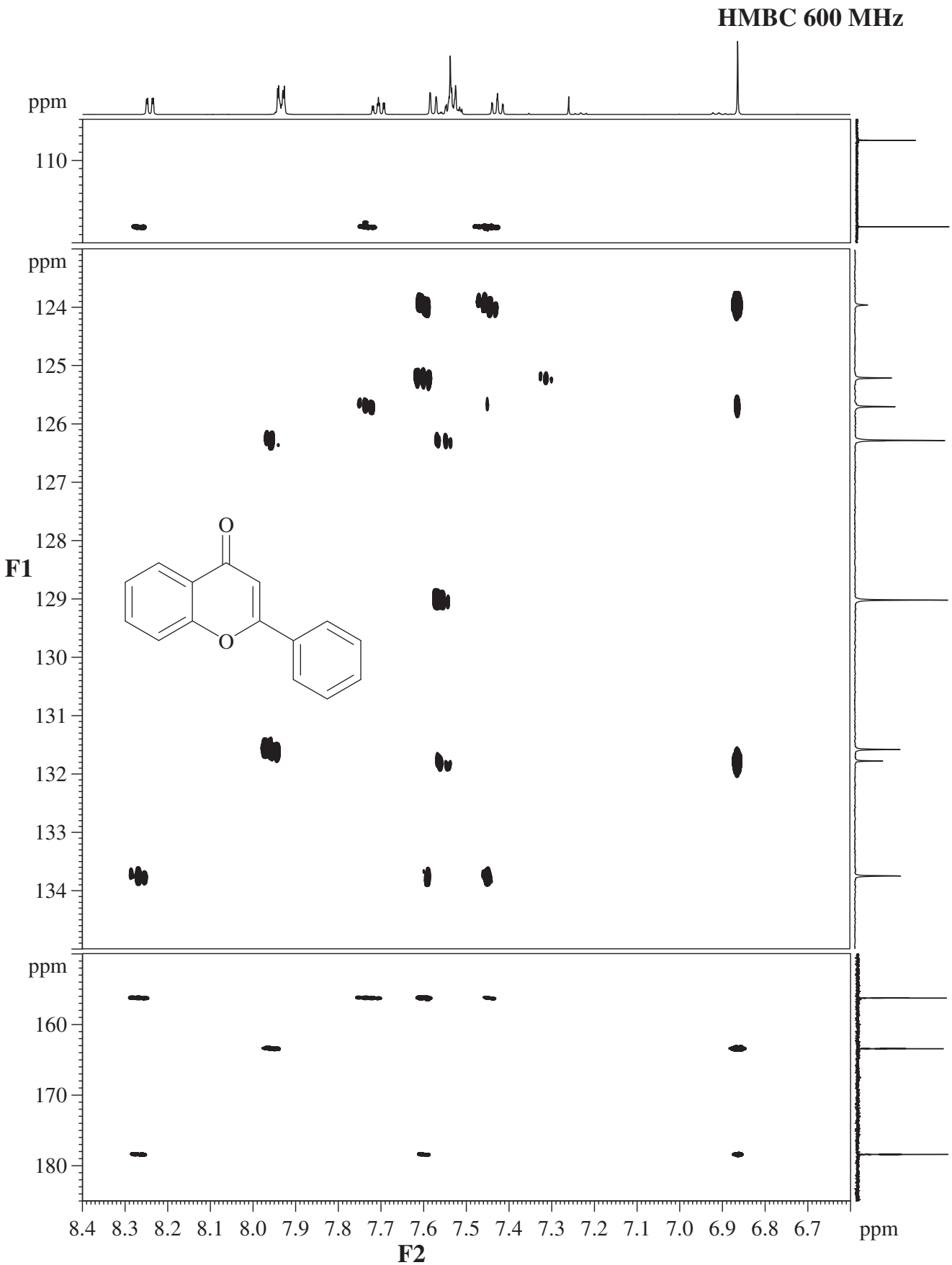
HMBC 600 MHz
ppm
110
ppm
124
125
126
127
128
129
130
131
132
133
134
F1
O
O
ppm
160
170
180
8.4 8.3 8.2 8.1 8.0 7.9 7.8 7.7 7.6 7.5 7.4 7.3 7.2 7.1 7.0 6.9 6.8 6.7
ppm
F2

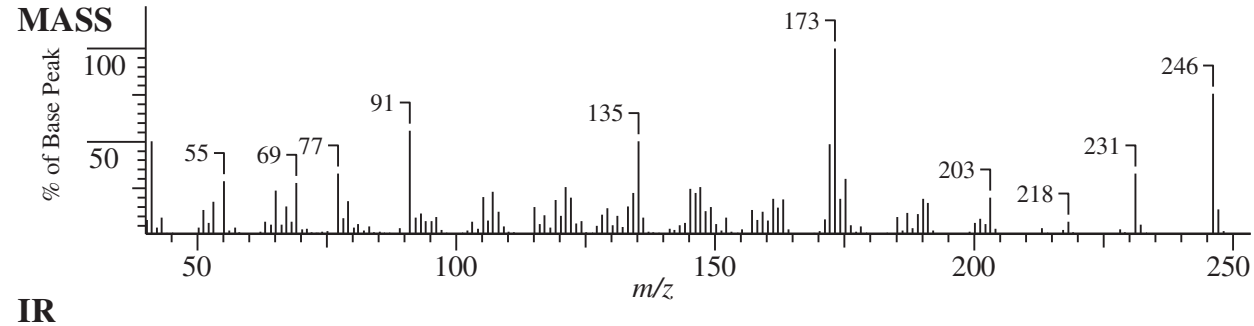
MASS
% of Base Peak
100
50
55
69
77
91
135
173
203
218
231
246
50
100
150
200
250
m/z

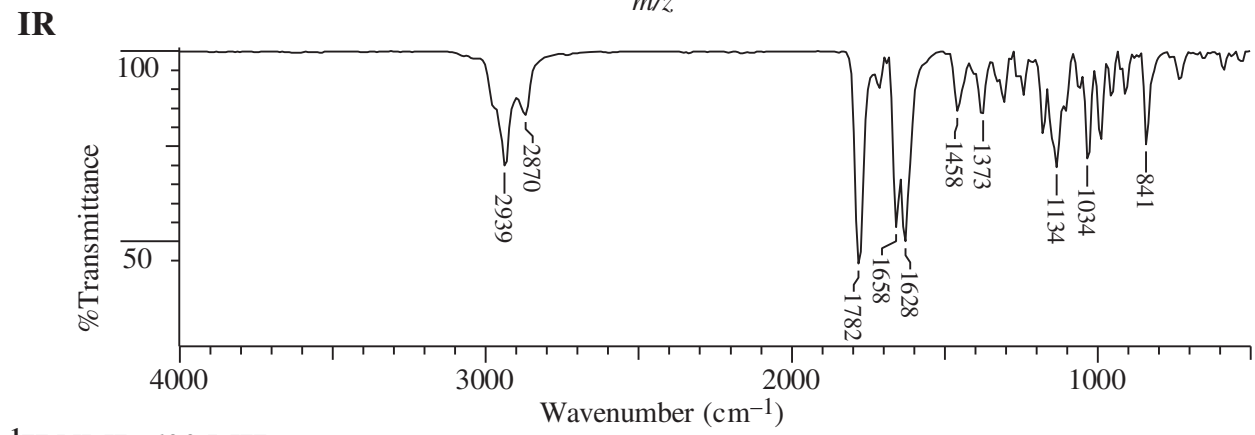
IR
%Transmittance
100
50
2939
2870
1782
1658
1628
1458
1373
1134
1034
841
4000
3000
2000
1000
Wavenumber (cm−1)

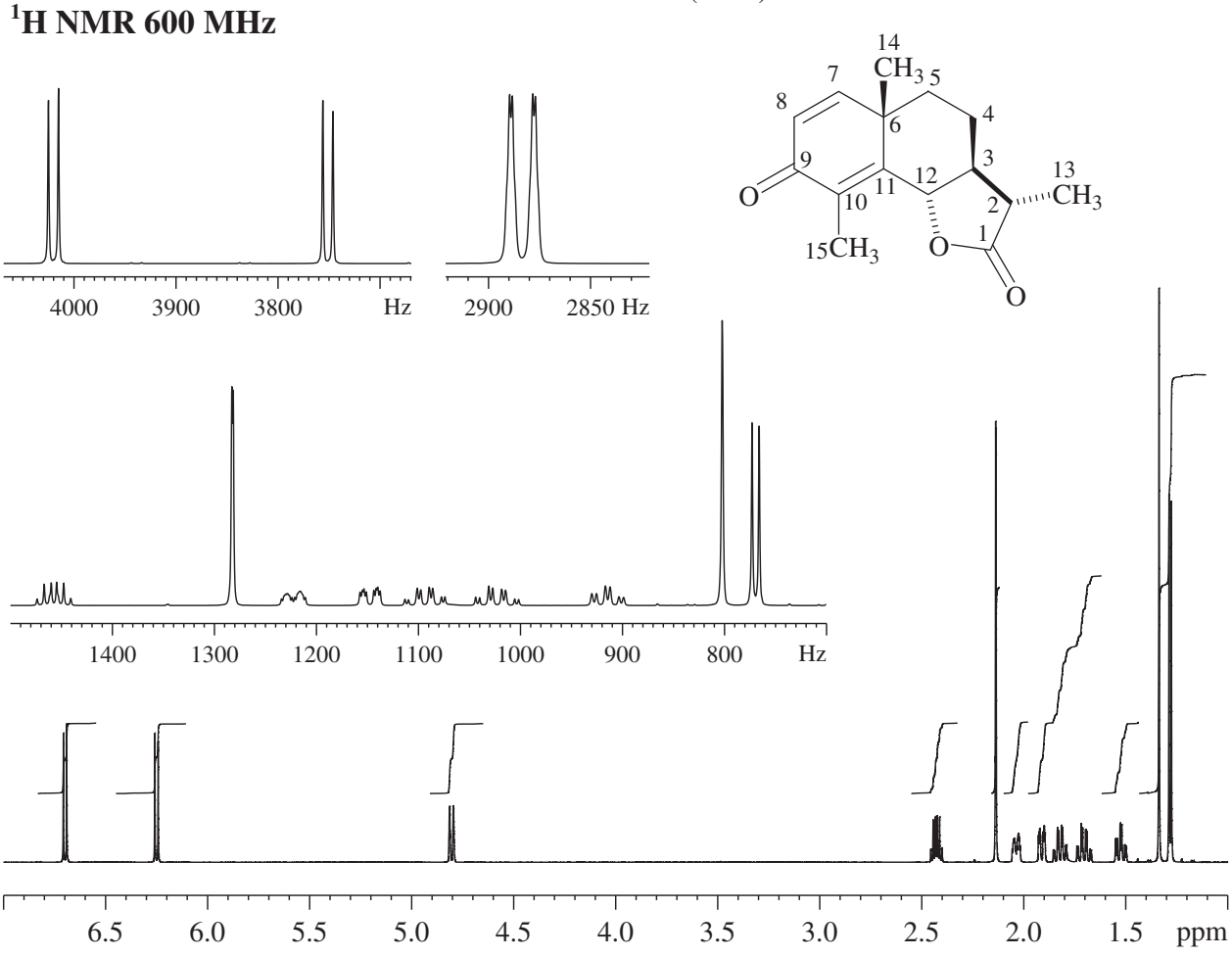
1H NMR 600 MHz
4000
3900
3800
Hz
2900
2850 Hz
1400
1300
1200
1100
1000
900
800
Hz
6.5
6.0
5.5
5.0
4.5
4.0
3.5
3.0
2.5
2.0
1.5
ppm
14
CH3
5
7
8
6
4
9
3
12
13
O
11
10
2
CH3
15CH3
O
1
O

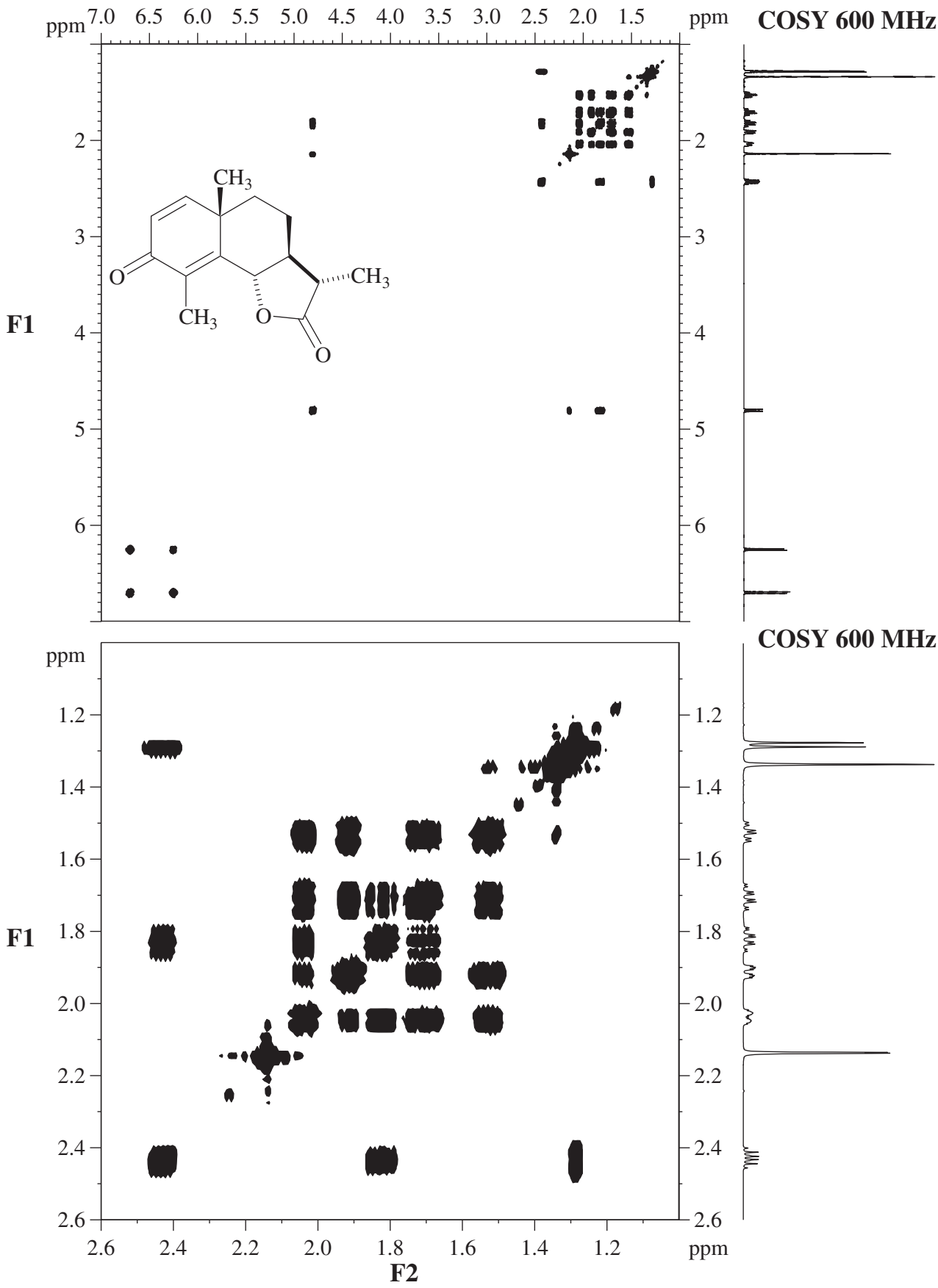
COSY 600 MHz
ppm
7.0 6.5 6.0 5.5 5.0 4.5 4.0 3.5 3.0 2.5 2.0 1.5
F1
2 3 4 5 6
CH3
O
CH3
CH3
O
O
COSY 600 MHz
ppm
F1
1.2 1.4 1.6 1.8 2.0 2.2 2.4 2.6
2.6 2.4 2.2 2.0 1.8 1.6 1.4 1.2
ppm
F2

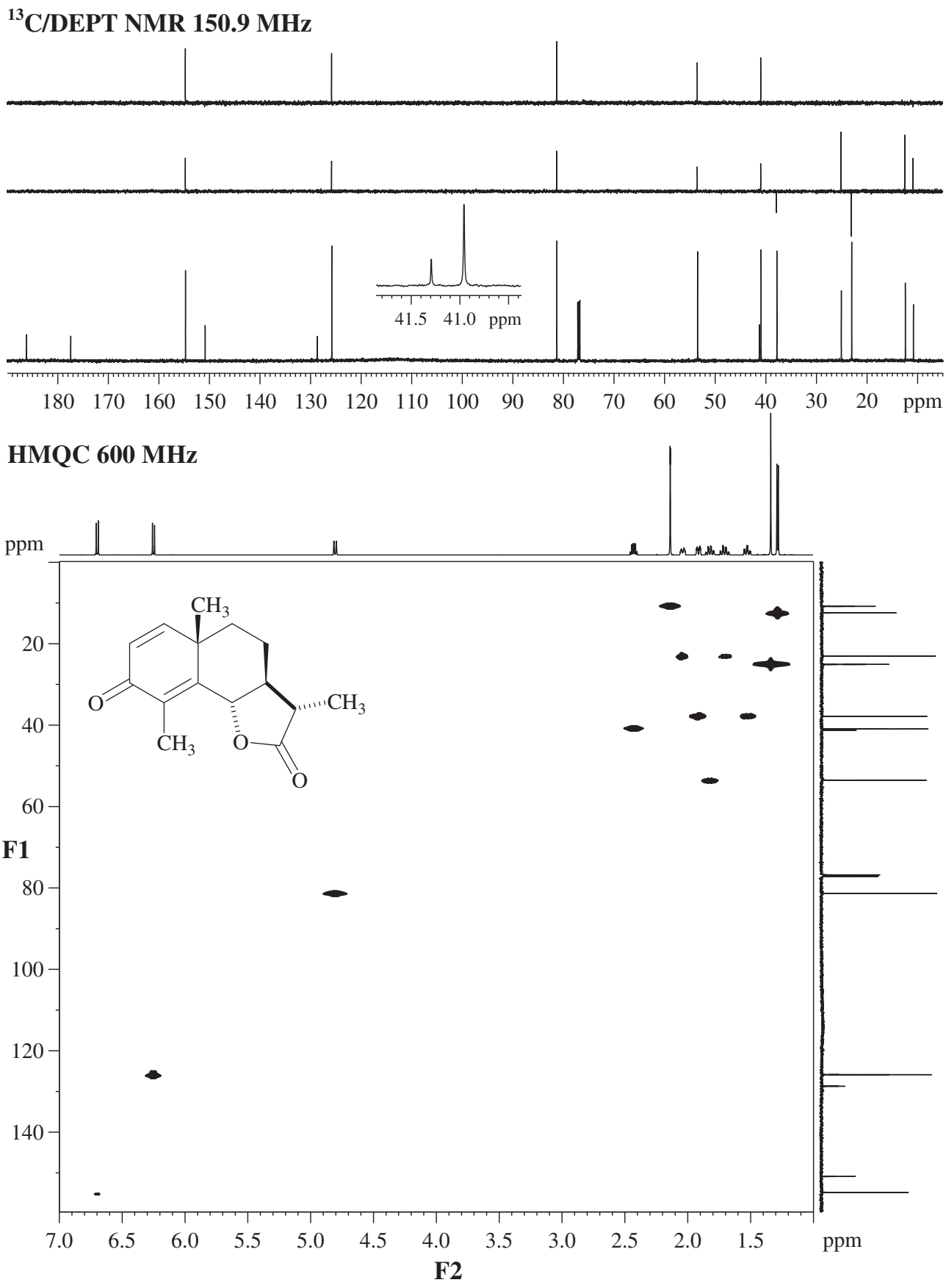
13C/DEPT NMR 150.9 MHz
41.5 41.0 ppm
180 170 160 150 140 130 120 110 100 90 80 70 60 50 40 30 20 ppm
HMQC 600 MHz
ppm
CH3
O
CH3
CH3
O
O
20
40
60
F1
80
100
120
140
7.0 6.5 6.0 5.5 5.0 4.5 4.0 3.5 3.0 2.5 2.0 1.5 ppm
F2

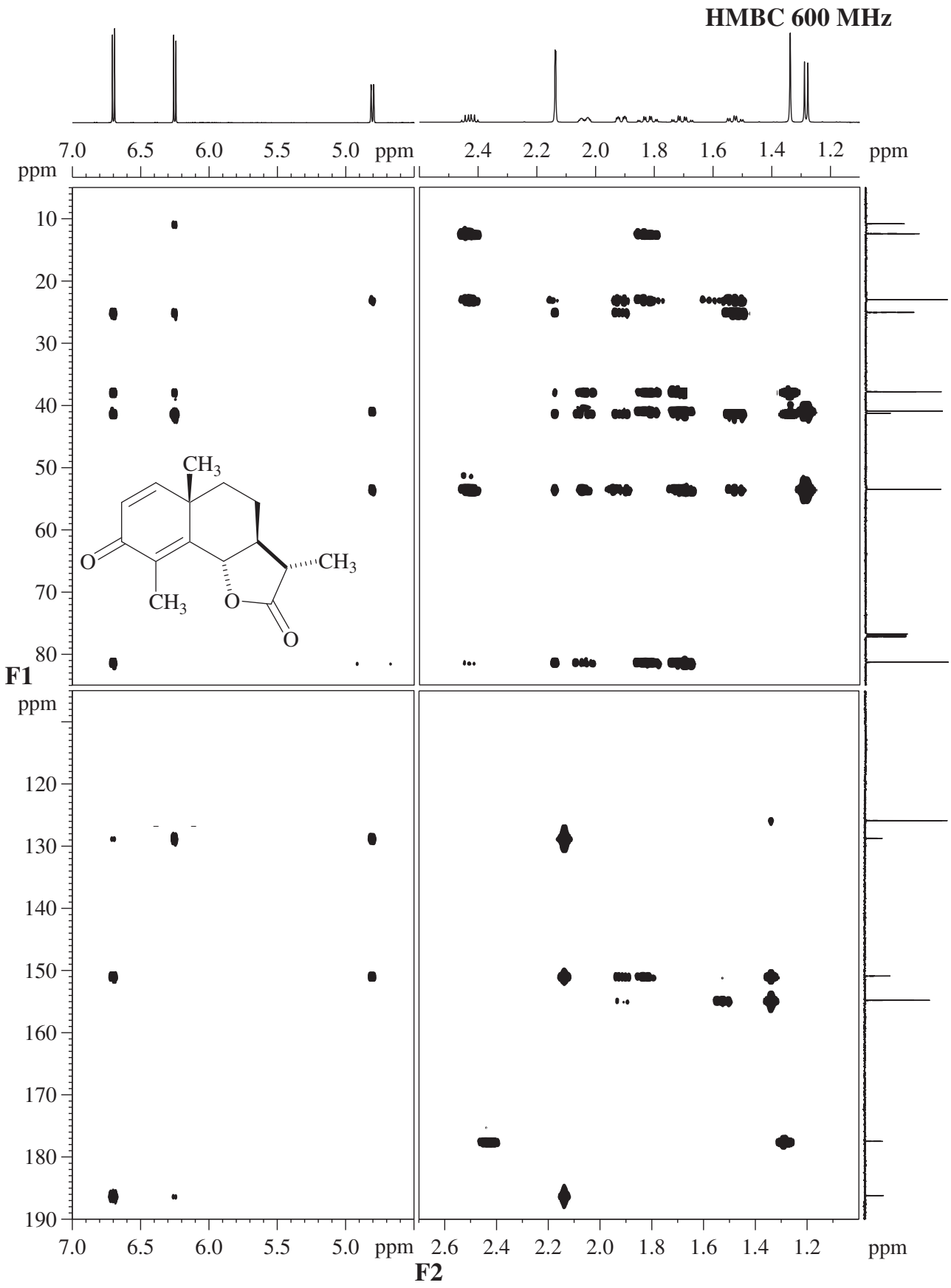
HMBC 600 MHz
7.0 6.5 6.0 5.5 5.0 ppm
2.4 2.2 2.0 1.8 1.6 1.4 1.2 ppm
ppm
10 20 30 40 50 60 70 80
CH3
O
CH3
CH3
O
O
F1
ppm
120 130 140 150 160 170 180 190
7.0 6.5 6.0 5.5 5.0 ppm 2.6 2.4 2.2 2.0 1.8 1.6 1.4 1.2 ppm
F2

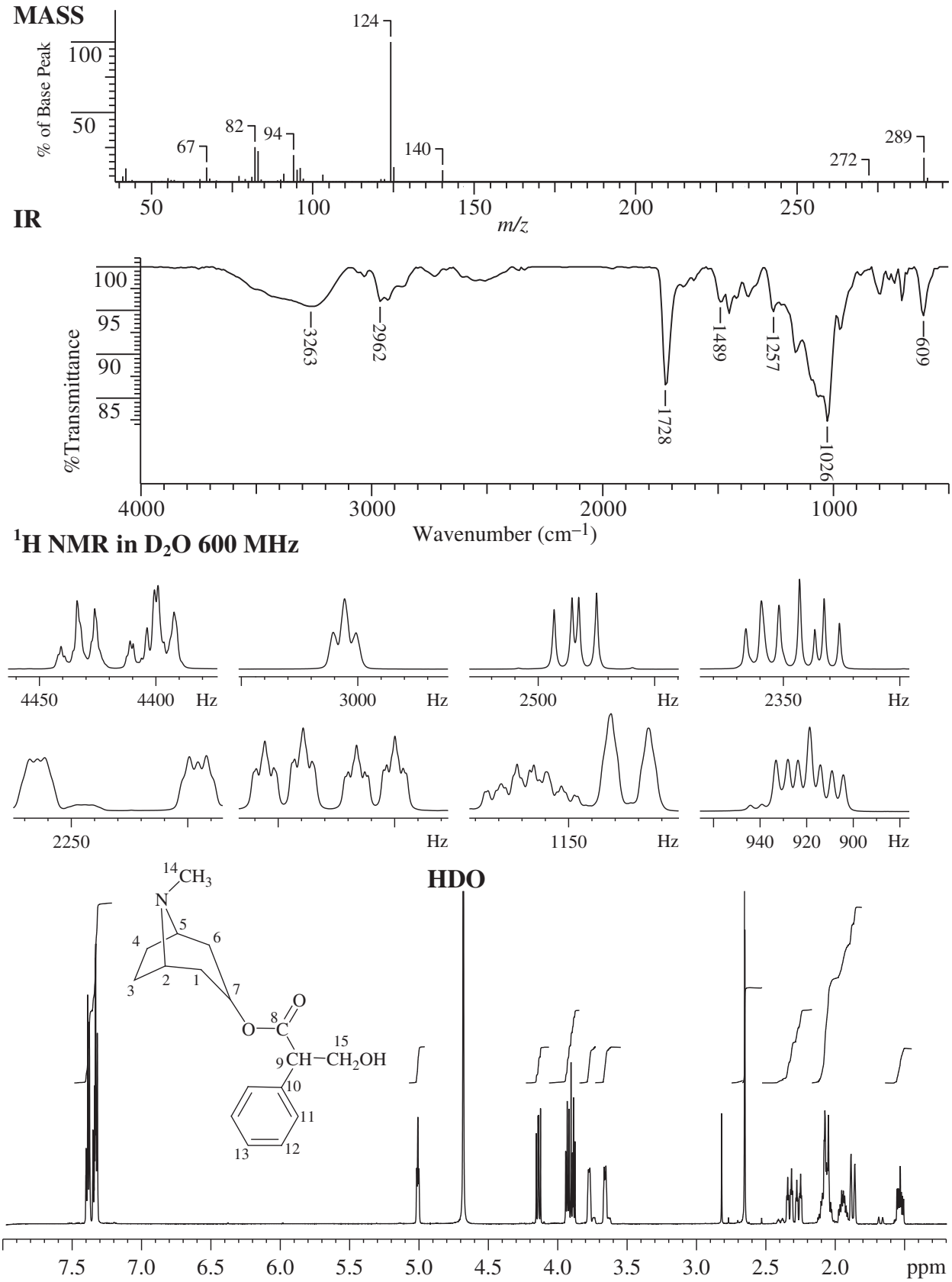
MASS
% of Base Peak
100
50
124
82
94
67
140
289
272
50
100
150
200
250
m/z
IR
%Transmittance
100
95
90
85
3263
2962
1728
1489
1257
1026
609
4000
3000
2000
1000
Wavenumber (cm−1)
1H NMR in D2O 600 MHz
4450
4400
Hz
3000
Hz
2500
Hz
2350
Hz
2250
Hz
1150
Hz
940
920
900
Hz
HDO
14CH3
N
5
4
6
3
2
1
7
O
8
O
C
O
15
9CH−CH2OH
10
11
13
12
7.5
7.0
6.5
6.0
5.5
5.0
4.5
4.0
3.5
3.0
2.5
2.0
ppm

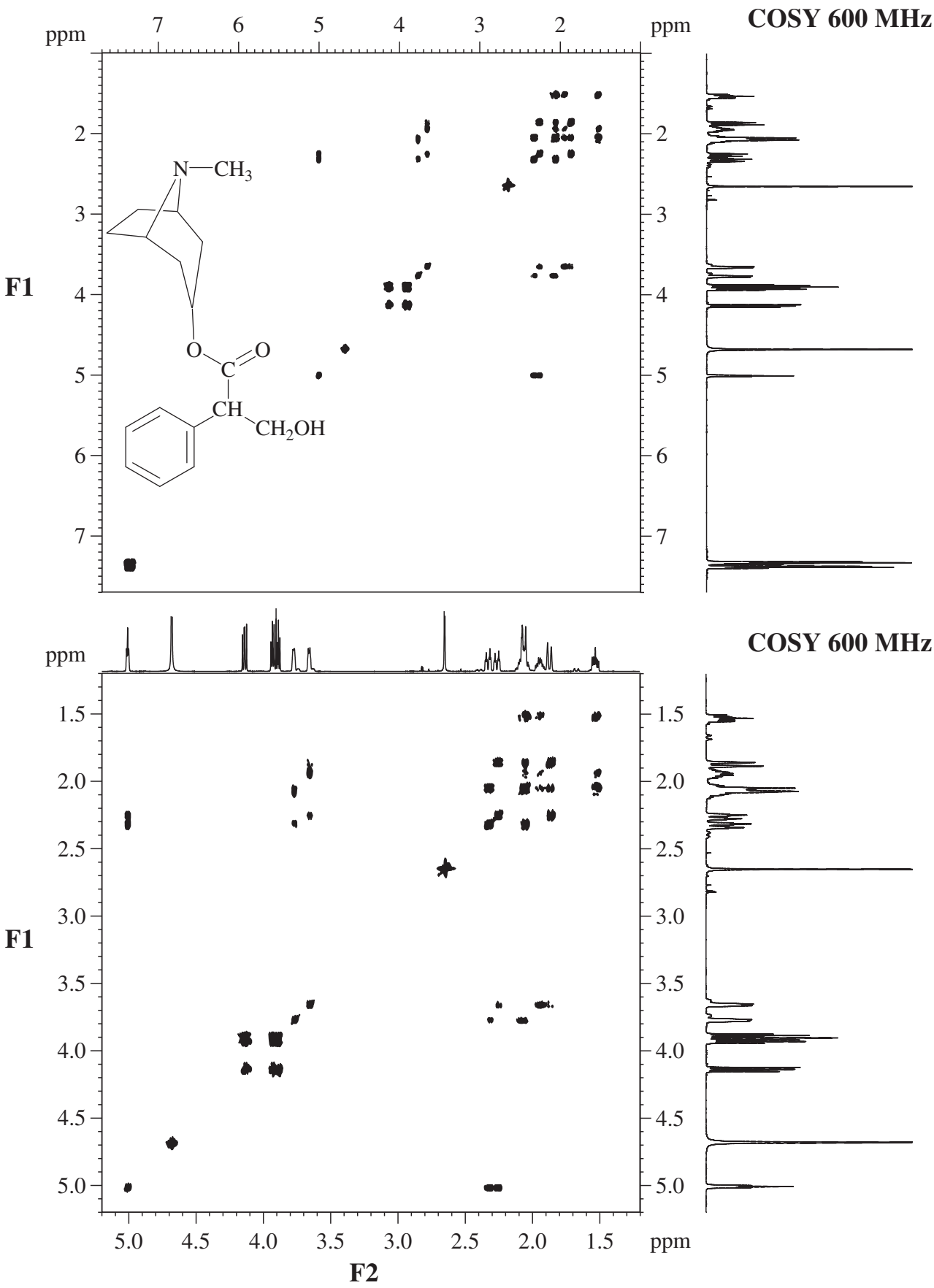
COSY 600 MHz
ppm
7
6
5
4
3
2
ppm
F1
N—CH3
O
C
O
CH
CH2OH
COSY 600 MHz
ppm
1.5
2.0
2.5
3.0
3.5
4.0
4.5
5.0
F1
5.0
4.5
4.0
3.5
3.0
2.5
2.0
1.5
ppm
F2

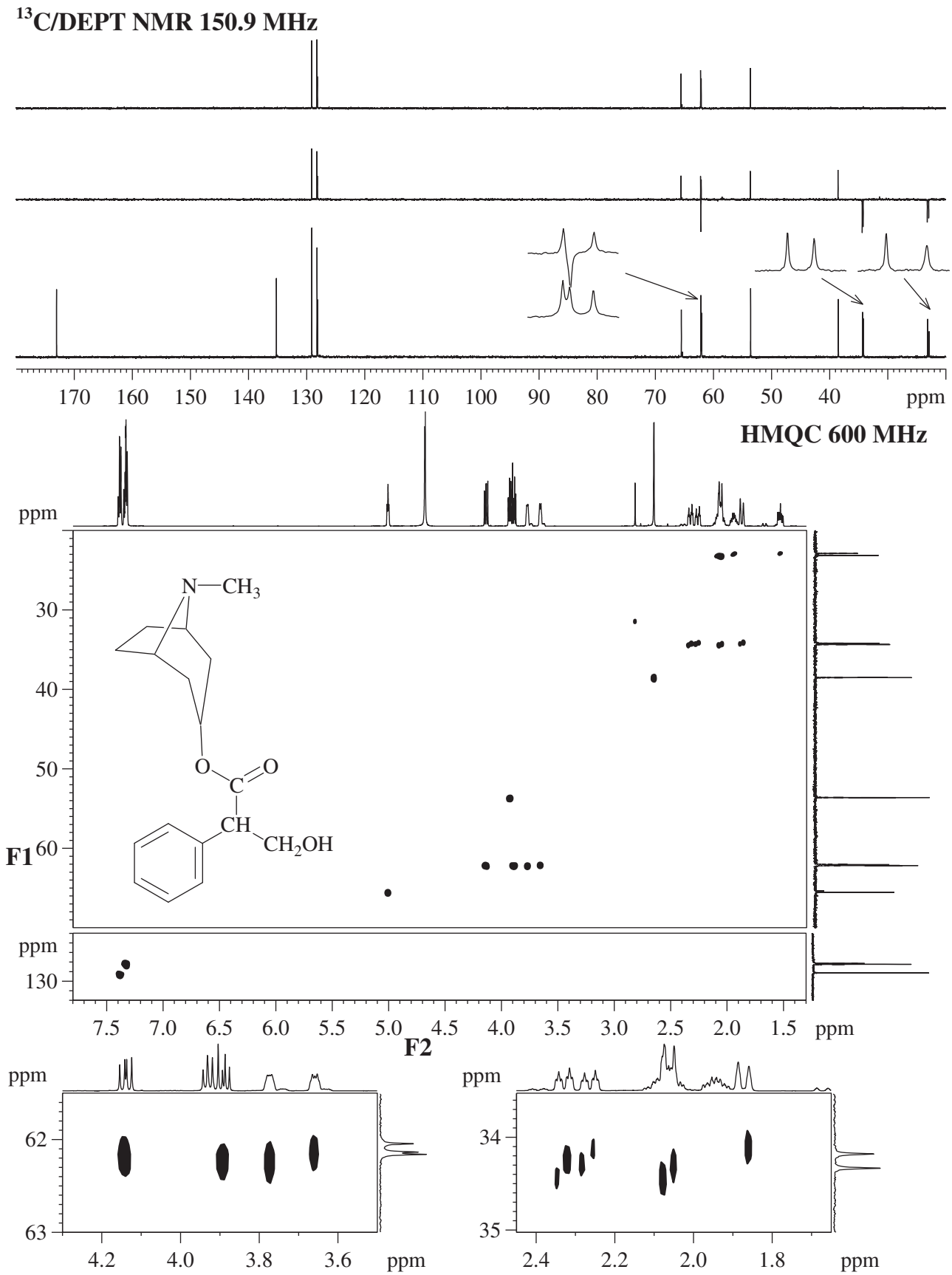
13C/DEPT NMR 150.9 MHz
170 160 150 140 130 120 110 100 90 80 70 60 50 40 ppm
HMQC 600 MHz
ppm
N—CH3
O
C
O
CH
CH2OH
F1
30
40
50
60
ppm
130
7.5 7.0 6.5 6.0 5.5 5.0 4.5 4.0 3.5 3.0 2.5 2.0 1.5 ppm
F2
ppm
62
63
4.2 4.0 3.8 3.6 ppm
ppm
34
35
2.4 2.2 2.0 1.8 ppm

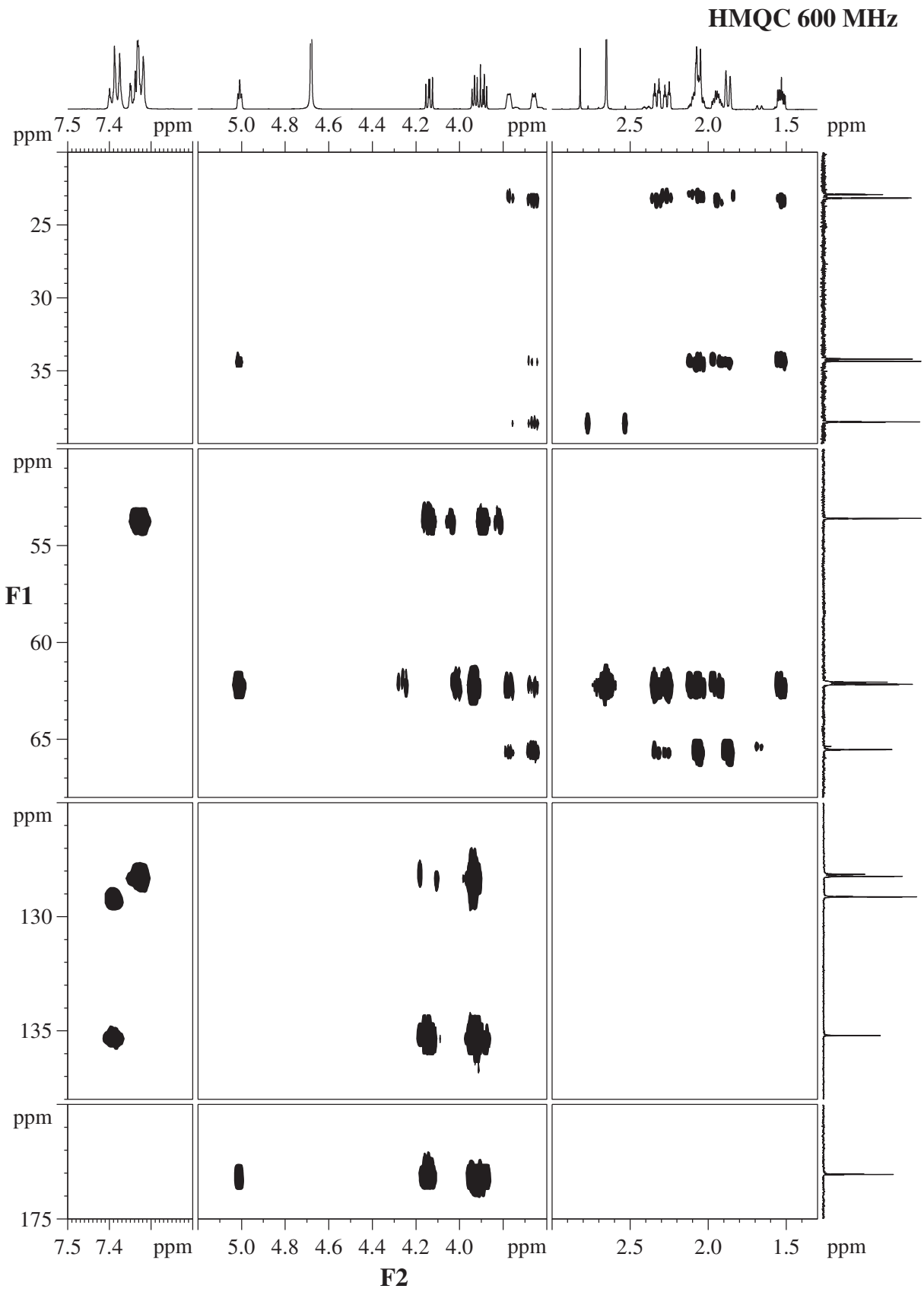
HMQC 600 MHz
7.5 7.4 ppm
5.0 4.8 4.6 4.4 4.2 4.0 ppm
2.5 2.0 1.5 ppm
ppm
25
30
35
ppm
55
60
65
F1
ppm
130
135
ppm
175
7.5 7.4 ppm
5.0 4.8 4.6 4.4 4.2 4.0 ppm
2.5 2.0 1.5 ppm
F2

INDEX

WILEY END USER LICENSE AGREEMENT

Go to www.wiley.com/go/eula to access Wiley’s ebook EULA.